frontiers | Research Topics

Abiotic stress signaling in plants: Functional genomic intervention, volume II

Edited by
Girdhar Kumar Pandey, Ashish Kumar Srivastava, Amita Pandey and Maik Böhmer

Published in
Frontiers in Plant Science

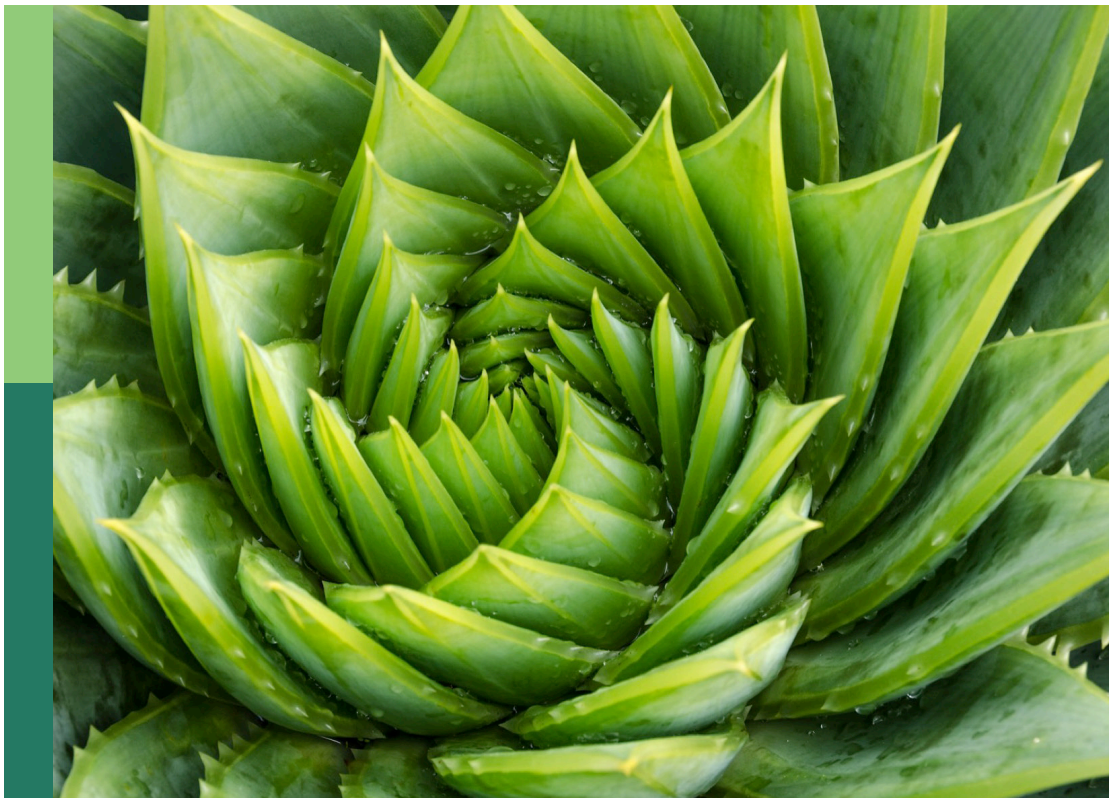

FRONTIERS EBOOK COPYRIGHT STATEMENT

The copyright in the text of individual articles in this ebook is the property of their respective authors or their respective institutions or funders. The copyright in graphics and images within each article may be subject to copyright of other parties. In both cases this is subject to a license granted to Frontiers.

The compilation of articles constituting this ebook is the property of Frontiers.

Each article within this ebook, and the ebook itself, are published under the most recent version of the Creative Commons CC-BY licence. The version current at the date of publication of this ebook is CC-BY 4.0. If the CC-BY licence is updated, the licence granted by Frontiers is automatically updated to the new version.

When exercising any right under the CC-BY licence, Frontiers must be attributed as the original publisher of the article or ebook, as applicable.

Authors have the responsibility of ensuring that any graphics or other materials which are the property of others may be included in the CC-BY licence, but this should be checked before relying on the CC-BY licence to reproduce those materials. Any copyright notices relating to those materials must be complied with.

Copyright and source acknowledgement notices may not be removed and must be displayed in any copy, derivative work or partial copy which includes the elements in question.

All copyright, and all rights therein, are protected by national and international copyright laws. The above represents a summary only. For further information please read Frontiers' Conditions for Website Use and Copyright Statement, and the applicable CC-BY licence.

ISSN 1664-8714
ISBN 978-2-8325-4397-9
DOI 10.3389/978-2-8325-4397-9

About Frontiers

Frontiers is more than just an open access publisher of scholarly articles: it is a pioneering approach to the world of academia, radically improving the way scholarly research is managed. The grand vision of Frontiers is a world where all people have an equal opportunity to seek, share and generate knowledge. Frontiers provides immediate and permanent online open access to all its publications, but this alone is not enough to realize our grand goals.

Frontiers journal series

The Frontiers journal series is a multi-tier and interdisciplinary set of open-access, online journals, promising a paradigm shift from the current review, selection and dissemination processes in academic publishing. All Frontiers journals are driven by researchers for researchers; therefore, they constitute a service to the scholarly community. At the same time, the *Frontiers journal series* operates on a revolutionary invention, the tiered publishing system, initially addressing specific communities of scholars, and gradually climbing up to broader public understanding, thus serving the interests of the lay society, too.

Dedication to quality

Each Frontiers article is a landmark of the highest quality, thanks to genuinely collaborative interactions between authors and review editors, who include some of the world's best academicians. Research must be certified by peers before entering a stream of knowledge that may eventually reach the public - and shape society; therefore, Frontiers only applies the most rigorous and unbiased reviews. Frontiers revolutionizes research publishing by freely delivering the most outstanding research, evaluated with no bias from both the academic and social point of view. By applying the most advanced information technologies, Frontiers is catapulting scholarly publishing into a new generation.

What are Frontiers Research Topics?

Frontiers Research Topics are very popular trademarks of the *Frontiers journals series*: they are collections of at least ten articles, all centered on a particular subject. With their unique mix of varied contributions from Original Research to Review Articles, Frontiers Research Topics unify the most influential researchers, the latest key findings and historical advances in a hot research area.

Find out more on how to host your own Frontiers Research Topic or contribute to one as an author by contacting the Frontiers editorial office: frontiersin.org/about/contact

Abiotic stress signaling in plants: Functional genomic intervention, volume II

Topic editors

Girdhar Kumar Pandey — University of Delhi, India
Ashish Kumar Srivastava — Bhabha Atomic Research Centre (BARC), India
Amita Pandey — Shriram Institute for Industrial Research, India
Maik Böhmer — Goethe University Frankfurt, Germany

Citation

Pandey, G. K., Srivastava, A. K., Pandey, A., Böhmer, M., eds. (2024). *Abiotic stress signaling in plants: Functional genomic intervention, volume II*. Lausanne: Frontiers Media SA. doi: 10.3389/978-2-8325-4397-9

Table of contents

05 Editorial: Abiotic stress signaling in plants: functional genomic intervention, volume II
Ashish Kumar Srivastava, Amita Pandey, Maik Böhmer and Girdhar Kumar Pandey

08 The *Paeonia qiui* R2R3-MYB Transcription Factor PqMYB113 Positively Regulates Anthocyanin Accumulation in *Arabidopsis thaliana* and Tobacco
Xiaokun Liu, Jingjing Duan, Dan Huo, Qinqin Li, Qiaoyun Wang, Yanlong Zhang, Lixin Niu and Jianrang Luo

22 Identification of a RelA/SpoT Homolog and Its Possible Role in the Accumulation of Astaxanthin in *Haematococcus pluvialis*
Hui Jin, Yong Min Lao, Jin Zhou and Zhong Hua Cai

33 Metabolic and Physiological Changes in the Roots of Two Oat Cultivars in Response to Complex Saline-Alkali Stress
Yugang Gao, Yongling Jin, Wei Guo, Yingwen Xue and Lihe Yu

51 Molecular Characterization Reveals the Involvement of Calcium Dependent Protein Kinases in Abiotic Stress Signaling and Development in Chickpea (*Cicer arietinum*)
Deepika Deepika, Nikita Poddar, Shailesh Kumar and Amarjeet Singh

69 Effect of *Piriformospora indica*-Induced Systemic Resistance and Basal Immunity Against *Rhizoctonia cerealis* and *Fusarium graminearum* in Wheat
Liang Li, Nannan Guo, Yu Feng, Mengmeng Duan and Chunhui Li

85 Sulfur Dioxide: An Emerging Signaling Molecule in Plants
Zhong-Guang Li, Xiao-Er Li and Hong-Yan Chen

94 Thermo-Priming Mediated Cellular Networks for Abiotic Stress Management in Plants
Ambreen Khan, Varisha Khan, Khyati Pandey, Sudhir Kumar Sopory and Neeti Sanan-Mishra

123 Core Components of Abscisic Acid Signaling and Their Post-translational Modification
Junsub Lim, Chae Woo Lim and Sung Chul Lee

135 Wheat ocs-Element Binding Factor 1 Enhances Thermotolerance by Modulating the Heat Stress Response Pathway
Harsha Samtani, Aishwarye Sharma and Paramjit Khurana

151 *GmWRKY21*, a Soybean WRKY Transcription Factor Gene, Enhances the Tolerance to Aluminum Stress in *Arabidopsis thaliana*
Zhenzhen Han, Jinyu Wang, Xinxin Wang, Xijia Zhang, Yanbo Cheng, Zhandong Cai, Hai Nian and Qibin Ma

168 OsSIDP301, a Member of the DUF1644 Family, Negatively Regulates Salt Stress and Grain Size in Rice
Li Ge, Hongming Guo, Xiu Li, Ming Tang, Chiming Guo, Han Bao, Linjuan Huang, Yin Yi, Yuchao Cui and Liang Chen

184 The interplay of DNA methyltransferases and demethylases with tuberization genes in potato (*Solanum tuberosum* L.) genotypes under high temperature
Madhushree Dutta, Vidhi Raturi, Vijay Gahlaut, Akhil Kumar, Paras Sharma, Vipasha Verma, Vijai Kishor Gupta, Salej Sood and Gaurav Zinta

200 Identification and analysis of proline-rich proteins and hybrid proline-rich proteins super family genes from *Sorghum bicolor* and their expression patterns to abiotic stress and zinc stimuli
Guddimalli Rajasheker, Marka Nagaraju, Rinku Polachirakkal Varghese, Naravula Jalaja, Anil Kumar Somanaboina, Prashant Singam, Chintala Ramakrishna, Suprasanna Penna, Nese Sreenivasulu and P. B. Kavi Kishor

223 Integrated transcriptomics and miRNAomics provide insights into the complex multi-tiered regulatory networks associated with coleoptile senescence in rice
Jyothish Madambikattil Sasi, Cheeni VijayaKumar, Bharti Kukreja, Roli Budhwar, Rohit Nandan Shukla, Manu Agarwal and Surekha Katiyar-Agarwal

245 Analysis of the response regulatory network of pepper genes under hydrogen peroxide stress
Bingqian Tang, Guangbin Yang, Juan Du, Lingling Xie, Jin Wang, Luzhao Pan, Yin Luo, Qingyun Shan, Xuexiao Zou, Cheng Xiong and Feng Liu

258 Physiology and transcriptome analysis of the response mechanism of *Solidago canadensis* to the nitrogen addition environment
Miao Wu, Huiyuan Liu, Ying Zhang, Bingbing Li, Tao Zhu and Man Sun

272 *GmABR1* encoding an ERF transcription factor enhances the tolerance to aluminum stress in *Arabidopsis thaliana*
Hongjie Wang, Cheng Li, Lidan Wang, Hongying Zhong, Xin Xu, Yanbo Cheng, Hai Nian, Wenhua Liu, Pei Chen, Aixia Zhang and Qibin Ma

frontiers | Frontiers in Plant Science

TYPE Editorial
PUBLISHED 16 January 2024
DOI 10.3389/fpls.2023.1334467

Check for updates

OPEN ACCESS

EDITED AND REVIEWED BY
Anna N. Stepanova,
North Carolina State University, United States

*CORRESPONDENCE
Ashish Kumar Srivastava
ashish@barc.gov.in
Girdhar Kumar Pandey
gkpandey@south.du.ac.in

RECEIVED 07 November 2023
ACCEPTED 28 December 2023
PUBLISHED 16 January 2024

CITATION
Srivastava AK, Pandey A, Böhmer M and Pandey GK (2024) Editorial: Abiotic stress signaling in plants: functional genomic intervention, volume II.
Front. Plant Sci. 14:1334467.
doi: 10.3389/fpls.2023.1334467

COPYRIGHT
© 2024 Srivastava, Pandey, Böhmer and Pandey. This is an open-access article distributed under the terms of the Creative Commons Attribution License (CC BY). The use, distribution or reproduction in other forums is permitted, provided the original author(s) and the copyright owner(s) are credited and that the original publication in this journal is cited, in accordance with accepted academic practice. No use, distribution or reproduction is permitted which does not comply with these terms.

Editorial: Abiotic stress signaling in plants: functional genomic intervention, volume II

Ashish Kumar Srivastava[1,2]*, Amita Pandey[3], Maik Böhmer[4] and Girdhar Kumar Pandey[5]*

[1]Nuclear Agriculture and Biotechnology Division, Bhabha Atomic Research Centre, Mumbai, Maharashtra, India, [2]Homi Bhabha National Institute, Mumbai, India, [3]Shriram Institute for Industrial Research, Delhi, India, [4]Institute of Molecular Biosciences, Faculty of Biological Sciences, Goethe University Frankfurt, Frankfurt, Germany, [5]Department of Plant Molecular Biology, University of Delhi South Campus, New Delhi, India

KEYWORDS

abiotic stress, stress signaling, stress tolerance, functional genomics, crop productivity

Editorial on the Research Topic
Abiotic stress signaling in plants: functional genomic intervention, volume II

Abiotic stresses such as high temperature, low temperature, drought, and salinity limit crop productivity worldwide. Understanding plant responses to these stresses is essential for the engineering of stress tolerance in plants. In Arabidopsis, the signal transduction pathways have been elucidated for perceiving and responding to different abiotic stress conditions (Zhu, 2016). A significant portion of plant genomes codes for proteins involved in signaling such as receptors, sensors, kinases, phosphatases, transcription factors, and transporters/channels (Pandey, 2020; Chen et al., 2021). Despite decades of physiological and molecular efforts, knowledge about how plants sense temperature fluctuations, drought, water submergence, and salinity signals is still limited. Further, the stress combinations pose another layer of complexity to this problem (Zandalinas et al., 2023). One of the major constraints hampering our understanding of these signal transduction processes has been the slow pace of gene-function studies in plants (Shinozaki and Yamaguchi-Shinozaki, 2022). In this post-genomic era, investigation and understanding of multiple genes and gene families regulating a particular physiological and developmental aspect of plant's life cycle is of utmost importance (Pandey et al., 2016; Baekelandt et al., 2023; Tyczewska et al., 2023). With a holistic understanding of the signaling pathways involving not only one gene but multiple genes from a signaling cascade, plant biologists can lay a foundation for designing and generating future crops that can withstand environmental stresses without jeopardizing the crop yield.

In the present Research Topic, various novel genes, mainly transcription factors, have been identified and characterized, that can serve as promising candidates for enhancing abiotic stress tolerance in crops. Han et al. have functionally characterized *GmWRKY21* that encodes a nuclear-localized WRKY transcription factor. *GmWRKY21* is expressed across different tissues including roots, leaves, and flowers of soybean and is substantially upregulated in response to aluminum stress. The overexpression of *GmWRKY21* in Arabidopsis increased the root growth of seedlings in transgenic lines under aluminum stress, which coincided with higher proline and

lower malondialdehyde (MDA) accumulation and upregulated expression of aluminum stress-specific as well as general stress marker genes. Similarly, Wang et al. identified *GLYCINE MAX ABA REPRESSOR1* (*GmABR1*) encoding an Ethylene Response Factor (ERF) transcription factor as a positive regulator of aluminum stress tolerance in *Arabidopsis thaliana*. The Basic Leucine Zipper (bZIP) family represents another large family of transcription factors that play an important role in mediating plant responses to abiotic stresses. Samtani et al. identified two homeologs of wheat *OCS-ELEMENT BINDING FACTOR1* (*TaOBF1-5B* and *TaOBF1-5D*) as heat-responsive TabZIP members. The heterologous overexpression of *TaOBF1-5B* resulted in enhanced thermotolerance in transgenic *Arabidopsis thaliana* and *Oryza sativa*. TaOBF1-5B has been shown to interact with HEAT SHOCK PROTEIN70 (TaHSP90) in the nucleus and TaSTI (a co-chaperone) in the nucleolus. MYBs (myeloblastosis) are another class of transcription factors that play a pivotal role in regulating anthocyanin synthesis. Liu et al. identified and characterized *PqMYB113* from the leaves of *Paeonia qiui*, a wild species of tree peony native to China. The overexpression of *PqMYB113* resulted in increased anthocyanin accumulation in *Arabidopsis thaliana* and *Nicotiana tabacum*.

Similarly, Jin et al. reported on a homolog of the RelA/SpoT protein (HpRSH) from *Haematococcus pluvialis*, which catalyzes Mg^{2+}-dependent synthesis and hydrolysis of guanosine tetraphosphate (ppGpp). The transcription of *HpRSH* was significantly upregulated by environmental stresses, such as darkness, high light, nitrogen limitation, and salinity stress. Apart from these positive regulators, Ge et al. identified *STRESS-INDUCED DUF1644* (*OsSIDP301*), a member of the DUF1644 (Domain of unknown function 1644) family, as a negative regulator of salt stress and grain size in rice. OsSIDP301 determines salt stress tolerance by modulating genes involved in the salt-response and ABA signaling pathways. Moreover, OsSIDP301 interacts with OsBUL1 COMPLEX1 (OsBC1), which positively regulates grain size in rice.

Another approach to identify the stress-responsive gene(s) and associated physiological processes is to compare the contrasting accessions/varieties. Gao et al. performed the phenotypic and metabolic level comparison of two oat cultivars, Baiyan7 (BY, tolerant cultivar) and Yizhangyan4 (YZY, sensitive cultivar) under saline-alkali stress, which is a major detrimental abiotic stress factor for reducing agricultural productivity. Saline-alkali induced metabolites were mainly associated with enhancements in energy metabolism and accumulations of organic acids. The differential abundances of these metabolites revealed that BY showed better adaptability to saline-alkali stress compared with YZY cultivars. Similarly, Dutta et al. performed a genome-wide analysis and identified 10 cytosine-5 DNA methyltransferases (C5-MTases) and 8 demethylases (DeMets) in potatoes. Based on comparative expression profiling in heat-sensitive (HS) and -tolerant (HT) genotypes, several positive [*SELF PRUNING 6A* (*StSP6A*) and *BEL1-LIKE HOMEODOMAIN* (*StBEL5*)] and negative [*SELF PRUNING 5G* (*StSP5G*), *SUCROSE TRANSPORTER4* (*StSUT4*), and *RELATED TO AP2 1* (*StRAP1*)] regulators were identified that regulate potato tuberization under high-temperature stress.

Genome-wide analyses of gene families followed by ranking analysis have also been reported in the Research Topic to identify the key genes. For instance, CALCIUM-DEPENDENT PROTEIN KINASES (CDPKs) are a major group of calcium (Ca^{2+}) sensors in plants. CDPKs play a dual function of "Ca^{2+} sensor and responder." Deepika et al. identified commonly induced *CaCDPKs* in response to drought, salt, and abscisic acid in chickpea. Rajasheker et al. reported the stress-responsive behavior of proline-rich proteins and hybrid proline-rich proteins super family genes in *Sorghum bicolor*. Further, "omics" based approaches have also been used for the identification of genes and regulatory networks associated with nitrogen (N) addition in *Solidago canadensis* (Wu et al.), hydrogen peroxide stress in pepper (Tang et al.) and coleoptile senescence in rice (Sasi et al.).

Apart from genetic engineering, priming with microbes and chemicals are also used as alternatives to enhance plant performance under stress conditions. Li et al. demonstrated the protective role of *Piriformospora indica* (a root endophytic fungus) in wheat against *Rhizoctonia cerealis* and *Fusarium graminearum* infections. RNA-seq suggested that transcriptome changes caused by *F. graminearum* were more severe than those caused by *R. cerealis*. Further, the supplementation of *P. indica* reduced the number of differentially expressed genes (DEGs) by 18% and 58% in wheat injected with *F. graminearum* and *R. cerealis*, respectively, indicating the activation of specific mechanisms. Further, the DEGs related to disease resistance, such as *WRKYs* and *MAPKs* were upregulated in wheat by *P. indica* colonization.

In addition to the research articles, the Research Topic also featured fundamental reviews. For instance, Lim et al. reviewed the core signaling and function of ABA, which is one of the major stress hormones in plants. In addition, the role of non-hormone signal mediators was also highlighted. Li et al. provided a comprehensive insight into sulfur dioxide, which has recently emerged as a signaling mediator in plants. Finally, Khan et al. reviewed the recent advances in the application of thermal techniques for inducing stress-priming during the seedling stage, which is another non-genetic approach.

Taken together, the Research Topic highlights the novel research findings in the field of abiotic stress signaling in plants, that may pave the path for developing "stress-tolerant" crops in the near future.

Author contributions

AS: Writing – original draft, Writing – review & editing. AP: Writing – review & editing. MB: Writing – review & editing. GP: Conceptualization, Funding acquisition, Writing – original draft, Writing – review & editing.

Funding

The author(s) declare that financial support was received for the research, authorship, and/or publication of this article. GP is thankful to the Department of Biotechnology (DBT), Govt. of India; Science and Engineering Research Board (SERB), Govt. of India; Council for

Scientific and Industrial Research (CSIR), Govt. of India; Delhi University (IoE/FRP grant), India for research funding.

Conflict of interest

The authors declare that the research was conducted in the absence of any commercial or financial relationships that could be construed as a potential conflict of interest.

Publisher's note

All claims expressed in this article are solely those of the authors and do not necessarily represent those of their affiliated organizations, or those of the publisher, the editors and the reviewers. Any product that may be evaluated in this article, or claim that may be made by its manufacturer, is not guaranteed or endorsed by the publisher.

References

Baekelandt, A., Saltenis, V. L., Nacry, P., Malyska, A., Cornelissen, M., Nanda, A. K., et al. (2023). Paving the way towards future-proofing our crops. *Food Energy Secur.* 12 (3), e441. doi: 10.1002/fes3.441

Chen, X., Ding, Y., Yang, Y., Song, C., Wang, B., Yang, S., et al. (2021). Protein kinases in plant responses to drought, salt, and cold stress. *J. Integr. Plant Biol.* 63 (1), 53–78. doi: 10.1111/jipb.13061

Pandey, G. K. (2020). *Protein phosphatases and stress management in plants: Functional genomics perspective* (Switzerland: Springer International Publishing).

G. K. Pandey, M. Prasad, A. Pandey and M. Böhmer (Eds.) (2016). *Abiotic Stress Signaling in Plants: Functional Genomic Intervention* (Lausanne: Frontiers Media). doi: 10.3389/978-2-88919-891-7

Shinozaki, K., and Yamaguchi-Shinozaki, K. (2022). Functional genomics in plant abiotic stress responses and tolerance: From gene discovery to complex regulatory networks and their application in breeding. *Proc. Japan Academy Ser. B* 98 (8), 470–492. doi: 10.2183/pjab.98.024

Tyczewska, A., Twardowski, T., and Woźniak-Gientka, E. (2023). Agricultural biotechnology for sustainable food security. *Trends Biotechnol.* 41, 331–341. doi: 10.1016/j.tibtech.2022.12.013

Zandalinas, S. I., Peláez-Vico, M. Á., Sinha, R., Pascual, L. S., and Mittler, R. (2023). The impact of multifactorial stress combination on plants, crops, and ecosystems: how should we prepare for what comes next? *Plant J.* doi: 10.1111/tpj.16557

Zhu, J. K. (2016). Abiotic stress signaling and responses in plants. *Cell* 167 (2), 313–324. doi: 10.1016/j.cell.2016.08.029

frontiers in Plant Science

ORIGINAL RESEARCH
published: 12 January 2022
doi: 10.3389/fpls.2021.810990

The *Paeonia qiui* R2R3-MYB Transcription Factor PqMYB113 Positively Regulates Anthocyanin Accumulation in *Arabidopsis thaliana* and Tobacco

Xiaokun Liu[1,2,3†], Jingjing Duan[1,2,4†], Dan Huo[1,2], Qinqin Li[1,2], Qiaoyun Wang[1,2], Yanlong Zhang[1,2], Lixin Niu[1,2] and Jianrang Luo[1,2]*

[1] College of Landscape Architecture and Arts, Northwest A&F University, Xianyang, China, [2] National Engineering Research Center for Oil Peony, Yangling, China, [3] Shanghai Key Laboratory of Plant Functional Genomics and Resource, Shanghai, China, [4] College of Plant Science, Tarim University, Alar, China

OPEN ACCESS

Edited by:
Ashish Kumar Srivastava, Bhabha Atomic Research Centre (BARC), India

Reviewed by:
Ying Chang, Northeast Agricultural University, China
Xiping Wang, Northwest A&F University, China
Tamara Gigolashvili, University of Cologne, Germany

***Correspondence:**
Jianrang Luo
luojianrang@nwafu.edu.cn

† These authors have contributed equally to this work and share first authorship

Specialty section:
This article was submitted to Plant Physiology, a section of the journal Frontiers in Plant Science

Received: *08 November 2021*
Accepted: *16 December 2021*
Published: *12 January 2022*

Citation:
Liu X, Duan J, Huo D, Li Q, Wang Q, Zhang Y, Niu L and Luo J (2022) The Paeonia qiui R2R3-MYB Transcription Factor PqMYB113 Positively Regulates Anthocyanin Accumulation in Arabidopsis thaliana and Tobacco. Front. Plant Sci. 12:810990. doi: 10.3389/fpls.2021.810990

Paeonia qiui is a wild species of tree peony native to China. Its leaves are purplish red from the bud germination to the flowering stage, and anthocyanin is the main pigment in purplish red leaves. However, the anthocyanin synthesis regulation mechanism in tree peony leaves remains unclear. In this study, an R2R3-MYB, PqMYB113 was identified from the leaves of *P. qiui*. Phylogenetic analysis revealed that PqMYB113 clustered with *Liquidambar* LfMYB113 and grape VvMYBA6. Subcellular location analysis showed that PqMYB113 was located in the cell nucleus. The transient reporter assay suggested that PqMYB113 was a transcriptional activator. The overexpression of *PqMYB113* in *Arabidopsis thaliana* and tobacco (*Nicotiana tabacum*) resulted in increased anthocyanin accumulation and the upregulation of *CHS*, *F3H*, *F3'H*, *DFR*, and *ANS*. The dual luciferase reporter assay showed that PqMYB113 could activate the promoters of *PqDFR* and *PqANS*. Bimolecular fluorescence complementation assays and yeast two-hybrid assays suggested that PqMYB113 could form a ternary MBW complex with PqbHLH1 and PqWD40 cofactors. These results provide insight into the regulation of anthocyanin biosynthesis in tree peony leaves.

Keywords: *Paeonia qiui*, anthocyanin, transcription factor, MYB, positive regulation

INTRODUCTION

Anthocyanins are widely distributed in plant flowers, fruits and other tissues (Jaakola, 2013). It provides plants with red, orange, purple, blue, and other different colors that attract pollinators and/or make plants resist abiotic and biotic stresses such as ultraviolet light, cold, drought and microbial agents (Shang et al., 2011; Song et al., 2016; Jin and Zhu, 2019; An et al., 2020). Over the past few decades, as a branch of the flavonoid pathway, anthocyanin biosynthesis has been extensively studied in *Arabidopsis*, grape, apple, and many other plants (Tanaka et al., 2008; Jaakola, 2013). It is well known that anthocyanin biosynthesis is controlled by a series of structural genes (enzyme genes), including the chalcone synthase gene (*CHS*), chalcone isomerase gene

(*CHI*), flavanone 3-hydroxylase gene (*F3H*), flavonoid 3′-hydroxylase gene (*F3′H*), flavonoid 3′,5′-hydroxylation gene (*F3′5′H*), dihydroflavonol 4-reductase gene (*DFR*), anthocyanin synthase gene (*ANS*), etc (Tanaka et al., 2008).

In addition to these structural genes, anthocyanin biosynthesis is also regulated by transcription factors, mainly myeloblastosis (MYB), basic helix loop helix (bHLH) and WD40/WDR (Allan et al., 2008; Hichri et al., 2011; Li, 2014). Among them, MYB plays a pivotal role in regulating anthocyanin synthesis (Dubos et al., 2010). It can act alone or with bHLH and WD40 constitutes the MYB-bHLH-WD40 complex (MBW) to regulate the structural genes of the anthocyanin pathway (Jaakola, 2013; Li, 2014; Xu et al., 2015). The MYB transcription factor family is divided into 4 categories according to the number of N-terminal conserved domains, namely, one conserved domain 1R (R1/2, R3-MYB), two conserved domains 2R (R2R3-MYB), three conserved domains 3R (R1R2R3-MYB) and four conserved domains 4R (Dubos et al., 2010). Among these four types of MYB transcription factors, R2R3-MYB is the most important in anthocyanin synthesis (Liu et al., 2015). Many R2R3-MYB transcription factors that positively regulate anthocyanin biosynthesis have been identified from various plants, such as AtMYB75 (PAP1), AtMYB90 (PAP2), AtMYB113, and AtMYB114 in *Arabidopsis* (Stracke et al., 2007; Gonzalez et al., 2008), PhAN2 and PhAN4 in *Petunia hybrid* (Albert et al., 2011), MdMYB1, MdMYBA, MdMYB10, and MdMYB110a in apple (Takos et al., 2006; Ban et al., 2007; Espley et al., 2007; Chagne et al., 2013), PpMYB10.1, PpMYB10.2, and PpMYB10.4 in peach (Rahim et al., 2014; Zhou et al., 2016). In addition to these activators, some MYB repressors were also found, such as FaMYB1 in *Fragaria* × *ananass*a (Paolocci et al., 2011), VvMYBC2-L1/L2/L3 and VvMYB4-like in *Vitis vinifera* (Cavallini et al., 2015), PtrMYB182 in *Populus spp*. (Yoshida et al., 2015) and PpMYB18 in *Prunus persica* (Hui et al., 2019). However, most of these studies focus on anthocyanin biosynthesis regulation in flowers or fruits, and the molecular mechanism of red color formation in leaves is still not well known.

As a wild tree peony native to China, *P. qiui* is a typical spring-red leaved plant that has purple–red leaves from the bud germination to the flowering stage, which has good foliage value. Based on our transcriptome sequencing, forty MYB genes were identified from differentially expressed genes. Among them, two R2R3-MYBs that may be related to anthocyanin biosynthesis were screened (Luo et al., 2017). One was designated as PqMYB4, its inhibitory function in anthocyanin biosynthesis was confirmed by our team (Huo et al., 2020). Another R2R3-MYB (Unigene0024459) showed highest consistency with LfMYB113 which regulated anthocyanin biosynthesis in *Liquidambar formosana*, so it was designated as PqMYB113 (Luo et al., 2017). In this study, PqMYB113 was isolated from *P. qiui* leaves, and the expression level of *PqMYB113* gene was consistent with the change in anthocyanin content in leaves. The stable transformation in *Arabidopsis* and tobacco showed that PqMYB113 could promote anthocyanin accumulation. The dual luciferase reporter assay showed that PqMYB113 could activate the promoters of *PqDFR* and *PqANS*. Bimolecular fluorescence complementation assays suggested that PqMYB113 could form a ternary MBW complex with PqbHLH1 and PqWD40. This study provided a basis for revealing the molecular mechanism of foliage color change in *P. qiui* and genetic resources for the molecular breeding of tree peony with colored leaves.

MATERIALS AND METHODS

Plant Materials

The *Paeonia qiui* plants used in this study were grown under field conditions at Northwest A&F University, Yangling, Shaanxi, China (altitude, 432 m above sea; 34°15′N, 108°3′E). Eight-year-old tree peonies were planted in loam, and the soil moisture content was approximately 17.5%. The second young leaves from the top of plants were collected in 10, 20, 30, 40, and 50 days after sprouting and designated as S1, S2, S3, S4, and S5, respectively. The samples were collected in the morning during March and April 2021 (10°C–18°C in the day and 5°C–8°C in the night). *Arabidopsis* and tobacco were cultivated in a climate chamber (22°C/80%; 16 h light and 8 h darkness). All samples were immediately frozen in liquid nitrogen and then stored at −80°C until use.

Total RNA Extraction and Quantitative Real-Time Polymerase Chain Reaction

Total RNA was isolated from the different leaf stages of *P. qiui* using the TIANGEN RNA Prep Pure Plant kit (Tiangen Biotech Co., Ltd., Beijing, China). The quality and concentration of RNA samples were tested by Goldview-stained agarose gel electrophoresis and spectrophotometric analysis, respectively. According to the manufacturer's instructions of the PrimeScript® RT reagent Kit (DRR047A, Takara, Japan), 1 μg DNA-free RNA sample was used to synthesize cDNA and stored at −20°C. qRT-PCR was conducted using SYBR® Premix Ex Taq™ II (DRR041A, Takara, Japan), and ubiquitin was used as an internal control (Luo et al., 2017). The primer sequences used for qRT-PCR are listed in **Supplementary Table 1**. The relative expression level of the qRT-PCR assay was calculated with the $2^{-\Delta\Delta CT}$ method, and a dissolution curve was automatically generated by software. Three biological replicates were performed.

Isolation of the Full-Length Coding Sequence of PqMYB113 and Bioinformatics Analysis

The gene specific primers *PqMYB113-F* and *PqMYB113-R* were designed by Oligo 7.0 software (**Supplementary Table 1**), and full-length gene amplification was carried out using the cDNA of *P. qiui* leaves as a template according to TransTaq-T DNA Polymerase. The specific bands of the expected size PCR products were recycled by the agarose gel DNA extraction kit (Takara, Japan). Then, the expected products were ligated into the pMD19-T vector placed at 4°C overnight, and the ligation products were transformed into *Escherichia coli* competent cells. After positive screening identification, the correct bacterial

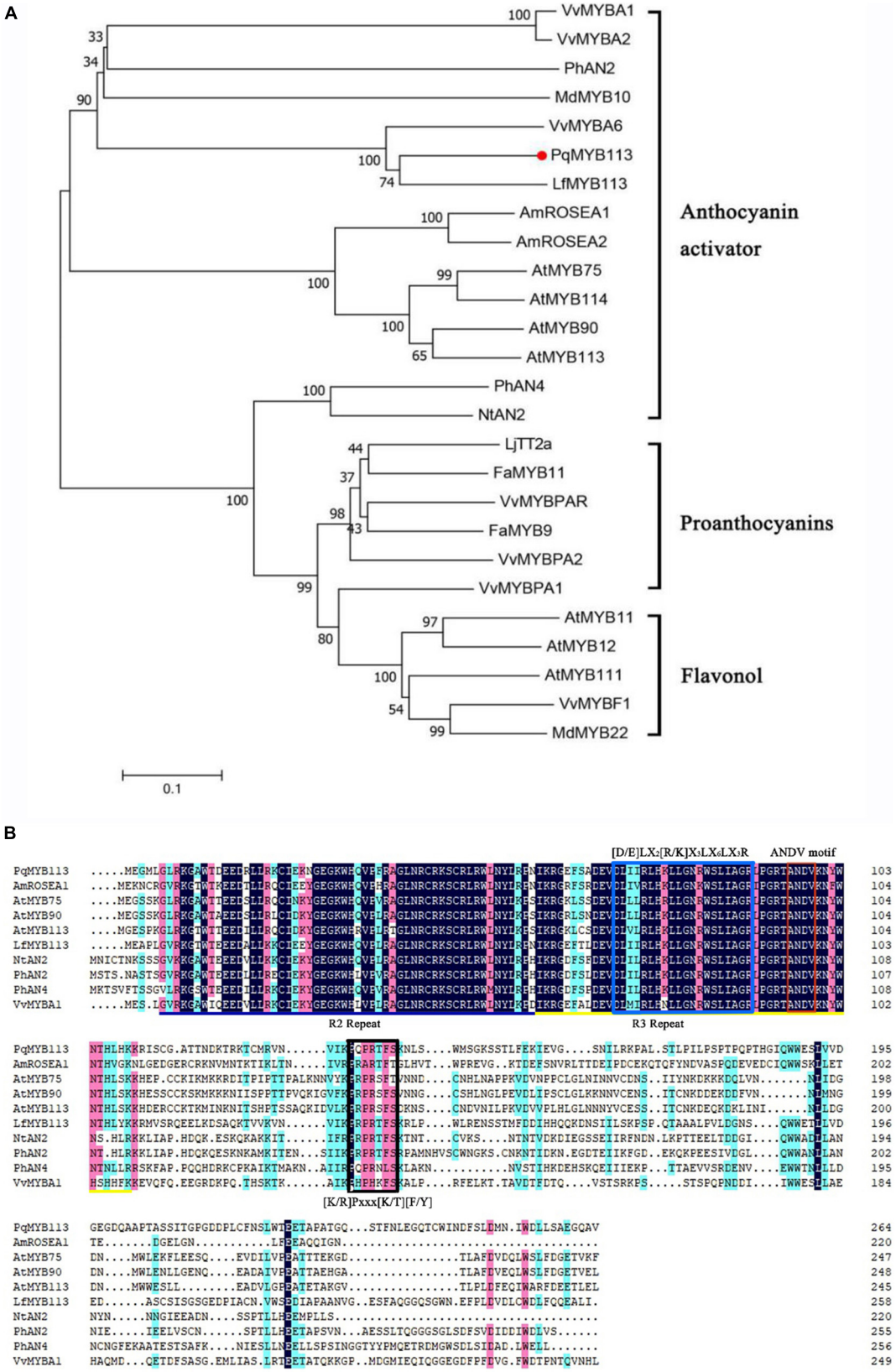

FIGURE 1 | (Continued)

FIGURE 1 | Phylogenetic analysis and sequence alignment of PqMYB113. **(A)** The phylogenetic analysis of PqMYB113 protein and MYB proteins from other species. PqMYB113 is highlighted with a red dot. The neighbor-joining method with MEGA software was used to construct the phylogenetic tree. Bootstrap values as a percentage of 1000 replicates are indicated at corresponding branch nodes. Putative functions of the R2R3-MYBs are listed on the right. **(B)** The alignment of deduced amino acid sequences of *PqMYB113* with other similar R2R3-MYB proteins. Alignment was conducted using DNAMAN Version 8. The R2 (black line) and R3 (yellow line) MYB domains shown refer to two repeats of the MYB DNA-binding domain of MYB proteins. The blue box shows the motif that interacts with bHLHs. The red and black boxes show the ANDV motif and motif 6, respectively.

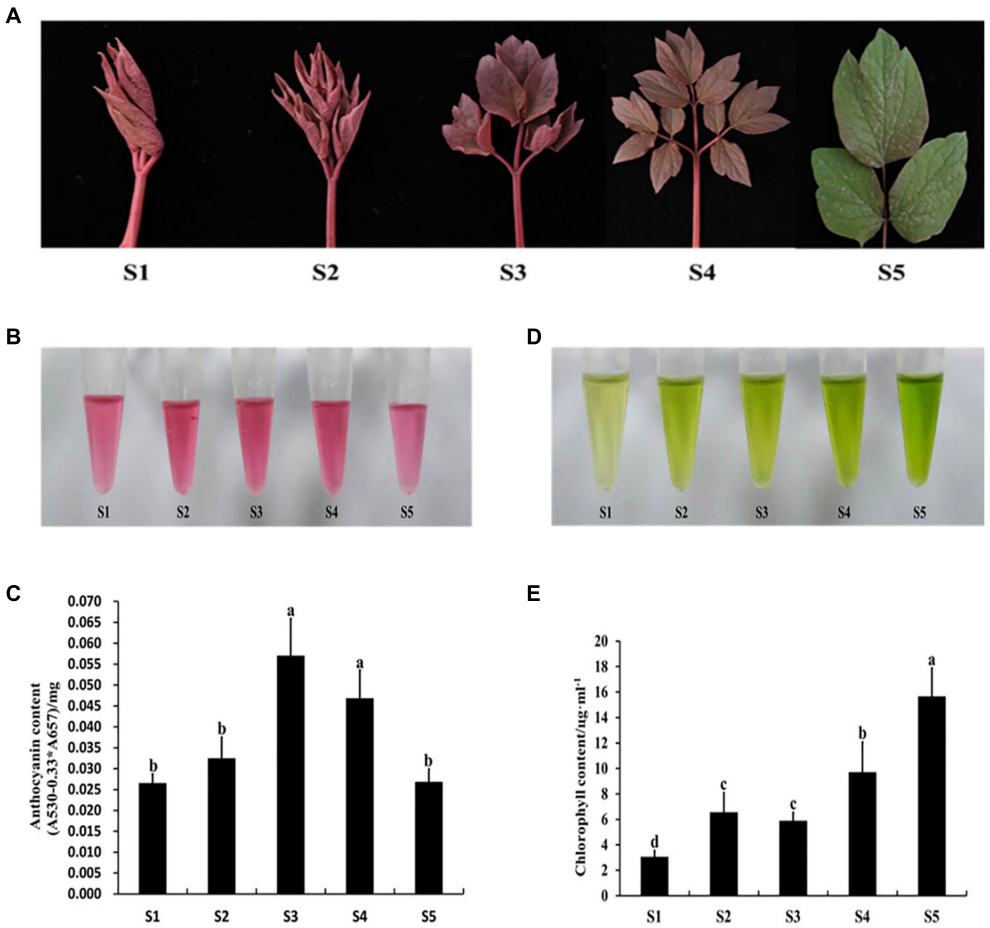

FIGURE 2 | Pigment content at different stages in *P. qiui*. **(A)** The leaves phenotype in different stages of *P. qiui*. **(B)** The anthocyanin extracting solution colors in leaf. **(C)** The anthocyanin content in leaf. **(D)** The chlorophyll extracting solution colors in leaf. **(E)** The chlorophyll content in leaf. S1, leaves of 10 days after sprouting; S2, leaves of 20 days after sprouting; S3, leaves of 30 days after sprouting; S4, leaves of 40 days after sprouting; S5, leaves of 50 days after sprouting. a, b, c, and d indicate significant difference at $p \leq 0.05$ level by Duncan's test.

solution was sent to the company for sequencing. The open reading frame of *PqMYB113* was found by the ORF Finder online tool in NCBI[1]. A homology search of sequences was carried out through BLAST in NCBI, and multiple alignments were analyzed using DNAMAN 8.0. A phylogenetic tree was constructed using the neighbor-joining method (NJ) with MEGA 7.0 software.

Subcellular Localization

The ORF of *PqMYB113* without the stop codon was inserted into the pCAMBIA1301-GFP vector. Then, the constructed plasmid was bombarded into onion epidermal cells using a Biolistic PDS1000 instrument (Bio-Rad, CA, United States). After incubation at 25°C for at least 16 h in the dark, the samples were observed under a confocal laser scanning microscope.

Overexpression Vector Construct and *Arabidopsis* and Tobacco Transformation

The full-length cDNA of *PqMYB113* was inserted in the sites between *Kpn*I and *Sal*I of the pCAMBIA1300 vector. Then, the recombinant vector was introduced into *Agrobacterium tumefaciens* strain GV3101 for

[1]https://www.ncbi.nlm.nih.gov/orffinder/

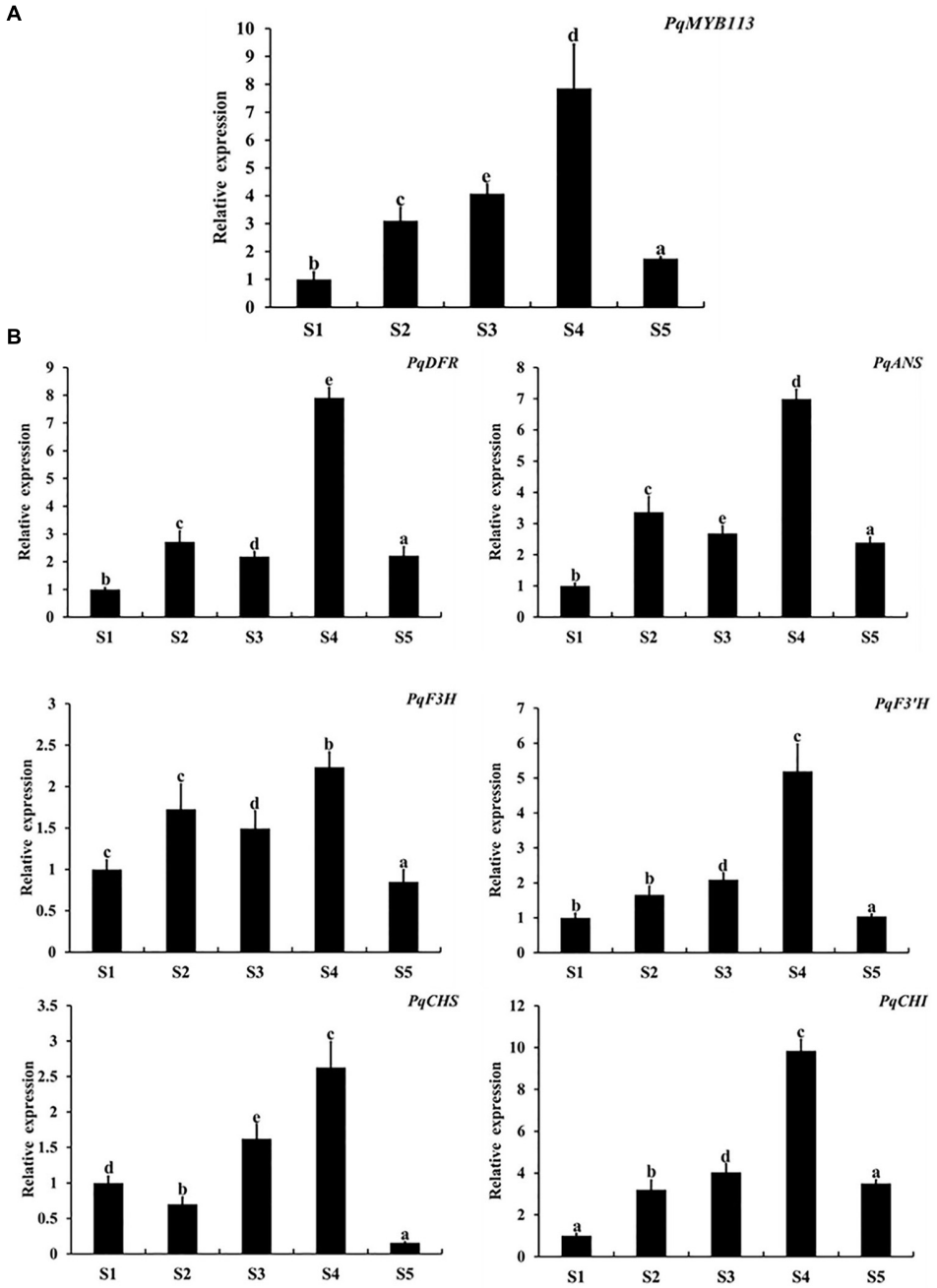

FIGURE 3 | Expression level of anthocyanin structural genes and *MYB113* at different stages in *P. qiui.* **(A)** The expression level of *PqMYB113* at different stages. **(B)** The expression level of anthocyanin structural genes at different stages. S1, leaves of 10 days after sprouting; S2, leaves of 20 days after sprouting; S3, leaves of 30 days after sprouting; S4, leaves of 40 days after sprouting; S5, leaves of 50 days after sprouting. Ubiquitin was used as an internal control. Error bars represent the standard errors. a, b, c, d, and e indicate significant differences at the $p \leq 0.05$ level by Duncan's test.

Arabidopsis and tobacco transformation. pCAMBIA1300-PqMYB113 in *Agrobacterium* strain GV3101 was transformed into wild-type *Arabidopsis* plants using the floral dip method. *Agrobacterium*-mediated transformation of tobacco plants was subsequently carried out. Hygromycin (200 mg/L) was used to select the transgenic tobacco lines.

Dual Luciferase Transient Transfection Assay and Dual Luciferase Reporter Assay

For the dual luciferase transient transfection assay, p35S-GAL4-BD, the effector plasmid, the reporter plasmid containing firefly luciferase and internal plasmids containing *Renilla* luciferase

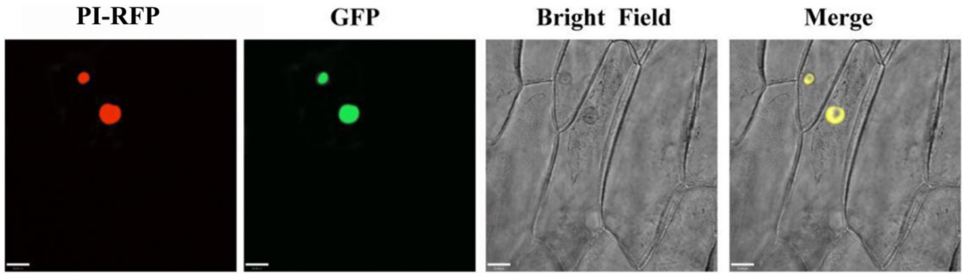

FIGURE 4 | The subcellular localization of GFP fusion of PqMYB113. Onion epidermal cells transiently expressing GFP and PqMYB113-GFP under the control of the CaMV 35S promoter. PI-RFP, mCherry fluorescence; GFP, GFP fluorescence; Merge, merged images of mCherry fluorescence; GFP fluorescence and bright-field microscopy. Bars = 33 μm.

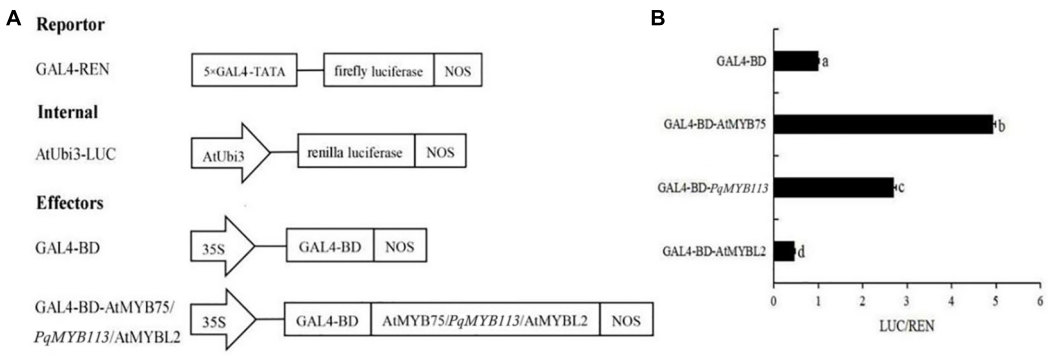

FIGURE 5 | The Dual Luciferase Transient Transfection Assay of *PqMYB113*. **(A)** The schematic depiction of the constructs used in the *Arabidopsis* protoplast co-transfection assay. **(B)** The relative luciferase activity (LUC/REN). a, b, c, and d indicate significant differences at the $p \leq 0.05$ level by Duncan's test.

were prepared as described previously (Zong et al., 2016). For the effector plasmid, AtMY75 (positive control), AtMYBL2 (negative control) and PqMYB113 cDNA fragments were inserted into the *Eco*RI site of p35S-GAL4-BD plasmids. The effector, reporter and internal plasmids were delivered into *Arabidopsis* protoplasts by PEG-mediated transformation of protoplasts. The relative luciferase (LUC/REN) activity was assayed with the Dual-Luciferase Reporter® Assay System (Promega) using a Promega GloMax 20/20 Microplate luminometer.

For the dual luciferase reporter assay, the promoters of *PqDFR* and *PqANS* were amplified using the Genome Walking Kit and inserted into the vector pGreenII 0800-LUC with the primers listed in **Supplementary Table 2**. PqMYB113 was joined with the pGreenII 62-SK vector, which was driven by 35S promoter. The primers used for reporter and effector constructions were listed in **Supplementary Table 3**. All of these recombinant plasmids were individually transformed into *Agrobacterium* strain GV3101. Activity data were expressed as the ratio of LUC activity to REN activity. Blank controls were run with only the promoter-LUC reporter construct (no transcription factor).

Bimolecular Fluorescence Complementation Experiment

PqMYB113 without the stop codon was constructed between the two restriction sites (*Bam*HI and *Xhol*) of the pSPYNE-35S expression vector. *PqbHLH*1 and *PqWD40* without the stop codon were constructed into *Bam*HI and *Xhol* of the pSPYCE-35S expression vector, respectively. In other words, PqMYB113 was connected to the N-terminus of YFP, and PqbHLH1 and PqWD40 were fused to the C-terminus of YFP. The constructed vector was transformed into *Agrobacterium* strain GV3101 and infiltrated into tobacco leaves. After 72 h of co-infiltration, samples were taken to detect the fluorescence signal by confocal laser scanning microscope.

Yeast Two Hybrid Assay

PqMYB113, PqbHLH1, and PqWD40 were constructed into the pGADT7 vector and pGBKT7 vector, respectively, and then co-transfected into yeast AH109. The medium lacking Leu and Trp (–T/–L) was used for selecting the transformed yeast strains at 30°C for 3 days. Subsequently, putative transformants were transferred to medium lacking Trp, Leu, His and adenine (–T/–L/–H/–A) with or without X-α-Gal, and cultured for 2–4 days. pGADT7-T and pGBKT7-Lam or pGADT7-T and pGBKT7-53 were co-transformed as negative and positive controls.

Anthocyanin Content Measurement

Ten milligrams of seedlings were ground in liquid nitrogen. Extraction of anthocyanins was performed in 250 μL of

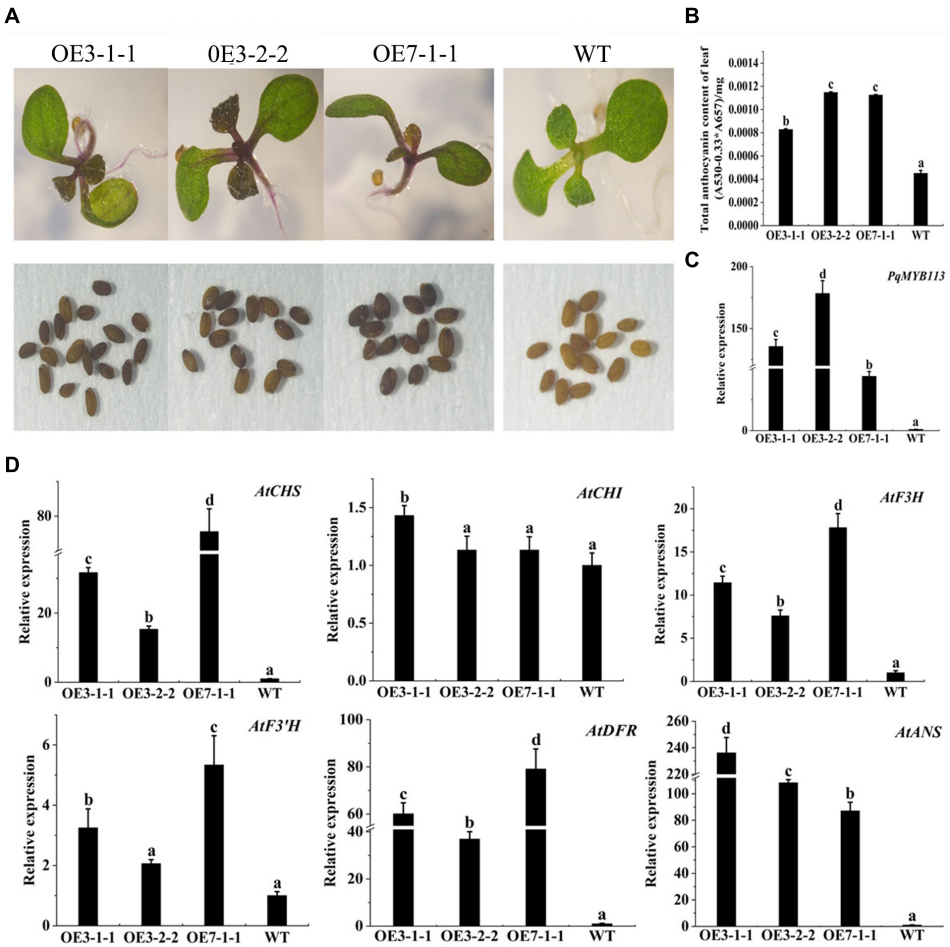

FIGURE 6 | The phenotype and the effect of *PqMYB113* overexpression in transgenic *Arabidopsis* plants. **(A)** The seeding and seeds phenotype of transgenic overexpression lines OE 3-1-1, OE 3-2-1, and OE 7-1-1 in comparison to WT. *Arabidopsis* seedlings were grown on MS plates at 22°C for 10 days. **(B)** The anthocyanin content in leaves. **(C)** The expression level of *PqMYB113* gene in leaves. **(D)** The expression level of anthocyanin biosynthesis structure genes in leaves. a, b, c, and d indicate significant differences at the $P \leq 0.05$ level by Duncan's test.

methanol containing 1% HCl in the dark at 4°C for 24 h. Then chlorophyll was eliminated by adding 250 μL chloroform and 250 μL water. Subsequently, the samples were centrifuged for 10 min at 10,000 × *g* at 4°C. The supernatant was used for anthocyanin measurement using a spectrophotometer at 530 and 657 nm. The relative anthocyanin level was calculated by the formula (A530-0.33 × A657)/mg.

RESULTS

Characterization of *PqMYB113*

PqMYB113 contained a 798 bp open reading frame (ORF) encoding 266 amino acids (GenBank accession number: QCF29938.1). The online software ProtParam analysis showed that the theoretical molecular weight of PqMYB113 was approximately 29.90 kD and the theoretical isoelectric point was 8.83. The protein instability coefficient was 55.91, indicating that it was an unstable protein. The maximum hydrophilicity/hydrophobicity of the protein encoded by *PqMYB113* was approximately 1.444, and the minimum was −2.578. The hydrophilic mean (GRAVY) was −0.557, suggesting that the protein was a hydrophilic protein (**Supplementary Figure 1A**). SignalP 4.1 Server and TMHMM predicted that PqMYB113 did not have a signal peptide site or transmembrane region, indicating that it is a non-secreted protein and non-transmembrane protein (**Supplementary Figures 1B,C**). Secondary structure prediction showed that PqMYB113 contained 35.09% α- helices, 4.91% β-turns, 10.19% extended chains and 49.81% random coils. The three-dimensional structure was constructed by SWISS-MODEL. The similarity of the model was 60.91% with the transcription factor WER (**Supplementary Figure 1D**). Conservative domain analysis showed that there were two conserved domains of SANT (repeat R) at the N-terminus, which revealed that PqMYB113 belonged to the 2R-MYB subfamily.

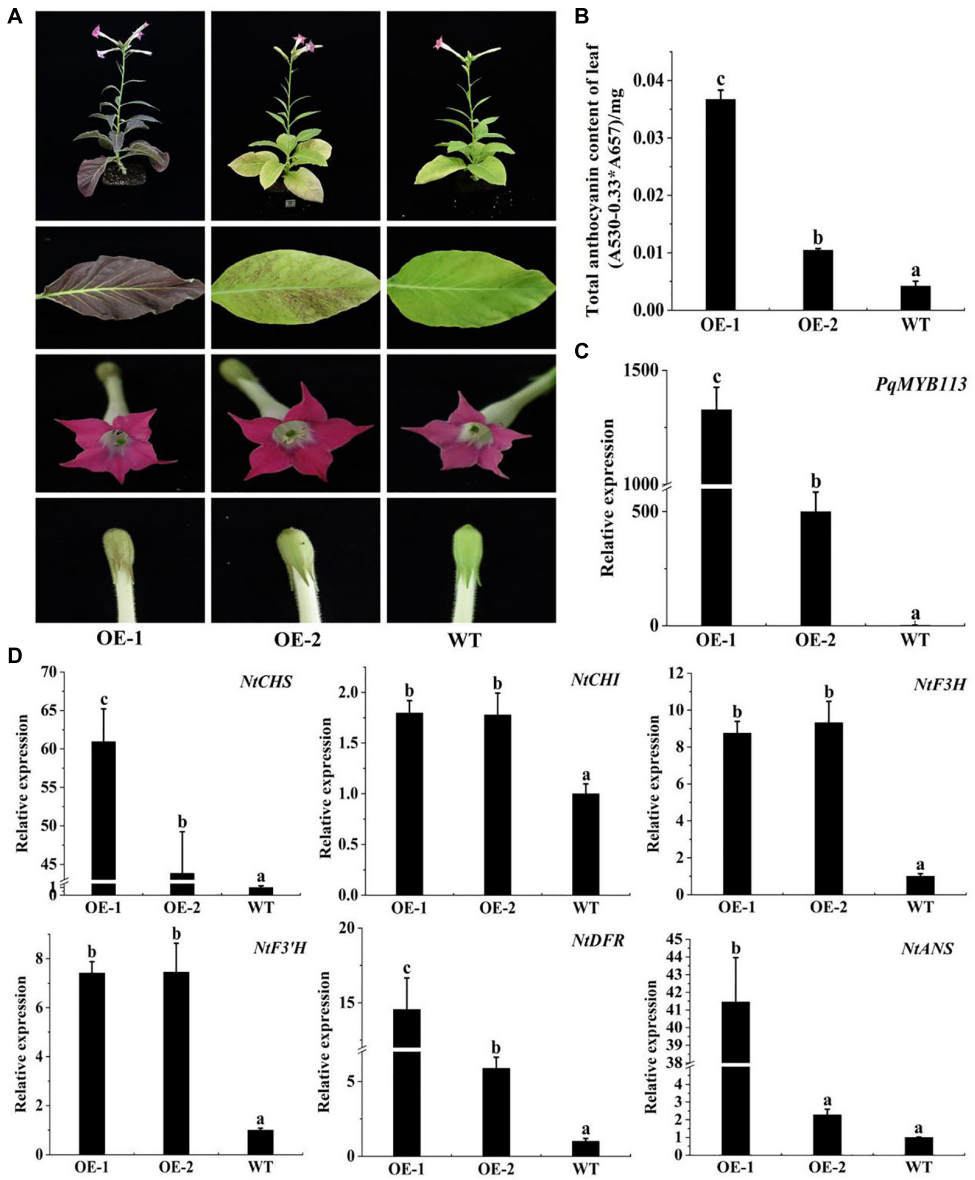

FIGURE 7 | The phenotype and the effect of *PqMYB113* overexpression in transgenic tobacco. **(A)**. The phenotype of OE-1 and OE-2 in comparison to WT. **(B)** The anthocyanin content in leaves. **(C)** The expression level of the *PqMYB113* gene in leaves. **(D)** The expression level of anthocyanin biosynthesis structure genes. a, b, and c indicate significant differences at the $P \leq 0.05$ level by Duncan's test.

Phylogenetic Analysis and Sequence Alignment of PqMYB113

Phylogenetic analysis showed that PqMYB113 was relatively far from the MYB transcription factors that regulate the synthesis of proanthocyanidins, such as grape VvMYBPA2, strawberry FaMYB9 and FaMYB11, and the synthesis of flavonols, such as *Arabidopsis* AtMYB11 and grape VvMYBF1 (**Figure 1A**). It was clustered with the MYB transcription factor that promotes anthocyanin synthesis in other plants, such as *Liquidambar* LfMYB113, *Arabidopsis* AtMYB75/90/113/114, grape VvMYBA1, VvMYBA6, apple MdMYB10, and petunia PhAN2 (**Figure 1A**), suggesting that PqMYB113 probably has the same function as these transcription factors.

Sequence analysis revealed that PqMYB113 contained R2 and R3 MYB DNA-binding domains in the N-terminus, indicating that PqMYB113 was an R2R3-MYB transcription factor (**Figure 1B**). The [D/E]LX2[R/K]X3LX6LX3R motif, which is responsible for interacting with bHLH proteins, was found in the R3 domain of PqMYB113 (**Figure 1B**; Zimmermann et al., 2004), suggesting that PqMYB113 could interact with bHLH. ANDV and KPRPR[S/T]F motifs, which are characteristics of anthocyanin biosynthesis regulators, were also found in

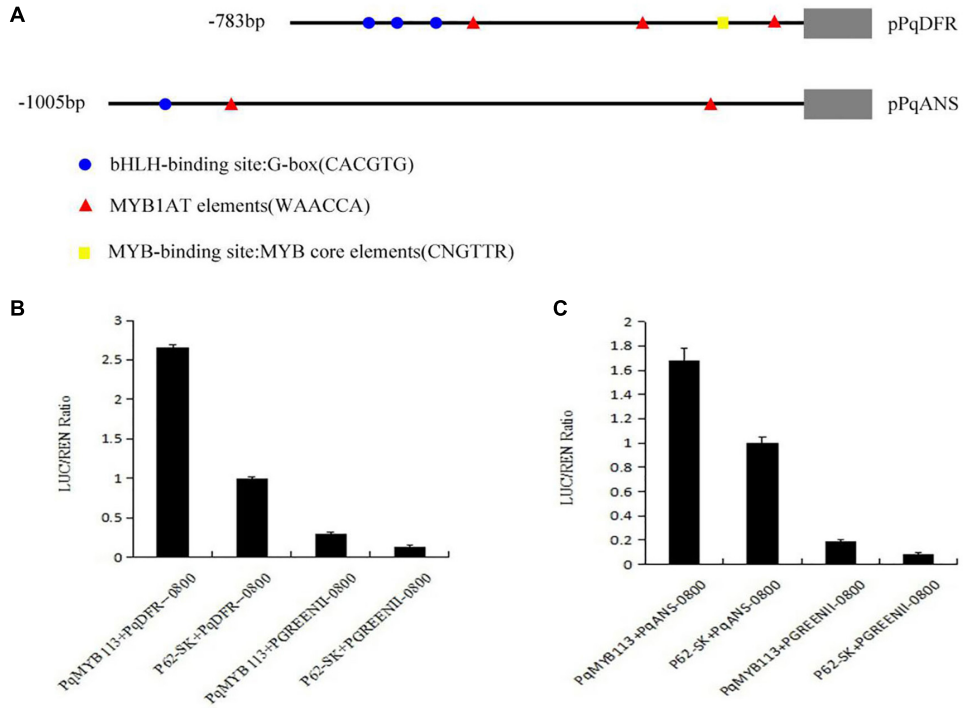

FIGURE 8 | Dual luciferase transient expression assay of *PqDFR, PqANS* promoters and PqMYB113. **(A)** The distribution of MYB binding and bHLH-binding elements in the promoter sequences of *PqDFR* and *PqANS*. **(B)** The effect of *PqDFR* promoter activity by PqMYB113. **(C)** The effect of *PqANS* promoter activity by PqMYB113. The ratio of LUC/REN of the empty vector (SK) plus promoter was used as calibrator (set as 1).

PqMYB113 (**Figure 1B**; Yamagishi et al., 2010), suggesting that PqMYB113 is probably involved in the regulation of anthocyanin synthesis.

Expression Analysis of *PqMYB113* and Anthocyanin Biosynthetic Genes in the Leaves of *P. qiui*

The expression levels of *PqMYB113* and anthocyanin biosynthetic genes in different leaf stages were revealed by qRT-PCR, and the anthocyanin content and chlorophyll content were measured with a UV spectrophotometer (**Figure 2**). The results showed that the anthocyanin content in leaves at S3 was the highest, followed by S4, the lowest at S1 and S5 (**Figures 2B,C**). Chlorophyll showed an increasing trend from S1 to S5 (**Figures 2D,E**). The expression level of *PqMYB113* was the highest at S4, followed by S2 and S3, and the lowest at S1, which was positively correlated with the anthocyanin content in leaves (**Figures 3A**, **2C**). In addition to *PqMYB113,* the anthocyanin pathway genes *PqCHS*, *PqDFR*, *PqANS, PqF3H, PqF3′H,* and *PqCHI* presented a basically consistent trend with the anthocyanin content in leaves (**Figure 3B**).

PqMYB113 Was a Transcriptional Activator

To investigate the subcellular localization of PqMYB113, the recombinant vector pCAMBIA1301-PqMYB113-GFP was transformed into onion cells and observed with confocal laser scanning microscopy. Onion cells expressing the PqMYB113-GFP fusion protein displayed a strong signal in the cell nucleus. The results revealed that PqMYB113 was localized in the cell nucleus (**Figure 4**).

To examine the transcriptional activity of PqMYB113, transient reporter assays were used (**Figure 5**). AtMYB75 was used as a positive control, and AtMYBL2 was used as a negative control. As shown in **Figure 5**, the relative luciferase activity was increased nearly three times by the expression of *GAL-BD-AtMYB113* compared with the *GAL4-BD* control. This result suggested that PqMYB113 was a transcriptional activator.

Overexpression of *PqMYB113* in *Arabidopsis* and Tobacco Promoted Anthocyanin Accumulation and the Expression of Anthocyanin Pathway Genes

To characterize the function of *PqMYB113*, the coding sequence of *PqMYB113*, driven by the 35S promoter, was transformed into *Arabidopsis* and tobacco. In *Arabidopsis*, three T3 overexpression (OE) transgenic lines, designated as OE 3-1-1, OE 3-2-2, and OE 7-1-1, were generated. Compared with the wild-type (WT), all *PqMYB113* OE lines showed increased anthocyanin pigments in young leaves (**Figures 6A,B**). In addition, the seed coat color of transgenic plants was also deeper than

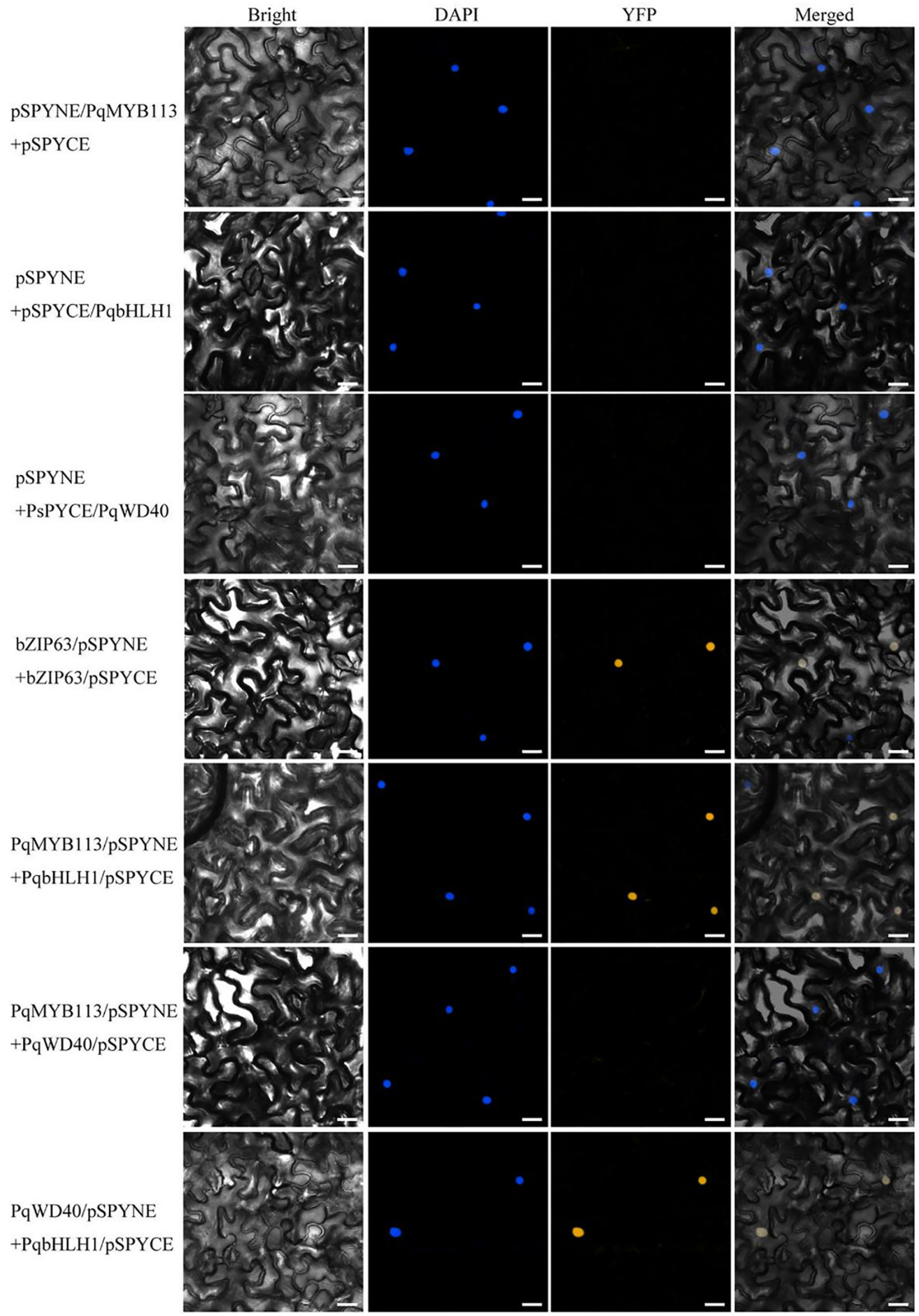

FIGURE 9 | Bimolecular fluorescence complementation in *Nicotiana benthamiana* leaves. Bright, field images show the complete epidermal cell profile in bright-field view; YFP, fluorescence of YFP; DAPI, nuclear staining; "Merge" is merged with chloroplast autofluorescence, YFP fluorescence and bright field images. Bars = 25 μm.

FIGURE 10 | The interaction between PqMYB113 and PqbHLH1, PqWD40 in the yeast two-hybrid system. pGBKT7-53/pGADT7-T served as a positive control; pGBKT7/-Lam/pGADT7-T served as a negative control.

that of WT (**Figure 6A**), suggesting more proanthocyanidin accumulation in the seed coat (Hui et al., 2019). In transgenic tobacco, the leaves of *PqMYB113* OE-1 lines were dark red, and the leaves of OE-2 plants had red spots (**Figure 7A**). The color of the petals and sepals of the OE lines was slightly redder than that of WT (**Figure 7A**). In *PqMYB113* OE *Arabidopsis* plants, the expression levels of anthocyanin biosynthesis pathway genes were analyzed with qRT-PCR. Compared with WT, the *PqMYB113* gene was highly expressed in the transgenic plants, and there was little or no expression in wild-type *Arabidopsis* (**Figure 6C**). The expression of *AtCHS, AtF3H*, *AtF3′H, AtDFR,* and *AtANS* in transgenic lines was higher than that of WT, especially *AtCHS, AtDFR,* and *AtANS*. The expression of *AtCHI* in *Arabidopsis* overexpression plants was similar to that in WT plants (**Figure 6D**). In *PqMYB113* OE tobacco, the results were similar to those in *Arabidopsis* (**Figure 7**). All of these results suggested that *PqMYB113* can promote anthocyanin accumulation by regulating anthocyanin pathway genes.

PqMYB113 Activates the Promoters of Anthocyanin Synthesis Pathway Genes

To test the effect of PqMYB113 on the key anthocyanin structural genes, a dual luciferase reporter assay was carried out. Among the anthocyanin pathway genes, *DFR* and *ANS* are the key structural genes (Zhong et al., 2020). Therefore, the promoters of *PqDFR* and *PqANS* were chosen as potential targets of PqMYB113 transcription activation. The promoter lengths of *PqDFR* and *PqANS* were 783 bp and 1005 bp, respectively. The key elements of the promoters were analyzed by PlantCARE online software, and it was found that these two promoters both have MYB binding sites (**Figure 8A**), suggesting that MYB may regulate their activity. As shown in **Figures 8B,C**, the promoter activities of *PqDFR* and *PqANS* increased approximately 2.6- and 1.7-fold by PqMYB113, respectively. The results suggested that PqMYB113 can activate the promoters of *PqDFR* and *PqANS*.

PqMYB113 Can Interact With Basic Helix Loop Helix and WD40

Bimolecular fluorescence complementation (BiFC) assays and yeast two-hybrid systems were performed to investigate whether PqMYB113 interacts with bHLH and WD40. In this study, PqbHLH1 and PqWD40 were used as candidate co-activators based on our previous study (Luo et al., 2017; **Supplementary Figure 2**).

In BiFC, pSPYNE/bZIP63 + pSPYCE/bZIP63 was used as a positive control, and pSPYNE/PqMYB113 + pSPYCE,

pSPYNE/PqbHLH1 + pSPYCE, pSPYNE/PqbWD40 + pSPYCE were used as negative controls. As shown in **Figure 9**, a yellow fluorescent protein (YFP) fluorescence signal was observed in the nuclei when pSPYNE/PqMYB113 was co-expressed with pSPYCE/PqbHLH1 or pSPYNE/PqbHLH1 with pSPYCE/PqbWD40 but not when pSPYNE/PqMYB113 was co-expressed with pSPYCE/PqbWD40 or any negative controls. The results suggested that PqMYB113 could interact with PqbHLH1 but not with PqWD40, and PqbHLH1 could interact with PqWD40.

In the yeast two-hybrid system, yeast colonies expressing pGBKT7-53 and pGADT7-T (positive control), PqMYB113 and PqbHLH1, PqbHLH1 and PqWD40, PqMYB113 and PqWD40 grew well on SD/-Leu/-Trp medium and became blue on SD/-Ade/-His/-Leu/-Trp/X-α-Gal medium (**Figure 10**). These results also indicated that PqMYB113 could interact with PqbHLH1 and PqWD40.

DISCUSSION

Increasing numbers of studies indicate that R2R3-MYB TFs are important regulators of anthocyanin biosynthesis in many plants (Liu et al., 2015). However, how R2R3-MYB TFs regulate anthocyanin biosynthesis is not clear in tree peony leaves. Here, an R2R3-MYB TF (PqMYB113) was isolated from *P. qiui*. The deduced amino acid sequence analysis of PqMYB113 revealed the presence of the highly conserved R2 and R3 domains at the N-terminus, which is characteristic of R2R3-MYB transcription factors (**Figure 1B**), indicating that PqMYB113 was an R2R3-MYB transcription factor. The characteristic motifs of anthocyanin biosynthesis regulators (ANDV and KPRPR[S/T]F) were also found in PqMYB113 (**Figure 1B**). Phylogenetic analysis showed that PqMYB113 belongs to subgroup 6 (SG6) and clustered with other anthocyanin MYB regulators together into the anthocyanin clade (**Figure 1A**). PqMYB113 shared the highest identity with *Liquidambar formosana* LfMYB113 (58.09%), followed by grapevine VvMYBA1 (48.87%), petunia PhAN2 (47.99%), and *Arabidopsis* AtMYB90 (44.36%) (**Figure 1B**). PqMYB113 showed the lowest identity with *Antirrhinum majus* AmROSEA1 (39.71%) (**Figure 1B**). Subcellular localization analysis revealed that PqMYB113 was localized in the cell nucleus (**Figure 4**). The luciferase assay revealed that PqMYB113 was a transcriptional activator (**Figure 5**). In addition, the [D/E]LX2[R/K]X3LX6LX3R motif, which is responsible for interacting with bHLH proteins, was found in the R3 domain of PqMYB113 (**Figure 1B**; Zimmermann et al., 2004). Taken together, these results suggested that PqMYB113 probably functions as an R2R3-MYB transcription activator that is dependent on bHLH proteins in regulating anthocyanin biosynthesis.

The anthocyanin biosynthesis MYB regulator can promote the accumulation of anthocyanin by regulating the expression level of flavonoid biosynthesis pathway genes. In apple skin, MdMYB3 can regulate anthocyanin biosynthesis and promote anthocyanin accumulation. Overexpression of *MdMYB3* in tobacco up-regulated the anthocyanin content and the expression levels of *NtCHS*, *NtCHI,* and *NtUFGT* (Vimolmangkang et al., 2013). In grape hyacinth, the expression level of *MaAN2* was positively correlated with the anthocyanin content and the expression level of *MaDFR* and *MaANS*; meanwhile, MaAN2 can also strongly activate the promoters of *MaDFR* and *MaANS* (Chen et al., 2017). Here, the expression of *PqMYB113* decreased gradually during tree peony leaf development, and it was positively correlated with anthocyanin accumulation and the expression profiles of *PqCHS*, *PqDFR,* and *PqANS*. In the transgenic *Arabidopsis* plants, compared with *AtF3H* and *AtF3′H*, the expression levels of *AtCHS*, *AtDFR* and *AtANS* in transgenic lines were much higher than those of the wild-type (**Figure 6**). Similar results were observed in transgenic tobacco (**Figure 7**). All of these results suggested that *PqCHS*, *PqDFR,* and *PqANS* (especially *PqDFR* and *PqANS*) may be the key structural genes of anthocyanin synthesis in tree peony leaves, and that PqMYB113 could activate these genes, which was also confirmed by a dual luciferase reporter assay (**Figure 8**).

In apple, overexpression of *MdbHLH3* independently promoted red fruit coloration, and this coloration was enhanced by low temperature. *MdbHLH3* suppression inhibited red coloration in the skin around the infiltration site, while the empty vector control did not influence red coloration (Xie et al., 2012). In the present study, overexpression of *PqMYB113* in tobacco and *Arabidopsis* plants promoted the accumulation of anthocyanin (**Figures 6**, **7**). However, overexpression of *PqbHLH1* did not promote anthocyanin accumulation (data not shown). This may be because the R2R3-MYB TFs play crucial roles in anthocyanin biosynthesis and are usually considered more specific in the MBW complex, while bHLH may function as an enhancer to promote the transcriptional activation activity of MYB. Bimolecular fluorescence complementation assays showed that PqMYB113 can interact with PqbHLH1 but not with PqWD40, and PqbHLH1 can interact with PqWD40 (**Figure 9**). Similar results were also found in apple and tomato (An et al., 2012; Gao et al., 2018). In apple, MdTTG1 (WD40) interacted with bHLH transcription factors but not MYB protein, whereas bHLH was known to interact with MYB (An et al., 2012). In tomato, SlAN11 (WD40) interacted with bHLH but not with MYB proteins in the ternary MBW complex, whereas bHLH interacted with MYB (Gao et al., 2018). The possible reason was that in addition to enhancing the activity of MYB, bHLH can bridge the MYB and WD40 proteins, while the function of WD40 was to stabilize the bHLH-MYB transcriptional complex, thus allowing the binding of the resulting MBW complex to promoters of anthocyanin pathway genes (*DFR*, *ANS*, etc.).

CONCLUSION

PqMYB113 is an R2R3-MYB transcription factor that has an ANDV motif and motif 6, which are characteristics of anthocyanin biosynthesis activators. Its expression is positively correlated with anthocyanin accumulation in tree peony

leaves. PqMYB113 could form a ternary MBW complex with PqbHLH1 and PqWD40 and promoted anthocyanin accumulation by up-regulating the expression levels of *PqDFR* and *PqANS*.

DATA AVAILABILITY STATEMENT

The original contributions presented in the study are included in the article/**Supplementary Material**, further inquiries can be directed to the corresponding author/s.

AUTHOR CONTRIBUTIONS

JL and YZ conceived and designed the research. XL, JD, DH, QL, and QW conducted the experiments and analyzed the data. XL and JD wrote the manuscript. JL and LN modified the manuscript. All authors have read and agreed to the manuscript.

FUNDING

This research was supported by the National Natural Science Foundation of China (Grant No. 31971709) and Shanghai Chenshan Botanical Garden Key Laboratory Opening Topic Fund.

ACKNOWLEDGMENTS

The authors would like to thank the reviewers for their comments. The authors would also like to thank Elsevier's Editing Service for language editing.

SUPPLEMENTARY MATERIAL

The Supplementary Material for this article can be found online at: https://www.frontiersin.org/articles/10.3389/fpls.2021.810990/full#supplementary-material

REFERENCES

Albert, N. W., Lewis, D. H., Zhang, H., Schwinn, K. E., Jameson, P. E., and Davies, K. M. (2011). Members of an R2R3-MYB transcription factor family in Petunia are developmentally and environmentally regulated to control complex floral and vegetative pigmentation patterning. *Plant J.* 65, 771–784. doi: 10.1111/j.1365-313X.2010.04465.x

Allan, A. C., Hellens, R. P., and Laing, W. A. (2008). MYB transcription factors that colour our fruit. *Trends Plant Sci.* 13, 99–102. doi: 10.1016/j.tplants.2007.11.012

An, J., Wang, X., Zhang, X., Xu, H., Bi, S., You, C., et al. (2020). An apple MYB transcription factor regulates cold tolerance and anthocyanin accumulation and undergoes MIEL1-mediated degradation. *Plant Biotechnol. J.* 18, 337–353. doi: 10.1111/pbi.13201

An, X., Tian, Y., Chen, K., Wang, X., and Hao, Y. (2012). The apple WD40 protein MdTTG1 interacts with bHLH but not MYB proteins to regulate anthocyanin accumulation. *J. Plant Physiol.* 169, 710–717. doi: 10.1016/j.jplph.2012.01.015

Ban, Y., Honda, C., Hatsuyama, Y., Igarashi, M., Bessho, H., and Moriguchi, T. (2007). Isolation and functional analysis of a MYB transcription factor gene that is a key regulator for the development of red coloration in apple skin. *Plant Cell Physiol.* 48, 958–970. doi: 10.1093/pcp/pcm066

Cavallini, E., Tomas Matus, J., Finezzo, L., Zenoni, S., Loyola, R., Guzzo, F., et al. (2015). The phenylpropanoid pathway is controlled at different branches by a set of R2R3-MYB c2 repressors in grapevine. *Plant Physiol.* 167, 1448–1470. doi: 10.1104/pp.114.256172

Chagne, D., Kui, L., Espley, R. V., Volz, R. K., How, N. M., Rouse, S., et al. (2013). An ancient duplication of apple MYB transcription factors is responsible for novel red fruit-flesh phenotypes. *Plant Physiol.* 161, 225–239. doi: 10.1104/pp.112.206771

Chen, K., Liu, H., Lou, Q., and Liu, Y. (2017). Ectopic expression of the grape hyacinth (*Muscari armeniacum*) R2R3-MYB transcription factor gene, MaAN2, induces anthocyanin accumulation in tobacco. *Front. Plant Sci.* 8:965. doi: 10.3389/fpls.2017.00965

Dubos, C., Stracke, R., Grotewold, E., Weisshaar, B., Martin, C., and Lepiniec, L. (2010). MYB transcription factors in *Arabidopsis*. *Trends Plant Sci.* 15, 573–581. doi: 10.1016/j.tplants.2010.06.005

Espley, R. V., Hellens, R. P., Putterill, J., Stevenson, D. E., Kutty-Amma, S., and Allan, A. C. (2007). Red colouration in apple fruit is due to the activity of the MYB transcription factor, MdMYB10. *Plant J.* 49, 414–427. doi: 10.1111/j.1365-313X.2006.02964.x

Gao, Y., Liu, J., Chen, Y., Tang, H., Wang, Y., He, Y., et al. (2018). Tomato SlAN11 regulates flavonoid biosynthesis and seed dormancy by interaction with bHLH proteins but not with MYB proteins. *Hortic. Res.* 5, 18–27. doi: 10.1038/s41438-018-0032-3

Gonzalez, A., Zhao, M., Leavitt, J. M., and Lloyd, A. M. (2008). Regulation of the anthocyanin biosynthetic pathway by the TTG1/bHLH/Myb transcriptional complex in *Arabidopsis* seedlings. *Plant J.* 53, 814–827. doi: 10.1111/j.1365-313X.2007.03373.x

Hichri, I., Barrieu, F., Bogs, J., Kappel, C., Delrot, S., and Lauvergeat, V. (2011). Recent advances in the transcriptional regulation of the flavonoid biosynthetic pathway. *J. Exp. Bot.* 62, 2465–2483. doi: 10.1093/jxb/erq442

Hui, Z., Kui, L., Wang, F., Espley, R. V., Ren, F., Zhao, J., et al. (2019). Activator-type R2R3-MYB genes induce a repressor-type R2R3-MYB gene to balance anthocyanin and proanthocyanidin accumulation. *New Phytol.* 221, 1919–1934. doi: 10.1111/nph.15486

Huo, D., Liu, X., Zhang, Y., Duan, J., Zhang, Y., Luo, J., et al. (2020). A novel R2R3-MYB transcription factor PqMYB4 inhibited anthocyanin biosynthesis in *Paeonia qiui*. *Int. J. Mol. Sci.* 21:5878. doi: 10.3390/ijms21165878

Jaakola, L. (2013). New insights into the regulation of anthocyanin biosynthesis in fruits. *Trends Plant Sci.* 18, 477–483. doi: 10.1016/j.tplants.2013.06.003

Jin, H., and Zhu, Z. (2019). Dark, light, and temperature: key players in plant morphogenesis. *Plant Physiol.* 180, 1793–1802. doi: 10.1104/pp.19.00331

Li, S. (2014). Transcriptional control of flavonoid biosynthesis fine-tuning of the MYB-bHLH-WD40 (MBW) complex. *Plant Signal. Behav.* 9:e27522. doi: 10.4161/psb.27522

Liu, J., Osbourn, A., and Ma, P. (2015). MYB transcription factors as regulators of phenylpropanoid metabolism in plants. *Mol. Plant* 8, 689–708. doi: 10.1016/j.molp.2015.03.012

Luo, J., Duan, J., Huo, D., Shi, Q., Niu, L., and Zhang, Y. (2017). Transcriptomic analysis reveals transcription factors related to leaf anthocyanin biosynthesis in *Paeonia qiui*. *Molecules* 22:2186. doi: 10.3390/molecules22122186

Paolocci, F., Robbins, M. P., Passeri, V., Hauck, B., Morris, P., Rubini, A., et al. (2011). The strawberry transcription factor FaMYB1 inhibits the biosynthesis of proanthocyanidins in *Lotus corniculatus* leaves. *J. Exp. Bot.* 62, 1189–1200. doi: 10.1093/jxb/erq344

Rahim, M. A., Busatto, N., and Trainotti, L. (2014). Regulation of anthocyanin biosynthesis in peach fruits. *Planta* 240, 913–929. doi: 10.1007/s00425-014-2078-2

Shang, Y., Venail, J., Mackay, S., Bailey, P. C., Schwinn, K. E., Jameson, P. E., et al. (2011). The molecular basis for venation patterning of pigmentation and its effect on pollinator attraction in flowers of Antirrhinum. *New Phytol.* 189, 602–615. doi: 10.1111/j.1469-8137.2010.03498.x

Song, X., Diao, J., Ji, J., Wang, G., Guan, C., Jin, C., et al. (2016). Molecular cloning and identification of a flavanone 3-hydroxylase gene from lycium chinense, and

its overexpression enhances drought stress in tobacco. *Plant Physiol. Biochem.* 98, 89–100. doi: 10.1016/j.plaphy.2015.11.011

Stracke, R., Ishihara, H., Barsch, G. H. A., Mehrtens, F., Niehaus, K., and Weisshaar, B. (2007). Differential regulation of closely related R2R3-MYB transcription factors controls flavonol accumulation in different parts of the *Arabidopsis thaliana* seedling. *Plant J.* 50, 660–677. doi: 10.1111/j.1365-313X.2007.03078.x

Takos, A. M., Jaffe, F. W., Jacob, S. R., Bogs, J., Robinson, S. P., and Walker, A. R. (2006). Light-induced expression of a MYB gene regulates anthocyanin biosynthesis in red apples. *Plant Physiol.* 142, 1216–1232. doi: 10.1104/pp.106.088104

Tanaka, Y., Sasaki, N., and Ohmiya, A. (2008). Biosynthesis of plant pigments: anthocyanins, betalains and carotenoids. *Plant J.* 54, 733–749. doi: 10.1111/j.1365-313X.2008.03447.x

Vimolmangkang, S., Han, Y., Wei, G., and Korban, S. S. (2013). An apple MYB transcription factor, MdMYB3, is involved in regulation of anthocyanin biosynthesis and flower development. *BMC Plant Biol.* 13:176. doi: 10.1186/1471-2229-13-176

Xie, X., Li, S., Zhang, R., Zhao, J., Chen, Y., Zhao, Q., et al. (2012). The bHLH transcription factor MdbHLH3 promotes anthocyanin accumulation and fruit colouration in response to low temperature in apples. *Plant Cell Environ.* 35, 1884–1897. doi: 10.1111/j.1365-3040.2012.02523.x

Xu, W., Dubos, C., and Lepiniec, L. (2015). Transcriptional control of flavonoid biosynthesis by MYB-bHLH-WDR complexes. *Trends Plant Sci.* 20, 176–185. doi: 10.1016/j.tplants.2014.12.001

Yamagishi, M., Shimoyamada, Y., Nakatsuka, T., and Masuda, K. (2010). Two R2R3-MYB genes, homologs of petunia AN2, regulate anthocyanin biosyntheses in flower tepals, tepal spots and leaves of asiatic hybrid lily. *Plant Cell Physiol.* 51, 463–474. doi: 10.1093/pcp/pcq011

Yoshida, K., Ma, D., and Constabel, C. P. (2015). The MYB182 protein down-regulates proanthocyanidin and anthocyanin biosynthesis in poplar by repressing both structural and regulatory flavonoid genes. *Plant Physiol.* 167:693. doi: 10.1104/pp.114.253674

Zhong, C., Tang, Y., Pang, B., Li, X., Yang, Y., Deng, J., et al. (2020). The R2R3-MYB transcription factor GhMYB1a regulates flavonol and anthocyanin accumulation in Gerbera hybrida. *Hortic. Res.* 7:78. doi: 10.1038/s41438-020-0296-2

Zhou, H., Peng, Q., Zhao, J., Owiti, A., Ren, F., Liao, L., et al. (2016). Multiple R2R3-MYB transcription factors involved in the regulation of anthocyanin accumulation in peach flower. *Front. Plant Sci.* 7:1557. doi: 10.3389/fpls.2016.01557

Zimmermann, I. M., Heim, M. A., Weisshaar, B., and Uhrig, J. F. (2004). Comprehensive identification of *Arabidopsis thaliana* MYB transcription factors interacting with R/B-like BHLH proteins. *Plant J.* 40, 22–34. doi: 10.1111/j.1365-313X.2004.02183.x

Zong, W., Tang, N., Yang, J., Peng, L., Ma, S., Xu, Y., et al. (2016). Feedback regulation of ABA signaling and biosynthesis by a bZIP transcription factor targets drought-resistance-related genes. *Plant Physiol.* 171, 2810–2825. doi: 10.1104/pp.16.00469

Conflict of Interest: The authors declare that the research was conducted in the absence of any commercial or financial relationships that could be construed as a potential conflict of interest.

Publisher's Note: All claims expressed in this article are solely those of the authors and do not necessarily represent those of their affiliated organizations, or those of the publisher, the editors and the reviewers. Any product that may be evaluated in this article, or claim that may be made by its manufacturer, is not guaranteed or endorsed by the publisher.

Copyright © 2022 Liu, Duan, Huo, Li, Wang, Zhang, Niu and Luo. This is an open-access article distributed under the terms of the Creative Commons Attribution License (CC BY). The use, distribution or reproduction in other forums is permitted, provided the original author(s) and the copyright owner(s) are credited and that the original publication in this journal is cited, in accordance with accepted academic practice. No use, distribution or reproduction is permitted which does not comply with these terms.

frontiers in Plant Science

ORIGINAL RESEARCH
published: 09 February 2022
doi: 10.3389/fpls.2022.796997

Identification of a RelA/SpoT Homolog and Its Possible Role in the Accumulation of Astaxanthin in *Haematococcus pluvialis*

*Hui Jin[1,2†], Yong Min Lao[3†], Jin Zhou[1] and Zhong Hua Cai[1]**

[1] Shenzhen Public Platform for Screening and Application of Marine Microbial Resources, Shenzhen International Graduate School, Institute for Ocean Engineering, Tsinghua University, Shenzhen, China, [2] School of Pharmaceutical Sciences, Sun Yat-sen University, Guangzhou, China, [3] Institute for Advanced Study, Shenzhen University, Shenzhen, China

A RelA/SpoT homolog, HpRSH, was identified in *Haematococcus pluvialis*. HpRSH was found to catalyze Mg^{2+}-dependent guanosine tetraphosphate (ppGpp) synthesis and Mn^{2+}-dependent ppGpp hydrolysis, respectively. The transcription of HpRSH was significantly upregulated by environmental stresses, such as darkness, high light, nitrogen limitation, and salinity stress. The intracellular ppGpp level was also increased when exposed to these stresses. In addition, the classical initiator of stringent response, serine hydroxamate (SHX), was found to upregulate the transcription of HpRSH and increase the level of ppGpp. Moreover, stringent response induced by SHX or environmental stresses was proven to induce the accumulation of astaxanthin. These results indicated that stringent response regulatory system involved in the regulation of astaxanthin biosynthesis in *H. pluvialis.* Furthermore, stringent response was unable to induce astaxanthin accumulation under dark condition. This result implied that stringent response may regulate astaxanthin biosynthesis in a light-dependent manner.

Keywords: environmental stresses, stringent response, ppGpp (guanosine 3′,5′ bisdiphosphate), astaxanthin, *Haematococcus pluvialis*

OPEN ACCESS

Edited by:
Maik Böhmer,
Goethe University Frankfurt, Germany

Reviewed by:
Shinji Masuda,
Tokyo Institute of Technology, Japan
Alexei E. Solovchenko,
Lomonosov Moscow State University, Russia

****Correspondence:***
Zhong Hua Cai
caizh@sz.tsinghua.edu.cn

† These authors have contributed equally to this work

Specialty section:
This article was submitted to Plant Physiology, a section of the journal Frontiers in Plant Science

Received: *18 October 2021*
Accepted: *06 January 2022*
Published: *09 February 2022*

Citation:
Jin H, Lao YM, Zhou J and Cai ZH (2022) Identification of a RelA/SpoT Homolog and Its Possible Role in the Accumulation of Astaxanthin in Haematococcus pluvialis. Front. Plant Sci. 13:796997. doi: 10.3389/fpls.2022.796997

INTRODUCTION

Haematococcus pluvialis is a unicellular biflagellate green microalga that inhabits in freshwater (Lorenz and Cysewski, 2000). Recently, this alga attracts considerable attention because it accumulates the highest content of astaxanthin (up to 4% by dry weight), which is a high-value carotenoid with excellent antioxidant activity (Han et al., 2013). Previous studies have proven that astaxanthin accumulation is occurring when algal cells are subjected to unfavorable environments, such as nutrient starvation, high light, and salt stress (Sarada et al., 2002). The accumulation of astaxanthin is generally believed to be a survival strategy of *H. pluvialis* under photo-oxidative stress or other adverse environmental conditions (Hagen et al., 1994; Hu et al., 2008). Astaxanthin confers *H. pluvialis* a remarkable ability to survive in extremely unfavorable environments (Hu et al., 2008; Li et al., 2008). Accompanied by the accumulation of astaxanthin, this alga also exhibits a dimorphic life cycle, mobile green vegetative cells in favorable environment and non-mobile red cyst cells in unfavorable environment (Droop, 1954; Zhang et al., 2017). During this process, *H. pluvialis* stops dividing, enters into a resting stage, and maintains a lower metabolic rate (Boussiba and Vonshak, 1991). Although many studies focus on the relationship between astaxanthin accumulation and environment stresses (Boussiba et al., 1999; Huir, 2000; Su et al., 2014), less is known about

the mechanism of how environmental stresses lead to the transformation of morphology and physiology and induce the accumulation of astaxanthin in *H. pluvialis*.

To survive in changing environments, organisms have evolved many stressful response systems. Stringent response is one of the most important bacterial adaptive responses to deal with nutrient limitation, which was first reported in *Escherichia coli* (Magnusson et al., 2005; Boutte and Crosson, 2013). In addition to nutrient limitation, it also mediates bacterial adaptations to other environmental stresses, such as oxidative damage and acid shock (Wells and Gaynor, 2006; Khakimova et al., 2013; Brown et al., 2014; Irving et al., 2021). Although described for the first time in *E. coli*, stringent response broadly exists in plants, algae, *Drosophila*, and human (Kasai, 2002; Takahashi et al., 2004; Sun et al., 2010). When cells are faced with adverse environmental stresses, stringent response is initiated by a small signal molecular, guanosine tetraphosphate (ppGpp) and/or guanosine pentaphosphate (pppGpp), collectively denoted as (p)ppGpp (Potrykus and Cashel, 2008; Hauryliuk et al., 2015). Once stringent response is activated, bacteria will reallocate their resources from growth support to survival prolonged by reprogramming relative genes transcription (Kanjee et al., 2012; Hauryliuk et al., 2015). A growing number of studies indicated that (p)ppGpp contributes to the regulation of many aspects of bacterial biology, such as growth adaption in *E. coli* (Traxler et al., 2011), antibiotic production in *Bacillus subtilis* (Ochi and Ohsawa, 1984), morphological differentiation in *Mycobacterium smegmatis* (Ojha et al., 2000), sporulation in *Streptomyces* (Ochi, 1987), social behavior in *pseudomonas aeruginosa* (Van Delden et al., 2001), and fruit body development in *Myxococcus xanthus* (Harris et al., 1998). Likewise, ppGpp was also operative in plant and algae, with the identification of ppGpp synthase homologs in *Arabidopsis thaliana* (Der Biezen et al., 2000) and *Chlamydomonas reinhardtii* (Kasai, 2002), the detection of ppGpp in pea, wheat, rice, and spinach (Takahashi et al., 2004), and the investigation of its roles in regulation of cell physiology in *Synechococcus elongatus* (Puszynska and O'Shea, 2017), red alga (Imamura et al., 2018), and *Phaeodactylum tricornutum* (Avilan et al., 2021).

Stringent response plays critical roles in cellular adaptation to environmental stresses (Potrykus and Cashel, 2008). The question of whether bacterial stringent response mediates adaption to stresses and induces accumulation of astaxanthin in *H. pluvialis* was raised. To validate this possibility, we attempted to clone and characterize the homolog of RelA/SpoT enzyme in *H. pluvialis*. And then, the interrelationship between stringent response and astaxanthin accumulation was investigated in detail through mimicking stringent response using serine hydroxamate (SHX), which is a classical initiator of stringent response (Nguyen et al., 2011). Finally, we showed that the RelA/SpoT homolog in *H. pluvialis*, HpRSH, is a double function enzyme, catalyzing Mg^{2+}-dependent ppGpp synthesis and Mn^{2+}-dependent ppGpp hydrolysis. Stringent response could be initiated by SHX and some stresses, such as nitrogen starvation, salinity stress, high light, and darkness. Moreover, stringent response activated by stresses or SHX caused a remarkable accumulation of astaxanthin and induced the upregulation of astaxanthin biosynthesis-related genes. Meanwhile, it was found that stringent response failed in inducing astaxanthin accumulation under dark condition. These results indicated that stringent response system involved in the accumulation of astaxanthin in a light-dependent manner in *H. pluvialis*.

MATERIALS AND METHODS

Algal Strain and Growth Conditions

Haematococcus pluvialis 797 strain was obtained from Institute of Hydrobiology, Chinese Academy of Sciences. The Blue-Green Medium (BG11, whose composition is shown in **Supplementary Table 1**) was used for the growth of *H. pluvialis*. Algae were cultured in conical flask containing 100 ml of growth medium under constant illumination. Cultures were incubated in an illumination incubator at 22°C and 20 μmol photons m^{-2} s^{-1} of light provided by HITACHI lamp (FH32EN, GY10q-9, HITACHI, Japan) under a 12-h light:12-h dark cycle and were shaken manually two times daily. Light intensities were measured by a photometer (LI-250A, LI-COR Inc., Lincoln, NE, United States).

Stresses Treatment

Haematococcus pluvialis in the logarithmic growth phase was treated by different stresses. For dark stress, cells were cultured in a black chamber; for high light stress, algal cells were cultured under illumination of 200 μmol photons m^{-2} s^{-1}; for salt stress, NaCl was added to fresh BG11 at a final concentration of 42 μM; for nitrogen (N^-) starvation, algal cells were washed three times using nitrogen-free (without nitrate) BG11 medium and inoculated into nitrogen-free BG11. For SHX treatment, SHX was added to the culture at a final concentration of 1 g/L. For the transcriptional analysis of HpRSH, algal cells were collected and exposed to different stresses for 0, 1, 2, 3, 6, and 9 h or SHX for 15 min, 30 min, 1, 2, 6, and 9 h. For the transcriptional analysis of some key genes related to astaxanthin accumulation and the determination of astaxanthin accumulation, algal cells were collected after stress exposure for 4 and 72 h, respectively.

Isolation of the Full-Length cDNA of *Hprsh* Gene

According to the sequence of bifunctional (p)ppGpp synthetase/guanosine-3′,5′-bis(diphosphate) 3′-pyrophosphohydrolase annotated in the transcriptome of *H. pluvialis* (GenBank: SRX765192), the ORF of *Hprsh* was amplified by PCR using eHpRelA F and eHpRelA R primers and RNA as template.

Based on the ORF sequence, two gene-specific primers (GSPs) were designed to amplify the 5′-end of *Hprsh* mRNA. 5′-RACE reactions were accomplished using the SMARTer®RACE 5′/3′ Kit (Clontech, United States) and two pairs of GSPs designed. All manipulations were according to the user manual. The full-length cDNAs were finally isolated using GSPs complementary with the 5′- and 3′-ends of the *Hprsh* gene, respectively. The parameters of PCRs were set as follows: 95°C for 5 min; 30 cycles of 95°C for

30 s, 55°C for 30 s, and 72°C for 4 min 30 s, with a final extension at 72°C for 10 min. The amplified sequences were cloned into pMD19-T vector (TaKaRa, China) and sequenced.

The localization of HpRSH was predicted by ChloroP 1.1[1] and WoLF PSORT[2]. Then, the truncate ORF was, respectively, cloned into pET-32a (+) vector between *Bam*HI and *Hin*dIII sites and into pUC19 between *Hin*dIII and *Eco*RI, generating pET-32a-*Hprsh* expression vector and pUC19-*Hprsh* for functional complementation in *E. coli*. Primes for *Hprsh* isolation are listed in **Supplementary Table 2**.

Complementation Analysis of *Hprsh* in *E. coli*

The *E. coli* wild-type strain CF1648 and its derived strain CF1693 ($relA^-/spoT^-$) were prepared as transformation strains. The plasmid pUC19-*Hprsh* including the truncate ORF without the transit peptide of HpRSH was transformed into CF1693 and CF1648. As a control, empty vector plasmid was also transformed into CF1693 and CF1648, respectively. All strains were coated to LB and M9M (M9 mineral medium) plate, respectively, and grown at 37°C for 24 h.

Protein Purification and Enzyme Assay

Recombinant protein was produced in *E. coli* BL-21(DE3) containing the plasmid pET-32a-*Hprsh*. Cells were pelleted by centrifugation at the speed of 12,000 × *g* for 2 min at 4°C. Enzyme extracts were then prepared by the Ni-NTA Spin Kit (QIAGEN, German) according to the user protocol and were eluted using 300 μl of PBS (50 mM NaH_2PO_4, 300 mM NaCl, pH 7.0) containing 500 mM imidazole. The PBS buffer was then exchanged to Tris–HCl buffer (0.1 M Tris–HCl, pH 8.0, 5 mM DTT, 1 mM EDTA) by using the Zeba Spin Desalting Columns and Plates, 7K MWCO (Thermo Fisher Scientific, United States). Protein extracts were quantitated at 25°C using the TaKaRa BCA Protein Assay Kit (TaKaRa, China). All steps were carried out at 4°C unless otherwise stated.

The synthetic or hydrolytic activities of HpRSH were assayed by a method described previously (Nanamiya et al., 2008; Ito et al., 2012). Briefly, for synthase activity assay, reaction mixture containing 50 μM GDP and 80 μM ATP was incubated with 5 mM Mg^{2+} in the presence of recombinant HpRSH protein at 37°C for 20 min. For hydrolase activity, reaction mixture containing 50 mM Tris–HCl (pH 8.0), 5 mM Mn^{2+}, 50 μM ppGpp, and 0.2–1.0 mg of the purified recombinant protein was incubated at 37°C for 20 min. The mixture was analyzed by UPLC on a HILIC chromatographic column (BEH Amide, Waters, United States). ppGpp and GDP were detected by their UV absorbance at 252 nm as reaction products of synthetic and hydrolytic activity, respectively.

Phylogenic Analysis

Sequence analysis was performed using BLAST Software[3]. Multiple alignments were conducted using Clustal X version 1.83. Molecular evolutionary analysis was conducted using the Neighbor-Joining method by the molecular evolution genetics analysis (MEGA) software, version 5.2. Bootstrap values were estimated (with 1,000 replicates) to assess the relative support for each branch, and they were labeled with a cutoff value of 50.

Extraction, Purification, and Detection of Guanosine Tetraphosphate

The analysis of ppGpp in algal cells was according to our published method (Jin et al., 2018). Notably, 2.4 g of cells were collected by centrifugation (8,000 × *g*, 10 min), frozen immediately in liquid nitrogen, crushed, and resuspended in 10 ml of 1 M cool formic acid. The broken cells were vigorously mixed, incubated on ice for 30 min, and then centrifuged (10,000 × *g*, 10 min). The upper layer was transferred into a new tube. The all supernatants were purified by solid-phase extract (SPE). First, the SPE column (OASIS@ WAX 3-cc Vac Cartridges, Waters) was pretreatment using 1 ml of MeOH and then 1% HCOOH. The supernatants were loaded immediately to SPE column. Then, the column loaded with supernatants was washed using 1 ml of 1% HCOOH and 1 ml of MeOH, respectively. Finally, the crude extracts were eluted by 1 ml of H_2O/NH_4OH (70:30) solution. The effluent was dried under vacuum. The resultant residue was dissolved in 100 μl H_2O/ACN (25/75, v/v), and 5 μl was detected using UPLC-MS/MS.

All MS analysis were performed on a Waters TQ-XS triple quadrupole mass analyzed connected to a Waters Aquity H-class UPLC (Waters, United States), and data were collected and analyzed using the MassLynx version 4.1 software (Waters, United States). Chromatographic separation was performed on a Waters BEH Amide column (2.1 × 50 mm, 1.7 μm) at the flow rate of 0.4 ml min^{-1}. The mobile phase was comprised by solvent A (0.1% NH_4OH) and solvent B (acetonitrile). The gradient was set according to the following profile: 0.0 min, 20% A + 80% B; 4.0 min, 25% A + 75% B; 13.0 min, 25% A + 75% B; 14.0 min 50% A + 50% B; 17.0 min, 50% A + 50% B; 17.5 min, 80% A + 20% B. The injection volume was 5 μl. MS was operated in negative electrospray ionization (ESI) and in multiple reactions monitoring (MRM) mode. The ion resource settings were as follows: capillary voltage = 2.5 kV; cone voltage = 30 V; desolvation gas flow = 1,200 L h^{-1}; cone gas flow = 150 L h^{-1}; nebulizer gas = 7.0 bar; desolvation temperature = 400°C; source temperature = 150°C. The ion transition at *m*/*z* 602/159 was used for ppGpp detection. The cone voltage (V) and collision energy (eV) are 44 V and 44 eV, respectively.

RT-PCR Analysis

For real-time quantitative reverse transcription PCR (qPCR) analysis, 30 ml of cells was collected by centrifugation at 12,000 × *g* for 2 min. Total RNA was isolated and purified using the TRIzol according to the manufacturer's instructions. Real-time qPCR was performed with a 7500 Real-Time PCR System (Applied Biosystems, United States) using PrimeScript®RT reagent Kit with gDNA Eraser (which supplies RNase-free DNase I to remove any co-isolated genomic DNA) and SYBR Green PCR Kit (product code: DRR041A and DRR047A, respectively;

[1]https://services.healthtech.dtu.dk/service.php?ChloroP-1.1

[2]https://wolfpsort.hgc.jp/

[3]http://blast.ncbi.nlm.nih.gov/

TaKaRa, China). Primers for quantitative analysis are listed in **Supplementary Table 2**.

The reaction mix contained 4 μl of cDNA, 0.5 μl of forward and reverse primer mix (20 μM each), 1 μl of 50 × ROX Reference Dye II and 25 μl 2 × TaKaRa SYBR Green PCR mix in a final volume of 50 μl. All reactions were set up in triplicate, and every sample was replicated in parallel three times to ensure statistical relevance. The following standard thermal conditions were used for all PCR reactions: 30 s at 95°C, 40 cycles of 30 s at 95°C, and 34 s at 60°C. Primer specificity was confirmed by RT-PCR amplification before Real-Time Quantitative PCR reaction, which produced single amplicon of the expected size for each primer set; these amplicons were sequenced to finally validate their specific amplification. The specificity of qPCR reaction was monitored by the presence of dissociation curves with single peak and sequencing of its products with unique bands of the expected size. Amplicon dissociation curves were obtained after cycle 40 with default settings suggested by the instrument. Data were analyzed using the SDS software (Applied Biosystems, United States).

Astaxanthin Extraction, Saponification, and Detection

Algal cells were collected by centrifugation at 12,000 × *g* for 15 min. The process of extraction, saponification, and detection was according to our published method (Jin et al., 2017). In brief, 100 ml of algae cells (OD_{600} at 0.45) were collected by centrifugation at 8,000 × *g* for 10 min at 25°C, lyophilized and weighed, sequentially. The freeze-dried cells were resuspended in 10 ml of 1 M cool chloroform and sonicated at 4°C for 5 min. The broken cells were vigorously mixed, incubated on ice for 30 min, and then centrifuged at 12,000 × *g* at 4°C for 15 min. The upper layer was collected. Second extraction was carried out, and the supernatant was then merged, evaporated to dryness, and dissolved with 5 ml acetonitrile. The extract was stored at -80°C until use. Then, 100 μl extract was diluted with 2 ml acetonitrile and hydrolyzed by adding 10 μl 1 M NaOH. The saponification process lasted for 6 h at 4°C in dark. The saponified extract was then washed several times with distilled water until the pH was neutral and analyzed by UPLC directly.

Carotenoids were separated at a flow rate of 0.4 ml min^{-1} on Waters BEH C18 column (2.1 × 50 mm, 1.7 μm), using mobile phases composed of methanol (A) and acetonitrile (B). The gradient elution was 10% A and 90% B at 0 min, followed by linear gradient to 0% A and 100% B to 4 min, maintained at 0% A and 100% B to 12 min, returned to initial condition by 12.1 min, re-equilibrated at initial condition by 15 min. The injection volume was 5 μl. Needle was washed using acetonitrile/methanol (9:1; v/v) mixture for 10 s after each injection. Column temperature was maintained at 35°C using a column oven. The detection of analysts was carried out by UV absorbance at 450 nm. The filter constant was set at 0.2.

Statistical Analysis

The analysis of variance was performed on SPSS software. Two-tailed Student's *t*-test (refer to **Figures 3–5**) was performed with assumptions of a Gaussian distribution and equal variance. The number of degrees of freedom for all tests was 4, for $n = 3$ in each set.

RESULTS

Functional Identification of HpRSH

TblastN against the *H. pluvialis* transcriptome by the *C. reinhardtii* RSH (CrRSH) retrieved a HpRSH candidate. Based on this sequence, RT-PCR was performed and a predicted 2,409 bp ORF was isolated. Then, 3′- and 5′-RACE reactions were conducted to isolate the full-length cDNA (**Supplementary Figure 1**). Results showed that the full-length *Hprsh* mRNA has a 166 bp 5′-UTR and 1,140 bp 3′-UTR, with an ORF of 2,409 bp encoding a polypeptide with 796 aa (**Figure 1A**). It has typical secondary structures of RelA/SpoT superfamily, e.g., HD domain (hydrolase), RelA_SpoT domain (synthase), TGS domain, and ACT domain (**Figure 1A**). These results implied that HpRSH may be a RelA/SpoT-like enzyme. Using ChloroP and WoLF PSORT, HpRSH is predicted to contain a 59 aa long transit peptide and, therefore, is localized in chloroplast.

The function of HpRSH was determined by functional complementation in *E. coli* strains CF1693 ($relA^{-}spoT^{-}$) and CF1648 (wild type). According to previous research, the high level of ppGpp is lethal for *E. coli* due to the lack of (p)ppGpp hydrolase activity (Xiao et al., 1991). Furthermore, it should be noted that $(p)ppGpp^{0}$ cell are unable to grow in nutritionally poor M9M medium because suitable concentration of ppGpp is needed for transcription of several operons involved in amino acid biosyntheses (Xiao et al., 1991; Ingraham et al., 1996). In this study, as shown in **Figure 1B**, on M9M plate, CF1693 with the pUC19 (empty vector) cannot grow, but transcribing the pUC19-HpRSH (carrying the full length of HpRSH) into CF1693 can restore the growth on M9M plate. These results indicate that HpRSH could complement $relA^{-}spoT^{-}$ phenotypes and function as an RSH, i.e., as a (p)ppGpp synthase and hydrolase bifunctional enzyme.

To further confirm the activity of HpRSH, we next examined *in vitro* synthetic and hydrolytic activities using recombinant protein (**Supplementary Figure 2**) at 35°C under different reaction condition (as shown in the section "Protein Purification and Enzyme Assay") and analyzed reaction products through UPLC. As expected, ppGpp was found when incubating recombinant protein with ATP and GDP at the presence of Mg^{2+} as cofactor, and GDP was detected in the mixture of hydrolytic assay which contained Mn^{2+} (**Figure 1C**), demonstrating HpRSH catalyzes Mg^{2+}-dependent ppGpp synthesis and Mn^{2+}-dependent ppGpp hydrolysis.

Molecular Evolutionary Relationships of HpRSH

Previous studies found that *C. reinhardtii* has a single RSH (CrRSH, GenBank: EFN56946) (Kasai, 2002); it does not cluster within any other plant RSH (Boniecka et al., 2017); CRSH appears to be present only in land plants (Tozawa et al., 2007). However, we used this CrRSH, AtRSH1-3

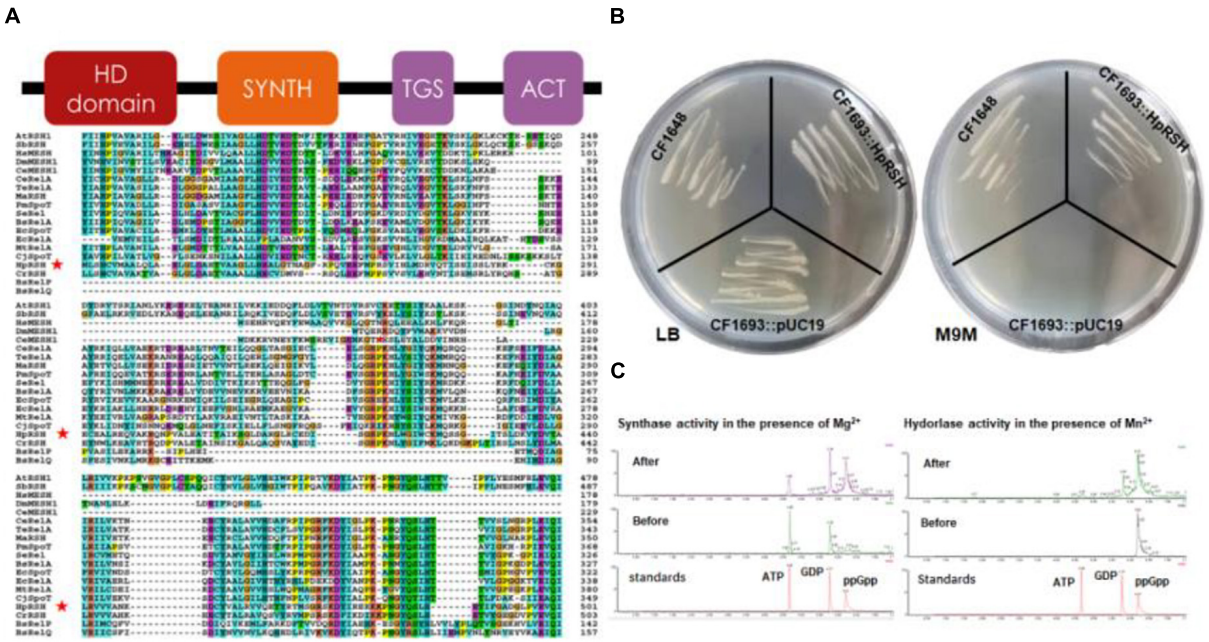

FIGURE 1 | Characterization of relA/spoT homologous gene *Hprsh* in *H. pluvialis*. **(A)** Secondary conserved domains and sequence alignment of MaRSH. Red stars indicate the sequence of HpRSH. **(B)** Functional complementation of HpRSH. **(C)** *In vitro* activities of HpRSH. Left: In the presence of Mg^{2+}, the enzyme utilized ATP and GDP as substrates (before the reaction, middle panel) to synthesize ppGpp (after the reaction, upper panel). Right: In the presence of Mn^{2+}, HpRSH displayed hydrolase activity to hydrolyze ppGpp (before the reaction, middle panel) into GDP (after the reaction, upper panel).

(GenBank: AAF37282, AAF37281, AAF37283, respectively), AtCRSH (GenBank: NP_001327078.1), and HpRSH (GenBank: KU744004) characterized here to tblastn search the newest version (v5.6) of C. *reinhardtii* genome[4] and found another RSH member, CrCRSH (GenBank: XP_042926693.1), with high query cover and confident score (**Supplementary Material** Phytozome BLAST file). Then, we used these RSHs, including CrRSH, CrCRSH, AtRSH1-3, and AtCRSH, to search the transcriptome of *H. pluvialis*, only the current HpRSH was retrieved. Based on the current HpRSH, a phylogenetic tree was constructed using RSH homologs. Results showed that HpRSH clustered with CrRSH, which was independent of other clusters of RSHs (**Figure 2**).

Stringent Response Could Be Initiated by Environmental Stresses

Previous studies have shown that stressful conditions such as light, nutrient limitation, and salinity stress could induce stringent response (Takahashi et al., 2004). Moreover, it was proven that environmental factors induce the expression of RSH in a time-dependent manner (Jin et al., 2020). Therefore, time-course expression profiles of HpRSH under different stresses were investigated in this study. As shown in **Figure 3A**, when algal cells were exposed to darkness, the transcription of HpRSH was upregulated gradually and rose to maximum level (about 3.1-fold, $p < 0.01$) after 2 h. High light induced a significant increase of the transcription of HpRSH (2.8-fold, $p < 0.01$) after 30 min and then resulted in the highest level (about 8.3-fold, $p < 0.001$) at 1 h (**Figure 3B**). Similarly, the transcription of HpRSH was raised to more than 6-fold at 2 h by nitrogen limitation and salinity stress, respectively (**Figures 3C,D**). In addition, since alarmone ppGpp is the arbiter of stringent response, its corresponding concentration at the highest transcriptional level of HpRSH (1 h for high light and 2 h for all other groups) was determined to further confirm the initiation of stringent response biochemically. As expected, the endogenous ppGpp level under environmental stresses was consistent with the transcription of HpRSH. As exhibited in **Figure 3E**, when subjected to darkness, high light, nitrogen starvation, and salt stress, the concentration of ppGpp reached to a level of 2.54 ± 0.19 ($p < 0.001$), 7.22 ± 0.68 ($p < 0.001$), 5.77 ± 0.30 ($p < 0.001$), and 5.58 ± 0.39 ($p < 0.001$) nmol/g DCW (dry cell weight), respectively, compared with that of control (1.11 ± 0.13 nmol/g DCW). These results show that environmental stresses could trigger stringent response in *H. pluvialis*.

Serine Hydroxamate Triggers Stringent Response in *H. pluvialis*

It is well-known that under amino acids starvation, uncharged tRNAs signal RelA to initiate stringent response in *E. coli* (Potrykus and Cashel, 2008). SHX, an inhibitor of serine tRNA synthetase, has been proven to elicit stringent response by simulating amino acid starvation in *E. coli*, *P. aeruginosa*, and some other bacteria (Van Delden et al., 2001; Potrykus and Cashel, 2008). To test whether SHX has the same effect on *H. pluvialis*, SHX was added to the algal culture media at a final

[4]https://phytozome-next.jgi.doe.gov/

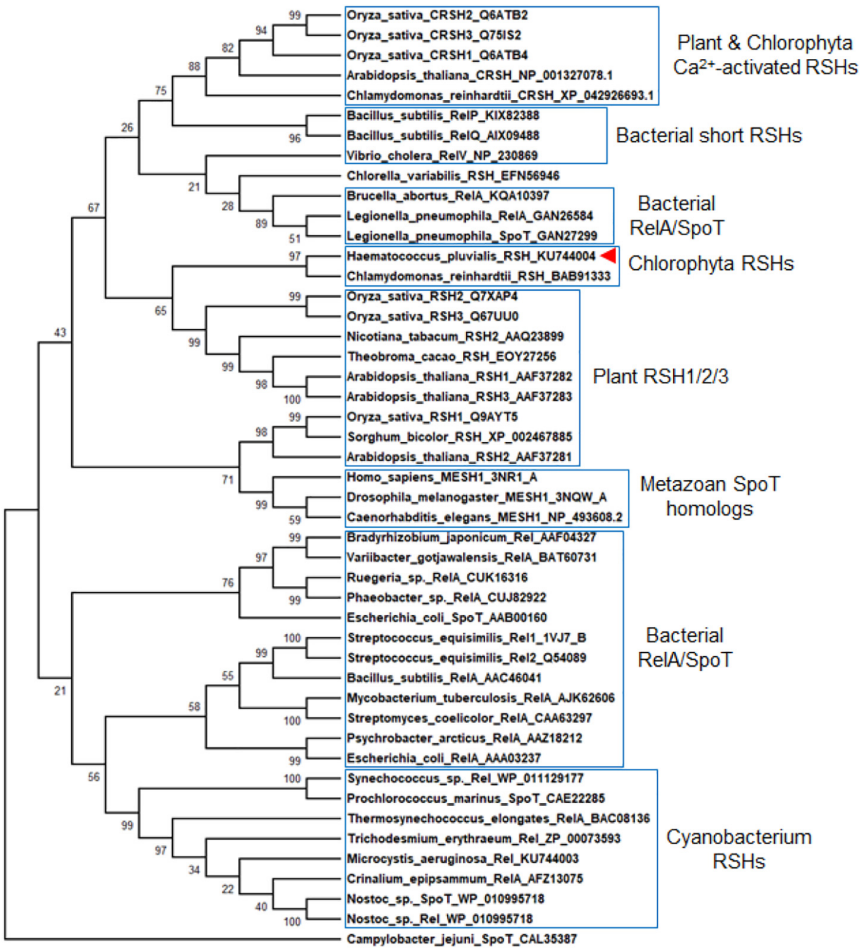

FIGURE 2 | Molecular evolutionary relationships of HpRSH by the Neighbor-Joining method. The nodes of gene duplication during evolution are dotted. The bootstrap consensus tree inferred from 1,000 replicates is taken to represent the evolutionary history of the taxa analyzed. Branches corresponding to partitions reproduced in less than 50% bootstrap replicates are collapsed. The percentage of replicate trees in which the associated taxa clustered together in the bootstrap test (1,000 replicates) are shown above the branches. Red arrow indicates the HpRSH isolated in this study.

concentration of 1.0 mg ml^{-1} and time-course transcriptional expression profile of HpRSH was determined in this study. As shown in **Figure 4A**, the transcription of HpRSH was upregulated after just 15 min, which reached the highest level at 1 h (about 9.8-fold, $p < 0.01$). Correspondingly, at the highest transcription level of HpRSH, the intracellular concentration of ppGpp was found to increase from 0.51 ± 0.12 at 0 h to 8.20 ± 0.31 nmol/g DCW ($p < 0.001$) at 1 h (**Figure 4B**). These results suggested that SHX was able to trigger stringent response in *H. pluvialis* and could be used as a positive control in this study.

Higher Guanosine Tetraphosphate Level Enhanced Astaxanthin Accumulation

In this study, some environmental stresses were found to elicit stringent response by upregulating the transcription of HpRSH and enhancing ppGpp synthesis in *H. pluvialis*. These stresses had been proven to induce astaxanthin accumulation in previous studies (Kobayashi et al., 1993; Boussiba et al., 1999; Boussiba, 2000; Sarada et al., 2002). This observation led to the hypothesis that stringent response involves in the regulation of astaxanthin biosynthesis. To evaluate the effect of stressful conditions on the accumulation of astaxanthin, the levels of astaxanthin under different stresses were determined by UPLC. As shown in **Figure 5A**, environment stresses could differentially regulate astaxanthin biosynthesis. Except for darkness, stresses led to astaxanthin accumulation when compared with the control. Among them, high light presented the most significant effect on astaxanthin accumulation. It enhanced the yield of astaxanthin to 5.65 ± 0.45, compared with 0.63 ± 0.05 mg/g DCW in the control. Nitrogen limitation could also raise the level of astaxanthin obviously to 4.22 ± 0.17 mg/g DCW. The addition of NaCl resulted in an increase of astaxanthin to 2.96 ± 0.37 mg/g DCW. This result indicated that with the exception of darkness, stressful conditions initiated stringent response and concomitantly led to astaxanthin accumulation, which implied a connection between the initiation of stringent response and the accumulation of astaxanthin.

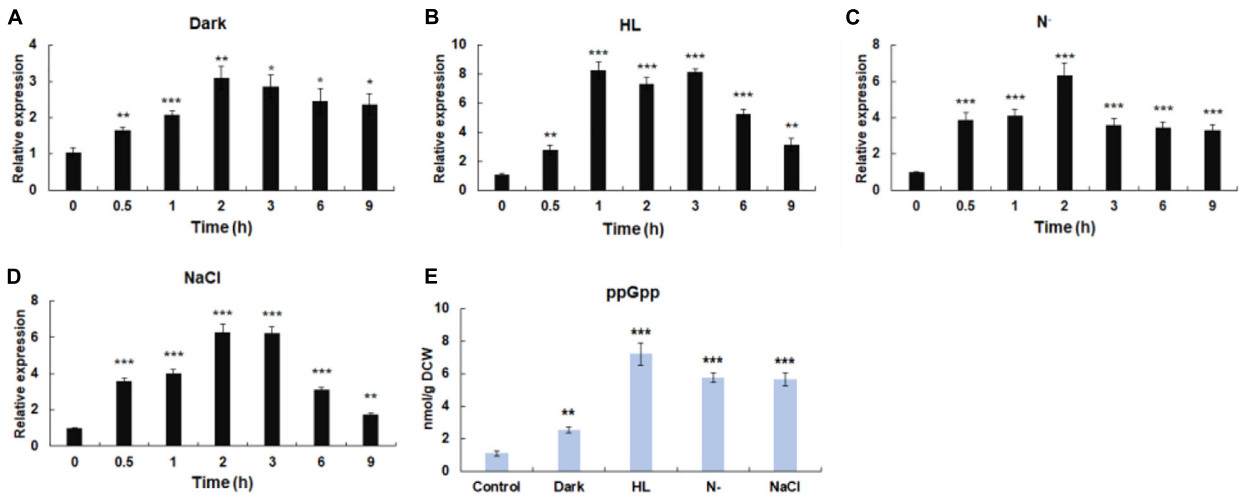

FIGURE 3 | Influence of environmental stresses on the initiation of stringent response. **(A)** The transcriptional expressions of *Hprsh* under different stresses. **(B)** The levels of ppGpp induced by different stresses. Dark, keep in dark place; HL, high light; N^-, nitrogen limitation (without nitrate sodium); NaCl, 42 μm NaCl; DCW, dry cell weight. Error bars indicate the standard deviation (SD) of the mean ($n = 3$) for *Hprsh* transcription analysis, or $n = 3$ for ppGpp determination. $^*p < 0.05$, $^{**}p < 0.01$, or $^{***}p < 0.001$ vs. 0 h **(A–D)** or control **(E)**.

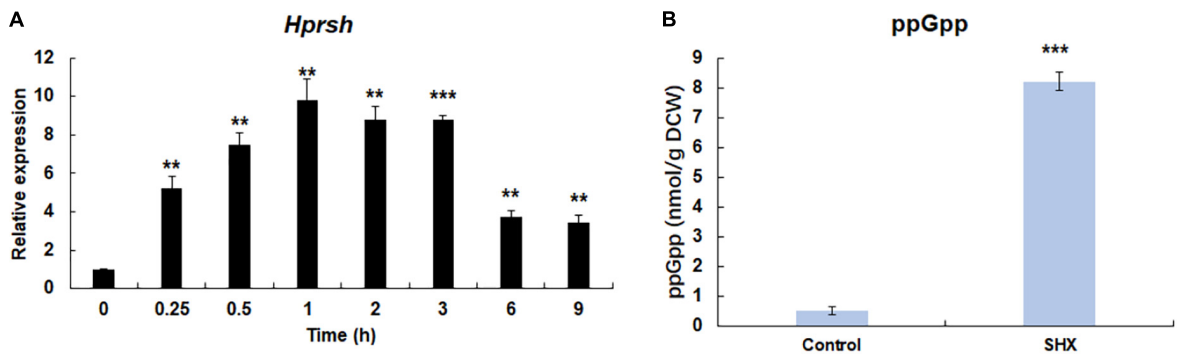

FIGURE 4 | SHX-triggered stringent response. **(A)** The transcription of *Hprsh* induced by SHX. **(B)** The levels of ppGpp induced by different stresses at the highest transcriptional level of *Hprsh* (1 h for SHX). DCW: dry cell weight. Error bars indicate the standard deviation (SD) of the mean ($n = 3$) for the transcription of *Hprsh* and ppGpp determination. $^{**}p < 0.01$, or $^{***}p < 0.001$ vs. 0 h **(A)** or control **(B)**.

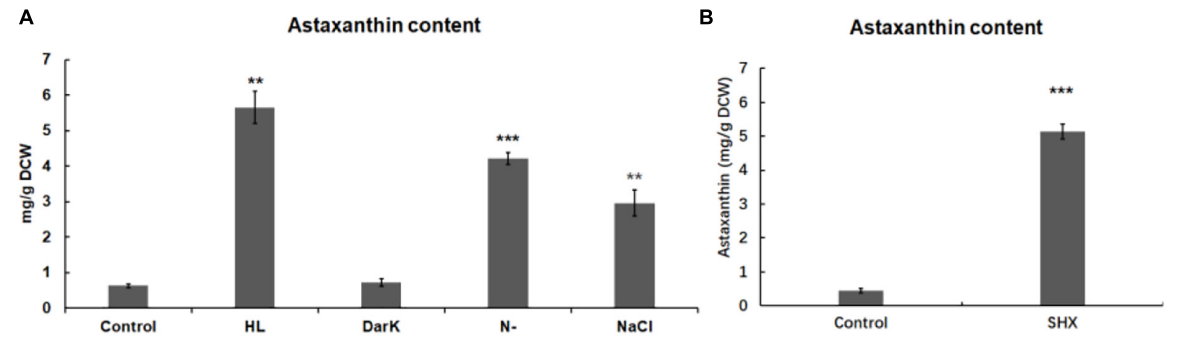

FIGURE 5 | Effect of environmental stresses and SHX on the accumulation of astaxanthin in *H. pluvialis*. The accumulation of astaxanthin induced by environmental stresses **(A)** and SHX (1 mg/ml) for 72 h **(B)**. DCW: dry cell weight. Error bars indicate the standard deviation (SD) of the mean ($n = 3$) for *Hprsh* transcription analysis or $n = 3$ for astaxanthin determination. $^{**}p < 0.01$, or $^{***}p < 0.001$ vs. control.

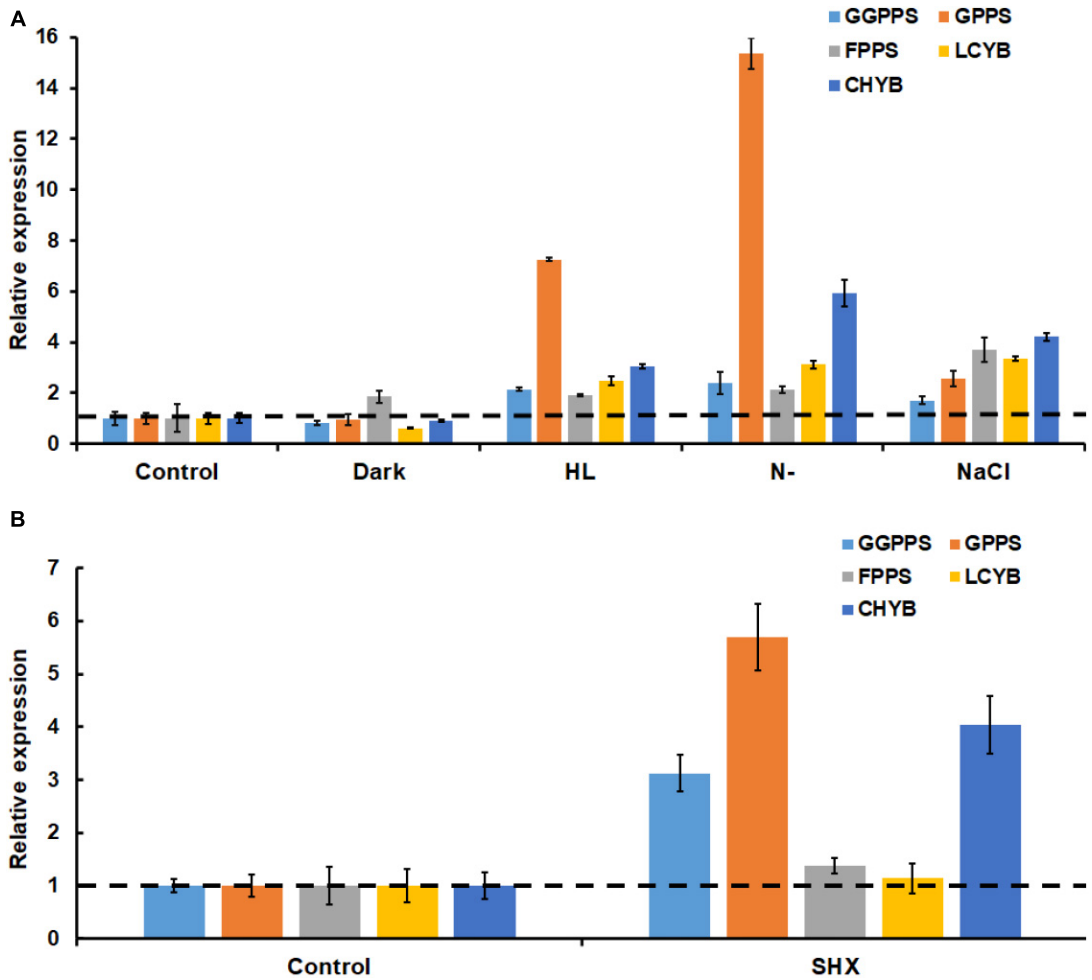

FIGURE 6 | Transcriptional expressions of key astaxanthin biosynthesis genes under SHX **(A)** and different environmental stresses **(B)**. CHYB, carotenoid β-hydroxylase; LCYB, lycopene ε-cyclase; GPPS, geranyl diphosphate synthase; FPPS, farnesyl diphosphate synthase; and GGPPS, geranylgeranyl diphosphate synthase.

To confirm this possibility, SHX was used to elicit stringent response, then the content of astaxanthin was determined. As depicted in **Figure 5B**, the content of astaxanthin was strikingly accumulated from 0.45 ± 0.07 to 5.13 ± 0.21 mg/g DCW. Furthermore, there was a marked change in algal morphology. As depicted in **Supplementary Figure 3**, when exposed to 1 mg ml^{-1} SHX, algae transformed from green motile cells to red non-motile cells after 10 days. Oppositely, the control cells were with almost no changes. These results further demonstrated that stringent response may be involved in the regulation of astaxanthin biosynthesis.

Stringent Response Induced the Upregulation of the Key Genes for Astaxanthin Biosynthesis

It was well-documented that environmental stresses caused the accumulation of astaxanthin through upregulating astaxanthin biosynthesis genes at the transcriptional level (Steinbrenner and Linden, 2003; Vidhyavathi et al., 2008). In this study, the transcription of general carotenogenic genes (e.g., *GPPS*, *FPPS*, and *GGPPS*) and specific astaxanthin synthesis genes (e.g., *LCYB* and *CHYB*) during stress exposure was investigated. As expected, both general carotenogenic genes and specific astaxanthin biosynthetic genes were found to be upregulated upon exposure to high light, nitrogen limitation, and salinity stress. Notably, 7.3- and 15.4-fold increases in the transcript of GGPPS were induced by nitrogen limitation and high light, respectively (**Figure 6A**). Meanwhile, both nitrogen limitation and high light resulted in more than 2-fold increase in the transcripts of GPPS, FPPS, LCYB, and CHYB (**Figure 6A**). In addition, salinity stress increased significantly the transcription of all the five genes. Darkness only upregulated the transcription of GGPP. Similarly, when stringent response was triggered by SHX, the expression levels of GGPPS, GPPS, FPPS, LCYB, and CHYB were found to be 4. 04-, 5. 69-, 1. 38-, 1. 14-, and 3.13-fold higher than the control group, respectively (**Figure 6B**). These results suggested environmental stresses (except darkness)

upregulated several key genes in astaxanthin biosynthesis by initiating stringent response.

DISCUSSION

Stringent Response May Be Involved in the Regulation of Astaxanthin Biosynthesis

Stringent response is highly conserved and regulates many important physiological functions in plant and algae (Kasai, 2002; Takahashi et al., 2004; Avilan et al., 2021). In this study, homologous protein of RelA/SpoT in *H. pluvialis*, HpRSH, was identified by function complement and enzyme assay *in vitro* (**Figure 1**). Both the transcription of *Hprsh* and the levels of ppGpp were stimulated by environmental stresses (**Figure 3**). In addition, a classic initiator of stringent response, SHX, was proven to elicit stringent response in *H. pluvialis* (**Figure 4**). These results suggested that stringent response system exists and possibly participates in the physiological regulation respond to stresses in *H. pluvialis*. Moreover, these environmental stresses were shown to stimulate *H. pluvialis* to produce astaxanthin (**Figure 4A**) and, meanwhile, SHX-activated stringent response to induce massive accumulation of astaxanthin under normal environment (**Figure 4B**). These results suggested that stringent response may be involved in the regulation of astaxanthin biosynthesis. The positive regulation of many key genes in astaxanthin biosynthesis by environmental stresses and SHX further validated the possibility (**Figure 6**). Astaxanthin accumulation is regarded as a responsive pathway against stresses to protect algal cells from damages under unfavorable conditions. Stringent response has been proven to be indispensable for organisms to adapt to diverse unfavorable environments (Boussiba, 2000). Moreover, stringent response is highly conserved and lies at the top network that governs global gene expression in response to environmental stresses (Hauryliuk et al., 2015). Therefore, on the basis of previous reports and our results, this study postulated that astaxanthin accumulation may be a consequence of stringent response induced by unfavorable environments. Algal cells sense stresses through stringent response, transmit this signal by ppGpp, and copy with stressful condition by redirection of transcription so that genes important for survival are favored, i.e., astaxanthin synthesis genes in this study.

Astaxanthin Accumulation Mediated by Stringent Response May Be Light-Dependent

Our results showed that stringent response may be involved in the regulation of astaxanthin biosynthesis in *H. pluvialis*. It is worthy noted that darkness triggered a clear stringent response, but it failed to induce astaxanthin accumulation (**Figures 3A**, 5A). The role of light in astaxanthin biosynthesis has been studied in previous studies. Goodwin and Jamikorn claimed that light is necessary for astaxanthin biosynthesis (Goodwin and Jamikorn, 1954). Droop showed that astaxanthin could be synthesized in dark only when culture medium contains sodium acetate (Droop, 1955). According to these points, it is reasonable that darkness was unable to induce astaxanthin accumulation in culture medium without sodium acetate, although it did initiate stringent response. These results may imply that stringent response regulates astaxanthin biosynthesis in a light-dependent manner. Actually, SHX-activated stringent response was also unable to induce astaxanthin accumulation under dark condition in culture medium without sodium acetate (**Supplementary Figure 4**), which further strengthens the light-dependent regulation hypothesis by stringent response.

CONCLUSION

In this study, HpRSH, a RelA/SpoT homolog, was identified by functional complement and *in vitro* enzyme activity in *H. pluvialis*. HpRSH was found to possess double functions and catalyzes Mg^{2+}-dependent ppGpp synthesis and Mn^{2+}-dependent ppGpp hydrolysis. Both the transcription of HpRSH and the level of ppGpp were raised by SHX and environmental stresses, such as darkness, nitrogen starvation, high light, and salinity stress. Moreover, stringent response induced by SHX or environmental stresses led to a significant accumulation of astaxanthin. Furthermore, key genes in astaxanthin biosynthesis were upregulated by SHX and these stresses. All these results showed that stringent response may be involved in the regulation of astaxanthin biosynthesis in *H. pluvialis*. In addition, darkness triggered stringent response but was unable to induce astaxanthin accumulation. Meanwhile, SHX-activated stringent response was unable to cause astaxanthin accumulation under dark condition. These results implied that the regulation of astaxanthin biosynthesis by stringent response may be light-dependent.

DATA AVAILABILITY STATEMENT

The datasets presented in this study can be found in online repositories. The names of the repository/repositories and accession number(s) can be found in the article/**Supplementary Material**.

AUTHOR CONTRIBUTIONS

HJ and YL contributed to conceptualization, methodology, investigation, writing – original draft and review and editing, and funding acquisition. JZ contributed to data analysis, validation, investigation, and writing – review and editing. ZC contributed to conceptualization, investigation, writing – review and editing, supervision, project administration, and funding acquisition. All authors contributed to the article and approved the submitted version.

FUNDING

This work was supported by the National Natural Science Foundation of China (32000071), Guangdong Basic and Applied Basic Research Foundation (2019A1515012227), S&T Projects of Shenzhen Science and Technology Innovation Committee (JCYJ20190808152805472, JCYJ20200109142822787, and JCYJ20200109142818589), Shenzhen Science and Technology Program (RCJC20200714114433069), and Project of Shenzhen Municipal Bureau of Planning and Natural Resources.

ACKNOWLEDGMENTS

We are grateful to Cashel for his kind donation of CF1648 and CF1693.

SUPPLEMENTARY MATERIAL

The Supplementary Material for this article can be found online at: https://www.frontiersin.org/articles/10.3389/fpls.2022.796997/full#supplementary-material

REFERENCES

Avilan, L., Lebrun, R., Puppo, C., Citerne, S., Cuine, S., LiBeisson, Y., et al. (2021). ppGpp influences protein protection, growth and photosynthesis in Phaeodactylum tricornutum. *New Phytol.* 230:1517. doi: 10.1111/nph.17286

Boniecka, J., Prusińska, J., Dąbrowska, G. B., and Goc, A. (2017). Within and beyond the stringent response-RSH and (p) ppGpp in plants. *Planta* 246, 817–842. doi: 10.1007/s00425-017-2780-y

Boussiba, S. (2000). Carotenogenesis in the green alga *Haematococcus pluvialis*: cellular physiology and stress response. *Physiol. Plantarum.* 108, 111–117.

Boussiba, S., Bing, W., Yuan, J., Zarka, A., and Chen, F. (1999). Changes in pigments profile in the green alga *Haeamtococcus pluvialis* exposed to environmental stresses. *Biotechnol. Lett.* 21, 601–604.

Boussiba, S., and Vonshak, A. (1991). Astaxanthin accumulation in the green alga *Haematococcus pluvialis*[1]. *Plant Cell Physiol.* 32, 1077–1082. doi: 10.1093/oxfordjournals.pcp.a078171

Boutte, C. C., and Crosson, S. (2013). Bacterial lifestyle shapes stringent response activation. *Trends Microbiol.* 21, 174–180. doi: 10.1016/j.tim.2013.01.002

Brown, D. R., Barton, G., Pan, Z., Buck, M., and Wigneshweraraj, S. (2014). Nitrogen stress response and stringent response are coupled in *Escherichia coli*. *Nat. Commun.* 5, 4115–4115. doi: 10.1038/ncomms5115

Der Biezen, E. A. V., Sun, J., Coleman, M. J., Bibb, M. J., and Jones, J. D. G. (2000). Arabidopsis RelA/SpoT homologs implicate (p)ppGpp in plant signaling. *P. Natl. Acad. Sci. USA* 97, 3747–3752. doi: 10.1073/pnas.060392397

Droop, M. (1955). Carotenogenesis in *Haematococcus pluvialis*. *Nature* 175, 42–42.

Droop, M. R. (1954). Conditions governing haematochrome formation and loss in the alga *haematococcus pluvialis* flotow. *Arch. Microbiol.* 20, 391–397. doi: 10.1007/BF00690882

Goodwin, T., and Jamikorn, M. (1954). Studies in carotenogenesis. 11. Carotenoid synthesis in the alga *Haematococcus pluvialis*. *Biochem. J.* 57, 376–381. doi: 10.1042/bj0570376

Hagen, C., Braune, W., and Bjorn, L. O. (1994). Functional aspects of secondary carotenoids in *Haematococcus lacustris* (Volvocales). III: Action as a Sunshade. *J. Phycol.* 30, 241–248.

Han, D., Li, Y., and Hu, Q. (2013). Astaxanthin in microalgae: pathways, functions and biotechnological implications. *Algae* 28, 131–147. doi: 10.1104/pp.122.4.1261

Harris, B. Z., Kaiser, D., and Singer, M. (1998). The guanosine nucleotide (p)ppGpp initiates development and A-factor production in *Myxococcus xanthus*. *Genes Dev.* 12, 1022–1035. doi: 10.1101/gad.12.7.1022

Hauryliuk, V., Atkinson, G. C., Murakami, K. S., Tenson, T., and Gerdes, K. (2015). Recent functional insights into the role of (p)ppGpp in bacterial physiology. *Nat. Rev. Microbiol.* 13, 298–309. doi: 10.1038/nrmicro3448

Hu, Z., Li, Y., Sommerfeld, M., Chen, F., and Hu, Q. (2008). Enhanced protection against oxidative stress in an astaxanthin-overproduction Haematococcus mutant (Chlorophyceae). *Eur. J. Phycol.* 43, 365–376. doi: 10.1080/09670260802227736

Huir, Z. (2000). The effect of nutritional stresses on accumulation of astaxanthin in *Haematococcus pluvialis*. *Acta Hydrobiol. Sin.* 24, 208–212.

Imamura, S., Nomura, Y., Takemura, T., Pancha, I., Taki, K., Toguchi, K., et al. (2018). The checkpoint kinase TOR (target of rapamycin) regulates expression of a nuclear-encoded chloroplast RelA-SpoT homolog (RSH) and modulates chloroplast ribosomal RNA synthesis in a unicellular red alga. *Plant J.* 94, 327–339. doi: 10.1111/tpj.13859

Ingraham, J. L., Marr, A., Neidhardt, F., and Curtiss, J. (1996). *Escherichia coli* and *Salmonella*: cellular and molecular biology. Washington, DC: ASM.

Irving, S. E., Choudhury, N. R., and Corrigan, R. M. (2021). The stringent response and physiological roles of (pp) pGpp in bacteria. *Nat. Rev. Microbiol.* 19, 256–271. doi: 10.1038/s41579-020-00470-y

Ito, D., Kato, T., Maruta, T., Tamoi, M., Yoshimura, K., and Shigeoka, S. (2012). Enzymatic and molecular characterization of Arabidopsis ppGpp pyrophosphohydrolase, AtNUDX26. *Biosci. Biotech. Bioch.* 76, 2236–2241. doi: 10.1271/bbb.120523

Jin, H., Lao, Y. M., Ying, K. Z., Zhou, J., and Cai, Z. H. (2020). Stringent response regulates stress resistance in cyanobacterium *Microcystis aeruginosa*. *Front. Microbiol.* 11:511801. doi: 10.3389/fmicb.2020.511801

Jin, H., Lao, Y. M., Zhou, J., Zhang, H. J., and Cai, Z. H. (2017). Simultaneous determination of 13 carotenoids by a simple C18 column-based ultra-high-pressure liquid chromatography method for carotenoid profiling in the astaxanthin-accumulating *Haematococcus pluvialis*. *J. Chromatogra. A* 1488, 93–103. doi: 10.1016/j.chroma.2017.01.088

Jin, H., Lao, Y. M., Zhou, J., Zhang, H. J., and Cai, Z. H. (2018). A rapid UHPLC-HILIC method for algal guanosine 5′-diphosphate 3′-diphosphate (ppGpp) and the potential separation mechanism. *J. Chromatogra. B* 1096, 143–153. doi: 10.1016/j.jchromb.2018.08.009

Kanjee, U., Ogata, K., and Houry, W. A. (2012). Direct binding targets of the stringent response alarmone (p)ppGpp. *Mol. Microbiol.* 85, 1029–1043. doi: 10.1111/j.1365-2958.2012.08177.x

Kasai, K. (2002). A ReIA-SpoT homolog (Cr-RSH) identified in *Chlamydomonas reinhardtii* generates stringent factor *in vivo* and localizes to chloroplasts *in vitro*. *Nucleic Acids Res.* 30, 4985–4992. doi: 10.1093/nar/gkf628

Khakimova, M., Ahlgren, H. G., Harrison, J. J., English, A. M., and Nguyen, D. (2013). The stringent response controls catalases in *Pseudomonas aeruginosa* and is required for hydrogen peroxide and antibiotic tolerance. *J. Bacteriol.* 195, 2011–2020. doi: 10.1128/JB.02061-12

Kobayashi, M., Kakizono, T., and Nagai, S. (1993). Enhanced carotenoid biosynthesis by oxidative stress in acetate-induced cyst cells of a green unicellular alga, *Haematococcus pluvialis*. *App. Environ. Microbiol.* 59, 867–873. doi: 10.1128/aem.59.3.867-873.1993

Li, Y., Sommerfeld, M., Chen, F., and Hu, Q. (2008). Consumption of oxygen by astaxanthin biosynthesis: a protective mechanism against oxidative stress in *Haematococcus pluvialis* (Chlorophyceae). *J. Plant Physiol.* 165, 1783–1797. doi: 10.1016/j.jplph.2007.12.007

Lorenz, R. T., and Cysewski, G. R. (2000). Commercial potential for Haematococcus microalgae as a natural source of astaxanthin. *Trends Biotechnol.* 18, 160–167. doi: 10.1016/s0167-7799(00)01433-5

Magnusson, L. U., Farewell, A., and Nystrom, T. (2005). ppGpp: a global regulator in *Escherichia coli*. *Trends Microbiol.* 13, 236–242. doi: 10.1016/j.tim.2005.03.008

Nanamiya, H., Kasai, K., Nozawa, A., Yun, C. S., Narisawa, T., Murakami, K., et al. (2008). Identification and functional analysis of novel (p) ppGpp synthetase genes in *Bacillus subtilis*. *Mol. microbiol.* 67, 291–304. doi: 10.1111/j.1365-2958.2007.06018.x

Nguyen, D., Joshidatar, A., Lepine, F., Bauerle, E., Olakanmi, O., Beer, K. D., et al. (2011). Active starvation responses mediate antibiotic tolerance in biofilms and nutrient-limited bacteria. *Science* 334, 982–986. doi: 10.1126/science.1211037

Ochi, K. (1987). Changes in nucleotide pools during sporulation of *Streptomyces griseus* in submerged culture. *Microbiol* 133, 2787–2795.

Ochi, K., and Ohsawa, S. (1984). Initiation of antibiotic production by the stringent response of *Bacillus subtilis* Marburg. *Microbiol* 130, 2473–2482. doi: 10.1099/00221287-130-10-2473

Ojha, A. K., Mukherjee, T. K., and Chatterji, D. (2000). High intracellular level of guanosine tetraphosphate in *Mycobacterium smegmatis* changes the morphology of the bacterium. *Infect. Immun.* 68, 4084–4091. doi: 10.1128/IAI.68.7.4084-4091.2000

Potrykus, K., and Cashel, M. (2008). (p)ppGpp: Still Magical ? *Annu. Rev. Microbiol.* 62, 35–51. doi: 10.1146/annurev.micro.62.081307.162903

Puszynska, A. M., and O'Shea, E. K. (2017). ppGpp controls global gene expression in light and in darkness in *S. elongatus*. *Cell Rep.* 21, 3155–3165. doi: 10.1016/j.celrep.2017.11.067

Sarada, R., Tripathi, U., and Ravishankar, G. A. (2002). Influence of stress on astaxanthin production in *Haematococcus pluvialis* grown under different culture conditions. *Proc. Biochem.* 37, 623–627.

Steinbrenner, J., and Linden, H. (2003). Light induction of carotenoid biosynthesis genes in the green alga *Haematococcus pluvialis*: regulation by photosynthetic redox control. *Plant Mol. Biol.* 52, 343–356. doi: 10.1023/a:1023948929665

Su, Y., Wang, J., Shi, M., Niu, X., Yu, X., Gao, L., et al. (2014). Metabolomic and network analysis of astaxanthin-producing *Haematococcus pluvialis* under various stress conditions. *Biores. Technol.* 170, 522–529. doi: 10.1016/j.biortech.2014.08.018

Sun, D., Lee, G., Lee, J. H., Kim, H. Y., Rhee, H., Park, S., et al. (2010). A metazoan ortholog of SpoT hydrolyzes ppGpp and functions in starvation responses. *Nat. Struct. Mol. Biol.* 17, 1188–1194. doi: 10.1038/nsmb.1906

Takahashi, K., Kasai, K., and Ochi, K. (2004). Identification of the bacterial alarmone guanosine 5′-diphosphate 3′-diphosphate (ppGpp) in plants. *P. Natl. Acad. Sci. USA* 101, 4320–4324. doi: 10.1073/pnas.0308555101

Tozawa, Y., Nozawa, A., Kanno, T., Narisawa, T., Masuda, S., Kasai, K., et al. (2007). Calcium-activated (p) ppGpp synthetase in chloroplasts of land plants. *J. Biol. Chem.* 282, 35536–35545. doi: 10.1074/jbc.M703820200

Traxler, M. F., Zacharia, V. M., Marquardt, S., Summers, S. M., Nguyen, H., Stark, S. E., et al. (2011). Discretely calibrated regulatory loops controlled by ppGpp partition gene induction across the 'feast to famine' gradient in *Escherichia coli*. *Mol. Microbiol.* 79, 830–845. doi: 10.1111/j.1365-2958.2010.07498.x

Van Delden, C., Comte, R., and Bally, M. (2001). Stringent response activates quorum sensing and modulates cell density-dependent gene expression in *Pseudomonas aeruginosa*. *J. Bacteriol.* 183, 5376–5384. doi: 10.1128/JB.183.18.5376-5384.2001

Vidhyavathi, R., Venkatachalam, L., Sarada, R., and Ravishankar, G. A. (2008). Regulation of carotenoid biosynthetic genes expression and carotenoid accumulation in the green alga *Haematococcus pluvialis* under nutrient stress conditions. *J. Exp. Bot.* 59, 1409–1418. doi: 10.1093/jxb/ern048

Wells, D. H., and Gaynor, E. C. (2006). *Helicobacter pylori* Initiates the Stringent Response upon Nutrient and pH Downshift. *J. Bacteriol.* 188, 3726–3729. doi: 10.1128/JB.188.10.3726-3729.2006

Xiao, H., Kalman, M., Ikehara, K., Zemel, S., Glaser, G., and Cashel, M. (1991). Residual guanosine 3′, 5′ -bispyrophosphate synthetic activity of relA null mutants can be eliminated by spoT null mutations. *J. Biol. Chem.* 266, 5980–5990.

Zhang, C., Liu, J., and Zhang, L. (2017). Cell cycles and proliferation patterns in *Haematococcus pluvialis*. *Chin. J. Oceanol. Limn.* 35, 1205–1211.

Conflict of Interest: The authors declare that the research was conducted in the absence of any commercial or financial relationships that could be construed as a potential conflict of interest.

Publisher's Note: All claims expressed in this article are solely those of the authors and do not necessarily represent those of their affiliated organizations, or those of the publisher, the editors and the reviewers. Any product that may be evaluated in this article, or claim that may be made by its manufacturer, is not guaranteed or endorsed by the publisher.

Copyright © 2022 Jin, Lao, Zhou and Cai. This is an open-access article distributed under the terms of the Creative Commons Attribution License (CC BY). The use, distribution or reproduction in other forums is permitted, provided the original author(s) and the copyright owner(s) are credited and that the original publication in this journal is cited, in accordance with accepted academic practice. No use, distribution or reproduction is permitted which does not comply with these terms.

frontiers in Plant Science

ORIGINAL RESEARCH
published: 29 March 2022
doi: 10.3389/fpls.2022.835414

Metabolic and Physiological Changes in the Roots of Two Oat Cultivars in Response to Complex Saline-Alkali Stress

*Yugang Gao, Yongling Jin, Wei Guo, Yingwen Xue and Lihe Yu**

Heilongjiang Bayi Agricultural University, Daqing, China

Saline-alkali stress is a major abiotic stress factor in agricultural productivity. Oat (*Avena sativa* L.) is a saline-alkali tolerant crop species. However, molecular mechanisms of saline-alkali tolerance in oats remain unclear. To understand the physiological and molecular mechanisms underlying seedling saline-alkali tolerance in oats, the phenotypic and metabolic responses of two oat cultivars, Baiyan7 (BY, tolerant cultivar) and Yizhangyan4 (YZY, sensitive cultivar), were characterized under saline-alkali stress conditions. Compared with YZY, BY showed better adaptability to saline-alkali stress. A total of 151 and 96 differential metabolites induced by saline-alkali stress were identified in roots of BY and YZY, respectively. More detailed analyses indicated that enhancements of energy metabolism and accumulations of organic acids were the active strategies of oat roots, in response to complex saline-alkali stress. The BY utilized sugars *via* sugar consumption more effectively, while amino acids strengthened metabolism and upregulated lignin and might be the positive responses of BY roots to saline-alkali stress, which led to a higher osmotic adjustment of solute concentrations and cell growth. The YZY mainly used soluble sugars and flavonoids combined with sugars to form glycosides, as osmotic regulatory substances or antioxidant substances, to cope with saline-alkali stress. The analyses of different metabolites of roots of tolerant and sensitive cultivars provided an important theoretical basis for understanding the mechanisms of saline-alkali tolerance and increased our knowledge of plant metabolism regulation under stress. Meanwhile, some related metabolites, such as proline, betaine, and *p*-coumaryl alcohol, can also be used as candidates for screening saline-alkali tolerant oat cultivars.

Keywords: growth, metabolites, oat, saline-alkali stress, root

OPEN ACCESS

Edited by:
Girdhar Kumar Pandey, University of Delhi, India

Reviewed by:
Suprasanna Penna, Bhabha Atomic Research Centre (BARC), India
Radwan Khalil, Benha University, Egypt
Kundan Kumar, Birla Institute of Technology and Science, India

****Correspondence:***
Lihe Yu
yulihe2002@126.com

Specialty section:
This article was submitted to Plant Physiology, a section of the journal Frontiers in Plant Science

Received: *14 December 2021*
Accepted: *28 February 2022*
Published: *29 March 2022*

Citation:
Gao Y, Jin Y, Guo W, Xue Y and Yu L (2022) Metabolic and Physiological Changes in the Roots of Two Oat Cultivars in Response to Complex Saline-Alkali Stress. Front. Plant Sci. 13:835414. doi: 10.3389/fpls.2022.835414

INTRODUCTION

Oats (*Avena sativa* L.) is an important economic crop used for multiple purposes, such as in food, forage, and medicine. Because of its wide range of ecological adaptability, oats have become an irreplaceable grain and feed crop in ecologically fragile areas (Łabanowska et al., 2016), and have been widely used as an alternative crop for saline-alkali soil amelioration (Fu et al., 2011; Han et al., 2012).

Soil saline-alkalization is a worldwide environmental and ecological problem. The total area of saline-alkali soils in the world exceeds 10×10^8 ha, and 10% of the total arable land is being affected by salinity (Shahid et al., 2018). In northeastern China, the Songnen Plain accounts for 3.73×10^6 ha (accounting for 21% of the total area) and is one of the three typical soda saline-alkali soil distribution areas; in this area, soil salinization is mainly caused by sodium-carbonate (i.e., Na_2CO_3 and $NaHCO_3$), which leads to increases in the pH of the soil to pH 10 in most areas (Yin et al., 2017; Fang et al., 2021). In addition, global warming, improper soil water-crop management, and pollution have led to constantly expanding areas undergoing salinization. According to the Food and Agricultural Organization, a manifested salinity is projected to affect 50% of global agricultural land by 2050 (Butcher et al., 2016). As two coexisting abiotic stresses, salt and alkali stress have severely restricted the development of global agriculture and food security (Bartels and Sunkar, 2005; Fang et al., 2021). Therefore, saline-alkalization is a major limiting factor for sustainable agricultural development and food security in the world. To solve this dilemma, developing and planting crop cultivars with high saline-alkali tolerance may be the most efficient approach.

The stress effects of soil saline-alkalization on plants include the effects of both salt stress and alkali stress. Salt stress, which results mainly from NaCl, Na_2SO_4, and other neutral salts, induces osmotic stress and ion injury by disrupting ion homeostasis and ion balance in plant cells (Fang et al., 2021; Wang et al., 2021). In addition, the superposition of osmotic stress and ionic stress can lead to secondary oxidative stress (Munns and Tester, 2008). The damage to plants caused by mixed salt-alkali stress is more serious (Rao et al., 2013), which is due to further increases in the pH during salt stress; a high pH, therefore, severely disturbs cell pH stability and destroys cell membrane integrity (Fang et al., 2021). It is well known that soil salinization and alkalization usually coexist. However, most studies have focused mainly on single salt stress (salt tress or alkali stress), and little attention has been given to combined saline-alkali stress.

Saline-alkali stress alters the physiological, biochemical, and molecular processes of plants (El-Esawi et al., 2019). Metabolomics studies can reflect the biological and physiological processes in response to stressful conditions at the cellular and molecular levels by monitoring the changes in metabolite levels and fluxes (Tinte et al., 2021). Therefore, metabolomics has become essential in studying the changes of metabolic pathways and tolerance mechanisms under environmental stress (Shao et al., 2011). Recent studies have shown that salinity induces several physiological processes, such as the osmotic and antioxidant adjustment defense mechanisms. To cope with osmotic stress, plants synthesize and accumulate compatible osmolytes, including organic acids, proline, betaine, *N*-containing compounds, sugars, straight-chain polyhydric polyols, and cyclic polyhydric alcohols (Yang et al., 2007; Zhao et al., 2013; Liu et al., 2015; Shen et al., 2018; Sun et al., 2019), to maintain cell turgor and osmotic potential. In oats (Liu et al., 2016), the salinity tolerance was associated with higher content of proline and soluble proteins. To cope with oxidative stress, the plant has two enzymatic and non-enzymatic active oxygen scavenging systems to avoid injury, which metabolizes reactive oxygen species (ROS) and their reaction products to avert oxidative stress conditions (Gill and Tuteja, 2010). Antioxidant enzymes mainly include superoxide dismutase (SOD), catalase (CAT), guaiacol peroxidase (GP), ascorbate peroxidase (APX), and glutathione reductase (GR) (Liu et al., 2020). Non-enzymatic antioxidants such as ascorbic acid, cysteine, carotenoids, alkaloids, α-tocopherol, flavonoids, and reduced glutathione can effectively help resist the damage caused by stress (Luo et al., 2009). Organic acids play an important role in maintaining the cell pH and ion balance (Fang et al., 2021). To cope with high pH, the accumulations of organic acids such as citrate, formate, lactate, acetate, succinate, malate, and oxalate, were observed in tomatoes (Wang et al., 2011), in *Chloris virgata* (Yang et al., 2010), and in grapevines (Xiang et al., 2019). Organic acids are synthesized to compensate for the deficiency of inorganic anions during saline-alkali stress, especially under alkaline stress (Guo et al., 2018), and they also play a role in osmotic regulation (Wang et al., 2021).

Oat crops are considered to be moderately tolerant to salinity and alkalinity, and some oat cultivars can grow in soil with pH values as high as 9 (Bai et al., 2018). However, the growth and physiological activities of oat plants are also affected by saline-alkali stress like other gramineous crops; the oat yield decreased by about 70% under 0.6% soil salinity (Zhao et al., 2013). Saline-alkali stress is therefore still an important limiting factor for the growth, development, yield, and quality of oats (Sun et al., 2010). Previous studies on salt or saltine-alkali tolerance of oats have focused on germplasm resource screening, and physiological and biochemical responses to saline-alkali stress (Zhang et al., 2011; Luo et al., 2012; Fu et al., 2018; Hou et al., 2018; Li et al., 2018; Zhang et al., 2018). To the best of our knowledge, the molecular mechanism for *A. sativa* L. saline-alkali tolerance remains largely unknown. An improved understanding of root metabolomics responses to saline-alkali treatment is, therefore, necessary to improve crop tolerance to this type of stress.

In this study, we described the metabolomics of BY and YZY seedling roots under complex saline-alkali stress using ultra-performance liquid chromatography–mass spectrometry (UPLC-MS/MS) analyses. The goals of this study were to (1) investigate the differences in growth and root metabolomics of oats under complex saline-alkali stress and (2) determine the differences in the saline-alkali tolerance mechanisms among tolerant and sensitive cultivars. This was a supplement to research on the mechanism of plant's saline-alkali tolerance and provided theoretical support for the innovation of saline-alkali tolerant germplasm resources.

MATERIALS AND METHODS

Preparation of Saline-Alkali Solutions

To simulate the saline-alkali composition and content of the soil in the central and western regions of Heilongjiang Province (Yin et al., 2017), which is one of the main oat producing areas in China, two neutral salts and two alkaline salts were mixed in a

2:1:2:1 molar ratio ($NaHCO_3$: Na_2CO_3: NaCl: Na_2SO_4), resulting in total ion concentrations of Na^+, Cl^-, HCO_3^-, CO_3^{2-}, and SO_4^{2-} of 150, 37.5, 37.5, 18.75, and 18.75 mM, respectively, with a pH of 9.8. The test design was conducted according to the method of Shi and Wang (2004), with appropriate adjustments.

Plant Materials and Cultivation Conditions

The seeds of two oat cultivars of BY and YZY were obtained from the oat Research Laboratory of Heilongjiang Bayi Agricultural University. The oat seeds were sand cultured in a rectangular plastic culture bowl (10 cm × 10 cm) under a 25/20°C (day/night), photoperiod 12/12 h (day/night), and 70% relative humidity. Hoagland nutrient solution (20 mL $bowl^{-1}$) was irrigated and replaced every 2 days until the first leaf of the seedlings emerged (i.e., tillering stage). Then, the control seedlings were irrigated with 20 mL of distilled water (0 mM Na^+, pH 6.8), instead of Hoagland nutrient solution, and the treatment seedlings were irrigated with 20 mL of saline-alkali mixed solution (150 mM Na^+, pH 9.8) instead of Hoagland nutrient solution. Each treatment contained three replicates. After 12 days of saline-alkali stress treatment, a total of 120 mL of saline-alkali solution was used for irrigation, then, the oat seedlings were ready for analysis.

Growth Performance and Physiological Indicators

Cultured seedlings were removed and rinsed, then, the plant height, root length, and accumulation of dry matter in the shoots and its root tissues were measured, and each measurement was conducted on 10 plants and was repeated three times. The soluble protein content was determined using the Bradford method, the soluble sugar content was determined using the anthrone colorimetric method, the proline content was determined using the acidic ninhydrin colorimetry method (Gao, 2006), and the content of betaine was determined using Reinecke's salt colorimetric method (Wang, 2006). The malondialdehyde (MDA) content was determined using the thiobarbituric acid method, the hydrogen peroxide (H_2O_2) content was determined using the titanium sulfate method, and the $O_2^{\cdot-}$ content was determined using the hydroxylamine method (Gao, 2006). The SOD activity was determined using nitro blue tetrazolium photoreduction, peroxidase (POD) activity was determined using guaiacol colorimetry, CAT activity was determined using the hydrogen peroxide method, and APX was determined according to the principle that H_2O_2 reduces the content of ascorbic acid (Zhang and Qu, 2003).

Metabolites of Oat Root Extracts

Sampling Methods

The oat seedlings were rinsed 2–3 times with phosphate-buffered saline (PBS) buffer (pH 7, 1 mol L^-), and the oat roots were then transferred to a cryotube, frozen with liquid nitrogen, and stored at −80°C for further metabolomics analyses. Three biological replicates were performed per treatment. The BY and YZY were labeled as CKby and CKyzy, and XPby and XPyzy for the control and salt-alkali treatments, respectively.

Sample Preparation

The freeze-dried oat root sample was crushed by using a grinder (MM400; Retsch, Germany) for 1.5 min at 30 Hz. Then, 100 mg of powder was weighed and extracted overnight in a refrigerator at 4°C with 1 mL of extract solution (methanol: water = 7: 3). The sample was vortexed three times during this period to increase the extraction efficiency. After centrifugation at 10,000 rpm for 10 min, the supernatant was collected, filtered with a microporous filter (0.22 μm), and stored in the injection bottle for further LC–MS/MS analysis. The quality control sample was prepared by mixing equal amounts of the four groups of oat root extracts from different treatments. One quality control sample, which was prepared by mixing an equal aliquot of the supernatants from all samples, was used and replicated three times to examine the repeatability of the entire analysis process.

LC–MS/MS Analysis

The ultra-performance liquid chromatography (UPLC) separation was conducted using a Shim-pack UFLC CBM30A System (Shimadzu, Kyoto, Japan), equipped with a UPLC HSS T3 C18 (1.8 μm, 2.1 mm × 100 mm; Waters, Milford, MA, United States). The mobile phase was composed of ultrapure water (with 0.04% acetic acid) and acetonitrile (with 0.04% acetic acid). An elution gradient with a water/acetonitrile ratio of 95:5 (v/v) at 0 min, 5:95 (v/v) at 11 min, 5:95 (v/v) at 12 min, 95:5 (v/v) 12.1 min, and 95:5 (v/v) at 15 min was performed. The flow rate was set to 0.4 mL min^{-1}, with a column temperature at 40°C and injection volume at 2 μl.

The Biosystems 6500 QTRAP was used to acquire MS/MS spectra of the metabolites. After the sample was chromatographically separated, it was subjected to MS for analysis, and the eluent was alternately connected to electrospray ionization (ESI)-triple quadrupole (QQQ). The MS conditions for a multiple reaction monitoring (MRM) test was set as follows: the electrospray ion source temperature 500°C, the ion spray voltage as 5500 or −4500 V in the positive or negative modes, respectively; the gas I as 55 psi gas II as 60 psi, the curtain gas as 25 psi, and the collision-activated dissociation as high. The QQQ scans were acquired as MRM experiments with the collision gas (nitrogen) set to 5 psi, and each ion pair was scanned according to the optimized declustering potential (DP) and collision energy (CE; Chen et al., 2013). The Analyst 1.6.3 software (AB Sciex, Waltham, MA, United States) was used to continuously evaluate the full scan survey of MS/MS data, as it was collected and triggered the acquisition of MS/MS spectra (**Supplementary Figure 1**).

Data Processing and Analysis

Qualitative and Quantitative of Metabolites

Metabolite identification was conducted based on the metabolite information MWDB (Metware Database built by BioMarker) and public databases, such as MassBank, KNAPSAcK, HMDB, and METLIN. A quantitative analysis of metabolites used MRM with QQQ mass spectrometry. Data were processed using

Analyst 1.6.3 software, and peak areas were integrated and corrected by the MultiaQuant software (Fraga et al., 2010; **Supplementary Figure 1**).

Data Preprocessing and Annotation

Metabolite data were $\log_{10}$-transformed for statistical analysis to improve the normality and were normalized. Unsupervised pattern recognition principal component analysis (PCA) on normalized data was performed using the R software, version 3.1.1. The supervised pattern recognition orthogonal partial least squares discriminant analysis (OPLS-DA) was tested for all samples, and the R (3.3.2) package *ropls* was adopted to analyze the differences between the samples and to identify differential metabolites. The OPLS-DA model was used with variable importance in the projection (VIP) values (VIP > 1) combined with FC (fold change) of metabolites values (FC > 2) to identify differential metabolites. The Kyoto Encyclopedia of Genes and Genomes (KEGG) database was used to perform functional annotations on differential metabolites. Based on the annotation results, a KEGG pathway enrichment analysis was performed.

Statistical Data Analysis

The effects of different concentrations of saline-alkali stress on the physiological parameters of roots were analyzed by one-way ANOVA with the Duncan's method for multiple comparisons at significance levels of $P \leq 0.05$ and 0.01. All statistical analyses of experimental data were performed using the SPSS software v.20.0 (SPSS, Chicago, IL, United States).

RESULTS

The Growth Phenotype Assay

Saline-alkali stress lasting for 12 days caused a decrease in plant heights by 5.68% (BY) and 7.57% (YZY), as compared to the respective controls; but there was no significant difference among cultivars under the same treatment (**Figure 1A**). For YZY, saline-alkali stress induced a significant decrease in the biomass of shoots and roots by 14.20 and 13.16%, respectively, in the stressed group when compared with its respective controls. For BY, saline-alkali stress did not induce a significant change in the biomass of shoots and resulted in a significant increase of root dry weight by 26.67% (**Figures 1B,C**). Under saline-alkali stress, shoots dry weight, root dry weight, and the ratio of roots to shoots in YZY decreased significantly by 26.77, 42.11, and 20.83%, respectively, compared to BY (**Figures 1B–D**).

The plant height of the two oat cultivars was significantly decreased ($P < 0.01$) after saline-alkali stress, but there was no significant difference among cultivars under the same treatment (**Figure 1A**). For BY, saline-alkali stress did not significantly reduce the biomass of shoots and roots, but it instead induced a significant increase ($P < 0.01$) in root's dry weight and the ratio of roots to shoots ratio ($P < 0.01$; **Figures 1B–D**). However, the saline-alkali stress resulted in a significant decrease ($P < 0.05$) in above-ground and below-ground biomasses in YZY (**Figures 1B,C**). These results showed that there were differences in growth phenotypes among cultivars after saline-alkali stress. At the same time, the chlorophyll content in leaves decreased during saline-alkali stress ($P < 0.01$; **Figure 1E**).

Reactive Oxygen Species and Malondialdehyde Accumulation

Under saline-alkali stress, distinct growth phenotype differences suggested that oat root cells were likely to face a serious threat. To verify this hypothesis, related physiological and biochemical analyses were conducted.

The significantly higher ROS content, which was induced by saline-alkali stress, was observed in the roots of both cultivars. The H_2O_2 concentration (0.69 μmol g^{-1} FW) in the treated roots of BY was the highest, which was significantly higher than that of YZY roots (**Figure 2A**). The roots of YZY had the highest $O_2^{\cdot-}$ concentration (8.14 μmol g^{-1} FW), which was significantly higher than that of BY roots (**Figure 2B**). Compared with the control, increases in H_2O_2 and $O_2^{\cdot-}$ were the largest in YZY roots, which was significantly increased by 111.54 and 282.16%, respectively. The MDA, which reflects cell membrane damage, increased significantly by 27.27 and 71.99% in BY and YZY roots, respectively. There was no significant difference in the content of MDA in roots between the two cultivars after treatment (**Figure 2C**).

Antioxidant Enzyme Activities of Oat Seedlings Roots

Saline-alkali stress-induced changes in the antioxidant enzyme activities of oat roots. After saline-alkali stress, the activity of SOD in YZY roots increased significantly by 54.15% ($P < 0.01$; **Figure 3A**); the activities of POD and APX in BY roots were significantly increased by 77.70 and 68.58% compared to control, respectively ($P < 0.01$; **Figures 3B,D**). The activity of CAT in the roots of both cultivars decreased significantly ($P < 0.01$; **Figure 3C**). Under saline-alkali stress, the activities of POD and CAT in BY roots were significantly higher than those in YZY roots; however, the APX activity was significantly lower than that of YZY root.

Osmo-Regulated Substance Changes of Oat Seedling Roots

The main osmoregulation substances such as proline, betaine, soluble sugar, and soluble protein were significantly affected by saline-alkali stress. The results showed that the contents of proline, soluble protein, and soluble sugar in the roots of both cultivars were significantly higher than those of the control ($P < 0.05$). Moreover, the content of betaine was significantly increased in BY roots ($P < 0.01$); but there was no significant change in YZY roots (**Figure 4**). After saline-alkali stress, the contents of proline, betaine, and soluble protein but not soluble sugar in the roots of BY, were significantly higher than those in the roots of YZY ($P < 0.05$), which increased by 55.88, 48.55, and 34.94%, respectively (**Figures 4A–C**). The soluble sugar content in the roots of BY was significantly increased by saline-alkali stress, but it was significantly lower than that of YZY after stress (**Figure 4D**).

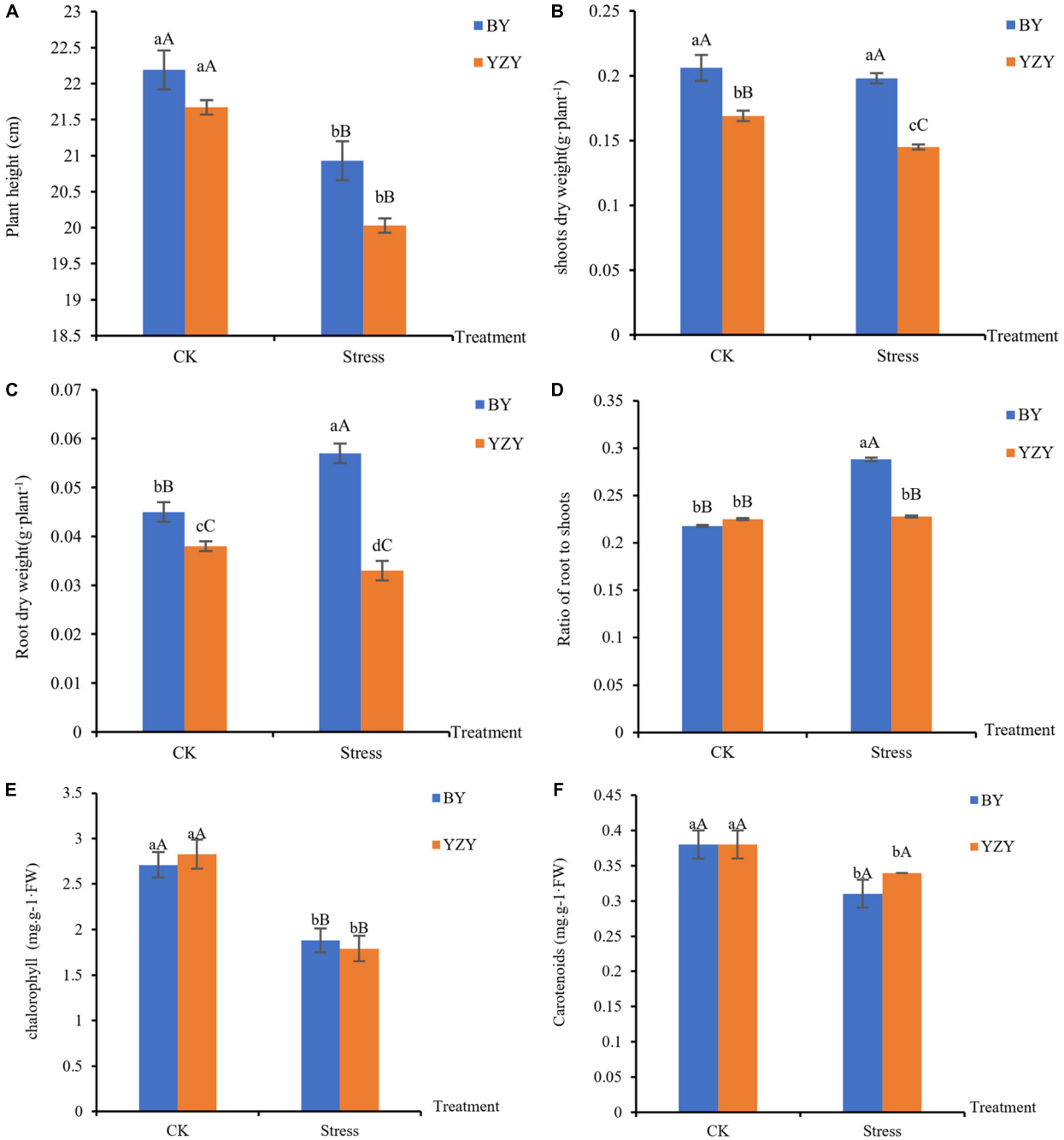

FIGURE 1 | Oat seedlings growth phenotypes of Baiyan7 (BY) and Yizhangyan4 (YZY) during saline-alkali stress. **(A)** Plant height (cm), **(B)** shoots dry weight (g plant^{-1}), **(C)** root dry weight (g plant^{-1}), **(D)** ratio of root weight to shoot weight, **(E)** chlorophyll content in the leaves (mg·g^{-1}·FW), and **(F)** carotenoids content in the leaves (mg·g^{-1}·FW). Different lowercase letters indicate significant differences among the treatments ($P < 0.05$) and different capital letters indicate significant differences ($P < 0.01$).

Principal Component Analysis of Oat Root Metabolites Under Saline-Alkali Stress

The results of the analysis of main osmoregulation substances showed that there were significant differences in osmotic adjustment responses to saline-alkali stress between the two cultivars. To further validate these results, a metabonomic analysis was conducted.

The chromatograms of oat seedling roots were obtained using LC–MS/MS analysis (**Supplementary Figure 1**). There were significant differences between the peaks. The score plots of PCA results (**Figure 5**) showed that the control and treatment clusters

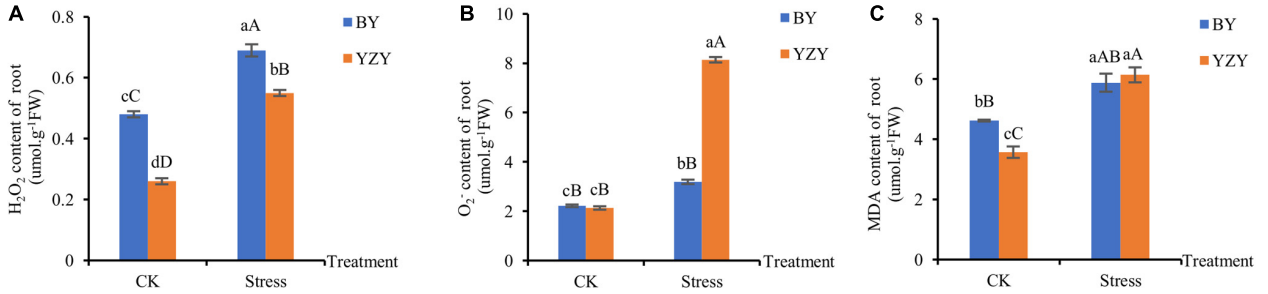

FIGURE 2 | Accumulation of H_2O_2, O_2^-, and malondialdehyde (MDA) in roots under saline-alkali stress. **(A)** H_2O_2, **(B)** O_2^-, and **(C)** MDA contents in roots under control and saline-alkali stress. FW, fresh weight.

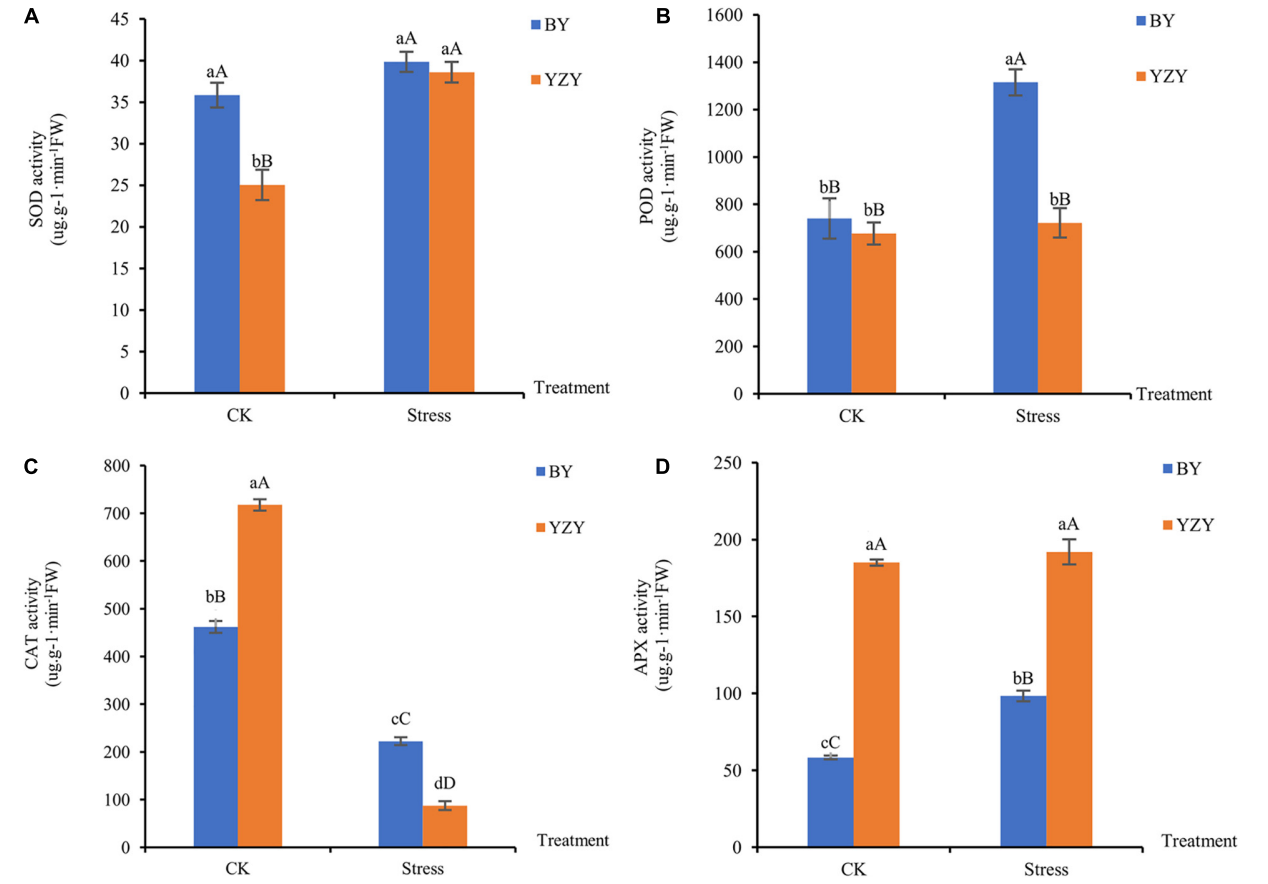

FIGURE 3 | Antioxidant enzyme activity of oat seedling roots during CK and saline-alkali stress conditions. **(A)** Activity of superoxide dismutase, **(B)** activity of peroxidase, **(C)** activity of catalase, and **(D)** activity of ascorbate peroxidase. FW, fresh weight; DW, dry weight.

were separated by the first principal (PC1), which accounted for 21.64% of the total variance, and the BY and YZY clusters were separated by the second principal (PC2), which accounted for 16.53% of the total variance. The separation performance of PCA analysis was not obvious. Given the complexity of the data, OPLS-DA was performed to accurately analyze the differences between the samples within each group (**Figure 6**). The score plots of the OPLS-DA results showed clear separations, and the Q2, which represented the model predictability, was greater than 0.5, indicating the effectiveness of the model. These results indicated that the samples within each group were significantly different in their metabolic levels, and the differential metabolites could be screened according to their VIP values.

Differential Metabolite Analysis

In BY and YZY roots, 752 metabolites were identified by LC–MS/MS. According to the OPLS-DA model, metabolites with VIP > 1 and FC > 2 were determined as differentially abundant

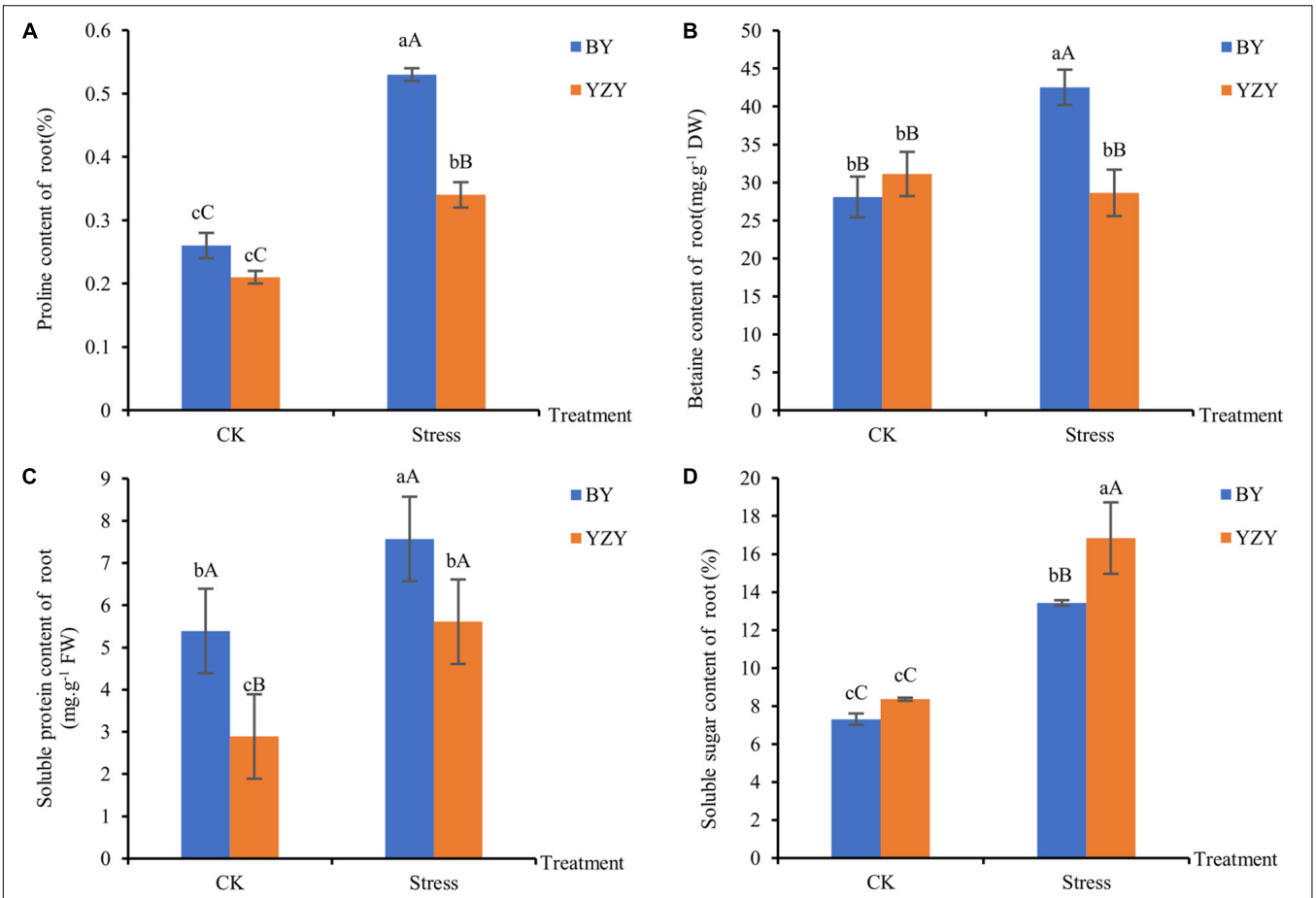

FIGURE 4 | Osmoregulation substances of oat seedling roots under CK and saline-alkali stress conditions. **(A)** Proline content of BY and YZY roots under saline-alkali stress treatment and CK conditions. **(B)** Betaine content, **(C)** soluble protein content, and **(D)** soluble sugar content. FW, fresh weight; DW, dry weight.

metabolites (DAMs). After saline-alkali stress, there were 42 upregulated DAMs and 109 downregulated DAMs in BY roots, and 56 upregulated DAMs and 40 DAMs in YZY roots (**Table 1** and **Supplementary Table 1**); while there were only 20 common DAMs, including 3 upregulated DAMs and 17 downregulated DAMs in groups G_1 and G_2 (**Figures 7A,B**). Compared with YZY, there were 86 upregulated DAMs and 71 downregulated DAMs in BY roots before treatment; and 54 upregulated DAMs and 88 downregulated DAMs in BY roots during stress (**Table 1** and **Supplementary Table 1**); there were only 54 common DAMs, including 24 upregulated DAMs and 30 downregulated DAMs in G_3 and G_4 (**Figures 7C,D**), which indicated that saline-alkali stress led to changes in metabolites and that there were differences in metabolic profiles between cultivars. We then focused on differential metabolites induced by saline-alkali stress in G1 (CkBY-vs-XpBY) and G2 (CkYZY-vs-XpYZY).

Difference significance analysis was conducted for DAMs induced by saline-alkali stress. Compared with the control, the significantly ($P < 0.05$) up-accumulated DAMs in BY roots were mainly amino acids and amino acid derivatives, phenylpropanoid compounds, including betaine (14.27-fold), 3-*O*-acetyl pinobanksin (11.00-fold), 1-*O*-feruloyl quinate (1.80-fold), *N*-acetyl-L-arginine (1.45-fold), L-cysteine (1.30-fold), proline (1.24-fold), *p*-coumaryl alcohol (1.29-fold), 3-methyl-1-pentanol (1.14-fold), pantothenol (1.12-fold), and 8-methoxy psoralen (1.09-fold). In contrast, the significantly ($P < 0.05$) up-accumulated DAMs in YZY roots were mainly organic acids, phenylpropanoid, and flavonoid compounds, including kaempferol 3-*O*-glucoside (2.80-fold), kaempferol 3-*O*-galactoside (2.34-fold), citric acid monohydrate (1.44-fold), *N*-feruloyl putrescine (1.36-fold), pantothenol (1.26-fold), citric acid (1.19-fold), 1-*O*-beta-D-glucopyranosyl sinapate (1.11-fold), and *cis*-aconitic acid (1.08-fold). Some lipids, phenylpropanoids, flavonoids, and other compounds were significantly ($P < 0.05$) down-accumulated metabolites, but there were differences in compound types and downregulation levels in the two cultivars (**Table 2**).

For BY roots, there were 42 upregulated DAMs and 109 downregulated DAMs in the saline-alkali stress-exposed samples, when compared to the control. A total of 151 DAMs included 5 sugars (such as trehalose 6-P, *N*-acetylglucosamine 1-P, and phytocassane, etc.), 35 organic acids and derivatives (such as fumaric acid, caffeic acid, cinnamate, and *trans*-cinnamate, etc.), 12 amino acids and derivatives (such as proline,

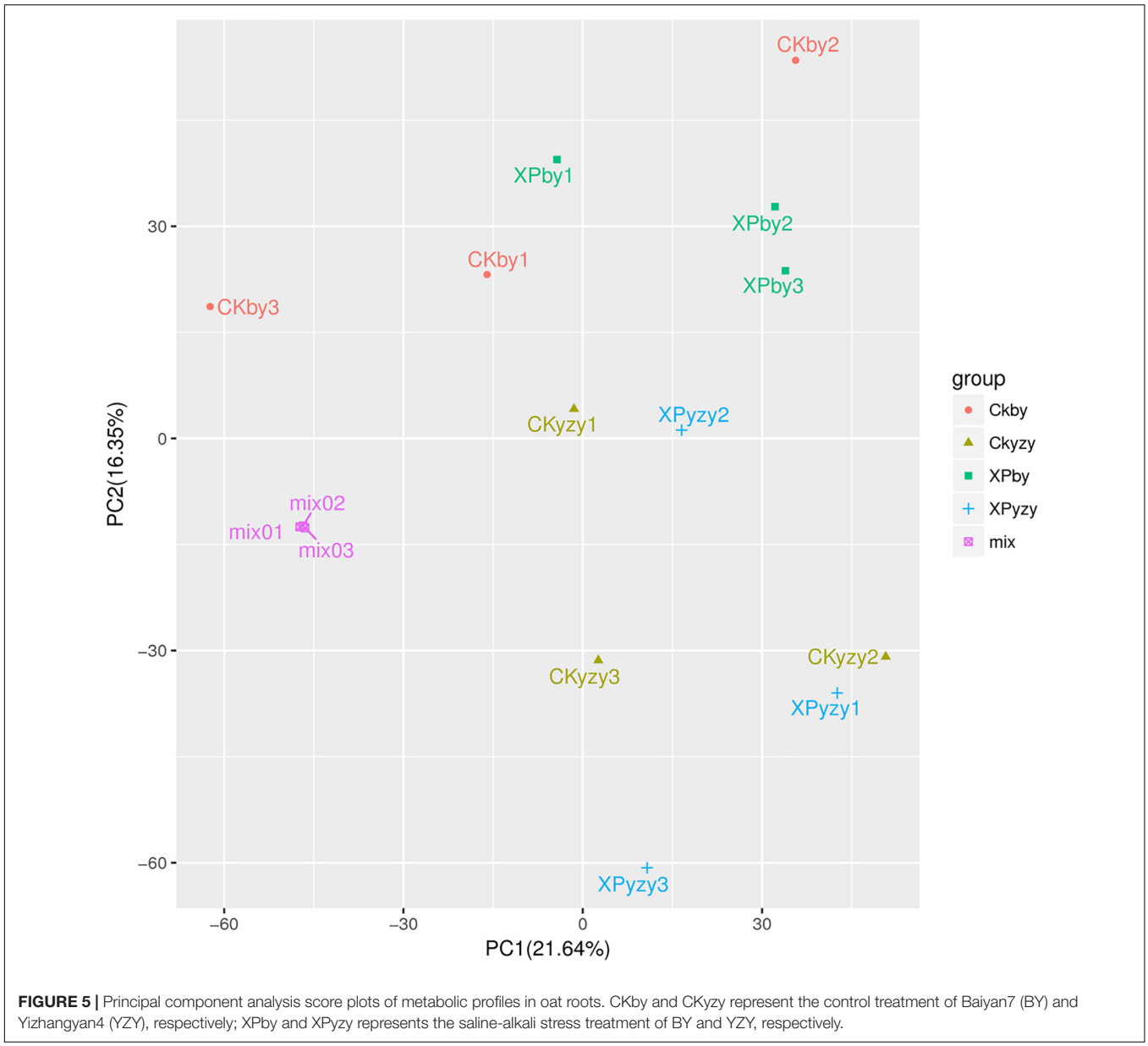

FIGURE 5 | Principal component analysis score plots of metabolic profiles in oat roots. CKby and CKyzy represent the control treatment of Baiyan7 (BY) and Yizhangyan4 (YZY), respectively; XPby and XPyzy represents the saline-alkali stress treatment of BY and YZY, respectively.

cysteine, and methionine, etc.), 33 lipids [most of which were monoacylglycerol (MAG) and its isomer, lysoPC and its isomer, and scope and its isomer, etc.], 11 phenylpropanoids (including 4 monolignols and 7 coumarins, etc.), 14 flavonoids (such as taxifolin, glabridin, 3-*O*-acetyl pinobanksin, and luteolin, etc.), 24 glycosides (most of them were formed by flavonoids and sugars; most of which were downregulated), 5 vitamins and cofactors (such as α-tocotrienol, pantothenol, and thiamine, etc.), 6 alkaloids, 2 peptides, 6-gingerol, phytol, and 4-hydroxy benzaldehyde (**Table 1** and **Supplementary Table 1**). Among them, the DAMs with larger multiples mainly included fumaric acid (16.38-fold), betaine (14.27-fold), rosmarinic acid (13.24-fold), L-isoleucine (12.98-fold), imperatorin (−13.92-fold), and α-tocotrienol (−12.20-fold) (**Figure 7**). The significantly ($P < 0.05$) increased DAMs were mainly amino acids and their derivatives, phenylpropanoid compounds, including betaine, 3-*O*-acetyl pinobanksin, 1-*O*-feruloyl quinate, *N*-acetyl-L-arginine, cysteine, proline, *p*-coumaryl alcohol, 3-methyl-1-pentanol pantothenol, and 8-methoxypsoralen. The significantly ($P < 0.05$) decreased DAMs were mainly lipids and organic acids (**Table 2**).

Compared to the control, there were 56 upregulated DAMs and 40 downregulated DAMs induced by saline-alkali stress in YZY roots. A total of 151 DAMs included 8 sugars (including upregulated maltotetraose, galactinol, mannitol, melezitose, panose, and downregulated sucrose and deoxyribose 5-P), 24 organic acids and derivatives (such as citric acid, *cis*-aconitic acid, citramalate, ureidoisobutyric acid, deoxycytidine, 2′-deoxyinosine, and *trans*-citridic acid), 4 amino acids and derivatives, 12 lipids, three phenylpropanoids, 10 flavonoids

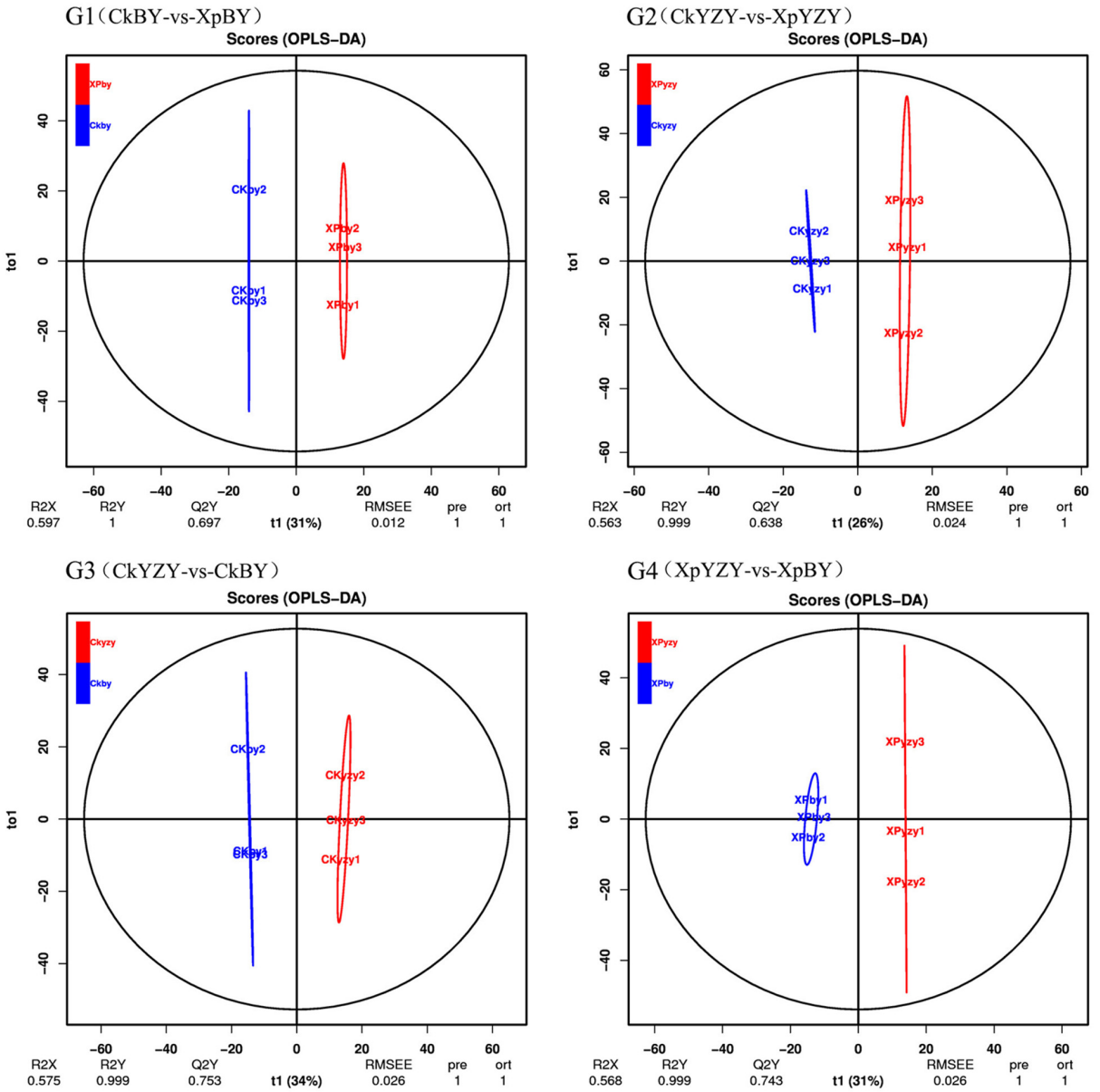

FIGURE 6 | The orthogonal partial least squares discriminant analysis model score plot of metabolic profiles in oat roots.

(such as liquiritigenin, tangeretin, tricin, and catechin), 19 glycosides (most of them were formed by flavonoids and sugar, and most of which were upregulated), two vitamins and cofactors (the reduced form of glutathione and pantothenol), 6 alkaloids, 3 peptides (*N*′-*p*-coumaroyl putrescine, *N*-*p*-coumaroyl putrescine, and *N*-feruloyl putrescine), 6-gingerol, gallic acid, ginkgolide A, and chlorpyrifos (**Table 1** and **Supplementary Table 1**). Among them, the more complex DAMs included *C*-hexosyl-chrysoeriol *O*-hexoside (15.5-fold), D (+)-melezitose *O*-rhamnoside (10.21-fold), maltotetraose (4.08-fold), melezitose (3.20-fold), gallic acid (−13.94-fold), deoxyribose 5-P (−11.67-fold), spinosin (−11.19-fold), rosmarinic acid (9.68-fold), and catechin (−2.86-fold) (**Figure 7**). The significantly ($P < 0.05$) increased DAMs included two metabolites related to the TCA cycle (citric acid and *cis*-aconitic acid), three glycosides, pantothenol, *N*-feruloyl putrescine, and citric acid monohydrate, and the decreased DAMs included gallic acid, spinosyn, ureidoisobutyric acid, and dimethylglycine (**Table 2**).

Functional Annotation and Enrichment Analysis of Differentially Abundant Metabolites in the Kyoto Encyclopedia of Genes and Genomes

The results of metabolic pathway annotation analyses identified 36 DAMs from BY and 26 DAMs from YZY of the corresponding metabolic pathways (**Table 1**). In BY roots, DAMs showing significantly increased accumulation levels under saline-alkali

TABLE 1 | Differential metabolites between different treatment groups of oat roots.

Group name	Differential metabolite	Down	Up	Differential metabolite in pathway
G1 (CkBY-vs-XpBY)	151	109	42	36
G2 (CkYZY-vs-XpYZY)	96	40	56	26
G3 (CkYZY-vs-CkBY)	157	71	86	46
G4 (XpYZY-vs-XpBY)	142	88	54	43

stress were mainly concentrated in amino acids and their derivatives (such as proline, *N*-acetyl-L-arginine, and L-cysteine) in the biosynthesis of amino acids pathway, in the serine and threonine metabolism pathway, and phenylpropanoids and their derivatives (such as *p*-coumaryl alcohol and 1-*O*-feruloyl quinate) in the phenylpropanoid biosynthesis pathway. The DAMs, showing significantly reduced accumulation levels under saline-alkali stress, were mainly concentrated in lipids and their derivatives [such as MAG, monogalactosyl diacylglycerol (DGMG), lysoPE, and lysoPC] in the glycerolipid metabolism pathway and the lipid metabolism pathway, phenylpropanoids and their derivatives in the phenylpropanoid biosynthesis pathway (such as 4-methoxy cinnamic acid, osthenol, caffeic acid, methyl *p*-coumarate, *trans*-4-hydroxycinnamic acid methyl ester, 3,4-dimethoxycinnamic acid, ethyl ferulate, and 1-*O*-caffeoyl quinate imperatorin), and flavonoid compounds (dihydroquercetin and glabridin) (**Table 2** and **Figure 9**). In YZY roots, significantly upregulated DAMs found under saline-alkali stress were mainly concentrated in the TCA cycle and its intermediate metabolites (such as citric acid, citric acid monohydrate, and *cis*-aconitic acid), and flavonol compounds in the flavone and flavonol biosynthesis pathways (such as kaempferol 3-*O*-glucoside, and kaempferol 3-*O*-galactoside). The significantly downregulated DAMs mainly included some flavonoid compounds (such as spinosyn, liquiritigenin, and apigenin *O*-hexosyl-*O*-pentoside) (**Table 2** and **Figure 9**).

Under saline-alkali stress, the TCA cycle of BY and YZY seeding roots was stimulated in the roots of BY and YZY, and the intermediates, such as citrate, *cis*-aconitate, succinate, fumarate, and malate, were increased. Compared with BY, the TCA cycle pathway components were enhanced by saline-alkali stress in YZY roots. The amino acid metabolism and related metabolism pathways were significantly altered in BY and YZY; in the arginine and proline metabolism pathway, proline in BY roots was upregulated, while a large amount of *N*-feruloyl putrescine, *N*-*p*-coumaroyl putrescine, and *N*′-*p*-coumaroyl putrescine accumulated in YZY roots. Compared with BY, the sugar and alcohol metabolisms in YZY roots were increased, as were melibiose, sucrose, galactinol, glucose-1P, glucose-6P, trehalose-6P, fructose-6P, maltotetraose, melezitose, and panose accumulation. For these metabolites, the increases were greater in YZY roots (**Figure 9**). In the phenylpropanoid biosynthesis pathway, saline-alkali stress induced the decrease of caffeate, methyl ferulate, methyl *p*-coumarate, *trans*-4-hydroxycinnamic acid methyl ester, 3,4-dimethoxycinnamic acid, 1-*O*-caffeoyl quinic acid, and 4-methoxycinnamic acid accumulation in BY roots, and increases of downstream products including *p*-coumaryl alcohol, coniferyl alcohol, and sinapyl alcohol. In contrast, saline-alkali stress led to the enhancement of the flavonoid biosynthesis pathway and the production of flavonoids, followed by glycosides (formed by flavonoids and sugar) accumulated in YZY roots (**Figure 9** and **Table 2**).

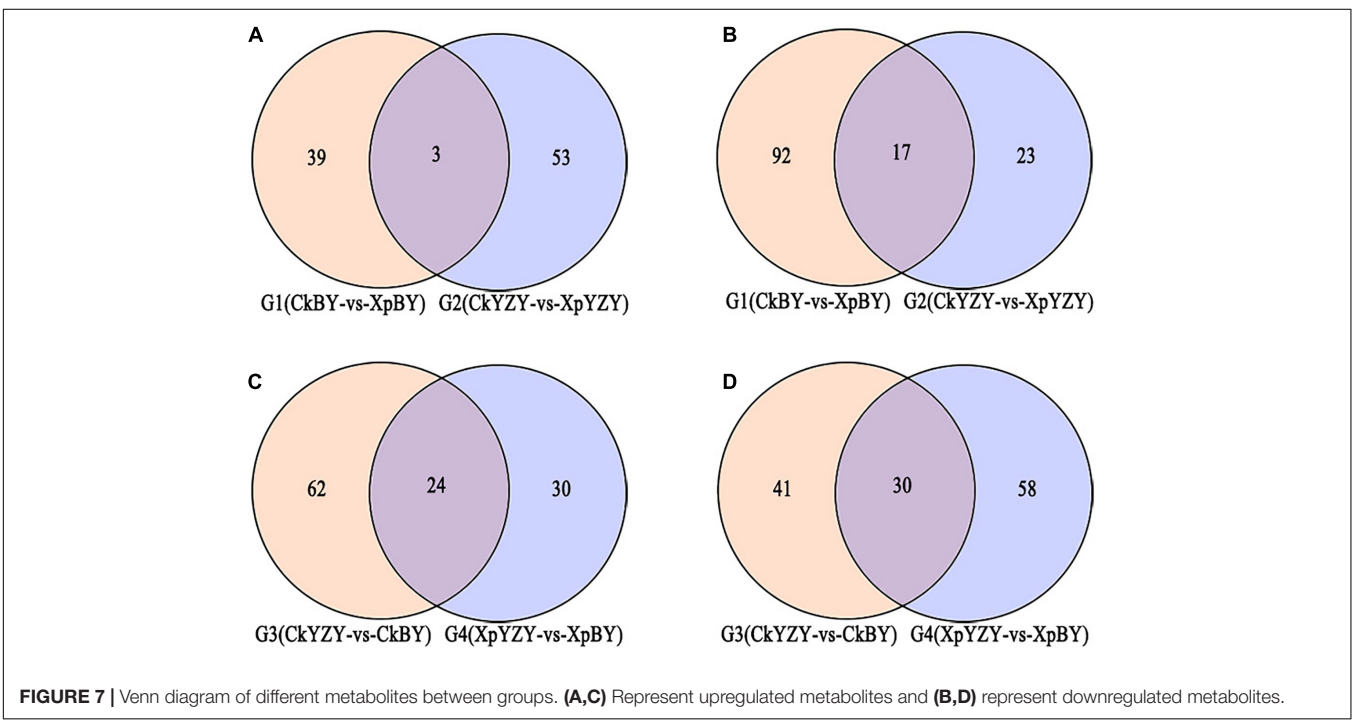

FIGURE 7 | Venn diagram of different metabolites between groups. **(A,C)** Represent upregulated metabolites and **(B,D)** represent downregulated metabolites.

TABLE 2 | The significant differential abundant metabolites in roots of Baiyan7 (BY) or Yizhangyan4 (YZY) after saline-alkali stress.

Compounds		BY roots			YZY roots		
		log_2FC	VIP	Regulated	log_2FC	VIP	Regulated
Amino acids and derivatives	L-Cysteine	1.30	1.76	$\uparrow^A$	0.41	1.74	–
	Betaine	14.27	1.72	$\uparrow^a$	0.18	0.20	–
	Proline	1.24	1.65	$\uparrow^a$	0.48	1.24	–
	N-acetyl-L-arginine	1.45	1.65	$\uparrow^a$	2.61	1.59	↑
	N-feruloyl putrescine	0.56	1.09	–	1.36	1.76	$\uparrow^a$
	N,*N*-dimethylglycine	−0.43	0.87	–	−1.11	1.78	$\downarrow^a$
Organic acids	Citric acid monohydrate	0.30	0.54	–	1.44	1.90	$\uparrow^A$
	Citric acid	0.26	0.57	–	1.19	1.84	$\uparrow^A$
	Cis-Aconitic acid	0.27	0.95	–	1.08	1.80	$\uparrow^a$
Lipids and derivatives	MAG (18:1) isomer2	−2.54	1.70	$\downarrow^A$	−1.09	1.01	$\downarrow^a$
	MAG (18:1) isomer1	−2.48	1.65	$\downarrow^A$	−1.13	1.01	$\downarrow^a$
	LysoPE 14:0	−2.11	1.56	$\downarrow^a$	−1.29	1.32	$\downarrow^a$
	LysoPC 16:1 (2n isomer)	−1.41	1.50	$\downarrow^a$	−1.26	1.26	$\downarrow^a$
	MAG (18:3) isomer2	−1.65	1.67	$\downarrow^A$	−0.43	0.46	–
	MAG (18:3) isomer3	−1.85	1.65	$\downarrow^a$	−0.52	0.52	–
	DGMG (18:1)	−1.98	1.61	$\downarrow^a$	−0.46	0.39	–
	DGMG (18:2) isomer2	−2.57	1.61	$\downarrow^a$	−0.52	0.39	–
	MAG (18:3) isomer5	−2.10	1.58	$\downarrow^a$	−0.71	0.57	–
	Ureido isobutyric acid	−0.20	0.16	–	−10.77	1.93	$\downarrow^A$
Phenylpropanoids	1-*O*-Feruloyl quinate	1.80	1.63	$\uparrow^a$	0.70	1.44	–
	p-Coumaryl alcohol	1.29	1.62	$\uparrow^a$	0.84	0.89	–
	8-Methoxy psoralen	1.09	1.65	$\uparrow^a$	0.41	0.61	–
	4-Methoxy cinnamic acid	−1.82	1.61	$\downarrow^a$	0.79	0.81	–
	Osthole	−1.81	1.59	$\downarrow^a$	−0.83	0.80	–
	trans-4-Hydroxycinnamic acid Methyl Ester	−1.79	1.61	$\downarrow^a$	0.78	0.82	–
	Methyl *p*-coumarate	−1.68	1.59	$\downarrow^a$	0.78	0.84	–
	Methyl ferulate	−1.60	1.50	$\downarrow^a$	0.65	0.59	–
	3,4-Dimethoxycinnamic acid	−1.60	1.50	$\downarrow^a$	0.66	0.60	–
	1-*O*-Caffeoyl quinate	−1.30	1.54	$\downarrow^a$	−0.43	0.65	–
	Caftaric acid	−1.02	1.50	$\downarrow^a$	0.77	1.35	–
	1-*O*-beta-D-Glucopyranosyl sinapate	0.63	0.95	–	1.11	1.83	$\uparrow^a$
	3,4,5-Trimethoxycinnamic acid	−0.01	0.02	–	−1.25	1.88	$\downarrow^a$
Flavonoids	3-*O*-Acetylpinobanksin	11.00	1.75	$\uparrow^A$	−0.26	0.21	
	Dihydroquercetin	−1.01	1.69	$\downarrow^A$	−0.24	1.27	–
	Glabridin	−1.89	1.63	$\downarrow^a$	−0.41	0.32	–
	Kaempferol 3-*O*-glucoside (astragalin)	−3.24	0.74	–	2.80	1.77	$\uparrow^a$
	Kaempferol 3-*O*-galactoside (trifolin)	−3.42	0.73	–	2.34	1.65	$\uparrow^a$
	Spinosin	0.42	0.46	–	−11.19	1.94	$\downarrow^A$
	Liquiritigenin	0.07	0.08	–	−2.49	1.74	$\downarrow^a$
	Apigenin *O*-hexosyl-*O*-pentoside	−0.49	1.69	–	−1.17	1.69	$\downarrow^a$
Others	Pantothenol	1.12	1.65	$\uparrow^A$	1.26	1.80	$\uparrow^a$
	3-Methyl-1-pentanol	1.14	1.60	$\uparrow^a$	0.41	1.12	–
	N-acetyl glucosamine 1-phosphate	−1.06	1.54	$\downarrow^a$	−0.49	1.24	–
	6-Gingerol	−1.09	1.09	$\downarrow^a$	−2.60	1.77	$\downarrow^a$
	Gallic acid	0.79	0.38	–	−13.94	1.94	$\downarrow^A$

The fold's change was calculated by the formula: $log_2^{(saline-alkali/control)}$; the $\uparrow^a$ and $\uparrow^A$ indicate significant and highly significant decreases, the $\downarrow^a$ and $\downarrow^A$ indicate significant and highly significant decreases, respectively.

DISCUSSION

The BY cultivar was bred by the Jilin Baicheng Academy of Agricultural Sciences (Guo et al., 2007); the YZY cultivar was bred by the Zhang Jiakou Academy of Agricultural Sciences. Both BY and YZY are the main cultivars of oats used for foods or feeds in the western Songnen Plain (Fu et al., 2018). According to the screening results (data not listed) of the experiments, the BY and YZY were identified as saline-alkali resistant and sensitive cultivars, respectively.

Saline-alkali stress severely inhibits plant growth and even leads to plant death, with seed germination and seedling growth

being the most sensitive stages affected (Ibrahim, 2016). Roots are the main site of nutrient uptake and salinity perception (Bai et al., 2016), which plays an important role in plant growth and development. Roots are in direct contact with soil, and are the first perceiver and responder of soil environmental stress; roots are more sensitive than shoots, responding to alkali stress (Xu et al., 2013; Wang et al., 2021). When roots are exposed to saline-alkali stress, the root is the first to perceive the stress information, which is gradually transmitted to the aboveground parts (Fang et al., 2021).

Inhibition of Seedling Growth and Physiological Parameters

The plant height of the two cultivars decreased significantly under saline-alkali stress, indicating that the plant growth of oats was significantly affected. Dry matter accumulation level is a comprehensive reflection of seedlings and one of the main indices of salt tolerance (Yang et al., 2009; Wang et al., 2018). A high pH stress mainly reduced the chlorophyll content (Bai et al., 2021), which caused a significant decrease in shoot and root dry weights of YZY (**Figure 1**). Saline-alkali stress did not have a negative impact on the BY root dry weight and even induced a significant increase in the root dry weight and root/shoot ratio. Maintaining vigorous root growth and increasing the root/shoot ratio may be a morphological adaptation for saline-alkali stress-tolerant cultivars (BY) (Wang et al., 2018). This is consistent with previous studies (Wu et al., 2009; Luo et al., 2012) and may be due to the difference in response mechanisms of different oat cultivars under saline-alkali stress, leading to differences in their growth performances.

Under saline-alkali stress, the rapid and excessive accumulation of ROS, including H_2O_2 and O_2^- can cause damage to cell membranes through lipid peroxidation and can even cause cell death (Gill and Tuteja, 2010; Liu et al., 2020). Among the antioxidant enzymes, CAT is sensitive to saline-alkali reaction, and, APX and POD play important roles in H_2O_2 clearance (Liu et al., 2016). In the present study, obvious effects of saline-alkali stress on the accumulation of H_2O_2 and $O_2^{\bullet-}$ were observed in the roots of both cultivars (**Figure 2**). The MDA, which reflects increased cell membrane damage, showed no significant differences among cultivars. This indicated that saline-alkali stress caused the accumulation of ROS in oat roots, but showed no significant difference in the degree of cell membrane damage between cultivars. Similar results for oats (*Avena nude* L.) have been reported (Zhao et al., 2013; Liu et al., 2016).

Osmotic stress has been identified as one of the main threats to plants under saline conditions (Munns, 2002). To cope with osmotic stress, plants synthesize and accumulate compatible solutes, and the most seen and compatible solutes are sucrose, proline, and betaine, which can generate a significant osmotic pressure and function as osmolytes during salt stress (Munns and Tester, 2008). Different plant species and different cultivars of the same species can respond to salt-alkali stress through changes in different osmotic adjustment substances. Accumulations of proline and betaine are generally higher in salt-tolerant plant species than in sensitive species (Liu et al., 2016; Fu et al., 2018). Consistent with these results, during saline-alkali stress, the contents of proline, betaine, soluble protein, and soluble sugar in BY roots were significantly increased, and were significantly higher than those in YZY roots, except for soluble sugar. The contents of proline, soluble sugar, and soluble protein in YZY roots were significantly increased, and the levels of soluble sugar were significantly higher than those in BY roots (**Figure 4**). These results indicated that proline and betaine were the main osmotic regulators in BY roots, and that soluble sugar played a more positive osmotic regulation role in YZY roots.

Sugar Metabolism Plays a Basic Function in Improving Saline-Alkali Tolerance

The regulation of sugar, induced by saline-alkali stress, was observed in the roots of oat (**Figure 9** and **Supplementary Table 1**). This may be related to the function of sugars in plant metabolic pathways. In plants, sucrose is a product of photosynthesis and it is an important energy source for metabolic activity; it has the function of osmotic adjustment, affecting redox homeostasis and the protection of macromolecular structures (Yang and Guo, 2018). Glucose was downregulated in the roots of BY and YZY, and this may be due to glucose being utilized in various metabolic pathways. Sufficient carbon sources and energy supplies are important for the assimilation of nitrogen and the synthesis of amino acids (Jia et al., 2019). Therefore, we speculated that the lack of significant accumulation of sugars may be related to other metabolic enhancements, including the TCA cycle and amino acid metabolism. In addition, the saline-alkali stress-induced mannitol (1.85-fold), galactinol (2.17-fold), maltotetraose (4.08-fold), melibiose (2.02-fold), panose (3.09-fold), melezitose (1.85-fold), and sucrose (2.25-fold), are consistent with the physiological parameters for soluble sugars.

Energy Metabolism Is an Active Strategy of Oat in Response to Saline-Alkali Stress

The TCA cycle is an important aerobic pathway in the final steps of the oxidation of carbohydrates and fatty acids (Wu et al., 2013) and is an important energy-producing process in plants. The TCA cycle plays an important role in resisting adverse environmental conditions, and is a central cycle in plant metabolism, giving rise to many primary and secondary metabolites including several intermediates involved in amino acid biosynthesis and nitrogen assimilation (Yang et al., 2017). The levels of *cis*-aconitic acid and citric acid in the TCA cycle were increased by saline-alkali stress in YZY roots. The intermediate metabolites of the TCA cycle, including citrate, fumarate, succinate, malate, and *cis*-aconitate, were upregulated in roots of BY and YZY (**Table 2** and **Figure 8**), revealing that saline-alkali stress induced the enhancement of the TCA cycle. Oats could, therefore, enhance the saline-alkali tolerance of its roots by increasing energy capacity and the levels of intermediate products during saline-alkali stress, which is similar to barley (Wu et al., 2013).

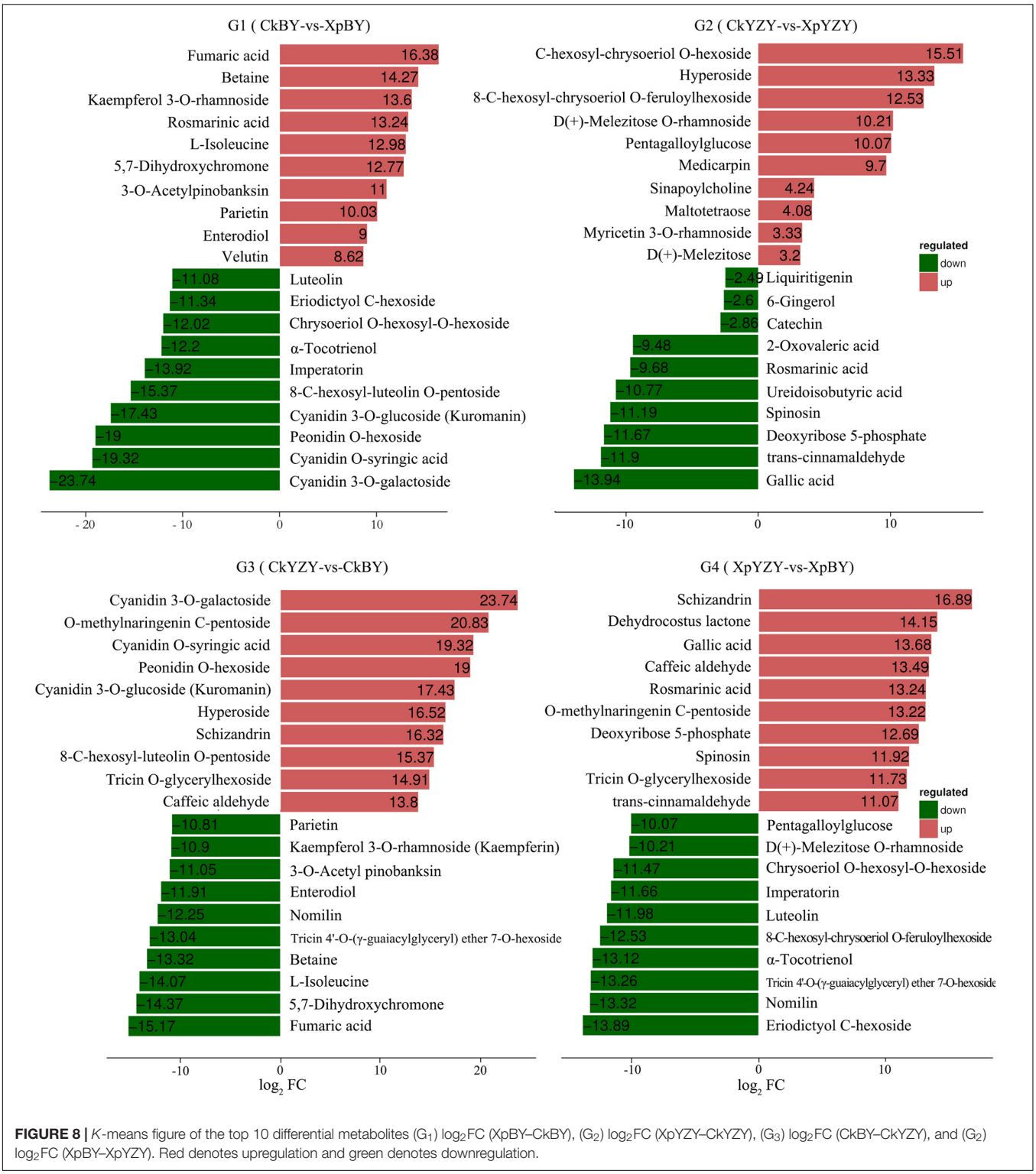

FIGURE 8 | *K*-means figure of the top 10 differential metabolites (G_1) log_2FC (XpBY–CkBY), (G_2) log_2FC (XpYZY–CkYZY), (G_3) log_2FC (CkBY–CkYZY), and (G_2) log_2FC (XpBY–XpYZY). Red denotes upregulation and green denotes downregulation.

Organic Acids Maintain the Intracellular pH Under Saline-Alkali Stress

Complex saline-alkali stress further increases the pH during salt stress (Fang et al., 2021), which results in reduced ion levels in the environment surrounding the roots. A high pH leads to root cells losing their normal physiological functions (Munns and Tester, 2008). Under saline-alkali stress, plants secrete organic acids to maintain the pH and ion balance of the internal environment, which is an adaptive response to stress (Yang et al., 2017; Jia et al., 2019). Similarly, saline-alkali stress induced the accumulation

of organic acids in oat roots. The plants of different families and genus (or even from the same family) have a different metabolic control mechanism for organic acids during alkali stress (Yang et al., 2007). We showed that saline-alkali stress induced the accumulation of organic acids, such as a citric acid monohydrate, *cis*-aconitic acid, citric acid, citramalate, oxalic acid, etc., in the roots of YZY. After saline-alkali stress, the organic acids accumulating in BY roots included fumaric acid, citric acid, malate, succinate, rosmarinic acid, linoleic acid, etc. The accumulation of organic acids can effectively compensate for the deficiency of inorganic anions (Wang et al., 2011). Organic acids are also involved in protein modification, nutrient uptake, signal transduction, and other physiological processes (Fang et al., 2021).

It is worth mentioning that fatty acids and their derivatives are also involved in plant resistance to abiotic stress, in addition to their roles in storing energy (Wang et al., 2021). We showed that in the roots of BY, four kinds of fatty acids, including ureidoisobutyric acid, punicic acid, octadecadien-6-ynoic acid, 16-hydroxyhexadecanoic acid, 9-hydroxy-(10E,12Z,15Z)-octadecatrienoic acid, 9,10-EODE, and 12,13-EODE, were downregulated by saline-alkali stress, which may be an effective way for BY roots to adapt to salt stress (Yang et al., 2017).

Differences of Amino Acids and Amino Acid-Associated Metabolism Between Cultivars

In higher plants, amino acids accumulate in response to various stresses and have multiple functions in plant growth (Less and Galili, 2008). Amino acid accumulation occurs in response to salt stress (Mutwakil et al., 2017). The results of the current study indicated that amino acid metabolism was significantly enhanced in BY roots during saline-alkali stress, leading to the significant accumulation of proline, cysteine, isoleucine, *N*′-acetyl-L-arginine aspartate, and 4-hydroxy-L-glutamate, whereas this was not observed in YZY roots. Metabolic analyses showed that there were differences in the arginine and proline metabolism pathways between the roots of the two studied cultivars (**Figure 9**), including the induced significant upregulation of proline accumulation in the roots of BY, and *N*-feruloyl putrescine in the roots of YZY ($P < 0.05$). In the roots of YZY, the compounds associated with putrescine biosynthesis, such as *N*-feruloyl putrescine, *N*′-*p*-coumaroyl putrescine, and *N*-*p*-coumaroyl putrescine, accumulated in the roots of YZY. The *N*-feruloyl putrescine is a feruloyl-CoA conjugate of putrescine, which shares ornithine as a common precursor with proline (Mohapatra et al., 2009; **Figure 9**). The accumulation of polyamine putrescine is correlated with slower growth and/or necrosis, rather than being an adaptive response to salinity (Widodo et al., 2009). The elevated levels of putrescine may indicate that the roots of sensitive cultivars, such as YZY, have been extensively damaged under the experimental conditions used in the study.

The L-cysteine is used as a sulfur donor in plants and is used for multiple processes catalyzed by multiple catabolic enzymes [(Less and Galili, 2008); its level is positively correlated with the methylation index (Kim et al., 2006)]. Cysteine has a structural function in proteins, as well as playing a role as a precursor for essential biomolecules, such as glutathione (GSH), phytochelatins (PCs), *S*-adenosyl-methionine (SAM), *S*-adenosyl-L-homocysteine (SAH), and methionine (Peng and Song, 2011; Sadak et al., 2019). Our results are supported by Peng and Song (2011), who reported that the L-cysteine treatment can efficiently activate the phenylpropanoid pathway, to promote the accumulation of phenolic substances (**Table 2** and **Figure 9**). The accumulation of isoleucine can alleviate salt stress by enhancing glycolysis (Kumar et al., 2010). In addition, these amino acids can increase the scavenging free oxygen radicals, in addition to regulating the osmotic pressure and alleviating salt stress. Moreover, amino acids serve as precursors for a large array of secondary metabolites, including pigments, alkaloids, hormones, and cell wall components (Jia et al., 2019).

Glycine betaine (GB) is synthesized from serine *via* ethanolamine, choline, and betaine aldehyde (Ashraf and Foolad, 2007), and is closely related to amino acid metabolism and lipid metabolism. Ethanolamine is essential for the synthesis of phospho-ethanolamine and phosphatidylethanolamine (PE) as well as choline and GB (Kim et al., 2006). MAG is degraded to ethanolamine *via* glycerone phosphate and PE in the glycerophospholipid metabolism pathway. In this study, the significant decrease of MAG contents in the roots of BY (**Table 2** and **Figure 9**), including MAG (18:1) isomer2, MAG (18:1) isomer1, and MAG (18:3) isomer5, may be related to its degradation and formation of choline, which, in turn, leads to significant up-accumulation of betaine (14.27-fold). In addition to important osmotic regulation functions, the GB and proline are thought to have positive effects on enzyme and membrane integrity during stress conditions (Ashraf and Foolad, 2007). When GB is present at high levels, together with proline, it is efficient in protecting plants from oxidative stress (Annunziata et al., 2019). Furthermore, GB is only accumulated during prolonged stress, does not normally break down in plants, and can be transported easily and efficiently from older to younger plant tissues (Bray et al., 2000; Carillo et al., 2008). These results suggest that GB plays a pivotal role in protecting young leaf and root tissues of BY against saline-alkali stress, and it may be one of the reasons why BY can maintain a relatively normal growth under saline-alkali stress.

Differences Between Cultivars of Secondary Metabolic Pathways

Generally, secondary metabolites, particularly the majority of phenolic compounds produced in the phenylpropanoid pathway, are usually a defense response to biotic or abiotic stress (Zhao et al., 2015). Compared with the control, the accumulations of secondary metabolites in oat roots, including some flavonoids and phenols, were significantly altered by saline-alkali stress (**Table 2**, **Figure 8**, and **Supplementary Table 1**). Considerable evidence suggests that phenylalanine, which is required for the biosynthesis of flavonoids and lignin, is an important precursor of phenylpropanoids (Santos et al., 1998).

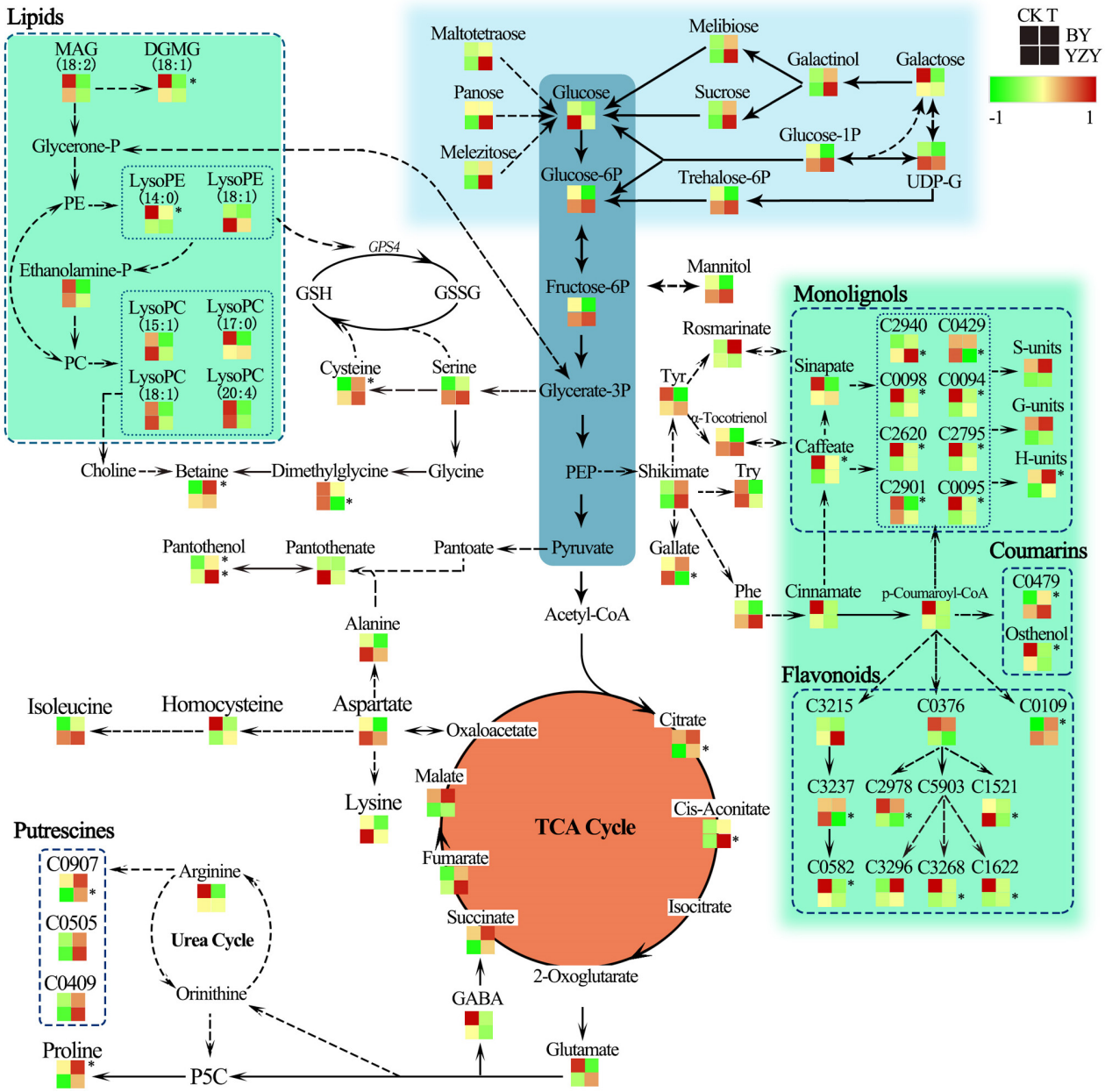

FIGURE 9 | Change in metabolites of the metabolic pathways in roots of oat seedlings after 12 days saline-alkali stress treatment. Proposed metabolic network changes in oat seedlings subjected to saline-alkali stress, as obtained using orthogonal partial least squares discriminant analysis. *H*-units, *p*-coumaryl alcohol; *S*-units, sinapyl alcohol; *G*-units, coniferyl alcohol; GABA, γ-aminobutyric acid; GPS4, phospholipid-hydroperoxide glutathione peroxidase; GSH, glutathione; GSSG, glutathione disulfide; LysoPE, 1-octadecanoyl-sn-glycero-3-phosphoethanolamine; MAG, monoacylglycerol; P5C, δ-pyrroline-5-carboxylate; PE, phosphatidylethanolamine; Phe, phenylalanine; PEP, phosphoenolpyruvate trisodium salt; SAH, *S*-adenosyl-L-homocysteine; Try, tryptophan; Tyr, tyrosine; C0094, methyl *p*-coumarate; C0095, methyl ferulate; C0098, *trans*-4-hydroxycinnamic acid methyl ester; C0109, 3-*O*-acetyl pinobanksin; C0376, naringenin; C0429, 3,4,5-trimethoxycinnamic acid; C0479, 8-methoxypsoralen (xanthotoxin); C0582, glabridin; C0907, *N*-feruloyl putrescine; C1521, dihydroquercetin (taxifolin); C1622, kaempferol 3-*O*-glucoside (astragalin); C2620, 3,4-dimethoxycinnamic acid; C2795, 4-methoxycinnamic acid; C2901, 1-*O*-caffeoyl quinic acid; C2940, 1-*O*-beta-D-glucopyranosyl sinapate; C2978, apigenin *O*-hexosyl-*O*-pentoside; C3215, isoliquiritigenin; C3237, liquiritigenin; C3268, kaempferol 3-*O*-galactoside (trifolin); C3296, kaempferol 3-*O*-rhamnoside (kaempferin); C0426, pentagalloylglucose; C5903, kaempferol. *Indicate significant ($P < 0.05$).

Phenylalanine accumulation was upregulated by saline-alkali stress in the roots of YZY, whereas it was downregulated in the roots of BY. This indicated that compared with YZY roots, the biosynthesis of the phenylpropanoids pathway in the roots of BY was at least partially inhibited. Analyses of metabolic pathways showed that during saline-alkali stress, phenylpropanoids and flavonoids in the roots of the two cultivars differed in metabolic pathways and metabolite accumulation levels (**Figure 9**).

The tolerance of plants to salinity is closely related to the formation of secondary cell walls and the deposition pattern of cellulose and lignin (Wang et al., 2016). Monolignols are synthesized from phenylalanine *via* cinnamate and *p*-coumaroyl-CoA, but this metabolic pathway can be diverted to the synthesis of flavonoids *via* *p*-coumaroyl-CoA (Wang, 2013). In BY roots, the increased monolignols, including coniferyl alcohol (*G*-units of lignin) and *p*-coumaryl alcohol (*H*-units of lignin) were induced by saline-alkali stress. In particular, the accumulation of *H*-units of lignin was significant (**Figure 9**). Increased lignin levels could contribute to the enhancement of cell wall strength, thus, maintaining and accelerating root cell growth. Unlike BY roots, lignin production in roots of YZY was not triggered by saline-alkali stress. Instead, the building blocks of phenylpropanoids were in part diverted to the production of flavonoids, suggesting suppression of root cell elongation. The tolerance of plants to salinity is closely related to the formation of secondary cell walls and the deposition pattern of cellulose and lignin (Wang et al., 2016). This may be the fundamental reason why BY roots could maintain vigorous growth under saline-alkali stress, while YZY roots were severely inhibited. The results suggested that under saline-alkali stress, the BY roots actively formed lignin units *via* the phenylpropanoid biosynthesis pathway to maintain cell structure stability and normal root growth, while the YZY roots formed flavonoids *via* the flavonoid biosynthesis pathway, and then flavonoids combined with sugars to form glycosides used for antioxidant regulation.

In addition, the panthenol in root tissues of both cultivars was significantly ($P < 0.05$) increased during stress (**Table 2** and **Figure 9**). Pantothenol is the precursor of pantothenic acid (vitamin B5). Pantothenic acid is not an antioxidant and exerts its major function as part of CoA. It is an essential acyl group carrier co-factor required for the growth of various organisms and plays a key role in numerous steps of cellular metabolism (Awasthy et al., 2010), controlling GSH biosynthesis by regulating cellular energy levels to maintain a stable GSH level to protect against peroxidative damage (Slyshenkov et al., 2004).

CONCLUSION

In summary, saline-alkali stress altered physiological, biochemical, and molecular processes, thereby affecting the growth and biomass of oat roots. The roots of oats, especially a sensitive cultivar (YZY), responded to saline-alkali stress by increasing the TCA cycle. Oat roots secreted and accumulated organic acids, which was an adaptive response to maintain pH and ion balance during saline-alkali stress. Saline-alkali stress induced the increase of amino acid metabolism in roots of tolerant cultivars (BY) and significantly increased the accumulation of osmotic substances, including proline, betaine, and L-cysteine. However, the roots of the sensitive cultivar (YZY) responded to osmotic stress by increasing the content of soluble sugars. Moreover, there were differences in the phenylpropanoid pathway between the tolerant cultivar and sensitive cultivar during saline-alkali stress. In the roots of BY, saline-alkali stress significantly induced the increase of monolignols, including coniferyl alcohol and *p*-coumaryl alcohol, which contributed to the enhancement of cell wall strength, and the maintenance and acceleration of root cell growth. However, the metabolism of phenylpropanoids was, in part, diverted to the production of flavonoids in the roots of YZY.

This is the first study that used an integrated approach to determine the possible molecular mechanisms of how *A. sativa* L. adapts to saline-alkali stress. The analyses of different metabolites of tolerant and sensitive cultivar roots provided an important theoretical basis for understanding the mechanisms of saline-alkali tolerance and increased our knowledge of plant metabolism regulation during stress.

DATA AVAILABILITY STATEMENT

The datasets presented in this study can be found in online repositories. The names of the repository/repositories and accession number(s) can be found in the article/ **Supplementary Material**.

AUTHOR CONTRIBUTIONS

YG and YJ proposed the study. YG, LY, and YJ designed the experiments and secured the funding. YG, YJ, and YX conducted the field and laboratory measurements and analyzed the data. WG contributed to planning the experimental protocols and data analyses. YG and YJ wrote the manuscript, which was edited by all authors. All authors have read and agreed to the present version of the manuscript.

FUNDING

This work was financially supported by the Heilongjiang Regional Characteristic Project-Coarse Cereals Production and Processing and the National Science and Technology Support Program "Research and Demonstration of Key Technologies for High-Efficiency Grain Production" (2014BAD07B05).

ACKNOWLEDGMENTS

We would like to thank Changjiang Zhao, Xilong Liang, Xiaoli Sun, Jingyu Xu, and Mingzhe Sun for their help in the implementation of the study and manuscript writing, as well as the International Science Editing (http://www.internationalscienceediting.com) for editing this manuscript.

SUPPLEMENTARY MATERIAL

The Supplementary Material for this article can be found online at: https://www.frontiersin.org/articles/10.3389/fpls.2022.835414/full#supplementary-material

REFERENCES

Annunziata, M. G., Ciarmiello, L., Woodrow, P., dell'Aversana, E., and Carillo, P. (2019). Spatial and Temporal Profile of Glycine Betaine Accumulation in Plants Under Abiotic Stresses. *Front. Plant Sci.* 10:230. doi: 10.3389/fpls.2019.00230

Ashraf, M., and Foolad, M. R. (2007). Roles of glycine betaine and proline in improving plant abiotic stress resistance. *Environ. Exp. Bot.* 59, 206–216. doi: 10.1016/J.ENVEXPBOT.2005.12.006

Awasthy, D., Ambady, A., Bhat, J., Sheikh, G., Ravishankar, S., Subbulakshmi, V., et al. (2010). Essentiality and functional analysis of type I and type III pantothenate kinases of Mycobacterium tuberculosis. *Microbiology* 156, 2691–2701. doi: 10.1099/mic.0.040717-0

Bai, J., Jin, K., Qin, W., Wang, Y., and Yin, Q. (2021). Proteomic Responses to Alkali Stress in Oats and the Alleviatory Effects of Exogenous Spermine Application. *Front. Plant Sci.* 12:627129. doi: 10.3389/fpls.2021.627129

Bai, J., Liu, J., Jiao, W., Sa, R., Zhang, N., and Jia, R. Z. (2016). Proteomic analysis of salt-responsive proteins in oat roots (Avena sativa L.). *J. Sci. Food Agri.* 96, 3867–3875. doi: 10.1002/jsfa.7583

Bai, J. H., Yan, W. K., Wang, Y. Q., Yin, Q., Liu, J. H., and Wight, C. (2018). Screening oat genotypes for tolerance to salinity and alkalinity. *Front. Plant Science* 9:1302. doi: 10.3389/fpls.2018.01302

Bartels, D., and Sunkar, R. (2005). Drought and Salt Tolerance in Plants. *Crit. Rev. Plant Sci.* 24, 23–58. doi: 10.1080/07352680590910410

Bray, E. A., Bailey-Serres, J., and Weretilnyk, E. (2000). "Responses to abiotic stress," in *Biochemistry and Molecular Biology of Plants*, eds B. Buchanan, W. Gruissem, and R. Jones (Rockville: American Society of Plant Physiology), 1158–1203.

Butcher, K., Wick, A., Desutter, T., Chatterjee, A., and Harmon, J. (2016). Soil Salinity: A Threat to Global Food Security. *Agronomy J.* 108, 2189–2200. doi: 10.2134/AGRONJ2016.06.0368

Carillo, P., Mastrolonardo, G., Nacca, F., Parisi, D., Verlotta, A., and Fuggi, A. (2008). Nitrogen metabolism in durum wheat under salinity: accumulation of proline and glycine betaine. *Funct. Plant Biol.* 35, 412–426. doi: 10.1071/FP08108

Chen, W., Gong, L., Guo, Z. L., Wang, W. S., and Zhang, H. Y. (2013). A Novel Integrated method for Large-Scale detection. Identification, and quantification of widely targeted metabolites: application in the study of rice metabolomics. *Mol. Plant.* 6, 1769–1780. doi: 10.1093/mp/sst080

El-Esawi, M. A., Al-Ghamdi, A. A., Ali, H. M., and Alayafi, A. A. (2019). Azospirillum lipoferum FK1 confers improved salt tolerance in chickpea (*Cicer a*rietinum icer arietinumoreali-Occidentaliars improved80" tion. Identification, and quantification. *Environ. Exper. Bot.* 159, 55–65. doi: 10.1016/J.ENVEXPBOT.2018.12.001

Fang, S., Hou, X., and Liang, X. (2021). Response Mechanisms of Plants Under Saline-Alkali Stress. *Front. Plant Sci.* 12:667458. doi: 10.3389/fpls.2021.667458

Fraga, C. G., Clowers, B. H., Moore, R. J., and Zink, E. M. (2010). Signature-discovery approach for sample matching of a nerve-agent precursor using liquid chromatography-mass spectrometry. XCMS, and chemometrics. *Anal. Chem.* 82, 4165–4173. doi: 10.1021/ac1003568

Fu, L. D., Wang, Y., Li, X., Sui, X., Ren, H., and Li, B. J. (2011). Study on cultivation techniques of oat in coastal saline-alkaline areas. *Agri. Res. Arid Areas* 29, 63–67.

Fu, L. H., Yu, S., Yu, L. H., Xue, Y. W., and Guo, W. (2018). Analysis of saline-alkaline tolerance and screening of identification indexes of different oat genotypes at the germination stage. *Crops* 06, 27–35.

Gao, J. F. (2006). Experimental guidance for plant physiology. Beijing: Higher Education Press.

Gill, S. S., and Tuteja, N. (2010). Reactive oxygen species and antioxidant machinery in abiotic stress tolerance in crop plants. *Plant Physiol. Biochem.* 48, 909–930. doi: 10.1016/j.plaphy.2010.08.016

Guo, C. L., Wei, L. M., Sha, L., and Deng, L. G. (2007). Breeding report of new oat variety Baiyan. *Crop Res.* 7, 340–342. doi: 10.16848/j.cnki.issn.1001-5280.2007.03.089

Guo, S., Niu, Y. J., Zhai, H., Han, N., and Du, Y. (2018). Effects of alkaline stress on organic acid metabolism in roots of grape hybrid rootstocks. *Sci. Horti.* 227, 255–260. doi: 10.1016/J.SCIENTA.2017.09.051

Han, L. P., Ma, F. J., Liu, J. T., Yu, S. H., Liu, H. T., and Tan, L. M. (2012). Analysis of oat-straw salt ion accumulation and the potential for improving saline-alkali soils in coastal Hebei Province. *Chin. J. Eco. Agri..* 20, 1706–1712. doi: 10.3724/SP.J.1011.2012.01606

Hou, X. D., Jia, Y. S., Bao, J., Fan, M. C., Zhao, M. Q., and Rong, R. (2018). Study on antisalinity characteristics of oat seed. *Grassland Prata.* 30, 49–55.

Ibrahim, E. A. (2016). Seed priming to alleviate salinity stress in germinating seeds. *J. Plant Physiol.* 192, 38–46. doi: 10.1016/j.jplph.2015.12.011

Jia, X., Zhu, Y., Hu, Y., Zhang, R., Cheng, L., Zhu, Z., et al. (2019). Integrated physiologic, proteomic, and metabolomic analyses of Malus halliana adaptation to saline-alkali stress. *Horti. Res.* 6:91 doi: 10.1038/s41438-019-0172-0

Kim, J., Bamba, T., Harada, K., Fukusaki, E., and Kobayashi, A. (2006). Time-course metabolic profiling in Arabidopsis thaliana cell cultures after salt stress treatment. *J. Exper Bot.* 58, 415–424. doi: 10.1093/JXB/ERL216

Kumar, V., Shriram, V., Kavi Kishor, P. B., Jawali, N., and Shitole, M. G. (2010). Enhanced proline accumulation and salt stress tolerance of transgenic *indica* rice by over-expressing *P5CSF129A* gene. *Plant Biotechnol. Rep.* 4, 37–48. doi: 10.1007/s11816-009-0118-3

Łabanowska, M., Kurdziel, M., Filek, M., and Wesełucha-Birczy'nska, A. (2016). The impact of biochemical composition and nature of paramagnetic species in grains on stress tolerance of oat cultivars. *J. Plant Physiol.* 199, 52–66. doi: 10.1016/j.jplph.2016.04.012

Less, H., and Galili, G. (2008). Principal Transcriptional Programs Regulating Plant Amino Acid Metabolism in Response to Abiotic Stresses1. *Plant Physiol.* 147, 316–330. doi: 10.1104/pp.108.115733

Li, H. C., Li, Y. F., Wang, B., Sha, N., Liu, J. Q., Du, C., et al. (2018). Response of different oat varieties to NaCl stress and its salt tolerance threshold. *J. North. Agri.* 46, 13–17.

Liu, J. H., Wang, W., Wu, H., Gong, X. Q., and Moriguchi, T. (2015). Polyamines function in stress tolerance: from synthesis to regulation. *Front. Plant Sci.* 6:827. doi: 10.3389/fpls.2015.00827

Liu, J. X., Wang, J. C., Wang, R. J., and Jia, H. Y. (2016). Effects of Complex Saline-alkali Stress on Seed Germination and Stress-resistance Physiological Characteristics of Naked Oat Seedlings. *Bull. Bot. Res.* 36, 224–231.

Liu, L. Y., Petchphankul, N., Ueda, A., and Saneoka, H. (2020). Differences in Physiological Responses of Two Oat (*Avena nuda* L.) Lines to Sodic-Alkalinity in the Vegetative Stage. *Plants* 9, 1188–1202. doi: 10.3390/plants9091188

Luo, Y. L., Song, S. Q., and Lan, Q. Y. (2009). Possible involvement of enzymatic and non-enzymatic antioxidant system in acquisition of desiccation tolerance of maize embryos. *Acta Bot. Yunnanica.* 31, 253–259. doi: 10.3724/SP.J.1143.2009.08227

Luo, Z. N., Zhao, G. Q., and Liu, H. (2012). The comprehensive evaluation of salt tolerance for 24 oat cultivars. *Grassl. Turf.* 32, 34–38+41.

Mohapatra, S., Minocha, R., Long, S., and Minocha, S. C. (2009). Transgenic manipulation of a single polyamine in poplar cells affects the accumulation of all amino acids. *Amino Acids* 38, 1117–1129. doi: 10.1007/s00726-009-0322-z

Munns, R. (2002). Comparative Physiology of Salt and Water Stress. *Plant Cell Environ.* 252, 239–250. doi: 10.1046/J.0016-8025.2001.00808.X

Munns, R., and Tester, M. (2008). Mechanisms of salinity tolerance. *Annu. Rev. Plant Biol.* 59, 651–681. doi: 10.1146/annurev.arplant.59.032607.092911

Mutwakil, M. Z., Hajrah, N. H., Atef, A., Edris, S., Sabir, M. J., Al-Ghamdi, A. K., et al. (2017). Transcriptomic and metabolic responses of *Calotropis procera* to salt and drought stress. *BMC Plant Biol.* 17:231. doi: 10.1186/s12870-017-1155-7

Peng, X. Y., and Song, M. (2011). Effects of exogenous cysteine on growth, copper accumulation and antioxidative systems in wheat seedlings under Cu stress. *Acta EcologicaSinica* 31, 3504–3511.

Rao, P. S., Mishra, B., and Gupta, S. (2013). Effects of Soil Salinity and Alkalinity on Grain Quality of Tolerant, Semi-Tolerant and Sensitive Rice Genotypes. *Rice Sci.* 20, 284–291. doi: 10.1016/S1672-6308(13)60136-5

Sadak, M. S., Abd El-Hameid, A. R., Zaki, F. S., Dawood, M. G., and El-Awadi, M. E. (2019). *Physiological and biochemical responses of soybean (Glycine max* L.) to cysteine application under sea salt stress.Bull. Natl. Res.Centre 44:1. doi: 10.1186/s42269-019-0259-7

Santos, A. C., Uyemura, S. A., Lopes, J. L., Bazon, J. N., Mingatto, F. E., and Curti, C. (1998). Effect of naturally occurring flavonoids on lipid peroxidation and membrane permeability transition in mitochondria. *Free Rad. Biol. Med.* 249, 1455–1461. doi: 10.1016/S0891-5849(98)00003-3

Shahid, S., Zaman, M., and Heng, L. (2018). *Soil Salinity: Historical Perspectives and a World Overview of the Problem. Guideline for Salinity Assessment, Mitigation*

and Adaptation Using Nuclear and Related Techniques. Cham: Springer, 43–53. doi: 10.1007/978-3-319-96190-3_2

Shao, C. R., Zhang, Y., Xie, L. N., and Li, Y. H. (2011). Progress in transcriptional regulation and metabolic profiling of plants response to abiotic stress. *Plant Physiol. J.* 47, 443–451.

Shen, Q. F., Yu, J. H., Fu, L. B., Wu, L. Y., Dai, F., Jiang, L. X., et al. (2018). Ionomic, metabolomic and proteomic analyses reveal molecular mechanisms of root adaption to salt stress in Tibetan wild barley. *Plant Physiol. Biochem.* 123, 319–330. doi: 10.1016/j.plaphy.2017.12.032

Shi, D., and Wang, D. (2004). Effects of various salt-alkaline mixed stresses on *Aneurolepidiumchinense* (*Trin.*) Kitag. *Plant Soil.* 271, 15–26. doi: 10.1007/s11104-004-1307-z

Slyshenkov, V. S., Dymkowska, D., and Wojtczak, L. (2004). Pantothenic acid and pantothenol increase biosynthesis of glutathione by boosting cell energetics. *Federat. Eur. Biochem. Soc.* 569, 169–172. doi: 10.1016/j.febslet.2004.05.044

Sun, J., He, L., and Li, T. (2019). Response of seedling growth and physiology of Sorghum bicolor (L.) Moench to saline-alkali stress. *PLoS One* 14:e0220340. doi: 10.1371/journal.pone.0220340

Sun, R. G., Zhao, G. Q., Hu, K. J., and Man, Y. R. (2010). Effect of Salinity Stress on Aboveground Dry Matter Accumulation of Oat and Photosynthesis at Grain Filling Stage. *Chinese J. Grassland* 32, 15–20.

Tinte, M. M., Chele, K. H., van der Hooft, J. J., and Tugizimana, F. (2021). Metabolomics-Guided Elucidation of Plant Abiotic Stress Responses in the 4IR Era: An Overview. *Metabolites* 11:445. doi: 10.3390/metabo11070445

Wang, P. (2013). *Study of lignin metabolism in Lyceum ruthenicum Murr. Under salt stress*. Lanzhou: Lanzhou university, 1–5.

Wang, Q. H., Han, W., Hou, Y. Y., Feng, L., Ye, Z. P., Gu, H. M., et al. (2018). Responses of main characters of root system to salt stress among cotton varieties with different salt tolerance. *J. Appl. Ecol.* 29, 865–873. doi: 10.13287/j.1001-9332.201803.025

Wang, S. H. (2006). *Betaine accumulations, partial cDNA cloning and the transcript expression of its related enzymes in Dendranthema lavandulifolium* L. under NaCI stress. Beijing: Beijing Forestry University Digital Repository.

Wang, T., McFarlane, H. E., and Persson, S. (2016). The impact of abiotic factors on cellulose synthesis. *J. Exper. Bot.* 67, 543–552. doi: 10.1093/jxb/erv488

Wang, W., Pang, J., Zhang, F., Sun, L., Yang, L., Zhao, Y., et al. (2021). Integrated transcriptomics and metabolomics analysis to characterize alkali stress responses in canola (*Brassica napus* L.). *Plant Physiol. Biochem.* 166, 605–620. doi: 10.1016/j.plaphy.2021.06.021

Wang, X., Geng, S., Ri, Y. J., Cao, D., Liu, J., Shi, D., et al. (2011). Physiological responses and adaptive strategies of tomato plants to salt and alkali stresses. *Sci. Hortic.* 130:255. doi: 10.1016/j.scienta.2011.07.006

Widodo, Patterson, J. H., Newbigin, E., Tester, M., Bacic, A., and Roessner, U. (2009). Metabolic responses to salt stress of barley (*Hordeum vulgare* L.) cultivars, Sahara and Clipper, which differ in salinity tolerance. *J. Experim. Bot.* 60, 4089–4103. doi: 10.1093/jxb/erp243

Wu, D. Z., Cai, S. G., Chen, M. X., Ye, L. Z., and Chen, Z. H. (2013). Tissue metabolic responses to salt stress in wild and cultivated barley. *PLoS One* 8:e55431. doi: 10.1371/journal.pone.0055431

Wu, J. Y., Liu, J. H., Zhai, L. J., Li, J., and Li, L. J. (2009). Salt-tolerance of seed germination and seedling growth of different oat varieties. *Chinese J. Ecol.* 28, 1960–1965.

Xiang, G., Ma, W., Gao, S., Jin, Z., Yue, Q., and Yao, Y. (2019). Transcriptomic and phosphoproteomic profiling and metabolite analyses reveal the mechanism of NaHCO3-induced organic acid secretion in grapevine roots. *BMC Plant Biol.* 19:383. doi: 10.1186/s12870-019-1990-9

Xu, A., Mu, C., Li, X., Lin, J., Li, Y., and Mu, Y. (2013). Salt and alkali stresses effects on contents of organic acids components in wheat seedings. *J. Plant Nutr.* 36, 1056–1064. doi: 10.1080/01904167.2013.766888

Yang, C., Guo, W., and Shi, D. (2010). Physiological roles of organic acids in alkali-tolerance of the alkali-tolerant halophyte *Chloris virgata. Agron. J.* 102:1089. doi: 10.2134/agronj2009.0471

Yang, C. W., Chong, J. N., Li, C., Kim, C., Shi, D. C., and Wang, D. L. (2007). Osmotic adjustment and ion balance traits of an alkali resistant halophyte *Kochia sieversiana* during adaptation to salt and alkali conditions. *Plant Soil.* 294, 263–276. doi: 10.1007/s11104-007-9251-3

Yang, D. S., Zhang, J., Li, M. X., and Shi, L. X. (2017). Metabolomics analysis reveals the salt-tolerant mechanism in Glycine soja. *J. Plant Growth Regul.* 36, 460–471. doi: 10.1007/s00344-016-9654-6

Yang, K., Zhang, B. J., Hu, Y. G., Wang, S. H., and Xue, X. F. (2009). Effects of complex saline-alkaline stress on seeds germination and physiological and biochemical parameters of oats seedlings. *Agri. Res. Arid Areas.* 27, 188–192.

Yang, Y., and Guo, Y. (2018). Elucidating the molecular mechanisms mediating plant salt-stress responses. *New phytol.* 217, 523–539. doi: 10.1111/nph.14920

Yin, H. M., Hu, J., Wang, Q. Q., Xu, X. H., and Zhang, Y. B. (2017). Advance and prospect of the research on improvement by dry farming measures of saline-alkali soils in Western Songnen Plain of China. *Chinese J. Soil Sci.* 48, 236–242. doi: 10.19336/j.cnki.trtb.2017.01.31

Zhang, X. Q., Liu, J. H., Qi, B. J., Guo, X. X., and He, P. C. (2011). Effects of mixed salt stress on seed germination index of seven Canadian naked oat varieties. *Agri. Res. Arid Areas.* 29, 233–238.

Zhang, Y. Q., Wu, N., Liu, J. L., Yang, N. N., and Yang, Y. Y. (2018). Effects of mild saline-alkali on photosynthetic physiology and yield of different oat cultivars. *Southwest China J. Agri. Sci.* 31, 2041–2046.

Zhang, Z. L., and Qu, W. Q. (2003). *Experimental guidance of Plant Physiology*. Beijing: Higher Education Press.

Zhao, B. P., Liu, J. H., Wu, J. Y., Liu, H., and Xu, H. (2013). Effects of salt stress on plasmalemma permeability, osmolyte accumulation and protective enzyme activities in oat plants. *J. Food Agric. Environ.* 11, 696–701.

Zhao, J. L., Zou, L., Zhong, L., Peng, L., Ying, P. L., and Tan, M. L. (2015). Effects of polysaccharide elicitors from endophytic *Bionectriapityrodes Fat6* on the growth and flavonoid production in tartary buckwheat sprout cultures. *Cereal Res. Commun.* 43, 661–671. doi: 10.1556/0806.43.2015.013

Conflict of Interest: The authors declare that the research was conducted in the absence of any commercial or financial relationships that could be construed as a potential conflict of interest.

Publisher's Note: All claims expressed in this article are solely those of the authors and do not necessarily represent those of their affiliated organizations, or those of the publisher, the editors and the reviewers. Any product that may be evaluated in this article, or claim that may be made by its manufacturer, is not guaranteed or endorsed by the publisher.

Copyright © 2022 Gao, Jin, Guo, Xue and Yu. This is an open-access article distributed under the terms of the Creative Commons Attribution License (CC BY). The use, distribution or reproduction in other forums is permitted, provided the original author(s) and the copyright owner(s) are credited and that the original publication in this journal is cited, in accordance with accepted academic practice. No use, distribution or reproduction is permitted which does not comply with these terms.

frontiers | Frontiers in Plant Science

ORIGINAL RESEARCH
published: 12 April 2022
doi: 10.3389/fpls.2022.831265

Molecular Characterization Reveals the Involvement of Calcium Dependent Protein Kinases in Abiotic Stress Signaling and Development in Chickpea (*Cicer arietinum*)

Deepika Deepika[1†], *Nikita Poddar*[2†], *Shailesh Kumar*[2*] *and Amarjeet Singh*[1*]

[1] *Stress Signaling Lab, National Institute of Plant Genome Research, New Delhi, India,* [2] *Bioinformatics Lab, National Institute of Plant Genome Research, New Delhi, India*

OPEN ACCESS

Edited by:
Girdhar Kumar Pandey, University of Delhi, India

Reviewed by:
Gaurav Zinta, Institute of Himalayan Bioresource Technology (CSIR), India
Sung Chul Lee, Chung-Ang University, South Korea
Aryadeep Roychoudhury, St. Xavier's College (Autonomous), Kolkata, India

***Correspondence:**
Amarjeet Singh
amarjeet.singh@nipgr.ac.in
orcid.org/0000-0001-9538-5406
Shailesh Kumar
shailesh@nipgr.ac.in
orcid.org/0000-0002-1872-9903

†These authors have contributed equally to this work and share first authorship

Specialty section:
This article was submitted to Plant Physiology, a section of the journal Frontiers in Plant Science

Received: *08 December 2021*
Accepted: *11 March 2022*
Published: *12 April 2022*

Citation:
Deepika D, Poddar N, Kumar S and Singh A (2022) Molecular Characterization Reveals the Involvement of Calcium Dependent Protein Kinases in Abiotic Stress Signaling and Development in Chickpea (Cicer arietinum). Front. Plant Sci. 13:831265. doi: 10.3389/fpls.2022.831265

Calcium-dependent protein kinases (CDPKs) are a major group of calcium (Ca^{2+}) sensors in plants. CDPKs play a dual function of "Ca^{2+} sensor and responder." These sensors decode the "Ca^{2+} signatures" generated in response to adverse growth conditions such as drought, salinity, and cold and developmental processes. However, knowledge of the CDPK family in the legume crop chickpea is missing. Here, we have identified a total of 22 *CDPK* genes in the chickpea genome. The phylogenetic analysis of the chickpea CDPK family with other plants revealed their evolutionary conservation. Protein homology modeling described the three-dimensional structure of chickpea CDPKs. Defined arrangements of α-helix, β-strands, and transmembrane-helix represent important structures like kinase domain, inhibitory junction domain, N and C-lobes of EF-hand motifs. Subcellular localization analysis revealed that CaCDPK proteins are localized mainly at the cytoplasm and in the nucleus. Most of the CaCDPK promoters had abiotic stress and development-related *cis*-regulatory elements, suggesting the functional role of CaCDPKs in abiotic stress and development-related signaling. RNA sequencing (RNA-seq) expression analysis indicated the role of the CaCDPK family in various developmental stages, including vegetative, reproductive development, senescence stages, and during seed stages of early embryogenesis, late embryogenesis, mid and late seed maturity. The real-time quantitative PCR (qRT-PCR) analysis revealed that several *CaCDPK* genes are specifically as well as commonly induced by drought, salt, and Abscisic acid (ABA). Overall, these findings indicate that the CDPK family is probably involved in abiotic stress responses and development in chickpeas. This study provides crucial information on the CDPK family that will be utilized in generating abiotic stress-tolerant and high-yielding chickpea varieties.

Keywords: abiotic stress, CDPK, chickpea, gene expression, signaling, development

INTRODUCTION

Chickpea, the world's second most important food legume, is majorly produced by South Asia. Importantly, as the largest producer of chickpea, India contributes about 70% (5.9 million tons (mt) annually) to the world's chickpeas production (Varshney et al., 2009). Chickpea seeds are of high nutrition value as they contain 20–30% crude protein, 40% carbohydrate, 3–6% oil, and an abundance of minerals, such as calcium, magnesium, potassium, phosphorus, iron, and zinc (Gil et al., 1996; Ibrikci et al., 2003). Unfortunately, due to continuously fluctuating and harsh environmental conditions in the semi-arid tropics where chickpea is majorly cultivated, its productivity is severely affected. An estimated 40–60% of annual global chickpea yield losses are accounted for by abiotic stress factors only. While drought inflicts severe damage and accounts for almost 50% of chickpea yield loss, temperature changes and soil salinity together account for about 25% of chickpea yield loss (Varshney et al., 2014). Consequently, a wide gap is developed between chickpea demand and supply. Importantly, damage to chickpea yield dents several chickpea-producing countries economically. Drought, cold, and salinity, respectively, are reported to cost ∼1.3 billion, 186, and 354 million US dollars (Ryan, 1997). Abiotic stresses negatively impact the flower set, pollen viability, pod set/abortion, and retention. As these developmental stages determine the seed number in chickpea, a negative impact on them significantly hampers chickpea yield. Thus, identification of crucial stress-related genes and their utilization in breeding programs to generate stress-tolerant chickpea varieties are urgently required.

Abiotic stresses are known to elicit a profound increase in cytosolic calcium (Ca^{2+}) levels. The spatio-temporal accumulation of Ca^{2+} develops a specific "Ca^{2+} signature" in the form of Ca^{2+} spikes, waves, and oscillations. The Ca^{2+} signature encoded by a specific stimulus is decoded by various Ca^{2+} sensors, toward a specific response (Tang et al., 2020). Major Ca^{2+} sensors that have been identified and characterized in plants include calmodulin (CaM) and CaM-like proteins (CMLs) (Zeng et al., 2015), calcineurin B-like proteins (CBLs) (Luan, 2009), and Ca^{2+}-dependent protein kinases (CDPKs) (Singh et al., 2017). Among these, CDPKs are one of the largest Ca^{2+} sensor groups in the plant kingdom and constitute a multi-gene family (Schulz et al., 2013; Xiao et al., 2017). A total of 34 CDPK have been found in the *Arabidopsis thaliana* genome (Cheng et al., 2002), 31 genes in the rice (*Oryza sativa*) genome (Ray et al., 2007), and 20 genes in the wheat (*Triticum aestivum* L.) genome (Li et al., 2008). CDPKs are unique enzymes with a dual function of a Ca^{2+} sensor and responder, attributed to their peculiar structural features. Differing from other Ca^{2+} sensors, CDPKs can sense, respond to, and translate Ca^{2+} signals into protein phosphorylation events (Poovaiah et al., 2013). Plant CDPKs are comprised of a conserved domain structure and are monomeric in nature. A variable N-terminal domain is followed by a ser/thr kinase domain and a CDPK activation domain (CAD). An auto-inhibitory region called as "inhibitory junction domain" and a calcium-binding CaM-like domain (CaM-LD) is located within CAD (Schulz et al., 2013). CaM-LD contains four elongation factors (EF) hand motifs that are responsible for Ca^{2+} binding. These EF hands are organized as N-terminal and C-terminal lobes (each consists of two EF hands) (Boudsocq and Sheen, 2013; Liese and Romeis, 2013). At the basal state, the C-terminal lobe shows high affinity to Ca^{2+} thus, it remains loaded with Ca^{2+} even at low Ca^{2+} concentration. The C-terminal lobe *via* interaction with auto-inhibitory junction maintains the kinase in an inactive state. The binding of Ca^{2+} induces a conformational change in the N-terminal lobe, which disrupts auto-inhibitory junction-kinase interaction. That removes auto-inhibition and leads to the activation of kinase (Boudsocq and Sheen, 2013). In plants, different CDPK isoforms have been found to exhibit distinct expression patterns, which possibly accounts for their functional specificity (Yang et al., 2017; Zhang et al., 2017). CDPK proteins localize in the cytosol and subcellular organelles, including the nucleus, plasma membrane, endoplasmic reticulum, tonoplast, mitochondria, and chloroplasts (Simeunovic et al., 2016). This suggests that CDPKs might target variable substrates throughout the plant cell. In plants, CDPKs have been involved in regulating important functions, including biotic and abiotic responses, hormone signaling, and development (Schulz et al., 2013). Knowledge of plants' CDPK functions has been generated majorly from the research with the model plant *Arabidopsis thaliana*. Information about molecular features of the CDPK family and its role in important legume crop chickpea is missing. Molecular characterization of the CDPK family will help in understanding their functions in chickpeas.

Here, we have unearthed the entire repertoire of CDPK encoding genes in the chickpea genome. Gene and domain structure analysis confirmed the authenticity and integrity of CDPKs. Phylogenetic analysis and chromosomal localization provided crucial insight into the evolution and expansion of the chickpea CDPK family. Homology modeling was used to understand the three-dimensional structure of chickpea CDPK proteins. Subcellular localization analysis showed that chickpea CDPK proteins are mainly nuclear and/or cytoplasmic. *In-silico* promoter analysis showed the presence of stress, hormone, and development-related *cis*-regulatory elements in CDPK promoters. Extensive expression analysis of the chickpea *CDPK* family was performed under abiotic stresses (drought, salinity, and cold) and during different developmental stages using public RNA-Seq data and qRT-PCR analysis. Expression analysis indicated the involvement of the CDPK family in abiotic stress signaling and plant development in chickpea.

MATERIALS AND METHODS

Identification of CDPKs in the Chickpea Genome

The chickpea genome at National Centre for Biotechnology Information (NCBI) (Varshney et al., 2013) was explored to identify the CDPK encoding genes. CDPK protein sequences of rice and *Arabidopsis thaliana* were retrieved from Uniprot (Swiss-Prot), and used for BLAST homology search in the chickpea genome database. Further, the Hidden Markov Model (HMM) profile of CDPK was extracted from the

Pfam (http://pfam.xfam.org/) database and was used as a query to search the chickpea database at NCBI. All obtained sequences were compiled, redundant entries were removed, and only unique entries were used in further analysis. Protein sequences of putative CDPKs were scrutinized for the presence of canonical domains using *in-silico* tools, such as SMART (http://smart.embl-heidelberg.de/), Interpro (https://www.ebi.ac.uk/interpro/), Prosite (https://prosite.expasy.org/) and Pfam (https://pfam. xfam.org/). Various attributes of CDPKs, such as gene ID, protein ID, CDS size, protein size, Introns, molecular weight (MW), isoelectric point (pI), and chromosomal coordinates were extracted from NCBI and ExPASy (https://web.expasy.~org/compute_pi/).

Phylogenetic Analysis

Multiple Sequence Alignment (MSA) was performed using non-redundant protein sequences of CDPKs from chickpea, *Arabidopsis*, rice, and soybean (*Glycine max*), using Clustal W at default settings. A phylogenetic tree was generated in MEGA X version 10.1.8 (Pennsylvania State University, USA) by the neighbor-joining method. Bootstrap values were calculated in 1,000 replicates to determine the phylogenetic relationship among the CDPKs. The web-server iTOL (Letunic and Bork, 2021) was used to mark the different clades of CIPKs with different colors for better visualization.

Gene Structures and Domain Prediction

To investigate the gene structure of *CDPKs*, their CDS and the genomic sequences were extracted from NCBI. These sequences were submitted at the Gene Structure Display Server 2.0. (http://gsds.cbi.pku.edu.cn/index.php?input=ite) to generate the gene structure diagram. Identification of domains was carried out using a standalone package of InterPro Scan. Co-ordinates of essential domains and active sites were extracted and used as input in Illustrator for Biological Sequences for the visualization.

Gene Nomenclature, Chromosomal Localization, and Gene Duplication

The nomenclature of chickpea *CDPK* genes was done based on sequence closeness to their *Arabidopsis* orthologs, and phylogenetic analysis. Genes were named as *CaCDPK* followed by a number (1–22) corresponding to their respective *Arabidopsis* orthologs. The information of chromosome co-ordinates of genes was obtained from NCBI and further used to display chromosomal localization. The MCScanX software package (Wang et al., 2012; Athens, USA) was used to assess the gene duplication within the chickpea *CDPK* gene family. Genes located within 20 kb distance on the same chromosome were considered as tandemly duplicated genes (Feng et al., 2015).

Homology Modeling of CaCDPK Proteins

The three-dimensional (3D) structures of all CaCDPK proteins were predicted by homology modeling using the PHYRE2 web portal (http://www.sbg.bio.ic.ac.uk/phyre2). PHYRE2 uses advanced remote homology detection methods to build 3D models for protein sequences (Kelley et al., 2015). All the proteins were modeled with 100% confidence by the single highest scoring template model.

In-Silico Subcellular Localization of CaCDPK Proteins

The full-length protein sequences of CaCDPKs were used as input in the subCELlular LOcalization predictor: CELLO online tool (Yu et al., 2006) to predict their subcellular localization.

Constructs Preparation for *In-Planta* Subcellular Localization

The protein coding sequence (ORF excluding their stop codon) of *CaCDPK5*, *CaCDPK16*, and *CaCDPK21* genes were amplified from chickpea complementary DNA (cDNA) with gene-specific primers using iProof high fidelity DNA polymerase (Bio-Rad) through PCR in a thermocycler (Applied Biosystems). The list of these primers is given in **Supplementary Table 1**. The ORFs after amplification cloned into gateway entry vector p-ENTR-D-TOPO (Invitrogen). Genes were subsequently mobilizing into a compatible destination vector pSITE3CA under the control of 2XCaMV35S promoter by LR recombination protocol. The authenticity of all the constructs was ensured by PCR and sequencing.

Agro-Infiltration Into *Nicotiana benthamiana* and Confocal Microscopy

Agrobacterium tumefaciens (GV3101::pMP90) cells were transformed with the YFP constructs of the respective genes. Transformed *Agrobacterium* cells were used to transfect 6-week-old *N. benthamiana* plant leaves. Plants were grown in a growth chamber with the following conditions: 12/12 h photoperiod, 25–26°C temperature, and 60% relative humidity for 48–72 h. Transiently transformed *Nicotiana* leaf discs were analyzed under Total confocal scanner (TCS) SP5 laser scanning electron microscope (Leica, Germany) to detect the florescence, according to Deepika et al. (2022).

In-Silico Promoter Analysis

The 2 kb sequence, upstream of translational start site of *CDPK* genes was retrieved from NCBI. This sequence was used as input in PlantCARE database (http://bioinformatics.psb. ugent.be/webtools/plantcare/html/) for the detection of various *cis*-regulatory elements and motifs. Important *cis*-regulatory related to abiotic stresses, hormonal response, and plant development were selected.

RNA-Seq Expression Analysis in Developmental Stages and Tissues

To investigate the expression pattern of *CaCDPK* genes during developmental stages, RNA-Seq data was extracted from the NCBI-Sequence Read Archive (SRA) (ID:SRP121085). The raw reads obtained from SRA were processed using the FASTP tool (Shenzhen, China). An index of the reference genome was built and mapping of raw reads onto the reference genome was done using HISAT2 (Kim et al., 2019). StringTie (Pertea et al., 2015) was used to assemble the aligned sequences into potential transcripts. Transcript abundance was calculated by fragments

per kilobase of transcript per million reads (FPKM) values. Expression dynamics were analyzed in 27 tissues representing different developmental stages, such as germination (radicle, plumule, and embryo), seedling (Epicotyl and primary root), vegetative (root, petiole, stem, and leaf), reproductive (Petiole, stem, nodules, root, flowers, buds, pods, immature seeds, and leaf), and senescence (immature seeds, mature seeds, seed coat, stem, petiole, root, nodules, leaf, and yellow leaf). Log_2 transformed expression values were used to generate the heat-map using the MeV4 tool (Maryland, USA). RNA-Seq data for different seed developmental stages (S1–S7) in two distinct desi chickpea varieties (JGK3 and Himchana 1) was extracted from SRA number SRP072563 and SRP072564.

Plant Growth and Stress Treatment

Desi chickpea (var. ICC4958) was used for gene expression analysis. The seeds were surface sterilized and plants were grown according to Sagar et al. (2020). Ten-day-old seedlings were subjected to different stress treatments. For drought stress, water was withdrawn and seedlings were air-dried within the folds of tissue paper at 22–23°C temperature. Samples were harvested in replicates after 0 (untreated control), 1, 3, and 6 h of drought treatment. For salt stress, seedlings were kept in 150 mM sodium chloride (NaCl) solution in a beaker, and samples were collected after 0, 3, 6, and 12 h. Abscisic Acid (ABA) seedlings were kept in 100 μM (±) ABA in sterile water in a beaker under light and samples were collected after 0, 3, 6, and 12 h treatment. Same aged seedlings were kept in sterile water for control at 22–23°C.

RNA Extraction and cDNA Synthesis

A total of 100 mg tissue of the control, drought, salinity, and ABA treated root and shoot samples were used for RNA extraction using the TRIzol reagent (Ambion, Life technologies, USA) according to the manufacturer's protocol. The RNA obtained was purified to remove any genomic DNA contamination using an RNeasy Min Elute Clean-up Kit (QIAGEN, Hilden, Germany). The quantity and quality of RNA were ascertained by the ratio 1.8–2.0 for A260:A280 and 2.0–2.3 for A260:A230 using a Nano Drop ONEc (Thermo Scientific, USA) nano-spectrophotometer. Subsequently, MOPS-agarose gel electrophoresis was done to confirm the integrity of the RNA. A total of 1 μg total RNA was used to synthesize the first strand cDNA using a RevertAid first-strand cDNA synthesis kit (Thermo Scientific) according to the manufacturer's protocol.

Expression Analysis by qRT-PCR

The qRT-PCR primers for selected genes were synthesized by the PRIMER EXPRESS SOFTWARE (Applied Biosystems, USA) according to Singh and Pandey (2015). Their specificity was analyzed using the RGAP BLAST tool and melt curve analysis after a real-time PCR run. The details of all the primers are given in **Supplementary Table 1**. Three biological replicate samples (with three technical replicates of each biological replicate) of control and nutrient-deficient root and shoots were used to assess the expression pattern. iTaq Universal SYBR Green supermix (Bio-Rad) was used to detect the expression in Bio-rad CFX96 real-time PCR system (Bio-Rad) according to Sagar et al. (2021).

Statistical Analysis

For statistical significance, all expression and quantitative experiments were replicated three times. The data have been presented as the mean of three replicates ± SD. A two-tailed student's *t*-test was performed to determine the statistical significance among the replicate samples. A $p < 0.05$ was considered statistically significant (denoted by *), $p < 0.01$ (denoted by **) and $p < 0.005$ (denoted by ***).

RESULTS AND DISCUSSION

Identification and Organization of CDPK Family in the Chickpea Genome

A thorough investigation of various databases resulted in the identification of 22 non-redundant CDPK encoding genes in the chickpea genome. This is consistent with previous findings, where different plant species including *Arabidopsis thaliana*, rice (*Oryza sativa*), wheat (*Triticum aestivum L.*), and tomato (*Solanum lycopersicum*) have been found to encode for about 20–30 *CDPK* genes (Cheng et al., 2002; Ray et al., 2007; Li et al., 2008; Hu et al., 2016; Wang et al., 2016). Gene structure analysis showed that *CaCDPKs* are made up of multiple exons and introns. Most *CDPK* genes are comprised of 6-8 introns except *CaCDPK16*, which is comprised of 11 introns. Domain analysis revealed that all the CaCDPKs harbored a canonical catalytic kinase domain toward the N-terminus with a typical Ser/Thr kinase active site and ATP binding site (**Figure 1**). In addition, four EF-hand motifs were present in all the CDPK proteins toward the C-terminus, which are crucial for Ca^{2+} binding. Strikingly, a crucial Ca^{2+} binding site was found to be missing in one of the EF hand motifs of CaCDPK6, CaCDPK7, CaCDPK8, CaCDPK13, and CaCDPK22. The absence of such an important site might impair the Ca^{2+} binding ability of these CDPKs. However, variations in the number of EF-hand motifs and Ca^{2+} binding sites have also been previously reported in other plants (Cheng et al., 2002; Asano et al., 2005; Kong et al., 2013; Zuo et al., 2013). The in-depth analysis of N-terminal sequences of CaCDPKs revealed that out of 22 proteins, 11 have a myristoylation site (**Table 1**). The N-terminal domain of many CDPKs in several plant species has been found to contain potential N-myristoylation and N-palmitoylation sites. For example, AtCPK2, AtCPK3, AtCPK6, AtCPK9, AtCPK13, AtCPK5, and AtCPK16 (Benetka et al., 2008; Mehlmer et al., 2010; Lu and Hrabak, 2013), *N. tabacum* NtCDPK2/NtCDPK3 (Witte et al., 2010) and potato (*Solanum tuberosum*) StCDPK4/StCDPK5 (Asai et al., 2013) have been marked with N-myristoylation. These N-terminal modifications determine the membrane targeting of plant CDPKs, as mutations in N-myristoylation or N-palmitoylation sites have been found to hamper their membrane targeting (Singh et al., 2017). CDPKs show a high degree of structural conservation in terms of gene and protein structure, as similar exon-intron and domain arrangement pattern has been observed in diverse plant species including tomato, barley (*Hordeum vulgare* L.), *Brachypodium distachyon,* and *Medicago truncatula* (Hu et al., 2016; Yang et al., 2017; Wen et al., 2020; Zhao et al., 2021). Chickpea

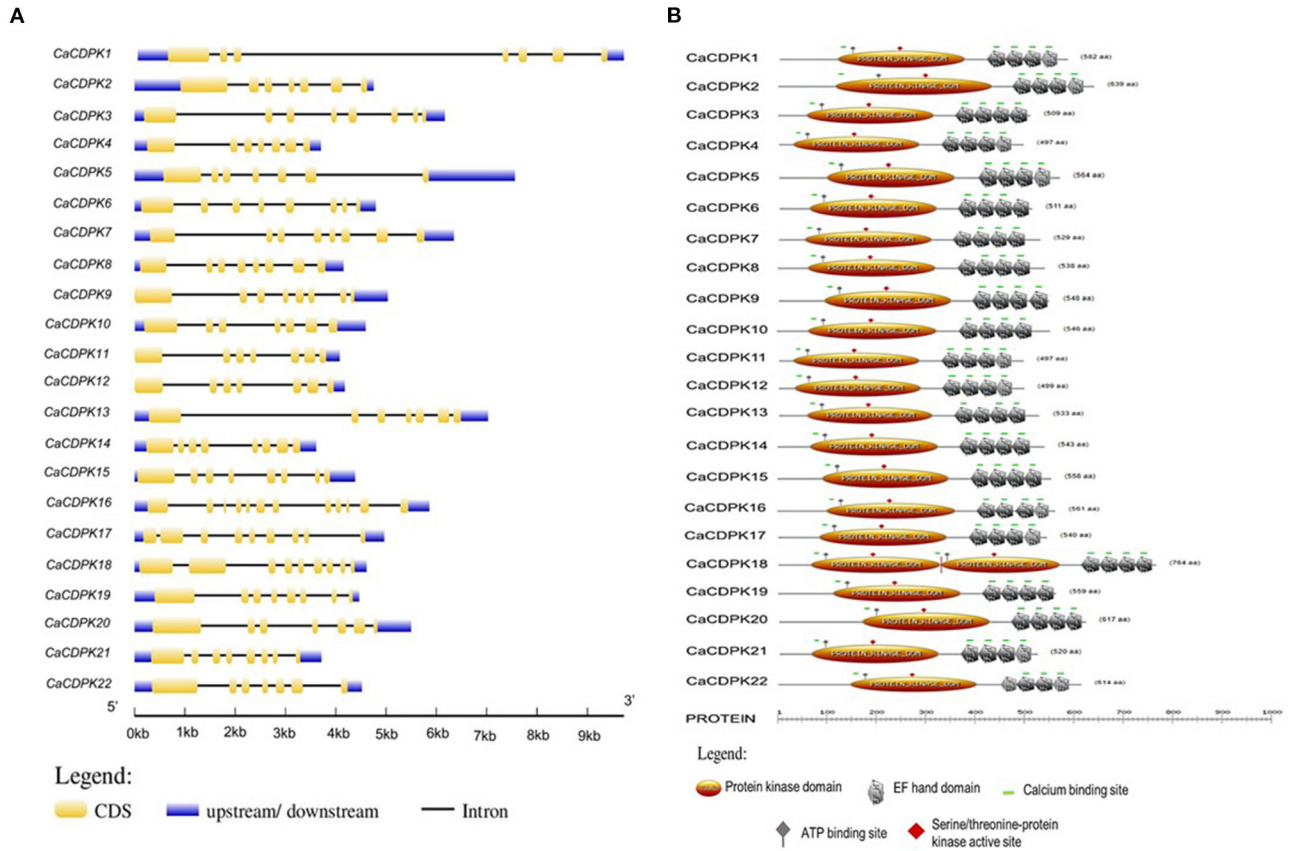

FIGURE 1 | Structural features of the chickpea calcium-dependent protein kinases (CDPK) family. **(A)** Exon-intron organization is shown for *CaCDPK* genes and gene names are mentioned at the left. The scale at the bottom represents gene length in kb. **(B)** Protein domain structure of the chickpea CDPK family is showing conserved protein kinase and EF-hand along with some important sites present. ATP binding site and Serine/threonine-protein kinase active site are located at the protein kinase domain.

CDPK proteins length was found to be in the range of 497–764 amino acids, and molecular weight varied between 56.16 and 68.74 KDa. Interestingly, CDPK protein had a highly variable isoelectric point (pI) falling in the range of 5.09 (CaCDPK22) and 8.99 (CaCDPK16) (**Table 1**). This indicates that the chickpea CDPK protein might function optimally in a diverse microenvironment.

Evolutionary Analysis of CDPK Family

To understand the evolution of chickpea CDPKs, phylogenetic analysis was performed with *Arabidopsis*, rice, soybean, and chickpea CDPK proteins. All the CDPKs from different plant species could be demarcated into four sub-clades; group I-IV(**Figure 2**). While, groups I and II each contained eight chickpea CDPK members, group III contained five CDPKs (CaCDPK7, 8, 10, 13, and 14), and group IV contained only a single CDPK member i.e., CaCDPK16. This phylogenetic distribution is conserved across different plant species, as group I comprises the highest number of CDPK members and group IV comprises the least members (Hu et al., 2016). This analysis suggests the evolutionary conservation of CDPKs across plant species. However, within the separate clades, chickpea CDPKs were closer to the dicot plants *Arabidopsis* and soybean, whereas distantly placed from monocot plant rice. Such distribution indicates the evolutionary divergence of monocot and dicot CDPKs.

Chickpea CDPK genes were mapped on the different chromosomes using their chromosomal coordinates. Out of 22 *CDPK* genes, 19 could be mapped on seven out of eight chickpea chromosomes. Three genes (*CaCDPK7*, *13,* and *17*) were placed on the scaffold region and none of the genes was localized on chromosome 1. *CaCDPK* genes were variably distributed on chromosomes, with chromosome 4 containing the highest five genes. Four and three *CDPK* genes were located on chromosomes 2 and 6, respectively. Two genes each were located on chromosomes 5, 7, and 8. Whereas, only a single gene, *CaCDPK8* was located on chromosome 3 (**Figure 3**). Gene duplication analysis revealed that three pairs of *CDPK* genes (*CaCDPK3/6*, *CaCDPK9/19,* and *CaCDPK11/12*) were segmentally duplicated. In addition, one gene pair, *CDPK2/20* was found to be tandemly duplicated. Gene duplication is considered an important process for the evolution of gene families in plants (Singh et al., 2010, 2014; Sagar et al., 2021). Similar to chickpea, the CDPK family has been evolved through

TABLE 1 | Summary of various features of the chickpea CDPK gene family.

S.No.	Gene name	Chromosome/Scaffolds	Protein ID	Exon number	CDS size	Proten length	pI	Mol. wt. (KDa)	N-Myristoylation
1	CaCDPK1	Ca4	XP_004498060.1	8	1,749	582	5.21	65.13	Non-Myristoylated
2	CaCDPK2	Ca4	XP_027189268.1	8	1,920	639	5.67	71.12	Non-Myristoylated
3	CaCDPK3	Ca8	XP_004511540.1	8	1,530	509	5.61	57.47	Myristoylated
4	CaCDPK4	Ca4	XP_004496370.1	7	1,494	497	5.33	55.85	N-terminal glycine absent
5	CaCDPK5	Ca2	XP_012568715.1	9	1,695	564	5.8	63.33	Non-Myristoylated
6	CaCDPK6	Ca6	XP_004503656.1	8	1,536	511	5.97	57.53	Non-Myristoylated
7	CaCDPK7	Unplaced scaffold	XP_004513770.1	8	1,590	529	6.62	59.88	Myristoylated
8	CaCDPK8	Ca3	NP_001266123.3	8	1,617	538	6.29	61.11	Myristoylated
9	CaCDPK9	Ca5	XP_004500067.1	8	1,647	548	6.15	61.79	Myristoylated
10	CaCDPK10	Ca7	XP_004508790.1	7	1,641	546	6.1	61.61	Myristoylated
11	CaCDPK11	Ca6	XP_004503860.1	7	1,494	497	5.33	56.16	N-terminal glycine absent
12	CaCDPK12	Ca5	XP_004503020.1	7	1,500	499	5.18	56.58	N-terminal glycine absent
13	CaCDPK13	Unplaced scaffold	XP_004514214.1	7	1,602	533	6.03	59.93	Non-Myristoylated
14	CaCDPK14	Ca6	XP_004507321.1	8	1,632	543	5.88	61.84	Myristoylated
15	CaCDPK15	Ca7	NP_001266075.1	8	1,671	556	5.92	62.15	Myristoylated
16	CaCDPK16	Ca8	XP_004512135.1	12	1,686	561	8.99	63.71	Myristoylated
17	CaCDPK17	Unplaced scaffold	XP_012574838.1	9	1,623	540	5.8	63.33	Myristoylated
18	CaCDPK18	Ca4	XP_004499307.1	9	2,295	764	6.89	86.37	Non-Myristoylated
19	CaCDPK19	Ca2	XP_004491400.1	8	1,680	559	6.46	63.38	Myristoylated
20	CaCDPK20	Ca4	XP_004497622.1	7	1,854	617	5.15	67.77	Non-Myristoylated
21	CaCDPK21	Ca2	XP_004491231.1	8	1,563	520	5.34	58.11	Myristoylated
22	CaCDPK22	Ca2	XP_004489857.1	7	1,845	614	5.09	68.74	Non-Myristoylated

segmental and tandem duplication in diverse plant species, such as *Arabidopsis*, rice, cotton, poplar, moss (*P. patens*), and cabbage (*Brassica rapa*) (Hrabak et al., 2003; Ray et al., 2007; Zuo et al., 2013; Hamel et al., 2014; Liu et al., 2014; Wu et al., 2017). However, the extent of duplication has been found to be varied in different species. For instance, chickpea had only three segmentally duplicated pairs, whereas nine and eight gene pairs were segmentally duplicated in the rice and *Arabidopsis* genomes, respectively (Ray et al., 2007). This indicates that gene duplication is a conserved mechanism of the evolution and expansion of the CDPK family in plants.

3D Protein Structure Analysis

To get an insight into the 3-D protein structure of chickpea CDPKs, homology-modeling was performed for all the CaCDPKs. The protein structures were obtained by comparing with related template protein pbanka-031420 (PDB id 3Q5I). All protein structures were modeled with the template protein with 100% confidence. Most proteins were modeled with a high coverage level ranging from 72 to 90%. The 3-D structures of different CaCDPKs were comprised of a variable number of α-helix, β-strands, disordered region, and transmembrane (TM) - helix (**Supplementary Table 2**). Among these, the most frequently occurring secondary structure was the α-helix, which warrants the stability of protein structure (Neelamathi et al., 2009). The percentage of α- helices varied from 36 to 48, whereas the β-strands contributed to 11–19% of the protein structure (**Supplementary Table 2**). In all the CaCDPK proteins, structural folds made up of blue and green α- helices and β-strands represent the catalytic kinase domain. Orange and red color ribbons represent the N-lobe and C-lobe, respectively with each lobe containing two EF hand motifs. Whereas, an inhibitory junction domain (JD) is represented by yellow helical ribbons (**Figure 4**). Thus, the presence of important characteristic domains and motifs in all the CaCDPK proteins confirms their authenticity and integrity. Similar features of the 3-D structure of CDPK proteins were obtained in different plant species including *Arabidopsis*, rice, maize, ginger (*Zingiber officinale*), and sorghum (Mittal et al., 2017; Vivek et al., 2017). Suggesting that the CDPK protein structure is highly conserved, with similar structural folds and conformational arrangements in higher plants. This also hints toward their conserved functional and structural mechanism.

Subcellular Localization of CaCDPK Proteins

To identify the possible sites of activity of CaCDPK proteins in order to have an insight into their function, *in-silico* subcellular localization was performed. By considering the highest reliability score, 15 CaCDPK proteins were exclusively localized in the cytoplasm, whereas only two proteins, CaCDPK16 and 19 were exclusively localized in the nucleus (**Figure 5A**). Five CDPK proteins, CaCDPK2, 5, 9, 15, and 18 could be localized both in the cytoplasm and nucleus. To validate the *in-silico* localization pattern, fluorescence-based subcellular localization was performed in *N. benthamiana* for three randomly selected candidates; CaCDPK5, 16, and 21. Confocal microscopy analysis

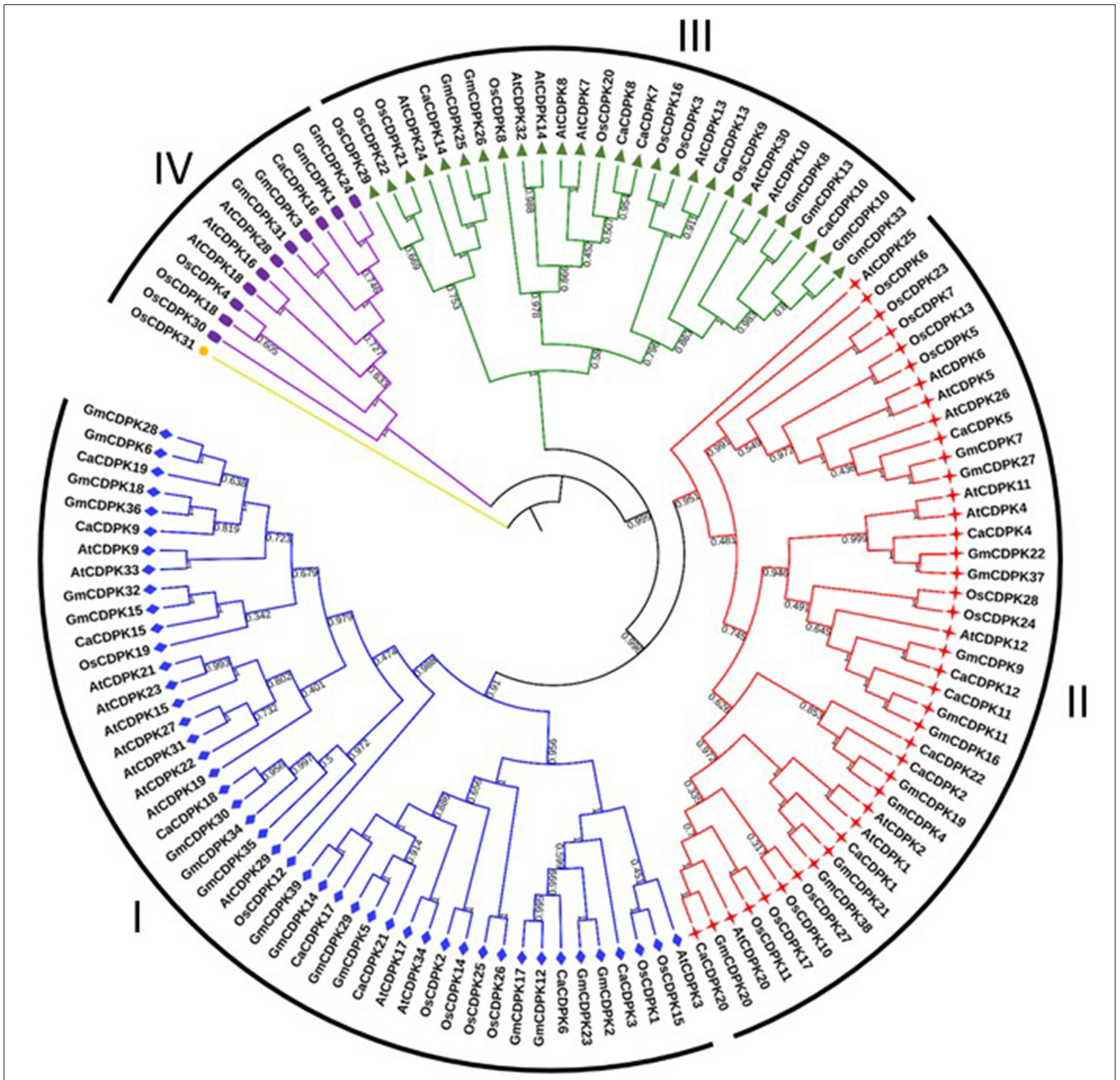

FIGURE 2 | Phylogenetic relationship among CDPKs from different plants. An un-rooted neighbor-joining phylogenetic tree was constructed from the CDPK protein sequences of *Arabidopsis thaliana*, rice, soybean, and chickpea. All the CDPKs could be divided into four groups; I- IV. Numbers above the nodes represent bootstrap values calculated from 1,000 replicates.

revealed that CaCDPK5 was localized in both the nucleus and cytoplasm and CaCDPK21 was localized at the cytoplasm (**Figure 5B**) which is consistent with *in-silico* prediction. Whereas, CaCDPK16, which was predicted to be nucleus localized was actually localized in the cytoplasm of *Nicotiana* cells. Thus, *in-planta* localization significantly supported and validated the *in-silico* localization pattern. These findings indicate that CaCDPKs might phosphorylate different substrates in the cytoplasm and in the nucleus to regulate various cellular functions in chickpea. CDPKs have been found to be localized at diverse subcellular locations in plants. Most of the CDPKs in Arabidopsis are either membrane-localized or are localized at both cytoplasm and membrane. Whereas, a few AtCDPKs are exclusively cytoplasm localized (Simeunovic et al., 2016). N-myristoylation and palmitoylation are crucial modifications of CDPK proteins that determine CDPK localization (Simeunovic

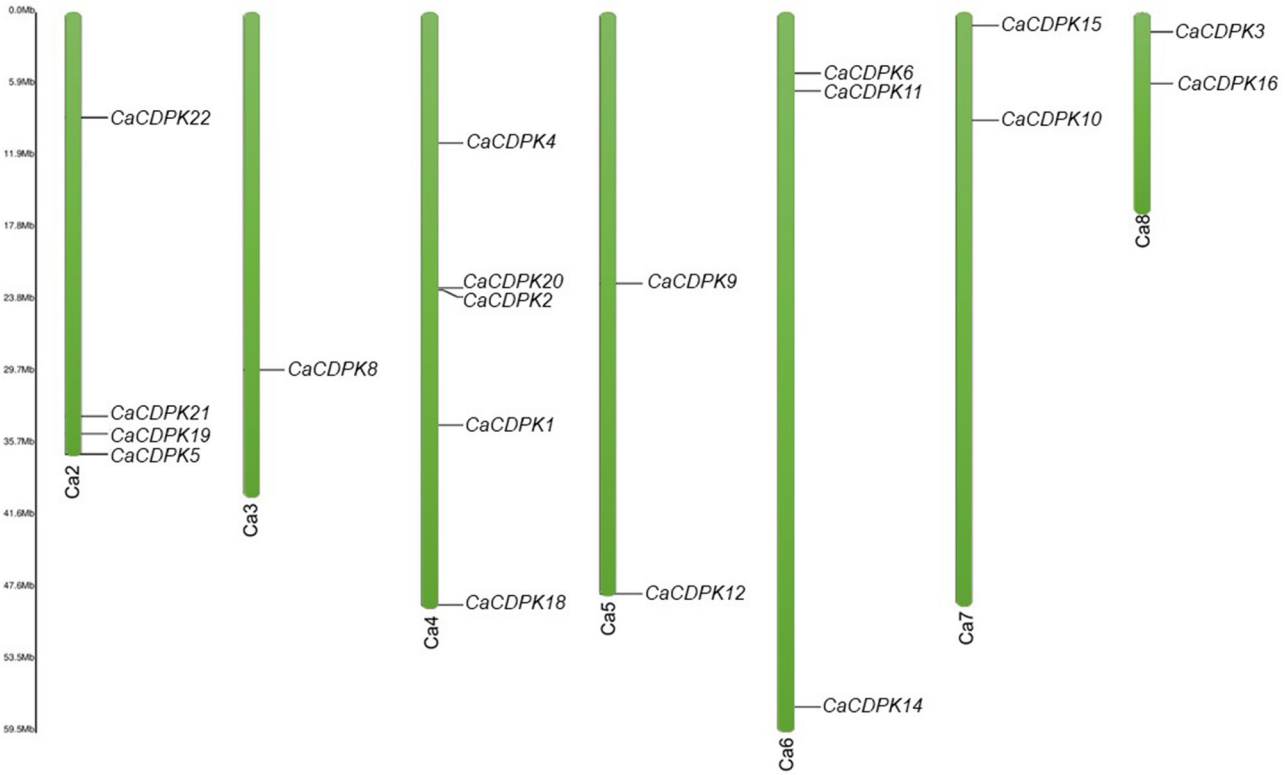

FIGURE 3 | Chromosomal locations of chickpea *CDPK* genes. Green color bars represent the chromosomes, the location of genes has been marked alongside. Chromosome numbers are given at the bottom of each chromosome. Except chromosome 1, the CDPK genes are distributed variably on seven chromosomes.

et al., 2016; Zheng et al., 2019). Recently, a study on legume plant *Medicago truncatula* showed that the CDPKs with N-terminal acylation sites were localized at the plasma membrane whereas, those lacking the N-acylation sites were distributed in cytosol and nucleus (Zhao et al., 2021). Consistently, in our study CaCDPK2, 5, and 18 were devoid of N- myristoylation site and distributed in nucleus and cytosol. Surprisingly, several CaCDPK proteins were marked with N- myristoylation site but none of them was found to be localized at the plasma membrane. It is known that N-myristoylation is an irreversible acylation, it requires a second post-translational signal i.e., reversible palmitoylation to sustain membrane localization of a CDPK (Witte et al., 2010). Therefore, the absence of a palmitoylation site in CaCDPK proteins could be a possible reason for them not to be localized at the plasma membrane. Also, the reversibility of the second post-translational signal could lead to the ferrying of CDPK between membrane and cytosol or nucleus (Boudsocq and Sheen, 2013). Moreover, the localization of CaCDPK proteins could be coupled with a stimulus, and a particular condition may lead to a change in their subcellular location. For example, the subcellular location of *Arabidopsis* AtCPK10, AtCPK30, and AtCPK32 proteins was changed due to variable NO_3^- availability (Liu et al., 2017).

cis-Elements in CDPK Promoters

The cis-regulatory elements in the promoter are crucial for the transcriptional regulation of a gene. Therefore, to get an insight into the transcriptional regulation of *CaCDPK* genes their promoters were investigated for *cis*-regulatory elements. A total of 16 types of *cis*-regulatory elements were found to be variably distributed in *CaCDPK* promoters (**Figure 6**, **Supplementary Table 3**). These elements majorly belong to three categories; stress-responsive (GT1-motif, LTR, WUN-motif, ARE, TC-rich repeats, Box-4, AE-box, MYB, Myb-like, MYC, chs-CMA1a, and STRE), hormone-responsive (ABRE, ERE), and plant development related (AAGAA-motif, GATA-motif) (Hughes et al., 2000; Abe et al., 2003; Yamaguchi-Shinozaki and Shinozaki, 2005; Sharma et al., 2011; Nakashima and Yamaguchi-Shinozaki, 2013; Deepika and Singh, 2021; Hou et al., 2021). Abiotic stress-related motif Box-4 (light-responsive) was present in all *CaCDPK* promoters, and MYB motif (drought, low temperature, salt stress-related) was found in all *CaCDPK* promoters except *CaCDPK2*. This suggests that by binding these motifs, specific TFs might regulate the expression of *CaCDPKs* under different abiotic stresses. Markedly, 14 out of 21 *CaCDPK* promoters which contain the MYB motif were also found to contain the ABRE motif (ABA-responsive element), suggesting that these genes could regulate abiotic stresses, such as drought and salinity *via* the ABA-dependent pathway. It has been well-understood that different developmental events and abiotic stresses are interconnected through ABA in plants (Schroeder et al., 2001; Singh et al., 2015). Especially, during the later stages of seed development,

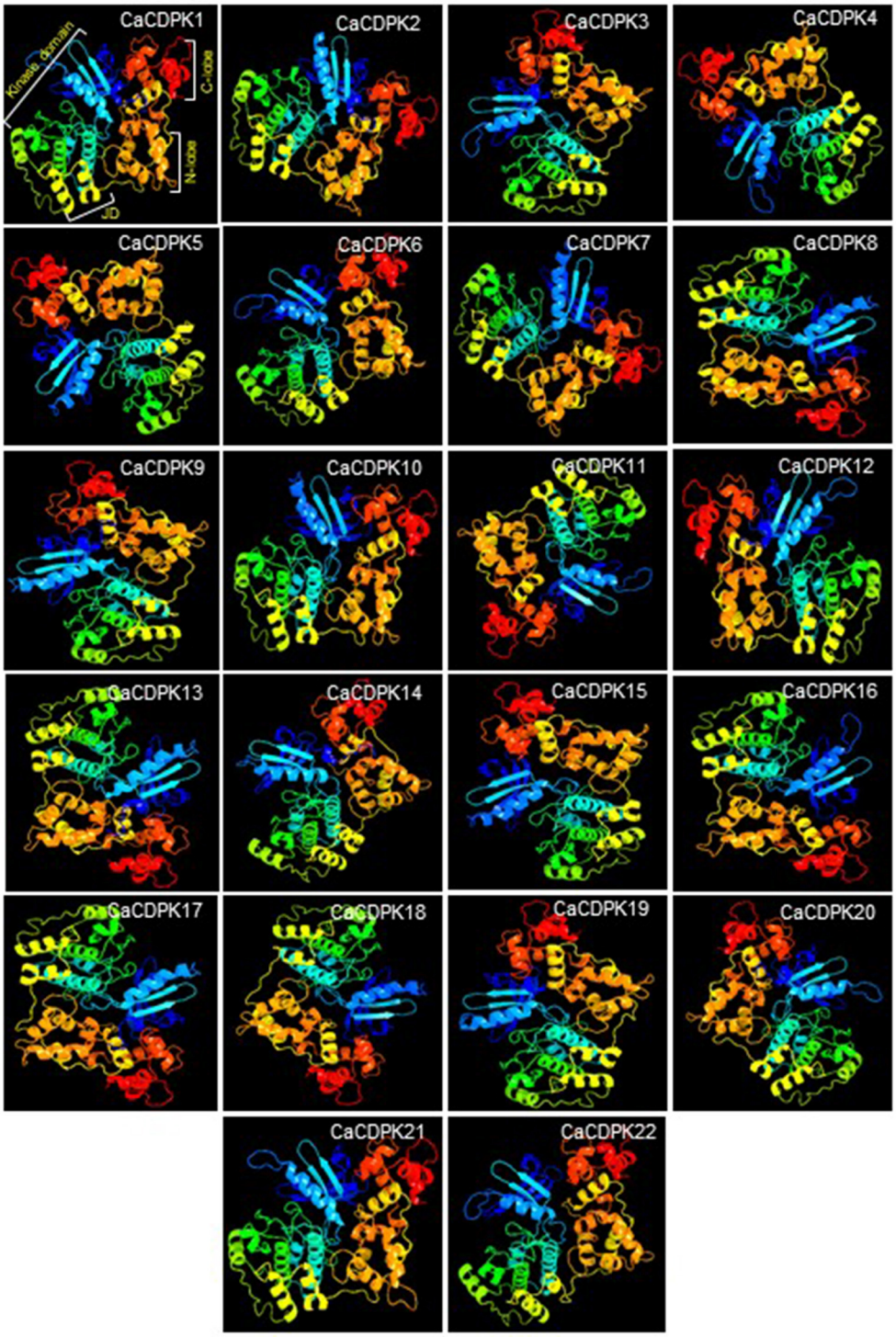

FIGURE 4 | Three-dimensional structure of chickpea CDPK proteins. A three-dimensional (3-D) structure was generated for all 22 members of the chickpea CDPK family. Each CDPK protein is made up of a variable number of α-helix, β-strands, transmembrane helix, and disordered region. Structure comprising blue and green α-helices and β-strands represents kinase domain, yellow helical ribbons represent inhibitory junction domain (JD), orange helices indicate N-lobe, and red helices indicate C-lobe with each containing two elongation factors (EF) hand motifs.

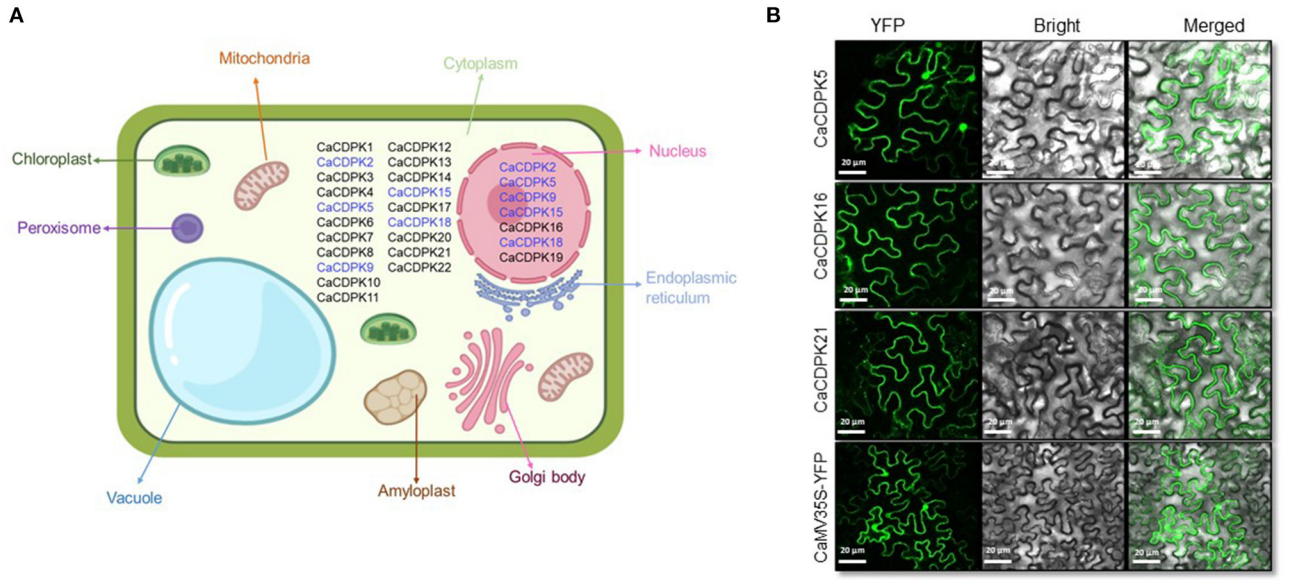

FIGURE 5 | Subcellular localization of chickpea CDPK proteins. **(A)** Localization was predicted using an online tool, CELLO. The figure shows chickpea CDPK proteins localized majorly in the cytoplasm and nucleus based on the highest reliability score with black color. Proteins that were predicted to be localized both in the cytoplasm and nucleus are shown by blue color at both locations. **(B)** *N. benthamiana* cells expressing the YFP- fusion protein driven by the 2XCaMV 35S promoter. Confocal images of fluorescence expressing CaCDPK proteins are showing their variable distribution in different compartments. CaCDPK5 is localized to the cytoplasm and nucleus, whereas CaCDPK16 and CaCDPK21 are localized at the cytoplasm. Cells transformed with vector only (CaMV35S-YFP) are shown in the lowermost row. Scale bar = 20 µm.

a programmed dehydration event is triggered that results in seed dormancy (Hetherington, 2001; Schroeder et al., 2001). ABA commonly regulates these developmental and abiotic stress responses (Nakashima et al., 2009; Hubbard et al., 2010), and genes, which are involved in the regulation of such responses have been found to contain ABRE elements in their promoters (Singh et al., 2012, 2013). Thus, *CaCDPK* promoters with elements like MYB and ABRE could be involved in regulating chickpea plant development under abiotic stress conditions. Apart from two promoters (*CaCDPK4* and *16*), all the *CaCDPK* promoters also contained one or more ethylene-responsive, ERE motifs. Ethylene is an important plant hormone that is involved in plant defense and development (Mishra et al., 2013). The presence of the ERE element in most of the *CaCDPK* promoters reinforces the involvement of the CDPK family in plant development, biotic and abiotic stress responses in chickpea. Consistently, CDPK family members have been found to regulate development during plant-pathogen interaction, herbivore attack, and wounding in diverse plant species (Cai et al., 2015; Zhang et al., 2015; Hettenhausen et al., 2016; Xiao et al., 2017).

Expression Pattern of *CaCDPKs* in Developmental Stages

To get an insight into the functional role of CDPK genes in plant development, expression analysis was undertaken during various stages of chickpea development. Expression profiles of all *CaCDPK* genes were generated during 27 development stages. These stages represent germination, seedling, vegetative stages, reproductive stages, and senescence. All genes except *CaCDPK2* showed a differential expression pattern during multiple developmental stages (**Figure 7**, **Supplementary Table 4**) A total of 10 genes showed ubiquitous expression during most developmental stages these include, *CaCDPK1, 5, 6, 8, 10, 11, 12, 13, 16,* and *19*. Out of these, *CaCDPK8* had the strongest expression during most stages of reproductive development, and some stages of vegetative development and senescence. Notably, the expression of all these 10 *CaCDPK* genes was relatively lower in three stages of senescence namely, immature seeds, mature seeds, and seed coat. This suggests that these *CaCDPK* genes could be involved in a range of developmental processes from germination to senescence. Some of the genes, including *CaCDPK7, 14, 17,* and *21* showed a significant and specific expression in flowers, suggesting their role in flower development. This observation is consistent with previous findings where CDPKs were implicated in flower development. FLOWERING LOCUS T (FT) is an important component of the regulatory network of flower development and it forms a complex with its interdependent partner AtFD (also known as AtbZIP14). *Arabidopsis* CDPK members, AtCPK4/AtCPK6/AtCPK33 phosphorylate AtFD at T282 *in-vitro* in presence of Ca^{2+}, which is crucial for the formation and function of this complex. This complex triggers the transcriptional activation of floral meristem identity genes which control floral transition (Abe et al., 2005; Kawamoto et al., 2015). Thus, genes like *CaCDPK7, 14, 17,* and *21* could be involved in similar regulatory networks controlling flower development in chickpea.

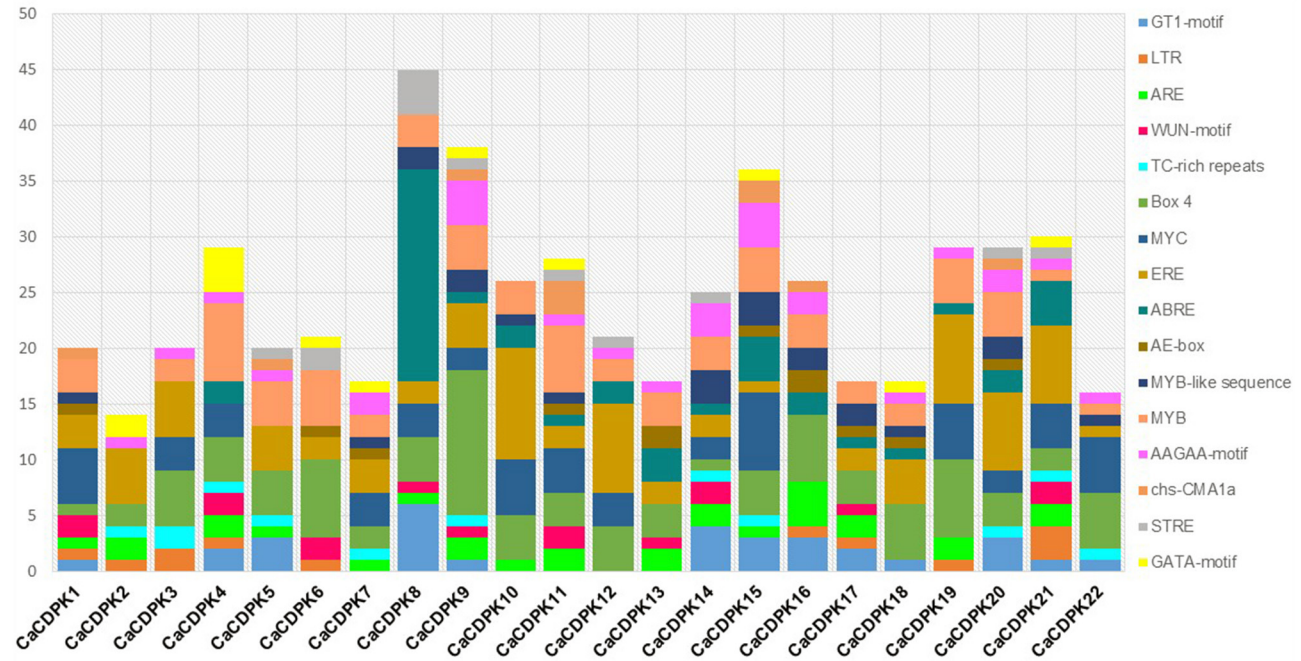

FIGURE 6 | Promoter analysis of chickpea *CDPK* genes. Different *cis*-regulatory elements in the 2 kb upstream promoter region of *CaCDPK* genes are illustrated by different colors in the bar chart. The X-axis represents the name of genes and Y-axis represents the number of different *cis*-elements in each promoter. The names of cis-regulatory elements are mentioned on the right.

In *Arabidopsis*, expression and functional analysis indicated the role of multiple CDPKs in pollen tube growth. Analysis of single and double mutants of *CDPK17* and *CDPK34* revealed that their redundant activity is required for pollen tube tip growth and pollen fitness (Myers et al., 2009). A shaker-type K^+ inward channel mediates the K^+ influx which is crucial for pollen tube growth in *Arabidopsis*. CPK11 and CPK24 work together to inhibit this channel, thereby suppressing pollen tube growth (Zhao et al., 2013). Similarly, CPK2 and CPK20 control pollen tube growth *via* regulating another ion channel SLAH3 (Gutermuth et al., 2013). Furthermore, CDPKs regulate plant development via modulating phytohormone signaling. AtCDPK28 regulates the expression of key GA biosynthesis genes (e.g., gene coding for GA3ox1) and thus, controls various facets of plant development, including petiole and stem elongation (Matschi et al., 2013). Similarly, in *Nicotiana attenuata,* NaCDPK4 and 5 regulating GA activity positively regulate stem elongation and plant height (Heinrich et al., 2013). In our study, *CaCDPK15* was specifically and strongly down-regulated during the germination stage of plumule, vegetative stage of petiole and stem, and senescence stage of the petiole. Thus, *CaCDPK15* could be a crucial regulator of the petiole, stem elongation, and plant height in chickpea.

Expression Pattern in Seed Development in Two Contrasting Chickpea Cultivars

The seed is the most important part of the chickpea plant from the yield point of view. Therefore, to understand the role of the CDPK family in seed development, expression analysis was performed in two contrasting chickpea cultivars i.e., large-seeded JGK3 and small-seeded Himchana 1. The expression pattern was analyzed during seven stages of chickpea seed development representing early-embryogenesis (S1), mid-embryogenesis (S2), late embryogenesis (S3–S4), mid-maturation (S5), and late-maturation (S6–S7) stages (Rajkumar et al., 2020). Total 17 *CaCDPK* genes expressed differentially in both chickpea cultivars. Out of these, nine genes (*CaCDPK2, 3, 6, 8, 9, 12, 14, 16,* and *20*) were found to be up-regulated, whereas eight genes (*CaCDPK4, 7, 11, 13, 15, 18, 19,* and *22*) were down-regulated in one or more seed stages in both the cultivars (**Figure 8**, **Supplementary Table 5**). Notably, most up-regulated *CaCDPK* genes were induced during S1–S4, while their expression was insignificant during later seed stages (S5–S7). In contrast, the most down-regulated genes had significant negative expression during later stages of seed development (S5–S7). This indicates that different sets of *CaCDPK* genes are involved in positively regulating early to late embryogenesis, and negatively regulating mid-late maturation phases of seed development, both in JGK3 and Himchana1 cultivars. *CaCDPK3* and *CaCDPK14* showed similar expression patterns (up-regulation) from the S1–S4 stages with the highest expression in the S4 stage. however, their expression level was higher in JGK3 than Himchana 1. *CaCDPK2* had significant expression during S3 and S4 stages in both the cultivars. *CaCDPK4* showed common as well as cultivar-specific expression as it was specifically down-regulated in the S6 stage of both JGK3 and Himchana1, and S5 and S7 stages of Himchana1

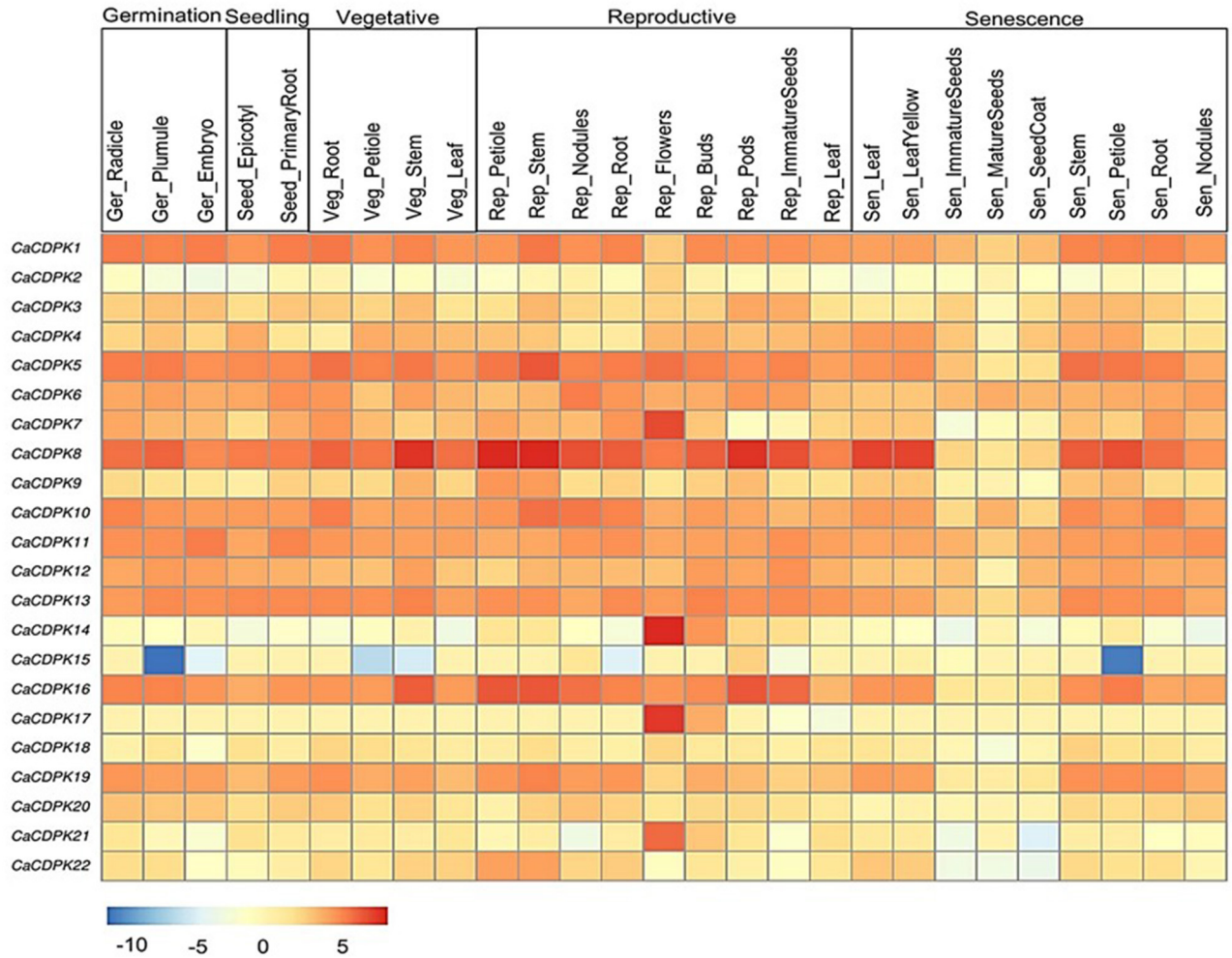

FIGURE 7 | Expression profiles of *CDPK* genes in different developmental stages of chickpea. The heatmap represents the expression pattern of *CaCDPK* genes in different tissues of developmental stages, such as germination, seedling, vegetative, reproduction, and senescence. The genes are named on the left and different tissues/developmental stages are labeled at the top. Scale bar represents the normalized log_2 FPKM values.

and JGK3, respectively. *CaCDPK15* showed a peculiar expression pattern, it was specifically down-regulated only in S2 and S4 stages of Himchana1. *CaCDPK7* could be a major negative regulator of the entire process of seed development as it was ubiquitously down-regulated during all the seed stages in both chickpea cultivars. Like chickpea, rice orthologs of CDPKs, such as *OsCPK21, OsCPK23,* and *OsCPK31* were found to be strongly up-regulated during different seed developmental stages (Ray et al., 2007). Overexpression of seed-specific *OsCPK31* results in early grain filling, and seed maturation in rice (Manimaran et al., 2015). As suggested by previous reports, CaCDPKs could phosphorylate specific targets/substrates which are important components of the seed development process in chickpea. For instance, a castor (*Ricinus communis*) CDPK protein, RcCDPK2 phosphorylate a sucrose synthase, RcSUS1 at Ser-11 in developing castor oil seed (COS). RcSUS1 cleaves the imported sucrose, thereby, it generated the storage end product in developing COS (Fedosejevs et al., 2016). Similarly, RcCDPK1 *in vivo* phosphorylates Phosphoenolpyruvate carboxylase (PEPC) interacting bacterial-type (BTPC) subunits at Ser-451, and this phosphorylation is inhibitory for BTPC activity. Thus, RcCDPK1 regulates respiratory CO_2 refixation and anaplerotic photosynthate partitioning in developing COS (Ying et al., 2017).

qRT-PCR Expression Analysis Under ABA, Drought, and Salinity Stress

The onslaught of abiotic stresses, such as drought and salinity triggers the increase in cytosolic Ca^{2+} concentration, leading to the generation of stimulus-specific "Ca^{2+} signatures." These signatures once sensed, trigger specific and overlapping downstream signaling cascades toward an adaptive response. CDPKs are a major class of Ca^{2+} sensors in plant cells that plays a crucial role in the plant's adaptation to stress conditions. Therefore, to understand their role in abiotic stress signaling in chickpea, qRT-PCR analysis was performed for 10 selected genes i.e., *CaCDPK3, 4, 5, 7, 8, 14, 16, 18, 21,* and 22 under abiotic

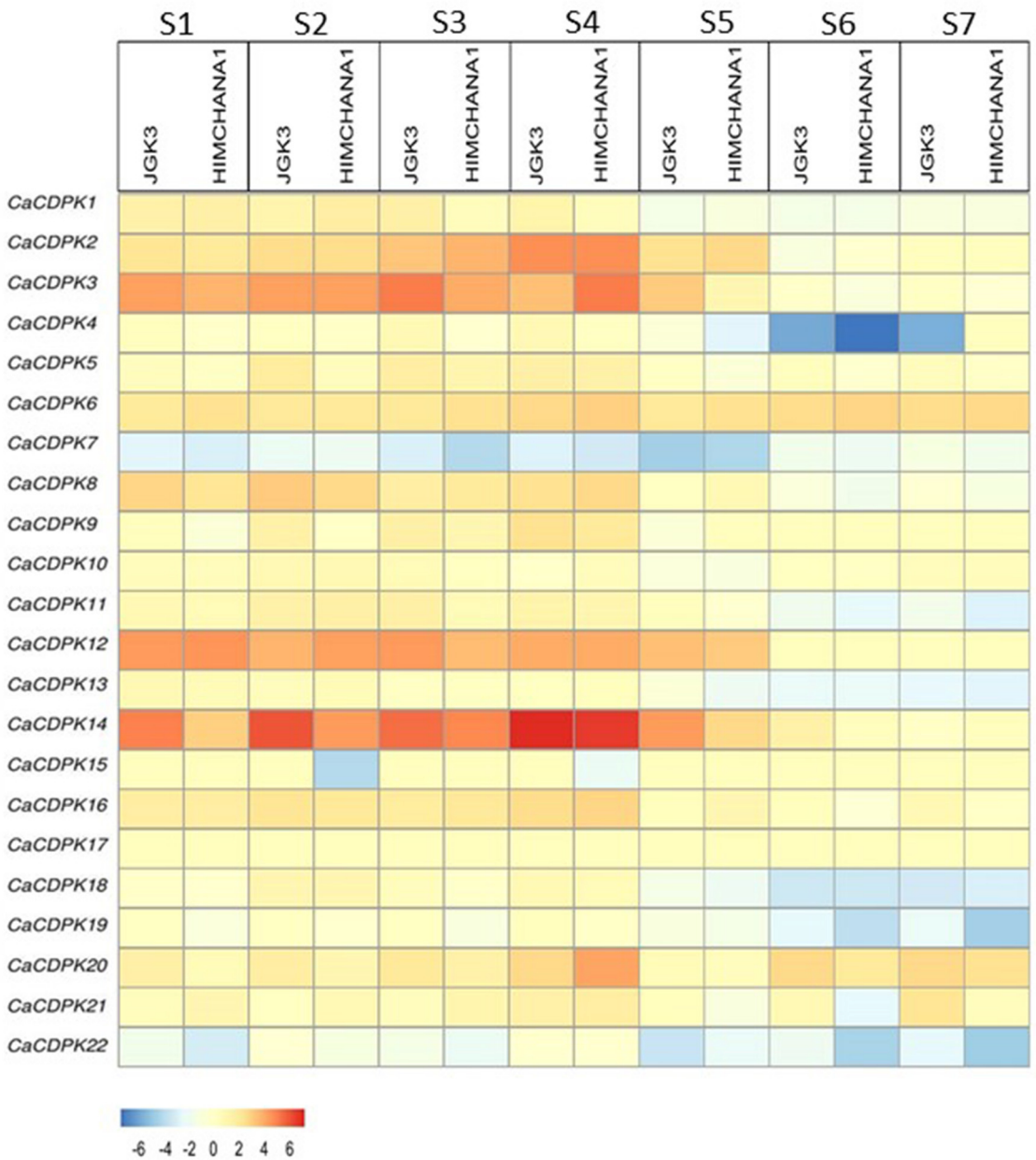

FIGURE 8 | Expression profiles of *CDPK* genes during different stages of seed development in chickpea. Expression profiles are shown for seven seed developmental stages (S1–S7) in two chickpea cultivars: large-seeded JGK3 and small-seeded Himchana1. The genes are named on the left and stages/cultivars are labeled at the top. The scale bar represents the log_2 Fold Change FPKM values.

stresses such as drought, salt stress, and phytohormone ABA. Expression profiles were generated at different time points, in root and shoot tissues separately. Based on the expression fold change value ≥1.5 w.r.t. untreated control, all 10 *CaCDPK* genes were found to be differentially expressed under one or more stress conditions (**Figure 9**, **Supplementary Table 6**). In roots, except *CaCDPK7* and *8*, eight genes express differentially under drought conditions. *CaCDPK5, 14,* and *21* were significantly up-regulated after 1, 3, and 6 h of drought treatment, while *CaCDPK22* was up-regulated after 3h and 6h of drought treatment. *CaCDPK3* and *16* were exclusively induced after 1h of drought treatment and *CaCDPK4* showed significant up-regulation after 6h drought only (**Figure 9**). Thus, these *CaCDPK* genes could be categorized as early inducing, late inducing, and ubiquitously expressed. Under ABA treatment, *CaCDPK4, 14, 16, 18,* and *22* were found to be differentially expressed.

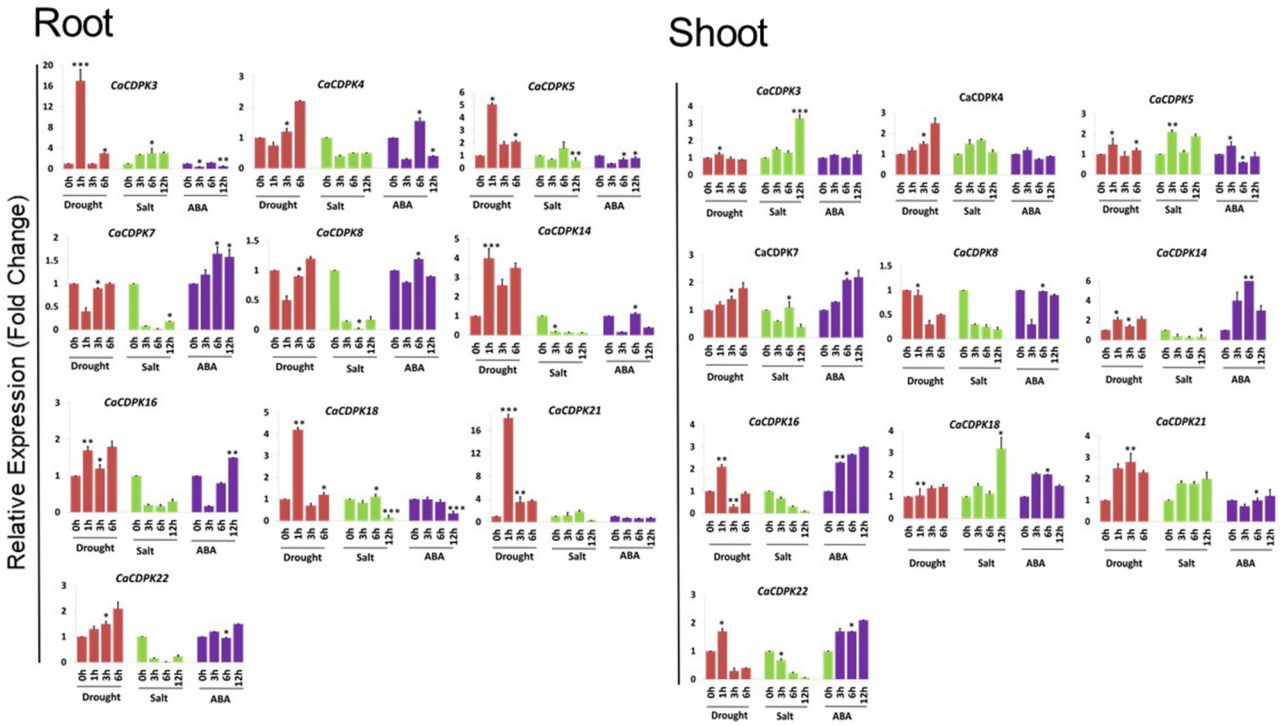

FIGURE 9 | Expression profiles of *CDPK* genes under drought, salt, and ABA treatments in chickpea. qRT-PCR analysis was performed to generate the expression profile of *CaCDPK* genes under drought, salt, and ABA treatment in root and shoot of desi chickpea (ICC4958). Different treatments and time points are indicated on X-axis and the relative expression level of the gene is indicated on Y-axis. Each bar represents the mean value of three replicates. Standard error among the samples is indicated by error bars. $^{*}p < 0.05$, $^{**}p < 0.01$ and $^{***}p < 0.005$ for treated samples w.r.t. untreated control.

Drought-induced *CaCDPK4, 16,* and *22* were also up-regulated during the mid (6 h) and late stages (12 h) of the ABA treatment. ABA is known to regulate various aspects of plant growth, including root growth and seed germination (Sagar and Singh, 2019). An overlapping expression of *CaCDPK4, 16,* and *22* under ABA and drought indicates that these CaCDPKs might be involved in regulating root growth *via* the ABA-dependent pathway, and improving water uptake under drought stress. The ABA pathway commonly regulates response to osmotic stresses, including drought and salinity stress (Singh et al., 2016). Numerous studies have revealed the co-regulation of several genes under drought and salinity stress (Ray et al., 2007; Singh et al., 2015, 2017). Surprisingly, in our study, except *CaCDPK3* most drought-induced *CaCDPK* genes were found to be down-regulated under salt stress. Salt stress is known to be inflicted through two components; osmotic and ionic stress (Verslues et al., 2006). The osmotic component is common in both drought and salt stress, whereas the ionic component is unique to salt stress. It is possible that CaCDPKs might regulate salt stress response through its ionic component only, however, it requires detailed functional investigation. Like in roots, *CaCDPK* genes are expressed differentially in one or more conditions in the shoot. Seven genes (*CaCDPK4, 7, 8, 14, 16, 21,* and *22*) showed differential expression under drought stress conditions. *CaCDPK8* was down-regulated in both the stresses and under ABA treatment. Similar to the root, *CaCDPK21* showed a continuous induction (1–6 h) under drought stress, and *CaCDPK4* was induced after 6 h. *CaCDPK22* which showed strong induction after 3 and 6 h drought in roots was found to be up-regulated after 1 h but down-regulated after 3 and 6 h drought treatment. Interestingly, *CaCDPK5* which was continuously expressed in roots showed insignificant expression in shoot whereas, *CaCDPK7* which had insignificant expression in roots was up-regulated after 6 h in the shoot, under drought. This suggests that some CaCDPKs preferentially express in the root or shoot tissues, and possibly regulate tissue-specific functions. Four genes, including *CaCDPK7, 14, 16,* and *22* were found to be up-regulated both under drought stress and ABA treatment. ABA is produced under drought conditions and it regulates the stomata closure. Drought-activated CaCDPKs might phosphorylate and regulate guard cell ion channels to regulate the stomata movement in an ABA-dependent manner, to reduce the transpiration rate and water loss under drought stress in chickpea. Previously, AtCPK3, AtCPK6, AtCPK21, and AtCPK23 have been shown to phosphorylate and regulate SLOW ANION CHANNEL (SLAC1), Ca^{2+} permeable channels, and SLOW ANION CHANNEL-ASSOCIATED (SLAH3) to promote ABA-dependent stomata closure (Mori et al., 2006;

Geiger et al., 2010, 2011). Besides phosphorylation, CaCDPKs may also regulate the stomata movement in chickpea through interaction with different proteins, as previously shown by the interaction of AtCPK8 with CATALASE3 (CAT3) and that of OsCPK21 with 14–3–3 protein (OsGF14e) (Zou et al., 2015; Chen et al., 2017). Strikingly, *CaCDPK14* which was strongly induced during most of the seed developmental stages (**Figure 8**), was also induced under drought and ABA treatment. Careful analysis showed that the promoter of *CaCDPK14* contains an ABRE element. As discussed earlier, seed development and drought stress are interconnected, and ABA is known to simultaneously regulate these processes. Probably by regulating drought response *CaCDPK14* might control seed development *via* the ABA-dependent pathway in chickpea. Such genes could be the potential targets for improving abiotic stress tolerance and crop yield, thus could be of great biotechnological importance.

Unlike roots, at least four genes, including *CaCDPK3, 5, 18,* and *21* were up-regulated under salt stress in the shoot. *CaCDPK21* showed continuous expression after 3, 6, and 12 h of salinity treatment, *CaCDPK5* was induced after 3 and 12 h whereas, *CaCDPK3* and *18* expressed during later stage (12 h) of salt stress (**Figure 9**, **Supplementary Table 6**). These CaCDPKs might regulate root-shoot translocation of Na^+ ion, sequestration of excess Na^+ from subcellular compartments into the vacuole, and in the maintenance of Na^+/K^+ homeostasis in plant cells under salinity stress. CPK3 (Mehlmer et al., 2010) and CPK27 (Zhao et al., 2015) have been shown to regulate Na^+ toxicity and K^+ uptake, respectively, in *Arabidopsis* that leads to salt stress tolerance. CDPKs also control oxidative damage or ROS homeostasis to protect the plants from the deleterious effects of stresses, including drought and salinity. For instance, OsCPK12 promotes the expression of ROS scavenger gene *OsAPX2/OsAPX8* and suppresses the expression of NADPH oxidase gene *OsRBOHI*, thereby regulating ROS homeostasis and improving tolerance to salt stress in rice (Asano et al., 2012). Overall, this analysis revealed the spatiotemporal pattern of *CaCDPK* genes expression in chickpea. This hints toward specific and common phosphorylation targets/substrates of CaCDPKs under abiotic stresses in the root and shoot tissues in chickpea.

CONCLUSIONS

In conclusion, a total of 22 non-redundant *CDPK* encoding genes are identified in the chickpea genome. Protein structure and phylogenetic analysis revealed that the CDPK family is highly conserved in terms of structure and evolution, in higher plants. Subcellular localization suggests that most CaCDPK members may target various substrates in the cytoplasm and nucleus to regulate diverse functions. The expression pattern suggests the crucial role of several CDPK members in abiotic stress tolerance and plant development in chickpea. Importantly, some candidate CaCDPKs might regulate drought stress response and seed development. Such genes could be important in determining the crop yield thus, will be of great biotechnological importance. In the future, efforts must be directed for the identification of targets/substrates of key CaCDPKs to delineate CDPK mediated signaling networks underlying abiotic stress response and plant development. Ultimately, knowledge obtained from this study will help in developing abiotic stress-tolerant and high yielding chickpea cultivars that will contribute to world food security.

DATA AVAILABILITY STATEMENT

The original contributions presented in the study are included in the article/**Supplementary Material**, further inquiries can be directed to the corresponding author/s.

AUTHOR CONTRIBUTIONS

AS and SK conceptualized the study, supervised the project, and designed all the analyses and experiments. DD and NP performed the experiments. DD, NP, SK, and AS analyzed the data. AS, DD, and NP wrote the manuscript. All authors read and approved the final version of manuscript.

FUNDING

The authors acknowledge financial support from NIPGR core grant. SK acknowledged the BT/PR40146/BTIS/137/4/2020 project grant from the Department of Biotechnology (DBT), Government of India. AS acknowledges research grant from Science and Engineering Research Board (SERB)—Department of Science and Technology (DST), Government of India (Grant No. EEQ/2018/000106).

ACKNOWLEDGMENTS

DD is thankful to the council of scientific and industrial research (CSIR), India for research fellowships. The authors are thankful to Mr. Ankit, senior research fellow in AS lab for compiling the references. DBT—eLibrary Consortium (DeLCON), is acknowledged for providing e-resources.

SUPPLEMENTARY MATERIAL

The Supplementary Material for this article can be found online at: https://www.frontiersin.org/articles/10.3389/fpls.2022.831265/full#supplementary-material

REFERENCES

Abe, H., Urao, T., Ito, T., Seki, M., Shinozaki, K., and Yamaguchi-Shinozaki, K. (2003). *Arabidopsis* AtMYC2 (bHLH) and AtMYB2 (MYB) function as transcriptional activators in abscisic acid signaling. *Plant Cell* 15, 63–78. doi: 10.1105/tpc.006130

Abe, M., Kobayashi, Y., Yamamoto, S., Daimon, Y., Yamaguchi, A., Ikeda, Y., et al. (2005). FD, a bZIP protein mediating signals. *Science* 309, 1052–1056. doi: 10.1126/science.1115983

Asai, S., Ichikawa, T., Nomura, H., Kobayashi, M., Kamiyoshihara, Y., Mori, H., et al. (2013). The variable domain of a plant calcium-dependent protein kinase (CDPK) confers subcellular localization and substrate recognition for NADPH oxidase. *J. Biol. Chem.* 288, 14332–14340. doi: 10.1074/jbc.M112.448910

Asano, T., Hayashi, N., Kikuchi, S., and Ohsugi, R. (2012). CDPK-mediated abiotic stress signaling. *Plant Signal. Behav.* 7, 817–821. doi: 10.4161/psb.20351

Asano, T., Tanaka, N., Yang, G., Hayashi, N., and Komatsu, S. (2005). Genome-wide identification of the rice calcium-dependent protein kinase. *Plant Cell Physiol.* 46, 356–366.

Benetka, W., Mehlmer, N., Maurer-Stroh, S., Sammer, M., Koranda, M., Neumüller, R., et al. (2008). Experimental testing of predicted myristoylation targets involved in asymmetric cell division and calcium-dependent signalling. *Cell Cycle* 7, 3709–3719. doi: 10.4161/cc.7.23.7176

Boudsocq, M., and Sheen, J. (2013). CDPKs in immune and stress signaling. *Trends Plant Sci.* 18, 30–40. doi: 10.1016/j.tplants.2012.08.008

Cai, H., Cheng, J., Yan, Y., Xiao, Z., Li, J., Mou, S., et al. (2015). Genome-wide identification and expression analysis of calcium-dependent protein kinase and its closely related kinase genes in *Capsicum annuum*. *Front. Plant Sci.* 6, 737. doi: 10.3389/fpls.2015.00737

Chen, Y., Zhou, X., Chang, S., Chu, Z., Wang, H., Han, S., et al. (2017). Calcium-dependent protein kinase 21 phosphorylates 14-3-3 proteins in response to ABA signaling and salt stress in rice. *Biochem. Biophys. Res. Commun.* 493, 1450–1456. doi: 10.1016/j.bbrc.2017.09.166

Cheng, S. H., Willmann, M. R., Chen, H. C., and Sheen, J. (2002). Calcium signaling through protein kinases. The *Arabidopsis* calcium-dependent protein kinase gene family. *Plant Physiol.* 129, 469–485. doi: 10.1104/pp.005645

Deepika, D., Ankit, J. S., Mali, K. V., Sinha, A. K., and Singh, A. (2022). Molecular analysis indicates the involvement of Jasmonic acid biosynthesis pathway in low-potassium (K+) stress response and development in chickpea (*Cicer arietinum*). *Environ. Exp. Bot.* 194, 104753. doi: 10.1016/j.envexpbot.2021.104753

Deepika, D., and Singh, A. (2021). Expression dynamics indicate the role of Jasmonic acid biosynthesis pathway in regulating macronutrient (N, P and K+) deficiency tolerance in rice (Oryza sativa L.). *Plant Cell Rep.* 40, 1495–1512. doi: 10.1007/s00299-021-02721-5

Fedosejevs, E. T., Gerdis, S. A., Ying, S., Pyc, M., Anderson, E. M., Snedden, W. A., et al. (2016). The calcium-dependent protein kinase RcCDPK2 phosphorylates sucrose synthase at Ser11 in developing castor oil seeds. *Biochem. J.* 473, 3667–3682. doi: 10.1042/BCJ20160531

Feng, Z. J., He, G. H., Zheng, W. J., Lu, P. P., Chen, M., Gong, Y. M., et al. (2015). Foxtail millet NF-Y families: genome-wide survey and evolution analyses identified two functional genes important in abiotic stresses. *Front. Plant Sci.* 6, 1142. doi: 10.3389/fpls.2015.01142

Geiger, D., Maierhofer, T., Al-Rasheid, K. A., Scherzer, S., Mumm, P., Liese, A., et al. (2011). Stomatal closure by fast abscisic acid signaling is mediated by the guard cell anion channel SLAH3 and the receptor RCAR1. *Sci. Signal.* 4, ra32. doi: 10.1126/scisignal.2001346

Geiger, D., Scherzer, S., Mumm, P., Marten, I. A. P. P. L., Ache, P., Matschi, S., et al. (2010). Guard cell anion channel SLAC1 is regulated by CDPK protein kinases with distinct Ca2+ affinities. *Proc. Nat. Acad. Sci U.S.A.* 107, 8023–8028. doi: 10.1073/pnas.0912030107

Gil, J., Nadal, S., Luna, D., Moreno, M. T., and Haro, A. D. (1996). Variability of some physico-chemical characters in Desi and Kabuli chickpea types. *J. Sci. Food Agric.* 71, 179–184. doi: 10.1002/(SICI)1097-0010(199606)71:2<179::AID-JSFA566>3.0.CO;2-7

Gutermuth, T., Lassig, R., Portes, M. T., Maierhofer, T., Romeis, T., Borst, J. W., et al. (2013). Pollen tube growth regulation by free anions depends on the interaction between the anion channel SLAH3 and calcium-dependent protein kinases CPK2 and CPK20. *Plant Cell* 25, 4525–4543. doi: 10.1105/tpc.113.118463

Hamel, L. P., Sheen, J., and Séguin, A. (2014). Ancient signals: comparative genomics of green plant CDPKs. *Trends Plant Sci.* 19, 79–89. doi: 10.1016/j.tplants.2013.10.009

Heinrich, M., Hettenhausen, C., Lange, T., Wünsche, H., Fang, J., Baldwin, I. T., et al. (2013). High levels of jasmonic acid antagonize the biosynthesis of gibberellins and inhibit the growth of N icotiana attenuata stems. *Plant J.* 73, 591–606. doi: 10.1111/tpj.12058

Hetherington, A. M. (2001). Guard cell signaling. *Cell* 107, 711–714. doi: 10.1016/S0092-8674(01)00606-7

Hettenhausen, C., Sun, G., He, Y., Zhuang, H., Sun, T., Qi, J., et al. (2016). Genome-wide identification of calcium-dependent protein kinases in soybean and analyses of their transcriptional responses to insect herbivory and drought stress. *Sci. Rep.* 6, 18973. doi: 10.1038/srep18973

Hou, F., Du, T., Qin, Z., Xu, T., Li, A., Dong, S., et al. (2021). Genome-wide *in silico* identification and expression analysis of beta-galactosidase family members in sweet potato [*Ipomoea batatas* (L.) Lam]. *BMC Genomics* 22, 140. doi: 10.1186/s12864-021-07436-1

Hrabak, E. M., Chan, C. W., Gribskov, M., Harper, J. F., Choi, J. H., Halford, N., et al. (2003). The *Arabidopsis* CDPK-SnRK superfamily of protein kinases. *Plant Physiol.* 132, 666–680. doi: 10.1104/pp.102.011999

Hu, Z., Lv, X., Xia, X., Zhou, J., Shi, K., Yu, J., et al. (2016). Genome-Wide identification and expression analysis of calcium-dependent protein kinase in tomato. *Front. Plant Sci.* 7, 469. doi: 10.3389/fpls.2016.00469

Hubbard, K. E., Nishimura, N., Hitomi, K., Getzoff, E. D., and Schroeder, J. I. (2010). Early abscisic acid signal transduction mechanisms: newly discovered components and newly emerging questions. *Genes Dev.* 24, 1695–1708. doi: 10.1101/gad.1953910

Hughes, J. D., Estep, P. W., Tavazoie, S., and Church, G. M. (2000). Computational identification of cis-regulatory elements associated with groups of functionally related genes in *Saccharomyces cerevisiae*. *J. Mol. Biol.* 296, 1205–1214. doi: 10.1006/jmbi.2000.3519

Ibrikci, H., Knewtson, S. J., and Grusak, M. A. (2003). Chickpea leaves as a vegetable green for humans: evaluation of mineral composition. *J. Sci. Food Agric.* 83, 945–950. doi: 10.1002/jsfa.1427

Kawamoto, N., Sasabe, M., Endo, M., Machida, Y., and Araki, T. (2015). Calcium-dependent protein kinases responsible for the phosphorylation of a bZIP transcription factor FD crucial for the florigen complex formation. *Sci. Rep.* 5, 8341. doi: 10.1038/srep08341

Kelley, L. A., Mezulis, S., Yates, C. M., Wass, M. N., and Sternberg, M. J. (2015). The Phyre2 web portal for protein modeling, prediction and analysis. *Nat. Protoc.* 10, 845–858. doi: 10.1038/nprot.2015.053

Kim, D., Paggi, J. M., Park, C., Bennett, C., and Salzberg, S. L. (2019). Graph-based genome alignment and genotyping with HISAT2 and HISAT-genotype. *Nat. Biotechnol.* 37, 907–915. doi: 10.1038/s41587-019-0201-4

Kong, X., Lv, W., Jiang, S., Zhang, D., Cai, G., Pan, J., et al. (2013). Genome-wide identification and expression analysis of calcium-dependent protein kinase in maize. *BMC Genomics* 14, 433. doi: 10.1186/1471-2164-14-433

Letunic, I., and Bork, P. (2021). Interactive tree of life (iTOL) v5: an online tool for phylogenetic tree display and annotation. *Nucleic Acids Res.* 49, W293–W296. doi: 10.1093/nar/gkab301

Li, A. L., Zhu, Y. F., Tan, X. M., Wang, X., Wei, B., Guo, H. Z., et al. (2008). Evolutionary and functional study of the CDPK gene family in wheat (*Triticum aestivum* L.). *Plant Mol. Biol.* 66, 429–443. doi: 10.1007/s11103-007-9281-5

Liese, A., and Romeis, T. (2013). Biochemical regulation of *in vivo* function of plant calcium-dependent protein kinases (CDPK). *Biochim. Biophys. Acta.* 1833, 1582–1589. doi: 10.1016/j.bbamcr.2012.10.024

Liu, K. H., Niu, Y., Konishi, M., Wu, Y., Du, H., Chung, H. S., et al. (2017). Discovery of nitrate–CPK–NLP signalling in central nutrient–growth networks. *Nature* 545, 311–316. doi: 10.1038/nature22077

Liu, W., Li, W., He, Q., Daud, M. K., Chen, J., and Zhu, S. (2014). Genome-wide survey and expression analysis of calcium-dependent protein kinase in Gossypium raimondii. *PLoS ONE* 9, e98189. doi: 10.1371/journal.pone.0098189

Lu, S. X., and Hrabak, E. M. (2013). The myristoylated amino-terminus of an *Arabidopsis* calcium-dependent protein kinase mediates plasma membrane localization. *Plant Mol. Biol.* 82, 267–278. doi: 10.1007/s11103-013-0061-0

Luan, S. (2009). The CBL-CIPK network in plant calcium signaling. *Trends Plant Sci.* 14, 37–42. doi: 10.1016/j.tplants.2008.10.005

Manimaran, P., Mangrauthia, S. K., Sundaram, R. M., and Balachandran, S. M. (2015). Constitutive expression and silencing of a novel seed specific calcium dependent protein kinase gene in rice reveals its role in grain filling. *J. Plant Physiol.* 174, 41–48. doi: 10.1016/j.jplph.2014.09.005

Matschi, S., Werner, S., Schulze, W. X., Legen, J., Hilger, H. H., and Romeis, T. (2013). Function of calcium-dependent protein kinase CPK 28 of *Arabidopsis* thaliana in plant stem elongation and vascular development. *Plant J.* 73, 883–896. doi: 10.1111/tpj.12090

Mehlmer, N., Wurzinger, B., Stael, S., Hofmann-Rodrigues, D., Csaszar, E., Pfister, B., et al. (2010). The Ca(2+) -dependent protein kinase CPK3 is required for MAPK-independent salt-stress acclimation in *Arabidopsis*. *Plant J.* 63, 484–498. doi: 10.1111/j.1365-313X.2010.04257.x

Mishra, M., Kanwar, P., Singh, A., Pandey, A., Kapoor, S., and Pandey, G. K. (2013). Plant omics: genome-wide analysis of ABA repressor1 (ABR1) related genes in rice during abiotic stress and development. *Omics* 17, 439–450. doi: 10.1089/omi.2012.0074

Mittal, S., Mallikarjuna, M. G., Rao, A. R., Jain, P. A., Dash, P. K., and Thirunavukkarasu, N. (2017). Comparative analysis of CDPK family in maize, arabidopsis, rice, and sorghum revealed potential targets for drought tolerance improvement. *Front. Chem.* 5, 115. doi: 10.3389/fchem.2017.00115

Mori, I. C., Murata, Y., Yang, Y., Munemasa, S., Wang, Y. F., Andreoli, S., et al. (2006). CDPKs CPK6 and CPK3 function in ABA regulation of guard cell S-type anion-and Ca2+-permeable channels and stomatal closure. *PLoS Biol.* 4, e327. doi: 10.1371/journal.pbio.0040327

Myers, C., Romanowsky, S. M., Barron, Y. D., Garg, S., Azuse, C. L., Curran, A., et al. (2009). Calcium-dependent protein kinases regulate polarized tip growth in pollen tubes. *Plant J.* 59, 528–539. doi: 10.1111/j.1365-313X.2009.03894.x

Nakashima, K., Fujita, Y., Kanamori, N., Katagiri, T., Umezawa, T., Kidokoro, S., et al. (2009). Three *Arabidopsis* SnRK2 protein kinases, SRK2D/SnRK2. 2, SRK2E/SnRK2. 6/OST1 and SRK2I/SnRK2. 3, involved in ABA signaling are essential for the control of seed development and dormancy. *Plant Cell Physiol.* 50, 1345–1363. doi: 10.1093/pcp/pcp083

Nakashima, K., and Yamaguchi-Shinozaki, K. (2013). ABA signaling in stress-response and seed development. *Plant Cell Rep.* 32, 959–970. doi: 10.1007/s00299-013-1418-1

Neelamathi, E., Vasumathi, E., Bagyalakshmi, S., and Kannan, R. (2009). *In silico* prediction of structure and functional aspects of a hypothetical protein of *Neurospora crassa*. *J. Cell Tissue Res.* 9, 1989.

Pertea, M., Pertea, G. M., Antonescu, C. M., Chang, T. C., Mendell, J. T., and Salzberg, S. L. (2015). StringTie enables improved reconstruction of a transcriptome from RNA-seq reads. *Nat. Biotechnol.* 33, 290–295. doi: 10.1038/nbt.3122

Poovaiah, B. W., Du, L., Wang, H., and Yang, T. (2013). Recent advances in calcium/calmodulin-mediated signaling with an emphasis on plant-microbe interactions. *Plant Physiol.* 163, 531–542. doi: 10.1104/pp.113.220780

Rajkumar, M. S., Gupta, K., Khemka, N. K., Garg, R., and Jain, M. (2020). DNA methylation reprogramming during seed development and its functional relevance in seed size/ weight determination in chickpea. *Commun. Biol.* 3, 340. doi: 10.1038/s42003-020-1059-1

Ray, S., Agarwal, P., Arora, R., Kapoor, S., and Tyagi, A. K. (2007). Expression analysis of calcium-dependent protein kinase gene family during reproductive development and abiotic stress conditions in rice (*Oryza sativa* L. ssp. indica). *Mol. Genet. Genom.* 278, 493–505. doi: 10.1007/s00438-007-0267-4

Ryan, J. G. (1997). "A global perspective on pigeonpea and chickpea sustainable production system : Present status and future potential," in *Recent Advances in Pulses Research*, eds A. N. Asthana and M. Ali (Kanpur: Indian Institute of Pulses Research), 1–32.

Sagar, S., Biswas, D. K., Chandrasekar, R., and Singh, A. (2021). Genome-wide identification, structure analysis and expression profiling of phospholipases D under hormone and abiotic stress treatment in chickpea (*Cicer arietinum*). *Int. J. Biol. Macromol.* 169, 264–273. doi: 10.1016/j.ijbiomac.2020.12.102

Sagar, S., Biswas, D. K., and Singh, A. (2020). Genomic and expression analysis indicate the involvement of phospholipase C family in abiotic stress signaling in chickpea (*Cicer arietinum*). *Gene* 753, 144797. doi: 10.1016/j.gene.2020.144797

Sagar, S., and Singh, A. (2019). "Abscisic acid, a principal regulator of plant abiotic stress responses," in *Plant Signaling Molecules*, eds I. Khan, S. P. Reddy, A. Ferrante, and N. S. Khan (Woodhead Publishing), 341–373. doi: 10.1016/B978-0-12-816451-8.00021-6

Schroeder, J. I., Kwak, J. M., and Allen, G. J. (2001). Guard cell abscisic acid signalling and engineering drought hardiness in plants. *Nature* 410, 327–330. doi: 10.1038/35066500

Schulz, P., Herde, M., and Romeis, T. (2013). Calcium-dependent protein kinases: hubs in plant stress signaling and development. *Plant Physiol.* 163, 523–530. doi: 10.1104/pp.113.222539

Sharma, N., Russell, S. D., Bhalla, P. L., and Singh, M. B. (2011). Putative cis-regulatory elements in genes highly expressed in rice sperm cells. *BMC Res. Notes* 4, 319. doi: 10.1186/1756-0500-4-319

Simeunovic, A., Mair, A., Wurzinger, B., and Teige, M. (2016). Know where your clients are: subcellular localization and targets of calcium-dependent protein kinases. *J. Exp. Bot.* 67, 3855–3872. doi: 10.1093/jxb/erw157

Singh, A., Baranwal, V., Shankar, A., Kanwar, P., Ranjan, R., Yadav, S., et al. (2012). Rice phospholipase A superfamily: organization, phylogenetic and expression analysis during abiotic stresses and development. *PLoS ONE* 7, e30947. doi: 10.1371/journal.pone.0030947

Singh, A., Giri, J., Kapoor, S., Tyagi, A. K., and Pandey, G. K. (2010). Protein phosphatase complement in rice: genome-wide identification and transcriptional analysis under abiotic stress conditions and reproductive development. *BMC Genomics* 11, 435. doi: 10.1186/1471-2164-11-435

Singh, A., Jha, S. K., Bagri, J., and Pandey, G. K. (2015). ABA inducible rice protein phosphatase 2C confers ABA insensitivity and abiotic stress tolerance in *Arabidopsis*. *PLoS ONE* 10, e0125168. doi: 10.1371/journal.pone.0125168

Singh, A., Kanwar, P., Pandey, A., Tyagi, A. K., Sopory, S. K., Kapoor, S., et al. (2013). Comprehensive genomic analysis and expression profiling of phospholipase C gene family during abiotic stresses and development in rice. *PLoS ONE* 8, e62494. doi: 10.1371/journal.pone.0062494

Singh, A., Kanwar, P., Yadav, A. K., Mishra, M., Jha, S. K., Baranwal, V., et al. (2014). Genome-wide expressional and functional analysis of calcium transport elements during abiotic stress and development in rice. *FEBS J.* 281, 894–915. doi: 10.1111/febs.12656

Singh, A., Pandey, A., Srivastava, A. K., Tran, L. S. P., and Pandey, G. K. (2016). Plant protein phosphatases 2C: from genomic diversity to functional multiplicity and importance in stress management. *Crit. Rev. Biotechnol.* 36, 1023–1035. doi: 10.3109/07388551.2015.1083941

Singh, A., and Pandey, G. K. (2015). "Primer design using primer express® for SYBR green-based quantitative PCR," in *PCR Primer Design* (New York, NY: Humana Press), 153–164. doi: 10.1007/978-1-4939-2365-6_11

Singh, A., Sagar, S., and Biswas, D. K. (2017). Calcium dependent protein kinase, a versatile player in plant stress management and development. *CRC Crit. Rev. Plant Sci.* 36, 336–352. doi: 10.1080/07352689.2018.1428438

Tang, R. J., Wang, C., Li, K., and Luan, S. (2020). The CBL–CIPK calcium signaling network: unified paradigm from 20 years of discoveries. *Trends Plant Sci.* 25, 604–617. doi: 10.1016/j.tplants.2020.01.009

Varshney, R. K., Hiremath, P. J., Lekha, P., Kashiwagi, J., Balaji, J., Deokar, A. A., et al. (2009). A comprehensive resource of drought- and salinity- responsive ESTs for gene discovery and marker development in chickpea (*Cicer arietinum* L.). *BMC Genomics* 10, 523. doi: 10.1186/1471-2164-10-523

Varshney, R. K., Song, C., Saxena, R. K., Azam, S., Yu, S., Sharpe, A. G., et al. (2013). Draft genome sequence of chickpea (*Cicer arietinum*) provides a resource for trait improvement. *Nat. Biotechnol.* 31, 240–246. doi: 10.1038/nbt.2491

Varshney, R. K., Thudi, M., Nayak, S. N., Gaur, P. M., Kashiwagi, J., Krishnamurthy, L., et al. (2014). Genetic dissection of drought tolerance in chickpea (*Cicer arietinum* L.). *Theor. Appl. Genet.* 127, 445–462. doi: 10.1007/s00122-013-2230-6

Verslues, P. E., Agarwal, M., Katiyar-Agarwal, S., Zhu, J., and Zhu, J. K. (2006). Methods and concepts in quantifying resistance to drought, salt and freezing, abiotic stresses that affect plant water status. *Plant J.* 45, 523–539. doi: 10.1111/j.1365-313X.2005.02593.x

Vivek, P. J., Resmi, M. S., Sreekumar, S., Sivakumar, K. C., Tuteja, N., and Soniya, E. V. (2017). Calcium-dependent protein kinase in ginger binds with Importin-α through its junction domain for nuclear localization, and further interacts with NAC transcription factor. *Front. Plant Sci.* 7, 1909. doi: 10.3389/fpls.2016.01909

Wang, J. P., Xu, Y. P., Munyampundu, J. P., Liu, T. Y., and Cai, X. Z. (2016). Calcium-dependent protein kinase (CDPK) and CDPK-related kinase (CRK) gene families in tomato: genome-wide identification and

functional analyses in disease resistance. *Mol. Genet. Genom.* 291, 661–676. doi: 10.1007/s00438-015-1137-0

Wang, Y., Tang, H., DeBarry, J. D., Tan, X., Li, J., Wang, X., et al. (2012). MCScanX: a toolkit for detection and evolutionary analysis of gene synteny and collinearity. *Nucleic Acids Res.* 40, e49–e49. doi: 10.1093/nar/gkr1293

Wen, F., Ye, F., Xiao, Z., Liao, L., Li, T., Jia, M., et al. (2020). Genome-wide survey and expression analysis of calcium-dependent protein kinase (CDPK) in grass Brachypodium distachyon. *BMC Genomics* 21, 53. doi: 10.1186/s12864-020-6475-6

Witte, C. P., Keinath, N., Dubiella, U., Demoulière, R., Seal, A., and Romeis, T. (2010). Tobacco calcium-dependent protein kinases are differentially phosphorylated in vivo as part of a kinase cascade that regulates stress response. *J. Biol. Chem.* 285, 9740–9748. doi: 10.1074/jbc.M109.052126

Wu, P., Wang, W., Duan, W., Li, Y., and Hou, X. (2017). Comprehensive analysis of the CDPK-SnRK superfamily genes in Chinese cabbage and its evolutionary implications in plants. *Front. Plant Sci.* 8, 162. doi: 10.3389/fpls.2017.00162

Xiao, X. H., Yang, M., Sui, J. L., Qi, J. Y., Fang, Y. J., Hu, S. N., et al. (2017). The calcium-dependent protein kinase (CDPK) and CDPK-related kinase gene families in Hevea brasiliensis—comparison with five other plant species in structure, evolution, and expression. *FEBS Open Bio* 7, 4–24. doi: 10.1002/2211-5463.12163

Yamaguchi-Shinozaki, K., and Shinozaki, K. (2005). Organization of cis-acting regulatory elements in osmotic-and cold-stress-responsive promoters. *Trends Plant Sci.* 10, 88–94. doi: 10.1016/j.tplants.2004.12.012

Yang, Y., Wang, Q., Chen, Q., Yin, X., Qian, M., Sun, X., et al. (2017). Genome-wide survey indicates diverse physiological roles of the barley (*Hordeum vulgare* L.) calcium-dependent protein kinase genes. *Sci. Rep.* 7, 5306. doi: 10.1038/s41598-017-05646-w

Ying, S., Hill, A. T., Pyc, M., Anderson, E. M., Snedden, W. A., Mullen, R. T., et al. (2017). Regulatory phosphorylation of bacterial-type PEP carboxylase by the Ca2+-dependent protein kinase RcCDPK1 in developing castor oil seeds. *Plant Physiol.* 174, 1012–1027. doi: 10.1104/pp.17.00288

Yu, C. S., Chen, Y. C., Lu, C. H., and Hwang, J. K. (2006). Prediction of protein subcellular localization. *Proteins* 64, 643–651. doi: 10.1002/prot.21018

Zeng, H., Xu, L., Singh, A., Wang, H., Du, L., and Poovaiah, B. W. (2015). Involvement of calmodulin and calmodulin-like proteins in plant responses to abiotic stresses. *Front. Plant Sci.* 6, 600. doi: 10.3389/fpls.2015.00600

Zhang, H., Wei, C., Yang, X., Chen, H., Yang, Y., Mo, Y., et al. (2017). Genome-wide identification and expression analysis of calcium-dependent protein kinase and its related kinase gene families in melon (*Cucumis melo* L.). *PLoS ONE* 12, e0176352. doi: 10.1371/journal.pone.0176352

Zhang, K., Han, Y. T., Zhao, F. L., Hu, Y., Gao, Y. R., Ma, Y. F., et al. (2015). Genome-wide identification and expression analysis of the CDPK gene family in grape, *Vitis* spp. *BMC Plant Biol.* 15, 164. doi: 10.1186/s12870-015-0552-z

Zhao, L. N., Shen, L. K., Zhang, W. Z., Zhang, W., Wang, Y., and Wu, W. H. (2013). Ca2+-dependent protein kinase11 and 24 modulate the activity of the inward rectifying K+ channels in *Arabidopsis* pollen tubes. *Plant Cell* 25, 649–661. doi: 10.1105/tpc.112.103184

Zhao, P., Liu, Y., Kong, W., Ji, J., Cai, T., and Guo, Z. (2021). Genome-Wide identification and characterization of calcium-dependent protein kinase (CDPK) and CDPK-related kinase (CRK) gene families in medicago truncatula. *Int. J. Mol. Sci.* 22, 1044. doi: 10.3390/ijms22031044

Zhao, R., Sun, H., Zhao, N., Jing, X., Shen, X., and Chen, S. (2015). The *Arabidopsis* Ca2+-dependent protein kinase CPK27 is required for plant response to salt-stress. *Gene* 563, 203–214. doi: 10.1016/j.gene.2015.03.024

Zheng, L., Liu, P., Liu, Q., Wang, T., and Dong, J. (2019). Dynamic protein S-acylation in plants. *Int. J. Mol. Sci.* 20, 560. doi: 10.3390/ijms20030560

Zou, J. J., Li, X. D., Ratnasekera, D., Wang, C., Liu, W. X., Song, L. F., et al. (2015). *Arabidopsis* CALCIUM-DEPENDENT PROTEIN KINASE8 and CATALASE3 function in abscisic acid-mediated signaling and H2O2 homeostasis in stomatal guard cells under drought stress. *Plant Cell* 27, 1445–1460. doi: 10.1105/tpc.15.00144

Zuo, R., Hu, R., Chai, G., Xu, M., Qi, G., Kong, Y., et al. (2013). Genome-wide identification, classification, and expression analysis of CDPK and its closely related gene families in poplar (*Populus trichocarpa*). *Mol. Biol. Rep.* 40, 2645–2662. doi: 10.1007/s11033-012-2351-z

Conflict of Interest: The authors declare that the research was conducted in the absence of any commercial or financial relationships that could be construed as a potential conflict of interest.

Publisher's Note: All claims expressed in this article are solely those of the authors and do not necessarily represent those of their affiliated organizations, or those of the publisher, the editors and the reviewers. Any product that may be evaluated in this article, or claim that may be made by its manufacturer, is not guaranteed or endorsed by the publisher.

Copyright © 2022 Deepika, Poddar, Kumar and Singh. This is an open-access article distributed under the terms of the Creative Commons Attribution License (CC BY). The use, distribution or reproduction in other forums is permitted, provided the original author(s) and the copyright owner(s) are credited and that the original publication in this journal is cited, in accordance with accepted academic practice. No use, distribution or reproduction is permitted which does not comply with these terms.

frontiers | Frontiers in Plant Science

ORIGINAL RESEARCH
published: 14 April 2022
doi: 10.3389/fpls.2022.836940

Effect of *Piriformospora indica*-Induced Systemic Resistance and Basal Immunity Against *Rhizoctonia cerealis* and *Fusarium graminearum* in Wheat

Liang Li, Nannan Guo, Yu Feng, Mengmeng Duan and Chunhui Li*

School of Chemical Engineering and Technology, Hebei University of Technology, Tianjin, China

Wheat is among the top 10 and most widely grown crops in the world. However, wheat is often infected with many soil-borne diseases, including sharp eyespot, mainly caused by the necrotrophic fungus *Rhizoctonia cerealis*, and Fusarium head blight (FHB), caused by *Fusarium graminearum*, resulting in reduced production. *Piriformospora indica* is a root endophytic fungus with a wide range of host plants, which increases their growth and tolerance to biotic and abiotic stresses. In this study, the capability of *P. indica* to protect wheat seedlings against *R. cerealis* and *F. graminearum* was investigated at the physiological, biochemical, and molecular levels. Our results showed that *P. indica* significantly reduced the disease progress on wheat caused by *F. graminearum* and *R. cerealis in vivo,* but not showed any antagonistic effect on *F. graminearum* and *R. cerealis in vitro*. Additionally, *P. indica* can induce systemic resistance by elevating H_2O_2 content, antioxidase activity, relative water content (RWC), and membrane stability index (MSI) compared to the plants only inoculated with *F. graminearum* or *R. cerealis* and control. RNA-seq suggested that transcriptome changes caused by *F. graminearum* were more severe than those caused by *R. cerealis.* The number of differentially expressed genes (DEGs) in the transcriptome can be reduced by the addition of *P. indica:* for *F. graminearum* reduced by 18% and for *R. cerealis* reduced 58%. The DEGs related to disease resistance, such as WRKY and MAPK, were upregulated by *P. indica* colonization. The data further revealed that the transcriptional resistance to *F. graminearum* and *R. cerealis* mediated by *P. indica* is quite different.

Keywords: *Piriformospora indica*, differentially expressed gene (DEGs), sharp eyesspot, root rot, reprogram

OPEN ACCESS

Edited by:
Girdhar Kumar Pandey, University of Delhi, India

Reviewed by:
Manoj Kumar Solanki, University of Silesia in Katowice, Poland
Rupam Kapoor, University of Delhi, India

****Correspondence:***
Liang Li
liangli@hebut.edu.cn

Specialty section:
This article was submitted to Plant Physiology, a section of the journal Frontiers in Plant Science

Received: *16 December 2021*
Accepted: *15 March 2022*
Published: *14 April 2022*

Citation:
Li L, Guo N, Feng Y, Duan M and Li C (2022) Effect of Piriformospora indica-Induced Systemic Resistance and Basal Immunity Against Rhizoctonia cerealis and Fusarium graminearum in Wheat. Front. Plant Sci. 13:836940. doi: 10.3389/fpls.2022.836940

INTRODUCTION

Wheat is an economically important crop worldwide and approximately 35∼40% of the world's population take wheat as the main food. As the world's largest producer and consumer of wheat, the stability of wheat production in China is of great significance to guarantee not only national but also world food security. However, one of the major problems of these crops is the ecological loss caused

by a variety of diseases, which has caused more than 1 billion yuan (RMB) of losses per year from 2005 to 2008 (Chen et al., 2008). Wheat sharp eyespot is a serious disease caused by *Rhizoctonia cerealis*, infecting both the stems and sheaths of wheat plants, blocking the transportation of nutrients required for growth (Chen et al., 2008; Wang et al., 2021). *Fusarium graminearum* is another necrotrophic fungus that can cause root rot and head blight in wheat around the world (Osborne and Stein, 2007). The *F. graminearum* produces mycotoxins, accumulates in wheat grains, and is harmful to food quality, thus, posing a severe threat to human and animal health (Zhang et al., 2013; Xiu et al., 2021).

In China, the increasing grain output is the primary goal of developing a modern agricultural path with Chinese characteristics. Studies have shown that despite a large number of measures that have been taken to protect crops from the threat of diseases and pests, the increase in yield is accompanied by an increased loss in crop production due to biotic and abiotic stresses (Lobell and Field, 2007; Schäfer et al., 2009). The methods to increase crop yield should be reliable for producers and safe for consumers, as well as the environment. Traditionally, agrochemicals played a critical role in disease control, but this has led to an increase in environmental pollution and induced pesticide resistance (Zhang et al., 2017). Hence, using endophytes in the rhizosphere to develop biological defenses against plant diseases, as a safer and more productive means of agricultural practices, has been attracting more attention to researchers and scientists. Those plant growth-promoting rhizobacteria (PGPR) have been well-evaluated and concluded by Gouda et al. (2018). Compared with endophytic bacteria, the role, and usages of endophytic fungi for sustainable agriculture remain controversial and restricted.

Generally, as a beneficial companion in plants, endophytic fungi help plants to resist both biotic and abiotic stresses by regulating the immune response of plant-microbe interactions and stimulating the production of metabolites (Tedersoo et al., 2020; Rajani et al., 2021). Therefore, endophytes have a broad application prospect for use as biological control agents and biological fortifiers. However, there is still a long way to go to integrate endophytes into conscious agricultural production because not all endophytes are inherently useful, which is strongly dependent on plant species and genotypes (Lu et al., 2021). Therefore, the complex and dynamic communication relationship between parasitic crops and endophytic fungi needs to be clarified.

Piriformospora indica is a root-endophytic basidiomycete member of the order Sebacinales, which was first discovered by Indian scientists in the Thar desert in northwestern India in 1998 (Verma et al., 1998). The *P. indica* is well-known to be able to establish beneficial interactions with many different hosts, including monocotyledons such as barley, wheat, rice, corn, and dicotyledons, such as *Arabidopsis* and tobacco (Qiang et al., 2012). The *P. indica* serves as an excellent model for beneficial microbes since it: (1) is genetically transformable and culturable in axenic conditions (Zuccaro et al., 2009); (2) promotes plant growth and yield (Kundu et al., 2021); (3) enhances plant tolerance against abiotic stress (Li et al., 2021a); and (4) primes plants for disease resistance against biotrophic and necrotrophic fungi (Stein et al., 2008), oomycetes (Trzewik et al., 2020), and viruses (Fakhro et al., 2010).

Among these advantages, its disease resistance develops it into a good biological control fungus and has been widely used. Studies have confirmed that *P. indica* can enhance plants' resistance against *Cochliobolus sativus* (Sahay and Varma, 2006) and can induce systemic resistance against Erysiphe in barley (Deshmukh and Kogel, 2007) and *Verticillium dahliae* in *Arabidopsis* (Sun et al., 2014). Rabiey and Shaw (2016) evaluated the inhibitory effect of *P. indica* against *F. graminearu*m, but did not elucidate the protective mechanism of *P. indica* to plants. Furthermore, Panda et al. (2019) showed that *P. indica* rapidly and effectively activates jasmonic acid/ethylene (JA/ET) mediated basic defense mechanisms against pathogen infection by inducing transcriptome reprogramming to change the expression of JA/ET-related genes. In addition, *P. indica* can induce changes in gibberellin (GA), salicylic acid (SA), and abscisic acid (ABA) hormone levels, thereby inducing host immunity of microbe-associated molecular model (MAMP) (Jacobs et al., 2011) and self-regulation of mutual-symbiosis (Ding et al., 2008; Waller et al., 2008). Roylawar et al. (2021) reported that *P. indica* primes onion response against stemphylium leaf blight disease. Colonization of *P. indica* enhances the complete signal transduction cascade, leading to systematic expression of host defense genes. Studies have also shown that the colonization of this fungus may increase the production of defensive secondary metabolites in plants, such as artemisinin (Arora et al., 2016), abricin (Prasad et al., 2013), trichroterpene (Das et al., 2014), and curcumin (Bajaj et al., 2014).

It follows, therefore, that *P. indica* itself is a member of a system that activates multiple defense signals in plants and, thus, provides durable defense against multiple pathogens. Harrach et al. (2013) showed that *P. indica* protects barley roots from the loss of antioxidant capacity caused by *Fusarium*. Pre-inoculation with *P. indic*a effectively prevented the decrease of ascorbic acid/oxidized ascorbic acid ratio and glutathione content caused by *F. culmorum* pathogens. Among them, the activities of key antioxidant enzymes increased about 35% in plant metabolism after *P. indica* colonization. The above results indicate that the colonization of *P. indica* can stimulate antioxidant enzymes in plants and destroy reactive oxygen species (ROS) in plant cells, thus, triggering the defense response and improving the resistance of plants to pathogens. In addition, *P. indica* can enhance the resistance of rice to sheath blight by reducing the content of H_2O_2 and increasing the activity of antioxidant enzymes (Nassimi and Taheri. 2017). Recent studies have shown that *P. indica* can increase the expression of resistance genes in potatoes, but does not increase the activities of ascorbate peroxidase, peroxidase, and superoxide dismutase (SOD) (Li et al., 2021b). The further study corroborates the idea that *P. indica* is not likely to affect the defense enzyme response by itself but has a role in modulating onion biochemical reaction to *Stemphylium vesicarium* infection (Roylawar et al., 2021). Those data implied that different signal transduction pathways are induced by *P. indica* in different hosts, and the in-depth mechanism remains to be elucidated.

In this study, the effects of *P. indica on* systemic resistance and basal immunity against sharp eyespot and root rot diseases in wheat were evaluated at the physiological, biochemical, and molecular levels. Also, the effects of *P. indica* on inducing wheat resistance to sharp eyespot and head blight were compared. With the *P. indica,* as an effective biocontrol agent, the potential for disease resistance was fully assessed.

MATERIALS AND METHODS

Fungal Inoculums Preparation and Inoculation

Rhizoctonia cerealis and *F. graminearum* isolated from wheat plants showing the symptoms of sharp eyespot and root rot were used in this study. The isolates of *P. indica* was obtained from the Professor Karl-Heinz-Kogel of Justus-Liebig-University, Gieseen, Germany. The *P. indica* was growing on complex medium (CM) medium plates and incubated at 23°C until used. The chlamydospores of *P. indica* were collected by flooding the surface of the 21-day-old CM plate with sterile distilled water by a spatula. Chlamydospore suspension was filtered through sterile Miracloth and the concentration of chlamydospores was adjusted to 1×10^5/mL using a hemocytometer (Nassimi and Taheri, 2017). The inoculum of *R. cerealis* was prepared using the method described by Qi et al. (2021). Briefly, at the tillering stage, the stem base of each plant was inoculated with toothpick fragments harboring well-developed mycelia of *R. cerealis*. The inoculated sites were covered with wet cotton to increase the humidity, which promotes *R. cerealis* infection. Conidia of *F. graminearum* were harvested as described previously (Gunnaiah et al., 2012). The *F. graminearum* isolate (obtained from Prof. Yang, Tianjin Academy of Agricultural Sciences, Tianjin, China) was maintained on potato dextrose agar (PDA) media. For spore production, cultures were grown on rye B agar media, under UV light and darkness, for 16 and 8 h, respectively, at 25°C. Macroconidia were harvested and the spore count was adjusted to 1×10^5 macroconidia ml^{-1}. Wheat spikelets were inoculated with 10 μl of spore suspension using a syringe with an auto dispenser. The inoculated plants were covered with moistened plastic bags to maintain a saturated atmosphere to facilitate infection, and the bags were removed 48 h post-inoculation (hpi).

Plant Materials

Seeds of wheat (*Triticum aestivum* L.) were surface sterilized by 15% sodium hypochlorite for 8 m and rinsed thoroughly with sterile distilled water. The seeds were treated by two methods: (1) Seed was germinated on wet and sterilized filter paper in a Petri dish at room temperature, after germination, the roots of germinated seeds were immersed into the suspension of *P. indica* for 6 h at 23°C. (2) Seeds of wheat were directly immersed into the suspension of *P. indica* at 23°C and change the fresh suspension of *P. indica* every 8 h until the seeds were germinated. The above treatments' seedlings were then transferred to cultivation trays containing sterilized sand (121°C and 15 psi for 1 h) under greenhouse conditions (28 ± 4°C; 14/10 h light/dark photoperiod). The seedlings were planted in the 15-cm diameter pots (five seedlings per pot) filled with a 1:1 (v:v) mixture of sand and soil, which were sterilized in three successive days at 121°C and 15 psi for 30 min. To guarantee the colonization of *P. indica* into the wheat root, the roots of wheat seedlings were irrigated with a 20 mL spore suspension of *P. indica* per day after being transferred into the soil. The plants used as controls were inoculated similarly with sterile distilled water containing 0.05% (v/v) between 20. Different time intervals (3, 5, 7, 10, 14, 21, and 35 days) between inoculation of *P. indica* and pathogen were set. The inoculated plants were kept at dark conditions at 85% relative humidity and 23°C for 48 h. Following disease assessment, root volume, wet and dry weight of the roots, and shoots were measured.

Plant Disease Evaluation

For disease evaluation, each plant was carefully pulled out and washed. Sharp eyespot disease severity was graded into six classes based on the site and number of diseased spots (1, $I \leq 5$; 2, $5 < I \leq 15$; 3, $15 < I \leq 25$; 4, $25 < I \leq 35$; and 5, $I > 35$) and the disease index (DI) was calculated, as described previously (Zhu et al., 2015). Fusarium head blight disease severity was graded into five classes based on the proportion of stem discoloration (0 = no discoloration; 1 = 1 to 25%; 2 = 26 to 50%; 3 = 51 to 75%; 4 = more than 75%; and 5 = dead plant) as described by Fernandez and Chen (2005).

Antagonistic Activity Assay

The interactions between *P. indica* and *R. cerealis,* the *P. indica* and *F. graminearum* were identified methodically. The 5-mm diameter plug of *P. indica* was placed on a side of a CM plate and incubated at 23°C. After 14 days, the same size plug of *R. cerealis* or *F. graminearum* from the margins of 7-day-old culture was placed at the other side of the plate. The interaction of two fungi was investigated macroscopically and microscopically (Rabiey et al., 2015) for 5 and 8 days post-co-cultivation.

Detection of *Piriformospora indica* in Colonized Wheat Roots

The *P. indica* colonization in wheat root was identified by staining the root fragments using chitin-specific dye WGA-AF 488 (Molecular Probes[1]) according to the method of Li et al. (2017). Root samples were then subjected to microscopic observation.

Relative Water Content Measurement

The Relative Water Content (RWC) displays the amount of water fraction in plant leaves and can be estimated by using the following formula as described by Weatherley (1950): RWC = FW−DW/TW−DW × 100. The weight of first leaf segments of wheat from each treatment and control plant was measured at 21 days after inoculation with *R. cerealis* and *F. graminearum* as fresh weight (FW). Afterward, leaf samples were immersed in distilled water at room temperature for 24 h and were weighted as turgid weight (TW), and the weights of

[1]www.invitrogen.com

leaf segments dried in an oven (70°C for 48 h) were recorded as dry weight (DW).

Electrolyte Leakage Determination

Cell membrane stability was estimated by the electrolyte leakage from crowns of wheat plants with different treatments. Wheat crowns without fungal inoculation were used as controls. Crown samples at 21 days after inoculation by the pathogen were washed three times by distilled water and then kept in 25 mL distilled water at room temperature for 24 h. The electrical conductivity of a solution (EC1) was calculated by a conductivity meter (Dingguo, Tianjin, China). Then, the solution containing the leaves was transferred to autoclave at 121°C for 20 m and after cooling to room temperature, the final electrical conductivity (EC2) was measured by a conductivity meter. Membrane stability index (MSI) percentage was measured by the following equation (Singh et al., 1992): MSI = 1−EC1/EC2 × 100.

Histochemical Detection of H_2O_2

Production of H_2O_2 in wheat plants was investigated using 3, 3'- diaminobenzidine (DAB) staining. The leaf samples with different treatments and controls without any inoculation or treatment were obtained at different time points and floated in the DAB solution (1 mg mL^{-1} DAB-HCL, pH 3.8) overnight. Alcohol and glycerin at the ratio of 8:2 were used to decolorize the leaf segments. The DAB polymerization at the site of H_2O_2 accumulation was produced in a reddish-brown polymer, which was microscopically investigated (Olympus IX83, Shibuya, Japan).

Protein Extraction and Antioxidant Analysis

Total protein extraction was done according to the method described by Kar and Mishra (1976). Leaf tissues (300 mg) were sampled at 0, 6, 12, 24, 48, and 72 hpi with *R. cerealis* for different treatments. The samples were ground in liquid nitrogen and homogenized in 3 mL of 100 mM potassium phosphate buffer (pH 6.8). The mixture was centrifuged at 14,000 *g* for 20 m at 4°C and supernatant was used as enzyme source. Soluble protein concentration was investigated using bovine serum albumin as a standard (Bradford, 1976). Guaiacol peroxidase (GPX) activity was determined using guaiacol as a hydrogen donor. The reaction mixture (1.18 mL) contained potassium phosphate buffer (100 mM, pH 6.8), guaiacol (10 mM), H_2O_2 (70 mM), and enzyme extract (10 μL), and absorbance of the mixture was recorded at 470 nm for 3 m (Chance and Maehly, 1955). The activities of catalase (CAT), superoxide dismutase (SOD), and peroxidase (POD) were calculated as described by Aebi (1984) and Chance and Maehly (1955). The GPX and CAT, SOD, and POD activities were expressed as μmol min^{-1} mg^{-1} protein.

Total RNA Extraction

The *P. indica* irrigation lasted for 2 weeks before *R. cerealis* and *F. graminearum* infection. Samples were harvested after respective treatments as shown in **Table 1** and subjectively subjected to RNA extraction. Ethanol precipitation protocol and CTAB-PBIOZOL reagent were used for the purification of total RNA from the plant tissue according to the manual instructions. Grind tissue samples about 80 mg with liquid nitrogen into powder and transfer the powder samples in 1.5 ml of preheated 65°C CTAB-pBIOZOL reagents. The samples were incubated by a Thermomixer for 15 m at 65°C to permit the complete dissociation of nucleoprotein complexes. After centrifuging at 12,000× *g* for 5 m at 4°C, the supernatant was added with 400 μl of chloroform per 1.5 ml of CTAB-pBIOZOL reagent and was centrifuged at 12,000× *g* for 10 m at 4°C. The supernatant was transferred to a new 2-ml tube that added 700 μl acidic phenol and 200 μl chloroform, followed by centrifuging 12,000× *g* for 10 m at 4°C. The aqueous phase was added with an equal volume of the aqueous phase of chloroform and centrifuged at 12,000× *g* for 10 m at 4°C. The supernatant was added an equal volume of supernatant of isopropyl alcohol and placed at −20°C for 2 h for precipitation. After that, the mix was centrifuged at 12,000× *g* for 20 m at 4°C and then remove the supernatant. After being washed with 1 ml of 75% ethanol, the RNA pellet was air-dried in the biosafety cabinet and was dissolved by adding 50 μL of diethylpyrocarbonate (DEPC)-treated water. Subsequently, total RNA was qualified and quantified using a NanoDrop and Agilent 2100 bioanalyzer (Thermo Fisher Scientific, MA, United States).

mRNA Library Construction

The mRNA Library were constructed using the samples in **Table 1**. The Oligo(dT)-attached magnetic beads were used to purify mRNA. Purified mRNA was fragmented into small pieces with fragment buffer at the appropriate temperature. Then, first-strand complement DNA (cDNA) was generated using random hexamer-primed reverse transcription, followed by second-strand cDNA synthesis. Afterward, A-Tailing Mix and RNA Index Adapters were added by incubating to end repair. The cDNA fragments obtained from the previous step were amplified by PCR, and products were purified by Ampure XP Beads, then dissolved in EB solution. The product was validated on the Agilent Technologies 2100 bioanalyzer for quality control. The double-stranded PCR products from the previous step were heated denatured and circularized by the splint oligo sequence to

TABLE 1 | Respective treatments for different sample.

Number	Treatments	Abbreviation	Repeats	*P. indica* pre-inoculation	Harvest at () dai
1	Mock	Mock	3	−	$14^0 + 14^0$
2	*Piriformospora indica*	Piri	3	+	$14^{pi} + 14^0$
3	*Fusarium graminearum*	Fg	3	−	$14^0 + 14^{fg}$
4	*Rhizoctonia cerealis*	Rh	3	−	$14^0 + 14^{rh}$
5	*P. indica* + *F. graminirum*	Piri + Fg	3	+	$14^{pi} + 14^{fg}$
6	*P. indica* + *R.cerealis*	Piri + Rh	3	+	$14^{pi} + 14^{rh}$

14^0 stands for days irrigation with water; 14^{fg} stands for Fusarium graminearum infection for 14 days; 14^{pi} stands for days pre-inoculation of P. indica; 14^{rh} stands for Rhizoctonia cerealis infection for 14 days.

get the final library. The single-strand circle DNA (ssCir DNA) was formatted as the final library. The final library was amplified with phi29 to make DNA nanoball (DNB), which had more than 300 copies of one molecular, DNBs were loaded into the patterned nanoarray and pair-end 100 bases reads were generated on the BGIseq500 platform (BGI-Shenzhen, China).

Quantitative Real-Time Polymerase Chain Reaction Analysis

Total RNAs (1 μg) from control and treatment were used to make cDNA using M-MLV Reverse Transcriptase (Takara, Beijing, Japan), according to the supplier's protocol, respectively. After treatment with DNase I (Sigma, Osterode am Harz, Germany), the cDNA was used as a template for quantitative real-time polymerase chain reaction (qRT-PCR) to quantify selected mRNAs using specific primers. The expression level of the respective gene was determined by quantitative RT-PCR. Quantitative RT-PCR was measured by SYBR Green fluorescence method as described previously (Livak and Schmittgen, 2001). In brief, quantitative PCR (qPCR) experiments were conducted on a Light Cycler96 Fast real-time PCR system (Roche, Basel, Switzerland)). The reaction solution contains 2 × Ultra SYBR Mixture 10 μL, 100 ng cDNA template, 10 μM forward, and reverse primers. Wheat actin was used as the control, and all experiments were conducted with at least three technical replications. Amplification program was applied as the following steps: the first initial activation step was performed at 95°C, 5 min, then followed by 30 cycles (95°C for 20 s, 56°C for 35 s, 72°C for 35 s, and 65°C for 20 s). At the end of each cycle, melting curves were determined respectively to guarantee the amplification of a single PCR product. The primers used in this work were listed in **Supplementary Table 1**.

Statistical Analysis

In this study, all data are expressed as the means ± SE and represent at least three independent biological experiments. The significance of differences was analyzed by using a one-way analysis of variance (ANOVA) with Duncan's multiple range test.

RESULTS

Interaction of *Piriformospora indica* With *Rhizoctonia cerealis* and *Fusarium graminearum* in Wheat

We set different time intervals including 7, 14, and 21 days between the infection of *P. indica* and the *R. cerealis,* and different time intervals including 3, 7, 10, and 14 days between the infection of *P. indica* and the *F. graminearum* based on disease progression (**Figure 1**). The disease index was assessed after infection. We found that sharp eyespot developed most slowly on the wheat seedlings inoculated by the pathogen at

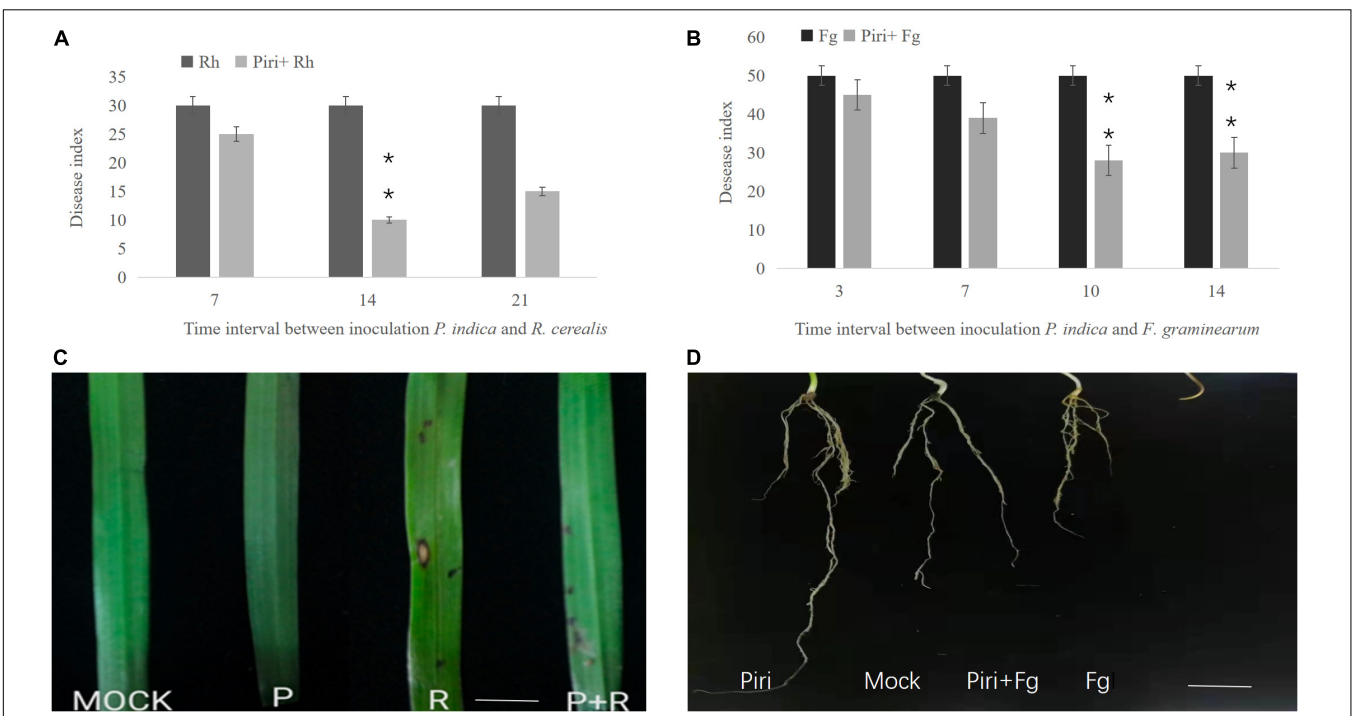

FIGURE 1 | Determination of the best time interval between inoculating wheat seedlings with *Piriformospora indica* and *Rhizoctonia cerealis* or *Fusarium graminearum*. **(A)** Time interval between inoculation *P. indica* and *R. cerealis*; **(B)** Time interval between inoculation *P. indica* and *F. graminearum*. **(C)** Symptoms of sharp eyespot caused by *R. cerealis* on wheat leaves under different treatment (*P. indica* inoculation was 14 days before *R. cerealis* infection); **(D)** Symptoms of root rot caused by *F. graminearum* on wheat roots under different treatment (*P. indica* inoculation was 10 days before *F. graminearum* infection). Piri, *P. indica*; Fg, *F. graminearum*; Rh, *R. cerealis*; Piri + Fg, *P. indica* + *F. graminearum*; Piri + Rh, *P. indica* + *R. cerealis*.

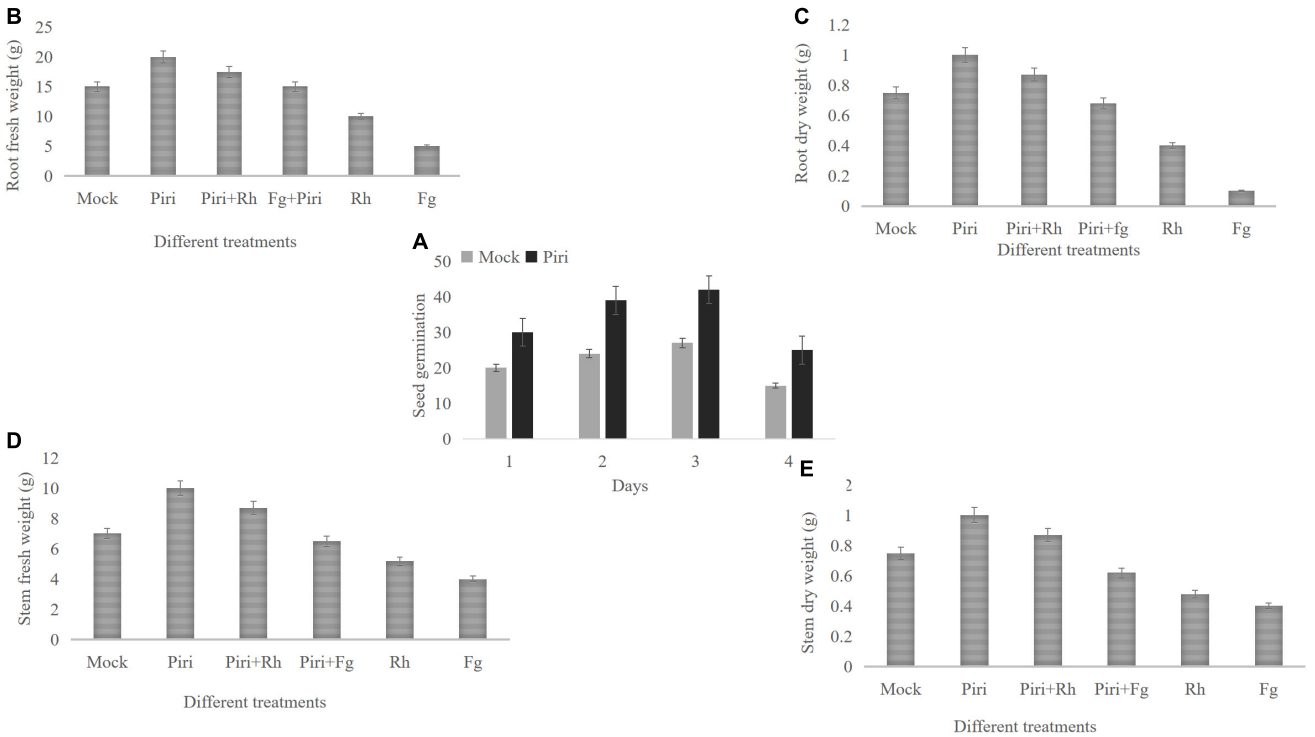

FIGURE 2 | Effect of various treatments of Piri, Fg, Piri + Fg, Rh, and Piri + Rh on wheat seedlings growth parameters. **(A)** Seed germination number; **(B)** root fresh weight; **(C)** root dry weight; **(D)** stem fresh weight; **(E)** stem dry weight. Samples were treated as shown in **Table 1** and harvested at 14 dpi with *F. graminearum* or *R. cerealis*. Piri, *P. indica*; Fg, *F. graminearum*; Rh, *R. cerealis*; Piri + Fg, *P. indica* + *F. graminearum*; Piri + Rh, *P. indica* + *R. cerealis*.

14 days post-inoculation (dpi) with *P. indica* (**Figure 1A**), whereas the lowest disease developing was observed on the wheat seedlings inoculation by *F. graminearum* at 10 dpi with *P. indica* (**Figure 1B**). The symptoms of damage caused by *R. cerealis* on leaves and caused by *F. graminearum* on roots were documented as shown in **Figures 1C,D**. The results indicated that pre-inoculation of spores of *P. indica* 14 days before *R. cerealis* infection could significantly reduce the eyesport number in the Piri + Rh treatment compared to the Rh (**Figure 1C**). And the pathogen of *F. graminearum* led to severe root rot, but this phenomenon could be remitted by *P. indica* pre-colonization 10 days before *F. graminearum* infection (**Figure 1D**).

Effect of *Piriformospora indica* on Wheat Growth Under Pathogens Infection

The seeds germination rate was calculated for those seeds directly immersed into the suspension of *P. indica*. Results indicated that pre-inoculation of *P. indica* before germination could significantly increase the rate of seeds germination (**Figure 2A**). Additionally, wheat seedlings inoculated by the pathogen at 14 dpi with *P. indica* were used to evaluate biomass production. The *P. indica* had a significant effect on growth characteristics of wheat seedlings such as root, stem fresh and dry weight of root, and shoot systems (**Figures 2B–E**). The biomass enhancement was obvious in wheat inoculated with *P. indica*, and pre-inoculation of *P. indica* significantly reduced the biomass loss caused by *R. cerealis* or *F. graminearum* (**Figures 2B–E**). In comparison, the side effects of *F. graminearum* on wheat yield were more serious than that of *R. cerealis*.

Disease Index Evaluation and Relative Water Content and Membrane Stability Index Determination

In this study, the effect of different treatments, including mock, *P. indica* (Piri), *F. graminearum* (Fg), *R. cerealis* (Rh), *P. indica* plus *F. graminearum* (Piri + Fg), and *P. indica* plus *R. cerealis* (Piri + Rh) on the progress of the disease on the wheat seedlings were evaluated at different time-points (dpi) with *P. indica*. With the increase of infection time, the inhibition effect on the pathogen in wheat that was pre-colonized by *P. indica* gradually appeared. From the 7 dpi, the Piri + Fg treatment had a higher effect on reduction of disease severity caused by *F. graminearum*, and until 21 dpi, this inhibition effect was quite obvious. As for *R. cerealis*, from the 14 dpi, the Piri + Rh treatment had a higher effect on reduction of disease severity caused by *R. cerealis*, and until 35 dpi (**Figures 3A,B**).

In addition, RWC and cell MSI, by measuring electrolyte leakage of wheat crowns of plant leaves, were evaluated among various treatments, inducing mock, Piri, Piri + Rh, Rh, Piri + Fg, and Fg (**Figures 3C,D**). The obtained results revealed that RWC in plants inoculated with *P. indica* was highest among the six treatments. In addition, RWCs in Piri + Rh and Piri + Fg were higher than Rh and Fg's, respectively, but lower than control. By

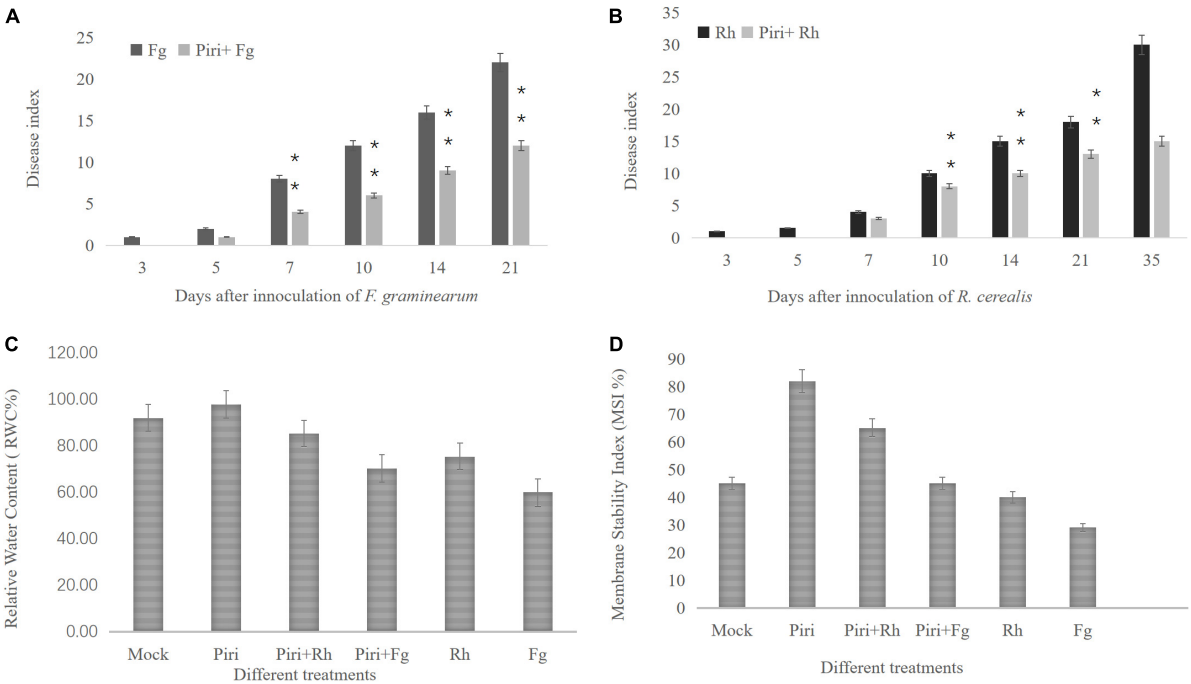

FIGURE 3 | Disease index evaluation and relative water content (RWC) and membrane stability index (MSI) determination. **(A)** The wheat seedlings were infected by *F. graminearum* at 14 days post inoculation (dpi) with *P. indica* and harvested at different time-points, including 3, 5, 7, 10, 14, and 21 days. Effect of different treatments, including Fg, Piri + Fg on progress of the disease on the wheat seedlings were evaluated. **(B)** The wheat seedlings were infected by *R. cerealis* at 14 days post inoculation (dpi) with *P. indica* and harvested at different time-points, including 3, 5, 7, 10, 14, 21, and 35 days. Effect of different treatments, including Rh and Piri + Rh on progress of the disease on the wheat seedlings were evaluated. **(C)** Effect of various treatments of Mock, Piri, Fg, Piri + Fg, Rh, and Piri + Rh on relative water content (RWC). **(D)** Effect of various treatments of Mock, Piri, Fg, Piri + Fg, Rh, and Piri + Rh on membrane stability index (MSI). Piri, *P. indica*; Fg, *F. graminearum*; Rh, *R. cerealis*; Piri + Fg, *P. indica* + *F. graminearum*; Piri + Rh, *P. indica* + *R. cerealis*.

contrast, the RWC in Rh was higher than in Fg (**Figure 3C**). On the other hand, the data trend of MSI was consistent with the RWC in the mock, Piri, Piri + Rh, Rh, Piri + Fg, and Fg (**Figure 3D**).

Interaction of *Piriformospora indica* With *Rhizoctonia cerealis* and *Fusarium graminearum in vitro*

Since *P. indica* can inhibit pathogens' infection in plants, we wanted to determine whether it can also inhibit pathogens' infection *in vitro*. Co-cultivation of *P. indica* with *R. cerealis* or with *F. graminearum* on PDA plate indicated that the endophytic fungi had no antagonistic effect on them, and no obvious inhibitory zone was found at the meeting point of the two colonies (**Figures 4A,B**).

Detection of H_2O_2 in Wheat Plants

The capabilities of six treatments, such as of mock, Piri, Piri + Rh, Rh, Piri + Fg, and Fg, for inducing H_2O_2 accumulation in wheat leaves, were investigated at 12, 24, 36, 48, 72, and 84 h, respectively, after inoculation (hai) (**Figure 5**). In the Piri + Rh group, the content of H_2O_2 reached the highest level at 48 hai, and then, gradually decreased. For the Rh, the content of H_2O_2 reached the peak level at 72 h after infection, which was later than that of the Piri + Rh group. Similarly, the content of H_2O_2 reached the peak after 72 h of infection in Piri + Fg treatment; whereas the highest level of H_2O_2 content was delayed to 84 hai in Fg treatment.

Determination of Antioxidant Enzymes Activity

To investigate the effect of various treatments on enzymatic antioxidants, activities of CAT, POD, SOD, and GPX were assayed in wheat seedlings at 12, 24, 36, 48, 72, and 84 hai, respectively (**Figures 6A–D**). The CAT activity in control plants without fungal inoculation had a stationary trend and was at the lowest level at all time points compared to other treatments tested. In Rh, CAT activity increased from 48 to 72 hai and then, decreased until 84 hai (**Figure 6A**). In Fg, the CAT activity increased from 36 hai. By contrast, the CAT activity in Piri + Rh, Piri + Fg was activated from 36 to72 hai and significantly higher than in Rh and Fg respectively. Also, CAT activity in the Pi treatment was higher than Rh and Fg, but lower than Piri + Rh and Piri + Fg.

The SOD activity in control plants exposed stationary estate and had the lowest level compared to other treatments tested. In Rh, SOD activity increased from 48 to 72 hai, followed by a decreasing trend until 84 hai (**Figure 6B**). In Pi + Rh treatment, an increasing trend of SOD activity was observed from 36 to 72 dai, and then, decreased. In Piri, a significant increase of SOD activity from 36 to 72 hai was observed, and then, displayed a

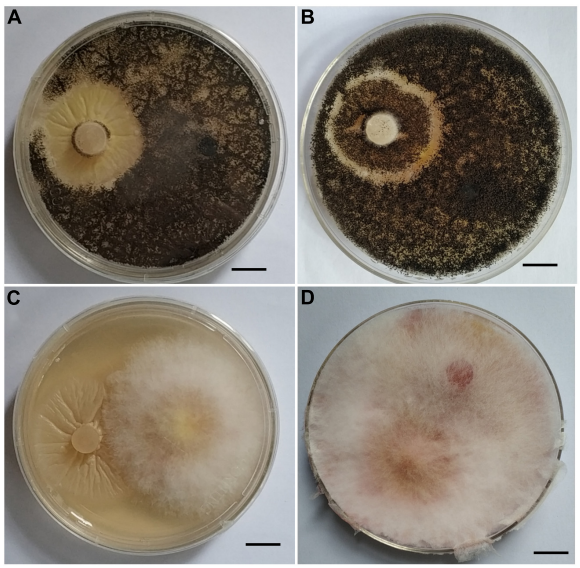

FIGURE 4 | Interaction of *Piriformospora indica* with *Fusarium graminearum* or *Rhizoctonia cerealis* on PDA plates. **(A)** *P. indica* and *R. cerealis* grow on PDA plate at the 13 and 5th, respectively; **(B)** *P. indica* and *R. cerealis* grow on PDA plate at the 16 and 8th, respectively. **(C)** *P. indica* and *F. graminearum* grow on PDA plate at the 13 and 5th, respectively. **(D)** *P. indica* and *F. graminearum* grow on PDA plate at the 16 and 8th, respectively.

stationary status until 84 hai. The highest level of SOD activity was observed at 48 hai in Fg treatment. In Pi + Fg treatment, an increasing trend of SOD activity was observed from 36 to 72 dai. The data indicated that pre-inoculation of *P. indica* spore could increase SOD activity either in Pi + Rh or Pi + Fg treatment from 36 to 72 dai, and then, remained approximately at the same level.

The POD activity in control plants without fungal inoculation had a stationary trend and was at the lowest level at all time points. In Rh and Fg, a similar trend was observed for the POD activity from 36 to 84 hai (**Figure 6C**). In Pi + Rh treatment, an increasing trend of POD activity was observed from 36 to 72 dai, and then, decreased. The POD activity in Pi + Fg has the same trend, but a higher POD activity was obtained than the Pi + Rh treatment. In Piri, significant increase of POD activity from 48 to 72 hai was observed. The highest level of POD activity was observed at 72 hai in Piri treatment. The data indicated that pre-inoculation of *P. indica* spore could increase POD activity either in Pi + Rh or Pi + Fg treatment from 36 to 72 dai.

The order of GPX activity in control plants without fungal inoculation had a stationary trend. In Rh and Fg, a similar trend was observed for the GPX activity from 36 to 84 hai (**Figure 6D**). By contrast, the GPX activity in Rh was a bit higher than in Fg treatment. However, In Piri, significant increase in GPX activity from 24 to 72 hai was observed. And the GPX activity in Pi + Rh treatment and Pi + Fg was higher than in Piri from 48 to 72 hai. In addition, Pi + Rh could promote higher GPX activity than Pi + Fg.

Profile of Different Expressed Genes in Wheat Responsive to *Piriformospora indica* and Pathogens Colonization

The transcriptomes of wheat responsive to *P. indica* and pathogens colonization (see **Table 1**) were obtained and

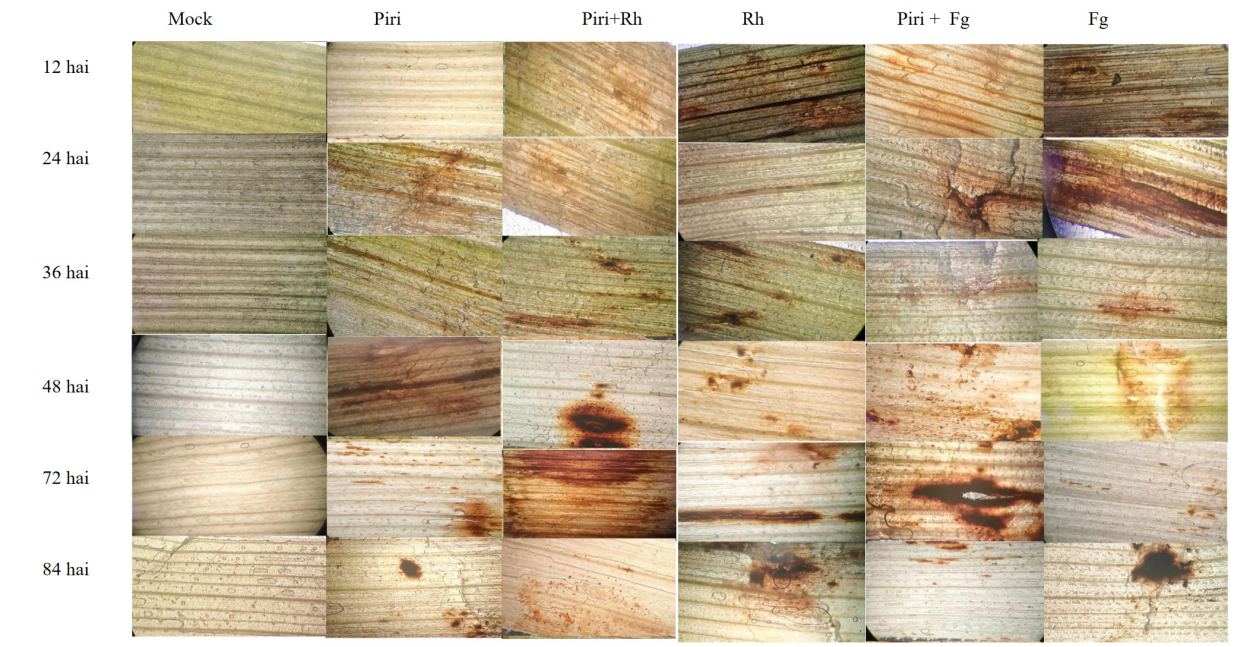

FIGURE 5 | Detection of H_2O_2 in wheat leaf segments using 3, 3- diaminobenzidine (DAB) at various hours post inoculation under different treatments. Piri, *P. indica*; Fg, *F. graminearum*; Rh, *R. cerealis*; Piri + Fg, *P. indica* + *F. graminearum*; Piri + Rh, *P. indica* + *R. cerealis*.

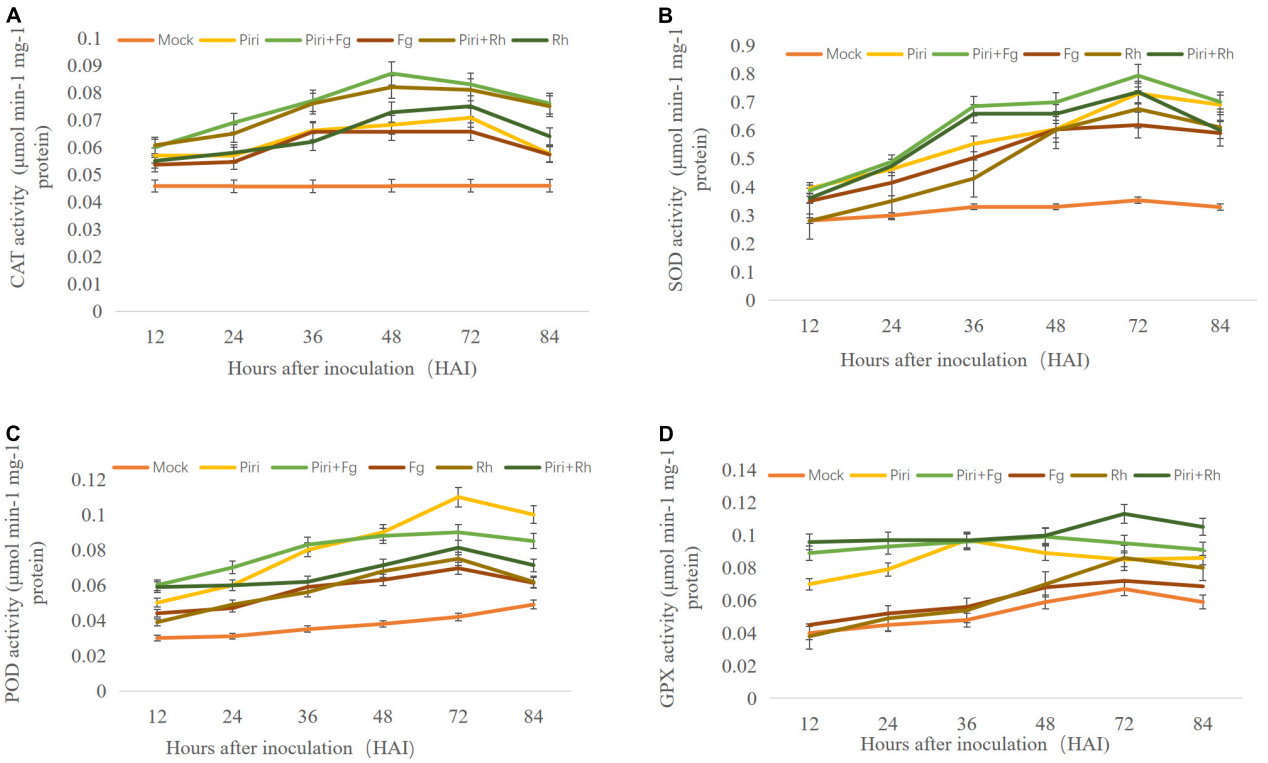

FIGURE 6 | Determination of antioxidant enzymes activity in wheat seedlings with various treatments at different time points after different fungi inoculation. **(A)** Catalase (CAT) activity; **(B)** superoxide dismutase (SOD) activity; **(C)** peroxidase (POD) activity; **(D)** Guaiacol peroxidase (GPX) activity. Piri, *P. indica*; Fg, *F. graminearum*; Rh, *R. cerealis*; Piri + Fg, *P. indica* + *F. graminearum*; Piri + Rh, *P. indica* + *R. cerealis*.

sequenced respectively by the BGI Seq500 platform. All the uni-genes were finally obtained by sequence splicing, a redundancy removal based on the sequence clustering software. Functional notation and cluster analysis of unigenes were performed by comparing unigenes to the database. Through data integration analysis, differentially expressed genes (DEGs) of wheat responsive to *P. indica* and pathogens colonization were analyzed (**Table 2**). The number of DEGs caused by root rot disease was 31,355, and the upregulation and downregulation genes were 17,859 and 13,496, respectively. The number of DEGs in wheat caused by sheath blight was 3,167, and the number of upregulated and downregulated genes was 1,988 and 1,179, respectively. However, *P. indica* had the least effect on the transcriptome of wheat, with only 641 DEGs, among which 147 genes were upregulated and 494 genes were downregulated, respectively.

It was shown that, compared to mock, Fg treatment produced 31,355 DEGs, by adding *P. indica*, the number of DEGs was reduced to 27,516 in Piri + Fg; whereas Rh treatment produced 3,167 DEGs and Rh + Piri produced 1,395 DEGs (**Figures 7A,B**). We can obtain some hints from the above data: (1) Transcriptome changes caused by *F. graminearum* were more severe than those caused by *R. cerealis*; (2) The number of DEGs in the transcriptome can be reduced by the addition of *P. indica*. The DEGs caused by *F. graminearum* reduced 18% and those caused by *R. cerealis* reduced 58% by the addition of *P. indica*. Additionally, the DEGs involved in the Kyoto Encyclopedia of Genes and Genomes (KEGG) pathway were analyzed (**Figures 7C–F**). In the Fg treatment group, the DEGs were mainly concentrated in the chloroplast-related pathways, including Chloroplast, chloroplast stroma, chloroplast envelope, chloroplast thylakoid, chloroplast membrane, and chloroplast inner membrane (**Figure 7C**). In the Piri + Fg group, besides the chloroplast-related pathways, DEGs in the plant Tpye cell wall, extracellular region, and photosystem I pathway were added,

TABLE 2 | Differentially expressed genes (DEG) in the different comparison group.

	Comparison group	DEG number	Up expression of DEG	Down expression of DEG
Fg Group	Fg vs. Mock	31,355	17,859	13,496
	Piri vs. Mock	641	147	494
	Piri + Fg vs. Mock	27,516	17,142	10,374
	Piri + Fg vs. Fg	3,941	2,559	1,382
	Piri + Fg vs. Piri	20,757	11,467	9,290
Rh Group	Rh vs. Mock	3,167	1,988	1,179
	Piri + Rh vs. Mock	1,395	375	1,020
	Piri + Rh vs. Rh	2,126	541	1,585
	Piri + Rh vs. Piri	796	224	572

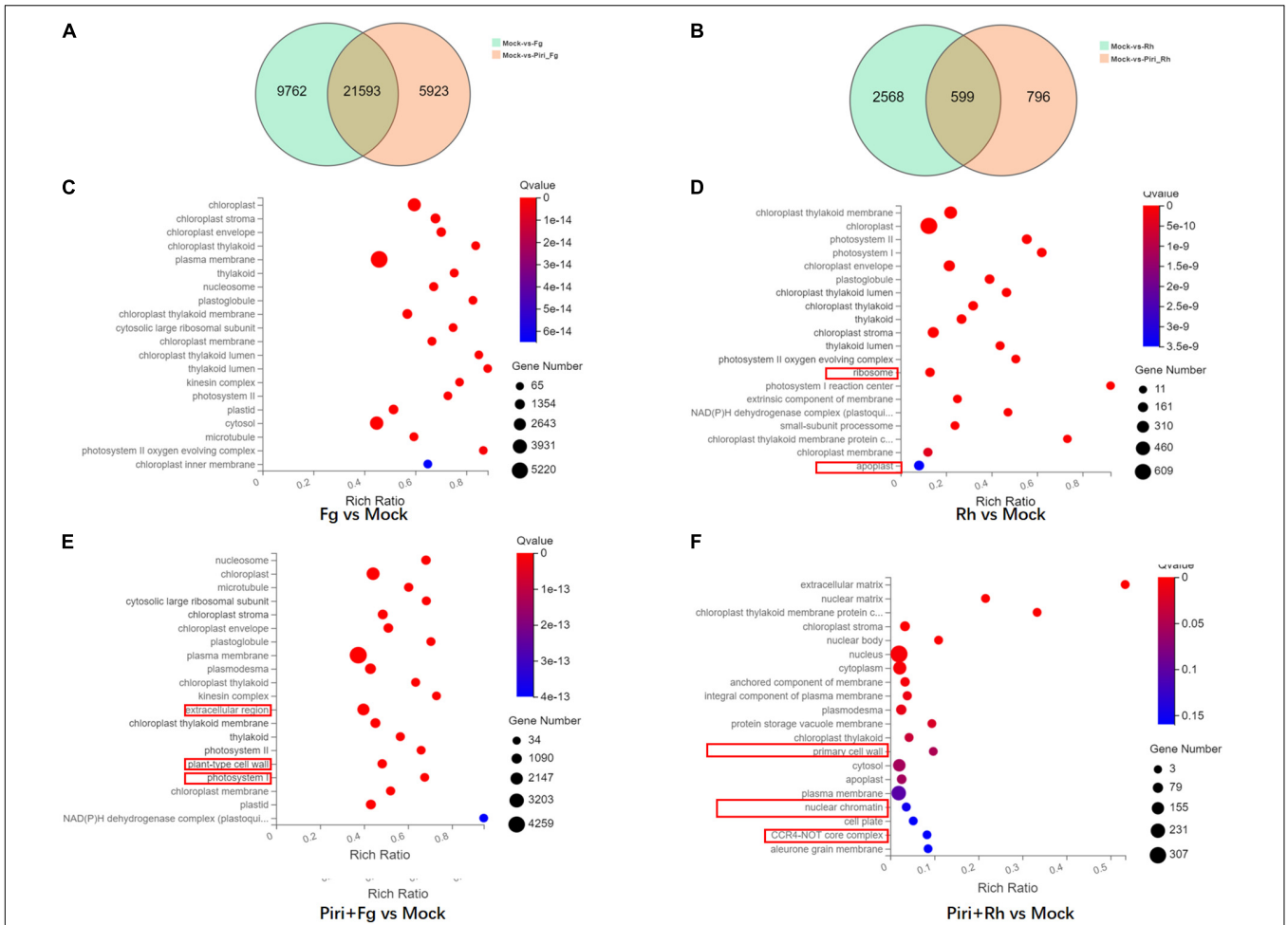

FIGURE 7 | Profile of different expressed genes in wheat responsive to *P. indica* and pathogens colonization. **(A)** Venn Diagram of the different expressed genes (DEGs) between Fg vs. Mock and Piri + Fg vs. Mock. **(B)** Venn Diagram of the DEGs between Rh vs. Mock and Piri + Rh vs. Mock. **(C)** DEGs enriched in KEEG pathway in Fg vs. Mock group. **(D)** DEGs enriched in KEEG pathway in Rh vs. Mock group. **(E)** DEGs enriched in KEEG pathway in Piri + Fg vs. Mock group. **(F)** DEGs enriched in KEEG pathway in Piri + Rh vs. Mock group (/log2 FC/ > = 1, Q-value < = 0.05). Piri, *P. indica*; Fg, *F. graminearum*; Rh, *R. cerealis*; Piri + Fg, *P. indica* + *F. graminearum*; Piri + Rh, *P. indica* + *R. cerealis*.

suggesting that these pathways probably play an important role in alleviating the effects of the disease (**Figure 7E**). Compared with the DEGs caused by *F. graminearum*, the DEGs caused by *R. cerealis* not only concentrated in the chloroplast-related pathway, but also involved in the ribosome and apoplast pathways, which implied that different pathways were activated by the two different pathogens (**Figure 7D**). By adding *P. indica*, another three pathways including the primary cell wall, Neclear chromatin, and CCR4-not Core complex pathway were added in the Piri + Rh group, and the defense role of these pathways also needs to be further explored (**Figure 7F**).

Identification of the Critical Genes in the Key Pathway

Because the addition of *P. indica* significantly alleviated the yield loss caused by *F. graminearum* and *R. cerealis*, we were curious to discover the molecular season of this difference at the transcriptome level. Significantly, DEGs were found in Piri + Fg vs. Fg comparison group (**Figure 8A**). There were 116 genes in the mitogen-activated protein kinase (MAPK) signaling pathway (plant), 71 of which were upregulated and 45 of which were downregulated. In the phenylalanine pathway, there were 167 DEGs, including 121 upregulated genes and 46 downregulated genes. In general, the number of upregulated genes was greater than that of downregulated genes in the Piri + Fg vs. Fg comparison group (**Table 3**).

In the Piri + Rh vs. Rh comparison group, significant DEGs were found mainly in phenylpropanoid biosynthesis, photosynthesis – antenna proteins, starch, and sucrose metabolism (**Figure 8B**). There were 87 DEGs, including 17 upregulated genes and 70 downregulated genes in the Phenylpropanoid biosynthesis pathway; In the fetish-antenna proteins pathway, 53 DEGs were downregulated. In Photosynthesis – antenna proteins pathway, there were 48 DEGs, 11 of which were upregulated and 37 of which were

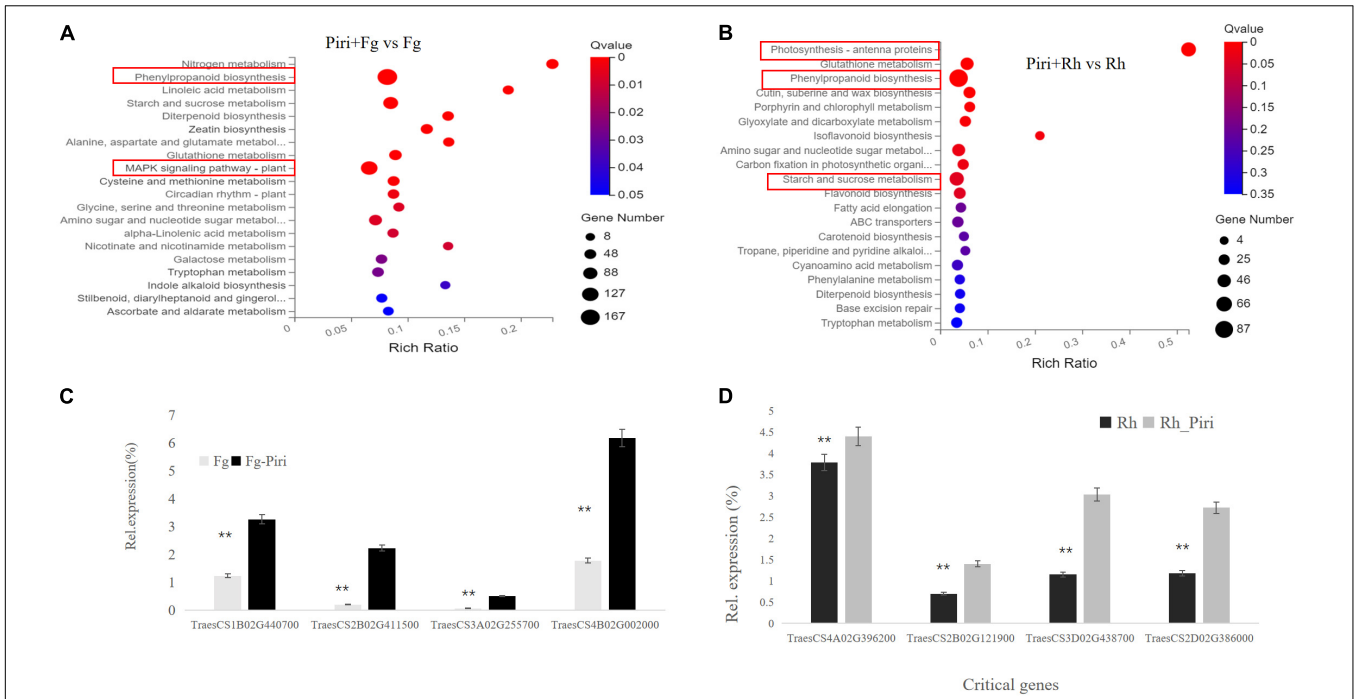

FIGURE 8 | Differentially expressed genes (DEGs) analysis in Kyoto Encyclopedia of Genes and Genomes (KEGG) pathway and QPCR identification by comparing Piri + Fg vs. Fg and Piri + Rh vs. Rh. **(A)** DEGs analysis in KEGG pathway by comparing Piri + Fg vs. Fg; **(B)** DEGs analysis in KEGG pathway by comparing Piri + Rh vs. Rh; **(C)** Identification of the critical genes by QPCR in Piri + Fg vs. Fg group; **(D)** Identification of the critical genes by QPCR in Piri + Rh vs. Rh group. Piri, *P. indica*; Fg, *F. graminearum*; Rh, *R. cerealis*; Piri + Fg, *P. indica* + *F. graminearum*; Piri + Rh, *P. indica* + *R. cerealis*.

downregulated. In general, the number of downregulated genes was greater than that of upregulated genes in the Piri + Rh vs. Rh comparison group (**Table 3**). The significant DEGs in the KEGG pathway were explored and their expression levels were quantitatively analyzed by QPCR (**Figures 8C,D**). The functions of these genes and their accession numbers in National Care for Biotechnology Information (NCBI) were listed in **Tables 4**, **5**. By comparing Piri + Fg vs. Fg, the significantly DEGs were functionally described as transcription factor WRKY19-like, ethylene-response factor C3/1B-like, mitogen-activated protein kinase kinase kinase 17-like, and were all upregulated in Piri + Fg (**Table 4**). In contrast, by comparing Piri + Rh vs. Rh, the significant DEGs were functionally described as WRKY transcription factor 70, LRR receptor-like serine/threonine-protein kinase, and cytochrome P450 84A1-like and were upregulated in Piri + Rh (**Table 5**).

TABLE 3 | Differentially expressed genes (DEG) involved in the key KEGG pathway in the comparison group of Piri + Fg vs. Fg and Piri + Rh vs. Rh.

	KEGG pathway	DEG number	Up expression of DEG	Down expression of DEG
Piri + Fg vs. Fg	MAPK signaling pathway – plant	116	71	45
	Phenylpropanoid biosynthesis	167	121	46
Piri + Rh vs. Rh	Phenylpropanoid biosynthesis	87	17	70
	Photosynthesis – antenna proteins	53	0	53
	Starch and sucrose metabolism	48	11	37

DISCUSSION

As an important worldwide food crop, wheat quality assurance plays an important role in maintaining the stability of food supply and food safety (Pehlivan-Karakas et al., 2021). However, wheat is often infected with many soil-borne diseases, resulting in reduced production. The sharp eyespot disease, caused by the necrotrophic fungus *R. cerealis*, and Fusarium head blight (FHB), caused mainly by the soil-borne fungus *F. graminearum*, are destructive diseases of wheat in many regions of the world (Gilbert and Tekauz, 2000; Hamada et al., 2011; Fernando et al., 2021). Therefore, the biological control capability of *P. indica* in wheat against sharp eyespot and FHB was investigated in this study.

In our effort, we have found that the germination rate of wheat seed that emerged in *P. indica* was significantly higher, and the germination time was 1 day earlier than the controls (soaked in water). In addition, our results proved that *P. indica* treatment was able to promote plant growth parameters, stimulating root biomass and fresh weight. Consistent with our data, colonization of *P. indica* has been confirmed to be able to increase the growth parameters of various plants (Deshmukh and Kogel, 2007;

TABLE 4 | Identification of DEGs involved in the key pathway by comparing Piri + Fg vs. Fg.

Seq-ID	Gene functional description	NCBI accession No.
TraesCS1B02G440700	*Triticum aestivum* transcription factor WRKY19-like (LOC123147334)	XM_044566571.1
TraesCS2B02G411500	*Triticum aestivum* ethylene-response factor C3-like	XM_037633443.1
TraesCS3A02G255700	*Triticum aestivum* mitogen-activated protein kinase kinase kinase 17-like	XM_044485046.1
TraesCS4B02G002000	*Triticum aestivum* ethylene-responsive transcription factor 1B-like	XM_044516187.1

TABLE 5 | Identification of DEGs involved in the key pathway by comparing Piri + Rh vs. Rh.

Seq-ID	Gene functional description	NCBI accession No.
TraesCS4A02G396200	*Triticum aestivum* WRKY transcription factor 72B-like	XM_044505189.1
TraesCS2B02G121900	Probable WRKY transcription factor 70	XM_044463411.1
TraesCS3D02G438700	Probable LRR receptor-like serine/threonine-protein kinase	XM_044495684.1
TraesCS2D02G386000	Cytochrome P450 84A1-like	XM_044477703.1

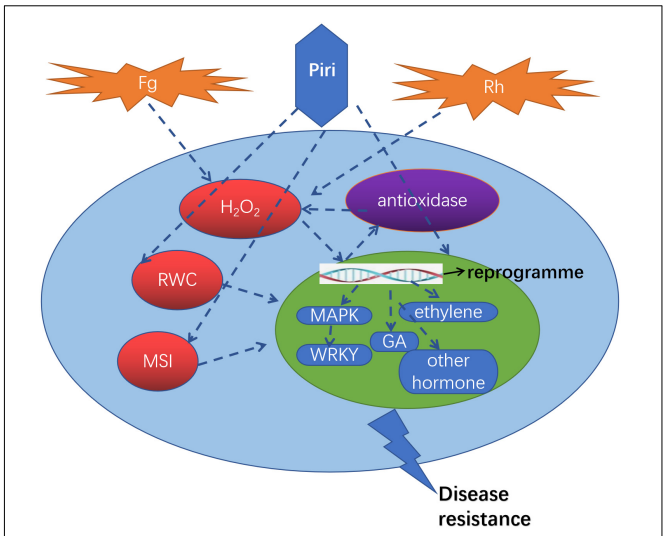

FIGURE 9 | A proposed model illustrating the roles of *P. indica* in wheat against *R. cerealis* and *F. graminearum*. Piri, *P. indica*; Fg, *F. graminearum*; Rh, *R. cerealis*; RWC, relative water content; MSI, membrane stability index; GA, gibberellin acid; MAPK, mitogen-activated protein kinases.

Waller et al., 2008; Sun et al., 2014; Nassimi and Taheri, 2017; Kundu et al., 2021; Liu et al., 2021), which undoubtedly makes us believe that *P. indica* can be considered as a biological fertilizer to improve plant yields. Several hypotheses have been formulated about the mechanisms of growth promotion of *P. indica,* which suggested that *P. indica* may actively promote auxin-regulated genes through the production of indole-3-acetic acid-like compounds (Lee et al., 2011; Franken, 2012). Of course, there are other possible reasons why *P. indica* promote plant growth. Studies have shown that root colonization by *P. indica* can hijack the ethylene signal pathway (Barazani et al., 2007). Because ethylene is used by plants to inhibit their growth under natural conditions, *P. indica* changes the ethylene pathway, which in turn may help promote host growth (Schäfer et al., 2009). A recent study indicated that Fe transporter (*PiFTR)* (Verma et al., 2021) and sulfate transporter (*SiSulT*) from *P. indica* (Narayan et al., 2021) play key roles in plant growth and development.

When we compare the difference between the treatment of *R. cerealis* and *F. graminearum*, it was clear that the disease effect of *F. graminearum* was more serious than *R. cerealis*. Previous physiological experiments have fully demonstrated that the colonization of wheat with *P. indica* can significantly inhibit the yield reduction caused by these two pathogens. In particular, we found that pre-soaking seeds in spore solution of *P. indica* could increase germination rates (**Figure 1**). These phenomena give us the confidence and motivation to unravel the mechanism behind them.

Our data demonstrated that dual culture on agar plate did not show any direct antagonistic effect of *P. indica* on *R. cerealis*, or *F. graminearum* (**Figures 2A–D**). These results were consistent with previous studies that *P. indica* has no resistance to the pathogen, including *F. graminearum*, *F. verticillioides*, *F. culmorum, Rhizoctonia solani*, and *Fusarium pseudograminearum in vitro* (Deshmukh and Kogel, 2007; Kumar et al., 2009; Rabiey et al., 2015; Nassimi and Taheri, 2017; Dehghanpour-Farashah et al., 2019). However, it has also been reported that *P. indica* can produce obvious inhibitory effects on *Verticillium dahliae* and *Gaeumannomyces graminis* on PDA plate (Ghahfarokhi and Goltapeh, 2010; Sun et al., 2014). This may indicate that the antagonistic effect of *P. indica* is species-specific *in vitro*.

In vivo, *P. indica* can inhibit disease effects caused by *R. cerealis and F. graminearum* (**Figure 3**). We found that a better antagonistic effect of *P. indica* would be produced *in vivo* when the time interval between *P. indica* and *R. cerealis* was 14 days (**Figure 3B**). As for *F. graminearum,* the best time interval between *P. indica* and *F. graminearum* was 10 days. And, in alleviating root rot, the role of *P. indica* is clear (**Figure 3D**). Previous evidence indicated that *P. indica* could induce resistance against *F. graminearum* and *F. culmorum* in barely (Deshmukh and Kogel, 2007; Waller et al., 2008; Harrach et al., 2013). Nassimi and Taheri (2017) reported that seedlings of rice pre-inoculated with *P. indica* showed a decreased level of disease caused by *R. solani,* which is consistent with our findings. Additionally, plants including barely, *Arabidopsis,* and maize pre-colonized *P. indica* significantly decreased the severity of the disease caused by *F. culmorum* and *Blumeria graminis* f. sp. Hordei, *Verticillium dahliae*, *F. verticillioides*, respectively (Waller et al., 2008; Kumar et al., 2009; Sun et al., 2014). Together with our data, this information strongly suggests that *P. indica* enhances plant resistance to pathogens through some indirect and complex mechanism.

Our study showed that RWC and MSI levels increased in the treatments of Pi and Pi + Rh compared to Fg/Rh and the control (**Figure 4**). The research demonstrated that electrolyte concentration in arbuscular mycorrhizal plants was higher than non-mycorrhizal plants because of the improved integrity and stability of membrane result from the colonization of arbuscular mycorrhizal fungi (Kaya et al., 2009). In addition, Naghashzadeh (2014) reported that the improved RWC and MSI were found in maize plants by applying mycorrhizal bio-fertilizers. The increased RWC and MSI in the *P. indica* colonized plant in our study implied that, like arbuscular mycorrhizal fungi, *P. indica* has the potential to be a biological fertilizer.

The results showed that both the disease of root rot and sheath blight could increase the content of H_2O_2 in leaves (**Figure 5**). This was consistent with previous studies, which have shown that soil-borne pathogens can accelerate plant cell death by increasing reactive oxygen species (ROS) and oxidative stress (Desmond et al., 2008; Cuzick et al., 2009). Our results further showed that the peak content of H_2O_2 appeared earlier in the Piri + Rh and Piri + Fg group, which indicated that the time point of hydrogen peroxide accumulation could be advanced by pre-inoculation of *P. indica*. In addition, our data showed that activity of SOD, POD, CAT, and GPX were activated in Piri, Piri + Rh, and Piri + Fg groups (**Figure 6**). Those data agreed with previously reported that *P. indica* can protect barley roots from loss of antioxidant enzymes caused by *F. culmorum* (Harrach et al., 2013). The research of Schäfer et al. (2009) and Jacobs et al. (2011) also clarified that *P. indica* intercepts MAMPs to induce immune responses, including oxidative bursts, induction of defense-related genes. Accordingly, it makes sense that the increased H_2O_2 content and enhanced antioxidant enzyme activity in plants pre-colonized by *P. indi*ca act as a signal to induce plants' immune system, thereby enhancing plants' resistance to pathogens. However, it is postulated that endophytes produce low levels of lytic enzymes as compared with pathogens, thus, avoiding triggering the plant immune response and gene products from mycorrhizal fungi are speculated to mimic the host cell signaling, thus, acting as decoys to circumvent plant defenses and gain entry into plant tissues (Trivedi et al., 2021). Obviously, *P. indica* acts as different patterns to participate in plant immune response. Overall, the interplay between plants and their endophytic microbiota is complex and still far from being fully elucidated.

Comparing the transcriptome of the different treatments, we found that transcriptome changes caused by *R. cerealis* were more intense than those caused by *F. graminearum* (**Table 2**). The growth promotion induced by *P. indica* was significant, although the transcriptome changes were not as large as those caused by the pathogen. Gene ontology (GO) analysis indicated enrichment in genes involved in various metabolic and catalytic processes. A previous study proved that the roots of the *Brachypodium distachyon* also displayed substantial transcriptional reprogramming following *P. indica* colonization (Šečić et al., 2021). These reprogramming genes must be responsible for the fungus-mediated growth promotion. In the Fg treatment group, the differential genes were mainly concentrated in the chloroplast-related pathways: Chloroplast, chloroplast stroma, chloroplast envelope, chloroplast thylakoid, chloroplast membrane, and chloroplast inner membrane. In the Piri + Fg group, different genes in the Tpye cell wall of the plant, in the extracellular region (1,733), and photosystem I pathway were added (**Figure 7**), suggesting that these pathways play an important role in alleviating the effects of the disease. The differential genes of sheath blight mainly concentrated in the pathways related to the chloroplast pathway, and involved in the ribosome and Apoplast pathways, suggesting that there were differences in the treatment pathways of the two strains. Compared with the Piri + Rh group, the differential genes of the primary cell wall, Neclear chromatin, and CCR4-not Core complex pathway were added, and the defense role of these pathways also needs to be further explored.

It was found that the addition of *P. indica* greatly alleviated the root rot caused by *F. graminearum* by comparing Piri + Fg to Fg treatment. Transcriptome sequencing showed that DEGs were mainly focused on the MAPK pathway and Phenylpropanoid biosynthesis (**Figure 8A**). Of them, 116 DEGs were found in the MAPK pathway, of which 71 were upregulated and 45 were downregulated. Accumulating data have demonstrated that MAPK cascades play central roles in plant immunity. In *Arabidopsis*, at least two complete MAPK cascades, the MEKK1-MKK1/MKK2-MPK4 and MAPKKK3/MAPKKK5-MKK4/MKK5-MPK3/MPK6 cascades, have been identified and reported to be involved in the elicitation of immune responses (Asai et al., 2002; Suarez-Rodriguez et al., 2007; Qiu et al., 2008; Yamada et al., 2016; Bi et al., 2018; Sun et al., 2018; Gao et al., 2021).

In rice, OsMAPKKK18 and OsMAPKKK24 also function downstream of receptor-like cytoplasmic kinases (RLCKs) and activate the OsMPKK4-OsMPK3/OsMPK6 cascade in the chitin signaling pathway (Kishi-Kaboshi et al., 2010; Wang et al., 2017; Yamada et al., 2017; Ma et al., 2021), suggesting similarity, as well as the diversity of MAPK cascades involved in immunity in different plant species. Therefore, we can determine that *P. indica* can participate in the activation of the plant immune system by activating the MAPK pathway. Thus, further experiments are warranted to determine which MAPK in wheat was involved in the elicitation of immune responses under the *P. indica* colonization.

On the other hand, we found that the phenylpropanoid biosynthesis pathway also participated in plant resistance to *F. graminearum*. Among 167 DEGs of phenylpropanoid biosynthesis pathway, 121 were upregulated and 67 downregulated. Plants have evolved exquisite mechanisms for the biosynthesis of secondary metabolites such as phenylpropanoids to cope with biotic and abiotic stresses (Dong and Lin, 2021). The significant DEGs in the phenylpropanoid biosynthesis pathway gave us reason to believe that *P. indica* can improve the wheat resistance to *F. graminearum via* regulating the phenylpropanoid biosynthesis.

In the case of *R. cerealis*, the pre-colonization of *P. indica* in wheat roots reduced the number of leaf spots caused by *R. cerealis* by comparing Piri + Rh to Rh treatment. Transcriptome sequencing showed that DEGs were mainly focused on phenylpropanoid biosynthesis, photosynthesis – antenna proteins, starch, and sucrose metabolism (**Figure 8B**). In the phenylpropanoid biosynthesis pathway, there were 87

differentially expressed genes, including 17 upregulated genes and 70 downregulated genes. In the photosynthesis – antenna proteins pathway, 53 differentially expressed genes were all downregulated. In the sucrose and sucrose pathway, the number of differentially expressed genes was 48, with 11 upregulated genes and 37 downregulated genes. By comparison, the responses of plants to the synergistic action of *P. indica* with the two respective pathogens were different. As reported, abiotic and biotic stresses widely reduce light-harvesting complex (LHC) gene expression in higher plants (Islam et al., 2020), which is consistent with our data that genes involved in Photosynthesis - antenna proteins pathway were all downregulated. However, control mechanisms and functions of these changes are not well-understood. Further research on the role of those defense components and their relationships with various types of reactive oxygen, antioxidant systems, in basal immunity will help us to design novel and effective disease management strategies to protect wheat plants against this destructive fungal pathogen.

CONCLUSION

A proposed model illustrating the roles of *P. indica* in wheat against *R. cerealis* and *F. graminearum* was drawn in **Figure 9**. The pathogens including *R. cerealis* and *F. graminearum* can induce the accumulation of H_2O_2 in plants, reduce the intracellular water content, and destroy the membrane stability. The addition of *P. indica* can reprogram the transcriptomic changes caused by *R. cerealis* and *F. graminearum*: (1) Inducing the expression of resistance-related genes, such as MAPK and WRKY; (2) Affecting the plant hormone signaling pathway; (3) Activating antioxidant pathway. Accordingly, wheat can directly resist the pathogen *via* the expression of resistance gene; Through the influence of the hormone metabolism pathway, *P. indica* colonization improved plant biological yield and enhanced plants tolerance to pathogens; By increasing the activity of antioxidant enzymes, the accumulation of reactive oxygen species in cells was decreased, and the water content in cells was further maintained and membrane stability was enhanced. Based on the above three modes, the resistance of wheat to these two pathogens was comprehensively improved.

DATA AVAILABILITY STATEMENT

The datasets presented in this study can be found in online repositories. The name of the repository and accession number can be found below: NCBI; PRJNA789469.

AUTHOR CONTRIBUTIONS

LL: conceptualization, methodology, investigation, formal analysis, visualization, and writing—original draft preparation, reviewing, and editing. NG and CL: investigation, formal analysis, and visualization. YF: software, data curation, and formal analysis. MD: software, investigation, and formal analysis. All authors approved the final manuscript.

FUNDING

We gratefully acknowledge support from the Natural Science Foundation of Hebei Province (Grant No. C2021202005) and the National Natural Science Foundation of China (Grant No. 31801948) as well as Key R&D Projects in Hebei Province (Grant No. 19226505D) for financial support.

ACKNOWLEDGMENTS

We would like to thank Prof. Karl-Heinz-Kogel for the gift of the *Piriformospora indica*. We gratefully acknowledge the Wu Hongqing for technical assistance in microscopy and macroscopy analyses. We also want to express our appreciation to students who contributed to this work, especially Yanze Zhang and Yuan Zhi. Lastly, we thank Mu Di for the critical reading and revision of the manuscript.

SUPPLEMENTARY MATERIAL

The Supplementary Material for this article can be found online at: https://www.frontiersin.org/articles/10.3389/fpls.2022.836940/full#supplementary-material

REFERENCES

Aebi, H. (1984). Catalase in vitro. *Methods Enzymol.* 105, 121–126. doi: 10.1016/S0076-6879(84)05016-3

Arora, M., Saxena, P., Choudhary, D. K., Abdin, M. Z., and Varma, A. (2016). Dual symbiosis between *Piriformospora indica* and *Azotobacter chroococcum* enhances the artemisinin content in *Artemisia annua* L. *World J Microbiol Biotechnol* 32:19. doi: 10.1007/s11274-015-1972-5

Asai, T., Tena, G., Plotnikova, J., Willmann, M. R., Chiu, W.-L., Gomez-Gomez, L., et al. (2002). MAP kinase signalling cascade in *Arabidopsis* innate immunity. *Nature* 415, 977–983. doi: 10.1038/415977a

Bajaj, R., Agarwal, A., Rajpal, K., Asthana, S., Prasad, R., Kharkwal, A. C., et al. (2014). Co-cultivation of *Curcuma longa* with *Piriformospora indica* enhances the yield and active ingredients. *Am. J Curr. Microbiol.* 2:12.

Barazani, O., von Dahl, C. C., and Baldwin, I. T. (2007). *Sebacina vermifera* promotes the growth and fitness of *Nicotiana attenuata* by inhibiting ethylene signaling. *Plant Physiol.* 144, 1223–1232. doi: 10.1104/pp.107.097543

Bi, G., Zhou, Z., Wang, W., Li, L., Rao, S., Wu, Y., et al. (2018). Receptor-Like cytoplasmic kinases directly link diverse pattern recognition receptors to the activation of mitogen-activated protein kinase cascades in *Arabidopsis*. *Plant Cell* 30, 1543–1561. doi: 10.1105/tpc.17.00981

Bradford, M. M. (1976). A rapid and sensitive method for the quantitation of microgram quantities of protein utilizing the principle of protein-dye binding. *Anal. Biochem.* 72, 248–254. doi: 10.1016/0003-2697(76)90527-3

Cuzick, A., Maguire, K., and Hammond-Kosack, K. E. (2009). Lack of the plant signalling component SGT1b enhances disease resistance to *Fusarium culmorum* in *Arabidopsis* buds and flowers. *New Phytol.* 181, 901–912. doi: 10.1111/j.1469-8137.2008.02712.x

Chance, B., and Maehly, A. C. (1955). Assay of catalases and peroxidases. *Methods Enzymol.* 2, 764–775. doi: 10.1016/S0076-6879(55)02300-8

Chen, L., Zhang, Z., Liang, H., Liu, H., Du, L., Xu, H., et al. (2008). Overexpression of TiERF1 enhances resistance to sharp eyespot in transgenic wheat. *J Exp. Bot.* 59, 4195–4204. doi: 10.1093/jxb/ern259

Das, A., Tripathi, S., and Varma, A. (2014). In vitro plant development and root colonization of *Coleus forskohlii* by *Piriformospora indica*. *World J. Microbiol. Biotechnol.* 30, 1075–1084. doi: 10.1007/s11274-013-1526-7

Desmond, O. J., Manners, J. M., Schenk, P. M., Maclean, D. J., and Kazan, K. (2008). Gene expression analysis of the wheat response to infection by *Fusarium pseudograminearum*. *Physiol. Mol. Plant Pathol.* 73, 40–47. doi: 10.1016/j.pmpp.2008.12.001

Dehghanpour-Farashah, S., Taheri, P., and Falahati-Rastegar, M. (2019). Effect of polyamines and nitric oxide in *Piriformospora indica*-induced resistance and basal immunity of wheat against *Fusarium pseudograminearum*. *Biol. Control* 136:104006. doi: 10.1016/j.biocontrol.2019.104006

Deshmukh, S. D., and Kogel, K.-H. (2007). Piriformospora indica protects barley from root rot caused by *Fusarium graminearum*. *J. Plant Dis. Prot* 114, 263–268. doi: 10.1007/BF03356227

Ding, Y., Kalo, P., Yendrek, C., Sun, J., Liang, Y., Marsh, J. F., et al. (2008). Abscisic acid coordinates nod factor and Cytokinin Signaling during the regulation of nodulation in *Medicago truncatula*. *Plant Cell* 20, 2681–2695. doi: 10.1105/tpc.108.061739

Dong, N., and Lin, H. (2021). Contribution of phenylpropanoid metabolism to plant development and plant–environment interactions. *J. Integr. Plant Biol.* 63, 180–209. doi: 10.1111/jipb.13054

Gunnaiah, R., Kushalappa, A. C., Duggavathi, R., Fox, S., and Somers, D. J. (2012). Integrated metabolo-proteomic approach to decipher the mechanisms by which wheat QTL (Fhb1) contributes to resistance against *Fusarium graminearum*. *PLoS One* 7:e40695. doi: 10.1371/journal.pone.0040695

Fakhro, A., Andrade-Linares, D. R., von Bargen, S., Bandte, M., Büttner, C., Grosch, R., et al. (2010). Impact of *Piriformospora indica* on tomato growth and on interaction with fungal and viral pathogens. *Mycorrhiza* 20, 191–200. doi: 10.1007/s00572-009-0279-5

Franken, P. (2012). The plant strengthening root endophyte *Piriformospora indica*: potential application and the biology behind. *Appl. Microbiol. Biotechnol.* 2012, 1455–1464. doi: 10.1007/s00253-012-4506-1

Fernandez, M. R., and Chen, Y. (2005). Pathogenicity of *Fusarium* species on different plant parts of spring wheat under controlled conditions. *Plant Dis.* 89, 164–169. doi: 10.1094/PD-89-0164

Fernando, W. G. D., Oghenekaro, A. O., Tucker, J. R., and Badea, A. (2021). Building on a foundation: advances in epidemiology, resistance breeding, and forecasting research for reducing the impact of *Fusarium* head blight in wheat and barley. *Can. J. Plant Pathol.* 43, 495–526. doi: 10.1080/07060661.2020.1861102

Gao, C., Sun, P., Wang, W., and Tang, D. (2021). *Arabidopsis* E3 ligase KEG associates with and ubiquitinates MKK4 and MKK5 to regulate plant immunity. *J. Integr. Plant Biol.* 63, 327–339. doi: 10.1111/jipb.13007

Gilbert, J., and Tekauz, A. (2000). Review: Recent developments in research on *Fusarium* head blight of wheat in Canada. *Can. J Plant Pathol* 22, 1–8. doi: 10.1080/07060660009501155

Gouda, S., Kerry, R. G., Das, G., Paramithiotis, S., Shin, and Kumar Patra, J. K. (2018). Revitalization of plant growth promoting rhizobacteria for sustainable development in agriculture. *Microbiol. Res.* 206, 131–140. doi: 10.1016/j.micres.2017.08.016

Hamada, M. S., Yin, Y., Chen, H., and Ma, Z. (2011). The escalating threat of *Rhizoctonia cerealis*, the causal agent of sharp eyespot in wheat. *Pest. Manag. Sci.* 67, 1411–1419. doi: 10.1002/ps.2236

Harrach, B. D., Baltruschat, H., Barna, B., Fodor, J., and Kogel, K. H. (2013). The mutualistic fungus *Piriformospora indica* protects barley roots from a loss of antioxidant capacity caused by the necrotrophic pathogen *Fusarium culmorum*. *MPMI* 26, 599–605. doi: 10.1094/MPMI-09-12-0216-R

Islam, S., Sabharwal, T., Wu, S., Bullock, T. J., and Mehdy, M. C. (2020). Early dynamics of photosynthetic Lhcf2 and Lhcf15 transcription and mRNA stabilities in response to herbivory-related decadienal in *Phaeodactylum tricornutum*. *Sci. Rep.* 10:2029. doi: 10.1038/s41598-020-58885-9

Jacobs, S., Zechmann, B., Molitor, A., Trujillo, M., Petutschnig, E., Lipka, V., et al. (2011). Broad-spectrum suppression of innate immunity is required for colonization of *Arabidopsis* roots by the fungus *Piriformospora indica*. *Plant Physiol.* 156, 726–740. doi: 10.1104/pp.111.176446

Kar, M., and Mishra, D. (1976). Catalase, peroxidase, and polyphenoloxidase activities during rice leaf senescence. *Plant Physiol.* 57, 315–319. doi: 10.1104/pp.57.2.315

Kaya, C., Ashraf, M., Sonmez, O., Aydemir, S., Tuna, A. L., and Cullu, M. A. (2009). The influence of arbuscular mycorrhizal colonization on key growth parameters and fruit yield of pepper plants grown at high salinity. *Sci. Hortic.* 121, 1–6. doi: 10.1016/j.scienta.2009.01.001

Kishi-Kaboshi, M., Okada, K., Kurimoto, L., Murakami, S., Umezawa, T., Shibuya, N., et al. (2010). A rice fungal MAMP-responsive MAPK cascade regulates metabolic flow to antimicrobial metabolite synthesis: Rice MAPK regulates antimicrobial biosynthesis. *Plant J.* 63, 599–612. doi: 10.1111/j.1365-313X.2010.04264.x

Kundu, A., Mishra, S., Kundu, P., Jogawat, A., and Vadassery, J. (2021). *Piriformospora indica* recruits host-derived putrescine for growth promotion in plants. *Plant Physiol.* 188, 2289–2307. doi: 10.1093/plphys/kiab536

Kumar, M., Yadav, V., Tuteja, N., and Johri, A. K. (2009). Antioxidant enzyme activities in maize plants colonized with *Piriformospora indica*. *Microbiology* 155, 780–790. doi: 10.1099/mic.0.019869-0

Lee, Y. C., Johnson, J. M., Chien, C. T., Sun, C., Cai, D., Lou, B., et al. (2011). Growth promotion of Chinese cabbage and *Arabidopsis* by *Piriformospora indica* is not stimulated by mycelium-synthesized auxin. *Mol. Plant Microbe Interact.* 24, 421–431. doi: 10.1094/MPMI-05-10-0110

Lobell, D. B., and Field, C. B. (2007). Global scale climate–crop yield relationships and the impacts of recent warming. *Environ. Res. Lett.* 2:014002. doi: 10.1088/1748-9326/2/1/014002

Li, D., Bodjrenou, D. M., Zhang, S., Wang, B., Pan, H., Yeh, K. W., et al. (2021a). The endophytic fungus *Piriformospora indica* reprograms banana to cold resistance. *Int. J Mol. Sci.* 22:4973. doi: 10.3390/ijms22094973

Li, L., Li, L., Wang, X., Zhu, P., Wu, H., and Qi, S. (2017). Plant growth-promoting endophyte *Piriformospora indica* alleviates salinity stress in *Medicago truncatula*. *Plant Physiol. Bioch.* 119, 211–223. doi: 10.1016/j.plaphy.2017.08.029

Li, Q., Kuo, Y. W., Lin, K. H., Huang, W., Deng, C., Yeh, K. W., et al. (2021b). *Piriformospora indica* colonization increases the growth, development, and herbivory resistance of sweet potato (*Ipomoea batatas* L.). *Plant Cell Rep.* 40, 339–350. doi: 10.1007/s00299-020-02636-7

Liu, Y., Zou, Y. N., Tian, Z. H., Wu, Q. S., and Kuča, K. (2021). Effects of beneficial endophytic fungal inoculants on plant growth and nutrient absorption of trifoliate orange seedlings. *Sci. Hortic.* 277:109815. doi: 10.1016/j.scienta.2020.109815

Livak, K. J., and Schmittgen, T. D. (2001). Analysis of relative gene expression data using real-time quantitative PCR and the 2(-Delta Delta C(T)) Method. *Methods* 25, 402–408. doi: 10.1006/meth.2001.1262

Lu, H., Wei, T., Lou, H., Shu, X., and Chen, Q. (2021). A critical review on communication mechanism within plant-endophytic fungi interactions to cope with biotic and abiotic stresses. *J. Fungi* 7:719. doi: 10.3390/jof7090719

Ma, H., Li, J., Ma, L., Wang, P., Xue, Y., Yin, P., et al. (2021). Pathogen-inducible OsMPKK10.2-OsMPK6 cascade phosphorylates the raf-like kinase OsEDR1 and inhibits its scaffold function to promote rice disease resistance. *Mol. Plant* 14, 620–632. doi: 10.1016/j.molp.2021.01.008

Naghashzadeh, M. (2014). Response of relative water content and cell membrane stability to mycorrhizal biofertilizer in maize. *eJBio.* 10, 68–72.

Narayan, O. P., Verma, N., Jogawat, A., Dua, M., and Johri, A. K. (2021). Sulfur transfer from the endophytic fungus *Serendipita indica* improves maize growth and requires the sulfate transporter SiSulT. *Plant Cell* 33, 1268–1285. doi: 10.1093/plcell/koab006

Nassimi, Z., and Taheri, P. (2017). Endophytic fungus *Piriformospora indica* induced systemic resistance against rice sheath blight via affecting hydrogen peroxide and antioxidants. *Biocontrol. Sci. Technol.* 27, 252–267. doi: 10.1080/09583157.2016.1277690

Osborne, L. E., and Stein, J. M. (2007). Epidemiology of *Fusarium* head blight on small-grain cereals. *Int. J. Food Microbiol.* 119, 103–108. doi: 10.1016/j.ijfoodmicro.2007.07.032

Panda, S., Busatto, N., Hussain, K., and Kamble, A. (2019). *Piriformospora indica*-primed transcriptional reprogramming induces defense response against early blight in tomato. *Sci. Hortic.* 255, 209–219. doi: 10.1016/j.scienta.2019.05.031

Pehlivan-Karakas, F., Keskin, C. N., Agil, F., and Zencirci, N. (2021). Profiles of vitamin B and E in wheat grass and grain of einkorn (*Triticum monococcum* spp. monococcum), emmer (*Triticum dicoccum* ssp. dicoccum Schrank.), durum (*Triticum durum* Desf.), and bread wheat (*Triticum aestivum* L.) cultivars

by LC-ESI-MS/MS analysis. *J. Cereal. Sci.* 98:103177. doi: 10.1016/j.jcs.2021.103177

Prasad, R., Kamal, S., Sharma, P. K., Oelmüller, R., and Varma, A. (2013). Root endophyte *Piriformospora indica* DSM 11827 alters plant morphology, enhances biomass and antioxidant activity of medicinal plant Bacopa monniera: Interaction of P. indica and *Bacopa monniera*. *J. Basic Microbiol.* 53, 1016–1024. doi: 10.1002/jobm.201200367

Qi, H., Zhu, X., Guo, F., Lv, L., and Zhang, Z. (2021). The wall-associated receptor-Like kinase TaWAK7D is required for defense responses to *Rhizoctonia cerealis* in wheat. *IJMS* 22:5629. doi: 10.3390/ijms22115629

Qiang, X., Weiss, M., Kogel, K.-H., and Schäfer, P. (2012). *Piriformospora indica*-a mutualistic basidiomycete with an exceptionally large plant host range: mutualistic root symbiosis. *Mol. Plant Pathol.* 13, 508–518. doi: 10.1111/j.1364-3703.2011.00764.x

Qiu, J. L., Zhou, L., Yun, B. W., Nielsen, H. B., Fiil, B. K., Petersen, K., et al. (2008). *Arabidopsis* mitogen-activated protein kinase kinases MKK1 and MKK2 Have overlapping functions in defense signaling mediated by MEKK1, MPK4, and MKS1. *Plant Physiol.* 148, 212–222. doi: 10.1104/pp.108.120006

Ghahfarokhi, R. M., and Goltapeh, M. E. (2010). Potential of the root endophytic fungus *Piriformospora indica*, *Sebacina vermifera* and *Trichoderma* species in biocontrol of take-all disease of wheat *Gaeumannomyces graminis* var. tritici in vitro, in Iran. *J Agric.Tech.* 6, 11–18.

Rajani, P., Rajasekaran, C., Vasanthakumari, M. M., Olsson, S. B., Ravikanth, G., and Shaanker, R. U. (2021). Inhibition of plant pathogenic fungi by endophytic *Trichoderma* spp. through mycoparasitism and volatile organic compounds. *Microbiol. Res.* 242:126595. doi: 10.1016/j.micres.2020.126595

Rabiey, M., and Shaw, M. W. (2016). *Piriformospora indica* reduces *Fusarium* head blight disease severity and mycotoxin DON contamination in wheat under UK weather conditions. *Plant Pathol.* 65, 940–952. doi: 10.1111/ppa.12483

Rabiey, M., Ullah, I., and Shaw, M. W. (2015). The endophytic fungus *Piriformospora indica* protects wheat from *Fusarium* crown rot disease in simulated UK autumn conditions. *Plant Pathol.* 64, 1029–1040. doi: 10.1111/ppa.12335

Roylawar, P., Khandagale, K., Randive, P., Shinde, B., Murumkar, C., Ade, A., et al. (2021). *Piriformospora indica* primes onion response against stemphylium leaf blight disease. *Pathogens* 10:1085. doi: 10.3390/pathogens10091085

Sahay, N. S., and Varma, A. (2006). *Piriformospora indica* : a new biological hardening tool for micropropagated plants. *FEMS Microbiol. Lett.* 181, 297–302. doi: 10.1111/j.1574-6968.1999.tb08858.x

Šečić, E., Zanini, S., Wibberg, D., et al. (2021). A novel plant-fungal association reveals fundamental sRNA and gene expression reprogramming at the onset of symbiosis. *BMC Biol.* 19:171. doi: 10.1186/s12915-021-01104-2

Schäfer, P., Pfiffi, S., Voll, L. M., Zajic, D., Chandler, P. M., Waller, F., et al. (2009). Manipulation of plant innate immunity and gibberellin as factor of compatibility in the mutualistic association of barley roots with *Piriformospora indica*. *Plant J.* 59, 461–474. doi: 10.1111/j.1365-313X.2009.03887.x

Singh, M., Srivastava, J. P., and Kumar, A. (1992). Cell membrane stability in relation to drought tolerance in wheat genotypes. *J. Agric. Crop Sci.* 168, 186–190. doi: 10.1111/j.1439-037x.1992.tb00997.x

Stein, E., Molitor, A., Kogel, K. H., and Waller, F. (2008). Systemic resistance in *Arabidopsis* conferred by the mycorrhizal fungus *Piriformospora indica* requires jasmonic acid signaling and the cytoplasmic function of NPR1. *Plant Cell Physiol.* 49, 1747–1751. doi: 10.1093/pcp/pcn147

Suarez-Rodriguez, M. C., Adams-Phillips, L., Liu, Y., Wang, H., Su, S. H., Jester, P. J., et al. (2007). MEKK1 is required for flg22-induced MPK4 activation in *Arabidopsis* plants. *Plant Physiol.* 143, 661–669. doi: 10.1104/pp.106.091389

Sun, C., Shao, Y., Vahabi, K., Lu, J., Bhattacharya, S., Dong, S., et al. (2014). The beneficial fungus *Piriformospora indica* protects *Arabidopsis* from *Verticillium dahliae* infection by downregulation plant defense responses. *BMC Plant Biol.* 14:268. doi: 10.1186/s12870-014-0268-5

Sun, T., Nitta, Y., Zhang, Q., Wu, D., Tian, H., Lee, J. S., et al. (2018). Antagonistic interactions between two MAP kinase cascades in plant development and immune signaling. *EMBO Rep.* 19:e45324. doi: 10.15252/embr.201745324

Tedersoo, L., Bahram, M., and Zobel, M. (2020). How mycorrhizal associations drive plant population and community biology. *Science* 367:867. doi: 10.1126/science.aba1223

Trivedi, P., Leach, J. E., Tringe, S. G., Sa, T. M., and Singh, B. K. (2021). Plant-microbiome interactions: from community assembly to plant health. *Nat. Rev. Microbiol.* 18, 607–621. doi: 10.1038/s41579-020-0412-1

Trzewik, A., Maciorowski, R., Klocke, E., and Orlikowska, T. (2020). The influence of *Piriformospora indica* on the resistance of two rhododendron cultivars to *Phytophthora cinnamomi* and P. plurivora. *Biol. Control.* 140:104121. doi: 10.1016/j.biocontrol.2019.104121

Verma, S., Varma, A., Rexer, K.-H., Hassel, A., Kost, G., Sarbhoy, A., et al. (1998). *Piriformospora indica*, gen. et sp. nov., a new root-colonizing fungus. *Mycologia* 90, 896–903. doi: 10.1080/00275514.1998.12026983

Verma, N., Narayan, O. P., Prasad, D., Jogawat, A., Panwar, S. L., Dua, M., et al. (2021). Functional characterization of a high-affinity iron transporter (PiFTR) from the endophytic fungus *Piriformospora indica* and its role in plant growth and development. *Environ. Microbiol* 24, 689–706. doi: 10.1111/1462-2920.15659

Waller, F., Mukherjee, K., Deshmukh, S. D., Achatz, B., Sharma, M., Schäfer, P., et al. (2008). Systemic and local modulation of plant responses by *Piriformospora indica* and related *Sebacinales* species. *Plant Physiol.* 165, 60–70. doi: 10.1016/j.jplph.2007.05.017

Wang, C., Wang, G., Zhang, C., Zhu, P., Dai, H., Yu, N., et al. (2017). OsCERK1-mediated chitin perception and immune signaling requires receptor-like cytoplasmic kinase 185 to activate an MAPK cascade in rice. *Molecular Plant* 10, 619–633. doi: 10.1016/j.molp.2017.01.006

Wang, K., Shao, Z. Y., Guo, F. L., Wang, K., and Zhang, Z. Y. (2021). The mitogen-activated protein kinase kinase TaMKK5 mediates immunity via the TaMKK5–TaMPK3–TaERF3 module. *Plant Physiol.* 187, 2323–2337. doi: 10.1093/plphys/kiab227

Weatherley, P. E. (1950). Studies in the water relations of the cotton plant. I. The field measurement of water deficits in leaves. *N. Phytol.* 49, 81–97. doi: 10.1111/j.1469-8137.1950.tb05146.x

Xiu, Q., Bi, L., Xu, H., Li, T., Zhou, Z., Wang, J., et al. (2021). Antifungal activity of quinofumelin against *Fusarium graminearum* and its inhibitory effect on DON biosynthesis. *Toxin* 13:348. doi: 10.3390/toxins13050348

Yamada, K., Yamaguchi, K., Shirakawa, T., Nakagami, H., Mine, A., Ishikawa, K., et al. (2016). The *Arabidopsis* CERK 1-associated kinase PBL 27 connects chitin perception to MAPK activation. *EMBO J* 35, 2468–2483. doi: 10.15252/embj.201694248

Yamada, K., Yamaguchi, K., Yoshimura, S., Terauchi, A., and Kawasaki, T. (2017). Conservation of chitin-induced MAPK signaling pathways in rice and *Arabidopsis*. *Plant Cell Physiol.* 58, 993–1002. doi: 10.1093/pcp/pcx042

Zhang, J., Liu, Y., Li, Q., Zhang, X., and Shang, J. K. (2013). Antifungal activity and mechanism of palladium-modified nitrogen-doped titanium oxide photocatalyst on agricultural pathogenic fungi *Fusarium graminearum*. *ACS Appl. Mater. Interfaces* 5, 10953–10959. doi: 10.1021/am4031196

Zhang, Z., Wang, H., Wang, K., Jiang, L., and Wang, D. (2017). Use of lentinan to control sharp eyespot of wheat, and the mechanism involved. *J. Agric. Food Chem.* 65, 10891–10898. doi: 10.1021/acs.jafc.7b04665

Zhu, X., Yang, K., Wei, X., Zhang, Q., Rong, W., Du, L., et al. (2015). The wheat AGC kinase TaAGC1 is a positive contributor to host resistance to the necrotrophic pathogen *Rhizoctonia cerealis*. *EXBOTJ* 66, 6591–6603. doi: 10.1093/jxb/erv367

Zuccaro, A., Basiewicz, M., Zurawska, M., Biedenkopf, D., and Kogel, K. H. (2009). Karyotype analysis, genome organization, and stable genetic transformation of the root colonizing fungus *Piriformospora indica*. *Fungal Genet. Biol.* 46, 543–550. doi: 10.1016/j.fgb.2009.03.009

Conflict of Interest: The authors declare that the research was conducted in the absence of any commercial or financial relationships that could be construed as a potential conflict of interest.

Publisher's Note: All claims expressed in this article are solely those of the authors and do not necessarily represent those of their affiliated organizations, or those of the publisher, the editors and the reviewers. Any product that may be evaluated in this article, or claim that may be made by its manufacturer, is not guaranteed or endorsed by the publisher.

Copyright © 2022 Li, Guo, Feng, Duan and Li. This is an open-access article distributed under the terms of the Creative Commons Attribution License (CC BY). The use, distribution or reproduction in other forums is permitted, provided the original author(s) and the copyright owner(s) are credited and that the original publication in this journal is cited, in accordance with accepted academic practice. No use, distribution or reproduction is permitted which does not comply with these terms.

frontiers | Frontiers in Plant Science

REVIEW
published: 09 May 2022
doi: 10.3389/fpls.2022.891626

Sulfur Dioxide: An Emerging Signaling Molecule in Plants

Zhong-Guang Li[1,2,3], Xiao-Er Li[1,2,3] and Hong-Yan Chen[1,2,3]*

[1]School of Life Sciences, Yunnan Normal University, Kunming, China, [2]Engineering Research Center of Sustainable Development and Utilization of Biomass Energy, Ministry of Education, Kunming, China, [3]Key Laboratory of Biomass Energy and Environmental Biotechnology, Yunnan Normal University, Kunming, China

Sulfur dioxide (SO_2) has long been viewed as toxic gas and air pollutant, but now is being verified as a signaling molecule in mammalian cells. SO_2 can be endogenously produced and rapidly transformed into sulfur-containing compounds (e.g., hydrogen sulfide, cysteine, methionine, glutathione, glucosinolate, and phytochelatin) to maintain its homeostasis in plant cells. Exogenous application of SO_2 in the form of gas or solution can trigger the expression of thousands of genes. The physiological functions of these genes are involved in the antioxidant defense, osmotic adjustment, and synthesis of stress proteins, secondary metabolites, and plant hormones, thus modulating numerous plant physiological processes. The modulated physiological processes by SO_2 are implicated in seed germination, stomatal action, postharvest physiology, and plant response to environmental stresses. However, the review on the signaling role of SO_2 in plants is little. In this review, the anabolism and catabolism of SO_2 in plants were summarized. In addition, the signaling role of SO_2 in seed germination, stomatal movement, fruit fresh-keeping, and plant response to environmental stresses (including drought, cold, heavy metal, and pathogen stresses) was discussed. Finally, the research direction of SO_2 in plants is also proposed.

Keywords: sulfur dioxide, signaling molecule, seed germination, fruit fresh-keeping, stomatal movement, stress response

OPEN ACCESS

Edited by:
Girdhar Kumar Pandey, University of Delhi, India

Reviewed by:
Gaurav Zinta, Institute of Himalayan Bioresource Technology (CSIR), India
Mohammad Yusuf, United Arab Emirates University, United Arab Emirates

****Correspondence:***
Zhong-Guang Li
zhongguang_li@163.com

Specialty section:
This article was submitted to Plant Physiology, a section of the journal Frontiers in Plant Science

Received: *08 March 2022*
Accepted: *25 April 2022*
Published: *09 May 2022*

Citation:
Li Z-G, Li X-E and Chen H-Y (2022) Sulfur Dioxide: An Emerging Signaling Molecule in Plants. Front. Plant Sci. 13:891626. doi: 10.3389/fpls.2022.891626

INTRODUCTION

For so long, sulfur dioxide (SO_2) has been viewed as a harmful gas and air pollutant. SO_2 can dissolve in water and form sulfurous acid (H_2SO_3), which in turn dissociates into sulfite (SO_3^{2-}), bisulfite (HSO_3^-), and hydrogen ion (H^+). In neutral solution, the ratio of SO_3^{2-} / HSO_3^- is 3/1 (M/M; Singh et al., 2012). Therefore, the toxicity of SO_2 mainly roots in three derivants, that is, SO_3^{2-}, HSO_3^-, and H^+. SO_3^{2-} and HSO_3^- are strong nucleophiles, which can deleteriously react with the sulfhydryl groups (–SH)-containing proteins (including enzymes) and then alter their functions and activities, thus disturbing physiological and biochemical metabolism (e.g., photosynthesis, respiration, and ion balance), and even leading to cell death. H^+ can lower the pH value of the cells and their compartmentations, followed by affecting the activities of the enzymes and interfering with the cellular metabolism (Huang et al., 2021). In addition, SO_2 can induce the accumulation of reactive oxygen species (ROS) by oxidizing sulfite into sulfate and/or activating NADPH oxidase (NOX), which in turn cause biomembrane damage, protein disintegration, DNA damage, chromosome aberration, gene mutation, Golgi body destruction, and programmed cell death (PCD) (Okpodu et al., 1996). Therefore, high

concentration of SO_2 can damage plant at morphological, physiological, biochemical, and molecular levels. For example, SO_2 can reduce photosynthesis by disrupting thylakoid function, interfering with electron transport chain and membrane permeability, destroying pigments, and affecting carbon allocation, leads to leaf damage (e.g., yellow spots, discoloration, and necrosis), growth inhibition, and even plant death (Lee et al., 2017; Huang et al., 2021; Li and Yi, 2022).

SO_2, as a signaling molecule, can endogenously produce by the catalysis of aspartate aminotransferase (AAT) and NOX using hydrogen sulfide (H_2S) as substrate in animal system (Huang et al., 2021). Endogenous SO_2 executes a positive role in reducing brain injury, lung injury, myocardial injury, and hypertension; regulating vascular remodeling, myocardial remodeling, collagen remodeling, ion channels, cell proliferation, endoplasmic reticulum stress, and protein posttranslational modification (mainly sulfenylation by H_2O_2). Therefore, the abnormal production of endogenous SO_2 commonly leads to colitis, hypertension, atherosclerosis, neuronal damage, vascular calcification, myocardial hypertrophy, myocardial injury, pulmonary hypertension, and acute lung injury (Huang et al., 2021). These studies indicate that SO_2, as signaling molecule, plays an essential role in many physiological and pathological processes.

In general, signaling molecules, such as calcium ion (Ca^{2+}), ROS, nitric oxide (NO), and H_2S, exhibit the common characteristics: small molecule, fast dispersal, dual effects, controllability of generation and elimination, biological activity, reprogramming gene expression, and so forth (Chen et al., 2011; Khan et al., 2019). Small molecules are easy to be quickly biosynthesized/released to initiate signaling, and then immediately eliminated to terminate signaling. In addition, signaling molecules can be rapidly spread from production sites to effect sites to exert their biological effects by their receptors/sensors. Dual effects of signaling molecules refer to their toxicity at high concentration and signaling role at low concentration. Therefore, they must be maintained homeostasis in cells (Khan et al., 2019). Finally, signaling molecules can specially bind to their receptors/sensors and then reprogram gene expression, further regulating cellular metabolism (Chen et al., 2011). It is quite clear that small molecule SO_2 meets these criterions, indicating its signaling role in organisms.

In plants, SO_2 can be generated in the form of SO_3^{2-} during sulfate $\left(SO_4^{2-}\right)$ reduction (Li et al., 2020). Recently, exogenous application of SO_2 in the form of gas ($mg\,m^{-3}$) or solution ($Na_2SO_3/NaHSO_3$, 3/1, M/M), at low concentrations, has been found to exert a positive role in seed germination (Wang et al., 2017; Sun et al., 2018; Guo et al., 2021), stomatal movement (Taylor et al., 1981; Wei et al., 2013; Hu et al., 2014; Yi et al., 2017), fruit fresh-keeping (Joradol et al., 2019; Zhang et al., 2022), and plant response to adverse environments (Hu et al., 2015; Zhu et al., 2015; Han et al., 2018, 2019; Xue and Yi, 2018; Li et al., 2021; Ma, 2021). These studies indicate that SO_2 is emerging as a signaling molecule in plants. However, the review on SO_2 signaling in plants is little summarized. In this review, SO_2 homeostasis in plants and its signaling role in seed germination, stomatal action, fruit fresh-keeping, and plant response to environmental stress (including drought, cold, heavy metal, and pathogen infection) were concluded. The aim of this paper highlighted that SO_2 is an emerging signaling molecule in plants.

METABOLISM OF SO_2

Anabolism of SO_2

Similar to other signaling molecules, SO_2 homeostasis in plants is maintained by its production (i.e., anabolism) and elimination (i.e., catabolism; **Figure 1**). In plants, the endogenous production of SO_2 mainly roots in the reduction of SO_4^{2-}. SO_4^{2-} absorbed by roots is activated by ATP sulfurylase (ATPS), producing adenosine 5′-phosphosulfate (APS), which is transformed into SO_3^{2-} (main form of SO_2 in solution) by APS reductase (APR) using glutathione (GSH) as reducing agent (Li et al., 2020). In addition, cysteine (Cys) can change into cysteine sulfinate (Cts) by the catalysis of cysteine dioxygenase (CDO), and then produce β-sulfinylpyruvate (SP), which automatically form SO_2 without any enzyme catalysis and release pyruvate (Pyr; Yu et al., 2020; Huang et al., 2022). Also, SO_2 can be released from hydrogen sulfide (H_2S) and its derivant thiosulfate (TS) under the catalysis of NOX, sulfide oxidase (SO), and TS sulfurtransferase (TST), respectively (Li et al., 2009). Similarly, sulfur-containing amino acids (SAA) also can generate SO_2 by the catalysis of amino acid oxidase (AAO; Rausch and Wachter, 2005). However, the detailed mechanisms of SO_2-producing pathways in plant growth, development, and response to environmental stress need to be further dissected in the coming days.

Catabolism of SO_2

Analogue to its production, the scavenging of excessive SO_2 is primarily achieved by the enzyme-catalysis pathways (**Figure 1**). Endogenous SO_2 is easy to dissolve in water and produce SO_3^{2-}, which is in turn reduced into H_2S by SO_3^{2-} reductase (SIR), followed by synthesizing Cys under the catalysis of Cys synthetase (CS; Hasanuzzaman et al., 2018; Li et al., 2020). Cys is a common precursor for biosynthesis of numerous biological molecules such as GSH, phytochelatin (PC), phytoalexins (PA), cystathionine (Cyst), homocystine (Hcy), methionine (Met), ethylene (ETH), and glucosinolate (GSL; **Figure 1**). GSH, as an important reducing agent in plant cells, which can be synthesized from Cys under the successive catalysis of γ-glutamycysteine synthetase (γ-ES) and GSH synthesis (GS; Yu et al., 2020; Huang et al., 2022). GSH and its oxidized form (GSSG) can mutually convert by dehydroascorbate reductase (DHAR) and glutathione reductase (GR) using dehydroascorbate and NADPH as electron acceptor and electron donor, respectively (Bartoli et al., 2017). Also, GSH can further synthesize PC to chelate heavy metal in plant cells, thus reducing the toxicity of heavy metal (Li et al., 2020). In addition to these, Cys can transform into other amino acids such as Cyst, Hcy, and Met (Li et al., 2009), further regulating the metabolism of amino acids in plants. These metabolic pathways are closely associated with the acquisition of stress tolerance in plants, also indicating the signaling role of SO_2.

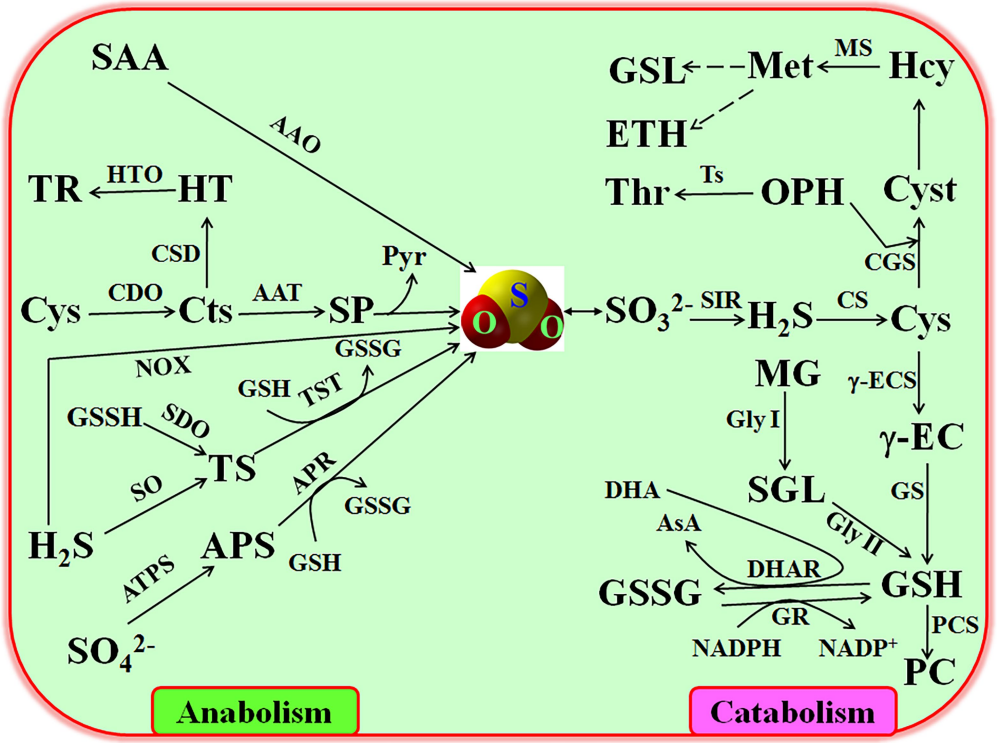

FIGURE 1 | Anabolism and catabolism of sulfur dioxide (SO_2) in plants. AAO, amino acid oxidase; APR, APS reductase; APS, adenosine 5′-phosphosulfate; ATPS, ATP sulfurylase; CDO, cysteine dioxygenase (CDO); CS, Cys synthetase; Cts, cysteine sulfinate; Cys, cysteine; Cyst, cystathionine; DHAR, dehydroascorbate reductase; γ-ECS, γ-glutamycysteine synthetase; Gly I, glyoxalase I; Gly II, glyoxalase II; GR, glutathione reductase; GS, GSH synthesis; GSH, glutathione; GSL, glucosinolate; GSSG, oxidized GSH; Hcy, homocystine; H_2S, hydrogen sulfide; Met, methionine; MG, methylglyoxal; NOX, NADPH oxidase; OPH, O-phosphohomoserine; PC, phytochelatin; Pry, pyruvate; SAA, sulfur-containing amino acids; SGL, S-D-lactoylglutathione; SIR, sulfite reductase; SO, sulfide oxidase; SP, β-sulfinylpyruvate; Thr, threonine; Ts, threonine synthetase; TS, thiosulfate; TST, TS sulfurtransferase.

SIGNALING ROLE OF SO_2

Increasing evidences show that exogenous application of SO_2 in a gas ($mg\,m^{-3}$, fumigation) or solution ($Na_2SO_3/NaHSO_3$, 3/1, irrigation) form could reprogramme the expression of thousands of genes. The physiological functions of these genes include antioxidant defense, osmotic adjustment, cell wall modification, and the synthesis of stress proteins (including heat shock proteins, HSP; and pathogen-related proteins, PR), secondary metabolites, and plant hormones (Li and Yi, 2012a,b, 2020; Zhao and Yi, 2014), which in turn modulated several physiological processes, such as seed germination, stomatal action, postharvest physiology, and plant response to environmental stresses, including drought, cold, heavy metal, and pathogen stresses (**Table 1**). In addition, the modulation of these physiological processes is involved in the interaction of SO_2 and other signaling molecules, such as H_2S, NO, ROS, cyclic guanosine monophosphate (cGMP), and plant hormones (**Figure 2**). In this section, the signaling role of SO_2 in plants will be stated in detail.

Seed Germination

Seed germination is the first and key stage of plant life cycle, which is sensitive to environmental stress, especially soil environment stress. Therefore, seed germination is the basis for crop production and vegetation recovery. In general, seed priming, especially chemical priming, can improve seed vigor, seed germination, and seedling viability, as well as the resistance of seedlings to adverse environments (Paul et al., 2022). In maize seeds, pretreatment with SO_2 (1 mM) facilitated seed germination and increased seed vigor. In addition, the SO_2-pretreated germinating seeds had higher NOX activity and ROS level, while NOX inhibitor, diphenyleneiodinium, inhibited ROS accumulation and germination and vigor of maize seeds pretreated with SO_2 (Guo et al., 2021). Also, SO_2 pretreatment up-regulated the expression and activity of α-amylase in germinating maize seeds (Guo et al., 2021). These data imply that SO_2 might function as signaling molecule in facilitating the germination of maize seeds by mobilizing reserves *via* activating NOX-dependent ROS production.

In wheat seeds, pretreatment with 100 μM SO_2 donor ($NaHSO_3/Na_2SO_3$, 1/3 M/M) postponed PCD, restrained the coalescence of small protein storage vacuoles, and reduced the accumulation of ROS (e.g., hydrogen peroxide, H_2O_2; and superoxide anion, O_2^-) in aleurone cells pretreated with gibberellin (Sun et al., 2018). In addition, SO_2-pretreated germinating seeds, compared to treatment with gibberelin alone, sustained higher activities of catalase (CAT), guaiacol peroxidase (POD), ascorbate peroxidase (APX), and superoxide dismutase (SOD),

TABLE 1 | Examples of the role of SO_2 signaling in plant growth and response to environmental stress.

Species	Response	SO_2 donor	Role	References
Maize	Seed germination	0 ~ 5 mM Na_2SO_3/$NaHSO_3$	Triggering NOX-dependent ROS signaling and elevating amylase activity	Guo et al., 2021
Wheat		0.1 mM Na_2SO_3/$NaHSO_3$	Delaying programmed cell death (PCD) and triggering H_2S/NO/ROS signaling	Sun et al., 2018
Barley		0.05 mM Na_2SO_3/$NaHSO_3$	Delaying PCD and triggering H_2S/NO/ROS signaling	Wang et al., 2017
Potato	Stomatal	0 ~ 5 mM Na_2SO_3/$NaHSO_3$	Triggering H_2S/NO signaling	Hu et al., 2014
H. fulva	movement	0 ~ 5 mM Na_2SO_3/$NaHSO_3$	Triggering PCD and NO/ROS/Ca^{2+} signaling	Wei et al., 2013
Vicia faba		0.25 ~ 6 mM Na_2SO_3/$NaHSO_3$	Triggering NO/ROS/Ca^{2+} signaling	Yi et al., 2017
Longan	Fruit fresh-	500 ~ 2,500 mg/L SO_2	Triggering NOX-dependent ROS signaling	Joradol et al., 2019
Grape	keeping	200 μl/L	Driving AsA-GSH cycle and regulating sulfur metabolism	Zhang et al., 2022
Wheat	Drought	0 ~ 20 mg/m^3 SO_2	Triggering H_2S signaling, synthesizing osmolyte, and activating antioxidant system	Li et al., 2021
Foxtail		30 mg/m^3 SO_2	Synthesizing osmolyte, triggering stomatal closure, and activating antioxidant system	Han et al., 2019
Arabidopsis	Cold	50 μM Na_2SO_3/$NaHSO_3$ 30 mg/m^3 SO_2	Activating C-repeated binding factor (CBF) pathway and antioxidant system, synthesizing anthocyanin	Ma (2021)
Wheat	Cadmium	1 and 2 mM Na_2SO_3/$NaHSO_3$	Triggering H_2S signaling, synthesizing osmolyte, and activating antioxidant system	Hu et al., 2015
Foxtail		0.5 mM Na_2SO_3/$NaHSO_3$	Triggering PCD, activating antioxidant system, and reducing metal transporters	Han et al., 2018
Wheat	Aluminium	1.2 mM Na_2SO_3/$NaHSO_3$	Triggering H_2S signaling, activating antioxidant system, and reducing aluminium accumulation	Zhu et al., 2015

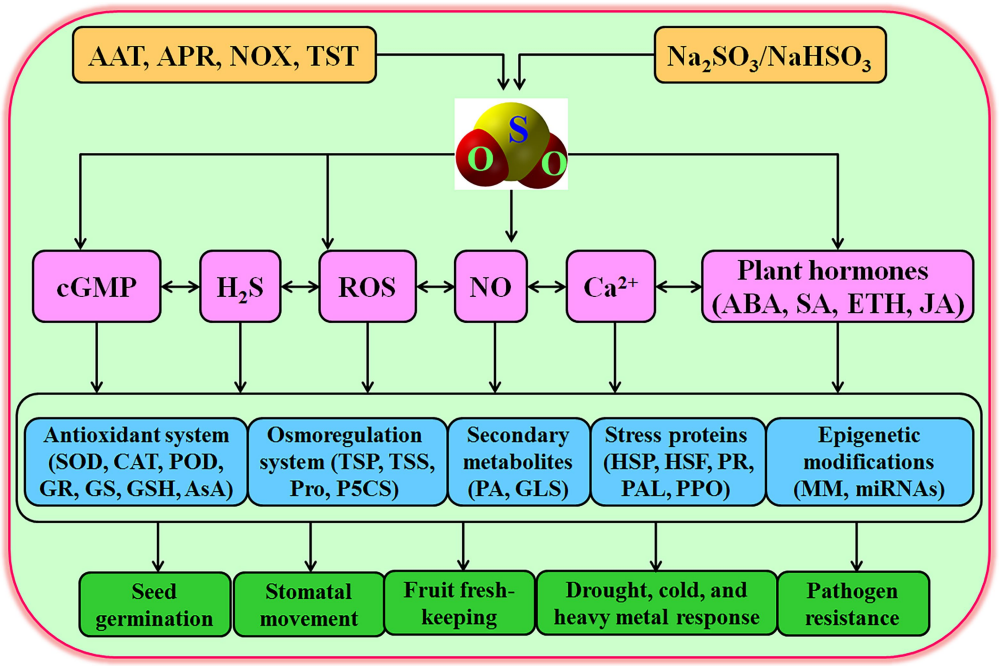

FIGURE 2 | Signaling role of sulfur dioxide (SO_2) in plants. AAT, aspartate aminotransferase; ABA, abscisic acid; APR, adenosine 5'-phosphosulfate reductase; AsA, ascorbic acid; CAT, catalase; cGMP, cyclic guanosine monophosphate; ETH, ethylene; GR, glutathione reductase; GS, glutathione synthetase; GSH, glutathione; GSL, glucosinolate; H_2S, hydrogen sulfide; HSF, heat shock factor; HSP, heat shock proteins; JA, jasmonic acid; MM, methylation modification; NO, nitric oxide; NOX, NADPH oxidase; PA, phytoalexins; PAL, phenylalanine ammonia-lyase; P5CS, Δ^1-pyrroline-5-carboxylate synthetase; POD, peroxidase; PPO, polyphenol oxidase; PR, pathogenesis-related proteins; Pro, proline; ROS, reactive oxygen species; SA, salicylic acid; SOD, superoxide dismutase; TSP, total soluble proteins; TSS, total soluble sugars; TST, thiosulfate sulfurtransferase.

while had lower activities of lipoxygenase (LOX) and polyphenol oxidase (PPO; Sun et al., 2018). Also, SO_2-pretreated aleurone layers induced the production of endogenous H_2S and NO, whereas the supplement of cPTIO (NO scavenger) accelerated PCD in both SO_2– and H_2S-pretreated aleurone cells (Sun et al., 2018). These results indicate that SO_2 can trigger H_2S/NO signaling to delay PCD in wheat aleurone layers pretreated with gibberellin *via* activating antioxidant enzyme system.

Similarly, in barley (*Hordeum vulgare* L.) seeds, pretreatment with SO_2 donor ($NaHSO_3/Na_2SO_3$, 50 μM) alleviated PCD induced by gibberelin in aleurone layers in a concentration-dependent fashion (Wang et al., 2017). Additionally, SO_2 pretreatment increased the activities of SOD, CAT, APX, POD, and glutathione reductase (GR), while weakened that of LOX, reduced the levels of H_2O_2, O_2^-, and malondialdehyde (MDA) in aleurone layers (Wang et al., 2017). Furthermore, SO_2 pretreatment triggered the accumulation of endogenous H_2S and NO in aleurone layers (Wang et al., 2017), similar to the results reported by Sun et al. (2018) in wheat. These data suggest that SO_2 might regulate the germination of barley seeds by attenuating PCD *via* the interaction among H_2S, NO, and ROS signaling.

Stomatal Movement

Stomata is a major gate that plants exchange with carbon dioxide, oxygen, and water, its movement (i.e., opening and closure) influences photosynthesis, respiration, and transpiration, as well as plant resistance to environmental stress, especially drought stress (Jia and Zhang, 2008). Stomatal movement is strictly controlled by a signaling network composed of many second messengers, such as Ca^{2+}, NO, ROS (mainly H_2O_2), H_2S, and plant hormones (especially abscisic acid, ABA; ethylene, ETH; and cytokinin, CTK; Qi et al., 2018). Therefore, priming with signaling molecules can alter stomatal aperture and enhance the tolerance of plants to environmental stress. In sweet potato (*Ipomoea batatas*), treatment of epidermal strips with the different concentrations (0 ~ 5 mM) of $Na_2SO_3/NaHSO_3$ solutions (SO_2 donor) rapidly increased the levels of endogenous H_2S and NO, and then induced stomatal closure in a dose-dependent manner (Hu et al., 2014). In addition, the stomatal closure induced by SO_2 was reversed by hypotaurine (H_2S scavenger) and cPTIO (NO scavenger; Hu et al., 2014), indicating that the SO_2-triggered stomatal closure might be mediated by the H_2S and NO signaling pathways. Also, in broad bean (*Vicia faba* L.), low concentrations (0.0001 ~ 0.1 μM) of sulfurous acid (H_2SO_3, as SO_2 donor) facilitated stomatal opening by reducing the level of endogenous ABA to antagonize its action (Taylor et al., 1981). Adversely, a high concentration (10 μM) of H_2SO_3 inhibited stomatal opening by increasing the level of endogenous ABA (Taylor et al., 1981).

In *Hemerocallis fulva*, the epidermal strips treated with the different concentrations (1 ~ 5 mM) of SO_2 donor ($Na_2SO_3/NaHSO_3$) were found to reduce the guard cells vigor and induce cell death in a concentration-dependent manner (Wei et al., 2013). The SO_2-induced death cells exhibited the features of apoptosis (i.e., nuclear condensation, nuclear elongation, and DNA fragmentation), indicating SO_2 could trigger PCD in guard cells. Additionally, the levels of endogenous NO, ROS, and Ca^{2+} were increased by SO_2, while reduced by NO scavenger (cPTIO), nitrate reductase (NO-producing enzyme) inhibitor (NaN_3), ROS scavengers (ascorbic acid, AsA; and CAT), Ca^{2+} chelating agent (EGTA), and plasma membrane Ca^{2+} channel blocker ($LaCl_3$), thus decreasing cell death (Wei et al., 2013). Also, AsA treatment decreased the levels of NO and Ca^{2+} compared with the SO_2 treatment alone, whereas NaN_3 treatment decreased ROS and Ca^{2+} levels, but $LaCl_3$ treatment had no significant effect on NO and ROS levels (Wei et al., 2013). These data imply that SO_2 could induce PCD in guard cells by intertwining NO, ROS, and Ca^{2+} signaling pathways in *H. fulva*, which might be a major cause for SO_2-induced stomatal closure.

Similarly, in *Vicia faba*, SO_2 hydrates ($Na_2SO_3/NaHSO_3$) induced guard cell death in a dose-dependent fashion (ranging from 0.25 to 6 mM; Yi et al., 2017). Meanwhile, SO_2 induced an increase in the level of endogenous NO, H_2O_2, and Ca^{2+} in guard cells of *Vicia faba*, similar to the data reported by Wei et al. (2013) in *H. fulva*. In addition, treatment with exogenous NO donor enhanced the toxicity of SO_2, whereas NO scavenger (cPTIO) and synthesis inhibitors (L-NAME and tungstate) weakened SO_2 toxicity (Yi et al., 2017). Likewise, the toxicity of SO_2 was also blocked by ROS scavenger (AsA and CAT), Ca^{2+} chelating agent (EGTA), and Ca^{2+} channel inhibitor ($LaCl_3$; Yi et al., 2017). Also, treatment with both cPTIO and AsA reversed SO_2-induced increase in Ca^{2+} level in guard cells, while cPTIO and AsA treatment alone blocked SO_2-induced H_2O_2 and NO accumulation (Yi et al., 2017). These data suggest that SO_2 toxicity might be achieved by joint action of NO, ROS, and Ca^{2+} signaling in guard cells of *Vicia faba*, further supporting the hypothesis proposed by Wei et al. (2013). In addition to stomatal movement, Haworth et al. (2012) reported that SO_2 could change stomatal density (SD), stomatal index (SI), and SD/SI ratio in *Lepidozamia hopei*, *Lepidozamia peroffskyana*, *Ginkgo biloba*, *Nageia nagi*, *Podocarpus macrophyllus*, *Araucaria bidwillii*, and *Aagathis australis*.

Fruit Fresh-Keeping

Shelf-life of the fruits and vegetables determines their quality and economic value. To lengthen the shelf-life, numerous physical and chemical methods are used in the process of fruits and vegetables storage (Joradol et al., 2019). The physical methods are involved in water, fertilizer, gas (e.g., oxygen and carbon dioxide), heat (temperature), and light; while chemical methods are mainly fresh-keeping agent treatments (Zhang et al., 2022). In Longan (*Dimocarpus longan* Lour. cv. Daw) fruits, SO_2 fumigation (500 ~ 2,500 mg L^{-1}) reduced pericarp browning, lengthened shelf-life, and improved the quality of fruits by enhancing antioxidant capacity compared with the control without SO_2 fumigation (Joradol et al., 2019). In addition, the fruits fumigated with SO_2 had a higher content of endogenous H_2O_2, which reached a maximum within 6 ~ 12 h. Also, SO_2 treatment up-regulated the gene expression of NOX and SOD (Joradol et al., 2019). These data indicate that SO_2 fumigation can induce the NOX-dependent H_2O_2 signaling, which in turn enhance the antioxidant capacity, thereby lengthening the shelf-life of fruits.

Similarly, in table grapes, SO_2 treatment (200 μl L^{-1}) inhibited fruit decay and reduced the levels of H_2O_2 and MDA compared to the control without SO_2 treatment (Zhang et al., 2022). Additionally, SO_2 treatment up-regulated the expression of *VvSiR, VvSAT1*, *VvSAT2*, and *VvOASTL*, which in turn increased

the activities of sulfite reductase, serine acetyltransferase, and *O*-acetylserine (thiol)-lyase, as well as the content of Cys (Zhang et al., 2022). Likewise, the gene expression level, enzyme activity, and antioxidant content related to AsA-GSH cycle was enhanced by SO_2 treatment in grapes. Also, the expression of *VvGS* (GSH synthetase) was up-regulated by SO_2 treatment in table grapes, while the transcription level of *VvHPCA1-4* and *VvHPCA3* (evaluating the degree of oxidative damage) was down-regulated (Zhang et al., 2022). These data indicate that SO_2 can lengthen the shelf-life of table grapes by maintaining H_2O_2 homeostasis to reduce postharvest oxidative damage *via* driving the AsA-GSH cycle.

Drought Response

Drought stress commonly leads to osmotic and oxidative stress due to the shortage of water and the overaccumulation of ROS in plant cells. The approaches alleviating osmotic and oxidative stresses can boost the resistance of plants to drought stress (Salehi-Lisar and Bakhshayeshan-Agdam, 2016). In wheat seedlings, under drought stress, pretreatment with SO_2 ($0 \sim 20\,mg\,m^{-3}$) improved the survival percentage and relative water content (Li et al., 2021), indicating that SO_2 could increase drought tolerance. The further experiments showed that SO_2 pretreatment improved the content of proline (Pro) and activities of SOD and POD, which in turn reduced the accumulation of H_2O_2 and MDA in drought-treated wheat seedlings. In addition, SO_2 pretreatment down-regulated the expression of *TaNAC69* (transcription factor gene), while the expression of other transcription factor genes (*TaERF1* and *TaMYB30*) insignificantly changed but maintained a higher levels in wheat seedlings under drought stress conditions (Li et al., 2021). Also, SO_2 pretreatment induced an increase in H_2S in wheat seedlings under drought stress, while H_2S scavenger hypotaurine decreased the activities of SOD and POD, as well as the expression of transcription factor genes, followed by increasing the accumulation of H_2O_2 and MDA, returning to the level of drought treatment alone (Li et al., 2021). These data suggest that SO_2 can increase the drought tolerance of wheat seedlings by accumulating osmolytes and activating antioxidant enzmyes *via* H_2S signaling pathway.

In like manner, in foxtail millet seedlings, SO_2 fumigation ($30\,mg\,m^{-3}$) decreased stomatal apertures and leaf transpiration rate, which in turn improved the relative water content in the leaves of drought-stressed seedlings (Han et al., 2019), thus improving the drought tolerance of seedlings. Additionally, SO_2 pretreatment increased the activity of Δ^1-pyrroline-5-carboxylate synthetase (P5CS), reduced that of Pro dehydrogenase (ProDH), and corresponding gene expression, followed by accumulating Pro in the leaves of drought-stressed seedlings (Han et al., 2019). Moreover, application of SO_2 up-regulated the gene expression of CAT and POD and increased the activities of corresponding enzymes in the leaves of drought-stressed plants, which in turn alleviated drought-induced oxidative damage (i.e., decreasing MDA content) by scavenging H_2O_2 (Han et al., 2019). These results imply that SO_2 fumigation can increase drought tolerance in foxtail millet seedlings by combined effect of stomatal closure, Pro accumulation, and antioxidant defense.

Similarly, under drought stress, SO_2 pre-exposure ($30\,mg\,m^{-3}$) increased SOD, POD, and O-acetylserine(thio)lyase (OASTL) activities and GSH, Cys, and nonprotein thiol (NPT) contents in Arabidopsis plants, which in turn alleviated oxidative stress (i.e., reducing H_2O_2 and MDA accumulation; Li and Yi, 2022). Meanwhile, SO_2 increased Pro level by up-regulating gene expression and activity of P5CS and down-regulating that of ProDH, followed by reducing water loss, stomatal conductance, and transpiration rate, thus increasing net photosynthetic rate, water use efficiency, and photosynthetic pigment contents (Li and Yi, 2022), indicating that SO_2 can improve the tolerance of Arabidopsis plants to drought stress.

Cold Response

Cold stress includes chilling (above freezing point, resulting in chilling injury) and freezing stress (below freezing point, leading to freezing injury). Both chilling and freezing stress can trigger osmotic and oxidative stresses (Ritonga and Chen, 2020). Therefore, the enhanced osmoregulation and antioxidant capacity by chemical priming are closely related with low temperature stress tolerance in plants. Presoaking of seeds with the different concentrations of (0, 10, 25, 50, and 100 μM) SO_2 alleviated the cold-induced growth inhibition. Among concentrations, 50 μM SO_2 presoaking was the most efficient (Ma, 2021). Similarly, pretreatment of *Arabidopsis thaliana* seeds with 50 μM SO_2 boosted the cold resistance of *A. thaliana* seedlings. Otherwise, SO_2 presoaking up-regulated the expression of *AtCAT3* and *AtPOD,* and increased the activities of corresponding CAT and POD, which in turn reduced the level of endogenous H_2O_2 (Ma, 2021). Meanwhile, 50 μM SO2 pretreatment up-regulated the expression of genes related to anthocyanin synthesis (i.e., *AtPAL2, AtCHS, AtCHI, and AtF3H*), followed by promoting the synthesis of anthocyanin. Interestingly, SO_2 pretreatment also activated the expression of genes (i.e., *AtICE1, AtICE2, AtCBF1, AtCBF2, AtCBF3, AtCOR15a, and AtCOR15b*) involved in C-repeated binding factor (CBF) signaling pathways, mainly cold-response signaling pathways (Ma, 2021).

Parallelly, SO_2 ($30\,mg\,m^{-3}$) exposure reduced stomatal aperture and ROS accumulation by enhancing POD activity under cold stress (Ma, 2021). Also, SO_2 exposure promoted Pro accumulation by increasing P5CS activity and lowering PDH activity as well as activated the gene expression of CBF signaling pathways (Ma, 2021), thus improving the cold adaptability of *Arabidopsis thaliana*. Similarly, exposure of *Arabidopsis thaliana* (Col-0) to the different concentrations of SO_2 increased O_2^- generation rate and H_2O_2 content in Arabidopsis shoots, and up-regulated the gene expression of POD, SOD, and glutathione peroxidase (GPX), as well as increased the activity of corresponding enzymes and the content of GSH. Additionally, SO_2 exposure increased isoenzymatic isoforms of SOD (FeSOD and Cu/ZnSOD) and POD, while decreased CAT isoforms (CAT2 and CAT3; Li and Yi, 2012b). Similarly, in Arabidopsis, SO_2 exposure ($30\,mg\,m^{-3}$) down-regulated the expression of miR398, which in turn increased the transcript level of its target genes Cu/Zn-SOD (*CSD1* and *CSD2*) and increased the activity of SOD (Li et al., 2017). Similarly, SO_2 up-regulated the expression of miR395 expression, followed by decline in the transcript level

of its target genes, ATP sulfurylases (*APS3* and *APS4*) and sulfate transporter (*SULTR2;1*), implying miR398 and miR395 participate in the resistance of Arabidopsis plants to oxidative stress induced by SO_2 exposure. These data suggest that SO_2-induced ROS act as a signal to trigger plant defense response.

Heavy Metal Response

Heavy metals, such as cadmium (Cd), mercury, arsenic, and aluminum, have become the major pollutants with the development of modern agriculture and industry. Heavy metals can disturb cellular metabolism, inhibit seed germination and plant growth, and even influence on human health by entering into food chain (Ghori et al., 2019). Therefore, heavy metal pollutions have become a huge challenge for crop production, food safety, and human health. How to improve the resistance of crop plants to heavy metal stress and reduce its endogenous accumulation is an urgent issue. In wheat seeds, Cd-inhibited seed germination, while the inhibiting effects were alleviated by exogenous application of SO_2 (Na_2SO_3/$NaHSO_3$ (3/1) solution as SO_2 donor) in a concentration-dependent manner and the optimal concentration was between 1 and 2 mM (Hu et al., 2015). Additionally, SO_2 donor pretreatment enhanced the activities of amylase and esterase, which in turn resulted in the accumulation of total soluble sugars (TSS) and total soluble protein (TSP) in germinating seeds under Cd stress (Hu et al., 2015). Also, SO_2 pretreatment reduced the overproduction of MDA, H_2O_2, and O_2^-, as well as the loss of plasma membrane integrity of the radicle tips of seedlings under Cd stress (Hu et al., 2015). Further experiment data showed that SO_2 increased the activities of POD, APX, SOD, and CAT, lowered level of LOX in germinating wheat seeds (Hu et al., 2015). Interestingly, compared with the control, SO_2 pretreatment increased the level of endogenous H_2S in germinating wheat seeds (Hu et al., 2015). These data suggest that SO_2 can promote the germination of wheat seeds under Cd stress by mobilizing reserves and activating antioxidant system *via* H_2S signaling pathway.

In foxtail millet seedlings, application of SO_2 derivatives (0.5 mM) reduced the Cd-inhibited seedling growth and Cd-induced oxidative damage (i.e., reducing MDA accumulation) in the leaves of seedlings (Han et al., 2018). Additionally, SO_2 treatment enhanced the activities of CAT and SOD and drove AsA-GSH cycle, which in turn reduced the accumulation of Cd-elicited O_2^- and H_2O_2 in the leaves of seedlings (Han et al., 2018). Furthermore, SO_2 application increased the contents of GSH and phytochelatin (PC) by promoting sulfur assimilation, followed by enhancing Cd-detoxification capacity in seedlings. Further experiments showed that SO_2 derivatives down-regulated the expression of genes related to Cd uptake and translocation (i.e., *NRAMP1*, *NRAMP6*, *IRT1*, *IRT2*, *HMA2*, and *HMA4*; Han et al., 2018), thus reducing Cd accumulation in the shoots and roots of Cd-stressed seedlings.

Similarly, in wheat seeds, pretreatment with SO_2 donor ($NaHSO_3$/Na_2SO_3, 1/3) at 1.2 mM increased the activities of POD, CAT, and APX, and lowered that of LOX, and reduced the accumulation of O_2^-, H_2O_2, and MDA in germinating seeds under aluminum stress (Zhu et al., 2015). As expected, SO_2 pretreatment increased the level of endogenous H_2S in wheat seeds, while reduced the content of ROS, which in turn maintained the integrity of biomembrane and reduced aluminum accumulation in wheat seedling radicles (Zhu et al., 2015). Also, SO_2 pretreatment down-regulated the expression of alumium-responsive genes (i.e., *TaWali1*, *TaWali2*, *TaWali3*, *TaWali5*, *TaWali6*, and *TaALMT1*) in seedling radicles under aluminum stress (Zhu et al., 2015). These data indicate that SO_2 can improve seed germination of wheat under aluminum stress by enhancing antioxidant capacity and reducing the accumulation of aluminum *via* H_2S signaling pathway.

Pathogen Response

Besides enhancing abiotic stress tolerance, exogenously applied SO_2 also can improve the resistance of plants to biotic stress (Zhao and Yi, 2014). In *Arabidopsis* plants, SO_2 pre-exposure (30 mg m^{-3}) increased the resistance to *Botrytis cinerea* (Xue and Yi, 2018). Further experiments showed that SO_2 pretreatment up-regulated the expression levels of the defense-related genes (*PAL*, *PPO*, *PR2*, and *PR3*), which encode phenylalanine ammonia-lyase (PAL), polyphenol oxidase (PPO), β-1,3-glucanase (BGL), and chitinase (CHI), and increased the activities of PAL, PPO, BGL, and CHI (Xue and Yi, 2018). Also, SO_2 pre-exposure increased the transcript levels of microRNAs (MIR393, MIR160, and MIR167), correspondingly decreased the gene expression of their targets involved in the auxin signaling pathway. Adversely, the expression levels of the primary auxin-response genes (*GH3-like*, *BDL/IAA12*, and *AXR3/IAA17*) were down-regulated by SO_2 pre-exposure in *Arabidopsis* plants (Xue and Yi, 2018). These data imply that SO_2 increases the disease resistance of Arabidopsis plants to *Botrytis cinerea* by enhancing the defense-related gene expression and enzyme activity as well as suppressing the auxin signaling pathway mediated by miRNA.

In addition, Arabidopsis plants, the transcriptome analysis identified that SO_2 fumigation (30 mg m^{-3}) led to the change in the expression of 2,780 genes, the genes involved in biotic stress resistance, ROS production and scavenging, and sulfur assimilation were up-regulated (Zhao and Yi, 2014). Likewise, Li and Yi (2012b) reported that SO_2 (30 mg m^{-3}) treatment triggered the different expression of 2,780 genes, the functions of which were mainly involved in signal transduction, transcription regulation, molecular structure, transport, binding, and metabolism. Many different expression genes encoding antioxidant enzymes (POD, GPX, and SOD), heat shock proteins (HSP), pathogenesis-related (PR) proteins, and cytochrome P450 were up-regulated by SO_2 in Arabidopsis shoots (Li and Yi, 2012b). In Arabidopsis, Li and Yi (2012a), using Affymetrix GeneChip technology, found that the expression of 494 genes was significantly changed by SO_2 exposure (30 mg m^{-3}), they encoded antioxidant enzymes (e.g., GST, POD, and thioredoxin), HSP, and PR, as well as were involved in the ETH signaling pathway, phenylpropanoid pathway, and cell wall modification. Similarly, SO_2 exposure enhanced the production of ROS, as signaling molecule, increased the activities of SOD, POD, glutathione peroxidase (GPX), and GST in Arabidopsis plants (Li and Yi, 2012a). Also, in fresh table grapes (*V. vinifera*

L. "Crimson Seedless"), transcriptomics approaches also found that SO_2 treatment ($140\,\mu l\,L^{-1}$) up-regulated the expression of enzymes genes related to sulfur-metabolizing enzymes (especially directing towards chelation and conjugation), redox homeostasis, and plant hormones (e.g., auxin, AUX; ethylene, ETH; and jasmonic acid, JA) signaling pathways (Giraud et al., 2012). Generally, salicylic acid (SA) level is closely related to plant disease resistance. In Arabidopsis thaliana plants, Hao et al. (2011) found that the *snc1* mutants (with high SA content) had higher tolerance to SO_2 than *nahG* plants (with low SA content), implying that endogenous SA and signaling might play an essential role in plant responses to SO_2 stress. These studies further support the fact that SO_2 increases disease resistance in Arabidopsis plants.

CONCLUSION AND PERSPECTIVES

Mounting evidences show that SO_2 can not only regulate seed germination, stomatal movement, and postharvest physiology, but also plants respond to environmental stresses, such as drought, cold, and heavy metal, and pathogen stresses. Numerous studies identified that SO_2 meets the requirements of signaling molecules in plants, emerging as a novel signaling role in many plant physiological processes. SO_2 as a novel signaling molecule can exert its physiological functions either alone or interaction with other signaling molecules, such as Ca^{2+}, H_2O_2, NO, H_2S, cGMP, and plant hormones (e.g., ABA, SA, ETH, and JA; **Figure 2**). SO_2 can enhance antioxidant system (e.g., SOD, CAT, POD, APX, GR, GSH, and AsA) and osmoregulation system (e.g., Pro, TTP, TSS, and P5CS), drive secondary metabolism (e.g., GLS and PA accumulation), synthesize stress proteins (e.g., HSP, HSF, PR, PAL, and PPO), and modulate epigenetic modifications (e.g., DNA methylation modification (MM) and miRNAs), thus regulating several plant physiological functions (**Figure 2**). Though, the signaling role of SO_2 in plants has been verified in a large amount of physiological processes, numerous open questions still need to be further answered in more detail in the coming days. In mammalian cells, the AAT/SO_2 pathway is contributed to SO_2 signaling; however, in plants, besides the APR/ SO_3^{2-} pathway (**Figure 1**), the detailed metabolic pathways of SO_2 are waiting for being further expounded. Correspondingly, the knowledge on the exact concentrations of SO_2 in plant cells and subcellular structures as well as its receptors/sensors remains to be found. Though SO_2 could improve multiple stress tolerance, whether SO_2 can induce the tolerance of plants to heat, salt, and flooding stresses and the underlying mechanisms requires to be further explored. In addition, the signaling interaction of SO_2 with Ca^{2+}, ROS, NO, H_2S, methylglyoxal, and cyclic nucleotide in plants under both physiological and stress conditions is necessary to be uncovered. With the development of omics, the effects of SO_2 on transcriptome, metabolome, proteome, and phenome in plants have to be settled urgently.

AUTHOR CONTRIBUTIONS

Z-GL conceived, designed, and wrote the manuscript, while X-EL and H-YC wrote the anabolism and catabolism of SO_2, respectively. All authors contributed to the article and approved the submitted version.

FUNDING

This research was funded by the National Natural Science Foundation of China (32160065 and 31760069).

REFERENCES

Bartoli, C. G., Buet, A., Gergoff Grozeff, G., Galatro, A., and Simontacchi, M. (2017). "Ascorbate-glutathione cycle and abiotic stress tolerance in plants" in *Ascorbic Acid in Plant Growth, Development and Stress Tolerance*. eds. M. Hossain, S. Munné-Bosch, D. Burritt, P. Diaz-Vivancos, M. Fujita and A. Lorence (Cham: Springer), 177–200.

Chen, S. S., Tang, C. S., Jin, H. F., and Du, J. B. (2011). Sulfur dioxide acts as a novel endogenous gaseous signaling molecule in the cardiovascular system. *Chin. Med. J.* 124, 1901–1905. doi: 10.3760/cma.j.issn.0366-6999.2011.12.024

Ghori, N. H., Ghori, T., Hayat, M. Q., Imadi, S. R., Gul, A., Altay, V., et al. (2019). Heavy metal stress and responses in plants. *Int. J. Environ. Sci. Technol.* 16, 1807–1828. doi: 10.1007/s13762-019-02215-8

Giraud, E., Ivanova, A., Gordon, C. S., Whelan, J., and Considine, M. J. (2012). Sulphur dioxide evokes a large scale reprogramming of the grape berry transcriptome associated with oxidative signalling and biotic defence responses. *Plant Cell Environ.* 35, 405–417. doi: 10.1111/j.1365-3040.2011.02379.x

Guo, Z., Zhao, J., Wang, M., Song, S., and Xia, Z. (2021). Sulfur dioxide promotes seed germination by modulating reactive oxygen species production in maize. *Plant Sci.* 312:111027. doi: 10.1016/j.plantsci.2021.111027

Han, Y., Wu, M., Hao, L., and Yi, H. (2018). Sulfur dioxide derivatives alleviate cadmium toxicity by enhancing antioxidant defence and reducing Cd^{2+} uptake and translocation in foxtail millet seedlings. *Ecotox. Environ. Safe.* 157, 207–215. doi: 10.1016/j.ecoenv.2018.03.084

Han, Y., Yang, H., Wu, M., and Yi, H. (2019). Enhanced drought tolerance of foxtail millet seedlings by sulfur dioxide fumigation. *Ecotox. Environ. Safe.* 178, 9–16. doi: 10.1016/j.ecoenv.2019.04.006

Hao, L., Wang, Y., Xu, J., Feng, S. D., Ma, C. Y., Liu, C., et al. (2011). Role of endogenous salicylic acid in Arabidopsis response to elevated sulfur dioxide concentration. *Biol. Plant.* 55, 297–304. doi: 10.1007/s10535-011-0042-6

Hasanuzzaman, M., Hossain, M. S., Bhuyan, M. H. M. B., Mahmud, J. A., Nahar, K., and Fujita, M. (2018). "The role of sulfur in plant abiotic stress tolerance: molecular interactions and defense mechanisms," in *Plant Nutrients and Abiotic Stress Tolerance*. eds. M. Hasanuzzaman, M. Fujita, H. Oku, K. Nahar and B. Hawrylak-Nowak (Singapore: Springer), 221–252.

Haworth, M., Elliott-Kingston, C., Gallagher, A., Fitzgerald, A., and McElwain, J. C. (2012). Sulphur dioxide fumigation effects on stomatal density and index of non-resistant plants: implications for the stomatal palaeo-[CO_2] proxy method. *Rev. Palaeobot. Palynol.* 182, 44–54. doi: 10.1016/j.revpalbo.2012.06.006

Hu, K. D., Bai, G. S., Li, W. J., Yan, H., Hu, L. Y., Li, Y. H., et al. (2015). Sulfur dioxide promotes germination and plays an antioxidant role in cadmium-stressed wheat seeds. *Plant Growth Regul.* 75, 271–280. doi: 10.1007/s10725-014-9951-7

Hu, K. D., Tang, J., Zhao, D. L., Hu, L. Y., Li, Y. H., Liu, Y. S., et al. (2014). Stomatal closure in sweet potato leaves induced by sulfur dioxide involves H2S and NO signaling pathways. *Biol. Plant.* 58, 676–680. doi: 10.1007/s10535-014-0440-7

Huang, Y., Zhang, H., Lv, B., Tang, C., Du, J., and Jin, H. (2021). Endogenous sulfur dioxide is a new gasotransmitter with promising therapeutic potential in cardiovascular system. *Sci. Bull.* 66, 1604–1607. doi: 10.1016/j.scib.2021.04.003

Huang, Y., Zhang, H., Lv, B., Tang, C., Du, J., and Jin, H. (2022). Sulfur dioxide: endogenous generation, biological effects, detection, and therapeutic potential. *Antioxidant Redox Signal.* 36, 256–274. doi: 10.1089/ars.2021.0213

Jia, W., and Zhang, J. (2008). Stomatal movements and long-distance signaling in plants. *Plant signal. behave.* 3, 772–777. doi: 10.4161/psb.3.10.6294

Joradol, A., Uthaibutra, J., Lithanatudom, P., and Saengnil, K. (2019). Induced expression of NOX and SOD by gaseous sulfur dioxide and chlorine dioxide enhances antioxidant capacity and maintains fruit quality of 'Daw' longan fruit during storage through H_2O_2 signaling. *Postharv. Biol. Technol.* 156:110938. doi: 10.1016/j.postharvbio.2019.110938

Khan, M. R., Reddy, P. S., Ferrante, A., and Khan, N. A. (2019). *Plant Signaling Molecules: Role and Regulation under Stressful Environments*. Cambridge: Elsevier.

Lee, H. K., Khaine, I., Kwak, M. J., Jang, J. H., Lee, T. Y., Lee, J. K., et al. (2017). The relationship between SO_2 exposure and plant physiology: a mini review. *Hortic. Environ. Biotechnol.* 58, 523–529. doi: 10.1007/s13580-017-0053-0

Li, X., Bazer, F. W., Gao, H., Jobgen, W., Johnson, G. A., Li, P., et al. (2009). Amino acids and gaseous signaling. *Amino Acids* 37, 65–78. doi: 10.1007/s00726-009-0264-5

Li, Q., Gao, Y., and Yang, A. (2020). Sulfur homeostasis in plants. *Int. J. Mol. Sci.* 21:8926. doi: 10.3390/ijms21238926

Li, L., and Yi, H. (2012a). Differential expression of Arabidopsis defense-related genes in response to sulfur dioxide. *Chemosphere* 87, 718–724. doi: 10.1016/j.chemosphere.2011.12.064

Li, L., and Yi, H. (2012b). Effect of sulfur dioxide on ROS production, gene expression and antioxidant enzyme activity in Arabidopsis plants. *Plant Physiol. Biochem.* 58, 46–53. doi: 10.1016/j.plaphy.2012.06.009

Li, L., and Yi, H. (2020). Photosynthetic responses of Arabidopsis to SO_2 were related to photosynthetic pigments, photosynthesis gene expression and redox regulation. *Ecotoxicol. Environ. Saf.* 203:111019. doi: 10.1016/j.ecoenv.2020.111019

Li, L., and Yi, H. (2022). Enhancement of drought tolerance in Arabidopsis plants induced by sulfur dioxide. *Ecotoxicology*. doi: 10.1007/s10646-022-02530-w [Epub ahead of print].

Li, L. H., Yi, H. L., Liu, X. P., and Qi, H. X. (2021). Sulfur dioxide enhance drought tolerance of wheat seedlings through H_2S signaling. *Ecotox. Environ. Safe.* 207:111248. doi: 10.1016/j.ecoenv.2020.111248

Li, L., Yi, H., Xue, M., and Yi, M. (2017). miR398 and miR395 are involved in response to SO_2 stress in Arabidopsis thaliana. *Ecotoxicology* 26, 1181–1187. doi: 10.1007/s10646-017-1843-y

Ma, L. (2021). *Sulfur Dioxide Enhanced Cold Stress Adaptability of Arabidopsis Thaliana*. Taiyuan: Shanxi University.

Okpodu, C. M., Alscher, R. G., Grabau, E. A., and Cramer, C. L. (1996). Physiological, biochemical and molecular effects of sulfur dioxide. *J. Plant Physiol.* 148, 309–316. doi: 10.1016/S0176-1617(96)80258-6

Paul, S., Dey, S., and Kundu, R. (2022). Seed priming: an emerging tool towards sustainable agriculture. *Plant Growth Regul.* doi: 10.1007/s10725-021-00761-1 (in press).

Qi, J., Song, C. P., Wang, B., Zhou, J., Kangasjärvi, J., Zhu, J. K., et al. (2018). Reactive oxygen species signaling and stomatal movement in plant responses to drought stress and pathogen attack. *J. Integr. Plant Biol.* 60, 805–826. doi: 10.1111/jipb.12654

Rausch, T., and Wachter, A. (2005). Sulfur metabolism: a versatile platform for launching defence operations. *Trends Plant Sci.* 10, 503–509. doi: 10.1016/j.tplants.2005.08.006

Ritonga, F. N., and Chen, S. (2020). Physiological and molecular mechanism involved in cold stress tolerance in plants. *Plan. Theory* 9:560. doi: 10.3390/plants9050560

Salehi-Lisar, S. Y., and Bakhshayeshan-Agdam, H. (2016). "Drought stress in plants: causes, consequences, and tolerance" in *Drought Stress Tolerance in Plants*. eds. M. Hossain, S. Wani, S. Bhattacharjee, D. Burritt and L. S. Tran (Cham: Springer), 1–16.

Singh, L. P., Gill, S. S., Gill, R., and Tuteja, N. (2012). "Mechanism of sulfur dioxide toxicity and tolerance in crop plants" in *Improving Crop Resistance to Abiotic Stress*. eds. N. Tuteja, S. S. Gill, A. F. Tiburcio and R. Tuteja (Weinheim: Wiley), 133–163.

Sun, K. K., Zhu, D. B., Yao, G. F., and Zhang, H. (2018). Sulfur dioxide acts as an antioxidant and delays programmed cell death in wheat aleurone layers upstream of H_2S and NO signaling pathways. *Biol. Plant.* 62, 809–816. doi: 10.1007/s10535-018-0796-1

Taylor, J. S., Reid, D. M., and Pharis, R. P. (1981). Mutual antagonism of sulfur dioxide and abscisic acid in their effect on stomatal aperture in broad bean (*Vicia faba* L.) epidermal strips. *Plant Physiol.* 68, 1504–1507. doi: 10.1104/pp.68.6.1504

Wang, S. S., Zhang, Y. X., Yang, F., Huang, Z. Q., Tang, J., Hu, K. D., et al. (2017). Sulfur dioxide alleviates programmed cell death in barley aleurone by acting as an antioxidant. *PLoS One* 12:e0188289. doi: 10.1371/journal.pone.0188289

Wei, A., Xin, X., Wang, Y., Zhang, C., and Cao, D. (2013). Signal regulation involved in sulfur dioxide-induced guard cell apoptosis in *Hemerocallis fulva*. *Ecotox. Environ. Safe.* 98, 41–45. doi: 10.1016/j.ecoenv.2013.09.029

Xue, M., and Yi, H. (2018). Enhanced Arabidopsis disease resistance against *Botrytis cinerea* induced by sulfur dioxide. *Ecotox. Environ. Safe.* 147, 523–529. doi: 10.1016/j.ecoenv.2017.09.011

Yi, M., Bai, H., Xue, M., and Yi, H. (2017). NO and H_2O_2 contribute to SO_2 toxicity via Ca^{2+} signaling in *Vicia faba* guard cells. *Environ. Sci. Pollut. Res.* 24, 9437–9446. doi: 10.1007/s11356-017-8612-6

Yu, B., Yuan, Z., Yang, X., and Wang, B. (2020). Prodrugs of persulfides, sulfur dioxide, and carbon disulfide: important tools for studying sulfur signaling at various oxidation states. *Antioxidant Redox Signal.* 33, 1046–1059. doi: 10.1089/ars.2019.7880

Zhang, Z., Wu, Z., Yuan, Y., Zhang, J., Wei, J., and Wu, B. (2022). Sulfur dioxide mitigates oxidative damage by modulating hydrogen peroxide homeostasis in postharvest table grapes. *Postharv. Biol. Technol.* 188:111877. doi: 10.1016/j.postharvbio.2022.111877

Zhao, J., and Yi, H. (2014). Genome-wide transcriptome analysis of Arabidopsis response to sulfur dioxide fumigation. *Mol. Gen. Genomics.* 289, 989–999. doi: 10.1007/s00438-014-0870-0

Zhu, D. B., Hu, K. D., Guo, X. K., Liu, Y., Hu, L. Y., Li, Y. H., et al. (2015). Sulfur dioxide enhances endogenous hydrogen sulfide accumulation and alleviates oxidative stress induced by aluminum stress in germinating wheat seeds. *Oxid. Med. Cell Long.* 2015:612363. doi: 10.1155/2015/612363

Conflict of Interest: The authors declare that the research was conducted in the absence of any commercial or financial relationships that could be construed as a potential conflict of interest.

Publisher's Note: All claims expressed in this article are solely those of the authors and do not necessarily represent those of their affiliated organizations, or those of the publisher, the editors and the reviewers. Any product that may be evaluated in this article, or claim that may be made by its manufacturer, is not guaranteed or endorsed by the publisher.

Copyright © 2022 Li, Li and Chen. This is an open-access article distributed under the terms of the Creative Commons Attribution License (CC BY). The use, distribution or reproduction in other forums is permitted, provided the original author(s) and the copyright owner(s) are credited and that the original publication in this journal is cited, in accordance with accepted academic practice. No use, distribution or reproduction is permitted which does not comply with these terms.

frontiers | Frontiers in Plant Science

REVIEW
published: 13 May 2022
doi: 10.3389/fpls.2022.866409

Thermo-Priming Mediated Cellular Networks for Abiotic Stress Management in Plants

*Ambreen Khan, Varisha Khan, Khyati Pandey, Sudhir Kumar Sopory and Neeti Sanan-Mishra**

Plant RNAi Biology Group, International Centre for Genetic Engineering and Biotechnology, New Delhi, India

Plants can adapt to different environmental conditions and can survive even under very harsh conditions. They have developed elaborate networks of receptors and signaling components, which modulate their biochemistry and physiology by regulating the genetic information. Plants also have the abilities to transmit information between their different parts to ensure a holistic response to any adverse environmental challenge. One such phenomenon that has received greater attention in recent years is called stress priming. Any milder exposure to stress is used by plants to prime themselves by modifying various cellular and molecular parameters. These changes seem to stay as memory and prepare the plants to better tolerate subsequent exposure to severe stress. In this review, we have discussed the various ways in which plants can be primed and illustrate the biochemical and molecular changes, including chromatin modification leading to stress memory, with major focus on thermo-priming. Alteration in various hormones and their subsequent role during and after priming under various stress conditions imposed by changing climate conditions are also discussed.

Keywords: priming, high temperature stress, phytohormones, chromatin modification, molecular mechanisms

OPEN ACCESS

Edited by:
Girdhar Kumar Pandey, University of Delhi, India

Reviewed by:
Suprasanna Penna, Bhabha Atomic Research Centre, India
Vasileios Fotopoulos, Cyprus University of Technology, Cyprus

***Correspondence:**
Neeti Sanan-Mishra
neeti@icgeb.res.in

Specialty section:
This article was submitted to Plant Physiology, a section of the journal Frontiers in Plant Science

Received: *31 January 2022*
Accepted: *25 February 2022*
Published: *13 May 2022*

Citation:
Khan A, Khan V, Pandey K, Sopory SK and Sanan-Mishra N (2022) Thermo-Priming Mediated Cellular Networks for Abiotic Stress Management in Plants. Front. Plant Sci. 13:866409. doi: 10.3389/fpls.2022.866409

INTRODUCTION

Plants being sessile by nature are perpetually manifested with various adverse abiotic and biotic conditions. These unfavorable conditions usually occur together; concurrently or sequentially and negatively impact plant growth, ultimately leading to loss of crop yields (Pandey et al., 2017; Hilker and Schmülling, 2019). Plants possess efficient signaling networks and a sophisticated innate immune system, which enables them to endure a combination of diverse stresses. They seem to have well-defined mechanisms and strategies to remember the impeding stresses by inducing "stress memory" (Martinez-Medina et al., 2016; Hossain et al., 2020).

The concept of memory in relation to plant biology was first indicated by Charles Darwin while analyzing the Venus flytrap (*Dionaea muscipula*), for its ability to recognize and grasp insects (Darwin and Darwin, 1880). The term "memory" has been used to

describe processes used for acquiring, storing, retaining and retrieving information. In humans and animals, it has been mainly linked with neuronal communications. In case of plants, however, "memory" has been used to describe three behaviors namely, keeping time, chemical talks within self and cross-talks with surroundings (Leopold, 2014).

The work on the retention of memory was demonstrated by Gagliano and her colleagues by using a potted touch-me-not plant (*Mimosa pudica*) (Gagliano et al., 2018). The beneficial adaptable behaviors in plants were considered to be similar to non-conscious, involuntary primitive qualities. Prof. Rainer Hedrich and his team elucidated that various action potentials elicited by an insect in insectivorous plants could be effectively mimicked by electric pulses. The pulses appraised and forewarned the plants with regards to the size of the prey and constitution of the nutrients (Böhm et al., 2016). These experiments demonstrated that plants could learn in terms of counting, memorizing and interpreting the action potentials evoked due to mechanical stimuli and further interpreting these stimuli to effectuate gene expression (Scherzer et al., 2017).

The ability of plants to retain memory in response to milder impact of various biotic and abiotic challenges is called stress priming. In this review we will discuss the biochemical and molecular events induced during stress priming, which may be the cause or effect for the retention of memory. This stress memory can even be passed on to the next generation (Bruce et al., 2007). These changes may eventually help the plants to ward off the negative impact of subsequent severe stress. The descriptions mainly include examples from thermo-priming but examples from other stress priming events are also discussed to better explain the cellular molecular mechanisms.

STRESS PRIMING

Stress can appear at any stage during the development of a plant and it affects essential processes like photosynthesis, membrane stability, gene expression, RNA splicing, protein synthesis, etc (Sah et al., 2016). When exposed to stress plants undergo several changes, which eventually allow them to tolerate stress and survive. When plants are subjected to a mild or sub-lethal stress treatment and permitted to regain, they form a "memory" which ensures that future stress stimuli are not as detrimental as the severe stress given at the first time, even in sensitive plants (Mittler et al., 2012; Crisp et al., 2016). The "memory" response forms the basis of the process of stress priming to facilitate protection of plants upon exposure to subsequent harsh stress. Stress priming is also referred to as stress hardening, stress training, or stress conditioning. Priming has attracted intensive research over the last decade as primed plants show better adaptability and improved stress tolerance. Recent research interests are now focused on understanding and developing stress priming as a viable technique for improving plant tolerance to diverse stresses (Balmer et al., 2015; Martinez-Medina et al., 2016; Xiao et al., 2017; Liu H. et al., 2021).

There are several reports to support that an earlier exposure to a modest high temperature stress (HTS) eliciting stimulus can prime a plant to acclimate to a further exposure of same or different stress (**Table 1**). Alexandrov (1956) first used the term "heat hardening" to describe this occurrence and he observed that hardening time and temperature are inversely proportional. Likewise, thermo-tolerance can be induced in plants after priming with other biotic or abiotic stress (**Table 1**). Plants can also be primed for a better response to unfavorable conditions by treatment with specific chemicals like salicylic acid (SA) or JA (Aranega-Bou et al., 2014; Conrath et al., 2015), herbivory and by colonization with microbes like rhizobacterium species (Conrath, 2011; Pieterse et al., 2014; Liu and Avramova, 2016).

The effect of priming can be short-term or long-term and the process can be achieved by exposing plants at three different developmental stages to different abiotic and/or biotic elicitors:

(a) Priming of seeds helps to evade diverse stresses at the time of germination by inducing cross-stress tolerance. Seed priming accelerated germination and emergence to allow seedlings to escape abiotic stress such as HTS (Banerjee and Roychoudhury, 2020; Kumari et al., 2021).

(b) Priming at the post-embryonic stage increases the likelihood of the plant for surviving through the environmental changes. Its effects are mainly observed in the existing generation so it is also categorized as intergenerational, mitotic or somatic stress memory. Yucel et al. (1992) demonstrated that pre-heat treated wheat seedlings displayed thermal tolerance to HTS and showed reduced loss in photosynthetic capacity.

(c) Priming of parental population, such that the effects are transmitted to progenies constitute *trans*-generational priming. Its effects influence the future generations so it is also categorized as meiotic stress memory (Munné-Bosch and Alegre, 2013). In *trans*-generational stress priming, the memory for response to environmental stresses are likely to be packaged into seeds along with other resources and these provide crucial information to the new seedling during germination and beginning of plant development (Herman and Sultan, 2011). Studies in *Brassica rapa* indicated that changes in the profiles of non-coding RNA due to HTS could be transmitted to the next generation (Bilichak, 2015). The effect of HTS on seed germination and seed vigor in the progeny from thermo-primed parents has been studied in wheat (Liu, 2020; Zhou et al., 2020).

Initially it was proposed that memory of biotic priming is conferred *trans*-generationally to protect the progeny against recurring biotic stresses (Luna et al., 2012), but soon it was discovered that memory of abiotic stresses is also passed on to the next generations.

Priming can also be categorized based on the nature of the stress signals into cis- and *trans*- priming. When the eliciting stimulus and the response-triggering stress are of the same nature it is termed as "cis-priming." If the eliciting stimulus is different from the response-triggering stress it is termed as "*trans*-priming" (Hilker et al., 2016).

Cis-Priming

Priming with a particular biotic or abiotic stress can stimulate plant tolerance to subsequent occurrence of same stress and such examples are categorized as *cis*-priming. It was unequivocally demonstrated using different plants that priming with high

TABLE 1 | Thermo-priming for enhancing plant tolerance to high temperature and other abiotic stresses.

Elicitor	Priming treatment			Subsequent stress			Effect of priming	Reference
	Plant stage	Duration	Plant	Stress	Duration	Plant Stage		
HTS tolerance through somatic thermo-priming								
30–38°C	2 weeks	Gradually increasing (30–36°C for 45 min each; 38°C for 90 min)	*Oryza sativa*	45°C	90 min	2 weeks	Up regulation of HSFs, HSPs and TFs due to changes in miRNA profiles	Kushawaha et al., 2021
29–38°C	Anthesis	Gradual increase from 29 to 38°C during the 1st h; 38°C for 6 h		38°C	2 days	Anthesis	Up regulation of HSPs	Jagadish et al., 2010
37°C	1 month	1 h	*Rhododendron hainanense*	42/35°C*	1 h; 7 days	1 month	Accumulation of HSPs, RCA1, CPN60b and pTAC5	Wang X. et al., 2020
37°C	5 days	1.5 h	*Arabidopsis thaliana*	44°C	45 min	5 days	Increased abundance and activity of ROF1, HSP90.1 and HSFA2; Rapid accumulation of HSP21 regulated by plastid localized metalloprotease FtsH6	Sedaghatmehr et al., 2016; Thirumalaikumar et al., 2021
	21 days	2 h			2 h	21 days	CSN5A regulated expression of HTS memory genes, *APX2* and *HSP22*	Singh et al., 2021
	5 weeks	1 h		45°C	3 h	5 weeks	Higher activity of APX, POD1; up regulation of ABA and ACC in roots	Prerostova et al., 2020
33.5°C	12 days	3 h		45°C	1.5 h	12 days	Increased production of branched chain amino acids, RFOs, lipolysis products and tocopherols	Serrano et al., 2019
38°C	27 days		*Solanum lycopersicum*	38°C		30 days	Improved stress avoidance by increase in evaporation and decrease in leaf temperature	Zhou et al., 2020
35°C	3 months	1 h	*Achillea millefolium*	45°C	5 min	3 months	Improved photosynthesis and synthesis of secondary compounds with antioxidative characteristics	Liu B. et al., 2021
5°C higher than control	Stem elongation, booting and anthesis	5 days	*Triticum aestivum*		5 days	Grain filling	Enhanced activities of antioxidant enzymes, reduction in ROS and malondialdehyde production; increased photosynthesis, stomatal conductance and chlorophyll content	Fan et al., 2018
36/32°C*	Tillering	48 h		36/32°C*	7 days	Anthesis	Primed plants were more efficient in re-mobilizing dry matter than non-primed plants	Mendanha et al., 2018
40°C	Germinating seeds	4 h		35/27°C*	5 days	Post anthesis	Leaf photosynthesis and antioxidation capacities were improved due to up regulation of photosynthesis, antioxidation and HSPs	Zhang et al., 2016b
32/24°C*	2 leaf seedlings	2 days		35/27°C*	5 days	2 leaf seedlings	Maintenance of a better redox homeostasis due to improved antioxidant capacity	Wang et al., 2014a; Fan et al., 2018
HTS tolerance through meiotic thermo-priming								
32/28°C*	Pre anthesis (9 leaf)	Pre anthesis: 2 days	*Triticum aestivum*	T-gen 34/30°C*	10th day post anthesis	6 days	Higher activities of antioxidant enzymes, increased rate of photosynthesis and dry matter translocation; up regulated LSD1	Wang et al., 2016
34/30°C*	Post anthesis (10th day)	Post anthesis: 7 days						
30°C	10 days	2 weeks	*Arabidopsis thaliana*	Seeds collected			memory of attenuated immunity, early flowering and post-transcriptional gene silencing (PTGS) release.	Liu J. et al., 2019

(Continued)

TABLE 1 | (Continued)

Elicitor	Priming treatment			Subsequent stress			Effect of priming	Reference
	Plant stage	Duration	Plant	Stress	Duration	Plant Stage		
40°C	12 days (seedlings); early rosette stage	Gradually increasing temperature over 7 h from 18°C to 40°C; 40°C for 2 h		T-gen till G4 40°C	72 h	12 days	Accelerated flowering; maternally and paternally inherited epigenetic changes induced by exposure to abiotic stress over multiple generations can lead to reversible, *trans*-generational phenotypic changes	Suter and Widmer, 2013
50°C	5 days	3 h per day for 5 days		T-gen 50°C	5 days, 3 h per day	5 days	Increased expression of HSFA2 and reduction in MSH2, ROS1 and several *SUVH* genes	Migicovsky et al., 2014
42°C	2 weeks	3 h per day for 7 days	*Brassica rapa*	T-gen 42°C	3 h per day for 7 days	2 weeks	Regulation of BR metabolism, H^+ ATPase activity, signaling by IMPL1, mRNA decay activity by RRP41 and epigenetic regulation by FAS2	Byeon et al., 2019
Tolerance to other biotic/abiotic stress(es) through thermo-priming								
45°C	12 days (3 leaf stage)	3 h	*Oryza sativa*	Cadmium (5 μM)	3 h, 30/25°C*	3 leaf stage seedlings	Transient induction of H_2O_2 followed by increased activity of GR and APX	Hsu and Kao, 2007; Chou et al., 2012
35/29°C*	seeds of IRBB61	35/29°C*		biotic stress	48 h post inoculation	rice plant	Resistance to *Xanthomonas oryzae*, by suppressing ABA responsive genes	Cohen et al., 2017
35, 45, 50, and 55°C	3 leaf (seedlings)	30 min	*Hordeum vulgare*	Salt (200 mM)	30 min	3 leaf stage seedlings	Increased root growth, osmotic potential in leaves and gene expression (APX, CAT2, Cu/Zn SOD, BAS1, DRF1, MT2, NHX1, HSP17, HSP18 and HSP90)	Faralli et al., 2015
38°C	mature green plants	12 h	*Solanum lycopersicum*	Chilling (arginase inhibitor NOHA, 30 μM)	12 h	mature green plants	Increased production of proline and putrescine; Increased activities of arginase, SOD, APX and CAT leading to reduced oxidative damage	Zhang et al., 2013b
40.5°C	2–3 months (plants)	2 h		*Pseudoidium neolycopersici* infection	9 days post inoculation	seedlings	Suppression of pathogen *Pseudoidium* by activating JA, ABA and peroxidase activity	Nožková et al., 2018
42°C	7 days (seedlings)	5 h	*Brassica campestris*	Salt (150 mM NaCl) and drought (20% PEG 6000)	48 h	7 day (seedling)	Higher activities of APX, GPX, GR, GST, DHAR, CAT, Gly I, Gly II and lower levels of GSSG, H_2O_2, MDA	Hossain et al., 2013b
42°C	Seedlings	4 h	*Zea mays*	Chilling (0.5°C), drought, salt (0.7 mol/L NaCl)	5 days	Seedlings	Induction of H_2O_2 production, diminished loss of coleoptiles vitality and reduced electrolyte leakage in primary roots	Gong et al., 2001
37°C	7 days (seedlings)	24 h	*Triticum aestivum*	Heavy metals (Al, Cd, Cu and Fe each at 0.02, 0.2, 2 and 20 mol $m-^3$)	2 h	7 days	Possible role of glutathione, phytochelatins, HSPs	Orzech and Burke, 1988
24/18°C*	3–5 leaf seedlings	21–24°C day time, 15–18°C night time		biotic stress (Stripe rust)	18–20 days post inoculation	Seedlings	Warm air provided resistant to stripe rust. Identified QTL, QYrlo.wpg 2BS associated with HTSAP	Carter et al., 2009
38°C	Young plants (10 leaves)	10 h	*Vitis vinifera*	Chilling stress (0.5°C)	10 h; 20	Young plants (10 leaves)	Organelle ultrastructure maintenance, reduced lipid peroxidation and membrane leakage	Zhang et al., 2005
40°C	hypocotyl	4 h	*Vigna radiata*	Chilling stress (2.5°C)	6 days	Hypocotyl	Chilling resistance by preventing membrane leakage	Collins et al., 1995

(Continued)

TABLE 1 | (Continued)

Elicitor	Priming treatment			Subsequent stress			Effect of priming	Reference
	Plant stage	Duration	Plant	Stress	Duration	Plant Stage		
40°C	Seedling	1 h	*Cucumis sativus*	Chilling stress (2.5°C)	96 h	Seedling	Chilling resistance by root elongation and ion leakage	Jennings and Saltveit, 1994
38°C	7 days cultured pith tissue	2 h	*Nicotiana tabacum*	Salinity stress (1.2 % NaCl)	3 h	Tobacco cells	H_2O_2 causes expression of CAT, SOD, APX, GR and MAPKs leading to salt tolerance	Harrington and Alm, 1988
38°C	7 days (seedlings)	1.5 h	*Arabidopsis thaliana*	Anoxia	28 h	Seedling	Production of HSPs induce anoxia tolerant mechanisms	Banti et al., 2008
Thermo-tolerance through priming with other biotic/abiotic stress								
Water stress (3.5L in pot)	fully expanded first leaf	14 days	*Phaseolus vulgaris*	38°C	38°C	Trifoliate leaf plant	Sustained lutein and xanthophyll pigments, enhanced PG concentration, reduced unsaturation of thylakoid lipids	González-Cruz and Pastenes, 2012
Drought stress	2 months	8 days	*Festuca arundinacea*	38/33°C*	25 days	2 months	Enhanced accumulation of phospholipids and glycolipids for membrane stabilization and stress signaling	Zhang et al., 2019b
Cold stress (8°C)	100 days berries after full bloom	3 h	*Vitis vinifera*	45°C	4 h	100 days berries	Regulates SA and phospholipase D; Reduces membrane permeability and MDA contents, increases HSP73	Wan et al., 2009
Cold stress (0°C)	Seedling	4 days	*Hordeum vulgare*	35°C	5 days	Seedling	Increased activities of antioxidant enzymes CAT, APX, GR and SOD	Mei and Song, 2010
Fungus *Paraphaeosphaeria quadriseptata*_25c.f.u	Seedling	4 days	*Arabidopsis thaliana*	45°C	75 min	Seedling	Fungal secondary metabolites MON and RAD can bind and inhibit plant HSP90. MON leads to expression of HSP101 and HSP70 to promote HTS tolerance	McLellan et al., 2007
Endophyte *Curvularia protuberata*	1 month	Symbiotic relationship	*Dichanthelium lanuginosum*	45–65°C	3–10 days	1 month	Fungal endophyte produces cell wall melanin that may dissipate heat along the hyphae and/or complex with ROS generated during HTS	Redman et al., 2002
Thermo-tolerance through priming with metabolites								
Proline and glycine betaine (20 mM)	Single noded buds	8 h	*Saccharum sp.*	42°C	5 h	Sprouting buds	Restricted H_2O_2 production, improved K^+ and Ca^{2+} content, increased concentration of free sugars	Rasheed et al., 2011
Ascorbic acid (70 ppm) and Hydrogen peroxide (30 ppm)	Sowing and reproductive stages	24 h spray	cotton plant	45/30°C*, 38/24°C*, 32/20°C*	7 days	Reproductive stage	Increased chlorophyll content, photosynthesis, fiber quality, SOD and CAT activity, net photosynthetic rate, chlorophyll content, fiber quality	Sarwar et al., 2018
Trehalose (30 mM)	6 years (plants)	3 days treatment	*Paeonia lactiflora* Pall.	40°C	3 days	6 years (plants)	Osmotic protection, decreased MDA, H_2O_2 and relative electric conductivity	Zhao et al., 2019
Glutathione (0.5 mM)	6 days (seedlings)	24 h	*Vigna radiata*	42°C	48 h	Seedling stage	Enhanced antioxidant and glyoxalase activities	Nahar et al., 2015
Sodium hydrosulfide (0.5 mM)	2.5 days (seedlings)	12 h	*Zea mays*	47°C	15 h	Seedling stage	Accumulation of endogenous betaine by activating BADH	Li and Zhu, 2015
Spermidine (1.5 mM)	grain filling	3 to 5 DAP	*Oryza sativa*	40°C	5 days	Grain filling	Enhanced seed germination percentage, grain quality, seedling shoot height and antioxidant enzyme activity	Fu et al., 2019

**indicates day/night temperatures.*

temperatures could help in increasing thermo-tolerance to subsequent HTS (Wang et al., 2014a; Zhang et al., 2016b). The preservation of thermo-memory involved expression of specific genes and epigenetic markings (Shi et al., 2016). In wheat seedlings, thermo-priming for two consecutive days with temperature which was 8°C higher than day/night temperatures, increased the tolerance of mature plants to subsequent HTS occurring after anthesis. The primed plants displayed enhanced photosynthetic capacity, higher scavenging capacity of reactive oxygen species (ROS) and greater grain starch accumulation, as compared to plants, which were not primed (Wang X. et al., 2012). These traits were attributed to the up regulation of

expression of antioxidant genes in the primed plants (Wang X. et al., 2012; Wang et al., 2014a). High temperature exposure to 10 days old *Arabidopsis thaliana* induced attenuated memory, early flowering and post-transcription gene silencing in the next generation (Suter and Widmer, 2013; Liu J. et al., 2019). Pre-exposure to sub-lethal high temperatures boosted thermo-tolerance of rice plants and their progenies at the vegetative stage (Shi et al., 2016).

Similarly, priming plants with low temperatures was shown to successfully boost their tolerance to cold stress (Li X. et al., 2014). Seven days pre-exposure of wheat plants at tillering stage to a temperature which was 5°C less than surrounding environmental temperature (10°C), could relieve the damaging impact of low temperature (14°C) stress (Li X. et al., 2014). Cold priming resulted in accumulation of metabolites like sucrose, proline and other osmolytes thereby contributing to the stability of cellular membranes against cold stress (Iba, 2002). It also induced the expression of genes encoding antioxidant enzymes, electron transport chain during photosynthesis, synthesis of chlorophyll and starch thereby ameliorating cell membrane damage and protecting photosynthesis apparatus (Byun et al., 2014; Li X. et al., 2014).

Trans-Priming

trans-priming includes all cases where pre-exposure to a particular biotic or abiotic stress can stimulate plant tolerance to subsequent occurrence of another stress. For instance, drought priming wheat plants at the stem elongation stage induced cross-tolerance to HTS at grain filling stage and reduced yield loss (Wang et al., 2015). Drought primed plants exhibited increase in rate of carboxylation and photosynthesis and reduction in rate of energy loss under HTS (Wang et al., 2015). Both drought primed and unstressed control wheat plants showed similar levels of total protein, glutenin macropolymers and high molecular weight glutenin subunits, which suggested that drought priming protected the grain quality under HTS (Zhang et al., 2013a). Similarly, intermediate drought stress during early seedling stage was found to reduce the damage of subsequent cold stress in wheat by activation of antioxidant enzymes and maintenance of photosynthesis (Li X. et al., 2015). In wheat, pre-treatment of the parent plants with drought or HTS during grain filling imparted *trans*-generational cross-tolerance to their offspring against HTS at post-anthesis stage (Wang X. et al., 2018). The progenies showed higher grain yield, better maintenance of leaf photosynthesis, enhanced activities of antioxidant enzymes and reduced cell membrane damage (Wang et al., 2016). Drought primed plant progenies also showed cross tolerance to HTS during grain filling due to increased in rate of photosynthesis, reduction of membrane damage and increase in grain yield (Zhang et al., 2016a). The imprint of *trans*-priming of stress tolerance was also observed in rice, tobacco, radish and alfalfa (Bruce et al., 2007; Choi and Sano, 2007; Vu et al., 2015).

Trans-priming may be facilitated as similar or overlapping signaling pathways are involved in the perception and response to most abiotic stresses in plant (Zhu, 2016). HTS resulted in acquired resistance against the heavy metals such as cadmium, aluminum, iron and copper (Orzech and Burke, 1988). It was shown that HTS treatment increased the production of antioxidant enzymes in plants, which helped to regulate the ROS production triggered by metals (Kochhar and Kochhar, 2005; Hsu and Kao, 2007). Thermo-priming could enhance the preservation of many fruits, particularly those from tropical or subtropical locations, prior to exposure to low temperatures. Response to thermo-priming was associated with accumulation of heat shock proteins (HSPs: HSP70 and HSP79), small HSPs (sHSP22, sHSP18.1, sHSP18.2) increase in antioxidant enzymes (APX, catalase), maintenance of ultrastructure, reduction of membrane leakage and lipid peroxidation. These processes were also associated with providing chilling tolerance (Lurie and Klein, 1991; Jennings and Saltveit, 1994; Collins et al., 1995; Sabehat et al., 1996; Sato et al., 2001; Rozenzvieg et al., 2004; Zhang et al., 2005). A variety of plants could develop cross-tolerance to salt stress after being pre-exposed to HTS. The thermo-memory prior to salt stress caused an increase in H_2O_2, which resulted in enhanced survival and decreased damage when later exposed to NaCl (Gong et al., 2001). Heat pre-treatment was also shown to increase salinity tolerance by improving antioxidant activity and glyoxalase metabolism in mustard, tobacco and cashew plants (Harrington and Alm, 1988; Hossain et al., 2013b; Pérez-Salamó et al., 2014).

Priming seeds with hormone solutions, bacteria and chemicals is also known to substantially improve seedling emergence, seed germination and plant growth under HTS (Hasanuzzaman and Fotopoulos, 2019). Seed priming with combination of ascorbic acid and SA improved rice growth under HTS (Kata et al., 2014). Priming seeds with bacteria such as *Bacillus* spp. and *Azospirillum* spp. improved tolerance against HTS by reducing ROS production (Abd El-Daim et al., 2014). Wheat seeds inoculated with rhizobacteria substantially increased thermo-tolerance of the seedlings (Yang et al., 2009; Anderson and Habiger, 2012). The endophytic bacteria present inside plant tissues have also been implicated in priming process to promote plant growth (Singh et al., 2021). Recently it was reported that colonization by Enterobacter sp. SA187, isolated from root nodules of the desert plant *Indigofera argentea* lead to HTS tolerance in wheat seedlings under field conditions (Shekhawat et al., 2021). Similarly, endophytic fungus, *Paecilomyces formosus* (Waqas et al., 2015) and arbuscular mycorrhizal fungi (AMF) (Begum et al., 2019) were shown to improve plant growth under HTS. AMF improved growth by enhancing uptake of water and nutrients, increasing the activity of antioxidant enzymes and improving the rates of photosynthesis (Zhu et al., 2011; Maya and Matsubara, 2013).

Priming of plants by foliar spray of various micronutrients also enhanced their performance under HTS. The foliar spray of boron and iron was effective in attenuating both HTS and drought stress by securing high water content (Kumari et al., 2019). Selenium acts as an osmo-protectant by improving membrane permeability and activities of anti-oxidant system under HTS (Djanaguiraman et al., 2010). Exogenously applied proline protected carbon metabolism and antioxidant enzymes in chickpea and thereby provided better tolerance to HTS (Kaushal et al., 2011).

The integration of priming memory in plants with different molecular techniques may have a major impact on vigor. Although common stress response mechanisms have been shown to provide cross-tolerance to a variety of abiotic and biotic stresses, different plant species have varied abiotic stress sensitivities and the mechanisms used to protect against stress and the cross-talk between these stresses may be species dependent.

MOLECULAR MECHANISMS BEHIND THERMO-PRIMING

The response of plants to stress depends on their ability to rapidly transmit the perceived signals for initiating appropriate physiological, biochemical and molecular adjustments (Hasanuzzaman et al., 2013; Kollist et al., 2019). The stress signals get amplified through various second messengers like calcium ions (Ca^{2+}) and ROS to regulate physiological and developmental responses. This leads to rapid alterations in the genetic machinery, which is achieved through a network of transcription factors (TFs) and microRNAs (miRNAs) (Kinoshita and Seki, 2014).

The same molecular pathways also conferred memory during priming by triggering an early, appropriate and successful acclimation response (Bruce et al., 2007; Conrath, 2011; Walter et al., 2011; Kollist et al., 2019). The activation of basal cellular processes possibly ensured increased capacity to tolerate future stress and maintain complete fitness of the plant (Li S. et al., 2014). The hypothesis thus proposed, suggested that the rapid stress response phase in plants could serve as an intermediate stage in which generic morphological, biochemical and metabolic changes occurred to effectively counteract the detrimental effects of subsequent stress (**Figure 1**). These processes might involve some overlap with the responses activated during later stages of stress. Together they help in preventing irreversible damage and pre-inducing the stress response cascades. It is possible that a cellular feedback mechanism from the early stress response of plants provides memory by modifying or altering the later plant response during re-occurring stress events (Kollist et al., 2019).

There are now several reports from studies on thermo-priming and other stress priming events that point towards the underlying mechanisms. Analysis of transcriptome and proteome of heat primed plants showed that the translation of genes encoding cellular receptors, signal transducers, chaperones, enzymes associated with the process of photosynthesis and sucrose synthesis, transcription factors and HSPs were positively regulated whereas genes encoding enzymes involved in metabolism were negatively regulated (Xin et al., 2016; Zhang et al., 2016b; Xiao et al., 2017; Wang X. et al., 2020). The priming information was transmitted to the progenies in the form of cellular signals, HSPs and structural alterations in protein (Zhang et al., 2016b). Similarly, during excess light stress some transcripts were elevated within seconds and these were found to be essential for light stress acclimation (Suzuki et al., 2015). Priming with pathogens or biotic stress elicitors induced primary metabolism, pattern-recognition receptors, Mitogen-activated protein kinases (MAPKs) and chromatin modifications (Slaughter et al., 2012; Balmer et al., 2015; Conrath et al., 2015). Priming with mild drought or waterlogging in wheat seedlings induced proteins participating in oxidative stress, cell defense, carbon metabolism and photosynthesis (Xiao et al., 2017).

Signaling Through Kinases

Synchronized phosphorylation and dephosphorylation of proteins play significant roles in priming plant tolerance to both abiotic and biotic stresses. The Receptor Like Kinases (RLKs) and MAPKs constitute two important signaling cascades for eliciting stress responses (Nakagami et al., 2005).

Receptor like kinases make-up one of the most extensive gene families found in plants and include a large subfamily of Leucine-Rich Repeats (LRR) that play essential roles in plant adaptation to diverse stresses (Monaghan and Zipfel, 2012). GbRLK, identified from *Gossypium barbadense* (cotton), plays a fundamental role in preventing wilt induced by *Verticillium dahliae* and tolerance to salinity and drought by regulation of stress-responsive genes (Zhao et al., 2013). Not much is, however, known about their role in HTS and thermo-priming responses as temperature-specific sensors or receptors are not yet known in plants (Liu J. et al., 2015). It is hypothesized that temperature-induced changes in membrane rigidity/fluidity might be involved in the perception of the temperature extremes (Guo et al., 2016).

Mitogen-activated protein kinases represent another large and conserved cascade of three sequentially functioning threonine and tyrosine (TXY) kinases, which mainly act downstream to the RLKs in the signaling events (Jonak et al., 2002; Sharma et al., 2020). They play a major role in amplification and transduction of intracellular signals. The MAPK (MPK) is the last enzyme in the cascade. It is phosphorylated and activated by its upstream MAPK kinase (MAPKK, MKK, or MEK) (Conrath, 2011). MAPKK activity is regulated by phosphorylation by the MAPKK kinase (MAPKKK or MEKK), which either directly or indirectly receives the stress signals from receptors or sensors (Takahashi et al., 2007). MAPKs can activate a variety of downstream effectors and TFs to control thousands of genes to ensure proper cellular functions. The involvement of MAPKs in HTS response has been experimentally validated (Sinha et al., 2011).

MPKs, MEKs, and MEKKs are considered as excellent candidates for transducing signals that mediate thermo-priming (Conrath, 2011). In wheat plants, genes encoding MAPK cascade, Ca^{2+} signaling kinases and other protein kinases were found to be up regulated in primed plants as compared to non-primed plants (Wang M. et al., 2016). In alfalfa, MKK1 and MKK4, which are intermediaries in wound-responsive MAP kinase signaling were also associated with priming for abiotic stress (Wassie et al., 2020). Transcriptome analysis also indicated a role for genes encoding Ca^{2+}-dependent protein kinases and MAPKK in cold priming response in Arabidopsis (Byun et al., 2014). The accumulation of MPK3 and MPK6 was crucial for priming Arabidopsis plants and was related to increased *pal1* and *pr1* gene activation, ROS homeostasis, cold stress regulation and pathogen signaling (Beckers et al., 2009). Treatment with benzo (1,2,3) thiadiazole-7-carbothioic acid S-methyl ester (BTH), a synthetic equivalent of the SA resulted in the accumulation of transcript

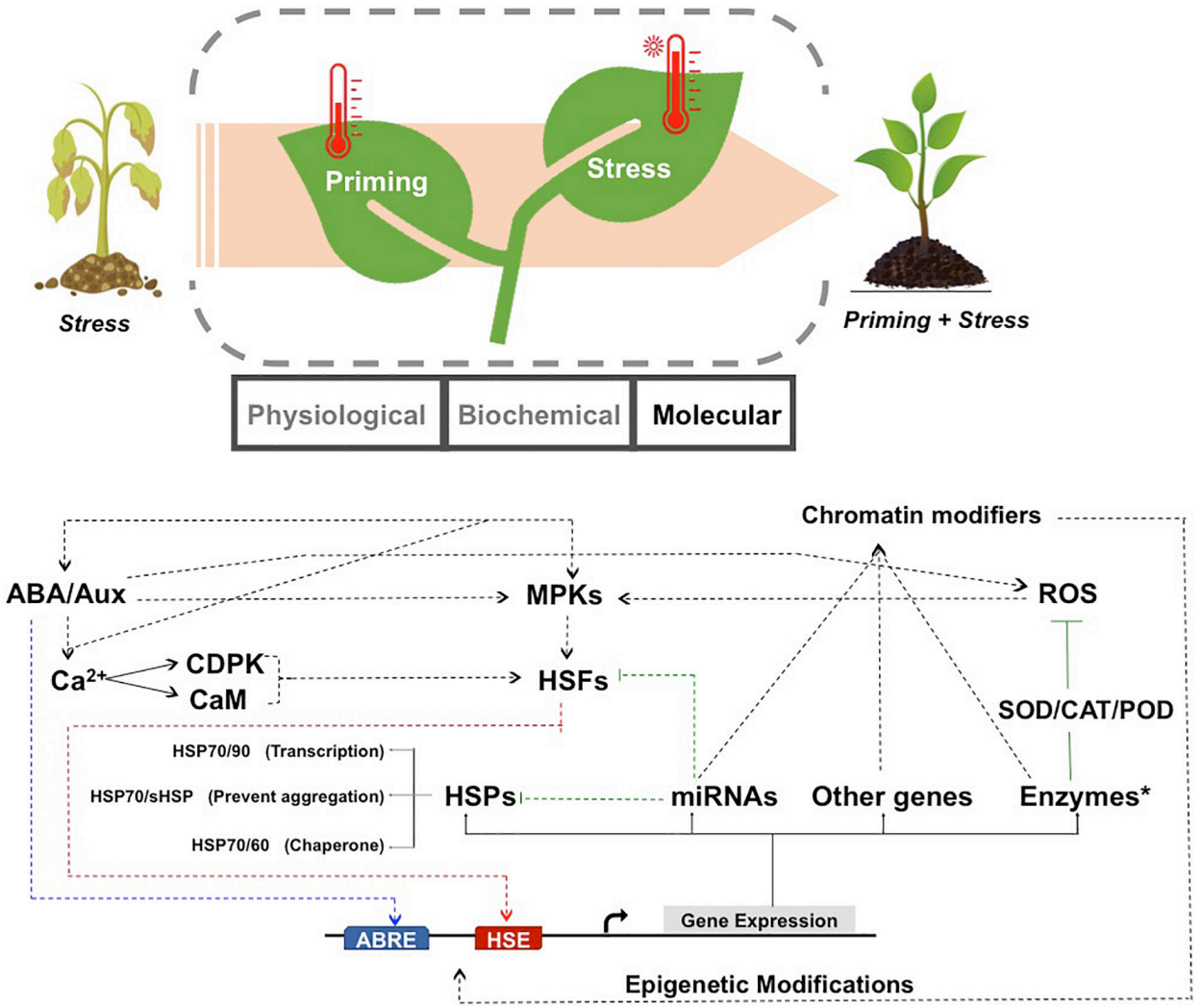

FIGURE 1 | Schematic representation to show the molecular networks operative during thermo-priming in plants. Plants under HTS perform better when primed with a short exposure to high temperature. Priming leads to changes in the physiological, biochemical and molecular framework. The molecular mechanisms responsible for thermo-tolerance and HTS memory are indicated below. Temperature priming activates the hormonal networks and ROS, which transmit the signals through the Ca^{2+} dependent pathways and/or MPKs to regulate HTS-responsive gene expression. The Ca^{2+} ions can be conducted through the CDPK or CaM pathways to activate the transcription factors. The HSFs (red) and hormones responsive transcription factors (blue) bind to their respective cis-elements and promote the transcription of HSPs, antioxidant enzymes (like SOD, POD, CAT), miRNAs and other genes. HSPs inhibit thermal denaturation of cellular proteins through increased chaperone capacity (HSP70/60), prevention of aggregation (sHSP/HSP70) and increased transcription (HSP70/90). miRNAs negatively regulate their targets genes, some of which include HSPs, HSFs and chromatin modifiers to trigger positive or negative feedback loops for retention of high temperature memory. On exposure to stress, primed plants show enhanced thermo-tolerance due to preparedness of the molecular machinery. ROS, reactive oxygen species; HSP, heat shock protein; HSF, heat stress transcription factor; MPK, mitogen-activated protein kinases; CDPK, calcium-dependent protein kinase; CaM, Calmodulin; ABA, abscisic acid; Aux, auxin; SOD, superoxide dismutase; CAT, catalase; POD, Peroxidases; HSE, heat shock sequence element; ABRE, abscisic acid response elements.

for *mpk3* and *mpk6*, as well as the gradual accumulation of MPK3 and MPK6 proteins (Beckers et al., 2009).

Forgetter2 (FGT2), a type 2C protein phosphatase, also plays an important role in HTS memory by maintaining the dynamics of cellular membranes (Castellanos et al., 2020). FGT2 also interacts with Phospholipase D (PLDα2) to produce phosphatidic acid (PA) and trigger lipid signaling for the maintenance of HTS memory. Mutants of *fgt2* and *pldα2* were defective in thermo-memory when exposed to reoccurring HTS.

In Arabidopsis, suppression of Target of Rapamycin (TOR) kinase is also well known for providing tolerance to different stresses (Bakshi et al., 2017; Wang P. et al., 2018; Dong et al., 2019). TOR overexpression lines were more immune to abiotic stress (Bakshi et al., 2017) but showed higher susceptibility to bacterial and fungal pathogens (De Vleesschauwer et al., 2018). TOR closely interacted with SnRK1 (Sucrose non-fermenting [SNF] related kinase 1) to regulate plant development and growth (Wang P. et al., 2018). It was demonstrated that in unstressed plants, TOR phosphorylated the ABA receptor to

repress the ABA signaling pathway and prevent activation of stress responses. Whereas, ABA-dependent repression of TOR and SnRK1 supported plant survival under extreme hypoxia, starvation and darkness (Baena-González and Sheen, 2008). The SnRK2 isoform, SnRK2.10, is implicated in osmotic stress response independent of ABA. SNRK2.10 mutant plants showed increased sensitivity to dehydration stress with respect to wild type plants. The target proteins of this kinase included dehydrins, ERD10 and ERD14, which are also induced during salinity stress (Maszkowska et al., 2019).

Ca^{2+}-sensing protein kinases (CPKS) or kinases interacting with Ca^{2+} sensors (CIPKs) and Ca^{2+} dependent protein kinases (CDPKs) are also associated with conferring stress resistance (Drerup et al., 2013; Mittler and Blumwald, 2015; Kudla et al., 2018). It was shown that exposure of apple trees to salt stress induced MdCIPK13, which phosphorylated to activate a sugar transporter, MdSUD2.2. The resulting sucrose accumulation provided the plants with protection from desiccation by increasing the osmotic pressure (Ma et al., 2019). The CDPKs take up a "primed conformation" as a first response to priming stimulus but their complete activation is possible upon exposure to subsequent harsh stress (Hake and Romeis, 2019).

Reactive Oxygen Species Pathway

Superoxide (O^{2-}), hydrogen peroxide (H_2O_2) and hydroxyl radicals (OH^-) are the most prominent ROS in early reaction of plants to many types of stresses. The burst of ROS production under abiotic stresses is usually analogous with the depression of photosynthesis (Kurepin et al., 2015). Plants have both enzyme dependent and non-enzyme dependent pathways for scavenging and detoxifying ROS. The common ROS-scavenging enzymes are superoxide dismutase (SOD), ascorbate peroxidase (APX), catalase (CAT), glutathione peroxidase (GPX), peroxiredoxin (PrxR) and glutathione reductase (GR). The major non-enzymatic antioxidants are ascorbic acid (ASA), reduced glutathione (GSH), carotenoids and flavonoids (Mittler et al., 2004).

Thermo-primed wheat plants produced significantly less amount of O^{2-} as compared to non-primed plants (Wang et al., 2014a). Low ROS rates are generally regarded as necessary secondary messengers for cellular metabolism. Accumulation of ROS likely has diverse functions in phytohormone biosynthesis, transport and signaling so it may affect the plant responses mediated by the hormones during priming (Xia et al., 2015). It also plays an important role in cross-tolerance to both abiotic and biotic stress by eliciting the respiratory burst oxidase homologs (RBOHs) and regulation of ABA signals (Xia et al., 2014). However, high ROS levels result in lipid peroxidation, degradation of pigments, DNA damage and carbohydrate oxidation eventually resulting in programmed cell death (Suzuki et al., 2012). Cold priming and drought priming were shown to individually increase SOD, APX and GR activities to shield photosynthetic machinery and protect the cellular membranes (Thomashow, 1999; Wang et al., 2014b).

H_2O_2 can act as a second messenger and play diverse roles in stress priming and cross-tolerance to multiple abiotic stressors (Suzuki et al., 2012; Hossain et al., 2015; Mittler and Blumwald, 2015). The ABA-dependent accumulation of H_2O_2 could stimulate the expression of *cat1* gene (Guan et al., 2000). Earlier investigations have demonstrated that exogenous application of 10 mM H_2O_2 solution could prime maize leaves to confer tolerance to salt stress by modulating various cellular processes associated with high antioxidant enzyme activity and increasing content of soluble proteins and carbohydrates (Gondim et al., 2013). Priming with H_2O_2 improved photosynthesis in leaves exposed to HTS in cucumber and salt stress in maize by enhancing the activity of carbon fixation enzyme, protection of chloroplasts and modulation of metabolites (Khan et al., 2018; dos Santos Araújo et al., 2021). It was shown that plants treated with brassinosteroid (BR) exhibited increased NADPH oxidase activity and enhanced the levels of H_2O_2 in cucumber apoplasts. These plants also showed resistance to CMV and tolerance to photo-oxidation and low temperature stress (Xia et al., 2009).

The ROS pathway interacts with Methylglyoxal (MG), a potentially toxic compound for plant cells that is produced rapidly as a result of abiotic stress. MG is primarily a by-product of glycolysis but it can also be produced during photosynthesis and metabolism of protein and lipids (Hoque et al., 2016). Excessive cellular accumulation of MG leads to protein glycation resulting in their degradation, endoreduplication and increased DNA strand breaks, sister chromatic exchange and point mutations (Kaur et al., 2014; Hoque et al., 2016). It has been shown that the application of exogenous GSH reduces MG levels via the glyoxalase pathway (Yadav et al., 2005). At low concentrations, MG was found to function as a signal molecule in plants (Li, 2016) and it was associated with the regulation of stomatal movement. MG can cross-talk with ROS and Ca^{2+} to activate MAPK and regulate the expression of stress tolerance-associated genes, *rd29b* and *rab18* in an ABA-dependent manner (Hoque et al., 2012, 2016). Exogenous application of MG could improve wheat seed germination and seedling establishment under salt and cadmium stresses (Li, 2016; Li X. D. et al., 2017; Li et al., 2017a,b). Recently, MG was reported to act as a HTS priming agent in maize seedlings by inducing AsA-GSH cycle and the ROS-scavenging system (Majláth et al., 2020).

Co-activation of the glyoxalase and ROS-antioxidant pathways is an important feature of abiotic stress and cross-stress tolerances in plants (Yadav et al., 2005; Upadhyaya et al., 2011). It was observed that a short spell of cold shock (6°C, 5.5 h) or heat shock (42°C, 5 h) promoted cross-tolerance to drought and salt stresses in mustard (*Brassica campestris L.*) seedlings, due to the induction of cellular detoxification of ROS and MG (Hossain et al., 2013a,b). The thermo-priming response involved both ROS and MG pathways, which were implicated in promoting cross-tolerance to HTS, cold stress, drought stress, salt stress and heavy metals in rice (Hsu and Kao, 2007), pea (Streb et al., 2008), maize (Gong et al., 2001), wheat (Lei et al., 2005), tomato (Zhang et al., 2013b), and cucumber (Kang and Saltveit, 2001).

The abiotic stresses also triggered the formation of nitric oxide (NO), which disturbed the redox potential of the cell by affecting the antioxidant and MG, detoxification systems. NO is also involved in the post-translational S-nitrosylation and nitration of target proteins. The exogenous application of NO and hydrogen

sulfide (H_2S) could induce a primed state which protected plants from the negative effects of salt stress (Antoniou et al., 2020) and low-temperature stress (Amooaghaie and Nikzad, 2013) but their role in thermo-priming has not been elucidated so far. The molecular oxygen and/or O^{2-} anion interact with NO to yield reactive nitrogen species (RNS). These molecules act together to transduce signals during stressed conditions and maintain redox equilibrium inside the cell (Suzuki et al., 2012). The redox hub formed by interaction between ROS, RNS and reactive sulphur species (RSS) is referred to as RONSS (reactive oxygen, nitrogen and sulfur species) and is considered essential for priming strategies to enhance cross-tolerance (Terrile et al., 2020). The RONSS primed state induced translation of a pool of transcripts inclusive of those coding for antioxidant enzymes, osmo-protectant proteins and polyamine biosynthesis.

Chaperons and Prions

One of the earliest indicators of the HTS response is the formation of heat shock proteins (HSPs). The HSPs act as molecular chaperones and are important for maintaining the structure and function of proteins, removing potentially toxic polypeptides and restoring protein homeostasis (Kotak et al., 2007; Timperio et al., 2008). They prevent the aggregation of non-native proteins by facilitating their refolding into their native conformation thereby minimizing toxicity of unfolded or denatured proteins during stress.

The HSPs are also associated with the maintenance of acquired thermo-tolerance (Xue et al., 2014). They are classified according to their molecular weight and functions into five broad families, namely HSP100, HSP90, HSP70, HSP60 and small HSP (sHSPs). The transcription of HSPs is stringently controlled by different members of HTS transcription factors (HSFs). The HSP90 and HSP70 represent the major families of HSPs and their activities are modulated by stress-induced HOP (Hsp70-Hsp90 organizing protein) protein (Carrigan et al., 2006). HSPs and HOP proteins were highly expressed in drought or thermo-primed plants, which helped in improving grain filling during HTS in wheat (Wang et al., 2014b; Zhang et al., 2016b) and rice (Kushawaha et al., 2021).

Under normal conditions, the HSP90.1 bound with ROF1 (rotamase FKBP 1), a member of the FKBP family, to form a cytoplasmic protein complex. Upon exposure to HTS, HSFA2 binds to HSP90.1-ROF1 and the resulting complex translocates to the nucleus, where it putatively functions to enhance the transcriptional activity of HSFA2 and maintain the expression of *hsp* genes regulated by it during HTS recovery (Meiri and Breiman, 2009). Accordingly, Arabidopsis plants overexpressing *rof1* displayed improved HTS memory while *rof1* mutant plants had impaired memory response. It was recently demonstrated that during the recovery phase NBR1 (Next to BRCA1) interacts with HSP90.1-ROF1 and facilitates their breakdown by autophagy to repress the response to HTS. Thus, HSP90 has a vital function in controlling of recovery from HTS and resetting the cellular memory of HTS in Arabidopsis. Loss-of-function mutants of NBR1 showed a stronger HTS memory (Thirumalaikumar et al., 2021). The HSP90 also displays hormonal cross talk by inducing TFs like ARFs and reducing the accumulation of transcriptional repressors like Aux/IAAs concentration (Wang R. et al., 2016; Watanabe et al., 2016). Studies in Arabidopsis and rice have indicated that HSP101-HSA32 interaction provides another conserved positive feedback loop during thermo-memory. Continuous accumulation of HSP101 during thermo-memory phase results in high abundance of HSA32. The HSFA32 in turn increases stability of HSP101 by retarding its degradation.

Several small HSPs like sHSP17.6II, sHSP22, sHSP18.2 are also associated with HTS memory. The Arabidopsis Hikeshi-Like Protein1 (HLP1) interacts with HSP70 to provide thermo-tolerance in plants (Koizumi et al., 2014). Induction of *Heat Stress Associated 32* (*hsa32*) gene by HSP101 is necessary for thermo-tolerance and HTS memory preservation (Wu et al., 2013). HSA32 works in tandem with Brushy1/Tonsoku/Mgoun3 (BRU1/TSK/MGO3) which is necessary for the sustained activation of HTS memory genes by inducing changes in chromatin structure (Suzuki et al., 2004; Takeda et al., 2004; Brzezinka et al., 2019).

Another interesting mode of biochemically reproducible memory is provided by sustainable changes in the protein conformation and function of prion domain proteins (PrD). These proteins are ubiquitously present in fungi, mammals and plants (Shorter and Lindquist, 2005; Chakrabortee et al., 2016). The PrDs were shown to switch between non-aggregated states and higher-order functional oligomers. The highly ordered aggregates acted as self-replicating entities that had the ability to propagate and could be transmitted to next generations. These characteristics enabled them to bestow stable alterations in biological states, which is important in molecular biology (Newby and Lindquist, 2013), but their significance in plant stress and memory remains largely unknown. A recent report has identified candidate PrDs in approximately 500 plant proteins using computational algorithms and predicted their diverse functional roles in stress and developmental responses including flowering time and thermo-sensory responsiveness (Garai et al., 2021). Transition from vegetative to reproductive stage also involves memorizing and integrating previously encountered environmental conditions. It was reported that Luminidependens (LD) proteins that are involved in regulating the timing of flowering in Arabidopsis behaved as prion-like conformational switch (Lee et al., 1994; Chakrabortee et al., 2016). The LD may be responsible for memorizing and assimilating the ambient signals required to control flower timing. Recently, an Arabidopsis PrD, ELF3, was found to be associated with thermo-sensory response (Jung et al., 2020).

REGULATION OF GENE EXPRESSION

Response to stress results in alterations in gene expression and the foremost amongst them involve activation of transcription, stabilization of mRNA and synthesis of new proteins. The genes can be grouped to differentiate those regulating the "non-memory" response from the group of genes that delineate the "transcriptional memory" (Ding et al., 2013). This became evident from whole-genome transcriptome studies

in Arabidopsis plants exposed to dehydration stress. Single exposure to stress identified >6500 differentially expressed genes, while upon repeated exposure, 4500 genes responded to each stimulus in a same way while 1963 genes generated considerably varied levels of transcripts each time.

Analysis of transcriptional changes, in *Arabidopsis thaliana* and *Zea mays* plants, in response to multiple stimuli indicated that transcriptional memory was based on an evolutionarily conserved mechanism that could discriminate between single and repeated stresses. The memory genes could induce or alter mRNA synthesis resulting in cellular changes and/or interactions between overlapping signaling pathways (Ding et al., 2014). These genes produced enzymes, osmolytes, dehydrins and chaperones, which were involved in cellular detoxification, protection and damage-repair. In Arabidopsis, stimuli like touch, wind, wounding, rain or transition of plants from light into darkness caused the translation of *tch* (touch induced) genes (Chehab et al., 2012). One of the members of this gene family was identified as a calmodulin homolog that could be involved in Ca^{2+} signaling (Chehab et al., 2009).

Transcription Factors

Transcriptome studies on stress challenged plant tissues identified changes in the transcripts coding for different TFs. Several genes from the MYB, NAC, HSFs, WRKY ethylene response factors (ERFs or AP2), and zinc finger (ZNF) super families have been shown to provide cross-tolerance to abiotic and biotic stressors in plants.

The responses to HTS and thermo-priming are transduced through the MAP kinase pathway to induce the translation of HSFs, which are prime regulators of plant response (Zhang et al., 2016b). HSFs are a conserved family of TFs that bind directly to heat shock elements (HSEs) to control HTS-related gene expression (Ohama et al., 2017). The HSEs consist of tandem inverted repeats of the pentameric consensus sequence nGAAn (nTTCnnGAAnnTTCn) and the AGGGG motifs (Swindell et al., 2007; von Koskull-Döring et al., 2007). Variable number of HSFs are observed in plants, *viz.* rice (25 members), wheat (56 members), Arabidopsis (21 members), soybean (52 members), tomato (26 members), maize (30 members), carrot (35 members), pepper (25 members), cotton (40 members) etc. (Scharf et al., 2012; Xue et al., 2014; Guo et al., 2016; Yang X. et al., 2016; Li et al., 2019). HSFs are divided into three structural classes: A, B and C, with class A serving as the principal activator of thermo-tolerance genes (Guo et al., 2008; Scharf et al., 2012).

Among the Class A HSF, the HSFA1 subfamily participates as early response genes for activating the other HTS response factors, for instance HSFA2 and DREB2A (Guo et al., 2008; Liu et al., 2011a; Scharf et al., 2012). Recent investigations have shown that HSFA1a directly senses HTS and gets activated through modifications in its redox state (Liu et al., 2013). HSFA1a is involved in the expression of genes coding for HLP1, dehydration-responsive element-binding protein 2a (DREB2a), HSFA7a, HSFBs, HSFA2 and multi-protein binding factor 1C (MBF1C) by binding to HSEs present in their upstream regions. HSFA2 is highly stimulated during HTS and is crucial for growth as well as maintaining the thermo-tolerance response during recovery period. It is regulated by three other TFs, HSFA1b, HSFA1d and HSFA1e (Yeh et al., 2012; Li X. D. et al., 2017). Thermo-priming-induced HSFA2 transiently binds at the promoter region of HTS memory genes, thereby facilitating di- and tri-methylation of histone H3 (Lämke et al., 2016). This chromatin modification triggers hyper-activation of transcription at these loci under subsequent HTS. HSFA3 expression is regulated by DREB2a and DREB2c and is essential for thermo-tolerance (Yoshida et al., 2011; Sato et al., 2014). In tomato, HsfA3 shows strong phosphorylation by HTS activated MAP kinases (Sinha et al., 2011). Other HSFs like HSFA4a and HSFA8 are also involved in sensing the ROS and induction of antioxidant system in plants (Qu et al., 2013). HSFA9 is exclusively expressed in late seed development stages.

The Class B HSFs, such as HSFB1 and HSFB2b primarily act as transcriptional repressors to inhibit HTS-induced gene expression (Ikeda et al., 2011). They act as co-activator in combination with class-A HSFs (Ikeda et al., 2011; Fragkostefanakis et al., 2015). The role of Class C HSFs in HTS is not clear. TF-HSFC1a was found to be negatively controlled by early HTS treatment in rice (Mittal et al., 2009), while overexpression of HSFC2a-B in wheat increased the expression of heat associated genes, resulting in improved thermo-tolerance (Hu et al., 2018).

NAC binding sites are known to be present in the promoters of several HSFs e.g., HSFA1b, HSFA6b, HSFA7a, and HSFC1 (Guo et al., 2015). The NAC TF family is found in plants and has been linked to the regulation of development and a stress related response. Overexpression of OsNAC6 improved tolerance of rice plants to drought and salt by activation of many stress-responsive genes (Nakashima et al., 2007). Heat priming elevated the expression of ATAF1 but its level again decreased during thermo recovery phase (Alshareef et al., 2019). JUB1 and ANAC019, members of NAC-TF family, were reported to regulate HTS and heat memory. JUB1 was reported to show thermo-memory related expression, which was similar to that of HSFA2 and HSFA32 (Shahnejat-Bushehri et al., 2012).

The stress induced increase in ABA, signaled the activation of R2R3-MYB TF, TaPIMP1 in wheat. This increased resistance to the fungus, *Bipolaris sorokiniana* and tolerance to drought stress (Zhang et al., 2012). The MYB-TFs also conferred cross tolerance to abiotic stimuli such as salinity and drought in transgenic tobacco by increasing the activity of phenylalanine ammonia lyase (PAL) and SOD (Liu et al., 2011b).

The expressions of ERF/AP2-TFs and ZNF proteins were induced in cold-primed plants indicating their crucial roles in priming plant response to cold tolerance (Byun et al., 2014). In cereals, long-term exposure to cold lead to the stable induction of VRN1, a TF related to AP1 (Trevaskis et al., 2003; Yan et al., 2003). This process was accompanied by accumulation of H3K4me at the VRN1 locus (Huan et al., 2018) indicating a possibility of analogous pathway for regulating chromatin in long-term memory of cold in cereals.

Priming by dehydration induced ABA-dependent memory through recruitment of MYC2-TFs, mobilization of mediator complex and accumulation of Ser5P RNA Pol II (Liu and Avramova, 2016). The ABA-dependent expression

of a stress inducible OsWRKY45 gene increased tolerance of Arabidopsis to salt and drought stress (Qiu and Yu, 2009). WRKY40 and Zat12, TFs showed a triphasic transient expression pattern during the response to stress. Their expression first peaked as a rapid response within a few seconds of stress (Suzuki et al., 2015), second time after a few minutes and third time after a few hours (Van Aken et al., 2016), indicating that TF pulses control the transcriptome in plants (Davletova et al., 2005).

MicroRNAs

Genome-wide transcriptome and small RNA analysis has linked the non-coding RNAs to stress response in plants. The stress responsive expressions of several conserved and novel miRNAs have been captured in a variety of plants like rice, tomato, populus, mustard, Arabidopsis, wheat, switch grass, cavendish banana and french beans (Chen L. et al., 2012; Yu et al., 2012; Kruszka et al., 2014; Raghuram et al., 2014; Jyothi and Rai, 2015; Liu W. et al., 2015; Hivrale et al., 2016; Pan et al., 2017). Different miRNAs such a miR156, miR159 and miR160 have been found to play essential roles in response to HTS (Stief et al., 2014). Many miRNAs induce response to HTS and thermo-memory by regulating key TFs and enzymes. For instance, miR159 acts on the *GAMYB* transcripts, miR396 regulates transcripts of *WRKY* TFs, miR528 regulates transcripts encoding F-box protein and miR5054 acts on *cat* transcripts (Giacomelli et al., 2012; Wang Y. et al., 2012). The miRNA168 acts in thermo-tolerance memory by regulating the function of AGO1 in thermo-memory, which generates a negative feedback loop and changes the expression of a larger number of miRNAs (Vaucheret et al., 2006).

It has been shown that miR156 was highly induced after HTS, to down regulate the *Squamosa Promoter Binding Protein-Like* (*spl*) TFs. Thermo-priming seems to generate HTS memory in Arabidopsis by repressing the transcription of *spl2* and *spl11* transcripts by inducing transcription of miR156 (Yu et al., 2012; Stief et al., 2014). During recovery from HTS, the *spl* levels were restored. The HTS also induced a positive feedback loop consisting of HSFA regulated miR398. The levels of miR398 were increased in response to HTS for down regulating the *copper/zinc superoxide dismutase* gene (Guan et al., 2013). This lead to increased levels of ROS, which in turn induced the HSFs and HSPs.

Another study showed that miR167 regulated DNA methylation process in response to HTS (Wu et al., 2010; Sanchez and Paszkowski, 2014; Naydenov et al., 2015), indicating a possible role for imprinting in HTS memory. The expression of osa-miR531 is regulated under different abiotic stress conditions including short duration HTS by signaling through MAPKs (Raghuram et al., 2014). HTS was shown to enhance the synthesis of vitamin E in chloroplasts, which up regulated miR398 biogenesis by retrograde signaling and provided protection to the Arabidopsis plants (Fang et al., 2019). A role for tRNA-derived siRNA fragments in *trans*-generational transmission of thermo-priming memory has recently been reported in durum wheat (Liu, 2020).

Our group has shown that miR169:NFY module may play a crucial role in integrating stress memory induced during HTS priming with light regulated development (Khan et al., 2017; Kushawaha et al., 2019). NGS analysis of rice transcriptome showed that levels of several miRNAs, HSPs, and HSFs were dis-regulated by thermo-priming (Kushawaha et al., 2021). Several heat responsive miRNAs like osa-miR531a, osa-miR5149, osa-miR168a-5p, osa-miR1846d-5p, osa-miR5077, osa-miR156b-3p, osa-miR167e-3p were identified that acted on respective HSF or HSP targets to differentially alter gene expression (Kushawaha et al., 2021). The other differentially expressed transcripts were mainly associated with redox pathway, protein phosphorylations and regulation of transcription.

ROLE OF CHROMATIN MODIFICATION IN STRESS PRIMING

Epigenetic regulation resulting in chromatin modification is a common mechanism used to regulate transcriptional activity in eukaryotes. Chromatin is composed of negatively charged DNA associated with positively charged histones that are arranged as nucleosomes. Each nucleosome consists of two molecules of each four histones (H2A, H2B, H3 and H4) forming an octamer, which is wrapped by DNA. The nucleosomes are connected to each other by a DNA strand linked with histone H1 (Kornberg, 1974; Thoma et al., 1979).

The DNA and histones are subjected to covalent modifications such as methylation, acetylation, ubiquitination and poly-ADP ribosylation during gene regulation. DNA methylation and histone modifications are two main mediators of epigenetic regulation. DNA methylation is a definitive chemical process in which a methyl group is added to DNA. It usually occurs when a cytosine (C) is linked to guanine (G) through the phosphate (p) linkage resulting in a CpG site. The methylation reaction is catalyzed by a large family of DNA-methyltransferase (DNMTs) and distinct enzymes perform *de novo* DNA methylation and maintenance DNA methylation (Kotkar and Giri, 2020).

The epigenetic modifications can be inherited via mitotic and meiotic cell divisions and act to synchronize the changes in gene expression, which form the basis of memory responses (Eichten et al., 2014; Kinoshita and Seki, 2014; Avramova, 2015; Crisp et al., 2016; Liu and Avramova, 2016). Initial indications for involvement of chromatin modification in priming response came from studies in which plants primed with benzothiadiazole showed increased levels of histone methylation (Jaskiewicz et al., 2011). The bi- and tri-methylation of lysine 4 in histone 3 (H3K4me2 and H3K4me3, respectively) is correlated with active transcription of genes (Ruthenburg et al., 2007; Jaskiewicz et al., 2011) and were recognized as potential abiotic stress memory markers.

Response to HTS comprises of two components, induction of stress memory-associated genes and differential expression of HTS regulated genes. Both components are related with increased levels of H3K4me3 and H3K4me2 and are dependent on functional TFs (Lämke et al., 2016; Liu Y. et al., 2019). An increase in H3K4me2 and H3K4me3 was observed after heat priming in Arabidopsis (Conrath et al., 2015). H3K4me2/3 accumulation was also seen in Arabidopsis plants that had been primed with JA (Liu and Avramova, 2016).

Stress related memory might particularly develop when the plant is recovering from stress. This has been best exemplified by studies on vernalization leading to development of memory for cold stress. During the cold phase, repressive chromatin marks were stored at the nucleation regions of FLC, but epigenetic modifications were triggered after reversing to warm conditions. During the recovery from cold signal, the Polycomb Repressive Complex 2 (PHD-PRC2) was deregulated across the entire FLC locus and H3K27me3 increased remarkably throughout the entire gene to achieve epigenetic silencing (De Lucia et al., 2008; Angel et al., 2011).

Modification of chromatin provided potential memory for stress during priming events by maintaining the basal transcriptional machinery at the promoters of these genes to facilitate their rapid or strong expression in response to recurring stress (Conrath et al., 2015). Increase in H3K4me3 was retained as a memory on the stress responsive genes during stress, while H3K4me3 accumulated at primed defense genes before their transcription (Conrath, 2011; Jaskiewicz et al., 2011). Repeated exposures of Arabidopsis plants to mild drought like conditions increased the levels of H3K4me3 and stalled RNA polymerase II at RD29B and RAB18 loci allowing their rapid activation during the stressed phase (Ding et al., 2012). Increased H3K4me3 levels also caused increase in the occupancy of TATA-binding protein (TBP), a key step in the formation of the pre-initiation complex (PIC), at the promoters of memory genes (Liu and Avramova, 2016). HTS memory was also maintained by H3K27me demethylases, Relative of Early Flowering 6 (REF6) and the Jumonji (JMJ30) proteins by controlling the level of histone modification of *HSP22* and *HSP17.6* genes (Yamaguchi and Ito, 2021).

Some stress-induced TFs were reported to function as prime components of transcriptional memory and are probably involved in recruiting specific chromatin-regulatory proteins to the target loci. For example, bZIP28/60 TFs were stimulated by the stress induced Unfolded Protein Response (UPR) protein (Liu and Howell, 2010) to recruit the COMPASS-like complex (Jiang et al., 2011) for initiating the accumulation of H3K4me during HTS (Song et al., 2015). It was shown that the same mechanism triggered the deposition of H3K4me3 at loci of dehydration memory genes. In yeast, both COMPASS and Mediator complexes were required for the H3K4me accumulation and transcriptional memory of the gene encoding inositol-1-phosphate synthase (Light et al., 2010, 2013; D'Urso et al., 2016). The composition of these protein complexes changed under memory and non-memory situations to allow differential regulation of transcription (D'Urso et al., 2016).

HSFA2 and HSFA1 are known to function in somatic HTS memory (Charng et al., 2007; Lämke et al., 2016; Liu Y. et al., 2019). Thermo-priming induced accumulation of H3K4me2 and H3K4me3 to generate HTS memory was dependent on HSFA2 (Lämke et al., 2016). Binding of HSFA2 occurred during first few hours of heat shock but the enhanced H3K4me3 and H3K4me2 levels persisted even after HSFA2 association with the gene had declined. The HSFA2 acts in trimeric complexes along with other HSFs like HSFA3 [reviewed in Scharf et al. (2012)], indicating that heat memory might be specific to few TF complexes and not individual TFs. HSEs were found to be the sites of active chromatin regions associated with histone (H3K9 and H3K14) acetylation and H3K4me3 (Guertin and Lis, 2010). Transcriptional activation of few HSF and HSP genes in Arabidopsis by HSF1A/B occurred through deposition of H3K56 acetylation under HTS (Weng et al., 2014).

The *trans*-generational HTS memory involves a heritable positive feedback loop consisting of REF6 and HSFA2 (Liu J. et al., 2019). The HSFA2 and REF6 promote the expression of each other to continuously maintain the active state of HSFA2. The HSFA2 in turn activates the expression of suppressor of gene silencing 3 (sgs3) interacting protein 1 (sgip1), an E3 ligase, to mediate SGS3 degradation. This represses biosynthesis of trans-acting siRNA (tasiRNA) and results in the release of its target, *Heat-Induced Tas1 Target 5* (*htt5*) to promote early flowering in the progeny plants. Subsequent studies demonstrated the role of FGT3 and HSFA3 in inducing transcription of memory-related genes during recovery from HTS.

Nucleosome remodeling has also been related to HTS induced memory. Arabidopsis FGT1 protein maintains low nucleosome occupancy at thermo-memory related genes like *hsa32, hsp22.0, hsp18.2, and hsp101*. FGT1 acts by interacting with proteins belonging to the chromatin remodeling complexes such as ATP-dependent Switch/Sucrose Non Fermentable (SWI/SNF), Imitation Switch family (ISWI) or Brahma (BRM), Chromo-domain Helicase DNA-binding (CHD) and INO80 complex ATPase subunit (INO80) to provide thermo-memory response (Brzezinka et al., 2016; Liu H. et al., 2021).

The *trans*-generational priming responses include both inheritable (DNA and chromatin structure change) and non-inheritable (metabolites, proteins or mRNA in the seeds) components (Boyko and Kovalchuk, 2011). The enzyme lysine-specific histone demethylase 1, which is involved in histone demethylation and epigenetic modification, was up regulated in the progenies of the primed plants. This suggested that the epigenetic modification could be involved in the *trans*-generational stress memory resulting in enhanced tolerance to stress.

The study of mechanism behind maintenance of epigenetic modifications over a longer period of time led to the discovery of trans factors that mediated faithful copying of the chromatin conformation through replication. One such protein, BRU, is necessary for the sustained activation of HTS memory genes (Suzuki et al., 2004; Takeda et al., 2004; Brzezinka et al., 2019). It is also essential to sustain the transcription of HTS responsive genes *hsa32*, *apx2*, *hsp22.0*, and *hsp21* (Stief et al., 2014). BRU1 has been implicated in the inheritance of chromatin states in transcriptional silencing and the DNA damage response across DNA replication and cell division.

Recently, a BRU1 orthologue from mammals was found to bind to single-stranded DNA and newly incorporated nucleosomes after replication (Huang et al., 2018). The histone chaperone, Chromatin Assembly Factor-1 (CAF-1) plays a key role in depositing histone H3H4 tetramers into newly replicated DNA. Mutants of *caf-1* showed a constitutive priming response against pathogens and increased H3K4me3 at primed defense-response genes. This suggested that regulated deposition of

histone tetramers may be essential for inheritance of priming responses (Mozgova et al., 2015).

DNA methylation is another mechanism of epigenetic modification and is shown to be a dynamic regulatory mechanism of defense genes and stress priming. Single base-resolution DNA methylome profiling of cold primed tissues revealed the global loss of DNA methylation with increase in some locally hypermethylated sites. The *de novo* methylation of cytosine residues (CG, CxG, Cxx) in plant DNA can be triggered by small interfering RNAs (siRNA). The onset of RNA-directed DNA methylation begins with the formation of siRNAs. The siRNAs may be produced through the Polymerase IV (Pol IV) pathway and loaded in Argonaute 4 (AGO4) complex. Alternatively, the siRNAs can be generated through Pol I-RNA Dependent RNA Polymerase 6 (RDR6) pathway and are loaded into AGO6 complex. The AGO4/6 complex, interact with Pol V to recruit a Nuclear RNA Polymerase E1 (NRPE1) complex, which subsequently establishes DNA methylation through Domains Rearranged Methyltransferase2 (DRM2). During cell divisions, the maintenance of known DNA methylation marks in CG and CxG are catalyzed by Methyltransferase1 (MET1) and Chromomethylase3 (CMT3), respectively (Ramirez-Prado et al., 2018; Zhang H. et al., 2018).

ROLE OF PHYTOHORMONES IN STRESS PRIMING

The classic growth promoting phytohormones viz. auxin, cytokinin (CK), strigolactones (SLs) and BR and the stress related hormones such as ABA, JA and SA, play an essential role in orchestrating protection in response high temperature and other abiotic stresses (Tang et al., 2008; Verma et al., 2016; Kumar et al., 2019; Li et al., 2021). Phytohormones act by positively regulating stress responsive gene expression, nutrient allocation, photosynthetic activity, osmolyte biosynthesis and antioxidant metabolism (Alam et al., 2013; Peng et al., 2014; Qiu et al., 2014; Shi et al., 2014; Jin and Pei, 2015; Cheng et al., 2016). Exogenous application of ABA, ethylene and SA or enhancing their endogenous levels helped to significantly overcome HTS induced damage and improved thermo-tolerance response (**Table 2**). Combined application of gibberellins and ABA in rice lead to increase in pollen germination and vigor. The phytohormones acted by improving anti-oxidant activity and membrane stability (Chhabra et al., 2009; Song et al., 2012). The role of ethylene in reducing HTS by reducing oxidative damage has been studied at seedling stage in Arabidopsis and rice (Larkindale and Knight, 2002; Wu and Yang, 2019).

Abscisic Acid

The primary stress hormone, ABA, modulates plant responses to multifarious environmental stresses. The involvement of ABA in response to HTS and thermo-priming has emerged through many different studies (Larkindale and Knight, 2002; Zhou et al., 2014; Li et al., 2021). ABA-mediated ROS accumulation in guard cells caused closure of stomata (Kwak et al., 2003) and helped to decrease loss of water. This resulted in cross-tolerance to temperature (heat or cold) and drought stresses. The ABA signals activated the expression of several stress responsive genes such as *dehydration-responsive 22* (*rd22*), *pr1a.205, thaumatin-like protein 4* (*tlp4*), and *myb* in wheat resulting in increased drought tolerance and fungus resistance (Zhang et al., 2012). ABA enhanced tolerance to HTS by up regulation of HSFs and HSPs, increase in sugar metabolism and reduction in electrolyte leakage (Larkindale and Knight, 2002; Wind et al., 2010; Wang X. et al., 2017; Rezaul et al., 2019). Arabidopsis plants treated with inhibitor of ABA biosynthesis showed impaired response to HTS and reduction in ROS levels (Larkindale et al., 2005). HTS also evoked a rapid and transient expression of endogenous ABA that in turn increased the levels of ROS like H_2O_2 thereby augmenting thermo-tolerance (Larkindale et al., 2005).

Interaction of ABA and ROS is considered as one of the prime factors for the acclimation of plants exposed simultaneously to drought and salt stresses (Suzuki et al., 2016; Zandalinas et al., 2016). Mutants in ABA biosynthesis or signaling components displayed suppressed H_2O_2 accumulation and increased HTS sensitivity in plants (Larkindale et al., 2005). Loss-of-function mutation in the ABA induced NADPH oxidases, also known as RBOHs exhibited impaired HTS tolerance as measured by decrease in seed survival and germination capacities (Larkindale et al., 2005; Silva-Correia et al., 2014). Heat- or cold- priming were also found to increase the endogenous concentration of ABA, SA and H_2O_2 (Liu et al., 2006; Wan et al., 2009). Cold priming induced frost tolerance in winter and spring wheat (*Triticum monococcum*) was associated with greater accumulation of ABA and dehydrins (Vanková et al., 2014). Priming with drought induced cold stress tolerance was associated with ABA and ROS accumulations in the leaf tissues of wheat (Li X. et al., 2015).

Jasmonic Acid and Salicylic Acid

The biotic stress-induced hormones, JA and SA, can prime transcription by stimulating the expression of defense genes after attack by the pests or pathogens (Beckers and Conrath, 2007; Chen R. et al., 2012). The basic helix–loop–helix (bHLH) TF, MYC2, is an important part of the JA signaling pathway and its activity is regulated by binding of repressor (JAZs) and co-repressors (TPL or related TRPs) proteins (Chini et al., 2007). The JA-induced proteolytic degradation of JAZ repressors allows MYC2 to bind with promoters. It then interacts with MED25 subunit to facilitate the assembly of Mediator complex (Elfving et al., 2011; Çevik et al., 2012), which in turn recruits the pre-initiation complex (PIC) to activate transcription. The cross-talk between JA- and ABA-mediated pathways, has been well established (Wasternack and Hause, 2013; de Ollas et al., 2015). Both JA and ABA mediate induction of drought-inducible genes in response to dehydration stress at the initial stage. However, in subsequent dehydration stress, ABA produced during the initial stress reduces the production of the MYC2 to inhibit biosynthesis of JA (Avramova, 2019).

The role of SA has been discussed in numerous HTS related studies in plants. Exogenous application of SA or its functional synthetic analogs like BTH or INA (2,6-dichloroisonicotinic acid) and the non-protein amino acid, BABA (b-amino butyric acid),

TABLE 2 | Role of hormones in priming plants to high temperature stress.

Elicitor	Priming treatment			Subsequent stress		Effect of priming	References
	Stage	Concentration	Plant	Stress	Duration		
Cytokinin	3 leaf seedling	BAP (60 mg L^{-1})	*Oryza sativa*	31.5 and 38.3°C*	15 days	Cytokinin transport from root to shoot for determining panicle size	Wu et al., 2017
	Anthesis	10 mg L^{-1} (6-BA)	*Triticum aestivum*	35/20°C*	5 days	Significantly ($P < 0.05$) enhanced the endosperm cell division, grain-filling and 1,000-grain weight	Yang D. et al., 2016
	Seedling	10 and 100 μM	*Agrostis stolonifera*	38°C /28°C*	4 weeks	Provides protection via antioxidants and shielding the photosynthetic apparatus	Wang et al., 2013
	Seedling	50 μM, 100 μM, 250 μM, and 500 μM	*Brassica juncea*	47.5°C	-	Soaking seeds in 50 and 100uM kinetin are effective in mitigating HTS.	Chhabra et al., 2009
	5 week plants	-	*Arabidopsis thaliana*	45°C	3 h	Enhanced activity of NADPH oxidases (NOX) and antioxidant enzymes [superoxide dismutases, guaiacol peroxidases, catalases, ascorbate peroxidases]	Prerostova et al., 2020
Gibberlic acid -3 (GA3)	3 months seedlings	100 μM	*Phoenix dactylifera*	44°C	6 weeks	Accumulation of polyphenol oxidase, peroxidase, and ascorbate peroxidase activities and up regulation of their synthesis, activation of HSF related genes (especially *hsfA3*)	Khan et al., 2020
	Seedling	50 μM, 100 μM, 250 μM, and 500 μM	*Brassica juncea*	47.5°C	-	Soaking seeds in GA was effective in mitigating HTS	Chhabra et al., 2009
	Post anthesis	100 μM in culture media	*Triticum aestivum*	45°C	2 h daily for 5 days	Positively regulates grain sink activity, sucrolytic and aminotransferases	Asthir and Bhatia, 2014
	Seedling stage	50 mM	*Arabidopsis thaliana*	50°C	3 h	Counter balances the inhibitory effects of stress during seed germination and seedling growth by modulation of SA biosynthesis	Alonso-Ramírez et al., 2009
Auxin	Anthesis	1, 10, 50 and 100 μM L^{-1} (NAA)	*Oryza sativa*	40°C	2 h	Prevents the inhibition of pollen tube elongation in pistil and crosstalk with ROS	Zhang C. et al., 2018
	5-leaf seedlings	10^{-6}, 10^{-5} or 10^{-4} M	*Hordeum vulgare*	31°C	5 days	Restores DNA replication licensing factor MCM5 expression and helped in normal proliferation and development of anther cells	Sakata et al., 2010
	Seedling stage	50 μM, 100 μM, 250 μM, and 500 μM	*Brassica juncea*	47.5°C	-	IAA is effective in mitigating HTS	Chhabra et al., 2009
ABA	5–6 leaf seedlings	1 μM L^{-1}, 10 μM L^{-1}, and 100 μM L^{-1}	*Oryza sativa*	45°C	24 h	Maintenance of energy homeostasis	Li et al., 2020
	Seedlings	1, 10, 100 μM L^{-1}		39–41°C	7 days	ABA prevents the decrease in pollen viability and spikelet fertility	Rezaul et al., 2019
	30 days old plants	30 μM	*Arabidopsis thaliana*	38°C	8 h	Induces accumulation of APX1 and MBF1c	Zandalinas et al., 2016
	2 months old plants	10 μM	*Festuca arundinacea*	38/33°C*	25 days	Up regulation of CDPK3, MPK3, DREB2A, AREB3, MYB2, MYC4, HsfA2, HSP18, and HSP70 for maintaining transcription	Zhang et al., 2019a
	4 weeks seedlings	5 μM		37/32°C*	35 days	Increased expression of HSFA2c, HSPs and ABA-responsive transcriptional factors, increased leaf photochemical efficiency and membrane stability	Wang X. et al., 2017
	4 days seedlings	2.5 μM	*Cicer arietinum*	30/20, 35/25, 40/30, and 45/35°C*	10 days	Reduced MDA and H_2O_2 concentrations and upregulated HSPs	Kumar et al., 2012
Ethylene	12 days old seedlings	10 μM ACC	*Oryza sativa*	45°C	4 days	Reduced electrolyte leakage and MDA Increased enzymatic activity of CAT, APX, and POX	Wu and Yang, 2019

(Continued)

TABLE 2 | (Continued)

Elicitor	Priming treatment			Subsequent stress		Effect of priming	References
	Stage	Concentration	Plant	Stress	Duration		
	Tomato plant	0.1 μL L^{-1} in air	*Solanum lycopersicum*	45°C	2 h	Ethylene synthesis genes SlACS3 and SlACS11 are increased	Jegadeesan et al., 2018
Salicylic acid	5 weeks old plants	0.5 mM NaSA	*Brachypodium distachyon*	35°C	4 h	Induction of chlorophyll-a and changes in various protective compounds, such as glutathione, flavonoids and antioxidant enzymes	Janda et al., 2020
	4-day-old seedlings	10 and 20 μM	*Brassica*	55°C	3 h	Help through enhancing seedling length, HSP expression, total soluble sugars and enzymatic activities of invertase, CAT, PO. Reduce electrolyte leakage and confer membrane protection thereby acquiring thermo-tolerance.	Kaur et al., 2009
	Fully expanded fifth leaf	1 mM	*Solanum lycopersicum*	42°C	36 h	SA enhanced gaseous exchange parameters, water use efficiency, decreased electrolyte leakage and increased SOD and improved thermotolerance.	Jahan et al., 2019
	Seven day seedlings	0.5 mM and 1 mM for 3 h	*Cajanus cajan*	45°C	3 h	Enhanced Antioxidant defense system.	Kaur et al., 2019
	Sowing and reproductive stages	50 ppm	*Gossypium hirsutum*	45/30°C, 38/24°C, 32/20°C*	7 days	Enhanced CAT, SOD activity, net photosynthetic rate chlorophyll content, number of sympodial branches, boll weight, and fiber quality	Sarwar et al., 2018
	Seedling	100 μL of 1 mM	*Pisum sativum*	28/24°C*	16 h	Enhanced net CO_2 assimilation and chlorophyll content	Martel and Qaderi, 2016
	pollen mother cell	0.01, 0.1, 1.0, 10, and 50 mM	*Oryza sativa*	40°C	10 days	H_2O_2 may play an important role in mediating SA to inhibit pollen abortion caused by heat stress by hampering the tapetum PCD.	Feng et al., 2018
	10 day seedlings	10 mM	*Triticum aestivum*	38°C	2 h	Enhanced total antioxidant capacity, accumulation of SAGs and osmolytes	Kumar et al., 2015
Brassinolide	16–18 cm high plant	0.01, 0.1, and 1.0 mgL^{-1}	*Leymus chinensis*	38/25°C*	10 h	increased biosynthesis of photosynthetic pigments, osmolytes, antioxidant enzyme and thus thermotolerance	Niu et al., 2016
	3 weeks old seedlings	10^{-6} M	*Brassica napus*	45°C	4 and 8 h	Enhanced endogenous ABA content	Kurepin et al., 2008
24-epibrassinolide	3–4 leaf seedling stage	0.05, 0.1, 0.5, 1.0, and 1.5 mg dm^{-3}	*Cucumis melo*	42/32°C*	2 days	Reduced MDA content and enhanced content of soluble proteins, free proline and antioxidant enzymes including guaiacol peroxidase, catalase, superoxide dismutase and ascorbate peroxidase	Zhang Y. et al., 2014
	12 days old seedlings	0.005 and 0.25 mg dm^{-3}	*Hordeum vulgare*	42°C	3 h	Increased the PSII efficiency	Janeczko et al., 2011
	20, 22, or 24 days after sowing	0.01 μM	*Triticum aestivum*	35/28 or 40/35°C*	24 h	Improved the growth features, photosynthetic efficacy and various biochemical parameters through enhanced antioxidant system and osmoprotectants	Hussain et al., 2019
Jasmonic acid	3 week plants	5 μm	*Arabidopsis thaliana*	45°C	2 h	Modulating ethylene levels. Ethylene mutant *ein2-1* conferred greater thermo-tolerance	Clarke et al., 2009
	Anthesis	50, 100, 150 μM JA and 50, 100, 150 μM MeJA,	*Oryza sativa*	25°C–35°C	6 days	Increase in soluble sugars, activities of catalase and α-amylase and reduction in H_2O_2 increased rate of spikelet opening	Yang et al., 2020
	37 days plants	20, 40, 60, 80, 100, 150, and 200 μM L^{-1}	*Lolium perenne*	38/30°C*	14 days	MeJA-induced heat tolerance by maintenance of chlorophyll loss, photosynthesis relative water content (RWC), electrolyte leakage (EL) and malondialdehyde (MDA) content under HTS	Su et al., 2021
Stringolactones	4 week plants	0.01 μM GR24	*Festuca arundinacea*	35/30°C*	8 days	Leaf elongation due to up regulation of cell-cycle-related genes and down regulation of auxin transport related genes	Hu et al., 2019
	14 days seedlings	10 μM rac-GR24	*Lupinus angustifolius*	40°C	1 h	Increased proline content and activities of antioxidant enzyme, reduced lipid peroxidation	Omoarelojie et al., 2020

**indicates day/night temperatures.*

prior to HTS were shown to enhance plant biomass, height and photosynthetic efficiency (Kauss et al., 1992; Oostendorp et al., 2001). Priming of plants with BABA also induced SA signals and activated the defense response (Ton et al., 2005). SA enhanced the activities of antioxidant enzymes like SOD, CAT and peroxidases to scavenge ROS and increased enzyme activities required for proline biosynthesis as an adaptive strategy to tolerate HTS. It also helped in reducing membrane damage caused by HTS and decreased the proline-metabolizing enzymes (Verbruggen and Hermans, 2008; Szabados and Savouré, 2010; Lv et al., 2011). Application of SA at seedling stage in plants such as maize, potato, wheat, cotton, pigeon pea, Arabidopsis, mung bean, grape and alfalfa lead to increase in antioxidant enzymes, photosynthetic activity and proline accumulation which reduced cellular damage. It also enhanced basal thermo-tolerance by up regulating HSP expression in some cases (Clarke et al., 2004; Saleh et al., 2007; Khan et al., 2013; Wang et al., 2014a; Hameed and Ali, 2016; Khanna et al., 2016; Makarova et al., 2018; Jahan et al., 2019; Kaur et al., 2019; Wassie et al., 2020).

The Set Domain Group 8 (SDG8) proteins which represent the major H3K36 di- and tri- methyltransferase in Arabidopsis have been implicated in the JA- and SA-mediated plant defense (Ding and Wang, 2015; Li Y. et al., 2015). SDG8 is essential for H3K36me3 for expression of the *R*-gene, *lazarus 5* (*LAZ5*), in response to fungal infection (Berr et al., 2010; Palma et al., 2010). This memory can be transmitted to the progeny plants and the off-springs were primed for enhanced activation of the WRKY6, PR1 and WRKY53 genes that play roles in immunity (Slaughter et al., 2012).

Auxin

Warm ambient temperature signals can promote a series of structural changes in plants like elongation, growth and flowering, which are collectively termed as thermo-morphogenesis (Quint et al., 2016) and auxin plays a major role in these processes. At normal growth temperatures, the exogenous application of auxin does not elicit hypocotyl elongation but at higher temperatures the auxin-responsive gene expression causes hypocotyl elongation and leaf hyponasty (Küpers et al., 2020). Auxin also act as thermo-protectant of anthers in barley and rice (Sakata et al., 2010; Oshino et al., 2011; Zhang C. et al., 2018).

The light responsive Phytochrome Interacting Factor 4 (PIF4) and PIF7 are involved in regulating hypocotyl elongation and leaf hyponasty. Recent studies showed that PIFs are inducible by HTS and they interact with at least one of the phytochromes thereby indicating their important role in transducing both light and temperature signals (Choi and Oh, 2016; Pham et al., 2018; Kim et al., 2020). The temperature-induced hypocotyl elongation is delayed by the suppression of PIF4 activity by blue light photoreceptor, Cryptochrome 1 (CRY1) (Ma et al., 2016). Loss-of-function mutants of *pif4* and *pif7* abrogate HTS mediated thermo-morphogenesis and show drastic reductions in auxin biosynthetic enzymes (aminotransferase, YUCCA and cytochrome P450s) (Sun et al., 2012; Fiorucci et al., 2020).

Cytokinin

Several studies have suggested the role of CK in acquisition of thermo-tolerance by inducing higher antioxidant activity and metabolism. When a part of the plant or whole plants were exposed to HTS, a rapid increase in CK was observed which further activated the carbohydrate metabolism and photosynthetic genes (Dobrá et al., 2015). Agrobacterium mediated ectopic transcription of *isopentenyltransferase* (ipt), which encodes a key enzyme in CK biosynthesis system, resulted in plants that were better adapted to HTS (Skalák et al., 2016). An interesting pattern of expression of interconnected proteins was observed in the chloroplasts, in response to HTS and CK. The adverse effect of HTS on spikelet formation and panicle differentiation is mitigated by CK application (Wu et al., 2017). In Arabidopsis and in crops like maize, wheat and rice, CKs were shown to provide HTS tolerance by reduction in kernel abortion, increase in rate of grain filling, modulating spikelet injury and regulating ROS production (Cheikh and Jones, 1994; Yang D. et al., 2016; Wu et al., 2017; Prerostova et al., 2020).

Brassinosteroids

Brassinosteroids are known to perform surveillance for HTS induced lipid peroxidation, ion leakage and survival rate (Mazorra et al., 2011). Treatment of plants with BR lead to a rise in basic thermo-tolerance due to higher translation of proteins like HSPs, aquaporins, etc. (Dhaubhadel et al., 2002; Sadura et al., 2020). The levels of ROS and expression of antioxidant enzymes also spiked up after the application of exogenous BR under HTS (Nie et al., 2013). However, in tomato seedlings both overproduction and deficiency of BR showed similar response to thermo-tolerance indicating that the process might be independent of BR homeostasis (Mazorra et al., 2011). Later it was shown that Brassinazole-resistant 1 (BZR1), the prime TF in BR signaling, activated PIF4 gene expression to integrate the plant response to different environmental stimuli (Ibañez et al., 2018). BRs also influenced the levels of other phytohormones like ABA, ethylene and SA to regulate oxidative stress under HTS and boost thermo-tolerance (Divi et al., 2010; Kothari and Lachowiec, 2021).

Melatonin

The role of phyto-melatonin is also implicated in governing the response and memory to plant stress (Arnao and Hernández-Ruiz, 2019). Melatonin, a predominantly animal hormone, is present in plants and performs a number of physiological activities including chlorophyll preservation, root and shoot growth, photosynthesis, reduction of oxidative damage and suppression of leaf senescence (Byeon et al., 2012; Tan et al., 2012; Zhang N. et al., 2014; Li X. et al., 2018). Exogenous application of melatonin to roots resulted in its absorption and mobilization in xylem and subsequent accumulation in the leaves (Yoon et al., 2019). Extracellular melatonin enhanced the level of *TaSNAT* transcripts, which encode a key enzyme in the melatonin biosynthetic pathway and increased the intracellular melatonin levels.

Various reports have also shown the protective effects of phyto-melatonin against biotic and abiotic stress (Li et al., 2012; Li X. et al., 2018; Bajwa et al., 2014; Meng et al., 2014; Shi et al., 2015b). Melatonin is an important master regulator of redox homeostasis in plants (Arnao and Hernández-Ruiz, 2019). It induced the DREB1/CBF TFs AtCBF1, AtCBF2, and AtCBF3 that caused increased tolerance to drought, cold, salt, and Pst-DC3000 (Shi et al., 2015a). Melatonin also up regulated polyamine levels by promoting the synthesis of polyamines from its precursor amino acids, arginine and methionine. In wheat seedlings, Melatonin attenuated the effect of salt stress by preventing polyamine degradation (Ke et al., 2018).

CONCLUSION AND PERSPECTIVES

According to Intergovernmental Panel on Climate Change (IPCC, 2018), the unprecedented increase in global mean temperatures has caused an upsurge in the incidence of extreme HTS. Its adverse effects on plant growth, reproduction and yield are proportional to the intensity and duration of high temperatures (Prasad et al., 2017; Ali et al., 2020). The increase in global temperatures accompanied by fluctuations or changes in climate regimes has increased the occurrence of abiotic stresses such as HTS, salinity, drought and flooding as well as biotic stresses such as pathogen infections and pest invasions. These challenges have emerged as major factors limiting crop production yield (Pandey et al., 2017).

High temperature stress results in various impairments including early leaf senescence, accumulation of ROS, reduced germination, decreased rate of photosynthesis, inhibition of root growth, lower seed set, reduced vigor and elevated rates of lipid peroxidation, protein denaturation, spikelet sterility and anther indehiscence (Wahid et al., 2007; Hasanuzzaman et al., 2013; Rodríguez et al., 2015; Narayanan et al., 2016; Iqbal et al., 2017; Ohama et al., 2017; Ali et al., 2020). Sustainable agriculture necessitates the adaptation of strategies to boost plant responses to improve their tolerance to these stresses. Although lot of efforts like conventional breeding, application phytohormones, comparative genetics, etc., have been initiated in this direction but a detailed understanding of the underlying mechanisms is still needed.

Priming has the potential to be developed as a very promising technique for improving the long-term sustainability of agriculture and increasing crop yields in the present context of global warming and climate change. Plants can be thermo-primed by moderately high temperatures to sustain extreme temperatures that are otherwise fatal to an unadapted plant (Bäurle, 2016). In our lab, experiments on thermo-priming mature rice before and after flowering, showed that priming allows the crops to tolerate HTS and help in prevention of seed loss and increase seed production by sustaining grain filling (Kushawaha et al., 2021). The response may vary from crop to crop depending upon their life cycle, habitat and stress tolerance levels. Therefore comprehensive investigations are required using a broad range of plant species to determine the most efficient and effective stage and duration of priming. The analyses also need to be extended from study of individual stresses to include a mixture of stressors so that plants can be acclimated to tolerate a wide range of temperatures.

Epigenetic regulations, transcript modifications, changes in protein conformations and generation of hormonal or metabolic signals are only a few of the cellular processes that have been studied in response to stress priming in the last decade. Epigenetic alterations resulting in changes in structure and composition of chromatin may play a vital role in stress memory by regulating transcription and/or plant response. The mechanisms overlap with the stress response pathways and often involve activation of epigenetic imprints and feedback loops to initiate faster recruitment of the stress response.

Advance investigations at the chromatin level will be fundamental for understanding the nature of modifications involved in inheriting tolerance to different stresses in the same species. Few features like accumulation of H3K4me may be commonly related to more than one type of stresses, while memory of individual stress may involve specific molecular elements. More research is required to recognize these patterns of stress memory and determine the exact mechanisms by which they are generated. The importance of synchronized gene silencing by miRNAs and other regulatory non-coding RNAs in stress primed plants is a significant question which will require an in-depth analysis. Their role and pathways for integration of priming with stress memory in regulation of plant development and productivity will be an important question to investigate.

It is apparent that our understanding of effects of priming and induced memory of stress in plants is far from clear. The maintenance of memory and its inheritance across cell divisions needs to be investigated. It will be essential to investigate how long the memory phase is maintained and regulated. Further studies are also required to comprehend the precise mechanisms that elicit and reset stress memory. The advancements in various omic-technologies will help in providing better understanding of priming induced cross-talk during stress tolerance in plants. It is evident that increased knowledge of the priming pathways will aid in designing strategies for improving plant performance and seed production. This will not only help them to pre-adapt to changing environmental conditions but also enable them to habituate in new domiciles.

AUTHOR CONTRIBUTIONS

NS-M and SKS conceptualized the idea of the study. AK, VK, and KP prepared the draft. SKS and NS-M edited the manuscript. All authors read and approved the final manuscript.

FUNDING

This research was supported by grants from the SERB (SPF/2021/000198), Government of India. SKS was thankful to SERB, Government of India, for providing Distinguished Fellowship award.

REFERENCES

Abd El-Daim, I. A., Bejai, S., and Meijer, J. (2014). Improved heat stress tolerance of wheat seedlings by bacterial seed treatment. *Plant Soil* 379, 337–350. doi: 10.1007/s11104-014-2063-3

Alam, M. M., Hasanuzzaman, M., Nahar, K., and Fujita, M. (2013). Exogenous salicylic acid ameliorates short-term drought stress in mustard (*Brassica juncea* L.) seedlings by up-regulating the antioxidant defense and glyoxalase system. *Australian J. Crop Sci.* 7:1053.

Alexandrov, V. Y. (1956). Cytophysiological and cytoecological investigations of heat resistance of plant cells toward the action of high and low temperature. *Q. Rev. Biol.* 39, 35–77. doi: 10.1086/404089

Ali, S., Rizwan, M., Arif, M. S., Ahmad, R., Hasanuzzaman, M., Ali, B., et al. (2020). Approaches in enhancing thermotolerance in plants: an updated review. *J. Plant Growth Regul.* 39, 456–480. doi: 10.1007/s00344-019-09994-x

Alonso-Ramírez, A., Rodríguez, D., Reyes, D., Jiménez, J. A., Nicolás, G., López-Climent, M., et al. (2009). Evidence for a role of gibberellins in salicylic acid-modulated early plant responses to abiotic stress in *Arabidopsis* seeds. *Plant Physiol.* 150, 1335–1344. doi: 10.1104/pp.109.139352

Alshareef, N. O., Rey, E., Khoury, H., Tester, M., and Schmöckel, S. M. (2019). Genome wide identification of NAC transcription factors and their role in abiotic stress tolerance in *Chenopodium quinoa*. *BioRxiv* [Preprint] BioRxiv: 693093, doi: 10.1101/693093

Amooaghaie, R., and Nikzad, K. (2013). The role of nitric oxide in priming-induced low-temperature tolerance in two genotypes of tomato. *Seed Sci. Res.* 23, 123–131. doi: 10.1017/S0960258513000068

Anderson, M., and Habiger, J. (2012). Characterization and identification of productivity-associated rhizobacteria in wheat. *Appl. Environ. Microbiol.* 78, 4434–4446. doi: 10.1128/AEM.07466-11

Angel, A., Song, J., Dean, C., and Howard, M. (2011). A Polycomb-based switch underlying quantitative epigenetic memory. *Nature* 476, 105–108. doi: 10.1038/nature10241

Antoniou, C., Xenofontos, R., Chatzimichail, G., Christou, A., Kashfi, K., and Fotopoulos, V. (2020). Exploring the potential of nitric oxide and hydrogen sulfide (NOSH)-releasing synthetic compounds as novel priming agents against drought stress in *Medicago sativa* plants. *Biomolecules* 10:120. doi: 10.3390/biom10010120

Aranega-Bou, P., de la O Leyva, M., Finiti, I., García-Agustín, P., and González-Bosch, C. (2014). Priming of plant resistance by natural compounds. Hexanoic acid as a model. *Front. Plant Sci.* 5:488. doi: 10.3389/fpls.2014.00488

Arnao, M. B., and Hernández-Ruiz, J. (2019). Melatonin: a new plant hormone and/or a plant master regulator? *Trends Plant Sci.* 24, 38–48. doi: 10.1016/j.tplants.2018.10.010

Asthir, B., and Bhatia, S. (2014). In vivo studies on artificial induction of thermotolerance to detached panicles of wheat (*Triticum aestivum* L) cultivars under heat stress. *J. Food Sci. Technol.* 51, 118–123. doi: 10.1007/s13197-011-0458-1

Avramova, Z. (2015). Transcriptional 'memory' of a stress: transient chromatin and memory (epigenetic) marks at stress-response genes. *Plant J.* 83, 149–159. doi: 10.1111/tpj.12832

Avramova, Z. (2019). Defence-related priming and responses to recurring drought: two manifestations of plant transcriptional memory mediated by the ABA and JA signalling pathways. *Plant Cell Environ.* 42, 983–997. doi: 10.1111/pce.13458

Baena-González, E., and Sheen, J. (2008). Convergent energy and stress signaling. *Trends Plant Sci.* 13, 474–482. doi: 10.1016/j.tplants.2008.06.006

Bajwa, V. S., Shukla, M. R., Sherif, S. M., Murch, S. J., and Saxena, P. K. (2014). Role of melatonin in alleviating cold stress in *Arabidopsis thaliana*. *J. Pineal Res.* 56, 238–245. doi: 10.1111/jpi.12115

Bakshi, A., Moin, M., Kumar, M. U., Reddy, A. B. M., Ren, M., Datla, R., et al. (2017). Ectopic expression of *Arabidopsis* Target of Rapamycin (AtTOR) improves water-use efficiency and yield potential in rice. *Sci. Rep.* 7, 1–16. doi: 10.1038/srep42835

Balmer, A., Pastor, V., Gamir, J., Flors, V., and Mauch-Mani, B. (2015). The 'prime-ome': towards a holistic approach to priming. *Trends Plant Sci.* 20, 443–452. doi: 10.1016/j.tplants.2015.04.002

Banerjee, A., and Roychoudhury, A. (2020). "Seed priming as a method to generate heat-stress tolerance in plants: a mini review," in *Heat Stress Tolerance in Plants: Physiological, Molecular and Genetic Perspectives*, eds S. H. Wani and V. Kumar (Hoboken, NJ: Wiley), 23–32. doi: 10.1002/9781119432401.ch2

Banti, V., Loreti, E., Novi, G., Santaniello, A., Alpi, A., and Perata, P. (2008). Heat acclimation and cross-tolerance against anoxia in *Arabidopsis*. *Plant Cell Environ.* 31, 1029–1037. doi: 10.1111/j.1365-3040.2008.01816.x

Bäurle, I. (2016). Plant heat adaptation: priming in response to heat stress. *F1000Research* 5:694. doi: 10.12688/f1000research.7526.1

Beckers, G. J., and Conrath, U. (2007). Priming for stress resistance: from the lab to the field. *Curr. Opin. Plant Biol.* 10, 425–431. doi: 10.1016/j.pbi.2007.06.002

Beckers, G. J., Jaskiewicz, M., Liu, Y., Underwood, W. R., He, S. Y., Zhang, S., et al. (2009). Mitogen-activated protein kinases 3 and 6 are required for full priming of stress responses in *Arabidopsis thaliana*. *Plant Cell* 21, 944–953. doi: 10.1105/tpc.108.062158

Begum, N., Qin, C., Ahanger, M. A., Raza, S., Khan, M. I., Ashraf, M., et al. (2019). Role of arbuscular mycorrhizal fungi in plant growth regulation: implications in abiotic stress tolerance. *Front. Plant Sci.* 10:1068. doi: 10.3389/fpls.2019.01068

Berr, A., McCallum, E. J., Alioua, A., Heintz, D., Heitz, T., and Shen, W. H. (2010). Arabidopsis histone methyltransferase SET DOMAIN GROUP8 mediates induction of the jasmonate/ethylene pathway genes in plant defense response to necrotrophic fungi. *Plant Physiol.* 154, 1403–1414. doi: 10.1104/pp.110.161497

Bilichak, A. I. (2015). The elucidation of stress memory inheritance in *Brassica rapa* plants. *Front. Plant Sci.* 6:5. doi: 10.3389/fpls.2015.00005

Böhm, J., Scherzer, S., Krol, E., Kreuzer, I., von Meyer, K., Lorey, C., et al. (2016). The Venus flytrap *Dionaea muscipula* counts prey-induced action potentials to induce sodium uptake. *Curr. Biol.* 26, 286–295. doi: 10.1016/j.cub.2015.11.057

Boyko, A., and Kovalchuk, I. (2011). Genome instability and epigenetic modification—heritable responses to environmental stress? *Curr. Opin. Plant Biol.* 14, 260–266. doi: 10.1016/j.pbi.2011.03.003

Bruce, T. J., Matthes, M. C., Napier, J. A., and Pickett, J. A. (2007). Stressful "memories" of plants: evidence and possible mechanisms. *Plant Sci.* 173, 603–608. doi: 10.1016/j.plantsci.2007.09.002

Brzezinka, K., Altmann, S., and Bäurle, I. (2019). BRUSHY1/TONSOKU/MGOUN3 is required for heat stress memory. *Plant Cell Environ.* 42, 771–781. doi: 10.1111/pce.13365

Brzezinka, K., Altmann, S., Czesnick, H., Nicolas, P., Gorka, M., Benke, E., et al. (2016). Arabidopsis FORGETTER1 mediates stress-induced chromatin memory through nucleosome remodeling. *Elife* 5:e17061. doi: 10.7554/eLife.17061.037

Byeon, B., Bilichak, A., and Kovalchuk, I. (2019). Transgenerational response to heat stress in the form of differential expression of noncoding RNA fragments in *Brassica rapa* plants. *Plant Genome* 12:180022. doi: 10.3835/plantgenome2018.04.0022

Byeon, Y., Park, S., Kim, Y. S., Park, D. H., Lee, S., and Back, K. (2012). Light-regulated melatonin biosynthesis in rice during the senescence process in detached leaves. *J. Pineal Res.* 53, 107–111. doi: 10.1111/j.1600-079X.2012.00976.x

Byun, Y. J., Koo, M. Y., Joo, H. J., Ha-Lee, Y. M., and Lee, D. H. (2014). Comparative analysis of gene expression under cold acclimation, deacclimation and reacclimation in *Arabidopsis*. *Physiol. Plant.* 152, 256–274. doi: 10.1111/ppl.12163

Carrigan, P. E., Sikkink, L. A., Smith, D. F., and Ramirez-Alvarado, M. (2006). Domain: domain interactions within Hop, the Hsp70/Hsp90 organizing protein, are required for protein stability and structure. *Protein Sci.* 15, 522–532. doi: 10.1110/ps.051810106

Carter, A. H., Chen, X., Garland-Campbell, K., and Kidwell, K. (2009). Identifying QTL for high-temperature adult-plant resistance to stripe rust (*Puccinia striiformis* f. sp. tritici) in the spring wheat (*Triticum aestivum* L.) cultivar 'Louise'. *Theor. Appl. Genet.* 119, 1119–1128. doi: 10.1007/s00122-009-1114-2

Castellanos, M., Mothi, N., and Muñoz, V. (2020). Eukaryotic transcription factors can track and control their target genes using DNA antennas. *Nat. Commun.* 11:540. doi: 10.1038/s41467-019-14217-8

Çevik, V., Kidd, B. N., Zhang, P., Hill, C., Kiddle, S., Denby, K. J., et al. (2012). MEDIATOR25 acts as an integrative hub for the regulation of jasmonate-responsive gene expression in *Arabidopsis*. *Plant Physiol.* 160, 541–555. doi: 10.1104/pp.112.202697

Chakrabortee, S., Kayatekin, C., Newby, G. A., Mendillo, M. L., Lancaster, A., and Lindquist, S. (2016). Luminidependens (LD) is an Arabidopsis protein with

prion behavior. *Proc. Natl. Acad. Sci. U.S.A.* 113, 6065–6070. doi: 10.1073/pnas.1604478113

Charng, Y. Y., Liu, H. C., Liu, N. Y., Chi, W. T., Wang, C. N., Chang, S. H., et al. (2007). A heat-inducible transcription factor, HsfA2, is required for extension of acquired thermotolerance in *Arabidopsis*. *Plant Physiol.* 143, 251–262. doi: 10.1104/pp.106.091322

Chehab, E. W., Eich, E., and Braam, J. (2009). Thigmomorphogenesis: a complex plant response to mechano-stimulation. *J. Exp. Bot.* 60, 43–56. doi: 10.1093/jxb/ern315

Chehab, E. W., Yao, C., Henderson, Z., Kim, S., and Braam, J. (2012). *Arabidopsis* touch-induced morphogenesis is jasmonate mediated and protects against pests. *Curr. Biol.* 22, 701–706. doi: 10.1016/j.cub.2012.02.061

Cheikh, N., and Jones, R. J. (1994). Disruption of maize kernel growth and development by heat stress (role of cytokinin/abscisic acid balance). *Plant Physiol.* 106, 45–51. doi: 10.1104/pp.106.1.45

Chen, L., Ren, Y., Zhang, Y., Xu, J., Sun, F., Zhang, Z., et al. (2012). Genome-wide identification and expression analysis of heat-responsive and novel microRNAs in Populus tomentosa. *Gene* 504, 160–165. doi: 10.1016/j.gene.2012.05.034

Chen, R., Jiang, H., Li, L., Zhai, Q., Qi, L., Zhou, W., et al. (2012). The Arabidopsis mediator subunit MED25 differentially regulates jasmonate and abscisic acid signaling through interacting with the MYC2 and ABI5 transcription factors. *Plant Cell* 24, 2898–2916. doi: 10.1105/tpc.112.098277

Cheng, Y., JalalAhammed, G., Yu, J., Yao, Z., Ruan, M., Ye, Q., et al. (2016). Putative WRKYs associated with regulation of fruit ripening revealed by detailed expression analysis of the WRKY gene family in pepper. *Sci. Rep.* 6, 1–11. doi: 10.1038/srep39000

Chhabra, M., Dhawan, A., Sangwan, N., Dhawan, K., and Singh, D. (2009). "Phytohormones induced amelioration of high temperature stress in *Brassica juncea* (L.) Czern and Coss," in *Proceedings of 16th Australian Research Assembly on Brassicas*, Ballarat, VIC, 10–14.

Chini, A., Fonseca, S. G. D. C., Fernandez, G., Adie, B., Chico, J. M., Lorenzo, O., et al. (2007). The JAZ family of repressors is the missing link in jasmonate signalling. *Nature* 448, 666–671. doi: 10.1038/nature06006

Choi, C.-S., and Sano, H. (2007). Abiotic-stress induces demethylation and transcriptional activation of a gene encoding a glycerophosphodiesterase-like protein in tobacco plants. *Mol. Genet. Genomics* 277, 589–600. doi: 10.1007/s00438-007-0209-1

Choi, H., and Oh, E. (2016). PIF4 integrates multiple environmental and hormonal signals for Plant growth regulation in *Arabidopsis*. *Mol. Cells* 39:587. doi: 10.14348/molcells.2016.0126

Chou, T.-S., Chao, Y.-Y., and Kao, C. H. (2012). Involvement of hydrogen peroxide in heat shock-and cadmium-induced expression of ascorbate peroxidase and glutathione reductase in leaves of rice seedlings. *J. Plant Physiol.* 169, 478–486. doi: 10.1016/j.jplph.2011.11.012

Clarke, S. M., Cristescu, S. M., Miersch, O., Harren, F. J., Wasternack, C., and Mur, L. A. (2009). Jasmonates act with salicylic acid to confer basal thermotolerance in *Arabidopsis thaliana*. *New Phytol.* 182, 175–187. doi: 10.1111/j.1469-8137.2008.02735.x

Clarke, S. M., Mur, L. A., Wood, J. E., and Scott, I. M. (2004). Salicylic acid dependent signaling promotes basal thermotolerance but is not essential for acquired thermotolerance in *Arabidopsis* thaliana. *Plant J.* 38, 432–447. doi: 10.1111/j.1365-313X.2004.02054.x

Cohen, S. P., Liu, H., Argueso, C. T., Pereira, A., Vera Cruz, C., Verdier, V., et al. (2017). RNA-Seq analysis reveals insight into enhanced rice Xa7-mediated bacterial blight resistance at high temperature. *PLoS One* 12:e0187625. doi: 10.1371/journal.pone.0187625

Collins, G. G., Nie, X., and Saltveit, M. E. (1995). Heat shock proteins and chilling sensitivity of mung bean hypocotyls. *J. Exp. Bot.* 46, 795–802. doi: 10.1093/jxb/46.7.795

Conrath, U. (2011). Molecular aspects of defence priming. *Trends Plant Sci.* 16, 524–531. doi: 10.1016/j.tplants.2011.06.004

Conrath, U., Beckers, G. J., Langenbach, C. J., and Jaskiewicz, M. R. (2015). Priming for enhanced defense. *Annu. Rev. Phytopathol.* 53, 97–119. doi: 10.1146/annurev-phyto-080614-120132

Crisp, P. A., Ganguly, D., Eichten, S. R., Borevitz, J. O., and Pogson, B. J. (2016). Reconsidering plant memory: intersections between stress recovery, RNA turnover, and epigenetics. *Sci. Adv.* 2:e1501340. doi: 10.1126/sciadv.1501340

Darwin, C., and Darwin, F. (1880). *The Power Of Movement In Plants*. London: John Murray. doi: 10.5962/bhl.title.102319

Davletova, S., Schlauch, K., Coutu, J., and Mittler, R. (2005). The zinc-finger protein Zat12 plays a central role in reactive oxygen and abiotic stress signaling in *Arabidopsis*. *Plant Physiol.* 139, 847–856. doi: 10.1104/pp.105.068254

De Lucia, F., Crevillen, P., Jones, A. M., Greb, T., and Dean, C. (2008). A PHD-polycomb repressive complex 2 triggers the epigenetic silencing of FLC during vernalization. *Proc. Natl. Acad. Sci. U.S.A.* 105, 16831–16836. doi: 10.1073/pnas.0808687105

de Ollas, C., Arbona, V., and Gómez-Cadenas, A. (2015). Jasmonic acid interacts with abscisic acid to regulate plant responses to water stress conditions. *Plant Signal. Behav.* 10:e1078953. doi: 10.1080/15592324.2015.1078953

De Vleesschauwer, D., Filipe, O., Hoffman, G., Seifi, H. S., Haeck, A., Canlas, P., et al. (2018). Target of rapamycin signaling orchestrates growth–defense trade-offs in plants. *New Phytol.* 217, 305–319. doi: 10.1111/nph.14785

Dhaubhadel, S., Browning, K. S., Gallie, D. R., and Krishna, P. (2002). Brassinosteroid functions to protect the translational machinery and heat-shock protein synthesis following thermal stress. *Plant J.* 29, 681–691. doi: 10.1046/j.1365-313X.2002.01257.x

Ding, B., and Wang, G.-L. (2015). Chromatin versus pathogens: the function of epigenetics in plant immunity. *Front. Plant Sci.* 6:675. doi: 10.3389/fpls.2015.00675

Ding, Y., Fromm, M., and Avramova, Z. (2012). Multiple exposures to drought 'train' transcriptional responses in *Arabidopsis*. *Nat. Commun.* 3, 1–9. doi: 10.1038/ncomms1732

Ding, Y., Liu, N., Virlouvet, L., Riethoven, J.-J., Fromm, M., and Avramova, Z. (2013). Four distinct types of dehydration stress memory genes in *Arabidopsis thaliana*. *BMC Plant Biol.* 13:229. doi: 10.1186/1471-2229-13-229

Ding, Y., Virlouvet, L., Liu, N., Riethoven, J.-J., Fromm, M., and Avramova, Z. (2014). Dehydration stress memory genes of *Zea mays*; comparison with *Arabidopsis thaliana*. *BMC Plant Biol.* 14:141. doi: 10.1186/1471-2229-14-141

Divi, U. K., Rahman, T., and Krishna, P. (2010). Brassinosteroid-mediated stress tolerance in Arabidopsis shows interactions with abscisic acid, ethylene and salicylic acid pathways. *BMC Plant Biol.* 10:151. doi: 10.1186/1471-2229-10-151

Djanaguiraman, M., Prasad, P. V., and Seppanen, M. (2010). Selenium protects sorghum leaves from oxidative damage under high temperature stress by enhancing antioxidant defense system. *Plant Physiol. Biochem.* 48, 999–1007. doi: 10.1016/j.plaphy.2010.09.009

Dobrá, J., Černý, M., Štorchová, H., Dobrev, P., Skalák, J., Jedelský, P. L., et al. (2015). The impact of heat stress targeting on the hormonal and transcriptomic response in *Arabidopsis*. *Plant Sci.* 231, 52–61. doi: 10.1016/j.plantsci.2014.11.005

Dong, Y., Teleman, A., Jedmowski, C., Wirtz, M., and Hell, R. (2019). The Arabidopsis THADA homologue modulates TOR activity and cold acclimation. *Plant Biol.* 21, 77–83. doi: 10.1111/plb.12893

dos Santos Araújo, G., de Oliveira Paula-Marinho, S., de Paiva Pinheiro, S. K., de Castro Miguel, E., de Sousa Lopes, L., Marques, E. C., et al. (2021). H2O2 priming promotes salt tolerance in maize by protecting chloroplasts ultrastructure and primary metabolites modulation. *Plant Sci.* 303:110774. doi: 10.1016/j.plantsci.2020.110774

Drerup, M. M., Schlücking, K., Hashimoto, K., Manishankar, P., Steinhorst, L., Kuchitsu, K., et al. (2013). The calcineurin B-like calcium sensors CBL1 and CBL9 together with their interacting protein kinase CIPK26 regulate the Arabidopsis NADPH oxidase RBOHF. *Mol. Plant* 6, 559–569. doi: 10.1093/mp/sst009

D'Urso, A., Takahashi, Y. H., Xiong, B., Marone, J., Coukos, R., Randise-Hinchliff, C., et al. (2016). Set1/COMPASS and Mediator are repurposed to promote epigenetic transcriptional memory. *Elife* 5:e16691. doi: 10.7554/eLife.16691.020

Eichten, S. R., Schmitz, R. J., and Springer, N. M. (2014). Epigenetics: beyond chromatin modifications and complex genetic regulation. *Plant Physiol.* 165, 933–947. doi: 10.1104/pp.113.234211

Elfving, N., Davoine, C., Benlloch, R., Blomberg, J., Brännström, K., Müller, D., et al. (2011). The *Arabidopsis thaliana* Med25 mediator subunit integrates environmental cues to control plant development. *Proc. Natl. Acad. Sci. U.S.A.* 108, 8245–8250. doi: 10.1073/pnas.1002981108

Fan, Y., Ma, C., Huang, Z., Abid, M., Jiang, S., Dai, T., et al. (2018). Heat priming during early reproductive stages enhances thermo-tolerance to post-anthesis

heat stress via improving photosynthesis and plant productivity in winter wheat (*Triticum aestivum* L.). *Front. Plant Sci.* 9:805. doi: 10.3389/fpls.2018.00805

Fang, X., Zhao, G., Zhang, S., Li, Y., Gu, H., Li, Y., et al. (2019). Chloroplast-to-nucleus signaling regulates microRNA biogenesis in *Arabidopsis*. *Dev. Cell* 48, 371–382. doi: 10.1016/j.devcel.2018.11.046

Faralli, M., Lektemur, C., Rosellini, D., and Gürel, F. (2015). Effects of heat shock and salinity on barley growth and stress-related gene transcription. *Biol. Plant.* 59, 537–546. doi: 10.1007/s10535-015-0518-x

Feng, B., Zhang, C., Chen, T., Zhang, X., Tao, L., and Fu, G. (2018). Salicylic acid reverses pollen abortion of rice caused by heat stress. *BMC Plant Biol.* 18:245. doi: 10.1186/s12870-018-1472-5

Fiorucci, A. S., Galvão, V. C., Ince, Y. Ç, Boccaccini, A., Goyal, A., Allenbach Petrolati, L., et al. (2020). Phytochrome interacting factor 7 is important for early responses to elevated temperature in Arabidopsis seedlings. *New Phytol.* 226, 50–58. doi: 10.1111/nph.16316

Fragkostefanakis, S., Röth, S., Schleiff, E., and Scharf, K. D. (2015). Prospects of engineering thermotolerance in crops through modulation of heat stress transcription factor and heat shock protein networks. *Plant Cell Environ.* 38, 1881–1895. doi: 10.1111/pce.12396

Fu, Y., Gu, Q., Dong, Q., Zhang, Z., Lin, C., Hu, W., et al. (2019). Spermidine enhances heat tolerance of rice seeds by modulating endogenous starch and polyamine metabolism. *Molecules* 24:1395. doi: 10.3390/molecules24071395

Gagliano, M., Abramson, C. I., and Depczynski, M. (2018). Plants learn and remember: lets get used to it. *Oecologia* 186, 29–31. doi: 10.1007/s00442-017-4029-7

Garai, S., Singla-Pareek, S. L., Sopory, S. K., Kaur, C., and Yadav, G. (2021). Complex networks of prion-like proteins reveal cross talk between stress and memory pathways in plants. *Front. Plant Sci.* 12:1513. doi: 10.3389/fpls.2021.707286

Giacomelli, J. I., Weigel, D., Chan, R. L., and Manavella, P. A. (2012). Role of recently evolved miRNA regulation of sunflower HaWRKY6 in response to temperature damage. *New Phytol.* 195, 766–773. doi: 10.1111/j.1469-8137.2012.04259.x

Gondim, F. A., Miranda, R. D. S., Gomes-Filho, E., and Prisco, J. T. (2013). Enhanced salt tolerance in maize plants induced by H2O2 leaf spraying is associated with improved gas exchange rather than with non-enzymatic antioxidant system. *Theor. Exp. Plant Physiol.* 25, 251–260. doi: 10.1590/S2197-00252013000400003

Gong, M., Chen, B., Li, Z.-G., and Guo, L.-H. (2001). Heat-shock-induced cross adaptation to heat, chilling, drought and salt stress in maize seedlings and involvement of H2O2. *J. Plant Physiol.* 158, 1125–1130. doi: 10.1078/0176-1617-00327

González-Cruz, J., and Pastenes, C. (2012). Water-stress-induced thermotolerance of photosynthesis in bean (*Phaseolus vulgaris* L.) plants: the possible involvement of lipid composition and xanthophyll cycle pigments. *Environ. Exp. Bot.* 77, 127–140. doi: 10.1016/j.envexpbot.2011.11.004

Guan, L. M., Zhao, J., and Scandalios, J. G. (2000). Cis-elements and trans-factors that regulate expression of the maize Cat1 antioxidant gene in response to ABA and osmotic stress: H2O2 is the likely intermediary signaling molecule for the response. *Plant J.* 22, 87–95. doi: 10.1046/j.1365-313x.2000.00723.x

Guan, Q., Lu, X., Zeng, H., Zhang, Y., and Zhu, J. (2013). Heat stress induction of mi R 398 triggers a regulatory loop that is critical for thermotolerance in *Arabidopsis*. *Plant J.* 74, 840–851. doi: 10.1111/tpj.12169

Guertin, M. J., and Lis, J. T. (2010). Chromatin landscape dictates HSF binding to target DNA elements. *PLoS Genet.* 6:e1001114. doi: 10.1371/journal.pgen.1001114

Guo, J., Wu, J., Ji, Q., Wang, C., Luo, L., Yuan, Y., et al. (2008). Genome-wide analysis of heat shock transcription factor families in rice and *Arabidopsis*. *J. Genet. Genomics* 35, 105–118. doi: 10.1016/S1673-8527(08)60016-8

Guo, M., Liu, J.-H., Ma, X., Luo, D.-X., Gong, Z.-H., and Lu, M.-H. (2016). The plant heat stress transcription factors (HSFs): structure, regulation, and function in response to abiotic stresses. *Front. Plant Sci.* 7:114. doi: 10.3389/fpls.2016.00114

Guo, M., Lu, J.-P., Zhai, Y.-F., Chai, W.-G., Gong, Z.-H., and Lu, M.-H. (2015). Genome-wide analysis, expression profile of heat shock factor gene family (CaHsfs) and characterisation of CaHsfA2 in pepper (*Capsicum annuum* L.). *BMC Plant Biol.* 15:1–20. doi: 10.1186/s12870-015-0512-7

Hake, K., and Romeis, T. (2019). Protein kinase-mediated signalling in priming: immune signal initiation, propagation, and establishment of long-term pathogen resistance in plants. *Plant Cell Environ.* 42, 904–917. doi: 10.1111/pce.13429

Hameed, S., and Ali, M. K. (2016). Exogenous application of salicylic acid: inducing thermotolerance in cotton (*Gossypium Hirsutum* L.) seedlings. *Int. J. Agric. Food Res.* 5, 9–18. doi: 10.24102/ijafr.v5i4.691

Harrington, H. M., and Alm, D. M. (1988). Interaction of heat and salt shock in cultured tobacco cells. *Plant Physiol.* 88, 618–625. doi: 10.1104/pp.88.3.618

Hasanuzzaman, M., and Fotopoulos, V. (2019). *Priming And Pretreatment Of Seeds And Seedlings*. Singapore: Springer. doi: 10.1007/978-981-13-8625-1

Hasanuzzaman, M., Nahar, K., Alam, M., Roychowdhury, R., and Fujita, M. (2013). Physiological, biochemical, and molecular mechanisms of heat stress tolerance in plants. *Int. J. Mol. Sci.* 14, 9643–9684. doi: 10.3390/ijms14059643

Herman, J. J., and Sultan, S. E. (2011). Adaptive transgenerational plasticity in plants: case studies, mechanisms, and implications for natural populations. *Front. Plant Sci.* 2:102. doi: 10.3389/fpls.2011.00102

Hilker, M., and Schmülling, T. (2019). *Stress Priming, Memory, And Signalling In Plants*. Hoboken, NJ: Wiley Online Library. doi: 10.1111/pce.13526

Hilker, M., Schwachtje, J., Baier, M., Balazadeh, S., Bäurle, I., Geiselhardt, S., et al. (2016). Priming and memory of stress responses in organisms lacking a nervous system. *Biol. Rev.* 91, 1118–1133. doi: 10.1111/brv.12215

Hivrale, V., Zheng, Y., Puli, C. O. R., Jagadeeswaran, G., Gowdu, K., Kakani, V. G., et al. (2016). Characterization of drought- and heat- responsive microRNAs in switchgrass. *Plant Sci.* 242, 214–223. doi: 10.1016/j.plantsci.2015.07.018

Hoque, T. S., Hossain, M. A., Mostofa, M. G., Burritt, D. J., Fujita, M., and Tran, L.-S. P. (2016). Methylglyoxal: an emerging signaling molecule in plant abiotic stress responses and tolerance. *Front. Plant Sci.* 7:1341. doi: 10.3389/fpls.2016.01341

Hoque, T., Uraji, M., Tuya, A., Nakamura, Y., and Murata, Y. (2012). Methylglyoxal inhibits seed germination and root elongation and up-regulates transcription of stress-responsive genes in ABA-dependent pathway in *Arabidopsis*. *Plant Biol.* 14, 854–858. doi: 10.1111/j.1438-8677.2012.00607.x

Hossain, M. A., Bhattacharjee, S., Armin, S. M., Qian, P., Xin, W., Li, H. Y., et al. (2015). Hydrogen peroxide priming modulates abiotic oxidative stress tolerance: insights from ROS detoxification and scavenging. *Front. Plant Sci.* 6:420. doi: 10.3389/fpls.2015.00420

Hossain, M. A., Liu, F., Burritt, D., Fujita, M., and Huang, B. (2020). *Priming-Mediated Stress and Cross-Stress Tolerance in Crop Plants*. Cambridge, MA: Academic Press.

Hossain, M. A., Mostofa, M. G., and Fujita, M. (2013a). Cross protection by cold-shock to salinity and drought stress-induced oxidative stress in mustard (*Brassica campestris* L.) seedlings. *Mol. Plant Breed.* 4, 50–70. doi: 10.5376/mpb.2013.04.0007

Hossain, M. A., Mostofa, M. G., and Fujita, M. (2013b). Heat-shock positively modulates oxidative protection of salt and drought-stressed mustard (*Brassica campestris* L.) seedlings. *J. Plant Sci. Mol. Breed.* 2:2. doi: 10.7243/2050-2389-2-2

Hsu, Y. T., and Kao, C. H. (2007). Heat shock-mediated H 2 O 2 accumulation and protection against Cd toxicity in rice seedlings. *Plant Soil* 300, 137–147. doi: 10.1007/s11104-007-9396-0

Hu, Q., Zhang, S., and Huang, B. (2019). Strigolactones promote leaf elongation in tall fescue through upregulation of cell cycle genes and downregulation of auxin transport genes in tall fescue under different temperature regimes. *Int. J. Mol. Sci.* 20:1836. doi: 10.3390/ijms20081836

Hu, X. J., Chen, D., Lynne Mclntyre, C., Fernanda Dreccer, M., Zhang, Z. B., Drenth, J., et al. (2018). Heat shock factor C2a serves as a proactive mechanism for heat protection in developing grains in wheat via an ABA-mediated regulatory pathway. *Plant Cell Environ.* 41, 79–98. doi: 10.1111/pce.12957

Huan, Q., Mao, Z., Chong, K., and Zhang, J. (2018). Global analysis of H3K4me3/H3K27me3 in Brachypodium distachyon reveals VRN 3 as critical epigenetic regulation point in vernalization and provides insights into epigenetic memory. *New Phytol.* 219, 1373–1387. doi: 10.1111/nph.15288

Huang, T.-H., Fowler, F., Chen, C.-C., Shen, Z.-J., Sleckman, B., and Tyler, J. K. (2018). The histone chaperones ASF1 and CAF-1 promote MMS22L-TONSL-mediated Rad51 loading onto ssDNA during homologous recombination in human cells. *Mol. Cell* 69, 879–892. E8. doi: 10.1016/j.molcel.2018.01.031

Hussain, M., Khan, T. A., Yusuf, M., and Fariduddin, Q. (2019). Silicon-mediated role of 24-epibrassinolide in wheat under high-temperature stress. *Environ. Sci. Pollut. Res.* 26, 17163–17172. doi: 10.1007/s11356-019-04938-0

Iba, K. (2002). Acclimative response to temperature stress in higher plants: approaches of gene engineering for temperature tolerance. *Annu. Rev. Plant Biol.* 53, 225–245. doi: 10.1146/annurev.arplant.53.100201.160729

Ibañez, C., Delker, C., Martinez, C., Bürstenbinder, K., Janitza, P., Lippmann, R., et al. (2018). Brassinosteroids dominate hormonal regulation of plant thermomorphogenesis via BZR1. *Curr. Biol.* 28, 303–310. doi: 10.1016/j.cub.2017.11.077

Ikeda, M., Mitsuda, N., and Ohme-Takagi, M. (2011). Arabidopsis HsfB1 and HsfB2b act as repressors of the expression of heat-inducible Hsfs but positively regulate the acquired thermotolerance. *Plant Physiol.* 157, 1243–1254. doi: 10.1104/pp.111.179036

IPCC (2018). "Summary for policymakers," in *Global Warming of 1.5°C. An IPCC Special Report on the Impacts of Global Warming of 1.5°C Above Pre-industrial Levels and Related Global Greenhouse gas Emission Pathways, in the Context of Strengthening the Global Response to the Threat of Climate Change, Sustainable Development, and Efforts to Eradicate Poverty,* eds V. Masson-Delmotte, P. Zhai, H.-O. Pörtner, D. Roberts, J. Skea, P. R. Shukla, et al. (Geneva: World Meteorological Organization), 32.

Iqbal, M., Raja, N. I., Yasmeen, F., Hussain, M., Ejaz, M., and Shah, M. (2017). Impacts of heat stress on wheat: a critical review. *Adv. Crop Sci. Technol.* 5, 01–09. doi: 10.4172/2329-8863.1000251

Jagadish, S., Muthurajan, R., Oane, R., Wheeler, T. R., Heuer, S., Bennett, J., et al. (2010). Physiological and proteomic approaches to address heat tolerance during anthesis in rice (*Oryza sativa* L.). *J. Exp. Bot.* 61, 143–156. doi: 10.1093/jxb/erp289

Jahan, M. S., Wang, Y., Shu, S., Zhong, M., Chen, Z., Wu, J., et al. (2019). Exogenous salicylic acid increases the heat tolerance in Tomato (*Solanum lycopersicum* L) by enhancing photosynthesis efficiency and improving antioxidant defense system through scavenging of reactive oxygen species. *Sci. Hortic.* 247, 421–429. doi: 10.1016/j.scienta.2018.12.047

Janda, T., Lejmel, M. A., Molnár, A. B., Majláth, I., Pál, M., Nguyen, Q. T., et al. (2020). Interaction between elevated temperature and different types of Na-salicylate treatment in *Brachypodium dystachion*. *PLoS One* 15:e0227608. doi: 10.1371/journal.pone.0227608

Janeczko, A., Oklešťková, J., Pociecha, E., Kościelniak, J., and Mirek, M. (2011). Physiological effects and transport of 24-epibrassinolide in heat-stressed barley. *Acta Physiol. Plant.* 33, 1249–1259. doi: 10.1007/s11738-010-0655-y

Jaskiewicz, M., Conrath, U., and Peterhänsel, C. (2011). Chromatin modification acts as a memory for systemic acquired resistance in the plant stress response. *EMBO Rep.* 12, 50–55. doi: 10.1038/embor.2010.186

Jegadeesan, S., Beery, A., Altahan, L., Meir, S., Pressman, E., and Firon, N. (2018). Ethylene production and signaling in tomato (*Solanum lycopersicum*) pollen grains is responsive to heat stress conditions. *Plant Reprod.* 31, 367–383. doi: 10.1007/s00497-018-0339-0

Jennings, P., and Saltveit, M. E. (1994). Temperature and chemical shocks induce chilling tolerance in germinating Cucumis sativus (cv. Poinsett 76) seeds. *Physiol. Plant.* 91, 703–707. doi: 10.1111/j.1399-3054.1994.tb03008.x

Jiang, D., Kong, N. C., Gu, X., Li, Z., and He, Y. (2011). *Arabidopsis* COMPASS-like complexes mediate histone H3 lysine-4 trimethylation to control floral transition and plant development. *PLoS Genet.* 7:e1001330. doi: 10.1371/journal.pgen.1001330

Jin, Z., and Pei, Y. (2015). Physiological implications of hydrogen sulfide in plants: pleasant exploration behind its unpleasant odour. *Oxid. Med. Cell. Longev.* 2015:397502. doi: 10.1155/2015/397502

Jonak, C., Ökrész, L., Bögre, L., and Hirt, H. (2002). Complexity, cross talk and integration of plant MAP kinase signalling. *Curr. Opin. Plant Biol.* 5, 415–424. doi: 10.1016/S1369-5266(02)00285-6

Jung, J. H., Barbosa, A. D., Hutin, S., Kumita, J. R., Gao, M., Derwort, D., et al. (2020). A prion-like domain in ELF3 functions as a thermosensor in *Arabidopsis*. *Nature* 585, 256–260. doi: 10.1038/s41586-020-2644-7

Jyothi, M., and Rai, D. (2015). Identification and characterization of high temperature stress responsive novel miRNAs in French bean (*Phaseolus vulgaris*). *Appl. Biochem. Biotechnol.* 176, 835–849. doi: 10.1007/s12010-015-1614-2

Kang, H. M., and Saltveit, M. E. (2001). Activity of enzymatic antioxidant defense systems in chilled and heat shocked cucumber seedling radicles. *Physiol. Plant.* 113, 548–556. doi: 10.1034/j.1399-3054.2001.1130414.x

Kata, L. P., Bhaskaran, M., and Umarani, R. (2014). Influence of priming treatments on stress tolerance during seed germination of rice. *Int. J. Agric. Environ. Biotechnol.* 7, 225–232. doi: 10.5958/2230-732X.2014.00238.1

Kaur, C., Singla-Pareek, S. L., and Sopory, S. K. (2014). Glyoxalase and methylglyoxal as biomarkers for plant stress tolerance. *Crit. Rev. Plant Sci.* 33, 429–456. doi: 10.1080/07352689.2014.904147

Kaur, N., Kaur, J., Grewal, S. K., and Singh, I. (2019). Effect of heat stress on antioxidative defense system and its amelioration by heat acclimation and salicylic acid pre-treatments in three pigeonpea genotypes. *Indian J. Agric. Biochem.* 32, 106–110. doi: 10.5958/0974-4479.2019.00014.5

Kaur, P., Ghai, N., and Sangha, M. K. (2009). Induction of thermotolerance through heat acclimation and salicylic acid in Brassica species. *African J. Biotechnol.* 8, 619–625.

Kaushal, N., Gupta, K., Bhandhari, K., Kumar, S., Thakur, P., and Nayyar, H. (2011). Proline induces heat tolerance in chickpea (*Cicer arietinum* L.) plants by protecting vital enzymes of carbon and antioxidative metabolism. *Physiol. Mol. Biol. Plants* 17, 203–213. doi: 10.1007/s12298-011-0078-2

Kauss, H., Theisinger-Hinkel, E., Mindermann, R., and Conrath, U. (1992). Dichloroisonicotinic and salicylic acid, inducers of systemic acquired resistance, enhance fungal elicitor responses in parsley cells. *Plant J.* 2, 655–660. doi: 10.1111/j.1365-313X.1992.tb00134.x

Ke, Q., Ye, J., Wang, B., Ren, J., Yin, L., Deng, X., et al. (2018). Melatonin mitigates salt stress in wheat seedlings by modulating polyamine metabolism. *Front. Plant Sci.* 9:914. doi: 10.3389/fpls.2018.00914

Khan, A., Bilal, S., Khan, A. L., Imran, M., Shahzad, R., Al-Harrasi, A., et al. (2020). Silicon and gibberellins: synergistic function in harnessing ABA signaling and heat stress tolerance in date palm (*Phoenix dactylifera* L.). *Plants* 9:620. doi: 10.3390/plants9050620

Khan, A., Goswami, K., Sopory, S. K., and Sanan-Mishra, N. (2017). "Mirador" on the potential role of miRNAs in synergy of light and heat networks. *Indian J. Plant Physiol.* 22, 587–607. doi: 10.1007/s40502-017-0329-5

Khan, M. I. R., Iqbal, N., Masood, A., Per, T. S., and Khan, N. A. (2013). Salicylic acid alleviates adverse effects of heat stress on photosynthesis through changes in proline production and ethylene formation. *Plant Signal. Behav.* 8:e26374. doi: 10.4161/psb.26374

Khan, T., Yusuf, M., and Fariduddin, Q. (2018). Hydrogen peroxide in regulation of plant metabolism: signalling and its effect under abiotic stress. *Photosynthetica* 56, 1237–1248. doi: 10.1007/s11099-018-0830-8

Khanna, P., Kaur, K., and Gupta, A. K. (2016). Salicylic acid induces differential antioxidant response in spring maize under high temperature stress. *Indian J. Exp. Biol.* 54, 386–393.

Kim, S., Hwang, G., Kim, S., Thi, T. N., Kim, H., Jeong, J., et al. (2020). The epidermis coordinates thermoresponsive growth through the phyB-PIF4-auxin pathway. *Nat. Commun.* 11, 1–13. doi: 10.1038/s41467-020-14905-w

Kinoshita, T., and Seki, M. (2014). Epigenetic memory for stress response and adaptation in plants. *Plant Cell Physiol.* 55, 1859–1863. doi: 10.1093/pcp/pcu125

Kochhar, S., and Kochhar, V. K. (2005). Expression of antioxidant enzymes and heat shock proteins in relation to combined stress of cadmium and heat in *Vigna mungo* seedlings. *Plant Sci.* 168, 921–929. doi: 10.1016/j.plantsci.2004.11.013

Koizumi, S., Ohama, N., Mizoi, J., Shinozaki, K., and Yamaguchi-Shinozaki, K. (2014). Functional analysis of the Hikeshi-like protein and its interaction with HSP70 in Arabidopsis. *Biochem. Biophys. Res. Commun.* 450, 396–400. doi: 10.1016/j.bbrc.2014.05.128

Kollist, H., Zandalinas, S. I., Sengupta, S., Nuhkat, M., Kangasjärvi, J., and Mittler, R. (2019). Rapid responses to abiotic stress: priming the landscape for the signal transduction network. *Trends Plant Sci.* 24, 25–37. doi: 10.1016/j.tplants.2018.10.003

Kornberg, R. D. (1974). Chromatin structure: a repeating unit of histones and DNA. *Science* 184, 868–871. doi: 10.1126/science.184.4139.868

Kotak, S., Larkindale, J., Lee, U., von Koskull-Döring, P., Vierling, E., and Scharf, K.-D. (2007). Complexity of the heat stress response in plants. *Curr. Opin. Plant Biol.* 10, 310–316. doi: 10.1016/j.pbi.2007.04.011

Kothari, A., and Lachowiec, J. (2021). Roles of brassinosteroids in mitigating heat stress damage in cereal crops. *Int. J. Mol. Sci.* 22:2706. doi: 10.3390/ijms22052706

Kotkar, H., and Giri, A. (2020). "Plant epigenetics and the 'intelligent'priming system to combat biotic stress," in *Epigenetics Of The Immune System*, eds D.

Kabelitz and J. Bhat (Amsterdam: Elsevier), 25–38. doi: 10.1016/B978-0-12-817964-2.00002-2

Kruszka, K., Pacak, A., Swida-Barteczka, A., Nuc, P., Alaba, S., Wroblewska, Z., et al. (2014). Transcriptionally and post-transcriptionally regulated microRNAs in heat stress response in barley. *J. Exp. Bot.* 65, 6123–6135. doi: 10.1093/jxb/eru353

Kudla, J., Becker, D., Grill, E., Hedrich, R., Hippler, M., Kummer, U., et al. (2018). Advances and current challenges in calcium signaling. *New Phytol.* 218, 414–431. doi: 10.1111/nph.14966

Kumar, M., Kesawat, M. S., Ali, A., Lee, S.-C., Gill, S. S., and Kim, H. U. (2019). Integration of abscisic acid signaling with other signaling pathways in plant stress responses and development. *Plants* 8:592. doi: 10.3390/plants8120592

Kumar, R. R., Sharma, S. K., Goswami, S., Verma, P., Singh, K., Dixit, N., et al. (2015). Salicylic acid alleviates the heat stress-induced oxidative damage of starch biosynthesis pathway by modulating the expression of heat-stable genes and proteins in wheat (*Triticum aestivum*). *Acta Physiol. Plant.* 37, 1–12. doi: 10.1007/s11738-015-1899-3

Kumar, S., Kaushal, N., Nayyar, H., and Gaur, P. (2012). Abscisic acid induces heat tolerance in chickpea (*Cicer arietinum* L.) seedlings by facilitated accumulation of osmoprotectants. *Acta Physiol. Plant.* 34, 1651–1658. doi: 10.1007/s11738-012-0959-1

Kumari, V. V., Banerjee, P., Nath, R., and Sengupta, K. (2019). Effect of foliar spray on phenology and yield of Lentil sown on different dates. *J. Crop Weed* 15, 54–58. doi: 10.22271/09746315.2019.v15.i3.1237

Kumari, V. V., Roy, A., Vijayan, R., Banerjee, P., Verma, V. C., Nalia, A., et al. (2021). Drought and heat stress in cool-season food legumes in sub-tropical regions: consequences, adaptation and mitigation strategies. *Plants* 10:1038. doi: 10.3390/plants10061038

Küpers, J. J., Oskam, L., and Pierik, R. (2020). Photoreceptors regulate plant developmental plasticity through auxin. *Plants* 9:940. doi: 10.3390/plants9080940

Kurepin, L. V., Ivanov, A. G., Zaman, M., Pharis, R. P., Allakhverdiev, S. I., Hurry, V., et al. (2015). Stress-related hormones and glycinebetaine interplay in protection of photosynthesis under abiotic stress conditions. *Photosynthesis Res.* 126, 221–235. doi: 10.1007/s11120-015-0125-x

Kurepin, L. V., Qaderi, M. M., Back, T. G., Reid, D. M., and Pharis, R. P. (2008). A rapid effect of applied brassinolide on abscisic acid concentrations in Brassica napus leaf tissue subjected to short-term heat stress. *Plant Growth Regul.* 55, 165–167. doi: 10.1007/s10725-008-9276-5

Kushawaha, A. K., Khan, A., Sopory, S. K., and Sanan-Mishra, N. (2019). Light regulated osa-miR169e is implicated during priming under high temperature stress in rice. *Am. J. Plant Sci.* 10:1662. doi: 10.4236/ajps.2019.109118

Kushawaha, A. K., Khan, A., Sopory, S. K., and Sanan-Mishra, N. (2021). Priming by High Temperature stress induces microRNA regulated heat shock modules indicating their involvement in thermopriming response in rice. *Life* 11:291. doi: 10.3390/life11040291

Kwak, J. M., Mori, I. C., Pei, Z. M., Leonhardt, N., Torres, M. A., Dangl, J. L., et al. (2003). NADPH oxidase AtrbohD and AtrbohF genes function in ROS-dependent ABA signaling in Arabidopsis. *EMBO J.* 22, 2623–2633. doi: 10.1093/emboj/cdg277

Lämke, J., Brzezinka, K., Altmann, S., and Bäurle, I. (2016). A hit-and-run heat shock factor governs sustained histone methylation and transcriptional stress memory. *EMBO J.* 35, 162–175. doi: 10.15252/embj.201592593

Larkindale, J., and Knight, M. R. (2002). Protection against heat stress-induced oxidative damage in *Arabidopsis* involves calcium, abscisic acid, ethylene, and salicylic acid. *Plant Physiol.* 128, 682–695. doi: 10.1104/pp.010320

Larkindale, J., Hall, J. D., Knight, M. R., and Vierling, E. (2005). Heat stress phenotypes of Arabidopsis mutants implicate multiple signaling pathways in the acquisition of thermotolerance. *Plant Physiol.* 138, 882–897. doi: 10.1104/pp.105.062257

Lee, I., Aukerman, M. J., Gore, S. L., Lohman, K. N., Michaels, S. D., Weaver, L. M., et al. (1994). Isolation of LUMINIDEPENDENS: a gene involved in the control of flowering time in *Arabidopsis*. *Plant Cell* 6, 75–83. doi: 10.1105/tpc.6.1.75

Lei, Y. B., Song, S. Q., and Fu, J. R. (2005). Possible involvement of anti-oxidant enzymes in the cross-tolerance of the germination/growth of wheat seeds to salinity and heat stress. *J. Integr. Plant Biol.* 47, 1211–1219. doi: 10.1111/j.1744-7909.2005.00152.x

Leopold, A. C. (2014). Smart plants: memory and communication without brains. *Plant Signal. Behav.* 9:e972268. doi: 10.4161/15592316.2014.972268

Li, C., Jiang, D., Wollenweber, B., Li, Y., Dai, T., and Cao, W. (2011). Waterlogging pretreatment during vegetative growth improves tolerance to waterlogging after anthesis in wheat. *Plant Sci.* 180, 672–678. doi: 10.1016/j.plantsci.2011.01.009

Li, C., Wang, P., Wei, Z., Liang, D., Liu, C., Yin, L., et al. (2012). The mitigation effects of exogenous melatonin on salinity-induced stress in *Malus hupehensis*. *J. Pineal Res.* 53, 298–306. doi: 10.1111/j.1600-079X.2012.00999.x

Li, G., Zhang, C., Zhang, G., Fu, W., Feng, B., Chen, T., et al. (2020). Abscisic acid negatively modulates heat tolerance in rolled leaf rice by increasing leaf temperature and regulating energy homeostasis. *Rice* 13, 1–16. doi: 10.1186/s12284-020-00379-3

Li, G., Zhang, Y., Zhang, H., Zhang, Y., Zhao, L., Liu, Z., et al. (2019). Characteristics and regulating role in thermotolerance of the heat shock transcription factor ZmHsf12 from *Zea mays* L. *J. Plant Biol.* 62, 329–341. doi: 10.1007/s12374-019-0067-5

Li, N., Euring, D., Cha, J. Y., Lin, Z., Lu, M., Huang, L. J., et al. (2021). Plant hormone-mediated regulation of heat tolerance in response to global climate change. *Front. Plant Sci.* 11:2318. doi: 10.3389/fpls.2020.627969

Li, S., Liu, J., Liu, Z., Li, X., Wu, F., and He, Y. (2014). Heat-induced TAS1 TARGET1 mediates thermotolerance via heat stress transcription factor A1a–directed pathways in *Arabidopsis*. *Plant Cell* 26, 1764–1780. doi: 10.1105/tpc.114.124883

Li, X., Brestic, M., Tan, D. X., Zivcak, M., Zhu, X., Liu, S., et al. (2018). Melatonin alleviates low PS I-limited carbon assimilation under elevated CO 2 and enhances the cold tolerance of offspring in chlorophyll b-deficient mutant wheat. *J. Pineal Res.* 64:e12453. doi: 10.1111/jpi.12453

Li, X., Cai, J., Liu, F., Dai, T., Cao, W., and Jiang, D. (2014). Cold priming drives the sub-cellular antioxidant systems to protect photosynthetic electron transport against subsequent low temperature stress in winter wheat. *Plant Physiol. Biochem.* 82, 34–43. doi: 10.1016/j.plaphy.2014.05.005

Li, X., Topbjerg, H. B., Jiang, D., and Liu, F. (2015). Drought priming at vegetative stage improves the antioxidant capacity and photosynthesis performance of wheat exposed to a short-term low temperature stress at jointing stage. *Plant Soil* 393, 307–318. doi: 10.1007/s11104-015-2499-0

Li, X.-D., Wang, X.-L., Cai, Y.-M., Wu, J.-H., Mo, B.-T., and Yu, E.-R. (2017). *Arabidopsis* heat stress transcription factors A2 (HSFA2) and A3 (HSFA3) function in the same heat regulation pathway. *Acta Physiol. Plant.* 39:67. doi: 10.1007/s11738-017-2351-7

Li, Y., Mukherjee, I., Thum, K. E., Tanurdzic, M., Katari, M. S., Obertello, M., et al. (2015). The histone methyltransferase SDG8 mediates the epigenetic modification of light and carbon responsive genes in plants. *Genome Biol.* 16, 1–15. doi: 10.1186/s13059-015-0640-2

Li, Z.-G. (2016). Methylglyoxal and glyoxalase system in plants: old players, new concepts. *Bot. Rev.* 82, 183–203. doi: 10.1007/s12229-016-9167-9

Li, Z.-G., and Zhu, L.-P. (2015). Hydrogen sulfide donor sodium hydrosulfide-induced accumulation of betaine is involved in the acquisition of heat tolerance in maize seedlings. *Braz. J. Bot.* 38, 31–38. doi: 10.1007/s40415-014-0106-x

Li, Z.-G., Duan, X.-Q., Min, X., and Zhou, Z.-H. (2017a). Methylglyoxal as a novel signal molecule induces the salt tolerance of wheat by regulating the glyoxalase system, the antioxidant system, and osmolytes. *Protoplasma* 254, 1995–2006. doi: 10.1007/s00709-017-1094-z

Li, Z.-G., Duan, X.-Q., Xia, Y.-M., Wang, Y., Zhou, Z.-H., and Min, X. (2017b). Methylglyoxal alleviates cadmium toxicity in wheat (*Triticum aestivum* L). *Plant Cell Rep.* 36, 367–370. doi: 10.1007/s00299-016-2070-3

Light, W. H., Brickner, D. G., Brand, V. R., and Brickner, J. H. (2010). Interaction of a DNA zip code with the nuclear pore complex promotes H2A. Z incorporation and INO1 transcriptional memory. *Mol. Cell* 40, 112–125. doi: 10.1016/j.molcel.2010.09.007

Light, W. H., Freaney, J., Sood, V., Thompson, A., D'Urso, A., Horvath, C. M., et al. (2013). A conserved role for human Nup98 in altering chromatin structure and promoting epigenetic transcriptional memory. *PLoS Biol.* 11:e1001524. doi: 10.1371/journal.pbio.1001524

Liu, B., Zhang, L., Rusalepp, L., Kaurilind, E., Sulaiman, H. Y., Püssa, T., et al. (2021). Heat priming improved heat tolerance of photosynthesis, enhanced terpenoid and benzenoid emission and phenolics accumulation in *Achillea millefolium*. *Plant Cell Environ.* 44, 2365–2385. doi: 10.1111/pce.13830

Liu, H. A. (2020). Transgenerational effects of water-deficit and heat stress on germination and seedling vigour—new insights from durum wheat microRNAs. *Plants* 9:89. doi: 10.3390/plants9020189

Liu, H. C., Liao, H. T., and Charng, Y. Y. (2011a). The role of class A1 heat shock factors (HSFA1s) in response to heat and other stresses in *Arabidopsis*. *Plant Cell Environ.* 34, 738–751. doi: 10.1111/j.1365-3040.2011.02278.x

Liu, H., Able, A. J., and Able, J. A. (2021). Priming crops for the future: rewiring stress memory. *Trends Plant Sci.* S1360–1385, 321–326. doi: 10.1016/j.tplants.2021.11.015

Liu, H., Zhou, X., Dong, N., Liu, X., Zhang, H., and Zhang, Z. (2011b). Expression of a wheat MYB gene in transgenic tobacco enhances resistance to *Ralstonia solanacearum*, and to drought and salt stresses. *Funct. Integr. Genomics* 11, 431–443. doi: 10.1007/s10142-011-0228-1

Liu, H.-T., Liu, Y.-Y., Pan, Q.-H., Yang, H.-R., Zhan, J.-C., and Huang, W.-D. (2006). Novel interrelationship between salicylic acid, abscisic acid, and PIP2-specific phospholipase C in heat acclimation-induced thermotolerance in pea leaves. *J. Exp. Bot.* 57, 3337–3347. doi: 10.1093/jxb/erl098

Liu, J., Feng, L., Gu, X., Deng, X., Qiu, Q., Li, Q., et al. (2019). An H3K27me3 demethylase-HSFA2 regulatory loop orchestrates transgenerational thermomemory in *Arabidopsis*. *Cell Res.* 29, 379–390.

Liu, J., Feng, L., Li, J., and He, Z. (2015). Genetic and epigenetic control of plant heat responses. *Front. Plant Sci.* 6:267. doi: 10.3389/fpls.2015.00267

Liu, J.-X., and Howell, S. H. (2010). bZIP28 and NF-Y transcription factors are activated by ER stress and assemble into a transcriptional complex to regulate stress response genes in *Arabidopsis*. *Plant Cell* 22, 782–796. doi: 10.1105/tpc.109.072173

Liu, N., and Avramova, Z. (2016). Molecular mechanism of the priming by jasmonic acid of specific dehydration stress response genes in *Arabidopsis*. *Epigenet. Chromatin* 9, 1–23. doi: 10.1186/s13072-016-0057-5

Liu, W., Xu, L., Wang, Y., Shen, H., Zhu, X., Zhang, K., et al. (2015). Transcriptome-wide analysis of chromium-stress responsive microRNAs to explore miRNA-mediated regulatory networks in radish (*Raphanus sativus* L.). *Sci. Rep.* 5, 1–17. doi: 10.1038/srep14024

Liu, Y., Liu, K., Yin, L., Yu, Y., Qi, J., Shen, W. H., et al. (2019). H3K4me2 functions as a repressive epigenetic mark in plants. *Epigenet. Chromatin* 12, 1–14. doi: 10.1186/s13072-019-0285-6

Liu, Y., Zhang, C., Chen, J., Guo, L., Li, X., Li, W., et al. (2013). Arabidopsis heat shock factor HsfA1a directly senses heat stress, pH changes, and hydrogen peroxide via the engagement of redox state. *Plant Physiol. Biochem.* 64, 92–98. doi: 10.1016/j.plaphy.2012.12.013

Luna, E., Bruce, T. J., Roberts, M. R., Flors, V., and Ton, J. (2012). Next-generation systemic acquired resistance. *Plant Physiol.* 158, 844–853. doi: 10.1104/pp.111.187468

Lurie, S., and Klein, J. D. (1991). Acquisition of low-temperature tolerance in tomatoes by exposure to high-temperature stress. *J. Am. Soc. Hortic. Sci.* 116, 1007–1012. doi: 10.21273/JASHS.116.6.1007

Lv, W.-T., Lin, B., Zhang, M., and Hua, X.-J. (2011). Proline accumulation is inhibitory to Arabidopsis seedlings during heat stress. *Plant Physiol.* 156, 1921–1933. doi: 10.1104/pp.111.175810

Ma, D., Li, X., Guo, Y., Chu, J., Fang, S., Yan, C., et al. (2016). Cryptochrome 1 interacts with PIF4 to regulate high temperature-mediated hypocotyl elongation in response to blue light. *Proc. Natl. Acad. Sci. U.S.A.* 113, 224–229. doi: 10.1073/pnas.1511437113

Ma, Q. J., Sun, M. H., Kang, H., Lu, J., You, C. X., and Hao, Y. J. (2019). A CIPK protein kinase targets sucrose transporter MdSUT2. 2 at Ser254 for phosphorylation to enhance salt tolerance. *Plant Cell Environ.* 42, 918–930. doi: 10.1111/pce.13349

Majláth, I., Éva, C., Tajti, J., Khalil, R., Elsayed, N., Darko, E., et al. (2020). Exogenous methylglyoxal enhances the reactive aldehyde detoxification capability and frost-hardiness of wheat. *Plant Physiol. Biochem.* 149, 75–85. doi: 10.1016/j.plaphy.2020.02.003

Makarova, S., Makhotenko, A., Spechenkova, N., Love, A. J., Kalinina, N. O., and Taliansky, M. (2018). Interactive responses of potato (*Solanum tuberosum* L.) plants to heat stress and infection with potato virus Y. *Front. Microbiol.* 9:2582. doi: 10.3389/fmicb.2018.02582

Martel, A. B., and Qaderi, M. M. (2016). Does salicylic acid mitigate the adverse effects of temperature and ultraviolet-B radiation on pea (*Pisum sativum*) plants? *Environ. Exp. Bot.* 122, 39–48. doi: 10.1016/j.envexpbot.2015.09.002

Martinez-Medina, A., Flors, V., Heil, M., Mauch-Mani, B., Pieterse, C. M., Pozo, M. J., et al. (2016). Recognizing plant defense priming. *Trends Plant Sci.* 21, 818–822. doi: 10.1016/j.tplants.2016.07.009

Maszkowska, J., Dêbski, J., Kulik, A., Kistowski, M., Bucholc, M., Lichocka, M., et al. (2019). Phosphoproteomic analysis reveals that dehydrins ERD10 and ERD14 are phosphorylated by SNF1-related protein kinase 2.10 in response to osmotic stress. *Plant Cell Environ.* 42, 931–946. doi: 10.1111/pce.13465

Maya, M. A., and Matsubara, Y.-I. (2013). Influence of arbuscular mycorrhiza on the growth and antioxidative activity in cyclamen under heat stress. *Mycorrhiza* 23, 381–390. doi: 10.1007/s00572-013-0477-z

Mazorra, L. M., Holton, N., Bishop, G. J., and Núñez, M. (2011). Heat shock response in tomato brassinosteroid mutants indicates that thermotolerance is independent of brassinosteroid homeostasis. *Plant Physiol. Biochem.* 49, 1420–1428. doi: 10.1016/j.plaphy.2011.09.005

McLellan, C. A., Turbyville, T. J., Wijeratne, E. K., Kerschen, A., Vierling, E., Queitsch, C., et al. (2007). A rhizosphere fungus enhances *Arabidopsis* thermotolerance through production of an HSP90 inhibitor. *Plant Physiol.* 145, 174–182. doi: 10.1104/pp.107.101808

Mei, Y. Q., and Song, S. Q. (2010). Response to temperature stress of reactive oxygen species scavenging enzymes in the cross-tolerance of barley seed germination. *J. Zhejiang Univ. Sci. B* 11, 965–972. doi: 10.1631/jzus.B1000147

Meiri, D., and Breiman, A. (2009). Arabidopsis ROF1 (FKBP62) modulates thermotolerance by interacting with HSP90. 1 and affecting the accumulation of HsfA2-regulated sHSPs. *Plant J.* 59, 387–399. doi: 10.1111/j.1365-313X.2009.03878.x

Mendanha, T., Rosenqvist, E., Hyldgaard, B., and Ottosen, C.-O. (2018). Heat priming effects on anthesis heat stress in wheat cultivars (*Triticum aestivum* L.) with contrasting tolerance to heat stress. *Plant Physiol. Biochem.* 132, 213–221. doi: 10.1016/j.plaphy.2018.09.002

Meng, J. F., Xu, T. F., Wang, Z. Z., Fang, Y. L., Xi, Z. M., and Zhang, Z. W. (2014). The ameliorative effects of exogenous melatonin on grape cuttings under water-deficient stress: antioxidant metabolites, leaf anatomy, and chloroplast morphology. *J. Pineal Res.* 57, 200–212. doi: 10.1111/jpi.12159

Migicovsky, Z., Yao, Y., and Kovalchuk, I. (2014). Transgenerational phenotypic and epigenetic changes in response to heat stress in *Arabidopsis thaliana*. *Plant Signal. Behav.* 9:e27971. doi: 10.4161/psb.27971

Mittal, D., Chakrabarti, S., Sarkar, A., Singh, A., and Grover, A. (2009). Heat shock factor gene family in rice: genomic organization and transcript expression profiling in response to high temperature, low temperature and oxidative stresses. *Plant Physiol. Biochem.* 47, 785–795. doi: 10.1016/j.plaphy.2009.05.003

Mittler, R., and Blumwald, E. (2015). The roles of ROS and ABA in systemic acquired acclimation. *Plant Cell* 27, 64–70. doi: 10.1105/tpc.114.133090

Mittler, R., Finka, A., and Goloubinoff, P. (2012). How do plants feel the heat? *Trends Biochem. Sci.* 37, 118–125. doi: 10.1016/j.tibs.2011.11.007

Mittler, R., Vanderauwera, S., Gollery, M., and Van Breusegem, F. (2004). Reactive oxygen gene network of plants. *Trends Plant Sci.* 9, 490–498. doi: 10.1016/j.tplants.2004.08.009

Monaghan, J., and Zipfel, C. (2012). Plant pattern recognition receptor complexes at the plasma membrane. *Curr. Opin. Plant Biol.* 15, 349–357. doi: 10.1016/j.pbi.2012.05.006

Mozgova, I., Wildhaber, T., Liu, Q., Abou-Mansour, E., L'Haridon, F., Metraux, J. P., et al. (2015). Chromatin assembly factor CAF-1 represses priming of plant defence response genes. *Nat. Plants* 1, 1–8. doi: 10.1038/nplants.2015.127

Munné-Bosch, S., and Alegre, L. (2013). Cross-stress tolerance and stress "memory" in plants. *Environ. Exp. Bot.* 94, 1–88. doi: 10.1016/j.envexpbot.2013.02.002

Nahar, K., Hasanuzzaman, M., Alam, M. M., and Fujita, M. (2015). Exogenous glutathione confers high temperature stress tolerance in mung bean (*Vigna radiata* L.) by modulating antioxidant defense and methylglyoxal detoxification system. *Environ. Exp. Bot.* 112, 44–54. doi: 10.1016/j.envexpbot.2014.12.001

Nakagami, H., Pitzschke, A., and Hirt, H. (2005). Emerging MAP kinase pathways in plant stress signalling. *Trends Plant Sci.* 10, 339–346. doi: 10.1016/j.tplants.2005.05.009

Nakashima, K., Tran, L. S. P., Van Nguyen, D., Fujita, M., Maruyama, K., Todaka, D., et al. (2007). Functional analysis of a NAC-type transcription factor OsNAC6 involved in abiotic and biotic stress-responsive gene expression in rice. *Plant J.* 51, 617–630. doi: 10.1111/j.1365-313X.2007.03168.x

Narayanan, S., Tamura, P. J., Roth, M. R., Prasad, P. V., and Welti, R. (2016). Wheat leaf lipids during heat stress: I. High day and night temperatures result in major lipid alterations. *Plant Cell Environ.* 39, 787–803. doi: 10.1111/pce.12649

Naydenov, M., Baev, V., Apostolova, E., Gospodinova, N., Sablok, G., Gozmanova, M., et al. (2015). High-temperature effect on genes engaged in DNA methylation and affected by DNA methylation in Arabidopsis. *Plant Physiol. Biochem.* 87, 102–108. doi: 10.1016/j.plaphy.2014.12.022

Newby, G. A., and Lindquist, S. (2013). Blessings in disguise: biological benefits of prion-like mechanisms. *Trends Cell Biol.* 23, 251–259. doi: 10.1016/j.tcb.2013.01.007

Nie, W. F., Wang, M. M., Xia, X. J., Zhou, Y. H., Shi, K., Chen, Z., et al. (2013). Silencing of tomato RBOH1 and MPK2 abolishes brassinosteroid-induced H2O2 generation and stress tolerance. *Plant Cell Environ.* 36, 789–803. doi: 10.1111/pce.12014

Niu, J. H., Ahmad Anjum, S., Wang, R., Li, J. H., Liu, M. R., Song, J. X., et al. (2016). Exogenous application of brassinolide can alter morphological and physiological traits of Leymus chinensis (Trin.) *Tzvelev* under room and high temperatures. *Chilean J. Agric. Res.* 76, 27–33. doi: 10.4067/S0718-58392016000100004

Nožková, V., Mieslerova, B., Luhova, L., Piterkova, J., Novák, O., Špundová, M., et al. (2018). Effect of heat-shock pre-treatment on tomato plants infected by powdery mildew fungus. *Plant Prot. Sci.* 55, 31–42. doi: 10.17221/24/2018-PPS

Ohama, N., Sato, H., Shinozaki, K., and Yamaguchi-Shinozaki, K. (2017). Transcriptional regulatory network of plant heat stress response. *Trends Plant Sci.* 22, 53–65. doi: 10.1016/j.tplants.2016.08.015

Omoarelojie, L. O., Kulkarni, M. G., Finnie, J. F., Pospíšil, T., Strnad, M., and Van Staden, J. (2020). Synthetic strigolactone (rac-GR24) alleviates the adverse effects of heat stress on seed germination and photosystem II function in lupine seedlings. *Plant Physiol. Biochem.* 155, 965–979. doi: 10.1016/j.plaphy.2020.07.043

Oostendorp, M., Kunz, W., Dietrich, B., and Staub, T. (2001). Induced disease resistance in plants by chemicals. *Eur. J. Plant Pathol.* 107, 19–28. doi: 10.1023/A:1008760518772

Orzech, K., and Burke, J. (1988). Heat shock and the protection against metal toxicity in wheat leaves 1. *Plant Cell Environ.* 11, 711–714. doi: 10.1111/j.1365-3040.1988.tb01154.x

Oshino, T., Miura, S., Kikuchi, S., Hamada, K., Yano, K., Watanabe, M., et al. (2011). Auxin depletion in barley plants under high-temperature conditions represses DNA proliferation in organelles and nuclei via transcriptional alterations. *Plant Cell Environ.* 34, 284–290. doi: 10.1111/j.1365-3040.2010.02242.x

Palma, K., Thorgrimsen, S., Malinovsky, F. G., Fiil, B. K., Nielsen, H. B., Brodersen, P., et al. (2010). Autoimmunity in *Arabidopsis* acd11 is mediated by epigenetic regulation of an immune receptor. *PLoS Pathog.* 6:e1001137. doi: 10.1371/journal.ppat.1001137

Pan, C., Ye, L., Zheng, Y., Wang, Y., Yang, D., Liu, X., et al. (2017). Identification and expression profiling of microRNAs involved in the stigma exsertion under high-temperature stress in tomato. *BMC Genomics* 18:843. doi: 10.1186/s12864-017-4238-9

Pandey, P., Irulappan, V., Bagavathiannan, M. V., and Senthil-Kumar, M. (2017). Impact of combined abiotic and biotic stresses on plant growth and avenues for crop improvement by exploiting physio-morphological traits. *Front. Plant Sci.* 8:537. doi: 10.3389/fpls.2017.00537

Peng, J., Li, Z., Wen, X., Li, W., Shi, H., Yang, L., et al. (2014). Salt-induced stabilization of EIN3/EIL1 confers salinity tolerance by deterring ROS accumulation in *Arabidopsis*. *PLoS Genet.* 10:e1004664. doi: 10.1371/journal.pgen.1004664

Pérez-Salamó, I., Papdi, C., Rigó, G., Zsigmond, L., Vilela, B., Lumbreras, V., et al. (2014). The heat shock factor A4A confers salt tolerance and is regulated by oxidative stress and the mitogen-activated protein kinases MPK3 and MPK6. *Plant Physiol.* 165, 319–334. doi: 10.1104/pp.114.237891

Pham, V. N., Kathare, P. K., and Huq, E. (2018). Phytochromes and phytochrome interacting factors. *Plant Physiol.* 176, 1025–1038. doi: 10.1104/pp.17.01384

Pieterse, C. M., Zamioudis, C., Berendsen, R. L., Weller, D. M., Van Wees, S. C., and Bakker, P. A. (2014). Induced systemic resistance by beneficial microbes. *Annu. Rev. Phytopathol.* 52, 347–375. doi: 10.1146/annurev-phyto-082712-102340

Prasad, P. V., Bheemanahalli, R., and Jagadish, S. K. (2017). Field crops and the fear of heat stress—opportunities, challenges and future directions. *Field Crops Res.* 200, 114–121. doi: 10.1016/j.fcr.2016.09.024

Prerostova, S., Dobrev, P. I., Kramna, B., Gaudinova, A., Knirsch, V., Spichal, L., et al. (2020). Heat acclimation and inhibition of cytokinin degradation positively affect heat stress tolerance of *Arabidopsis*. *Front. Plant Sci.* 11:87. doi: 10.3389/fpls.2020.00087

Qiu, Y., and Yu, D. (2009). Over-expression of the stress-induced OsWRKY45 enhances disease resistance and drought tolerance in *Arabidopsis*. *Environ. Exp. Bot.* 65, 35–47. doi: 10.1016/j.envexpbot.2008.07.002

Qiu, Z., Guo, J., Zhu, A., Zhang, L., and Zhang, M. (2014). Exogenous jasmonic acid can enhance tolerance of wheat seedlings to salt stress. *Ecotoxicol. Environ. Saf.* 104, 202–208. doi: 10.1016/j.ecoenv.2014.03.014

Qu, A.-L., Ding, Y.-F., Jiang, Q., and Zhu, C. (2013). Molecular mechanisms of the plant heat stress response. *Biochem. Biophys. Res. Commun.* 432, 203–207. doi: 10.1016/j.bbrc.2013.01.104

Quint, M., Delker, C., Franklin, K. A., Wigge, P. A., Halliday, K. J., and Van Zanten, M. (2016). Molecular and genetic control of plant thermomorphogenesis. *Nat. Plants* 2, 1–9. doi: 10.1038/nplants.2015.190

Raghuram, B., Sheikh, A. H., and Sinha, A. K. (2014). Regulation of MAP kinase signaling cascade by microRNAs in *Oryza sativa*. *Plant Signal. Behav.* 9:e972130. doi: 10.4161/psb.29804

Ramirez-Prado, J. S., Abulfaraj, A. A., Rayapuram, N., Benhamed, M., and Hirt, H. (2018). Plant immunity: from signaling to epigenetic control of defense. *Trends Plant Sci.* 23, 833–844. doi: 10.1016/j.tplants.2018.06.004

Rasheed, R., Wahid, A., Farooq, M., Hussain, I., and Basra, S. M. (2011). Role of proline and glycinebetaine pretreatments in improving heat tolerance of sprouting sugarcane (*Saccharum* sp.) buds. *Plant Growth Regul.* 65, 35–45. doi: 10.1007/s10725-011-9572-3

Redman, R. S., Sheehan, K. B., Stout, R. G., Rodriguez, R. J., and Henson, J. M. (2002). Thermotolerance generated by plant/fungal symbiosis. *Science* 298, 1581–1581. doi: 10.1126/science.1078055

Rezaul, I. M., Baohua, F., Tingting, C., Weimeng, F., Caixia, Z., Longxing, T., et al. (2019). Abscisic acid prevents pollen abortion under high-temperature stress by mediating sugar metabolism in rice spikelets. *Physiol. Plant.* 165, 644–663. doi: 10.1111/ppl.12759

Rodríguez, V. M., Soengas, P., Alonso-Villaverde, V., Sotelo, T., Cartea, M. E., and Velasco, P. (2015). Effect of temperature stress on the early vegetative development of *Brassica oleracea* L. *BMC Plant Biol.* 15:145. doi: 10.1186/s12870-015-0535-0

Rozenzvieg, D., Elmaci, C., Samach, A., Lurie, S., and Porat, R. (2004). Isolation of four heat shock protein cDNAs from grapefruit peel tissue and characterization of their expression in response to heat and chilling temperature stresses. *Physiol. Plant.* 121, 421–428. doi: 10.1111/j.1399-3054.2004.00334.x

Ruthenburg, A. J., Allis, C. D., and Wysocka, J. (2007). Methylation of lysine 4 on histone H3: intricacy of writing and reading a single epigenetic mark. *Mol. Cell* 25, 15–30. doi: 10.1016/j.molcel.2006.12.014

Sabehat, A., Weiss, D., and Lurie, S. (1996). The correlation between heat-shock protein accumulation and persistence and chilling tolerance in tomato fruit. *Plant Physiol.* 110, 531–537. doi: 10.1104/pp.110.2.531

Sadura, I., Libik-Konieczny, M., Jurczyk, B., Gruszka, D., and Janeczko, A. (2020). Plasma membrane ATPase and the aquaporin HvPIP1 in barley brassinosteroid mutants acclimated to high and low temperature. *J. Plant Physiol.* 244:153090. doi: 10.1016/j.jplph.2019.153090

Sah, S. K., Reddy, K. R., and Li, J. (2016). Abscisic acid and abiotic stress tolerance in crop plants. *Front. Plant Sci.* 7:571. doi: 10.3389/fpls.2016.00571

Sakata, T., Oshino, T., Miura, S., Tomabechi, M., Tsunaga, Y., Higashitani, N., et al. (2010). Auxins reverse plant male sterility caused by high temperatures. *Proc. Natl. Acad. Sci. U.S.A.* 107, 8569–8574. doi: 10.1073/pnas.1000869107

Saleh, A. A., Abdel-Kader, D. Z., and El Elish, A. M. (2007). Role of heat shock and salicylic acid in antioxidant homeostasis in mungbean (*Vigna radiata* L.) plant subjected to heat stress. *Am. J. Plant Physiol.* 2, 344–355. doi: 10.3923/ajpp.2007.344.355

Sanchez, D. H., and Paszkowski, J. (2014). Heat-induced release of epigenetic silencing reveals the concealed role of an imprinted plant gene. *PLoS Genet.* 10:e1004806. doi: 10.1371/journal.pgen.1004806

Sarwar, M., Saleem, M. F., Ullah, N., Rizwan, M., Ali, S., Shahid, M. R., et al. (2018). Exogenously applied growth regulators protect the cotton crop from heat-induced injury by modulating plant defense mechanism. *Sci. Rep.* 8, 1–15. doi: 10.1038/s41598-018-35420-5

Sato, H., Mizoi, J., Tanaka, H., Maruyama, K., Qin, F., Osakabe, Y., et al. (2014). Arabidopsis DPB3-1, a DREB2A interactor, specifically enhances heat stress-induced gene expression by forming a heat stress-specific transcriptional complex with NF-Y subunits. *Plant Cell* 26, 4954–4973. doi: 10.1105/tpc.114.132928

Sato, Y., Murakami, T., Funatsuki, H., Matsuba, S., Saruyama, H., and Tanida, M. (2001). Heat shock-mediated APX gene expression and protection against chilling injury in rice seedlings. *J. Exp. Bot.* 52, 145–151. doi: 10.1093/jexbot/52.354.145

Scharf, K.-D., Berberich, T., Ebersberger, I., and Nover, L. (2012). The plant heat stress transcription factor (Hsf) family: structure, function and evolution. *Biochim. Biophys. Acta BBA Gene Regul. Mechanisms* 1819, 104–119. doi: 10.1016/j.bbagrm.2011.10.002

Scherzer, S., Shabala, L., Hedrich, B., Fromm, J., Bauer, H., Munz, E., et al. (2017). Insect haptoelectrical stimulation of Venus flytrap triggers exocytosis in gland cells. *Proc. Natl. Acad. Sci. U.S.A.* 114, 4822–4827. doi: 10.1073/pnas.1701860114

Sedaghatmehr, M., Mueller-Roeber, B., and Balazadeh, S. (2016). The plastid metalloprotease FtsH6 and small heat shock protein HSP21 jointly regulate thermomemory in *Arabidopsis*. *Nat. Commun.* 7, 1–14. doi: 10.1038/ncomms12439

Serrano, N., Ling, Y., Bahieldin, A., and Mahfouz, M. M. (2019). Thermopriming reprograms metabolic homeostasis to confer heat tolerance. *Sci. Rep.* 9, 1–14. doi: 10.1038/s41598-018-36484-z

Shahnejat-Bushehri, S., Mueller-Roeber, B., and Balazadeh, S. (2012). Arabidopsis NAC transcription factor JUNGBRUNNEN1 affects thermomemory-associated genes and enhances heat stress tolerance in primed and unprimed conditions. *Plant Signal. Behav.* 7, 1518–1521. doi: 10.4161/psb.22092

Sharma, D., Verma, N., Pandey, C., Verma, D., Bhagat, P. K., Noryang, S., et al. (2020). "MAP kinase as regulators for stress responses in plants: an overview," in *Protein Kinases And Stress Signaling In Plants*, ed. G. K. Pandey (Hoboken, NJ: Wiley), 369–392. doi: 10.1002/9781119541578.ch15

Shekhawat, K., Saad, M. M., Sheikh, A., Mariappan, K., Al-Mahmoudi, H., Abdulhakim, F., et al. (2021). Root endophyte induced plant thermotolerance by constitutive chromatin modification at heat stress memory gene loci. *EMBO Rep.* 22:e51049. doi: 10.15252/embr.202051049

Shi, H., Tan, D. X., Reiter, R. J., Ye, T., Yang, F., and Chan, Z. (2015b). Melatonin induces class A1 heat-shock factors (HSFA 1s) and their possible involvement of thermotolerance in *Arabidopsis*. *J. Pineal Res.* 58, 335–342. doi: 10.1111/jpi.12219

Shi, H., Qian, Y., Tan, D. X., Reiter, R. J., and He, C. (2015a). Melatonin induces the transcripts of CBF/DREB1s and their involvement in both abiotic and biotic stresses in *Arabidopsis*. *J. Pineal Res.* 59, 334–342. doi: 10.1111/jpi.12262

Shi, H., Wang, X., Ye, T., Chen, F., Deng, J., Yang, P., et al. (2014). The Cysteine2/Histidine2-type transcription factor zinc finger of *Arabidopsis thaliana* 6 modulates biotic and abiotic stress responses by activating salicylic acid-related genes and C-repeat-binding factor genes in *Arabidopsis*. *Plant Physiol.* 165, 1367–1379. doi: 10.1104/pp.114.242404

Shi, W., Lawas, L., Raju, B., and Jagadish, S. (2016). Acquired thermo-tolerance and trans-generational heat stress response at flowering in rice. *J. Agron. Crop Sci.* 202, 309–319. doi: 10.1111/jac.12157

Shorter, J., and Lindquist, S. (2005). Prions as adaptive conduits of memory and inheritance. *Nat. Rev. Genet.* 6, 435–450. doi: 10.1038/nrg1616

Silva-Correia, J., Freitas, S., Tavares, R. M., Lino-Neto, T., and Azevedo, H. (2014). Phenotypic analysis of the *Arabidopsis* heat stress response during germination and early seedling development. *Plant Methods* 10, 1–11. doi: 10.1186/1746-4811-10-7

Singh, A. K., Dhanapal, S., Finkelshtein, A., and Chamovitz, D. A. (2021). CSN5A subunit of COP9 signalosome is required for resetting transcriptional stress memory after recurrent heat stress in Arabidopsis. *Biomolecules* 11:668. doi: 10.3390/biom11050668

Sinha, A. K., Jaggi, M., Raghuram, B., and Tuteja, N. (2011). Mitogen-activated protein kinase signaling in plants under abiotic stress. *Plant Signal. Behav.* 6, 196–203. doi: 10.4161/psb.6.2.14701

Skalák, J., Černý, M., Jedelský, P., Dobrá, J., Ge, E., Novák, J., et al. (2016). Stimulation of ipt overexpression as a tool to elucidate the role of cytokinins in high temperature responses of *Arabidopsis thaliana*. *J. Exp. Bot.* 67, 2861–2873. doi: 10.1093/jxb/erw129

Slaughter, A., Daniel, X., Flors, V., Luna, E., Hohn, B., and Mauch-Mani, B. (2012). Descendants of primed *Arabidopsis* plants exhibit resistance to biotic stress. *Plant Physiol.* 158, 835–843. doi: 10.1104/pp.111.191593

Song, L., Jiang, Y., Zhao, H., and Hou, M. (2012). Acquired thermotolerance in plants. *Plant Cell Tissue Organ Cult.* 111, 265–276. doi: 10.1007/s11240-012-0198-6

Song, Z.-T., Sun, L., Lu, S.-J., Tian, Y., Ding, Y., and Liu, J.-X. (2015). Transcription factor interaction with COMPASS-like complex regulates histone H3K4 trimethylation for specific gene expression in plants. *Proc. Natl. Acad. Sci. U.S.A.* 112, 2900–2905. doi: 10.1073/pnas.1419703112

Stief, A., Altmann, S., Hoffmann, K., Pant, B. D., Scheible, W.-R., and Bäurle, I. (2014). Arabidopsis miR156 regulates tolerance to recurring environmental stress through SPL transcription factors. *Plant Cell* 26, 1792–1807. doi: 10.1105/tpc.114.123851

Streb, P., Aubert, S., Gout, E., Feierabend, J., and Bligny, R. (2008). Cross tolerance to heavy-metal and cold-induced photoinhibiton in leaves of Pisum sativum acclimated to low temperature. *Physiol. Mol. Biol. Plants* 14, 185–193. doi: 10.1007/s12298-008-0018-y

Su, Y., Huang, Y., Dong, X., Wang, R., Tang, M., Cai, J., et al. (2021). Exogenous methyl jasmonate improves heat tolerance of perennial ryegrass through alteration of osmotic adjustment, antioxidant defense, and expression of jasmonic acid-responsive genes. *Front. Plant Sci.* 12:664519. doi: 10.3389/fpls.2021.664519

Sun, J., Qi, L., Li, Y., Chu, J., and Li, C. (2012). PIF4–mediated activation of YUCCA8 expression integrates temperature into the auxin pathway in regulating *Arabidopsis* hypocotyl growth. *PLoS Genet.* 8:e1002594. doi: 10.1371/journal.pgen.1002594

Suter, L., and Widmer, A. (2013). Environmental heat and salt stress induce transgenerational phenotypic changes in *Arabidopsis thaliana*. *PLoS One* 8:e60364. doi: 10.1371/journal.pone.0060364

Suzuki, N., Bassil, E., Hamilton, J. S., Inupakutika, M. A., Zandalinas, S. I., Tripathy, D., et al. (2016). ABA is required for plant acclimation to a combination of salt and heat stress. *PLoS One* 11:e0147625. doi: 10.1371/journal.pone.0147625

Suzuki, N., Devireddy, A. R., Inupakutika, M. A., Baxter, A., Miller, G., Song, L., et al. (2015). Ultra-fast alterations in mRNA levels uncover multiple players in light stress acclimation in plants. *Plant J.* 84, 760–772. doi: 10.1111/tpj.13039

Suzuki, N., Koussevitzky, S., Mittler, R., and Miller, G. (2012). ROS and redox signalling in the response of plants to abiotic stress. *Plant Cell Environ.* 35, 259–270. doi: 10.1111/j.1365-3040.2011.02336.x

Suzuki, T., Inagaki, S., Nakajima, S., Akashi, T., Ohto, M. A., Kobayashi, M., et al. (2004). A novel *Arabidopsis* gene TONSOKU is required for proper cell arrangement in root and shoot apical meristems. *Plant J.* 38, 673–684. doi: 10.1111/j.1365-313X.2004.02074.x

Swindell, W. R., Huebner, M., and Weber, A. P. (2007). Transcriptional profiling of Arabidopsis heat shock proteins and transcription factors reveals extensive overlap between heat and non-heat stress response pathways. *BMC Genomics* 8:125. doi: 10.1186/1471-2164-8-125

Szabados, L., and Savouré, A. (2010). Proline: a multifunctional amino acid. *Trends Plant Sci.* 15, 89–97. doi: 10.1016/j.tplants.2009.11.009

Takahashi, F., Yoshida, R., Ichimura, K., Mizoguchi, T., Seo, S., Yonezawa, M., et al. (2007). The mitogen-activated protein kinase cascade MKK3–MPK6 is an important part of the jasmonate signal transduction pathway in *Arabidopsis*. *Plant Cell* 19, 805–818. doi: 10.1105/tpc.106.046581

Takeda, S., Tadele, Z., Hofmann, I., Probst, A. V., Angelis, K. J., Kaya, H., et al. (2004). BRU1, a novel link between responses to DNA damage and epigenetic gene silencing in *Arabidopsis*. *Genes Dev.* 18, 782–793. doi: 10.1101/gad.295404

Tan, D. X., Hardeland, R., Manchester, L. C., Korkmaz, A., Ma, S., Rosales-Corral, S., et al. (2012). Functional roles of melatonin in plants, and perspectives in nutritional and agricultural science. *J. Exp. Bot.* 63, 577–597. doi: 10.1093/jxb/err256

Tang, R.-S., Zheng, J.-C., Jin, Z.-Q., Zhang, D.-D., Huang, Y.-H., and Chen, L.-G. (2008). Possible correlation between high temperature-induced floret sterility and endogenous levels of IAA, GAs and ABA in rice (*Oryza sativa* L.). *Plant Growth Regul.* 54, 37–43. doi: 10.1007/s10725-007-9225-8

Terrile, M., Iglesias, M., Casalongué, C., and París, R. (2020). "Reactive nitrogen species mediated cross-stress tolerance in plants," in *Priming-Mediated Stress and Cross-Stress Tolerance in Crop Plants*, eds B. Huang, D. J. Burritt, F. Liu, M. Fujita, and M. A. Hossain (Amsterdam: Elsevier), 133–148. doi: 10.1016/B978-0-12-817892-8.00008-8

Thirumalaikumar, V. P., Gorka, M., Schulz, K., Masclaux-Daubresse, C., Sampathkumar, A., Skirycz, A., et al. (2021). Selective autophagy regulates heat stress memory in *Arabidopsis* by NBR1-mediated targeting of HSP90. 1 and ROF1. *Autophagy* 17, 2184–2199. doi: 10.1080/15548627.2020.1820778

Thoma, F., Koller, T., and Klug, A. (1979). Involvement of histone H1 in the organization of the nucleosome and of the salt-dependent superstructures of chromatin. *J. Cell Biol.* 83, 403–427. doi: 10.1083/jcb.83.2.403

Thomashow, M. F. (1999). Plant cold acclimation: freezing tolerance genes and regulatory mechanisms. *Annu. Rev. Plant Biol.* 50, 571–599. doi: 10.1146/annurev.arplant.50.1.571

Timperio, A. M., Egidi, M. G., and Zolla, L. (2008). Proteomics applied on plant abiotic stresses: role of heat shock proteins (HSP). *J. Proteomics* 71, 391–411. doi: 10.1016/j.jprot.2008.07.005

Ton, J., Jakab, G., Toquin, V., Flors, V., Iavicoli, A., Maeder, M. N., et al. (2005). Dissecting the β-aminobutyric acid–induced priming phenomenon in *Arabidopsis*. *Plant Cell* 17, 987–999. doi: 10.1105/tpc.104.029728

Trevaskis, B., Bagnall, D. J., Ellis, M. H., Peacock, W. J., and Dennis, E. S. (2003). MADS box genes control vernalization-induced flowering in cereals. *Proc. Natl. Acad. Sci. U.S.A.* 100, 13099–13104. doi: 10.1073/pnas.1635053100

Upadhyaya, C. P., Venkatesh, J., Gururani, M. A., Asnin, L., Sharma, K., Ajappala, H., et al. (2011). Transgenic potato overproducing L-ascorbic acid resisted an increase in methylglyoxal under salinity stress via maintaining higher reduced glutathione level and glyoxalase enzyme activity. *Biotechnol. Lett.* 33, 2297–2307. doi: 10.1007/s10529-011-0684-7

Van Aken, O., De Clercq, I., Ivanova, A., Law, S. R., Van Breusegem, F., Millar, A. H., et al. (2016). Mitochondrial and chloroplast stress responses are modulated in distinct touch and chemical inhibition phases. *Plant Physiol.* 171, 2150–2165. doi: 10.1104/pp.16.00273

Vanková, R., Kosová, K., Dobrev, P., Vítámvás, P., Trávníčková, A., Cvikrová, M., et al. (2014). Dynamics of cold acclimation and complex phytohormone responses in Triticum monococcum lines G3116 and DV92 differing in vernalization and frost tolerance level. *Environ. Exp. Bot.* 101, 12–25. doi: 10.1016/j.envexpbot.2014.01.002

Vaucheret, H., Mallory, A. C., and Bartel, D. P. (2006). AGO1 homeostasis entails coexpression of MIR168 and AGO1 and preferential stabilization of miR168 by AGO1. *Mol. Cell* 22, 129–136. doi: 10.1016/j.molcel.2006.03.011

Verbruggen, N., and Hermans, C. (2008). Proline accumulation in plants: a review. *Amino Acids* 35, 753–759. doi: 10.1007/s00726-008-0061-6

Verma, V., Ravindran, P., and Kumar, P. P. (2016). Plant hormone-mediated regulation of stress responses. *BMC Plant Biol.* 16:86. doi: 10.1186/s12870-016-0771-y

von Koskull-Döring, P., Scharf, K.-D., and Nover, L. (2007). The diversity of plant heat stress transcription factors. *Trends Plant Sci.* 12, 452–457. doi: 10.1016/j.tplants.2007.08.014

Vu, W. T., Chang, P. L., Moriuchi, K. S., and Friesen, M. L. (2015). Genetic variation of transgenerational plasticity of offspring germination in response to salinity stress and the seed transcriptome of *Medicago truncatula*. *BMC Evol. Biol.* 15:59. doi: 10.1186/s12862-015-0322-4

Wahid, A., Gelani, S., Ashraf, M., and Foolad, M. R. (2007). Heat tolerance in plants: an overview. *Environ. Exp. Bot.* 61, 199–223. doi: 10.1016/j.envexpbot.2007.05.011

Walter, J., Nagy, L., Hein, R., Rascher, U., Beierkuhnlein, C., Willner, E., et al. (2011). Do plants remember drought? Hints towards a drought-memory in grasses. *Environ. Exp. Bot.* 71, 34–40. doi: 10.1016/j.envexpbot.2010.10.020

Wan, S. B., Tian, L., Tian, R. R., Pan, Q. H., Zhan, J. C., Wen, P. F., et al. (2009). Involvement of phospholipase D in the low temperature acclimation-induced thermotolerance in grape berry. *Plant Physiol. Biochem.* 47, 504–510. doi: 10.1016/j.plaphy.2008.12.010

Wang, K., Zhang, X., and Ervin, E. (2013). Effects of nitrate and cytokinin on creeping bentgrass under supraoptimal temperatures. *J. Plant Nutr.* 36, 1549–1564. doi: 10.1080/01904167.2013.799184

Wang, M., Yue, H., Feng, K., Deng, P., Song, W., and Nie, X. (2016). Genome-wide identification, phylogeny and expressional profiles of mitogen activated protein kinase kinase kinase (MAPKKK) gene family in bread wheat (*Triticum aestivum* L.). *BMC Genomics* 17:668. doi: 10.1186/s12864-016-2993-7

Wang, P., Zhao, Y., Li, Z., Hsu, C. C., Liu, X., Fu, L., et al. (2018). Reciprocal regulation of the TOR kinase and ABA receptor balances plant growth and stress response. *Mol. Cell* 69, 100–112. doi: 10.1016/j.molcel.2017.12.002

Wang, R., Zhang, Y., Kieffer, M., Yu, H., Kepinski, S., and Estelle, M. (2016). HSP90 regulates temperature-dependent seedling growth in *Arabidopsis* by stabilizing the auxin co-receptor F-box protein TIR1. *Nat. Commun.* 7, 1–11. doi: 10.1038/ncomms10269

Wang, X., Cai, J., Liu, F., Dai, T., Cao, W., Wollenweber, B., et al. (2014a). Multiple heat priming enhances thermo-tolerance to a later high temperature stress via improving subcellular antioxidant activities in wheat seedlings. *Plant Physiol. Biochem.* 74, 185–192. doi: 10.1016/j.plaphy.2013.11.014

Wang, X., Vignjevic, M., Jiang, D., Jacobsen, S., and Wollenweber, B. (2014b). Improved tolerance to drought stress after anthesis due to priming before anthesis in wheat (*Triticum aestivum* L.) var. Vinjett. *J. Exp. Bot.* 65, 6441–6456. doi: 10.1093/jxb/eru362

Wang, X., Cai, J., Liu, F., Jin, M., Yu, H., Jiang, D., et al. (2012). Pre-anthesis high temperature acclimation alleviates the negative effects of post-anthesis heat stress on stem stored carbohydrates remobilization and grain starch accumulation in wheat. *J. Cereal Sci.* 55, 331–336. doi: 10.1016/j.jcs.2012.01.004

Wang, X., Li, Z., Liu, B., Zhou, H., Elmongy, M. S., and Xia, Y. (2020). Combined proteome and transcriptome analysis of heat-primed azalea reveals new insights into plant heat acclimation memory. *Front. Plant Sci.* 11:1278. doi: 10.3389/fpls.2020.01278

Wang, X., Vignjevic, M., Liu, F., Jacobsen, S., Jiang, D., and Wollenweber, B. (2015). Drought priming at vegetative growth stages improves tolerance to drought and heat stresses occurring during grain filling in spring wheat. *Plant Growth Regul.* 75, 677–687. doi: 10.1007/s10725-014-9969-x

Wang, X., Xin, C., Cai, J., Zhou, Q., Dai, T., Cao, W., et al. (2016). Heat priming induces trans-generational tolerance to high temperature stress in wheat. *Front. Plant Sci.* 7:501. doi: 10.3389/fpls.2016.00501

Wang, X., Zhang, X., Chen, J., Wang, X., Cai, J., Zhou, Q., et al. (2018). Parental drought-priming enhances tolerance to post-anthesis drought in offspring of wheat. *Front. Plant Sci.* 9:261. doi: 10.3389/fpls.2018.00261

Wang, X., Zhuang, L., Shi, Y., and Huang, B. (2017). Up-regulation of HSFA2c and HSPs by ABA contributing to improved heat tolerance in tall fescue and *Arabidopsis*. *Int. J. Mol. Sci.* 18:1981. doi: 10.3390/ijms18091981

Wang, Y., Sun, F., Cao, H., Peng, H., Ni, Z., Sun, Q., et al. (2012). TamiR159 directed wheat TaGAMYB cleavage and its involvement in anther development and heat response. *PLoS One* 7:e48445. doi: 10.1371/journal.pone.0048445

Waqas, M., Khan, A. L., Shahzad, R., Ullah, I., Khan, A. R., and Lee, I.-J. (2015). Mutualistic fungal endophytes produce phytohormones and organic acids that promote japonica rice plant growth under prolonged heat stress. *J. Zhejiang Univ. Sci. B* 16, 1011–1018. doi: 10.1631/jzus.B1500081

Wassie, M., Zhang, W., Zhang, Q., Ji, K., Cao, L., and Chen, L. (2020). Exogenous salicylic acid ameliorates heat stress-induced damages and improves growth and photosynthetic efficiency in alfalfa (*Medicago sativa* L.). *Ecotoxicol. Environ. Saf.* 191:110206. doi: 10.1016/j.ecoenv.2020.110206

Wasternack, C., and Hause, B. (2013). Jasmonates: biosynthesis, perception, signal transduction and action in plant stress response, growth and development. An update. *Ann. Bot.* 111, 1021–1058. doi: 10.1093/aob/mct067

Watanabe, C. K., Yamori, W., Takahashi, S., Terashima, I., and Noguchi, K. (2016). Mitochondrial alternative pathway-associated photoprotection of photosystem II is related to the photorespiratory pathway. *Plant Cell Physiol.* 57, 1426–1431. doi: 10.1093/pcp/pcw036

Weng, M., Yang, Y. U. E., Feng, H., Pan, Z., Shen, W. H., Zhu, Y. A. N., et al. (2014). Histone chaperone ASF1 is involved in gene transcription activation in response to heat stress in *Arabidopsis thaliana*. *Plant Cell Environ.* 37, 2128–2138. doi: 10.1111/pce.12299

Wind, J., Smeekens, S., and Hanson, J. (2010). Sucrose: metabolite and signaling molecule. *Phytochemistry* 71, 1610–1614. doi: 10.1016/j.phytochem.2010.07.007

Wu, C., Cui, K., Wang, W., Li, Q., Fahad, S., Hu, Q., et al. (2017). Heat-induced cytokinin transportation and degradation are associated with reduced panicle cytokinin expression and fewer spikelets per panicle in rice. *Front. Plant Sci.* 8:371. doi: 10.3389/fpls.2017.00371

Wu, L., Zhou, H., Zhang, Q., Zhang, J., Ni, F., Liu, C., et al. (2010). DNA methylation mediated by a microRNA pathway. *Mol. Cell* 38, 465–475. doi: 10.1016/j.molcel.2010.03.008

Wu, T. Y., Juan, Y. T., Hsu, Y. H., Wu, S. H., Liao, H. T., Fung, R. W., et al. (2013). Interplay between heat shock proteins HSP101 and HSA32 prolongs heat acclimation memory posttranscriptionally in *Arabidopsis*. *Plant Physiol.* 161, 2075–2084. doi: 10.1104/pp.112.212589

Wu, Y.-S., and Yang, C.-Y. (2019). Ethylene-mediated signaling confers thermotolerance and regulates transcript levels of heat shock factors in rice seedlings under heat stress. *Bot. Stud.* 60, 1–12. doi: 10.1186/s40529-019-0272-z

Xia, X. J., Gao, C. J., Song, L. X., Zhou, Y. H., Shi, K., and Yu, J. Q. (2014). Role of H2O2 dynamics in brassinosteroid-induced stomatal closure and opening in *Solanum lycopersicum*. *Plant Cell Environ.* 37, 2036–2050. doi: 10.1111/pce.12275

Xia, X. J., Wang, Y. J., Zhou, Y. H., Tao, Y., Mao, W. H., Shi, K., et al. (2009). Reactive oxygen species are involved in brassinosteroid-induced stress tolerance in cucumber. *Plant Physiol.* 150, 801–814. doi: 10.1104/pp.109.138230

Xia, X.-J., Zhou, Y.-H., Shi, K., Zhou, J., Foyer, C. H., and Yu, J.-Q. (2015). Interplay between reactive oxygen species and hormones in the control of plant development and stress tolerance. *J. Exp. Bot.* 66, 2839–2856. doi: 10.1093/jxb/erv089

Xiao, W., Liu, F.-l, and Jiang, D. (2017). Priming: a promising strategy for crop production in response to future climate. *J. Integr. Agric.* 16, 2709–2716. doi: 10.1016/S2095-3119(17)61786-6

Xin, C., Wang, X., Cai, J., Zhou, Q., Liu, F., Dai, T., et al. (2016). Changes of transcriptome and proteome are associated with the enhanced post-anthesis high temperature tolerance induced by pre-anthesis heat priming in wheat. *Plant Growth Regul.* 79, 135–145. doi: 10.1007/s10725-015-0119-x

Xue, G.-P., Sadat, S., Drenth, J., and McIntyre, C. L. (2014). The heat shock factor family from *Triticum aestivum* in response to heat and other major abiotic stresses and their role in regulation of heat shock protein genes. *J. Exp. Bot.* 65, 539–557. doi: 10.1093/jxb/ert399

Yadav, S. K., Singla-Pareek, S. L., Ray, M., Reddy, M., and Sopory, S. (2005). Methylglyoxal levels in plants under salinity stress are dependent on glyoxalase I and glutathione. *Biochem. Biophys. Res. Commun.* 337, 61–67. doi: 10.1016/j.bbrc.2005.08.263

Yamaguchi, N., and Ito, T. (2021). Expression profiling of H3K27me3 demethylase genes during plant development and in response to environmental stress in *Arabidopsis*. *Plant Signal. Behav.* 16:1950445. doi: 10.1080/15592324.2021.1950445

Yan, L., Loukoianov, A., Tranquilli, G., Helguera, M., Fahima, T., and Dubcovsky, J. (2003). Positional cloning of the wheat vernalization gene VRN1. *Proc. Natl. Acad. Sci. U.S.A.* 100, 6263–6268. doi: 10.1073/pnas.0937399100

Yang, D., Li, Y., Shi, Y., Cui, Z., Luo, Y., Zheng, M., et al. (2016). Exogenous cytokinins increase grain yield of winter wheat cultivars by improving stay-green characteristics under heat stress. *PLoS One* 11:e0155437. doi: 10.1371/journal.pone.0155437

Yang, J., Fei, K., Chen, J., Wang, Z., Zhang, W., and Zhang, J. (2020). Jasmonates alleviate spikelet-opening impairment caused by high temperature stress during anthesis of photo-thermo-sensitive genic male sterile rice lines. *Food Energy Security* 9:e233. doi: 10.1002/fes3.233

Yang, J., Kloepper, J. W., and Ryu, C.-M. (2009). Rhizosphere bacteria help plants tolerate abiotic stress. *Trends Plant Sci.* 14, 1–4. doi: 10.1016/j.tplants.2008.10.004

Yang, X., Zhu, W., Zhang, H., Liu, N., and Tian, S. (2016). Heat shock factors in tomatoes: genome-wide identification, phylogenetic analysis and expression profiling under development and heat stress. *PeerJ* 4:e1961. doi: 10.7717/peerj.1961

Yeh, C.-H., Kaplinsky, N. J., Hu, C., and Charng, Y.-Y. (2012). Some like it hot, some like it warm: phenotyping to explore thermotolerance diversity. *Plant Sci.* 195, 10–23. doi: 10.1016/j.plantsci.2012.06.004

Yoon, Y. H., Kim, M., and Park, W. J. (2019). Foliar accumulation of melatonin applied to the roots of maize (*Zea mays*) seedlings. *Biomolecules* 9:26. doi: 10.3390/biom9010026

Yoshida, T., Ohama, N., Nakajima, J., Kidokoro, S., Mizoi, J., Nakashima, K., et al. (2011). Arabidopsis HsfA1 transcription factors function as the main positive regulators in heat shock-responsive gene expression. *Mol. Genet. Genomics* 286, 321–332. doi: 10.1007/s00438-011-0647-7

Yu, X., Wang, H., Lu, Y., de Ruiter, M., Cariaso, M., Prins, M., et al. (2012). Identification of conserved and novel microRNAs that are responsive to heat stress in *Brassica rapa*. *J. Exp. Bot.* 63, 1025–1038. doi: 10.1093/jxb/err337

Yucel, M., Burke, J. J., and Nguyen, H. T. (1992). Inhibition and recovery of photosystem II following exposure of wheat to heat shock. *Environ. Exp. Bot.* 32, 133–135. doi: 10.1016/0098-8472(92)90037-3

Zandalinas, S. I., Balfagón, D., Arbona, V., Gómez-Cadenas, A., Inupakutika, M. A., and Mittler, R. (2016). ABA is required for the accumulation of APX1 and MBF1c during a combination of water deficit and heat stress. *J. Exp. Bot.* 67, 5381–5390. doi: 10.1093/jxb/erw299

Zhang, C., Li, G., Chen, T., Feng, B., Fu, W., Yan, J., et al. (2018). Heat stress induces spikelet sterility in rice at anthesis through inhibition of pollen tube elongation interfering with auxin homeostasis in pollinated pistils. *Rice* 11, 1–12. doi: 10.1186/s12284-018-0206-5

Zhang, H., Lang, Z., and Zhu, J.-K. (2018). Dynamics and function of DNA methylation in plants. *Nat. Rev. Mol. Cell Biol.* 19, 489–506. doi: 10.1038/s41580-018-0016-z

Zhang, J. H., Huang, W. D., Liu, Y. P., and Pan, Q. H. (2005). Effects of temperature acclimation pretreatment on the ultrastructure of mesophyll cells in young grape plants (*Vitis vinifera* L. cv. Jingxiu) under cross-temperature stresses. *J. Integr. Plant Biol.* 47, 959–970. doi: 10.1111/j.1744-7909.2005.00109.x

Zhang, N., Zhang, H. J., Zhao, B., Sun, Q. Q., Cao, Y. Y., Li, R., et al. (2014). The RNA-seq approach to discriminate gene expression profiles in response to melatonin on cucumber lateral root formation. *J. Pineal Res.* 56, 39–50. doi: 10.1111/jpi.12095

Zhang, X., Cai, J., Wollenweber, B., Liu, F., Dai, T., Cao, W., et al. (2013a). Multiple heat and drought events affect grain yield and accumulations of high molecular weight glutenin subunits and glutenin macropolymers in wheat. *J. Cereal Sci.* 57, 134–140. doi: 10.1016/j.jcs.2012.10.010

Zhang, X., Shen, L., Li, F., Meng, D., and Sheng, J. (2013b). Arginase induction by heat treatment contributes to amelioration of chilling injury and activation of antioxidant enzymes in tomato fruit. *Postharvest Biol. Technol.* 79, 1–8. doi: 10.1016/j.postharvbio.2012.12.019

Zhang, X., Zhou, Q., Wang, X., Cai, J., Dai, T., Cao, W., et al. (2016b). Physiological and transcriptional analyses of induced post-anthesis thermo-tolerance by heat-shock pretreatment on germinating seeds of winter wheat. *Environ. Exp. Bot.* 131, 181–189. doi: 10.1016/j.envexpbot.2016.08.002

Zhang, X., Wang, X., Zhong, J., Zhou, Q., Wang, X., Cai, J., et al. (2016a). Drought priming induces thermo-tolerance to post-anthesis high-temperature in offspring of winter wheat. *Environ. Exp. Bot.* 127, 26–36. doi: 10.1016/j.envexpbot.2016.03.004

Zhang, X., Xu, Y., and Huang, B. (2019b). Lipidomic reprogramming associated with drought stress priming-enhanced heat tolerance in tall fescue (*Festuca arundinacea*). *Plant Cell Environ.* 42, 947–958. doi: 10.1111/pce.13405

Zhang, X., Wang, X., Zhuang, L., Gao, Y., and Huang, B. (2019a). Abscisic acid mediation of drought priming-enhanced heat tolerance in tall fescue (*Festuca arundinacea*) and *Arabidopsis*. *Physiol. Plant.* 167, 488–501. doi: 10.1111/ppl.12975

Zhang, Y., He, J., Yang, S., and Chen, Y. (2014). Exogenous 24-epibrassinolide ameliorates high temperature-induced inhibition of growth and photosynthesis in *Cucumis melo*. *Biol. Plant.* 58, 311–318. doi: 10.1007/s10535-014-0395-8

Zhang, Z., Liu, X., Wang, X., Zhou, M., Zhou, X., Ye, X., et al. (2012). An R2R3 MYB transcription factor in wheat, Ta PIMP 1, mediates host resistance to *Bipolaris sorokiniana* and drought stresses through regulation of defense-and stress-related genes. *New Phytol.* 196, 1155–1170. doi: 10.1111/j.1469-8137.2012.04353.x

Zhao, D.-Q., Li, T.-T., Hao, Z.-J., Cheng, M.-L., and Tao, J. (2019). Exogenous trehalose confers high temperature stress tolerance to herbaceous peony by enhancing antioxidant systems, activating photosynthesis, and protecting cell structure. *Cell Stress Chaperones* 24, 247–257.

Zhao, J., Gao, Y., Zhang, Z., Chen, T., Guo, W., and Zhang, T. (2013). A receptor-like kinase gene (GbRLK) from Gossypium barbadense enhances salinity and drought-stress tolerance in *Arabidopsis*. *BMC Plant Biol.* 13:110. doi: 10.1186/1471-2229-13-110

Zhou, J., Wang, J., Li, X., Xia, X. J., Zhou, Y. H., Shi, K., et al. (2014). H2O2 mediates the crosstalk of brassinosteroid and abscisic acid in tomato responses to heat and oxidative stresses. *J. Exp. Bot.* 65, 4371–4383. doi: 10.1093/jxb/eru217

Zhou, R., Yu, X., Li, X., Dos Santos, T. M., Rosenqvist, E., and Ottosen, C. O. (2020). Combined high light and heat stress induced complex response in tomato with better leaf cooling after heat priming. *Plant Physiol. Biochem.* 151, 1–9. doi: 10.1016/j.plaphy.2020.03.011

Zhu, J. K. (2016). Abiotic stress signaling and responses in plants. *Cell* 167, 313–324. doi: 10.1016/j.cell.2016.08.029

Zhu, X.-C., Song, F.-B., Liu, S.-Q., and Liu, T.-D. (2011). Effects of arbuscular mycorrhizal fungus on photosynthesis and water status of maize under high temperature stress. *Plant Soil* 346, 189–199. doi: 10.1007/s11104-011-0809-8

Conflict of Interest: The authors declare that the research was conducted in the absence of any commercial or financial relationships that could be construed as a potential conflict of interest.

Publisher's Note: All claims expressed in this article are solely those of the authors and do not necessarily represent those of their affiliated organizations, or those of the publisher, the editors and the reviewers. Any product that may be evaluated in this article, or claim that may be made by its manufacturer, is not guaranteed or endorsed by the publisher.

Copyright © 2022 Khan, Khan, Pandey, Sopory and Sanan-Mishra. This is an open-access article distributed under the terms of the Creative Commons Attribution License (CC BY). The use, distribution or reproduction in other forums is permitted, provided the original author(s) and the copyright owner(s) are credited and that the original publication in this journal is cited, in accordance with accepted academic practice. No use, distribution or reproduction is permitted which does not comply with these terms.

frontiers | Frontiers in Plant Science

MINI REVIEW
published: 30 May 2022
doi: 10.3389/fpls.2022.895698

Core Components of Abscisic Acid Signaling and Their Post-translational Modification

*Junsub Lim†, Chae Woo Lim† and Sung Chul Lee**

Department of Life Science (BK21 Program), Chung-Ang University, Seoul, South Korea

Abscisic acid (ABA) is a major phytohormone that regulates plant growth, development, and abiotic/biotic stress responses. Under stress, ABA is synthesized in various plant organs, and it plays roles in diverse adaptive processes, including seed dormancy, growth inhibition, and leaf senescence, by modulating stomatal closure and gene expression. ABA receptor, clade A protein phosphatase 2C (PP2C), and SNF1-related protein kinase 2 (SnRK2) proteins have been identified as core components of ABA signaling, which is initiated *via* perception of ABA with receptor and subsequent activation or inactivation by phosphorylation/dephosphorylation. The findings of several recent studies have established that the post-translational modification of these components, including phosphorylation and ubiquitination/deubiquitination, play important roles in regulating their activity and stability. In this review, we discuss the functions of the core components of ABA signaling and the regulation of their activities *via* post-translational modification under normal and stress conditions.

Keywords: abscisic acid, core component of ABA signaling, phosphorylation, post-translational modification, ubiquitination

OPEN ACCESS

Edited by:
Girdhar Kumar Pandey, University of Delhi, India

Reviewed by:
Andreas Bachmair, University of Vienna, Austria

***Correspondence:**
Sung Chul Lee
sclee1972@cau.ac.kr

†These authors have contributed equally to this work

Specialty section:
This article was submitted to Plant Physiology, a section of the journal Frontiers in Plant Science

Received: *14 March 2022*
Accepted: *03 May 2022*
Published: *30 May 2022*

Citation:
Lim J, Lim CW and Lee SC (2022) Core Components of Abscisic Acid Signaling and Their Post-translational Modification. Front. Plant Sci. 13:895698. doi: 10.3389/fpls.2022.895698

INTRODUCTION

Abscisic acid (ABA) is a major hormone that regulates growth, development, and responses to abiotic/biotic stress throughout the life cycle of plants. Under environmental conditions perceived as unsuitable for plant growth, ABA helps maintain seed dormancy and inhibits germination, whereas during the post-germination stage, this hormone inhibits growth to conserve energy (Chinnusamy et al., 2008; Raghavendra et al., 2010). In addition, ABA plays key roles in stomatal opening and closure, thereby contributing to the regulation of water loss under drought stress (Melotto et al., 2006; Hirayama and Shinozaki, 2007; Cutler et al., 2010; Finkelstein, 2013).

The core components of ABA signaling, along with their roles and regulatory mechanisms, are well known. As ABA receptors, pyrabactin resistance 1 (PYR1)/PYR1-like (PYL)/regulatory components of the ABA receptor (RCAR) family bind ABA in response to abiotic stress and positively regulate ABA signaling (Ma et al., 2009; Park et al., 2009; Santiago et al., 2009; Gonzalez-Guzman et al., 2012; Antoni et al., 2013). Under normal conditions, clade A protein phosphatase 2Cs (PP2Cs) play roles as negative regulator of ABA signaling by binding to subclass III sucrose nonfermenting 1 (SNF1)-related protein kinase 2 (SnRK2) proteins, and subsequently these interactions inactivate downstream ABA signaling factors and inhibit ABA

responses to facilitate growth and development (Mustilli et al., 2002; Yoshida et al., 2006a; Fujii et al., 2007; Umezawa et al., 2009; Vlad et al., 2009). Under stress conditions, ABA receptors interact with PP2Cs and SnRK2s are released from PP2Cs-mediated inhibition, leading to autophosphorylation or phosphorylation by other kinases, whereupon the activated SnRK2s phosphorylate downstream targets, including transcription factors and channel proteins, thereby facilitating abiotic stress responses (Fujii and Zhu, 2009; Geiger et al., 2009; Yin et al., 2009; Nishimura et al., 2010; Ng et al., 2011; Xue et al., 2011; Brandt et al., 2012; Soon et al., 2012).

The different components of ABA signaling are modulated to varying extents by post-translational modification (**Table 1**), with the ubiquitination/deubiquitination and phosphorylation of these components being generally well studied. Ubiquitination of ABA core components can influence ABA signaling and responses both positively and negatively (Coego et al., 2021). Deubiquitination mediated by members of the UBIQUITIN-SPECIFIC PROTEASE (UBP) protein family affects a range of plant physiological processes, including growth, development, immunity, and stress response (Zhou et al., 2017). However, the biochemical mechanisms underlying the involvement of UBPs in ABA signaling have yet to be sufficiently elucidated. A further major category of post-translational modification is phosphorylation; ABA receptors, PP2Cs, and SnRK2s can be positively or negatively regulated by phosphorylation. For example, SnRK2s can undergo autophosphorylation and activation (Yang et al., 2017; Chen et al., 2020). In this review, we focus on the roles of ABA, core ABA signaling pathways, and post-transcriptional regulation of ABA signaling components in plants.

TABLE 1 | Post-translational regulation factors of ABA core components in *Arabidopsis*.

Post-translational regulation	Enzyme	Targets	References
Ubiquitination	RSL1	PYR1/PYL4	Bueso et al., 2014
Ubiquitination	$CRL4^{DDA1}$	PYL8	Irigoyen et al., 2014
Ubiquitination	RFA1/RFA4	PYR1/PYL4	Fernandez et al., 2020
Ubiquitination	PUB12/13	ABI1	Kong et al., 2015
Ubiquitination	$CRL3^{BPM3/5}$	PP2CA, ABI1, HAB1	Julian et al., 2019
Ubiquitination	AIRP3	ABI1	Pan et al., 2020
Ubiquitination	PIR1/2	PP2CA	Baek et al., 2019b
Ubiquitination	RGLG1/5	PP2CA, ABI2, HAB2	Wu et al., 2016
Endosomal degradation	FYVE1/FREE1	PYR1/PYL4	Belda-Palazon et al., 2016
Endosomal degradation	VPS23A	PYR1/PYL4	Yu et al., 2016
Endosomal degradation	ALIX	PYL4	Garcia-Leon et al., 2019
Phosphorylation	TOR	PYL1/PYL4	Wang et al., 2018a
Phosphorylation	AEL	PYR1/PYL1	Chen et al., 2018
Phosphorylation	CEPR2	PYL1/PYL2/PYL4	Yu et al., 2019
Phosphorylation	CARK1	PYR1/PYL1/PYL2/PYL3/PYL8	Zhang et al., 2018; Li et al., 2019
Phosphorylation	PR5K2	ABI1/2	Baek et al., 2019a
Phosphorylation	BIN2	SnRK2.2/2.3	Cai et al., 2014
Phosphorylation	RAF10	SnRK2.2/2.3/2.6	Nguyen et al., 2019

THE ROLE OF ABA IN ABIOTIC STRESS RESPONSES

Regulation of Stomatal Closure

In response to drought stress, ABA induces stomatal closure to reduce transpirational water loss (Bauer et al., 2013). ABA modulates stomatal movement *via* both Ca^{2+}-dependent and -independent pathways. In the former, ABA induces Ca^{2+} channel opening to facilitate the influx of calcium ions, in response to which upregulated reactive oxygen species levels and inositol-1-4-5-triphosphate contribute to increases in cytosolic Ca^{2+} content (Lee et al., 1996; Pei et al., 2000; Murata et al., 2001; Mustilli et al., 2002), which in turn modulates multiple signal transduction. Calcium-dependent protein kinases (CPKs) 3/4/6/10/11 phosphorylate and activate slow-type anion efflux channels, including SLOW ANION CHANNEL-ASSOCIATED 1 (SLAC1) and SLAC1 HOMOLOG 3 (SLAH3; Mori et al., 2006; Zhu et al., 2007; Zou et al., 2010; Brandt et al., 2012), whereas CPK21 phosphorylates K^+ outward rectifying channel GORK to promote the efflux of K^+ ions; KAT1 and KAT2 are inactivated by CPK13 to inhibit K^+ ion influx (Hosy et al., 2003; van Kleeff et al., 2018). In contrast, the Ca^{2+}-independent pathway is associated with SnRK2.6 (Li et al., 2000), which activates SLAC1 and KUP6, the latter of which is a KUP/HAK/KT family K^+ efflux transporter, thereby suppressing KAT1 activity *via* phosphorylation (Kwak et al., 2001; Geiger et al., 2009; Lee et al., 2009; Sato et al., 2009a; Osakabe et al., 2013). SnRK2.6 has also been shown to phosphorylate the ABA-responsive kinase substrate AKS1, which binds to the *KAT1* promoter, thereby promoting the downregulated expression of *KAT1* (Takahashi et al., 2013). Collectively, these Ca^{2+}-dependent and Ca^{2+}-independent pathways contribute to reductions in guard cell turgor, thereby leading to stomatal closure.

Regulation of Dormancy and Germination

As sessile organisms, plants are particularly responsive to environmental cues with respect to the initiation of germination. Under unfavorable environmental conditions, ABA contributes to the suppression of germination by promoting seed dormancy, as revealed by the reduced seed dormancy of ABA biosynthesis and signaling-impaired mutants (Koornneef et al., 1982; Leon-Kloosterziel et al., 1996; Lefebvre et al., 2006; Nakashima et al., 2009a; Zhao et al., 2018). For example, the Raf-like MAKKKs, Raf10 and Raf11, influence seed dormancy by phosphorylating SnRK2s and ABRE-binding factors (ABFs; Lee et al., 2015; Nguyen et al., 2019). ABA can also influence seed germination by modifying hormonal balance. In contrast to ABA, gibberellic acid (GA) is a phytohormone that promotes seed germination (Debeaujon and Koornneef, 2000; Ogawa et al., 2003), and the activities of these two hormones antagonistically regulate seed dormancy and germination in

higher plants (Weiss and Ori, 2007; Golldack et al., 2013). Notably, compared with wild-type plants, ABA-deficient mutants are characterized by higher levels of GA, and it has accordingly been suggested that ABA plays a role in regulating the GA metabolic pathway (Seo et al., 2006). As a key repressor of GA signaling, REPRESSOR OF GA-LIKE 2 (RGL2) plays a negative role in seed germination, as indicated by the loss-of-function mutant *rgl2*, in which ABA concentrations are reduced and germination is promoted (Piskurewicz et al., 2008; Lee et al., 2010). RGL2 also promotes *ABI5* expression levels, thereby inducing the ABA-mediated suppression of germination (Liu et al., 2016). Exogenous ABA activates the expression of *RGL2* and *ABI5* (Piskurewicz et al., 2008), and thus RGL2 is believed to modulate the balance between ABA and GA contents during seed germination.

Regulation of Drought-Responsive Gene Expression

On exposure to drought stress, ABA induces the expression of several genes in mature plants that play roles in the drought stress response. Representative ABA-responsive marker genes in this context include *RESPONSIVE TO DESICCATION 29B (RD29B), RESPONSIVE TO ABA18 (RAB18), LATE EMBRYOGENESIS ABUNDANT 1 (EM1),* and *EM6*, the expression of which is induced under conditions of water limitation (Yamaguchi-Shinozaki and Shinozaki, 1994; Mantyla et al., 1995; Uno et al., 2000; Carles et al., 2002; Umezawa et al., 2006; Wang et al., 2018b). The expression of these genes is regulated by a number ABA-inducible transcription factors, including ABA-responsive element (ABRE)-binding proteins (AREBs) and ABFs, which contribute to the regulation of ABA-dependent gene expression under drought stress conditions (Nakashima et al., 2009b; Yoshida et al., 2015). It has also been established that a number drought stress-induced genes are also responsive to exogenous ABA, which is mediated *via* promoter region ABREs (Nakashima et al., 2009b; Fujita et al., 2011). For example, plants overexpressing (OX) the *AREB1/ABF2, AREB2/ABF4, ABF1,* and *ABF3* genes are characterized by enhanced ABA sensitivity and drought tolerance (Kang et al., 2002; Fujita et al., 2005). In contrast, *areb1*, *areb2*, and *abf3* mutants show reduced drought tolerance and ABA sensitivity (Yoshida et al., 2010). The transcripts of other transcription factors, such as *AtMYC2* and *AtMYB2*, have been found to accumulate in response to exogenous ABA, and in *AtMYC2*-OX and *AtMYB2*-OX plants, the ABA-inducible gene *RESPONSIVE TO DESICCATION 22 (RD22)* is upregulated, leading to ABA-sensitive and drought-tolerant phenotypes (Abe et al., 2003). Similarly, expression of the NAC transcription factor *RD26* is induced by drought and ABA treatment, with *RD26*-OX plants being characterized by hypersensitivity to exogenous ABA, whereas contrastingly, *RD26* dominant repressor plants exhibit an ABA-insensitive phenotype (Fujita et al., 2004). Collectively, these findings thus indicate that ABA induces ABA-responsive transcription factors, which in turn regulate the expression of ABA-responsive genes, thereby enhancing drought stress tolerance.

Regulation of Leaf Senescence

Exogenous ABA treatment has been widely demonstrated to induce leaf senescence (Gepstein and Thimann, 1980; Pourtau et al., 2004; Raab et al., 2009; Lee et al., 2011). Moreover, it has been observed that as leaves senesce, there is a corresponding increase in endogenous ABA levels (Gepstein and Thimann, 1980; Leon-Kloosterziel et al., 1996; Cheng et al., 2002; Breeze et al., 2011; Yang et al., 2014). In terms of gene expression, ABA signaling-associated genes have been found to be upregulated during leaf senescence and the expression of various senescence-associated genes can also be induced by the application of exogenous ABA (Tan et al., 2003; Parkash et al., 2014). An important factor associated with the induction of leaf senescence is chlorophyll degradation, which is mediated *via* genes such as *STAY-GREEN 1 (SGR1)*, *NON-YELLOW COLORING 1 (NYC1), PHEOPHYYTINASE (PPH),* and *PHEIDE a OXYGENASE (PaO)* (Pruzinska et al., 2005; Ren et al., 2007; Hortensteiner, 2009; Sato et al., 2009b; Schelbert et al., 2009). In this regard, *Arabidopsis thaliana* NAC-LIKE, ACTIVATED BY AP3/PI (AtNAP) has been found to bind to the promoter of *ABSCISIC ALDEHYDE OXIDASE 3 (AAO3)* to enhance *AAO3* transcription and ABA production, and this accumulation of ABA contributes to the induction of chlorophyll degradation-associated genes (Yang et al., 2014). ABA core components have also been established to be involved in chlorophyll degradation. For example, SnRK2s regulate the bZIP transcription factors ABI5 and ABF2/3/4, which directly activate *NYC1*, *PAO*, and *SENESCENCE-ASSOCIATED GENE 12* (*SAG12*), which are considered senescence marker genes (Gao et al., 2016; Zhao et al., 2016b).

ABA CORE COMPONENTS

Under abiotic stress conditions, ABA mediates responses *via* a core signaling pathway. As ABA receptors, PYR1 and PYLs were initially identified based on the characterization of ABA-insensitive mutants, whereas RCARs were identified *via* yeast two-hybrid screens with clade A PP2Cs (Ma et al., 2009; Park et al., 2009). As positive regulators of ABA signaling, PYRs, PYLs, and RCARs (Ma et al., 2009; Park et al., 2009; Santiago et al., 2009; Gonzalez-Guzman et al., 2012; Antoni et al., 2013) are characterized by star-related lipid-transfer domains that contain a conserved ligand-binding pocket and are localized to the nucleus, cytoplasm, and plasma membrane (Iyer et al., 2001; McConnell et al., 2001; Radauer et al., 2008). *Arabidopsis* also expresses a group of 13 genes that are similar to *Pyr1,* namely, *Pyl1* to *Pyl13* (*PYR1-Like*; Fujii et al., 2009; Li et al., 2013; Zhao et al., 2013), among which, *Pyr1/Pyl1/pyl2/pyl4* mutant alleles show an ABA insensitive phenotype in terms of seed germination and root growth with diminished ABA-responsive gene expression and SnRK2.6 kinase activity (Park et al., 2009). Under normal conditions, PP2Cs negatively regulate ABA signaling by interacting with SnRK2s and inhibiting kinase activity, whereas under stress conditions, PYR1 and PYLs interact with group A PP2Cs, leading to the release and activation of SnRK2s. PYLs have different binding properties

with respect to ABA and PP2Cs (Szostkiewicz et al., 2010; Hao et al., 2011; Antoni et al., 2012; Li et al., 2013; Zhao et al., 2013; Tischer et al., 2017), with two discrete binding types being identified, namely ABA-enhanced and ABA-dependent. In the former PYLs, including PYL4-6 and PYL8-10, bind with PP2Cs, whereas in the latter, dimeric PYLs, including PYR1 and PYL1-2, bind with PP2Cs (Hao et al., 2011).

In *Arabidopsis*, six of the nine identified clade A PP2Cs (ABI1, ABI2, HAB1, HAB2, AHG1, and PP2CA) function as ABA negative regulators (Merlot et al., 2001; Kuhn et al., 2006; Robert et al., 2006; Saez et al., 2006; Yoshida et al., 2006b; Nishimura et al., 2007; Rubio et al., 2009). Under normal conditions, PP2Cs bind to SnRK2s, thereby suppressing stress signal transmission, and thus facilitating appropriate plant growth. PP2Cs interact with C-terminal subdomain II of SnRK2s in an ABA-independent manner (Bhaskara et al., 2012) and repress ABA signaling *via* interaction with and dephosphorylation of SnRK2s (Mustilli et al., 2002; Yoshida et al., 2006a; Fujii et al., 2007; Lee et al., 2009; Umezawa et al., 2009; Vlad et al., 2009). In the presence of ABA, the different PP2Cs interact with specific ABA receptors and release SnRK2s, thereby inducing downstream signal transduction. Released subclass III SnRK2s are autophosphorylated and activated, with their activity being enhanced *via* phosphorylation by other protein kinases, including Raf kinases (Cai et al., 2014; Nguyen et al., 2019). In turn, these activated SnRK2s phosphorylate downstream transcription factors, including AREB and ABFs (Kobayashi et al., 2005; Furihata et al., 2006; Sirichandra et al., 2010).

POST-TRANSLATIONAL MODIFICATION OF ABA COMPONENTS

Ubiquitination and Deubiquitination

The core components of ABA signaling are modulated by different types of post-translational modification, among which, ubiquitination influences the responses to environmental factors. Ubiquitination is mediated by the activity of a series of enzymes, including ubiquitin-activating enzyme E1, ubiquitin-conjugating enzyme E2, and ubiquitin-protein ligase E3, and the substrate proteins thus ubiquitinated are subsequently degraded by 26S proteasome proteolysis (Stone, 2019). ABA components are regulated by E3 ligase complexes *via* successional steps (**Figure 1**). These complexes are classified into four groups, namely, really interesting new gene (RING), cullin-RING ligase (CRLs), U-box, and homologous to E6-AP carboxyl terminus (HECT; Vierstra, 2009), among which, RING, CRLs, and U-box E3 ligases are involved in ABA signaling.

Deubiquitination is catalyzed by the ubiquitin deconjugating enzymes (Chung and Baek, 1999). In contrast to E3 ligases, members of the deubiquitinase superfamily (DUB) proteins cleave ubiquitin from target proteins *via* the deconjugation or degradation of ubiquitin (Amerik and Hochstrasser, 2004). These processes contribute to enhancing target protein stability and activity *in vivo* (Taya et al., 1999; Lim et al., 2021b). There are five superfamilies among the DUBs, namely, ubiquitin-specific-processing proteases (UBPs), ubiquitin carboxy-terminal (UCH) proteases, the ovarian tumor proteases (OTUs), the Machado-Joseph disease protein domain proteases (MJDs), and JAB1/MPN^{+}/MOV34 (JAMM) proteases. UBPs, UCHs, OTUs, and MJDs are cysteine proteases, whereas JAMMs are zinc metalloisopeptidases (Nijman et al., 2005). Of these five families, the UBPs are well studied in plants, and have been shown to play important roles in cellular processes, including signal transduction, protein degradation, and gene regulation (Yan et al., 2000; Liu et al., 2008).

Ubiquitination of ABA Receptors

CRL E3 ligase complexes and RING-type E3 ligases degrade PYR/PYLs *via* the 26S proteasome, and yeast two-hybrid screening has revealed that in this pathway, Cullin 4 (CUL4)/De-etiolated 1 (DET1)-damaged DNA binding protein 1 (DDB1)-associated 1 (DDA1) E3 ligase interacts with PYL4, PYL8, and PYL9 (Irigoyen et al., 2014). Furthermore, DDA1 promotes PYL8 protein degradation *via* the 26S proteasome and reduces ABA sensitivity in *DDA1* overexpression mutants (Irigoyen et al., 2014), whereas in MG132-treated plants, accumulated PYL8 is polyubiquitinated and DDA1 promotes polyubiquitination, but ABA opposes this effect (Irigoyen et al., 2014). These findings provide evidence to indicate that ABA protects PYL8 from $CRL4^{DDA1}$-mediated degradation, either by affecting the CDD-DDA1 complex or by promoting the formation of degradation-resistant PYL8-PP2C complexes (Irigoyen et al., 2014).

Ring finger of seed longevity 1 (RSL1), a member of the RBR-type E3 ligase family (Marin, 2010; Callis, 2014) interacts with PYR1 and PYL4 in the plasma membrane and subsequently polyubiquitinates these to promote their degradation *via* the 26S proteasome. Phenotypic analysis has revealed that RNA interference mutants of *RSL1* are characterized by an ABA-hypersensitive phenotype, whereas an *RSL1* overexpression line was found to show reduced ABA sensitivity during seed germination and early seedling growth (Bueso et al., 2014). These observations indicate that RSL1 plays a negative role in ABA signaling *via* the degradation of ABA receptors (Bueso et al., 2014). In the same gene family as *RSL1*, the RING finger ABA-related 1–9 (RFA1 to RFA9) proteins are similarly associated with ABA receptor degradation, among which, RFA1 and RFA4 are localized in the nucleus and promote the nuclear degradation of PYR1 and PYL4 *via* activity of the nuclear E2 enzyme UBC26 (Fernandez et al., 2020). Compared with wild-type plants, PYR1 and PYL4 were observed to show higher expression in an *RFA1*/*RFA4* double knock-out mutant (Fernandez et al., 2020). The endosomal trafficking pathway functions as an important route for the modification of membrane proteins *via* the endosomal sorting complex required for transport (ESCRT) machinery. Ubiquitinated PYL4 is localized in the plasma membrane and degraded *via* a vacuolar degradation pathway mediated by the ESCRT components, in which ESCRT-I components FIVE1, VPS23A, and ALIX promote PYL4 degradation. Knock-down mutations of these ESCRT components are characterized a reduction in the degradation of PYL4 and enhanced ABA responses (Belda-Palazon et al., 2016; Yu et al., 2016; Garcia-Leon et al., 2019).

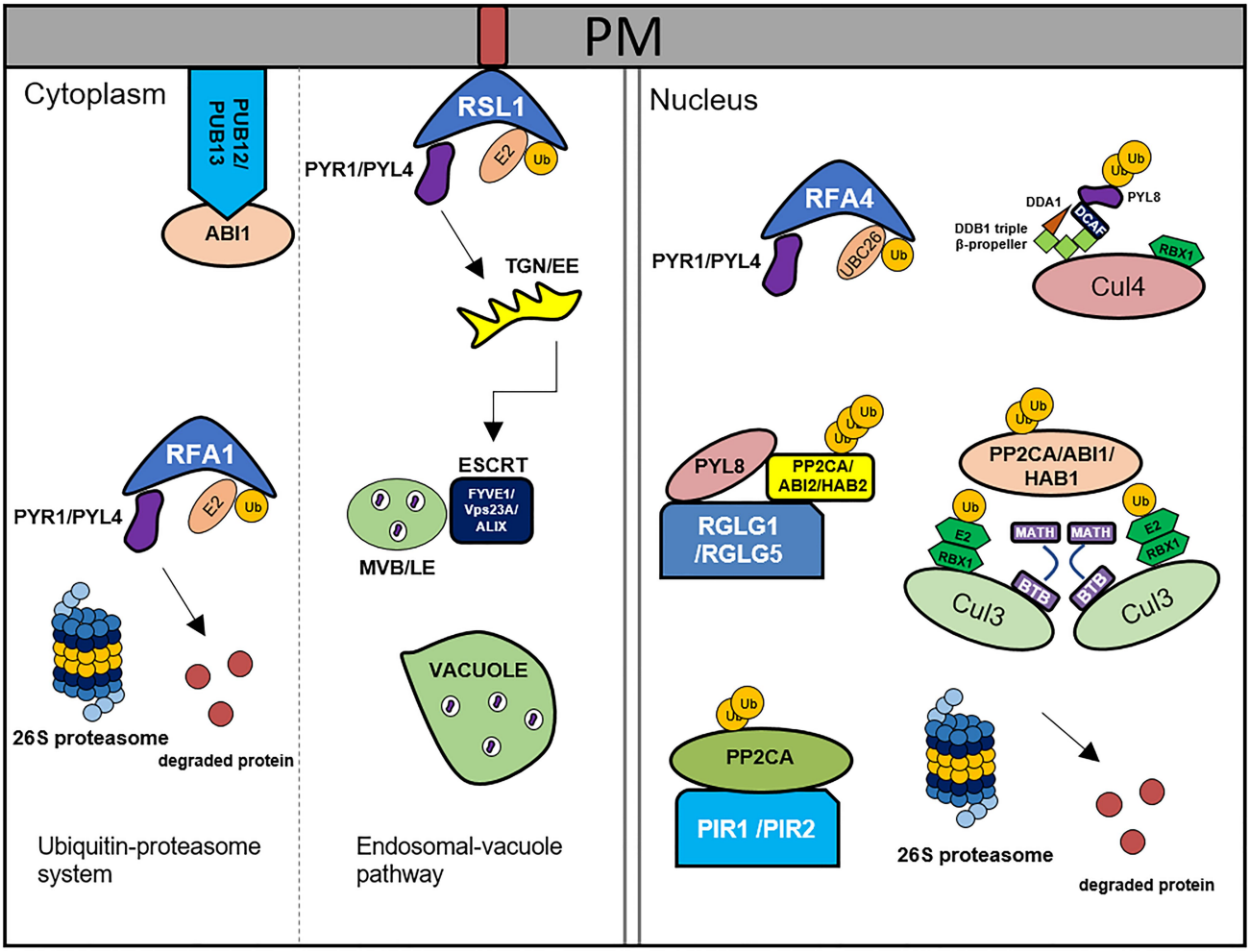

FIGURE 1 | Degradation of ABA core components by the 26S ubiquitin-proteasome system and endosomal-vacuole pathway. PYR1/PYLs are degraded by RSL1, RFA1/RFA4, and $CRL4^{DDA1}$ through ubiquitin-proteasome system. RSL1 ubiquitinates PYR1/PYL4 on the plasma membrane (PM), after that ubiquitinated substrates are degraded by ESCRT components, FIVE1/VPS23A/ALIX *via* endosomal-vacuole pathway. RFA1- and RFA4/$CRL4^{DDA1}$-mediated ubiquitination processes occur in the cytosol and nucleus, respectively. PP2Cs are degraded by PUB12/13, $CRL3^{BPM3/5(BTB\text{-}MATH)}$, PIR1/2, and RGLG1/5 through 26S proteasome. PUB12/13 degrade ABI1 by ubiquitination in the PM. RGLG1/5 ubiquitinate PP2CA/ABI2/HAB2, $CRL3^{BPM3/5(BTB\text{-}MATH)}$ ubiquitinate PP2CA/ABI1/HAB1, and PIR1/2 ubiquitinates PP2CA in the nucleus. This figure has been modified from Coego et al. (2021).

Ubiquitination of Clade A PP2Cs

Plant U-box type E3 ubiquitin ligase (PUB)12/13, Ring domain ligase (RGLG)1/5, CUL3-RING-based E3 ligases, and other E3 ligases collectively play roles in the proteolytic degradation of PP2Cs. PUB12/13 interact with ABI1 and thereby promote the ubiquitination of ABI1 in response to exogenous ABA, which induces the production of the dimeric form of PYR1 or monomeric forms of PYL4/PYL9 (Kong et al., 2015). A *pub12 pub13* double mutant was found to be characterized by a high accumulation of ABI1 and an ABA-insensitive phenotype, the latter of which was recovered following the crossing of double mutant plants with those containing an *abi1-3* mutation. These findings thus indicate that PUB12 and PUB13 play roles in controlling ABI1 stability (Kong et al., 2015). RGLG1/5 E3 ligases contribute to the degradation of PP2CA. *In vivo* analysis has revealed that RGLG1 interacts with PP2CA, which is enhanced by ABA, and promotes ubiquitination. *In vitro*, however, it has been observed that RGLG1 ubiquitinates PP2CA in the absence of either ABA or PYL4 (Wu et al., 2016). In contrast to PP2CA, which is nuclear localized, myristoylated RGLG1 is localized in the plasma membrane. ABA prevents the myristoylation of RGLG1 and induces cycloheximide-insensitive translocation to the nucleus (Belda-Palazon et al., 2019). Thus, RGLG1 plays a positive role in the ABA response by repressing PP2CA (Wu et al., 2016). PP2CA has also been demonstrated to interact with BTB/POZ and MATH domain proteins (BPMs) in plants, based on co-immunoprecipitation analysis performed in conjunction with liquid chromatography–tandem mass spectrometry. Compared with wild-type plants, those overexpressing *BPM3* and *BPM5* were found to accumulate lower amounts of PP2CA protein following ABA treatment. Contrastingly, in response

to ABA treatment, the levels of PP2CA accumulated in plants harboring a *bpm3 bpm5* double knock mutation were observed to be higher than those in the wild-type plants. Consistently, *BPM3* and *BPM5* overexpressing plants are characterized by enhanced ABA sensitivity, whereas the *bpm3 bpm5* mutant shows reduced ABA sensitivity. Consequently, $CRL3^{BPM}$ complexes appear to play vital roles in ABA responses and signaling (Julian et al., 2019).

By interacting with UBC27, AIRP3 contributes to ABI1 degradation *via* E3 ligase activity. The UBC27-AIRP3 ubiquitination complex modulates ABA responses by enhancing ABI1 protein stability. In *ubc27* and *airp3* mutant plants, the rate of ABI1 degradation is reduced, and with respect to cotyledon greening and stomatal movement, *ubc27* and *airp3* mutant plants are characterized by ABA-insensitive phenotypes (Pan et al., 2020). Among other RING proteins, PP2CA interacting ring finger protein (PIR)1 and PIR2 have been shown to interact with PP2CA, both *in vitro* and *in vivo*, thereby promoting its ubiquitination. *pir1 pir2* double knock-out mutants were found to be characterized by higher PP2CA protein levels, thus indicating that PIR1 and PIR2 degrade PP2CA *via* the 26S proteasome (Baek et al., 2019b).

Regulation of SnRK2s Stability by E3 Ligases

Although E3 ligases have been established to contribute indirectly to the stability of SnRK2s, there has as yet been no conclusive evidence to indicate that E3 ligases directly target SnRK2s. To date, only AtPP2-B11, a component of the SKP1/Cullin/F-box complex, has been shown to interact directly with SnRK2.3, with cell-free degradation assays performed using *AtPP2-B11-OE* and *amiR-AtPP2-B11* cell extracts indicating that AtPP2-B11 negatively influences SnRK2.3 stability. However, there is no evidence to indicate that AtPP2-B11 directly ubiquitinates SnRK2.3 (Cheng et al., 2017). In addition, the E3-ubiquitin ligase HOS15 has been found to interact with SnRK2.6, thereby influencing its stability, and compared with wild-type plants, those harboring a *hos15-2* mutation were found to accumulate higher levels of SnRK2.6 (Ali et al., 2019). However, in common with AtPP2-B11, the mechanisms whereby HOS15 regulates SnRK2 stability have yet to be established.

Modulation of ABA Signaling by Ubiquitin-Specific Processing Proteases

With respect to ABA signaling, plant tolerance to high salinity and drought stresses is modulated by UBP24 *via* the regulation of stomatal closure. Knock-out of the *UBP24* gene confers an ABA-hypersensitive phenotype during seedling growth, although contrastingly it reduces ABA sensitivity in the guard cells of mature plants. The latter effect results in a drought-sensitive phenotype, owing to a higher water loss compared with wild-type plants (Zhao et al., 2016a). In pepper plants, CaUBP12 has been observed to suppress the degradation of CaSnRK2.6 (Arabidopsis OST1 homolog; Lim et al., 2021b). CaUBP12 interacts with CaSnRK2.6 both *in vitro* and *in vivo*, and cell-free degradation analysis has revealed higher levels of CaSnRK2.6 degradation when incubated with crude extracts of the *CaUBP12* knock-down pepper plants, although lower levels in the presence of crude extracts of *CaUBP12* overexpressing *Arabidopsis* and tobacco plants (Lim et al., 2021a,b). These findings thus provide evidence to indicate that deubiquitinase-mediated post-transcriptional modification is implicated in the modulation of ABA signaling.

Phosphorylation of ABA Core Components

In response to the perception of stress, ABA signaling is regulated *via* the phosphorylation activity of a diverse range of kinases particularly with respect to ABA-induced responses under drought stress (Zhu, 2016). In the ABA core signaling pathway, SnRK2s phosphorylate downstream transcription factors (Merlot et al., 2001; Yoshida et al., 2002, 2006b; Saez et al., 2004, 2006; Kuhn et al., 2006; Robert et al., 2006; Rubio et al., 2009), whereas other kinases contribute to the phosphorylation of ABA receptor PYR/PYLs, PP2Cs, SnRK2s, and downstream transcription factors (**Figure 2**; Cai et al., 2014; Chen et al., 2018; Wang et al., 2018a; Zhang et al., 2018; Baek et al., 2019a; Li et al., 2019; Nguyen et al., 2019; Yu et al., 2019).

Phosphorylation of ABA Receptors

Several studies have provided evidence indicating the phosphorylation of ABA receptors. For example, TOR kinase, *Arabidopsis* Early flowering 1 (EL1)-like casein kinase (AEL), C-terminally encoded peptide receptor 2 (CEPR2), and cytosolic ABA receptor kinase 1 (CARK1) have been established to phosphorylate PYLs (Chen et al., 2018; Wang et al., 2018a; Zhang et al., 2018; Li et al., 2019; Yu et al., 2019). Among these, TOR kinase inactivates PYL1 and PYL4 by phosphorylating the Ser119 and Ser114 residues, respectively. Phosphomimic mutants of PYL1 and PYL4 are characterized by an inability to inhibit ABI1 phosphatase activity. Moreover, ABA has been shown to inhibit TOR kinase activity, thereby enhancing the ABA response. Thus, these observations indicate that TOR kinase functions as a negative regulator of ABA signaling by phosphorylating PYL1 and PYL4 (Wang et al., 2018a). AEL phosphorylates PYR1 and PYL1 at residues Ser109/152 and Ser136/182, respectively, and in doing so, promotes PYR1 and PYL1 degradation. Compared with wild-type plants, PYR1 and PYL1 proteins show greater stability in *ael* triple mutants. The ABA- and NaCl-sensitive phenotypes in knock-out mutants thus tend to indicate that AEL negatively regulates ABA signaling (Chen et al., 2018). CEPR2 has been found to interact with PYL4 in the plasma membrane, in which it phosphorylates Ser54, thus promoting an accelerated degradation of the PYL4 protein. Consistently, the levels of PYL4 protein in *CEPR2* overexpressing and *cepr2* mutant plants have been shown to be less and more stable, respectively (Yu et al., 2019). CARK1 phosphorylates PYR1 Thr78, PYL1 Thr105, PYL2 Ser81, and PYL3 Thr101, thereby enhancing ABA responses implicated in the inhibition of seed germination, root growth, and the expression of a number of ABA-responsive genes (Zhang et al., 2018; Li et al., 2019).

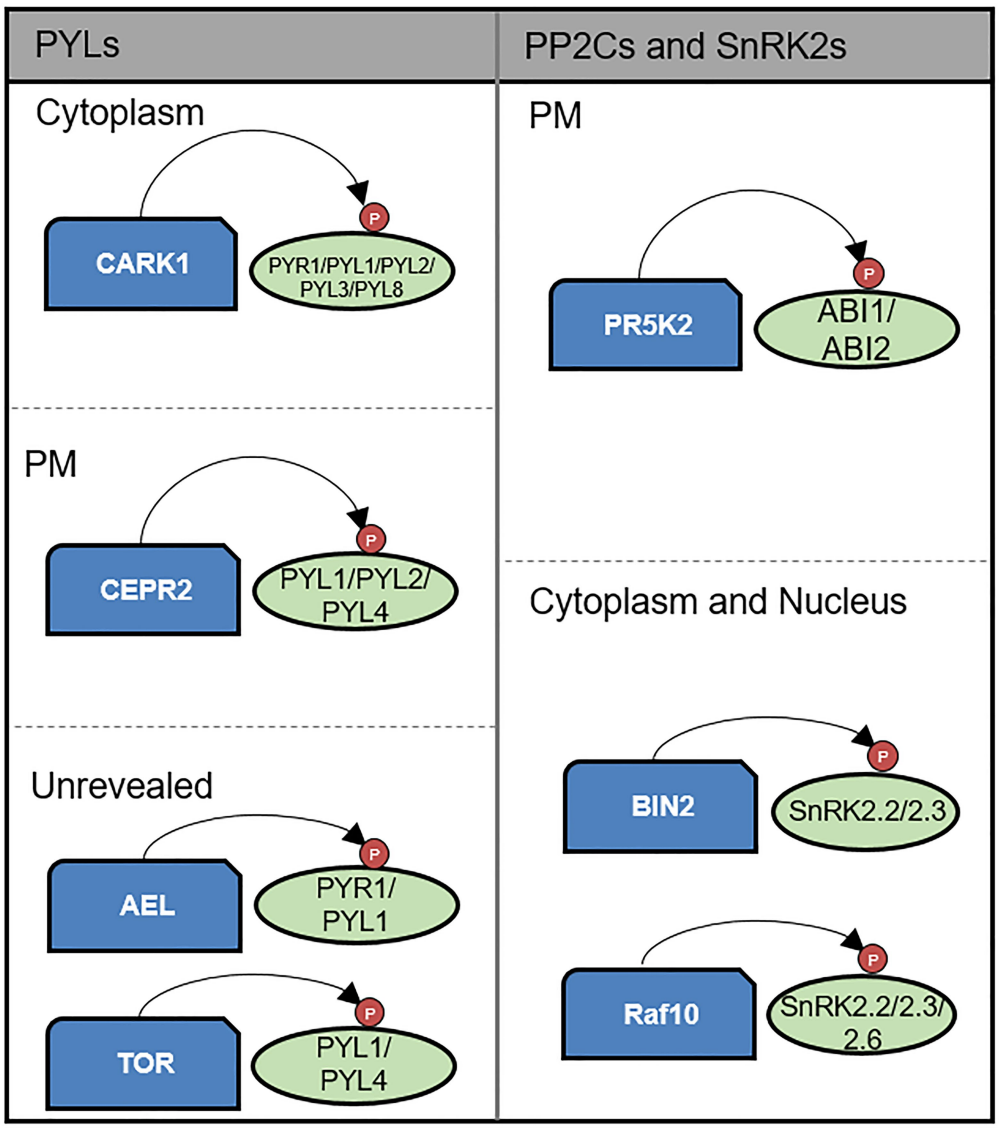

FIGURE 2 | Kinase-mediated post-translational modification of core components of the ABA signaling pathway. CARK1, CEPR2, TOR kinase, and AEL phosphorylate PYLs. CARK1 positively regulates ABA signaling by enhancing PYLs activity on the cytoplasm. In contrast, CEPR2 and AEL negatively regulate ABA signaling by promoting degradation of PYLs. TOR kinase also plays negative role in ABA signaling by preventing PYL activation. CEPR2 acts on PM. ABI1 and ABI2 are phosphorylated and enhanced in their phosphatase activity by PR5K2 on the PM. BIN2 and RAF10 phosphorylate SnRK2s enhancing their kinase activity on the cytoplasm and nucleus.

Phosphorylation of Clade A PP2Cs and Subclass III SnRK2s

PP2Cs are also phosphorylated by specific kinases. For example, ABI1 and ABI2 are phosphorylated by PR5 receptor-like kinase 2 (PR5K2), which phosphorylates the putative ABI1 phosphorylation site Ser 314 and ABI2 Ser304, thereby enhancing their respective phosphatase activities (Baek et al., 2019a). Plants overexpressing PR5K2 are characterized by ABA-insensitive and drought-sensitive phenotypes, whereas *atpr5k2* mutant plants show the opposite phenotypes. SnRK2s are phosphorylated and activated by Raf-like MAKKKs, among which RAF10 phosphorylates SnRK2s at a site within C-terminal domain II, referred to as the ABA box. *raf10 raf11* double-knock-out mutants are characterized by reduced levels of SnRK2 phosphorylation and germination is significantly delayed in the presence of ABA. In brassinosteroid (BR) signaling, BRASSINOSTEROID INSENSITIVE 2 (BIN2) plays a negative regulatory role by phosphorylating several transcription factors, which contrast with ABA signaling, wherein BIN2 plays the role of a positive regulator promoting ABA responses *via* the phosphorylation of SnRK2.2 and SnRK2.3, thus enhancing their kinase activities. These observations indicate that the modulation of stress responses in plants involves a certain degree of crosstalk between the ABA and BR signaling pathways (Cai et al., 2014).

CONCLUSIONS AND PERSPECTIVES

Abscisic acid plays vital roles in plant growth, development, and biotic/abiotic stress responses, particularly with respect to seed dormancy/germination, stomatal opening and closure, and leaf senescence. Moreover, the ABA core signaling pathway and post-translational modification of pathway components have been extensively studied. Ubiquitination, catalyzed by E3 ligases, contributes to the 26S proteasome-mediated degradation of ABA receptor PYR/PYL and clade A PP2C proteins, and numerous E3 ligases have been found to regulate the stability of these target proteins, either *via* direct or indirect interactions. However, it has yet to be conclusively determined whether E3 ligases directly ubiquitinate SnRK2 proteins, which accordingly limits our current understanding of the E3 ligase-mediated modulation of SnRK2 protein stability. The regulation of target protein stability is also modulated by deubiquitination, although in *Arabidopsis*, the mechanisms underlying the deubiquitination of ABA signaling core components remain to be ascertained. The involvement of UBPs in stress responses and other developmental processes is well characterized; however, to date there have been few studies that have examined the mechanisms associated with protein deubiquitination. To determine whether target proteins are deubiquitinated by UBPs, it will be necessary to isolate either mono- or poly-ubiquitinated proteins. The phosphorylation of target proteins also contributes to their activity and/or stability. In this regard, several kinases that phosphorylate key ABA signaling factors have been shown to regulate drought stress responses, either positively or negatively. However, only a few kinases involved in the ABA core signaling-associated regulation of drought responses have been examined, and it can be assumed that there are numerous other functional kinases that await identification. Consequently, to gain a better understanding of the post-translational modification of ABA core components, it will be necessary to conduct further studies that focus on identifying and characterizing these undiscovered proteins, which will illustrate potentially novel routes for the regulation of ABA signaling and stress responses.

AUTHOR CONTRIBUTIONS

JL, CL, and SL: conceptualization and writing. JL and CL: data analysis. All authors contributed to the article and approved the submitted version.

FUNDING

This work was supported by a grant from the Agriculture & Technology Development (project no. PJ01652101), the National Research Foundation of Korea (NRF) grant funded by the Korea Government (MSIT; 2021R1A2C2006338), and Rural Development Administration, Republic of Korea.

REFERENCES

Abe, H., Urao, T., Ito, T., Seki, M., Shinozaki, K., and Yamaguchi-Shinozaki, K. (2003). Arabidopsis AtMYC2 (bHLH) and AtMYB2 (MYB) function as transcriptional activators in abscisic acid signaling. *Plant Cell* 15, 63–78. doi: 10.1105/tpc.006130

Ali, A., Kim, J. K., Jan, M., Khan, H. A., Khan, I. U., Shen, M., et al. (2019). Rheostatic control of ABA signaling through HOS15-mediated OST1 degradation. *Mol. Plant* 12, 1447–1462. doi: 10.1016/j.molp.2019.08.005

Amerik, A. Y., and Hochstrasser, M. (2004). Mechanism and function of deubiquitinating enzymes. *Biochim. Biophys. Acta* 1695, 189–207. doi: 10.1016/j.bbamcr.2004.10.003

Antoni, R., Gonzalez-Guzman, M., Rodriguez, L., Peirats-Llobet, M., Pizzio, G. A., Fernandez, M. A., et al. (2013). PYRABACTIN RESISTANCE1-LIKE8 plays an important role for the regulation of abscisic acid signaling in root. *Plant Physiol.* 161, 931–941. doi: 10.1104/pp.112.208678

Antoni, R., Gonzalez-Guzman, M., Rodriguez, L., Rodrigues, A., Pizzio, G. A., and Rodriguez, P. L. (2012). Selective inhibition of clade A phosphatases type 2C by PYR/PYL/RCAR abscisic acid receptors. *Plant Physiol.* 158, 970–980. doi: 10.1104/pp.111.188623

Baek, D., Kim, M. C., Kumar, D., Park, B., Cheong, M. S., Choi, W., et al. (2019a). AtPR5K2, a PR5-Like receptor kinase, modulates plant responses to drought stress by phosphorylating protein phosphatase 2Cs. *Front. Plant Sci.* 10:1146. doi: 10.3389/fpls.2019.01146

Baek, W., Lim, C. W., Luan, S., and Lee, S. C. (2019b). The RING finger E3 ligases PIR1 and PIR2 mediate PP2CA degradation to enhance abscisic acid response in Arabidopsis. *Plant J.* 100, 473–486. doi: 10.1111/tpj.14507

Bauer, H., Ache, P., Lautner, S., Fromm, J., Hartung, W., Al-Rasheid, K. A., et al. (2013). The stomatal response to reduced relative humidity requires guard cell-autonomous ABA synthesis. *Curr. Biol.* 23, 53–57. doi: 10.1016/j.cub.2012.11.022

Belda-Palazon, B., Julian, J., Coego, A., Wu, Q., Zhang, X., Batistic, O., et al. (2019). ABA inhibits myristoylation and induces shuttling of the RGLG1 E3 ligase to promote nuclear degradation of PP2CA. *Plant J.* 98, 813–825. doi: 10.1111/tpj.14274

Belda-Palazon, B., Rodriguez, L., Fernandez, M. A., Castillo, M. C., Anderson, E. M., Gao, C., et al. (2016). FYVE1/FREE1 interacts with the PYL4 ABA receptor and mediates its delivery to the vacuolar degradation pathway. *Plant Cell* 28, 2291–2311. doi: 10.1105/tpc.16.00178

Bhaskara, G. B., Nguyen, T. T., and Verslues, P. E. (2012). Unique drought resistance functions of the highly ABA-induced clade A protein phosphatase 2Cs. *Plant Physiol.* 160, 379–395. doi: 10.1104/pp.112.202408

Brandt, B., Brodsky, D. E., Xue, S., Negi, J., Iba, K., Kangasjarvi, J., et al. (2012). Reconstitution of abscisic acid activation of SLAC1 anion channel by CPK6 and OST1 kinases and branched ABI1 PP2C phosphatase action. *Proc. Natl. Acad. Sci. U. S. A.* 109, 10593–10598. doi: 10.1073/pnas.1116590109

Breeze, E., Harrison, E., McHattie, S., Hughes, L., Hickman, R., Hill, C., et al. (2011). High-resolution temporal profiling of transcripts during Arabidopsis leaf senescence reveals a distinct chronology of processes and regulation. *Plant Cell* 23, 873–894. doi: 10.1105/tpc.111.083345

Bueso, E., Rodriguez, L., Lorenzo-Orts, L., Gonzalez-Guzman, M., Sayas, E., Munoz-Bertomeu, J., et al. (2014). The single-subunit RING-type E3 ubiquitin ligase RSL1 targets PYL4 and PYR1 ABA receptors in plasma membrane to modulate abscisic acid signaling. *Plant J.* 80, 1057–1071. doi: 10.1111/tpj.12708

Cai, Z., Liu, J., Wang, H., Yang, C., Chen, Y., Li, Y., et al. (2014). GSK3-like kinases positively modulate abscisic acid signaling through phosphorylating subgroup III SnRK2s in Arabidopsis. *Proc. Natl. Acad. Sci. U. S. A.* 111, 9651–9656. doi: 10.1073/pnas.1316717111

Callis, J. (2014). The ubiquitination machinery of the ubiquitin system. *Arabidopsis Book* 12:e0174. doi: 10.1199/tab.0174

Carles, C., Bies-Etheve, N., Aspart, L., Léon-Kloosterziel, K. M., Koornneef, M., Echeverria, M., et al. (2002). Regulation of *Arabidopsis thaliana* Em genes: role of ABI5. *Plant J.* 30, 373–383. doi: 10.1046/j.1365-313X.2002.01295.x

Chen, K., Li, G. J., Bressan, R. A., Song, C. P., Zhu, J. K., and Zhao, Y. (2020). Abscisic acid dynamics, signaling, and functions in plants. *J. Integr. Plant Biol.* 62, 25–54. doi: 10.1111/jipb.12899

Chen, H. H., Qu, L., Xu, Z. H., Zhu, J. K., and Xue, H. W. (2018). EL1-like casein kinases suppress ABA signaling and responses by phosphorylating and destabilizing the ABA receptors PYR/PYLs in Arabidopsis. *Mol. Plant* 11, 706–719. doi: 10.1016/j.molp.2018.02.012

Cheng, W. H., Endo, A., Zhou, L., Penney, J., Chen, H. C., Arroyo, A., et al. (2002). A unique short-chain dehydrogenase/reductase in Arabidopsis glucose signaling and abscisic acid biosynthesis and functions. *Plant Cell* 14, 2723–2743. doi: 10.1105/tpc.006494

Cheng, C., Wang, Z., Ren, Z., Zhi, L., Yao, B., Su, C., et al. (2017). SCFAtPP2-B11 modulates ABA signaling by facilitating SnRK2.3 degradation in *Arabidopsis thaliana*. *PLoS Genet.* 13:e1006947. doi: 10.1371/journal.pgen.1006947

Chinnusamy, V., Gong, Z., and Zhu, J. K. (2008). Abscisic acid-mediated epigenetic processes in plant development and stress responses. *J. Integr. Plant Biol.* 50, 1187–1195. doi: 10.1111/j.1744-7909.2008.00727.x

Chung, C. H., and Baek, S. H. (1999). Deubiquitinating enzymes: their diversity and emerging roles. *Biochem. Biophys. Res. Commun.* 266, 633–640. doi: 10.1006/bbrc.1999.1880

Coego, A., Julian, J., Lozano-Juste, J., Pizzio, G. A., Alrefaei, A. F., and Rodriguez, P. L. (2021). Ubiquitylation of ABA receptors and protein phosphatase 2C Coreceptors to modulate ABA signaling and stress response. *Int. J. Mol. Sci.* 22:7103. doi: 10.3390/ijms22137103

Cutler, S. R., Rodriguez, P. L., Finkelstein, R. R., and Abrams, S. R. (2010). Abscisic acid: emergence of a core signaling network. *Annu. Rev. Plant Biol.* 61, 651–679. doi: 10.1146/annurev-arplant-042809-112122

Debeaujon, I., and Koornneef, M. (2000). Gibberellin requirement for Arabidopsis seed germination is determined both by testa characteristics and embryonic abscisic acid. *Plant Physiol.* 122, 415–424. doi: 10.1104/pp.122.2.415

Fernandez, M. A., Belda-Palazon, B., Julian, J., Coego, A., Lozano-Juste, J., Inigo, S., et al. (2020). RBR-type E3 ligases and the ubiquitin-conjugating enzyme UBC26 regulate Abscisic acid receptor levels and signaling. *Plant Physiol.* 182, 1723–1742. doi: 10.1104/pp.19.00898

Finkelstein, R. (2013). Abscisic acid synthesis and response. *Arabidopsis Book* 11:e0166. doi: 10.1199/tab.0166

Fujii, H., Chinnusamy, V., Rodrigues, A., Rubio, S., Antoni, R., Park, S. Y., et al. (2009). In vitro reconstitution of an abscisic acid signalling pathway. *Nature* 462, 660–664. doi: 10.1038/nature08599

Fujii, H., Verslues, P. E., and Zhu, J. K. (2007). Identification of two protein kinases required for abscisic acid regulation of seed germination, root growth, and gene expression in Arabidopsis. *Plant Cell* 19, 485–494. doi: 10.1105/tpc.106.048538

Fujii, H., and Zhu, J. K. (2009). Arabidopsis mutant deficient in 3 abscisic acid-activated protein kinases reveals critical roles in growth, reproduction, and stress. *Proc. Natl. Acad. Sci. U. S. A.* 106, 8380–8385. doi: 10.1073/pnas.0903144106

Fujita, M., Fujita, Y., Maruyama, K., Seki, M., Hiratsu, K., Ohme-Takagi, M., et al. (2004). A dehydration-induced NAC protein, RD26, is involved in a novel ABA-dependent stress-signaling pathway. *Plant J.* 39, 863–876. doi: 10.1111/j.1365-313X.2004.02171.x

Fujita, Y., Fujita, M., Satoh, R., Maruyama, K., Parvez, M. M., Seki, M., et al. (2005). AREB1 is a transcription activator of novel ABRE-dependent ABA signaling that enhances drought stress tolerance in Arabidopsis. *Plant Cell* 17, 3470–3488. doi: 10.1105/tpc.105.035659

Fujita, Y., Fujita, M., Shinozaki, K., and Yamaguchi-Shinozaki, K. (2011). ABA-mediated transcriptional regulation in response to osmotic stress in plants. *J. Plant Res.* 124, 509–525. doi: 10.1007/s10265-011-0412-3

Furihata, T., Maruyama, K., Fujita, Y., Umezawa, T., Yoshida, R., Shinozaki, K., et al. (2006). Abscisic acid-dependent multisite phosphorylation regulates the activity of a transcription activator AREB1. *Proc. Natl. Acad. Sci. U. S. A.* 103, 1988–1993. doi: 10.1073/pnas.0505667103

Gao, S., Gao, J., Zhu, X., Song, Y., Li, Z., Ren, G., et al. (2016). ABF2, ABF3, and ABF4 promote ABA-mediated chlorophyll degradation and leaf senescence by transcriptional activation of chlorophyll catabolic genes and senescence-associated genes in Arabidopsis. *Mol. Plant* 9, 1272–1285. doi: 10.1016/j.molp.2016.06.006

Garcia-Leon, M., Cuyas, L., El-Moneim, D. A., Rodriguez, L., Belda-Palazon, B., Sanchez-Quant, E., et al. (2019). Arabidopsis ALIX regulates Stomatal aperture and turnover of Abscisic acid receptors. *Plant Cell* 31, 2411–2429. doi: 10.1105/tpc.19.00399

Geiger, D., Scherzer, S., Mumm, P., Stange, A., Marten, I., Bauer, H., et al. (2009). Activity of guard cell anion channel SLAC1 is controlled by drought-stress signaling kinase-phosphatase pair. *Proc. Natl. Acad. Sci. U. S. A.* 106, 21425–21430. doi: 10.1073/pnas.0912021106

Gepstein, S., and Thimann, K. V. (1980). Changes in the abscisic acid content of oat leaves during senescence. *Proc. Natl. Acad. Sci. U. S. A.* 77, 2050–2053. doi: 10.1073/pnas.77.4.2050

Golldack, D., Li, C., Mohan, H., and Probst, N. (2013). Gibberellins and abscisic acid signal crosstalk: living and developing under unfavorable conditions. *Plant Cell Rep.* 32, 1007–1016. doi: 10.1007/s00299-013-1409-2

Gonzalez-Guzman, M., Pizzio, G. A., Antoni, R., Vera-Sirera, F., Merilo, E., Bassel, G. W., et al. (2012). Arabidopsis PYR/PYL/RCAR receptors play a major role in quantitative regulation of stomatal aperture and transcriptional response to abscisic acid. *Plant Cell* 24, 2483–2496. doi: 10.1105/tpc.112.098574

Hao, Q., Yin, P., Li, W., Wang, L., Yan, C., Lin, Z., et al. (2011). The molecular basis of ABA-independent inhibition of PP2Cs by a subclass of PYL proteins. *Mol. Cell* 42, 662–672. doi: 10.1016/j.molcel.2011.05.011

Hirayama, T., and Shinozaki, K. (2007). Perception and transduction of abscisic acid signals: keys to the function of the versatile plant hormone ABA. *Trends Plant Sci.* 12, 343–351. doi: 10.1016/j.tplants.2007.06.013

Hortensteiner, S. (2009). Stay-green regulates chlorophyll and chlorophyll-binding protein degradation during senescence. *Trends Plant Sci.* 14, 155–162. doi: 10.1016/j.tplants.2009.01.002

Hosy, E., Vavasseur, A., Mouline, K., Dreyer, I., Gaymard, F., Poree, F., et al. (2003). The Arabidopsis outward K+ channel GORK is involved in regulation of stomatal movements and plant transpiration. *Proc. Natl. Acad. Sci. U. S. A.* 100, 5549–5554. doi: 10.1073/pnas.0733970100

Irigoyen, M. L., Iniesto, E., Rodriguez, L., Puga, M. I., Yanagawa, Y., Pick, E., et al. (2014). Targeted degradation of abscisic acid receptors is mediated by the ubiquitin ligase substrate adaptor DDA1 in Arabidopsis. *Plant Cell* 26, 712–728. doi: 10.1105/tpc.113.122234

Iyer, L. M., Koonin, E. V., and Aravind, L. (2001). Adaptations of the helix-grip fold for ligand binding and catalysis in the START domain superfamily. *Proteins* 43, 134–144. doi: 10.1002/1097-0134(20010501)43:2<134::AID-PROT1025>3.0.CO;2-I

Julian, J., Coego, A., Lozano-Juste, J., Lechner, E., Wu, Q., Zhang, X., et al. (2019). The MATH-BTB BPM3 and BPM5 subunits of Cullin3-RING E3 ubiquitin ligases target PP2CA and other clade A PP2Cs for degradation. *Proc. Natl. Acad. Sci. U. S. A.* 116, 15725–15734. doi: 10.1073/pnas.1908677116

Kang, J. Y., Choi, H. I., Im, M. Y., and Kim, S. Y. (2002). Arabidopsis basic leucine zipper proteins that mediate stress-responsive abscisic acid signaling. *Plant Cell* 14, 343–357. doi: 10.1105/tpc.010362

Kobayashi, Y., Murata, M., Minami, H., Yamamoto, S., Kagaya, Y., Hobo, T., et al. (2005). Abscisic acid-activated SNRK2 protein kinases function in the gene-regulation pathway of ABA signal transduction by phosphorylating ABA response element-binding factors. *Plant J.* 44, 939–949. doi: 10.1111/j.1365-313X.2005.02583.x

Kong, L., Cheng, J., Zhu, Y., Ding, Y., Meng, J., Chen, Z., et al. (2015). Degradation of the ABA co-receptor ABI1 by PUB12/13 U-box E3 ligases. *Nat. Commun.* 6:8630. doi: 10.1038/ncomms9630

Koornneef, M., Jorna, M. L., Brinkhorst-van der Swan, D. L., and Karssen, C. M. (1982). The isolation of abscisic acid (ABA) deficient mutants by selection of induced revertants in non-germinating gibberellin sensitive lines of *Arabidopsis thaliana* (L.) heynh. *Theor. Appl. Genet.* 61, 385–393. doi: 10.1007/BF00272861

Kuhn, J. M., Boisson-Dernier, A., Dizon, M. B., Maktabi, M. H., and Schroeder, J. I. (2006). The protein phosphatase AtPP2CA negatively regulates abscisic acid signal transduction in Arabidopsis, and effects of abh1 on AtPP2CA mRNA. *Plant Physiol.* 140, 127–139. doi: 10.1104/pp.105.070318

Kwak, J. M., Murata, Y., Baizabal-Aguirre, V. M., Merrill, J., Wang, M., Kemper, A., et al. (2001). Dominant negative guard cell K+ channel mutants reduce inward-rectifying K+ currents and light-induced Stomatal opening in Arabidopsis. *Plant Physiol.* 127, 473–485. doi: 10.1104/pp.010428

Lee, Y., Choi, Y. B., Suh, S., Lee, J., Assmann, S. M., Joe, C. O., et al. (1996). Abscisic acid-induced phosphoinositide turnover in guard cell protoplasts of *Vicia faba*. *Plant Physiol.* 110, 987–996. doi: 10.1104/pp.110.3.987

Lee, I. C., Hong, S. W., Whang, S. S., Lim, P. O., Nam, H. G., and Koo, J. C. (2011). Age-dependent action of an ABA-inducible receptor kinase, RPK1, as a positive regulator of senescence in Arabidopsis leaves. *Plant Cell Physiol.* 52, 651–662. doi: 10.1093/pcp/pcr026

Lee, S. C., Lan, W., Buchanan, B. B., and Luan, S. (2009). A protein kinase-phosphatase pair interacts with an ion channel to regulate ABA signaling in plant guard cells. *Proc. Natl. Acad. Sci. U. S. A.* 106, 21419–21424. doi: 10.1073/pnas.0910601106

Lee, S. J., Lee, M. H., Kim, J. I., and Kim, S. Y. (2015). Arabidopsis putative MAP kinase kinase kinases Raf10 and Raf11 are positive regulators of seed dormancy and ABA response. *Plant Cell Physiol.* 56, 84–97. doi: 10.1093/pcp/pcu148

Lee, K. P., Piskurewicz, U., Tureckova, V., Strnad, M., and Lopez-Molina, L. (2010). A seed coat bedding assay shows that RGL2-dependent release of abscisic acid by the endosperm controls embryo growth in Arabidopsis dormant seeds. *Proc. Natl. Acad. Sci. U. S. A.* 107, 19108–19113. doi: 10.1073/pnas.1012896107

Lefebvre, V., North, H., Frey, A., Sotta, B., Seo, M., Okamoto, M., et al. (2006). Functional analysis of Arabidopsis NCED6 and NCED9 genes indicates that ABA synthesized in the endosperm is involved in the induction of seed dormancy. *Plant J.* 45, 309–319. doi: 10.1111/j.1365-313X.2005.02622.x

Leon-Kloosterziel, K. M., Gil, M. A., Ruijs, G. J., Jacobsen, S. E., Olszewski, N. E., Schwartz, S. H., et al. (1996). Isolation and characterization of abscisic acid-deficient Arabidopsis mutants at two new loci. *Plant J.* 10, 655–661. doi: 10.1046/j.1365-313X.1996.10040655.x

Li, X., Kong, X., Huang, Q., Zhang, Q., Ge, H., Zhang, L., et al. (2019). CARK1 phosphorylates subfamily III members of ABA receptors. *J. Exp. Bot.* 70, 519–528. doi: 10.1093/jxb/ery374

Li, W., Wang, L., Sheng, X., Yan, C., Zhou, R., Hang, J., et al. (2013). Molecular basis for the selective and ABA-independent inhibition of PP2CA by PYL13. *Cell Res.* 23, 1369–1379. doi: 10.1038/cr.2013.143

Li, J., Wang, X. Q., Watson, M. B., and Assmann, S. M. (2000). Regulation of abscisic acid-induced stomatal closure and anion channels by guard cell AAPK kinase. *Science* 287, 300–303. doi: 10.1126/science.287.5451.300

Lim, C. W., Baek, W., and Lee, S. C. (2021a). Tobacco ubiquitin-specific protease 12 (NbUBP12) positively modulates drought resistance. *Plant Signal. Behav.* 16:1974725. doi: 10.1080/15592324.2021.1974725

Lim, C. W., Baek, W., Lim, J., Hong, E., and Lee, S. C. (2021b). Pepper ubiquitin-specific protease, CaUBP12, positively modulates dehydration resistance by enhancing CaSnRK2.6 stability. *Plant J.* 107, 1148–1165. doi: 10.1111/tpj.15374

Liu, X., Hu, P., Huang, M., Tang, Y., Li, Y., Li, L., et al. (2016). The NF-YC-RGL2 module integrates GA and ABA signalling to regulate seed germination in Arabidopsis. *Nat. Commun.* 7:12768. doi: 10.1038/ncomms12768

Liu, Y., Wang, F., Zhang, H., He, H., Ma, L., and Deng, X. W. (2008). Functional characterization of the Arabidopsis ubiquitin-specific protease gene family reveals specific role and redundancy of individual members in development. *Plant J.* 55, 844–856. doi: 10.1111/j.1365-313X.2008.03557.x

Ma, Y., Szostkiewicz, I., Korte, A., Moes, D., Yang, Y., Christmann, A., et al. (2009). Regulators of PP2C phosphatase activity function as abscisic acid sensors. *Science* 324, 1064–1068. doi: 10.1126/science.1172408

Mantyla, E., Lang, V., and Palva, E. T. (1995). Role of abscisic acid in drought-induced freezing tolerance, cold acclimation, and accumulation of LT178 and RAB18 proteins in *Arabidopsis thaliana*. *Plant Physiol.* 107, 141–148. doi: 10.1104/pp.107.1.141

Marin, I. (2010). Diversification and specialization of plant RBR ubiquitin ligases. *PLoS One* 5:e11579. doi: 10.1371/journal.pone.0011579

McConnell, J. R., Emery, J., Eshed, Y., Bao, N., Bowman, J., and Barton, M. K. (2001). Role of PHABULOSA and PHAVOLUTA in determining radial patterning in shoots. *Nature* 411, 709–713. doi: 10.1038/35079635

Melotto, M., Underwood, W., Koczan, J., Nomura, K., and He, S. Y. (2006). Plant stomata function in innate immunity against bacterial invasion. *Cell* 126, 969–980. doi: 10.1016/j.cell.2006.06.054

Merlot, S., Gosti, F., Guerrier, D., Vavasseur, A., and Giraudat, J. (2001). The ABI1 and ABI2 protein phosphatases 2C act in a negative feedback regulatory loop of the abscisic acid signalling pathway. *Plant J.* 25, 295–303. doi: 10.1046/j.1365-313x.2001.00965.x

Mori, I. C., Murata, Y., Yang, Y., Munemasa, S., Wang, Y. F., Andreoli, S., et al. (2006). CDPKs CPK6 and CPK3 function in ABA regulation of guard cell S-type anion- and Ca(2+)-permeable channels and stomatal closure. *PLoS Biol.* 4:e327. doi: 10.1371/journal.pbio.0040327

Murata, Y., Pei, Z. M., Mori, I. C., and Schroeder, J. (2001). Abscisic acid activation of plasma membrane Ca(2+) channels in guard cells requires cytosolic NAD(P)H and is differentially disrupted upstream and downstream of reactive oxygen species production in abi1-1 and abi2-1 protein phosphatase 2C mutants. *Plant Cell* 13, 2513–2523. doi: 10.1105/tpc.010210

Mustilli, A. C., Merlot, S., Vavasseur, A., Fenzi, F., and Giraudat, J. (2002). Arabidopsis OST1 protein kinase mediates the regulation of stomatal aperture by abscisic acid and acts upstream of reactive oxygen species production. *Plant Cell* 14, 3089–3099. doi: 10.1105/tpc.007906

Nakashima, K., Fujita, Y., Kanamori, N., Katagiri, T., Umezawa, T., Kidokoro, S., et al. (2009a). Three Arabidopsis SnRK2 protein kinases, SRK2D/SnRK2.2, SRK2E/SnRK2.6/OST1 and SRK2I/SnRK2.3, involved in ABA signaling are essential for the control of seed development and dormancy. *Plant Cell Physiol.* 50, 1345–1363. doi: 10.1093/pcp/pcp083

Nakashima, K., Ito, Y., and Yamaguchi-Shinozaki, K. (2009b). Transcriptional regulatory networks in response to abiotic stresses in Arabidopsis and grasses. *Plant Physiol.* 149, 88–95. doi: 10.1104/pp.108.129791

Ng, L. M., Soon, F. F., Zhou, X. E., West, G. M., Kovach, A., Suino-Powell, K. M., et al. (2011). Structural basis for basal activity and autoactivation of abscisic acid (ABA) signaling SnRK2 kinases. *Proc. Natl. Acad. Sci. U. S. A.* 108, 21259–21264. doi: 10.1073/pnas.1118651109

Nguyen, Q. T. C., Lee, S. J., Choi, S. W., Na, Y. J., Song, M. R., Hoang, Q. T. N., et al. (2019). Arabidopsis Raf-Like kinase Raf10 is a regulatory component of Core ABA signaling. *Mol. Cell* 42, 646–660. doi: 10.14348/molcells.2019.0173

Nijman, S. M., Luna-Vargas, M. P., Velds, A., Brummelkamp, T. R., Dirac, A. M., Sixma, T. K., et al. (2005). A genomic and functional inventory of deubiquitinating enzymes. *Cell* 123, 773–786. doi: 10.1016/j.cell.2005.11.007

Nishimura, N., Sarkeshik, A., Nito, K., Park, S. Y., Wang, A., Carvalho, P. C., et al. (2010). PYR/PYL/RCAR family members are major in-vivo ABI1 protein phosphatase 2C-interacting proteins in Arabidopsis. *Plant J.* 61, 290–299. doi: 10.1111/j.1365-313X.2009.04054.x

Nishimura, N., Yoshida, T., Kitahata, N., Asami, T., Shinozaki, K., and Hirayama, T. (2007). ABA-hypersensitive Germination1 encodes a protein phosphatase 2C, an essential component of abscisic acid signaling in Arabidopsis seed. *Plant J.* 50, 935–949. doi: 10.1111/j.1365-313X.2007.03107.x

Ogawa, M., Hanada, A., Yamauchi, Y., Kuwahara, A., Kamiya, Y., and Yamaguchi, S. (2003). Gibberellin biosynthesis and response during Arabidopsis seed germination. *Plant Cell* 15, 1591–1604. doi: 10.1105/tpc.011650

Osakabe, Y., Arinaga, N., Umezawa, T., Katsura, S., Nagamachi, K., Tanaka, H., et al. (2013). Osmotic stress responses and plant growth controlled by potassium transporters in Arabidopsis. *Plant Cell* 25, 609–624. doi: 10.1105/tpc.112.105700

Pan, W., Lin, B., Yang, X., Liu, L., Xia, R., Li, J., et al. (2020). The UBC27-AIRP3 ubiquitination complex modulates ABA signaling by promoting the degradation of ABI1 in Arabidopsis. *Proc. Natl. Acad. Sci. U. S. A.* 117, 27694–27702. doi: 10.1073/pnas.2007366117

Park, S. Y., Fung, P., Nishimura, N., Jensen, D. R., Fujii, H., Zhao, Y., et al. (2009). Abscisic acid inhibits type 2C protein phosphatases via the PYR/PYL family of START proteins. *Science* 324, 1068–1071. doi: 10.1126/science.1173041

Parkash, J., Vaidya, T., Kirti, S., and Dutt, S. (2014). Translation initiation factor 5A in Picrorhiza is up-regulated during leaf senescence and in response to abscisic acid. *Gene* 542, 1–7. doi: 10.1016/j.gene.2014.03.032

Pei, Z. M., Murata, Y., Benning, G., Thomine, S., Klusener, B., Allen, G. J., et al. (2000). Calcium channels activated by hydrogen peroxide mediate abscisic acid signalling in guard cells. *Nature* 406, 731–734. doi: 10.1038/35021067

Piskurewicz, U., Jikumaru, Y., Kinoshita, N., Nambara, E., Kamiya, Y., and Lopez-Molina, L. (2008). The gibberellic acid signaling repressor RGL2 inhibits Arabidopsis seed germination by stimulating abscisic acid synthesis and ABI5 activity. *Plant Cell* 20, 2729–2745. doi: 10.1105/tpc.108.061515

Pourtau, N., Mares, M., Purdy, S., Quentin, N., Ruel, A., and Wingler, A. (2004). Interactions of abscisic acid and sugar signalling in the regulation of leaf senescence. *Planta* 219, 765–772. doi: 10.1007/s00425-004-1279-5

Pruzinska, A., Tanner, G., Aubry, S., Anders, I., Moser, S., Muller, T., et al. (2005). Chlorophyll breakdown in senescent Arabidopsis leaves. Characterization of chlorophyll catabolites and of chlorophyll catabolic enzymes involved in the degreening reaction. *Plant Physiol.* 139, 52–63. doi: 10.1104/pp.105.065870

Raab, S., Drechsel, G., Zarepour, M., Hartung, W., Koshiba, T., Bittner, F., et al. (2009). Identification of a novel E3 ubiquitin ligase that is required for suppression of premature senescence in Arabidopsis. *Plant J.* 59, 39–51. doi: 10.1111/j.1365-313X.2009.03846.x

Radauer, C., Lackner, P., and Breiteneder, H. (2008). The bet v 1 fold: an ancient, versatile scaffold for binding of large, hydrophobic ligands. *BMC Evol. Biol.* 8:286. doi: 10.1186/1471-2148-8-286

Raghavendra, A. S., Gonugunta, V. K., Christmann, A., and Grill, E. (2010). ABA perception and signalling. *Trends Plant Sci.* 15, 395–401. doi: 10.1016/j.tplants.2010.04.006

Ren, G., An, K., Liao, Y., Zhou, X., Cao, Y., Zhao, H., et al. (2007). Identification of a novel chloroplast protein AtNYE1 regulating chlorophyll degradation during leaf senescence in Arabidopsis. *Plant Physiol.* 144, 1429–1441. doi: 10.1104/pp.107.100172

Robert, N., Merlot, S., N'Guyen, V., Boisson-Dernier, A., and Schroeder, J. I. (2006). A hypermorphic mutation in the protein phosphatase 2C HAB1 strongly affects ABA signaling in Arabidopsis. *FEBS Lett.* 580, 4691–4696. doi: 10.1016/j.febslet.2006.07.047

Rubio, S., Rodrigues, A., Saez, A., Dizon, M. B., Galle, A., Kim, T. H., et al. (2009). Triple loss of function of protein phosphatases type 2C leads to partial constitutive response to endogenous abscisic acid. *Plant Physiol.* 150, 1345–1355. doi: 10.1104/pp.109.137174

Saez, A., Apostolova, N., Gonzalez-Guzman, M., Gonzalez-Garcia, M. P., Nicolas, C., Lorenzo, O., et al. (2004). Gain-of-function and loss-of-function phenotypes of the protein phosphatase 2C HAB1 reveal its role as a negative regulator of abscisic acid signalling. *Plant J.* 37, 354–369. doi: 10.1046/j.1365-313X.2003.01966.x

Saez, A., Robert, N., Maktabi, M. H., Schroeder, J. I., Serrano, R., and Rodriguez, P. L. (2006). Enhancement of abscisic acid sensitivity and reduction of water consumption in Arabidopsis by combined inactivation of the protein phosphatases type 2C ABI1 and HAB1. *Plant Physiol.* 141, 1389–1399. doi: 10.1104/pp.106.081018

Santiago, J., Rodrigues, A., Saez, A., Rubio, S., Antoni, R., Dupeux, F., et al. (2009). Modulation of drought resistance by the abscisic acid receptor PYL5 through inhibition of clade A PP2Cs. *Plant J.* 60, 575–588. doi: 10.1111/j.1365-313X.2009.03981.x

Sato, Y., Morita, R., Katsuma, S., Nishimura, M., Tanaka, A., and Kusaba, M. (2009b). Two short-chain dehydrogenase/reductases, NON-YELLOW COLORING 1 and NYC1-LIKE, are required for chlorophyll b and light-harvesting complex II degradation during senescence in rice. *Plant J.* 57, 120–131. doi: 10.1111/j.1365-313X.2008.03670.x

Sato, A., Sato, Y., Fukao, Y., Fujiwara, M., Umezawa, T., Shinozaki, K., et al. (2009a). Threonine at position 306 of the KAT1 potassium channel is essential for channel activity and is a target site for ABA-activated SnRK2/OST1/SnRK2.6 protein kinase. *Biochem. J.* 424, 439–448. doi: 10.1042/BJ20091221

Schelbert, S., Aubry, S., Burla, B., Agne, B., Kessler, F., Krupinska, K., et al. (2009). Pheophytin pheophorbide hydrolase (pheophytinase) is involved in chlorophyll breakdown during leaf senescence in Arabidopsis. *Plant Cell* 21, 767–785. doi: 10.1105/tpc.108.064089

Seo, M., Hanada, A., Kuwahara, A., Endo, A., Okamoto, M., Yamauchi, Y., et al. (2006). Regulation of hormone metabolism in Arabidopsis seeds: phytochrome regulation of abscisic acid metabolism and abscisic acid regulation of gibberellin metabolism. *Plant J.* 48, 354–366. doi: 10.1111/j.1365-313X.2006.02881.x

Sirichandra, C., Davanture, M., Turk, B. E., Zivy, M., Valot, B., Leung, J., et al. (2010). The Arabidopsis ABA-activated kinase OST1 phosphorylates the bZIP transcription factor ABF3 and creates a 14-3-3 binding site involved in its turnover. *PLoS One* 5:e13935. doi: 10.1371/journal.pone.0013935

Soon, F. F., Ng, L. M., Zhou, X. E., West, G. M., Kovach, A., Tan, M. H., et al. (2012). Molecular mimicry regulates ABA signaling by SnRK2 kinases and PP2C phosphatases. *Science* 335, 85–88. doi: 10.1126/science.1215106

Stone, S. L. (2019). Role of the ubiquitin proteasome system in plant response to abiotic stress. *Int. Rev. Cell Mol. Biol.* 343, 65–110. doi: 10.1016/bs.ircmb.2018.05.012

Szostkiewicz, I., Richter, K., Kepka, M., Demmel, S., Ma, Y., Korte, A., et al. (2010). Closely related receptor complexes differ in their ABA selectivity and sensitivity. *Plant J.* 61, 25–35. doi: 10.1111/j.1365-313X.2009.04025.x

Takahashi, Y., Ebisu, Y., Kinoshita, T., Doi, M., Okuma, E., Murata, Y., et al. (2013). bHLH transcription factors that facilitate K^+ uptake during stomatal opening are repressed by abscisic acid through phosphorylation. *Sci. Signal.* 6:ra48. doi: 10.1126/scisignal.2003760

Tan, B. C., Joseph, L. M., Deng, W. T., Liu, L., Li, Q. B., Cline, K., et al. (2003). Molecular characterization of the Arabidopsis 9-cis epoxycarotenoid dioxygenase gene family. *Plant J.* 35, 44–56. doi: 10.1046/j.1365-313X.2003.01786.x

Taya, S., Yamamoto, T., Kanai-Azuma, M., Wood, S. A., and Kaibuchi, K. (1999). The deubiquitinating enzyme Fam interacts with and stabilizes beta-catenin. *Genes Cells* 4, 757–767. doi: 10.1046/j.1365-2443.1999.00297.x

Tischer, S. V., Wunschel, C., Papacek, M., Kleigrewe, K., Hofmann, T., Christmann, A., et al. (2017). Combinatorial interaction network of abscisic acid receptors and coreceptors from *Arabidopsis thaliana*. *Proc. Natl. Acad. Sci. U. S. A.* 114, 10280–10285. doi: 10.1073/pnas.1706593114

Umezawa, T., Okamoto, M., Kushiro, T., Nambara, E., Oono, Y., Seki, M., et al. (2006). CYP707A3, a major ABA 8′-hydroxylase involved in dehydration and rehydration response in *Arabidopsis thaliana*. *Plant J.* 46, 171–182. doi: 10.1111/j.1365-313X.2006.02683.x

Umezawa, T., Sugiyama, N., Mizoguchi, M., Hayashi, S., Myouga, F., Yamaguchi-Shinozaki, K., et al. (2009). Type 2C protein phosphatases directly regulate abscisic acid-activated protein kinases in Arabidopsis. *Proc. Natl. Acad. Sci. U. S. A.* 106, 17588–17593. doi: 10.1073/pnas.0907095106

Uno, Y., Furihata, T., Abe, H., Yoshida, R., Shinozaki, K., and Yamaguchi-Shinozaki, K. (2000). Arabidopsis basic leucine zipper transcription factors involved in an abscisic acid-dependent signal transduction pathway under drought and high-salinity conditions. *Proc. Natl. Acad. Sci. U. S. A.* 97, 11632–11637. doi: 10.1073/pnas.190309197

van Kleeff, P. J. M., Gao, J., Mol, S., Zwart, N., Zhang, H., Li, K. W., et al. (2018). The Arabidopsis GORK K(+)-channel is phosphorylated by calcium-dependent protein kinase 21 (CPK21), which in turn is activated by 14-3-3 proteins. *Plant Physiol. Biochem.* 125, 219–231. doi: 10.1016/j.plaphy.2018.02.013

Vierstra, R. D. (2009). The ubiquitin-26S proteasome system at the nexus of plant biology. *Nat. Rev. Mol. Cell Biol.* 10, 385–397. doi: 10.1038/nrm2688

Vlad, F., Rubio, S., Rodrigues, A., Sirichandra, C., Belin, C., Robert, N., et al. (2009). Protein phosphatases 2C regulate the activation of the Snf1-related kinase OST1 by abscisic acid in Arabidopsis. *Plant Cell* 21, 3170–3184. doi: 10.1105/tpc.109.069179

Wang, Z., Wang, F., Hong, Y., Yao, J., Ren, Z., Shi, H., et al. (2018b). The flowering repressor SVP confers drought resistance in Arabidopsis by regulating Abscisic acid catabolism. *Mol. Plant* 11, 1184–1197. doi: 10.1016/j.molp.2018.06.009

Wang, P., Zhao, Y., Li, Z., Hsu, C. C., Liu, X., Fu, L., et al. (2018a). Reciprocal regulation of the TOR kinase and ABA receptor balances plant growth and stress response. *Mol. Cell* 69, 100–112.e6. doi: 10.1016/j.molcel.2017.12.002

Weiss, D., and Ori, N. (2007). Mechanisms of cross talk between gibberellin and other hormones. *Plant Physiol.* 144, 1240–1246. doi: 10.1104/pp.107.100370

Wu, Q., Zhang, X., Peirats-Llobet, M., Belda-Palazon, B., Wang, X., Cui, S., et al. (2016). Ubiquitin ligases RGLG1 and RGLG5 regulate Abscisic acid signaling by controlling the turnover of phosphatase PP2CA. *Plant Cell* 28, 2178–2196. doi: 10.1105/tpc.16.00364

Xue, S., Hu, H., Ries, A., Merilo, E., Kollist, H., and Schroeder, J. I. (2011). Central functions of bicarbonate in S-type anion channel activation and OST1 protein kinase in CO2 signal transduction in guard cell. *EMBO J.* 30, 1645–1658. doi: 10.1038/emboj.2011.68

Yamaguchi-Shinozaki, K., and Shinozaki, K. (1994). A novel cis-acting element in an Arabidopsis gene is involved in responsiveness to drought, low-temperature, or high-salt stress. *Plant Cell* 6, 251–264. doi: 10.1105/tpc.6.2.251

Yan, N., Doelling, J. H., Falbel, T. G., Durski, A. M., and Vierstra, R. D. (2000). The ubiquitin-specific protease family from Arabidopsis. AtUBP1 and 2 are required for the resistance to the amino acid analog canavanine. *Plant Physiol.* 124, 1828–1843. doi: 10.1104/pp.124.4.1828

Yang, J., Worley, E., and Udvardi, M. (2014). A NAP-AAO3 regulatory module promotes chlorophyll degradation via ABA biosynthesis in Arabidopsis leaves. *Plant Cell* 26, 4862–4874. doi: 10.1105/tpc.114.133769

Yang, W., Zhang, W., and Wang, X. (2017). Post-translational control of ABA signalling: the roles of protein phosphorylation and ubiquitination. *Plant Biotechnol. J.* 15, 4–14. doi: 10.1111/pbi.12652

Yin, P., Fan, H., Hao, Q., Yuan, X., Wu, D., Pang, Y., et al. (2009). Structural insights into the mechanism of abscisic acid signaling by PYL proteins. *Nat. Struct. Mol. Biol.* 16, 1230–1236. doi: 10.1038/nsmb.1730

Yoshida, T., Fujita, Y., Maruyama, K., Mogami, J., Todaka, D., Shinozaki, K., et al. (2015). Four Arabidopsis AREB/ABF transcription factors function predominantly in gene expression downstream of SnRK2 kinases in abscisic acid signalling in response to osmotic stress. *Plant Cell Environ.* 38, 35–49. doi: 10.1111/pce.12351

Yoshida, T., Fujita, Y., Sayama, H., Kidokoro, S., Maruyama, K., Mizoi, J., et al. (2010). AREB1, AREB2, and ABF3 are master transcription factors that cooperatively regulate ABRE-dependent ABA signaling involved in drought stress tolerance and require ABA for full activation. *Plant J.* 61, 672–685. doi: 10.1111/j.1365-313X.2009.04092.x

Yoshida, R., Hobo, T., Ichimura, K., Mizoguchi, T., Takahashi, F., Aronso, J., et al. (2002). ABA-activated SnRK2 protein kinase is required for dehydration stress signaling in Arabidopsis. *Plant Cell Physiol.* 43, 1473–1483. doi: 10.1093/pcp/pcf188

Yoshida, T., Nishimura, N., Kitahata, N., Kuromori, T., Ito, T., Asami, T., et al. (2006b). ABA-hypersensitive germination3 encodes a protein phosphatase 2C (AtPP2CA) that strongly regulates abscisic acid signaling during germination among Arabidopsis protein phosphatase 2Cs. *Plant Physiol.* 140, 115–126. doi: 10.1104/pp.105.070128

Yoshida, R., Umezawa, T., Mizoguchi, T., Takahashi, S., Takahashi, F., and Shinozaki, K. (2006a). The regulatory domain of SRK2E/OST1/SnRK2.6 interacts with ABI1 and integrates abscisic acid (ABA) and osmotic stress signals controlling stomatal closure in Arabidopsis. *J. Biol. Chem.* 281, 5310–5318. doi: 10.1074/jbc.M509820200

Yu, F., Lou, L., Tian, M., Li, Q., Ding, Y., Cao, X., et al. (2016). ESCRT-I component VPS23A affects ABA signaling by recognizing ABA receptors for Endosomal degradation. *Mol. Plant* 9, 1570–1582. doi: 10.1016/j.molp.2016.11.002

Yu, Z., Zhang, D., Xu, Y., Jin, S., Zhang, L., Zhang, S., et al. (2019). CEPR2 phosphorylates and accelerates the degradation of PYR/PYLs in Arabidopsis. *J. Exp. Bot.* 70, 5457–5469. doi: 10.1093/jxb/erz302

Zhang, L., Li, X., Li, D., Sun, Y., Li, Y., Luo, Q., et al. (2018). CARK1 mediates ABA signaling by phosphorylation of ABA receptors. *Cell Discov.* 4:30. doi: 10.1038/s41421-018-0029-y

Zhao, Y., Chan, Z., Gao, J., Xing, L., Cao, M., Yu, C., et al. (2016b). ABA receptor PYL9 promotes drought resistance and leaf senescence. *Proc. Natl. Acad. Sci. U. S. A.* 113, 1949–1954. doi: 10.1073/pnas.1522840113

Zhao, Y., Chan, Z., Xing, L., Liu, X., Hou, Y. J., Chinnusamy, V., et al. (2013). The unique mode of action of a divergent member of the ABA-receptor protein family in ABA and stress signaling. *Cell Res.* 23, 1380–1395. doi: 10.1038/cr.2013.149

Zhao, Y., Zhang, Z., Gao, J., Wang, P., Hu, T., Wang, Z., et al. (2018). Arabidopsis duodecuple mutant of PYL ABA receptors reveals PYL repression of ABA-independent SnRK2 activity. *Cell Rep.* 23, 3340.e5–3351.e5. doi: 10.1016/j.celrep.2018.05.044

Zhao, J., Zhou, H., Zhang, M., Gao, Y., Li, L., Gao, Y., et al. (2016a). Ubiquitin-specific protease 24 negatively regulates abscisic acid signalling in *Arabidopsis thaliana*. *Plant Cell Environ.* 39, 427–440. doi: 10.1111/pce.12628

Zhou, H., Zhao, J., Cai, J., and Patil, S. B. (2017). UBIQUITIN-SPECIFIC PROTEASES function in plant development and stress responses. *Plant Mol. Biol.* 94, 565–576. doi: 10.1007/s11103-017-0633-5

Zhu, J. K. (2016). Abiotic stress signaling and responses in plants. *Cell* 167, 313–324. doi: 10.1016/j.cell.2016.08.029

Zhu, S. Y., Yu, X. C., Wang, X. J., Zhao, R., Li, Y., Fan, R. C., et al. (2007). Two calcium-dependent protein kinases, CPK4 and CPK11, regulate abscisic acid signal transduction in Arabidopsis. *Plant Cell* 19, 3019–3036. doi: 10.1105/tpc.107.050666

Zou, J. J., Wei, F. J., Wang, C., Wu, J. J., Ratnasekera, D., Liu, W. X., et al. (2010). Arabidopsis calcium-dependent protein kinase CPK10 functions in abscisic acid- and Ca^{2+}−mediated stomatal regulation in response to drought stress. *Plant Physiol.* 154, 1232–1243. doi: 10.1104/pp.110.157545

Conflict of Interest: The authors declare that the research was conducted in the absence of any commercial or financial relationships that could be construed as a potential conflict of interest.

Publisher's Note: All claims expressed in this article are solely those of the authors and do not necessarily represent those of their affiliated organizations, or those of the publisher, the editors and the reviewers. Any product that may be evaluated in this article, or claim that may be made by its manufacturer, is not guaranteed or endorsed by the publisher.

Copyright © 2022 Lim, Lim and Lee. This is an open-access article distributed under the terms of the Creative Commons Attribution License (CC BY). The use, distribution or reproduction in other forums is permitted, provided the original author(s) and the copyright owner(s) are credited and that the original publication in this journal is cited, in accordance with accepted academic practice. No use, distribution or reproduction is permitted which does not comply with these terms.

frontiers | Frontiers in Plant Science

ORIGINAL RESEARCH
published: 31 May 2022
doi: 10.3389/fpls.2022.914363

Wheat ocs-Element Binding Factor 1 Enhances Thermotolerance by Modulating the Heat Stress Response Pathway

*Harsha Samtani†, Aishwarye Sharma† and Paramjit Khurana**

Department of Plant Molecular Biology, University of Delhi South Campus, New Delhi, India

The basic leucine zipper family (bZIP) represents one of the largest families of transcription factors that play an important role in plant responses to abiotic stresses. However, their role in contributing to thermotolerance in plants is not well explored. In this article, two homoeologs of wheat ocs-element binding factor 1 (TaOBF1-5B and TaOBF1-5D) were found to be heat-responsive TabZIP members. Their expression analysis in Indian wheat cultivars revealed their differential expression pattern and TaOBF1-5B was found to be more receptive to heat stress. Consistent with this, the heterologous overexpression of TaOBF1-5B in *Arabidopsis thaliana* and *Oryza sativa* promoted the expression of stress-responsive genes, which contributed to thermotolerance in transgenic plants. TaOBF1-5B was seen to interact with TaHSP90 in the nucleus and TaSTI in the nucleolus and the ER. Thus, the results suggest that TaOBF1-5B might play an important regulatory role in the heat stress response and is a major factor governing thermotolerance in plants.

Keywords: bZIP, endoplasmic reticulum (ER), heat stress, nucleus, ocs-element binding factor 1 (OBF1), thermotolerance, wheat

OPEN ACCESS

Edited by:
Amita Pandey,
Shriram Institute for Industrial Research, India

Reviewed by:
Sung Chul Lee,
Chung-Ang University, South Korea
Necla Pehlivan,
Recep Tayyip Erdoğan University, Turkey

***Correspondence:**
Paramjit Khurana
param@genomeindia.org
orcid.org/0000-0002-8629-1245

†These authors have contributed equally to this work

Specialty section:
This article was submitted to Plant Physiology, a section of the journal Frontiers in Plant Science

Received: *06 April 2022*
Accepted: *28 April 2022*
Published: *31 May 2022*

Citation:
Samtani H, Sharma A and Khurana P (2022) Wheat ocs-Element Binding Factor 1 Enhances Thermotolerance by Modulating the Heat Stress Response Pathway. Front. Plant Sci. 13:914363. doi: 10.3389/fpls.2022.914363

INTRODUCTION

Transcription factors function as important components of regulatory networks present inside the cell. They modulate the expression of the target genes by binding to specific sequences in their promoter region (Kong et al., 2015; Yamaguchi, 2021). Amongst the various transcription factor families in plants, basic leucine zipper family (bZIP) represents one of the family, which participates in regulating diverse biological functions, such as stress and hormone signaling, floral induction and development, seed maturation and germination, photomorphogenesis, and pathogen defense (Jakoby et al., 2002; Nijhawan et al., 2008).

bZIP proteins possess the characteristic bZIP domain composed of the basic region and a leucine zipper (Dröge-Laser and Weiste, 2018). The bZIP domain spans over 60–80 amino acids. The basic region consists of 16 amino acids which are further characterized by the presence of an invariant N-x$_7$-R/K motif. The leucine zipper is composed of a heptad repeat of leucine or other hydrophobic amino acids, such as isoleucine, valine, methionine, and phenylalanine, situated nine amino acids toward the C-terminal. While the basic region binds to DNA in a sequence-specific manner, the leucine zipper is in the form of a coiled-coil amphipathic sequence, which is less conserved and determines dimerization aspects, i.e., homodimerization and heterodimerization (Nijhawan et al., 2008; Dröge-Laser et al., 2018).

bZIP is one of the most diverse proteins and is reported in many eukaryotes. Several members of this family have been reported in organisms, such as *Arabidopsis* (75), rice (89), human (56), *Sorghum* (92), Soybean (131) and maize (125), *Brachipodium distachyon* (96), *Triticum aestivum* (191), *Musa acuminata* (121), and *Manihot esculanta* (77) (Riechmann et al., 2000; Deppmann et al., 2004; Liao et al., 2008; Nijhawan et al., 2008; Wang et al., 2011; Wei et al., 2012; Liu and Chu, 2015; Hu et al., 2016a,b; Agarwal et al., 2019). Studies suggest that plant bZIPs can bind to DNA sequences with an ACGT core *cis*-element, such as ABRE, G-box (CACGTG), C-box (GACGTC), A-box (TACGTA), T-box (AACGTT), and a GCN4 motif [TGA (G/C)TCA] (Foster et al., 1994; Agarwal et al., 2019).

Several bZIPs have been implicated to play an important role in abiotic stresses, such as drought stress, saline stress, and cold stress. In the case of *Arabidopsis*, *AtbZIP17* and *AtbZIP24* were reported to enhance salt tolerance by regulating the expression of stress-responsive genes (Liu et al., 2008; Yang et al., 2009). *AtbZIP1* was found to be upregulated by cold, salt, and drought stress and its overexpression promoted salt and drought tolerance, thereby making it a positive regulator of the stress response (Sun et al., 2012). *AtbZIP62* has been reported as a negative regulator of salt stress response in *Arabidopsis thaliana* (Rolly et al., 2020). In the case of rice, overexpression of *OsbZIP23* in rice plants significantly enhanced drought and salt tolerance and led to increased ABA sensitivity (Xiang et al., 2008). Similarly, Lu et al. (2009) reported the role of *OsbZIP72* in ABA signaling and drought tolerance. OsbZIP52 was found to function as a negative regulator in cold and drought stress, as the rice plants overexpressing *OsbZIP52,* were found to be cold and drought-sensitive, and various stress-regulated genes were observed to be down-regulated in the transgenic plants (Liu et al., 2012). The role of *OsbZIP39* was reported in regulating the ER stress response, as its overexpression enhanced the expression of ER stress marker genes (Takahashi et al., 2012).

As compared to *Arabidopsis* and *Oryza sativa*, there have been very limited reports elucidating the functional role of *TabZIPs*. In wheat, overexpression of *TabZIP60* enhanced multiple stress tolerance in *Arabidopsis* through the ABA signaling pathway (Zhang et al., 2015). Further, the splicing of *TabZIP60* was found to provide heat stress tolerance in *Arabidopsis* plants by regulating the expression of ER stress-related genes (Geng et al., 2018). Similarly, *TabZIP14-B* was found to participate in freezing and salt tolerance in transgenic *Arabidopsis* plants (Zhang et al., 2017). Agarwal et al. (2019) identified *TabZIP,* which provided tolerance against environmental stress, such as heat, salinity, and dehydration. *TabZIP6* was identified to negatively regulate cold stress response, as it was found to bind to CBF and decrease the expression of downstream COR genes in *Arabidopsis* overexpression lines (Cai et al., 2018).

Ocs-element binding factor (OBF) proteins belong to group S bZIPs, which bind to promoters containing 20 bp element named as *ocs* (Katagiri and Chua, 1992; Zhang et al., 1993). This *cis*-acting *ocs*-element was first discovered in the promoter of the octopine synthase (*ocs*) gene of *A. tumefaciens* (Zhang et al., 1993). The proteins that belong to the OBF bZIP subfamily are also classified as TGA transfactors (Rieping et al., 1994). Maize OBF1 was reported to accumulate in response to low temperature (Kusano et al., 1995). In the case of *O. sativa*, OsOBF1 has been identified as an interacting protein of low-temperature induced lip19 protein, although the transcripts of *OsOBF1* were found to decrease under low-temperature treatment. Thus, *OsOBF1* is speculated to be involved in a low-temperature signal switching mechanism in rice (Shimizu et al., 2005). Similarly, in the case of wheat, the transcript of *TaOBF1* was found to increase under cold and drought stress, and TaOBF1 heterodimerized with Wlip19 (wheat lip19 homoeolog) (Kobayashi et al., 2008). However, till now TaOBF1 has not been functionally characterized in any plant.

In this study, we have identified *TaOBF1-5B* as a heat-responsive bZIP. Its interaction with TaSTI and TaHSP90 suggested its potential role in heat stress response. Overexpression of *TaOBF1-5B* in both *Arabidopsis* and *O. sativa* provided thermotolerance by increasing the expression of stress-responsive genes. Thus, this data suggests that apart from being involved in low-temperature response, *TaOBF1* might also play an important role under heat stress conditions.

MATERIALS AND METHODS

Phylogenetic Analysis

The protein sequences of all the OBF1 members were downloaded from the NCBI database. The multiple sequence alignment was performed by using the MUSCLE program and the neighbor-joining (NJ) phylogenetic tree was constructed by using MEGA 7 software.

Expression Analysis of *TaOBF1* in *Triticum aestivum*

For analyzing the expression of *TaOBF1-5B* and *TaOBF1-5D* in various developmental stages, the wheat expression database hosted at http://wheatexpression.com was used (Borrill et al., 2016). As this database harbored the normalized data, therefore, transcripts per kilobase millions (TPM) values were Log transformed (Log_2X) to generate a heatmap using gplot package and Rcolorbrewer package. For seedling-based studies, wheat plants of Indian cultivar PBW-343 and K7903 were germinated on a cotton bed in sterile petri-dishes in a growth chamber maintained at 24/20°C temperature under a daily cycle of 16 h light/8 h dark photoperiod, having 200–300 μmol m^{-2} s^{-1} of light intensity. For studying the effect of high temperature, the seedlings of K7903 and PBW-343 cultivar were kept in a growth chamber, that was set at 30, 35, 40, and 45°C and were collected at 2 hrs after the stress treatment (Agarwal and Khurana, 2019). For checking the expression of *TaOBF1* homoeologs in various tissues, plants of PBW-343 were grown in potting soil in the departmental net house. For heat stress treatment, the plants were transferred for 4 h to a growth chamber maintained at 42°C for 5, 10, 15, and 20 days after anthesis (Agarwal and Khurana, 2019). A sampling of tissues like root, flag leaf, anther, ovary, lodicule, and developing grain was done from the spike of the control and stressed plants simultaneously. The tissue was immediately frozen in liquid nitrogen and stored at −80°C until RNA isolation.

Transactivation Assay

For checking the transactivation of TaOBF1-5B, the full-length CDS was subcloned into the GAL4 DNA-binding domain of the pGBKT7 vector (Clonetech, USA) by using the Gateway™ cloning technology (Directional TOPO cloning kit and LR clonase Enzyme mix II kit, Invitrogen Inc., USA). The recombinant plasmids were then transformed into yeast strain AH109 harboring the HIS3 reporter gene. The transformants were selected on tryptophan lacking media (SD-W) and the transactivation activity was screened by dropout assay performed on tryptophan and histidine lacking media (SD-HW).

Subcellular Localization and BiFC Assay

To determine the subcellular localization of TaOBF1-5B, the full-length CDS was amplified from the 2 h heat stress cDNA, using the HF phusion enzyme (NEB), and then cloned into the pENTR/D-TOPO vector. It was then mobilized into the destination vector, i.e., pSITE3CA, having the CaMV35S promoter (Directional TOPO cloning kit and LR clonase Enzyme mix II kit, Invitrogen Inc., USA). The ORF of the gene was fused in frame with the C terminal of YFP. This plasmid construct was then used for coating the gold particles and bombarded at a pressure of 1,100 psi into the onion epidermal peel cells by using the PDS-1000 bombardment system (Bio-Rad, Canada). Transformed onion peels were incubated at 27°C for 16 h under dark conditions and the fluorescence was observed in the confocal microscope (Leica, Germany).

For the BiFC assay, the CDS of *TaHSP90* and *TaSTI-2A* were first cloned into pENTR/D-TOPO vector and then mobilized into pSITE-cEYFP. Similarly, the CDS of *TaOBF1-5B* was cloned into pSITE-nEYFP. The plasmid combinations were used for coating the gold particles and then bombarded at a pressure of 1,100 psi into the onion epidermal peel cells by using the PDS-1000 bombardment system (Bio-Rad, Canada). Transformed onion peels were incubated at 27°C for 16 h under dark conditions and the fluorescence was observed in the confocal microscope (Leica, Germany).

For checking the interaction between putative interactors, the genes of *TaOBF1-5B*, *TaOBF1-5D*, *TaHSP90,* and *TaSTI-2A* were cloned into the pENTR/D-TOPO vector and further into pDEST-GADT7 and pDEST-GBKT7 vectors (Clonetech, United States). The plasmid combinations were transformed into the yeast AH109 strain harboring the HIS3 reporter gene. The reporter gene activity was confirmed by the viability test on a medium lacking histidine, leucine, and tryptophan (-HLW) supplemented with 0.5 mM 3AT (3-Amino-1,2,4-triazole).

TaOBF1-5B Cloning and Overexpression in *Arabidopsis thaliana*

For generating the *TaOBF1-5B* overexpression lines in *Arabidopsis*, the full-length CDS was amplified and cloned into the pENTR/D-TOPO vector. It was then mobilized into a pMDC32 destination vector having the CaMV35S promoter using the Gateway™ cloning technology (Directional TOPO cloning kit and LR clonase Enzyme mix II kit, Invitrogen Inc., USA). The EHA105 strain of *Agrobacterium tumefaciens* harboring the pMDC32-*TaOBF1-5B* was used for the transformation of *Arabidopsis* plants by the floral dip method (Zhang et al., 2006). Positive transgenic plants were selected after successive generations of selection on MS-agar medium supplemented with 50 μg/μl of hygromycin. The plants were further confirmed by PCR by using the hygromycin and gene-specific primers. Members of the T_3 generation with 100% resistance to hygromycin were considered to be homozygous. The level of ectopic expression in homozygous plants was checked by RT-PCR analysis.

TaOBF1-5B Overexpression in *Oryza sativa*

For generating the *TaOBF1-5B* overexpression lines in rice, the full length CDS was cloned into pIPKb002 gateway-based vector under the control of maize ubiquitin promoter (Himmelbach et al., 2007; accession no - EU161568). This construct was then transformed into *O. sativa* Indica rice through *Agrobacterium*-mediated transformation by using a protocol described by Toki et al. (2006). Briefly, 7-day-old scutellum-derived embryogenic calli were infected with *Agrobacterium* EHA105 strain harboring the above-mentioned construct. These calli were washed after three days of co-cultivation and kept on the selection medium supplemented with 50 μg/L hygromycin. The secondary calli that developed after four rounds of selection were then transferred to regeneration media for the development of shoots. The regenerated shoots were then transferred to the rooting media. The regenerated plantlets were maintained at 30 ± 2°C at a photosynthetic flux density of 300 μmol $m^{-2}s^{-1}$, 75–80% of humidity, and photoperiod duration of 16/10 h light/dark phase in rice growth medium (RGM) for 1 month. Thereafter, the plants were transferred to pots containing soil in the greenhouse having the same growth conditions as mentioned above.

Heat Stress Treatment and Expression Profile of Marker Genes in *TaOBF1-5B* Overexpression Lines in *Arabidopsis thaliana* and *Oryza sativa*

For checking the basal thermotolerance in plants, the *Arabidopsis* Col-0 seeds and the overexpression line seeds were germinated on half strength MS media and allowed to grow in a culture room maintained at 22 ± 2°C at a photosynthetic flux density of 300 μmol $m^{-2}s^{-1}$, 60% of humidity and photoperiod duration of 16/10 h light/dark phase for 2 weeks. For basal heat stress, the plants were transferred to a growth chamber maintained at 42°C for 2 h and then returned to their original growth conditions for recovery. The phenotype was recorded after 5 days of recovery.

For checking the thermotolerance in rice, T_2 seeds were germinated on MS medium supplemented with hygromycin. The WT seeds were germinated on only MS media. Five days after germination, the plants were transferred to a growth chamber maintained at 42°C at a photosynthetic flux density of 300 μmol $m^{-2}s^{-1}$, 60% of humidity, and a photoperiod duration of 16/10 h light/dark phase. After 5 days of heat stress, the plants were then transferred back to normal temperature and allowed to recover. The phenotype was observed after 4 days of recovery. For checking the expression of heat stress marker genes, plants were grown in the greenhouse until the heading

stage and then were then subjected to alternate days of heat stress followed by recovery. The flag leaf tissue was harvested after the stress treatment and stored at −80°C until RNA isolation. For analyzing the ROS levels, 15-day-old seedlings were subjected to 42°C for 24 h followed by a single day of recovery after which both leaf and root tissues were used for NBT staining.

Histochemical ROS Detection

For vizualization the ROS levels in *TaOBF1-5B Arabidopsis* overexpression lines and WT, staining with nitro blue tetrazolium (NBT) was done (Meena et al., 2020; Samtani et al., 2022). The seeds were germinated on half strength MS medium and then 1- and 2-week-old plants were subjected to 42°C for 2 h, after which the overnight staining of the seedlings was done with NBT (2 mM NBT powder, 20 mM phosphate buffer). The seedlings were washed with water and subjected to chlorophyll removal by dipping them in a bleaching solution (ethanol, acetic acid, and glycerol in a ratio of 3:1:1). The seedlings were then visualized under a bright field light microscope (Leica, Germany) and pictures were taken for comparison of ROS in transgenics and the wild-type plants.

Similarly, NBT staining was done in *TaOBF1-5B* rice overexpression lines and the WT plants after heat stress for analyzing the ROS levels. For this, 15-day-old seedlings grown hydroponically were subjected to 42°C for 24 h and then allowed to recover for 24 h after which the staining was done overnight as described above.

Estimation of Chlorophyll Content and Fresh Weight

Two-week-old *TaOBF1-5B* transgenic and WT plants *A. thaliana* were subjected to 42°C for 2 h. For estimation of chlorophyll,

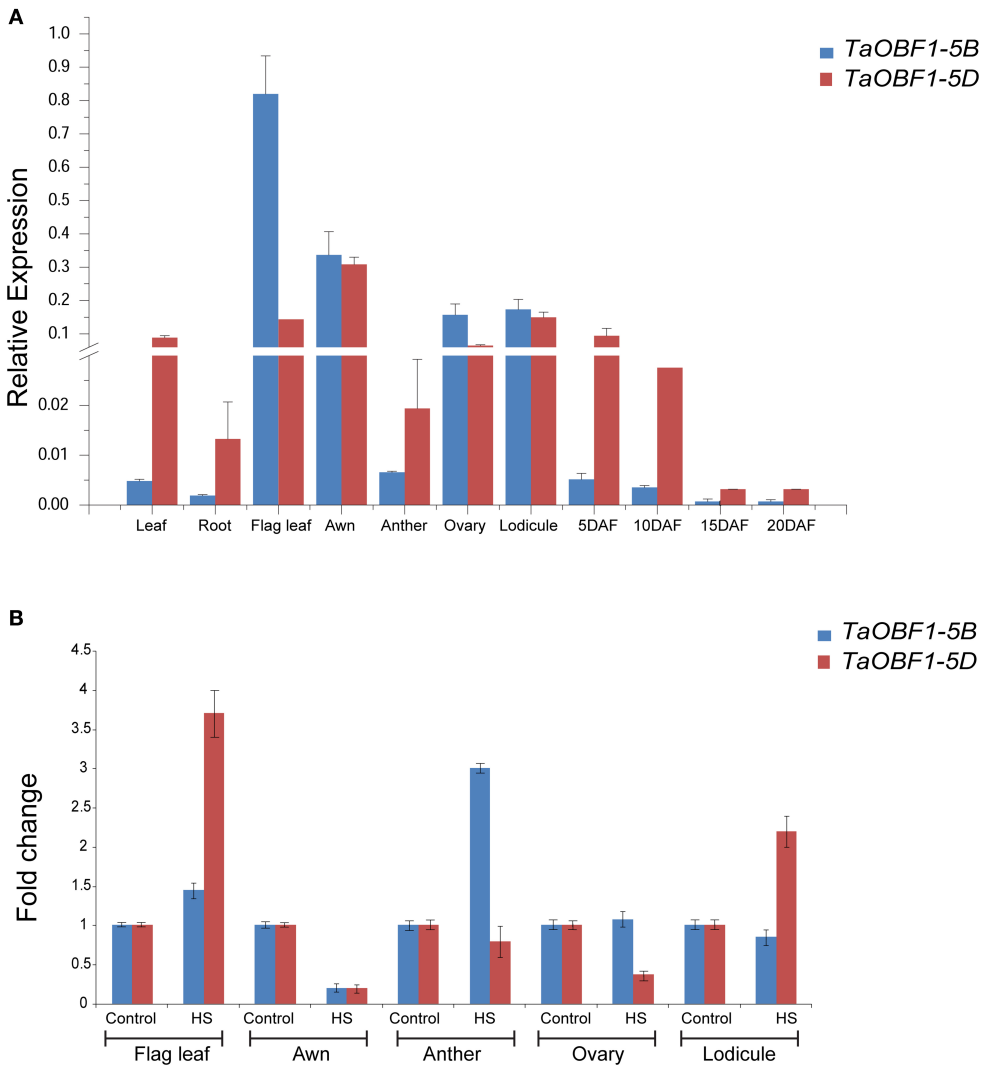

FIGURE 1 | Expression analysis of TaOBF1 homoeologs in different tissues of wheat cv. PBW343 seedlings under **(A)** control and **(B)** heat stress conditions. Relative expression was checked in different tissues by qRT-PCR. *TaGAPDH* was used as an internal control gene. Error bars indicate values ±SD. DAF, days after fertilization.

50 mg of the seedling tissue was taken in a test tube containing 2.5 ml of Dimethyl Sulfoxide and incubated overnight for chlorophyll bleaching. The absorbance of the samples was then measured at 645 nm and 663 nm in a UV-Vis spectrophotometer (Hitachi U-2810, Tokyo, Japan), and the chlorophyll content was calculated according to Arnon (1949), Agarwal and Khurana (2018). For fresh weight estimation, 2-week-old seedlings were subjected to the above-mentioned HS regime, and after 4 days of recovery, the fresh weight was measured. Three biological replicates having 50 seedlings each were taken for calculations.

RNA Isolation and Quantitative Real-Time PCR Analysis

Total RNA was extracted using the TRIzol Reagent (Ambion) according to the manufacturer's protocol. Isolated RNA was converted into cDNA using the Applied Biosystems™ High-Capacity cDNA Reverse Transcription kit (Thermo Fisher Scientific). Quantitative Real-Time PCR (qRT-PCR) was conducted using the SYBR Green (Applied Biosystems) in QuantStudio™ 3 Real-time PCR system (Thermo Fisher Scientific) to study the expression of selected genes (primer sequences provided in **Supplementary Table 1**) with three biological and three technical replicates. For internal control, *GAPDH* was used in the case of *T. aestivum*, *Actin 2* in the case of *A. thaliana*, and *Ubiquitin5* was used in the case of *O. sativa*. Relative gene expression was calculated according to the $2^{-\Delta\Delta}$Ct method (Livak and Schmittgen, 2001). Further, the relative expression of *TaOBF1* homoeologs in different tissues was calculated according to Borah and Khurana (2018).

The real-time data presented in graphs depict the mean ± standard deviation of mean (SD). The distribution of the data was assumed to be normal and thus paired Student's t-test was used for statistical analyses of the results. The statistical significant differences were shown at $p \leq 0.05$ (marked *), $p \leq 0.01$ (marked **), and $p \leq 0.001$ (marked ***).

RESULTS

Identification and Phylogenetic Analysis of *TaOBF1-5B* and *TaOBF1-5D*

Genome-wide identification of *TabZIPs* in wheat showed the expression profile of all the bZIPs under heat stress conditions (Agarwal et al., 2019). In this data, Traes_5B_FF44610EF1.3 and Traes_5D_011851EE7.1 were identified as two *TabZIPs*, which showed upregulation by heat stress. Using the Ensembl database, these genes were found to be homoeologs and the domain analysis of the database identified them as *OBF1*. The Traes_5B_FF44610EF1.3 gene was found to be located on chromosome 5B (hereafter denoted as *TaOBF1-5B*) with CDS of 474 bp, protein of 157 amino acids, and 5' and 3' non-coding region of 598 and 372 bp, respectively. On the other hand, Traes_5D_011851EE7.1 was also found to be located on chromosome 5D (hereafter denoted as *TaOBF1-5D*) with CDS of 474 bp, protein of 157 amino acids, and 5' and 3' non-coding region of 320 and 295 bp, respectively. Sequence analysis revealed that the CDS of *TaOBF1-5B* and *TaOBF1-5D* differed only by the presence of eight SNPs as the rest of the sequence was found to be identical (**Supplementary Figure S1A**). At the protein level, differences of only two amino acids were found in these homoeologs. TaOBF1-5B had Ala and Asp, while in TaOBF1-5D Ser and Thr were present at respective positions (**Supplementary Figure S1B**). By using the differences in their UTR regions, the CDS of *TaOBF1-5B* and *TaOBF1-5D* was cloned into the pENTR/D-TOPO vector and subsequently mobilized into various destination vectors (**Supplementary Figure S2**).

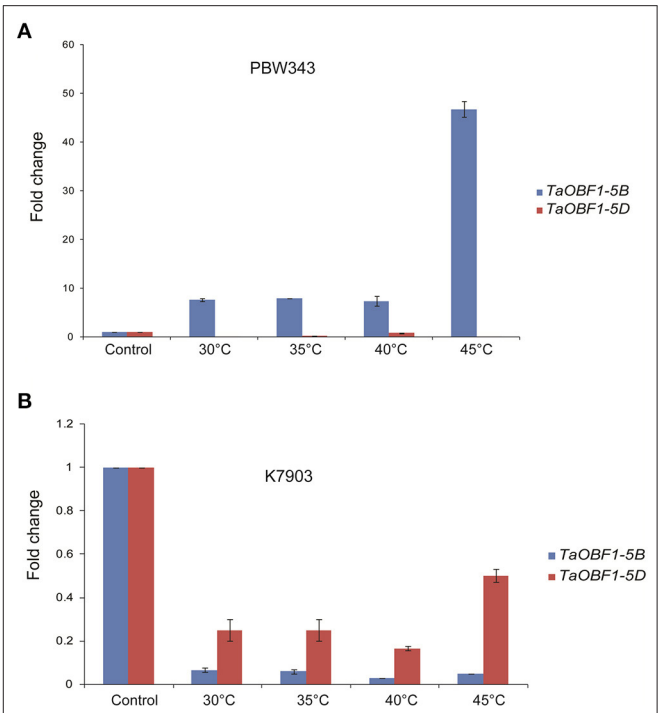

FIGURE 2 | Expression analysis of *TaOBF1* homoeologs under heat stress conditions in *Triticum aestivum* cv. **(A)** PBW343 (heat sensitive) **(B)** K7903 (heat tolerant) seedlings at various temperatures. Relative fold change was checked by qRT-PCR. *TaGAPDH* was used as an internal control gene. Error bars indicate values ± SD.

For finding the evolutionary links of TaOBF1, a phylogenetic tree was constructed using OBF and TGA sequences from different species (**Supplementary Figure S1C**). Interestingly, all the OBFs appeared in a separate clade, whereas all the TGAs grouped in different clades. This grouping pattern indicates their functional divergence as well. Moreover, TaOBF1-5B and TaOBF1-5D were found to be closest to OBF1 of *Secale cereale* (**Supplementary Figure S1C**).

Comparison of Expression Profile and Subcellular Localization of TaOBF1-5B and TaOBF1-5D

A wheat expression database was used to investigate the differences in the expression profile of *TaOBF1-5B* and *TaOBF1-5D*. **Supplementary Figure S3** depicts the expression

of *TaOBF1-5B* and *TaOBF1-5D* across various Zadok stages and in different developmental tissues. It was observed that both of them had similar expression profiles, as among different Zadok stages their expression was found in stem (Zadok stage 65) and root (Zadokstage 13 and Zadokstage 23) (**Supplementary Figure S3A**). Amongst the various tissues, *TaOBF1-5B* and *TaOBF1-5D* showed the highest expression in the stamen, although it was found to be higher for *TaOBF1-5B* (**Supplementary Figure S3B**). The stress responsiveness of *TaOBF1* was also analyzed by the wheat expression database (**Supplementary Figure S3C**). Both *TaOBF1-5B* and *TaOBF1-5D* were found to be upregulated by 6 h of heat stress.

Further, the relative expression pattern of both the homoeologs of *TaOBF1* was analyzed in different tissues in Indian cultivars, i.e., PBW 343 by RT-PCR (**Figure 1A**). Interestingly, as compared to the online expression data of the cultivar Chinese Spring, a differential expression pattern of *TaOBF1* homoeologs, was observed in PBW-343. *TaOBF1-5B* had higher expression levels in flag leaf, awn, and lodicule tissues as compared to *TaOBF-5D*. Moreover, their expression was also compared in control and under heat stress conditions in flag leaf, awn, anther, ovary, and lodicule tissues (**Figure 1B**). *TaOBF1-5D* was found to be heat-induced in the flag leaf and lodicule tissues, whereas *TaOBF1-5B* was observed to be specifically upregulated by the heat stress in the anther tissues. Their expression was also validated at different time points of heat stress in the Indian wheat cultivar PBW-343. As shown in **Supplementary Figure S4**, *TaOBF1-5B* was induced by heat stress within 30 mins and its expression peaked at 4 h. Surprisingly, *TaOBF1-5D* was not found to be upregulated by heat stress. The expression *TaOBF1-5B* and *5D* were also compared in heat-sensitive (PBW-343) and heat tolerant (K7903) wheat varieties at different temperatures (**Figure 2**). Higher transcript levels of *TaOBF1-5B* were observed with increasing temperatures in the heat-sensitive variety, i.e., PBW-343, with its highest expression at 45°C (**Figure 2A**). The expression of *TaOBF1-5D* did not show any increase with the rise in temperature in PBW-343. In the case of heat-tolerant wheat varieties, the expression of both the homoeologs of TaOBF1 were found to be down-regulated with the increase in temperature (**Figure 2B**). However, lesser down-regulation of *TaOBF1-5B* was observed as compared to *TaOBF1-5D*. Since a differential expression pattern was noticed for *TaOBF1* homoeologs, therefore, their subcellular localization pattern was also checked by bombarding their YFP-fusion constructs in onion epidermal peel cells. Both TaOBF1-5B and TaOBF1-5D were found to localize to the nucleus and in the cytoplasm (**Figure 3**). No difference in their localization pattern was observed. Thus, these studies indicate that among the TaOBF1 homoeologs,

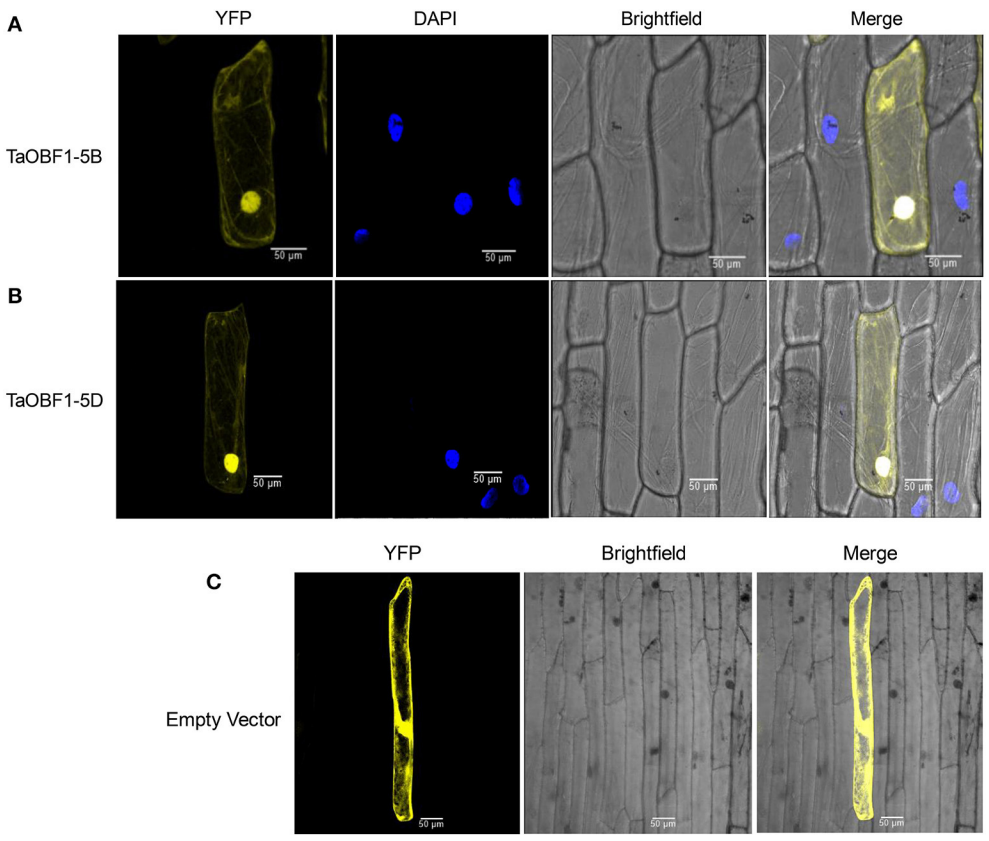

FIGURE 3 | Subcellular localization of selected TaOBF1 homoeologs **(A)** TaOBF1-5B, **(B)** TaOBF1-5D, and **(C)** localization of pSIT3CA empty vector. DAPI stain was used to highlight the nucleus along with the YFP (YFP, yellow fluorescent protein) (scale bar 50 µm).

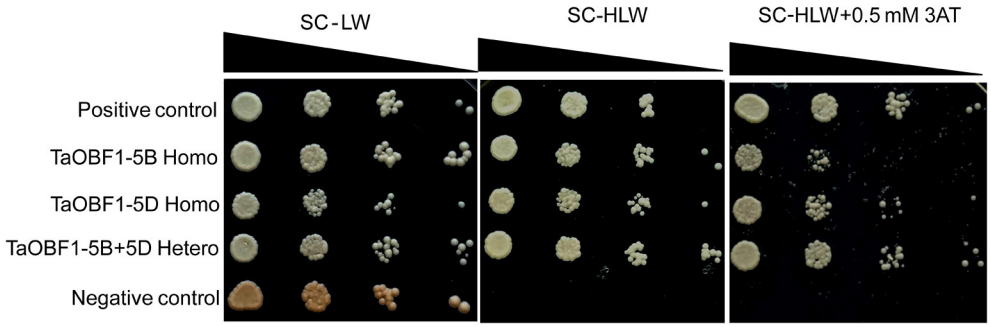

FIGURE 4 | Homo-dimerization and hetero-dimerization of TaOBF1-5B and TaOBF1-5D. Yeast-two-hybrid (Y2H) assay was performed to check the homodimerization of TaOBF1-5B and TaOBF1-5D by co-transforming pGBKT7-5B and pGADT7-5B (labeled as TaOBF1-5B Homo) and pGBKT7-5D and pGADT7-5D (labeled as TaOBF1-5D Homo), respectively. The Y2H assay was performed to check the heterodimerization of TaOBF1-5B and TaOBF1-5D by co-transforming pGBKT7-5B and pGADT7-5D (labeled as TaOBF1-5B-5D Hetero). The growth of co-transformed yeast cells was analyzed by drop assay on SD/-Leu/-Trp (-LW) medium, SD/-Leu/-Trp/-His (-HLW) medium, and SD/-Leu/-Trp/-His (-HLW) + 0.5 mM 3-aminotriazole medium (3AT). Pair of plasmids pGBKT7-53 and pGADT7-T were used as positive control, and pGBKT7-Lam and pGADT7-T were used as the negative control.

TaOBF1-5B has a probable role in the heat stress response, and thus it was taken further for in-depth characterization.

Homo and Hetro-Dimerization Between TaOBF1-5B and TaOBF1-5D

As *TaOBF1* belongs to a bZIP family, which is well known for controlling the transcription of various genes. Therefore, the transactivation potential of TaOBF1-5B was checked by a yeast one-hybrid system. As shown in **Supplementary Figure S5**, no growth of the transformed cells was observed on histidine lacking media thereby indicating the absence of transactivation. The leucine zipper motif of bZIPs is known to dimerize (Jakoby et al., 2002). Therefore, the homo and hetero-dimerization of both the homoeologs of TaOBF1 were checked using the yeast two-hybrid assay. To see the interaction, the growth of co-transformed colonies was analyzed on SC-HLW and SC-HLW + 0.5 mM 3AT media. Homo-dimerization was observed with both TaOBF1-5B and TaOBF1-5D (**Figure 4**). TaOBF1-5D showed slightly better strength of homodimerization as compared to TaOBF1-5B as observed by their growth on SC-HLW + 0.5 mM 3AT media. Apart from this, TaOBF1-5B and TaOBF1-5D were also found to hetero-dimerize as the co-transformed cells were able to grow on 3AT-containing media. The strength of hetero-dimerization was found to be more as compared to the individual homo-dimerization.

In vivo Interaction of TaOBF1-5B With TaSTI and TaHSP90

Shimizu et al. (2005) reported that the low-temperature induced Lip19 protein interacted with OsOBF1 to work in the cold-signaling pathway. As *TaOBF1-5B* was found heat-responsive, therefore, we checked its interaction with TaSTI, which is a stress-induced protein known to function in heat stress. Also, previously we had reported the interaction between TaSTI and TaHSP90 (Meena et al., 2020), therefore, we also checked the interaction of TaOBF1-5B with TaHSP90 and TaHSP70 using the yeast two-hybrid method. Interestingly, TaOBF1-5B was found to interact both with TaHSP90 and with TaSTI as the co-transformed yeast cells were able to grow in an SC-HLW medium (**Figure 5A**). Interaction with TaSTI appeared to be stronger in comparison to TaHSP90. However, no interaction was observed with TaHSP70. These interactions were further confirmed by the BiFC assay. Interaction between TaOBF1-5B and TaSTI was found to occur in the nucleolus and the ER (**Figure 5B**). On the other hand, the interaction between TaOBF1-5B and TaHSP90 was seen only in the nucleus (**Figure 5C**).

TaOBF1-5B Enhances Basal Thermotolerance in *Arabidopsis thaliana*

To investigate the role of TaOBF1-5B in heat stress response, it was overexpressed in the *A. thaliana* plants. The overexpression lines were confirmed by using hygromycin-specific PCR, gene-specific PCR (**Supplementary Figures S6A,B**). The level of ectopic overexpression was detected by RT-PCR, and the overexpression lines were found to have higher expression in comparison to the WT (**Supplementary Figure S6C**). For checking the basal thermotolerance, *Arabidopsis* seedlings were subjected to heat stress of 42°C for 2 h and then allowed to recover for 8 days (**Figure 6C**). The overexpression lines were able to recover better as observed by lesser senescence, more fresh weight, and more chlorophyll levels in comparison to the wild-type plants (**Figures 6A,D,E**). Similarly, when the 1-week-old plants were subjected to heat stress in pots, they grew better than wild-type plants, as observed by their rosettes (**Figure 6B**). It is well reported that heat stress accelerates ROS accumulation in plants, which leads to oxidative damage (Suzuki and Mittler, 2006). Therefore, the levels of ROS accumulation were checked in both WT and over-expression lines after giving heat stress at two different stages (**Figure 7**). The overexpression lines had lesser ROS levels in comparison to WT as evident by the NBT staining.

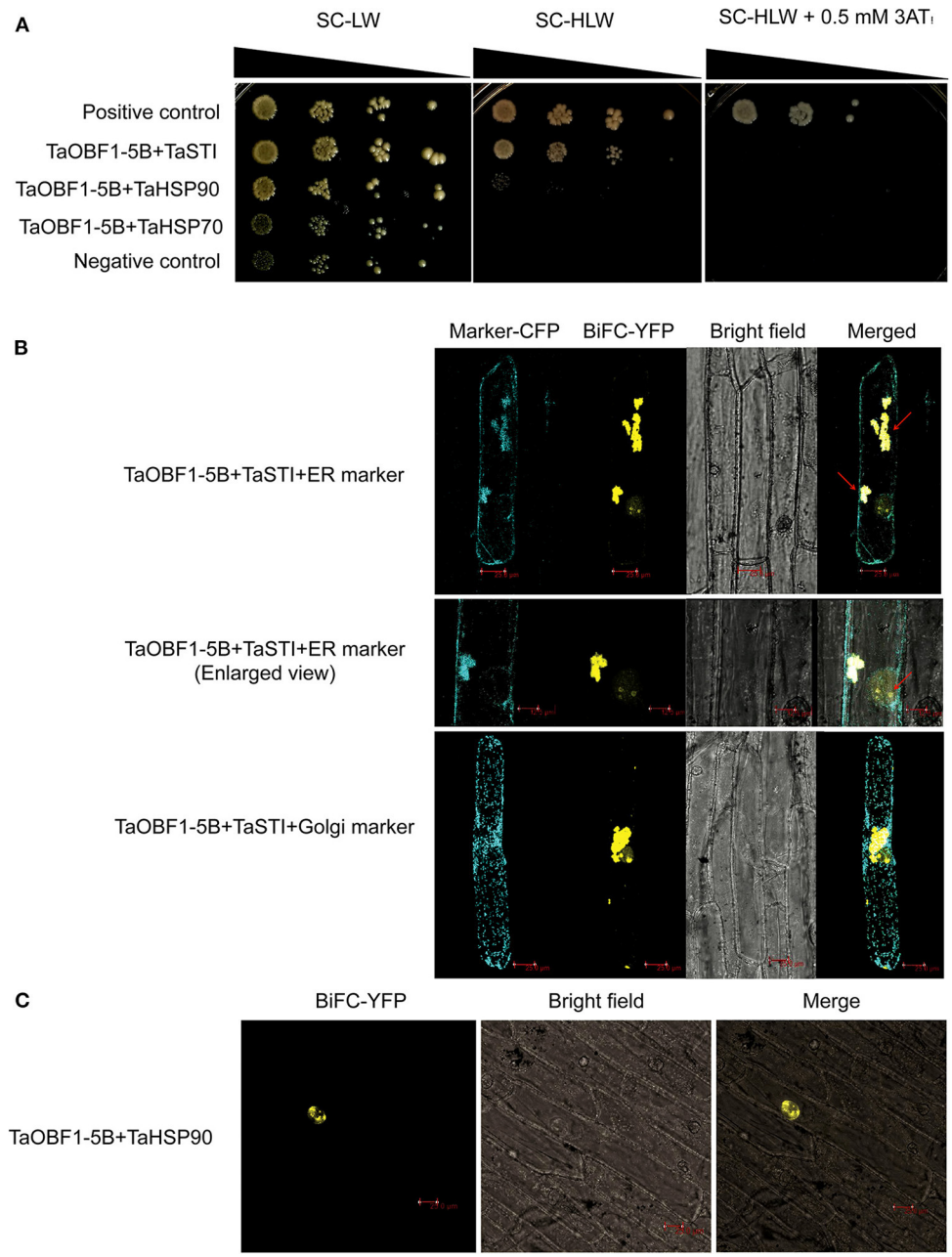

FIGURE 5 | Interaction of TaOBF1-5B with TaSTI and TaHSP90. **(A)** The yeast-two-hybrid assay was performed to check the interaction of TaOBF1-5B with TaSTI, TaHSP90, and TaHSP70 proteins. The growth of co-transformed yeast cells was analyzed on SD/-Leu/-Trp (-LW) medium and on SD/-Leu/-Trp/-His (-HLW) medium. Drop assay was performed on media lacking histidine, leucine, and tryptophan (-HLW) along with 0.5 mM 3-aminotriazole (3AT). Pair of plasmids pGBKT7-53 and pGADT7-T were used as positive control, and pGBKT7-Lam and pGADT7-T were used as the negative control. **(B)** BiFC assay showing the interaction of TaOBF1-5B with TaSTI-2A in the nucleolus and ER in onion epidermal cells. The localization of the BiFC signal was comparable with the ER marker localization. Red arrows indicate the interaction occurring in the ER and in the nucleolus [ER (endoplasmic reticulum); Scale bar 25 μm]. **(C)** BiFC assay showing the interaction of TaOBF1-5B with TaHSP-90 in the nucleus in onion epidermal cells (scale bar 25 μm).

Transcription Profiling of Stress Marker Genes in *Arabidopsis*

TaOBF1-5B Overexpression Lines

To understand the molecular basis of *TaOBF1-5B* mediated heat stress tolerance in *A. thaliana*, we checked the expression levels of different *Hsfs* and *HSPs*, which are major components of HSR. It was observed that relative expression levels of *AtHsfA2, AtHsfA6*, and *AtHsfA3* were higher in the overexpression lines as compared to the WT under heat stress conditions (**Figure 8**). Moreover, an increase in the expression of *AtHSP100* was also

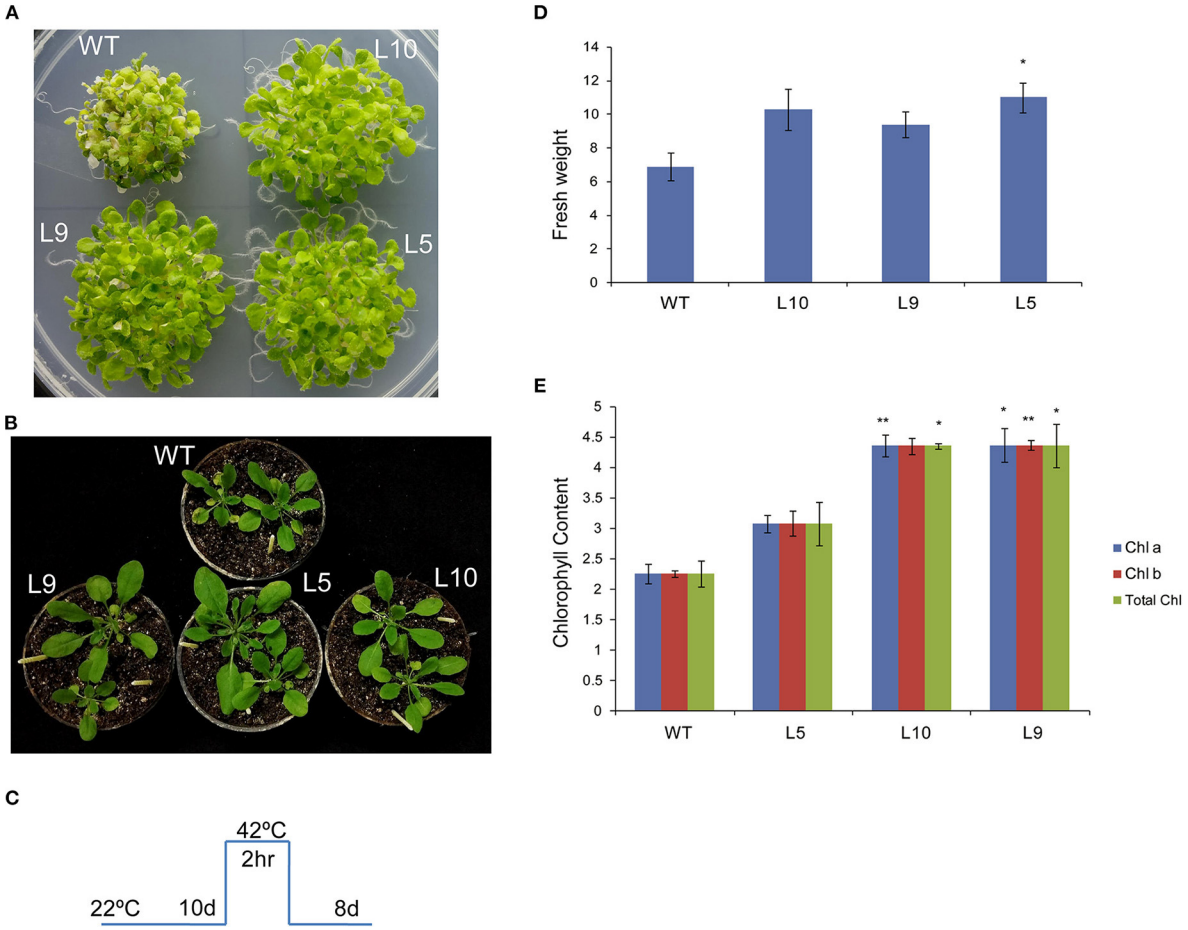

FIGURE 6 | Overexpression of *TaOBF1-5B* in Arabidopsis *thaliana* promoted better growth and more chlorophyll levels under basal heat stress conditions. **(A,B)** Photographs showing thermotolerance in *Arabidopsis* TaOBF1-5B-overexpression lines. **(C)** Depiction of stress regime. **(D,E)** Graphs representing fresh weight chlorophyll content, respectively. Asterisks indicates statistically significant difference. (Student *t*-test: $^{*}p \leq 0.05$; $^{**}p \leq 0.01$).

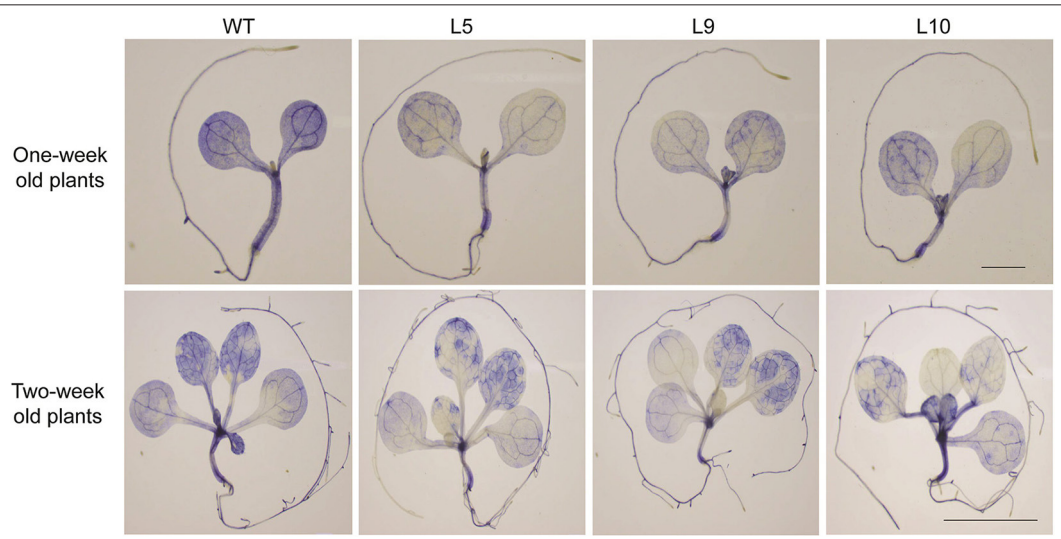

FIGURE 7 | NBT staining of 1 week (scale bar 1 mm) and 2 weeks (scale bar 1 cm) old seedlings. Plants were given heat stress and were then stained with NBT to visualize the superoxide anion accumulation after the stress treatment.

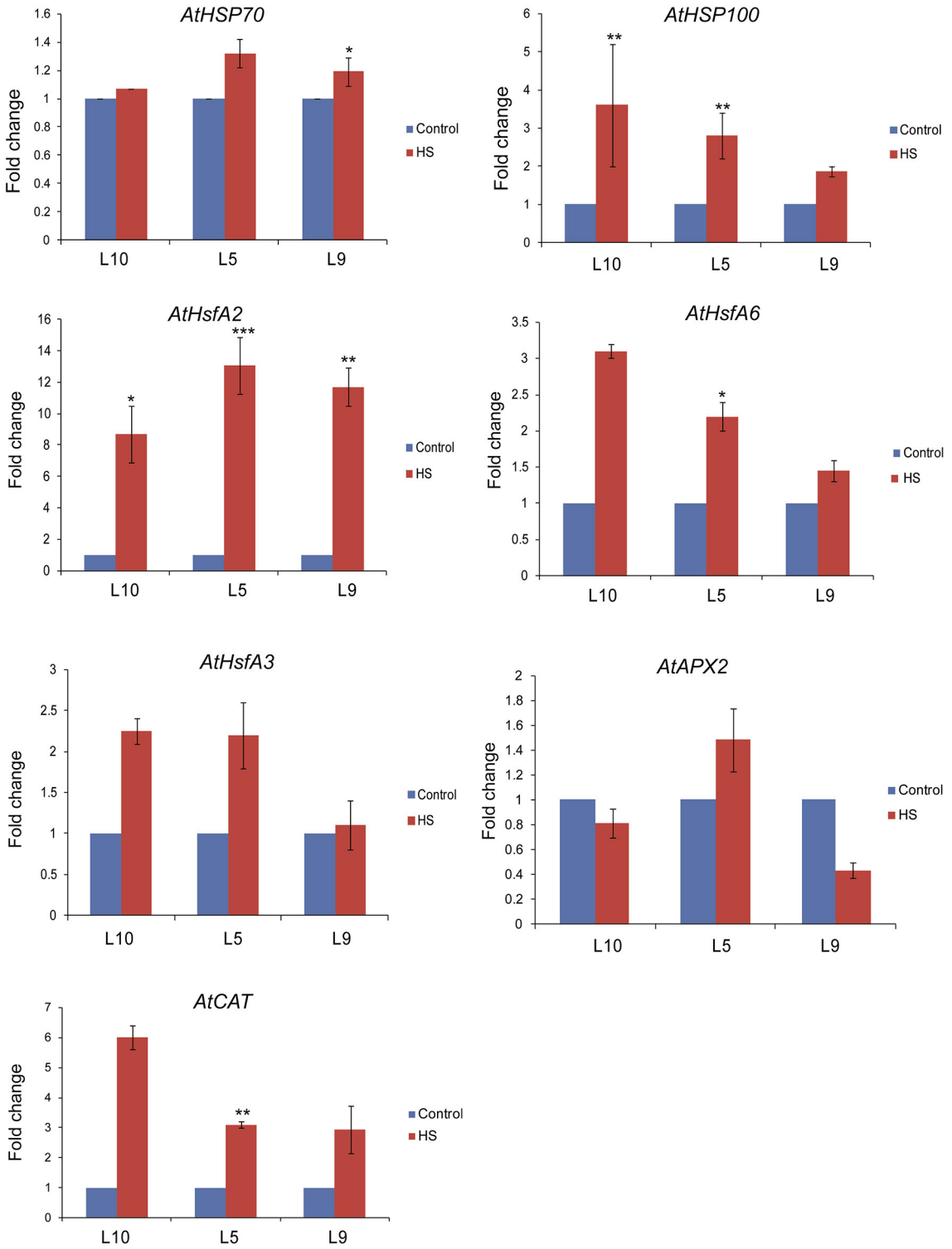

FIGURE 8 | Expression analysis of heat stress marker genes by qRT-PCR of WT and *Arabidopsis* transgenics under control and heat stress. Transcript levels were normalized to WT and *AtActin* was used as an internal control. Error bars indicate values ± SD. Asterisks on top of the error bars represent the significance levels (Students *t*-test; $p \leq 0.05$).

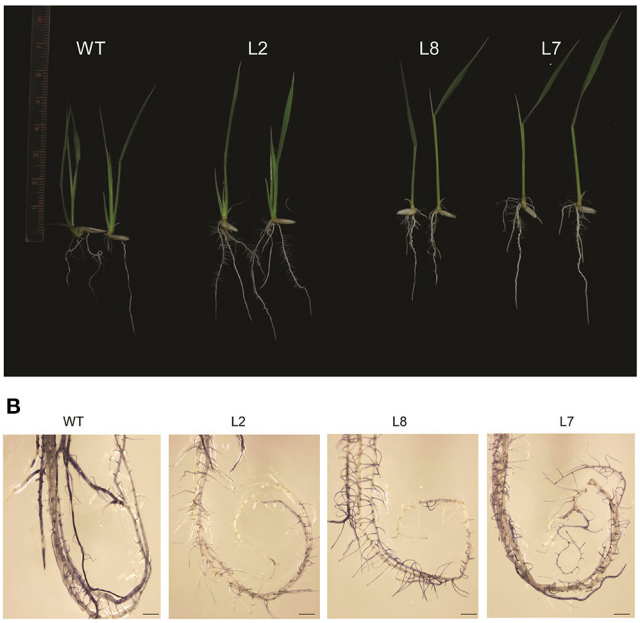

FIGURE 9 | Phenotypic analysis of rice *TaOBF1-5B*-overexpression lines under heat stress conditions. **(A)** Photographs showing thermotolerance in TaOBF1-5B rice overexpression lines. Transgenic plants showed better growth as compared to WT. **(B)** NBT staining of roots of WT and *TaOBF1-5B* transgenics. Plants subjected to heat stress followed by the recovery were stained with NBT to analyze the superoxide anion accumulation after the stress treatment (scale bar 3 mm).

observed in overexpression lines under stress conditions in comparison to WT. However, no difference in *AtHSP70* levels was observed between the overexpression and the WT plants. As the overexpression lines showed lower ROS accumulation under heat stress conditions, therefore, the expression levels of antioxidant enzymes, such as *Ascorbate peroxidase 2 (APX2)* and *Catalase (CAT),* were also analyzed. All the overexpression lines had higher levels of *AtCAT* as compared to WT (**Figure 8**). No significant difference was observed in the case of *AtAPX2*.

Analysis of *TaOBF1-5B* Rice Transgenics Showed Lesser ROS Accumulation Under Heat Stress Conditions

After observing the thermotolerance in *A. thaliana*, *TaOBF1-5B* was then overexpressed in a monocot model organism, i.e., *O. sativa,* for confirming its role in providing thermotolerance. *Agrobacterium*-mediated transformation method was used for transforming rice calli with *TaOBF1-5B* and the regenerated plants were selected on hygromycin-containing media (**Supplementary Figure S7**). The transgenic lines were confirmed by using hygromycin specific PCR, and gene-specific PCR (**Supplementary Figures S8A,B**). The level of ectopic overexpression was detected by RT-PCR and high expression levels were detected in the overexpression lines 2, 8, and 7 with relative transcript levels of 175, 140, and 150, respectively, as compared to 1 in WT (**Supplementary Figure S8C**). Thus, these three independent transgenic lines were selected for further analysis.

For checking the thermotolerance in the selected over-expression lines of rice, the 5-day-old seedlings were subjected to 42°C for 5 days and then allowed to recover. The *TaOBF1-5B* overexpression lines were seen to perform better than the WT (**Figure 9A**). The transgenic plants showed better shoot and root growth, while the growth of WT halted during heat stress. Apart from this, the level of the oxidative load was also analyzed in the transgenic plants after the heat stress. For this, 15-day-old seedlings were subjected to 42°C for 24 h followed by a single day of recovery after which both leaf and root tissues were used for NBT staining. Although no significant difference was observed among the leaf tissues, *TaOBF1-5B* overexpression lines showed lesser ROS accumulation in the roots as compared to the wild-type plants (**Figure 9B**). This indicated the potential role of *TaOBF1-5B* in providing thermotolerance.

Transcript Profiling of Stress Marker Genes in Rice *TaOBF1-5B* Overexpression Lines

To explore the mechanism behind *TaOBF1-5B* attributed thermotolerance in rice, we analyzed the expression levels of stress marker genes in *TaOBF1-5B* overexpression lines. As observed in **Figure 10**, higher transcript levels of *OsHSP100 and OsHsfA2* were observed in the transgenic plants in comparison to WT under heat stress conditions. A slight but significant increase was observed in the case of *OsHSP90* levels in transgenics, whereas no difference was observed in the levels of OsHSP17. Apart from these, the expression levels of antioxidant enzymes, such as *Superoxide dismutase* (*OsSOD*) and *Catalase* (*OsCAT*), were also analyzed. Higher expression levels of *OsSOD* were detected in the overexpression lines as compared to WT after exposure to heat stress conditions. No significant difference in the expression of *OsCAT* was observed between the transgenic and WT plants (**Figure 10**).

DISCUSSION

bZIP transcription factors have been well documented to work in various abiotic stresses, such as drought, salinity, and cold stress (Nijhawan et al., 2008; Sornaraj et al., 2016). However, till now there have been limited reports regarding the role of bZIPs in heat stress response in plants. Previously, Agarwal et al. (2019) identified *bZIPs* in *T. aestivum* and had reported the role of one of the TabZIP (Traes_7AL_25850F96F.1) in providing thermotolerance in *A. thaliana*. Using this genome-wide data, we have identified *TaOBF1* as one of the most heat-responsive bZIP present in *T. aestivum*. Moreover, both the homoeologs of *TaOBF1* (*TaOBF1-5B* and *TaOBF1-5D*) appeared to be heat-responsive in this data. Therefore, in this study, we tried to find the

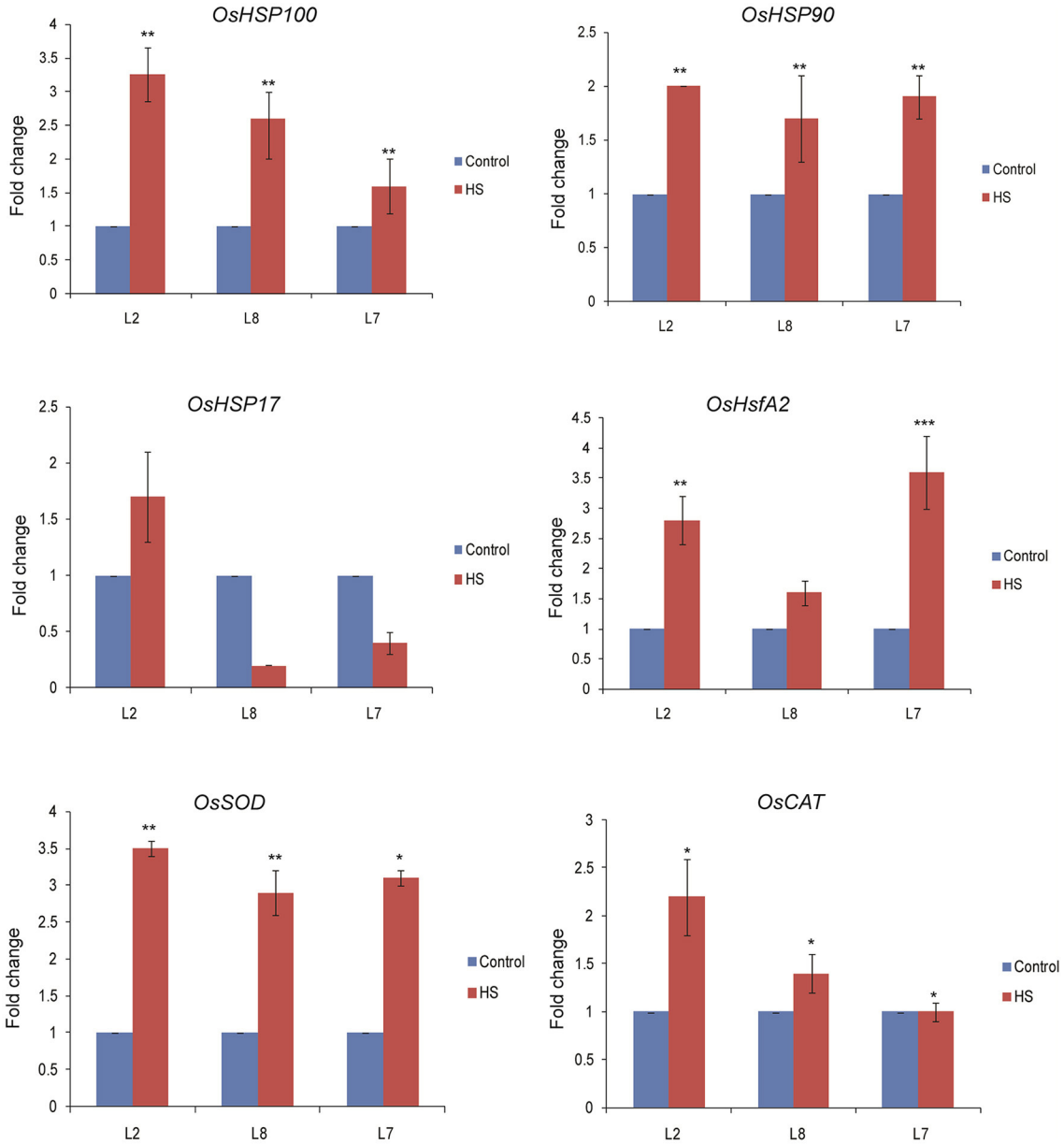

FIGURE 10 | Expression analysis of heat stress marker genes by qRT-PCR of WT and *TaOBF1-5B rice* transgenics under control and heat stress. Transcript levels were normalized to WT and *OsUbiquitin* was used as an internal control. Error bars indicate values ± SD. Asterisks on top of the error bars represent the significance levels (Students *t*-test; $p \leq 0.05$).

functional role of *TaOBF1* during the heat stress response in plants.

Wheat being a hexaploid plant has three sub-genomes, which leads to the presence of homoeologs of each gene. Although it has been speculated that there may be partitioned expression patterns among the homoeologous genes, the experimental evidence is still limited (Zhang et al., 2016). To elucidate the differences between *TaOBF1* homoeologous, their CDS sequence and protein sequences were analyzed. It was observed that at the gene level they differ by 8 SNPs whereas at the protein level a change in two amino acids was seen (**Supplementary Figure S1**). The change of Ala to Ser and Asp to Thr was found between *TaOBF1-5B* and *TaOBF1-5D*. Ser and Thr residues have been documented as the potential targets of phosphorylation in bZIPs (Smykowski et al., 2015). Therefore, it can be speculated that TaOBF1-5D might work after being phosphorylated and activated by a kinase. Both TaOBF1-5B and TaOBF1-5D showed localization in the nucleus and

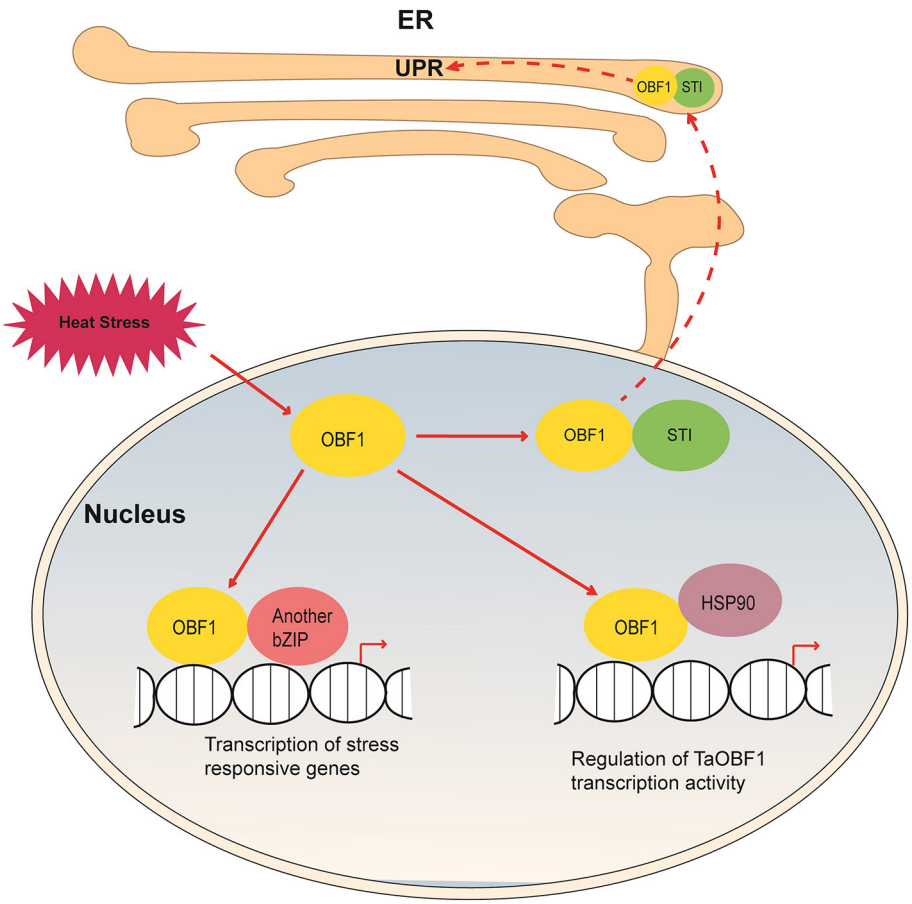

FIGURE 11 | Hypothetical model depicting the role of TaOBF1 in heat stress response. Upon heat stress, TaOBF1 by interacting with TaHSP90 translocates from nucleus to the ER where it participates in the protein unfolding response. Also inside the nucleus, it forms homodimers and heterodimers (by interaction with other bZIPs) and regulates the transcription of heat stress-responsive genes, which aid in providing thermotolerance. Apart from this, TaHSP90 also interacts with TaOBF1 and regulates its transcriptional activity.

the cytoplasm, which indicates that they might work in these compartments (**Figure 3**).

The available online expression database suggested a similar expression pattern of both the homeologues of *TaOBF1* under heat stress conditions. However, a significant difference in their expression pattern was noticed after running RT-PCR for the Indian cultivar PBW-343 (**Figure 2A**). This observed difference could be explained by the fact that the data present in the wheat expression database is from the Chinese Spring variety. Moreover, *TaOBF1-5B* and *TaOBF1-5D* showed differential expression in various tissues under control and heat stress conditions (**Figure 1**). This indicates their tissue preferential expression pattern, as the D homoeologs of TaOBF1 might function in flag leaf and lodicule under heat stress, whereas the B homoeologs might function in the anthers. A recent report by Meena et al. (2022) showed that the homoeologs of TaHsfA6b showed differential expression patterns in various tissues under control conditions. Apart from the comparison in tissues, their expression profiling under heat stress conditions in the seedling stage revealed *TaOBF1-5B* as a heat-inducible gene. *TaOBF1-5D* was not found to be heat inducible at the seedling stage. Moreover, in heat-tolerant cultivar its expression was found to be severely down-regulated (**Figure 2B**). Thus, overall, these studies hint toward the expression partitioning of *TaOBF1* homoeologs in response to heat stress. This could be further supported by the observations by Liu et al. (2015) and Meena et al. (2020), wherein differences in homoeologs expression have been observed under heat stress conditions for other genes.

Since TaOBF1-5B was chosen for further analysis, its transcriptional activity was checked and it was found that TaOBF1-5B lacked the transactivation potential (**Supplementary Figure S5**). Previous studies have reported that OsOBF1 and TaOBF1 work by interacting with another bZIP i.e. lip19 (Shimizu et al., 2005; Kobayashi et al., 2008). So, it can be speculated that TaOBF1 might regulate its target genes *via* interaction with other bZIPs. Interestingly, TaOBF1-5B was found to interact with TaSTI and TaHSP90, which

are known to work in heat stress response (**Figure 5**). This was found to be in accordance with earlier reports, which have highlighted the role of OBF1 in cold-signaling in rice and abiotic stress tolerance in wheat through its interaction with lip19 protein (Shimizu et al., 2005; Kobayashi et al., 2008).

Overexpression of *TaOBF1-5B* enhanced the thermal stress tolerance of *A. thaliana*, as the plants recovered better after heat stress as compared to the WT (**Figures 6**, **7**). Similarly, in the case of rice, the transgenic lines showed thermotolerance and accumulated lesser superoxide ions after heat stress (**Figure 9**). Thus, this data suggested that *TaOBF1-5B* might have a role in providing basal thermal tolerance. In support of this, the expression levels of various stress marker genes, such as *AtHsfA2*, *AtHSfA6*, *AtHSfA3*, *AtHSP100*, and *AtCat,* were found to be higher in overexpression lines of *A. thaliana* (**Figure 8**). On the other hand, levels of *OsHsfA2*, *OsHSP100*, *OsSOD*, and *OsHSP90* were observed to be higher in rice transgenics after exposure to heat stress (**Figure 10**). The role of these marker genes in attributing to thermotolerance has been reported earlier (Jacob et al., 2017; Samtani et al., 2022). Also, it is worth noticing that overexpression of *TaSTI* and *TaHSP90* has been documented to promote thermotolerance and *TaSTI* overexpression lines of *Arabidopsis* had higher levels of *AtHsfA2* and *AtHsfA6* transcripts under heat stress conditions (Vishwakarma et al., 2018; Meena et al., 2020). In this study as well, expression levels of *AtHsfA2* and *AtHsfA6* were found to be high in overexpression lines of *Arabidopsis* under heat stress conditions. So, this highlights the probability of TaOBF1 working in concert with *TaSTI* and *TaHSP90* in the HSR to promote thermotolerance.

Apart from this, we had previously shown that TaSTI interacts with TaHSP90 in the nucleus and the ER-Golgi complex (Meena et al., 2020). Since TaOBF1-5B was found to interact with both of these proteins, we speculated that three of them might work in a complex. However, the BiFC assay showed that TaSTI and TaOBF1-5B interacted in the nucleolus and the ER, whereas interaction with TaHSP90 was observed in the nucleus (**Figures 5B,C**). Moreover, ER retention signals have been documented in TaSTI (Meena et al., 2020). Thus, this ruled out the possibility of the three working together. Therefore, it is possible that TaOBF1-5B by interacting with TaSTI moves in the ER and might function in the protein unfolding response. Apart from this, it is well known that HSP90 binds to Hsfs and regulates their activity (Yamada and Nishimura, 2008). As TaOBF1-5B interacted with TaHSP90 in the nucleus, it could be possible that TaHSP90 might regulate its activity, though further experimental evidence is needed to confirm this.

Based on our findings, we propose a hypothetical model depicting the role of TaOBF1 in response to high temperatures (**Figure 11**). Upon heat stress, TaOBF1-5B on interacting with TaSTI translocates into the ER, where it might participate in protein unfolding response. Apart from this, homo-dimerization of TaOBF1-5B or hetero-dimerization with some other bZIP transcription factor leads to the transcription of heat stress-responsive genes, which help in imparting thermotolerance. Its interaction with TaHSP90 probably regulates its transcriptional activity. However, the molecular mechanisms behind TaHSP90 mediated regulation need further investigation. Also, how these three types of interactions help in providing thermotolerance is a potential area of future research. Overall, this study identifies TaOBF1-5B as a positive regulator of heat stress tolerance and provides insights into the mechanisms involved in the heat stress response pathway in crops, such as wheat.

DATA AVAILABILITY STATEMENT

The raw data supporting the conclusions of this article will be made available by the authors, without undue reservation.

AUTHOR CONTRIBUTIONS

PK conceived the idea, concept of the research work, and provided all the facilities for the experiments. HS and AS performed the experiments and wrote the manuscript. All authors have read and agreed to the submitted version of the manuscript.

FUNDING

HS and AS are thankful to the University Grant Commission (UGC) for the research fellowship. This work has been supported by a grant from the JC Bose Fellowship Award and Science and Engineering Research Board, Government of India.

SUPPLEMENTARY MATERIAL

The Supplementary Material for this article can be found online at: https://www.frontiersin.org/articles/10.3389/fpls.2022.914363/full#supplementary-material

Supplementary Figure 1 | Sequence and phylogenetic analysis of TaOBF1. **(A)** Sequence alignment of CDS of *TaOBF1-5B* and *TaOBF1-5D*. SNPs are depicted by #. **(B)** Protein sequence alignment of TaOBF1-5B and TaOBF1-5D.The difference in amino acids is depicted in yellow color. **(C)** Phylogenetic tree of TaOBF1 protein and OBF1 protein from other plant species. The unrooted tree was made using MEGA (version 7) with the neighbor joining method (1,000 replicates).

Supplementary Figure 2 | Cloning of *TaOBF1* homeologues in different vectors. **(A)** Confirmation of *TaOBF1-5B* cloned in pDRIVE, pENTR/D-TOPO, and pMDC-32 vectors by digestion. **(B)** Confirmation of *TaOBF1-5D* cloned in pDRIVE, pENTR/D-TOPO, and pMDC-32 vectors by digestion.

Supplementary Figure 3 | Expression analysis of TaOBF1 homoeologs in different developmental stages of wheat. **(A)** Heatmap showing the relative expression profile of the *TaOBF1-5B* and *TaOBF1-5D* across the various zadok stages of wheat. **(B)** Heatmap showing the relative expression profile of the *TaOBF1-5B* and *TaOBF1-5D* across the various tissues of wheat. **(C)** Heatmap showing the relative expression profile of the *TaOBF1-5B* and *TaOBF1-5D* under abiotic stresses and biotic stresses. MI, mock inoculation; HS, heat stress; DS, drought stress; CS, cold stress; FGI, *Fusarium graminearum* inoculation; PEG, polyethylene glycol.

Supplementary Figure 4 | Expression analysis of TaOBF1 homoeologs in wheat cv. PBW343 seedlings at different time points of heat stress conditions. Relative fold change was checked by qRT-PCR. *TaGAPDH* was used as an internal control gene. Error bars indicate values ± SD.

Supplementary Figure 5 | Transcriptional activation assay of TaOBF1-5B in yeast cells. TaOBF1-5B lacked transcriptional activation, as AH109 yeast cells containing TaOBF1-5B::pGBKT7 construct were unable to grow on SC-HW media.

Supplementary Figure 6 | Confirmation of *TaOBF1-5B Arabidopsis* overexpression transgenic lines by **(A)** Hygromycin resistance gene specific PCR **(B)** Gene-specific PCR **(C)** RT-PCR.

Supplementary Figure 7 | Generation of rice transgenics by tissue culture. Transformation of rice calli with *Agrobacterium* harboring *TaOBF1-5B* gene.

Supplementary Figure 8 | Confirmation of *TaOBF1-5B* overexpression rice transgenic lines by **(A)** Hygromycin resistance gene specific PCR **(B)** Gene and vector-specific PCR **(C)** RT-PCR.

Supplementary Table 1 | List of primers used in this study.

REFERENCES

Agarwal, P., Baranwal, V. K., and Khurana, P. (2019). Genome-wide analysis of bZIP transcription factors in wheat and functional characterization of a TabZIP under abiotic stress. *Sci. Rep.* 9, 4608. doi: 10.1038/s41598-019-40659-7

Agarwal, P., and Khurana, P. (2018). Characterization of a novel zinc finger transcription factor (TaZnF) from wheat conferring heat stress tolerance in *Arabidopsis*. *Cell Stress Chaperones* 23, 253–267. doi: 10.1007/s12192-017-0838-1

Agarwal, P., and Khurana, P. (2019). Functional characterization of HSFs from wheat in response to heat and other abiotic stress conditions. *Funct. Integr. Genomics* 19, 497–513. doi: 10.1007/s10142-019-00666-3

Arnon, D. I. (1949). Copper enzymes in isolated chloroplasts polyphenoloxidase in beta vulgaris. *Plant Physiol.* 24, 1–15. doi: 10.1104/pp.24.1.1

Borah, P., and Khurana, J. P. (2018). The OsFBK1 E3 ligase subunit affects anther and root secondary cell wall thickenings by mediating turnover of a cinnamoyl-CoA reductase. *Plant Physiol.* 176, 2148–2165. doi: 10.1104/pp.17.01733

Borrill, P., Ramirez-Gonzalez, R., and Uauy, C. (2016). expVIP: a customizable RNA-seq data analysis and visualization platform. *Plant Physiol.* 170, 2172–2186. doi: 10.1104/pp.15.01667

Cai, W., Yang, Y., Wang, W., Guo, G., Liu, W., and Bi, C. (2018). Overexpression of a wheat (*Triticum aestivum* L.) bZIP transcription factor gene, TabZIP6, decreased the freezing tolerance of transgenic *Arabidopsis* seedlings by down-regulating the expression of CBFs. *Plant Physiol. Biochem.* 124, 100–111. doi: 10.1016/j.plaphy.2018.01.008

Deppmann, C. D., Acharya, A., Rishi, V., Wobbes, B., Smeekens, S., Taparowsky, E. J., et al. (2004). Dimerization specificity of all 67 B-ZIP motifs in *Arabidopsis thaliana*: a comparison to *Homo sapiens* B-ZIP motifs. *Nucleic Acids Res.* 32, 3435–3445. doi: 10.1093/nar/gkh653

Dröge-Laser, W., Snoek, B. L., Snel, B., and Weiste, C. (2018). The *Arabidopsis* bZIP transcription factor family-an update. *Curr. Opin. Plant Biol.* 45, 36–49. doi: 10.1016/j.pbi.2018.05.001

Dröge-Laser, W., and Weiste, C. (2018). The C/S1 bZIP network: a regulatory hub orchestrating plant energy homeostasis. *Trends Plant Sci.* 23, 422–433. doi: 10.1016/j.tplants.2018.02.003

Foster, R., Izawa, T., and Chua, N. H. (1994). Plant bZIP proteins gather at ACGT elements. *FASEB J.* 8, 192–200. doi: 10.1096/fasebj.8.2.8119490

Geng, X., Zang, X., Li, H., Liu, Z., Zhao, A., Liu, J., et al. (2018). Unconventional splicing of wheat TabZIP60 confers heat tolerance in transgenic *Arabidopsis*. *Plant Sci. Int. J. Exp. Plant Biol.* 274, 252–260. doi: 10.1016/j.plantsci.2018.05.029

Himmelbach, A., Zierold, U., Hensel, G., Riechen, J., Douchkov, D., Schweizer, P., et al. (2007). A set of modular binary vectors for transformation of cereals. *Plant Physiol.* 145, 1192–1200. doi: 10.1104/pp.107.111575

Hu, W., Wang, L., Tie, W., Yan, Y., Ding, Z., Liu, J., et al. (2016a). Genome-wide analyses of the bZIP family reveal their involvement in the development, ripening and abiotic stress response in banana. *Sci. Rep.* 6, 30203. doi: 10.1038/srep30203

Hu, W., Yang, H., Yan, Y., Wei, Y., Tie, W., Ding, Z., et al. (2016b). Genome-wide characterization and analysis of bZIP transcription factor gene family related to abiotic stress in cassava. *Sci. Rep.* 6, 22783. doi: 10.1038/srep22783

Jacob, P., Hirt, H., and Bendahmane, A. (2017). The heat-shock protein/chaperone network and multiple stress resistance. *Plant Biotechnol. J.* 15, 405–414. doi: 10.1111/pbi.12659

Jakoby, M., Weisshaar, B., Dröge-Laser, W., Vicente-Carbajosa, J., Tiedemann, J., Kroj, T., et al. (2002). bZIP transcription factors in *Arabidopsis*. *Trends Plant Sci.* 7, 106–111. doi: 10.1016/S1360-1385(01)02223-3

Katagiri, F., and Chua, N. H. (1992). Plant transcription factors: present knowledge and future challenges. *Trends Genet.* 8, 22–27. doi: 10.1016/0168-9525(92)90020-5

Kobayashi, F., Maeta, E., Terashima, A., Kawaura, K., Ogihara, Y., and Takumi, S. (2008). Development of abiotic stress tolerance via bZIP-type transcription factor LIP19 in common wheat. *J. Exp. Bot.* 59, 891–905. doi: 10.1093/jxb/ern014

Kong, S., Park, S.-Y., and Lee, Y.-H. (2015). Systematic characterization of the bZIP transcription factor gene family in the rice blast fungus, *Magnaporthe oryzae*. *Environ. Microbiol.* 17, 1425–1443. doi: 10.1111/1462-2920.12633

Kusano, T., Berberich, T., Harada, M., Suzuki, N., and Sugawara, K. (1995). A maize DNA-binding factor with a bZIP motif is induced by low temperature. *Mol. Gen. Genet.* 248, 507–517. doi: 10.1007/BF02423445

Liao, Y., Zou, H.-F., Wei, W., Hao, Y.-J., Tian, A.-G., Huang, J., et al. (2008). Soybean GmbZIP44, GmbZIP62 and GmbZIP78 genes function as negative regulator of ABA signaling and confer salt and freezing tolerance in transgenic *Arabidopsis*. *Planta* 228, 225–240. doi: 10.1007/s00425-008-0731-3

Liu, C., Wu, Y., and Wang, X. (2012). bZIP transcription factor OsbZIP52/RISBZ5: a potential negative regulator of cold and drought stress response in rice. *Planta* 235, 1157–1169. doi: 10.1007/s00425-011-1564-z

Liu, J.-X., Srivastava, R., and Howell, S. H. (2008). Stress-induced expression of an activated form of AtbZIP17 provides protection from salt stress in *Arabidopsis*. *Plant Cell Environ.* 31, 1735–1743. doi: 10.1111/j.1365-3040.2008.01873.x

Liu, X., and Chu, Z. (2015). Genome-wide evolutionary characterization and analysis of bZIP transcription factors and their expression profiles in response to multiple abiotic stresses in *Brachypodium distachyon*. *BMC Genomics* 16, 227. doi: 10.1186/s12864-015-1457-9

Liu, Z., Xin, M., Qin, J., Peng, H., Ni, Z., Yao, Y., et al. (2015). Temporal transcriptome profiling reveals expression partitioning of homeologous genes contributing to heat and drought acclimation in wheat (*Triticum aestivum* L.). *BMC Plant Biol.* 15, 152. doi: 10.1186/s12870-015-0511-8

Livak, K. J., and Schmittgen, T. D. (2001). Analysis of relative gene expression data using real-time quantitative PCR and the 2(-ΔΔCT) method. *Methods* 25, 402–408. doi: 10.1006/meth.2001.1262

Lu, G., Gao, C., Zheng, X., and Han, B. (2009). Identification of OsbZIP72 as a positive regulator of ABA response and drought tolerance in rice. *Planta* 229, 605–615. doi: 10.1007/s00425-008-0857-3

Meena, S., Deb, S., Samtani, H., and Khurana, P. (2020). Dissecting the molecular function of *Triticum aestivum* STI family members under heat stress. *Front. Genet.* 11, 873. doi: 10.3389/fgene.2020.00873

Meena, S., Samtani, H., and Khurana, P. (2022). Elucidating the functional role of heat stress transcription factor A6b (TaHsfA6b) in linking heat stress response and the unfolded protein response in wheat. *Plant Mol. Biol.* 108, 621–634. doi: 10.1007/s11103-022-01252-1

Nijhawan, A., Jain, M., Tyagi, A. K., and Khurana, J. P. (2008). Genomic survey and gene expression analysis of the basic leucine zipper transcription factor family in rice. *Plant Physiol.* 146, 333–350. doi: 10.1104/pp.107.112821

Riechmann, J. L., Heard, J., Martin, G., Reuber, L., Jiang, C., Keddie, J., et al. (2000). *Arabidopsis* transcription factors: genome-wide comparative analysis among eukaryotes. *Science* 290, 2105–2110. doi: 10.1126/science.290.5499.2105

Rieping, M., Fritz, M., Prat, S., and Gatz, C. (1994). A dominant negative mutant of PG13 suppresses transcription from a cauliflower mosaic virus 35S truncated promoter in transgenic tobacco plants. *Plant Cell* 6, 1087–1098. doi: 10.1105/tpc.6.8.1087

Rolly, N. K., Imran, Q. M., Lee, I.-J., and Yun, B.-W. (2020). Salinity stress-mediated suppression of expression of salt overly sensitive signaling pathway genes suggests negative regulation by AtbZIP62 transcription factor in *Arabidopsis thaliana*. *Int. J. Mol. Sci.* 21, 1726. doi: 10.3390/ijms21051726

Samtani, H., Sharma, A., and Khurana, P. (2022). Overexpression of HVA1 enhances drought and heat stress tolerance in *Triticum aestivum* doubled haploid plants. *Cells* 11, 912. doi: 10.3390/cells11050912

Shimizu, H., Sato, K., Berberich, T., Miyazaki, A., Ozaki, R., Imai, R., et al. (2005). LIP19, a basic region leucine zipper protein, is a Fos-like molecular switch in the cold signaling of rice plants. *Plant Cell Physiol.* 46, 1623–1634. doi: 10.1093/pcp/pci178

Smykowski, A., Fischer, S. M., and Zentgraf, U. (2015). Phosphorylation affects DNA-binding of the senescence-regulating bZIP transcription factor GBF1. *Plants* 4, 691–709. doi: 10.3390/plants4030691

Sornaraj, P., Luang, S., Lopato, S., and Hrmova, M. (2016). Basic leucine zipper (bZIP) transcription factors involved in abiotic stresses: a molecular model of a wheat bZIP factor and implications of its structure in function. *Biochim. Biophys. Acta* 1860, 46–56. doi: 10.1016/j.bbagen.2015.10.014

Sun, X., Li, Y., Cai, H., Bai, X., Ji, W., Ding, X., et al. (2012). The *Arabidopsis* AtbZIP1 transcription factor is a positive regulator of plant tolerance to salt, osmotic and drought stresses. *J. Plant Res.* 125, 429–438. doi: 10.1007/s10265-011-0448-4

Suzuki, N., and Mittler, R. (2006). Reactive oxygen species and temperature stresses: a delicate balance between signaling and destruction. *Physiol. Plant.* 126, 45–51. doi: 10.1111/j.0031-9317.2005.00582.x

Takahashi, H., Kawakatsu, T., Wakasa, Y., Hayashi, S., and Takaiwa, F. (2012). A rice transmembrane bZIP transcription factor, OsbZIP39, regulates the endoplasmic reticulum stress response. *Plant Cell Physiol.* 53, 144–153. doi: 10.1093/pcp/pcr157

Toki, S., Hara, N., Ono, K., Onodera, H., Tagiri, A., Oka, S., et al. (2006). Early infection of scutellum tissue with *Agrobacterium* allows high-speed transformation of rice. *Plant J. Cell Mol. Biol.* 47, 969–976. doi: 10.1111/j.1365-313X.2006.02836.x

Vishwakarma, H., Junaid, A., Manjhi, J., Singh, G. P., Gaikwad, K., and Padaria, J. C. (2018). Heat stress transcripts, differential expression, and profiling of heat stress tolerant gene TaHsp90 in Indian wheat (*Triticum aestivum* L.) cv C306. *PLoS ONE* 13, e0198293. doi: 10.1371/journal.pone.0198293

Wang, J., Zhou, J., Zhang, B., Vanitha, J., Ramachandran, S., and Jiang, S.-Y. (2011). Genome-wide expansion and expression divergence of the basic leucine zipper transcription factors in higher plants with an emphasis on sorghum. *J. Integr. Plant Biol.* 53, 212–231. doi: 10.1111/j.1744-7909.2010.01017.x

Wei, K., Chen, J., Wang, Y., Chen, Y., Chen, S., Lin, Y., et al. (2012). Genome-wide analysis of bZIP-encoding genes in maize. *DNA Res.* 19, 463–476. doi: 10.1093/dnares/dss026

Xiang, Y., Tang, N., Du, H., Ye, H., and Xiong, L. (2008). Characterization of OsbZIP23 as a key player of the basic leucine zipper transcription factor family for conferring abscisic acid sensitivity and salinity and drought tolerance in rice. *Plant Physiol.* 148, 1938–1952. doi: 10.1104/pp.108.128199

Yamada, K., and Nishimura, M. (2008). Cytosolic heat shock protein 90 regulates heat shock transcription factor in *Arabidopsis thaliana*. *Plant Signal. Behav.* 3, 660–662. doi: 10.4161/psb.3.9.5775

Yamaguchi, N. (2021). LEAFY, a pioneer transcription factor in plants: a mini-review. *Front. Plant Sci.* 12, 1274. doi: 10.3389/fpls.2021.701406

Yang, O., Popova, O. V., Süthoff, U., Lüking, I., Dietz, K.-J., and Golldack, D. (2009). The *Arabidopsis* basic leucine zipper transcription factor AtbZIP24 regulates complex transcriptional networks involved in abiotic stress resistance. *Gene* 436, 45–55. doi: 10.1016/j.gene.2009.02.010

Zhang, B., Foley, R. C., and Singh, K. B. (1993). Isolation and characterization of two related *Arabidopsis* ocs-element bZIP binding proteins. *Plant J. Cell Mol. Biol.* 4, 711–716. doi: 10.1046/j.1365-313X.1993.04040711.x

Zhang, L., Zhang, L., Xia, C., Gao, L., Hao, C., Zhao, G., et al. (2017). A novel wheat C-bZIP gene, TabZIP14-B, participates in salt and freezing tolerance in transgenic plants. *Front. Plant Sci.* 8, 710. doi: 10.3389/fpls.2017.00710

Zhang, L., Zhang, L., Xia, C., Zhao, G., Liu, J., Jia, J., et al. (2015). A novel wheat bZIP transcription factor, TabZIP60, confers multiple abiotic stress tolerances in transgenic *Arabidopsis*. *Physiol. Plant.* 153, 538–554. doi: 10.1111/ppl.12261

Zhang, X., Henriques, R., Lin, S.-S., Niu, Q.-W., and Chua, N.-H. (2006). *Agrobacterium*-mediated transformation of *Arabidopsis thaliana* using the floral dip method. *Nat. Protoc.* 1, 641–646. doi: 10.1038/nprot.2006.97

Zhang, Y., Liu, Z., Khan, A. A., Lin, Q., Han, Y., Mu, P., et al. (2016). Expression partitioning of homeologs and tandem duplications contribute to salt tolerance in wheat (*Triticum aestivum* L.). *Sci. Rep.* 6, 21476. doi: 10.1038/srep21476

Conflict of Interest: The authors declare that the research was conducted in the absence of any commercial or financial relationships that could be construed as a potential conflict of interest.

The handling editor declared a shared affiliation with the author PK at the time of the review.

Publisher's Note: All claims expressed in this article are solely those of the authors and do not necessarily represent those of their affiliated organizations, or those of the publisher, the editors and the reviewers. Any product that may be evaluated in this article, or claim that may be made by its manufacturer, is not guaranteed or endorsed by the publisher.

Copyright © 2022 Samtani, Sharma and Khurana. This is an open-access article distributed under the terms of the Creative Commons Attribution License (CC BY). The use, distribution or reproduction in other forums is permitted, provided the original author(s) and the copyright owner(s) are credited and that the original publication in this journal is cited, in accordance with accepted academic practice. No use, distribution or reproduction is permitted which does not comply with these terms.

frontiers | Frontiers in Plant Science

ORIGINAL RESEARCH
published: 25 July 2022
doi: 10.3389/fpls.2022.833326

GmWRKY21, a Soybean WRKY Transcription Factor Gene, Enhances the Tolerance to Aluminum Stress in *Arabidopsis thaliana*

Zhenzhen Han[1,2,3,4,5†], *Jinyu Wang*[1,2,3,4,5†], *Xinxin Wang*[1,2,3,4,5], *Xijia Zhang*[1,2,3,4,5], *Yanbo Cheng*[1,2,3,4,5], *Zhandong Cai*[1,2,3,4,5], *Hai Nian*[1,2,3,4,5*] and *Qibin Ma*[1,2,3,4,5*]

[1] The State Key Laboratory for Conservation and Utilization of Subtropical Agro-Bioresources, South China Agricultural University, Guangzhou, China, [2] The Key Laboratory of Plant Molecular Breeding of Guangdong Province, College of Agriculture, South China Agricultural University, Guangzhou, China, [3] The Guangdong Subcenter of the National Center for Soybean Improvement, College of Agriculture, South China Agricultural University, Guangzhou, China, [4] The Guangdong Provincial Laboratory of Lingnan Modern Agricultural Science and Technology, South China Agricultural University, Guangzhou, China, [5] Zengcheng Teaching and Research Bases, South China Agricultural University, Guangzhou, China

OPEN ACCESS

Edited by:
Girdhar Kumar Pandey,
University of Delhi, India

Reviewed by:
Branka Salopek Sondi,
Rudjer Boskovic Institute, Croatia
Sung Chul Lee,
Chung-Ang University, South Korea

***Correspondence:**
Qibin Ma
maqibin@scau.edu.cn
Hai Nian
hnian@scau.edu.cn

†These authors have contributed equally to this work

Specialty section:
This article was submitted to Plant Physiology, a section of the journal Frontiers in Plant Science

Received: 11 December 2021
Accepted: 15 June 2022
Published: 25 July 2022

Citation:
Han Z, Wang J, Wang X, Zhang X, Cheng Y, Cai Z, Nian H and Ma Q (2022) GmWRKY21, a Soybean WRKY Transcription Factor Gene, Enhances the Tolerance to Aluminum Stress in Arabidopsis thaliana. Front. Plant Sci. 13:833326. doi: 10.3389/fpls.2022.833326

The WRKY transcription factors (TFs) are one of the largest families of TFs in plants and play multiple roles in plant growth and development and stress response. In this study, *GmWRKY21* encoding a WRKY transcription factor was functionally characterized in Arabidopsis and soybean. The GmWRKY21 protein containing a highly conserved WRKY domain and a C_2H_2 zinc-finger structure is located in the nucleus and has the characteristics of transcriptional activation ability. The *GmWRKY21* gene presented a constitutive expression pattern rich in the roots, leaves, and flowers of soybean with over 6-fold of relative expression levels and could be substantially induced by aluminum stress. As compared to the control, overexpression of *GmWRKY21* in Arabidopsis increased the root growth of seedlings in transgenic lines under the $AlCl_3$ concentrations of 25, 50, and 100 μM with higher proline and lower MDA accumulation. The results of quantitative real-time polymerase chain reaction (qRT-PCR) showed that the marker genes relative to aluminum stress including *ALMT*, *ALS3*, *MATE*, and *STOP1* were induced in *GmWRKY21* transgenic plants under $AlCl_3$ treatment. The stress-related genes, such as *KIN1*, *COR15A*, *COR15B*, *COR47*, *GLOS3*, and *RD29A*, were also upregulated in *GmWRKY21* transgenic Arabidopsis under aluminum stress. Similarly, stress-related genes, such as *GmCOR47, GmDREB2A*, *GmMYB84, GmKIN1*, *GmGST1*, and *GmLEA*, were upregulated in hair roots of *GmWRKY21* transgenic plants. In summary, these results suggested that the GmWRKY21 transcription factor may promote the tolerance to aluminum stress mediated by the pathways regulating the expression of the acidic aluminum stress-responsive genes and abiotic stress-responsive genes.

Keywords: transcription factor, *GmWRKY21*, soybean, Al stress, *Arabidopsis thaliana*

INTRODUCTION

Aluminum (Al) mainly existing in the forms of harmless oxides and aluminosilicates is the third most abundant metal in the earth's crust next to oxygen and silicon (Kochian et al., 2004). Acidic soils are widespread with ∼30% of the world's land area and about 50% of the potential of the world's potentially arable lands (Silambarasan et al., 2019). In acidic soil (pH < 5), Al^{3+} ions are activated and dissolved into the soil solution from clay minerals, which can quickly inhibit root growth resulting in reduced crop yield (Kochian et al., 2015). Therefore, Al toxicity is the main factor restricting plant growth in acidic soil (Bojorquez-Quintal et al., 2017). The solubility of aluminum increases with the decrease in pH value (Brautigan et al., 2012). In an acidic solution, Al^{3+} exists as the octahedral hexahydrate Al $(H_2O)_6^{3+}$ commonly known as Al^{3+} (Kochian et al., 2015), while the Al toxicity in acidic soil is mainly caused by Al^{3+}(Singh et al., 2017). The most apparent feature of Al toxicity is to inhibit the root tip cell elongation and cell division. It was generally believed that the root tip is the central part of Al toxicity (Kochian, 1995). The transition zone (DTZ) of the root tip 1–2 mm between the meristematic zone and the elongation zone is the most sensitive area for aluminum poisoning (Kollmeier et al., 2000). Al^{3+} is electrostatically bound to the pectin of the negatively charged root tip cell wall (Kochian, 1995), which reduces the rate of cell division and extension and affects root elongation.

Previous studies showed that the higher concentration of Al^{3+} will cause severe toxicity to plants because it will inhibit cell elongation and cell division in the roots, which will lead to enlarged root tips, reduced root hairs, or no root hair development, thus hindering the absorption of nutrients and water (Kochian et al., 2015). Al^{3+} toxicity increases the formation of reactive oxygen species (ROS) in plants by leading to lipid membrane peroxidation, ion leakage, protein oxidation, callose accumulation, and cell death (Ezaki et al., 2000; Yamamoto et al., 2002; Boscolo et al., 2003).

In adaptation to Al stress, plants have evolved two resistance mechanisms: external and internal tolerance mechanisms (Liu et al., 2014; Kochian et al., 2015; Wang N. et al., 2017). Several main components exist in the external mechanism including the cell wall of Al^{3+} fixation, induced pH increase, organic acid (OA) anions chelate Al^{3+} ions, and Al^{3+} transmembrane outflow, while some main components are involved in the internal tolerance mechanism including plants chelate aluminum ions through organic acids and proteins in cells and transporting aluminum ions from sensitive cytoplasmic areas to non-sensitive areas, such as vacuoles (Feng, 2000; Ryan et al., 2001; Kochian et al., 2015; Silambarasan et al., 2019). Aluminum-activated malate transporter (ALMT) and multidrug and toxic compound extrusion (MATE) identified in plants are two transporter families that confer Al tolerance through the secretion of the organic acids. *TaALMT1* was the first identified malate efflux gene in wheat (Sasaki et al., 2004). Another organic acid efflux transporter family MATEs as a plasma membrane efflux transporter are responsible for the Al-activated citrate release (Liu et al., 2009, 2012).

Transcription factors are proteins that regulate gene transcription to adapt to the environmental stimulus (Finatto et al., 2018). WRKY proteins have one or two conserved WRKY domains of about 60 amino acids with an invariable sequence motif WRKYGQK at the N-terminus and a zinc-finger domain-like ($CX_{4-5}CX_{22-23}HXH$ or $CX_7CX_{23}HXC$) (Eulgem et al., 2000; Rushton et al., 2010). The WRKY TFs can be classified into three main groups (I–III) based on the number of WRKY domains and the type of their zinc-finger motifs. The WRKY TFs in group I have two WRKY domains and a C_2H_2-type zinc-finger structure. The TFs in group II have a single WRKY domain and contain the zinc-finger motif C_2H_2, which is divided into five subgroups (IIa–e). The TFs in group III hold a WRKY domain and contain a C_2-HC motif (Eulgem et al., 2000; Zhang and Wang, 2005; Song et al., 2018; Xie et al., 2018).

WRKY is a superfamily of transcription factors in plants that play an essential role in many life processes, especially in biotic and abiotic stresses (Eulgem et al., 2000; Zhang and Wang, 2005; Rushton et al., 2010; Chen et al., 2012; Li et al., 2013). *SPF1* was the first WRKY gene isolated from sweet potato in 1994 (Ishiguro and Nakamura, 1994), and then, the *ABF1* and *ABF2* genes were discovered in wild oats (Rushton et al., 1995). The genes of *WRKY1*, *WRKY2,* and *WRKY3* from parsley were confirmed for the first time that WRKY protein could regulate the response of plants to pathogens (Rushton et al., 1996).

In Arabidopsis, overexpression of *AtWRKY25* and *AtWRKY33* increased salt tolerance in transgenic plants (Jiang and Deyholos, 2009). Overexpression of *AtWRKY57, ABO3, AtWRKY70, AtWRKY46,* and *AtWRKY54* in Arabidopsis conferred the tolerance of transgenic plants to drought stress (Ren et al., 2010; Jiang et al., 2012; Chen et al., 2017). Overexpression of *GhWRKY34* enhanced the tolerance of transgenic Arabidopsis to salt stress by selectively taking up Na^+ and K^+ (Zhou et al., 2015). *GhWRKY1-like* encodes a WRKY TF-mediated drought tolerance in Arabidopsis *via* modulating ABA biosynthesis (Hu et al., 2021). Besides these, *AtWRKY3* and *AtWRKY4* increased salt stress tolerance in transgenic Arabidopsis (Li C. et al., 2021). In rice, overexpression of *OsWRKY11* controlled by the *HSP101* promoter resulted in the enhancement of drought resistance, which was characterized by slower leaf wilting and a higher survival rate (Wu et al., 2009). *OsWRKY30* in transgenic rice enhanced the tolerance to drought stress (Shen et al., 2012). Overexpression of *OsWRKY45* and *OsWRKY72* can change the drought resistance of transgenic Arabidopsis, which may be related to the induction of genes related to abscisic acid stress (Qiu and Yu, 2009; Song et al., 2010). Recent studies have shown that OsWRKY108 was an integrative regulator of P homeostasis and leaf inclination (Wang et al., 2021). The inactivated *OsWRKY5* enhanced drought tolerance through abscisic acid signaling pathways (Lim et al., 2021). At 4°C, overexpression of *OsWRKY76* improved the tolerance to low-temperature stress (Babitha et al., 2013). OsWRKY50 enhanced salt stress tolerance *via* an ABA-independent pathway (Huang et al., 2021). In wheat, *TaWRKY2* overexpression improved salt and drought tolerance by reducing the expression of *STZ* and *RD29B* (Niu et al., 2012). *TaWRKY146* enhanced drought tolerance by inducing

stomatal closure in Arabidopsis (Ma et al., 2017). *TaWRKY1* and *TaWRKY33* made transgenic Arabidopsis resistant to drought and high-temperature stress (He et al., 2016). The heterologous transgenic plants of the *TaWRKY19* gene had salt and drought tolerance and showed tolerance to low temperatures (Niu et al., 2012). *TaWRKY74* participated in copper tolerance through regulation of *TaGST1* expression and GSH content (Li G. Z. et al., 2021). Ectopic expression of *TaWRKY75-A* improved drought and salt resistance in transgenic Arabidopsis (Ye et al., 2021). Among the WRKY genes in soybean, overexpression of *GmWRKY21* enhanced the tolerance to cold stress in Arabidopsis (Zhou et al., 2008). *GmWRKY54* and *GmWRKY49* enhanced the tolerance to salt and drought stress in transgenic Arabidopsis (Zhou et al., 2008; Xu et al., 2018), whereas *GmWRKY16* conferred salt and drought tolerance (Ma et al., 2019). Overexpression of *GmWRKY12* increased the tolerance of transgenic soybean seedlings to drought and salt stress by proline accumulation and malondialdehyde decrease. *GmWRKY46* overexpression showed that it was involved in hairy root development and subsequently affected plant growth and Pi uptake (Li C. et al., 2021). It was found that the research progresses on the functions of WRKY family genes in soybean mostly focused on the abiotic stress response. However, there are few reports on the functions of WRKY family genes in acidic aluminum stress in soybean. In this study, *GmWRKY21*, an abiotic stress-responsive gene induced by Al stress, was investigated for its functional characterization of Al stress tolerance both in Arabidopsis and in soybean. The systems of Arabidopsis genetic transformation and soybean hairy root transformation were used to study the resistance and molecular mechanism of *GmWRKY21* responding to acidic aluminum stress.

MATERIALS AND METHODS

Plant Materials and Stress Treatments

A soybean cultivar, "Huaxia 3" (HX3), bred by the Guangdong Subcenter of the National Center for Soybean Improvement in South China Agricultural University, was used to investigate the tissue expression pattern of *GmWRKY21* and its responses to Al stress. Soybean seeds of HX3 were germinated in vermiculite with room temperature set at 28/26°C and the light time set as 14-h light/10-h dark under a light intensity of 100 μmol/(m^2·s) (Zeng et al., 2012). For the Al dose–response experiment, seedlings were subjected to a modified 0.5 mM $CaCl_2$ solution containing 0, 25, 50, 75, or 100 μM of $AlCl_3$ for 24 h. During the time-course experiment, seedlings were subjected to a modified 0.5 mM $CaCl_2$ solution with 50 μM $AlCl_3$ for 0, 6, 9, 12, 24, 36, or 48 h.

Plasmid Construction and Transformation of *GmWRKY21* in *Arabidopsis*

The cDNA sequences of *GmWRKY21* gene were isolated using specific primers (**Supplementary Table 1**) and inserted into the multicloning sites of the pLB vector to form the *GmWRKY21*-pLB construct. Then, the full-length coding sequence of *GmWRKY21* amplified from the *GmWRKY21*-pLB vector was inserted into the *Sac*I and *Xba*I sites of a pTF101.1 vector. The non-conserved region sequence 200 bp of *GmWRKY21* amplified by PCR using the specific primers was inserted into the *Avr*II and *Asc*I sites, and then, the 200-bp sequence was reversely inserted into the *Sac*I and *Spe*I sites of a pMU103 vector using the ClonExpressR II One Step Cloning Kit (C112, Vazyme, Nanjing, China). The *GmWRKY21*-pTF101 and *GmWRKY21*-pMU103 plasmids were then transformed into *Agrobacterium* strains, GV3101 and K599 competent cells by heat shock, respectively. The subsequent transformations were carried out by the methods of the *Agrobacterium*-mediated floral dip (Clough and Bent, 2010) and *Agrobacterium rhizogenes*-based transformation (Matthews and Youssef, 2016).

The Isolation and Sequence Analysis of the *GmWRKY21* Gene

The sequence information of the *GmWRKY21* gene was obtained from the database of the National Center for Biotechnology Information (NCBI) with the accession number NP_001237327.2 (Wang et al., 2019). The full-length sequence of *GmWRKY21* was amplified by RT-PCR using specific primers (**Supplementary Table 1**) and Super-Fidelity DNA polymerase (Phanta Max, Vazyme Biotech Co., Ltd., Nanjing, China). The seedlings of soybean cultivar HX3 under the treatment of 50 μM $AlCl_3$ (1 mM $CaCl_2$, pH 4.5) were used to extract total RNA by TRIzol reagent (Invitrogen). The methods of generated cDNA, RT-PCR, and agarose gel electrophoresis were described in detail previously (Lu et al., 2015). The purified PCR product was then inserted into the multiple cloning sites of the pLB vector (Tiangen Rapid DNA Ligation Kit, Beijing, China). The positive clones in *Escherichia coli* were used to obtain the full cDNA sequence of *GmWRKY21* identified by PCR, enzyme digestion, and sequencing (Sangon Biotech Co., Ltd., Shanghai, China) (Lu et al., 2015; Ma et al., 2018).

The nucleotide sequence of *GmWRKY21* and the amino acid sequence of GmWRKY21 protein were used to search its homologous genes and proteins using the database of NCBI. The alignment of nucleotide sequences was performed with the software of DNAMAN. The structure prediction of the GmWRKY21 protein was carried out using the NCBI blast results. The phylogenetic analysis was enforced by using the software of MEGA X (Kumar et al., 2016). The alignment was adjusted manually, while the unrooted phylogenetic trees were constructed by the neighbor-joining method (Sievers et al., 2011).

Intracellular Localization of *GmWRKY21* Protein

Localization of the 'protein was carried out using the method described previously (Lu et al., 2015). The complete coding sequence of *GmWRKY21* without a stop codon amplified by PCR using the specific primers was inserted into the *Nco*I and *Spe*I sites to generate a fusion construct of the GmWRKY21-pCAMBIA1302 vector under the control of CaMV 35S promoter. The plasmids of pCAMBIA1302 and GmWRKY21-pCAMBIA1302 were transformed into

Agrobacterium tumefaciens strain GV3101 by the heat shock method. The young leaves of 4-week-old tobacco plants were contaminated by the recombinant Agrobacterium tumefaciens using the method described previously in detail (Kokkirala et al., 2010). The agro-infiltration leaves of tobacco plants cultured for 48h to 72 h were photographed with a confocal laser scanning microscope (Leica, Germany).

Transactivation Assay of *GmWRKY21* Protein

The ORF sequence of *GmWRKY21* amplified by PCR using the specific primers was inserted into the *Eco*RI and *Bam*HI sites to create a fusion construct of GmWRKY21-pGBKT7 (**Supplementary Table 1**). The GmWRKY21-pGBKT7 and pGBKT7 plasmids were transformed into the cells of yeast strain Y2H. Transcriptional activation of GmWRKY21 protein was analyzed according to the methods described previously (Yang et al., 2010).

Expression Analysis by qRT-PCR

Total RNA was extracted from the seedlings of soybean or Arabidopsis using the Plant Total RNA Kit (GeneMark, Taiwan, China). Reversing transcription for the first-strand cDNA synthesis was performed with 2 μg of total RNA using a PrimeScriptTM RT reagent Kit (Takara, Beijing, China). The qRT-PCR analysis was performed on a CFX96TM Real-Time System (Bio-Rad, Hercules, CA, USA) with SYBR Premix Ex Taq II (Takara, Beijing, China). The inner reference gene *Actin* 3 was used to normalize the data. The quantitative variations of gene expression between the examined replicates were evaluated by the $2^{-\Delta\Delta Ct}$ method described previously (Willems et al., 2008; Lu et al., 2015). Three independent biological repeats were performed to ensure accurate statistical analysis. The specific primers are listed in **Supplementary Table 1**.

Acidic Aluminum Treatment in Transgenic Arabidopsis

Two homozygous lines of T_3 generation of *GmWRKY21* transgenic plants were used for Al sensitivity assay by measuring relative root elongation according to the method described previously (Yokosho et al., 2016). After seed germination in the MS medium, 5-day-old seedlings of wild-type and *GmWRKY21* transgenic plants were transferred to a solid agar medium supplied with 1 mM $CaCl_2$ and 1% sucrose containing different concentrations of $AlCl_3$ (0, 25, 50, and 100 μM; pH 4.5). To prepare 100 mM of $AlCl_3$ stock solution, 2.414 g of $AlCl_3{\cdot}6H_2O$ was dissolved in 100 ml of distilled water and sterile-filtered. The root lengths were measured before and after 3 days of different treatments. The relative root elongation (RRE) was computed as the formula, that is, RRE = (root elongation with different treatments/root elongation without treatments) ×100 (Cai et al., 2020).

Hair Root Transformation in Soybean

The plasmids of the empty vector (EV), *GmWRKY21*-pTF101 (OE), and *GmWRKY21*-pMU103 (RNAi) constructs were transformed into the competent cells of *Agrobacterium* strains K599 by heat shock. Hairy root transformation was performed according to previous reports (Kereszt et al., 2007; Ren et al., 2019). Hypocotyls of 5-day-old soybean seedlings were injected with *Agrobacterium rhizogenes* K599 and kept at high humidity (>90%) with plastic lids until hairy roots at the injection sites were developed to 5–10 cm long. Then, the main roots of the original seedlings were cut, and the hairy roots were immersed in water for ∼5 days before the plants with hairy roots were transferred into the solutions of 0 and 50 μM $AlCl_3$ (0.5 mM $CaCl_2$, pH 4.3) for 24 h.

Data Analysis

All data were presented as the mean of three biological replicates ± SEM. Student's *t*-test at $P = 0.01$ or $P = 0.05$ was used to identify the difference between observation values (Lu et al., 2015).

RESULTS

Cloning and Bioinformatics Analysis of *GmWRKY21*

Based on recent reports of QTL mapping for the aluminum tolerance of soybean (Wang et al., 2019), an aluminum stress-induced gene encoding a transcription factor of WRKY protein was obtained from the database under the gene locus GLYMA_04G218700 and the protein accession number of NP_001237327.2. The WRKY gene designed as *GmWRKY21* is located on chromosome 4 of soybean. The *GmWRKY21* open reading frame (ORF) was isolated from the soybean variety Huaxia 3 based on putative sequence information available from the Phytozome database. The sequence analysis showed that the *GmWRKY21* gene contained three exons and two introns, which encoded a 196-amino-acid protein with an estimated molecular mass of 22.521 KDa and an isoelectric point of 6.143 (data not shown).

The protein BLAST analysis using the complete amino acid sequences indicated that the GmWRKY21 protein had a WRKY DNA-binding domain at the location of the peptide chain between 111 aa and 168 aa. The relationship analysis between GmWRKY21 and other WRKY proteins in soybean and Arabidopsis by the phylogenetic tree showed that *Glyma.06g147100* was 91.3% sequence similar to its homology of the *GmWRKY21* gene in soybean (**Figure 1A**), while *AT5G64810* with the highest homology in Arabidopsis was 40.8% sequence similar to that of the *GmWRKY21* gene. The results of multiple sequence alignment indicated there were three groups for all the WRKY proteins with the largest subgroup of group II. The GmWRKY21 protein was a member of group IIc containing a typical WRKY domain and a C_2H_2 zinc-finger motif (Eulgem et al., 2000; **Figure 1B**). In group IIc, some genes had higher sequence similarity to that of *GmWRKY21*. Among them, *GmWRKY6* held the tolerance to salt and drought stress (Zhou et al., 2008). The results suggested that GmWRKY21 protein was a WRKY TF in soybean which may play certain roles in responding to abiotic stress.

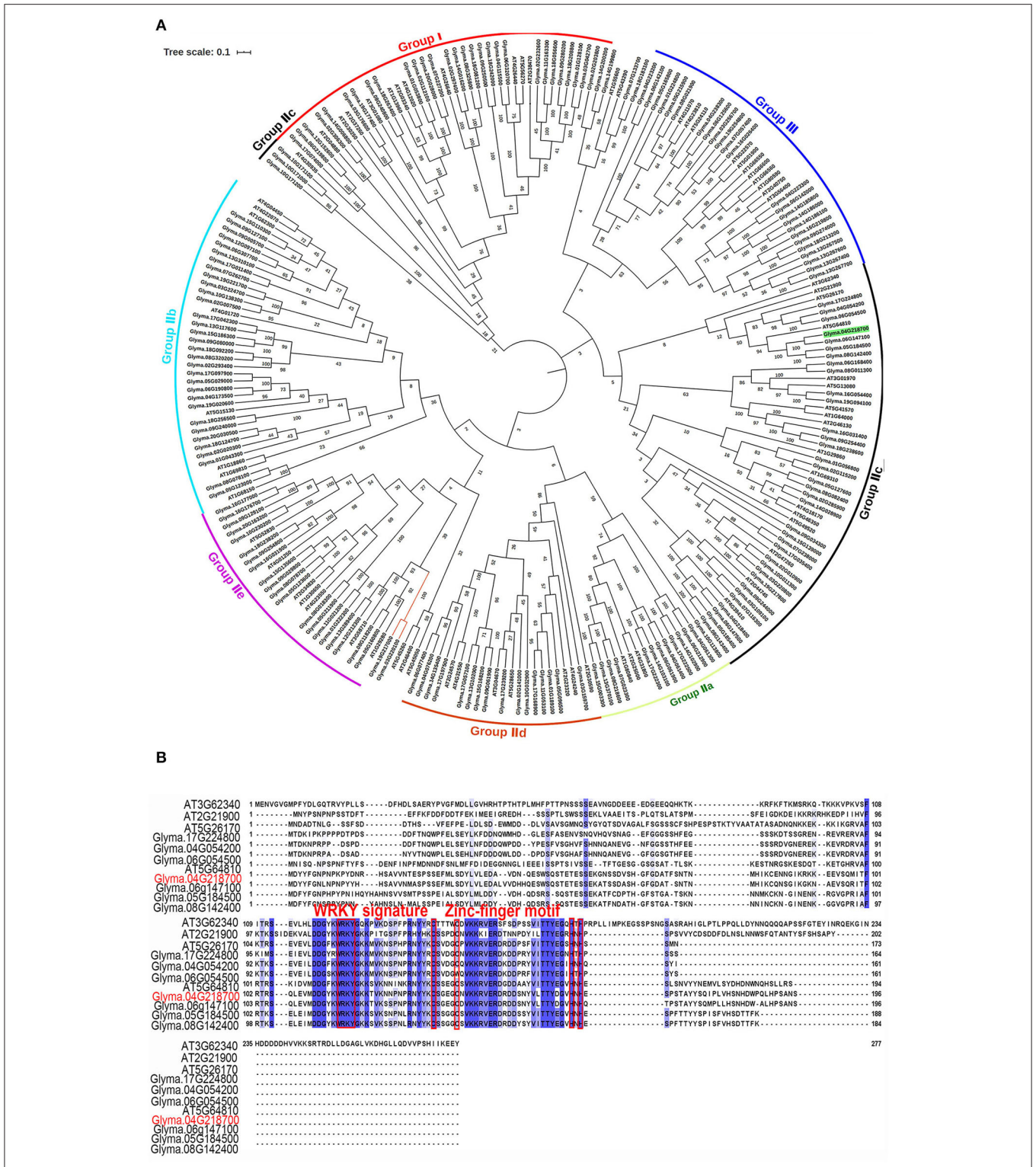

FIGURE 1 | Bioinformatics analysis of the *GmWRKY21* gene. **(A)** Phylogenetic tree was constructed to analyze GmWRKY21 and WRKY proteins in soybean and Arabidopsis by the neighbor-joining method using the software of MEGA X. We selected 177 and 71 WRKT family genes in soybean and *Arabidopsis*, respectively (**Supplementary Table 1**). The amino acid sequences and the accession numbers of WRKY proteins from soybean and Arabidopsis were obtained from the databases of NCBI (https://www.ncbi.nlm.nih.gov/). **(B)** Multiple sequence alignment of genes belonged to the same branch of GmWRKY21 from the phylogenetic tree in **(A)**. Red box highlights the WRKY domains and the zinc-finger motifs.

Characteristics of Localization and Transcriptional Activation Ability of *GmWRKY21* Protein

To determine the transcriptional activity of GmWRKY21 protein, the complete GmWRKY21 ORF was inserted into the pGBKT7 vector. The results showed that the cell deposits transformed by the GmWRKY21-pGBKT7 construct turned blue on the SD/-Trp/X-α-Gal medium. However, the yeast cells transformed by the pGBKT7 vector did not turn blue (**Figure 2A**). These results indicated that the GmWRKY21 protein had transcriptional activity in yeast cells.

To investigate the subcellular localization of GmWRKY21 protein, the GmWRKY21-GFP (green fluorescent protein) recombinant was transformed into the cells of tobacco leaves. The results showed that the green fluorescence was observed in both cytoplasm and nucleus in the cells transformed with the pCAMBIA1302 vector, while the green fluorescence was only observed in the nucleus in the cells transformed with the GmWRKY21-pCAMBIA1302 vector (**Figure 2B**). The results indicated that the GmWRKY21 protein is localized in the nucleus.

Expression Patterns of *GmWRKY21*

The qRT-PCR was used to investigate the expression patterns of *GmWRKY21*. The results showed that *GmWRKY21* presented a constitutive expression pattern, which was rich in soybean roots with about a 10-fold expression value, and more transcripts in leaves and flowers than those in stems or pods (**Figure 3A**). The *GmWRKY21* gene was upregulated under the dose treatments of $AlCl_3$ with more than 160-fold relative expression values, and the *GmWRKY21* transcripts reached the maximum value under the treatment of 50 μM $AlCl_3$ with about 350-fold relative expression value compared with that under the control treatment (**Figure 3B**). While under the time-course treatments of 50 μM $AlCl_3$, the *GmWRKY21* gene was promptly upregulated with over 50-fold relative expression value and reached its much higher value after the treatment of 50 μM $AlCl_3$ for 24 h (**Figure 3C**). After 50 μM $AlCl_3$ treatment for 48 h, the expression of *GmWRKY21* was still at a relatively high level with over 250-fold relative expression (**Figure 3C**).

GmWRKY21 Transgenic Plants Confer Al Tolerance

To investigate *GmWRKY21* response to Al stress, three homozygous lines (OE-2, OE-5, and OE-10) and wild type were used to observe the phenotypes under the treatments of $AlCl_3$ in *Arabidopsis*. As shown in **Figure 4A**, no statistical difference was observed in root growth between WT and *GmWRKY21* transgenic lines in the absence of $AlCl_3$. However, in the presence of 25 and 50 μM $AlCl_3$, the root elongation of WT was inhibited by 15 and 16% after 5 days, but the root elongation of *GmWRKY21* transgenic lines was not significantly influenced. The root elongation of both WT and transgenic lines was inhibited with the increase in Al concentrations. At 100 μM $AlCl_3$, the root elongation of WT was inhibited by 38% and that of the transgenic lines was inhibited by 12% (**Figure 4B**). The determination results showed that MDA was accumulated in both WT and *GmWRKY21* transgenic lines with 0.2733 and 0.1643 μg/g fresh weight, respectively (**Figure 4C**). In contrast, proline contents in both wild-type plants and *GmWRKY21* transgenic lines were 24 and 38–51 μg/g fresh weight, respectively, under the treatment of 100 μM $AlCl_3$ (**Figure 4D**).

To assess the effect of *GmWRKY21* overexpression on Al tolerance in soybean, transgenic hairy roots were produced using the A. rhizogenes-mediated transformation system (**Figure 5A**). Transcript analysis revealed that *GmWRKY21* was upregulated in the overexpression lines at an average fold of 16 and the expression of *GmWRKY21* was downregulated in the RNAi transgenic lines at an average fold of 0.5 (**Figure 5B**). Hematoxylin staining analysis of root tips showed that the *GmWRKY21*-silenced transgenic lines accumulated more Al^{3+} than those of the overexpression lines. The determination in root tips showed that the Al^{3+} contents were 88.1, 162.4, and 120.7 μg/g in the tips of OE, RNAi, and WT plants, respectively (**Figure 5C**). The results indicated that overexpression of *GmWRKY21* improves the tolerance of the hairy roots to Al stress by reducing Al^{3+} accumulation in soybean roots.

Expression Patterns of Genes Responsive to Al Stress

The qRT-PCR was carried out to analyze the molecular regulation mechanism of the *GmWRKY21* gene tolerant to acidic aluminum. The results showed that the expression of *AtALMT1*, *AtALS3*, *AtMATE*, and *AtSTOP1* was all upregulated under Al stress in transgenic Arabidopsis (**Figure 6**). The transcripts of *AtALMT1* and *AtALS3* induced by Al stress were much higher than those of them under the control; however, the expression of *AtMATE* and *AtSTOP1* was not significantly higher compared with that of the control (**Figure 6**). The results showed that *GmWRKY21* enhances the transgenic plants tolerant to Al stress mediated by the multiple genes through the pathway responding to aluminum toxicity.

Expression Patterns of Stress-Responsive Genes Regulated by *GmWRKY21* in *Arabidopsis*

To further investigate the pathways regulated by *GmWRKY21* under Al stress, the expression patterns of stress-responsive genes were performed by qRT-PCR. The results showed that the stress-responsive genes, such as *KIN1*, *COR15A*, *COR15B*, *COR47*, *GLOS3,* and *RD29A*, were upregulated by the treatment of 100 μM $AlCl_3$ (**Figure 7**). Among them, the transcripts of *KIN1*, *GLOS3*, *COR15A,* and *COR15B* genes were significantly higher in the OE-10 line than those of WT under Al stress. However, only the expression levels of *KIN1*, *GLOS3*, and *RD29A* were significantly different from those in the OE-2 lines. The results showed that the GmWRKY21 TF enhances the tolerance of transgenic *Arabidopsis* to acidic aluminum stress mediated by regulating the expression of the stress-responsive genes.

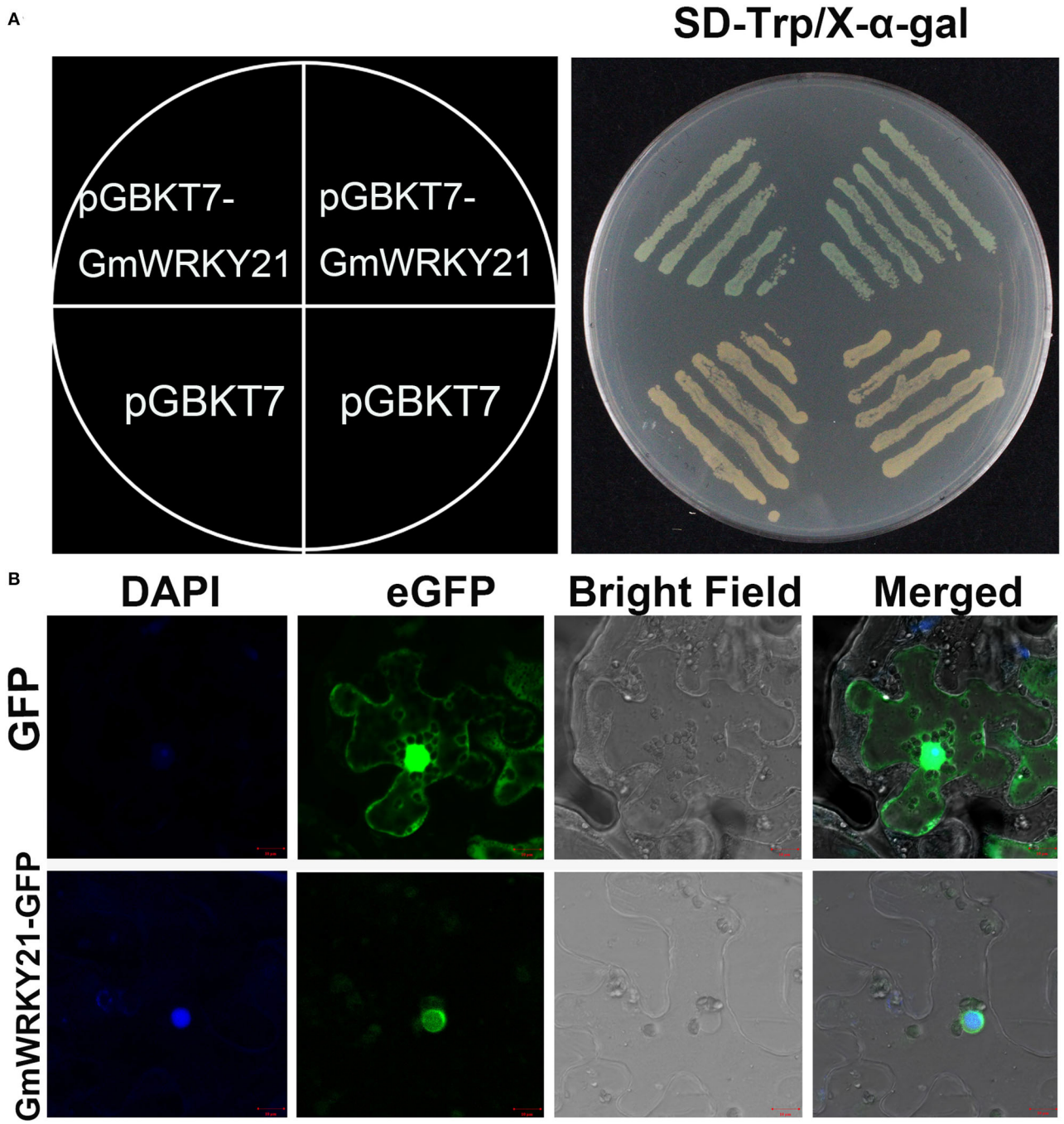

FIGURE 2 | Transcriptional activation and subcellular localization of GmWRKY21 protein. **(A)** Transcriptional activation analysis of GmWRKY21 protein. **(B)** Subcellular localization of GmWRKY21 protein in leaf epidermal cells of tobacco. The ORF sequence of GmWRKY21 was inserted into the sites of *Eco*RI and *Bam*HI of pGBKT7 vector to form the fusion carrier of GmWRKY21-pGBKT7. The fusion plasmid of GmWRKY21-pGBKT7 and pGBKT7 alone (negative control) were transformed into the cells of yeast strain Y2H. The cell deposits were colored with a chromogenic substrate of X-gal. The full coding sequence of GmWRKY21 (without TGA) was inserted into the *Nco*I and *Spe*I sites of pCAMBIA1302 vector to obtain the GmWRKY21-GFP fusion construct. The pCAMBIA1302-GFP vector was transformed as a control. Scale bar **(A,B)**: 10 μm.

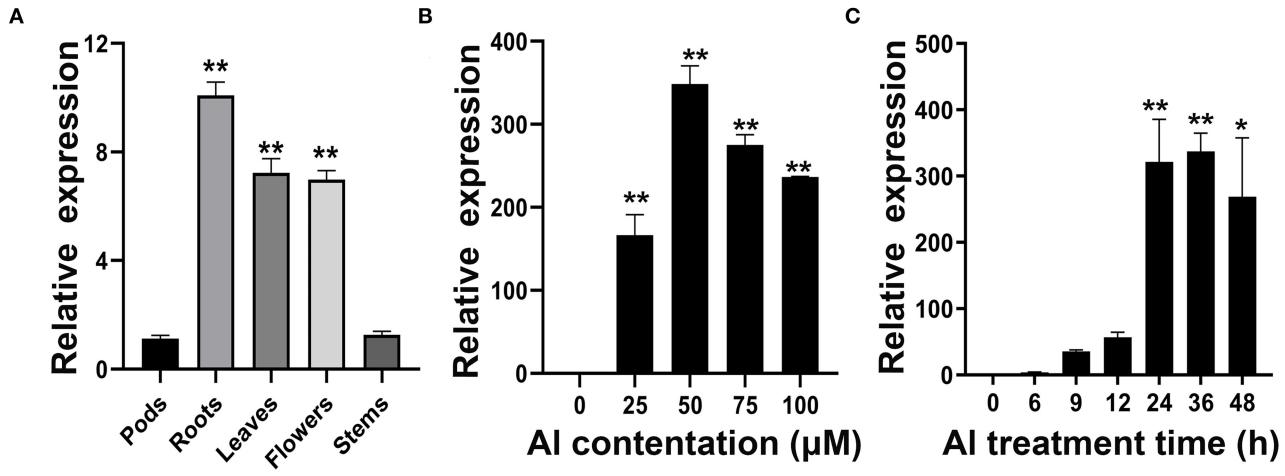

FIGURE 3 | Analysis of *GmWRKY21* expression patterns in different tissues and in response to Al stress. **(A)** qRT-PCR analysis of the *GmWRKY21* transcript in different tissues of the soybean variety Huaxia 3. The total RNA was isolated from the samples of soybean roots, stems, leaves, flowers, and pods. **(B)** Dose-dependent *GmWRKY21* expression pattern in the roots of soybean seedlings. The root samples were taken from the seedlings exposed to different treatments of $AlCl_3$ concentrations (0, 25, 50, 75, and 100 μM) for 24 h. **(C)** The time-course *GmWRKY21* expression pattern in the roots of soybean seedlings. The soybean seedlings were exposed to 50 μM $AlCl_3$ for 0, 6, 9, 12, 24, 36, or 48 h. The root samples were separately harvested for qRT-PCR analysis. The expressing values are designed as the means ± SEM ($n = 3$). The experiments were performed with at least three independent biological replicates. Significant differences according to the one-way analysis of variance are denoted as follows: $^{*}P < 0.05$ and $^{**}P < 0.01$.

GmWRKY21 Transgenic Hairy Roots Increased Transcripts of Abiotic Stress-Related Marker Genes

Several genes such as *GmCOR47* (Guo et al., 1992), *GmDREB2A* (Agarwal et al., 2007), *GmMYB84* (Wang Y. Q. et al., 2017), *GmKIN1* (Wang et al., 1995), *GmGST1* (Qi et al., 2018), and *GmLEA* (Magwanga et al., 2018) play significant roles in abiotic stress. The expression levels of these marker genes were analyzed between EV and *GmWRKY21* transgenic (OE or RNAi) hairy roots under normal and Al stress conditions by qRT-PCR analysis. There was no significant difference between the EV roots and either of the *GmWRKY21* transgenic soybean hairy roots under normal growth conditions. The expression levels of *GmCOR47, GmDREB2A*, *GmMYB84, GmKIN1*, *GmGST1,* and *GmLEA* in the OE soybean hairy roots were significantly higher than those in the EV roots. Conversely, the expression levels of these stress-responsive genes in the RNAi soybean hairy roots were significantly lower than those in the EV-control soybean hairy roots (**Figure 8**).

DISCUSSION

Since the first WRKY transcription factor gene *SPF1* was found in sweet potato in 1994 (Ishiguro and Nakamura, 1994), the WRKY family genes have been broadly investigated for the diverse biological roles in plant growth and development and responses to biotic and abiotic stress (Dai et al., 2016; Kiranmai et al., 2018). However, few genes are known about the WRKYs' roles and their mechanisms responsive to Al stress in soybean. In this study, the candidate gene *GmWRKY21* derived from the RIL (recombinant inbred line, F_{12}) population of Zhonghuang 24 and Huaxia 3 (160 lines) was investigated for its functional characterization of tolerance to aluminum stress in Arabidopsis (Wang et al., 2019). The GmWRKY21 protein located in subgroup IIc contained the WRKY domain and C_2H_2-type zinc-finger structure with the classical characteristic of WRKY proteins from soybean and Arabidopsis (**Figures 1A,B**). The GmWRKY21 protein had more similarities to other WRKY proteins, such as GmWRKY6, GmWRKY25, GmWRKY45, GmWRKY53, GmWRKY8, GmWRKY54, and GmWRKY45, in soybean and AtWRKY57, AtWRKY45, AtWRKY71, AtWRKY28, AtWRKY75, and AtWRKY12 in Arabidopsis (**Supplementary Figure 1**). Previous reports indicated that these genes were all related to biotic and abiotic stress. For example, *GmWRKY6*, *GmWRKY25*, *GmWRKY53*, and *GmWRKY8* all respond to salt and drought stress (Zhou et al., 2008). *GmWRKY45* enhanced the adaptation to phosphate deficiency and salt tolerance in transgenic Arabidopsis (Zhou et al., 2008; Li et al., 2019; Wei et al., 2019). Overexpression of *GmWRKY54* resulted in the tolerance to salt and drought stress in Arabidopsis and the resistance to drought stress through activating genes in Ca^{2+} signaling pathways and abscisic acid in transgenic soybean (Wei et al., 2019). In addition, the WRKY family genes also play multiple roles in regulating plant growth and development, responding to biotic and abiotic stresses. Previous reports indicated that *AtWRKY57* conferred drought tolerance in Arabidopsis (Jiang et al., 2012). AtWRKY45 transcription factor activated *PHT1; 1* expression in response to phosphate starvation (Wang et al., 2014). *AtWRKY71* accelerated flowering in Arabidopsis in the presence of salt stress (Yu Z. Y. et al., 2018). Co-expression of *AtWRKY28* and *AtbHLH17* conferred resistance to abiotic stress in Arabidopsis (Babitha et al., 2013). AtWRKY75 interacted with DELLA protein to positively regulate Arabidopsis flowering

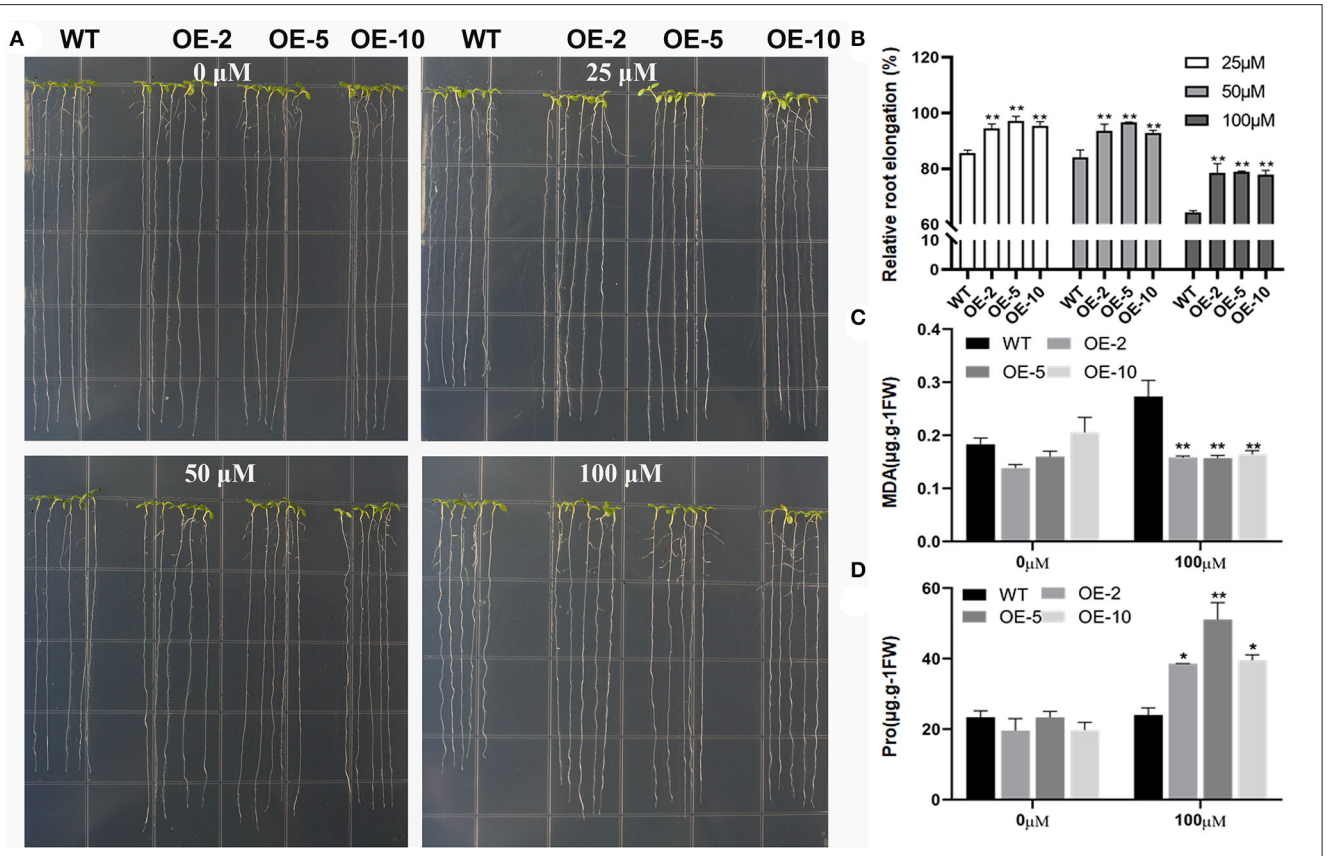

FIGURE 4 | Overexpression of *GmWRKY21* conferred enhanced Al tolerance in transgenic Arabidopsis. **(A)** The phenotypes of *GmWRKY21* transgenic lines (OE-2, 5, and 10) and wild type (WT) under different treatments of $AlCl_3$ solutions. Five-day-old seedlings were transferred to solid agar medium supplied with 1 mM $CaCl_2$ and 1% sucrose containing different concentrations of $AlCl_3$ (0, 25, 50, or 100 μM; pH 4.5) for 5 days. **(B)** The analysis of relative root elongation for the *GmWRKY21* transgenic lines and WT. **(C)** The determination of MDA content. **(D)** The determination of free proline content. All data are presented as means ± SEM. A significant difference according to the one-way analysis of variance is denoted as follows: $^{*}P < 0.05$, $^{**}P < 0.01$.

(Zhang et al., 2018), while *AtWRKY12* negatively regulated cadmium tolerance in Arabidopsis by directly targeting GSH1 (Han et al., 2019). Furthermore, the phylogenetic tree indicated that the GmWRKY21 protein responding to salt and drought stress had more similarities to the GmWRKY6 protein (**Supplementary Figure 1**). Previous reports showed that overexpression of *GmWRKY21* responding to various abiotic stresses, such as salt and drought, enhanced the tolerance of low-temperature stress in transgenic Arabidopsis (Zhou et al., 2008). Therefore, the GmWRKY21 protein was identified to be a WRKY transcription factor to participate in abiotic stress and/or development in plants.

Previous studies revealed that WRKY TFs were widely investigated for key roles in acidic aluminum stress (Ding et al., 2013; Li et al., 2018, 2020). In this study, the *GmWRKY21* gene was rich in soybean root and quickly upregulated under $AlCl_3$ treatment with the differences in Al^{3+} concentrations and temporal differences (**Figure 3**). Aluminum stress increased the formation of reactive oxygen species (ROS) in plants, leading to lipid membrane peroxidation, ion leakage, and protein oxidation (Ezaki et al., 2000; Boscolo et al., 2003). Malondialdehyde (MDA) was one of the most commonly used indicators for the destruction of ROS under stress conditions (Shi et al., 2013), while proline was a multifunctional amino acid to protect plant growth by accumulating in large quantities when plants were subjected to adversity stress (Natarajan et al., 2012). In this study, overexpression of *GmWRKY21* enhanced the tolerance of transgenic Arabidopsis and soybean hairy roots to acid–aluminum stress with the corresponding changes of MDA and proline (**Figures 4**, **6**). Hematoxylin was easy to combine with the root aluminum to form a purplish red complex, and the root tip aluminum ion content can be indirectly judged by the depth of root tip color so as to obtain the sensitivity of plants to aluminum toxicity (Rincon and Gonzales, 1992). In this study, the lines of *GmWRKY21* overexpression were dyed shallower by hematoxylin staining with less Al^{3+} content in the root tips compared to those of WT and RNAi plants (**Figure 5**). Recent reports indicated that other WRKY TFs also have the function of coping with acidic aluminum stress. For example, *AtWRKY46* was a transcriptional suppressor of *ALMT1* that regulates alumina-induced Arabidopsis malic acid secretion. The

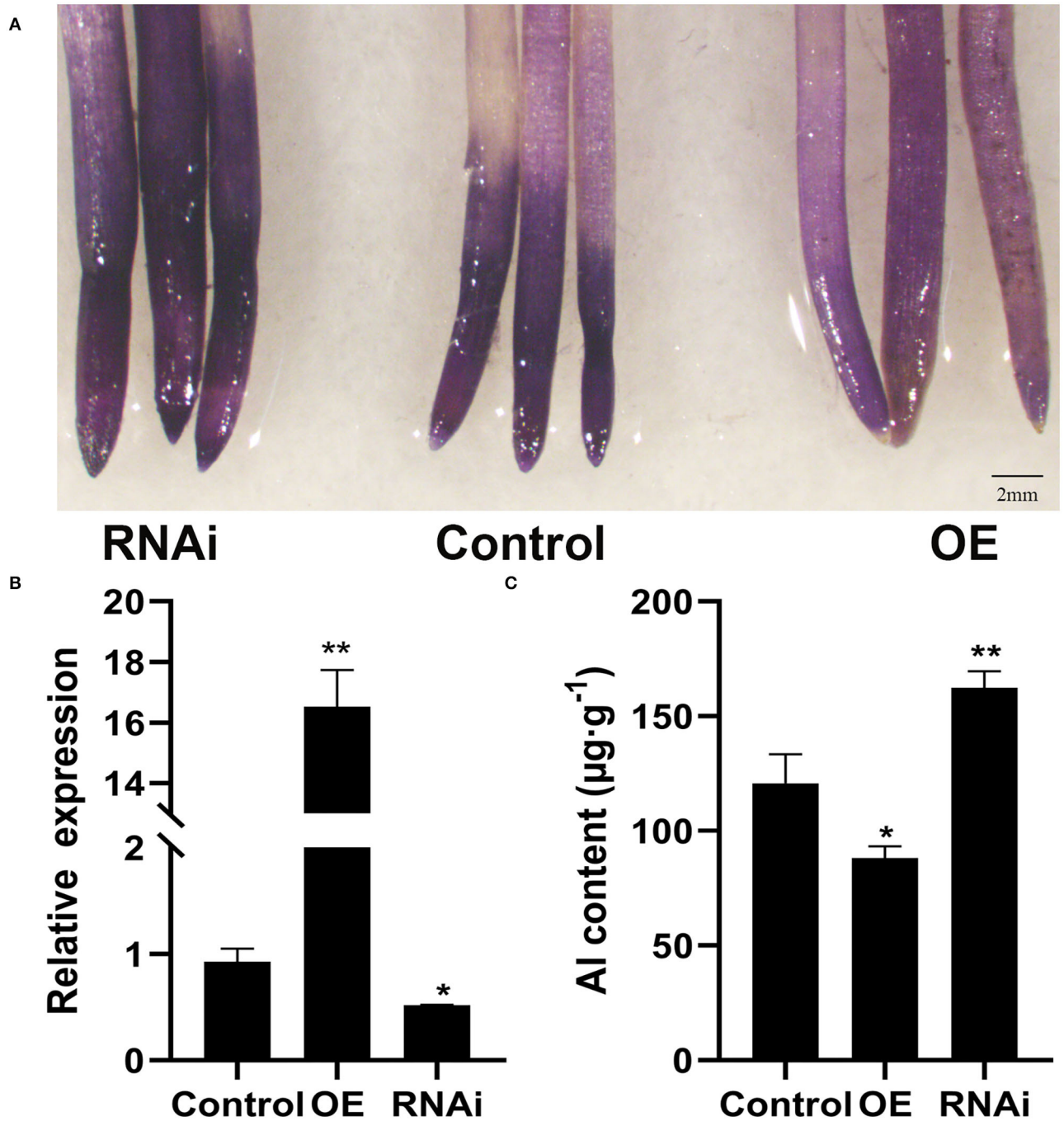

FIGURE 5 | Hematoxylin staining in soybean hairy roots. **(A)** Hematoxylin staining in soybean hairy roots. **(B)** Detection of RNA level in soybean hairy roots. **(C)** Determination of Al^{3+} content in root tips. OE: the hairy roots of *GmWRKY21*-overexpressing transgenic soybean; RNAi: the hairy roots of *GmWRKY21*-RNAi transgenic soybean; Control: the hairy roots of Agrobacterium rhizogenes pathogenic strain K599 in soybean. The experiments were performed with at least three independent biological replicates. Significant differences according to the one-way analysis of variance are denoted as follows: $^{*}P < 0.05$ and $^{**}P < 0.01$.

mutation of *AtWRKY46* led to increased malic acid secretion and reduced aluminum accumulation in the root tip resulting in higher aluminum tolerance in Arabidopsis (Ding et al., 2013). *OsWRKY22* enhanced the tolerance to aluminum stress by activating the expression of *OsFRDL4* and enhancing the secretion of citric acid in rice (Li et al., 2018). *AtWRKY47* made Arabidopsis aluminum tolerant by regulating cell wall modification genes (Li et al., 2020). Therefore, the *GmWRKY21* gene may play an important role in the response of plants to acidic aluminum stress.

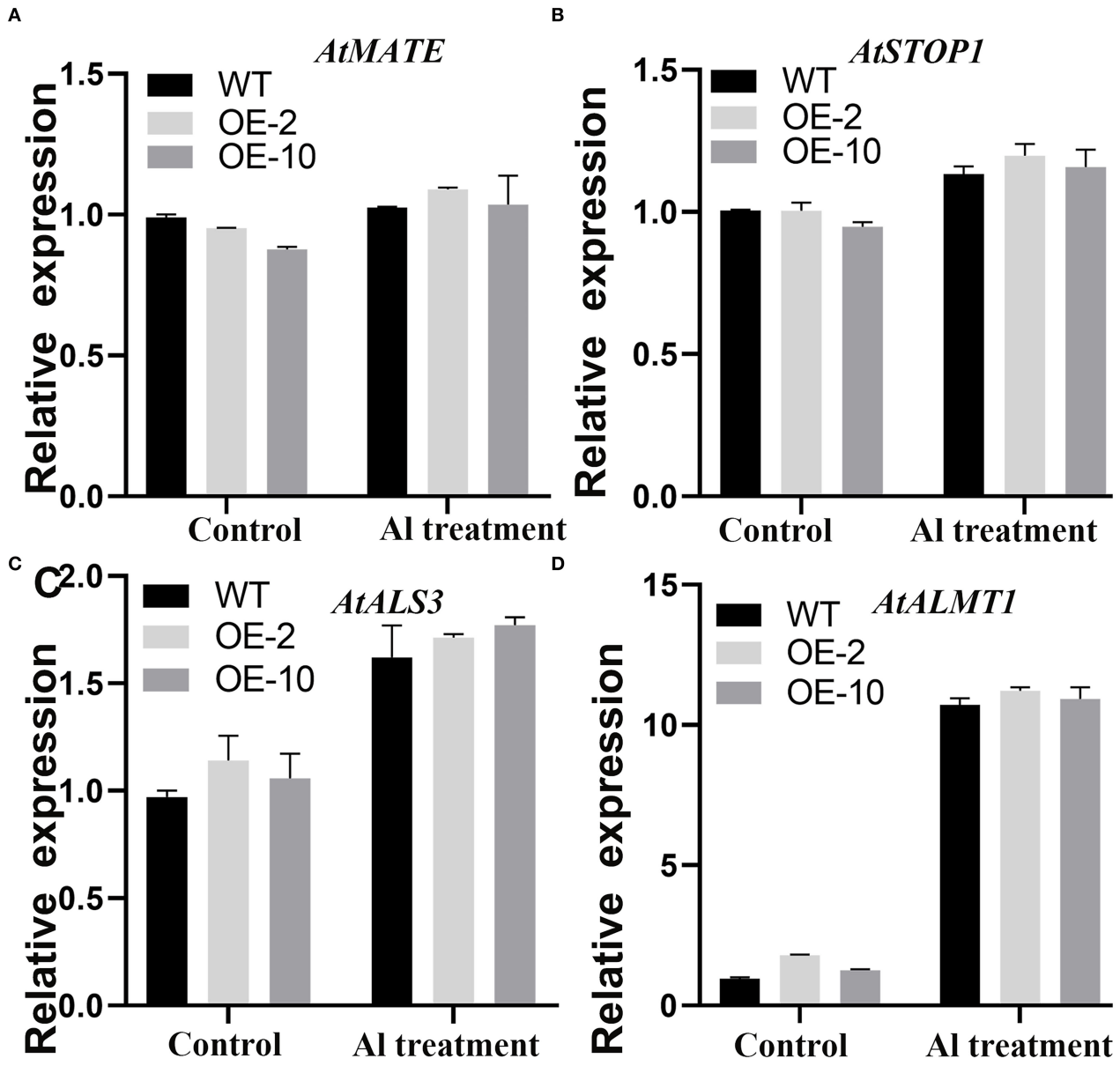

FIGURE 6 | (A–D) Expression patterns of genes responsive to Al stress. WT: wild-type Arabidopsis; OE-2, OE-10: *GmWRKY21* overexpression transgenic lines. WT and transgenic *Arabidopsis* were grown on 0 or 100 μM $AlCl_3$ (pH 4.3) 1/2 MS medium for about 10 days. All data are presented as means ± SEM ($n = 3$). Significant differences according to the one-way analysis of variance are denoted.

Previous studies have found that the ALMT protein family can transport malic acid in the root system to the rhizosphere conferring plants tolerant to aluminum toxicity (Sasaki et al., 2004). The MATE protein family was also involved in the aluminum rejection mechanism by transporting citric acid from the root system to the rhizosphere (Ryan et al., 2011; Kochian et al., 2015). In Arabidopsis, *ALMT1*, *MATE,* and *ALS3* were upregulated by the STOP1 transcription factor (Sawaki et al., 2009). In this study, the *STOP1*, *ALMT1*, *ALS3,* and *MATE* genes were upregulated under aluminum acid stress, while the *STOP1*, *ALMT1*, and *ALS3* genes were dramatically induced by *GmWRKY21* in transgenic lines. However, the transcripts of the four genes in transgenic Arabidopsis under Al stress were statistically non-significant differences compared to those under the control (**Figure 6**). The results suggested that *GmWRKY21* enhances the tolerance to Al stress in transgenic plants by the comprehensive effect of multiple genes. Previous research found that *GmWRKY21* was involved in a variety of abiotic stresses, such as low-temperature, salt, and drought stress (Zhou et al., 2008). In this study, the stress-related genes of *KIN1*, *GLOS3,* and *RD29A* were significantly upregulated in transgenic Arabidopsis

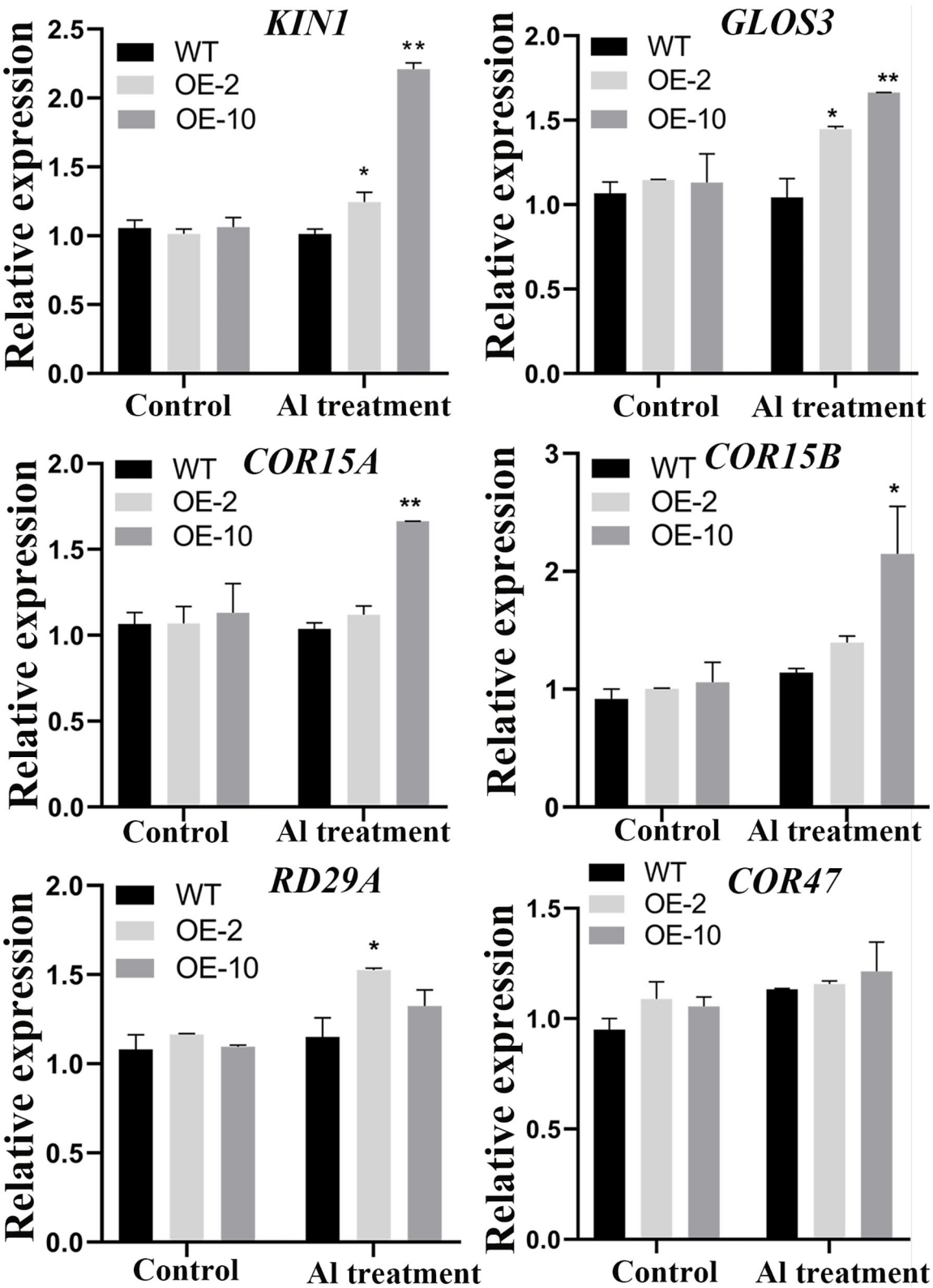

FIGURE 7 | Expression patterns of stress-responsive genes regulated by *GmWRKY21*in Arabidopsis. WT, wild-type Arabidopsis; OE-2, OE-10: *GmWRKY21* overexpression transgenic lines. WT and transgenic *Arabidopsis* were grown on 0 or 100 μM $AlCl_3$ (pH 4.3) 1/2 MS medium for about 10 days. All data are presented as means ± SEM ($n = 3$). Significant differences according to the one-way analysis of variance are denoted as follows: $^{**}P < 0.01$ and $^{*}P < 0.05$.

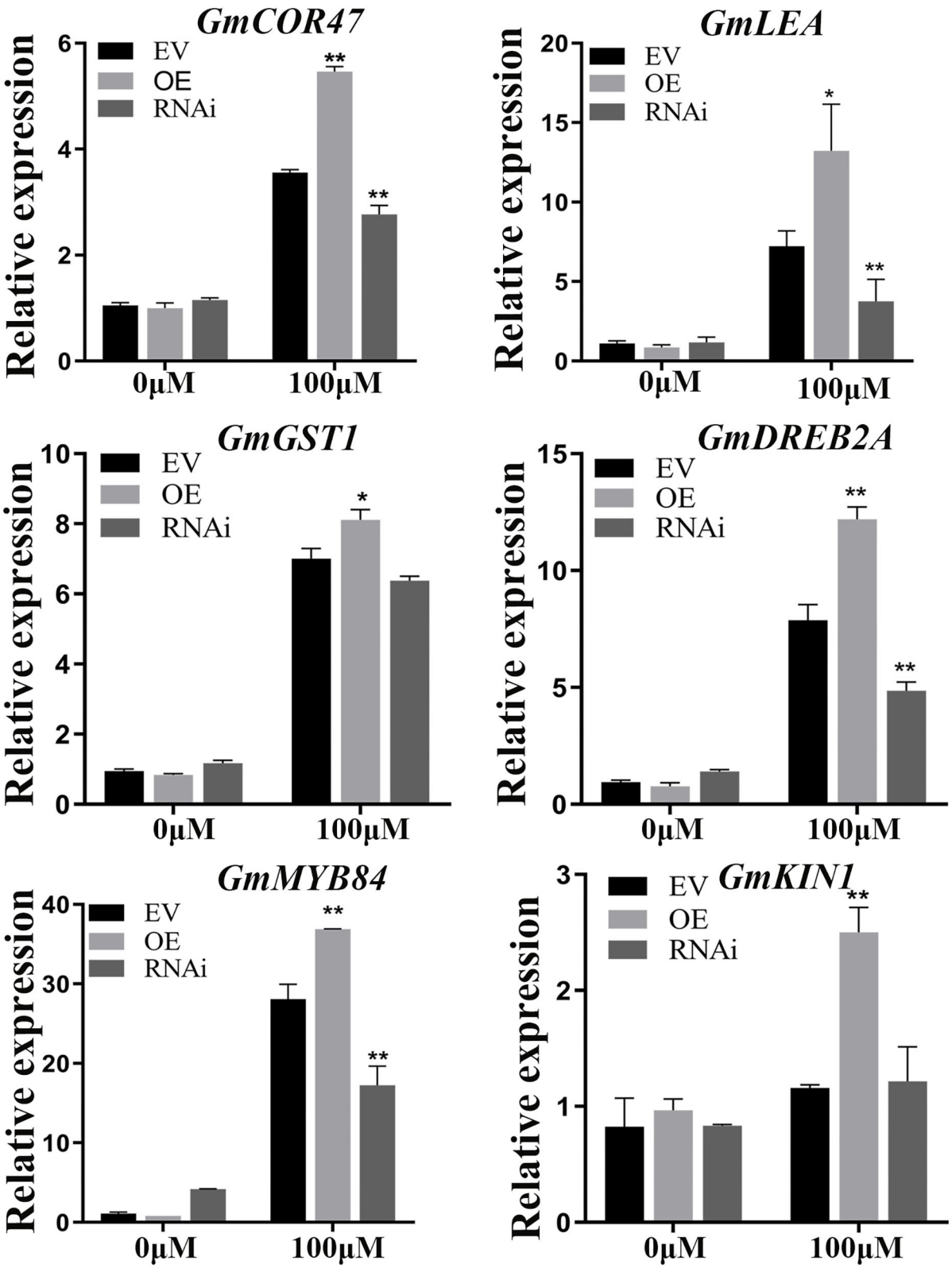

FIGURE 8 | Expression patterns of the stress-responsive genes including *GmCOR47*, *GmLEA*, *GmGST1*, *GmDREB2A*, *GmMYB84*, and *GmKIN1*. EV, empty vector; OE, overexpressing *GmWRKY21* soybean hair roots; RNAi: the hairy roots of *GmWRKY21*-RNAi transgenic soybean. The EV, OE, and RNAi soybean hair roots under normal and Al stress conditions. The hair roots were exposed to 0 and 100 μM $AlCl_3$ (pH 4.3) for 24 h. All data are presented as means ± SEM ($n = 3$). Significant differences according to the one-way analysis of variance are denoted as follows: $^{**}P < 0.01$ and $^{*}P < 0.05$.

plants under the $AlCl_3$ treatment (**Figure 7**; Yu et al., 2016; Chu et al., 2018; Wang et al., 2018; Ma et al., 2019). The LEA genes of *COR15A* and *COR15B* were upregulated with more transcripts in transgenic Arabidopsis plants (**Figure 7**), which were abundantly present in vegetative plant tissues under drought, low-temperature or salt, and other environmental stresses (Hundertmark and Hincha, 2008). Overexpression of *COR15A* or *COR15B* significantly improved the freezing resistance of Arabidopsis, while silencing these two genes at the same time reduced the freezing resistance of Arabidopsis (Artus et al., 1996; Thalhammer et al., 2014). The results indicated that *GmWRKY21* enhanced the tolerance to aluminum stress in Arabidopsis by several genes mediated by certain stress-responsive pathways.

A previous study indicated that some genes such as *GmCOR47*, *GmMYB84*, *GmDREB2A*, *GmGST1*, *GmKIN1,* and *GmLEA* play certain roles in regulating plant response to abiotic stress by potential mechanism. *GmGST1* helps in maintaining redox homeostasis of cells, thus enhancing plant ability to resist abiotic stress (Qi et al., 2018). *GmMYB84* can improve the expression levels of *GmRBOHB-1* and *GmRBOHB-2* genes by binding to the MBS cis-elements in their promoter, enhancing stress tolerance in soybean (Wang N. et al., 2017). The COR47 and LEA as group 2 LEA (LEA II) proteins encode dehydrins, which are cold-inducible proteins that are supposed to sustain membrane stabilization and prevent protein aggregation (Guo et al., 1992; Yu Y. C. et al., 2018; Yu Z. Y. et al., 2018; Li P. et al., 2021). The DREB protein plays an important role in regulating abiotic stress-related genes and thereby imparting stress tolerance to the plant system (Dubouzet et al., 2003). *KIN1* was induced by low temperature, ABA, osmoticum, and dehydration (Wang et al., 1995). These stress-responsive genes were significantly upregulated in the hairy root of transgenic *GmWRKY21* soybean (**Figure 8**). This indicates that *GmWRKY21* improved soybean resistance to aluminum stress by regulating the expression of several stress-responsive genes.

DATA AVAILABILITY STATEMENT

The original contributions presented in the study are included in the article/**Supplementary Material**, further inquiries can be directed to the corresponding author/s.

AUTHOR CONTRIBUTIONS

QM, HN, and ZH conceived and designed the study. ZH, JW, XW, XZ, YC, and ZC conducted the experiments. ZH, JW, and QM performed the data and statistical analysis. ZH wrote the manuscript which was reviewed and edited by HN and QM. All authors contributed to the article and approved the submitted version.

FUNDING

This work was supported by grants from the National Natural Science Foundation of China (31971965 and 31771816), the Major Project of New Varieties Cultivation of Genetically Modified Organisms (2016ZX08004002-007), the Special Supervision on Quality and Safety of Agricultural Products of the Ministry of Agriculture and Rural Areas (4100-C17106 and 21301091702101), the Key Projects of International Scientific and Technological Innovation Cooperation among Governments under National Key R&D Plan (2018YFE0116900-06), the Key Area Research and Development Program of Guangdong Province (2020B020220008), the China Agricultural Research System (CARS-04-PS09), and the Project of Science and Technology of Guangzhou (201804020015).

SUPPLEMENTARY MATERIAL

The Supplementary Material for this article can be found online at: https://www.frontiersin.org/articles/10.3389/fpls.2022.833326/full#supplementary-material

REFERENCES

Agarwal, P., Agarwal, P. K., Nair, S., Sopory, S. K., and Reddy, M. K. (2007). Stress-inducible DREB2A transcription factor from *Pennisetum glaucum* is a phosphoprotein and its phosphorylation negatively regulates its DNA-binding activity. *Mol. Genet. Genomics* 277, 189–198. doi: 10.1007/s00438-006-0183-z

Artus, N. N., Uemura, M., Steponkus, P. L., Gilmour, S. J., Lin, C., and Thomashow, M. F. (1996). Constitutive expression of the cold-regulated *Arabidopsis thaliana COR15a* gene affects both chloroplast and protoplast freezing tolerance. *Proc. Natl. Acad. Sci. U.S.A.* 93, 13404–13409. doi: 10.1073/pnas.93.23.13404

Babitha, K. C., Ramu, S. V., Pruthvi, V., Mahesh, P., Nataraja, K. N., and Udayakumar, M. (2013). Co-expression of *AtbHLH17* and *AtWRKY28* confers resistance to abiotic stress in *Arabidopsis*. *Transgenic Res.* 22, 327–341. doi: 10.1007/s11248-012-9645-8

Bojorquez-Quintal, E., Escalante-Magana, C., Echevarria-Machado, I., and Martinez-Estevez, M. (2017). Aluminum, a friend or foe of higher plants in acid soils. *Front. Plant Sci.* 8, 1767. doi: 10.3389/fpls.2017.01767

Boscolo, P., Menossi, M., and Jorge, R. A. (2003). Aluminum-induced oxidative stress in maize. *Phytochemistry* 62, 181–189. doi: 10.1016/S0031-9422(02)00491-0

Brautigan, D. J., Rengasamy, P., and Chittleborough, D. J. (2012). Aluminium speciation and phytotoxicity in alkaline soils. *Plant Soil* 360, 187–196. doi: 10.1007/s11104-012-1232-5

Cai, Z. D., Xian, P. Q., Lin, R. B., Cheng, Y. B., Lian, T. X., Ma, Q. B., et al. (2020). Characterization of the soybean GmIREG family genes and the function of GmIREG3 in conferring tolerance to aluminum stress. *Int. J. Mol. Sci.* 21, 497. doi: 10.3390/ijms21020497

Chen, J. N., Nolan, T. M., Ye, H. X., Zhang, M. C., Tong, H. N., Xin, P. Y., et al. (2017). Arabidopsis WRKY46, WRKY54, and WRKY70 transcription factors are involved in brassinosteroid-regulated plant growth and drought responses. *Plant Cell* 29, 1425–1439. doi: 10.1105/tpc.17.00364

Chen, L. G., Song, Y., Li, S. J., Zhang, L. P., Zou, C. S., and Yu, D. Q. (2012). The role of WRKY transcription factors in plant abiotic stresses. *Biochim. Biophys. Acta* 1819, 120–128. doi: 10.1016/j.bbagrm.2011.09.002

Chu, M. X., Li, J. J., Zhang, J. Y., Shen, S. F., Li, C. N., Gao, Y. J., et al. (2018). AtCaM4 interacts with a Sec14-like protein, PATL1, to regulate freezing tolerance in Arabidopsis in a CBF-independent manner. *J. Exp. Bot.* 69, 5241–5253. doi: 10.1093/jxb/ery278

Clough, S. J., and Bent, A. F. (2010). Floral dip: A simplified method for *Agrobacterium*-mediated transformation of *Arabidopsis thaliana*. *Plant J.* 16, 735–743. doi: 10.1046/j.1365-313x.1998.00343.x

Dai, X. Y., Wang, Y. Y., and Zhang, W. H. (2016). *OsWRKY74*, a WRKY transcription factor, modulates tolerance to phosphate starvation in rice. *J. Exp. Bot.* 67, 947–960. doi: 10.1093/jxb/erv515

Ding, Z. J., Yan, J. Y., Xu, X. Y., Li, G. X., and Zheng, S. J. (2013). WRKY46 functions as a transcriptional repressor of *ALMT1*, regulating aluminum-induced malate secretion in *Arabidopsis*. *Plant J.* 76, 825–835. doi: 10.1111/tpj.12337

Dubouzet, J. G., Sakuma, Y., Ito, Y., Kasuga, M., Dubouzet, E. G., Miura, S., et al. (2003). *OsDREB* genes in rice, *Oryza sativa* L., encode transcription activators that function in drought-, high-salt- and cold-responsive gene expression. *Plant J.* 33, 751–763. doi: 10.1046/j.1365-313X.2003.01661.x

Eulgem, T., Rushton, P. J., Robatzek, S., and Somssich, I. E. (2000). The WRKY superfamily of plant transcription factors. *Trends Plant Sci.* 5, 199–206. doi: 10.1016/S1360-1385(00)01600-9

Ezaki, B., Gardner, R. C., Ezaki, Y., and Matsumoto, H. (2000). Expression of aluminum-induced genes in transgenic *Arabidopsis* plants can ameliorate aluminum stress and/or oxidative stress. *Plant Physiol.* 122, 657–665. doi: 10.1104/pp.122.3.657

Feng, M. J. (2000). Role of organic acids in detoxification of aluminum in higher plants. *Plant Cell Physiol.* 41, 383–390. doi: 10.1093/pcp/41.4.383

Finatto, T., Viana, V. E., Woyann, L. G., Busanello, C., Maia, L. C. D., and Oliveira, A. C. (2018). Can WRKY transcription factors help plants to overcome environmental challenges? *Genet. Mol. Biol.* 41, 533–544. doi: 10.1590/1678-4685-gmb-2017-0232

Guo, W., Ward, R. W., and Thomashow, M. F. (1992). Characterization of a cold-regulated wheat gene related to *Arabidopsis cor47*. *Plant Physiol.* 100, 915–922. doi: 10.1104/pp.100.2.915

Han, Y. Y., Fan, T. T., Zhu, X. Y., Wu, X., Ouyang, J., Jiang, L., et al. (2019). WRKY12 represses *GSH1* expression to negatively regulate cadmium tolerance in *Arabidopsis*. *Plant Mol. Biol.* 99, 149–159. doi: 10.1007/s11103-018-0809-7

He, G. H., Xu, J. Y., Wang, Y. X., Liu, J. M., Li, P. S., Chen, M., et al. (2016). Drought-responsive WRKY transcription factor genes *TaWRKY1* and *TaWRKY33* from wheat confer drought and/or heat resistance in *Arabidopsis*. *BMC Plant Biol.* 16, 116. doi: 10.1186/s12870-016-0806-4

Hu, Q., Ao, C. W., Wang, X. R., Wu, Y. F., and Du, X. Z. (2021). *GhWRKY1-like*, a WRKY transcription factor, mediates drought tolerance in *Arabidopsis* via modulating ABA biosynthesis. *BMC Plant Biol.* 21, 458. doi: 10.1186/s12870-021-03238-5

Huang, S. Z., Hu, L. J., Zhang, S. H., Zhang, M. X., Jiang, W. Z., Wu, T., et al. (2021). Rice OsWRKY50 mediates ABA-dependent seed germination and seedling growth, and ABA-independent salt stress tolerance. *Int. J. Mol. Sci.* 22, 8625. doi: 10.3390/ijms22168625

Hundertmark, M., and Hincha, D. K. (2008). LEA (late embryogenesis abundant) proteins and their encoding genes in *Arabidopsis thaliana*. *BMC Genomics* 9, 118. doi: 10.1186/1471-2164-9-118

Ishiguro, S., and Nakamura, K. (1994). Characterization of a cDNA encoding a novel DNA-binding protein, SPF1, that recognizes SP8 sequences in the 5′ upstream regions of genes coding for sporamin and β-amylase from sweet potato. *Mol. Gen. Genet.* 244, 563–571. doi: 10.1007/BF00282746

Jiang, Y. J., Liang, G., and Yu, D. Q. (2012). Activated expression of WRKY57 confers drought tolerance in *Arabidopsis*. *Mol. Plant* 5, 1375–1388. doi: 10.1093/mp/sss080

Jiang, Y. Q., and Deyholos, M. K. (2009). Functional characterization of *Arabidopsis* NaCl-inducible *WRKY25* and *WRKY33* transcription factors in abiotic stresses. *Plant Mol. Biol.* 69, 91–105. doi: 10.1007/s11103-008-9408-3

Kereszt, A., Li, D. X., Indrasumunar, A., Nguyen, C. D. T., Nontachaiyapoom, S., Kinkema, M., et al. (2007). Agrobacterium rhizogenes-mediated transformation of soybean to study root biology. *Nat. Protoc.* 2, 948–952. doi: 10.1038/nprot.2007.141

Kiranmai, K., Rao, G. L., Pandurangaiah, M., Nareshkumar, A., Reddy, V. A., Lokesh, U., et al. (2018). A novel WRKY transcription factor, *MuWRKY3* (*Macrotyloma uniflorum* Lam. Verdc.) enhances drought stress tolerance in transgenic groundnut (*Arachis hypogaea* L.) plants. *Front. Plant Sci.* 9, 346. doi: 10.3389/fpls.2018.00346

Kochian, L. V. (1995). Cellular mechanism of aluminum toxicity and resistance in plants. *Annu. Rev. Plant Biol.* 46, 675–681. doi: 10.1146/annurev.pp.46.060195.001321

Kochian, L. V., Hoekenga, O. A., and Pineros, M. A. (2004). How do crop plants tolerate acid soil? Mechanisms of aluminum tolerance and phosphorous efficiency. *Ann. Rev. Plant Biol.* 55, 459–493. doi: 10.1146/annurev.arplant.55.031903.141655

Kochian, L. V., Pineros, M. A., Liu, J., and Magalhaes, J. V. (2015). Plant adaptation to acid soils: the molecular basis for crop aluminum resistance. *Annu. Rev. Plant Biol.* 66, 571. doi: 10.1146/annurev-arplant-043014-114822

Kokkirala, V. R., Yonggang, P., Abbagani, S., Zhu, Z., and Umate, P. (2010). Subcellular localization of proteins of *Oryza sativa* L. In the model tobacco and tomato plants. *Plant Signal. Behav.* 5, 1336–1341. doi: 10.4161/psb.5.11.13318

Kollmeier, M., Felle, H. H., and Horst, W. J. (2000). Genotypical differences in aluminum resistance of maize are expressed in the distal part of the transition zone. Is reduced basipetal auxin flow involved in inhibition of root elongation by aluminum? *Plant Physiol.* 122, 945–956. doi: 10.1104/pp.122.3.945

Kumar, S., Stecher, G., and Tamura, K. (2016). MEGA7: Molecular evolutionary genetics analysis version 7.0 for bigger datasets. *Mol. Biol. Evol.* 33, 1870–1874. doi: 10.1093/molbev/msw054

Li, C., Li, K. N., Liu, X. Y., Ruan, H., Zheng, M. M., Yu, Z. J., et al. (2021). Transcription factor *GmWRKY46* enhanced phosphate starvation tolerance and root development in transgenic plants. *Front. Plant Sci.* 12, 700651. doi: 10.3389/fpls.2021.700651

Li, C., Liu, X. Y., Ruan, H., Zhang, J. Y., Xie, F. B., Gai, J. Y., et al. (2019). *GmWRKY45* enhances tolerance to phosphate starvation and salt stress, and changes fertility in transgenic *Arabidopsis*. *Front. Plant Sci.* 10, 1714. doi: 10.3389/fpls.2019.01714

Li, C. X., Yan, J. Y., Ren, J. Y., Sun, L., Xu, C., Li, G. X., et al. (2020). A WRKY transcription factor confers aluminum tolerance via regulation of cell wall modifying genes. *J. Integr. Plant Biol.* 62, 1176–1192. doi: 10.1111/jipb.12888

Li, G. Z., Wang, Z. Q., Yokosho, K., Ding, B., Fan, W., Gong, Q. Q., et al. (2018). Transcription factor WRKY22 promotes aluminum tolerance via activation of *OsFRDL4* expression and enhancement of citrate secretion in rice (*Oryza sativa*). *New Phytol.* 219, 149–162. doi: 10.1111/nph.15143

Li, G. Z., Zheng, Y. X., Chen, S. J., Liu, J., Wang, P. F., Wang, Y. H., et al. (2021). TaWRKY74 participates copper tolerance through regulation of TaGST1 expression and GSH content in wheat. *Ecotoxicol. Environ. Saf.* 221, 112469. doi: 10.1016/j.ecoenv.2021.112469

Li, J., Besseau, S., Trnen, P., Sipari, N., Kollist, H., Holm, L., et al. (2013). Defense-related transcription factors WRKY70 and WRKY54 modulate osmotic stress tolerance by regulating stomatal aperture in *Arabidopsis*. *New Phytol.* 200, 457–472. doi: 10.1111/nph.12378

Li, P., Li, X., and Jiang, M. (2021). CRISPR/Cas9-mediated mutagenesis of *WRKY3* and *WRKY4* function decreases salt and Me-JA stress tolerance in *Arabidopsis thaliana*. *Mol. Biol. Rep.* 48, 5821–5832. doi: 10.1007/s11033-021-06541-4

Lim, C., Kang, K., Shim, Y., Yoo, S. C., and Paek, N. C. (2021). Inactivating transcription factor *OsWRKY5* enhances drought tolerance through abscisic acid signaling pathways. *Plant Physiol.* 188, 1900–1916. doi: 10.1093/plphys/kiab492

Liu, J. P., Luo, X. Y., Shaff, J., Liang, C. Y., Jia, X. M., Li, Z. Y., et al. (2012). A promoter-swap strategy between the *AtALMT* and *AtMATE* genes increased *Arabidopsis* aluminum resistance and improved carbon-use efficiency for aluminum resistance. *Plant J.* 71, 327–373. doi: 10.1111/j.1365-313X.2012.04994.x

Liu, J. P., Magalhaes, J. V., Shaff, J., and Kochian, L. V. (2009). Aluminum-activated citrate and malate transporters from the MATE and ALMT families function independently to confer *Arabidopsis* aluminum tolerance. *Plant J.* 57, 389–399. doi: 10.1111/j.1365-313X.2008.03696.x

Liu, J. P., Pineros, M. A., and Kochian, L. V. (2014). The role of aluminum sensing and signaling in plant aluminum resistance. *J. Integr. Plant Biol.* 56, 221–230. doi: 10.1111/jipb.12162

Lu, J., Suo, H. C., Yi, R., Ma, Q. B., and Nian, H. (2015). *Glyma11g13220*, a homolog of the vernalization pathway gene *VERNALIZATION 1* from soybean [*Glycine max* (L.) Merr.], Promotes flowering in *Arabidopsis thaliana*. *BMC Plant Biol.* 15, 232. doi: 10.1186/s12870-015-0602-6

Ma, J. H., Gao, X. L., Liu, Q., Shao, Y., Zhang, D. J., Jiang, L. N., et al. (2017). Overexpression of *TaWRKY146* increases drought tolerance through inducing stomatal closure in *Arabidopsis thaliana*. *Front. Plant Sci.* 8, 2036. doi: 10.3389/fpls.2017.02036

Ma, Q. B., Xia, Z. L., Cai, Z. D., Li, L., Cheng, Y. B., Liu, J., et al. (2019). *GmWRKY16* enhances drought and salt tolerance through an ABA-mediated pathway in *Arabidopsis thaliana*. *Front. Plant Sci.* 9, 1979. doi: 10.3389/fpls.2018.01979

Ma, Q. B., Yi, R., Li, L., Liang, Z. Y., Zeng, T. T., Zhang, Y., et al. (2018). *GsMATE* encoding a multidrug and toxic compound extrusion transporter enhances aluminum tolerance in *Arabidopsis thaliana*. *BMC Plant Biol.* 18, 212. doi: 10.1186/s12870-018-1397-z

Magwanga, R. O., Lu, P., Kirungu, J. N., Lu, H. J., Wang, X. X., Cai, X. Y., et al. (2018). Characterization of the late embryogenesis abundant (LEA) proteins family and their role in drought stress tolerance in upland cotton. *BMC Genet.* 19, 6. doi: 10.1186/s12863-017-0596-1

Matthews, B., and Youssef, R. (2016). Agrobacterium rhizogenes-based transformation of soybean roots to form composite plants. *Bio-Protocol* 6, e1708. doi: 10.21769/BioProtoc.1708

Natarajan, S. K., Zhu, W. D., Liang, X. W., Zhang, L., Demers, A. J., Zimmerman, M. C., et al. (2012). Proline dehydrogenase is essential for proline protection against hydrogen peroxide-induced cell death. *Free Radic. Biol. Med.* 53, 1181–1191. doi: 10.1016/j.freeradbiomed.2012.07.002

Niu, C. F., Wei, W., Zhou, Q. Y., Tian, A. G., Hao, Y. J., Zhang, W. K., et al. (2012). Wheat *WRKY* genes *TaWRKY2* and *TaWRKY19* regulate abiotic stress tolerance in transgenic *Arabidopsis* plants. *Plant Cell Environ.* 35, 1156–1170. doi: 10.1111/j.1365-3040.2012.02480.x

Qi, J. S., Song, C. P., Wang, B. S., Zhou, J. M., Kangasjarvi, J., Zhu, J. K., et al. (2018). Reactive oxygen species signaling and stomatal movement in plant responses to drought stress and pathogen attack. *J. Integr. Plant Biol.* 60, 805–826. doi: 10.1111/jipb.12654

Qiu, Y. P., and Yu, D. Q. (2009). Over-expression of the stress-induced *OsWRKY45* enhances disease resistance and drought tolerance in *Arabidopsis*. *Environ. Exp. Bot.* 65, 35–47. doi: 10.1016/j.envexpbot.2008.07.002

Ren, B., Wang, X. T., Duan, J. B., and Ma, J. X. (2019). Rhizobial tRNA-derived small RNAs are signal molecules regulating plant nodulation. *Science* 365, 919–922. doi: 10.1126/science.aav8907

Ren, X. Z., Chen, Z. Z., Liu, Y., Zhang, H. R., Zhang, M., Liu, Q. A., et al. (2010). ABO3, a WRKY transcription factor, mediates plant responses to abscisic acid and drought tolerance in *Arabidopsis*. *Plant J.* 63, 417–429. doi: 10.1111/j.1365-313X.2010.04248.x

Rincon, M., and Gonzales, R. A. (1992). Aluminum partitioning in intact roots of aluminum-tolerant and aluminum-sensitive wheat (*Triticum aestivum* L.) cultivars. *Plant Physiol.* 99, 1021–1028. doi: 10.1104/pp.99.3.1021

Rushton, P. J., Macdonald, H., Huttly, A. K., Lazarus, C. M., and Hooley, R. (1995). Members of a new family of DNA-binding proteins bind to a conserved cis-element in the promoters of α-*Amy2* genes. *Plant Mol. Biol.* 29, 691–702. doi: 10.1007/BF00041160

Rushton, P. J., Somssich, I. E., Ringler, P., and Shen, Q. J. (2010). WRKY transcription factors. *Trends Plant Sci.* 15, 247–258. doi: 10.1016/j.tplants.2010.02.006

Rushton, P. J., Torres, J. T., Parniske, M., Wernert, P., Hahlbrock, K., and Somssich, I. E. (1996). Interaction of elicitor-induced DNA-binding proteins with elicitor response elements in the promoters of parsley PR1 genes. *Embo J.* 15, 5690–5700. doi: 10.1002/j.1460-2075.1996.tb00953.x

Ryan, P. R., Delhaize, E., and Jones, D. L. (2001). Function and mechanism of organic anion exudation from plant roots. *Annu. Rev. Plant Physiol. Plant Mol. Biol.* 52, 527–560. doi: 10.1146/annurev.arplant.52.1.527

Ryan, P. R., Tyerman, S. D., Sasaki, T., Furuichi, T., Yamamoto, Y., Zhang, W. H., et al. (2011). The identification of aluminium-resistance genes provides opportunities for enhancing crop production on acid soils. *J. Exp. Bot.* 62, 9–20. doi: 10.1093/jxb/erq272

Sasaki, T., Yamamoto, Y., Ezaki, B., Katsuhara, M., Ahn, S. J., Ryan, P. R., et al. (2004). A wheat gene encoding an aluminum-activated malate transporter. *Plant J.* 37, 645–653. doi: 10.1111/j.1365-313X.2003.01991.x

Sawaki, Y., Iuchi, S., Kobayashi, Y., Kobayashi, Y., Ikka, T., Sakurai, N., et al. (2009). STOP1 regulates multiple genes that protect arabidopsis from proton and aluminum toxicities. *Plant Physiol.* 150, 281–294. doi: 10.1104/pp.108.134700

Shen, H. S., Liu, C. T., Zhang, Y., Meng, X. P., Zhou, X., Chu, C. C., et al. (2012). OsWRKY30 is activated by MAP kinases to confer drought tolerance in rice. *Plant Mol. Biol.* 80, 241–253. doi: 10.1007/s11103-012-9941-y

Shi, H. T., Ye, T. T., and Chan, Z. L. (2013). Exogenous application of hydrogen sulfide donor sodium hydrosulfide enhanced multiple abiotic stress tolerance in bermudagrass [*Cynodon dactylon* (L). Pers.]. *Plant Physiol. Biochem.* 71, 226–234. doi: 10.1016/j.plaphy.2013.07.021

Sievers, F., Wilm, A., Dineen, D., Gibson, T. J., Karplus, K., Li, W. Z., et al. (2011). Fast, scalable generation of high-quality protein multiple sequence alignments using clustal omega. *Mol. Syst. Biol.* 7, 539. doi: 10.1038/msb.2011.75

Silambarasan, S., Logeswari, P., Valentine, A., and Cornejo, P. (2019). Role of *Curtobacterium herbarum* strain CAH5 on aluminum bioaccumulation and enhancement of *Lactuca sativa* growth under aluminum and drought stresses. *Ecotoxicol. Environ. Saf.* 183, 109571–109573. doi: 10.1016/j.ecoenv.2019.109573

Singh, S., Tripathi, D. K., Singh, S., Sharma, S., Dubey, N. K., Chauhan, D. K., et al. (2017). Toxicity of aluminium on various levels of plant cells and organism. *Environ. Exp. Bot.* 137, 177–193. doi: 10.1016/j.envexpbot.2017.01.005

Song, H., Sun, W. H., Yang, G. F., and Sun, J. (2018). WRKY transcription factors in legumes. *BMC Plant Biol.* 18, 243. doi: 10.1186/s12870-018-1467-2

Song, Y., Chen, L. G., Zhang, L. P., and Yu, D. Q. (2010). Overexpression of *OsWRKY72* gene interferes in the abscisic acid signal and auxin transport pathway of *Arabidopsis*. *J. Biosci.* 35, 459–471. doi: 10.1007/s12038-010-0051-1

Thalhammer, A., Bryant, G., Sulpice, R., and Hincha, D. K. (2014). Disordered cold regulated15 proteins protect chloroplast membranes during freezing through binding and folding, but do not stabilize chloroplast enzymes *in vivo*. *Plant Physiol.* 166, 190–201. doi: 10.1104/pp.114.245399

Wang, H., Datla, R., Georges, F., Loewen, M., and Cutler, A. J. (1995). Promoters from *kin1* and *cor6.6*, two homologous *Arabidopsis tha*liana genes: transcriptional regulation and gene expression induced by low temperature, ABA, osmoticum and dehydration. *Plant Mol. Biol.* 28, 605–617. doi: 10.1007/BF00021187

Wang, H., Xu, Q., Kong, Y. H., Chen, Y., Duan, J. Y., Wu, W. H., et al. (2014). Arabidopsis WRKY45 transcription factor activates *PHOSPHATE TRANSPORTER1;1* expression in response to phosphate starvation. *Plant Physiol.* 164, 2020–2029. doi: 10.1104/pp.113.235077

Wang, N., Zhang, W. X., Qin, M. Y., Li, S., Qiao, M., Liu, Z. H., et al. (2017). Drought tolerance conferred in soybean (*Glycine max*. L) by GmMYB84, a novel R2R3-MYB transcription factor. *Plant Cell Physiol* 58, 1764–1776. doi: 10.1093/pcp/pcx111

Wang, S. C., Zhang, J., Gu, M., and Xu, G. H. (2021). OsWRKY108 is an integrative regulator of phosphorus homeostasis and leaf inclination in rice. *Plant Signal. Behav.* 16, 1976545. doi: 10.1080/15592324.2021.1976545

Wang, X. L., Wang, Y., Wang, L., Liu, H., Zhang, B., Cao, Q. J., et al. (2018). *Arabidopsis* PCaP2 functions as a linker between ABA and SA signals in plant water deficit tolerance. *Front. Plant Sci.* 9, 578. doi: 10.3389/fpls.2018.01062

Wang, X. X., Cheng, Y. B., Yang, C., Yang, C. Y., Mu, Y. H., Xia, Q. J., et al. (2019). QTL mapping for aluminum tolerance in RIL population of soybean (*Glycine max* L.) by RAD sequencing. *PLoS ONE* 14, e223674. doi: 10.1371/journal.pone.0223674

Wang, Y. Q., Li, R. H., Li, D. M., Jia, X. M., Zhou, D. W., Li, J. Y., et al. (2017). NIP1;2 is a plasma membrane-localized transporter mediating aluminum uptake, translocation, and tolerance in *Arabidopsis*. *Proc. Natl. Acad. U.S.A.* 114, 5047. doi: 10.1073/pnas.1618557114

Wei, W., Liang, D. W., Bian, X. H., Shen, M., Xiao, J. H., Zhang, W. K., et al. (2019). GmWRKY54 improves drought tolerance through activating genes in abscisic acid and Ca^{2+} signaling pathways in transgenic soybean. *Plant J.* 100, 384–398. doi: 10.1111/tpj.14449

Willems, E., Leyns, L., and Vandesompele, J. (2008). Standardization of real-time PCR gene expression data from independent biological replicates. *Anal. Biochem.* 379, 127–129. doi: 10.1016/j.ab.2008.04.036

Wu, X. L., Shiroto, Y., Kishitani, S., Ito, Y., and Toriyama, K. (2009). Enhanced heat and drought tolerance in transgenic rice seedlings overexpressing *OsWRKY11* under the control of *HSP101* promoter. *Plant Cell Rep.* 28, 21–30. doi: 10.1007/s00299-008-0614-x

Xie, T., Chen, C. J., Li, C. H., Liu, J. R., Liu, C. Y., and He, Y. H. (2018). Genome-wide investigation of WRKY gene family in pineapple: Evolution and expression profiles during development and stress. *BMC Genomics* 19, 490. doi: 10.1186/s12864-018-4880-x

Xu, Z. L., Raza, Q., Xu, L., He, X. L., Huang, Y. H., Yi, J. X., et al. (2018). GmWRKY49, a salt-responsive nuclear protein, improved root length and

governed better salinity tolerance in transgenic *Arabidopsis*. *Front. Plant Sci.* 9, 809. doi: 10.3389/fpls.2018.00809

Yamamoto, Y., Kobayashi, Y., Devi, S. R., Rikiishi, S., and Matsumoto, H. (2002). Aluminum toxicity is associated with mitochondrial dysfunction and the production of reactive oxygen species in plant cells. *Plant Physiol.* 128, 63–72. doi: 10.1104/pp.010417

Yang, L. A., Ji, W., Zhu, Y. M., Gao, P., Li, Y., Cai, H., et al. (2010). GsCBRLK, a calcium/calmodulin-binding receptor-like kinase, is a positive regulator of plant tolerance to salt and ABA stress. *J. Exp. Bot.* 61, 2519–2533. doi: 10.1093/jxb/erq084

Ye, H., Qiao, L. Y., Guo, H. Y., Guo, L. P., Ren, F., Bai, J. F., et al. (2021). Genome-wide identification of wheat *WRKY* gene family reveals that *TaWRKY75-A* is referred to drought and salt resistances. *Front. Plant Sci.* 12, 663118. doi: 10.3389/fpls.2021.663118

Yokosho, K., Yamaji, N., Mitani-Ueno, N., Shen, R. F., and Ma, J. F. (2016). An aluminum-inducible IREG gene is required for internal detoxification of aluminum in buckwheat. *Plant Cell Physiol.* 57, 1169–1178. doi: 10.1093/pcp/pcw065

Yu, X. W., Liu, Y. M., Wang, S., Tao, Y., Wang, Z. K., Shu, Y. J., et al. (2016). CarNAC4, a NAC-type chickpea transcription factor conferring enhanced drought and salt stress tolerances in *Arabidopsis*. *Plant Cell Rep.* 35, 613–627. doi: 10.1007/s00299-015-1907-5

Yu, Y. C., Wang, L., Chen, J. C., Liu, Z. H., Park, C. M., and Xiang, F. N. (2018). WRKY71 acts antagonistically against salt-delayed flowering in *Arabidopsis thaliana*. *Plant Cell Physiol.* 59, 414–422. doi: 10.1093/pcp/pcx201

Yu, Z. Y., Wang, X., and Zhang, L. S. (2018). Structural and functional dynamics of dehydrins: A plant protector protein under abiotic stress. *Int. J. Mol. Sci.* 19, 3420. doi: 10.3390/ijms19113420

Zeng, Q. Y., Yang, C. Y., Ma, Q. B., Li, X. P., Dong, W. W., and Nian, H. (2012). Identification of wild soybean miRNAs and their target genes responsive to aluminum stress. *BMC Plant Biol.* 12, 182. doi: 10.1186/1471-2229-12-182

Zhang, L. P., Chen, L. G., and Yu, D. Q. (2018). Transcription factor WRKY75 interacts with DELLA proteins to affect flowering. *Plant Physiol.* 176, 790–803. doi: 10.1104/pp.17.00657

Zhang, Y. J., and Wang, L. J. (2005). The WRKY transcription factor superfamily: Its origin in eukaryotes and expansion in plants. *BMC Evol. Biol.* 5, 1. doi: 10.1186/1471-2148-5-1

Zhou, L., Wang, N. N., Gong, S. Y., Lu, R., Li, Y., and Li, X. B. (2015). Overexpression of a cotton (Gossypium hirsutum) WRKY gene, GhWRKY34, in Arabidopsis enhances salt-tolerance of the transgenic plants. *Plant Physiol. Biochem.* 96, 311–320. doi: 10.1016/j.plaphy.2015.08.016

Zhou, Q. Y., Tian, A. G., Zou, H. F., Xie, Z. M., Lei, G., Huang, J., et al. (2008). Soybean WRKY-type transcription factor genes, *GmWRKY13*, *GmWRKY21*, and *GmWRKY54*, confer differential tolerance to abiotic stresses in transgenic *Arabidopsis* plants. *Plant Biotechnol. J.* 6, 486–503. doi: 10.1111/j.1467-7652.2008.00336.x

Conflict of Interest: The authors declare that the research was conducted in the absence of any commercial or financial relationships that could be construed as a potential conflict of interest.

Publisher's Note: All claims expressed in this article are solely those of the authors and do not necessarily represent those of their affiliated organizations, or those of the publisher, the editors and the reviewers. Any product that may be evaluated in this article, or claim that may be made by its manufacturer, is not guaranteed or endorsed by the publisher.

Copyright © 2022 Han, Wang, Wang, Zhang, Cheng, Cai, Nian and Ma. This is an open-access article distributed under the terms of the Creative Commons Attribution License (CC BY). The use, distribution or reproduction in other forums is permitted, provided the original author(s) and the copyright owner(s) are credited and that the original publication in this journal is cited, in accordance with accepted academic practice. No use, distribution or reproduction is permitted which does not comply with these terms.

frontiers | Frontiers in Plant Science

ORIGINAL RESEARCH
published: 28 July 2022
doi: 10.3389/fpls.2022.863233

OsSIDP301, a Member of the DUF1644 Family, Negatively Regulates Salt Stress and Grain Size in Rice

Li Ge[1], Hongming Guo[1], Xiu Li[1], Ming Tang[2], Chiming Guo[3], Han Bao[1], Linjuan Huang[1], Yin Yi[2], Yuchao Cui[1] and Liang Chen[1]**

[1] Xiamen Key Laboratory for Plant Genetics, School of Life Sciences, Xiamen University, Xiamen, China, [2] Key Laboratory of National Forestry and Grassland Administration on Biodiversity Conservation in Karst Mountainous Areas of Southwestern China, School of Life Sciences, Guizhou Normal University, Guiyang, China, [3] Fujian Key Laboratory of Subtropical Plant Physiology and Biochemistry, Fujian Institute of Subtropical Botany, Xiamen, China

As a major environmental factor, salt stress substantially retards growth and reduces the productivity of rice (*Oryza sativa*). Members of the DUF1644 family, "the domains of unknown function 1644 motif" are predicted to play an essential regulatory role in response to abiotic stress. However, the specific molecular mechanisms of most members of this family remain elusive. Here, we report that the *OsSIDP301* (stress-induced DUF1644 protein) was induced by salt stress and abscisic acid (ABA). We found that overexpression of *OsSIDP301* (OE) in plants conferred salt hypersensitivity and reduced grain size, whereas plants with *OsSIDP301* RNA interference (RNAi) exhibited salt tolerance and increased grain size in rice. *OsSIDP301* determines salt stress tolerance by modulating genes involved in the salt-response and ABA signaling pathways. Further studies suggest that *OsSIDP301* regulates grain size by influencing cell expansion in spikelet hulls. Moreover, OsSIDP301 interacts with OsBUL1 COMPLEX1 (OsBC1), which positively regulates grain size in rice. Our findings reveal that *OsSIDP301* functions as a negative regulator of salt stress and grain size, and repressing its expression represents a promising strategy for improving salt stress tolerance and yield in rice.

Keywords: OsSIDP301, salt stress, ABA signaling, grain size, cell expansion

OPEN ACCESS

Edited by:
Maik Böhmer,
Goethe University Frankfurt, Germany

Reviewed by:
Jian Zhang,
China National Rice Research Institute (CAAS), China
Weiqiang Li,
RIKEN, Japan

****Correspondence:***
Yuchao Cui
yuchaocui@xmu.edu.cn
Liang Chen
chenlg@xmu.edu.cn

Specialty section:
This article was submitted to Plant Physiology, a section of the journal Frontiers in Plant Science

Received: *26 January 2022*
Accepted: *13 June 2022*
Published: *28 July 2022*

Citation:
Ge L, Guo H, Li X, Tang M, Guo C, Bao H, Huang L, Yi Y, Cui Y and Chen L (2022) OsSIDP301, a Member of the DUF1644 Family, Negatively Regulates Salt Stress and Grain Size in Rice. Front. Plant Sci. 13:863233. doi: 10.3389/fpls.2022.863233

INTRODUCTION

Adverse environmental conditions limiting agricultural productivity and threatening security, such as saline alkalization of soil, severely affect plant development and damage one-fifth of the irrigated land (Rasool et al., 2013; Roy et al., 2014; Zhu, 2016; Morton et al., 2019). Rice (*Oryza sativa*), which is one of the most important cereal crops, is sensitive to saline alkalinization (Hussain et al., 2017; Chang et al., 2019). To meet the demand for food for a rapidly growing population and to compensate for the ever-reducing availability of arable land, it is necessary to urgently develop salt-tolerant rice varieties through efficient molecular breeding technologies (Godfray et al., 2010; Qian et al., 2016). Extensive studies have demonstrated that salt stress usually causes ion toxicity (e.g., Na^+ and Cl^-), hyperosmotic stress, and secondary stress (e.g., oxidative damage; Zhu, 2002). Plants

have evolved various strategies to cope with salt stress, such as the accumulation of antioxidants, osmolytes, phytohormones, and salt-tolerant plant growth-promoting rhizobacteria (Singh et al., 2022; Sinha et al., 2022), which are involved in an intricate signaling network (Zhao et al., 2020). First, the signals are triggered by sodium ion sensing and a cytosolic Ca^{2+} concentration increase, which depend on salt stress signaling sensors, namely, glycosyl inositol phosphoryl ceramides, and diverse Ca^{2+}-dependent proteins (Jiang et al., 2019). Subsequently, the salt sensitivity signaling pathway is activated to exclude Na^+ and activate downstream salt stress-responsive genes (Yang and Guo, 2018). Recent studies on rice have shown that multiple ion transporters, such as *HIGH-AFFINITY* K^+ *TRANSPORTER 1* (*HKT1*) (Wei et al., 2021), *HKT4* (Wang et al., 2015), *HKT8* (Hauser and Horie, 2010), *HIGH-AFFINITY POTASSIUM* (K^+) *TRANSPORTER 1* (*OsHAK1*) (Chen et al., 2015), and *OsHAK21* (Shen et al., 2015), are involved in regulating the homeostasis of Na^+/K^+ and play a positive role in salt stress management.

Rice yield is determined by the number of effective tillers, number of grains per panicle, and grain weight. Moreover, the grain length, width, and thickness directly influence grain weight. In recent decades, numerous quantitative trait loci and genes that regulate grain size have been identified, such as *GRAIN WEIGHT 2* (Song et al., 2007), *BIG GRAIN 1* (Liu et al., 2015), *RICE SQUAMOSA PROMOTER-BINDING-LIKE 13* (Si et al., 2016), and *GRAIN SIZE and ABIOTIC STRESS TOLERANCE 1* (GSA1; Dong et al., 2020). Various studies indicated that the regulation of grain size is associated with multiple signaling factors, including phytohormones, protein kinases, and transcription factors (Zuo and Li, 2014; Li et al., 2019). Notably, brassinosteroid (BR) has been highlighted in connection with grain shape (Li et al., 2019), and mutants with *dwarf2* and *dwarf11* (involved in BR biosynthesis) displayed a typical BR-deficient phenotype and have small and short grains (Hong et al., 2005; Tanabe et al., 2005; Fang et al., 2016; Wu et al., 2016). The BRASSINOSTEROID UPREGULATED 1 (BU1), a putative helix–loop–helix (HLH) transcription factor, displays typical BR phenotypes and enlarged grains, and also functions as a brassinosteroid UPREGULATED-LIKE 1 (BUL1) and OsBC1 (Tanaka et al., 2009; Jang et al., 2017).

To date, although *EARLY FLOWERING 4a* (OsELF4a; Wang et al., 2021) and *PSEUDO-RESPONSE REGULATOR 73* (OsPRR73; Wei et al., 2021) were reported to positively regulate salt tolerance and grain yield by modulating downstream genes and related proteins, and *GSA1* positively regulates salt tolerance and grain size by modulating metabolic flux redirection (Dong et al., 2020), the synergistic regulatory network between abiotic stress and grain yield remains largely unknown (Dong et al., 2020).

Domains of unknown function 1644 (DUF1644) is a large group of proteins (Bateman et al., 2010). Although *OsSIDP366* and *OsSIDP361* have been reported to be involved in abiotic stress (Guo et al., 2016; Li et al., 2016), the coordinated regulatory network between salt tolerance and grain size remains unclear. In this study, to explore the function of *OsSIDP301*, which encodes a DUF1644 protein, we developed plants with gene overexpression (OE), gene silencing (RNA interference; RNAi), and gene knock-out. To better understand the role of *OsSIDP301* in plant growth and development, we screened for OsSIDP301 interacting proteins, and OsBC1, a basic HLH transcription factor, was identified. In addition, gene silencing plants of *OsBC1* also showed a smaller grain size in rice. Our findings revealed that *OsSIDP301* was involved in synergistic regulation of salt stress tolerance and grain size, and may have a direct application value in rice.

MATERIALS AND METHODS

Plant Materials and Trait Measurements

In this study, rice (japonica variety TaiPei309, TP309) plants were cultivated with an interplant spacing of 20 cm × 20 cm in the field at Xiamen University, Fujian Province, China, under natural growing conditions. The grain length, width, thickness, and 1,000-grain weight were measured using filled grains after maturation using a Vernier caliper. TP309 was used as the background for the genetic transformation and control of physiological experiments.

Generation of Transgenic Lines

OsSIDP301 was amplified from TP309 and cloned into the pCXUN-Flag (Chen et al., 2009) vector to generate the overexpression line p*Ubi*: *OsSIDP301* (*OsSIDP301*^{OE}). Knockdown and knockout plants were generated using RNAi technology and clustered regularly interspaced short palindromic repeats (CRISPR/Cas9) technology. *OsSIDP301* gene-specific RNA sequences and guide sequences were cloned into the pH7GWIWGII vector (*OsSIDP301*^{RNAi}) and pH-Ubi-cas9 vector (*OsSIDP301*^{cas9}). For the p*OsSIDP301*: glucuronidase (*GUS*) vector, a DNA fragment containing the *OsSIDP301* promoter was inserted into the pCXGUS-P vector (Chen et al., 2009). These constructs were introduced into TP309 *via Agrobacterium*-mediated transformation. The primers used are listed in **Supplementary Table 1**.

β-Glucuronidase Staining Analysis

To localize the transcripts of *OsSIDP301* in TP309 tissue, a 988-bp sequence upstream of the start codon was cloned into the pCXGUS-P vector, and the construct pro*OsSIDP301*:*GUS* was introduced into TP309 by *Agrobacterium tumefaciens* with the EHA105-mediated transformation method. The activity of GUS in transgenic plants was detected using a histochemistry assay, as previously described (Jefferson, 1987). The panicles and spikelets of different developmental stages were soaked in a staining solution (50 mM phosphate buffer saline at pH = 7.2, 2 mM potassium ferricyanide, 2 mM potassium ferrocyanide, 0.2% Triton-X-100, and 1 mg/ml X-Gluc) at 37 °C in an incubator with constant temperature. The materials were washed in 70% ethanol after 24 h and images were taken using a stereoscope.

Subcellular Localization of OsSIDP301

To investigate the subcellular localization of the OsSIDP301 protein, the coding sequence of *OsSIDP301* was fused with

a green fluorescent protein (GFP) cloned into the plasmid of pXDG (Chen et al., 2009) by using ligation-independent cloning technology. Then the constructs of pXDG-OsSIDP301, membrane localization maker (Scamp-mCherry), and nuclear localization maker (NLS-RFP) were co-expressed in tobacco leaves or rice protoplast. The GFP fluorescence signal was observed with a laser scanning confocal microscope (Zeiss LSM, Germany).

Stress Treatments

For phenotype analysis after germination growth, rice seeds of the WT and transgenic lines were sterilized with 70% ethanol for 1 min and then soaked in sodium hypochlorite solution [containing 0.8% (W/V) effective chlorine] for 20 min. After washing with sterile distilled water, the seeds were first germinated on standard 1/2 MS or selection solid medium (1/2 MS + hygromycin) and then transferred to 1/2 MS medium with or without NaCl (100 mM and 150 mM) or abscisic acid (ABA) (3 and 5 μM). After 1 week of growth in the incubator with a photoperiod of 12 h light (30 °C)/12 h dark (25 °C), the shoot length, root length, fresh weight, and dry weight were measured. Two-week-old seedlings grown on 1/2 MS medium were treated with liquid NaCl (150 mM) for 5 days and then recovered in 1/2 MS solution. Survival rates were counted after 7–30 days, and the criterion for death was the absence of the green shoots.

Physiology Parameter Characterization

The total chlorophyll content was detected following a previously described method (Zhou et al., 2018). Briefly, the leaf samples (100 mg) of 3-week-old seedlings were soaked and sealed in 4 ml of 95% (W/V) ethanol and then placed in an incubator at 37 °C in the dark for 2 weeks. The soaking liquid was centrifuged at 8,000 *g*, and the supernatant absorbance (*A*) was read at 665, 649, and 470 nm, respectively.

The malondialdehyde (MDA) content was measured following a previously described method (Du et al., 2018a). Briefly, the leaf samples (20 mg) of 3-week-old seedlings were homogenized in 5 ml of 10% (W/V) trichloroacetic acid and centrifuged at 2,000 *g* for 10 min at 4 °C. The supernatant was reacted with an equal volume 0.67% (W/V) thiobarbituric acid and then boiled for 15 min and centrifuged at 5,000 *g*. The *A* of the supernatant was read at 450, 532, and 600 nm, respectively.

The proline concentration was measured following a previously described method (Du et al., 2018b). Leaf samples (100–200 mg) of 3-week-old seedlings were soaked in 5 ml of 3% (W/V) sulfosalicylic acid in 10-ml tubes and boiled for 30 min, and then a reaction mixture was prepared using the supernatant, 2.5% (W/V) ninhydrin reagent, and glacial acetic acid in equal volume and boiled for 30 min. The reaction mixture was added to a double toluene solution of glacial acetic acid and reacted for 24 h. The *A* of the supernatant was read at 520 nm.

The Na^+ content was measured using the previously described method (Fang et al., 2018). Briefly, the leaves were oven-dried at 65 °C for 10 days, 100 mg samples were extracted in 20 ml of 1 M HCl at 25 °C, and the supernatant was filtered and diluted. Finally, Na^+ was quantified using flame atomic absorption spectrophotometry (FP6410).

The activity of antioxidant enzyme catalase (CAT) was determined based on the rate of decomposition of H_2O_2 as described protocols with the reagent test kit of Nanjing jiancheng (A007-1-1). The leaves (100 mg) were homogenized in 50 mM phosphate buffer sodium (pH = 7.8), centrifuged (1,000 *g*, 20 min, 4 °C), and then the supernatant was used for the analysis of CAT activity.

The diaminobenzidine (DAB) staining assays were performed as described previously (You et al., 2018).

RNA Isolation and Quantitative Real-Time PCR

Total RNA was extracted using an RNA extraction kit (Promega, Shanghai, China). Subsequently, RNA (2–4 μg) was reverse-transcribed into complementary DNA with a reverse transcription kit (Promega). Quantitative real-time PCR (RT-qPCR) was performed using gene-specific primers (**Supplementary Table 1**) and a detection system on a ROCHE LightCycler 96 instrument (Switzerland). Samples from the wild-type or unstressed wild-type tissue were selected as controls, the gene for *OsACTINI* was detected in parallel and used as an internal reference, and the data were analyzed using the comparative Ct method. Each experiment was performed in triplicates. The primers used are listed in **Supplementary Table 1**.

RNA-Seq

For Illumina sequencing, 2.5–3 cm panicle and 20-day-old leaves of TP309 were collected with three biological replicates and RNA was isolated for library preparation using Illumina sequencing by Novogene Bioinformatics Technology Co., Ltd., Beijing, China. RNA-seq reads were aligned to rice cultivar NP reference genome and gene information.[1]

Yeast Two-Hybrid Library

A Y187 yeast cDNA library of young seedlings was constructed using the pGADT7 vector (TaKaRa Bio, Dalian, China). The coding sequence of *OsSIDP301* was introduced into the pGBKT7 vector and transformed into Y2H-Gold yeast cells to screen the cDNA library. Library screening was performed using the mating method, according to TaKaRa Bio. Putative interaction proteins were characterized by sequencing the positive colonies. The coding region of the putative gene was cloned into PGADT7 and co-transformed with PGBKT7-OsSIDP301 to confirm the interaction in the Y2H-Gold strain. The positive control (PGBKT7-53 + PGADT7-T) was used as previously described by using the Y2H system. Primers used are listed in **Supplementary Table 1**.

Bimolecular Fluorescence Complementation Analysis

OsSIDP301 was cloned into the *Pac*I/*Asc*I restriction sites of the 2YN [pSAT6-n(1–174)EYFP-C1] and 2YC (pSAT6-cEYFP-C1-B vector) to generate constructs for the bimolecular fluorescence complementation (BiFC), respectively (Citovsky et al., 2006).

[1] https://rapdb.dna.affrc.go.jp/

For transient expression, *A. tumefaciens* strain Gv3101 carrying the combined constructs (*OsSIDP301*^{YC} + *OsSIDP301*^{YN}) was co-expressed with the P19 strains into leaves of 1-month-old *Nicotiana benthamiana*. The YFP fluorescence signal was examined using a Zeiss laser scanning confocal microscope at 48–72 h after infiltration. Primers used are listed in **Supplementary Table 1**.

Statistical Analysis

Each experiment contained three biological replicates. All data analyses were performed using GraphPad Prism version 7.0.0 for Windows (GraphPad Software, San Diego, CA, United States[2]). Statistical analysis was performed using IBM SPSS Statistics for Windows (version 25.0; IBM Corp., Armonk, NY, United States), and means were compared by computing unpaired Student's *t*-tests. Pairwise multiple parameter comparisons were made using Duncan's multiple range test to obtain the significance groups (Duncan, 1955).

RESULTS

Expression Analysis and Subcellular Localization of OsSIDP301

To investigate the expression pattern of *OsSIDP301*, real-time quantitative PCR (RT-qPCR) assay was performed. *OsSIDP301* was expressed in all tissues of rice, including sheath, leaf lamina joints, and panicle (**Figure 1A**). To further explore the expression pattern of *OsSIDP301* in more detail, transgenic plants harboring the β-glucuronidase (GUS) reporter were generated under the control of the *OsSIDP301* promoter, and GUS staining showed that *OsSIDP301* was highly expressed in stamen, pistil, and grain (**Figures 1B–H**). To analyze the protein subcellar localization of OsSIDP301, the GFP-OsSIDP301 fused protein was constructed and introduced into the *N. benthamiana* leaves and rice protoplasts. Confocal results showed that GFP signals can be co-localized with membrane localization signal (SCAMP1-mCherry) and nuclear localization signal (NLS-RFP) (**Figures 1I,J**). Therefore, OsSIDP301 was localized in both the cell membrane and nucleus.

[2]www.graphpad.com/

OsSIDP301 Knockdown Confers Salt Tolerance in Rice

DUF1644 members have been reported to play important roles in abiotic stress. For example, *OsSIDP366* and *OsSIDP361* are involved in salt and drought stress (Guo et al., 2016; Li et al., 2016). To determine whether *OsSIDP301* responds to abiotic stress, *OsSIDP301* was first detected in leaves treated with NaCl or ABA. *OsSIDP301* expression was induced by salt stress and ABA treatment (**Figures 2A,B**). Subsequently, RNAi technology was used to generate *OsSIDP301* knockdown transgenic lines (referred to as *OsSIDP301*^{RNAi}), and *OsSIDP301* was driven by a maize (*Zea mays*) *ubiquitin* promoter to obtain its overexpression lines (referred to as *OsSIDP301*^{OE}), both in the TP309 background. Two lines of each transgenic plant were selected for the study and their expressions were confirmed by RT-qPCR (**Figure 2C**).

Thereafter, salt-stress response analysis was performed during different growth periods. For the germination stage (**Figure 2D**), the seeds were germinated in 1/2 MS medium with or without NaCl for 7 days. There was no difference between the WT and *OsSIDP301* transgenic plants grown in 1/2 MS medium (**Figure 2E**). When treated with NaCl, although there was no obvious difference between the WT and *OsSIDP301*^{RNAi} plants, it was significantly decreased in the *OsSIDP301*^{OE} plants compared with the WT plants (**Figures 2F,G**). For the seedling stage (**Figure 2H**), the seeds of all plants were germinated in 1/2 MS medium and then transferred to the medium with or without NaCl for continuous 7 days of treatment. There was no substantial difference between the WT and *OsSIDP301* plants grown in 1/2 MS medium. However, *OsSIDP301*^{RNAi} lines showed higher salt tolerance, with shoot

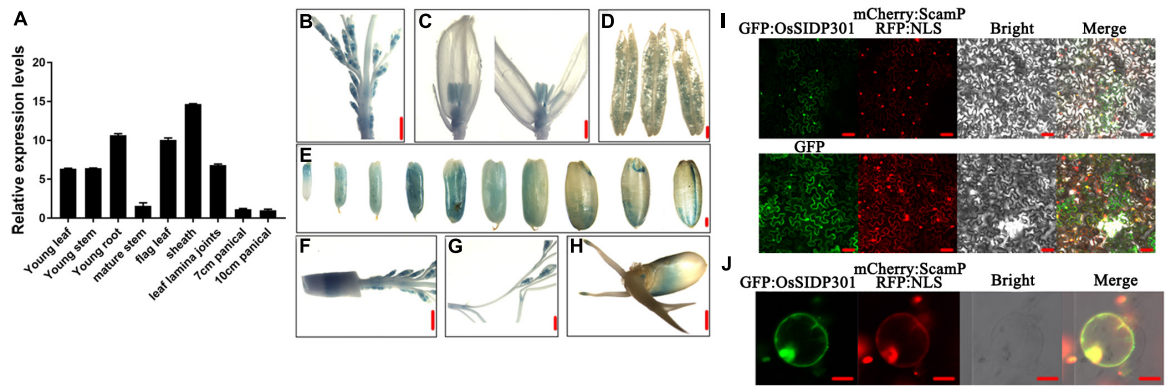

FIGURE 1 | Expression profiling and subcellular localization. **(A)** Transcript levels of *OsSIDP301* in various tissues. *OsACTIN1* was used normalized and data are shown as mean ± SD (*n* = 3). Promoter–GUS activity of *OsSIDP301* in young panicle **(B,F,G)**, pollen **(D)**, stigma **(C)**, seed maturation stage, **(E)** and germination stage **(H)**, bar = 1 mm **(B,C,E–H)**, bar = 10 μm **(D)**. Subcellular localization of OsSIDP301-GFP in *N. benthamiana* leaves **(I)**, bar = 50 μm and rice protoplast **(J)**, bar = 20 μm.

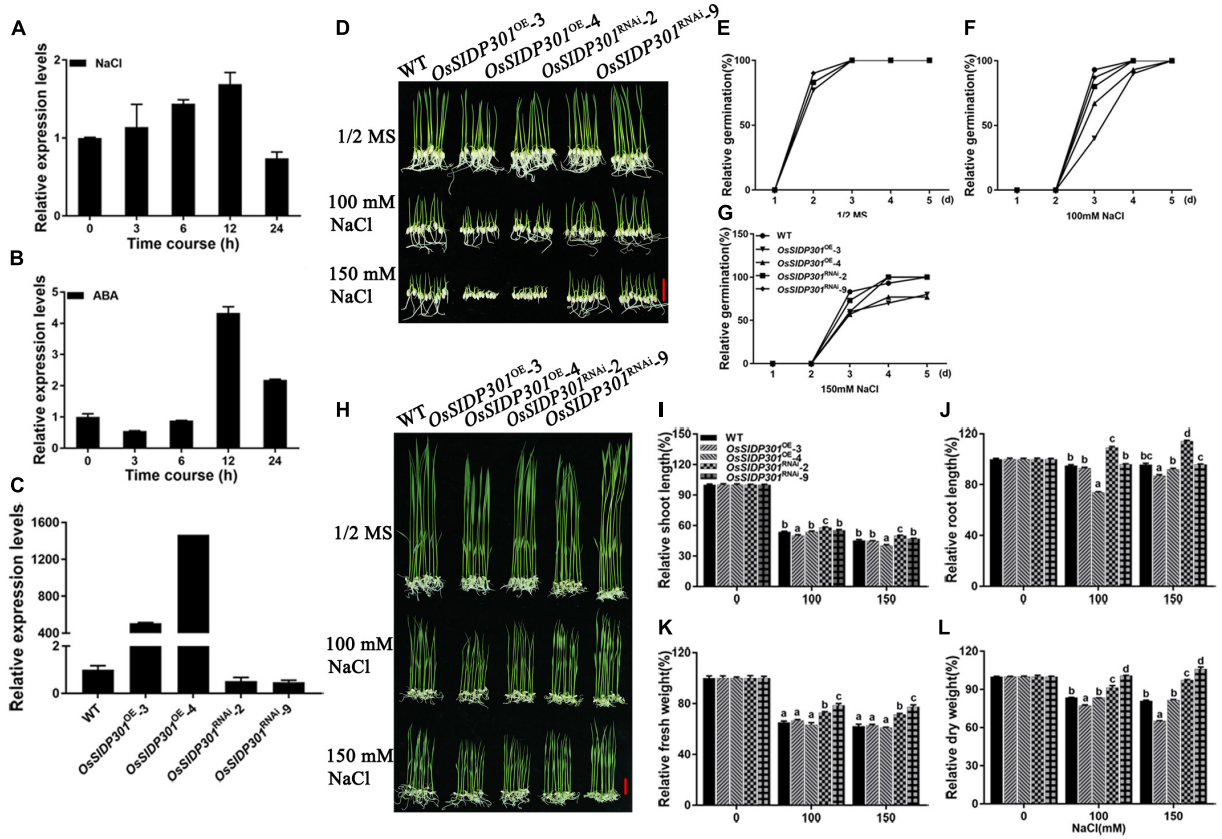

FIGURE 2 | Phenotype of *OsSIDP301* transgenic plants with NaCl treatment. Transcript levels of *OsSIDP301* were induced by 100 mM NaCl **(A)** and 100 μM ABA **(B)** in 3-week-old seedlings. **(C)** Relative expression levels of *OsSIDP301* between WT, *OsSIDP301*^{OE}, and *OsSIDP301*^{RNAi} plants. **(D)** Phenotype of *OsSIDP301* transgenic plants with NaCl treatment at germination stage, bar = 2 cm. Comparisons of germination rate between WT, *OsSIDP301*^{OE}, and *OsSIDP301*^{RNAi} plants under normal condition **(E)** and with NaCl treatment for 7 days **(F,G)**. **(H)** Phenotype of *OsSIDP301* transgenic plants with NaCl treatment at the seedling stage, bar = 2 cm. Comparisons of shoot length **(I)**, root length **(J)**, fresh weight **(K)**, and dry weight **(L)** between WT, *OsSIDP301*^{OE}, and *OsSIDP301*^{RNAi} plants with or without NaCl treatment for 7 days. Data are shown as mean ± SD (n = 8), different letters suggest significant difference at $P < 0.05$.

length (+4.29%, +4.96%), root length (+14.27%, +18.26%), fresh weight (+7.48%, +9.2%), and dry weight (+7.79%, +16.23%) remarkably higher than that of the WT with NaCl treatment (**Figures 2I–L**). In contrast, *OsSIDP301*^{OE} plants were more sensitive than WT plants, with shoot length (–3.54%, –0.67%), root length (–2.01%, –8.96%), fresh weight (–1.29%, –0.57%), and dry weight (–6.29%, –15.98%) dramatically reduced compared to WT plants (**Figures 2I–L**). In addition, 20-day-old WT and *OsSIDP301* plants were treated with 150 mM NaCl solution for 5 days and then re-watered for 20 days. As expected, compared with WT, the survival rate of *OsSIDP301*^{OE} lines was significantly decreased but was elevated in *OsSIDP301*^{RNAi} (**Figures 3A,B**). These results indicate that *OsSIDP301* may act as a negative regulator of salt stress in rice.

To further verify the salt tolerance phenotype, mutants were generated using the CRISPR/Cas9 genome-editing system. Two mutants of *OsSIDP301*, designated as *OsSIDP301*^{cas9}-2 and *OsSIDP301*^{cas9}-3, were chosen for further characterization (**Figure 4A**). The results showed that *OsSIDP301*^{cas9} plants displayed a similar tendency to *OsSIDP301*^{RNAi} lines when treated with NaCl. The 20-day-old *OsSIDP301*^{cas9} mutants were treated with 150 mM NaCl for 5 days and then re-watered for 7 days. Consequently, the survival rate of *OsSIDP301*^{cas9} lines was significantly increased compared with WT (**Figures 4B–E**). In addition, 3-day-old seedlings of the WT and *OsSIDP301*^{cas9} lines were grown with or without NaCl treatment for 7 days, respectively (**Figure 4F**). *OsSIDP301*^{cas9} lines showed higher salt tolerance than the corresponding WT, with an increase in shoot length, root length, and fresh weight (**Figures 4G–I**). In addition, there was also no significant difference at the germination stage between *OsSIDP301*^{cas9} and WT plants with or without NaCl treatment (**Supplementary Figures 1A–C**).

Knockdown of *OsSIDP301* Reduces the ROS Levels in Rice Under Salt Stress

To further verify the effect of *OsSIDP301*, physiological parameters (including the total chlorophyll content, malondialdehyde [MDA], proline content, and CAT activity) were measured. The total chlorophyll content, which represents the presence of chlorosis, was less downregulated in *OsSIDP301*^{RNAi} lines than that of WT, whereas it was severely

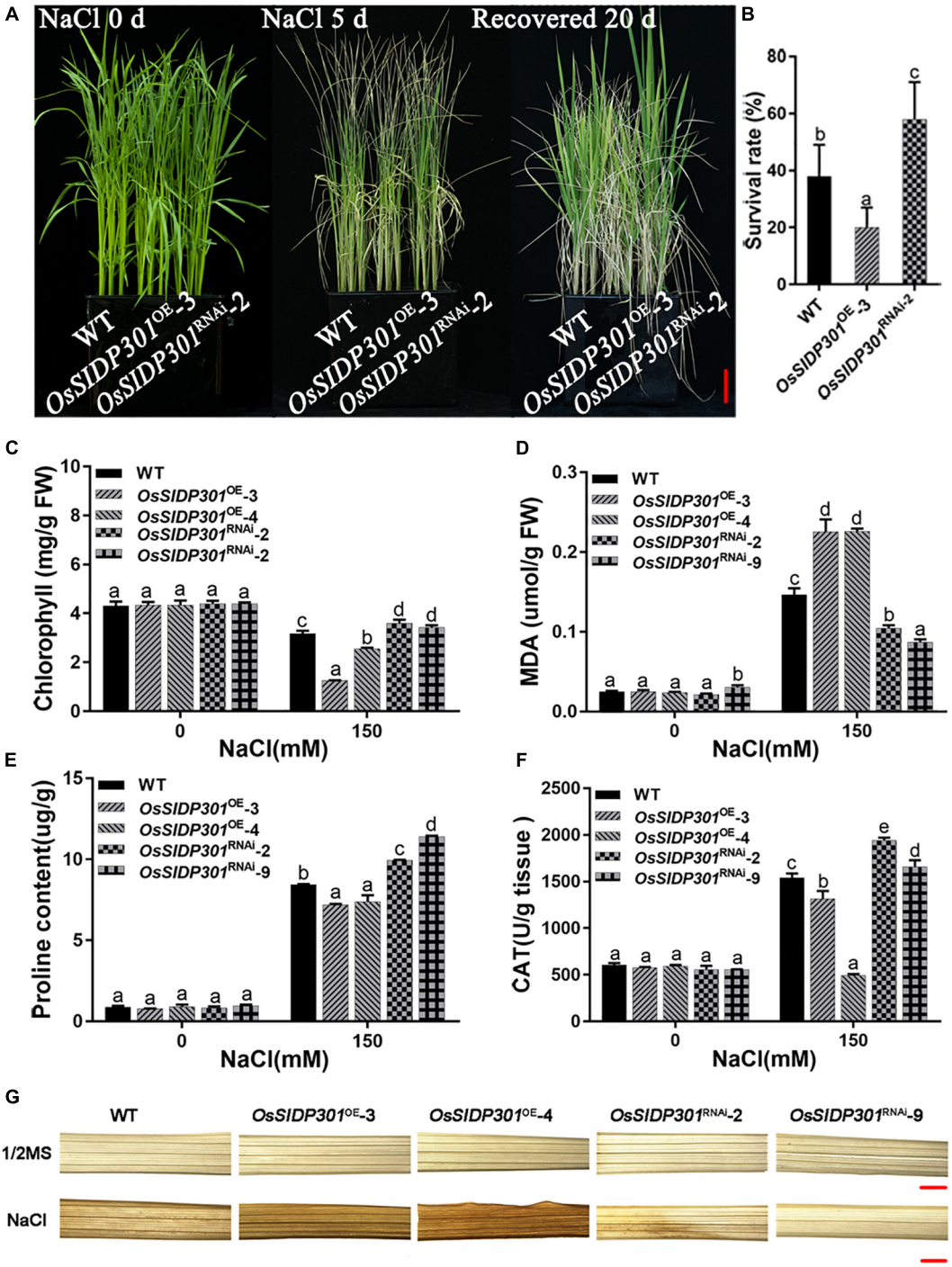

FIGURE 3 | Physiological changes in *OsSIDP301* transgenic plants. **(A)** Phenotype of *OsSIDP301* transgenic plants that were treated with 150 mM NaCl solution for 5 days and then recovered for 20 days, bar = 3 cm. **(B)** Survival rate of the panel **(A)**. **(C)** The chlorophyll content of 3-week-old plant leaves with or without 150 mM NaCl treatment. **(D)** The MDA content of 3-week-old plant leaves with or without 150 mM NaCl treatment. **(E)** The proline content of 3-week-old plant leaves with or without 150 mM NaCl treatment. **(F)** The CAT activity of 3-week-old plant leaves with or without 150 mM NaCl treatment. **(G)** The DAB staining of 3-week-old plant leaves with or without 150 mM NaCl treatment, bar = 1 mm. Data are shown as mean ± SD (n = 3), different letters suggested significant differences at $P < 0.05$.

decreased in *OsSIDP301*^{OE} lines compared with WT under saline conditions (**Figure 3C**). MDA, which induces lipid peroxidation and represents cell oxidative damage, was markedly higher in *OsSIDP301*^{OE} lines but lower in *OsSIDP301*^{RNAi} lines than in the WT plants under salt stress (**Figure 3D**). In addition, proline and CAT, which play an essential role in protecting cells against

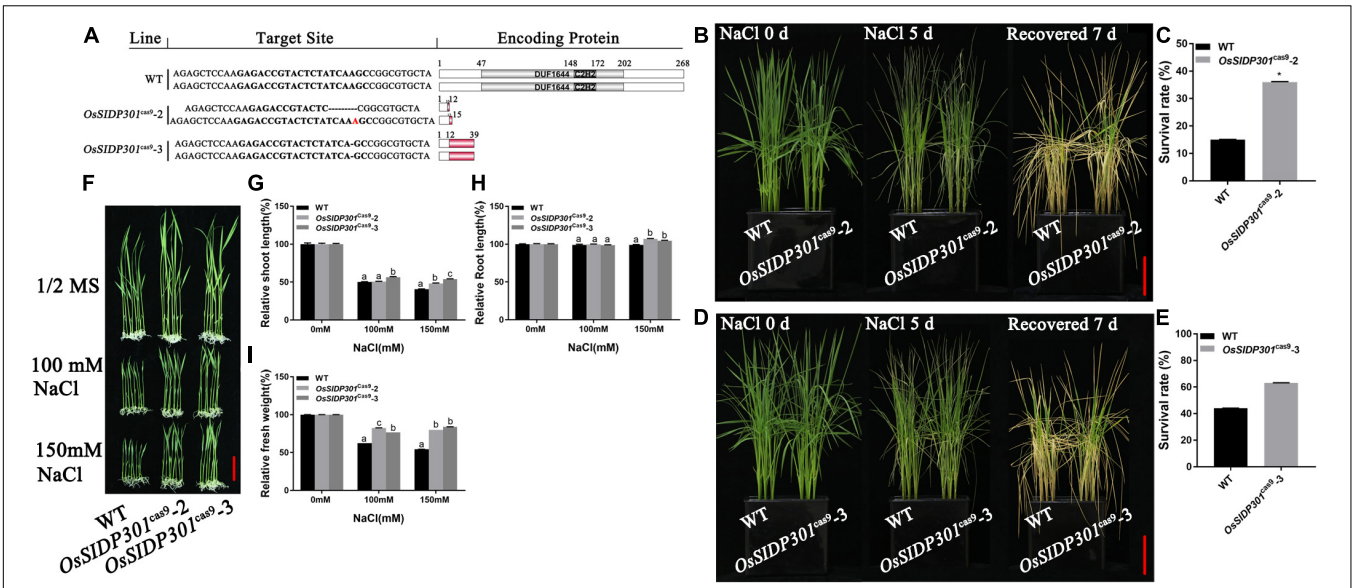

FIGURE 4 | Mutants of *OsSIDP301* were conferred salt tolerance. **(A)** Mutation types of *OsSIDP301* mutants. **(B–E)** Phenotype and survival rate of mutants were treated with containing 150 mM NaCl solution for 5 days and then recovered for 7 days, bar = 4 cm. **(F)** Phenotypes of mutants with NaCl treatment at the seedling stage, bar = 2 cm. Comparisons of shoot length **(G)**, root length **(H)**, fresh weight **(I)** between WT and mutants with or without NaCl treatment for 7 days. Data are shown as mean ± SD (n = 8), different letters suggested significant difference at $P < 0.05$.

oxidative stress caused by ROS, were increased in *OsSIDP301*^{RNAi} lines and decreased in *OsSIDP301*^{OE} lines compared to that of WT plants with salt treatment (**Figures 3E,F**). Moreover, 3,3′-diaminobenzidine (DAB) staining assay was used to determine the H_2O_2 content, which reflects the ROS levels. In comparison with WT leaves, *OsSIDP301*^{OE} leaves showed stronger staining, whereas only weak staining was observed in *OsSIDP301*^{RNAi} lines (**Figure 3G**). Taken together, these results suggested that *OsSIDP301* is crucial for maintaining cellular redox homeostasis.

Knockdown of *OsSIDP301* Reduces the Na^+ Content in Rice Under Salt Stress

To examine whether the reduced growth and biomass of *OsSIDP301*^{OE} plants were also caused by osmotic stress, 3-day-old seedlings were planted with 0, 120, or 150 mM mannitol. Interestingly, there were no significant differences in *OsSIDP301* compared to the WT (**Supplementary Figures 1D,E**), indicating that ion toxicity rather than osmotic stress was the reason why *OsSIDP301*^{OE} plants exhibited reduced tolerance to salt stress. Subsequently, the Na^+ content of the leaves of 4-week-old seedlings was measured in seedlings grown with and without NaCl treatment (**Figures 5A,B**). The results showed that Na^+ content was significantly higher in the *OsSIDP301*^{OE} plants than in the WT plants, whereas it decreased in the *OsSIDP301*^{RNAi} plants with NaCl treatment. These data suggest that the enhanced salt tolerance in the *OsSIDP301*^{RNAi} lines may be due to reduced Na^+ accumulation.

Additionally, we detected the expressions of salt ion transporters *OsHKT1;1* (Wang et al., 2015), *OsHAK21* (Shen et al., 2015), *OsHAK22* (He et al., 2019), and salt-response genes, including *Δ′-PYRROLINE-5-CARBOXYLATE SYNTHETASE* (P5CS; Zhang et al., 1995) and *9-CIS-EPOXYCAROTENOID DIOXYGENASE 1* (OsNCED1; Liu, 2017), which have been reported to positively regulate salt stress. *ABA INSENSITIVE 5* (*ABI5*) has been reported to negatively modulate salt stress (Zou et al., 2008). Our results showed that the expression levels of *OsHKT1;1*, *OsHAK21*, *OsHAK22*, *OsP5CS*, and *OsNCED1* were decreased, while *OsABI5* transcript was increased in *OsSIDP301*^{OE} plants (**Figures 5C–H**). However, an opposite trend was observed in *OsSIDP301*^{RNAi} plants. Taken together, these results demonstrate that *OsSIDP301* may enhance salt sensitivity by influencing the Na^+ content and salt-response genes in rice.

Transcriptome Analysis of *OsSIDP301*^{OE} and *OsSIDP301*^{RNAi} Plants

To elucidate the molecular mechanism of *OsSIDP301*, transcriptome deep sequencing (RNA-seq) was performed in the leaves of salt-stressed 3-week-old plants. With the threshold of significantly differentially expressed genes (DEGs) set at $\log_2$ (fold change) > 1 or $\log_2$ (fold change) < -1 and adjusted to $P < 0.05$, 4,002 DEGs (1,796 upregulated and 2,206 downregulated) were identified in *OsSIDP301*^{RNAi} compared with WT, and 2,951 DEGs (1,321 upregulated and 1,630 downregulated) in *OsSIDP301*^{OE} compared with WT under salt stress (**Supplementary Figures 2A,B**). We also identified that 255 DEGs were downregulated in *OsSIDP301*^{OE} and upregulated in *OsSIDP301*^{RNAi} plants, and 236 DEGs were upregulated in *OsSIDP301*^{OE} and downregulated in *OsSIDP301*^{RNAi} plants (**Figure 6A**). Gene Ontology (GO) enrichment analysis on these 491 DEGs revealed that genes were related to stress responses, and the GO term with the

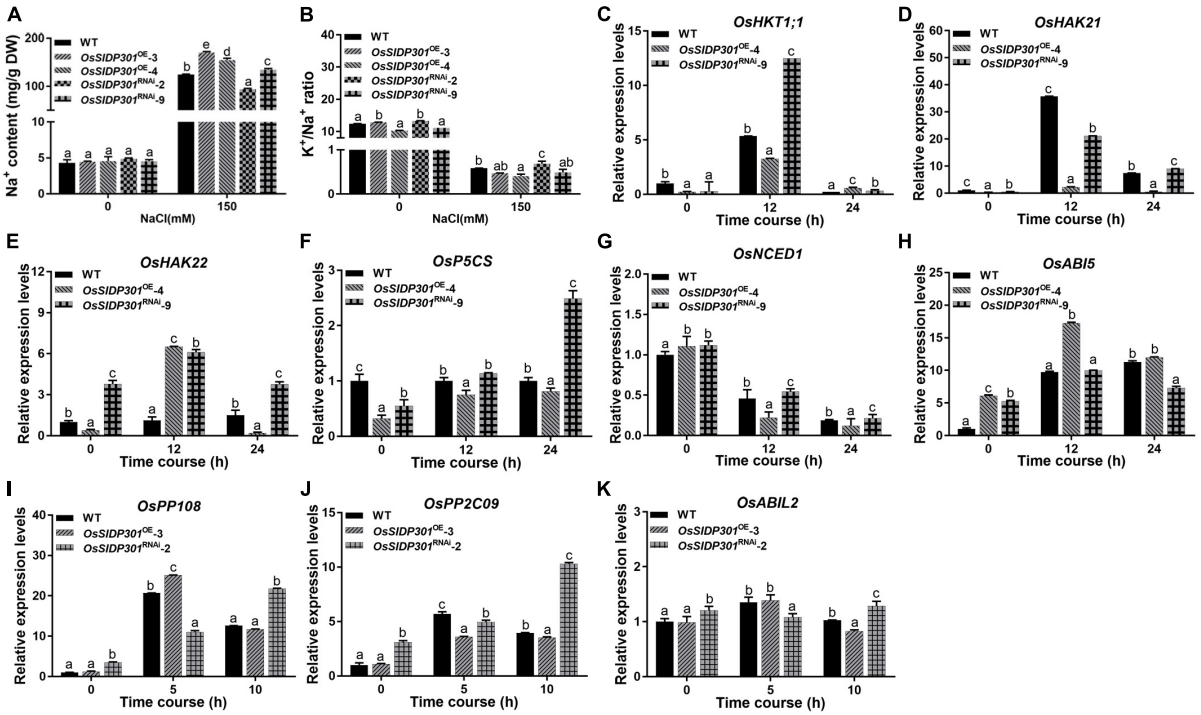

FIGURE 5 | The expression levels of salt stress and ABA-related genes. The Na^+ content **(A)** and K^+/Na^+ ratio **(B)** of 3-week-old plant leave with or without 150 mM NaCl treatment. **(C–H)** The expression level analysis of ion transporter *OsHKT1;1*, *OsHAK21*, *OsHAK22*, and salt-response genes *OsNCED1*, *OsP5CS*, and *OsABI5* with or without 150 mM NaCl treatment by using 2-week-old seedlings. **(I–K)** The expression level analysis of ABA signaling regulators *OsPP108*, *OsPP2C09*, and *OsABIL2* with 100 μM ABA treatment by using 2-week-old seedlings. Data are shown as mean ± SD ($n = 3$), different letters suggested significant differences at $P < 0.05$.

DEGs included "response to stress (heat, oxidative, antibiotic, etc.)," "protein folding," "metabolic process," and "catabolic process" (**Figure 6B**). Then, the Kyoto Encyclopedia of Genes and Genomes (KEGG) enrichment analysis showed that these DEGs were enriched in the "biosynthesis and metabolism" pathway that may be conducive to salt tolerance (**Figure 6C**). These salt-related DEGs encode diverse proteins, such as transcription factors (e.g., *Os05g0322900*, *Os02g0649300*), receptor-like kinases (e.g., *Os02g0822900*, *Os11g0168600*), antioxidant enzymes (e.g., *Os01g0963000*, *Os02g0115700*), and ion transporters (e.g., *Os04g0445000*, *Os01g0930400*) (**Figure 6D**).

As shown in **Supplementary Figure 2**, several representative genes from RNA-seq data were selected for confirmation using RT-qPCR. For example, *K^+-efflux channels stelar K^+ outward rectifier* was significantly upregulated in *OsSIDP301*^{OE} and downregulated in *OsSIDP301*^{RNAi} plants, but sodium transporter *OsHKT3*, Na^+–K^+ co-transport *OsHKT9*, and potassium transporters *OsHAK5* and *OsHAK17* were considerably upregulated in *OsSIDP301*^{RNAi} plants, whereas the opposite results were observed in *OsSIDP301*^{OE} plants. The salt-related positive regulators, such as *RECEPTOR-LIKE CYTOPLASMIC KINASE 311*, *WRKY TRANSCRIPTION FACTOR 45*, and *C2 DOMAIN-CONTAINING PROTEIN* were significantly upregulated in *OsSIDP301*^{RNAi} plants. However, the salt-related negative regulators, such as *HOMEOBOX-LEUCINE ZIPPER PROTEIN HOX24*, *HEAT STRESS TRANSCRIPTION FACTOR B2b*, *PLASMA MEMBRANE PROTEIN 1*, and *MEDIATOR 37_1* were significantly upregulated in *OsSIDP301*^{OE} plants. These results were consistent with RNA-seq data and the role of *OsSIDP301* in salt-tolerance signaling, revealing that *OsSIDP301* acts as a negative regulator of salt stress.

OsSIDP301 Positively Regulates Abscisic Acid Signaling

As the expression of *OsSIDP301* was induced by ABA treatment, we hypothesized that *OsSIDP301* is associated with ABA signaling. To confirm this, the ABA sensitivity of *OsSIDP301* transgenic plants was first examined at the germination stage at different ABA concentrations (**Figure 7A**). The germination rate of *OsSIDP301*^{OE} lines was significantly lower than that of WT at 3 and 5 μM ABA treatments, whereas *OsSIDP301*^{RNAi} lines showed opposite results (**Figures 7B–D**). There were no significant differences between the transgenic and WT plants under normal conditions. For the seedling stage (**Figure 7E**), with different concentrations (3 and 5 μM) of ABA treatment for 7 days, the *OsSIDP301*^{OE} lines exhibited a severe decrease in shoot length (–15.1%, –11.9%), root length (–70.5%, –54.9%), fresh weight (–27.03%, –7.8%), and dry weight (–28.4%, –21.7%) compared with WT. In contrast, *OsSIDP301*^{RNAi} lines showed an obvious increase in shoot length (+0.9%,

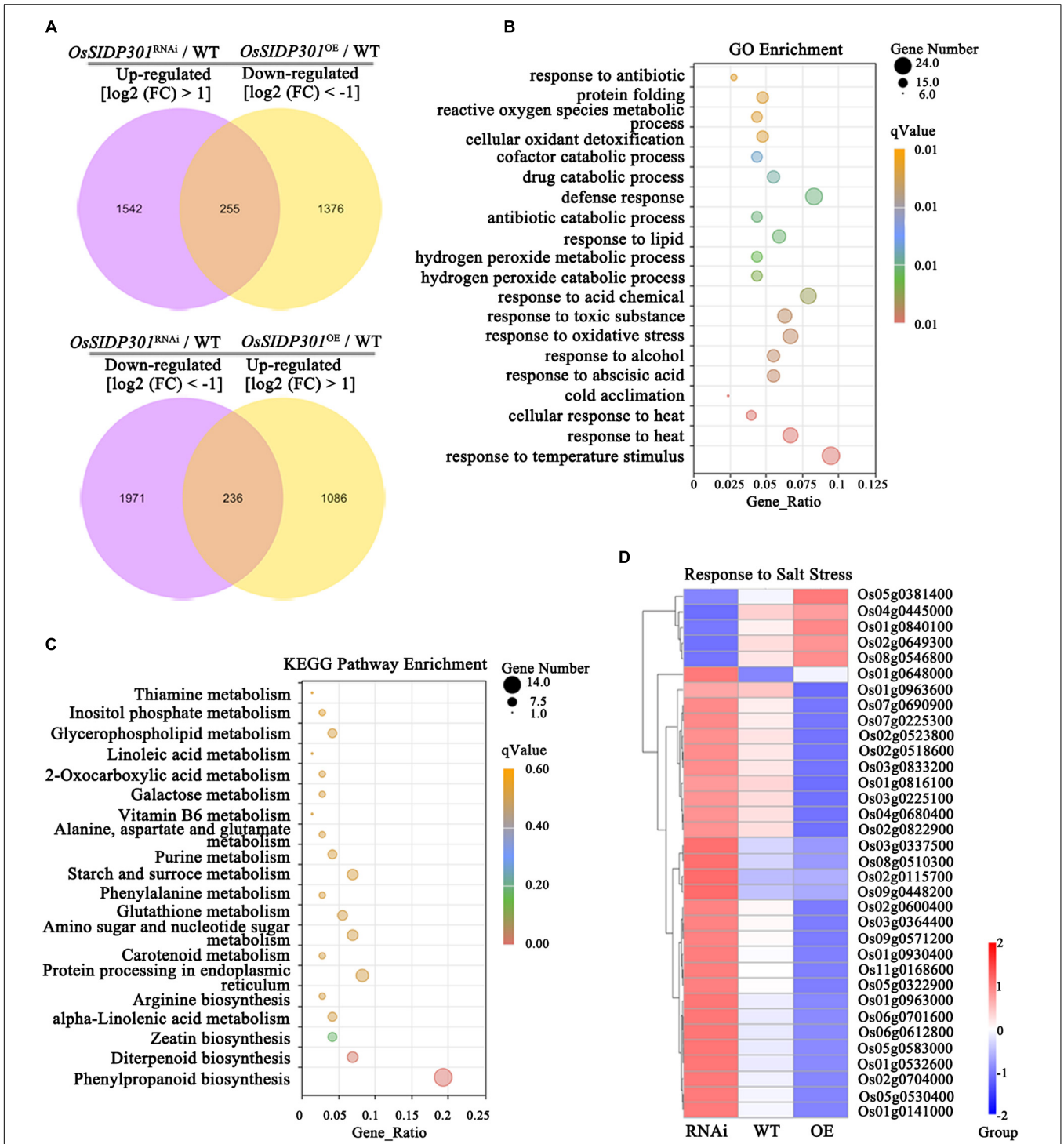

FIGURE 6 | Transcriptome analysis of *OsSIDP301* transgenic plants. **(A)** Venn diagrams for the upregulated in *OsSIDP301*^{RNAi} and downregulated in *OsSIDP301*^{OE} DEGs, and downregulated in *OsSIDP301*^{RNAi} and upregulated in *OsSIDP301*^{OE} DEGs with NaCl treatment. **(B)** Gene Ontology (GO) enrichment analysis of the **(A)** DEGs. **(C)** Kyoto Encyclopedia of Genes and Genomes (KEGG) enrichment analysis of the **(A)** DEGs. **(D)** Heatmaps showing the partially representative salt-related gene expression patterns between WT and transgenic plants under salt stress.

+2.8%), root length (+4.4%, +37.4%), fresh weight (+9.28%, +2.06%), and dry weight (+2.2%, +5.7%) after ABA treatment (**Figures 7F–I**).

In addition, we examined the expression of ABA signaling-related genes, including *PROTEIN PHOSPHATASE 2C 09* (*OsPP2C09*) (Miao et al., 2020), *PROTEIN PHOSPHATASE 108*

(*OsPP108*) (Singh et al., 2015), and *OsABI-LIKE2* (*OsABIL2*) (Li et al., 2015), which negatively regulate ABA signaling. Their expression levels were upregulated in *OsSIDP301*^{RNAi}, whereas slightly downregulated in *OsSIDP301*^{OE} lines compared to WT plants treated with 100 μM ABA (**Figures 5I–K**). Taken together, these results suggest that *OsSIDP301* plays a positive role in the ABA signaling pathway and participates in the ABA-mediated complex abiotic stress signal transduction pathway.

OsSIDP301 Negatively Regulates Grain Size

Since GUS staining showed that *OsSIDP301* was highly expressed in grains, it would be worthwhile to investigate whether *OsSIDP301* can function in grain development. As expected, the homozygous *OsSIDP301*^{RNAi} lines markedly increased in grain length (+1.13%, +3.8%), grain width (+2.8%, +5%), and 1,000-grain weight (+2.4%, +3.7%) (**Figures 8A–D,F** and **Supplementary Figures 3A–E**). Moreover, the number of secondary branches in the *OsSIDP301*^{RNAi} plants' panicle increased compared to the WT (**Supplementary Figures 3K,N**). However, the homozygous *OsSIDP301*^{OE} lines showed opposite phenotypes. *OsSIDP301*^{OE} plants displayed decreased grain length (–2.96%, –4.5%), grain width (–3.1%, –5%), and 1,000-grain weight (–6%, –11.7%) (**Figures 8A–D,F** and **Supplementary Figures 3A–E**). Additionally, panicle length and the number of secondary branches in *OsSIDP301*^{OE} lines were significantly decreased than those in the WT plants (**Supplementary Figures 3K–N**). Furthermore, our results showed that the mutants displayed a significant increase in grain length (+3.8%, +3.9%), grain width (+2.5%, +2.2%), and 1,000-grain weight (+3.3%, +7.4%) compared to the WT (**Figures 8C,D,F**), but no obvious changes in grain thickness and panicle length were observed (**Figure 8E** and **Supplementary Figures 3F–N**). Together, these results indicate that *OsSIDP301* negatively regulates grain size and weight.

OsSIDP301 Regulates Grain Size by Promoting Cell Expansion

Cell proliferation and expansion are major factors that influence grain development. As the grain length of *OsSIDP301*^{cas9} mutants and *OsSIDP301*^{RNAi} plants increased, scanning electron microscopy (SEM) and paraffin section assays were used to observe the cells in spikelet hulls (**Figure 8G** and **Supplementary Figures 4A,B**). Compared with those of the WT, the epidermal cells of the glume were smaller in *OsSIDP301*^{OE} lines and enlarged in *OsSIDP301*^{RNAi} lines (**Supplementary Figure 4B**). Moreover, SEM results showed that the cell length of the glume was significantly increased in *OsSIDP301*^{RNAi} and *OsSIDP301*^{cas9} lines compared to the WT, but no significant difference in cell width was observed between *OsSIDP301*^{cas9} mutants and WT (**Figures 8H,I**). However, the cell length and width of the glume were significantly decreased in *OsSIDP301*^{OE} lines than those in WT. These results suggest that *OsSIDP301* negatively regulates grain size by influencing cell expansion.

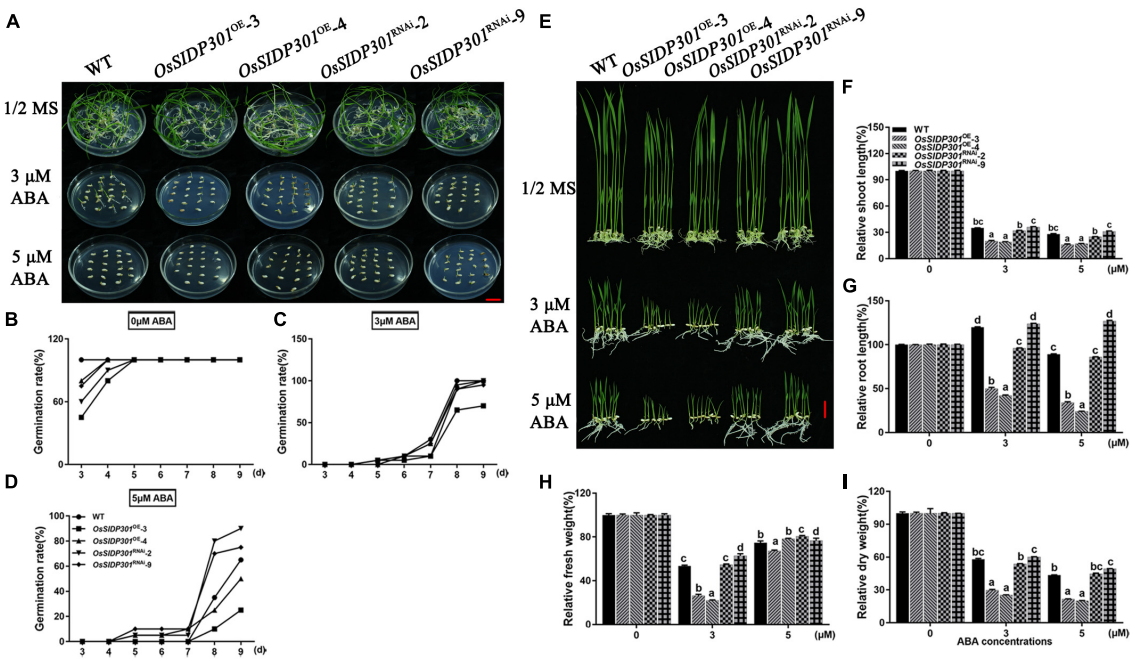

FIGURE 7 | Phenotype of *OsSIDP301* transgenic plants with ABA treatment. **(A)** Phenotype of *OsSIDP301* transgenic plants with ABA treatment at germination stage, bar = 2 cm. Comparisons germination rate between WT, *OsSIDP301*^{OE}, and *OsSIDP301*^{RNAi} plants with **(C,D)** or without ABA treatment **(B)**. **(E)** Phenotype of *OsSIDP301* transgenic plants with ABA treatment at the seedling stage, bar = 2 cm. Comparisons of shoot length **(F)**, root length **(G)**, fresh weight **(H)**, and dry weight **(I)** between WT, *OsSIDP301*^{OE}, and *OsSIDP301*^{RNAi} plants with or without ABA treatment for 7 days. Data are shown as mean ± SD (n = 8), different letters suggested significant differences at $P < 0.05$.

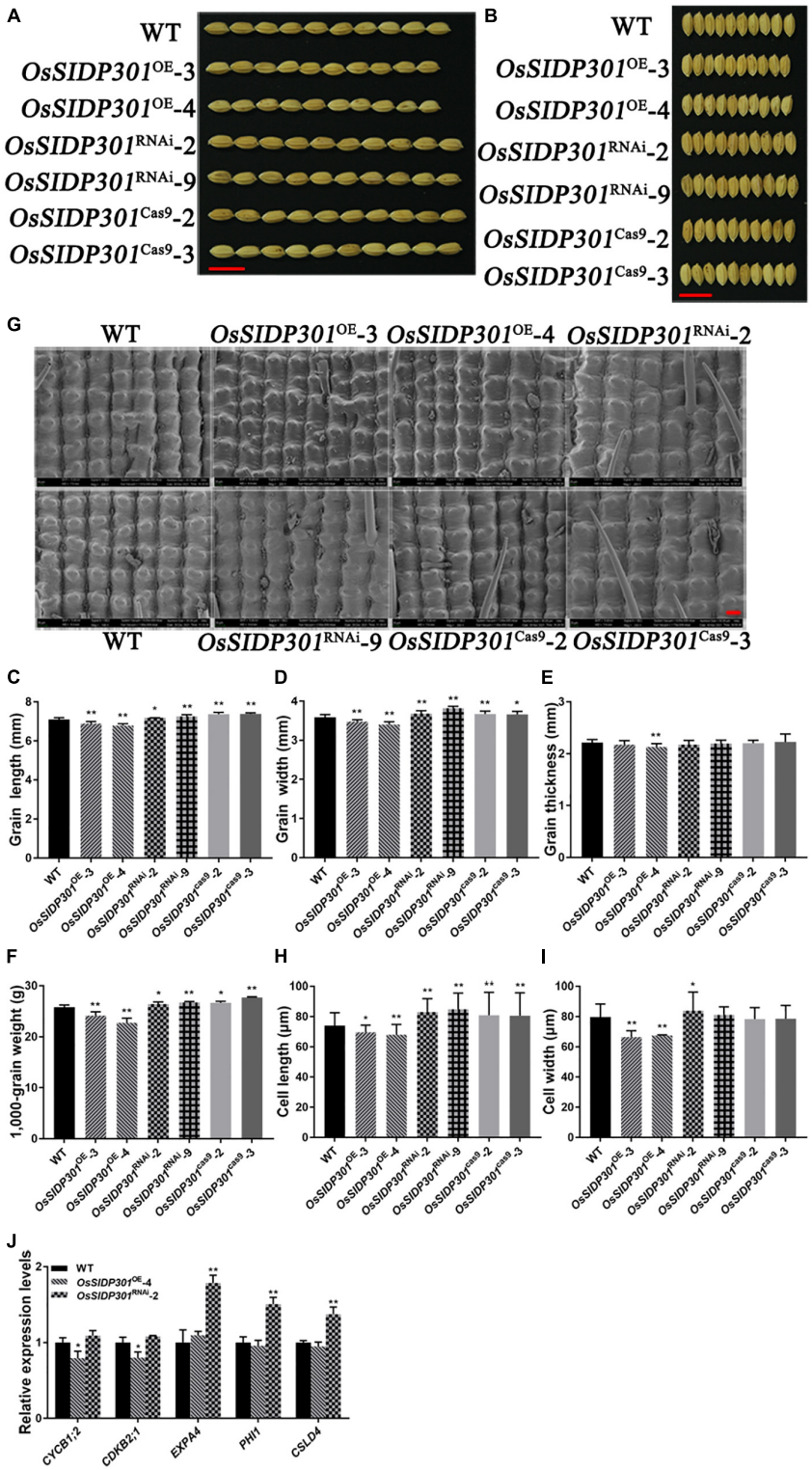

FIGURE 8 | *OsSIDP301* regulates grain length and grain width. Morphology of grain length **(A)** and grain width **(B)** in WT, *OsSIDP301*^{OE}, *OsSIDP301*^{RNAi} lines, and mutants, bar = 1 cm. Comparisons of grain length **(C)**, grain width **(D)**, grain thickness **(E)**, and 1,000-grain weight **(F)** between WT, *OsSIDP301*^{OE}, *OsSIDP301*^{RNAi}, and mutants (n = 100). **(G)** Scanning electron micrographs of the local outer surfaces of glumes in WT, *OsSIDP301*^{OE}, *OsSIDP301*^{RNAi}, and mutants, bar = 40 μm. Comparisons cell length **(H)** and cell width **(I)** between WT, *OsSIDP301*^{OE}, *OsSIDP301*^{RNAi}, and mutants on the surfaces of glumes. **(J)** Relative expression levels of cell cycle-related and cell expansion-related genes from RNA-seq analysis in WT and transgenic lines. Data are shown as mean ± SD (n = 3), Student's t-test was used, $^{*}P < 0.05$, $^{**}P < 0.01$.

To explore the possible molecular pathway of *OsSIDP301* in the regulation of seed development, RNA-seq was performed in the young panicle of WT and *OsSIDP301* lines. A total of 514 differentially expressed genes (DEGs) were identified (**Supplementary Figure 4C**). GO enrichment and KEGG analysis showed that these DEGs were involved in biosynthesis and metabolism pathways (**Supplementary Figures 4D,E**). Among them, cell-expansion related genes, including *ALPHA-EXPANSIN 4* (*EXPA4*) (Choi et al., 2003), *PHOSPHATE-INDUCED PROTEIN 1* (Aya et al., 2014), and the cell-cycle related gene *CELLULOSE SYNTHASE-LIKE* (Yoshikawa et al., 2013), were significantly upregulated in *OsSIDP301*^{RNAi} lines compared to that in WT and *OsSIDP301*^{OE} plants (**Figure 8J**), indicating that the increased cell size in *OsSIDP301*^{RNAi} may result from the upregulated expression of genes that promote cell expansion. Taken together, these results indicate that *OsSIDP301* negatively regulates grain size by altering glume cell expansion.

OsSIDP301 Interacts With OsBC1

A yeast two-hybrid assay (Y2H) was used to screen for OsSIDP301-interacting proteins, with the OsSIDP301 protein used as a bait. *OsBC1*, which encodes a basic helix–loop–helix transcription activator and has been reported to positively regulate grain size (Jang et al., 2017), was identified as one of the interactive proteins (**Figure 9A**). Overexpression of *BC1* increases the grain size by promoting the expression of cell expansion-related genes, including *ALPHA-EXPANSIN 1* (*EXPA1*), *ALPHA-EXPANSIN 2* (*EXPA2*), *ALPHA-EXPANSIN 3* (*EXPA3*), and *EXPA4* (Tanaka et al., 2009, Jang et al., 2017). In addition, we observed that OsSIDP301 could interact with itself, suggesting that OsSIDP301 might exert its function by forming dimers (**Figure 9A**). Subsequently, we cloned three types of truncations of full-length *OsSIDP301* based on the DUF1644 domain, including OsSIDP301N, OsSIDP301DUF, and OsSIDP301C, as shown in **Figure 9B**. The Y2H results showed that all truncations of OsSIDP301 could interact with OsBC1 and OsSIDP301, respectively (**Figures 9C,D**). BiFC assays were performed to further confirm the interaction between OsSIDP301 and OsBC1 *in vivo*. OsSIDP301 and OsBC1 were fused to the N-terminal (nYFP) and C-terminal (cYFP) of YFP, respectively. Confocal microscopy showed strong YFP fluorescence in the nucleus of *N. benthamiana* cells with OsBC1-cYFP and OsSIDP301-nYFP, OsSIDP301-cYFP and OsBC1-nYFP, or OsSIDP301-cYFP and OsSIDP301-nYFP, but not in the negative controls (**Figure 9E**). Taken together, these results indicate that OsSIDP301 could interact with OsBC1 and form homo-dimers in rice.

DISCUSSION

Several studies have reported that the DUF640 family is involved in grain development in rice (Li et al., 2012; Yan et al., 2013); the

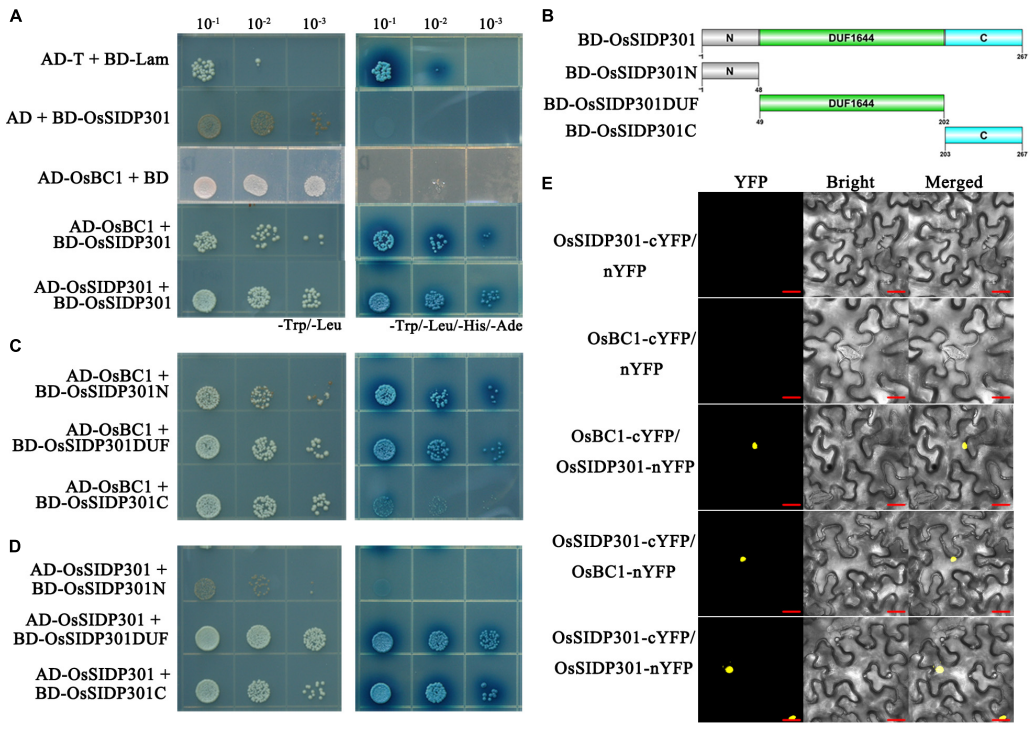

FIGURE 9 | OsSIDP301 interacts with OsBC1. Yeast two-hybrid assay demonstrated the OsSIDP301 interacts with OsBC1 **(C)** and itself **(D)** by the full length **(A)**, N terminal, the DUF1644 domain, and the C terminal of OsSIDP301, respectively. **(B)** The protein truncation sites of OsSIDP301. **(E)** BiFC assay demonstrated the OsSIDP301 interacts with OsBC1 *in vivo*, the YFP fluorescence signals located in nuclear of *N. benthamiana* leaves, bar = 20 μm.

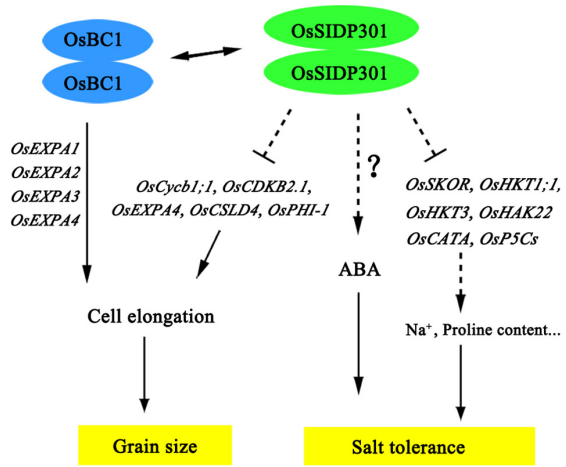

FIGURE 10 | The proposed working model of *OsSIDP301* regulates salt tolerance and grain size. The dotted lines indicated indirect regulation, the two-way arrows indicate interaction of protein, and the solid lines indicate direct regulation.

DUF966 family has been shown to respond to abiotic stress in rice (Luo et al., 2014); and the DUF1644 family is responsible for abiotic stress in rice and affects crop yield in maize (Guo et al., 2016; Li et al., 2016; Chen et al., 2022). The DUF1644 family is a plant-specific protein, and there are nine DUF1644 homologous genes in rice, while the functions of only two members have been identified and that of the others are still unclear. In this study, we provide evidence that the DUF1644 protein OsSIDP301 negatively regulates grain size and salt tolerance in rice.

OsSIDP301 Negatively Regulates Salt Tolerance

The major staple crops for eating are glycophytes, which are unable to complete their life cycle when salt concentrations in soil exceed 200 mM compared to halophytes (Munns and Tester, 2008; Flowers et al., 2015). Therefore, improving abiotic tolerance is essential for global food security and productivity. *OsSIDP361* and *OsSIDP366*, which encode the DUF1644 proteins with a conserved DUF1644 domain and zinc finger domain, respectively, have been reported to be associated with abiotic stress (Guo et al., 2016; Li et al., 2016). In this study, the overexpression of *OsSIDP301* was observed in response to salt stress (**Figure 2A**). Moreover, salt stress simulation at the germination and seedling stages showed that *OsSIDP301* might have a negative effect on salt tolerance (**Figures 2**, **3**, **4**). These results suggested that *OsSIDP301* plays an important role in abiotic stress tolerance. Previous studies have shown that salt stress induces the accumulation of MDA, proline, ROS, and Na^+, as well as high activities of superoxide dismutase, peroxidase, and CAT, leading to disruption of cellular homeostasis and threatening plant development (Zhang et al., 2013; Kaur and Asthir, 2015; Liang et al., 2018). In this study, proline content was decreased in *OsSIDP301*^{OE} lines, whereas MDA content was increased with NaCl treatment; DAB staining also suggested that H_2O_2 content in *OsSIDP301*^{OE} lines was higher than that of the WT, which was consistent with inhibited CAT activity (**Figure 3**); and *OsSIDP301*^{OE} plants had a higher level of Na^+ content when compared with WT under NaCl treatment (**Figure 5A**). The HKT, HAK, and AKT family members and salt-response genes have been reported to be related to the K^+/Na^+ balance in cells. For example, *OsHKT1;1* (*HKT4*) encodes a high-affinity potassium transporter that plays an essential role in controlling Na^+ content and inhibiting Na^+ toxicity in leaves, leading to enhanced salt tolerance in rice (Wang et al., 2015); *OsHAK21* encodes a potassium transporter and its mutants exhibit hypersensitivity to salt stress (He et al., 2019); and *OsABI5* encodes a bZIP transcription factor that negatively regulates salt tolerance *via* an ABA-dependent pathway (Zou et al., 2008). In this study, the expressions of *OsHKT1;1*, *OsHAK21*, *OsHAK22*, *OsABI5*, and *OsNCED1* were consistent with salt tolerance of *OsSIDP301* with NaCl treatment (**Figures 5C–G**). *P5Cs* has been reported to participate in proline biosynthesis (Zhang et al., 1995), and the overexpression of *P5Cs* in *OsSIDP301*^{RNAi} plants (**Figure 5H**) was consistent with higher proline content compared to WT (**Figure 3E**). In addition, RNA-seq data and RT-qPCR results confirmed that many positive factors were upregulated in *OsSIDP301*^{RNAi} plants (**Figure 6** and **Supplementary Figure 2**), suggesting that *OsSIDP301* is involved in salt tolerance by regulating salt-related gene expression. Put together, these findings reveal that *OsSIDP301* negatively regulates salt tolerance by changing physiological parameters and participating in abiotic stress signaling pathways in rice.

OsSIDP301 Responds to Abscisic Acid Signaling

Abiotic stress-resistance systems are complex networks that include signal transduction, phytohormones, and functional gene regulation. ABA has been widely reported to respond to abiotic stress (Zhu, 2002). In this study, an obvious hypersensitive phenotype to ABA treatment was exhibited in *OsSIDP301*^{OE} plants at the seed germination and seedling growth stages (**Figure 7**), which was contrary to previous results on the relationship between ABA and stress resistance. However, *Oshox22* (Zhang et al., 2012), *bZIP TRANSCRIPTION FACTOR 05* (Tong et al., 2021), *OsABI5* (Zou et al., 2008), and *SlbZIP38* (Pan et al., 2017) have been found to negatively regulate salt or drought stress, but positively regulate ABA responses. In addition, *WRKY GENE 20* (Luo et al., 2013) and *OsbZIP71* (Liu et al., 2014) have been reported to positively regulate abiotic stress, but negatively regulate ABA responses. In this study, the overexpression of negative regulators in ABA signaling were observed in *OsSIDP301*^{RNAi} lines with ABA treatment, including *OsPP2C09* (Miao et al., 2020), *OsPP108* (Singh et al., 2015), and *OsABIL2* (Li et al., 2015). These results demonstrated that *OsSIDP301* is involved in the salt stress response through an ABA-dependent pathway.

OsSIDP301 Is Associated With Yield-Related Traits in Rice

Grain size (grain length and width)/weight is an important agronomic trait for crop production (Xing and Zhang, 2010). In rice, grain shape is related to cell expansion or proliferation. *SMALL GRAIN 11*, a new allele of *DWARF2*, positively regulates grain size and weight by promoting cell expansion in rice (Fang et al., 2016); *MEI2-LIKE PROTEIN 4* negatively regulates grain length and weight by controlling cell expansion in rice (Lyu et al., 2020); and *GRAIN WIDTH 6* enhances grain size and weight by promoting cell expansion (Shi et al., 2020). In this study, intense GUS staining and grain shape were observed in the seeds of transgenic plants, which showed that *OsSIDP301* plays an important role in grain development. Moreover, SEM and paraffin section results suggested that the smaller grain shape in *OsSIDP301*^{OE} lines might be caused by decreasing cell expansion (**Figure 8** and **Supplementary Figures 4A,B**). BR has been reported to be associated with regulating grain shape (Li et al., 2019). *DWARF 61* encodes a BR receptor that positively regulates grain size by regulating downstream genes, and the overexpression of *BU1* showed typical BR phenotypes and larger grain size (Tanaka et al., 2009); *BC1* increased grain size by upregulating cell expansion-related genes, including *EXPA1*, *EXPA2*, *EXPA*3, and *EXPA*4 (Tanaka et al., 2009; Jang et al., 2017). In this study, OsSIDP301 was found to interact with OsBC1, and overexpression of *EXPA4* was observed in *OsSIDP301*^{RNAi} lines (**Figures 9**, **8J**). These results suggest that *OsSIDP301* negatively regulates grain size by controlling cell expansion.

In conclusion, our findings indicate that *OsSIDP301* plays a negative role in salt tolerance by regulating salt-related genes and negatively regulating grain size and weight by promoting cell expansion in spikelet hulls. Moreover, OsSIDP301 interacts with OsBC1, which also plays an important role in regulating grain size (**Figure 10**). Taken together, the knockdown of *OsSIDP301* can enhance grain size/weight and salt tolerance in rice. These findings of the functional characteristics of *OsSIDP301* complement the mechanism of yield and resistance synergy, which could provide a new target for cultivating high-yield and stress-resistant varieties in rice.

DATA AVAILABILITY STATEMENT

The datasets presented in this study can be found in online repositories. The names of the repository/repositories and accession number can be found below: NCBI SRA, PRJNA852225, and PRJNA852226.

AUTHOR CONTRIBUTIONS

LC and YC supervised the project and revised the article. LC, YC, and LG designed the experiments. LG performed most of the experiments, analyzed the data, and wrote the article. YC, HG, and CG helped with manuscript revision. XL conducted the screening of some transgenic plants and yeast. HB, MT, LH, and YY assisted in the experiments. All authors contributed to the article and approved the submitted version.

FUNDING

This study was supported by grants from the Joint Fund of the National Natural Science Foundation of China and the Karst Science Research Center of Guizhou Province (U1812401) and the Major Science and Technology Special Project of Fujian Province (2020NZ08016).

ACKNOWLEDGMENTS

We thank Xiaoling Guo (College of the Environment and Ecology, Xiamen University) for generously providing technical assistance.

SUPPLEMENTARY MATERIAL

The Supplementary Material for this article can be found online at: https://www.frontiersin.org/articles/10.3389/fpls.2022.863233/full#supplementary-material

Supplementary Figure 1 | The germination rate with NaCl treatment in mutants and osmotic stress for *OsSIDP301* lines. **(A)** Phenotype of mutants at germination stage with or without NaCl treatment, bar = 2 cm. Comparisons germination rate between WT and mutants with or without NaCl treatment for 2 days **(B)** and 3 days **(C)**, data was shown as mean ± SD (n = 8). **(D)** Phenotype of *OsSIDP301* transgenic plants at the seedling stage with or without Mannitol treatment, bar = 2 cm. **(E)** Comparisons of shoot length between WT, *OsSIDP301*^{OE}, and *OsSIDP301*^{RNAi} plants for 7 days with Mannitol treatment, data was showed as mean ± SD (n = 7).

Supplementary Figure 2 | (A, B) Volcano plots comparing the transcriptomes between *OsSIDP301*^{RNAi} and *OsSIDP301*^{OE} with the WT. The green and red dots represent downregulated DEGs with $\log_2$(FC) < -1 and upregulated DEGs with $\log_2$(FC) > 1, respectively. The blue dots represent no significant difference in transcriptomes. **(C–V)** Relative expression levels of DEGs from RNA-seq by RT-qPCR analysis. Data were shown as mean ± SD (n = 3).

Supplementary Figure 3 | Increased *OsSIDP301* expression caused smaller grains and shorter panicles. **(A)** Morphology of grain length and grain width in WT, *OsSIDP301*^{OE}, and *OsSIDP301*^{RNAi} lines. Comparisons of grain length **(B)**, grain width **(C)**, grain thickness **(D)**, and 1,000-grain weight **(E)** between WT, *OsSIDP301*^{OE} and *OsSIDP301*^{RNAi} lines (n = 100). **(F)** Morphology of grain length and grain width in WT and mutants. Comparisons of grain length **(G)**, grain width **(H)**, grain thickness **(I)**, and 1,000-grain weight **(J)** between WT and mutants. **(K)** Morphology of panicle length in WT, *OsSIDP301*^{OE}, *OsSIDP301*^{RNAi} lines, and mutants, bar = 3 cm. Comparisons of panicle length **(M)**, primary branches **(L)**, and secondary branches **(N)** between WT, *OsSIDP301*^{OE}, *OsSIDP301*^{RNAi} lines, and mutants (n = 4). Data were shown as mean ± SD, Student's t-test was used, $^{*}P < 0.05$, $^{**}P < 0.01$.

Supplementary Figure 4 | Cytological analysis of spikelet before fertilization and transcriptome analysis between WT and *OsSIDP301* plants in panicle. **(A)** Longitudinal sections of spikelet before fertilization, bar = 1 mm. **(B)** The local longitudinal sections of spikelet regions that were indicated by a red rectangle on panel **(A)** were enlarged 20-fold, the local cell length was indicated by the red line, bar = 250 μm. **(C)** Venn diagrams of the DEGs between WT and *OsSIDP301* plants in panicle. **(D)** GO enrichment analysis of all the **(C)** DEGs. **(E)** KEGG enrichment of all the **(C)** DEGs.

Supplementary Table 1 | Primers in this study.

Supplementary Table 2 | Differentially Expressed Genes (DEGs) between WT, *OsSIDP301*^{OE}, and *OsSIDP301*^{RNAi} from RNA-seq analysis, and using leaves as the material with 150 mM NaCl treatment for 3 days.

Supplementary Table 3 | Differentially Expressed Genes (DEGs) between WT, *OsSIDP301*^{OE}, and *OsSIDP301*^{RNAi} from RNA-seq analysis, and using young panicle as the material.

REFERENCES

Aya, K., Hobo, T., Sato-Izawa, K., Ueguchi-Tanaka, M., Kitano, H., and Matsuoka, M. (2014). A novel AP2-type transcription factor, SMALL ORGAN SIZE1, controls organ size downstream of an auxin signaling pathway. *Plant Cell Physiol.* 55, 897–912. doi: 10.1093/pcp/pcu023

Bateman, A., Coggill, P., and Finn, R. D. (2010). DUFs: families in search of function. *Acta Crystallogr. Sect. F Struct. Biol. Cryst. Commun.* 66, 1148–1152. doi: 10.1107/S1744309110001685

Chang, J., Cheong, B. E., Natera, S., and Roessner, U. (2019). Morphological and metabolic responses to salt stress of rice (*Oryza sativa* L.) cultivars which differ in salinity tolerance. *Plant Physiol. Biochem.* 144, 427–435. doi: 10.1016/j.plaphy.2019.10.017

Chen, G., Hu, Q. D., Luo, L., Yang, T. Y., Zhang, S., Hu, Y. B., et al. (2015). Rice potassium transporter OsHAK1 is essential for maintaining potassium-mediated growth and functions in salt tolerance over low and high potassium concentration ranges. *Plant Cell Environ.* 38, 2747–2765. doi: 10.1111/pce.12585

Chen, S. B., Songkumarn, P., Liu, J. L., and Wang, G. L. (2009). A versatile zero background T-vector system for gene cloning and functional genomics. *Plant Physiol.* 150, 1111–1121. doi: 10.1104/pp.109.137125

Chen, W. K., Chen, L., Zhang, X., Yang, N., Guo, J. H., Wang, M., et al. (2022). Convergent selection of a WD40 protein that enhances grain yield in maize and rice. *Science* 375:eabg7985. doi: 10.1126/science.abg7985

Choi, D., Lee, Y., Cho, H. T., and Kende, H. (2003). Regulation of expansin gene expression affects growth and development in transgenic rice plants. *Plant Cell* 15, 1386–1398. doi: 10.1105/tpc.011965

Citovsky, V., Lee, L. Y., Vyas, S., Glick, E., Chen, M. H., Vainstein, A., et al. (2006). Subcellular localization of interacting proteins by bimolecular fluorescence complementation in planta. *J. Mol. Biol.* 362, 1120–1131. doi: 10.1016/j.jmb.2006.08.017

Dong, N. Q., Sun, Y. W., Guo, T., Shi, C. L., Zhang, Y. M., Kan, Y., et al. (2020). UDP-glucosyltransferase regulates grain size and abiotic stress tolerance associated with metabolic flux redirection in rice. *Nat. Commun.* 1:2629. doi: 10.1038/s41467-020-16403-5

Du, H., Wang, N. L., and Xiong, L. Z. (2018a). Determination of malondialdehyde (MDA) content in rice leaves. *Bio* 101:e1010148. doi: 10.21769/BioProtoc.1010148

Du, H., You, J., and Xiong, L. Z. (2018b). Measurement of proline content in rice tissue. *Bio* 101:e1010146. doi: 10.21769/BioProtoc.1010146

Duncan, D. B. (1955). Multiple range and multiple F tests. *Biometrics* 11, 1–42. doi: 10.2307/3001478

Fang, N., Xu, R., Huang, L. J., Zhang, B. L., Duan, P. G., Li, N., et al. (2016). SMALL GRAIN 11 controls grain size, grain number and grain yield in rice. *Rice* 9:64.

Fang, Y. J., Qin, Y. H., and Xiong, L. Z. (2018). Determination of Na^+, K^+ in rice leaf (flame photometric method). *Bio* 101:e1010149. doi: 10.21769/BioProtoc.1010149

Flowers, T. J., Munns, R., and Colmer, T. D. (2015). Sodium chloride toxicity and the cellular basis of salt tolerance in halophytes. *Ann. Bot.* 115, 419–431. doi: 10.1093/aob/mcu217

Godfray, H. C., Beddington, J., Crute, I., Haddad, L., Lawrence, D., Muir, J., et al. (2010). Food security: the challenge of feeding 9 billion people. *Science* 327, 812–818. doi: 10.1126/science.1185383

Guo, C. M., Luo, C. K., Guo, L. J., Li, M., Guo, X. L., Zhang, Y. X., et al. (2016). OsSIDP366, a DUF1644 gene, positively regulates responses to drought and salt stresses in rice. *J. Integr. Plant Biol.* 58, 492–502. doi: 10.1111/jipb.12376

Hauser, F., and Horie, T. (2010). A conserved primary salt tolerance mechanism mediated by HKT transporters: a mechanism for sodium exclusion and maintenance of high K^+/Na^+ ratio in leaves during salinity stress. *Plant Cell Environ.* 33, 552–565. doi: 10.1111/j.1365-3040.2009.02056.x

He, Y. Q., Yang, B., He, Y., Zhan, C. F., Cheng, Y. H., Zhang, J. H., et al. (2019). A quantitative trait locus, qSE3, promotes seed germination and seedling establishment under salinity stress in rice. *Plant J.* 97, 1089–1104. doi: 10.1111/tpj.14181

Hong, Z., Ueguchi-Tanaka, M., Fujioka, S., Takatsuto, S., Yoshida, S., Hasegawa, Y., et al. (2005). The Rice brassinosteroid-deficient dwarf2 mutant, defective in the rice homolog of *Arabidopsis* DIMINUTO/DWARF1, is rescued by the endogenously accumulated alternative bioactive brassinosteroid, dolichosterone. *Plant Cell* 17, 2243–2254. doi: 10.1105/tpc.105.030973

Hussain, S., Zhang, J. H., Zhong, C., Zhu, L. F., Cao, X. C., Yu, S. M., et al. (2017). Effects of salt stress on rice growth, development characteristics, and the regulating ways: a review. *J. Integr. Agric.* 16, 2357–2374. doi: 10.1016/S2095-3119(16)61608-8

Jang, S., An, G., and Li, H. Y. (2017). Rice leaf angle and grain size are affected by the OsBUL1 transcriptional activator complex. *Plant Physiol.* 173, 688–702. doi: 10.1104/pp.16.01653

Jefferson, R. A. (1987). Assaying chimeric genes in plants: the GUS gene fusion system. *Plant Mol. Biol. Rep.* 5, 387–405. doi: 10.1007/bf02667740

Jiang, Z. H., Zhou, X. P., Tao, M., Yuan, F., Liu, L. L., Wu, F. H., et al. (2019). Plant cell-surface GIPC sphingolipids sense salt to trigger Ca^{2+} influx. *Nature* 572, 341–346. doi: 10.1038/s41586-019-1449-z

Kaur, G., and Asthir, B. (2015). Proline: a key player in plant abiotic stress tolerance. *Biol. Plant* 59, 609–619. doi: 10.1007/s10535-015-0549-3

Li, C. X., Shen, H. Y., Wang, T., and Wang, X. L. (2015). ABA regulates subcellular redistribution of OsABI-LIKE2, a negative regulator in ABA signaling, to control root architecture and drought resistance in *Oryza sativa*. *Plant Cell Physiol.* 56, 2396–2408. doi: 10.1093/pcp/pcv154

Li, M., Guo, L. J., Guo, C. M., Wang, L. J., and Chen, L. (2016). Over-expression of a DUF1644 protein gene, SIDP361, enhances tolerance to salt stress in transgenic rice. *J. Plant Biol.* 59, 62–73. doi: 10.1007/s12374-016-0180-7

Li, N., Xu, R., and Li, Y. H. (2019). Molecular networks of seed size control in plants. *Annu. Rev. Plant Biol.* 70, 435–463.

Li, X., Sun, L., Tan, L., Liu, F. X., Zhu, Z. F., Fu, Y. C., et al. (2012). TH1, a DUF640 domain-like gene controls lemma and palea development in rice. *Plant Mol. Biol.* 78, 351–359. doi: 10.1007/s11103-011-9868-8

Liang, W. J., Ma, X. L., Wan, P., and Liu, L. Y. (2018). Plant salt-tolerance mechanism: a review. *Biochem. Biophys. Res. Commun.* 495, 286–291.

Liu, C., Mao, B., Ou, S. J., Wang, W., Liu, L. C., Wu, Y. B., et al. (2014). OsbZIP71, a bZIP transcription factor, confers salinity and drought tolerance in rice. *Plant Mol. Biol.* 84, 19–36. doi: 10.1007/s11103-013-0115-3

Liu, L. C., Tong, H. N., Xiao, Y. H., Che, R. H., Xu, F., Hu, B., et al. (2015). Activation of big grain 1 significantly improves grain size by regulating auxin transport in rice. *Proc. Natl. Acad. Sci. U.S.A.* 112, 11102–11107. doi: 10.1073/pnas.1512748112

Liu, Y. T. (2017). *The preliminary function analysis on OsNCED1 gene in rice (Oryza sativa L)* (in Chinese). MA thesis. Hunan: Hunan Normal University. doi: 10.27137/d.cnki.ghusu.2017.000707

Luo, C. K., Guo, C. M., Wang, W. J., Wang, L. J., and Chen, L. (2014). Overexpression of a new stress-repressive gene OsDSR2 encoding a protein with a DUF966 domain increases salt and simulated drought stress sensitivities and reduces ABA sensitivity in rice. *Plant Cell Rep.* 33, 323–336. doi: 10.1007/s00299-013-1532-0

Luo, X., Bai, X., Sun, X. L., Zhu, D., Liu, B. H., Ji, W., et al. (2013). Expression of wild soybean WRKY20 in *Arabidopsis* enhances drought tolerance and regulates ABA signaling. *J. Exp. Bot.* 64, 2155–2169. doi: 10.1093/jxb/ert073

Lyu, J., Wang, D. K., Duan, P. G., Liu, Y. P., Huang, K., Zeng, D. L., et al. (2020). Control of grain size and weight by the GSK2-LARGE1/OML4 pathway in rice. *Plant Cell* 32, 1905–1918. doi: 10.1105/tpc.19.00468

Miao, J., Li, X. F., Li, X. B., Tan, W. C., You, A. Q., Wu, S. J., et al. (2020). OsPP2C09, a negative regulatory factor in abscisic acid signalling, plays an essential role in balancing plant growth and drought tolerance in rice. *New Phytol.* 227, 1417–1433. doi: 10.1111/nph.16670

Morton, M., Awlia, M., Al-Tamimi, N., Saade, S., Pailles, Y., Negrão, S., et al. (2019). Salt stress under the scalpel-Dissecting the genetics of salt tolerance. *Plant J.* 97, 148–163. doi: 10.1111/tpj.14189

Munns, R., and Tester, M. (2008). Mechanisms of salinity tolerance. *Annu. Rev. Plant Biol.* 59, 651–681. doi: 10.1146/annurev.arplant.59.032607.092911

Pan, Y. L., Hu, X., Li, C. Y., Xu, X., Su, C. G., Li, J. H., et al. (2017). SlbZIP38, a tomato bZIP family gene downregulated by abscisic acid, is a negative regulator of drought and salt stress tolerance. *Genes* 8:402. doi: 10.3390/genes8120402

Qian, Q., Guo, L. B., Smith, S. M., and Li, J. Y. (2016). Breeding high-yield superior quality hybrid super rice by rational design. *Natl. Sci. Rev.* 3, 283–294. doi: 10.1093/nsr/nww006

Rasool, S., Hameed, A., Azooz, M. M., Muneeb-u-Rehman, Siddiqi, T. O., and Ahmad, P. (2013). "Salt stress: causes, types and responses of plants," in *Ecophysiology and Responses of Plants Under Salt Stress*, eds P. Ahmad, M. Azooz, and M. Prasad (Berlin: Springer), doi: 10.1007/978-1-4614-4747-4_1

Roy, S. J., Negrao, S., and Tester, M. (2014). Salt resistant crop plants. *Curr. Opin. Biotechnol.* 26, 115–124. doi: 10.1016/j.copbio.2013.12.004

Si, L. Z., Chen, J. Y., Huang, X. H., Gong, H., Luo, J. H., Hou, Q. Q., et al. (2016). OsSPL13 controls grain size in cultivated rice. *Nat. Genet*. 48, 447–456. doi: 10.1038/ng.3518

Shen, Y., Shen, L. K., Shen, Z. X., Jing, W., Ge, H. L., Zhao, J. Z., et al. (2015). The potassium transporter OsHAK21 functions in the maintenance of ion homeostasis and tolerance to salt stress in rice. *Plant Cell Environ.* 38, 2766–2779. doi: 10.1111/pce.12586

Shi, C. L., Dong, N. Q., Guo, T., Ye, W. W., Shan, J. X., and Lin, H. X. (2020). A quantitative trait locus GW6 controls rice grain size and yield through the gibberellin pathway. *Plant J.* 103, 1174–1188. doi: 10.1111/tpj.14793

Singh, A., Jha, S. K., Bagri, J., and Pandey, G. K. (2015). ABA inducible rice protein phosphatase 2C confers ABA insensitivity and abiotic stress tolerance in *Arabidopsis*. *PLoS One* 10:e0125168. doi: 10.1371/journal.pone.0125168

Singh, A. L., Reddy, K. K., Singh, S., and Rani, K. (2022). "Salt stress alleviation strategies to maintain potassium homeostasis in plants," in *Role of Potassium in Abiotic Stress*, eds N. Iqbal and S. Umar (Singapore: Springer), doi: 10.1007/978-981-16-4461-0_9

Sinha, N., Chaudhary, S., Rani, R., Karuna, K., and Ahmad, M. (2022). Impact of salt stress on fruits and its mitigation strategies; a review. *Ann. Plant Sci.* 11, 4692–4704. doi: 10.21746/aps.2022.11.01.17

Song, X. J., Huang, W., Shi, M., Zhu, M. Z., and Lin, H. X. (2007). A QTL for rice grain width and weight encodes a previously unknown RING-type E3 ubiquitin ligase. *Nat. Genet.* 39, 623–630. doi: 10.1038/ng2014

Tanabe, S., Ashikari, M., Fujioka, F., Takatsuto, S., Yoshida, S., Yano, M., et al. (2005). A novel cytochrome P450 is implicated in brassinosteroid biosynthesis via the characterization of a rice dwarf mutant, dwarf11, with reduced seed length. *Plant Cell* 17, 776–790. doi: 10.1105/tpc.104.024950

Tanaka, A., Nakagawa, H., Tomita, C., Shimatani, Z., Ohtake, M., Nomura, T., et al. (2009). BRASSINOSTEROID UPREGULATED1, encoding a helix-loop-helix protein, is a novel gene involved in brassinosteroid signaling and controls bending of the lamina joint in rice. *Plant Physiol.* 151, 669–680. doi: 10.1104/pp.109.140806

Tong, Y., Wang, C., Zhao, L. L., Lian, J., Liu, X. M., and Zhao, B. C. (2021). Transcription factor OsbZIP5 negatively regulates drought-tolerance in rice. *Chinese J. Biochem. Mol. Biol.* 37, 798–810. doi: 10.13865/j.cnki.cjbmb.2021.03.1427

Wang, R., Jing, W., Xiao, L. Y., Jin, Y. K., Shen, L. K., and Zhang, W. H. (2015). The rice high-affinity potassium transporter1;1 is involved in salt tolerance and regulated by an MYB-type transcription factor. *Plant Physiol.* 168, 1076–1090. doi: 10.1104/pp.15.00298

Wang, X. L., He, Y. Q., Wei, H., and Wang, L. (2021). A clock regulatory module is required for salt tolerance and control of heading date in rice. *Plant Cell Environ.* 44, 3283–3301. doi: 10.1111/pce.14167

Wei, H., Wang, X. L., He, Y. Q., Xu, H., and Wang, L. (2021). Clock component *OsPRR73* positively regulates rice salt tolerance by modulating OsHKT2;1-mediated sodium homeostasis. *EMBO J.* 40:e105086. doi: 10.15252/embj.2020105086

Wu, Y., Fu, Y., Zhao, S., Gu, P., Zhu, Z., Sun, C., et al. (2016). CLUSTERED PRIMARY BRANCH 1, a new allele of DWARF11, controls panicle architecture and seed size in rice. *Plant Biotechnol. J.* 14, 377–386. doi: 10.1111/pbi.12391

Xing, Y. Z., and Zhang, Q. F. (2010). Genetic and molecular bases of rice yield. *Annu. Rev. Plant Biol.* 61, 421–442. doi: 10.1146/annurev-arplant-042809-112209

Yan, D., Zhou, Y., Ye, S., Zeng, L. J., Zhang, X. M., and He, Z. H. (2013). BEAK-SHAPED GRAIN 1/TRIANGULAR HULL 1, a DUF640 gene, is associated with grain shape, size and weight in rice. *Sci. China-Life Sci.* 56, 275–283. doi: 10.1007/s11427-013-4449-5

Yang, Y., and Guo, Y. (2018). Elucidating the molecular mechanisms mediating plant salt-stress responses. *New Phytol.* 217, 523–539. doi: 10.1111/nph.14920

Yoshikawa, T., Eiguchi, M., Hibara, K., Ito, J., and Nagato, Y. (2013). Rice slender leaf 1 gene encodes cellulose synthase-like D4 and is specifically expressed in M-phase cells to regulate cell proliferation. *J. Exp. Bot.* 64, 2049–2061. doi: 10.1093/jxb/ert060

You, J., Fang, Y. J., and Xiong, L. Z. (2018). Reactive oxygen detection. *Bio* 101:e1010170. doi: 10.21769/BioProtoc.1010170

Zhang, C. S., Lu, Q., and Verma, D. P. (1995). Removal of feedback inhibition of Δ1-Pyrroline-5-carboxylate synthetase, a bifunctional enzyme catalyzing the first two steps of proline biosynthesis in plants. *J. Biol. Chem.* 270, 20491–20496. doi: 10.1074/jbc.270.35.20491

Zhang, M., Fang, Y. M., Ji, Y. H., Jiang, Z. P., and Wang, L. (2013). Effects of salt stress on ion content, antioxidant enzymes and protein profile in different tissues of *Broussonetia papyrifera*. *S. Afr. J. Bot.* 85, 1–9. doi: 10.1016/j.sajb.2012.11.005

Zhang, S. X., Haider, I., Kohlen, W., Jiang, L., Bouwmeester, H., Meijer, A. H., et al. (2012). Function of the HD-Zip I gene Oshox22 in ABA-mediated drought and salt tolerances in rice. *Plant Mol. Biol.* 80, 571–585. doi: 10.1007/s11103-012-9967-1

Zhao, C., Zhang, H., Song, C., Zhu, J. K., and Shabala, S. (2020). Mechanisms of plant responses and adaptation to soil salinity. *Innovation* 1:100017. doi: 10.1016/j.xinn.2020.100017

Zhou, Y., Fan, X. L., Lin, Y. J., and Chen, H. (2018). Determination of chlorophyll content in rice. *Bio* 101:e1010147. doi: 10.21769/BioProtoc.1010147

Zhu, J. K. (2002). Salt and drought stress signal transduction in plants. *Annu. Rev. Plant Biol.* 53, 247–273. doi: 10.1146/annurev.arplant.53.091401.143329

Zhu, J. K. (2016). Abiotic stress signaling and responses in plants. *Cell* 167, 313–324. doi: 10.1016/j.cell.2016.08.029

Zou, M. J., Guan, Y. C., Ren, H. B., Zhang, F., and Chen, F. (2008). A bZIP transcription factor, OsABI5, is involved in rice fertility and stress tolerance. *Plant Mol. Biol.* 66, 675–683. doi: 10.1007/s11103-008-9298-4

Zuo, J. R., and Li, J. Y. (2014). Molecular genetic dissection of quantitative trait loci regulating rice grain size. *Annu. Rev. Genet.* 48, 99–118. doi: 10.1146/annurev-genet-120213-092138

Conflict of Interest: The authors declare that the research was conducted in the absence of any commercial or financial relationships that could be construed as a potential conflict of sdainterest.

Publisher's Note: All claims expressed in this article are solely those of the authors and do not necessarily represent those of their affiliated organizations, or those of the publisher, the editors and the reviewers. Any product that may be evaluated in this article, or claim that may be made by its manufacturer, is not guaranteed or endorsed by the publisher.

Copyright © 2022 Ge, Guo, Li, Tang, Guo, Bao, Huang, Yi, Cui and Chen. This is an open-access article distributed under the terms of the Creative Commons Attribution License (CC BY). The use, distribution or reproduction in other forums is permitted, provided the original author(s) and the copyright owner(s) are credited and that the original publication in this journal is cited, in accordance with accepted academic practice. No use, distribution or reproduction is permitted which does not comply with these terms.

frontiers | Frontiers in Plant Science

TYPE Original Research
PUBLISHED 16 August 2022
DOI 10.3389/fpls.2022.933740

Check for updates

OPEN ACCESS

EDITED BY
Girdhar Kumar Pandey,
University of Delhi, India

REVIEWED BY
Jonathan Fresnedo Ramirez,
The Ohio State University,
United States
Muthusamy Ramakrishnan,
Nanjing Forestry University, China
Wen-Feng Nie,
Yangzhou University, China

*CORRESPONDENCE
Gaurav Zinta
gzinta@gmail.com;
gauravzinta@ihbt.res.in

†These authors have contributed equally to this work and share first authorship

SPECIALTY SECTION
This article was submitted to Plant Physiology, a section of the journal Frontiers in Plant Science

RECEIVED 01 May 2022
ACCEPTED 08 July 2022
PUBLISHED 16 August 2022

CITATION
Dutta M, Raturi V, Gahlaut V, Kumar A, Sharma P, Verma V, Gupta VK, Sood S and Zinta G (2022) The interplay of DNA methyltransferases and demethylases with tuberization genes in potato (*Solanum tuberosum* L.) genotypes under high temperature. *Front. Plant Sci.* 13:933740. doi: 10.3389/fpls.2022.933740

COPYRIGHT
© 2022 Dutta, Raturi, Gahlaut, Kumar, Sharma, Verma, Gupta, Sood and Zinta. This is an open-access article distributed under the terms of the Creative Commons Attribution License (CC BY). The use, distribution or reproduction in other forums is permitted, provided the original author(s) and the copyright owner(s) are credited and that the original publication in this journal is cited, in accordance with accepted academic practice. No use, distribution or reproduction is permitted which does not comply with these terms.

The interplay of DNA methyltransferases and demethylases with tuberization genes in potato (*Solanum tuberosum* L.) genotypes under high temperature

Madhushree Dutta[1,2†], Vidhi Raturi[1,2†], Vijay Gahlaut[1], Akhil Kumar[3], Paras Sharma[1], Vipasha Verma[3], Vijai Kishor Gupta[4], Salej Sood[5] and Gaurav Zinta[1,2*]

[1]Biotechnology Division, CSIR-Institute of Himalayan Bioresource Technology, Palampur, India, [2]Academy of Scientific and Innovative Research (AcSIR), Ghaziabad, Uttar Pradesh, India, [3]Agrotechnology Division, CSIR-Institute of Himalayan Bioresource Technology, Palampur, India, [4]ICAR-Central Potato Research Institute, Modipuram, Uttar Pradesh, India, [5]Division of Crop Improvement, ICAR-Central Potato Research Institute, Shimla, Himachal Pradesh, India

Potato is a temperate crop consumed globally as a staple food. High temperature negatively impacts the tuberization process, eventually affecting crop yield. DNA methylation plays an important role in various developmental and physiological processes in plants. It is a conserved epigenetic mark determined by the dynamic concurrent action of cytosine-5 DNA methyltransferases (*C5-MTases*) and demethylases (*DeMets*). However, *C5-MTases* and *DeMets* remain unidentified in potato, and their expression patterns are unknown under high temperatures. Here, we performed genome-wide analysis and identified 10 C5-MTases and 8 DeMets in potatoes. Analysis of their conserved motifs, gene structures, and phylogenetic analysis grouped *C5-MTases* into four subfamilies (*StMET*, *StCMT3*, *StDRM*, and *StDNMT2*) and *DeMets* into three subfamilies (*StROS*, *StDML*, and *StDME*). Promoter analysis showed the presence of multiple cis-regulatory elements involved in plant development, hormone, and stress response. Furthermore, expression dynamics of *C5-MTases* and *DeMets* were determined in the different tissues (leaf, flower, and stolon) of heat-sensitive (HS) and heat-tolerant (HT) genotypes under high temperature. qPCR results revealed that high temperature resulted in pronounced upregulation of *CMT* and *DRM* genes in the HT genotype. Likewise, demethylases showed strong upregulation in HT genotype as compared to HS genotype. Several positive (*StSP6A* and *StBEL5*) and negative (*StSP5G*, *StSUT4*, and *StRAP1*) regulators are involved in the potato tuberization. Expression analysis of these genes revealed that high temperature induces the expression of positive regulators in the leaf and stolon samples of HT genotype, possibly through active DNA demethylation and RNA-directed DNA methylation (RdDM) pathway components. Our findings lay a framework for understanding how epigenetic pathways synergistically

or antagonistically regulate the tuberization process under high-temperature stress in potatoes. Uncovering such mechanisms will contribute to potato breeding for developing thermotolerant potato varieties.

KEYWORDS

DNA methylation, epigenetics, climate change, tuberization, heat stress, thermotolerance

Introduction

Global climate change is a serious threat to sustainable crop production. The global mean surface air temperature is expected to rise from 0.5°C to 4.5°C by the end of the twenty-first century (Change, 2013), which is predicted to result in a 17–24% loss in crop productivity (Zhou et al., 2019). The temperate crops are more vulnerable to global temperature rise, negatively affecting their development and final harvest (Lesk et al., 2016).

Potato is a temperate staple food crop with global production of 370.43 million tons (FAOSTAT, 2021). It is one of the richest sources of carbohydrates, fibers, vitamins, and antioxidants (Beals, 2019), feeding the global nutritional requirements (Birch et al., 2012). Potato is vegetatively propagated through tubers, which develop from underground stems known as stolons (Zierer et al., 2021). The stages of tuberization involve different phases, *viz.* stolon induction, elongation/branching, termination of stolon longitudinal growth, tuber induction by sub-apical stolon swelling, tuber growth, and bulking (Vreugdenhil and Struik, 1989).

Tuberization is a complex biological phenomenon affected by several environmental cues (Dutt et al., 2017). Short days, cool temperature, and low nitrogen supply favors tuberization, whereas long days, high temperature, and high nitrogen supply oppose the tuberization process (Gao et al., 2014). The optimal temperature requirement for tuberization is 15–20°C (Rykaczewska, 2015). High temperatures and long days impede the tuberization process (Dutt et al., 2017). The process of tuberization under high temperature involves altered assimilate partitioning and change in the source to sink balance (Hastilestari et al., 2018). Even a slight increase in temperature (e.g., 30°C Day/20°C night) can impact the process of tuberization, affecting crop yield severely (Hancock et al., 2014; Kim et al., 2017). Additionally, phytohormones are involved in the tuberization process. The high GA levels impair tuber development, whereas ABA, cytokinin, and sucrose promote tuberization (Chatterjee et al., 2007). The tuberization signaling network involves several key players, including promoters (*StSP6A*, *StBEL5*, *StPOTH1*, and *StCDF*) and inhibitors (*StSUT4*, *StSP5G*, and *StRAP1*) of tuberization (Dutt et al., 2017).

DNA methylation is a conserved epigenetic mark that regulates gene expression, transposable elements, and stress-mediated responses, eventually contributing to genomic stability (Zhang et al., 2018). DNA methylation in eukaryotes is determined by the concurrent activity of methyltransferases and demethylases (Zhang et al., 2018). In plants, DNA methylation occurs at cytosine residues in three sequence contexts: CpG, CpHpG, and CpHpH (H depicts A, C, T; Law and Jacobsen, 2010). DNA methylation is broadly categorized into *de novo* and maintenance methylation (Zhang et al., 2018). The basic function of any C5-MTase is to recognize specific nucleotide sequences and mark the transfer of methyl group from co-factor S-adenosyl-L methionine (SAM) to 5'-cytosine residue on the pyrimidine ring (Cheng et al., 1993). This function is attributed to the N-terminal regulatory and C-terminal catalytic domain (Pavlopoulou and Kossida, 2007). Plant cytosine DNA methylases (C5-MTase) are much more diverse and less explored than mammalian C5-MTase. Till now, four major types of C5-MTases have been identified including METHYLTRANSFERASE (MET), CHROMO METHYLTRANSFERASE (CMT), DOMAINS REARRANGED METHYLASE (DRM), and DNA METHYLASE HOMOLOG 2 (DNMT2; Cao et al., 2003). DNA demethylation occurs either passively by loss of maintenance methylation enzymes during consecutive DNA replication or actively by the action of a special set of DNA glycosylases (HhH-GPD); DNA glycosylases/lyases that excise 5-meC and operate through the base excision pathway (Roldán-Arjona et al., 2019). Also, two additional conserved domains named RNA recognition motif (RRM) and methylated CpG discriminating CXXC domain are found (Iyer et al., 2011). Thus, active DNA demethylation requires a set of DNA demethylases to initiate the process (Gallego-Bartolomé et al., 2018; Liu et al., 2021).

The concurrent action of methyltransferase and demethylases regulate several developmental features such as plant size, leaf size and shape, flowering time, and fruit ripening (Finnegan et al., 1996). Also, methyltransferases and demethylases are involved in regulating stress-responsive genes in plants (Zhu et al., 2020). For instance, the role of DNA methylation has been suggested in drought and salinity stress responses while studying the contrasting rice genotypes (Garg et al., 2015). Likewise, the role of DNA methylation

in conferring plant immunity in *A. thaliana* has also been demonstrated (Dowen et al., 2012).

In the present study, DNA methyltransferase and demethylases were characterized in potato (*Solanum tuberosum*) for the first time. Also, their expression patterns were determined in several tissues such as the leaf, flower, and stolon in the heat-sensitive (HS) and heat-tolerant (HT) potato genotypes under high temperature. Furthermore, the expression of tuberization genes and heat shock factors (HSFs) were studied in these genotypes to delineate how epigenetic components are linked with tuberization under high temperature.

Materials and methods

Collection of candidate genes

Protein sequences were downloaded from the potato genome database (Spud DB; Hirsch et al., 2014) by using Pfam ID (PF00145, PF15628, PF00730, and PF15629) to identify the C5-MTases and demethylases. The resultant protein sequences were also verified by downloading the hidden Markov model (HMM) file from the HMMER search and identified through the ENSEMBL database (Potter et al., 2018). The identified potato C5-MTase and demethylase protein sequences were then classified based on the presence of conserved domain using available online software SMART (Schultz et al., 2000) and NCBI_CDD (Marchler-Bauer et al., 2015). Domain Graph 2.0 (DOG 2.0) was used to construct the figures of conserved domains of each class of proteins (Ren et al., 2009). The ExPASy server (http://www.expasy.org/) (Artimo et al., 2012) was used to predict the relative molecular weight (MW) and isoelectric point (PI) of potato C5-MTase and demethylase.

Analysis of conserved motif and gene structure

The conserved motifs of C5-MTase and demethylases were analyzed using MEME suite vs 5.05 (Bailey et al., 2009), and a total of 15 conserved motifs were identified which was further constructed using TBtool (Chen et al., 2018). Gene Structure Display Server (GSDS 2.0) was used to draw the gene structure of potato C5-MTase and demethylase (Hu et al., 2015).

Identification of promoter cis-regulatory elements

The sequence retrieval tab of the potato genome database (Spud DB) was used to extract 2 kb sequences that lie upstream of the Transcription Start Site (TSS) of genomic sequences of C5-MTases and demethylases. The online software PlantCare (Lescot et al., 2002) was used to list out the conserved elements of promoter sequences.

Analysis of multiple sequence alignment and phylogenetic tree

Full-length amino acid sequences of C5-MTase (*Arabidopsis thaliana*, *Solanum lycopersicum*, *Solanum tuberosum*, *Glycine max*, *Zea mays*, and *Oryza sativa*) and DNA demethylase (*Arabidopsis thaliana*, *Solanum lycopersicum*, *Solanum tuberosum, Cucumis sativa*, and *Glycine max*) were subjected to multiple sequence alignments by using muscle program of MEGA X (10.05) software (Kumar et al., 2018). The aligned protein sequences were used to construct a phylogenetic tree, using the Neighbor-Joining (NJ) program for 1,000 bootstrap replicates with Poisson correction (Yang, 2007).

Prediction of subcellular localization

The subcellular localization of candidate genes was determined by using the protein sequences in the web tool CELLO v.2.5 (Yu et al., 2014). The localization of genes was further used to map them.

Experimental set-up

Heat-sensitive (Kufri Chandramukhi, CP2141/A-2708) and -tolerant (Kufri Kiran, CP4803/A-2708) potato tubers were obtained from the Central Potato Research Institute (CPRI), Shimla, India. Well-sprouted tubers were grown in 0.2 L and 12 cm pots containing soil mixture (soil: vermicompost:sand, 2:1:1). Six replicates per genotype were raised in a Percival growth chamber under 16 h light and 8 h darkness conditions with day and night temperatures of 22 and 18°C, respectively. The light intensity of the growth chamber was 300 μmol/s/m^2. The plants were watered and rotated daily to avoid water deficit and minimize positional effects. After 50 days, half of the plants were subjected to 14 days high-temperature stress (32°C day and 27°C night). The leaves, flowers, and stolon tissues were harvested from both the control and heat treatments around 10 AM (4 h of light onset). The harvested tissues, *viz.* leaf, flower, and stolon of similar size/age, were collected in aluminum zippers, frozen immediately in liquid nitrogen, and stored at −80°C.

RNA isolation, cDNA synthesis, and quantitative real-time PCR (qPCR)

About 100 mg of the frozen tissue was finely ground with a mortar and pestle (Yu et al., 2007). RNA was isolated with Spectrum Plant Total RNA Kit (Sigma Aldrich, USA) by following the manufacturer's protocol. The isolated RNA was treated with 1 U/μl of DNase I (ThermoFisher Scientific Baltics, UAB, Lithuania). Further, 1 μg of RNA was used to synthesize cDNA using the Verso cDNA synthesis kit (ThermoFisher Scientific Baltics, UAB, Lithuania). qPCR primers were designed from the CDS sequence using the ApE software (Davis and Jorgensen, 2022) (Supplementary Table S1). The quantitative real-time PCR was carried out using the Dynamo Colorflash SYBR Green (ThermoFisher Scientific Baltics, UAB, Lithuania) in an Applied Biosystem step-plus real-time PCR system. Three biological and three technical replicates were used to perform qPCR analysis. The expression of the housekeeping gene tubulin was found to be stable across tissues, treatments, and genotypes. Hence, tubulin was used as an internal control to measure target gene expression using the 2−ΔΔCt method (Schmittgen and Livak, 2008).

Statistical analysis

The gene expression data obtained by qPCR were expressed as mean ± standard error (SE) for three biological and technical replicates. Statistical analysis was carried out by using the SPSS 16.0 software (SPSS Science, UK). The significant difference between control and heat-treated plants was analyzed based on two-tailed Student's *t*-test. The significant difference between control and heat-treated samples at $p < 0.05$, $p < 0.01$, and $p < 0.001$ are denoted by one, two, and three asterisks.

Results

Gene identification, structure analysis, and chromosome localization of *C5-MTase* and *demethylase* genes

In our present study, we identified 10 C5-MTase (*StMET1-4A*, *StMET2-11A*, *StCMT3-1A*, *StCMT3-8A*, *StCMT3-12A*, *StDNMT2-8A*, *StDNMT2-8B*, *StDRM1-2A*, *StDRM2-4A*, and *StDRM3-10A)* and 8 DNA demethylase genes (*StDeMet1*, *StDeMet2*, *StDeMet3*, *StDeMet4*, *StDeMet5*, *StDeMet6*, *StDeMet7*, and *StDeMet8).* The CDS and protein length of methyltransferase genes varied from 363 bp (*StDNMT2-8B)* to 4,674 bp *(StMET2-11A)* and 120 amino acids (aa) (*StDNMT2-8B)* to 1,557 aa *(StMET2-11A)*, respectively. Similarly, gene transcript length and polypeptide length of demethylase genes ranges from 906 bp (*StDeMet8)* to 5,556 bp *(StDeMet1)* and 301aa (*StDeMet8)* to 1,851 aa *(StDeMet1)*, respectively (Figure 1). The predicted molecular weight and pI value range from 174.27 to 13.7 kDa and 4.63 to 9.51 in C5-MTase; and 207.46 to 33.51 kDa and 6.24 to 9.46 in DeMets (Table 1). The chromosome localization of the candidate proteins has also been incorporated (Table 1). Interestingly, the classification of C5-MTase is based on the linear arrangement of distinct and conserved domains across members of a different enzyme family (Pavlopoulou and Kossida, 2007). Pfam analysis revealed that all C5-MTases (PF00145) have conserved DNA_Methylase (DNA_M) domain. However, different C5-MTase are characterized due to the presence of distinctive domains at their N-terminal: (i) CMT family possesses CHROMO (Chromatin organization modifier) and one BAH (Bromo Adjacent Homology) in contrast to (ii) MET which has two BAH and an RFD domains (iii) DRM family has unique UBA domain (Ubiquitin-associated), whereas (iv) DNMT has shorter protein length as compared to other C5-MTase owing to lack of N-terminal regulatory domain (Figure 2). Additionally, DeMets have conserved HhH-GPD (PF00730), Perm-CXXC (PF15629), and RRM_DME (PF15628). The distribution of conserved motifs in the StC5-MTase and StDeMets proteins were predicted using the MEME online suite. A total of 15 conserved motifs were explored in StC5-MTase and StDeMets proteins. Motifs 9, 11, and 12 were highly conserved in the MET subfamily. Motifs 5, 13, and 15 were major motifs in DRM, while Motif 8 was unique to CMT3 subfamilies. The motif distribution in StDeMets proteins showed that Motifs 1, 3, 4, 5, 6, 7, 8, 9, 11, and 13 were highly conserved in StDeMet 1- 5 proteins, while DeMet 2 and 3 have additional unique Motif 14 (Figure 2). The structure of *StC5-MTase* and *StDeMets* of potato is identical to *Arabidopsis thaliana* and is presumed to catalyze similar functions as that of *Arabidopsis thaliana* in potato.

Phylogenetic analysis

To exemplify the evolutionary relationship among C5-MTase subfamilies in plants, we used 55 protein sequences from four dicots (*Arabidopsis thaliana*, *Solanum lycopersicum*, *Solanum tuberosum*, and *Glycine max*) and two monocots (*Zea mays* and *Oryza sativa*) to construct a phylogenetic tree (Supplementary Table S2). C5-MTase is grouped into four subfamilies: DRM, CMT, MET, and DNMT having 21, 15, 13, and six members, respectively (Figure 1). Subsequently, the largest and smallest group in the tree were DRM and DNMT subfamily. Further, the subfamilies could also be divided into monocot and dicot distinct subgroups, based upon the significant differences in protein sequences. Interestingly, in almost all clades, tomato C5-MTase was closer to potato C5-MTase protein, suggesting that they are the members of the same taxonomic family, *Solanaceae*, and predicted to share functional similarity.

As for DNA Demethylases, 24 protein sequences from four dicots (*Arabidopsis thaliana*, *Solanum lycopersicum*, *Solanum*

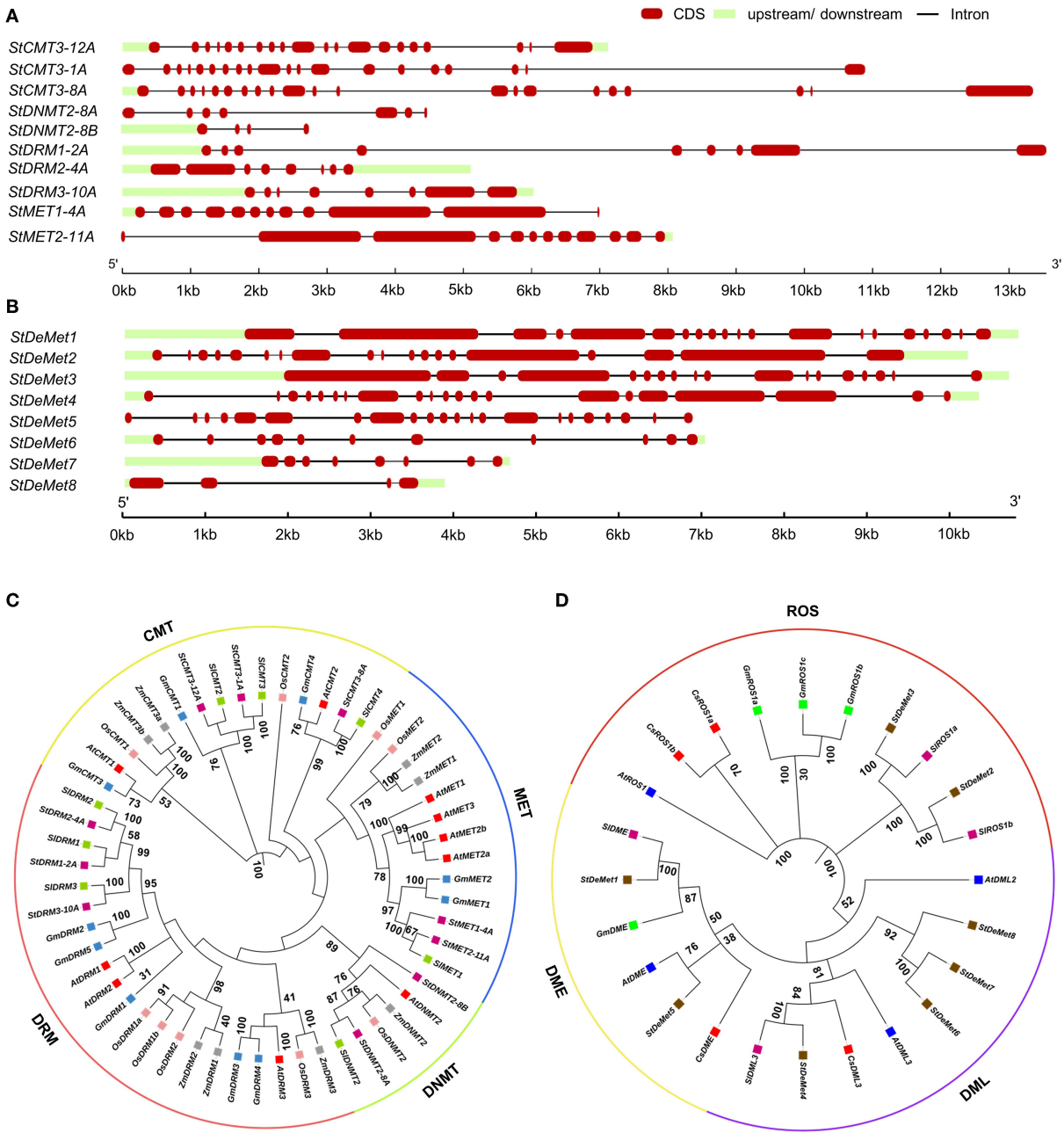

FIGURE 1
Gene structures of *StC5-MTase* **(A)** and *StDeMets* **(B)** in *S. tuberosum*. Phylogenetic tree analysis of C5-MTase **(C)** and DeMet proteins **(D)** with 1,000 bootstrap replicates. The lines in gene structure represent introns and filled red and light green boxes represent CDS and UTR, respectively. The lengths of CDS and introns can be determined using the scale bar on the bottom.

tuberosum and Cucumis sativa, and *Glycine max*) were extracted to construct a phylogenetic tree (Supplementary Table S3) arranged in ascending order in accordance to the number of members: DME, DML, and ROS. However, we analyzed *DeMets* from dicots as DME evolved monophyletically in dicots, such results are consistent with the previous report (Yu et al., 2021). We also observed DML group constituting four out of eight *StDeMets* genes as compared to ROS and DME.

Analysis of regulatory elements in the promoter region

Cis-regulatory elements are the core components governing biological processes. A sum of 30 major elements was represented that were predicted in the 2 kb upstream of the TSS in the promoter region. They were further categorized into light, development, hormone, and stress-responsive cis

TABLE 1 Basic information of C5-MTase and DNA demethylase genes in *Solanum tuberosum*.

Protein name	Gene ID	Chromosome number	Chromosome location		Protein			CDS length (bp)
Cytosine-5 DNA methyltransferases					**PI**	**Mw (kDa)**	**Length (aa)**	
StMET1-4A	Soltu.DM.04G014710	Chr04	23868453	23875446	6.15	174.27	1547	4644
StMET2-11A	Soltu.DM.11G013230	Chr11	16840303	16848391	6.2	175.13	1557	4674
StCMT3-1A	Soltu.DM.01G001630	Chr01	1678832	1689723	4.72	94.08	832	2499
StCMT3-8A	Soltu.DM.08G003560	Chr08	4677712	4691064	8.96	121.97	1086	3261
StCMT3-12A	Soltu.DM.12G000130	Chr12	355235	362351	5.25	104.5	933	2802
StDNMT2-8A	Soltu.DM.08G015570	Chr08	43136073	43140542	5.03	37.11	325	978
StDNMT2-8B	Soltu.DM.08G015580	Chr08	43143967	43146720	9.51	13.7	120	363
StDRM1-2A	Soltu.DM.02G006560	Chr02	20245172	20258718	4.8	77.1	684	2055
StDRM2-4A	Soltu.DM.04G000230	Chr04	452787	457895	4.63	68.47	608	1827
StDRM3-10A	Soltu.DM.10G030090	Chr10	60637223	60643251	5.12	69.03	609	1830
DNA demethylases								
StDeMet1	Soltu.DM.11G005260	Chr11	5686999	5397802	7.47	207.46	1851	5556
StDeMet2	Soltu.DM.09G004240	Chr09	3690956	3701147	6.24	204.72	1834	5505
StDeMet3	Soltu.DM.10G024770	Chr10	56407648	56417613	6.63	181.56	1624	4875
StDeMet4	Soltu.DM.03G037240	Chr03	60022718	60033043	7.76	165.45	1468	4407
StDeMet5	Soltu.DM.04G021680	Chr04	49931927	49938794	9.23	105.71	931	2796
StDeMet6	Soltu.DM.06G028750	Chr06	53964389	53971402	9.46	41.5	378	1137
StDeMet7	Soltu.DM.09G025490	Chr09	61584476	61589128	9.17	33.8	299	900
StDeMet8	Soltu.DM.03G027780	Chr03	52412404	52416269	8.31	33.51	301	906

elements (Figure 3). C5-MTase genes showed several stress-responsive cis elements, such as CAAT and TATA box, which were predominant across the subfamilies/members (MET, CMT3, DRM, and DNMT2). Among all the subfamilies, CMT3 had the largest number of stress-involved elements. We found nine hormone-responsive elements such as ABRE and ERE that were abundant in all members. However, AuxRR-core is present exclusively in *StDNMT2-8A*. Elements involved in plant development were also screened, and five major elements including A box, CCGTCC, CAT box, ACA motif, and Circadian were identified. A box and CCGTCC were present only in *StCMT3-12A*, while circadian control element and ACA motif were found exclusively in *DNMT2* and *MET* subfamilies. Further, eight CRE elements of the light-responsive module were also identified, out of which G box and Box 4 were found in all the naturally grouped subfamilies.

Similarly, cis-regulatory elements were also analyzed in the potato DNA methyltransferase proteins. ARE, CAAT, and TATA control elements were present in all the eight *DeMet* genes. Surprisingly, the abscisic hormone element ABRE was not found in *StDeMet6* and *StDeMet7,* while TCA elements involved in salicylic acid response were present in *StDeMet6* and *StDeMet7*. Furthermore, light module Box4 was present in all members. Altogether, our results suggest that C5-MTase and demethylase genes are involved in plant growth, development, and various abiotic stress responses.

Sub-cellular localization of potato C5-MTase and DeMets

The *in silico* subcellular localization revealed that all DeMets were localized in the nucleus; however, *StDeMet7* was additionally found in mitochondria. The C5-MTases were localized in the nucleus (*StMET1-4A*, *StMET2-11A*, *StCMT3-8A*, *StCMT3-12A*, *StDRM1-2A*, *StDRM2-4A*, and *StDRM3-10A)* and cytoplasm (*StCMT3-1A*, *StDNMT2-8A*, and *StDNMT2-8B).* Apart from being in the nucleus, a couple of DRM members (*StDRM1-2A* and *StDRM2-4A)* were also localized in the cytoplasm (Figure 4).

Expression patterns of *C5-MTase* and *DeMet* genes

The expression dynamics of *C5-MTase* and *DeMet* genes were studied in different tissues, *viz*. leaf, flower, and stolon in the heat-sensitive (HS) and heat-tolerant (HT) potato genotypes under high temperature (Figures 5, 6). The expression

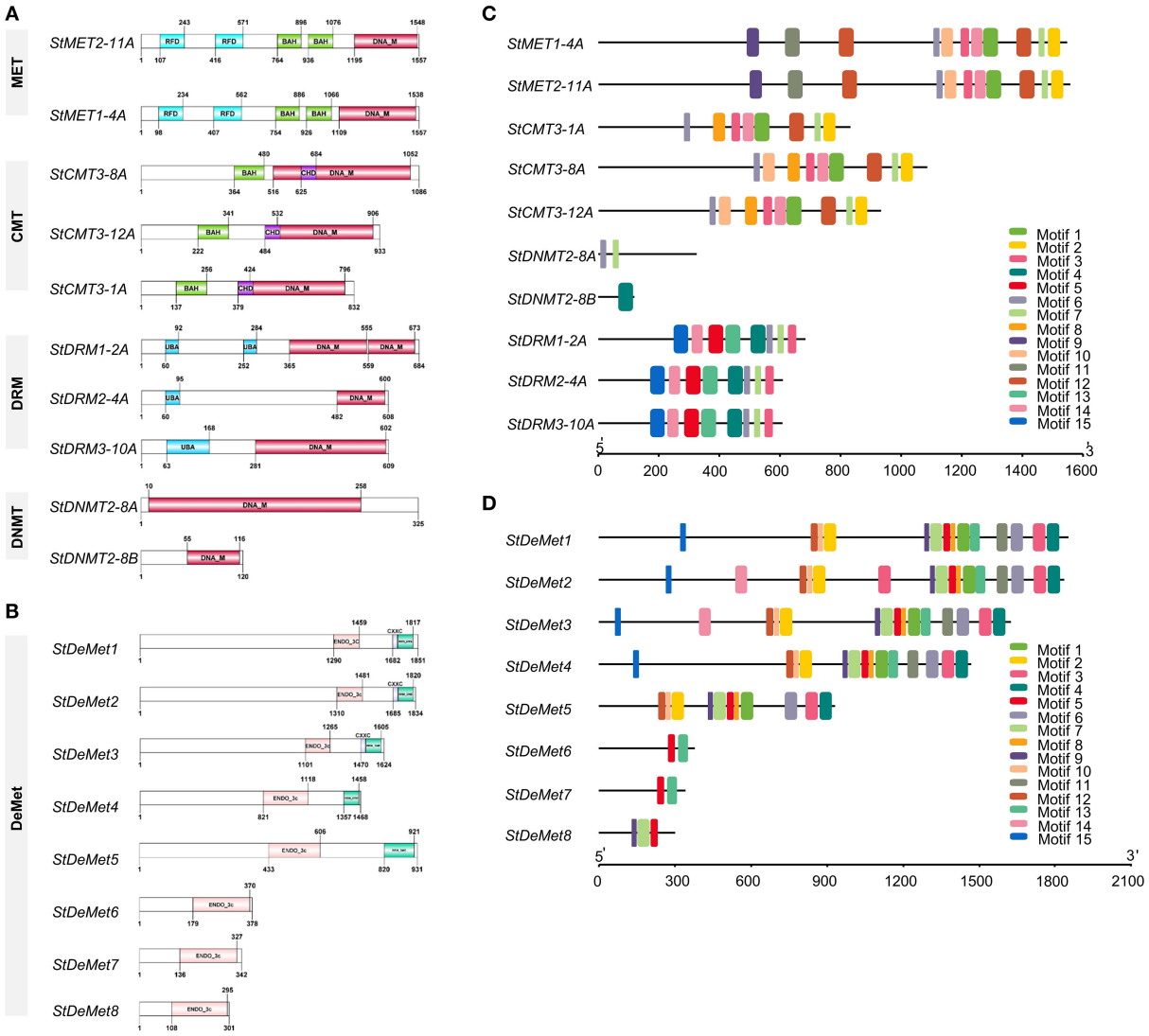

FIGURE 2
Schematic structures of conserved domains present in *StC5-MTase* **(A)** and *StDeMet* **(B)** proteins. The conserved motifs present in C5-MTase **(C)** and DNA demethylase **(D)** genes in *Solanum tuberosum*. (i) The conserved domains in the CMT family possess CHROMO (Chromatin organization modifier) and one BAH (Bromo Adjacent Homology); (ii) MET has two BAH and an RFD domains; (iii) DRM family has a unique UBA domain (Ubiquitin-associated); whereas (iv) DNMT has shorter protein length due to lack of N-terminal regulatory domain. *StDeMet* family possesses DNA glycosylase (ENDO_3C), RNA Recognition Motif (RRM), and methylated CpG discriminating (CXXC). The color boxes in the motif represent the position of different motifs and box sizes show the length (aa) of motifs.

of *StMET1-4A* and *StMET2-11A* showed a significant decline both in leaf and floral tissues in heat-sensitive genotype as compared to heat tolerant. However, stolon tissue shows upregulation and downregulation of *StMET1-4A* and *StMET2-11A*, respectively, in heat-sensitive cultivar. *StDNMT-8A* and *StDNMT-8B* expression level is predominantly detected in stolon tissues of HS. Moreover, heat induced the expression of *StDNMT-8B* in the flower of HT. The expression profile of the CMT subfamily is significantly higher in HT as compared to HS across three tissues (leaf, flower, and stolon) except *StCMT3-1A*. *StDRM1-2A* is downregulated in HT and HS in all samples. Interestingly, the expression level of *StDRM2-4A* increased in leaves, flowers, and stolon in heat-tolerant genotype. Overall, *C5-MTase* genes respond differently in different tissues of two genotypes, wherein CMT and DRM subfamilies showed pronounced heat-induced upregulation in the tolerant genotype.

DeMets are involved in DNA demethylation, and we observed a varied expression pattern across different tissues and genotypes. Heat resulted in the downregulation of *StDeMet1* in flower; however, the stolon tissue showed upregulation in the HS genotype. In contrast, *StDeMet1* showed upregulation in flower. In general, *StDeMet2* expression was downregulated in all the tissues of both the genotypes under heat stress, except the stolon of HT where it showed upregulation. Importantly,

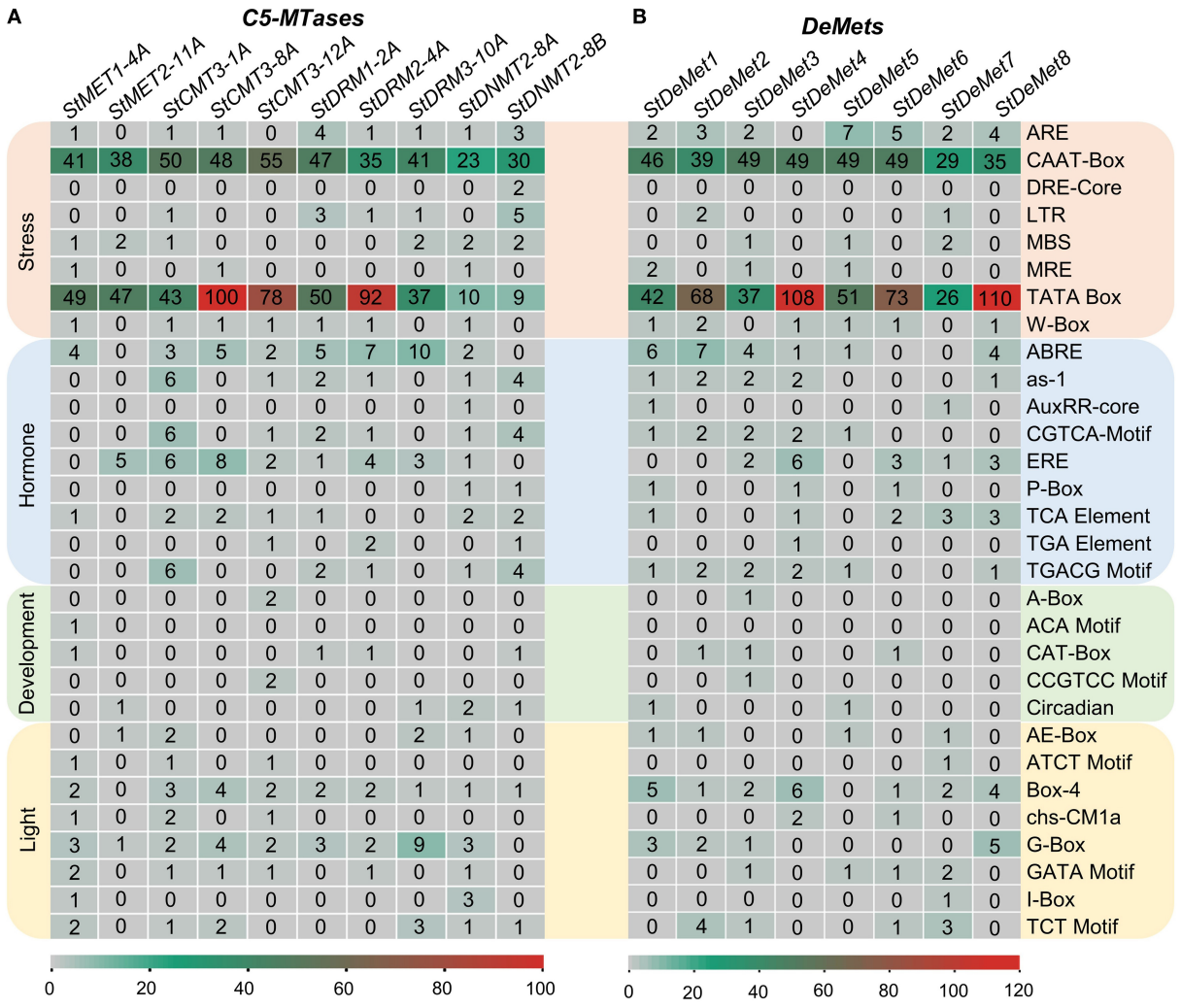

FIGURE 3
Cis-acting regulatory elements in the promoters of **(A)** *StC5-MTase* and **(B)** *StDeMets*. Cis-regulatory elements are classified into four categories (light, development, hormones and stress responses). The numbers in the heat map depict the abundance of cis-regulatory elements in the promoter region.

the expression of *StDeMet3*, *StDeMet5*, *StDeMet6*, and *StDeMet7* was induced under heat in the leaf and stolon tissues of the HT genotype. The expression of *StDeMet4*, *StDeMet5*, and *StDeMet6* were downregulated in the flower of HS. In the case of *StDeMet8*, HS leaf showed upregulation, while flower showed downregulation; however, the stolon tissue showed upregulation in both the genotypes.

Expression patterns of tuberization and HSFs genes

Several genes play an important role in tuber formation in potato, wherein the concurrent action of positive (e.g., *StSP6A* and *StBEL5*) and negative regulators (e.g., *StSUT4*, *StSP5G*, and *StRAP1*) determine the tuber yield. Also, Heat Shock Factors (HSFs) are well-known to impart thermotolerance in plants. Thus, we analyzed the expression of tuberization and HSF genes in the leaf and stolon tissues (Figure 7).

Heat resulted in the downregulation of *StSUT4* expression in the leaf tissues of the HT genotype, whereas *StSP5G* showed significant upregulation in stolon tissues of the HS genotype. *StSP6A* is a master regulator of tuberization that is affected by high-temperature stress. Heat resulted in the significant suppression of *StSP6A* in leaves of HS genotype compared to HT genotype (Figure 7). However, unexpectedly intrinsic basal transcript level was maintained in stolon tissues of HS and HT genotypes. *StBEL5* expression was downregulated by high temperature in the leaf tissue of the HS genotype,

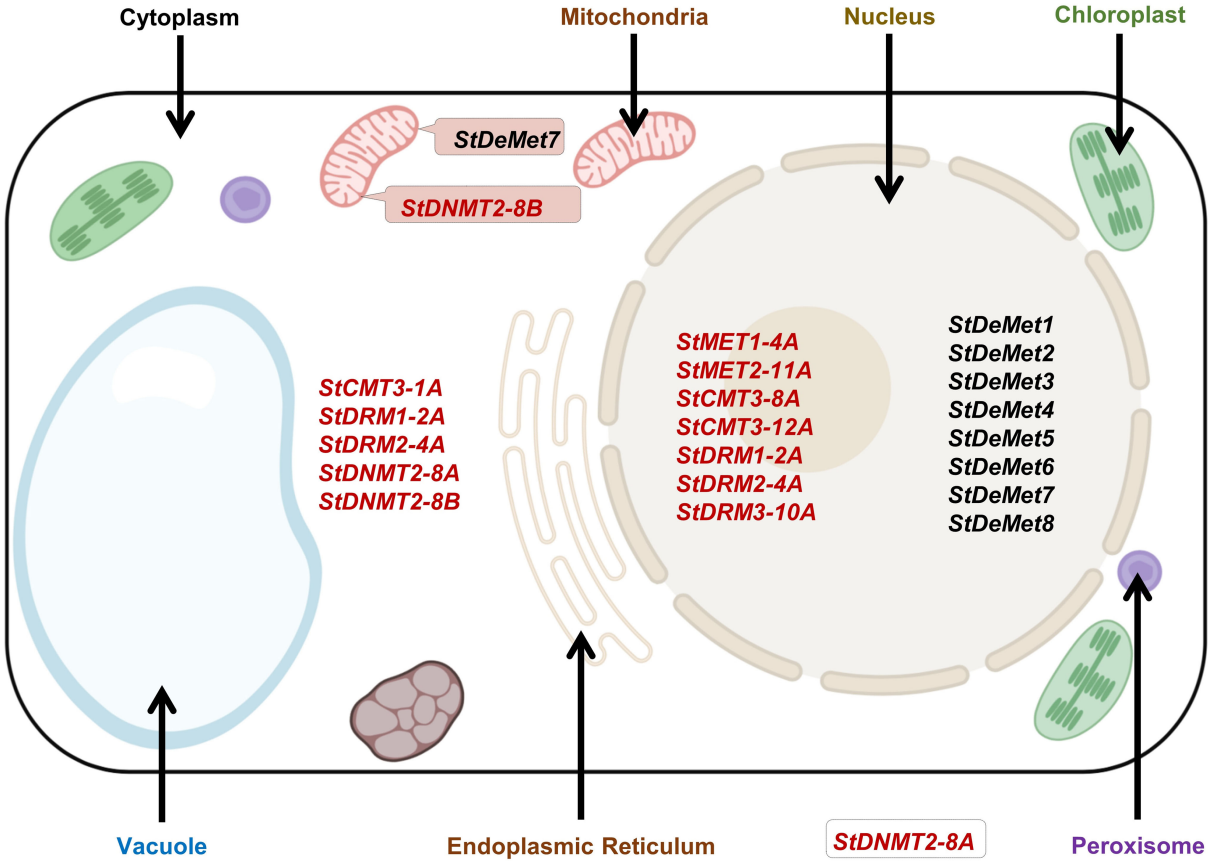

FIGURE 4
Subcellular localization of StC5-MTase and StDeMet proteins in potato predicted using the CELLO program. Partially adapted from Gahlaut et al. (2020).

while it was stable across leaf and stolon tissues of the HT genotype. *StRAP1* showed enhanced expression in leaves while it remained unaltered in stolons of HS genotype. Furthermore, the expression of HSFs was quantified. We found that *StHSFA5* and *StHSFA8* were strongly upregulated in the HT genotype both in leaves and stolons tissues under heat stress, suggesting its role in thermotolerance.

Discussion

Potato is a temperate crop that is challenged by several environmental cues such as high temperature. High-temperature exposure alters the partitioning of assimilates and accumulation of biomass in plant organs, which results in stem elongation, an increase in leaf number, and a decline in tuber yield (Wolf et al., 1991; Lafta and Lorenzen, 1995). A complex gene regulatory network comprising FT orthologs SELF PRUNING 6A (*StSP6A*) and SELF PRUNING 5G (*StSP5G*), CONSTANS-LIKE 1 (*StCOL1*), BEL1-like homeodomain (*StBEL5*), and an AP2-like gene (*StRAP1*) plays an important role in potato tuberization (Navarro et al., 2011; Hancock et al., 2014). For example, SP6A is a master regulator that interacts with its FD partner (*StFDL*) and scaffold protein St14-3-3 to form Tuber Activating Complex (TAC) to induce stolon–tuber induction (Hannapel and Banerjee, 2017). Recent developments have established that the *StSP6A* transcript is suppressed under elevated temperature, possibly through another FT homolog, *StSP5G*, which functions to repress tuberization through the accumulation of *StCO*. Similarly the antagonistic role of FT homologs in controlling flowering time in sugar beet has been reported (Pin et al., 2010). Furthermore, high temperature causes *SP6A* repression by a micro-RNA named SUPPRESSING OF SP6A (SES; Lehretz et al., 2019). Also, recently it has been shown that *SP6A* is suppressed transcriptionally and post-transcriptionally under high-temperature stress (Park et al., 2022). Epigenetic components are also involved in potato tuberization, wherein Polycomb Repressive Complex (PRC)-mediated histone modifications repress several target genes by H3K27 trimethylation (Kumar et al., 2021). The role

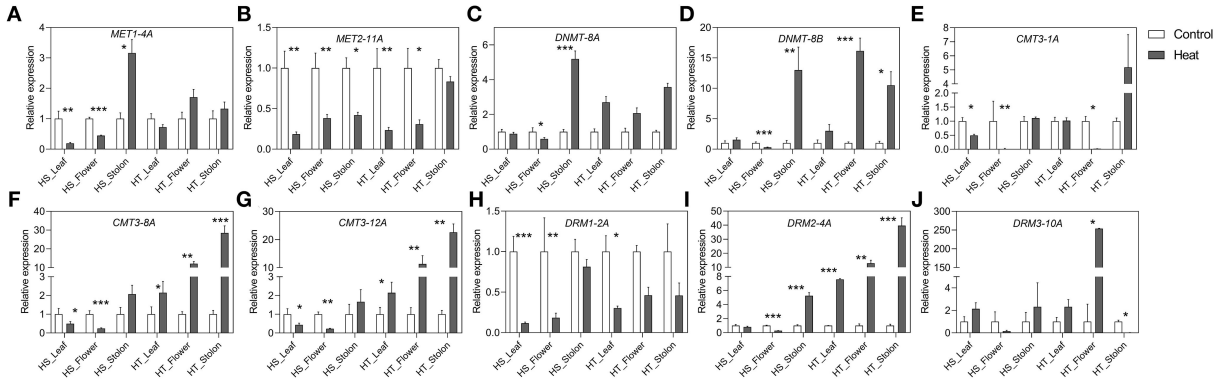

FIGURE 5
(A–J) Relative expression levels of potato *C5-MTase* genes in different tissues in heat sensitive (HS) and tolerant (HT) genotypes under high-temperature stress. Three biological samples were measured with three technical replicates. The fold change in RNA levels was calculated as the $2-\Delta\Delta Ct$ value relative to the mean values obtained in the leaf, flower and stolon samples (set at a value of 1.0). Standard errors of the means are shown with one, two and three asterisks indicating significant differences ($p < 0.05$, $p < 0.01$, $p < 0.001$, respectively) using a student's *t*-test.

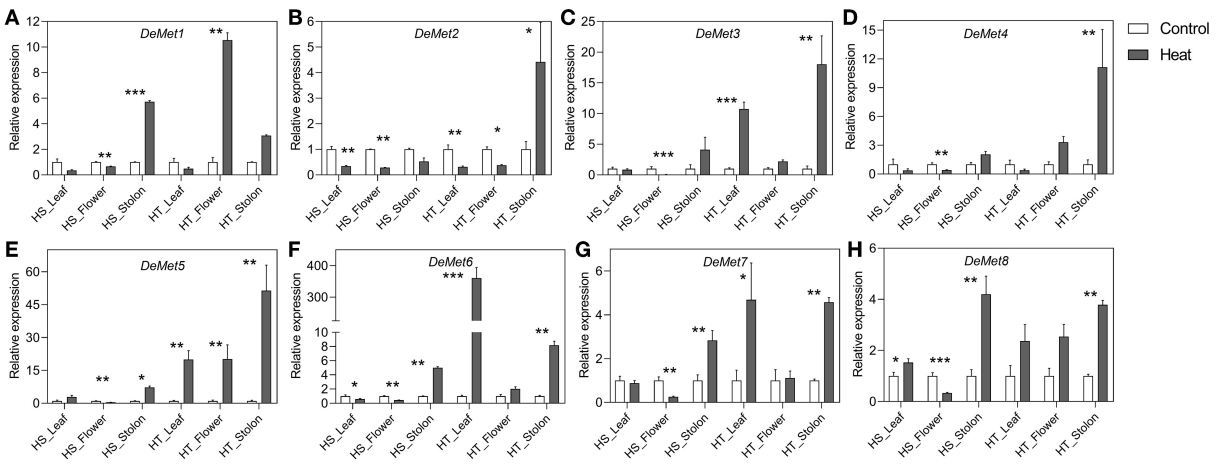

FIGURE 6
(A–H) Relative expression levels of potato DeMet genes in different tissues in heat sensitive (HS) and tolerant (HT) genotypes under high temperature stress. Three biological samples were measured with three technical replicates. The fold change in RNA levels was calculated as the $2-\Delta\Delta Ct$ value relative to the mean values obtained in the leaf, flower and stolon samples (set at a value of 1.0). Standard errors of the means are shown with one, two and three asterisks indicating significant differences ($p < 0.05$, $p < 0.01$, $p < 0.001$, respectively) using a student's *t*-test.

of DNA methylation in photoperiod-mediated tuberization has also been recently reported (Ai et al., 2021). However, DNA methylation and demethylation enzymes remain uncharacterized in potatoes and their role in potato tuberization under high temperature is unexplored. The concurrent action of DNA methyltransferase and demethylase carries out DNA methylation and demethylation respectively (Lang et al., 2017).

In the present study, we identified several *C5-MTases* and *DeMets* in potatoes and studied their expression dynamics in the different tissues of the two contrasting genotypes, *viz.* Kufri Chandramukhi (heat sensitive) and Kufri Kiran (heat tolerant) under high temperature stress. We found 10 *C5-MTase* and 8 *DeMets* in potato, and several C5-MTase and DeMets were also reported in other allotetraploid soybean and peanut (Song et al., 2013; Wang et al., 2016), which is comparatively higher than the diploid species (Kong et al., 2020). This suggests that polyploidization events potentially contribute to the enhancement of plant epigenetic factors. Furthermore, based on their domain structure and phylogenetic analysis, C5-MTases were divided into four different subfamilies, *viz.* METs, CMTs, DRMs, and DNMTs. The members within the same subfamily shared similar domain architecture and exon-intron boundary, but it differed between sub-families. Our results are consistent with the previous reports on *Solanum lycopersicum*

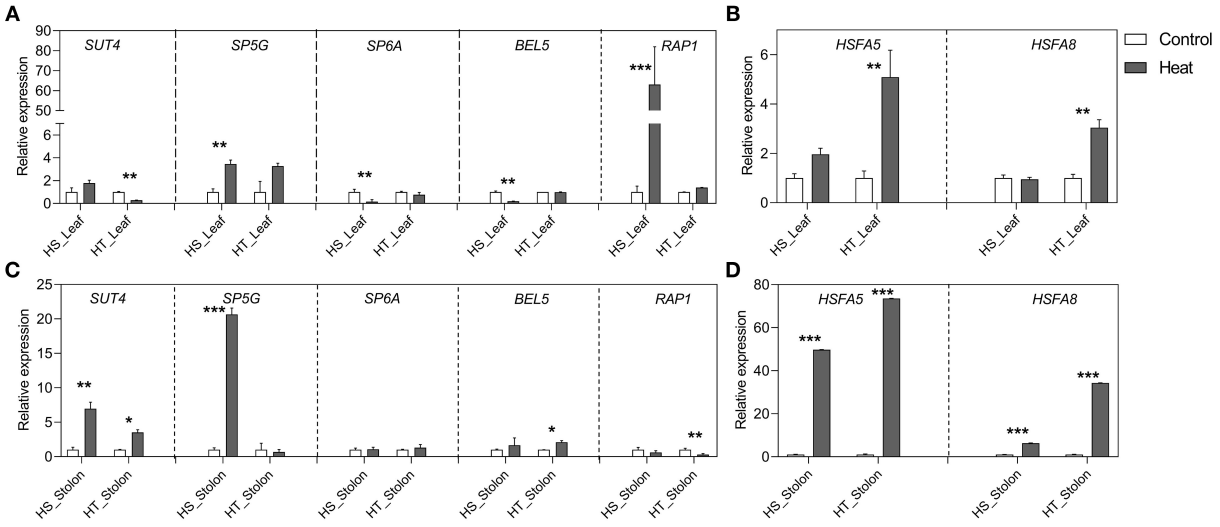

FIGURE 7
Relative expression levels of potato tuberization genes and HSFs in leaf **(A,B)** and stolon **(C,D)** tissues in heat-sensitive (HS) and -tolerant (HT) genotypes under high-temperature stress. Three biological samples were measured with three technical replicates. The fold change in RNA levels was calculated as the $2-\Delta\Delta Ct$ value relative to the mean values obtained in the leaf and stolon samples (set at a value of 1.0). Standard errors of the means are shown with one, two, and three asterisks indicating significant differences ($p < 0.05$, $p < 0.01$, $p < 0.001$, respectively) using a Student's *t*-test.

(Cao et al., 2014). The principal maintenance of symmetric CG methylation is operated by METs, an ortholog of mammalian DNMT1 (Zhang et al., 2018). Contrastingly, METs in plants cannot distinguish hemimethylated CG dinucleotides from non-methylated CG, unlike DNMT1, as it lacks a cysteine-rich CXXC domain (Song et al., 2011). BAH domain of METs facilitates protein-protein interactions, which result in inhibition of gene expression and establish an interconnection among cytosine methylation, replication, and transcription (Callebaut et al., 1999). CMTs are involved in maintaining CHG methylation in centromeric and transposable regions (Gehring and Henikoff, 2008). The chromodomain of CMTs is responsible for protein association with heterochromatin (Gehring and Henikoff, 2008). The protein structure of maize revealed the association of chromo and BAH domain with H3K9me2 and shed light on the functional activity of CMTs (Stroud et al., 2014). The maintenance of "non-symmetrical" CHH methylation is catalyzed by DRMs that operates through the RNA-directed DNA methylation pathway (RdDM). The N-terminal UBA domain provides a connecting link between DNA methylation and ubiquitin-mediated protein degradation. This domain also promotes the degradation of DRMs at specific points in the cell cycle (Cao et al., 2000).

DeMets in potato also has conserved domains that are responsible for functional identity and activity (Zhang et al., 2018). The functional demethylases contain HhH-GPD (Endo_3c) domain that is responsible for cleaving glycosidic bonds and generating AP sites (Gehring and Henikoff, 2008). Sometimes, two additional conserved domains named RNA recognition motif (RRM) and methylated CpG discriminating CXXC domain are also found (Iyer et al., 2011). The evolutionary studies revealed that *DeMets* expression varied across species of different genotypes (Yang et al., 2019).

The sub-cellular localization of any protein is important for determining its function in plants. Therefore, we performed *in-silico* subcellular prediction to identify the location of *C5-MTases* and *DeMets*. *C5-MTases* were localized either in the nucleus or in the cytoplasm. These results are consistent with the previous studies on *Solanum lycopersicum*, which reported the localization of *C5-MTase* in the nucleus and cytoplasm (Cao et al., 2014). The presence of *C5-MTase* in both these organelles indicates its possible involvement in stress management machinery (Gahlaut et al., 2020). The exclusive nuclear localization of *DeMets* suggests its potential role in replication and transcriptional regulation (Wang et al., 2016).

Cis-regulatory elements play an important role in the regulation of biological processes and molecular function under developmental transitions and stress episodes (Yamaguchi-Shinozaki and Shinozaki, 2005). The promoter analysis of potato *C5-MTase* and *DeMets* revealed that cis-regulatory elements are classified into four categories such as light response, development, hormones, and stress responses. The presence of CAAT box in the promoter region plays an essential role in leaf development by modulating jasmonate pathways in proliferating tissues as reported in *Nicotiana benthamiana* (*NbCMT3–2*; Lin et al., 2015). The predominance of TATA box

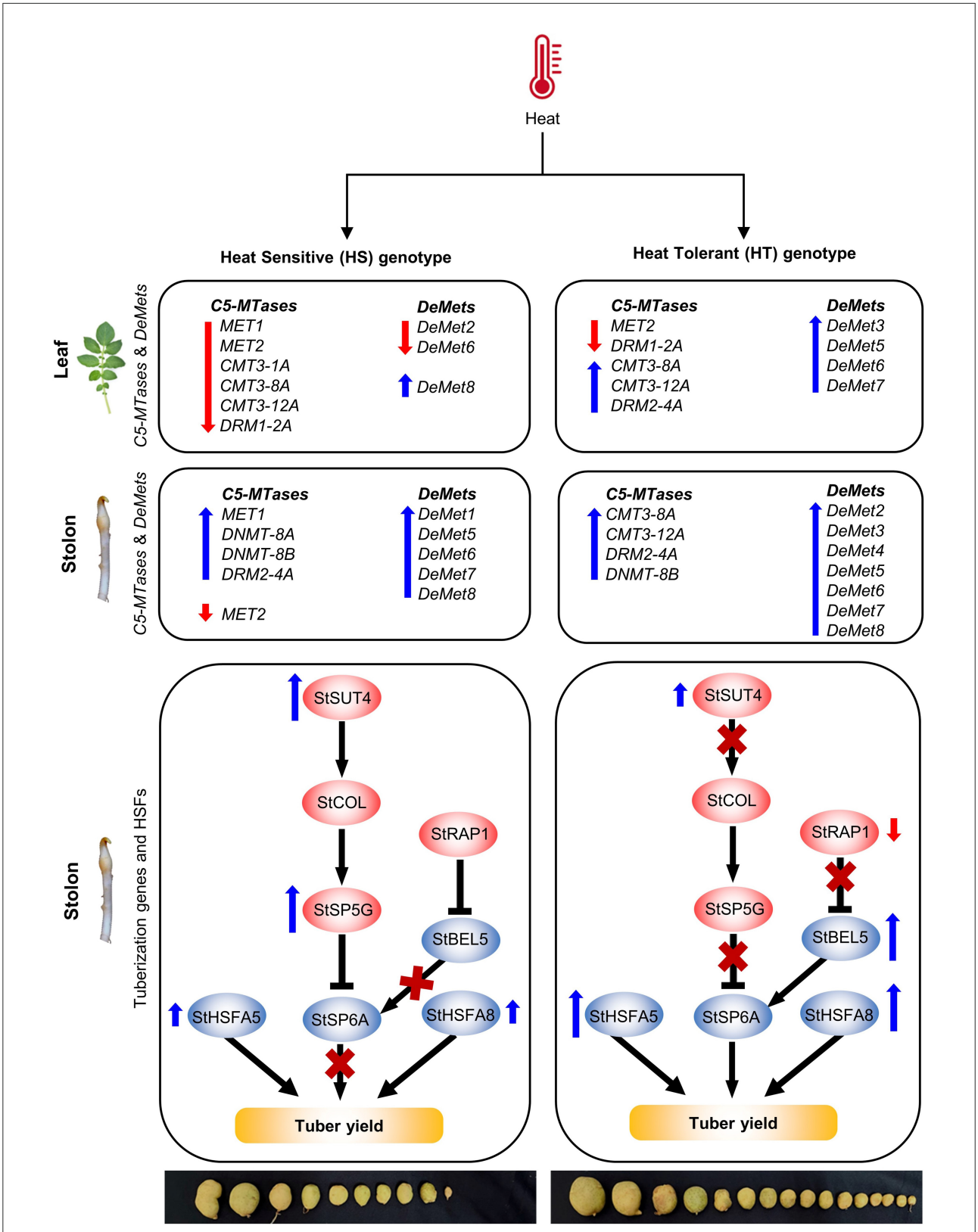

FIGURE 8
The schematic model depicting the role of *C5-MTase* and *DeMets* gene with potato tuberization genes under high temperature in heat-tolerant (HT) and heat-sensitive (HS) genotype: Tuberization is regulated by positive (*StSP6A and StBEL5*) and negative regulators (*StSUT4*, *StSP5G*, and *StRAP1*). Under high temperature, the positive regulators were relatively stable in the HT genotype as compared to the HS genotype. The

(Continued)

FIGURE 8 (Continued)
stability might be attributed by reduced expression of upstream negative regulators, increased DNA demethylation (*StDeMet2*, *StDeMet3*, *StDeMet4*, *StDeMet5*, *StDeMet6*, *StDeMet7*, and *StDeMet8*) and active RdDM (DRM and CMT subfamilies) pathway in leaves and stolon samples of HT genotype. On the contrary, the HS genotype has heat-induced upregulation of negative regulators, thereby affecting the process of tuberization. Stronger upregulation of HSFs (*StHSFA5* and *StHSFA8*) was observed in leaves and stolon tissues of HT genotype as compared to HS genotype maintaining the health status of the tolerant cultivar.

elements in the promoter region confers stress responsiveness, whereas TATA-less genes are related to cell growth or housekeeping activity (Bae et al., 2015). The abundance of ABRE and ERE in all the members demonstrates the active role of *C5-MTase* and *DeMets* in abscisic acid and ethylene responsiveness (Kaur and Asthir, 2017). Also, stress-specific regulatory elements such as ARE and MBS were found in the *C5-MTase* of the tea plant (Zhu et al., 2020). Overall, these findings highlight the role of potato's *C5-MTase* and *DeMets* in plant development and stress responses (Gahlaut et al., 2020).

The relationship between DNA methylation and heat stress is less explored. DNA methylation level in different tissues regulates plant growth and development *via* controlling the transcript levels of developmentally important genes (Zhang et al., 2018). We investigated the expression pattern of *C5-MTase* and *DeMets* in two contrasting genotypes across different tissues and observed differential DNA methylation. Our results are similar to studies on rice and rapeseed (Karan et al., 2012; Gao et al., 2014). The decline in expression of *StMET1-4A* and *StMET2-11A* in leaf and floral tissues in heat-sensitive genotype possibly led to reduced CG methylation.

Similarly, Arabidopsis *met1* mutant with reduced MET level showed delayed flowering and juvenile-to-adult transition (Kankel et al., 2003). Such delayed flowering was due to hypomethylation of transposable element (TE) upstream of the *FLOWERING WAGENINGEN* (*FWA*) gene (Kankel et al., 2003). This shows how MET regulates the morphological characteristics and flowering time of plants (Finnegan and Kovac, 2000). We also found that CMT and DRM subfamilies showed pronounced heat-induced upregulation in the tolerant genotype. These findings indicate the role of CMT and DRM in the suppression of TEs (Ramakrishnan et al., 2021). High-temperature stress causes genomic instability and impairs plant health by activating TEs such as *ONSEN* (Chang et al., 2020). Several plant developmental abnormalities have been observed in the DNA methylation-free *C5-MTase* mutants of Arabidopsis, suggesting their role in controlling gene expression and developmental processes in plants (He et al., 2022). However, the reduced expression of CMT and DRM subfamilies in heat-sensitive genotypes across different tissues might be an alternative strategy to recover from heat stress by causing activation of SUPPRESSOR OF DRM1 DRM2 CMT3 (SDC), thus leading to loss of non-CG methylation (Popova et al., 2013). Differential methylation landscapes between genotypes can potentially contribute to stress adaptation (Eriksson et al., 2020).

Heat-induced DNA demethylase gene expression was observed in both genotypes. The expression of the demethylase gene family was more pronounced in HT genotype as compared to the HS genotype. Our results showed that *DeMets-like StDeMet2,StDeMet3*, *StDeMet4*, *StDeMet5*, *StDeMet6*, and *StDeMet7,* were significantly expressed in stolons of HT genotype. Such results are consistent with the increased expression of *ROS* and *DML* like demethylase gene family in Arabidopsis (Hsieh et al., 2009), suggesting its involvement in combating abiotic stress events. Consistently, active DNA demethylation is also associated with the upregulation of stress-responsive genes (Verhoeven et al., 2010).

DNA methylation and demethylation events are correlated with the gene expression patterns, thus regulating plant development and stress responses (Choi and Sano, 2007). Also, the genetic control of potato tuberization is well-studied. We observed that the expression of positive regulators of tuberization (*StSP6A* and *StBEL5*) was found to be stable in the leaves and stolon tissues in the HT genotype as compared to the HS genotype under high-temperature stress (Figure 8). The stability of the *StSP6A* transcript under high temperature in HT genotype might be due to the reduced expression of upstream negative regulators (*StSUT4*, *StSP5G*, and *StRAP1*). Heat induced the expression of *StSUT4* in the leaves and stolons of the HS genotype, which might have led to the activation of the *StCOL1-StSP5G* regulatory module. Such studies are consistent with the recent finding that elevated temperature caused higher *StCOL1* accumulation and suppressed potato tuberization (Park et al., 2022). Our expression analysis revealed the higher expression of *StSP5G* transcript under high temperature in the HS genotype. However, such enhanced expression of *StSP5G* did not alter the basal transcription of *StSP6A* in stolons of HS genotype. The expression levels of *StSP5G* and *StSP6A* are usually difficult to interpret in vegetative tissues like stolons and tubers (Hancock et al., 2014). In addition, different regulatory pathways operate for photoperiod and temperature-dependent tuberization, suggesting that a complex regulatory network is involved in the regulation of potato tuberization (Park et al., 2022).

Additionally, we observed a spike in *StRAP1* expression (<50-fold) in leaves of HS genotype, which acts to suppress a phloem mobile transcript (*StBEL5*), thereby delaying tuber induction (Banerjee et al., 2006). Other than genetic factors,

the role of DNA methylation machinery components was sought in potato tuberization under high temperature. The increased expression of positive regulators of tuberization in HT genotype might be due to increased DNA demethylation and the active RdDM pathway in the stolons. Furthermore, we observed stronger upregulation of *StHSFA5 and StHSFA8* (<3 and <5-fold, respectively) in leaves and (<50- and <30-fold) in stolons of the tolerant genotype as compared to the HS genotype. This may contribute to the better heat stress resilience of the HT genotype (Tang et al., 2016; Ramakrishnan et al., 2022). Altogether, a complex interplay of genetic and epigenetic factors controls potato tuberization under high-temperature conditions.

Conclusion

Over the last few decades, the mechanisms underlying plant responses to abiotic stresses have been studied in most of the model plants such as Arabidopsis, rice, and tomato. However, only a few studies are available on other important crops such as potato. More detailed studies are needed to shed light on the signaling networks and downstream target genes controlling potato response to heat stress. Importantly, understanding the interplay of genetic and epigenetic factors in plant stress response will provide new avenues for crop improvement. In this work, we report the characterization of DNA methyltransferase and demethylase gene families in the potato. The expression of *C5-MTases* and *DeMets* were studied in the different tissues of heat-tolerant and heat-sensitive genotypes followed by the expression analysis of tuberization genes. We found enhanced expression of *DeMets* and RdDM genes in HT genotype as compared to HS genotype. These results suggest that increased activity of *DeMets* might have contributed to transcriptional activation of tuberization genes wherein *RdDM* stabilized genomic integrity of HT genotype. Overall, this work will open new research directions on the role of DNA methylation machinery in potato tuberization under high temperature, which is important in the context of global temperature rise.

Data availability statement

The raw data supporting the conclusions of this article will be made available by the authors, without undue reservation.

Author contributions

MD performed *in silico* analysis, experiments, analyzed data, and wrote the original draft with figures. VR performed *in silico* analysis and experiments. VG performed *in silico* analysis and writing. AK, PS, and VV performed experiments. VKG and SS provided material and discussed data. GZ conceived the idea, edited, and finalized the manuscript. All authors contributed to the article and approved the submitted version.

Acknowledgments

MD and VR acknowledge UGC for Junior Research Fellowship. SS and VKG acknowledge the support of institutional project from ICAR-CPRI, Shimla. GZ acknowledges the financial support obtained from the projects *viz*. MLP-201, CSIR-FIRST (MLP-178), and DST-SERB-SRG (GAP-294). This manuscript represents CSIR-IHBT publication number 5102.

Conflict of interest

The authors declare that the research was conducted in the absence of any commercial or financial relationships that could be construed as a potential conflict of interest.

Publisher's note

All claims expressed in this article are solely those of the authors and do not necessarily represent those of their affiliated organizations, or those of the publisher, the editors and the reviewers. Any product that may be evaluated in this article, or claim that may be made by its manufacturer, is not guaranteed or endorsed by the publisher.

Supplementary material

The Supplementary Material for this article can be found online at: https://www.frontiersin.org/articles/10.3389/fpls.2022.933740/full#supplementary-material

References

Ai, Y., Jing, S., Cheng, Z., Song, B., Xie, C., Liu, J., et al. (2021). DNA methylation affects photoperiodic tuberization in potato (*Solanum tuberosum* L.) by mediating the expression of genes related to the photoperiod and GA pathways. *Hortic. Res.* 8, 181. doi: 10.1038/s41438-021-00619-7

Artimo, P., Jonnalagedda, M., Arnold, K., Baratin, D., Csardi, G., De Castro, E., et al. (2012). ExPASy: SIB bioinformatics resource portal. *Nucl. Acids Res.* 40, W597–W603. doi: 10.1093/nar/gks400

Bae, S.-H., Han, H. W., and Moon, J. (2015). Functional analysis of the molecular interactions of TATA box-containing genes and essential genes. *PLoS ONE* 10, e0120848. doi: 10.1371/journal.pone.0120848

Bailey, T. L., Boden, M., Buske, F. A., Frith, M., Grant, C. E., Clementi, L., et al. (2009). MEME SUITE: tools for motif discovery and searching. *Nucleic Acid. Res.* 37, W202–W208. doi: 10.1093/nar/gkp335

Banerjee, A. K., Chatterjee, M., Yu, Y., Suh, S.-G., Miller, W. A., and Hannapel, D. J. (2006). Dynamics of a mobile RNA of potato involved in a long-distance signaling pathway. *Plant Cell* 18, 3443–3457. doi: 10.1105/tpc.106.042473

Beals, K. A. (2019). Potatoes, nutrition, and health. *Am. J. Potato Res.* 96, 102–110. doi: 10.1007/s12230-018-09705-4

Birch, P. R., Bryan, G., Fenton, B., Gilroy, E. M., Hein, I., Jones, J. T., et al. (2012). Crops that feed the world 8: potato: are the trends of increased global production sustainable? *Food Secur.* 4, 477–508. doi: 10.1007/s12571-012-0220-1

Callebaut, I., Courvalin, J.-C., and Mornon, J.-P. (1999). The BAH (bromo-adjacent homology) domain: a link between DNA methylation, replication and transcriptional regulation. *FEBS Lett.* 446, 189–193. doi: 10.1016/S0014-5793(99)00132-5

Cao, D., Ju, Z., Gao, C., Mei, X., Fu, D., Zhu, H., et al. (2014). Genome-wide identification of cytosine-5 DNA methyltransferases and demethylases in *Solanum lycopersicum*. *Gene* 550, 230–237. doi: 10.1016/j.gene.2014.08.034

Cao, X., Aufsatz, W., Zilberman, D., Mette, M. F., Huang, M. S., Matzke, M., et al. (2003). Role of the DRM and CMT3 methyltransferases in RNA-directed DNA methylation. *Curr. Biol.* 13, 2212–2217. doi: 10.1016/j.cub.2003.11.052

Cao, X., Springer, N. M., Muszynski, M. G., Phillips, R. L., Kaeppler, S., and Jacobsen, S. E. (2000). Conserved plant genes with similarity to mammalian *de novo* DNA methyltransferases. *Proc. National Acad. Sci. U. S. A.* 97, 4979–4984. doi: 10.1073/pnas.97.9.4979

Chang, Y. N., Zhu, C., Jiang, J., Zhang, H., Zhu, J. K., and Duan, C. G. (2020). Epigenetic regulation in plant abiotic stress responses. *J. Intergrat. Plant Biol.* 62, 563–580. doi: 10.1111/jipb.12901

Change, I. C. (2013). *The Physical Science Basis*. Cambridge: Cambridge University Press.

Chatterjee, M., Banerjee, A. K., and Hannapel, D. J. (2007). A BELL1-like gene of potato is light activated and wound inducible. *Plant Physiol.* 145, 1435–1443. doi: 10.1104/pp.107.105924

Chen, C., Chen, H., He, Y., and Xia, R. (2018). TBtools, a toolkit for biologists integrating various biological data handling tools with a user-friendly interface. *BioRxiv* 2018, 289660. doi: 10.1101/289660

Cheng, X., Kumar, S., Posfai, J., Pflugrath, J. W., and Roberts, R. J. (1993). Crystal structure of the Hhal DNA methyltransferase complexed with S-adenosyl-L-methionine. *Cell* 74, 299–307. doi: 10.1016/0092-8674(93)90421-L

Choi, C.-S., and Sano, H. (2007). Abiotic-stress induces demethylation and transcriptional activation of a gene encoding a glycerophosphodiesterase-like protein in tobacco plants. *Mol. Genet. Genom.* 277, 589–600. doi: 10.1007/s00438-007-0209-1

Davis, M. W., and Jorgensen, E. M. (2022). ApE, A plasmid Editor: a freely available DNA manipulation and visualization program. *Front. Bioinf.* 2, 818619. doi: 10.3389/fbinf.2022.818619

Dowen, R. H., Pelizzola, M., Schmitz, R. J., Lister, R., Dowen, J. M., Nery, J. R., et al. (2012). Widespread dynamic DNA methylation in response to biotic stress. *Proc. National Acad. Sci. U. S. A.* 109, E2183–E2191. doi: 10.1073/pnas.1209329109

Dutt, S., Manjul, A. S., Raigond, P., Singh, B., Siddappa, S., Bhardwaj, V., et al. (2017). Key players associated with tuberization in potato: potential candidates for genetic engineering. *Crit. Rev. Biotechnol.* 37, 942–957. doi: 10.1080/07388551.2016.1274876

Eriksson, M. C., Szukala, A., Tian, B., and Paun, O. (2020). Current research frontiers in plant epigenetics: an introduction to a Virtual Issue. *New Phytol.* 226, 285. doi: 10.1111/nph.16493

FAOSTAT (2021). *Food and Agriculture Data*. Available online at: http://faostat.fao.org (accessed April 15, 2022).

Finnegan, E., and Kovac, K. (2000). Plant DNA methyltransferases. *Plant Mol. Biol.* 43, 189–201. doi: 10.1023/a:1006427226972

Finnegan, E. J., Peacock, W. J., and Dennis, E. S. (1996). Reduced DNA methylation in *Arabidopsis thaliana* results in abnormal plant development. *Proc. Natl. Acad. Sci. U. S. A.* 93, 8449–8454. doi: 10.1073/pnas.93.16.8449

Gahlaut, V., Samtani, H., and Khurana, P. (2020). Genome-wide identification and expression profiling of cytosine-5 DNA methyltransferases during drought and heat stress in wheat (*Triticum aestivum*). *Genomics* 112, 4796–4807. doi: 10.1016/j.ygeno.2020.08.031

Gallego-Bartolomé, J., Gardiner, J., Liu, W., Papikian, A., Ghoshal, B., Kuo, H. Y., et al. (2018). Targeted DNA demethylation of the Arabidopsis genome using the human TET1 catalytic domain. *Proc. National Acad. Sci. U. S. A.* 115, E2125–E2134. doi: 10.1073/pnas.1716945115

Gao, Y., Jia, L., Hu, B., Alva, A., and Fan, M. (2014). Potato stolon and tuber growth influenced by nitrogen form. *Plant Prod. Sci.* 17, 138–143. doi: 10.1626/pps.17.138

Garg, R., Narayana Chevala, V., Shankar, R., and Jain, M. (2015). Divergent DNA methylation patterns associated with gene expression in rice cultivars with contrasting drought and salinity stress response. *Sci. Rep.* 5, 1–16. doi: 10.1038/srep14922

Gehring, M., and Henikoff, S. (2008). DNA methylation and demethylation in Arabidopsis. *Arabidopsis Book* 6, e0102. doi: 10.1199/tab.0102

Hancock, R. D., Morris, W. L., Ducreux, L. J., Morris, J. A., Usman, M., Verrall, S. R., et al. (2014). Physiological, biochemical and molecular responses of the potato (*Solanum tuberosum* L.) plant to moderately elevated temperature. *Plant Cell Environ.* 37, 439–450. doi: 10.1111/pce.12168

Hannapel, D. J., and Banerjee, A. K. (2017). Multiple mobile mRNA signals regulate tuber development in potato. *Plants* 6, 8. doi: 10.3390/plants6010008

Hastilestari, B. R., Lorenz, J., Reid, S., Hofmann, J., Pscheidt, D., Sonnewald, U., et al. (2018). Deciphering source and sink responses of potato plants (*Solanum tuberosum* L.) to elevated temperatures. *Plant Cell Environ.* 41, 2600–2616. doi: 10.1111/pce.13366

He, L., Huang, H., Bradai, M., Zhao, C., You, Y., Ma, J., et al. (2022). DNA methylation-free Arabidopsis reveals crucial roles of DNA methylation in regulating gene expression and development. *Nat. Commun.* 13, 1–16. doi: 10.1038/s41467-022-28940-2

Hirsch, C. D., Hamilton, J. P., Childs, K. L., Cepela, J., Crisovan, E., Vaillancourt, B., et al. (2014). Spud DB: A resource for mining sequences, genotypes, and phenotypes to accelerate potato breeding. *Plant Genome* 7, plantgenome2013.12.0042. doi: 10.3835/plantgenome2013.12.0042

Hsieh, T.-F., Ibarra, C. A., Silva, P., Zemach, A., Eshed-Williams, L., Fischer, R. L., et al. (2009). Genome-wide demethylation of Arabidopsis endosperm. *Science* 324, 1451–1454. doi: 10.1126/science.1172417

Hu, B., Jin, J., Guo, A.-Y., Zhang, H., Luo, J., and Gao, G. (2015). GSDS 2.0: an upgraded gene feature visualization server. *Bioinformatics* 31, 1296–1297. doi: 10.1093/bioinformatics/btu817

Iyer, L. M., Abhiman, S., and Aravind, L. (2011). Natural history of eukaryotic DNA methylation systems. *Progr. Mol. Biol. Trans. Sci.* 101, 25–104. doi: 10.1016/B978-0-12-387685-0.00002-0

Kankel, M. W., Ramsey, D. E., Stokes, T. L., Flowers, S. K., Haag, J. R., Jeddeloh, J. A., et al. (2003). Arabidopsis MET1 cytosine methyltransferase mutants. *Genetics* 163, 1109–1122. doi: 10.1093/genetics/163.3.1109

Karan, R., Deleon, T., Biradar, H., and Subudhi, P. K. (2012). Salt stress induced variation in DNA methylation pattern and its influence on gene expression in contrasting rice genotypes. *PLoS ONE* 7, e40203. doi: 10.1371/journal.pone.0040203

Kaur, G., and Asthir, B. (2017). Molecular responses to drought stress in plants. *Biol. Plant.* 61, 201–209. doi: 10.1007/s10535-016-0700-9

Kim, Y.-U., Seo, B.-S., Choi, D.-H., Ban, H.-Y., and Lee, B.-W. (2017). Impact of high temperatures on the marketable tuber yield and related traits of potato. *Eur. Agron.* 89, 46–52. doi: 10.1016/j.eja.2017.06.005

Kong, W., Xia, X., Wang, Q., Liu, L.-W., Zhang, S., Ding, L., et al. (2020). Impact of DNA demethylases on the DNA methylation and transcription of Arabidopsis NLR Genes. *Front. Genet.* 11, 460. doi: 10.3389/fgene.2020.00460

Kumar, A., Kondhare, K. R., Malankar, N. N., and Banerjee, A. K. (2021). The Polycomb group methyltransferase StE (z) 2 and deposition of H3K27me3 and

H3K4me3 regulate the expression of tuberization genes in potato. *J. Exp. Bot.* 72, 426–444. doi: 10.1093/jxb/eraa468

Kumar, S., Stecher, G., Li, M., Knyaz, C., and Tamura, K. (2018). MEGA X: molecular evolutionary genetics analysis across computing platforms. *Mol. Biol. Evol.* 35, 1547. doi: 10.1093/molbev/msy096

Lafta, A. M., and Lorenzen, J. H. (1995). Effect of high temperature on plant growth and carbohydrate metabolism in potato. *Plant Physiol.* 109, 637–643. doi: 10.1104/pp.109.2.637

Lang, Z., Wang, Y., Tang, K., Tang, D., Datsenka, T., Cheng, J., et al. (2017). Critical roles of DNA demethylation in the activation of ripening-induced genes and inhibition of ripening-repressed genes in tomato fruit. *Proc. Natl. Acad. Sci. U. S. A.* 114, E4511–E4519. doi: 10.1073/pnas.1705233114

Law, J. A., and Jacobsen, S. E. (2010). Establishing, maintaining and modifying DNA methylation patterns in plants and animals. *Nat. Rev. Genet.* 11, 204–220. doi: 10.1038/nrg2719

Lehretz, G. G., Sonnewald, S., Hornyik, C., Corral, J. M., and Sonnewald, U. (2019). Post-transcriptional regulation of FLOWERING LOCUS T modulates heat-dependent source-sink development in potato. *Curr. Biol. 29* 1614–1624. e1613. doi: 10.1016/j.cub.2019.04.027

Lescot, M., Déhais, P., Thijs, G., Marchal, K., Moreau, Y., Van De Peer, Y., et al. (2002). PlantCARE, a database of plant cis-acting regulatory elements and a portal to tools for *in silico* analysis of promoter sequences. *Nucleic Acids Res.* 30, 325–327. doi: 10.1093/nar/30.1.325

Lesk, C., Rowhani, P., and Ramankutty, N. (2016). Influence of extreme weather disasters on global crop production. *Nature* 529, 84–87. doi: 10.1038/nature16467

Lin, Y.-T., Wei, H.-M., Lu, H.-Y., Lee, Y.-I., and Fu, S.-F. (2015). Developmental- and tissue-specific expression of NbCMT3-2 encoding a chromomethylase in *Nicotiana benthamiana*. *Plant Cell Physiol.* 56, 1124–1143. doi: 10.1093/pcp/pcv036

Liu, P., Nie, W. F., Xiong, X., Wang, Y., Jiang, Y., Huang, P., et al. (2021). A novel protein complex that regulates active DNA demethylation in Arabidopsis. *J. Int. Plant Biol.* 63, 772–786. doi: 10.1111/jipb.13045

Marchler-Bauer, A., Derbyshire, M. K., Gonzales, N. R., Lu, S., Chitsaz, F., Geer, L. Y., et al. (2015). CDD: NCBI's conserved domain database. *Nucleic Acids Res.* 43, D222–D226. doi: 10.1093/nar/gku1221

Navarro, C., Abelenda, J. A., Cruz-Oró, E., Cuéllar, C. A., Tamaki, S., Silva, J., et al. (2011). Control of flowering and storage organ formation in potato by FLOWERING LOCUS T. *Nature* 478, 119–122. doi: 10.1038/nature10431

Park, J.-S., Park, S.-J., Kwon, S.-Y., Shin, A.-Y., Moon, K.-B., Park, J. M., et al. (2022). Temporally distinct regulatory pathways coordinate thermo-responsive storage organ formation in potato. *Cell Rep.* 38, 110579. doi: 10.1016/j.celrep.2022.110579

Pavlopoulou, A., and Kossida, S. (2007). Plant cytosine-5 DNA methyltransferases: structure, function, and molecular evolution. *Genomics* 90, 530–541. doi: 10.1016/j.ygeno.2007.06.011

Pin, P. A., Benlloch, R., Bonnet, D., Wremerth-Weich, E., Kraft, T., Gielen, J. J., et al. (2010). An antagonistic pair of FT homologs mediates the control of flowering time in sugar beet. *Science* 330, 1397–1400. doi: 10.1126/science.1197004

Popova, O. V., Dinh, H. Q., Aufsatz, W., and Jonak, C. (2013). The RdDM pathway is required for basal heat tolerance in Arabidopsis. *Mol. Plant* 6, 396–410. doi: 10.1093/mp/sst023

Potter, S. C., Luciani, A., Eddy, S. R., Park, Y., Lopez, R., and Finn, R. D. (2018). HMMER web server: 2018 update. *Nucleic Acids Res.* 46, W200–W204. doi: 10.1093/nar/gky448

Ramakrishnan, M., Papolu, P. K., Satish, L., Vinod, K. K., Wei, Q., Sharma, A., et al. (2022). Redox status of the plant cell determines epigenetic modifications under abiotic stress conditions and during developmental processes. *J. Adv. Res.* 4, 7. doi: 10.1016/j.jare.2022.04.007

Ramakrishnan, M., Satish, L., Kalendar, R., Narayanan, M., Kandasamy, S., Sharma, A., et al. (2021). The dynamism of transposon methylation for plant development and stress adaptation. *Int. J. Mol. Sci.* 22, 11387. doi: 10.3390/ijms222111387

Ren, J., Wen, L., Gao, X., Jin, C., Xue, Y., and Yao, X. (2009). DOG 1.0: illustrator of protein domain structures. *Cell Res.* 19, 271–273. doi: 10.1038/cr.2009.6

Roldán-Arjona, T., Ariza, R. R., and Córdoba-Cañero, D. (2019). DNA base excision repair in plants: an unfolding story with familiar and novel characters. *Front. Plant Sci.* 10, 1055. doi: 10.3389/fpls.2019.01055

Rykaczewska, K. (2015). The effect of high temperature occurring in subsequent stages of plant development on potato yield and tuber physiological defects. *Am. J. Potato Res.* 92, 339–349. doi: 10.1007/s12230-015-9436-x

Schmittgen, T. D., and Livak, K. J. (2008). Analyzing real-time PCR data by the comparative CT method. *Nat. Protocols* 3, 1101–1108. doi: 10.1038/nprot.2008.73

Schultz, J., Copley, R. R., Doerks, T., Ponting, C.P., and Bork, P. (2000). SMART: a web-based tool for the study of genetically mobile domains. *Nucleic Acid. Res.* 28, 231–234. doi: 10.1093/nar/28.1.231

Song, J., Rechkoblit, O., Bestor, T. H., and Patel, D. J. (2011). Structure of DNMT1-DNA complex reveals a role for autoinhibition in maintenance DNA methylation. *Science* 331, 1036–1040. doi: 10.1126/science.1195380

Song, Q.-X., Lu, X., Li, Q.-T., Chen, H., Hu, X.-Y., Ma, B., et al. (2013). Genome-wide analysis of DNA methylation in soybean. *Mol. Plant* 6, 1961–1974. doi: 10.1093/mp/sst123

Stroud, H., Do, T., Du, J., Zhong, X., Feng, S., Johnson, L., et al. (2014). Non-CG methylation patterns shape the epigenetic landscape in Arabidopsis. *Nat. Struct. Mol. Biol.* 21, 64–72. doi: 10.1038/nsmb.2735

Tang, R., Zhu, W., Song, X., Lin, X., Cai, J., Wang, M., et al. (2016). Genome-wide identification and function analyses of heat shock transcription factors in potato. *Front. Plant Sci.* 7, 490. doi: 10.3389/fpls.2016.00490

Verhoeven, K. J., Jansen, J. J., Van Dijk, P. J., and Biere, A. (2010). Stress-induced DNA methylation changes and their heritability in asexual dandelions. *New Phytol.* 185, 1108–1118. doi: 10.1111/j.1469-8137.2009.03121.x

Vreugdenhil, D., and Struik, P. C. (1989). An integrated view of the hormonal regulation of tuber formation in potato (*Solanum tuberosum*). *Physiol. Plant.* 75, 525–531. doi: 10.1111/j.1399-3054.1989.tb05619.x

Wang, P., Gao, C., Bian, X., Zhao, S., Zhao, C., Xia, H., et al. (2016). Genome-wide identification and comparative analysis of cytosine-5 DNA methyltransferase and demethylase families in wild and cultivated peanut. *Front. Plant Sci.* 7, 7. doi: 10.3389/fpls.2016.00007

Wolf, S., Marani, A., and Rudich, J. (1991). Effect of temperature on carbohydrate metabolism in potato plants. *J. Exp. Bot.* 42, 619–625. doi: 10.1093/jxb/42.5.619

Yamaguchi-Shinozaki, K., and Shinozaki, K. (2005). Organization of cis-acting regulatory elements in osmotic-and cold-stress-responsive promoters. *Trends Plant Sci.* 10, 88–94. doi: 10.1016/j.tplants.2004.12.012

Yang, X., Lu, X., Chen, X., Wang, D., Wang, J., Wang, S., et al. (2019). Genome-wide identification and expression analysis of DNA demethylase family in cotton. *J. Cotton Res.* 2, 1–9. doi: 10.1186/s42397-019-0033-2

Yang, Z. (2007). PAML 4: phylogenetic analysis by maximum likelihood. *Mol. Biol. Evol.* 24, 1586–1591. doi: 10.1093/molbev/msm088

Yu, C.-S., Cheng, C.-W., Su, W.-C., Chang, K.-C., Huang, S.-W., Hwang, J.-K., et al. (2014). CELLO2GO: a web server for protein subCELlular LOcalization prediction with functional gene ontology annotation. *PLoS ONE* 9, e99368. doi: 10.1371/journal.pone.0099368

Yu, Y., Lashbrook, C., and Hannapel, D. J. (2007). Tissue integrity and RNA quality of laser microdissected phloem of potato. *Planta* 226, 797–803. doi: 10.1007/s00425-007-0509-z

Yu, Z., Zhang, G., Teixeira Da Silva, J. A., Li, M., Zhao, C., He, C., et al. (2021). Genome-wide identification and analysis of DNA methyltransferase and demethylase gene families in *Dendrobium officinale* reveal their potential functions in polysaccharide accumulation. *BMC Plant Biol.* 21, 1–17. doi: 10.1186/s12870-020-02811-8

Zhang, H., Lang, Z., and Zhu, J.-K. (2018). Dynamics and function of DNA methylation in plants. *Nat. Rev. Mo. Cell Biol.* 19, 489–506. doi: 10.1038/s41580-018-0016-z

Zhou, R., Kong, L., Yu, X., Ottosen, C.-O., Zhao, T., Jiang, F., et al. (2019). Oxidative damage and antioxidant mechanism in tomatoes responding to drought and heat stress. *Acta. Physiol. Plant.* 41, 1–11. doi: 10.1007/s11738-019-2805-1

Zhu, C., Zhang, S., Zhou, C., Chen, L., Fu, H., Li, X., et al. (2020). Genome-wide investigation and transcriptional analysis of cytosine-5 DNA methyltransferase and DNA demethylase gene families in tea plant (*Camellia sinensis*) under abiotic stress and withering processing. *PeerJ.* 8, e8432. doi: 10.7717/peerj.8432

Zierer, W., Rüscher, D., Sonnewald, U., and Sonnewald, S. (2021). Tuber and tuberous root development. *Ann. Rev. Plant Biol.* 72, 551–580. doi: 10.1146/annurev-arplant-080720-084456

frontiers | Frontiers in Plant Science

TYPE Original Research
PUBLISHED 26 September 2022
DOI 10.3389/fpls.2022.952732

Check for updates

OPEN ACCESS

EDITED BY
Ashish Kumar Srivastava,
Bhabha Atomic Research Centre (BARC), India

REVIEWED BY
Anuj Kumar,
Dalhousie University, Canada
Nicolás M. Cecchini,
National University of Córdoba (CIQUIBIC), Argentina

*CORRESPONDENCE
P. B. Kavi Kishor
pbkavi@yahoo.com

SPECIALTY SECTION
This article was submitted to Plant Physiology, a section of the journal Frontiers in Plant Science

RECEIVED 25 May 2022
ACCEPTED 16 August 2022
PUBLISHED 26 September 2022

CITATION
Rajasheker G, Nagaraju M, Varghese RP, Jalaja N, Somanaboina AK, Singam P, Ramakrishna C, Penna S, Sreenivasulu N and Kishor PBK (2022) Identification and analysis of proline-rich proteins and hybrid proline-rich proteins super family genes from *Sorghum bicolor* and their expression patterns to abiotic stress and zinc stimuli.
Front. Plant Sci. 13:952732.
doi: 10.3389/fpls.2022.952732

COPYRIGHT
© 2022 Rajasheker, Nagaraju, Varghese, Jalaja, Somanaboina, Singam, Ramakrishna, Penna, Sreenivasulu and Kishor. This is an open-access article distributed under the terms of the Creative Commons Attribution License (CC BY). The use, distribution or reproduction in other forums is permitted, provided the original author(s) and the copyright owner(s) are credited and that the original publication in this journal is cited, in accordance with accepted academic practice. No use, distribution or reproduction is permitted which does not comply with these terms.

Identification and analysis of proline-rich proteins and hybrid proline-rich proteins super family genes from *Sorghum bicolor* and their expression patterns to abiotic stress and zinc stimuli

Guddimalli Rajasheker[1], Marka Nagaraju[2], Rinku Polachirakkal Varghese[3,4], Naravula Jalaja[3], Anil Kumar Somanaboina[3], Prashant Singam[1], Chintala Ramakrishna[5], Suprasanna Penna[6], Nese Sreenivasulu[7] and P. B. Kavi Kishor[3]*

[1]Department of Genetics and Biotechnology, Osmania University, Hyderabad, India, [2]Biochemistry Division, ICMR-National Institute of Nutrition, Hyderabad, India, [3]Department of Biotechnology, Vignan's Foundation for Science, Technology & Research (Deemed to be University), Vadlamudi, India, [4]School of Biosciences and Technology, Vellore Institute of Technology, Vellore, India, [5]Department of Environmental Sciences, GITAM University, Visakhapatnam, India, [6]Nuclear Agriculture and Biotechnology, Bhabha Atomic Research Center, Mumbai, India, [7]Consumer-driven Grain Quality and Nutrition Research Unit, International Rice Research Institute, Los Baños, Philippines

Systematic genome-wide analysis of *Sorghum bicolor* revealed the identification of a total of 48 homologous genes comprising 21 proline-rich proteins (*PRPs*) and 27 hybrid proline-rich proteins (*HyPRPs*). Comprehensive scrutiny of these gene homologs was conducted for gene structure, phylogenetic investigations, chromosome mapping, and subcellular localization of proteins. Promoter analysis uncovered the regions rich with phosphorous- (BIHD), ammonium-, sulfur-responsive (SURE), and iron starvation-responsive (IRO2) along with biotic, abiotic, and development-specific *cis*-elements. Further, PRPs exhibit more methylation and acetylation sites in comparison with HyPRPs. miRNAs have been predicted which might play a role in cleavage and translation inhibition. Several of the *SbPRP* genes were stimulated in a tissue-specific manner under drought, salt, heat, and cold stresses. Additionally, exposure of plants to abscisic acid (ABA) and zinc (Zn) also triggered PRP genes in a tissue-dependent way. Among them, *SbPRP17* has been found upregulated markedly in all tissues irrespective of the stress

imposed. The expressions of *SbHyPRPs*, especially *SbHyPRP2*, *SbHyPRP6*, and *SbHyPRP17* were activated under all stresses in all three tissues. On the other hand, *SbHyPRP8* (root only) and *SbHyPRP12* (all three tissues) were highly responsive to cold stress and ABA while *SbHyPRP26* was induced by drought and Zn in the stem. Taken together, this study indicates the critical roles that *SbPRPs* and *SbHyPRPs* play during diverse abiotic stress conditions and notably the plausible roles that these genes play upon exposure to zinc, the crucial micronutrient in plants.

KEYWORDS

proline-rich proteins, hybrid proline-rich proteins, gene expressions, abiotic stresses, *Sorghum bicolor*

Introduction

Plants are constantly exposed to both biotic and abiotic stresses because of which a lion's share of the final productivity is lost globally. Plants can cope with them by deploying several complex physiological and molecular mechanisms depending upon the type, severity, and duration of stress. But unraveling the underlying mechanisms is crucial for us to design crops with superior tolerance to stresses. Extreme environmental conditions cause membrane damage, denaturation of proteins, and accumulation of excessive reactive oxygen species (ROS) that eventually dismantle the cellular fabric (Bokszczanin, 2013; Wang et al., 2019). To combat these stress-induced damages, plants accumulate osmotic agents, antioxidants, and also antioxidative enzymatic machinery (Bohnert et al., 2006; Bokszczanin, 2013). Plant cell wall proteins consist of both structural [arabinogalactan proteins, (AGPs) and extensins or hydroxyproline-rich *O*-glycoproteins (HRGPs)] and enzymatic proteins. They play key roles in cell wall formation, cell differentiation, development, and oxidative cross-linking mediated by extension peroxidases (McNeil et al., 1984; Jose-Estanyol and Puigdomenech, 1993; Showalter, 1993; Sommer-Knudsen et al., 1998). Proline rich-proteins (PRPs) and hybrid proline-rich proteins (HyPRPs) contain proline and hydroxyproline and are a part of the HRGPs super family proteins, widely distributed in plants and implicated in biotic and abiotic stress tolerance. PRPs contain at least two consecutive proline residues organized in the peptides and the domains contain 70% of proline residues (Zhang et al., 2021). Based on the presence or absence of N-terminal signal peptides and also differences in the domains, PRPs are divided into (1) PRPs that have two domains with signal peptides and highly rich repeat regions of proline at the N-terminus (Dvorakova et al., 2007), (2) PRPs that have three domains with N-terminal signal peptide, repeat regions of proline, aside cysteine-rich regions in the C-terminal end, and (3) PRPs that are devoid of any signal peptide, but with similar PPVYK repeat sequences at the C-terminus (Jose-Estanyol and Puigdomenech, 1994, 2000). The presence of signal peptides in these proteins infers that they are secreted-type of proteins in plants (Keller, 1993; Showalter, 1993; Cassab, 1998). The signal peptides permit their sorting into the rough endoplasmic reticulum and other cellular organelles. Newman and Cooper (2011) identified 31 distinct proline-rich tandem repeat protein classes targeted for secretion using a systems-level computational approach. Further, PRPs have been classified as an 8-cysteine motif or 8CM proteins, with 90–100 amino acids but the proteins are not integrated within the membrane. The 8-cysteine residues appear indispensable for the three-dimensional structure of these proteins. The 8-cysteine residues have a versatile structure in plant proteins domain and lipid transfer proteins (Jose-Estanyol et al., 2004; Dvorakova et al., 2012). In general, proline-rich repeats precede the 8CM, and such proteins are named as HyPRPs, but the N-terminus features like that of PRPs (Jose-Estanyol and Puigdomenech, 1994, 2000). HyPRPs differ from that of PRPs in the amino acid motif size and composition of proline repeats (Jose-Estanyol et al., 2004; Dvorakova et al., 2007). HyPRPs are subdivided into two groups based on cysteine residue positions in the peptidic sequence (Jose-Estanyol and Puigdomenech, 1994). Proline-rich domains of SbrHyPRP from *Solanum brevidens* contains repeated motifs PPHVKPPSTPK and PTPPIVSPP extended with TPKYP and TPKPPS motifs at N- or C-termini, respectively (Fischer et al., 2002). PRPs having tandem repeats of a hexapeptide PPPVHL were first characterized by corn endosperm (Esen et al., 1982). Function, localization, and differential expression of three PRPs from *Glycine max* (PRP1, PRP2, and PRP3) were studied (Hong et al., 1990; Wyatt et al., 1992). PRPs and PRP-like proteins have been found to play a crucial role during plant growth, germination of seeds (Bouton et al., 2005; Chen et al., 2014), and elongation of root hairs in *Arabidopsis* (Boron et al., 2014). Blocking *OsPRP3* by RNAi

leads to defects in floral organogenesis in *Oryza sativa* implying its role during plant development (Gothandam et al., 2010). Further, PRPs modulate both biotic and abiotic stresses such as chilling, drought, and salinity stresses (Zhan et al., 2012; Kavi Kishor et al., 2015). Pathogen-derived molecules usually trigger systemic acquired resistance (SAR) in plants, which can be abolished in a wide spectrum of pathogens. Many experiments have shown that HyPRPs are closely related to biotic stress resistance (Yu et al., 2013; Cecchini et al., 2015, 2021). HyPRPs with plastid pools modulates systemic immunity either positively or negatively against *Pseudomonas syringae* (Banday et al., 2022). It appears that HyPRPs are obligatory for both SAR and induced-systemic resistance (ISR), and SAR signal movement or action (Gao et al., 2015; Cecchini et al., 2019, 2021; Kachroo and Kachroo, 2020). Therefore, HyPRPs have distinct roles to play in plant immunity. Also, when useful bacteria attack the roots of plants, ISR occurs, which leads to the transport of mobile signals from the tissues or organs that are immunized (Cecchini et al., 2015, 2019; Carella, 2020; Kachroo and Kachroo, 2020). Signal molecules such as azelaic acid (AZA) work as mobile signals for SAR, and such signals alongside free radicals are imperative in imparting SAR (Jung et al., 2009; Wang et al., 2014; Kachroo and Kachroo, 2020). The experiments infer that HyPRPs may have a critical role to play in biotic stress tolerance. In *Arabidopsis*, *FUSED OUTER CUTICULAR LEDGE1* (*FOCL1*) encodes a guard cell-expressed, secreted PRP protein. Interestingly, *focl1* mutants display enhanced drought tolerance compared to wild-type plants (Hunt et al., 2017). HyPRPs are poorly glycosylated cell wall glycoproteins and also play critical roles during plant ontogeny and abiotic stress tolerance like PRPs (Holk et al., 2002; Blanco-Portales et al., 2004; Kavi Kishor et al., 2015; Gujjar et al., 2019).

Information on the number of PRPs in diverse taxa is scanty. Showalter et al. (2016) discovered 49 *PtPRPs* in *Populus trichocarpa* and *Malus domestica,* 9 *MdPRP* genes have been identified (Zhang et al., 2021). Surprisingly, no HyPRPs have been found in algae, mosses, and ferns, but *Pinus taeda* contains 21 *PtHyPRPs* (Dvorakova et al., 2007). While in dicots such as *Arabidopsis thaliana* 28 *AtHyPRPs* have been found, 16 *StHyPRPs* were recorded in *Solanum tuberosum* (Dvorakova et al., 2012), 19 complete or nearly complete from *S. lycopersicon* (*SlHyPRPs*) (Kapoor et al., 2019) and 14 from *Medicago truncatula* (*MtHyPRPs*) have been recorded from the publicly available sequence data (Dvorakova et al., 2012). In *Glycine max*, 35 *GmHyPRP*-encoding genes were identified by Neto et al. (2013). In monocots, like *Oryza sativa* genome, conflicting reports exist. Studies by Dvorakova et al. (2007), Boutrot et al. (2008), and Kapoor et al. (2019) showed 21, 31, and 45 *OsHyPRP* genes, respectively, in rice whereas, in *Zea mays*, 52 members of *ZmHyPRPs* have been detected (Dvorakova et al., 2007). Such a large variation could be because of different methods that researchers have employed for identification.

Sorghum [*Sorghum bicolor* (L.) Moench] is an important C_4 cereal crop and the fifth largest grown in arid and semi-arid regions, globally utilized for both food and fodder (FAOSTAT[1]). In the semi-arid tropics of Asia and Africa, it serves as a staple food, animal feed, fodder, and notably a promising multipurpose feedstock crop for bioethanol production (Silva et al., 2022). It is moderately tolerant to both drought and heat and requires very low inputs. Traits that impart alkalinity, salt, water deficit, waterlogging, and high-temperature stresses make this crop attractive for research purposes in comparison to other cereal crops (Hadebe et al., 2017; Huang, 2018). Fujino et al. (2014) have detected 21 *HyPRPs* in *Oryza sativa*, 12 in *Hordeum vulgare*, 10 in *Brachypodium*, 20 in *Zea mays,* and 28 in *S. bicolor* using a BLAST search of qLTG3-1 as the query. Though 28 *HyPRPs* have been reported in sorghum, their subcellular localizations, *cis*-element characterization, and their tissue-specific expressions and implications under abiotic stress conditions have not been undertaken. So, the number of PRPs and HyPRPs, their tissue-specific expressions under cold, high temperature, salt, drought stress conditions, and their response to ABA have not yet been elucidated. Similarly, little is known if these genes play a molecular function in response to soil nutrients especially sulfur (S), zinc (Zn), and iron (Fe). In the present study, we have presented results on the genome-wide analysis of sorghum for both PRP and HyPRP homolog genes, their characterization, and tissue-specific expressions under abiotic stress conditions besides their response to ABA and Zn.

Materials and methods

Plant material

Seeds of *S. bicolor* variety BTx623 (an inbred line) were obtained from ICRISAT, Patancheru, Hyderabad. This line is moderately tolerant to water deficit conditions and its genome sequencing information is publicly available. Seeds were sown in the pots filled with 5 kg of garden soil, and seedlings were grown for 40-days under glasshouse conditions (28/20°C day/night temperatures). Seedlings were subjected to drought stress by imposing a 200 mM mannitol solution, and salt stress was induced by saturating the seedlings with 200 mM NaCl solution for 4 h. Seedlings were subjected to cold stress by keeping them at 4°C and high-temperature stress by exposing them to 40°C for 4 h. Seedlings were also treated with 100 μM ABA and 25 mM zinc chloride

1 https://www.fao.org/faostat/en#data

solution (based on literature search) for 4 h separately. After completion of treatment, roots, stems, and leaves were collected along with respective controls (without treatment) and frozen immediately in liquid nitrogen and stored at –80°C refrigerator for isolation of RNA and gene expression analysis by qRT-PCR. Biological triplicates and technical duplicates were maintained for gene expression analysis for each treatment.

In silico identification of proline-rich proteins and hybrid proline-rich proteins genes in sorghum

Proline-rich proteins and HyPRP gene sequences of *Oryza*, and *Arabidopsis* were retrieved from Plant GDB[2] and Gramene database[3] (Tello-Ruiz et al., 2021). These gene sequences were blasted against *S. bicolor* genome in Gramene database to find out their homologs. Genscan[4] (Burge and Karlin, 1998) was used to retrieve genes and their respective protein sequences. Based on the homology, the identified putative protein sequences were subjected to motif search[5] to check the reliability and for identifying the conserved domains (Letunic et al., 2004).

In silico prediction of potential *cis*-regulatory elements

To predict the putative *cis*-acting elements of *PRP* and *HyPRP* promoter regions, the 2,000 bp genomic sequences upstream of the start codon were extracted and PLANTCARE (Lescot et al., 2002) software was used to identify putative *cis*-acting elements responsible for plant development and biotic and abiotic stress tolerance.

Chromosomal localization, and gene structure analysis of sorghum *SbPRPs* and *SbHyPRPs*

The identified *SbPRP* and *SbHyPRP* genes were mapped to their respective chromosomes based on the information provided in the Gramene Genome Database. Gene Structure Display Server [6]software was used for obtaining the gene structures of *SbPRPs* and *SbHyPRPs* – exons, introns, and untranslated sequence regions (UTRs) by aligning their gene and coding sequences (Guo et al., 2007).

Synteny of proline-rich proteins and hybrid proline-rich proteins genes across *Sorghum*, *Oryza,* and *Arabidopsis*

TBtools (Chen et al., 2020) was used for identifying the synteny of *PRP* and *HyPRP* genes across *S. bicolor* (*Sb*), *O. sativa* (*Os*), and *A. thaliana* (*At*).

Phylogenetic analysis and non-synonymous and synonymous substitution ratios of proline-rich proteins and hybrid proline-rich proteins

The Maximum Likelihood phylogenetic tree was constructed using MEGA 6.2 software (Tamura et al., 2013) by employing the Poisson correction, partial deletion, and bootstrap value (1,000 replicates) parameters to know the evolutionary relationships. The PAL2NAL[7] (Suyama et al., 2006) software was used to calculate the substitution rates for non-synonymous and synonymous sites of each of the identified paralogs (sorghum) and orthologous gene pairs (between *Sorghum/Oryza*, and *Sorghum/Arabidopsis*) from phylogeny.

Protein analysis of SbPRPs and SbHyPRPs

Molecular weight (MW), isoelectric point (pI), and GRAVY (grand average of hydropathy) of PRPs and HyPRPs were identified by using ProtParam Expasy tools[8] (Gasteiger et al., 2005), while phosphorylation sites were predicted by employing NetPhos3.1 software of Expasy tools (Blom et al., 2004). The putative transmembrane helices within these genes were identified using TMHMM software (Moller et al., 2001). The sub-cellular localization of PRPs and HyPRPS was identified by the WOLFPSORT program[9] (Horton et al., 2007). MEME software (Bailey and Gribskov, 1998) was employed to analyze new sequence patterns and their significance (Bailey et al., 2006). The software helped to identify the nature of motifs by setting different default parameters, number of motifs from 1

2 http://www.plantgdb.org/
3 http://www.gramene.org/
4 http://genes.mit.edu/GENSCAN.html
5 http://www.genome.jp/tools/motif/
6 http://gsds.cbi.pku.edu.cn
7 http://www.bork.embl.de/pal2nal/
8 http://web.expasy.org/protparam
9 http://wolfpsort.org/

to 10 with a motif width of 5–50, and the number of motif sites from 5 to 10.

Prediction of 3D structures and verification of their stability

The 3D structures for the highly expressed 12 proteins encoded by *SbPRP* (*SbPRP3*, *SbPRP6*, *SbPRP10*, *SbPRP12*, *SbPRP17*, and *SbPRP19*) and *SbHyPRP* genes (*SbHyPRP2*, *SbHyPRP5*, *SbHyPRP6*, *SbHyPRP13*, *SbHyPRP17*, and *SbHyPRP26*) were predicted using SWISS-MODEL server (Biasini et al., 2014). The predicted 3D structures of proteins for the highly expressed genes were evaluated for stability using PROCHECK and protein structure verification server (PSVS)[10]. The stability of the proteins was analyzed by Ramachandran plots through the calculation of phi (F) and psi (ψ) torsion angles.

Analysis of acetylation, methylation sites, and miRNA target sites

The acetylation of the internal lysines was predicted by using PAIL[11] (Li et al., 2006), the PRmePRed[12] (Kumar et al., 2017) was used to predict the methylation sites. The putative miRNAs in targeting the *SbPRP and SbHyPRP* genes were identified using the psRNATarget server (Dai and Zhao, 2011) by default parameters.

Prediction of simple sequence repeats

The simple sequence repeats (SSRs), the gene-specific molecular markers of PRPs and HyPRPs were identified within the transcripts by employing MISA-web[13] (Beier et al., 2017).

Digital expressions of *SbPRP* and *HyPRP* genes in diverse tissues and developmental stages under cold and drought stresses

Digital expression profiling of *SbPRP* and *SbHyPRP* genes was analyzed using Genevestigator[14]. *S. bicolor* mRNA-seq data available for all the 21 *SbPRP* and 27 *SbHyPRP* genes for stress conditions like cold and drought, three tissues, and five developmental stages were collected and used for analysis. Gene expression profiles were developed using hierarchical clustering and heat maps were generated for anatomy, development, and perturbations separately.

qRT-PCR gene expression analysis of SbPRP and SbHyPRPs under diverse abiotic stress conditions

The transcriptional profiling of *PRPs* and *HyPRPs* was further investigated using qRT-PCR. Total RNA from root, stem, and leaf tissues under various stresses was extracted by using a nucleo-spin plant RNA isolation kit (MACHEREY-NAGEL) according to the manufacturer's instructions. A total of 3 μg of total RNA was transcribed into cDNA by using first-strand synthesis kit (Thermo Scientific, Waltham, MA, USA). The SYBR Green Master Mix (2×) (Takara, Kasatsu, Shiga, Japan) was used according to the manufacturer's recommendations. The qRT-PCR analysis was conducted by using ABI 7500 real-time PCR system (Applied Biosystems, Waltham, MA, USA) and Takara SYBR Green Master Mix (2 ×) with the following thermal cycles: 1 cycle at 95^{o}C for 10 min, followed by 40 cycles alternatively at 95°C for 15 s and 60°C for 1 min. The amplicon dissociation curves were recorded with a fluorescence lamp after the 40th cycle by heating from 58 to 95^{o}C within 20 min. Three biological replicates and two technical replicates were taken for the study. The gene expression data were normalized with Acyl Carrier Protein 2 (*SbACP2*) and Elongation Factor P (*SbEF-P*) genes of sorghum (Reddy et al., 2016). The *PRP* and *HyPRP* gene-specific primers used for qRT-PCR and reference genes are listed in **Supplementary Table 1**. The relative gene expressions were calculated by employing REST software (Pfaffl et al., 2002).

Results

Genome-wide characterization, chromosomal localization, and gene structure analysis of sorghum *PRPs* and *HyPRP* genes

The workflow of genome-wide screening and characterization of SbPRPs and SbHyPRPs is shown in **Figure 1**. Genome-wide analysis of sorghum resulted in the identification of a total of 48 homologous genes encompassing 21 *SbPRPs* and 27 *SbHyPRPs*. After checking their reliability by conserved domain search using the MOTIF search tool for convenience, the predicted PRPs, HyPRPs have been named as *SbPRP1* to *SbPRP21*, and *SbHyPRP1* to *SbHyPRP27*, respectively. Out of 21 *SbPRP* genes, 7 genes were localized on chromosome 1, followed

10 https://saves.mbi.ucla.edu/
11 http://bdmpail.biocuckoo.org/
12 http://bioinfo.icgeb.res.in/PRmePRed/
13 http://misaweb.ipk-gatersleben.de/
14 https://genevestigator.com/

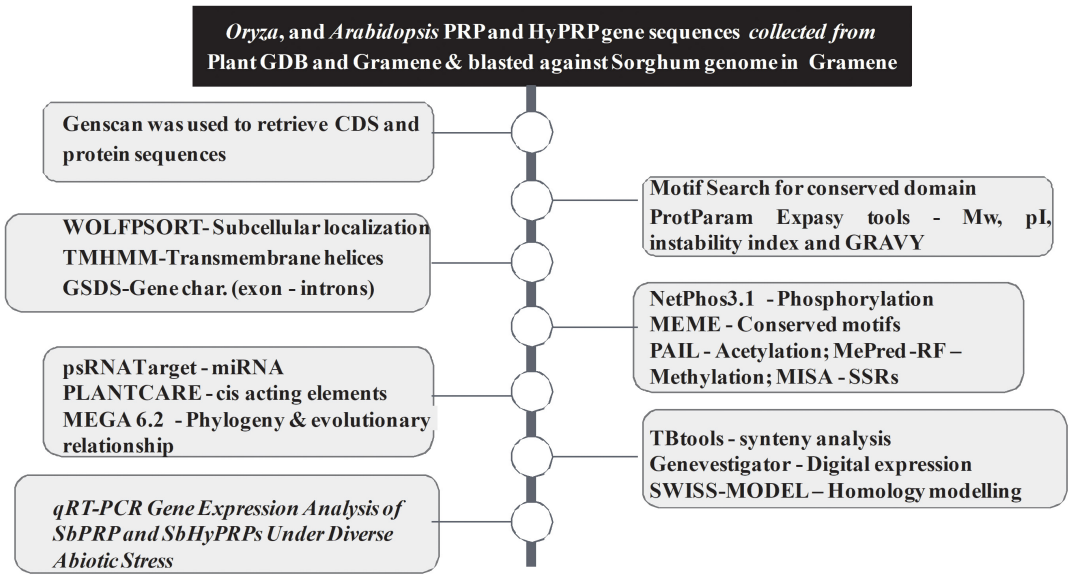

FIGURE 1
Methods, softwares, and pipelines used for genome-wide screening and characterization of SbPRPs and SbHyPRPs.

TABLE 1 List of identified PRPs exhibiting chromosomal location, sub group, length, DNA binding domains (DBD), molecular weight, (MW), iso-electric point (pI), GRAVY, no. of exons, localization, and instability and aliphatic indexes.

Gene	Common name	AA	Chr loc.	Pi/MW	DBD	Exon	Localization	GRAVY	Instability index	Aliphatic index	TMH MM
SORBI_3001G265900	SbPRP-1	624	1	9.37/71127.19	133–209	4	C	−1.066	59.37	42.88	0
SORBI_3001G266100	SbPRP-2	324	1	7.74/34937.58	34–108	2	E/V	−0.630	51.39	51.54	1
SORBI_3001G266200	SbPRP-3	210	1	6.93/22303.42	31–107	2	E	−0.305	47.66	64.24	0
SORBI_3001G266300	SbPRP-4	266	1	9.09/29111.79	35–117	2	E	−0.318	40.84	68.98	1
SORBI_3001G438400	SbPRP-5	256	1	7.49/27050.04	32–113	7	E	−0.455	44.55	61.48	0
SORBI_3001G438500	SbPRP-6	259	1	6.51/26803.38	34–116	2	E	−0.177	71.97	45.27	1
SORBI_3001G493300	SbPRP-7	195	1	7.52/19452.47	35–109	3	P	0.313	43.46	97.74	2
SORBI_3003G195000	SbPRP-8	312	3	11.11/32187.12	44–75	1	C	−0.054	54.54	73.91	1
SORBI_3003G315500	SbPRP-9	69	3	4.59/25020.34	11–60	3	C	−0.220	84.11	53.77	0
SORBI_3003G336300	SbPRP-10	2477	3	6.67/278911.49	142–276	4	N	−0.622	40.73	71.53	0
SORBI_3004G060600	SbPRP-11	511	4	9.31/57657.25	320–421	12	Cy	−0.094	36.47*	106.71	0
SORBI_3004G180900	SbPRP-12	519	4	5.05/58183.27	308–345	8	N	−1.061	50.76	54.66	0
SORBI_3005G191600	SbPRP-13	481	5	7.03/52432.65	261–335	12	N/P/ER	−0.441	43.8	70.58	0
SORBI_3005G197700	SbPRP-14	264	5	6.95/29229.79	57–98	6	V	−0.406	48.76	86.44	1
SORBI_3006G031100	SbPRP-15	309	6	10.99/33712.72	118–150	3	Cy/M/ER	−0.219	44.26	95.34	0
SORBI_3006G211701	SbPRP-16	148	6	8.68/15027.87	65–147	1	C	0.388	53.06	96.89	0
SORBI_3006G238000	SbPRP-17	380	6	6.54/41092.34	321–375	10	Cy	0.126	42.81	92.45	0
SORBI_3007G074200	SbPRP-18	1016	7	8.61/112336.86	977–1016	12	N	−0.476	40.98	72.33	0
SORBI_3008G082400	SbPRP-19	205	8	9.33/22334.14	13–118	1	V	−1.491	77.34	34.39	1
SORBI_3010G054600	SbPRP-20	324	10	9.43/34162.79	238–319	1	C	−0.347	87.66	68.83	0
SORBI_3010G278800	SbPRP-21	814	10	5.42/91773.76	537–582	4	C	−0.970	47.90	64.05	1

a.a, amino acids; Chrom, chromosome; C, chloroplast; Cy, cytoplasm; N, nucleus; P, plastid; V, vacuole; E, extra cellular; ER, endoplasmic reticulum; GRAVY, grand average hydropathy.
* Stable.

by 3 and 6 (3 genes each). Chromosomes 4, 5, and 10 have 2 genes each, and chromosomes 7 and 8 have 1 gene each in *S. bicolor* (Table 1 and Figure 2A). Chromosome 1 also displays 9 HyPRP genes in *S. bicolor* out of 27 *SbHyPRPs*, followed by chromosomes 4 and 6 with 4 each, chromosome 3 with 3, chromosome 8 with 2, chromosome 5, 7, 10, 11, 12 with 1 gene

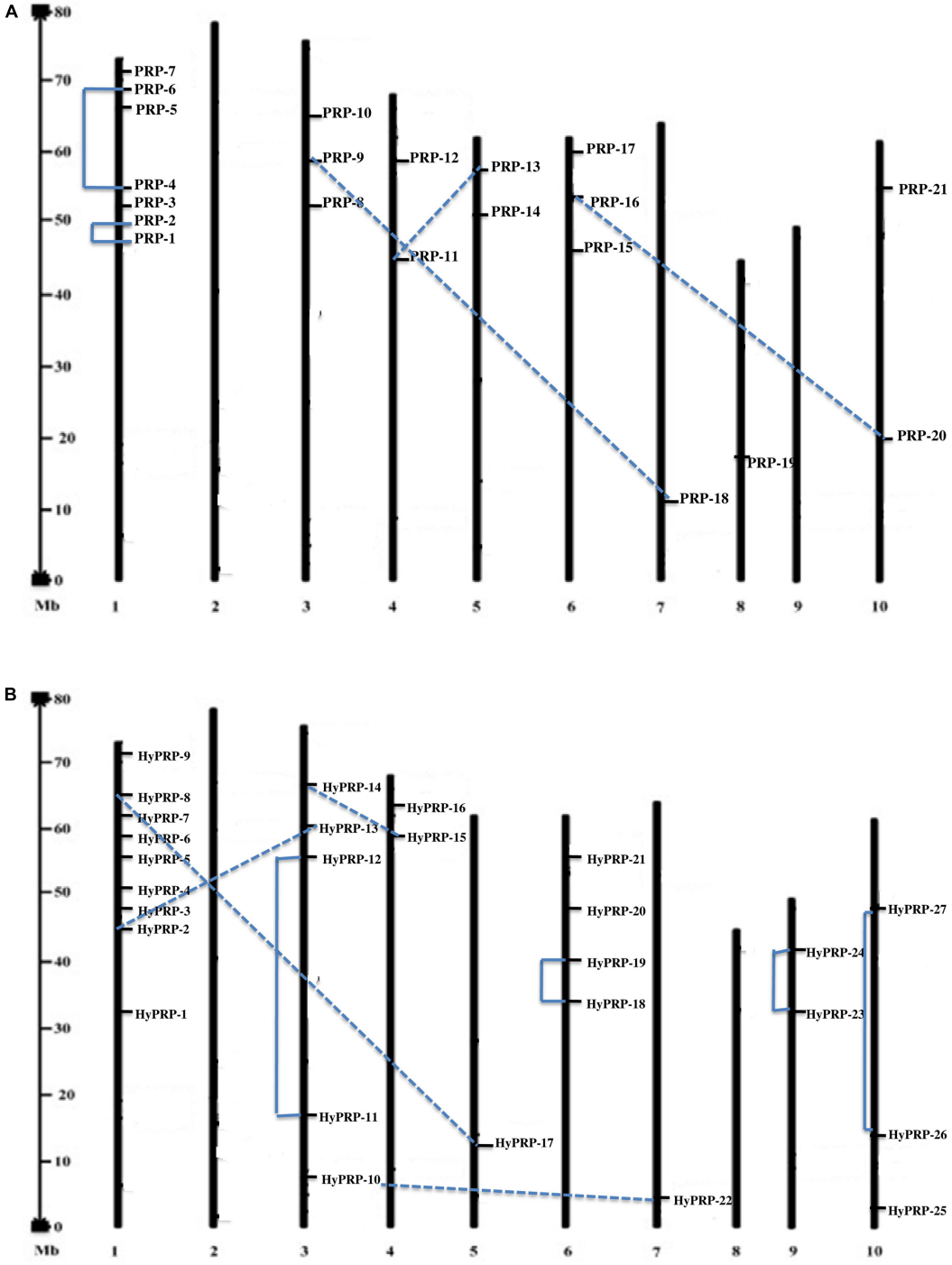

FIGURE 2
Location and duplications of SbPRP and SbHyPRP. **(A)** Location and duplication of *SbPRPs* on chromosomes. **(B)** Location and duplication of *SbHyPRPs* on chromosomes.

each (Table 2 and Figure 2B). Chromosomes 2 and 9 totally lack the distribution of these genes. Thus, chromosome 1 has been found as the hot spot with 7 *SbPRP* and 8 *SbHyPRP* genes. The gene structure analysis provides possible mechanisms of structural evolution of *SbPRP* and *SbHyPRP* genes in sorghum and hence an attempt was made to compare the exon–intron structures of all the identified genes. Out of 21 *SbPRP* genes, 4 have no introns, 2 exons were found in 4 genes, 3 exons in 3 genes, 4 in 3, 6 in 1, 7 in 1, 8 in 1, 10 in 1, and 12 in 3 (Table 1 and Figure 3A). The *SbPRP11*, *13*, and *18* have the highest

TABLE 2 List of identified HyPRPs exhibiting chromosomal location, length of aa, DNA binding domains (DBD), molecular weight (MW), iso-electric point (pI), GRAVY, no. of exons, localization, and instability and aliphatic indexes.

Gene	Common name	AA	Chr loc.	Pi/MW	DBD	Exon	Localization	GRAVY	Instability index	Aliphatic index	TMHMM
SORBI_3001G302600	SbHyPRP-1	287	1	7.52/27092.47	142–214	2	E	0.192	44.22	78.89	0
SORBI_3001G304201	SbHyPRP-2	218	1	8.90/22653.51	86–147	2	C	0.321	49.09	102.39	0
SORBI_3001G304300	SbHyPRP-3	129	1	6.00/13201.74	53–126	1	E	0.676	45.72	118.68	0
SORBI_3001G473200	SbHyPRP-4	252	1	8.88/26375.49	42–120	1	C	0.175	49.82	87.54	1
SORBI_3001G541300	SbHyPRP-5	150	1	8.00/14891.71	69–149	1	C	0.594	58.85	100.07	0
SORBI_3001G541400	SbHyPRP-6	175	1	8.82/15975.22	91–173	1	E	0.334	60.61	84.17	1
SORBI_3001G542000	SbHyPRP-7	137	1	8.03/13709.31	54–135	1	E	0.587	49.89	107.66	1
SORBI_3001G112200	SbHyPRP-8	415	1	9.66/45451.14	354–386	3	M	− 0.147	50.26	88.63	0
SORBI_3003G126100	SbHyPRP-9	613	3	9.33/66940.26	209–286	2	C	− 0.359	58.43	72.92	0
SORBI_3003G058900	SbHyPRP-10	198	3	6.58/21159.92	61–157	1	E	− 0.257	35.37*	70.96	0
SORBI_3003G149800	SbHyPRP-11	636	3	9.00/70134.60	48–63	3	N	− 0.575	51.65	74.47	0
SORBI_3003G329400	SbHyPRP-12	171	3	9.40/19721.55	81–119	2	N	− 0.559	58.31	75.91	0
SORBI_3004G291500	SbHyPRP-13	131	4	8.05/12991.45	49–130	1	C	0.664	43.56	105.80	0
SORBI_3004G292001	SbHyPRP-14	122	4	7.45/12258.61	41–122	1	C	0.833	38.84*	116.72	0
SORBI_3004G292250	SbHyPRP-15	122	4	7.45/12255.61	41–122	1	C	0.831	37.27*	117.54	0
SORBI_3004G292900	SbHyPRP-16	621	4	9.13/69704.92	38–115	2	C	− 0.303	44.73	81.24	1
SORBI_3005G046700	SbHyPRP-17	131	5	5.99/13456.17	65–129	1	E	0.722	48.17	122.82	0
SORBI_3006G172550	SbHyPRP-18	132	6	8.36/13331.89	50–131	1	E	0.597	35.81*	107.95	1
SORBI_3006G172601	SbHyPRP-19	328	6	8.75/36189.90	48–125	4	E/V	0.200	66.33	99.02	1
SORBI_3006G211701	SbHyPRP-20	148	6	8.68/15027.87	65–147	1	C	0.388	53.06	96.89	0
SORBI_3006G238100	SbHyPRP-21	380	6	6.54/41092.34	321–375	3	Cy	0.126	42.81	92.45	0
SORBI_3007G030100	SbHyPRP-22	148	7	9.66/15852.42	26–111	1	E	− 0.299	68.58	78.58	0
SORBI_3008G158501	SbHyPRP-23	229	8	7.45/19735.64	146–228	1	E	0.181	36.93*	69.48	1
SORBI_3008G158600	SbHyPRP-24	273	8	7.45/ 22529.25	190–272	1	E	0.107	42.70	61.87	1
SORBI_3010G003600	SbHyPRP-25	249	10	8.71/26495.94	166–248	2	C	0.208	56.48	100.68	1
SORBI 3010G054800	SbHyPRP-26	324	10	9.43/34162.79	238–319	2	C	− 0.347	87.66	68.83	0
SORBI_3010G204700	SbHyPRP-27	309	10	9.10/31575.13	135–192	1	E/V	− 0.189	69.42	77.80	0

a.a, amino acids; Chrom, chromosome; C, chloroplast; Cy, cytoplasm; N, nucleus; M, mitochondria; V, vacuole; E, extra cellular; ER, endoplasmic reticulum; GRAVY, grand average hydropathy.
* Stable.

number of exons, i.e., 12, while the least number of exons (one) was noticed in *SbPRP8*, *16*, *19,* and *20*. Of the 27 *SbHyPRPs*, 16 genes have been found without any introns, but comprise only one exon, 2 exons in 7 genes, 3 in 3, and 4 exons in one gene. The majority of the *SbHyPRPs* were intron less in comparison with *SbPRPs* (**Table 2** and **Figure 3B**).

In silico prediction of potential *cis*-regulatory elements

Promoter analysis predicted that *SbPRP* and *SbHyPRP* genes have potential *cis*-regulatory elements such as Dc3 Promoter Binding Factor (DPBF, participate in seed specific and/or ABA-inducible expression), MYC, MYB, etiolation, G-box, I-box, ANAERO, associated with abiotic stress, hormone-specific (ABRE, and ERE), T/GBOX for jasmonic acid, biotic stress-responsive WBox, development-specific (pollen, endosperm, and meristem specific) and guard cell-specific elements. Phosphorous (BIHD)-, ammonium-, sulfur-responsive (SURE), and iron (IRO2) starvation-responsive elements have also been predicted. They were rich with EECCRCAH1 elements, the binding site of MYB transcription factor; rbcS general consensus sequence; XYLAT, the core xylem gene set; Telo-box elements for activation of expression in root primordia (**Supplementary Tables 2, 3**).

Phylogenetic and gene duplication analysis of SbPRP, SbHyPRPs, and gene synteny in sorghum, rice, and *Arabidopsis*

The phylogenetic analysis of SbPRPs has been clustered into two clades, based on homology and conserved motifs. Clade I is subdivided into 7, whereas clade II is grouped into 4. A total of five paralogous pairs were observed in the SbPRP family, of which two tandem (SbPRP1/2 and SbPRP4/6

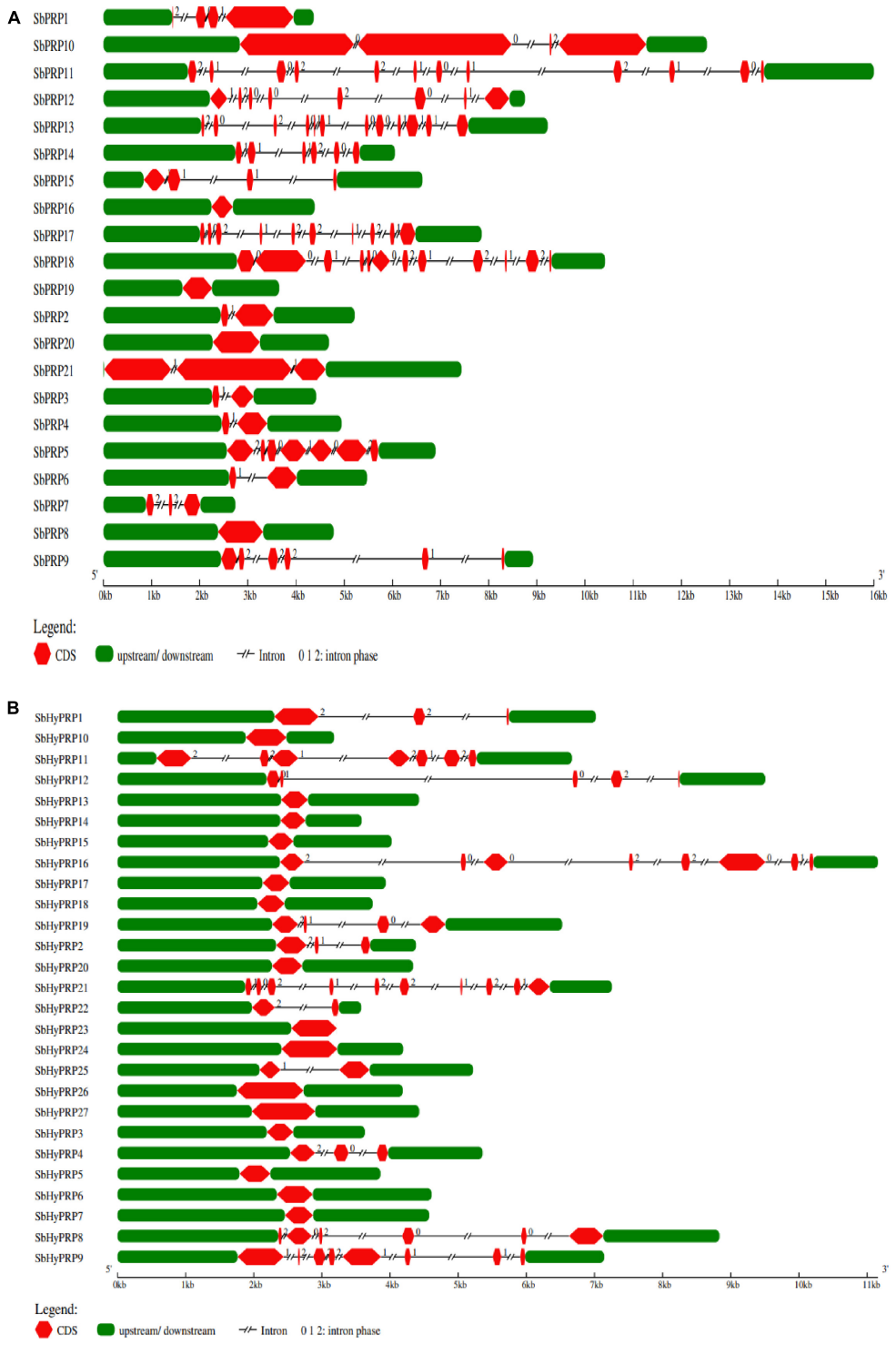

FIGURE 3
Gene characterization of SbPRP and SbHyPRP genes. **(A)** Distribution of exons, introns, upstream, and downstream regions in *SbPRPs*, **(B)** distribution of exons, introns, upstream, and downstream regions in *SbHyPRPs*.

on chromosome 1) and the remaining segmental duplications (Figures 2A, 4A). A phylogenetic tree was constructed to see the evolutionary relationship of SbPRPs with *Oryza* and *Arabidopsis* ancestors for monocot and dicots. All of them exhibited lesser evolutionary relationships, but species-specific clusters were noticed. SbPRPs showed five orthologous relationships, of

10.3389/fpls.2022.952732

which four are with *Oryza* and only one with *Arabidopsis* (Sorbi_3001G266100/AT5G9170) (**Supplementary Figure 1**). The phylogenetic tree of SbHyPRPs clustered into two clades, based on their conserved motifs and subcellular localizations. Clade I is divided into two groups, whereas clade II is clustered into eight groups. A total of nine paralogs were predicted, of which four tandem (SbHyPRP11/12 on chromosome 3; SbHyPRP18/19 on 6; SbHyPRP23/24 on chromosome 9; SbHyPRP26/27 on chromosome 10) and five segmental duplications (**Figures 2B**, **4B**). The SbHyPRPS have been predicted to have 10 orthologous relationships with *Oryza*, and only one with *Arabidopsis* (Sorbi_3010G204700/AT2G10940) (**Supplementary Figure 2**). Comprehensive phylogenetic trees were constructed by including *Oryza, Arabidopsis, Zea, Medicago, Lycopersicum, Solanum, Medicago, Hordeum, Beta vulgaris, and Setaria* for PRP and HyPRPs. They display species and family specificities. While SbPRPs showed 12 orthologous relationships with *Zea*, SbHyPRPS depicted 3 with *Zea* (**Supplementary Figures 3, 4**). Darwinian selection in paralogous and orthologous duplications was uncovered by calculating the non-synonymous substitution (d_N) to synonymous (d_S) ratios. Among the five paralogs of SbPRPs, only one event (SbPRP9/SbPRP18) showed the dN/dS ratio below 1, implying purifying selection, while the remaining four followed a positive/Darwinian selection (**Supplementary Table 4**). Out of the 5 PRP orthologous events, three events (SORBI_3006G211701/Os06G0104800; SORBI_3010G054600/Os06G0168700; SORBI_3001G266100/At5G59170) exhibited the d_N/d_S ratio less than 1, while the remaining two showed Darwinian/positive selection (**Supplementary Table 5**). Of the nine paralogous events of SbHyPRPs, only two (SbHyPRP14/SbHyPRP15, SbHyPRP18/SbHyPRP19) exhibited purifying selection (**Supplementary Table 6**). Out of six orthologs of SbHyPRPs, only one event (SORBI_3001G304201/Os10G40420) followed purifying selection and the remaining positive selection (**Supplementary Table 7**). Syntenic genes for sorghum PRP and HyPRPs were mapped to *Oryza* and *Arabidopsis*. For *SbPRP* genes, chromosome 1 displays seven genes, followed by chromosomes 3 and 6 with three genes, chromosomes 4, 5, and 10 with two genes, and chromosomes 7 and 8 with one gene each, respectively (**Figure 5A**). For *SbHyPRP*, *S. bicolor* chromosome 1 displays nine genes, followed by chromosomes 4 and 6 with 4, chromosome 3 with 3, chromosome 8 with 2, and chromosomes 5, 7, 10, 11, and 12 with one gene each, respectively (**Figure 5B**).

In silico characterization of SbPRP and SbHyPRP proteins

It has been predicted that *SbPRP* genes encoding peptides span from 69 (SbPRP9) to 2477 (SbPRP10) amino acids with

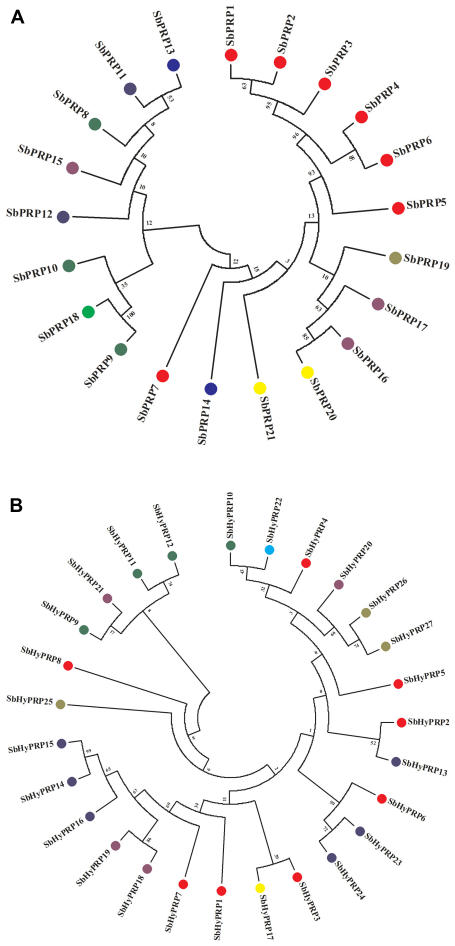

FIGURE 4
Phylogenetic analysis of SbPRP and SbHyPRP genes. **(A)** Phylogenetic tree of PRPs in *Sorghum*. Sub-groups are distinguished by different colors based on their chromosome locations, **(B)** phylogenetic tree of HyPRPs in *Sorghum*. Sub-groups are distinguished by different colors based on their chromosome locations.

the pI value varying from 4.59 (SbPRP9) to 11.11 (SbPRP8). The molecular weights range from 15027.87 (SbPRP-16) to 278911.49 (SbPRP10) Da. The pI values ranges between 5.99 (SbHyPRP17) and 9.66 (SbHyPRP8 and 22), and the molecular weights extend from 12255.61 (SbHyPRP15) to 70134.60 Da (SbHyPRP11). The analyses reveal that majority of them are basic in nature with few exceptions. All the predicted SbPRPs are unstable, (if instability index > 40, considered stable in nature) and the instability index ranges between 40.73 (SbPRP10) and 87.66 (SbPRP20). In the case of SbHyPRPs, 81.48% of proteins were unstable and the remaining were stable (**Table 1**). The instability index varies from 35.37 (SbHyPRP1) to −87.66 (SbHyPRP26) (**Table 2**). SbPRPs are hydrophilic proteins (86%) with lower aliphatic indices. When compared, the majority of the SbHyPRPs (66.66%) are found to be hydrophobic in nature, with a high aliphatic index. Out of

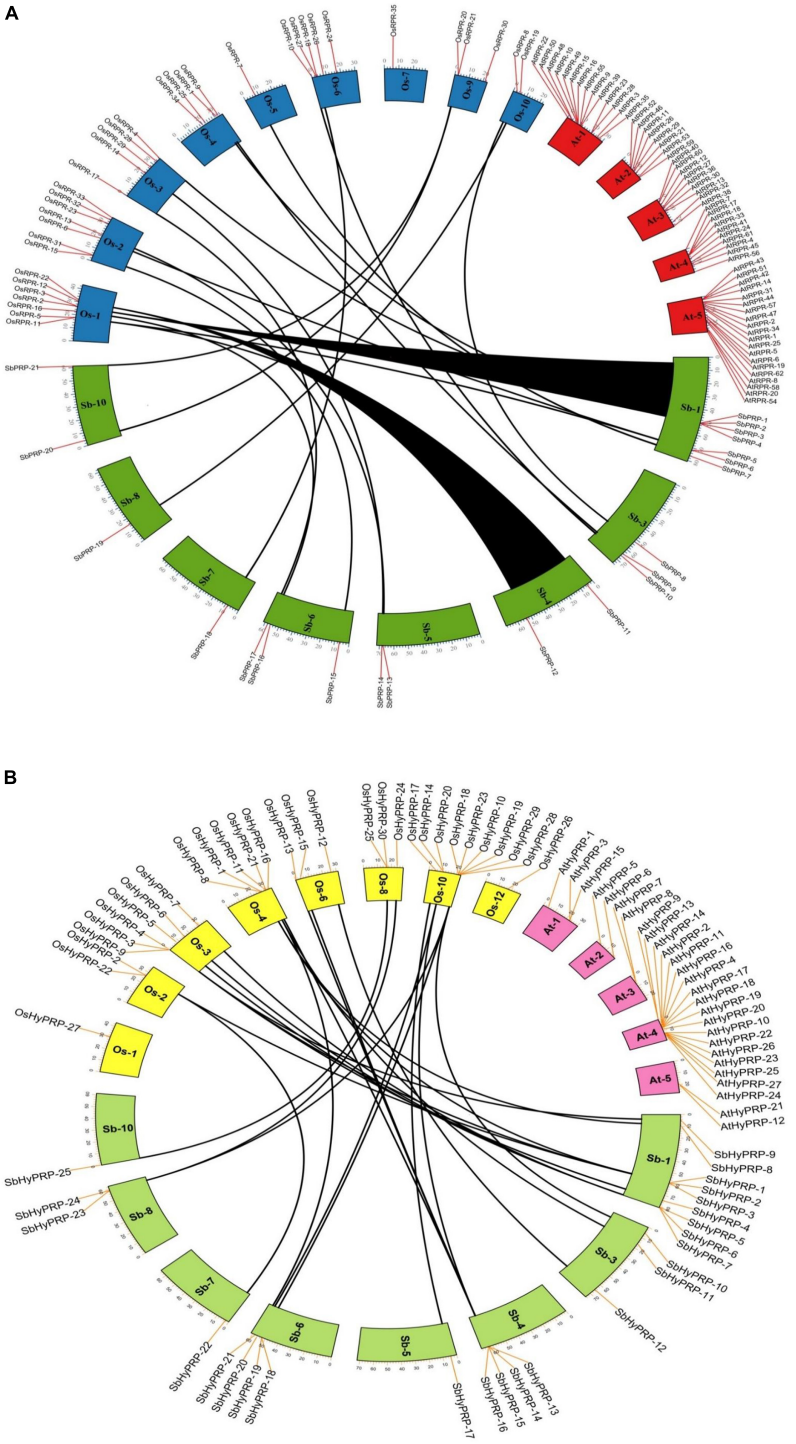

FIGURE 5
Synteny analysis of SbPRP and SbHyPRP genes. **(A)** Synteny analysis of PRP in *Sorghum bicolor, Oryza sativa,* and *Arabidopsis thaliana*. **(B)** Synteny analysis of HyPRP in *Sorghum bicolor, Oryza sativa,* and *Arabidopsis thaliana*. The map was built with TB tools software. Sb, *Sorghum bicolor*; Os, *Oryza sativa;* PRP, Proline-rich proteins; HyPRP, Hybrid proline-rich proteins.

21 SbPRPs, only 38.09% contain transmembrane helices, while 33.33% of SbHyPRPs consist of the same (Tables 1, 2). Six (28.57%) of the SbPRPs target chloroplasts, four extracellular, one plastid, two the cytoplasm, three the nucleus, two the vacuole, and the remaining three target different localizations (Table 1). Out of 27 SbHyPRPs, 11 have been distributed in

the chloroplast, 10 extracellular, one in mitochondria, two in the nucleus, one in the cytoplasm, and two extracellular or vacuolar (Table 2). Based on the analysis, it has been predicted that chloroplast and extracellular are the major target sites for their localization. Most of the SbPRPs have been predicted in the cytoplasm, indicating that they are secretary proteins. SbPRPs have been predicted to have a signal peptide at the N-terminus and a hydrophobic cysteine-rich region at the C-terminus. These results indicate that PRP proteins are secreted to the extracellular matrix through the signal peptide. The majority of the SbPRP proteins phosphorylate at serine and threonine sites and very few of them at tyrosine residues, threonine being the predominant one. Protein kinase C (PKC) and unspecified (unsp) are the most dominant types present in higher amounts in all the SbPRP proteins. Next to CKII, PKA P38MAPK, CDK5, PKG, and GSK3 are the most common kinases associated with phosphorylation (Supplementary Table 8). Whereas, in the case of SbHyPRPs, serine is the governing phosphorylation site followed by threonine and tyrosine. TPKC, unsp, PKA, CKII, cdc2, P38MAPK, CDK5, PKG, and GSK3 are the common kinases for SbHyPRP protein phosphorylations (Supplementary Table 9).

Conserved motif analysis

The MEME web server was used to analyze the motif distribution of SbPRPs and SbHyPRPs. In SbPRPs, the predicted motif 1 appears as the biggest and motif 10, the smallest. The SbPRP family does not exhibit a common motif distribution pattern. Motif 1 is the common motif found at N-terminus in fewer proteins. The motifs 2, 3, 4, and 5 are the structural conserved motifs, present in the middle of the proteins (Supplementary Figures 5, 6). In SbHyPRPs, motif 6 is the largest with 43 amino acids in length, and motifs 7 and 8 with 11 amino acids, are the smallest. Motif 4 is the common conserved motif present at N-terminus, while motif 3 is at C-terminus. Motif 8 exhibited repeated distribution in SbHyPRP 11, 26, and 27 (Supplementary Figures 7, 8). These conserved motifs reflect features for PRP and HyPRP proteins as shown by Wang et al. (2006) and hence provide confirmatory identification of proteins from the sorghum genome.

Homology modeling and validation of proline-rich proteins and hybrid proline-rich proteins

Protein models help to understand structure-function relationships (Rasheed et al., 2020). So, the 3D structures of SbPRP and SbHyPRP proteins were predicted with the best PDB templates (Supplementary Figure 9). The template PDB id, template description, chain, model of the oligomer, and their structure validations are represented in Supplementary Table 10. 3D structures of one SbPRP (SbPRP12) and six SbHyPRP (SbHyPRP2, SbHyPRP5, SbHyPRP6, SbHyPRP13, SbHYPRP17, and SbHYPRP26) proteins displayed significant sequence similarity percent ranging from 31.1% (SbPRP12) to 55.26% (SbHyPRP6). 3D structures of five SbPRP proteins (SbPRP3, SbPRP6, SbPRP10, SbPRP17, and SbPRP19) did not show any significant (<30%) sequence similarity (Supplementary Table 10). All the generated Ramachandran plots for structure validation are represented in Supplementary Figure 10.

miRNA target site prediction and analysis of acetylation and methylation sites

Plant regulatory small RNAs (sRNAs) include microRNAs (miRNAs) and small interfering RNAs (siRNAs) like phasiRNAs which regulate gene expressions, thus, modulating plant growth as well as stress tolerance (Haak et al., 2017). The psRNA Target Server predicts the miRNAs and their target sites in *SbPRP* and *SbHyPRP* genes. The 21 SbPRPS predicted in the present study appear to be the targets for 34 different miRNAs. The sbi-miR437 and sbi-miR5568 have been predicted to target the SbPRP family. The miRNAs participate in cleavage and translation inhibition events. The SbPRP13, 18, and 20 appear as the major targets for different miRNAs (Supplementary Table 11). Interestingly, 29 different miRNAs target 25 *SbHyPRPs* and moderate the activity. The *SbHyPRP2*, *3*, *14*, *16*, *18*, and *24* are the major gene targets for the majority of the miRNAs (Supplementary Table 12). SbPRP9 and SbPRP21 showed a high number of acetylations (Supplementary Table 13). When compared with SbPRPs, SbHyPRPs displayed a diminished number of acetylation and methylation sites. SbHyPRP 11 and 16 have been predicted to have myriad acetylation, and methylation sites (Supplementary Table 14). Prediction of miRNAs, methylation and acetylation sites indicate that *SbPRP* and *SbHyPRP* genes might be regulated epigenetically.

Prediction of simple sequence repeats

Out of a total of 36 SSRs, 18 were predicted in PRPs and HyPRPS. They were present on chromosomes 1, 3, 4, 5, 6, 7, and 10. Chromosome 1 has been found as the hot spot with three PRPs and five HyPRPs. While the majority of them carried single SSRs, PRP8, 10, HyPRP1, 4, and 6, have 2, and PRP6 and 8 have 3 SSRs. Tri-nucleotide repeats have been predicted as the major repeats (25), followed by hexamer (7) and tetra-nucleotide repeats (4) (Supplementary Table 15).

Digital expressions of *SbPRP* and *SbHyPRP* genes in diverse tissues, stages, and stress conditions

Using digital data, the expression of 21 *SbPRP* genes was analyzed in the root, shoot, and leaf tissues exposed to cold and drought stress conditions. Overall, high expression levels of *SbPRPs* were noticed in the leaf compared to root and shoot tissues. Out of 21 *SbPRPs*, *SbPRP16*, *SbPRP17*, *SbPRP19*, *SbPRP1*, and *SbPRP3* displayed high expressions in shoot tissues (Figure 6A). Among diverse developmental stages such as maturity, dough, milking, flowering, and seedling, the seedling stage showed superior expressions followed by the flowering stage. *SbPRP19*, *SbPRP16*, *SbPRP17*, *SbPRP1*, *SbPRP13*, *SbPRP13*, and *SbPRP20* showed high expression levels in seedlings treated with cold and drought stresses in comparison with other developmental stages (Figure 6B). SbPRP18 displayed higher expression levels, followed by 16, and 19 under both the stresses (Figure 6C). *SbHyPRP5*, *SbHyPRP20*, *SbHyPRP13*, and *SbHyPRP21* showed elevated expressions in the leaf. Expressions of *SbHyPRP12*, *SbHyPRP17*, and *SbHyPRP11* were strikingly high in roots (Figure 7A). *SbHyPRP12* and *SbHyPRP26* were markedly upregulated during maturity, dough, milking, and flowering stages in comparison with other genes. The majority of the *SbHyPRP* genes are also expressed during the seedling stage (Figure 7B). The heat map of *SbHyPRPs* showed both up- and down-regulation up to 2.5-folds under cold and drought stresses (Figure 7C). *SbHyPRP17*, *SbHyPRP2*, *SbHyPRP18*, and *SbHyPRP20* showed upregulation in comparison with other genes under stress conditions. *SbHyPRP2*, *SbHyPRP8*, and *SbHyPRP17* displayed high expressions under drought compared to cold stress conditions (Figure 7C).

Expression analysis of *SbPRP* genes in different tissues, varying stress conditions, and Zn treatment

Expression analysis of *SbPRP* and *SbHyPRP* genes were carried out in root, stem, and leaf to address their role in diverse organs. There is no single gene that has exhibited uniform levels of expression in all the three tissues. Under control conditions (without any stress), only *SbPRP2* (1.303-folds) and

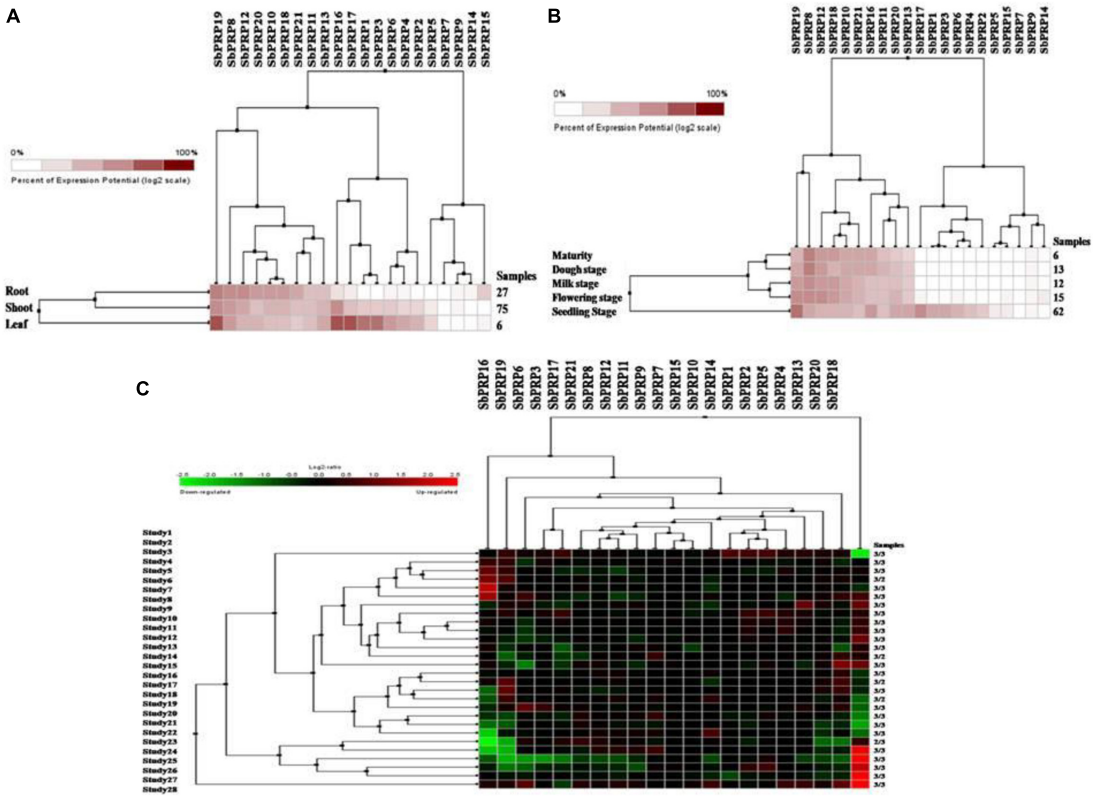

FIGURE 6
Digital expression profile of *SbPRP* genes in different organs, developmental stages under cold and drought stresses. **(A)** *SbPRP* in anatomical tissues, **(B)** *SbPRP* genes in developmental stages, **(C)** *SbPRP* gene expressions under cold and drought stress conditions.

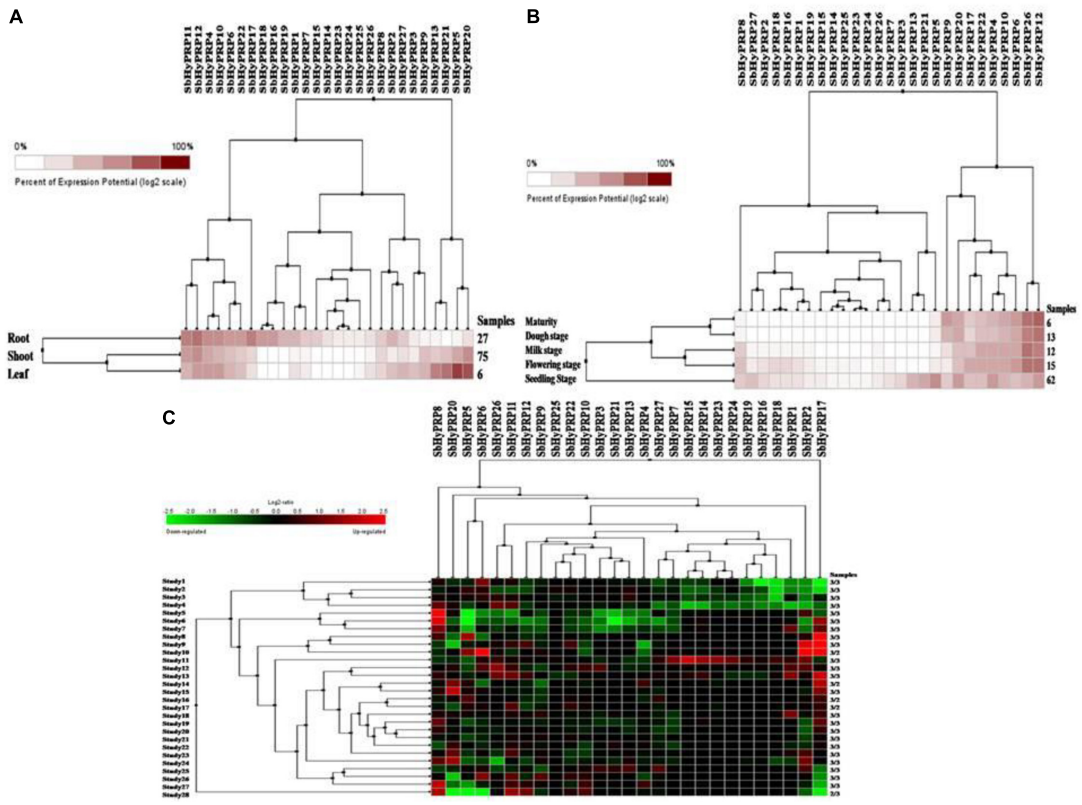

FIGURE 7
Digital expression profile of *SbHyPRP* genes in different organs, developmental stages under cold and drought stresses. **(A)** *SbHyPRP* in anatomical tissues, **(B)** *SbHyPRP* in developmental stages, **(C)** *SbHyPRP* gene expressions under cold and drought stresses.

SbPRP4 (0.824-folds) were constitutively expressed in roots, while *SbPRP11* (1.820-folds) and *SbPRP18* (1.473-folds) in the stem, and *SbPRP3* (0.985) in leaf tissues (Figure 8A and Supplementary Table 16). Drought has considerably stimulated the expression of *SbPRP17* in leaf (4.73-folds), stem (4.08-folds), and root (3.94-folds), but only in the roots of *SbPRP12* (3.61-folds). Salt stress induced the activity of *SbPRP17* by 4. 25-, 3. 53-, and 4.44-folds in leaf, stem, and root tissues, respectively, and also only in the roots of *SbPRP19* (4.34-folds). Heat stress has upregulated *SbPRP3* (3.31-folds), *SbPRP6* (3.34-folds) and *SbPRP17* (4.94-folds), and PRP19 (4.00-folds) in the leaf, *SbPRP8* (4.58-folds) and *SbPRP17* (3.744-folds) in the stem, *SbPRP6*, *SbPRP12* and *SbPRP17* by 4. 05-, 3. 84-, and 3.65-folds respectively in the root (Figure 8B and Supplementary Table 16). Cold stress has stimulated *SbPRP4*, *SbPRP5*, *SbPRP6*, *SbPRP7*, *SbPRP9*, *SbPRP10*, *SbPRP13*, *SbPRP15*, *SbPRP17*, *SbPRP20,* and *SbPRP21* in the leaf between 3.08 to 4.99-folds. The fold-wise increase in the stem of *SbPRP3*, *SbPRP6*, *SbPRP12*, *SbPRP13*, *SbPRP17*, and *SbPRP19* ranged from 3.01 to 5.20-folds. In the case of roots, the elevated transcript levels were 4.53, 5.38, 4.82, 3.03, 4.82, 3.24, and 4.59-folds in *SbPRP3*, *SbPRP6*, *SbPRP12*, *SbPRP13*, *SbPRP15*, *SbPRP17,* and *SbPRP19*, respectively. While ABA stimulated *SbPRP6* and *SbPRP17* by 3. 85-, 3.65- (*SbPRP6*), 4. 94-, and 4.20-folds (*SbPRP17*) in the leaf and root, it activated *SbPRP3*, *SbPRP12*, and *SbPRP17* in the stems by 4.00, 3.04, and 4.00-folds, respectively (Figure 8B and Supplementary Table 16). Zn has jacked up only *SbPRP17* by 3.58-folds in the leaf, *SbPRP3* and *SbPRP17* in the stems by 3.51- and 3. 37-, and in the roots by 4.81- and 3.52-folds respectively. From the results obtained, it is inferred that *SbPRP17* is critical for stress tolerance since it is expressed under various abiotic stress conditions in all three tissues, followed by *SbPRP3*, *SbPRP6,* and *SbPRP12* (Figure 8B, Supplementary Figure 11, and Supplementary Table 16).

Transcript profiling of *SbHyPRP* genes in different tissues, diverse abiotic stresses, and Zn treatment

Unlike *SbPRPs*, *SbHyPRPs* displayed uniform constitutive expressions in all the tissues. In roots, *SbHyPRP12* was enhanced by 1. 75-, *SbHyPRP10* by 1. 60-, and *SbHyPRP21* by 1.54-folds when compared to the expression levels of the housekeeping gene actin. In the case of the stem, *SbHyPRP3*

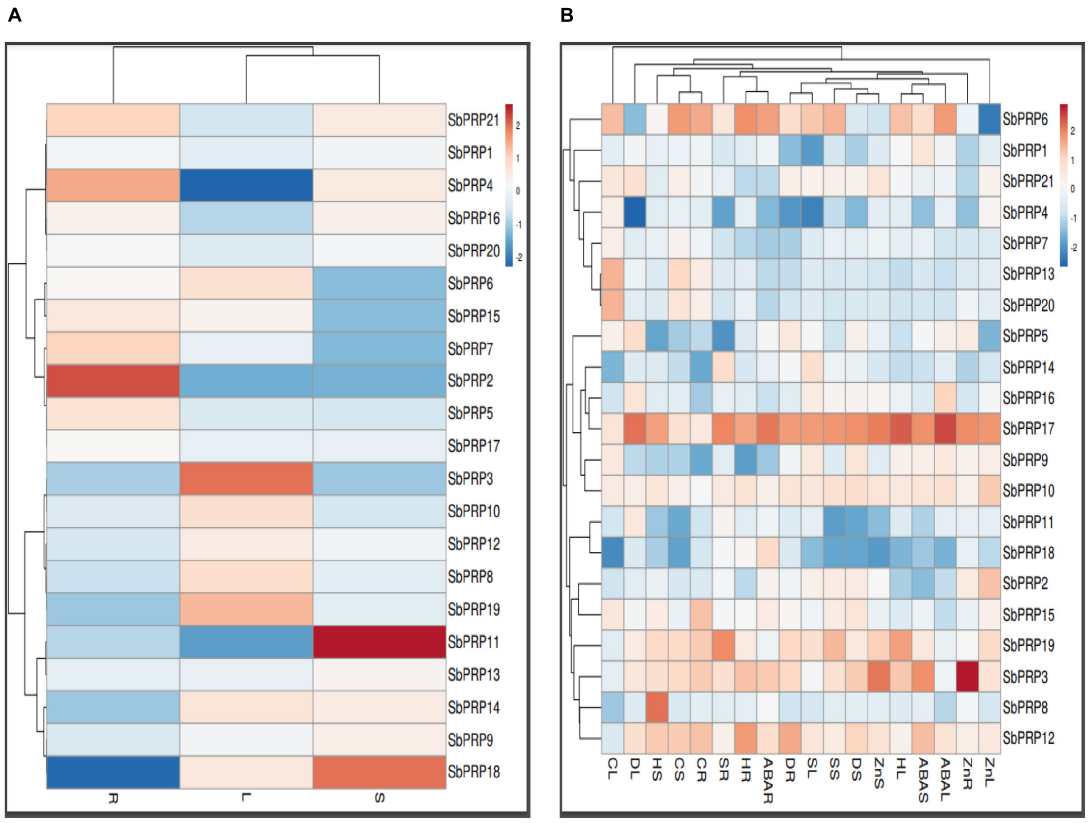

FIGURE 8
qRT-PCR expression profiling of *SbPRP*s. **(A)** Native expression analysis in root, stem, and leaf, **(B)** relative expression analysis in root, stem, and leaf under drought, salt, heat, cold, ABA, and Zn stresses. R, root; S, stem; L, leaf.

was upregulated by 2. 77-, *SbHyPRP20* by 2. 03-, *SbHyPRP16* by 1.95, and *SbHyPRP13* by 1.91-folds. While in leaf tissues, gene expressions increased by 1.77- in *SbHyPRP14*, 1.35- in *SbHyPRP11*, and 1.32-folds in *SbHyPRP18* devoid of any stress (**Figure 9A** and **Supplementary Table 17**). Significant upregulation of the *SbHyPRP2* and *SbHyPRP17* genes was noticed in comparison with control tissues regardless of the tissue and type of stress imposed. Drought stress has increased the expressions of *SbHyPRP2* by 5. 16-, 9. 67-, and 8.17-folds in the leaf, stem, and root, respectively. *SbHyPRP17* registered an upregulation of 26. 66-, 17. 01-, and 15.35-folds in leaf, stem, and root, respectively, under drought. The highest expression of 44.15-folds was recorded in *SbHyPRP20* in the stem tissues under water-deficit conditions. Expressions varied between 3. 45-, and 24.00-folds in *SbHyPRP5*, *SbHyPRP6*, *SbHyPRP10*, *SbHyPRP13*, *SbHyPRP16*, *SbHyPRP27* genes under drought stress (**Figure 9B** and **Supplementary Table 17**). Under salt stress, the highest expression of 21.79-folds was noticed in the root tissues of *SbHyPRP17*, followed by leaf tissues (19.10-folds). *SbHyPRP2* was upregulated by 15.60-folds in the leaf under saline conditions. Activities were also high under salt stress in *SbHyPRP6*, *SbHyPRP7*, *SbHyPRP10*, *SbHyPRP14*, and *SbHyPRP26*. *SbHyPRP17* displayed a dramatic increase in the activity (30.82-folds) under heat stress in the leaves, followed by *SbHyPRP2* in the leaf (23.44-folds). *SbHyPRP2* and *SbHyPRP17* also recorded markedly high activities in the stem and root tissues (15. 3-, 12. 58-, 8. 54-, 13.40-folds respectively). Cold temperature induced the transcript levels of *SbHyPRP2*, *SbHyPRP6*, *SbHyPRP9*, *SbHyPRP12*, *SbHyPRP17*, *SbHyPRP26*, and *SbHyPRP27* in the leaves in the range of 3.34- (*SbHyPRP26*) to 19.96-folds (*SbHyPRP12*). Again in the stem, the expression level was high in *SbHyPRP12* (11.35-folds). *SbHyPRP2* and *SbHyPRP13* exhibited 10.13- and 17.83-folds enhanced transcript levels in the roots under cold stress (**Figure 9B** and **Supplementary Table 17**). Significant upregulation in the activity of *SbHyPRP17* was noticed in the leaf, stem, and root tissues (30. 87-, 16. 10-, and 18.46-folds), and the activities ranged between 3.13- and 9.57-folds in other genes when exposed to the phytohormone ABA. Zn treatment boosted the activities of *SbHyPRP26* (25.39-folds) and *SbHyPRP17* (11.96-folds) in the leaves. While *SbHyPRP2* displayed the maximum activity (16.83-folds) in the stem, the roots of *SbHyPRP17* showed 11.47-fold higher activities compared

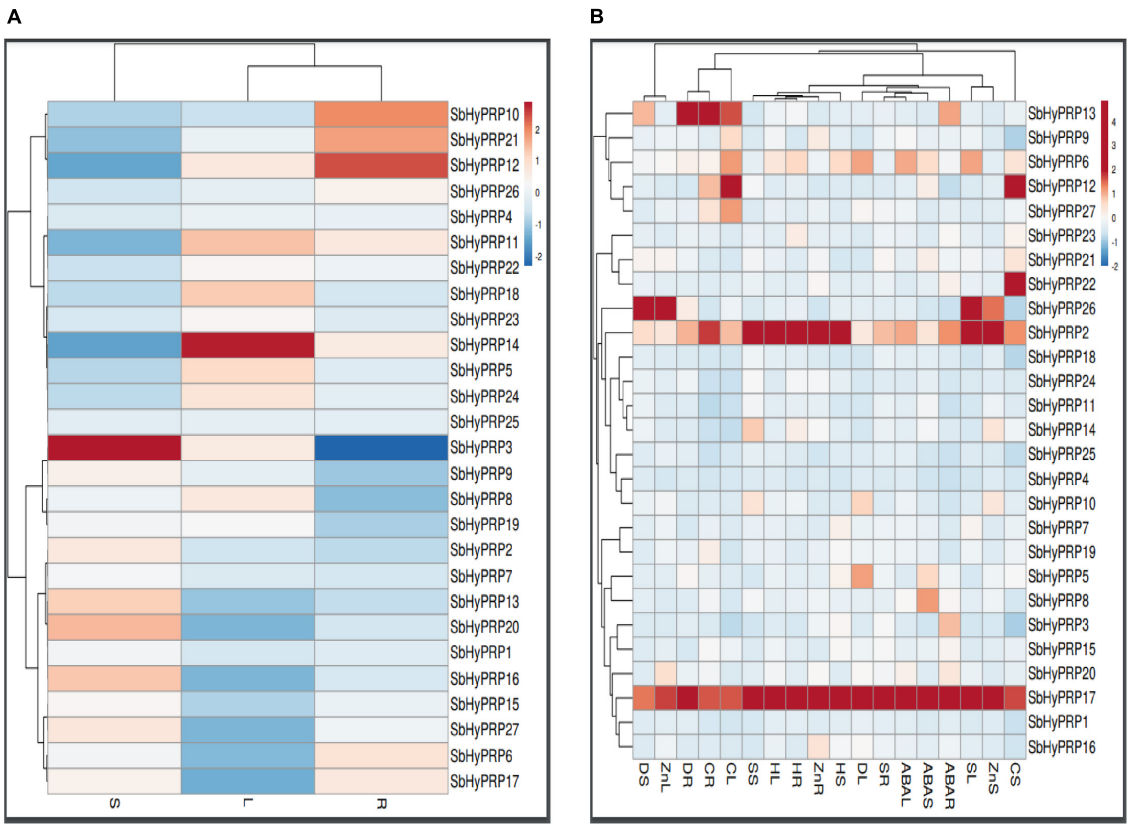

FIGURE 9
qRT-PCR expression profiling of *SbHyPRP*s. **(A)** Native expression analysis in root, stem, and leaf, **(B)** relative expression analysis in root, stem, and leaf under drought, salt, heat, cold, ABA, and Zn stresses. R, root; S, stem; L, leaf.

to the controls (**Figure 9B**, **Supplementary Figure 12**, and **Supplementary Table 17**).

Discussion

Characterization of *SbPRP* and *SbHyPRP* gene homologs

The accessibility of the whole sorghum genome sequence (Paterson et al., 2009) has provided an excellent opportunity for genome annotation, comparative genomic analysis, and understanding of the structural and functional variations among the diverse gene families. Publicly available genome sequence data have helped us in identifying different gene families in sorghum (Kumari et al., 2018; Maheshwari et al., 2019; Nagaraju et al., 2020, 2021). PRPs and HyPRPs play crucial roles in abiotic stress and growth functions as well (Zhang and Schläppi, 2007; Priyanka et al., 2010; Huang et al., 2011; Berendsen et al., 2012; Li et al., 2016; Efthimiadou et al., 2020). Recently, *OsHyPRP06/R3L1* has been found to modulate root system development besides salt tolerance via apoplastic ROS homeostasis in rice (Zhao et al., 2021). Great variability exists in the number of *PRPs* and *HyPRPs* in different taxa (Dvorakova et al., 2007; Neto et al., 2013; Fujino et al., 2014; Showalter et al., 2016; Kapoor et al., 2019; Zhang et al., 2021), which could be due to differences in the genera or the method employed. Genome-wide analyses of sorghum resulted in the identification of 21 *SbPRPs* and 27 *SbHyPRPs* in the present study. Detection of both *SbPRPs* and *SbHyPRPs* in the present study in *S. bicolor* indicates their conservation in evolution.

Prediction of exons and introns

The exon-intron structure in the genomic sequences furnishes an insight into evolutionary relationships among the genes or organisms and perhaps needs intensified investigations (Koralewski and Krutovsky, 2011). Our predicted results on intron-exon structure organization both in *SbPRPs* and *SbHyPRPs* conform to the results obtained from other species (Fujino et al., 2014; Kapoor et al., 2019; Zhang et al., 2021). Several *SbPRP* and *SbHyPRP* genes have been found with

no or few introns. It has been shown in yeast, *A. thaliana*, and mice that genes with rapidly changing expression levels in response to environmental stresses contain lower intron densities (Jeffares et al., 2008). Introns delay the regulatory responses, hence genes that need rapid adjustment for survival against the changing environment are intron poor (Jeffares et al., 2008; Lan et al., 2013). It appears, therefore, that there is an intron loss during the evolution of a few eukaryotic lineages. Besides structural diversity, the complexity of the eukaryotic genes might contribute to the evolution of gene families. Our results show that the *SbPRP* and *SbHyPRP* genes have been distributed randomly on different chromosomes.

Predicted *cis*-regulatory elements

In the present study, *cis*-elements such as DPBF, MYC, MYB, G-box, ABRE, and ERE have been identified in sorghum besides phosphorous, ammonium, sulfur, and iron starvation-responsive elements. SbPRPs have been found rich in phosphorous, iron, ammonium, and sulfur-responsive elements, while SbHyPRPs in sulfur-responsive elements, indicating the diverse roles they play in nutrient homeostasis. These elements might target transcription factors like SPB, zinc finger, WRKY, WD-40, NAC, MYB, HSFs, GRAS, ARFs, and bHLH families and play a vital role in abiotic stress tolerance (Katiyar et al., 2015). MYB and ABRE elements might play a role in the ABA-dependent signaling pathway in response to drought, salt, and cold stresses. Promoter analysis also revealed the presence of elements that participate in sugar signaling, nuclear factor binding, and biotic stress-responsive *cis*-elements such as WBOXNTERF3, WBOXATNPR1, and CGTCA that respond to wounds, pathogens, and salicylic acid (Hwang et al., 1998; Schumann et al., 2017). In cotton, the *GhHyPRP4* promoter is cold-inducible (Huang et al., 2011). Kapoor et al. (2019) reported a good correlation between inducible expression in *OsHyPRP16* in response to the pathogen *Magnaporthe oryzae*, hormones ABA, methyl jasmonate, salicylic acid, and abiotic stresses like cold, and salt in the promoter sequences of rice.

Phylogenetic analysis

Phylogenetic trees infer that PRPs are highly conserved in different taxa. Analysis of the phylogenetic trees reveals that homologous gene pairs have high sequence identities with other taxa compared, thus displaying their evolutionary relationships. The clustering of the PRP and HyPRPs of sorghum, rice, maize, and disconnection from Arabidopsis indicates their evolutionary divergence during monocotyledon lineage-specific evolution. Expansion of gene families occurs through segmental, and tandem duplications besides transposition events (Kong et al., 2007). In the present study, a total of eight paralogs were observed including two regional and six segmental duplication events in *SbPRPs*, while three regional and five segmental duplications in *SbHyPRPs*, indicating that segmental and tandem duplications are responsible for gene family expansion. Gene order conservation of PRP and HyPRP has been identified by circos maps. High conservation of *PRP* and *HyPRP* genes has been noticed between *Sorghum* and *Oryza* when compared to *Sorghum* and *Arabidopsis*, indicating that rice and sorghum are closely related.

Subcellular localization of protein predictions

Predictions related to the subcellular localization of the proteins in the extracellular matrix, identification of signal peptides, and also cysteine-rich regions indicate that all these proteins might not be secretory type as has also been pointed out by Banday et al. (2022). PRPs and HyPRPs are located on the cell wall and plasma membrane and regulate the synthesis of cell walls aside from responding to abiotic stresses (Jose-Estanyol et al., 2004; Kavi Kishor et al., 2015; Mellacheruvu et al., 2016; Gujjar et al., 2018; Li et al., 2019; Zhang et al., 2021). In citrus, CsPRP4 protein was localized in the plasma membrane (Ma et al., 2013), and in *Juglans sigillata*, JsPRP1 in the epidermal cells (Liu et al., 2018). While HyPRP protein from *Arabidopsis* has been identified on the cell wall (Zhang and Schläppi, 2007), GhHyPRP3 from cotton has been noticed on the plasma membrane (Qin et al., 2013). In apple, PRP proteins have been detected in the cell membrane, nucleus, and chloroplast (Zhang et al., 2021). AZELAIC ACID INDUCED 1 (AZI1) is a HyPRP, a member of the HyPRP superfamily (Dvorakova et al., 2007), and a signal-anchored protein that has a proline-rich region (PRR) for targeting the protein to plastids (Cecchini et al., 2015, 2021). HyPRPs possess transmembrane domains besides a PRR and a lipid transfer domain. A feedback regulatory loop exists between glycerol-3-phosphate (G3P) and lipid transfer protein Defective in Induced Resistance (DIR1) in plants and AZI1 mediates azelaic-acid-induced systemic immunity (Yu et al., 2013). But, the subcellular locations of HyPRPs and their precise functions during development and biotic and abiotic stress tolerance have mostly not yet been identified. HyPRPs may be localized to the plastid outer membranes, thylakoid membranes, membranes of the endoplasmic reticulum, plasma membrane, or plasmodesmata (Banday et al., 2022). Few of the HyPRPs have a set of proteins that target the outer membrane of the plastid with the aid of PRRs. HyPRPs modulate systemic immunity against *Pseudomonas syringae* and also help in the colonization of *P. simiae* WCS417 in the roots. Taken together, it appears that HyPRPs may facilitate signal molecule transport and help in plant immunity, growth, and development besides abiotic stress tolerance. Similar to the studies carried out by He et al. (2002), Fujino et al. (2014), and Kapoor et al. (2019), our

findings suggest that SbPRP and SbHyPRP proteins are localized in different subcellular locations.

Homology modeling

The highly expressed SbPRP and SbHyPRP protein structures were predicted and structurally validated for accuracy using Ramachandran plots. Similar studies were reported previously by Kumar et al. (2018). Understanding the prediction of protein structures can facilitate the understanding of their function (Jumper et al., 2021).

Methylation sites, identification of micro RNAs

SbPRPs and *SbHyPRPs* showed methylation as well as acetylation sites. Elements of epigenetic regulation such as histone variants, chromatin remodeling, non-coding RNAs, and DNA methylations are highly conserved among plant systems and represent an important component of the omnifarious biological process (Goldberg et al., 2007; Allis and Jenuwein, 2016; Ueda and Seki, 2020). It is known that epigenetic regulation including acetylation and methylation coordinates abiotic stress responses (Kim et al., 2015; Asensi-Fabado et al., 2017; Luo et al., 2017; Ueda and Seki, 2020). Methylations and acetylations found in sorghum might regulate the genes post-transcriptionally which are implicated in abiotic stresses.

Micro RNAs (miRNAs) are small, non-coding, regulatory elements, which play overriding roles in gene regulation by disturbing the transcripts of genes and mediating the plant adaptation to the changing environmental conditions (Bartel, 2004). In the present study, miRNAs that target SbPRPs and SbHyPRPs have been predicted. We assume that these miRNAs regulate these genes. miRNAs are critical not only for stress responses but also for plant development (Sunkar et al., 2007; Rubio-Somoza et al., 2009). In the present investigation, miR437 and miR5568 have been identified as dominant miRNAs, specific for monocots and absent from eudicots (Sunkar et al., 2007). The conservation and divergence of miRNAs may help to understand miRNA evolution and identify the species-specific miRNAs and the roles that they play in gene regulation. SICKLE (*SIC*), a proline-rich protein has been found vital in *A. thaliana* for development and abiotic stress tolerance. It is also involved in microRNA biogenesis (Zhan et al., 2012). Loss-of-function *sic-1* mutant *Arabidopsis* displayed higher levels of introns, sickle-like margin, delayed flowering, hypersensitivity to chilling, and salt stresses. The *SIC* protein has been observed to colocalize with the miRNA biogenesis component hyponastic leaves 1 (HYL1). These observations have led Zhan et al. (2012) to conclude that *SIC* is necessary for the biogenesis of some miRNAs and spliced introns. DNA and chromatin modifications modulate the expression of stress-responsive genes. Such modifications are also heritable inferring their role in the evolutionary mechanisms associated with abiotic stress tolerance (Singroha et al., 2022).

Predicted simple sequence repeats

Simple sequence repeats are used generally to study genetic relatedness or variation among the species. SSRs get mutated quickly; hence, differentiation of closely related species is possible. So far, several QTLs associated with diverse traits were identified in many crops. The predicted SSRs associated with PRPs and HyPRPs could be informative and used to evaluate the genetic diversity and relationships among diverse sorghum lines. Such markers may also be useful to the breeders who are aiming to generate abiotic stress tolerant sorghum lines.

Digital expressions of *SbPRP* and *SbHyPRP* genes at diverse organs and developmental stages and transcript profiling of *SbPRP* and *SbHyPRP* genes under abiotic stresses, abscisic acid, and zinc

Digital expression data indicated that the expressions of *PRP* and *HyPRP* genes were higher in leaf tissues during the seedling stage of plant development. The results indicate the importance of *SbPRP19*, *SbPRP16*, *SbPRP17*, *SbPRP1*, *SbPRP13*, *SbPRP13*, and *SbPRP20* genes during seedling when compared to other stages. Such genes need to be functionally validated to find out the seedling specific roles they play especially under water-deficit conditions. Increased expressions of both *SbHyPRP12* and *SbHyPRP26* during maturity, dough, milking, and flowering stages infer the crucial role they might play during these stages. High expressions of *SbHyPRP2*, *SbHyPRP8*, and *SbHyPRP17* under water-deficit conditions compared to cold stress surmise that functional validation of these genes needs to be carried out.

Insolubilization of PRPs leads to the formation of protein–protein or protein–carbohydrate linkages within cell walls and assists in the stability of extracellular matrix in plants (Bernhardt and Tierney, 2000; Akiyama and Pillai, 2003). PRPs respond to the changing environments and thus abet in coping with stress situations (Kavi Kishor et al., 2015; Zhang et al., 2021). Literature on the transcript expressions of PRPs is scanty. Munoz et al. (1998) in *Cicer arietinum* and Xu et al. (2007) in *Gossypium hirsutum* have shown tissue-specific expression of PRP genes. *GmPRP1* mRNAs have been found in elongating and mature regions of the seedling hypocotyl cells in *Glycine max*, *GmPRP2* in phloem cells, and *GmPRP3* in the endodermoid layer of cells in the hypocotyl elongating region (Wyatt et al.,

1992). In the case of *Arabidopsis*, *AtPRP1* and *AtPRP3* gene expressions were noticed in roots, and *AtPRP2* and *AtPRP4* in aerial organs (Fowler et al., 1999; Bernhardt and Tierney, 2000). *SbPRP* genes were activated under different abiotic stress conditions aside from ABA and Zn treatments in a tissue-specific manner in sorghum. This reveals that these genes are spatially regulated during plant development in a specific tissue or cell type as has been shown by others (Munoz et al., 1998; Xu et al., 2007; Zhang et al., 2021). Out of 21 *SbPRPs*, *SbPRP17* appeared to have ubiquitous expressions in all tissues though the magnitude differed, suggesting that *SbPRPs* function in many physiological processes during stress. It is known that *PRP* genes are up- and down-regulated, involved in plant growth and environmental challenges. In support of this statement, Gothandam et al. (2010) overexpressed rice *OsPRP3* and showed that transgenics acquire cold tolerance, but knockdown mutants display defects in flower morphogenesis. In *Arabidopsis*, *PRP* is critical for development, and abiotic stress tolerance is associated with microRNA biogenesis (Zhan et al., 2012). When *Gossypium hirsutum GhPRP5* gene was overexpressed in *Arabidopsis*, transgenics exhibited diminished growth in comparison with wild-type plants. On the other hand, *GhPRP5* knock-down mutants in cotton improved fiber development with longer fiber length (Xu et al., 2013). Thus, PRPs have been proved to be associated with positive or negative regulation of plant growth. In the present study, it has been noticed that *SbPRPs* respond to drought, salt, heat, cold, ABA, and Zn inferring that *SbPRPs* play critical roles, but the responses differ among various environmental stimuli and Zn treatment. Such a phenomenon was noticed in *Brassica napus*, and *BnPRP* responds to low and high temperatures, and drought, but not injury (Goodwin et al., 1996). In *Glycine max*, *GmPRP* was triggered by salicylic acid, an endogenous circadian rhythm and diverse abiotic stress conditions (He et al., 2002). Contrary to the above, *OsPRP* was down-regulated during submergence in *Oryza sativa* (Akiyama and Pillai, 2003). In the case of Arabidopsis, out of 18 *PRP* genes, nematode infection upregulated the expression of *PRP4*, *PRP11*, and *PRP16* and *P. syringae* infection induced *PRP9* and *PRP10* (Showalter et al., 2010). Overexpression of *Juglans sigillata JsPRP1* resulted in drought tolerance, $CdCl_2$ stress, *Colletotrichum gloeosporiodes* infection (Liu et al., 2018). In apple also, many *MdPRP* genes were expressed in all tissues except *MdPRP4*, *MdPRP5*, *MdPRP7,* and *MdPRP8* (Zhang et al., 2021). Interestingly, Zn also stimulated *SbPRP3* and *SbPRP17* genes in all three tissues, but their implication in zinc nutrition or starvation await functional assays to demonstrate the precise role of ABA and Zn in *PRP* functioning. Overall, these findings indicate that *PRPs* are differentially regulated under diverse abiotic stress conditions and might play decisive roles in modulating growth in addition to stress responses.

HyPRPs are a large family of cell wall protein with a variable N-terminal domain and a conserved C-terminal domain which is related to non-specific lipid transfer proteins. Initially, they have been regarded as only cell wall proteins, but slowly their multifunctional nature is being unraveled. *HyPRPs* take an active part in abscission, cell elongation, cell wall synthesis, growth, development, and biotic and abiotic stress tolerance (Wu et al., 1993; Zhang and Schläppi, 2007; Dvorakova et al., 2012; Sundaresan et al., 2018). Compared to *SbPRP* genes, multiple *SbHyPRP* genes have been found upregulated upon exposure to different abiotic stress conditions. Several *HyPRP* genes have been cloned and overexpressed and the transgenics displayed freezing or low-temperature stress tolerance inferring their positive regulatory role in stress response (Zhang and Schläppi, 2007; Huang et al., 2011; Peng et al., 2015). Overexpression of other *HyPRP* genes such as *CcHyPRP* (*Cajanus cajan*), *GhHyPRP3* (*Gossypium hirsutum*), and *MfHyPRP* (*Medicago falcata*) increased the levels of tolerance to multiple abiotic stresses like salt, and cold temperature (Priyanka et al., 2010; Qin et al., 2013; Tan et al., 2013). Pitzschke et al. (2014) identified and characterized AZI1, a lipid transfer protein (LTP)-related HyPRP, a target of mitogen-activated protein kinase 3 (MPK3). While null mutants of *azi1* are salt susceptible, overexpressing lines exhibit tolerance. Thus, MPK3 appears as a positive regulator of AZI1 and a key interactant. *HyPRP* from *Arabidopsis* has been found to play a key role in SAR when infected with *Pseudomonas syringae* (Jung et al., 2009). Neto et al. (2013) identified soybean HyPRP family members and their responses to Asian soybean rust disease. *EARLI1* is an Arabidopsis *HyPRP*, protects plants against cold stress, and improves germination under low temperatures and salt stress conditions (Zhang and Schläppi, 2007). Experiments performed by Li et al. (2012) using recombinant EARLI1 protein indicate that its application to *Botrytis cinerea*, *Fusarium oxysporum* inhibits the growth and cell viability. These results point out that *HyPRPs* are positively associated with biotic stress tolerance. Conversely, Yeom et al. (2012) identified the *HyPRP1* gene in *Capsicum annuum* and *Nicotiana benthamiana* which is constitutively expressed in different organs. But the gene was down-regulated when inoculated with pathogens. Overexpression of the gene resulted in accelerated death along with the down-regulation of ROS-scavenging genes. Gene silencing suppressed pathogen-induced cell death but increased disease resistance. It appears therefore that *HyPRP* acts as a positive regulator of cell death and a negative regulator of basal defense against pathogens. A DOUBLE HYBRID PROLINE-RICH PROTEIN 1 (*AtDHyPRP1*) detected in *Arabidopsis* contains two tandem proline-rich domain-eight cysteine motifs (PRD-8CMs) and is a novel *HyPRP* and induced by salicylic acid, methyl jasmonate, virulent and non-virulent strains of the pathogen

P. synringae. Overexpression of this gene resulted in increased pathogen resistance, but RNAi lines of *AtDHyPRP1* exhibited susceptibility, indicating its involvement in defense response (Li et al., 2014). Li et al. (2016) noticed that the *SpHyPRP1* gene isolated from *Solanum pennellii* play a negative role in abiotic stress tolerance in tomato. Similarly, *GhHyPRP1* negatively regulates the resistance to *Verticillium dahliae* in cotton via the thickening of cell walls and ROS accumulation (Yang et al., 2018). These studies underpin the significant role that *HyPRPs* play during biotic and abiotic stress tolerance.

Conclusion

Proline-rich proteins and HyPRPs are dominant constituents of cell wall proteins and help in the stability of the extracellular matrix. Their role in plant growth, development, and biotic and abiotic stresses are being rolled in recent times. The present study predicts the identification of 21 PRPs and 27 HyPRPs in sorghum and also the presence of *cis*-regulating elements implicated in abiotic stress tolerance, and nutritional starvation. Further, qRT-PCR analysis indicates that *SbPRP* and *SbHyPRP* genes are stimulated under cold, drought, high temperature, and salt stress conditions in sorghum. However, it is necessary to understand the molecular regulation of PRP and HyPRP proteins and also the functional validation of these genes in a wide array of biotic and abiotic stress conditions.

Data availability statement

The original contributions presented in this study are included in the article/Supplementary material, further inquiries can be directed to the corresponding author.

Author contributions

PK and NS designed the experiments. MN, RV, and GR carried out the bioinformatics analysis. GR performed the qRT-PCR experiments. PK, NS, GR, MN, RV, NJ, AKS, PS, and SP prepared the manuscript and refined it. PK, MN, GR, NS, and AKS revised the manuscript. All authors have read and approved the final version of the manuscript.

Funding

This work was financially supported from the German Federal Ministry for Economic Cooperation and Development (BMZ) commissioned and administered through the Deutsche Gesellschaft für Internationale Zusammenarbeit (GIZ) Fund for International Agricultural Research (FIA), grant number: 81206686 and the Bill & Melinda Gates Foundation AGGRi Alliance (grant No. OPP1194925), and Stress Tolerant Rice for Africa and South Asia (STRASA) Phase III (grant No. OPP1088843).

Acknowledgments

PK acknowledges VFSTR, Guntur for providing emeritus fellowship. GR is grateful to ICMR for providing fellowship. RV is a graduate student worked in the laboratory of PK and is grateful to VFSTR.

Conflict of interest

The authors declare that the research was conducted in the absence of any commercial or financial relationships that could be construed as a potential conflict of interest.

Publisher's note

All claims expressed in this article are solely those of the authors and do not necessarily represent those of their affiliated organizations, or those of the publisher, the editors and the reviewers. Any product that may be evaluated in this article, or claim that may be made by its manufacturer, is not guaranteed or endorsed by the publisher.

Supplementary material

The Supplementary Material for this article can be found online at: https://www.frontiersin.org/articles/10.3389/fpls.2022.952732/full#supplementary-material

References

Akiyama, T., and Pillai, M. A. (2003). Isolation and characterization of a gene for a repetitive proline-rich protein (OsPRP) down-regulated during submergence in rice (*Oryza sativa*). *Physiol. Plant.* 118, 507–513.

Allis, C. D., and Jenuwein, T. (2016). The molecular hallmarks of epigenetic control. *Nat. Rev. Genet.* 17, 487–500. doi: 10.1038/nrg.2016.59

Asensi-Fabado, M. A., Amtmann, A., and Perrella, G. (2017). Plant responses to abiotic stress: The chromatin context of transcriptional regulation. *Biochim. Biophys. Acta Gene Regul. Mech.* 1860, 106–122. doi: 10.1016/j.bbagrm.2016.07.015

Bailey, T. L., and Gribskov, M. (1998). Combining evidence using p-values: Application to sequence homology searches. *Bioinformatics* 14, 48–54. doi: 10.1093/bioinformatics/14.1.48

Bailey, T. L., Williams, N., Misleh, C., and Li, W. W. (2006). MEME: Discovering and analyzing DNA and protein sequence motifs. *Nucleic Acids Res.* 34, W369–W373. doi: 10.1093/nar/gkl198

Banday, Z. Z., Cecchini, N. M., Speed, D. J., Scott, A. T., Parent, C., Hu, C. T., et al. (2022). Friend or foe: Hybrid proline-rich proteins determine how plants respond to beneficial and pathogenic microbes. *Plant Physiol.* 1:kiac263. doi: 10.1093/plphys/kiac263

Bartel, D. P. (2004). MicroRNAs: Genomics, biogenesis, mechanism, and function. *Cell* 116, 281–297. doi: 10.1016/S0092-8674(04)00045-5

Beier, S., Thiel, T., Münch, T., Scholz, U., and Mascher, M. (2017). MISA-web: A web server for microsatellite prediction. *Bioinformatics* 33, 2583–2585. doi: 10.1093/bioinformatics/btx198

Berendsen, R. L., Pieterse, C. M. J., and Bakker, P. A. H. M. (2012). The rhizosphere microbiome and plant health. *Trends Plant Sci.* 17, 478–486. doi: 10.1016/j.tplants.2012.04.001

Bernhardt, C., and Tierney, M. L. (2000). Expression of AtPRP3, a proline-rich structural cell wall protein from *Arabidopsis*, is regulated by cell-type-specific developmental pathways involved in root hair formation. *Plant Physiol.* 122, 705–714. doi: 10.1104/pp.122.3.705

Biasini, M., Bienert, S., Waterhouse, A., Arnold, K., Studer, G., Schmidt, T., et al. (2014). SWISS-MODEL:modeling protein tertiary and quaternary structure using evolutionary information. *Nucleic Acids Res.* 42, W252–W258. doi: 10.1093/nar/gku340

Blanco-Portales, R., Lopez-Raez, J. A., Bellido, M. L., Moyano, E., Dorado, G., Gonzalez-Reyes, A., et al. (2004). A strawberry fruit-specific and ripening-related gene codes for a HyPRP protein involved in polyphenol anchoring. *Plant Mol. Biol.* 55, 763–780. doi: 10.1007/s11103-004-1966-4

Blom, N., Sicheritz-Ponten, T., Gupta, R., Gammeltoft, S., and Brunak, S. (2004). Prediction of post-translational glycosylation and phosphorylation of proteins from the amino acid sequence. *Proteomics* 4, 1633–1649. doi: 10.1002/pmic.200300771

Bohnert, H. J., Gong, Q., Li, P., and Ma, S. (2006). Unraveling abiotic stress tolerance mechanisms-getting genomics going. *Curr. Opin. Plant Biol.* 9, 180–188. doi: 10.1016/j.pbi.2006.01.003

Bokszczanin, K. (2013). Perspectives on deciphering mechanisms underlying plant heat stress response and thermotolerance. *Front. Plant Sci.* 4:315. doi: 10.3389/fpls.2013.00315

Boron, A. K., Orden, J. V., Markakis, M. N., Mouille, G., Adriaensen, D., Verbelen, J., et al. (2014). Proline-rich protein-like PRPL1 controls elongation of root hairs in *Arabidopsis thaliana*. *J. Exp. Bot.* 65, 5485–5495. doi: 10.1093/jxb/eru308

Bouton, S., Viau, L., Lelievre, E., and Limami, A. M. (2005). A gene encoding a protein with a proline-rich domain (MtPPRD1), revealed by suppressive subtractive hybridization (SSH), is specifically expressed in the *Medicago truncatula* embryo axis during germination. *J. Exp. Bot.* 56, 825–832. doi: 10.1093/jxb/eri077

Boutrot, F., Chantret, N., and Gautier, M. F. (2008). Genome-wide analysis of the rice and *Arabidopsis* non-specific lipid transfer protein (nsLtp) gene families and identification of wheat nsLtp genes by EST data mining. *BMC Genom.* 9:86. doi: 10.1186/1471-2164-9-86

Burge, C. B., and Karlin, S. (1998). Finding the genes in genomic DNA. *Curr. Opin. Struct. Biol.* 8, 346–354. doi: 10.1016/s0959-440x(98)80069-9

Carella, P. (2020). Xylem-mobile oxylipins are critical regulators of induced systemic resistance in maize. *Plant Cell* 32, 13–14. doi: 10.1105/tpc.19.00924

Cassab, G. I. (1998). Plant cell wall proteins. *Annu. Rev. Plant Biol. Plant Mol. Biol.* 49, 281–309. doi: 10.1146/annurev.arplant.49.1.281

Cecchini, N. M., Roychoudhry, S., Speed, D. J., Steffes, K., Tambe, A., Zodrow, K., et al. (2019). Underground azelaic acid-conferred resistance to *Pseudomonas syringae* in *Arabidopsis*. *Mol. Plant Microbe Interact.* 32, 86–94. doi: 10.1094/MPMI-07-18-0185-R

Cecchini, N. M., Speed, D. J., Roychoudhry, S., and Greenberg, J. T. (2021). Kinases and protein motifs required for AZI1 plastid localization and trafficking during plant defense induction. *Plant J.* 105, 1615–1629. doi: 10.1111/tpj.15137

Cecchini, N. M., Steffes, K., Schlappi, M. R., Gifford, A. N., and Greenberg, J. T. (2015). *Arabidopsis* AZI1 family proteins mediate signal mobilization for systemic defence priming. *Nat. Commun.* 6:7658. doi: 10.1038/ncomms8658

Chen, C., Chen, H., Zhang, Y., Thomas, H. R., Frank, M. H., He, Y., et al. (2020). TBtools: An integrative toolkit developed for interactive analyses of big biological data. *Mol. Plant* 13, 1194–1202. doi: 10.1016/j.molp.2020.06.009

Chen, J., Zhao, J., Ning, J., Liu, Y., Xu, J., Tian, S., et al. (2014). NtProRP1, a novel proline-rich protein, is an osmotic stress-responsive factor and specifically functions in pollen tube growth and early embryogenesis in *Nicotiana tabacum*. *Plant Cell Environ.* 37, 499–511. doi: 10.1111/pce.12174

Dai, X., and Zhao, P. X. (2011). psRNATarget: A plant small RNA target analysis server. *Nucleic Acids Res.* 39, W155–W159. doi: 10.1093/nar/gkr319

Dvorakova, L., Cvrckova, F., and Fischer, L. (2007). Analysis of the hybrid proline-rich protein families from seven plant species suggests rapid diversification of their sequences and expression patterns. *BMC Genom.* 8:412. doi: 10.1186/1471-2164-8-412

Dvorakova, L., Srba, M., Opatrny, Z., and Fischer, L. (2012). Hybrid proline-rich proteins: Novel players in plant cell elongation?. *Ann. Bot.* 109, 453–462. doi: 10.1093/aob/mcr278

Efthimiadou, A., Katsenios, N., Chanioti, S., Giannoglou, M., Djordjevic, N., and Katsaros, G. (2020). Effect of foliar and soil application of plant growth promoting bacteria on growth, physiology, yield and seed quality of maize under Mediterranean conditions. *Sci. Rep.* 10:21060. doi: 10.1038/s41598-020-78034-6

Esen, A., Bietz, J. A., Paulis, J. W., and Wall, J. S. (1982). Tandem repeats in the N-terminal sequence of a proline-rich protein from corn endosperm. *Nature* 296, 678–679. doi: 10.1038/296678a0

Fischer, L., Lovas, A., Opatrny, Z., and Banfalvi, Z. (2002). Structure and expression of a hybrid proline-rich protein gene in the *Solanaceous* species, *Solanum brevidens*, *Solanum tuberosum* and *Lycopersicum esculentum*. *J. Plant Physiol.* 159, 1271–1275. doi: 10.1078/0176-1617-00744

Fowler, T. J., Bernhardt, C., and Tierney, M. L. (1999). Characterization and expression of four proline-rich cell wall protein genes in *Arabidopsis* encoding two distinct subsets of multiple domain proteins. *Plant Physiol.* 121, 1081–1091. doi: 10.1104/pp.121.4.1081

Fujino, K., Obara, M., and Sato, K. (2014). Diversification of the plant-specific hybrid glycine-rich protein (HyGRP) genes in cereals. *Front. Plant Sci.* 5:489. doi: 10.3389/fpls.2014.00489

Gao, Q. M., Zhu, S., Kachroo, P., and Kachroo, A. (2015). Signal regulators of systemic acquired resistance. *Front. Plant Sci.* 6:228. doi: 10.3389/fpls.2015.00228

Gasteiger, E., Hoogland, C., Gattiker, A., Wilkins, M. R., Appel, R. D., and Bairoch, A. (2005). "Protein identification and analysis tools on the ExPASy server," in *The Proteomics Protocols Handbook. Springer Protocols Handbooks*, ed. J. M. Walker (Totowa, NJ: Humana Press), 571–607. doi: 10.1385/1-59259-890-0:571

Goldberg, A. D., Allis, C. D., and Bernstein, E. (2007). Epigenetics: A landscape takes shape. *Cell* 128, 635–638. doi: 10.1016/j.cell.2007.02.006

Goodwin, W., Pallas, J. A., and Jenkins, G. I. (1996). Transcripts of a gene encoding a putative cell wall-plasma membrane linker protein are specifically cold-induced in *Brassica napus*. *Plant Mol. Biol.* 31, 771–781. doi: 10.1007/BF00019465

Gothandam, K. M., Nalini, E., Karthikeyan, S., and Shin, J. S. (2010). OsPRP3, a flower specific proline-rich protein of rice, determines extracellular matrix structure of floral organs and its overexpression confers cold-tolerance. *Plant Mol. Biol.* 72, 125–135. doi: 10.1007/s11103-009-9557-z

Gujjar, R. S., Karkute, S. G., Rai, A., Singh, M., and Singh, B. (2018). Proline-rich proteins may regulate free cellular proline levels during drought stress in tomato. *Curr. Sci.* 114, 915–920. doi: 10.18520/cs/v114/i04/909-915

Gujjar, R. S., Pathak, A. D., Karkute, S. G., and Watana, K. S. (2019). Multifunctional proline rich proteins and their role in regulating cellular proline content in plants under stress. *Biol. Plant* 63, 448–454. doi: 10.32615/bp.2019.078

Guo, A. Y., Zhu, Q. H., Chen, X., and Luo, J. C. (2007). GSDS: A gene structure display server. *Yi Chuan Hered.* 29, 1023–1026.

Haak, D. C., Fukao, T., Grene, R., Hua, Z., Ivanov, R., Perrella, G., et al. (2017). Multilevel regulation of abiotic stress responses in plants. *Front. Plant Sci.* 8:1564. doi: 10.3389/fpls.2017.01564

Hadebe, S. T., Modi, A. T., and Mahabudhi, T. (2017). Drought tolerance and water use of cereal crops: A focus on sorghum as a food security crop in sub-saharan Africa. *J. Agron. Crop Sci.* 203, 177–191. doi: 10.1111/jac.12191

He, C. Y., Zhang, J. S., and Chen, S. Y. (2002). A soybean gene encoding a proline-rich protein is regulated by salicylic acid, an endogenous circadian rhythm

and by various stresses. *Theor. Appl. Genet.* 104, 1125–1131. doi: 10.1007/s00122-001-0853-5

Holk, A., Klumpp, L., and Scherer, G. F. E. (2002). A cell wall protein down-regulated by auxin suppressed cell expansion in *Daucus carota* (L.). *Plant Mol. Biol.* 50, 295–305. doi: 10.1023/a:1016052613196

Hong, J. C., Nagao, R. T., and Key, J. L. (1990). Characterization of a proline-rich cell wall protein gene family of soybean. A comparative analysis. *J. Biol. Chem.* 265, 2470–2475. doi: 10.1016/S0021-9258(19)39823-0

Horton, P., Park, K. J., Obayashi, T., Fujita, N., Harada, H., Adams-Collier, C. J., et al. (2007). WoLF PSORT: Protein localization predictor. *Nucleic Acids Res.* 35, W585–W587. doi: 10.1093/nar/gkm259

Huang, G., Gong, S., Xu, W., Li, P., Zhang, D., Qin, L., et al. (2011). GhHyPRP4, a cotton gene encoding putative hybrid proline-rich protein, is preferentially expressed in leaves and involved in plant response to cold stress. *Acta Biochim. Biophys. Sin.* 43, 519–527. doi: 10.1093/abbs/gmr040

Huang, R. (2018). Research progress on plant tolerance to soil salinity and alkalinity in *Sorghum*. *J. Integr. Agric.* 17, 739–746. doi: 10.1016/S2095-3119(17)61728-3

Hunt, L., Amsbury, S., Baillie, A., Movahedi, M., Mitchell, A., Afsharinafar, M., et al. (2017). Formation of the stomatal outer cuticular ledge requires a guard cell wall proline-rich protein. *Plant Physiol.* 174, 689–699. doi: 10.1104/pp.16.01715

Hwang, Y. S., Karrer, E. E., Thomas, B. R., Chen, L., and Rodriguez, R. L. (1998). Three cis-elements required for rice α-amylase Amy3D expression during sugar starvation. *Plant Mol. Biol.* 36, 331–341. doi: 10.1023/A:1005956104636

Jeffares, D. C., Penkett, C. J., and Bähler, J. (2008). Rapidly regulated genes are intron poor. *Trends Genet.* 24, 375–378. doi: 10.1016/j.tig.2008.05.006

Jose-Estanyol, M., Gomis-Ruth, F. X., and Puigdomènech, P. (2004). The eight-cysteine motif, a versatile structure in plant proteins. *Plant Physiol. Biochem.* 42, 355–365. doi: 10.1016/j.plaphy.2004.03.009

Jose-Estanyol, M., and Puigdomenech, P. (1993). Structure and expression of genes coding for structural proteins of the plant cell wall. *New Phytol.* 125, 259–282. doi: 10.1111/j.1469-8137.1993.tb03881.x

Jose-Estanyol, M., and Puigdomenech, P. (1994). Hybrid-proline rich and related proteins. *Curr. Top. Mol. Genet.* 2, 109–126.

Jose-Estanyol, M., and Puigdomenech, P. (2000). Plant cell wall glycoproteins and their genes. *Plant Physiol. Biochem.* 38, 97–108. doi: 10.1016/S0981-9428(00)00165-0

Jumper, J., Evans, R., Pritzel, A., Green, T., Figurnov, M., Ronneberger, O., et al. (2021). Highly accurate protein structure prediction with AlphaFold. *Nature* 596, 583–589. doi: 10.1038/s41586-021-03819-2

Jung, H. W., Tschaplinski, T. J., Wang, L., Glazebrook, J., and Greenberg, J. T. (2009). Priming in systemic plant immunity. *Science* 324, 89–91. doi: 10.1126/science.1170025

Kachroo, A., and Kachroo, P. (2020). Mobile signals in systemic acquired resistance. *Curr. Opin. Plant Biol.* 58, 41–47. doi: 10.1016/j.pbi.2020.10.004

Kapoor, R., Kumar, G., Arya, P., Jaswal, R., Jain, P., Singh, K., et al. (2019). Genome-wide analysis and expression profiling of rice hybrid proline-rich proteins in response to biotic and abiotic stresses, and hormone treatment. *Plants* 8:343. doi: 10.3390/plants8090343

Katiyar, A., Smita, S., Muthusamy, S. K., Chinnusamy, V., Pandey, D. M., and Bansal, K. C. (2015). Identification of novel drought-responsive microRNAs and trans-acting siRNAs from *Sorghum bicolor* (L.) Moench by high-throughput sequencing analysis. *Front. Plant Sci.* 6:506. doi: 10.3389/fpls.2015.00506

Kavi Kishor, P. B. K., Hima Kumari, P., Sunita, M. S. L., and Sreenivasulu, N. (2015). Role of proline in cell wall synthesis and plant development and its implications in plant ontogeny. *Front. Plant Sci.* 6:544. doi: 10.3389/fpls.2015.00544

Keller, B. (1993). Structural cell wall proteins. *Plant Physiol.* 101, 1127–1130. doi: 10.1104/pp.101.4.1127

Kim, J. M., Sasaki, T., Ueda, M., Sako, K., and Seki, M. (2015). Chromatin changes in response to drought, salinity, heat, and cold stresses in plants. *Front. Plant Sci.* 6:114. doi: 10.3389/fpls.2015.00114

Kong, H., Landherr, L., Frohlich, M., Leebens-Mack, J., Ma, H., and dePamphilis, C. (2007). Patterns of gene duplication in the plant SKP1 gene family in angiosperms: Evidence for multiple mechanisms of rapid gene birth. *Plant J.* 50, 873–885. doi: 10.1111/j.1365-313X.2007.03097.x

Koralewski, T. E., and Krutovsky, K. V. (2011). Evolution of exon-intron structure and alternative splicing. *PLoS One* 6:e18055. doi: 10.1371/journal.pone.0018055

Kumar, A., Batra, R., Gahlaut, V., Gautam, T., Kumar, S., Sharma, M., et al. (2018). Genome-wide identification and characterization of gene family for RWP-RK transcription factors in wheat (*Triticum aestivum* L.). *PLoS One* 13:e0208409. doi: 10.1371/journal.pone.0208409

Kumar, P., Joy, J., Pandey, A., and Gupta, D. (2017). PRmePRed: A protein arginine methylation prediction tool. *PLoS One* 12:e0183318. doi: 10.1371/journal.pone.0183318

Kumari, P. H., Anil Kumar, S., Katam, R., Reddy, P. S., Nagaraju, M., Bhanu Prakash, A., et al. (2018). Genome-wide identification and analysis of *Arabidopsis* sodium proton antiporter (NHX) and human sodium proton exchanger (NHE) homologs in *Sorghum bicolor*. *Genes* 9:236. doi: 10.3390/genes9050236

Lan, P., Li, W., Lin, W. D., Santi, S., and Schmidt, W. (2013). Mapping gene activity of *Arabidopsis* root hairs. *Genome Biol.* 14:R67. doi: 10.1186/gb-2013-14-6-r67

Lescot, M., Dehais, P., Thijs, G., Marchal, K., Moreau, Y., Van de Peer, Y., et al. (2002). PlantCARE, a database of plant cis-acting regulatory elements and a portal to tools for *in silico* analysis of promoter sequences. *Nucleic Acids Res.* 30, 325–327. doi: 10.1093/nar/30.1.325

Letunic, I., Copley, R. R., Schmidt, S., Ciccarelli, F. D., Doerks, T., Schultz, J., et al. (2004). SMART 4.0: Towards genomic data integration. *Nucleic Acids Res.* 32, D142–D144. doi: 10.1093/nar/gkh088

Li, A., Xue, Y., Jin, C., Wang, M., and Yao, X. (2006). Prediction of Nepsilon-acetylation on internal lysines implemented in Bayesian discriminant method. *Biochem. Biophys. Res. Commun.* 350, 818–824. doi: 10.1016/j.bbrc.2006.08.199

Li, B. C., Zhang, C., Chai, Q. X., Han, Y. Y., Wang, X. Y., Liu, M. X., et al. (2014). Plasmalemma localisation of double hybrid proline-rich protein 1 and its function in systemic acquired resistance of *Arabidopsis thaliana*. *Funct. Plant Biol.* 41, 768–779. doi: 10.1071/FP13314

Li, J., Ouyang, B., Wang, T., Luo, Z., Yang, C., Li, H., et al. (2016). HyPRP1 gene suppressed by multiple stresses play a negative role in abiotic stress tolerance in tomato. *Front. Plant Sci.* 7:967. doi: 10.3389/fpls.2016.00967

Li, L., Zhang, C., Xu, D., Schläppi, M., and Xu, Z. Q. (2012). Expression of recombinant EARLI1, a hybrid proline-rich protein of *Arabidopsis*, in *Escherichia coli* and its inhibition effect to the growth of fungal pathogens and *Saccharomyces cerevisiae*. *Gene* 506, 50–61. doi: 10.1016/j.gene.2012.06.070

Li, S., Zhang, Y., Ding, C., Gao, X., Wang, R., Mo, W., et al. (2019). Proline-rich protein gene PdPRP regulates secondary wall formation in poplar. *J. Plant Physiol.* 233, 58–72. doi: 10.1016/j.jplph.2018.12.007

Liu, D. Q., Han, Q., Shah, T., Chen, C. Y., Wang, Q., Tang, B. F., et al. (2018). A hybrid proline-rich cell-wall protein gene JsPRP1 from *Juglans sigillata* Dode confers both biotic and abiotic stresses in transgenic tobacco plants. *Trees* 32, 1199–1209. doi: 10.1007/s00468-018-1702-3

Luo, M., Cheng, K., Xu, Y., Yang, S., and Wu, K. (2017). Plant responses to abiotic stress regulated by histone deacetylases. *Front. Plant Sci.* 8:2147. doi: 10.3389/fpls.2017.02147

Ma, Y. Y., Wu, T. L., Zhong, G. Y., and Zheng, Y. Q. (2013). Overexpression of a new proline-rich protein encoding gene CsPRP4 increases starch accumulation in *Citrus*. *Sci. Hortic.* 260:108744. doi: 10.1016/j.scienta.2019.108744

Maheshwari, P., Divya, K., Reddy, P. S., Tejaswi, U. N., Nagaraju, M., Rajasheker, G., et al. (2019). Genome-wide identification and expression profile analysis of NUCLEAR FACTOR Y family genes in *Sorghum bicolor* L. (Moench). *PLoS One* 14:e0222203. doi: 10.1371/journal.pone.0222203

McNeil, M., Darvill, A. G., Fry, S. C., and Albersheim, P. (1984). Structure and function of the primary cell walls of plants. *Annu. Rev. Biochem.* 53, 625–663. doi: 10.1146/annurev.bi.53.070184.003205

Mellacheruvu, S., Tamirisa, S., Vudem, D. R., and Khareedu, V. R. (2016). Pigeonpea hybrid-proline-rich protein (CcHyPRP) confers biotic and abiotic stress tolerance in transgenic rice. *Front. Plant Sci.* 6:1167. doi: 10.3389/fpls.2015.01167

Moller, S., Croning, M. D., and Apweiler, R. (2001). Evaluation of methods for the prediction of membrane spanning regions. *Bioinformatics* 17, 646–653. doi: 10.1093/bioinformatics/17.7.646

Munoz, F. J., Dopico, B., and Labrador, E. (1998). A cDNA encoding a proline-rich protein from *Cicer arietinum*. changes in expression during development and abiotic stresses. *Physiol. Plant.* 102, 582–590. doi: 10.1111/j.1467-7652.2009.00467.x

Nagaraju, M., Anuj Kumar, S., Jalaja, N., Rao, D. M., and Kavi Kishor, P. B. (2021). Functional exploration of chaperonin (HSP60/10) family genes and their abiotic stress-induced expression patterns in *Sorghum bicolor*. *Curr. Genom.* 22, 137–155. doi: 10.2174/1389202922666210324154336

Nagaraju, M., Reddy, P. S., Anil Kumar, S., Kumar, A., Rajasheker, G., Rao, D. M., et al. (2020). Genome-wide identification and transcriptional profiling of

small heat shock protein gene family under diverse abiotic stress conditions in *Sorghum bicolor* (L.). *Int. J. Biol. Macromol.* 142, 822–834. doi: 10.1016/j.ijbiomac.2019.10.023

Neto, L. B., de Oliveira, R. R., Wiebke-Strohm, B., Bencke, M., Weber, R. L. M., Cabreira, C., et al. (2013). Identification of the soybean HyPRP family and specific gene response to Asian soybean rust disease. *Genet. Mol. Biol.* 36, 214–224. doi: 10.1590/S1415-47572013005000017

Newman, A. M., and Cooper, J. B. (2011). Global analysis of proline-rich tandem repeat proteins reveals broad phylogenetic diversity in plant secretomes. *PLoS One* 6:e23167. doi: 10.1371/journal.pone.0023167

Paterson, A. H., Bowers, J. E., Bruggmann, R., Dubchak, I., Grimwood, J., Gundlach, H., et al. (2009). The *Sorghum bicolor* genome and the diversification of grasses. *Nature* 457, 551–556. doi: 10.1038/nature07723

Peng, L., Jia, M. M., and Liu, J. H. (2015). RNAi-based functional elucidation of PtrPRP, a gene encoding a hybrid proline rich protein, in cold tolerance of *Poncirus trifoliata*. *Front. Plant Sci.* 6:808. doi: 10.3389/fpls.2015.00808

Pfaffl, M. W., Horgan, G. W., and Dempfle, L. (2002). Relative expression software tool (REST) for group-wise comparison and statistical analysis of relative expression results in real-time PCR. *Nucleic Acids Res.* 30:e36. doi: 10.1093/nar/30.9.e36

Pitzschke, A., Datta, S., and Persak, H. (2014). Salt stress in *Arabidopsis*: Lipid transfer protein AZI1 and its control by mitogen-activated protein kinase MPK3. *Mol. Plant* 7, 722–738. doi: 10.1093/mp/sst157

Priyanka, B., Sekhar, K., Reddy, V. D., and Rao, K. V. (2010). Expression of pigeonpea hybrid-proline-rich protein encoding gene (CcHyPRP) in yeast and *Arabidopsis* affords multiple abiotic stress tolerance. *Plant Biotechnol. J.* 8, 76–87. doi: 10.1111/j.1467-7652.2009.00467.x

Qin, L. X., Zhang, D. J., Huang, G. Q., Li, L., Li, J., Gong, S. Y., et al. (2013). Cotton GhHyPRP3 encoding a hybrid proline-rich protein is stress inducible and its overexpression in *Arabidopsis* enhances germination under cold temperature and high salinity stress conditions. *Acta Physiol. Plant.* 35, 1531–1542. doi: 10.1007/s11738-012-1194-5

Rasheed, F., Markgren, J., Hedenqvist, M., and Johansson, E. (2020). Modeling to understand plant protein structure-function relationships-implications for seed storage proteins. *Molecules* 25:873. doi: 10.3390/molecules25040873

Reddy, P. S., Reddy, D. S., Sivasakthi, K., Bhatnagar-Mathur, P., Vadez, V., and Sharma, K. K. (2016). Evaluation of sorghum [*Sorghum bicolor* (L.)] reference genes in various tissues and under abiotic stress conditions for quantitative real-time PCR data normalization. *Front. Plant Sci.* 7:529. doi: 10.3389/fpls.2016.00529

Rubio-Somoza, I., Cuperus, J. T., Weigel, D., and Carrington, J. C. (2009). Regulation and functional specialization of small RNA-target nodes during plant development. *Curr. Opin. Plant Biol.* 12, 622–627. doi: 10.1016/j.pbi

Schumann, U., Lee, J., Kazan, K., Ayliffe, M., and Wang, M. B. (2017). DNA-demethylase regulated genes show methylation-independent spatiotemporal expression patterns. *Front. Plant Sci.* 8:1449. doi: 10.3389/fpls.2017.01449

Showalter, A. M. (1993). Structure and function of plant cell wall proteins. *Plant Cell* 5, 9–23. doi: 10.1105/tpc.5.1.9

Showalter, A. M., Keppler, B., Lichtenberg, J., Gu, D. Z., and Welch, L. R. (2010). A bioinformatics approach to the identification, classification, and analysis of hydroxyproline-rich glycoproteins. *Plant Physiol.* 153, 485–513. doi: 10.1104/pp.110.156554

Showalter, A. M., Keppler, B. D., Liu, X., Lichtenberg, J., and Welch, L. R. (2016). Bioinformatic identification and analysis of hydroxyproline-rich glycoproteins in *Populus trichocarpa*. *BMC Plant Biol.* 16:229. doi: 10.1186/s12870-016-0912-3

Silva, T. N., Thomas, J. B., Dahlberg, J., Rhee, S. Y., and Mortimer, J. C. (2022). Progress and challenges in sorghum biotechnology, a multipurpose feedstock for the bioeconomy. *J. Exp. Bot.* 73, 646–664. doi: 10.1093/jxb/erab450

Singroha, G., Kumar, S., Gupta, O. P., Singh, G. P., and Sharma, P. (2022). Uncovering the epigenetic marks involved in mediating salt stress tolerance in plants. *Front. Genet.* 13:811732. doi: 10.3389/fgene.2022.811732

Sommer-Knudsen, J., Bacic, A., and Clarke, A. E. (1998). Hydroxyproline-rich plant glycoproteins. *Phytochem* 47, 483–497. doi: 10.1016/S0031-9422(97)00724-3

Sundaresan, S., Philosoph-Hadas, S., Ma, C., Jiang, C. Z., Riov, J., Mugasimangalam, R., et al. (2018). The tomato hybrid proline-rich protein regulates the abscission zone competence to respond to ethylene signals. *Hortic. Res.* 5:28. doi: 10.1038/s41438-018-0033-2

Sunkar, R., Chinnusamy, V., Zhu, J., and Zhu, J. K. (2007). Small RNAs as big players in plant abiotic stress responses and nutrient deprivation. *Trends Plant Sci.* 12, 301–309. doi: 10.1016/j.tplants.2007.05

Suyama, M., Torrents, D., and Bork, P. (2006). PAL2NAL: Robust conversion of protein sequence alignments into the corresponding codon alignments. *Nucleic Acids Res.* 34, W609–W612. doi: 10.1093/nar/gkl315

Tamura, K., Stecher, G., Peterson, D., Filipski, A., and Kumar, S. (2013). MEGA6: Molecular evolutionary genetics analysis version 6.0. *Mol. Biol. Evol.* 30, 2725–2729. doi: 10.1093/molbev/mst197

Tan, J., Zhuo, C., and Guo, Z. (2013). Nitric oxide mediates cold- and dehydration-induced expression of a novel MfHyPRP that confers tolerance to abiotic stress. *Physiol. Plant.* 149, 310–320. doi: 10.1111/ppl.12032

Tello-Ruiz, M. K., Naithani, S., Gupta, P., Olson, A., Wei, S., Preece, J., et al. (2021). Gramene 2021: Harnessing the power of comparative genomics and pathways for plant research. *Nucleic Acids Res.* 49, D1452–D1463. doi: 10.1093/nar/gkaa979

Ueda, M., and Seki, M. (2020). Histone modifications form epigenetic regulatory networks to regulate abiotic stress response. *Plant Physiol.* 182, 15–26. doi: 10.1104/pp.19.00988

Wang, C., El-Shetehy, M., Shine, M. B., Yu, K., Navarre, D., Wendehenne, D., et al. (2014). Free radicals mediate systemic acquired resistance. *Cell Rep.* 7, 348–355. doi: 10.1016/j.celrep.2014.03.032

Wang, R., Chong, K., and Wang, T. (2006). Divergence in spatial expression patterns and in response to stimuli of tandem-repeat paralogues encoding a novel class of proline-rich proteins in *Oryza sativa*. *J. Exp. Bot.* 57, 2887–2897. doi: 10.1093/jxb/erl057

Wang, X., Liu, H., Yu, F., Hu, B., Jia, Y., Sha, H., et al. (2019). Differential activity of the antioxidant defence system and alterations in the accumulation of osmolyte and reactive oxygen species under drought stress and recovery in rice (*Oryza sativa* L.) tillering. *Sci. Rep.* 9:8543. doi: 10.1038/s41598-019-44958-x

Wu, H., Zou, J., May, B., Gu, Q., and Cheung, A. Y. (1993). A tobacco gene family for flower cell wall proteins with a proline-rich domain and a cysteine-rich domain. *Proc. Natl. Acad. Sci. U. S. A.* 90, 6829–6833. doi: 10.1073/pnas.90.14.6829

Wyatt, R. E., Nagao, R. T., and Key, J. L. (1992). Patterns of soybean proline-rich protein gene expression. *Plant Cell* 4, 99–110. doi: 10.1105/tpc.4.1.99

Xu, W. L., Huang, G. Q., Wang, X. L., Wang, H., and Li, X. B. (2007). Molecular characterization and expression analysis of five novel genes encoding proline-rich proteins in cotton (*Gossypium hirsutum*). *Prog. Biochem. Biophys.* 34, 509–517. doi: 10.1104/pp.005538

Xu, W. L., Zhang, D. J., Wu, Y. F., Qin, L. X., Huang, G. Q., Li, J., et al. (2013). Cotton PRP5 gene encoding a proline-rich protein is involved in fiber development. *Plant Mol. Biol.* 82, 353–365. doi: 10.1007/s11103-013-0066-8

Yang, J., Zhang, Y., Wang, X., Wang, W., Li, Z., Wu, J., et al. (2018). HyPRP1 performs a role in negatively regulating cotton resistance to *Verticillum dahliae* via the thickening of cell walls and ROS accumulation. *BMC Plant Biol.* 18:339. doi: 10.1186/s12870-018-1565-1

Yeom, S., Seo, E., Oh, S., Kim, K. W., and Choi, D. (2012). A common plant cell-wall protein HyPRP1 has dual roles as a positive regulator of cell death and a negative regulator of basal defense against pathogens. *Plant J.* 69, 755–768. doi: 10.1111/j.1365-313X.2011.04828.x

Yu, K., Soares, J. M., Mandal, M. K., Wang, C., Chanda, B., Gifford, A. N., et al. (2013). A feedback regulatory loop between G3P and lipid transfer proteins DIR1 and AZI1 mediates azelaic-acid-induced systemic immunity. *Cell Rep.* 3, 1266–1278. doi: 10.1016/j.celrep.2013.03.030

Zhan, X., Wang, B., Li, H., Liu, R., Kalia, R., Zhu, J. K., et al. (2012). *Arabidopsis* proline-rich protein important for development and abiotic stress tolerance is involved in microRNA biogenesis. *Proc. Nat. Acad. Sci. U. S. A.* 109, 18198–18203. doi: 10.1073/pnas.1216199109

Zhang, X., Gong, X., Li, D., Yue, H., Qin, Y., Liu, Z., et al. (2021). Genome-wide identification of PRP genes in apple genome and the role of MdPRP6 in response to heat stress. *Int. J. Mol. Sci.* 22:5942. doi: 10.3390/ijms22115942

Zhang, Y., and Schläppi, M. (2007). Cold responsive EARLI1 type HyPRPs improve freezing survival of yeast cells and form higher order complexes in plants. *Planta* 227, 233–243. doi: 10.1007/s00425-007-0611-2

Zhao, W., Wang, K., Chang, Y., Zhang, B., Li, F., Meng, Y., et al. (2021). OsHyPRP06/R3L1 regulates root system development and salt tolerance via apoplastic ROS homeostasis in rice (*Oryza sativa* (L.). *Plant Cell Environ.* 45, 900–914. doi: 10.1111/pce.14180

frontiers | Frontiers in Plant Science

TYPE Original Research
PUBLISHED 12 October 2022
DOI 10.3389/fpls.2022.985402

Check for updates

OPEN ACCESS

EDITED BY
Ashish Kumar Srivastava,
Bhabha Atomic Research Centre (BARC), India

REVIEWED BY
Omar Borsani,
Universidad de la República, Uruguay
László Szabados,
Hungarian Academy of Sciences (MTA), Hungary

*CORRESPONDENCE
Surekha Katiyar-Agarwal
katiyars@south.du.ac.in;
katiyarsurekha@gmail.com

SPECIALTY SECTION
This article was submitted to Plant Physiology, a section of the journal Frontiers in Plant Science

RECEIVED 03 July 2022
ACCEPTED 20 September 2022
PUBLISHED 12 October 2022

CITATION
Sasi JM, VijayaKumar C, Kukreja B, Budhwar R, Shukla RN, Agarwal M and Katiyar-Agarwal S (2022) Integrated transcriptomics and miRNAomics provide insights into the complex multi-tiered regulatory networks associated with coleoptile senescence in rice.
Front. Plant Sci. 13:985402.
doi: 10.3389/fpls.2022.985402

COPYRIGHT
© 2022 Sasi, VijayaKumar, Kukreja, Budhwar, Shukla, Agarwal and Katiyar-Agarwal. This is an open-access article distributed under the terms of the Creative Commons Attribution License (CC BY). The use, distribution or reproduction in other forums is permitted, provided the original author(s) and the copyright owner(s) are credited and that the original publication in this journal is cited, in accordance with accepted academic practice. No use, distribution or reproduction is permitted which does not comply with these terms.

Integrated transcriptomics and miRNAomics provide insights into the complex multi-tiered regulatory networks associated with coleoptile senescence in rice

Jyothish Madambikattil Sasi[1], Cheeni VijayaKumar[1], Bharti Kukreja[2], Roli Budhwar[3], Rohit Nandan Shukla[3], Manu Agarwal[2] and Surekha Katiyar-Agarwal[1]*

[1]Department of Plant Molecular Biology, University of Delhi South Campus, New Delhi, India, [2]Department of Botany, University of Delhi, Delhi, India, [3]Bionivid Technology Pvt. Limited, Bengaluru, Karnataka, India

Coleoptile is the small conical, short-lived, sheath-like organ that safeguards the first leaf and shoot apex in cereals. It is also the first leaf-like organ to senesce that provides nutrition to the developing shoot and is, therefore, believed to play a crucial role in seedling establishment in rice and other grasses. Though histochemical studies have helped in understanding the pattern of cell death in senescing rice coleoptiles, genome-wide expression changes during coleoptile senescence have not yet been explored. With an aim to investigate the gene regulation underlying the coleoptile senescence (CS), we performed a combinatorial whole genome expression analysis by sequencing transcriptome and miRNAome of senescing coleoptiles. Transcriptome analysis revealed extensive reprogramming of 3439 genes belonging to several categories, the most prominent of which encoded for transporters, transcription factors (TFs), signaling components, cell wall organization enzymes, redox homeostasis, stress response and hormone metabolism. Small RNA sequencing identified 41 known and 21 novel miRNAs that were differentially expressed during CS. Comparison of gene expression and miRNA profiles generated for CS with publicly available leaf senescence (LS) datasets revealed that the two aging programs are remarkably distinct at molecular level in rice. Integration of expression data of transcriptome and miRNAome identified high confidence 140 miRNA-mRNA pairs forming 42 modules, thereby demonstrating multi-tiered regulation of CS. The present study has generated a comprehensive resource of the molecular networks that enrich our understanding of the fundamental pathways regulating coleoptile senescence in rice.

KEYWORDS

rice, coleoptile, senescence, transcriptome, miRNAs, regulation

Introduction

Plant senescence, the terminal phase of plant development, is a regimented degradation process which ensures efficient nutrient recycling, fitness and reproductive success. It is a natural phenomenon primarily governed by developmental age and has a multi-layered regulation in which phytohormones play a pivotal role in integrating developmental signals with extrinsic factors, thereby fine-tuning the senescence program by an intricate network of signaling pathways (Lim et al., 2007). Abscisic acid (ABA), jasmonic acid (JA), salicylic acid (SA), ethylene, brassinosteroids (BRs) and strigolactones are well-acknowledged positive regulators of plant senescence, while cytokinins, gibberellins and auxins are generally known to negatively regulate plant senescence. Eventually all the cells and tissues undergo slow death in the plant organs that are destined for senescence. Among different plant organs, extensive studies have been carried out for understanding the molecular mechanism underlying the regulation of leaf senescence in plants. The senescence-associated deterioration process is tightly controlled at transcriptional, post-transcriptional and epigenetic level. The transcriptional regulation of senescence refers to the changes in the expression pattern of genes which are known as senescence-associated genes (SAGs). Several transcriptome studies have revealed massive reprogramming of a large repertoire of genes predominantly belonging to families such as transcription factors (TFs), proteases, receptor-like kinases, and nucleases. Members of TF families such as NAC, WRKY, bHLH, Zinc finger, MYB, TCP and AP2 participate in the senescence programme and many of these represent nodal points for mediating crosstalk between external and internal factors to initiate the aging process. Like many other processes of plant development, the last stage is also regulated at post-transcriptional level by small non-coding RNAs (Thatcher et al., 2015). High-throughput sequencing has fuelled the discovery of a large number of miRNAs associated with leaf senescence in multiple plant species (Xu et al., 2014; Huo et al., 2015; Wu et al., 2016). Three miRNA regulatory modules and their cognate TF targets i.e., miR164-ORE1, miR319-TCP4 and miR390-TAS3-ARF2 play critical role in regulating leaf senescence in Arabidopsis (Ellis et al., 2005; Kim et al., 2009; Li et al., 2013). Senescence is also regulated epigenetically by DNA methylation, histone modifications and chromatin alterations (Ay et al., 2014). Overall, the complex regulatory interactive network comprising SAGs (mainly TFs), miRNAs, hormones and chromatin modifications modulate leaf senescence in plants.

Among different plant organs, coleoptile is the first organ to undergo senescence post-germination in cereal plants. It is a protective sheath that emerges two days after sowing and covers emerging shoots in monocotyledonous plants. In addition to providing physical protection to first true leaves, the coleoptile also provides nutrition, mainly carbohydrates, to the growing parts of developing seedlings (Fröhlich and Kutschera, 1995). During seed germination under submerged conditions, coleoptile rapidly elongates and acts like a 'snorkel' to uptake oxygen from the water surface and transfer it to the underwater parts for their optimal growth (Narsai et al., 2015). It is evidently clear that the coleoptile, along with the first leaf, play a crucial role in seedling establishment, which is a key determinant of plant fitness and productivity of the cereal crops. Interestingly, the coleoptile continues to elongate under anaerobic conditions, however, on transfer to aerobic conditions it rapidly attains maturation followed by growth cessation and initiation of senescence (Inada et al., 2002). Under optimum growth condition, the coleoptile turns green from white within 3 days of seedling transfer to air. This is followed by emergence of the first leaf along with splitting of coleoptile in the next 24 h. Senescence of coleoptile is initiated rapidly afterwards and is evident by the formation of lysigenous aerenchyma, chlorophyll degradation and DNA fragmentation (Inada et al., 2002). Other than coleoptile, leaf senescence also occurs naturally in rice plants. Though deterioration events such as chloroplast breakdown followed by nuclear condensation are conserved in coleoptile and leaf senescence, aging within an individual leaf is highly asynchronous, thereby making it difficult to accurately characterize its senescence program and associated regulatory pathways (Inada et al., 1998). On the contrary, the senescence in coleoptile is relatively synchronous because of its simple cellular architecture consisting of only two vascular bundles and few layers of mesophyll cells. Owing to the simple cellular architecture, short life-span and quick and uniform pattern of aging, coleoptile is often proposed as a model organ for studying the mechanism of senescence in cereals.

Comprehensive understanding of the senescence process in coleoptile has been gained with respect to the pattern of cell death events and major changes that occur at tissue and cellular level, however, till date there is no genomic-scale study on discovering the gene expression changes during coleoptile senescence in any cereal plant. With an aim to gain insights into the components of regulatory pathway(s) and possible interaction among these components/pathways that contribute to coleoptile senescence, we employed an integrated omics approach and performed high-throughput sequencing of coding as well as non-coding RNAs to identify the differentially expressed genes and their regulation by miRNAs. A comparative analysis of the coleoptile transcriptome dataset with the publicly available leaf senescence dataset revealed the unique and common components between the two senescing organs. Efforts were made to validate some of the transcripts and miRNAs that exhibited differential expression during senescence. Regulatory networks involving differentially expressed genes and their probable miRNA regulators were integrated with protein-protein interaction (PPI) datasets,

which vividly supported a multi-tiered regulation of senescence program in rice coleoptiles.

Materials and methods

Plant material

The surface-sterilized rice seeds (var. Pusa Basmati 1) were submerged in autoclaved water for seven days at 28^0C in test tubes (8-10 cm below the water surface) placed in a growth room. After seven days of growth under submergence, the seeds with elongated coleoptiles were transferred to cotton beds soaked with rice growth media (Yoshida et al., 1976). Immediately after transferring to aerobic conditions, the unsenesced elongated coleoptile tissues (control-Day 0) were harvested. Senescence of coleoptiles was monitored on Day 1 and Day 2 under aerobic conditions, and tissues were harvested at each time point. Tissues from three biological replicates were harvested, frozen in liquid nitrogen and stored in -80°C for future use. Out of the three replicates, two replicates of control and Day 2 tissues were employed for high-throughput sequencing of RNA and small RNA. For quantitative PCR experiments three biological replicates comprising all three timepoints (control, Day 1 and Day 2) were utilized.

mRNA and small RNA library preparation and high-throughput sequencing

Total RNA was isolated from the harvested tissues using a modified GITC method (Chomczynski and Sacchi, 1987). The quantity and quality of the isolated RNA were evaluated using a spectrophotometer (Bio-Rad, USA) and MOPS-formaldehyde-agarose denaturing gel electrophoresis. Four RNA-Seq libraries were constructed from control (Control_BR1 and Control_BR2) and Day 2 (Day 2_BR1 and Day 2_BR2) samples followed by their 101 bp paired-end sequencing using Illumina's HiSeq4000 sequencing platform (Illumina, Inc., USA). For mRNA library preparation, RNA integrity of the control and Day 2 samples were assessed using Agilent Bioanalyzer 2100 system (Agilent Technologies, USA). TruSeq RNA Sample Preparation Kit v2 (Illumina, Inc., USA) was used according to the manufacturer's instructions to construct the RNA sequencing libraries. The transcriptome library preparation and sequencing were outsourced to M/s Bionivid Technology Pvt. Ltd., India.

For small RNA library preparation, total RNA was resolved on TBE-urea-PAGE gel and the 15-30 nt portion corresponding to the low molecular weight (LMW) RNA fraction was excised and extracted for LMW RNA. The extracted LMW RNA was ligated with RNA adapters (5' and 3') using T4 RNA ligase and subsequently used for first-strand cDNA synthesis using Superscript III reverse transcriptase (Invitrogen, USA). A 3' adapter specific reverse primer was used for the first-strand cDNA synthesis (Supplementary Table 11). The cDNA library was enriched and purified before quality check using Bioanalyzer (Agilent Technologies, USA). The small RNA-cDNA libraries were sequenced using Illumina HiSeq4000 sequencing platform by M/s Bionivid Technology Pvt. Ltd., India. The transcriptome and small RNA sequencing datasets were submitted to the SRA database as accession nos. GSE199139 and GSE199238, respectively.

Differential gene expression analysis, gene ontology and functional enrichment analysis

The sequencing data obtained by RNA sequencing was analyzed for quality assessment. In brief, filtering of high quality (HQ) reads was performed with 'NGS QC Toolkit (Patel and Jain, 2012). The HQ reads with an average Phred score ≥20 and ≥70% high-quality bases were included in the downstream analysis. *Oryza sativa*-Nipponbare-Reference-IRGSP-1.0 was used as the reference genome for mapping HQ adapter-trimmed reads. TopHat v2.0.11 was employed for mapping with default parameters (Trapnell et al., 2009). Subsequently, Cufflink (Cufflink_2.2.1) and Cuffmerge (Trapnell et al., 2009) tools were used for reference-based assembly of the reads. Fragments per transcript kilobase per million fragments mapped (FPKM) for each transcript was calculated from the number of mapped reads of the transcripts. Transcripts with normalized FPKM value ≥1 were considered for differential expression analysis with the Cuffdiff module of Cufflink. A comparative analysis of FPKM values of all the transcripts from Day 2 with that of control tissue was performed for identifying differentially expressed genes (DEGs). Identification of DEGs in coleoptile senescence was performed by calculating log (base 2) of FPKM of senescence sample divided by FPKM of control condition sample. A fold change of ±2 in the log2 scale was set as a cutoff for the categorization of DEGs. For the transcripts which were either specifically expressed in control or Day 2, fold change could not be calculated owing to FPKM value 0 in one of the samples. Since there were two biological replicates p-value was calculated to identify the transcripts which exhibited significant differential expression during senescence in the two biological replicates and transcripts with p-value <0.05 were shortlisted as a sub-dataset for downstream analyses.

GO ontologies were carried out using DAVID Functional Annotation Tool (DAVID Bioinformatics Resources 6.8, NIAID/NIH), and functional enrichment analysis was performed using MapMan annotation tool (http://mapman.gabipd.org/).

Small RNA analysis and target prediction

The UEA Small RNA Workbench (version 2.4) was used to analyze purity-filtered raw reads (Stocks et al., 2012). The adapter sequences were removed from the raw reads and the resulting reads were converted into FASTA format by using the Adapter removal tool. Further, the reads were filtered according to the length and complexity. The invalid sequences, tRNAs, rRNAs and other non-coding RNA sequences were removed by filtering tools. For predicting mature miRNAs (novel and conserved), the miRCat tool was employed. Further, the Reference genome (*Oryza sativa* -Nipponbare-Reference-IRGSP-1.0) was used for mapping. miRBase v21 was used to identify the conserved miRNAs wherein two mismatches in the miRNA sequence were allowed. After filtering conserved miRNAs, novel miRNA predictions were carried out in the remaining small RNA population. Furthermore, the putative miRNAs were also screened manually according to criteria proposed by Meyers et al. (2008) and Kozomara and Griffiths-Jones (2014). To identify differentially expressed miRNAs, read counts were normalized and fold change was calculated as described by Xin et al. (2010). For target prediction, Plant small RNA target server (psRNATarget; https://www.zhaolab.org/psRNATarget/) was employed with default parameters and the expectation value was set to 4. MSU rice genome annotation, version 7 was used as the reference genome dataset. To generate a regulatory network of miRNA and target genes, we identified the predicted target IDs in the coleoptile transcriptome dataset generated using the VLOOKUP function in Microsoft excel.

Gene expression profiling and validation of miRNAs

For the validation of transcriptome data, SYBR green based-qPCR method was employed, and the rice *eEF1α* was employed as an internal control for normalization. For validation and evaluation of expression of predicted rice miRNAs, poly A tailing method of qPCR method was employed with SYBR chemistry. 2 µg total RNA was poly-adenylated by using poly A polymerase enzyme (Ambion, USA) followed by a purification step using the RNAeasy MinElute Cleanup Kit (Qiagen, GmBH). The RTQ primer (Supplementary Table 11) along with Superscript III reverse transcriptase (Invitrogen, USA) was used to reverse transcribe poly A-tailed RNA population. The universal reverse primer and miRNA-specific forward primer were used for Real-time PCR amplification in Mastercycler Realplex 2 (Eppendorf, Germany) with KAPA PROBE FAST Universal qPCR kit (KAPA Biosystems, USA). For the normalization, rice 5S ribosomal RNA was used as an endogenous control. Relative expression levels were calculated after normalization against the control sample. Fold change was calculated using $2^{-\Delta\Delta ct}$ method (Livak and Schmittgen, 2001) and an average of all the replicates was plotted along with the calculated standard error (SE).

Protein-protein interaction network creation and visualization

The protein-protein interaction of the high confidence putative miRNA target genes which exhibited inverse expression patterns in the transcriptome data with respect to the corresponding miRNA profile were analyzed using the STRING 11 database. The output obtained was integrated with the miRNAs and their predicted targets to generate the miRNA-target-PPI network using Cytoscape_v3.7.2 software.

Results

Characterization of coleoptile senescence at morphological and molecular level

With an aim to obtain elongated coleoptiles with synchronized growth and senescence, rice seeds were grown under submerged conditions for seven days. To induce rapid maturation and initiate senescence in coleoptiles, submerged seedlings were transferred to aerobic conditions (taken as 'control'), and progression of senescence was subsequently monitored on day 1, day 2 and day 3 as depicted in Figure 1A. Closer examination of morphological alterations during coleoptile senescence revealed that wilting, curling and yellowing/browning of the coleoptile, especially at tips, was discernible at day 2 stage. On day 3, while the first leaf emerged, there was extensive wilting and browning of coleoptiles indicating late stage of senescence. Physio-morphological changes during progression of coleoptile senescence were confirmed at the molecular level by determining relative gene expression levels of senescence-associated marker genes (SAGs): *RED CHLOROPHYLL CATABOLITE REDUCTASE (RCC reductase)* and *WRKY88*. Increased expression of *RCC reductase* gene encoding for RCC reductase enzyme (which catabolizes chlorophyll) is a hallmark of senescence in leaves and other plant organs (Tang et al., 2011). Similarly, increased expression of *WRKY88* is reported during flag leaf senescence in rice (Lee et al., 2017). Quantitative PCR analysis demonstrated significant upregulation in steady state mRNA levels of both the genes during the progression of coleoptile senescence. The level of expression dramatically increased on day 1 and day 2. Notably, *RCC reductase* exhibited higher levels of induction at all the stages as compared to that of *WRKY88* (Figure 1B). These findings ratify the staging of coleoptile senescence in the present study.

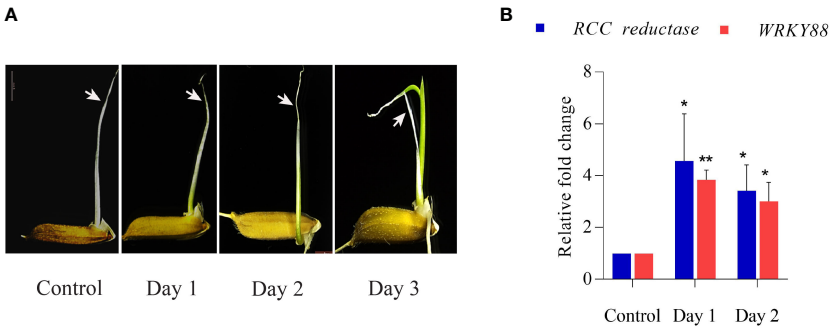

FIGURE 1
Coleoptile senescence in rice. **(A)** Different stages of coleoptile senescence in rice seedlings after transfer from anaerobic (submergence) to aerobic conditions. **(B)** Expression profile of senescence associated genes (*SAGs)* at different stages of coleoptile senescence using quantitative PCR. For normalization *eEF-1α* was used as an internal control. Three biological replicates and two technical replicates were included in the study. White arrows highlight the progression of senescence in the coleoptile. Asterisks indicate a significant difference between the control and senescence tissues (Student's *t*-test, $*P < 0.05$, $**P < 0.01$). *RCC reductase: red chlorophyll catabolite reductase*.

In view of these observations, day 2 was considered as the middle stage of coleoptile senescence which could be utilized for studying the changes occurring at molecular level by transcriptome and small RNAome analysis.

Transcriptome sequencing, differential gene expression analysis and GO enrichment of differentially expressed genes during coleoptile senescence

Sequencing of four RNA-Seq libraries [control (Control_BR1 and Control_BR2) and Day 2 (Day 2_BR1 and Day 2_BR2)] yielded an aggregate of 119.82 million HQ reads which were processed to calculate normalized FPKM values (Supplementary Table 1). Scatter plots plotted for comparing gene expression between the two independent biological replicates of control and day 2 samples showed good correlation (Supplementary Figures 1A, B). As evident from the volcano plot, the number of significantly upregulated transcripts (1970) were higher compared to the downregulated ones (1195) (Figures 2A, B). Overall, 3166 transcripts were differentially expressed (DEGs) in senesced coleoptile samples when compared to the control, while 44 and 273 genes exhibited specific expression in control and senesced coleoptiles, respectively (Figure 2B; Supplementary Table 3). These observations indicate that a large number of genes are regulated, during progression of senescence in rice coleoptiles. The genes exclusively regulated during senescence at Day 2 were also included under DEGs for further downstream analyses. To predict the function of genes exhibiting altered expression, GO analysis was carried out and GO terms could be assigned to 1792 out of 3439 DEGs. Maximum number of genes were associated with molecular function (77%) followed by cellular components (71%) and biological processes (58%) (Figure 2C, Supplementary Table 3). The top terms enriched under molecular function, cellular component and biological process GO categories were "integral component of ATP binding", "integral component of membrane", and "transcription" respectively (Figure 2D).

Functional category enrichment analysis of differentially expressed genes during coleoptile senescence

To predict the functional categories associated with the DEGs, enrichment analysis was performed using the MapMan annotation tool (Thimm et al., 2004). Out of the 3439 DEGs, 438 and 823 genes mapped to the metabolism and regulation pathways, respectively (Figures 3A, B). Genes belonging to different functional categories such as transcriptional regulators (RNA category), transporters, hormone metabolism, redox related, stress response and signalling pathways are already known to play a role in the senescence of leaves (Guo et al., 2004; Gregersen and Holm, 2007; Zhang et al., 2014; Lin et al., 2015) and our analyses showed that 176, 37, 183, 134, 143, 94 and 105 transcripts belonging to signaling, redox, transcription factors, transporters, stress, cell wall and hormone signalling were differentially expressed during coleoptile senescence, respectively (Figure 3; Supplementary Figure 2; Supplementary Table 4). Detailed analysis of the selected categories revealed that out of the 176 signaling-related genes only 3 genes were specifically expressed in senescing coleoptiles. A greater number of signaling genes displayed downregulation (108) as compared to those that exhibited upregulation (65) (Supplementary Figure 2A; Supplementary Table 4). More genes belonging to receptor

10.3389/fpls.2022.985402

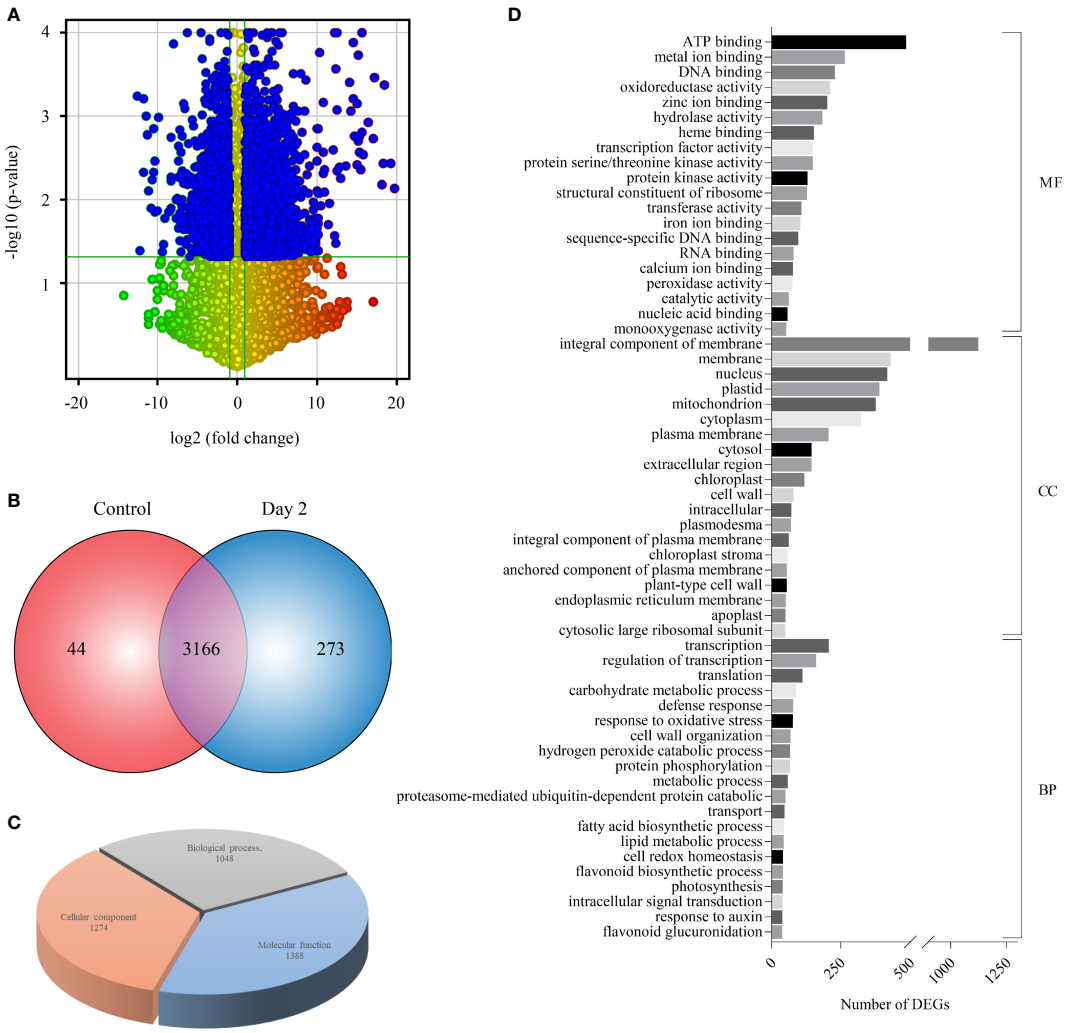

FIGURE 2
Expression profiling and GO enrichment of differentially expressed genes (DEGs) during coleoptile senescence in rice. **(A)** Volcano scatter plot depicting the expression pattern of DEGs in RNA-Seq data of rice coleoptile senescence. Statistically significant downregulated (top left) and upregulated (top right) genes in day 2 of senescence relative to control coleoptiles are highlighted in blue color. **(B)** Venn diagram representing the number of DEGs specific to control and senesced coleoptiles, and the ones which were expressed commonly in the two samples. **(C)** Gene Ontology (GO) enrichment analysis of DEGs. **(D)** Top twenty GO enrichment terms belonging to 3 separate sub-ontologies: molecular function (MF), cellular component (CC), and biological process (BP) and number of DEGs classified in each term are presented.

kinases (81), calcium (15) and sugar and nutrient (6) categories were downregulated; whereas higher numbers of genes from G-proteins (7) and light (11) categories exhibited upregulation. Relatively fewer genes belonging to receptor kinases (2) and G-proteins (1) were specifically expressed in senescing coleoptiles (Supplementary Figure 2A; Supplementary Table 4). Of the 37 redox-related transcripts, 29 and 8 were up- and down-regulated, respectively. While the entire set of DEGs grouped under sub-categories 'dismutases, catalases, peroxiredoxin' (17) were exclusively expressed in senescing tissue, all the 3 genes belonging to glutaredoxins category were exclusively expressed in control coleoptiles. A larger number of genes belonging to 'ascorbate and glutathione' (17) and thioredoxin (4) were upregulated (Supplementary Figure 2B; Supplementary Table 4). Of the 134 transporters identified, 98 were upregulated, 22 were downregulated and 14 were specifically expressed during coleoptile senescence. The transporter classes whose gene expression was upregulated majorly belonged to ABC (15), peptide (14), amino acid (13), metabolite (13), major intrinsic proteins or MIPs (11), sugar (8) nucleotide (6), ammonium (3), potassium (3) and sulphate (3) transporters. Whereas, genes of ABC (4), peptide (5), amino acid (2), metal (2) and nitrate (2) class of transporters were also found to be downregulated (Figure 3C; Supplementary Table 4). In the

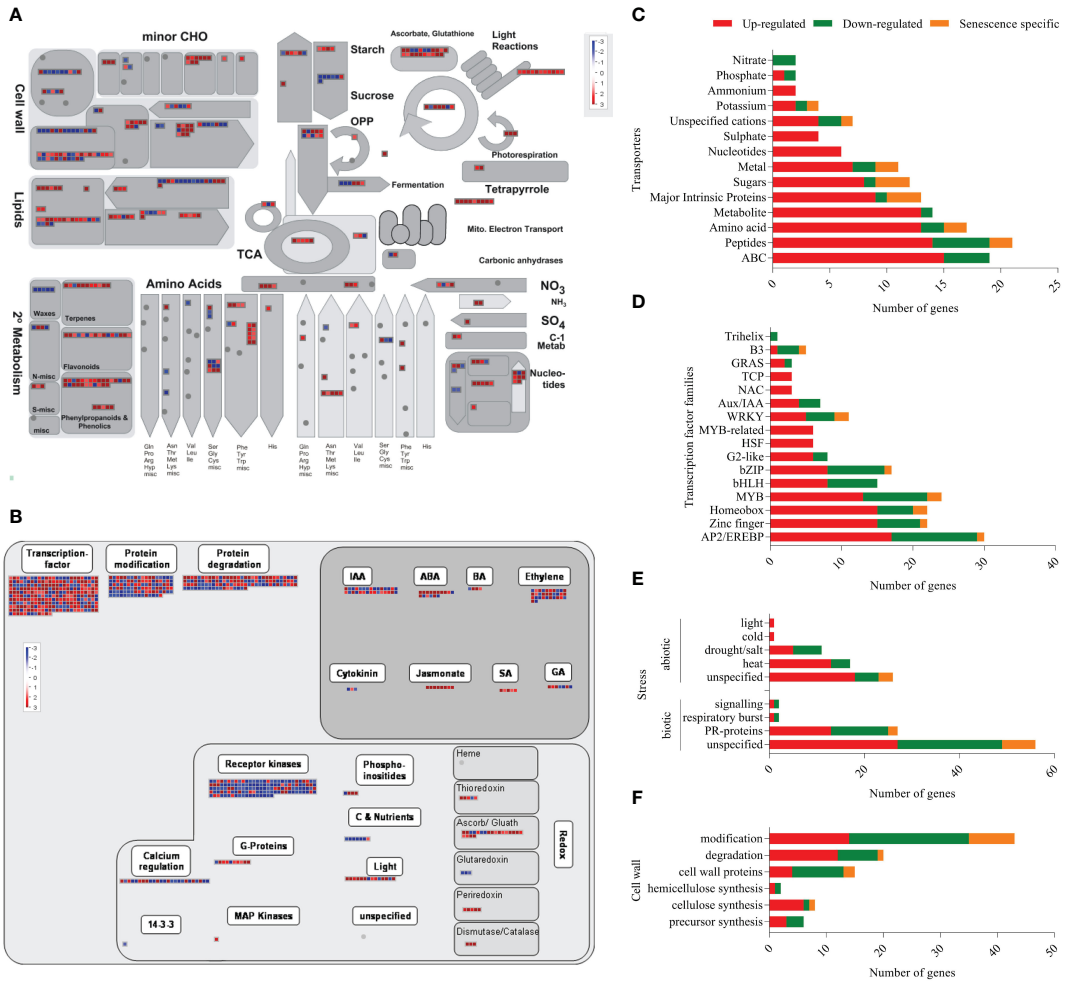

FIGURE 3
Functional annotation of DEGs using MapMan tool. The functional annotation of DEGs were analysed using MapMan tool and overviews of metabolism **(A)** and regulation **(B)** are depicted. In the overviews, red boxes represent up-regulated/senescence specific transcripts and the blue boxes represent down-regulated transcripts. The major functional categories of genes: Transporters **(C)**, Transcription factors **(D)**, Stress **(E)** and Cell wall-related **(F)** are represented as stacked bar graphs. In the stacked bar graphs red bar indicates upregulated genes, green bar shows down regulated genes and orange bar represents senescence-specific genes (day 2-specific).

transcription factor category, 112, 61 and 12 genes belonging to 16, 12 and 8 TF families exhibited upregulation, downregulation and specific expression during coleoptile senescence, respectively. Maximum number of upregulated genes were of AP2/EREBP (17) TF family, followed by Zinc finger (15), Homeobox (15), MYB (13), bHLH (8), bZIP (8), G2-like (6), HSF (6), MYB-related (6) and WRKY (5). Furthermore, the main TF families whose transcripts showed downregulation were Zinc finger (6), AP2/EREBP (12), Homeobox (5), MYB (9), bHLH (7), bZIP (8), G2-like (2), WRKY (4), Aux/IAA (3) and B3 (3). Senescence-specific expression was observed for only a few transcripts, which were members of the zinc finger (1), AP2/EREBP (1), Homeobox (4), MYB (2), bZIP (1), WRKY (2) and B3 (1) TF families (Figure 3D; Supplementary Table 4).

Out of the 143 stress-associated genes, 56 belonged to abiotic stresses category (37 upregulated, 15 downregulated and 4 senescence-specific), while 87 were related to biotic stresses (44 upregulated, 34 downregulated and 9 senescence-specific) (Figure 3E; Supplementary Table 4). One of the limitations of the MapMan tool is that many annotated genes are not associated with any specific pathway and are listed as 'unspecified'. Consequently, 56 and 19 genes under biotic and abiotic stress categories, respectively, were not assigned any sub-category. However, from the ones that were assigned a sub-category, PR proteins (13 upregulated, 12 downregulated and 3 senescence-specific) constituted a large number of differentially expressed biotic stress genes. In case of abiotic stresses, many heat stress (13 upregulated, 4 downregulated) and drought/salt stress (5

upregulated, 6 downregulated) related transcripts showed altered expression during coleoptile senescence. Because of extensive changes that occur in the cell wall during senescence (Serafini-Fracassini et al., 2002), we also analyzed genes associated with the term 'cell wall' and found that 94 genes associated with the cell wall exhibited differential expression. These included 42 downregulated, 40 upregulated, and 12 senescence-specific genes. Overall, genes associated with the degradation and cellulose synthesis were largely up-regulated, whereas genes associated with modification and cell wall proteins were down-regulated during senescence (Figure 3F; Supplementary Table 4).

Phytohormones regulate multiple aspects of plant growth and development (Gray, 2004). Therefore, we surveyed 105 genes belonging to the hormone signalling category and found that the number of upregulated transcripts (61) was higher than that of the downregulated (38) ones. In addition, few members (6) belonging to brassinosteroid (1), ethylene (2), SA (2) and cytokinin (1) signaling were exclusively expressed in the senescing tissue. The upregulated hormone signalling pathways include ethylene (17), auxin (15), ABA (12), JA (8), SA (3), gibberellic acid (4), and brassinosteroid (2). It is worthwhile to highlight that all the identified genes of JA and SA pathways exhibited dramatic upregulation. Whereas down-regulation of several transcripts belonging to auxin (15), ethylene (13), gibberellic acid (3), cytokinin (2), ABA (4) and brassinosteroid (1) was noted in coleoptile senescence (Figure 3B; Supplementary Figure 2; Supplementary Table 4).

Comparison of transcriptome datasets of coleoptile and leaf senescence in rice

To delineate the core and specific components involved in the two physiologically different senescence programs in plants, we compared the DEGs of coleoptile transcriptome (3439 DEGs) with the publicly available combined transcriptome data of second and flag leaf senescence, henceforth referred to as LS (3778 DEGs; Lee et al., 2017). While the majority of genes were specifically up- and down-regulated in LS and CS (1603, 1691 up-regulated and 1638, 913 down-regulated in LS, CS, respectively), a smaller, albeit significant, number of genes exhibited similar expression pattern in both LS and CS (194 showed upregulation and 85 were downregulated). These genes probably constitute the core components of senescence in rice. Based on these observations it is evident that CS is remarkably distinct from the LS program in rice. This is further supported by an inverse expression pattern of a substantial number of genes (258) in LS and CS (Figure 4A; Supplementary Table 5). To obtain insights into the biological function of core components of the senescence process, GO analysis of the commonly upregulated genes was carried out. The analysis revealed that maximum number of upregulated genes were associated with cellular components (enrichment of subcategories such as "integral components of membrane", "nucleus" and "membrane") followed by molecular function (subcategories such as "DNA binding" and "TF activity") (Figure 4B; Supplementary Table 5). Functional enrichment analysis identified several transporters (amino acid transporters, aquaporins, MATE efflux protein, ion transporters), TFs (MYB, NAC, homeobox domain, Zinc finger proteins, and WRKY family proteins), cytochrome P450, heat shock transcription factors or HSFs (HSFA7a, HSFA3a and HSFC1b), hormone signaling pathway genes (ABA, auxin, ethylene and gibberellin) and chlorophyll degradation genes (RCC reductase and senescence-inducible chloroplastic stay green 1 protein) among the commonly upregulated genes (Supplementary Table 5). Genes encoding for 1-aminocyclopropane-1-carboxylate oxidase proteins, TFs such as MYB, bZIP, WRKY118, FBXs (FBX27, FBX 28), receptor like protein kinases, lectin-like receptor kinases and certain enzymes such as GDSL-like lipase/acid hydrolase and glycosyl hydrolase showed down regulation in both CS and LS. Among the genes that exhibited inverse correlation in expression during LS and CS, a large number of genes encoded for proteins belonging to subcategory "integral component of membrane" followed by 'plastid'. Besides, during CS several genes associated with "secondary metabolite synthesis", "photosynthesis", "metal ion binding", "oxidoreductases" and "response to stress" categories were significantly upregulated whereas they exhibited downward trend in expression in LS. On the other hand, several genes coding for proteins of subcategories "plasma membrane", "DNA binding" and "transcription" showed significant induction in LS while their expression declined in CS (Supplementary Table 5). It is noteworthy that several membrane proteins, especially transporters (amino acid transporter, aquaporin, malic acid transporter, phosphate transporter and potassium transporter), were commonly upregulated, while some membrane proteins (citrate transporter, amino acid transporter) exhibited inverse correlation in their expression in CS and LS.

Validation of rice coleoptile senescence transcriptome data

RNA-seq derived expression data was reconfirmed with the help of qRT-PCR by examining the expression of 8 DEGs. Relative expression of genes belonging to functional categories such as transporters (*amino acid, ABC transporter*), signalling (*receptor kinase*), hormone signalling and transduction (*hydrolase, cytochrome P450* and *12-oxophytodienoate*), cell wall (*pectinesterase*), and photosynthesis (*ribulose bisphosphate*

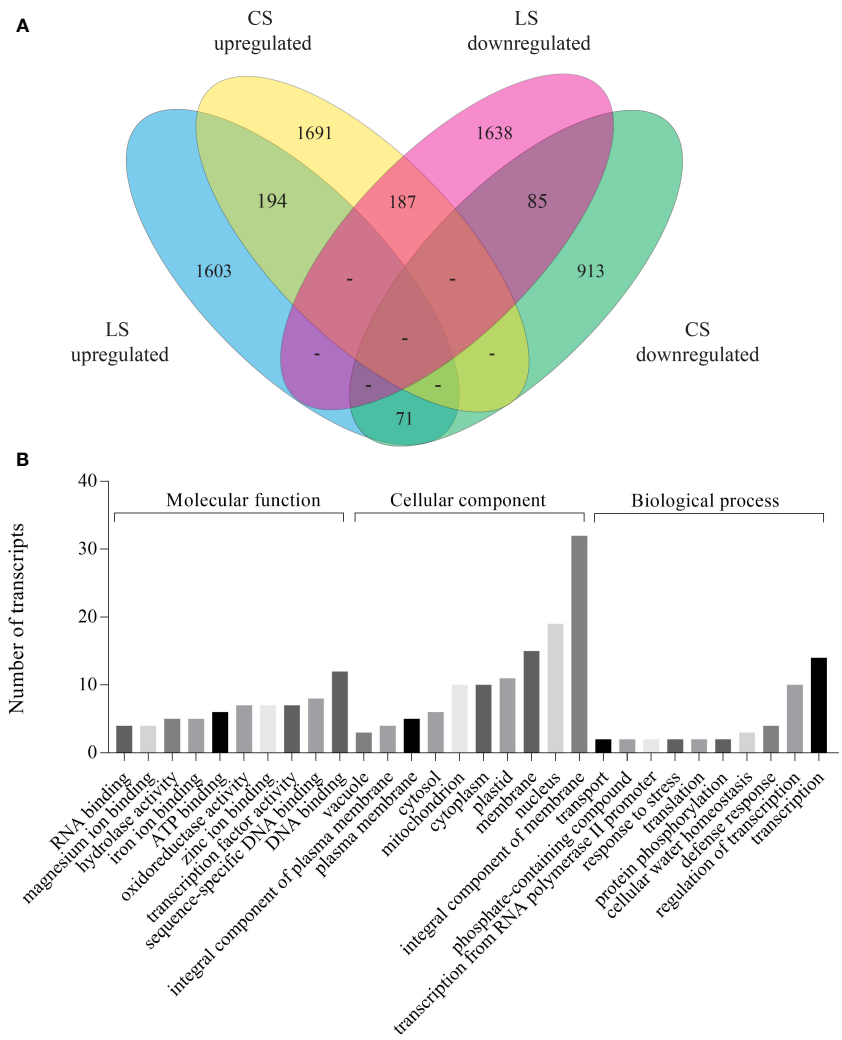

FIGURE 4
Comparison of DEGs identified in coleoptile senescence with those reported in natural leaf senescence in rice. Leaf senescence data (both second and flag leaf) was retrieved (Lee et al., 2017) and was compared with coleoptile senescence dataset obtained in the present study. DEGs identified in the 36 days post heading (36 DPH) tissues of LS dataset were used for the analysis. **(A)** Venn diagram of DEGs shows overlap between CS and LS. **(B)** GO enrichment analysis of DEGs which were commonly upregulated during leaf as well as coleoptile senescence in rice.

carboxylase) was determined in control and at day 1 and day 2 of senescing coleoptiles. Both transporters and hydrolase genes showed consistent upregulation in day 1 and day 2 of senescence (Figures 5A, B, D). Expression of receptor kinase, cytochrome P450 and 12-oxophytodienoate increased massively on day 1, followed by a slight decline (although upregulated) on day 2 (Figures 5C, E, F). Both pectinesterase and ribulose bisphosphate carboxylase showed significant downregulation during progression of senescence. However, pectinesterase exhibited a more severe decline in expression levels on day 2 as compared to ribulose bisphosphate carboxylase (Figures 5G, H). The expression patterns of the genes by qPCR analysis were consistent with that of the RNA-sequencing results.

Identification, digital expression profiling and validation of conserved and novel miRNAs during coleoptile senescence

Small RNAs are known regulators of gene expression in diverse biological processes in plants such as growth, development and response to biotic and abiotic stresses (Li et al., 2017). The role of miRNAs in regulating induced and natural senescence in leaves has been demonstrated by several studies (Huo et al., 2015; Kim et al., 2018), however, no miRNAs have been identified which have a potential role in controlling the progression of senescence in coleoptile, which is the first organ to senesce in cereals. Therefore, small RNA libraries of

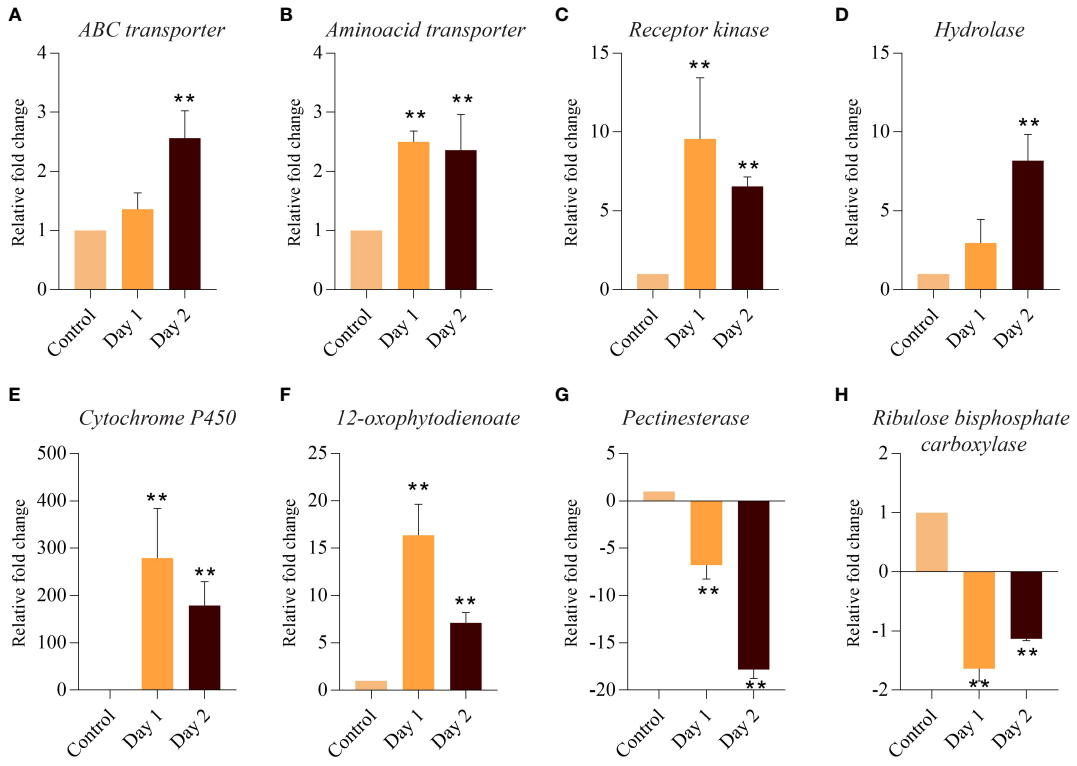

FIGURE 5
Quantitative PCR-based validation of DEGs associated with coleoptile senescence in rice. Relative expression of genes belonging to functional categories such as transporters: *ABC transporter* **(A)**, *amino acid transporter* **(B)**; signaling: *Receptor kinase* **(C)**; hormone signaling and transduction: *Hydrolase* **(D)**, *cytochrome P450* **(E)** and *12-oxophytodienoate* **(F)**; cell wall: *Pectinesterase* **(G)**; and photosynthesis: *Ribulose bisphosphate carboxylase* **(H)** was determined in control and at day 1 and day 2 of senescing coleoptiles. For normalization *eEF-1α* was used as an internal control. Three biological replicates and two technical replicates were included in the study. Asterisks indicate a significant difference between the control and the senescence sample (Student's *t*-test, $^{**}P < 0.01$).

control and senescing coleoptiles were sequenced and the data so obtained was analyzed. Scatter plots for comparing small RNA expression pattern between the two biological replicates of control and day 2 samples showed good correlation (Supplementary Figures 1C, D). Our analysis identified 66 known miRNAs belonging to thirty-one miRNA families and 41 true novel miRNAs (with star sequences) in the small RNA dataset (Supplementary Table 6). For finding the miRNAs that could potentially regulate coleoptile senescence in rice, digital expression levels were analyzed and the miRNAs exhibiting ±2-fold change (log2 scale; average of two biological replicates) in senescing coleoptiles were considered as 'differentially regulated'. Of the 41 conserved miRNAs, 17 showed upregulation while 24 exhibited downregulation in senescing coleoptiles (Figure 6A; Supplementary Table 7). The major upregulated miRNA families were miR396 (3 members), miR167 and miR160 (2 members each). Some of the conserved miRNAs; osa-miR160e-5p, osa-miR160f-3p, osa-miR164c, osa-miR167d-3p, osa-miR171h, osa-miR1428e-3p, osa-miR394, osa-miR396a-3p, osa-miR396a-5p, and osa-miR531a were highly upregulated (>4-fold) during coleoptile senescence (Figure 6A; Supplementary Table 7). The predominantly downregulated miRNA families were miR169 (6 members) and miR390 (3 members). Expression of nine miRNAs (osa-miR159f, osa-miR164d, osa-miR169h, osa-miR169n, osa-miR169p, oss-miR390-5p, osa-miR398b, osa-miR528-3p, and osa-miR529a) declined considerably (more than 3-fold) during coleoptile senescence (Figure 6A; Supplementary Table 7).

Similar to the conserved miRNAs, novel miRNAs were also regulated during coleoptile senescence. A total of 21 novel miRNAs were differentially expressed, of which 9 miRNAs were upregulated and 12 miRNAs exhibited downregulation (Figure 6B; Supplementary Table 7). Among the upregulated novel miRNAs, miRNA_16, miRNA_24, miRNA_26, miRNA_79, and miRNA_82 showed more than 4-fold upregulation. Further, greater than 3-fold downregulation was observed in the expression levels of miRNA_18, miRNA_22, miRNA_25, miRNA_45, miRNA_47, miRNA_49, miRNA_52 and miRNA_75 (Figure 6B; Supplementary Table 7). Expression

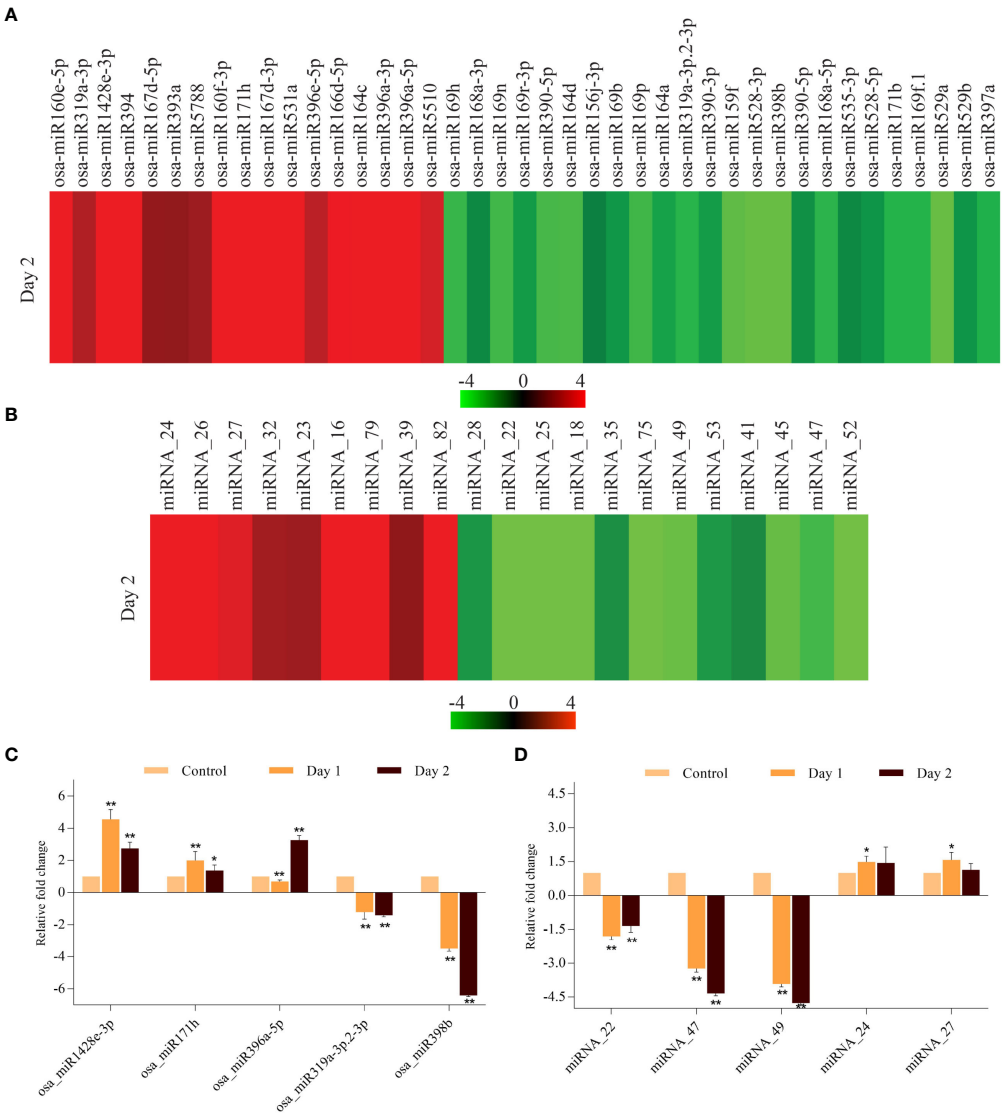

FIGURE 6
Expression profiling of miRNAs that are differentially expressed during coleoptile senescence in rice. Heat map of differentially expressed miRNAs belonging to 'conserved miRNAs' **(A)** and 'novel miRNAs' **(B)** categories during coleoptile senescence in rice. Quantitative PCR-based validation of few conserved **(C)** and novel **(D)** miRNAs. For normalization, 5S ribosomal RNA was used as internal control. Three biological replicates and two technical replicates were included in the study. Asterisks indicate significant differences between the control and the senescence sample (Student's *t*-test, $*P < 0.05$, $**P < 0.01$).

of 5 conserved and 5 novel miRNAs was validated by poly(T) adaptor RT-PCR method. It was observed that expression of osa_miR1428e-3p and osa_miR171h elevated on day 1 and although their levels declined slightly on day 2, they remained upregulated (Figure 6C). On the other hand, levels of osa_miR396c-5p were lower on day 1, but increased rapidly on day 2 of senescence (Figure 6C). Among the downregulated conserved miRNAs, osa_miR398b exhibited significantly higher decline than osa_miR319a-3p.2-3p during senescence (Figure 6C). The expression of novel miRNAs, miRNA_24 and miRNA_27 increased moderately, while miRNA_47 and miRNA_49 downregulated significantly during coleoptile senescence (Figure 6D). Notably, the expression pattern of conserved and novel miRNAs as observed by qRT-PCR was similar with their digital expression profiles.

Comparison of coleoptile and rice flag leaf senescence miRNAs

To gain insights into the conservation or differences in the miRNA-dependent regulation of senescence in coleoptile and

flag leaf, expression of 66 conserved miRNAs was compared with the 38 miRNAs previously identified by our group in flag leaf senescence (FLS) (Sasi et al., 2019). The analysis revealed that 17 conserved miRNAs were detected in both CS and FLS (Supplementary Table 8). While 3 conserved miRNAs (osa-miR164a, osa-miR171b, osa-miR535-3p) showed similar expression patterns, 6 miRNAs (osa-miR1428e-3p, osa-miR160e-5p, osa-miR168a-5p, osa-miR171h, osa-miR1432-5p, and osa-miR1861e) displayed an inverse expression pattern in CS and FLS datasets. The remaining 8 miRNAs did not display any remarkable comparative pattern during the two senescence programs. We further compared the expression trends of the 41 true novel miRNAs in CS with 203 true novel miRNAs in FLS and found that 3 miRNAs [(miRNA_2, 24 and 30 which were named as N_osa_619, N_osa_595 and N_osa_176, respectively, in Sasi et al. (2019)] were present in both the datasets. Out of the 3 commonly present novel miRNAs, miR_30 was slightly downregulated in both CS and FLS, while miR_23 was slightly downregulated in FLS, but was upregulated in CS. miR_2 exhibited no significant change in expression level in FLS, however, it was downregulated in CS. The comparative study led to the identification of few miRNAs which probably comprise the core regulatory pathway of senescence programs in rice. It would be worthwhile to determine the expression of their putative targets in the senescence datasets to identify the functionally conserved miRNA-mRNA modules regulating senescence in different tissues of rice.

Computational prediction of targets of miRNAs, their GO analysis and expression profiling-based validation of selected targets

To elucidate the biological function of miRNAs and other small RNAs it is pertinent to identify the genes targeted by them. The information generated is utilized to unravel the complex regulatory network of miRNA-target interaction and their possible role(s) in regulating different biological processes. We predicted 301 targets for 62 miRNAs (41 conserved and 21 true novel) that were differentially expressed during coleoptile senescence in our dataset (Supplementary Table 9). Targets could not be predicted for four conserved (osa-miR169b, osa-miR390-3p, osa-miR394 and osa-miR5788) and one novel (miRNA_47) miRNAs. Except osa-miR1428e-3p, osa-miR169f.1, osa-miR169h, osa-miR319a-3p.2-3p, osa-miR396a-3p, osa-miR5510 and miRNA_23 which were predicted to hit only a single target gene, all other miRNAs were predicted to target multiple genes. The maximum number of targets were 44 for osa-miR531a, followed by 14 for osa-miR156j-3p. Gene ontology clustering analysis of the predicted targets revealed that the maximum number of targets were associated with molecular function (207) followed by biological process (145) (Supplementary Table 9). The top sub-categories in each gene function cluster belonged to ATP-binding, transferase activity, membrane proteins, protein phosphorylation, oxidation-reduction process and regulation of transcription. All these observations indicate that these miRNAs might regulate diverse processes in coleoptile senescence program.

To validate the predicted regulatory relationship between the senescence-associated miRNAs and their target, we performed qRT-PCR of osa-miR164d, osa-miR169r-3p, miRNA_45 and miRNA_75 and their corresponding putative target genes. The expression patterns of all miRNAs and their targets exhibited consistency with the digital expression data obtained in RNA-seq and small RNA-seq experiments (Figure 7). osa-miR164d was predicted to target OsNAC2 or OsORE1 (encoded by LOC_Os04g38720) which was significantly upregulated during progression of coleoptile senescence. Similarly, osa-miR169r-3p exhibited downregulation and its target ABC transporter (encoded by LOC_Os11g07600) accumulated to high levels. One of the targets of novel miRNA_45 was MYB TF encoded by LOC_Os05g07010 whose expression levels were upregulated. The expression profiling analyses of miRNA-mRNA interactions indicated the high confidence level of the prediction of the targets and the requirement of testing more such pairs to gain an insight into the regulation of coleoptile senescence in rice.

Regulatory network of miRNAs and their target genes

To identify the key regulatory components and their interactors in coleoptile senescence, a combinatorial approach was employed to integrate the regulatory dataset of RNA-seq and small RNA-seq with publicly available protein-protein interaction (PPI) dataset (Szklarczyk et al., 2021). Expression of putative miRNA-targets was searched in the transcriptome data and the target genes whose expression correlated inversely with that of corresponding miRNAs were interrogated for their protein interactions (Supplementary Tables 9, 10). The PPI analysis output was used to generate miRNA-target regulatory networks using the Cytoscape software (Figure 8). It was noted that 105 known miRNA-target pairs and 35 novel miRNA-target pairs showed an inverse correlation in the expression profile (Figure 8). The biological regulatory network model consisted of 14 and 28 modules composed of upregulated and downregulated miRNAs targeting the genes that exhibited significant decline and elevation in expression level during coleoptile senescence, respectively (Figure 8). An important module was controlled by an upregulated miR531a whose all the 15 target genes exhibited decline in their expression levels during senescence. Among these 15 targets, two genes encoded for LRR transmembrane protein kinase and an expressed protein and they are known to interact which has been validated experimentally (Szklarczyk et al., 2021). It would be worthwhile to validate the targets and

10.3389/fpls.2022.985402

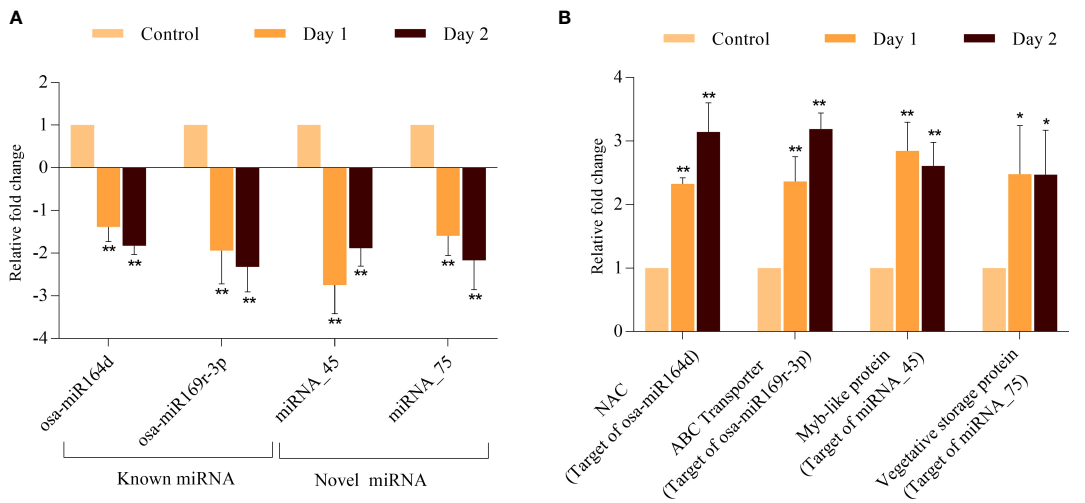

FIGURE 7
Validation of expression profile of miRNAs and their predicted target genes during coleoptile senescence in rice. Expression analysis of selected miRNAs **(A)** and one of their predicted targets genes **(B)** using qPCR. For normalization of real-time PCR results, *eEF-1α* was used as internal control. Three biological replicates and two technical replicates were included in the study. Asterisks indicate significant differences between the control and the senescence sample (Student's *t*-test, $*P < 0.05$, $**P < 0.01$).

identify which of these contribute to coleoptile senescence. Similarly, other downregulated conserved miRNAs such as miR397a and miR156j could target 9 genes each, while miR164a was found to target 7 genes, expression of all of which was suppressed during senescence. Two novel miRNAs, miRNA_45 and miRNA_75 were predicted to target 6 genes each and these genes also exhibited an inverse correlation in expression. Majority of the modules in the regulatory network consisted of senescence-repressed miRNAs and their corresponding senescence-upregulated targets and therefore protein-protein interactions were largely predicted within these modules.

At the center of the predominant hub were two members of the MIR164 family, miR164a and miR164d. The sequences of miR164a and miR164d are similar except that miR164a had an extra nucleotide at its 3' end. However, this did not affect the ability of these miRNAs to target the same genes (Supplementary Tables 9, 10). Interestingly, proteins coded by two of their targets i.e. LOC_Os01g62490 (coding for a laccase precursor) and LOC_Os04g38720 (a NAC TF), appeared to be interacting with each other. These proteins further served as connectors with four additional modules; a) NAC protein interacted with OsSPL2 protein encoded by LOC_01g69830 (a target of miRNA_41 and osa-miR529b; b) laccase precursor interacted with a plastocyanin-domain containing protein encoded by LOC_06g11490 (a target of osa-miR528-3p); c) laccase precursor is also a target of osa-miR397a, thereby connecting the osa-miR164 and osa-miR397a nodes; d) laccase precursor interacted with an auxin-responsive protein encoded by LOC_Os05g48270 (a target of osa-miR169n). Additional connections between different modules were seen such as the Molybdenum cofactor biosynthesis protein 1 encoded by LOC_Os02g15870 (target of osa-miR529b) interacted with CTP synthase protein encoded by LOC_Os01g46570 (target of osa-miR156j-3p). Intermodular connection was also observed between the module regulated by miRNA_75 and module regulated by miRNA_41 and osa-miR529b, wherein 1,3-beta-glucan synthase component domain containing protein (encoded by LOC_Os03g03610) was a target of both osa-miR529b and miRNA_75. Intramodular connections were seen in the module regulated by miRNA_41 and osa-miR529, both of which shared two targets i.e., LOC_Os01g69830 and LOC_01g22954. Only few interactions among different proteins encoded by miRNA-targeted genes in the dataset were observed. However, most of the PPIs identified in the network are predicted on the basis of their co-expression or database or text mining. It is, therefore, necessary to validate these interactions experimentally and then characterize their role in coleoptile senescence in rice. It is expected that with the enrichment of PPI data in the public domain, more connectivity between the modules (both inter-modular and intra-modular) will be observed which would highlight the functional and dynamic complexity of proteins and miRNA regulation of their target genes.

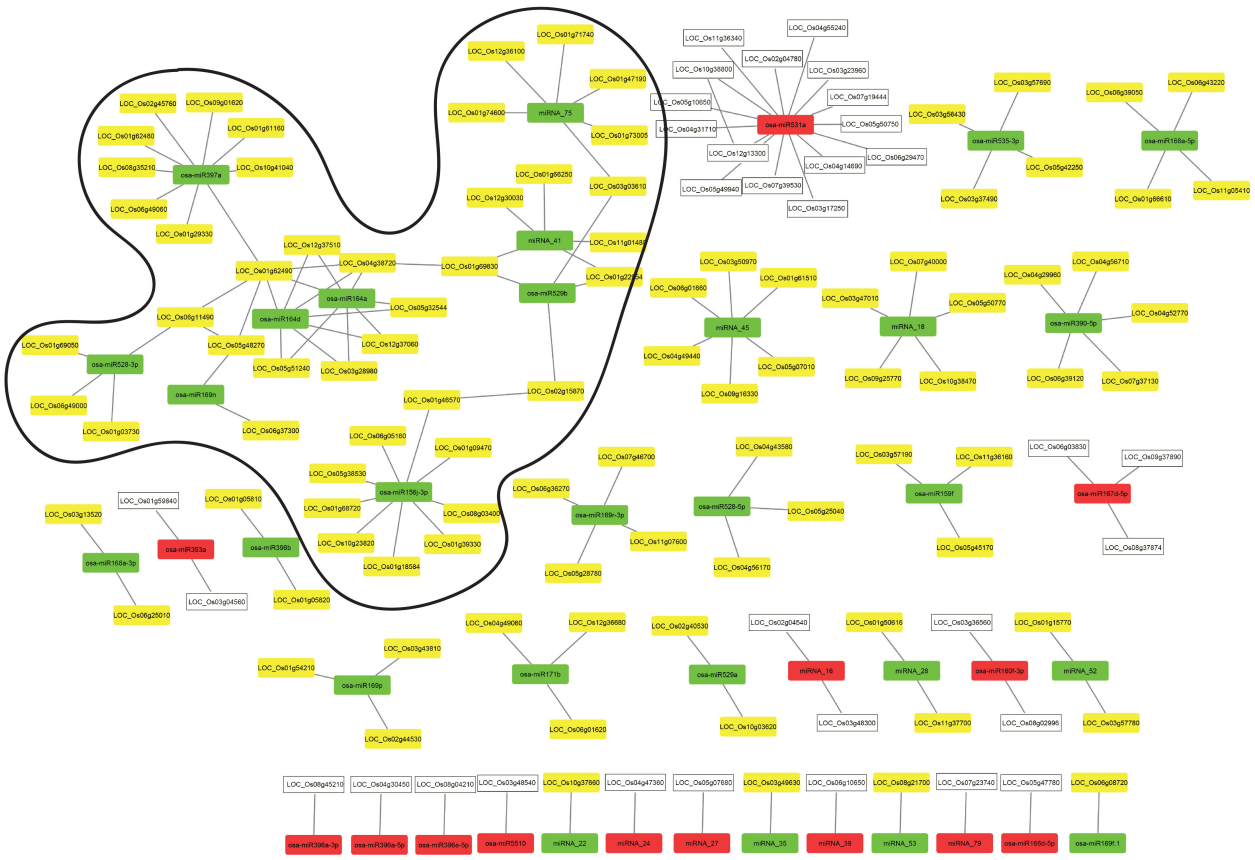

FIGURE 8
Integration of regulatory miRNA-mRNA network with PPI network during coleoptile senescence in rice. Protein-protein interaction network for the predicted target genes of conserved and novel miRNAs was generated using Cytoscape visualization software. The expression of miRNAs and target genes is presented based on the RNA-seq and small RNAome data obtained for coleoptile senescence in rice, respectively. Upregulated and downregulated miRNAs are represented by red and green boxes, respectively. Upregulated and downregulated predicted target genes are represented by yellow and white boxes, respectively. The predominant hub identified in the present study is highlighted.

Discussion

Senescence is a precise and highly orchestrated degradation process that is essential for reallocation of resources to developing organs and overall fitness of the plants. The genetic complexity and molecular mechanisms underlying natural leaf senescence have been well-studied, however, owing to slow progression of flag leaf senescence and long experimental duration with flag leaf being the last leaf to emerge, studying flag leaf senescence is challenging. On the other hand, coleoptile the first organ to senesce after seed germination in monocotyledonous plants undergoes a rapid transition from growth to death phase and due to which there is more uniformity in the coleoptile senescence as compared to that of leaves (Kawai and Uchimiya, 2000). Nevertheless, the key changes at tissue and cellular levels associated with senescence in coleoptiles and leaves are conserved (Inada et al., 2002). The unique features of coleoptile senescence thus advocates the possibility of its utilization as a convenient and rapid system for studying the cellular and molecular mechanisms of senescence in cereals. With an aim to unravel the functional biological networks of coleoptile senescence in rice, an integrative multi-omics approach was designed which combined high-throughput RNA-seq and small RNA-seq data of the senescing coleoptile generated in the present study with publicly available protein-protein interaction (PPI) datasets.

Our study reports identification of 3166 differentially expressed and 273 senescence-specific genes (jointly referred to as DEGs) in rice coleoptile senescence. Several of these DEGs encodes for transporter proteins, more interestingly, proportion of upregulated transporters (112) was nearly 5 times higher than those exhibiting downregulation (22). Transport of ions and other macromolecules across cellular boundaries is a key event that ensures remobilization of nutrients from source to sink (Guo et al., 2021). Previous studies on elucidating the molecular changes occurring during leaf senescence reported an increased

expression of genes encoding for several transporters, especially ABC and MATE type, amino acid and ion transporters (Buchanan-Wollaston et al., 2005; Graaff et al., 2006; Lee et al., 2017). ABC, peptides, amino acids, metabolites, sugar, and metal transporters were abundantly expressed during CS, which is in agreement with earlier reports (Guo et al., 2004; Zhang et al., 2014). Among the upregulated transporters, 11 genes each for MATE (Multidrug And Toxic compound Extrusion) and aquaporins (AQPs) were identified. MATE protein family in rice has 46 members and are involved in transport of secondary metabolites, ions and phytohormones and are therefore associated with regulation of several agronomic traits by mediating growth, development and response to environmental stimuli (Upadhyay et al., 2019; Du et al., 2021). Overexpression of *ELS1* (a MATE transporter) in Arabidopsis accelerated the senescence (Wang et al., 2016). Further, ABS3 (abnormal shoot 3), a MATE transporter protein, interacts with ATG8 (autophagy-related protein 8) and promotes senescence under natural and carbon-deprivation conditions (Jia et al., 2019). Functional characterization of the differentially expressed MATE transporters will help in identifying the transported molecules during CS. Another transporter family which attracted our attention was aquaporins (AQPs), which are expressed under a myriad of physiological conditions and regulate plant development and stress in plants (Maurel et al., 2008). These channel proteins are actively involved in water transport and trafficking of small solutes such as silicon, urea, reactive oxygen species (ROS) and even gasses such as CO_2 and ammonia (Maurel et al., 2008). Interestingly, CS involved upregulation and downregulation of 11 and 1 aquaporins, respectively. Functionally, AQPs are involved in plant senescence as the suppression of TIP1;1, a member of tonoplast AQPs, compromised carbohydrate transport, had excessive water loss and accelerated leaf senescence (Ma et al., 2004), while overexpression of the cotton TIP1;1-like protein in Arabidopsis promoted premature bolting and delayed senescence of rosette leaves (Cheng et al., 2022). AQPs promote diffusion of H_2O_2 across the membranes during senescence which may act as a signal for triggering senescence in the adjoining cells (Zentgraf et al., 2022). During senescence, generation of ROS, especially H_2O_2 is one of the early responses and it acts as a potent signaling reactive oxygen species. H_2O_2 further reprograms expression of AQPs and other SAGs. In addition to regulating the expression, H_2O_2 is also believed to modulate the AQPs transportation efficiency, structure and localization (Luu and Maurel, 2005). Owing to the multitasking roles of different transporters in plants, it would be worth exploring the function of these transporters in plant senescence.

Members of TF families such as NAC, MYB, WRKY, TCP, AP2/EREBP, bZIP and bHLH are associated with senescence (Guo et al., 2004; Gregersen and Holm, 2007; Breeze et al., 2011; Zhang et al., 2014; Lin et al., 2015; Moschen et al., 2016; Hinckley and Brusslan, 2020; Dong et al., 2021). The number of upregulated members of TF families AP2/EREBP, Zinc finger, homeobox, MYB, bHLH and WRKY TFs was greater than the down regulated members during CS, thus conforming to the previous observations (Zhang et al., 2014; Lin et al., 2015). Heat shock transcription factors (HSFs) have been indirectly associated with senescence and an early senescence phenotype was reported in the knock-out mutant of *AtHSFB1* in Arabidopsis (Breeze et al., 2008). Wu et al. (2012) demonstrated that JUNGBRUNNEN1 (JUB1), a NAC TF, functions as a negative regulator of senescence through its action on HSFA3 which elevates accumulation of HSPs and lowers H_2O_2 levels (Wu et al., 2012). Our results indicate that HSF family members play a more crucial role in regulating senescence as 5 members of HSF family (*OsHSFA2b, OsHSFA3a, OsHSFA7a, OsHSFB2b* and *OsHSFC1b*) were significantly upregulated during CS. Comprehensive expression profiling of HSFs has also revealed differential regulation of several HSFs in natural and induced flag leaf senescence in rice (Sasi et al., unpublished). Further, we found that the putative promoter regions of approximately 5% of SAGs in rice possess canonical and non-canonical heat shock elements (HSEs), thus indicating that HSFs might regulate the expression of SAGs by binding to their promoters (Sasi et al., unpublished).

Phytohormone homeostasis genes, together with an active involvement of regulatory factors such as TFs and small RNAs, fine tune senescence program in plants by integrating the developmental and environmental signals (Staden, 1995; Schippers et al., 2007; Khan et al., 2014). We observed exclusive upregulation for several SA and JA pathway genes. Additionally, the proportion of upregulated genes associated with cytokinin metabolism were largely downregulated, but those related with the auxin metabolism were upregulated. The levels of cytokinins decline during leaf senescence and exogenous application of cytokinins delay senescence (Guo et al., 2021). Although, upregulation of a few IAA (indole acetic acid) biosynthesis genes during leaf senescence has also been previously observed (Quirino et al., 1999), auxin also appears to play a negative role by suppressing expression of WRK57 and its downstream target SAG12, thereby delaying senescence in Arabidopsis (Noh and Amasino, 1999). A comparative transcriptome study revealed that SA, JA and ethylene are predominantly associated with developmental and dark-induced leaf and cell-suspension senescence, respectively (Buchanan-Wollaston et al., 2005). Transcript profiling of hormone pathway genes in senescing leaves in Arabidopsis and cotton demonstrated the involvement of several hormones such as salicylic acid (SA), ethylene, auxin, jasmonic acid and cytokinin, ABA and BR (Graaff et al., 2006; Lin et al., 2015). BRs accelerate senescence in detached cotyledons and leaves in wheat and pea (Sağlam-Çağ, 2007; Fedina et al., 2016) and acts synergistically with auxin to induce senescence in soybean cotyledons (Baris and Saglam-Cag, 2016).

ABA enhances plant senescence by positively regulating the expression of various chlorophyll degradation genes (*NON-YELLOW COLORING1, STAY-GREEN, PHEOPHYTINASE* and *PHEIDE A OXYGENASE*) and NAC TF family members (*VND-INTERACTING2 (VNI2), A SUBFAMILY OF STRESS-RESPONSIVE NAC (SNAC-A), ORESARA1 (ORE1), NAC-LIKE ACTIVATED BY APETALA3/PISTILLATA (OsNAP)* and *OsNAC2*) (Pruzinská et al., 2005; Kusaba et al., 2007; Park et al., 2007; Schelbert et al., 2009; Kim et al., 2011; Yang et al., 2011; Liang et al., 2014; Takasaki et al., 2015; Mao et al., 2017).

Unfavorable growth conditions such as salinity, extreme temperatures, dehydration, oxidative and nutrient deprivation induce premature senescence in plants. In fact, gene expression analyses have shown that several stress-responsive genes, including regulatory genes, are induced during progression of senescence (Breeze et al., 2011; Dong et al., 2021; Li et al., 2021). It is, therefore, believed that the molecular pathways of leaf senescence cross-talk with stress responsive pathways in plants (Guo and Gan, 2012). Our study revealed that several PR genes, conventionally associated with biotic stress, were differentially expressed in senescing coleoptiles, which is consistent with the previous studies where PR protein encoding genes were categorized as SAGs (Barth et al., 2004; Sillanpää et al., 2005). Accumulation of PR proteins was also observed in the intercellular spaces of barley leaves during natural senescence (Tamás et al., 1998). Protein profiling of apoplastic proteins of naturally, but not dark-induced, senescing leaves of Arabidopsis revealed that the most abundant SAG proteins were PR2 and PR5 (Borniego et al., 2020). Pathogens interfere with the host development by modifying the signalling pathways and regulating progression of plant senescence to meet their nutritional demands, whereas plants counteract by inducing a hypersensitive response to kill its own cells. When plants are challenged by a pathogen, induction of PR proteins along with several TFs is necessary for triggering the defense-related responses (Häffner et al., 2015). It would be worth comparing the induction patterns of PR genes in genotypes with contrasting senescence timing as well as correlating the progression of senescence with steady state levels of PR genes in pathogen-resistant versus susceptible genotypes. It is, therefore, pertinent to understand how the complex interaction of host and pathogen triggers senescence so as to pinpoint the cross-talk, signaling branches and regulatory nodes that play crucial roles in both pathogen response and senescence. Under abiotic stress category, heat stress-related genes such as DnaJ-related heat shock proteins (HSPs), several HSP70s, small HSPs (HSP18.2, HSP17.4, mitochondrial HSP23) exhibited significant upregulation during senescence. Although the potency of heat shock response (HSR) declines at the terminal stages of development, several components of HSR accumulate specifically during aging (Taylor and Dillin, 2011). One class of such proteins is molecular chaperones, which prevent protein aggregation observed during senescence and stress (Calderwood et al., 2009; Trivedi and Jurivich, 2020). Induction of HSFs and HSPs during stress and senescence thus indicate the existence of cross-talk between the senescence and abiotic stress pathways.

Although senescence of coleoptile and flag leaf supplies nutrition to growing seedlings and developing seeds respectively, the overall physiology of senescence in these tissues is vastly different. Whereas coleoptile emerges from the seed and exhibits rapid senescence, second leaf and flag leaf emerge from photosynthesizing plants and have a slow progression of senescence. To explore the extent of similarity and highlight the core components involved in senescence of two spatially and temporally different organs in rice (coleoptile and leaves) DEGs of CS and LS were compared. We observed that approximately 92% of the DEGs had different expression profiles in CS and LS, which is a reflection of their divergent physiologies at the level of gene expression. Among the 8% genes that were similarly regulated, 3 AQP-coding genes were commonly induced during both leaf and coleoptile senescence, however, overrepresentation of upregulated AQPs in CS (11) as compared to LS (4) also highlight specific roles of the aquaporins during coleoptile senescence. It would be worth performing additional functional studies to understand the convergent and divergent roles that the common and specific AQPs play during senescence in rice. Among the TFs, few members such as *WRKY*s, *MYB*s, *NAC*s and *Zinc finger proteins* along with 3 HSFs (*OsHSFA3a*, *OsHSFA7a* and *OsHSFC1b*) were commonly upregulated in CS and LS. The roles of transporters and TFs during plant senescence have been discussed previously in this article. Since AQPs, HSFs and other TFs are also involved in stress-responsive pathways, stress and aging pathways appear to be closely related.

Several genes encoding ELIPs (early light-induced proteins) were also upregulated in both CS and LS. ELIPs bind to free chlorophyll released from pigment-protein complexes and provide protection against oxidative stress during senescence (Binyamin et al., 2001; Hutin et al., 2003). Similarly RCCR (red chlorophyll catabolite reductase) induced in both types of senescence is involved in chlorophyll degradation, an integral component of plant senescence (Pruzinská et al., 2005). Another important gene associated with the initial step of the chlorophyll degradation pathway, *OsSGR* (stay-green), was also expressed at high levels during senescence in coleoptiles and flag leaves in rice. OsSGR encodes a vital enzyme, magnesium (Mg) dechelatase that removes Mg from chlorophyll-a resulting in its conversion to pheophytin A (Phein A), an intermediate in the universal chlorophyll breakdown pathway (Shimoda et al., 2016). Furthermore, SGR binds to LHCII and accelerates the breakdown of chlorophyll-protein complexes (Sakuraba et al., 2012). Several CYPs (cytochrome P450 monooxygenases) exhibited upregulation in both CS and LS. CYPs are known as 'versatile biocatalysts' because of their involvement with biosynthesis of antioxidants, secondary metabolites and phytohormones (Pandian et al., 2020), whose levels change

with progression of senescence. The role of cytochrome P450 members in brassinosteroid signaling is well-documented in the studies on rice dwarf mutant, *dwarf11* (Tanabe, 2005). Cell wall breakdown and a decline in photosynthesis are often associated with the senescence process (Mohapatra et al., 2010) and we also observed that several genes belonging to the cell wall such as pectinesterase and photosynthesis-related categories such as *Ribulose bisphosphate carboxylase small chain precursor*, displayed significant decline in expression levels. Pectinesterase is involved in cellular adhesion and stem elongation (Li et al., 2017) and its level decreases in senescing strawberries (Castillejo et al., 2004). Ribulose bisphosphate carboxylase small chain precursor is the core component of photosynthesis (Bannenberg et al., 2009) and systematic degradation of chlorophyll during senescence could possibly be related to the decreased expression of Ribulose bisphosphate carboxylase small chain precursor. One and two genes encoding for 1-aminocyclopropane-1-carboxylate oxidase (ACO) family were upregulated and downregulated, respectively, during both CS and LS. ACO members are differentially expressed developmentally and in tissue-specific manner (Houben and Van de Poel, 2019) and regulate various developmental processes and stress responses in plants (Houben and Van de Poel, 2019). Since ACOs exert a precise control on spatial and temporal levels of ethylene it will be interesting to correlate change in expression of individual ACO members with ethylene levels and senescence programs.

In addition to the genes that were co-expressed, multiple genes showed an inverse expression profile during the two senescence programs. GO enrichment revealed that the top category of genes belonged to the 'integral component of membrane' followed by DNA binding/transcription. Additionally, several TFs belonging to the MYB family, CYPs, GSTs (glutathione-S-transferase), LTPLs (lipid transfer proteins), glycosyl hydrolases, transporters and stress-responsive proteins exhibited differential expression patterns during progression of senescence in two tissues. We believe that finding the downstream constituents of the inversely correlated genes will help in finding the basis of the different physiologies seen in these senescence programs. An important gene involved in ABA synthesis, i.e., *NCED1* encoding for 9-cis-epoxycarotenoid dioxygenase accumulated in CS, while its levels declined in LS. Modulating expression of NCED genes can affect the timing of senescence e.g., overexpression of *OsNCED3*, and *OsNCED5* genes that are strongly induced by dark, accelerate leaf senescence in rice (Huang et al., 2018; Huang et al., 2019). NCED1 is a rate-limiting enzyme in the ABA biosynthesis pathway and since ABA is a positive regulator of senescence in plants, upregulation of NCED1 explains the positive correlation between the NCED1 expression and CS. However, the reason for its downregulation in LS is not known. The downregulation of NCED1 in LS was observed by comparing the expression levels at 36 days post heading (DPH) with 4 DPH stage and it is possible that NCED1 levels elevate at a later stage of senescence in flag leaves. The effect of modulating the expression levels of other members of NCED gene family on natural and dark-induced senescence in rice is not known and worth exploring. Since ABA is synthesized from β-carotene, we analyzed the expression pattern of carotenoid biosynthesis genes in CS as well. At least 16 genes involved in carotenoid production have been identified in rice (Chaudhary et al., 2010), of which two genes, *Phytoene synthase* (LOC Os09g38320) and *Lycopene ϵ-cyclase* (LOC Os01g39960), were found to be up-regulated in our dataset. During α-carotene biosynthesis, lycopene ϵ-cyclase catalyzes the cyclization of linear lycopene to produce cyclic lycopene (Bai et al., 2009). Phytoene synthase is the major rate-limiting enzyme in the carotenoid biosynthesis pathway (Simpson et al., 2018). It is well documented that ABA can induce Phytoene synthase to activate the production of its precursors (Simpson et al., 2018). This suggests that phytoene synthase and carotenes may participate in an auto-activating ABA biosynthesis pathway during CS in rice.

Small RNAs play an important role in regulating gene expression during growth and development and response to different stresses in plants (Li et al., 2017). A number of miRNAs associated with regulation of leaf senescence have been identified in multiple plant species (Xu et al., 2014; Huo et al., 2015; Thatcher et al., 2015; Qin et al., 2016; Wu et al., 2016; Swida-Barteczka and Szweykowska-Kulinska, 2019; Sasi et al., 2019). However, the contribution of miRNAs in controlling coleoptile senescence has not been elucidated so far. Therefore, in the present study miRNAs that are differentially expressed during progression of senescence in coleoptiles and their target genes were predicted. Further miRNAs and their corresponding target genes which exhibited an inverse expression pattern during coleoptile senescence were identified. Overall, 41 conserved and 21 novel miRNAs exhibiting differential expression patterns in senescing coleoptiles were identified. To find out the commonality in the senescence programs of different tissues of rice, we compared the miRNAs identified in the CS and flag leaf senescence (Sasi et al., 2019) and found that 3 miRNAs were commonly downregulated in both datasets. Interestingly, when the expression pattern of the predicted target genes of these miRNAs was determined in CS (present study) and FLS (Lee et al., 2017) RNA-seq datasets, we found that the targets of 2 commonly downregulated miRNAs (osa-miR164a: LOC_Os04g38720 which encodes for NAC2 and osa-miR535-3p: LOC_Os05g42250 which encodes for cyclic nucleotide-gated ion channel 2 or OsCNGC16) exhibited remarkable upregulation which indicates that these miRNA-mRNA pairs could play an important role in plant senescence. OsCNGC16 is a plasma-membrane localized protein which triggers an increase in calcium levels when plants are exposed to extreme temperatures (heat or chilling) and imparts thermotolerance in rice (Cui et al., 2020). Calcium also plays an important role in triggering senescence in plants as exogenous application of

calcium delays senescence in detached leaves (Poovaiah and Leopold, 1973). The importance of calcium in senescence is further evident by the action of calcium-dependent protein kinase 1 (CPK1) in phosphorylating ORE, the master regulator of senescence in Arabidopsis (Durian et al., 2020). It would be interesting to validate these miRNAs and their respective targets in different senescence tissues and perform their functional characterization for possible involvement in regulation of senescence in plants.

Integration of expression datasets of RNA-seq and small RNA-seq of coleoptile senescence unraveled the important miRNA-mRNA modules and provided a thorough understanding of the associated multiple regulatory networks. Only high confidence miRNA-target pairs which exhibited inverse expression patterns in miRNAome and transcriptome datasets generated by us, respectively, were utilized for the construction of regulatory network. Further, publicly available protein-protein interaction (PPI) data was also integrated with the miRNA-mRNA network and visualization of regulatory network unravelled 140 miRNA-mRNA modules, while only 6 protein interactions were identified. Based on the network generated we concluded that:

a. A predominant hub consists of 9 upregulated miRNAs, including two members of MIR164 family at the center, targeting 42 genes during coleoptile senescence. Previous studies have reported few of these reliable miRNA-target pairs in rice and other plant species: osa-miR164a/d-NAC2, osa-miR397a-laccase, osa-miR528-plastocyanin, osa-miR529b-SPL2 (Fang et al., 2014; Pan et al., 2017; Tsuzuki et al., 2019; Zhu et al., 2020). Some of these miRNAs such as osa-miR164, osa-miR528 and their targets genes NAC2 and COPPER ION BINDING PROTEIN1 have been implicated in regulation of leaf senescence (Yuan et al., 2015; Mao et al., 2017). SPLs are also associated with regulation of flowering time, phase transition and developmental aging (Jung et al., 2016).
b. The coregulatory miRNA-target pairs are connected by the characteristic nature of miRNAs targeting more than one gene or one gene targeted by several miRNAs. For example: While osa-miR164a/d target NAC2 and laccase, laccase is also a target of osa-miR397a. SPL2 and serine carboxypeptidase are targets of both osa-miR529b and miRNA_41. 1,3 beta glucan synthase, being the common target of osa-miR529b and miRNA_75, links the two miRNA modules. The autolysis of cellular components during PCD has been linked to serine carboxypeptidases (Schaller, 2004). However, no reports were found that directly implicate 1,3 beat glucan synthase and laccases in plant senescence.
c. Several targets of miRNAs are TFs which regulate diverse biological processes at different stages of plant development and few of these have been implicated in regulation of senescence such as WRKY, NAC, SPL, MYB, TCP, and F-box protein as discussed earlier (Woo et al., 2001; Schommer et al., 2008; Zhang et al., 2011; Jiang et al., 2014; Liang et al., 2014; Jung et al., 2016).
d. miR169n is predicted to target two genes, LOC_Os05g48270 (DOMON domain-containing protein-cytochromeb561/ferric reductase transmembrane protein/auxin responsive protein) and LOC_Os06g37300 (cytochrome P450 or CYP). In rice, CYPs belong to a large multigene family, the members of which are associated with metabolism of fatty acids, phenylpropanoids and steroids and more importantly, with hormone homeostasis, thereby regulating plant development and stress responses (Wei and Chen, 2018). A recent report demonstrated that a mutant of *ELL1* which encodes for CYP monooxygenase displayed high accumulation of ROS and cell death in rice (Cui et al., 2021). DOMON gene was identified as a strong candidate in the QTLs for functional stay-green (FSG) trait in rice (Lim and Paek, 2015). However, it is important to investigate the exact function of LOC_Os05g48270 and how it regulates coleoptile senescence in rice.
e. Two copper-containing proteins, laccase (multi-copper) and plastocyanin (mono-copper), are part of the hub wherein one member (LOC_Os01g62490) of laccase family is targeted by three miRNAs, osa-miR164a/d and osa-miR397a, while the two other members (LOC_Os01g61160, LOC_Os01g62480) are targeted by osa-miR397a only. The gene (LOC_Os06g11490) encoding endomembrane plastocyanin is targeted by osa-miR528-3p. In plants Cu-miRNAs such as miR397, miR408, miR528 and miR857 target copper-containing proteins: laccases, plastocyanin, polyphenol oxidase (PPO), ascorbate oxidase (AAO), amino oxidase (AO), Cu/Zn superoxide dismutases (CSDs; Zhu et al., 2020). These Cu-containing proteins are actively involved in diverse processes such as ROS metabolism, Cu homeostasis and stress tolerance (Zhu et al., 2020). In Arabidopsis, a pair of interacting proteins belonging to blue copper protein family: plantacyanin (PCY) and SAG14 are induced during dark-induced senescence which is crucial for chloroplast copper efflux and this module is regulated by miR408 and PIF3/4/5 (Hao et al., 2022). Plant laccases are Cu-oxidases which catalyze lignin and anthocyanin biosynthesis and are involved in diverse plant processes: growth and development, defense against biotic and abiotic stresses (Ranocha et al., 2002; Wan et al., 2022). However, as per our understanding no studies have directly linked laccase with regulation of senescence in plants. In the present study we show that three laccase-encoding genes are

upregulated and 3 miRNAs that are possibly regulating their expression are clearly downregulated. Our results highlight the possible involvement of laccases in regulating coleoptile senescence in rice, however, the underlying mechanism needs to be explored. It is hypothesized that the copper-proteins might contribute to regulation of senescence by modulating Cu and redox homeostasis in plants.

Conclusions

We employed an integrated omics approach by combining transcriptome and small RNAome sequencing of coleoptile senescence in rice. Analysis of the RNA-seq dataset identified 3439 DEGs many of which were TFs, transporters, and involved in hormone metabolism, redox and stress responses. Comparison of CS dataset with publicly available leaf senescence (LS) dataset discovered a set of core senescence associated genes. Small RNA sequencing identified many differentially expressed miRNAs, targets for some of which displayed an inverse expression profile in transcriptome dataset. The regulatory network generated by integrating the high confidence miRNA-RNA target pairs with PPI dataset was comprised of 42 modules. A distinguished hub of miR164a/d targeting copper-containing proteins, laccases and plastocyanin, indicated that copper and ROS homeostasis regulate coleoptile senescence in rice. Overall, our study reports a comprehensive atlas on the expression dynamics of genes, miRNA regulators and their interactions and provides insights into the fundamental pathways regulating coleoptile senescence in rice.

Data availability statement

The datasets presented in this study can be found in online repositories. The names of the repository/repositories and accession number(s) can be found in the article/Supplementary Material.

Author contributions

SK: Conceptualization, Supervision, Investigation, Formal analysis, Funding acquisition, Methodology, Resources, Validation, Writing-original draft, review and editing; MA: Investigation, Methodology, Resources, Writing-critical review and editing; JMS: Investigation, Methodology, Validation, Data curation, Formal Analysis, Writing-original draft, review and editing; CV: Data analysis, curation and Writing-review and editing; BK: Data analysis and curation; RB: Data curation, formal analysis, software; RS: Data curation, formal analysis, software. All authors contributed to the article and approved the submitted version.

Funding

The financial support from University Grants Commission (sanction order # 41-512/2012), Government of India; Department of Biotechnology, Government of India and Faculty Research Programme (Institute of Eminence), University of Delhi (sanction orders # IoE/FRP/2020/27 and IoE/2021/12/FRP) are acknowledged. JMS and CV are thankful to UGC for Basic Science Research (BSR) fellowships.

Conflict of interest

Authors RB and RS are employed by the company Bionivid Technology Pvt. Limited, Bengaluru, Karnataka, India. The remaining authors declare that the research was conducted in the absence of any commercial or financial relationships that could be construed as a potential conflict of interest..

Publisher's note

All claims expressed in this article are solely those of the authors and do not necessarily represent those of their affiliated organizations, or those of the publisher, the editors and the reviewers. Any product that may be evaluated in this article, or claim that may be made by its manufacturer, is not guaranteed or endorsed by the publisher.

Supplementary material

The Supplementary Material for this article can be found online at: https://www.frontiersin.org/articles/10.3389/fpls.2022.985402/full#supplementary-material

References

Ay, N., Janack, B., and Humbeck, K. (2014). Epigenetic control of plant senescence and linked processes. *J. Exp. Bot.* 65 (14), 3875–3887. doi: 10.1093/jxb/eru132

Bai, L., Kim, E. H., Dellapenna, D., and Brutnell, T. P. (2009). Novel lycopene epsilon cyclase activities in maize revealed through perturbation of carotenoid biosynthesis. *Plant J.* 59 (4), 588–599. doi: 10.1111/J.1365-313X.2009.03899.X

Bannenberg, G., Martínez, M., Rodríguez, M. J., López, M. A., Ponce de León, I., Hamberg, M., et al. (2009). Functional analysis of alpha-DOX2, an active alpha-dioxygenase critical for normal development in tomato plants. *Plant Physiol.* 151 (3), 1421–1432. doi: 10.1104/pp.109.145094

Baris, C., and Saglam-Cag, S. (2016). The effects of brassinosteroids on sequential leaf senescence occurring in glycine max l. *Int. J. Bio-Technology Res. (IJBTR)* 6 (4), 7–16.

Barth, C., Moeder, W., Klessig, D. F., and Conklin, P. L. (2004). The timing of senescence and response to pathogens is altered in the ascorbate-deficient arabidopsis mutant vitamin c-1. *Plant Physiol.* 134 (4), 1784–1792. doi: 10.1104/pp.103.032185

Binyamin, L., Falah, M., Portnoy, V., Soudry, E., and Gepstein, S. (2001). The early light-induced protein is also produced during leaf senescence of nicotiana tabacum. *Planta* 212 (4), 591–597. doi: 10.1007/S004250000423

Borniego, M. L., Molina, M. C., Guiamét, J. J., and Martinez, D. E. (2020). Physiological and proteomic changes in the apoplast accompany leaf senescence in arabidopsis. *Front. Plant Sci.* 10. doi: 10.3389/fpls.2019.01635

Breeze, E., Harrison, E., McHattie, S., Hughes, L., Hickman, R., Hill, C., et al. (2011). High-resolution temporal profiling of transcripts during arabidopsis leaf senescence reveals a distinct chronology of processes and regulation. *Plant Cell* 23 (3), 873–894. doi: 10.1105/tpc.111.083345

Breeze, E., Harrison, E., Page, T., Warner, N., Shen, C., and Zhang, C. (2008). Transcriptional regulation of plant senescence : from functional genomics to systems biology *Plant Bio.* 10, 99–109. doi: 10.1111/j.1438-8677.2008.00076.x

Buchanan-Wollaston, V., Page, T., Harrison, E., Breeze, E., Lim, P. O., Nam, H. G., et al. (2005). Comparative transcriptome analysis reveals significant differences in gene expression and signalling pathways between developmental and dark / starvation-induced senescence in arabidopsis. *Plant J.* 42, 567–585. doi: 10.1111/j.1365-313X.2005.02399.x

Calderwood, S. K., Murshid, A., and Prince, T. (2009). The shock of aging: molecular chaperones and the heat shock response in longevity and aging–a mini-review. *Gerontology* 55 (5), 550–558. doi: 10.1159/000225957

Castillejo, C., de la Fuente, J. I., Iannetta, P., Botella, M.Á., and Valpuesta, V. (2004). Pectin esterase gene family in strawberry fruit: study of FaPE1, a ripening-specific isoform. *J. Exp. Bot.* 55 (398), 909–918. doi: 10.1093/jxb/erh102

Chaudhary, N., Nijhawan, A., Khurana, J. P., and Khurana, P. (2010). Carotenoid biosynthesis genes in rice: Structural analysis, genome-wide expression profiling and phylogenetic analysis. *Mol. Genet. Genomics* 283 (1), 13–33. doi: 10.1007/S00438-009-0495-X

Cheng, G., Wang, M., Zhang, L., Wei, H., Wang, H., Lu, J., et al. (2022). Overexpression of a cotton aquaporin gene GhTIP1;1-like confers cold tolerance in transgenic arabidopsis. *Int. J. Mol. Sci.* 23 (3), 1361. doi: 10.3390/ijms23031361

Chomczynski, P., and Sacchi, N. (1987). Single-step method of RNA isolation by acid guanidinium thiocyanate-phenol-chloroform extraction. *Analytical Biochem.* 162 (1), 156–159. doi: 10.1006/abio.1987.9999

Cui, Y., Lu, S., Li, Z., Cheng, J., Hu, P., Zhu, T., et al. (2020). CYCLIC NUCLEOTIDE-GATED ION CHANNELs 14 and 16 promote tolerance to heat and chilling in rice. *Plant Physiol.* 183 (4), 1794–1808. doi: 10.1104/PP.20.00591

Cui, Y., Peng, Y., Zhang, Q., Xia, S., Ruan, B., Xu, Q., et al. (2021). Disruption of EARLY LESION LEAF 1, encoding a cytochrome P450 monooxygenase, induces ROS accumulation and cell death in rice. *Plant J.* 105 (4), 942–956. doi: 10.1111/TPJ.15079

Dong, S., Sang, L., Xie, H., Chai, M., and Wang, Z. Y. (2021). Comparative transcriptome analysis of salt stress-induced leaf senescence in medicago truncatula. *Front. Plant Sci.* 12. doi: 10.3389/FPLS.2021.666660

Durian, G., Sedaghatmehr, M., Matallana-Ramirez, L. P., Schilling, S. M., Schaepe, S., Guerra, T., et al. (2020). Calcium-dependent protein kinase CPK1 controls cell death by *In vivo* phosphorylation of senescence master regulator ORE1. *Plant Cell* 32 (5), 1610–1625. doi: 10.1105/TPC.19.00810

Du, Z., Su, Q., Wu, Z., Huang, Z., Bao, J., Li, J., et al. (2021). Genome-wide characterization of MATE gene family and expression profiles in response to abiotic stresses in rice (Oryza sativa). *BMC Ecol. Evol.* 21 (1), 1–14. doi: 10.1186/S12862-021-01873-Y

Ellis, C. M., Nagpal, P., Young, J. C., Hagen, G., Guilfoyle, T. J., and Reed, J. W. (2005). AUXIN RESPONSE FACTOR1 and AUXIN RESPONSE FACTOR2 regulate senescence and floral organ abscission in arabidopsis thaliana. *Dev. (Cambridge England)* 132 (20), 4563–4574. doi: 10.1242/DEV.02012

Fang, Y., Xie, K., and Xiong, L. (2014). Conserved miR164-targeted NAC genes negatively regulate drought resistance in rice. *J. Exp. Bot.* 65 (8), 2119–2135. doi: 10.1093/JXB/ERU072

Fedina, E., Yarin, A., Mukhitova, F., Blufard, A., and Chechetkin, I. (2016). Brassinosteroid-induced changes of lipid composition in leaves of pisum sativum l. *during senescence. Steroids* 117, 25–28. doi: 10.1016/j.steroids.2016.10.009

Fröhlich, M., and Kutschera, U. (1995). Changes in soluble sugars and proteins during development of rye coleoptiles. *J. Plant Physiol.* 146 (1–2), 121–125. doi: 10.1016/S0176-1617(11)81977-2

Graaff, E., Schwacke, R., Schneider, A., Desimone, M., Flügge, U.-I., and Kunze, R. (2006). Transcription analysis of arabidopsis membrane transporters and hormone pathways during developmental and induced leaf senescence. *Plant Physiol.* 141 (2), 776–792. doi: 10.1104/pp.106.079293

Gray, W. M. (2004). Hormonal regulation of plant growth and development. *PloS Biol.* 2 (9), e311. doi: 10.1371/JOURNAL.PBIO.0020311

Gregersen, P. L., and Holm, P. B. (2007). Transcriptome analysis of senescence in the flag leaf of wheat (triticum aestivum l .). *Plant Biotechnol. J.* 5 (1), 192–206. doi: 10.1111/j.1467-7652.2006.00232.x

Guo, Y., Cai, Z., and Gan, S. (2004). Transcriptome of arabidopsis leaf senescence. *Plant Cell Environ.* 27 (5), 521–549. doi: 10.1111/j.1365-3040.2003.01158.x

Guo, Y., and Gan, S.-S. (2012). Convergence and divergence in gene expression profiles induced by leaf senescence and 27 senescence-promoting hormonal, pathological and environmental stress treatments. *Plant Cell Environ.* 35 (3), 644–655. doi: 10.1111/j.1365-3040.2011.02442.x

Guo, Y., Ren, G., Zhang, K., Li, Z., Miao, Y., and Guo, H. (2021). Leaf senescence: progression, regulation, and application. *Mol. Horticulture* 1, 1. doi: 10.1186/S43897-021-00006-9

Häffner, E., Konietzki, S., and Diederichsen, E. (2015). Keeping control: The role of senescence and development in plant pathogenesis and defense. *Plants* 4 (3), 449–488. doi: 10.3390/PLANTS4030449

Hao, C., Yang, Y., Du, J., Deng, X. W., and Li, L. (2022). The PCY-SAG14 phytocyanin module regulated by PIFs and miR408 promotes dark-induced leaf senescence in arabidopsis. *Proc. Natl. Acad. Sci. U.S.A.* 119 (3), 1–10. doi: 10.1073/pnas.2116623119

Hinckley, W. E., and Brusslan, J. A. (2020). Gene expression changes occurring at bolting time are associated with leaf senescence in arabidopsis. *Plant Direct* 4 (11), e00279. doi: 10.1002/pld3.279

Houben, M., and Van de Poel, B. (2019). 1-aminocyclopropane-1-carboxylic acid oxidase (ACO): The enzyme that makes the plant hormone ethylene. *Front. Plant Sci.* 10. doi: 10.3389/FPLS.2019.00695

Huang, Y., Guo, Y., Liu, Y., Zhang, F., Wang, Z., Wang, H., et al. (2018). 9-cis-epoxycarotenoid dioxygenase 3 regulates plant growth and enhances multi-abiotic stress tolerance in rice. *Front. Plant Sci.* 9. doi: 10.3389/FPLS.2018.00162/BIBTEX

Huang, Y., Jiao, Y., Xie, N., Guo, Y., Zhang, F., Xiang, Z., et al. (2019). OsNCED5, a 9-cis-epoxycarotenoid dioxygenase gene, regulates salt and water stress tolerance and leaf senescence in rice. *Plant Sci.* 287, 110188. doi: 10.1016/J.PLANTSCI.2019.110188

Huo, X., Wang, C., Teng, Y., and Liu, X. (2015). Identification of miRNAs associated with dark-induced senescence in arabidopsis. *BMC Plant Biol.* 15 (1), 1–12. doi: 10.1186/s12870-015-0656-5

Hutin, C., Nussaume, L., Moise, N., Moya, I., Kloppstech, K., and Havaux, M. (2003). Early light-induced proteins protect arabidopsis from photooxidative stress. *Proc. Natl. Acad. Sci. U.S.A.* 100 (8), 4921–4926. doi: 10.1073/PNAS.0736939100

Inada, N., Sakai, A., Kuroiwa, H., and Kuroiwa, T. (1998). Three-dimensional analysis of the senescence program in rice (Oryza sativa l.) coleoptiles: Investigations by fluorescence microscopy and electron microscopy. *Planta* 206 (4), 585–597. doi: 10.1007/s004250050307

Inada, N., Sakai, A., Kuroiwa, H., and Kuroiwa, T. (2002). "Three-dimensional progression of programmed death in the rice coleoptile," in *International review of cytology*, vol. 218). (USA: Elsevier Masson SAS). doi: 10.1016/S0074-7696(02)18014-4

Jia, M., Liu, X., Xue, H., Wu, Y., Shi, L., Wang, R., et al. (2019). Noncanonical ATG8-ABS3 interaction controls senescence in plants. *Nat. Plants* 5 (2), 212–224. doi: 10.1038/S41477-018-0348-X

Jiang, Y., Liang, G., Yang, S., and Yu, D. (2014). Arabidopsis WRKY57 functions as a node of convergence for jasmonic acid – and auxin-mediated signaling in

jasmonic acid-Induced leaf senescence. *The Plant Cell* 26 (1), 230–245. doi: 10.1105/tpc.113.117838

Jung, J. H., Lee, H. J., Ryu, J. Y., and Park, C. M. (2016). SPL3/4/5 integrate developmental aging and photoperiodic signals into the FT-FD module in arabidopsis flowering. *Mol. Plant* 9 (12), 1647–1659. doi: 10.1016/J.MOLP.2016.10.014

Kawai, M., and Uchimiya, H. (2000). Coleoptile senescence in rice (Oryza sativa l.). *Ann. Bot.* 86 (2), 405–414. doi: 10.1006/anbo.2000.1199

Khan, M., Rozhon, W., and Poppenberger, B. (2014). The role of hormones in the aging of plants - a mini-review. *Gerontology* 60 (1), 49–55. doi: 10.1159/000354334

Kim, J. H., Chung, K. M., and Woo, H. R. (2011). Three positive regulators of leaf senescence in arabidopsis, ORE1, ORE3 and ORE9, play roles in crosstalk among multiple hormone-mediated senescence pathways. *Genes Genomics* 33, 373–381. doi: 10.1007/s13258-011-0044-y

Kim, J., Kim, J. H., Lyu, J., Woo, H. R., and Lim, P. O. (2018). New insights into the regulation of leaf senescence in arabidopsis. *J. Exp. Bot.* 69 (4), 787–799. doi: 10.1093/JXB/ERX287

Kim, J. H., Woo, H. R., Kim, J., Lim, P. O., Lee, I. C., Choi, S. H., et al. (2009). Trifurcate feed-forward regulation of age-dependent cell death involving miR164 in arabidopsis. *Science* 323 (5917), 1053–1057. doi: 10.1126/science.1166386

Kozomara, A., and Griffiths-Jones, S. (2014). miRBase: annotating high confidence microRNAs using deep sequencing data. *Nucleic Acids Res.* 42 (D1), D68–D73. doi: 10.1093/NAR/GKT1181

Kusaba, M., Ito, H., Morita, R., Iida, S., Sato, Y., Fujimoto, M., et al. (2007). Rice NON-YELLOW COLORING1 is involved in light-harvesting complex II and grana degradation during leaf senescence. *Plant Cell* 19 (4), 1362–1375. doi: 10.1105/tpc.106.042911

Lee, S., Jeong, H., Lee, S., Lee, J., Kim, S., Park, J., et al. (2017). Molecular bases for differential aging programs between flag and second leaves during grain-filling in rice. *Sci. Rep.* 7 (1), 1–16. doi: 10.1038/s41598-017-07035-9

Liang, C., Wang, Y., Zhu, Y., Tang, J., Hu, B., Liu, L., et al. (2014). OsNAP connects abscisic acid and leaf senescence by fine-tuning abscisic acid biosynthesis and directly targeting senescence-associated genes in rice. *Proc. Natl. Acad. Sci. U. S. A.* 111 (27), 10013–10018. doi: 10.1073/pnas.1321568111

Li, S., Castillo-González, C., Yu, B., and Zhang, X. (2017). The functions of plant small RNAs in development and in stress responses. *Plant J.* 90 (4), 654–670. doi: 10.1111/TPJ.13444

Li, L., He, Y., Zhang, Z., Shi, Y., Zhang, X., Xu, X., et al. (2021). OsNAC109 regulates senescence, growth and development by altering the expression of senescence- and phytohormone-associated genes in rice. *Plant Mol. Biol.* 105 (6), 637–654. doi: 10.1007/S11103-021-01118-Y

Lim, P. O., Kim, H. J., and Gil Nam, H. (2007). Leaf senescence. *Annu. Rev. Plant Biol.* 58 (1), 115–136. doi: 10.1146/annurev.arplant.57.032905.105316

Lim, J.-H., and Paek, N.-C. (2015). Quantitative trait locus mapping and candidate gene analysis for functional stay-green trait in rice. *Plant Breed. Biotechnol.* 3 (2), 95–107. doi: 10.9787/pbb.2015.3.2.095

Lin, M., Pang, C., Fan, S., Song, M., Wei, H., and Yu, S. (2015). Global analysis of the gossypium hirsutum l. transcriptome during leaf senescence by RNA-seq. *BMC Plant Biol.* 15 (1), 1–18. doi: 10.1186/S12870-015-0433-5

Li, Z., Peng, J., Wen, X., and Guo, H. (2013). ETHYLENE-INSENSITIVE3 is a senescence-associated gene that accelerates age-dependent leaf senescence by directly repressing miR164 transcription in arabidopsis. *Plant Cell* 25 (9), 3311. doi: 10.1105/TPC.113.113340

Livak, K. J., and Schmittgen, T. D. (2001). Analysis of relative gene expression data using real-time quantitative PCR and the 2(-delta delta C(T)) method. *Methods (San Diego Calif.)* 25 (4), 402–408. doi: 10.1006/METH.2001.1262

Li, N., Zhao, M., Liu, T., Dong, L., Cheng, Q., Wu, J., et al. (2017). A novel soybean dirigent gene GmDIR22 contributes to promotion of lignan biosynthesis and enhances resistance to phytophthora sojae. *Front. Plant Sci.* 8, 1–12. doi: 10.3389/fpls.2017.01185

Luu, D. T., and Maurel, C. (2005). Aquaporins in a challenging environment: molecular gears for adjusting plant water status. *Plant Cell Environ.* 28 (1), 85–96. doi: 10.1111/J.1365-3040.2004.01295.X

Mao, C., Lu, S., Lv, B., Zhang, B., Shen, J., He, J., et al. (2017). A rice NAC transcription factor promotes leaf senescence *via* ABA biosynthesis. *Plant Physiol.* 174 (3), 1747–1763. doi: 10.1104/pp.17.00542

Ma, S., Quist, T. M., Ulanov, A., Joly, R., and Bohnert, H. J. (2004). Loss of TIP1;1 aquaporin in arabidopsis leads to cell and plant death. *Plant Journal : For Cell Mol. Biol.* 40 (6), 845–859. doi: 10.1111/J.1365-313X.2004.02265.X

Maurel, C., Verdoucq, L., Luu, D. T., and Santoni, V. (2008). Plant aquaporins: membrane channels with multiple integrated functions. *Annu. Rev. Plant Biol.* 59, 595–624. doi: 10.1146/ANNUREV.ARPLANT.59.032607.092734

Meyers, B. C., Axtell, M. J., Bartel, B., Bartel, D. P., Baulcombe, D., Bowman, J. L., et al. (2008). Criteria for annotation of plant MicroRNAs. *THE Plant Cell Online* 20 (12), 3186–3190. doi: 10.1105/tpc.108.064311

Mohapatra, P. K., Patro, L., Raval, M. K., Ramaswamy, N. K., Biswal, U. C., and Biswal, B. (2010). Senescence-induced loss in photosynthesis enhances cell wall β-glucosidase activity. *Physiologia Plantarum* 138 (3), 346–355. doi: 10.1111/J.1399-3054.2009.01327.X

Moschen, S., Bengoa Luoni, S., Di Rienzo, J. A., Caro, M., del, P., Tohge, T., et al. (2016). Integrating transcriptomic and metabolomic analysis to understand natural leaf senescence in sunflower. *Plant Biotechnol. J.* 14 (2), 719–734. doi: 10.1111/PBI.12422

Narsai, R., Edwards, J. M., Roberts, T. H., Whelan, J., Joss, G. H., and Atwell, B. J. (2015). Mechanisms of growth and patterns of gene expression in oxygen-deprived rice coleoptiles. *Plant J.* 82 (1), 25–40. doi: 10.1111/TPJ.12786

Noh, Y. S., and Amasino, R. M. (1999). Identification of a promoter region responsible for the senescence-specific expression of SAG12. *Plant Mol. Biol.* 41, 2. doi: 10.1023/A:1006342412688

Pandian, B. A., Sathishraj, R., Djanaguiraman, M., Prasad, P. V. V., and Jugulam, M. (2020). Role of cytochrome P450 enzymes in plant stress response. *Antioxidants (Basel Switzerland)* 9 (5), E454–E454. doi: 10.3390/ANTIOX9050454

Pan, L., Zhao, H., Yu, Q., Bai, L., and Dong, L. (2017). miR397/laccase gene mediated network improves tolerance to fenoxaprop-p-ethyl in beckmannia syzigachne and oryza sativa. *Front. Plant Sci.* 8. doi: 10.3389/FPLS.2017.00879/BIBTEX

Park, S.-Y., Yu, J.-W., Park, J.-S., Li, J., Yoo, S.-C., Lee, N.-Y., et al. (2007). The senescence-induced staygreen protein regulates chlorophyll degradation. *Plant Cell* 19 (5), 1649–1664. doi: 10.1105/tpc.106.044891

Patel, R. K., and Jain, M. (2012). NGS QC toolkit: A toolkit for quality control of next generation sequencing data. *PloS One* 7 (2):e30619. doi: 10.1371/journal.pone.0030619

Poovaiah, B. W., and Leopold, A. C. (1973). Deferral of leaf senescence with calcium. *Plant Physiol.* 52 (3), 236. doi: 10.1104/PP.52.3.236

Pruzinská, A., Tanner, G., Aubry, S., Anders, I., Moser, S., Müller, T., et al. (2005). Chlorophyll breakdown in senescent arabidopsis leaves. characterization of chlorophyll catabolites and of chlorophyll catabolic enzymes involved in the degreening reaction. *Plant Physiol.* 139 (1), 52–63. doi: 10.1104/pp.105.065870

Qin, J., Ma, X., Yi, Z., Tang, Z., and Meng, Y. (2016). A transcriptome-wide study on the microRNA- and the argonaute 1-enriched small RNA-mediated regulatory networks involved in plant leaf senescence. *Plant Biol.* 18 (2), 197–205. doi: 10.1111/PLB.12373

Quirino, B. F., Normanly, J., and Amasino, R. M. (1999). Diverse range of gene activity during arabidopsis thaliana leaf senescence includes pathogen-independent induction of defense-related genes. *Plant Mol. Biol.* 40, 2. doi: 10.1023/A:1006199932265

Ranocha, P., Chabannes, M., Chamayou, S., Danoun, S., Jauneau, A., Boudet, A. M., et al. (2002). Laccase down-regulation causes alterations in phenolic metabolism and cell wall structure in poplar. *Plant Physiol.* 129 (1), 145. doi: 10.1104/PP.010988

Sağlam-Çağ, S. (2007). The effect of epibrassinolide on senescence in wheat leaves. *Biotechnol. Biotechnol. Equip.* 21 (1), 63–65. doi: 10.1080/13102818.2007.10817415

Sakuraba, Y., Schelbert, S., Park, S. Y., Han, S. H., Lee, B. D., Andrès, C. B., et al. (2012). STAY-GREEN and chlorophyll catabolic enzymes interact at light-harvesting complex II for chlorophyll detoxification during leaf senescence in arabidopsis. *Plant Cell* 24 (2), 507–518. doi: 10.1105/TPC.111.089474

Sasi, J. M., Kumar, C. V., Mani, B., Bhardwaj, A. R., Agarwal, M., and Katiyar-Agarwal, S. (2019). Identification and characterization of miRNAs during flag leaf senescence in rice by high-throughput sequencing. *Plant Physiol. Rep.* 24 (1), 1–14. doi: 10.1007/S40502-019-0436-6

Schaller,A. (2004). A cut above the rest: The regulatory function of plant proteases. *Planta* 220 (2), 183 –197. doi: 10.1007/s00425-004-1407-2

Schelbert, S., Aubry, S., Burla, B., Agne, B., Kessler, F., Krupinska, K., et al. (2009). Pheophytin pheophorbide hydrolase (pheophytinase) is involved in chlorophyll breakdown during leaf senescence in arabidopsis. *Plant Cell* 21 (3), 767–785. doi: 10.1105/tpc.108.064089

Schippers, J. H. M., Jing, H., Hille, J., and Dijkwel, P. P. (2007). "Developmental and hormonal control of leaf senescence," in *Senescence processes in plants* (Oxford: Blackwell Publishing), 145–170.

Schommer, C., Palatnik, J. F., Aggarwal, P., Chételat, A., Cubas, P., Farmer, E. E., et al. (2008). Control of jasmonate biosynthesis and senescence by miR319 targets. *PloS Biol.* 6 (9), e230. doi: 10.1371/journal.pbio.0060230

Serafini-Fracassini, D., Del Duca, S., Monti, F., Poli, F., Sacchetti, G., Bregoli, A. M., et al. (2002). Transglutaminase activity during senescence and programmed cell

death in the corolla of tobacco (Nicotiana tabacum) flowers. *Cell Death Differentiation* 9, 309–321. doi: 10.1038/sj.cdd.4400954

Shimoda, Y., Ito, H., and Tanaka, A. (2016). Arabidopsis STAY-GREEN, mendel's green cotyledon gene, encodes magnesium-dechelatase. *Plant Cell* 28 (9), 2147–2160. doi: 10.1105/TPC.16.00428

Sillanpää, M., Kontunen-Soppela, S., Luomala, E. M., Sutinen, S., Kangasjärvi, J., Häggman, H., et al. (2005). Expression of senescence-associated genes in the leaves of silver birch (Betula pendula). *Tree Physiol.* 25 (9), 1161–1172. doi: 10.1093/TREEPHYS/25.9.1161

Simpson, K., Fuentes, P., Quiroz-Iturra, L. F., Flores-Ortiz, C., Contreras, R., Handford, M., et al. (2018). Unraveling the induction of phytoene synthase 2 expression by salt stress and abscisic acid in daucus carota. *J. Exp. Bot.* 69 (16), 4113–4126. doi: 10.1093/JXB/ERY207

Staden, J. (1995). Hormonal control of carnation flower senescence. *Acta Hortic.* 405, 232–239. doi: 10.17660/ACTAHORTIC.1995.405.30

Stocks, M. B., Moxon, S., Mapleson, D., Woolfenden, H. C., Mohorianu, I., Folkes, L., et al. (2012). The UEA sRNA workbench: a suite of tools for analysing and visualizing next generation sequencing microRNA and small RNA datasets. *Bioinf. (Oxford England)* 28 (15), 2059–2061. doi: 10.1093/bioinformatics/bts311

Swida-Barteczka, A., and Szweykowska-Kulinska, Z. (2019). Micromanagement of developmental and stress-induced senescence: The emerging role of MicroRNAs. *Genes* 10 (3), 210. doi: 10.3390/GENES10030210

Szklarczyk, D., Gable, A. L., Nastou, K. C., Lyon, D., Kirsch, R., Pyysalo, S., et al. (2021). The STRING database in 2021: customizable protein-protein networks, and functional characterization of user-uploaded gene/measurement sets. *Nucleic Acids Res.* 49 (D1), 605–612. doi: 10.1093/nar/gkaa1074

Takasaki, H., Maruyama, K., Takahashi, F., Fujita, M., Yoshida, T., Nakashima, K., et al. (2015). SNAC-as, stress-responsive NAC transcription factors, mediate ABA-inducible leaf senescence. *Plant journal: Cell Mol. Biol.* 84 (6), 1114–1123. doi: 10.1111/tpj.13067

Tamás, L., Čiamporová, M., and Luxová, M. (1998). Accumulation of pathogenesis-related proteins in barley leaf intercellular spaces during leaf senescence. *Biol. Plantarum* 41, 3. doi: 10.1023/A:1001814930794

Tanabe, S. (2005). A novel cytochrome P450 is implicated in brassinosteroid biosynthesis *via* the characterization of a rice dwarf mutant, dwarf11, with reduced seed length. *Plant Cell Online* 17, 776–790. doi: 10.1105/tpc.104.024950

Tang, Y., Li, M., Chen, Y., Wu, P., Wu, G., and Jiang, H. (2011). Knockdown of OsPAO and OsRCCR1 cause different plant death phenotypes in rice. *J. Plant Physiol.* 168 (16), 1952–1959. doi: 10.1016/J.JPLPH.2011.05.026

Taylor, R. C., and Dillin, A. (2011). Aging as an event of proteostasis collapse. *Cold Spring Harbor Perspect. Biol.* 3 (5), 1–17. doi: 10.1101/CSHPERSPECT.A004440

Thatcher, S. R., Burd, S., Wright, C., Lers, A., and Green, P. J. (2015). Differential expression of miRNAs and their target genes in senescing leaves and siliques: insights from deep sequencing of small RNAs and cleaved target RNAs. *Plant Cell Environ.* 38 (1), 188–200. doi: 10.1111/pce.12393

Thimm, O., BlaÈ sing, O., Gibon, Y., Nagel, A., Meyer, S., KruÈ ger, P., et al. (2004). MAPMAN: A user-driven tool to display genomics data sets onto diagrams of metabolic. *Plant J.* 37, 914–939. doi: 10.1111/j.1365-313x.2004.02016.x

Trapnell, C., Pachter, L., and Salzberg, S. L. (2009). TopHat: Discovering splice junctions with RNA-seq. *Bioinformatics* 25 (9), 1105–1111. doi: 10.1093/bioinformatics/btp120

Trivedi, R., and Jurivich, D. A. (2020). A molecular perspective on age-dependent changes to the heat shock axis. *Exp. Geronto.* 137, 110969. doi: 10.1016/J.EXGER.2020.110969

Tsuzuki, M., Futagami, K., Shimamura, M., Inoue, C., Kunimoto, K., Oogami, T., et al. (2019). An early arising role of the MicroRNA156/529-SPL module in reproductive development revealed by the liverwort marchantia polymorpha. *Curr. Biology : CB* 29 (19), 3307–3314.e5. doi: 10.1016/J.CUB.2019.07.084

Upadhyay, N., Kar, D., Deepak Mahajan, B., Nanda, S., Rahiman, R., Panchakshari, N., et al. (2019). The multitasking abilities of MATE transporters in plants. *J. Exp. Bot.* 70 (18), 4643–4656. doi: 10.1093/JXB/ERZ246

Wang, Z., Qian, C., Guo, X., Liu, E., Mao, K., Mu, C., et al. (2016). ELS1, a novel MATE transporter related to leaf senescence and iron homeostasis in arabidopsis thaliana. *Biochem. Biophys. Res. Commun.* 476 (4), 319–325. doi: 10.1016/J.BBRC.2016.05.121

Wan, F., Zhang, L., Tan, M., Wang, X., Wang, G. L., Qi, M., et al. (2022). Genome-wide identification and characterization of laccase family members in eggplant (Solanum melongena l.). *PeerJ* 10, 1–24. doi: 10.7717/peerj.12922

Wei, K., and Chen, H. (2018). Global identification, structural analysis and expression characterization of cytochrome P450 monooxygenase superfamily in rice. *BMC Genomics* 19 (1), 1–18. doi: 10.1186/s12864-017-4425-8

Woo, H. R., Chung, K. M., Park, J.-H., Oh, S. A., Ahn, T., Hong, S. H., et al. (2001). ORE9, an f-box protein that regulates leaf senescence in arabidopsis. *Plant Cell* 13 (8), 1779. doi: 10.1105/TPC.010061

Wu, A., Allu, A. D., Garapati, P., Siddiqui, H., Dortay, H., Zanor, M. I., et al. (2012). JUNGBRUNNEN1, a reactive oxygen species–responsive NAC transcription factor, regulates longevity in arabidopsis. *Plant Cell* 24 (2), 482–506. doi: 10.1105/TPC.111.090894

Wu, X., Ding, D., Shi, C., Xue, Y., Zhang, Z., Tang, G., et al. (2016). microRNA-dependent gene regulatory networks in maize leaf senescence. *BMC Plant Biol.* 16, 73. doi: 10.1186/s12870-016-0755-y

Xin, M., Wang, Y., Yao, Y., Xie, C., Peng, H., Ni, Z., et al. (2010). Diverse set of microRNAs are responsive to powdery mildew infection and heat stress in wheat (Triticum aestivum l.). *BMC Plant Biol.* 10, 123. doi: 10.1186/1471-2229-10-123

Xu, X., Bai, H., Liu, C., Chen, E., Chen, Q., Zhuang, J., et al. (2014). Genome-wide analysis of microRNAs and their target genes related to leaf senescence of rice. *PloS One* 9 (12), e114313. doi: 10.1371/journal.pone.0114313

Yang, S. D., Seo, P. J., Yoon, H. K., and Park, C. M. (2011). The arabidopsis NAC transcription factor VNI2 integrates abscisic acid signals into leaf senescence *via* the COR/RD genes. *Plant Cell* 23 (6), 2155–2168. doi: 10.1105/tpc.111.084913

Yoshida, S., Forno, D. A., Cock, J. H., and Gomez, K. A. (1976). *Laboratory manual for physiological studies of rice* (Manila: International Rice Research Institute;), 61–66.

Yuan, S., Li, Z., Li, D., Yuan, N., Hu, Q., and Luo, H. (2015). Constitutive expression of rice MicroRNA528 alters plant development and enhances tolerance to salinity stress and nitrogen starvation in creeping bentgrass. *Plant Physiol.* 169 (1), 576. doi: 10.1104/PP.15.00899

Zentgraf, U., Andrade-Galan, A. G., and Bieker, S. (2022). Specificity of H2O2 signaling in leaf senescence: is the ratio of H2O2 contents in different cellular compartments sensed in arabidopsis plants? *Cell. Mol. Biol. Lett.* 27 (1), 1–19. doi: 10.1186/S11658-021-00300-W

Zhang, X., Ju, H. W., Chung, M. S., Huang, P., Ahn, S. J., and Kim, C. S. (2011). The r-r-type MYB-like transcription factor, AtMYBL, is involved in promoting leaf senescence and modulates an abiotic stress response in arabidopsis. *Plant Cell Physiol.* 52 (1), 138–148. doi: 10.1093/pcp/pcq180

Zhang, W. Y., Xu, Y. C., Li, W. L., Yang, L., Yue, X., Zhang, X. S., et al. (2014). Transcriptional analyses of natural leaf senescence in maize. *PloS One* 9 (12), e115617. doi: 10.1371/journal.pone.0115617

Zhu, H., Chen, C., Zeng, J., Yun, Z., Liu, Y., Qu, H., et al. (2020). MicroRNA528, a hub regulator modulating ROS homeostasis ***via*** targeting of a diverse set of genes encoding copper-containing proteins in monocots. *New Phytol.* 225 (1), 385–399. doi: 10.1111/NPH.16130

frontiers | Frontiers in Plant Science

TYPE Original Research
PUBLISHED 08 December 2022
DOI 10.3389/fpls.2022.1018991

Check for updates

OPEN ACCESS

EDITED BY
Girdhar Kumar Pandey,
University of Delhi, India

REVIEWED BY
Chenliang Yu,
Zhejiang Agriculture and Forestry University, China
Liangsheng Zhang,
Zhejiang University, China

*CORRESPONDENCE
Cheng Xiong
xiongchenghzau@163.com
Feng Liu
liufengrich@126.com

†These authors have contributed equally to this work

SPECIALTY SECTION
This article was submitted to Plant Physiology, a section of the journal Frontiers in Plant Science

RECEIVED 14 August 2022
ACCEPTED 15 November 2022
PUBLISHED 08 December 2022

CITATION
Tang B, Yang G, Du J, Xie L, Wang J, Pan L, Luo Y, Shan Q, Zou X, Xiong C and Liu F (2022) Analysis of the response regulatory network of pepper genes under hydrogen peroxide stress.
Front. Plant Sci. 13:1018991.
doi: 10.3389/fpls.2022.1018991

COPYRIGHT
© 2022 Tang, Yang, Du, Xie, Wang, Pan, Luo, Shan, Zou, Xiong and Liu. This is an open-access article distributed under the terms of the Creative Commons Attribution License (CC BY). The use, distribution or reproduction in other forums is permitted, provided the original author(s) and the copyright owner(s) are credited and that the original publication in this journal is cited, in accordance with accepted academic practice. No use, distribution or reproduction is permitted which does not comply with these terms.

Analysis of the response regulatory network of pepper genes under hydrogen peroxide stress

Bingqian Tang[1,2,3†], Guangbin Yang[2†], Juan Du[2], Lingling Xie[3], Jin Wang[1], Luzhao Pan[1], Yin Luo[2], Qingyun Shan[1], Xuexiao Zou[1,2,3,4], Cheng Xiong[1,3*] and Feng Liu[1,2,3,4*]

[1]College of Horticulture, Hunan Agricultural University, Changsha, Hunan, China, [2]Longping Branch, Graduate School of Hunan University, Changsha, Hunan, China, [3]Engineering Research Center for Germplasm Innovation and New Varieties Breeding of Horticultural Crops, Key Laboratory for Vegetable Biology of Hunan Province, College of Horticulture, Hunan Agricultural University, Changsha, China, [4]Laboratory of Lingnan Modern Agriculture, Guangzhou, Guangdong, China

Hydrogen peroxide (H_2O_2) is a regulatory component related to plant signal transduction. To better understand the genome-wide gene expression response to H_2O_2 stress in pepper plants, a regulatory network of H_2O_2 stress-gene expression in pepper leaves and roots was constructed in the present study. We collected the normal tissues of leaves and roots of pepper plants after 40 days of H_2O_2 treatment and obtained the RNA-seq data of leaves and roots exposed to H_2O_2 for 0.5–24 h. By comparing the gene responses of pepper leaves and roots exposed to H_2O_2 stress for different time periods, we found that the response in roots reached the peak at 3 h, whereas the response in leaves reached the peak at 24 h after treatment, and the response degree in the roots was higher than that in the leaves. We used all datasets for K-means analysis and network analysis identified the clusters related to stress response and related genes. In addition, *CaEBS1*, *CaRAP2*, and *CabHLH029* were identified through a co-expression analysis and were found to be strongly related to several reactive oxygen species-scavenging enzyme genes; their homologous genes in Arabidopsis showed important functions in response to hypoxia or iron uptake. This study provides a theoretical basis for determining the dynamic response process of pepper plants to H_2O_2 stress in leaves and roots, as well as for determining the critical time and the molecular mechanism of H_2O_2 stress response in leaves and roots. The candidate transcription factors identified in this study can be used as a reference for further experimental verification.

KEYWORDS

hydrogen peroxide stress, reactive oxygen species, pepper, gene regulatory network, tissue specificity

Introduction

Biotic and abiotic stresses are the main environmental factors that restrict normal growth and development of plants by decreasing the yield, thereby posing a threat to food safety (Fedoroff et al., 2010; Zhu, 2016).

Hydrogen peroxide (H_2O_2), an important regulatory component of plant signal transduction, affects plant growth in a concentration-dependent manner (Xiong et al., 2015). In a root dipping treatment of *Solanum lycopersicum*, low doses of H_2O_2 (0.1 or 0.5 mM) were reported to be potentially advantageous for the development of plants (Nazir et al., 2019). In a study, the dose of 0.1 mM H_2O_2 was found to be optimum as it caused a maximum increase in the length, fresh mass, and dry mass of *Solanum lycopersicum* roots and shoots (Nazir et al., 2019). In cucumbers, a low concentration of H_2O_2 improved the germination capability, germination rate, tap root length, and hypocotyledonary axis, whereas high H_2O_2 concentration inhibited these processes (Sun et al., 2009). On the one hand, the production of reactive oxygen species (ROS) is a byproduct of aerobic metabolism (Sandalio and Romero-Puertas, 2015; Dietz et al., 2016; Huang et al., 2016). On the other hand, anaerobic metabolism can be induced in plants under biotic or abiotic stress including pathogens, strong light, drought, low temperature, high temperature, and salinization (He et al., 2018b). Different ROS such as H_2O_2, singlet oxygen, and superoxide can trigger specific changes in a transcriptome (Gadjev et al., 2006; Willems et al., 2016).

The biological effects of ROS on cell cytotoxicity or signaling mainly depend on the balance between generating and scavenging systems. The normal concentration of ROS plays a crucial role in maintaining normal plant growth and improving plant stress resistance (Karuppanapandian et al., 2011; Huang et al., 2019).

High ROS concentrations hinder the growth and development of plants and even lead to plant death, thereby causing an irreversible damage to plants (Sachdev et al., 2021). To cope with the ever-changing external environment, plants have evolved a complex mechanism for excessive ROS scavenging (Huang et al., 2019). The scavenging mechanism of ROS in plants can be divided into two types. First, the enzymatic scavenging mechanism, which mainly includes superoxide dismutase (SOD), ascorbate peroxidase (APX), glutathione peroxidase (GPX), catalase (CAT), and glutathione S-transferase. Second, the non-enzymatic scavenging mechanism, which mainly depends on ascorbic acid, reduced glutathione, α-tocopherol, proline, alkaloids (carotenoids), and flavonoids (Gill and Tuteja, 2010; Miller et al., 2010; Sarvajeet Singh Gill et al., 2011; Das and Roychoudhury, 2014).

ROS also affect some transcription factors such as HSF, NPR1, WRKY, and MYB. The upregulation of the expression of these transcription factor genes eventually leads to changes in the expression of downstream genes. Gene expression changes triggered by ROS are mediated by stress-responsive cis-regulated promoter elements, redox regulation of transcription regulators, and upstream signal cascades such as the mitogen-activated kinase module (Dietz, 2014; He et al., 2018a).

The present study investigated changes in whole-genome expression in hot peppers under H_2O_2 stress and determined the ROS-scavenging gene response mechanism at the gene level. Data were obtained from the transcriptome data of leaves and roots of peppers cultured in water for 40 days with 30 mM H_2O_2 at six time points and compared with those of the control group. A regulatory network of pepper genes that respond to H_2O_2 stress was constructed. In addition, the genes related to key ROS-scavenging enzymes in peppers, important time nodes of the response, and the key transcription factors co-expressing with the key enzymes were identified.

Materials and methods

Plant materials and data sources

Total RNA-seq data from H_2O_2-treated pepper leaves and roots was isolated according to the method described in a previous study (Liu et al., 2017). Line 6421, an elite-breeding pepper (*Capsicum annuum*) line, was selected from a long-red pepper landrace that is widely grown on the west side of Xiangjiang River, Hunan Province, China.

The seeds were disinfected with sodium hypochlorite and grown in vermiculite at 25/18°C under short-day growth conditions (8 h light/16 h dark, light intensity of 6000 Lux, pH 6.0) and 60%–70% humidity. The stress treatments were applied on 40-day-old seedlings, and samples for RNA extraction were collected from the leaves and roots of the seedlings. The leaves and roots were treated with 30 mM H_2O_2 for 0.5, 1, 3, 6, 12, and 24 h to induce oxidative stress. Control plants were mock treated with the nutrient solution only. Leaf and root tissues were collected from both treated and control plants at 0.5, 1, 3, 6, 12, and 24 h after treatment.

Abbreviations: H_2O_2, Hydrogen peroxide; ROS, Reactive Oxygen Species; SOD, Superoxide Dismutase; APX, Ascorbate Peroxidase; GPX, Glutathione Peroxidase; CAT, Catalase; DEGs, Differentially Expressed Genes; TFs, Transcription Factors; RNA-seq, RNA sequence; HPT, hours post-treatment; TPM, Transcripts Per Million; HCL, Hierarchical clustering; PCA, Principal Component Analysis; GO, Gene Ontology; KEGG, Kyoto Encyclopedia of Genes and Genomes; BP, Biological Process; MF, Molecular Function; CC, Cellular Component; FC, Fold Changes; FDR, False Discovery Rate; BRs, Brassinosteroid Signaling.

Differential gene expression analysis

We quality-tested gene sequences by using (Chen et al., 2018) FastQC v. 0.11.7 (Andrews, 2017) with default mapping parameters (10 mismatches/read; nine multimapping locations/read) and aligned using HISAT (Kim et al., 2015). Differential gene expression analysis was performed using DESeq2 v1.20.0, an R-based package available from Bioconductor (Love et al., 2014). The reference genome of *C. annuum L.* (Zunla_1) was used in this analysis (Qin et al., 2014).

Transcripts expressing differentially under two conditions were identified by examining the difference in their abundance under these conditions. The abundance of a transcript was measured as the mean-normalized count of reads mapping onto the transcript (Love et al., 2014). The difference in the expression was quantified using the logarithm (the logarithmic multiple change) of the mean-normalized count ratio between the two conditions. The differentially expressed transcripts in our experiments were defined as those with adjusted P values < 0.05 fold changes (FC) (negative binomial Wald test and Benjamini-Hochberg correction; both are part of the DESeq2 package). Differentially expressed genes (DEGs) were classified as upregulated or downregulated according to the significant positive or negative logarithmic change value. upregulated and downregulated DEGs were represented using the Venn diagram (Lin et al., 2016). Heat maps were generated using the seaborn heatmap available in python. Summary statistics for the sequencing performed are presented in Table S1 and all expression genes in Table S2.

Co-expression cluster identification and gene enrichment analysis

Co-expression/coregulation analysis was performed on the samples from 12 control tissues and 12 H_2O_2-treated tissues by using the K-means (Gasch and Eisen, 2002) method (Gasch and Eisen, 2002) in python. The normalized expression values of genes were calculated by dividing their expression values in all samples with their maximum observed TPM (Transcripts Per Kilobase Million) Hierarchical clustering (HCL) and principal component analysis (PCA) were performed using the Kernel Principal Component Analysis in python with default settings to facilitate the graphical interpretation of the relatedness among the 24 samples. The transformed- and normalized-gene and -metabolite expression values with Z-scores were used for HCL and PCA. The clusters that were identified to respond to H_2O_2 stress were followed up for gene enrichment analysis with GOATOOLS (Klopfenstein et al., 2018), which is a python package for Gene Ontology (GO) enrichment analysis; false discovery rate (FDR) values of <0.01 was considered to denote statistically significant GO terms. The Kyoto Encyclopedia of Genes and Genomes (KEGG) pathway analysis was performed by KofamKOALA (Aramaki et al., 2020) to protein sequences by homology search, and the enrichment analysis use P-value Cutoff = 0.05 was carried by package clusterProfiler (Yu et al., 2012).

Analysis of orthologous genes and homologous evolutionary genes

The *Arabidopsis thaliana* (TAIR10) and *C. annuum L.* (Zunla_1) proteomes were downloaded from The Arabidopsis Information Resource and National Center for Biotechnology Information, respectively. Protein sequences from the primary transcripts were used for the construction of orthogroups between the two species by using OrthoMCL (https://orthomcl.org/orthomcl/). The information on transcription factors (TFs) was retrieved from PlantTFDB (http://planttfdb.gao-lab.org/).

The multiple sequence alignment of capsicum and *Arabidopsis* genes was performed using MUSCLE (Multiple Protein Sequence Alignment) in Linux. A contiguous algorithm was used to build phylogenetic tree files by using treebest software (Edgar, 2004), and a phylogenetic tree was constructed using the online tool iTOL (Interactive Tree Of Life; https://itol.embl.de/) (Letunic and Bork, 2016).

Network analysis of ROS scavenging genes in pepper

The Python NetworkX package (https://networkx.org/) was used to visualize the co-expression network relationship between the candidate target transcription factors and ROS-scavenging enzyme-related genes.

Results

Generation of the pepper H_2O_2 dataset

To comprehensively and accurately record the gene response network in leaves and roots of pepper plants treated with H_2O_2, we used the transcriptome data set (Figure 1A). To determine the gene expression in the 24 samples, a Z-score normalized expression heat map (Figure 1C) was obtained. The Pearson's correlation matrix among the transcriptome samples showed that the gene expression pattern was tissue-specific. The same tissues clustered together (Figure 1C). PCA (Figure 1B) also showed that the samples from the same tissues gathered at different time points during stress treatment (Figure 1B). These results showed that the difference in gene expression because of H_2O_2 stress is much smaller than the tissue-specific expression

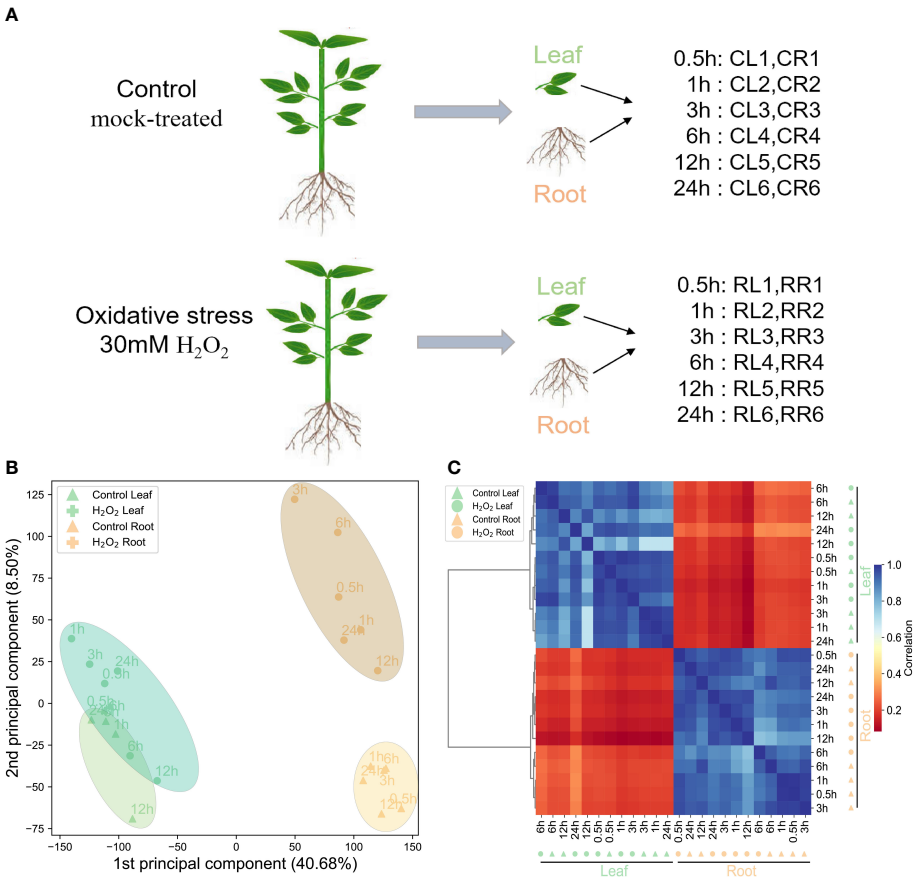

FIGURE 1
Summary of the transcriptome data of the H_2O_2 datasets. **(A)**: Schematic representation of the design for the datasets. Leaf (L) and root (R) of these samples at six time points in the control and H_2O_2-treatment groups, respectively. **(B)**: Principal component analysis of the transcriptome data from the control and H_2O_2-treatment samples (leaf and root). **(C)**: The hierarchical clustering analysis of the expression profiles of 35,336 genes from the 24 samples; the color scale 0–1 represents the Pearson's correlation coefficient.

of the whole gene of the pepper roots and leaves, which is consistent with our general cognition.

The pepper transcriptomes are coregulated in 12 clusters that corresponded to different tissues and treatment times

To further understand the trend in the classification of gene expression in pepper roots and leaves after H_2O_2 stress, we used the K-means clustering algorithm to divide the genes into 12 clusters according to the expression patterns of all 29,065 genes expressed in at least one sample (Figure 2). The expressions of genes in Cluster 1, Cluster 5, and Cluster 12 were significantly increased in the roots at 3 h, 6 h, and 12 h after the stress, respectively, whereas the expressions of genes in Cluster 3 and Cluster 11 were significantly increased in the leaves at 6 h and 24 h, respectively, after the stress. In the early stage of the stress treatment, we observed that the genes in Cluster 10 were the first to respond within 0.5 h–1 h. Despite the increase or decrease in gene expression observed after the stress treatment at a certain time point, genes in Cluster 2, Cluster 4, Cluster 7, and Cluster 9 showed no significant changes in expression in the leaves and roots at the six time points before and after the stress treatment. The reason for dividing the genes into 12 clusters was to classify these genes according to dynamic changes in them to facilitate their follow-up and better targeted analysis.

Identification of differentially expressed genes under hydrogen peroxide stress

To capture a comprehensive overview of the response, H_2O_2-responsive genes in the peppers were identified by analyzing the temporal changes in the transcriptome after up

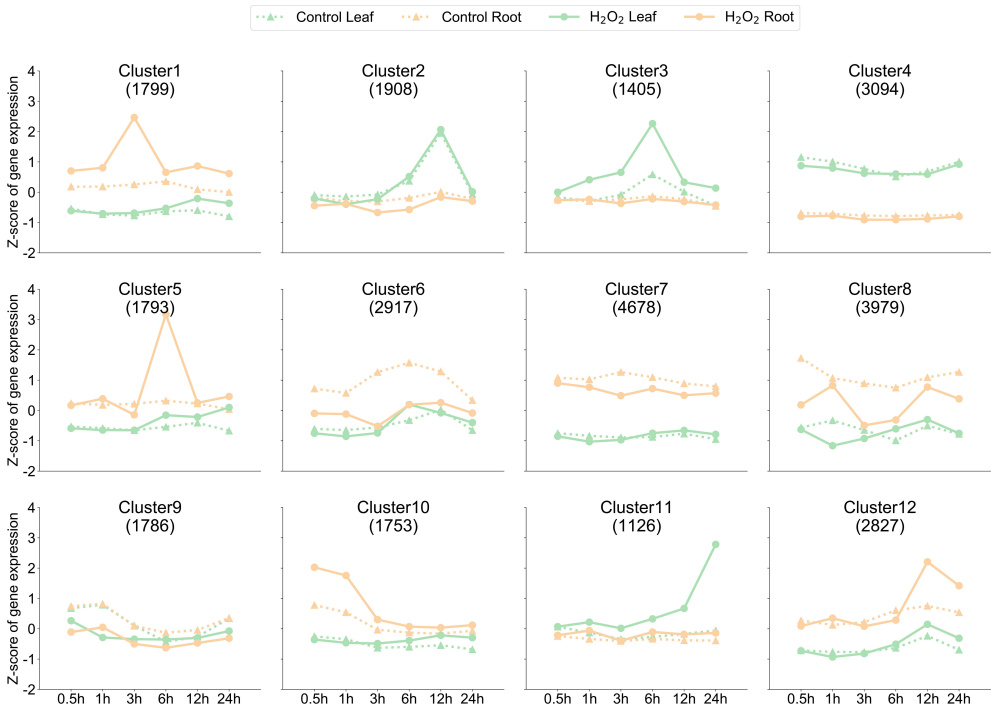

FIGURE 2
Dynamics of gene expression in the samples. K-means clustering grouped the expression profiles of the transcriptome into 12 clusters. The x-axis depicts the 24 samples, and the y-axis depicts the Z-score standardized cluster gene expression trend. The numbers shown in each box (for example, 1,799 genes for Cluster 1) were derived from the number of genes.

to 24 h of treatment with 30 mM H_2O_2 (Figure 1A). Overall, 1,116 upregulated and 309 downregulated genes were identified in the leaves, whereas 1,144 upregulated and 394 downregulated genes were identified in the roots at different time points. The analyses collectively yielded 2,382 DEGs, constituting approximately 8.20% of the expressed genes in the datasets.

The difference in differential expression between the leaves and roots was that the highest amount of DEGs in the leaves was observed at 12 and 24 h (Figures 3A, C) and that in the roots was observed at 3 and 6 h (Figures 3B, D); in leaves, 349 DEGs were upregulated and 17 DEGs were downregulated at 12 and 24 h. Consequently, the gene response speed in the roots was faster than that in the leaves of peppers under H_2O_2 stress. The distribution of upregulated and downregulated DEGs identified in the leaves and roots in each cluster is shown in Table 1, and the results of the distribution corresponding to the trend map are shown in Figure 2.

Functional enrichment analysis of DEGs

The main functions of DEGs (shown in Figure 3) identified in the leaf (Figure 4A) and root (Figure 4B) were analyzed by GO, and the aggregation of upregulated DEGs and

TABLE 1 Distribution of the leaf and root DEGs identified in this study across different cluster.

	Cluster												
	1	2	3	4	5	6	7	8	9	10	11	12	
Genes	**1799**	**1908**	**1405**	**3094**	**1793**	**2917**	**4678**	**3979**	**1786**	**1753**	**1126**	**2827**	**Number**
Leaf Upregulated DEGs	213	36	116	41	94	19	91	9	3	139	135	220	1116
Leaf Downregulated DEGs	30	14	2	22	5	24	93	33	46	21	1	18	309
Root Upregulated DEGs	297	41	46	93	222	0	8	1	22	140	101	173	1144
Root Downregulated DEGs	0	30	11	112	5	90	58	39	36	2	6	5	394

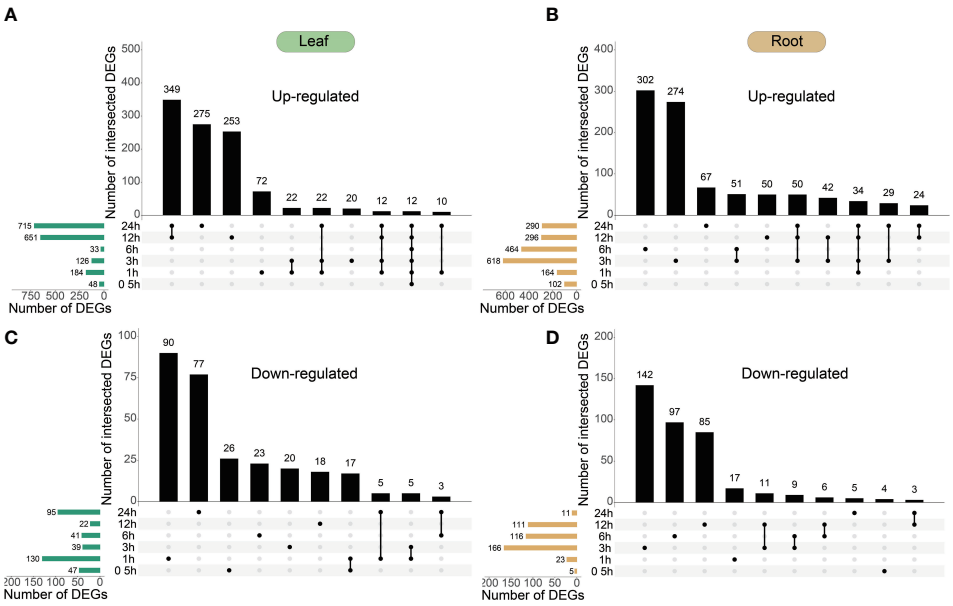

FIGURE 3
Temporal dynamics of *Capsicum annuum L.* transcriptome during H_2O_2 treatment. **(A–D)**, the 40-day-old *C. annuum L.* plants were treated with 30 mM H_2O_2 in liquid media and harvested at the given time points for transcriptome analysis. UpSet plots of the number of upregulated and downregulated genes (cut-off threshold, |log2(FC)| ≥2; FDR <0.01) demonstrating different temporal expression patterns (top bar graphs). The total number of upregulated and downregulated genes at each time point is shown on the left. All leaf and root DEGs show in Supplementary Table S3.

downregulated DEGs in the leaf and root is shown by the Wayne diagram (Figure 4C). Most identified DEGs encode the enzymes involved in basic biological metabolism and nucleotide binding (Figures 4A, B), and the amount of GO terms enriched by DEGs in leaves was more than that in roots.

Several key points identified in GO term enrichment in the leaf and root DEGs were related to the oxidoreductase activity, which implied that the H_2O_2 treatment of pepper plants affected key physiological metabolic pathways *in vivo*. In the leaves, GO terms such as "ATP metabolic process", "chloroplast thylakoid membrane", "proton-transporting ATP synthase activity, rotational mechanism" and "oxidoreductase activity, acting on peroxide as acceptor", leaf photosynthesis, and energy transformation were closely related; in roots, GO terms such as "response to water", "intracellular membrane-bounded organelle," "DNA-binding transcription factor activity," and "oxidoreductase activity" were also related to cell redox and important organelle membranes.

Through the KEGG pathway analysis of the DEGs identified in leaf and root at 6 time points, it was found that the common enrichment in "MAPK signaling pathway", "Phenylpropanoid biosynthesis", "Photosynthesis", "Glutathione metabolism", "Cytochrome P450" and "Sesquiterpenoid and triterpenoid biosynthesis" (Figure 5). However, "Plant hormone signal transduction", "Oxidative phosphorylation", "alpha–Linolenic acid metabolism", "Zeatin biosynthesis" and "Diterpenoid biosynthesis" were unique in leaf (Figure 5A).

We selected 43 and 27 genes in the MAPK-signaling pathway (ko04016) and photosynthesis pathway (ko00195), respectively, those genes were enriched in both the DEGs identified in leaves and roots (Figures 5C, D). In plants, several MAPK-signaling pathways are triggered by different biotic and abiotic stress stimuli, such as pathogen infection, injury, low temperature, drought, osmotic shock, high salinity, and reactive oxygen species (Asai et al., 2002; Colcombet and Hirt, 2008; Rodriguez et al., 2010). The Photosynthesis pathway is an important route for energy conversion in plants (Jones and Fyfe, 2001; Ferreira et al., 2004). DEGs identified in leaves and roots are enriched in these two pathways, indicating that the fluctuation of gene expression in response to external stimuli is conserved to a certain extent in different tissues, and the genes shown in Figures 5C, D are important candidate genes.

Evolution and expression analysis of genes associated with ROS scavenging

Because of the increase in the ROS content in plants observed under H_2O_2 stress, we evaluated the response of the genes associated with ROS scavenging. The experiment was

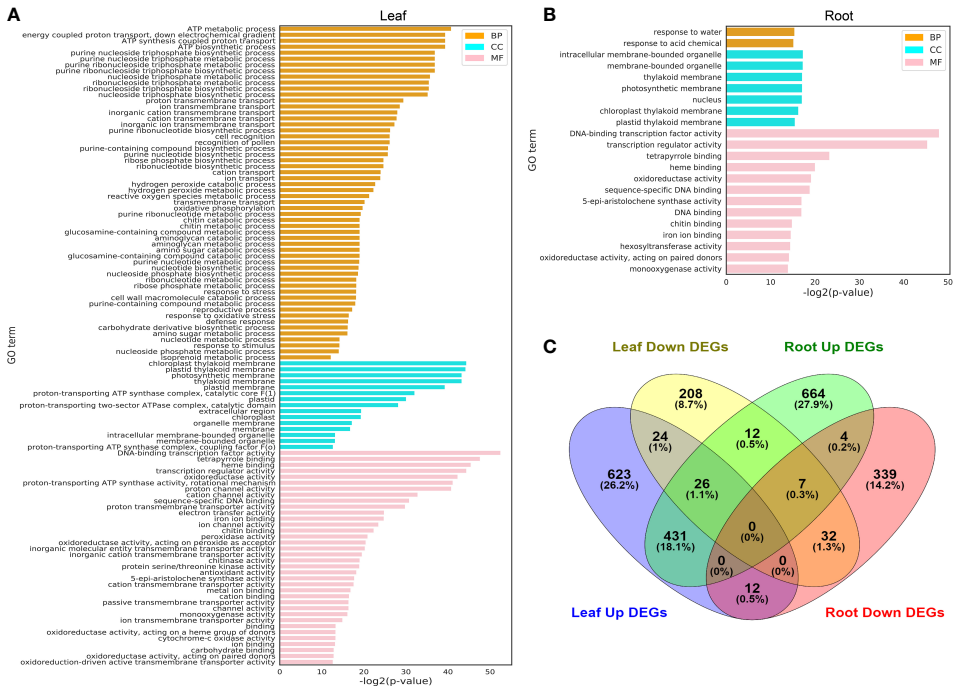

FIGURE 4
GO terms of leaf and root DEGs under hydrogen peroxide stress. **(A)** GO terms identified from the different treatment time points of leaf DEGs (FDR < 0.01). **(B)**: GO terms identified from the different treatment time points of root DEGs (FDR < 0.01). **(C)**: Venn diagrams of upregulated and downregulated DEGs identified in the leaf and root tissues. The full lists of DEGs and GO terms from the enrichment analysis are shown in Supplementary Tables S4, S5.

designed to evaluate changes in the expression patterns of ROS-scavenging genes such as SOD, APX, GPX, and CAT that are involved in the enzymatic scavenging mechanism (Gill and Tuteja, 2010; Miller et al., 2010; Sarvajeet Singh Gill et al., 2011). Additionally, we determined whether these genes have different response nodes and levels in the leaves and roots, according to the sequence of these genes in *A. thaliana*. The respective lineal homologous genes were identified in the pepper genome; 28 genes synthesizing these key enzymes in *A. thaliana* and 28 lineal homologous genes in pepper were identified. The evolutionary relationship of these 58 genes is shown in Figure 5A, which were mainly divided into three subfamilies, and a close sequence alignment relationship between *A. thaliana* genes and the corresponding pepper lineal homologous genes was obvious. The results reflected the significance of identifying direct homologous genes. Subfamily I was mainly from *A. thaliana* and capsicum and included *DHAR3*, *MDHAR1*, *GR*, *SOD1/2*, and *CAT2*. Subfamily II mainly included *MDHAR2* and *PrxR1*. All *APXs*, *DHAR1*, *SOD3*, and all *GPXs* were included in subfamily III (Figure 6A). Figure 3B shows the expression patterns of the genes encoding for these ROS-scavenging enzymes in untreated leaves and roots, as well as in the treated leaves and roots. *CAT3* expression in root tissues under H_2O_2 stress was significantly decreased compared with that in untreated roots; *PrxR1* gene expression in root tissues after12 h and 24 h was also decreased after root treatment (Figure 6B).

However, the expression of six genes, namely *APX1, SOD1, MDHAR1, APX2, GPX6*, and *GPX2*, was higher at 3 h after root treatment than that in the untreated root tissues; however, no significant difference was observed in the gene expression across other time periods and tissues. These six genes may be important in response to ROS clearance in the roots treated for 3 h. Follow-up studies on H_2O_2 stress must focus on the expression of genes in roots at 3 h, which can also be seen from Figures 3B, D. The number of DEGs in the roots treated with H_2O_2 for 3 h was the highest, and among these genes, 618 genes were upregulated genes and 196 genes were downregulated. The effect of H_2O_2 stress on plant roots reached a peak at 3 h compared with that in the control, and most of the DEGs were expressed in the roots.

According to the expression profiles of 29 genes related to ROS-scavenging enzyme synthesis at different time points in the control and H_2O_2 stress of leaves and roots shown in Figure 6B, 10 obvious genes are marked on the basis of different expression patterns after H_2O_2 stress. The genes whose expression levels changed and the expression profiles of these 10 genes are shown separately to avoid the influence of data normalization in Figure 6C. *PrxR1*, *DHAR1*, *GPX3*, *SOD2*, and *SOD1* were significantly up-regulated at different time points in leaves under

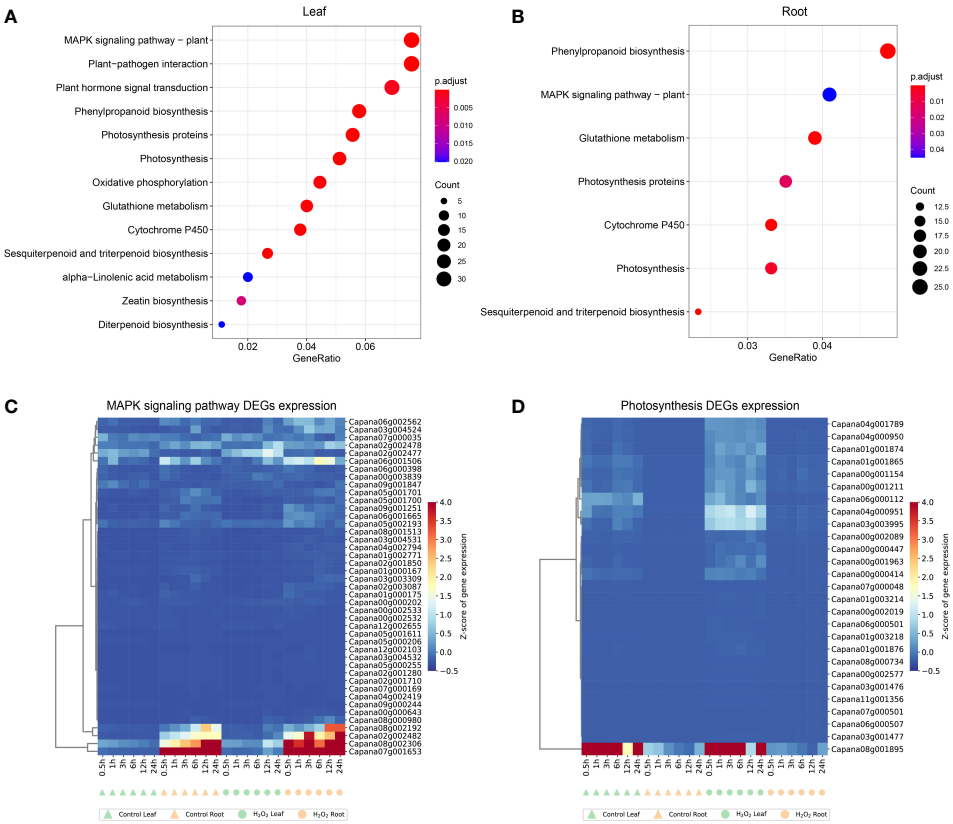

FIGURE 5
Kyoto encyclopedia of genes and genomes (KEGG) pathway enrichment analysis results for the DEGs in leaf **(A)** and root **(B)**. Expression profiles of DEGs enriched in MAPK-signaling pathway **(C)** and photosynthesis pathway **(D)** in leaves and roots. The complete list of DEGs and KEGG pathways for enrichment analysis is shown in Supplementary Tables S6, S7.

hydrogen peroxide stress; *APX1*, *SOD1*, *MDHAR1*, and *GPX6* were up-regulated in roots after H_2O_2 stress, which may be related to the fact that the roles of these enzymes in pepper were tissue related.

Discovery and functional analysis of transcription factors of important regulatory genes responding to H_2O_2 stress and the analysis of key clusters

Several key clusters identified through the K-means cluster analysis may have a certain role in response to ROS clearance. Most genes showed a rapid increase in the expression in leaves or roots at a certain time point, which may be because of plant response to irreversible damage caused by an increase in the ROS level, and the study of genes in these key clusters can be helpful in determining the response mechanism of plants to H_2O_2 stress. Moreover, these clusters have an increase in expression in different tissues at different time points, indicating an important area of research for determining time nodes and patterns of gene response to ROS. For instance, the genes in Cluster 10 (1,753 genes) were the first to respond to H_2O_2 stress in root tissues. Within 0.5 and 1 h, the expression of genes in Cluster 10 in roots under H_2O_2 stress was much higher than that in untreated roots; however, the difference in the expression of these genes was not significant in the leaves during the same period. The expression of genes in Cluster 1 (1,799 genes) increased significantly in roots under 3-h stress, and at this time point, the largest number of DEGs was observed in the roots (Figures 3B, D), indicating that the 3-h time point is the most favorable time point for gene response to stress in pepper roots.

To further study the function of genes in Cluster 1 and Cluster 10, we performed GO enrichment analysis of all genes in these clusters. A total of 1,799 genes in Cluster 1 were mainly enriched in the GO terms such as “L-phenylalanine metabolic process”, “DNA-binding transcription factor activity,” and “acyltransferase activity”. GO terms enriched by 1,753 genes in Cluster 10 were “oligosaccharide metabolic process”, “protein serine/threonine kinase activity”, “kinase activity,” and “ubiquitin-protein transferase activity”.

By analyzing the constructed gene co-expression relationship network, we found that the correlation coefficient

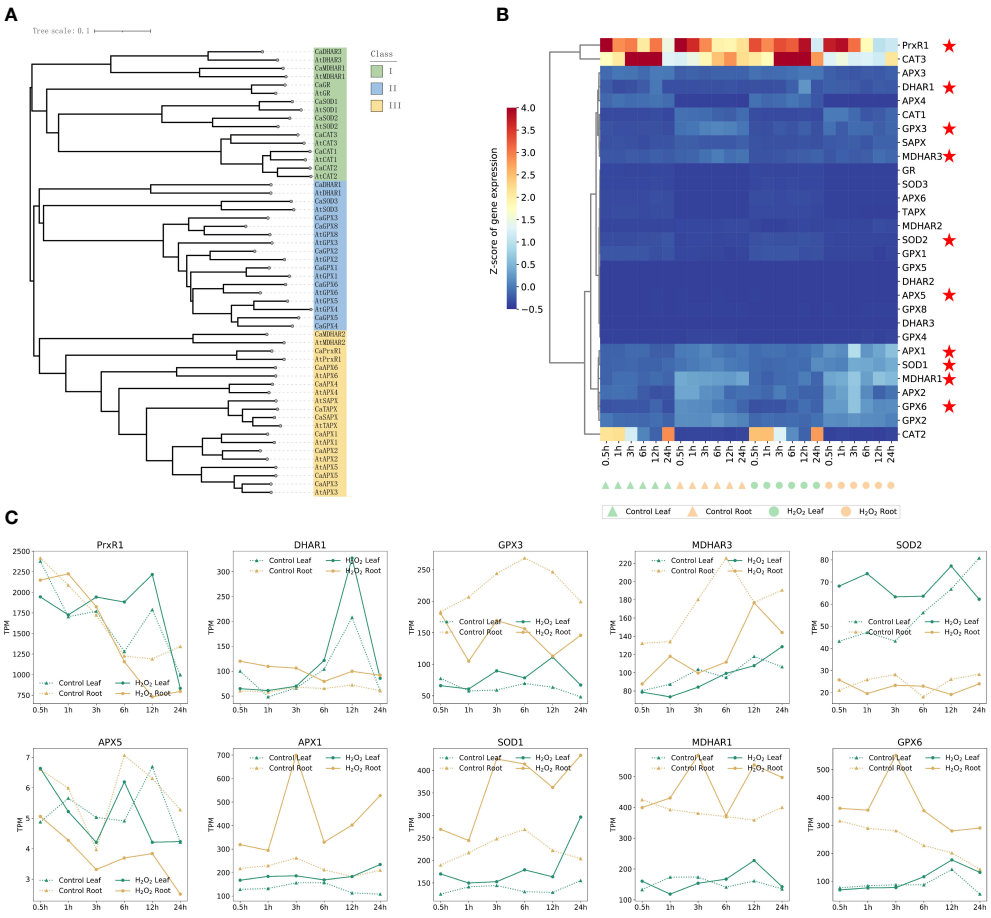

FIGURE 6
The genetic relationship of enzymes related to ROS scavenging in *Arabidopsis thaliana* and capsicum **(A)**, and the gene expression patterns in Pepper **(B)**. All those pepper genes expression in Supplementary Table S8. **(C)** Expression profiles of 10 typical ROS-scavenging enzyme synthesis genes in different clustering modules at different time points in leaves and roots of control and H_2O_2 stress.

of key transcription factors in Cluster 1 and Cluster 10 was closely related to those of ROS-scavenging genes. The relationship between these three typical transcription factors and ROS-scavenging enzyme-related genes (Figure 7B) is shown in the form of a network map (Figures 7D, E). The genes in the middle red circle represent the key transcription factors that were identified. The genes in the blue circle on the edge are the genes related to ROS-scavenging enzymes in capsicum. The blue lines between the two genes indicate negative regulatory relationships, whereas the red lines indicate positive regulatory relationships. These three key transcription factors were verified as the key factors in subsequent experiments, providing a new conjecture for studying the molecular mechanism of ROS scavenging in plants.

Through sequence alignment, the corresponding orthologous genes of three transcription factors, namely *BES1*, *RAP2* and *bHLH029*, in Arabidopsis were identified, and the sequence similarity was more than 70%. Therefore, we named the corresponding pepper genes as *CaBES1* (Figures 7B, F), *CaRAP2* (Figures 7D, G), and *CabHLH029* (Figures 7E, H) according to the gene names of Arabidopsis thaliana. The gene expression profile data of these were extracted. These data are displayed as line graphs in Figures 7F–H. The expression levels of *CaBES1* and *CabHLH029* were significantly up-regulated at H_2O_2 stress 3 and 6 h, respectively, but there was no significant difference at other time points. *CaRAP2* was significantly up-regulated in the early stage of H_2O_2 stress (0.5–3 h), and its expression returned to normal in the later stage of H_2O_2 stress. They may be involved in regulation at different stages.

Discussion

Pepper is an important vegetable belonging to the Solanaceae family that is widely cultivated worldwide. According to FAO statistics (www.fao.org), peppers were

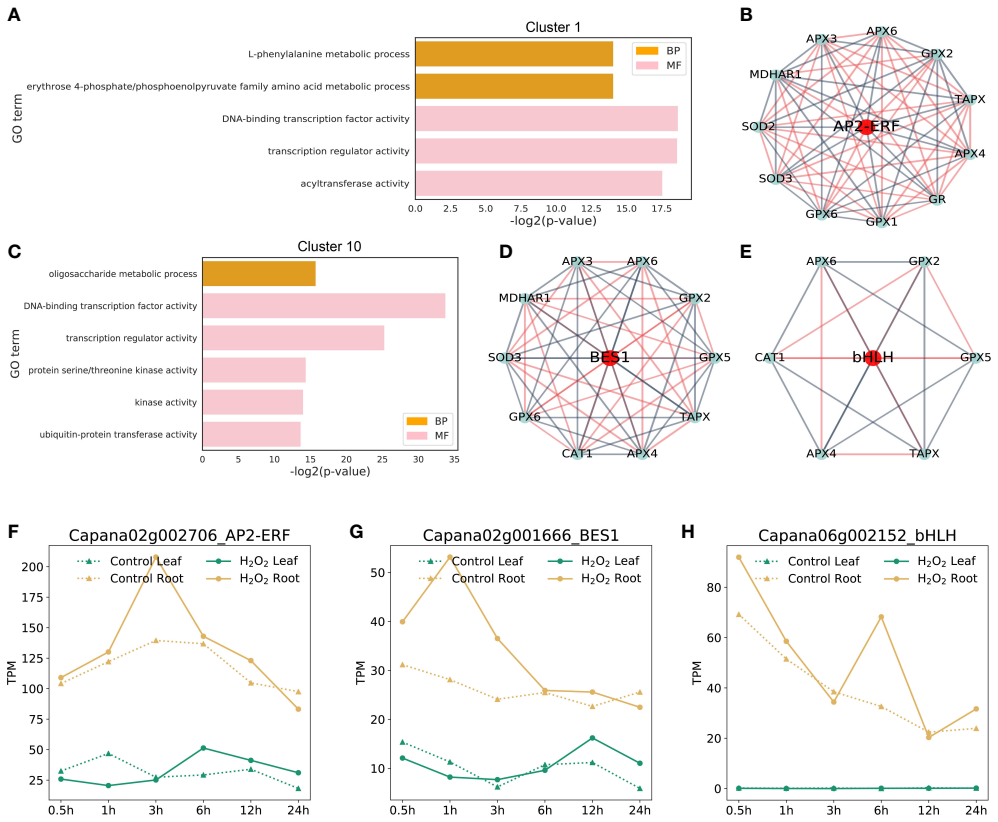

FIGURE 7
Important clusters in GO enrichment and TF networks. **(A, C)**: GO terms of the identified DEGs from Cluster 1 and Cluster 10 (FDR < 0.01)). The complete lists of cluster genes and GO terms from the enrichment analysis are shown in Supplementary Tables S9, S10. **(B, D, E)**: The transcriptional factors that co-expressed with ROS-scavenging genes were identified using the constructed network. **(F–H)**: Expression profiles of the three candidate transcription factors at different time points in control and H_2O_2 stress in leaves and roots.

grown in 118 countries and regions of the world in 2018. Pepper is the third largest vegetable crop in the world; in 2014, Mexico and China successively completed the whole-genome sequencing of two pepper varieties, namely CM334 and Zunla-1 (Kim et al., 2014; Qin et al., 2014). The pepper genome sequence is ~3.3 Gb, which is approximately three times that of the tomato genome (~900 Mb) (Tomato Genome, 2012). Because of the presence of many tandem repeats in the pepper genome, the research on pepper gene annotation is relatively lagging. The present study analyzed the RNA-seq data of the leaves and roots of 40-day-old pepper plants under H_2O_2 stress at six time points and compared the obtained data with those of the control plant, we used data from this database (Liu et al., 2017). Moreover, the study analyzed the dynamic expression network of genes in leaves and roots in response to H_2O_2 stress from 0.5 h to 24 h at the genomic level. Based on the gene expression trend, the K-means value was used to divide genes into 12 expression clusters (Figure 2) from Cluster 1 to Cluster 10. The GO enrichment of genes in the clusters was analyzed (Figures 7A, C), and the genes in the chili peppers were identified through the orthologous alignment of the determined gene sequences in *Arabidopsis*. A total of 28 synthesis genes related to ROS-scavenging enzymes were identified, which showed their dynamic expression at six time points under H_2O_2 stress. We constructed a co-expression network matrix based on the Pearson correlation coefficient and found three transcription factors that exhibited a strong correlation with the synthesis genes of multiple ROS-scavenging enzymes (Figures 4C–F). Subsequent experiments are required to study in detail the mechanism through which these transcription factors regulate the associated enzymes when plants are under H_2O_2 stress, as well as the mechanism through which plants balance the ROS concentration.

The pepper plants in the present study are based on hydroponic culture and 30 mM H_2O_2 treatment in the aqueous solution. The roots most directly sense the changes in ROS concentrations, whereas the leaves after the stress. The response to H_2O_2 stress was higher and the response time was earlier in pepper roots than in leaves (Figure 3). After H_2O_2 stress, it reached to genes in pepper roots within 3 h, denoting

the peak of the response (Figures 3B, D) and indicating that the number of DEGs was the largest at 3 h. Unlike the response speed in the roots, the peak of gene response in the leaves appeared 24 h after H_2O_2 stress (Figures 3A, C). Relative to roots, the leaves responded gradually, and previous studies have shown that ROS play a crucial role in controlling root hair growth (Carol and Dolan, 2006). Some studies have used large quantities of transcriptome data processed by *Arabidopsis* oxidative stress and found that the time of oxidative stress is the determinant of the footprint of different transcriptomes (Gadjev et al., 2006; Willems et al., 2016). Thus, exploring the differences in gene expression in plants at different time points after oxidative stress treatment can be valuable.

Through the cluster analysis of identified genes related to ROS clearance and key responses in peppers, the key transcription factors, including *CaARP2* (Figure 7B) in Cluster 10 and *CaBES1* and *CabHLH029* in Cluster 1, were identified (Figures 7D, E). These transcription factors were co-expressed with the genes encoding for multiple ROS-scavenging enzymes, and their K-means analysis results showed their distribution in Cluster 1 and Cluster 10. The genes in Cluster 10 showed the earliest response in pepper root tissues. The genes in Cluster 1 had the largest number of DEGs at the 3-h time point in the root tissues of pepper under H_2O_2 stress compared with the unstressed root tissues. Therefore, these Clusters 1 and 10 were used to analyze the response of genes in pepper roots to peroxidation. The co-expression of the three transcription factors and multiple genes encoding for ROS-scavenging enzymes provides an important reference for the subsequent verification of their functional mechanisms. Studies on *Arabidopsis* have confirmed that *BES1* encodes for brassinosteroid-signaling (BRs) protein that accumulates in the nucleus in the dephosphorylated form in response to BRs and coordination of chloroplast development (Wang et al., 2002; Yin et al., 2005; Zubo et al., 2018; Clark et al., 2021; Van Nguyen et al., 2021) in *A. thaliana*, which is in line with our results that *CaBES1* also affected the expression of genes in response to H_2O_2 stress in pepper, thus indicating that the aforementioned mechanism may also be involved in pepper. For Arabidopsis, many studies have shown that *RAP2* is involved in oxygen sensing, which plays a key role in controlling root bending in response to hypoxia (Hartman et al., 2019; Smit et al., 2020; Tang et al., 2021; Seok et al., 2022); *bHLH029*, as a putative transcription factor encoding the regulation of iron uptake responses, mRNA was detected in the outer cell layer of roots and accumulated in iron deficiency, similar to FER in tomato, as a regulator of iron uptake (Cai et al., 2021; Kanwar et al., 2021; Song et al., 2022). The functions of these three important transcription factors of pepper identified in the gene expression network of pepper seedlings under hydrogen peroxide stress may show some functional conservation with their homologous genes in Arabidopsis, but to obtain exact evidence further experiments are required.

In this study, based on the control and processed RNA-seq data of the leaves and roots of 40-day-old pepper plants subjected to H_2O_2 stress at six time points, the genome-wide regulatory network was analyzed, and three possible key transcription factors were identified. A balanced candidate transcription factor can provide reliable evidence for in-depth verification and analysis.

Conclusion

In this study, the gene dynamic expression network of pepper leaves and roots at six time points in response to H_2O_2 stress was analyzed at the whole-genome level. A total of 29,065 genes were found to be expressed in at least one sample. These genes were divided into 12 clusters based on their dynamic expression in different tissues and time points. In addition, based on the research on ROS-scavenging enzymes in *Arabidopsis*, we identified 28 orthologous genes in peppers that were associated with Cluster 1 and 10 and identified three transcription factors. Multiple ROS-scavenging enzyme synthesis-related genes in pepper were highly co-expressed. We also performed GO and KEGG analysis for the DEGs identified in leaves and roots to identify key cluster genes and analyzed the GO terms and KEGG pathways that are mainly enriched in these important genes. This study provides insights into the effects of H_2O_2 stress on pepper at the whole-genome level and may serve as a reference for research on other crops.

Data availability statement

The datasets presented in this study can be found in online repositories. The names of the repository/repositories and accession number(s) can be found below: China National Center for Bioinformation, accession number CRA007961.

Author contributions

Conceptualization, LX, GY, and JW; Data curation, BT; Funding acquisition, FL, CX and XZ; Investigation, LP, YL, QS, and JD; Visualization, BT; Writing – original draft, BT and CX; Writing – review & editing, BT and FL. All authors contributed to the article and approved the submitted version.

Funding

This work was supported by Laboratory of Lingnan Modern Agriculture Project (NT2021004), Special Funds for Construction of Innovative Provinces in Hunan Province (2021NK1006), the National Key Research and Development

Program of China (Grant No. 2019YFD1000300) and A Project Supported by Scientific Research Fund of Hunan Provincial Education Department (19B271).

Acknowledgments

We thank the high-performance computing platform of Bioinformatics Center, Nanjing Agricultural University.

Conflict of interest

The authors declare that the research was conducted in the absence of any commercial or financial relationships that could be construed as a potential conflict of interest.

Publisher's note

All claims expressed in this article are solely those of the authors and do not necessarily represent those of their affiliated organizations, or those of the publisher, the editors and the reviewers. Any product that may be evaluated in this article, or claim that may be made by its manufacturer, is not guaranteed or endorsed by the publisher.

Supplementary material

The Supplementary Material for this article can be found online at: https://www.frontiersin.org/articles/10.3389/fpls.2022.1018991/full#supplementary-material

References

Andrews, S. (2017). FastQC: a quality control tool for high throughput sequence data. 2010. doi: 10.12688/f1000research.21142.2

Aramaki, T., Blanc-Mathieu, R., Endo, H., Ohkubo, K., Kanehisa, M., Goto, S., et al. (2020). KofamKOALA: KEGG ortholog assignment based on profile HMM and adaptive score threshold. *Bioinformatics* 36, 2251–2252. doi: 10.1093/bioinformatics/btz859

Asai, T., Tena, G., Plotnikova, J., Willmann, M. R., Chiu, W.-L., Gomez-Gomez, L., et al. (2002). MAP kinase signalling cascade in arabidopsis innate immunity. *Nature* 415 (6875), 977–983. doi: 10.1038/415977a

Cai, Y., Li, Y., and Liang, G. (2021). FIT and bHLH ib transcription factors modulate iron and copper crosstalk in arabidopsis. *Plant Cell Environ.* 44, 1679–1691. doi: 10.1111/pce.14000

Carol, R. J., and Dolan, L. (2006). The role of reactive oxygen species in cell growth: Lessons from root hairs. *J. Exp. Bot.* 57, 1829–1834. doi: 10.1093/jxb/erj201

Chen, S., Zhou, Y., Chen, Y., and Gu, J. (2018). Fastp: an ultra-fast all-in-one FASTQ preprocessor. *Bioinformatics* 34, i884–i890. doi: 10.1093/bioinformatics/bty560

Clark, N. M., Nolan, T. M., Wang, P., Song, G., Montes, C., Valentine, C. T., et al. (2021). Integrated omics networks reveal the temporal signaling events of brassinosteroid response in arabidopsis. *Nat. Commun.* 12, 5858. doi: 10.1038/s41467-021-26165-3

Colcombet, J., and Hirt, H. (2008). Arabidopsis MAPKs: A complex signalling network involved in multiple biological processes. *Biochem. J.* 413, 217–226. doi: 10.1042/BJ20080625

Das, K., and Roychoudhury, A. (2014). Reactive oxygen species (ROS) and response of antioxidants as ROS-scavengers during environmental stress in plants. *Front. Environ. Sci.* 2. doi: 10.3389/fenvs.2014.00053

Dietz, K. J. (2014). Redox regulation of transcription factors in plant stress acclimation and development. *Antioxid Redox Signal* 21, 1356–1372. doi: 10.1089/ars.2013.5672

Dietz, K. J., Turkan, I., and Krieger-Liszkay, A. (2016). Redox- and reactive oxygen species-dependent signaling into and out of the photosynthesizing chloroplast. *Plant Physiol.* 171, 1541–1550. doi: 10.1104/pp.16.00375

Edgar, R. C. (2004). MUSCLE: multiple sequence alignment with high accuracy and high throughput. *Nucleic Acids Res.* 32, 1792–1797. doi: 10.1093/nar/gkh340

Fedoroff, N. V., Battisti, D. S., Beachy, R. N., Cooper, P. J., Fischhoff, D. A., Hodges, C. N., et al. (2010). Radically rethinking agriculture for the 21st century. *Science* 327, 833–834. doi: 10.1126/science.1186834

Ferreira, K. N., Iverson, T. M., Maghlaoui, K., Barber, J., and Iwata, S. (2004). Architecture of the photosynthetic oxygen-evolving center. *Science* 303, 1831–1838. doi: 10.1126/science.1093087

Gadjev, I., Vanderauwera, S., Gechev, T. S., Laloi, C., Minkov, I. N., Shulaev, V., et al. (2006). Transcriptomic footprints disclose specificity of reactive oxygen species signaling in arabidopsis. *Plant Physiol.* 141, 436–445. doi: 10.1104/pp.106.078717

Gasch, A. P., and Eisen, M. B. (2002). Exploring the conditional coregulation of yeast gene expression through fuzzy k-means clustering. *Genome Biol.* 3, 1–22. doi: 10.1186/gb-2002-3-11-research0059

Gill, S. S., and Tuteja, N. (2010). Reactive oxygen species and antioxidant machinery in abiotic stress tolerance in crop plants. *Plant Physiol. Biochem.* 48, 909–930. doi: 10.1016/j.plaphy.2010.08.016

Hartman, S., Liu, Z., Van Veen, H., Vicente, J., Reinen, E., Martopawiro, S., et al. (2019). Ethylene-mediated nitric oxide depletion pre-adapts plants to hypoxia stress. *Nat. Commun.* 10, 4020. doi: 10.1038/s41467-019-12045-4

He, M., He, C. Q., and Ding, N. Z. (2018b). Abiotic stresses: General defenses of land plants and chances for engineering multistress tolerance. *Front. Plant Sci.* 9, 1771. doi: 10.3389/fpls.2018.01771

He, H., Van Breusegem, F., and Mhamdi, A. (2018a). Redox-dependent control of nuclear transcription in plants. *J. Exp. Bot.* 69, 3359–3372. doi: 10.1093/jxb/ery130

Huang, H., Ullah, F., Zhou, D. X., Yi, M., and Zhao, Y. (2019). Mechanisms of ROS regulation of plant development and stress responses. *Front. Plant Sci.* 10, 800. doi: 10.3389/fpls.2019.00800

Huang, S., Van Aken, O., Schwarzlander, M., Belt, K., and Millar, A. H. (2016). The roles of mitochondrial reactive oxygen species in cellular signaling and stress response in plants. *Plant Physiol.* 171, 1551–1559. doi: 10.1104/pp.16.00166

Jones, M. R., and Fyfe, P. K. (2001). Photosynthesis new light on biological oxygen production. *Curr. Biol.* 11(8):R318–R321. doi: 10.1016/s0960-9822(01)00174-9

Kanwar, P., Baby, D., and Bauer, P. (2021). Interconnection of iron and osmotic stress signalling in plants: is FIT a regulatory hub to cross-connect abscisic acid responses? *Plant Biol. (Stuttg)* 23 Suppl 1, 31–38. doi: 10.1111/plb.13261

Karuppanapandian, T., Moon, J.-C., Kim, C., and Kim, W. (2011). Reactive oxygen species in plants their generation, signal transduction, and scavenging mechanisms. *Aust. J. Crop Sci.* 5 (6), 709–725. doi: 10.1111/j.1365-3040.2009.02041.x

Kim, D., Langmead, B., and Salzberg, S. L. (2015). HISAT: a fast spliced aligner with low memory requirements. *Nat. Methods* 12, 357–360. doi: 10.1038/nmeth.3317

Kim, S., Park, M., Yeom, S. I., Kim, Y. M., Lee, J. M., Lee, H. A., et al. (2014). Genome sequence of the hot pepper provides insights into the evolution of pungency in capsicum species. *Nat. Genet.* 46, 270–278. doi: 10.1038/ng.2877

Klopfenstein, D. V., Zhang, L., Pedersen, B. S., Ramirez, F., Warwick Vesztrocy, A., Naldi, A., et al. (2018). GOATOOLS: A Python library for gene ontology analyses. *Sci. Rep.* 8, 10872. doi: 10.1038/s41598-018-28948-z

Letunic, I., and Bork, P. (2016). Interactive tree of life (iTOL) v3: an online tool for the display and annotation of phylogenetic and other trees. *Nucleic Acids Res.* 44, W242–W245. doi: 10.1093/nar/gkw290

Lin, G., Chai, J., Yuan, S., Mai, C., Cai, L., Murphy, R. W., et al. (2016). VennPainter: A tool for the comparison and identification of candidate genes based on Venn diagrams. *PloS One* 11, e0154315. doi: 10.1371/journal.pone.0154315

Liu, F., Yu, H., Deng, Y., Zheng, J., Liu, M., Ou, L., et al. (2017). PepperHub, an informatics hub for the chili pepper research community. *Mol. Plant* 10, 1129–1132. doi: 10.1016/j.molp.2017.03.005

Love, M. I., Huber, W., and Anders, S. (2014). Moderated estimation of fold change and dispersion for RNA-seq data with DESeq2. *Genome Biol.* 15, 550. doi: 10.1186/s13059-014-0550-8

Miller, G., Suzuki, N., Ciftci-Yilmaz, S., and Mittler, R. (2010). Reactive oxygen species homeostasis and signalling during drought and salinity stresses. *Plant Cell Environ.* 33 (4), 453–467. doi: 10.1111/j.1365-3040.2009.02041.x

Nazir, F., Hussain, A., and Fariduddin, Q. (2019). Hydrogen peroxide modulate photosynthesis and antioxidant systems in tomato (Solanum lycopersicum l.) plants under copper stress. *Chemosphere* 230, 544–558. doi: 10.1016/j.chemosphere.2019.05.001

Qin, C., Yu, C., Shen, Y., Fang, X., Chen, L., Min, J., et al. (2014). Whole-genome sequencing of cultivated and wild peppers provides insights into capsicum domestication and specialization. *Proc. Natl. Acad. Sci. U.S.A.* 111, 5135–5140. doi: 10.1073/pnas.1400975111

Rodriguez, M. C., Petersen, M., and Mundy, J. (2010). Mitogen-activated protein kinase signaling in plants. *Annu. Rev. Plant Biol.* 61, 621–649. doi: 10.1146/annurev-arplant-042809-112252

Sachdev, S., Ansari, S. A., Ansari, M. I., Fujita, M., and Hasanuzzaman, M. (2021). Abiotic stress and reactive oxygen species: Generation, signaling, and defense mechanisms. *Antioxidants (Basel)* 10 (2), 277. doi: 10.3390/antiox10020277

Sandalio, L. M., and Romero-Puertas, M. C. (2015). Peroxisomes sense and respond to environmental cues by regulating ROS and RNS signalling networks. *Ann. Bot.* 116, 475–485. doi: 10.1093/aob/mcv074

Sarvajeet Singh Gill,, Khan, N. A., Anjum, N. A., and Tuteja, N. (2011). Amelioration of cadmium stress in crop plants by nutrient management: Morphological, physiological and biochemical aspects. *Plant Stress* 5 (1), 1–23. doi: 10.4161/psb.6.2.14880

Seok, H. Y., Tran, H. T., Lee, S. Y., and Moon, Y. H. (2022). AtERF71/HRE2, an arabidopsis AP2/ERF transcription factor gene, contains both positive and negative cis-regulatory elements in its promoter region involved in hypoxia and salt stress responses. *Int. J. Mol. Sci.* 23 (10), 5310. doi: 10.3390/ijms23105310

Smit, M. E., Mcgregor, S. R., Sun, H., Gough, C., Bagman, A. M., Soyars, C. L., et al. (2020). A PXY-mediated transcriptional network integrates signaling mechanisms to control vascular development in arabidopsis. *Plant Cell* 32, 319–335. doi: 10.1105/tpc.19.00562

Song, H., Chen, F., Wu, X., Hu, M., Geng, Q., Ye, M., et al. (2022). MNB1 gene is involved in regulating the iron-deficiency stress response in arabidopsis thaliana. *BMC Plant Biol.* 22, 151. doi: 10.1186/s12870-022-03553-5

Sun, Y., Zhang, C., Qi, A., and Luo, W. (2009). "Effects of hydrogen peroxide on the germination characteristics of cucumber seeds". in *International Conference on Environmental Science and Information Application Technology*. (IEEE), 272–275.

Tang, H., Bi, H., Liu, B., Lou, S., Song, Y., Tong, S., et al. (2021). WRKY33 interacts with WRKY12 protein to up-regulate RAP2.2 during submergence induced hypoxia response in arabidopsis thaliana. *New Phytol.* 229, 106–125. doi: 10.1111/nph.17020

Tomato Genome, C. (2012). The tomato genome sequence provides insights into fleshy fruit evolution. *Nature* 485, 635–641. doi: 10.1038/nature11119

Van Nguyen, T., Park, C. R., Lee, K. H., Lee, S., and Kim, C. S. (2021). BES1/BZR1 homolog 3 cooperates with E3 ligase AtRZF1 to regulate osmotic stress and brassinosteroid responses in arabidopsis. *J. Exp. Bot.* 72, 636–653. doi: 10.1093/jxb/eraa458

Wang, Z.-Y., Gendron, J., Nakano, T., He, J., Chen, M., Vafeados, D., et al. (2002). Nuclear-localized BZR1 mediates brassinosteroid-induced growth and feedback suppression of brassinosteroid biosynthesis. *Developmental Cell* 2 (4), 505–513. doi: 10.1016/S1534-5807(02)00153-3

Willems, P., Mhamdi, A., Stael, S., Storme, V., Kerchev, P., Noctor, G., et al. (2016). The ROS wheel: Refining ROS transcriptional footprints. *Plant Physiol.* 171, 1720–1733. doi: 10.1104/pp.16.00420

Xiong, J., Yang, Y., Fu, G., and Tao, L. (2015). Novel roles of hydrogen peroxide (H(2)O(2)) in regulating pectin synthesis and demethylesterification in the cell wall of rice (Oryza sativa) root tips. *New Phytol.* 206, 118–126. doi: 10.1111/nph.13285

Yin, Y., Vafeados, D., Tao, Y., Yoshida, S., Asami, T., and Chory, J. (2005). A new class of transcription factors mediates brassinosteroid-regulated gene expression in arabidopsis. *Cell* 120, 249–259. doi: 10.1016/j.cell.2004.11.044

Yu, G., Wang, L. G., Han, Y., and He, Q. Y. (2012). clusterProfiler: An r package for comparing biological themes among gene clusters. *OMICS* 16, 284–287. doi: 10.1089/omi.2011.0118

Zhu, J. K. (2016). Abiotic stress signaling and responses in plants. *Cell* 167, 313–324. doi: 10.1016/j.cell.2016.08.029

Zubo, Y. O., Blakley, I. C., Franco-Zorrilla, J. M., Yamburenko, M. V., Solano, R., Kieber, J. J., et al. (2018). Coordination of chloroplast development through the action of the GNC and GLK transcription factor families. *Plant Physiol.* 178, 130–147. doi: 10.1104/pp.18.00414

frontiers | Frontiers in Plant Science

TYPE Original Research
PUBLISHED 14 February 2023
DOI 10.3389/fpls.2023.1005023

Check for updates

OPEN ACCESS

EDITED BY
Girdhar Kumar Pandey,
University of Delhi, India

REVIEWED BY
Sezai Ercisli,
Atatürk University, Türkiye
Ayub Oduor,
Technical University of Kenya, Kenya

*CORRESPONDENCE
Miao Wu
wumiao@hncj.edu.cn

SPECIALTY SECTION
This article was submitted to Plant Physiology, a section of the journal Frontiers in Plant Science

RECEIVED 27 July 2022
ACCEPTED 30 January 2023
PUBLISHED 14 February 2023

CITATION
Wu M, Liu H, Zhang Y, Li B, Zhu T and Sun M (2023) Physiology and transcriptome analysis of the response mechanism of *Solidago canadensis* to the nitrogen addition environment. *Front. Plant Sci.* 14:1005023. doi: 10.3389/fpls.2023.1005023

COPYRIGHT
© 2023 Wu, Liu, Zhang, Li, Zhu and Sun. This is an open-access article distributed under the terms of the Creative Commons Attribution License (CC BY). The use, distribution or reproduction in other forums is permitted, provided the original author(s) and the copyright owner(s) are credited and that the original publication in this journal is cited, in accordance with accepted academic practice. No use, distribution or reproduction is permitted which does not comply with these terms.

Physiology and transcriptome analysis of the response mechanism of *Solidago canadensis* to the nitrogen addition environment

Miao Wu*, Huiyuan Liu, Ying Zhang, Bingbing Li, Tao Zhu and Man Sun

School of Life Science and Engineering, Henan University of Urban Construction, Pingdingshan, Henan, China

Solidago canadensis is an invasive plant that can adapt to variable environmental conditions. To explore the molecular mechanism of the response to nitrogen (N) addition conditions in *S. canadensis*, physiology and transcriptome analysis were performed with samples that cultured by natural and three N level conditions. Comparative analysis detected many differentially expressed genes (DEGs), including the function of plant growth and development, photosynthesis, antioxidant, sugar metabolism and secondary metabolism pathways. Most genes encoding proteins involved in plant growth, circadian rhythm and photosynthesis were upregulated. Furthermore, secondary metabolism-related genes were specifically expressed among the different groups; for example, most DEGs related to phenol and flavonoid synthesis were downregulated in the N-level environment. Most DEGs related to diterpenoid and monoterpenoid biosynthesis were upregulated. In addition, many physiological responses, such as antioxidant enzyme activities and chlorophyll and soluble sugar contents, were elevated by the N environment, which was consistent with the gene expression levels in each group. Collectively, our observations indicated that *S. canadensis* may be promoted by N deposition conditions with the alteration of plant growth, secondary metabolism and physiological accumulation.

KEYWORDS

plant invasion, nitrogen deposition, *Solidago canadensis*, gene expression, physiological analysis

Introduction

Biological invasion is a global phenomenon and a threat to global biodiversity and the global economy (Simberloff et al., 2013; Diagne et al., 2021), representing a significant element of global change. Numerous studies have shown that plant invasion can reduce native plant performance. Therefore, invasive species will threaten global biodiversity, and

experts are required to effectively determine the main causes of biological invasion (Pysek et al., 2012; Hui et al., 2021). The ecological and economic impact of species invasions showed that managers urgently need to provide meaningful suggestions for how to prevent invasions and how to prioritize the management of invasive species (Luo et al., 2020). To understand the impact of environmental changes caused by human activities on biological invasion, many studies have been performed to explore the responses of invasive plants in common environments (Huang et al., 2022).

The invasiveness of species or habitat conditions can be changed through environmental changes, which may facilitate or inhibit alien invaders (Nguyen et al., 2016; Merow et al., 2017). Global environmental change from human activities acts as the main factor influencing plant invasion in general (Bradley et al., 2010; Carboni et al., 2018; Questad et al., 2021). The main reason for the successful invasion of alien plants is related to the environment in which they grow (Heshmati et al., 2019). Thus, plant invasion can be significantly affected by environmental factors in the receptor habitat, affecting social stability and sustainable development (Ren et al., 2020). Human-mediated interference may increase the invasiveness of alien plants, such as nutrient fluctuations in nitrogen (N) and phosphorus (Zhang et al., 2022). Recently, the distribution of anthropogenic N, which is usually caused by social and urban development, rapid agricultural intensification, and increased fuel utilization, has rapidly increased global N deposition and significantly impacts ecosystems (Yu et al., 2019).

Previous studies have proven that N deposition is accelerated by profound effects on both natural and anthropogenic ecosystems (Yu et al., 2019). Recent research and analysis of the changes in N deposition in China have increased by approximately 60%, which is the highest value in the world (Dentener et al., 2006; Liu et al., 2013). Many studies have shown that N plays an essential role in the rapid growth of invasive plants (Parepa et al., 2013; Ribeiro et al., 2017; Luo et al., 2019). Therefore, N enrichment has become an increasingly important element in global environmental change and has been widely focused on its effect on plant biodiversity and invasive plant ranges (Payne et al., 2017; Midolo et al., 2019). Although some studies have implied that high N levels in soil will promote invasive species to develop into a peak or drop (Mattingly and Reynolds, 2014; Nguyen et al., 2016), there are some evidences that suggests that N addition and enrichment will increase the opportunity to form invasive species and finally facilitate plant flourishing into invasion (Bradley et al., 2010; Vallano et al., 2012; Seabloom et al., 2015; Liu et al., 2017; Liu et al., 2019). To better understand the mechanism of how global climate change affects the mechanism of plant invasion, many novel studies are being conducted. With the development of biology, next-generation RNA sequencing technologies (RNA-seq) have supplied an approach to describe the whole genome or transcriptomes and are being used to explore the regulatory mechanisms of plant responses to many conditions in which they grow (Chu et al., 2019; Khan et al., 2022). Therefore, transcriptomic profiling can be used as an emerging method to reveal the molecular mechanism of plants in response to different environments (Asim et al., 2021; Kayihan et al., 2021; Qu et al., 2021; Li et al., 2022).

Solidago canadensis L., native to North America, is an aggressive invasive plant that successfully invaded Europe, Australia, Asia and New Zealand (Dong et al., 2006; Szymura and Szymura, 2013; Nolf et al., 2014; Gusev, 2015; Dong et al., 2017; Ye et al., 2019). The species can colonize different growth environments and exhibit a variety of phenotypes to adapt to these environments (Li et al., 2016; Jin et al., 2020). Furthermore, recent studies have attempted to suggest that N deposition and enrichment may facilitate *S. canadensis* invasion and rapid adaptation (Peng et al., 2019; Wan et al., 2019). Extended studies will provide a meaningful model for exploring invasive plants in response to the climate change environment.

Some studies have proved that invasive plants may have corresponding changes in physiological, biochemical and related gene expression levels for the environmental changes (Chuang et al., 2022; Cocozza et al., 2022; Liu Z et al., 2022). Invasive plants may be affected their enzyme activities and the synthesis process of secondary metabolites for the altered external environment (Cocozza et al., 2022; Hura et al., 2022). In this study, to explore the response of *S. canadensis* to the N addition climate change in physiology and related gene expression, we conducted a simulated N addition environment to detect the effects of altered levels on the physiology and gene expression of *S. canadensis*. Our aims were as follows: (i) explore physiological differences in plants among different levels of N addition; (ii) screen the differentially expressed transcripts; and (iii) determine the mechanism by which N addition may enhance the invasive ability of *S. canadensis*.

Materials and methods

Plant materials and experimental design

S. canadensis, as an ornamental plant, was introduced into China in 1935. At present, it is distributed in many provinces of China (Oduor et al., 2022). Mature seeds were collected from a suburb of Wuhan city (30°32′N, 114°25′E) and sown into plastic pots with a diameter of 25 cm.

To simulate increasing rates of N deposition, a total of 12 samples from four differential levels of treatments with three independent replicates for each treatment were carried out. The control group was established by pure water, and the other three levels of simulated N deposition were added by a polyethylene injector with prepared NH_4NO_3 solution, which included low N with a deposition rate of 5 g m^{-2} yr^{-1} (N5), intermediate N with 10 g m^{-2} yr^{-1} (N10), and high N with 15 g m^{-2} yr^{-1} (N15). All treatments were applied for 5 weeks, and N solution was applied to the corresponding pots. In addition, to provide daily basic water needs, 500 ml of pure water was added every two days in each pot.

Physiological measurements

The soluble sugars, MDA, chlorophyll, superoxide dismutase (SOD), catalase (CAT), and peroxidase (POD) were quantified. Each measurement was performed with three biological replicates. The chlorophyll content, which included total chlorophyll (Chl a+b) was detected by Wu et al. (2020b).

The content of soluble sugars was detected according to Quinet et al. (2012) with some modifications. The frozen samples (1 g) were put into liquid N, ground to powder, and then incubated at room temperature

with 10 mL of pure water. The mixture solution was transferred into a centrifuge tube and centrifuged at 7000 rpm for 10 minutes. The supernatant was collected for estimation by anthrone reagent.

The measurements of malonaldehyde (MDA) and antioxidant enzyme activities were performed based on Cao et al. (2017) with minor modification. The powder of each sample was collected at 0.1 g to prepare 10 mL of 10% TCA solution and then centrifuged at 7000 rpm for 10 minutes. The supernatant (2 mL) was added to 2 mL of 0.6% thiobarbituric acid (TBA). The samples were heated in boiling water for 15 minutes and cooled immediately. The mixture solution was centrifuged at 7000 rpm for 10 minutes, and then the absorbance values were detected at 532 nm, 600 nm and 450 nm.

Antioxidant enzyme activities were assayed according to Zhong et al. (2017). Fresh leaf powder (0.1 g) was collected and incubated in phosphate buffer solution, which was precooled at 4 °C. The mixture was homogenized and then centrifuged at 7000 rpm at 4°C for 15 minutes. We collected the supernatant to detect the activity of SOD, CAT and POD.

RNA and cDNA library preparation

TRIzol reagent (Invitrogen, Carlsbad, CA, USA) was used to isolate total RNA according to the protocol's instructions, and the quantification of isolated RNA was detected by using a NanoDrop spectrophotometer (Thermo Fisher Scientific, Inc.). The quality and integrity of the RNA samples were assessed with a Bioanalyzer 2100 (Agilent, CA, USA). The total RNA of each sample that satisfied the range of OD260/280 values between 1.8 and 2.2 and an RNA integrity number (RIN) above 7.5 was used for cDNA library preparation. We collected 1 μg of RNA per sample and used it to construct a paired-end cDNA library, and each library was sequenced by the Illumina NovaSeq 6000 sequencing platform at Biomarker Technology (Beijing, China). All the clean data of this study were deposited in the National Genomics Data Center (https://ngdc.cncb.ac.cn/) and are accessible through BioProject accession number PRJCA010244.

De novo transcriptome assembly and annotation

Trinity software (v2.5.1) was used to assemble transcripts (Grabherr et al., 2011), which satisfied the assumption that the assembly length should not be less than 200 bp. The redundant sequences were removed by cd-hit (v4.6.1) and clustered with Tgicl (v2.1) to merge the sequences with a similarity over 90%. The functions of the assembled unigenes were identified by searching against public databases, such as the nonredundant protein (Nr), Kyoto Encyclopedia of Genes and Genomes (KEGG), Gene Ontology (GO), and eggNOG databases, with a significance threshold of E-value ≤ 10^{-5}.

Gene expression pattern analysis

The assembled unigenes were used to map clean reads by Bowtie software, and the gene expression level was analysed and represented by using RSEM software based on fragments per kilobase of transcript sequence per million base pairs (FPKM) (Li and Dewey, 2011). The differentially expressed genes (DEGs) in each comparison group were identified by DESeq2, and the significant DEGs were collected based on a q-value < 0.01 and a fold change value ≥ 2. To explore which DEGs may play an important role in each comparison group, GO and KEGG pathway enrichment analyses of the DEGs were applied by the topGO R packages and KOBAS software, respectively.

Gene coexpression network analysis

The weighted gene correlation network analysis (WGCNA) approach is usually performed to identify gene coexpression networks, which can be used to thoroughly investigate the correlation patterns across multiple samples. All DEGs between the different N level treatments and the control were applied with the R package WGCNA.

Statistical analysis

The evaluation of statistical data, which observed under different N level treatment groups, was tested by normality (Shapiro-Wilk) and homogeneity (Bartlett). We would transform and normalize the data that need to reduce the heterogeneity of variance. ANOVAs were performed to evaluate the significant differences of physiological changes in *S. canadensis* under different nitrogen levels. *Post hoc* LSD tests were used to separate differences between pairs of treatments. Three biological replicates were collected and analysed by using variance, and the mean (± SD) with the significant difference analysis was satisfied a p value < 0.05.

Validation of qRT-PCR analysis

The isolated RNA was reverse transcribed into cDNA by an M-MuLV cDNA Synthesis Kit (Sangon Biotech). The primers of this study for qRT-PCR were designed by Primer Premier 5.0 software to verify the relative expression level of randomly selected genes with the 18S gene as an internal control. The relative expression of these randomly selected genes was calculated with the $2^{-\triangle\triangle Ct}$ method. The PCR conditions were set as follows: predenaturation at 95°C for 10 min and 40 cycles of 95°C for 10 s and 60°C for 30 s (Wu et al., 2021).

Result

Physiological and biochemical responses to different N level environments

The physiological and biochemical response analysis showed accumulation of proline, MDA and soluble sugar among different N level environments in *S. canadensis*. The levels of MDA increased with increasing N levels, while no significant changes were detected among the groups (Figure 1A). The result may show little harm to the cell membrane in *S. canadensis*. In addition, the soluble sugar contents

reached a maximum in the N10 environment with significant changes (Figure 1B). This result showed a significant effect of energy metabolism in *S. canadensis* among different N level environments.

The detected antioxidant enzymes (POD, CAT and SOD) at the different N levels are depicted in Figures 1C–E. The activity of POD was increased in the N environment groups. No significant effect was found between the CK and N5 groups, and a significant increase was observed between the CK and N10 and N15 groups (Figure 1C). The activities of CAT and SOD reached a maximum in the N10 groups, with significant differences among the groups (Figures 1D, E).

The contents of photosynthetic pigment (total chlorophyll) in each group were all affected by the N environment, and a significant difference was also detected among the CK with N5, N10, and N15 groups (Figure 1F). This result indicates that photosynthesis may be promoted by the N environment.

Overview of gene expression patterns

We performed transcriptome analysis to explore the molecular changes in *S. canadensis* exposed to different doses of N. Fresh leaf samples with different N level conditions and one control check were used for RNA-seq analysis. Based on the deep sequencing of RNA-seq, 96.50 Gb clean reads with no less than 7 Gb per sample was obtained. A total of 106,423 unigenes were obtained according to the assembly result. As a result of the expression analysis, 91,550 unigenes were detected by FPKMs, with 61,981, 56,716, 63,714, and 59,236 unigenes in the CK, N5, N10, and N15 groups, respectively. Among these expressed genes in each group, 38,610 genes were detected in each of the four experimental groups, and 7,799, 5,383, 10,022 and 6,024 genes were specifically expressed in the CK, N5, N10 and N15 groups, respectively (Figure 2A).

Analysis of differentially expressed genes

To better determine the difference in response to various N level conditions in *S. canadensis* leaves, three comparison groups were constructed, including N5-vs.-CK, N10-vs.-CK, and N15-vs.-CK. There were 654 DEGs in the comparison of N5-vs.-CK, with 372 being upregulated and 282 downregulated (Table 1). Furthermore, in the N10-vs.-CK comparison, 1,536 DEGs (745 upregulated and 791 downregulated) (Table 1) were detected. Under the N15 condition compared with the control group, we detected 640 DEGs (331 upregulated and 309 downregulated) (Table 1). It is possible that with the addition of N in the environment, some genes may be depressed. The overlap of DEGs showed that 134 DEGs were detected in all three groups; furthermore, 265 DEGs were specifically expressed in the N5-vs.-CK group, 1,001 in N10-vs.-CK, and 272 in N15-vs.-CK (Figure 2B).

GO functional analysis of DEGs

To identify and classify the functions of the DEGs, we performed GO classification analysis. In the N5-vs.-CK group, 471 DEGs were classified into 56 GO terms with three main categories: cellular component, molecular function and biological process. In the cellular component category, most DEGs were classified into the 'membrane', 'cell', 'cell part' and 'membrane part' subcategories (Supplementary Table S1). Most DEGs were classified into 'catalytic activity' and 'binding' in the molecular function category (Supplementary Table S1). In the biological process category, most DEGs were classified into 'metabolic process', 'cellular process' and 'single-organism process' (Supplementary Table S1). In addition, we performed GO functional enrichment analysis to identify insight genes that may be vital for each comparison group,

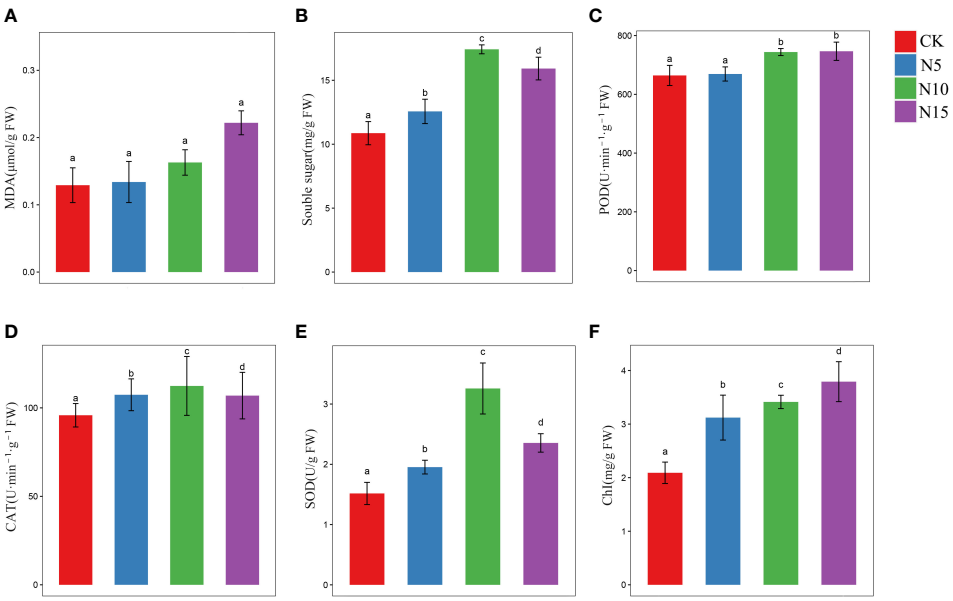

FIGURE 1
Physiological evaluate of *S. canadensis* in different N addition conditions. **(A, B, F)** The content of MDA, soluble sugar and total chlorophyll in leaves of various N level environment. **(C–E)** The activities of POD, SOD and CAT enzymes. The color bar represented each group (mean ± SE), and the significant differences among different N level groups was marked by letters ($p < .05$). The red, blue, green, and purple color bar represents CK, N5, N10, and N15 group, respectively.

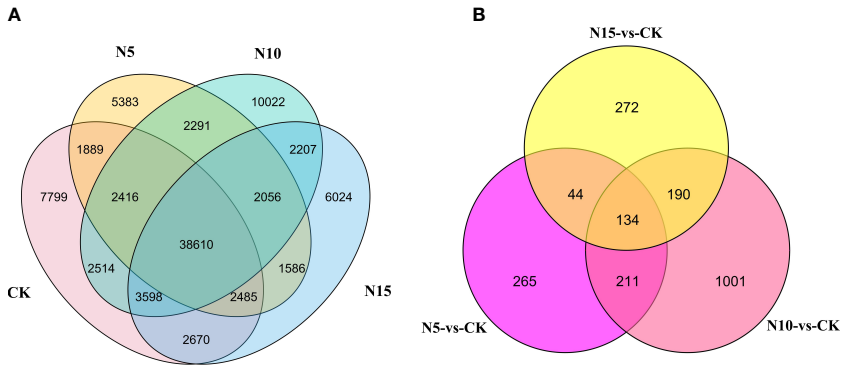

FIGURE 2
The overlap of expressed genes in each group and DEGs among three comparison groups. **(A)** The overlap of expressed genes in the CK, N5, N10, and N15 group. **(B)** The overlap of DEGs at CK-vs-N5, CK-vs-N10 and CK-vs-N15 comparison group.

and the significantly enriched GO terms were further identified by REVIGO. Many GO terms with biological functions, such as 'tetrapyrrole biosynthetic process', 'photosystem I reaction center', 'negative regulation of brassinosteroid mediated signalling pathway', 'monooxygenase activity', 'chlorophyll binding', 'urea transmembrane xyloglucan transport', and 'photosynthesis' (Figure 3A). These significantly enriched genes might play an essential functional role in the N5-vs.-CK group. In the N10-vs.-CK group, 1067 DEGs were classified into 46 GO terms of three categories. Most DEGs were classified into subcategories similar to those in the N5-vs.-CK group (Supplementary Table S2). The GO enrichment and REVIGO analysis found that except for some enriched GO items that were similar to the N5-vs.-CK group, many other items were also enriched, such as 'regulation of monopolar cell growth', 'nitrate assimilation', 'nitrogen cycle metabolic process' and 'nitrogen utilization' (Figure 3B). In the N15-vs.-CK comparison, 449 DEGs were classified into 39 GO terms. Most DEGs were classified into subcategories similar to the other two comparison groups (Supplementary Table S3). According to the GO enrichment and REVIGO analysis, some enriched GO terms were the same as those in the other two comparison groups, while some specifically enriched GO terms were also collected, such as 'protein autophosphorylation', 'isoprenoid metabolic process' and 'terpene synthase activity' (Figure 3C).

KEGG pathway analysis of DEGs

Based on the KEGG pathway enrichment analysis, 96 pathways were enriched DEGs in the N5-vs.-CK comparison group, which included 'plant hormone signal transduction', 'starch and sucrose metabolism' and 'phenylpropanoid biosynthesis' (Supplementary Table S4). To explore significant enrichment, the pathways were ranked by collected Q-values, which included 'phenylpropanoid biosynthesis', 'monoterpenoid biosynthesis', 'plant hormone signal transduction', 'photosynthesis-antenna proteins' and 'brassinosteroid biosynthesis' (Figure 4A). The significantly enriched DEGs in these pathways may be essential to respond to N5 conditions. In the N10-vs.-CK comparison group, DEGs were mapped into 106 pathways (Supplementary Table S5), and most of the DEGs were distributed in pathways similar to those in N5-vs.-CK. Based on the significant enrichment analysis, some of the collected pathways of the top 20 were the same as those in N5-vs.-CK, while some other pathways were also enriched, such as the 'zeatin biosynthesis', 'sesquiterpenoid and triterpenoid biosynthesis', 'circadian rhythm-plant', 'MAPK signalling pathway' and 'glutathione metabolism' pathways (Figure 4B). In the N15-vs.-CK comparison group, DEGs were mapped into 89 pathways (Supplementary Table S6), and most of the DEGs distributed similar pathways with the other two comparison groups. Some of the top 20 significant enriched pathways in this comparison group were same as N5-vs.-CK group, such as 'riboflavin metabolism', 'linoleic acid metabolism' and 'brassinosteroid biosynthesis', and some of the top 20 enriched pathways were same as N10-vs.-CK group, such as 'plant-pathogen interaction', 'sesquiterpenoid and triterpenoid biosynthesis' and 'circadian rhythm-plant'. Three pathways of the top 20 were all collected in each comparison group that included pathways of 'plant hormone signal transduction', 'isoflavonoid biosynthesis' and 'starch and sucrose metabolism'. Other pathways, such as 'anthocyanin biosynthesis' and 'carotenoid biosynthesis', were specifically enriched (Figure 4C). DEGs enriched in these pathways may be important in the response to N10 and N15 conditions. Thus, we inferred that with increasing N levels, the expressed functional genes may have changed.

TABLE 1 The number of DEGs in three comparison groups.

Groups	Total number	Up-regulated	Down-regulated
CK-vs-N5	654	372	282
CK-vs-N10	1536	745	791
CK-vs-N15	640	331	309

Plant growth and development related DEGs

According to the pathway functional enrichment analysis in the three comparison groups, a total of 10 DEGs were involved in the photosynthesis pathway. In the N5-vs.-CK comparison group, 6 DEGs were collected, with 5 upregulated and 1 downregulated DEGs, and in the N10-vs.-CK comparison group, 10 DEGs were

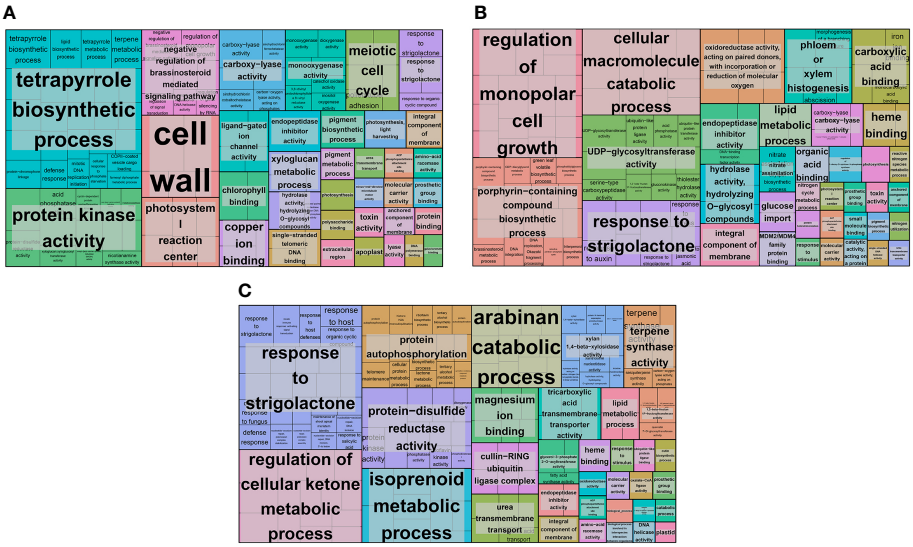

FIGURE 3
The distribution of DEGs and GO functional enrichment analysis. **(A)** The GO enrichment of CK-vs-N5 comparison; **(B)** The GO enrichment of CK-vs-N10 comparison. **(C)** The GO enrichment of CK-vs-N15 comparison. The enriched GO terms were presented in rectangles.

collected, with 8 upregulated and 2 downregulated DEGs. In the N15-vs.-CK comparison group, one downregulated DEG was detected (Figure 5A). This result showed that with increasing N addition level, the expression and number of photosynthesis-related DEGs first increased and then decreased. Furthermore, 9 auxin-related DEGs were collected in the three comparison groups. In the N5-vs.-CK comparison group, 5 DEGs were detected, with 3 upregulated and 2 downregulated. Furthermore, 7 DEGs were collected in the N10-vs.-CK and N15-vs.-CK comparison groups, with 5 upregulated and 2 downregulated DEGs in the N10-vs.-CK comparison and 6 upregulated and 1 downregulated DEGs in the N15-vs.-CK comparison (Figure 5B). In addition, 12 DEGs were detected in the 'circadian rhythm-plant' pathway in the three comparison groups. In the N5-vs.-CK comparison group, 2 *CO* genes were detected and upregulated. In the N10-vs.-CK comparison group, 8 DEGs with 5 upregulated and 3 downregulated genes were detected, which included 2 *LHY*, 3 *CO*, 1 *TOC1*, 2 *COP1* and 1 *CHS* genes. In the N15-vs.-CK comparison group, 9 DEGs, including 8 upregulated and 1 downregulated DEGs, were detected, and except for most of the DEGs in the N10-vs.-CK comparison group, 3 *PIF3* genes were also detected (Figure 5C). These DEGs may play important functions in responding to different N level environments and regulating plant growth and development in *S. canadensis*.

Secondary metabolism related DEGs

In this study, most secondary metabolism-related DEGs were collected and enriched in related pathways. For example, in the 'phenylpropanoid biosynthesis' pathway, 10 DEGs were collected, with 8 upregulated, such as the *F6H* and *HCT* genes, and 2 downregulated in the N5-vs.-CK comparison group. In the N10-vs.-CK comparison group, 17 DEGs, 12 downregulated, including the *F5H*, *HCT*, cinnamyl-alcohol dehydrogenase (*CAD*) and *CCR* genes, and 5 upregulated. In the N15-vs.-CK comparison group, most DEGs were also downregulated, such as the *PAL*, *CAD* and *HCT* genes (Figure 5D). Furthermore, in the flavonoid biosynthesis pathway, most DEGs were downregulated in the three comparison groups,

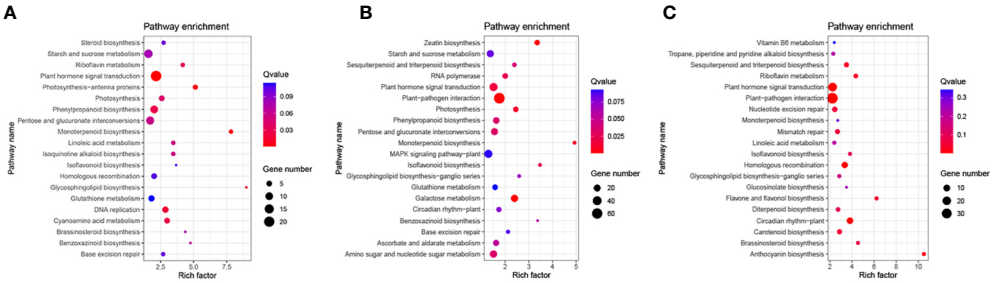

FIGURE 4
KEGG pathway functional enrichment analysis of DEGs. **(A)** The CK-vs-N5 comparison; **(B)** The CK-vs-N10 comparison. **(C)** The CK-vs-N15 comparison. The KEGG pathway name were presented in Y-axis, and the rich factor were presented in X-axis. The color bar and bubble size represent the corresponding q-value and number of genes respectively.

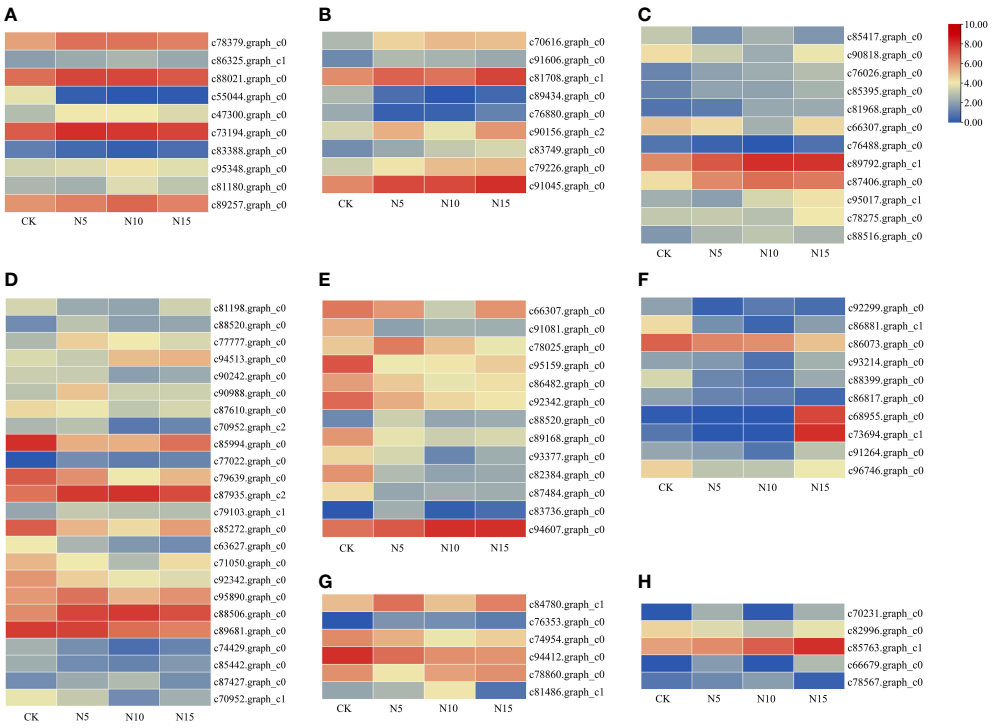

FIGURE 5
The expression profile of collected functional genes in various N level environments. **(A)** Photosynthesis; **(B)** Auxin; **(C)** Circadian rhythm; **(D)** Phenylpropanoid biosynthesis; **(E)** Flavonoids synthesis; **(F)** sesquiterpenoid and triterpenoid biosynthesis; **(G)** diterpenoid biosynthesis; **(H)** monoterpenoid biosynthesis.

including *CHS*, *CHI* and *FLS* genes (Figure 5E). Phenol and flavonoid synthesis may be depressed in *S. canadensis* in an elevated N level environment. Terpenoid biosynthesis-related DEGs, such as those in the 'monoterpenoid biosynthesis' and 'diterpenoid biosynthesis' pathways, were collected in the three comparison groups. In the comparison groups of N5-vs.-CK and N10-vs.-CK, all of the detected sesquiterpenoid and triterpenoid biosynthesis-related genes were downregulated, such as *GERD*, beta-amyrin synthase (*β-AS*) and *CYP* genes. Nevertheless, in the N15-vs.-CK comparison group, 2 *GERD* genes were upregulated (Figure 5F). In addition, most of the diterpenoid and monoterpenoid biosynthesis-related DEGs, such as kaurene synthase (*KS*), momilactone synthase (*MS*) and carboxylinalool synthase-related genes, were upregulated in the three comparison groups (Figures 5G, H). These results provided different regulation patterns of terpenoid synthesis in response to changes in the N environment.

Gene expression network analysis

Based on the differentially expressed gene analysis, we collected 2117 DEGs from three comparison groups and analysed them with the method of WGCNA. A total of 18 gene expression modules were collected (Figure 6A), and according to the module and trait correlation analysis, the coregulatory modules were identified by correlation coefficient > 0.5 and p value < 0.05 (Figure 6B).

In the N5-vs.-CK comparison group, the green-yellow, salmon and black modules were collected. The expression profiles of genes in these three modules were depicted by heatmaps across all samples. A total of 61 DEGs were collected in the green-yellow module, and most of the upregulated genes were detected in the N5 group (Figure 7A). Based on the functional annotation, the collected genes in the green-yellow module included plant growth- and photosynthesis-related genes, such as *ARF* (c91123.graph_c0), auxin efflux carrier family protein (c90097.graph_c0) gene, sucrose synthase (*SuSy*, c90097.graph_c0) and chlorophyll a/b binding protein 2 (*Lhcb2*, c82134.graph_c0) genes, and secondary metabolism-related genes, which were enriched in 'monoterpenoid biosynthesis' and 'flavonoid biosynthesis' pathways, such as *CHI* (c78025.graph_c0), neomenthol dehydrogenase (*NMR*, c78860.graph_c0) gene (Figure 8A). In the black module, 100 DEGs were collected, and most of the upregulated genes were also detected in the N5 group (Figure 7B). In addition to *Lhcb3* (c88539.graph_c0) gene during photosynthesis and sugar metabolism related genes, other functional genes, such as the *POD* (c77777.graph_c0) gene, elongation factor (*EF*, c88198.graph_c0) gene, histone H3 (c69025.graph_c0) gene and E3 ubiquitin-protein ligase (*EL*, c71740.graph_c0) gene were collected in the network analysis (Figure 8B).

In the N10-vs.-CK comparison, the brown, blue, cyan and midnight blue modules were collected. A total of 212 DEGs were collected in the brown module, most of which were upregulated in the N10 group, while some of the genes were also upregulated in the N5 group (Figure 7C). The network analysis showed that some genes related to photosynthesis, such as the *psbP* (c78379.graph_c0) gene, *psaD* (c73194.graph_c0) gene and blue-light photoreceptor (c91454.graph_c0) gene, were upregulated in the N10 group. Furthermore, some enzyme synthesis and plant hormone related genes, such as *SOD* (c80060.graph_c0), *GST* (c81884.graph_c1), *POD* (c91380.graph_c0), and auxin-binding

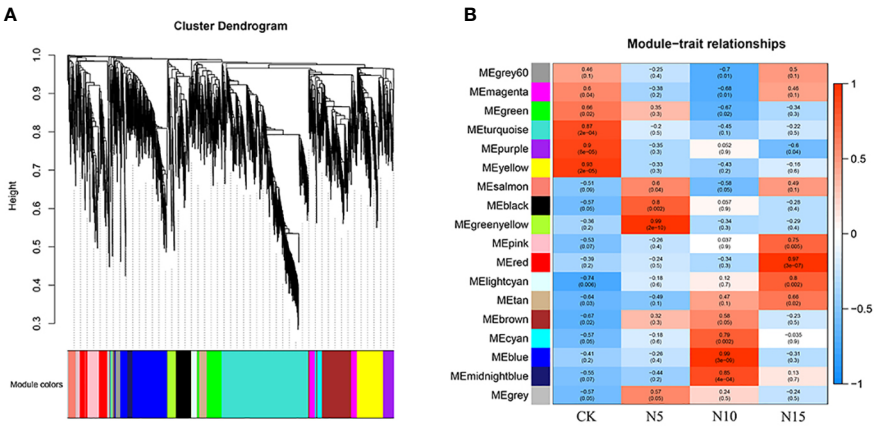

FIGURE 6
The analysis of WGCNA. **(A)** The collected genes were clustered and merged into different modules. **(B)** Module–trait associations. Each cell contains the corresponding correlation and p-value. The color bar indicates the correlation of each module with each sample.

protein (c72444.graph_c0) gene were upregulated. In addition, some transcription factor genes were collected in this module, such as *MYB* (c84062.graph_c0, c92964.graph_c0), *bHLH* (c69458.graph_c0, c85512.graph_c0, c71271.graph_c0), *TCP* (c76145.graph_c0) and *ERF* (c76763.graph_c0) transcription factor genes, all of which were upregulated (Figure 8C). In the blue module, 275 DEGs were most of which were upregulated in the N10 group (Figure 7D). Except for some photosynthesis, plant hormone-related and transcription factor genes, such as *Lhcb2* (c81347.graph_c0) gene, *psaA* and *psaB* (c81180.graph_c0) gene, auxin responsive protein (c69869.graph_c0) gene, *ERF* (c68175.graph_c0), *SBP* (c84523.graph_c1) and *MYB* (c76609.graph_c0) transcription factor genes and other metabolism and functional genes include the nitronate monooxygenase (c82612.graph_c0) gene, *SuSy* (c81588.graph_c1) gene, *β-AS* (c91264.graph_c0), histone H3 (c57400.graph_c0) gene, histone H4 (c30533.graph_c0) gene and zinc finger protein (c93267.graph_c0, c91298.graph_c0) gene were collected in the network (Figure 8D).

In the N15-vs.-CK comparison group, four modules with red, pink, tan and lightcyan were collected. A total of 101 DEGs were collected in the red module, most of which were upregulated in the N15 group (Figure 7E). The network analysis of these DEGs showed that metabolism biosynthesis-related genes, such as the *SuSy* (c95043.graph_c0) gene and germacrene D synthase (c73694.graph_c1, c95043.graph_c0) gene, were collected. Furthermore, other functional genes included transcription factors and plant hormone-related genes, such as brassinosteroid insensitive 1-associated kinase 1 (*BRI1*, c86844.graph_c1) gene, PIN-FORMED (PIN) protein (*PIN*, c89411.graph_c0) gene, zinc finger protein (*COL3*, c78275.graph_c0) gene and *AP2* (c89411.graph_c0) gene were also collected (Figure 8E). In the tan module, 52 DEGs were most of which were upregulated in the N15 and N10 groups (Figure 7F). Many of the upregulated genes in the network, such as *POD* (c94513.graph_c0), *ERF* (c67768.graph_c0, c77988.graph_c0), *LHY* (c81968.graph_c0), zinc finger protein (*COL2*, c89792.graph_c1) gene and *SuSy* (c86075.graph_c0) gene, were identified (Figure 8F), some of which were also upregulated in the N10 groups. Secondary metabolism related genes, such *CAD* (c89681.graph_c0) gene was downregulated in both the N15 and N10 groups. The functional analysis of these collected modules shown that most of DEGs may involved in photosynthesis, plant growth and development and secondary metabolism process (Table 2). These collected genes may be vital for the regulation of the response in the N additional environment.

Verification of gene expression by qRT-PCR

We randomly selected 12 candidate genes for qRT-PCR to validate the gene expression results, which were obtained from RNA-seq (Figure 9). As a result of qRT-PCR, the relative expression of each selected gene was detected and was basically in agreement with the RNA-seq data. The primer sequences are listed in the Supplementary Table S7.

Discussion

Physiological responses of *S. canadensis* in the N addition environment

Physiological investigations are essential and effective means to evaluate the real influence of various environments (Hu et al., 2019). Physiological traits such as photosynthetic pigments, antioxidant enzymes, and soluble sugars have often been implicated in survival and ecological strategies in plants under different conditions (Mao et al., 2017). Plants, especially invasive plants, in different N-level environments exhibit various physiological and morphological responses (Wan et al., 2019; Huang et al., 2022; Sun et al., 2022). The increased N supply environment can induce a significant effect on resource use in plants (Wang et al., 2017; Wan et al., 2019); therefore, continuous N addition conditions will promote plant invasion (Liu et al., 2018a; Luo et al., 2020), such as facilitating invasive plants to synthesize more photosynthetic compounds in the leaves, which supports plant growth (Huang et al., 2022). The physiological analysis showed that Chl contents increased with elevated N levels, which may contribute to the photosynthetic capacity and growth of *S. canadensis*. The GO and KEGG pathway

10.3389/fpls.2023.1005023

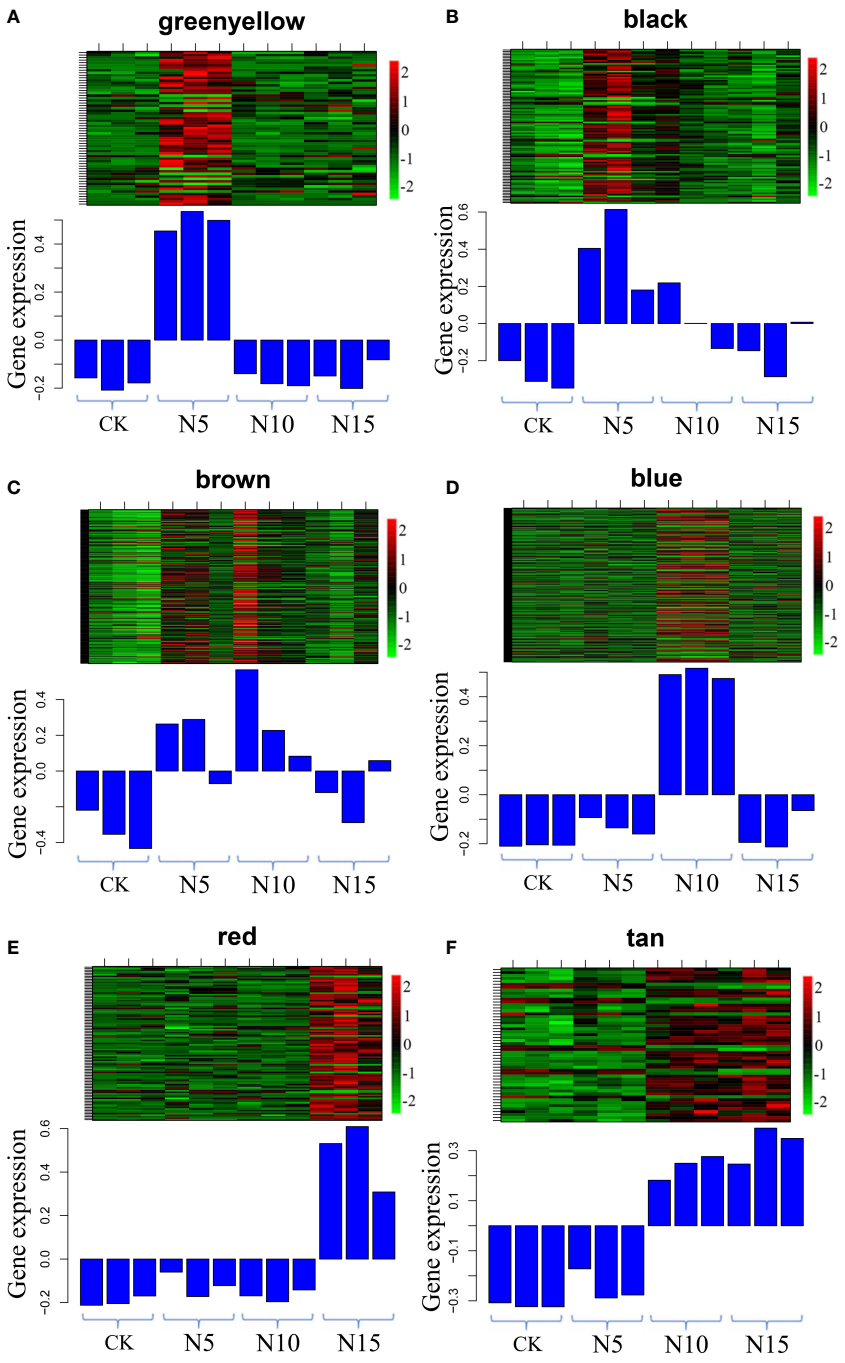

FIGURE 7
Gene expression profiles of selected modules. The color bar represent the relative expression, red denotes up-regulation and green denotes down-regulation. **(A-F)** The modules represented greenyellow, black, brown, blue, red and tan respectively.

enrichment analyses also showed that many genes were related to the GO terms 'photosynthesis' and 'photosystem I reaction center' and the KEGG pathway 'photosynthesis-antenna proteins', which may be related to the Chl contents in response to the N addition environment. Sugars, as energy sources in plants, the metabolism of which can be regulated by N levels (Sun et al., 2019; Zhang et al., 2021), play regulatory roles in plant growth and development (Lastdrager et al., 2014; Ciereszko, 2018). In this study, the soluble sugar content was upaccumulated with the N levels and reached the highest in the N10 environment. This suggests that the N environment may have an effect on the metabolic process of sugars in *S. canadensis*. Gene expression pattern analysis has shown that the transcription of numerous sucrose and starch metabolism-related genes will change sugar content levels (Gao et al., 2018; Zhu et al., 2018; Shao et al., 2020). The KEGG pathway enrichment analysis found that 35 DEGs were enriched in the 'starch and sucrose metabolism' pathway, with 12 enriched in the N5-vs.-CK and N15-vs.-CK comparison groups and 22 DEGs in the N10-vs.-CK comparison groups. The collected functional DEGs might be affected by the N environment and play an essential role in sugar

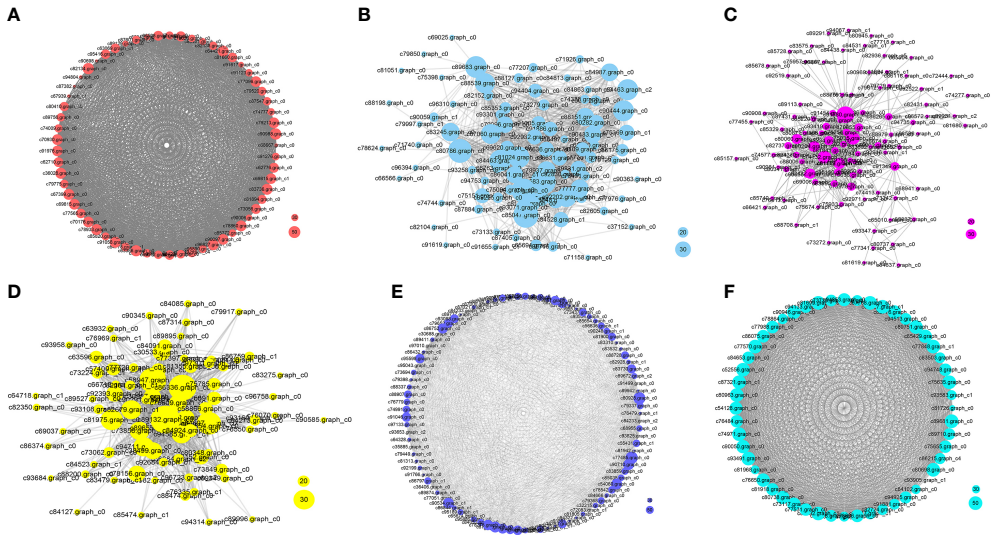

FIGURE 8
Network analysis of the collected modules. The bubble size indicates connect degree of each gene. **(A–F)** The networks represented greenyellow, black, brown, blue, red and tan respectively.

metabolism in *S. canadensis*. In addition, previous studies have shown that antioxidant enzyme activity in plants is altered in N supplementation and fertilizer environments (Liao et al., 2019; Wang et al., 2022). With the results of this study, all three enzyme activities were elevated with N supplementation levels. For instance, the increased activities of SOD, POD and CAT were significantly elevated in the N-supplemented environment. Based on the RNA-seq dataset, DEGs encoding these enzymes were identified among the comparison groups, which might contribute to the enhanced activity of these enzymes in *S. canadensis* under the N level environment. Therefore, we can reasonably infer that the activity of these enzymes might be highly regulated at the protein level. Further research into higher levels of regulation will expand our current understanding of how *S. canadensis* responds to the N-supplemented environment.

Secondary metabolite synthesis in *S. canadensis* may be altered by the N environment

Plants respond to global changes by simulating special physiological and molecular responses and by modulating distinct metabolism in plant growth and development (Zandalinas et al., 2022). Therefore, plants can adapt to new energy requirements brought about by different climate and environmental scenarios (Dusenge et al., 2019; Fernie et al., 2020). In alien invasive plants, allelopathy is one of the important approaches for successful invasion. Thus, the production of allelopathic chemicals makes introduced invasive plants more competitive against local plants than natives. The allelopathic potential of *S. canadensis* has significantly affected the production of secondary metabolites, which contribute to its competitive abilities and its successful invasion (Wu et al., 2020a). Previous researchers found that simulated N deposition can reduce phenolic compound synthesis in plants (Sun et al., 2020). The mechanistic evidence of this phenomenon was driven by the effects on PAL, which acts as the rate-limiting enzyme for the generation of phenylpropanoids. Therefore, both *PAL* gene expression and PAL enzyme activity were markedly inhibited by simulated N deposition. Furthermore, other phenylpropanoid metabolism- and phenolic synthesis-related enzymes of chalcone synthase (CHS) and flavanone-3-hydroxylase (FHT) have also been reported (Deng et al., 2019). In this study, most DEGs involved in phenylpropanoid and flavonoid synthesis were collected and downregulated under N environmental conditions, such as the *PAL*, *CAD*, *CHS*, chalcone isomerase (*CHI*) and *FHT* genes, encoding enzymes that promote phenylpropanoid and flavonoid secondary metabolite accumulation.

In addition, based on the KEGG enrichment analysis, some terpenoid synthesis-related DEGs were also collected. Many of these DEGs enriched in the sesquiterpenoid and triterpenoid synthesis pathways were downregulated in the N addition environment, such as the squalene monooxygenase gene, nerolidol synthase gene, α-farnesene synthase gene and *β-AS* gene. In the monoterpenoid and diterpenoid pathways, except for some of the downregulated DEGs in the N addition environment, such as the 8-hydroxygeraniol dehydrogenase gene, neomenthol dehydrogenase gene, gibberellin 3β-dioxygenase gene, some DEGs were upregulated, such as the (E)-8-carboxylinalool synthase gene, *KS* gene and gibberellin 2beta-dioxygenase gene. The results suggest that the difference in secondary metabolism-related genes may especially respond to the N environment, which may give rise to the specific accumulation of secondary metabolites. It is thought that the ability of plants to synthesize large numbers of specialized secondary metabolites helps them adapt to changing environments (Panda et al., 2021). These results indicate that the N addition environment may alter the secondary metabolism process in *S. canadensis*, which would affect allelopathic abilities and change plant chemical defenses with climate change.

10.3389/fpls.2023.1005023

TABLE 2 Functional analysis of collected modules with network analysis.

Module names	Number of genes	GO terms	KEGG pahtways	Related genes
greenyellow	61	Photosynthesis, light harvesting in photosystem I	Monoterpenoid biosynthesis	*ARF*, *CHI*, *Lhcb2*, *MNR*, *SuSy*, etc.
		Regulation of ARF protein signal transduction	Isoflavonoid biosynthesis	
		Chloroplast organization	Phenylpropanoid biosynthesis	
		Developmental growth	Photosynthesis - antenna proteins	
			Flavonoid biosynthesis	
			Starch and sucrose metabolism	
black	100	Protein heterodimerization activity	Photosynthesis - antenna proteins	*EF*, *POD*, *Lhcb3*, *Lhcb4*, etc.
		Integral component of membrane	Phenylpropanoid biosynthesis	
		Photosynthesis, light harvesting in photosystem I		
brown	212	Photosystem II oxygen evolving complex	Photosynthesis	*PsbP*, *PsaD*, *CRY*, *EL*, etc.
		Superoxide dismutase activity	Peroxisome	
		Regulation of transcription		
		peroxidase activity		
		DNA-binding transcription factor activity		
		Antioxidant activity		
blue	275	Integral component of membrane	Sesquiterpenoid and triterpenoid biosynthesis	*EL*, *Lhcb2*, *ERF*, *SBP*, *psaA*, *psaB*, *SuSy*, *β-AS*, etc.
		Signal transduction	Starch and sucrose metabolism	
		Nitronate monooxygenase activity	Photosynthesis	
			Nitrogen metabolism	
red	101	Auxin-activated signaling pathway	Plant hormone signal transduction	*SuSy*, *BRI1*, *PIN*, *AP2*, *COL3*, etc.
		Zinc ion binding	Starch and sucrose metabolism	
		Terpene synthase activity	MAPK signaling pathway - plant	
			Sesquiterpenoid and triterpenoid biosynthesis	
			Circadian rhythm - plant	
tan	52	DNA-binding transcription factor activity	Plant hormone signal transduction	*POD*, *ERF*, *LHY*, *CAD*, *COL2*, etc.
		Starch biosynthetic process	Circadian rhythm - plant	
		Hydrogen peroxide catabolic process	Phenylpropanoid biosynthesis	

Transcriptome analysis of the effects of the N addition response of *S. canadensis*

Plant invasion is a major component of global change that could affected by other components of global change (Liu et al., 2018b; Ren et al., 2020). It is predicted that plant invasions will further increase as the global environment continues to change (Liu et al., 2017). Environmental change can increase the dispersal rate and population growth of alien species and may promote their invasion range (Sandel and Dangremond, 2012; Liu et al., 2017). In this study, some DEGs were detected of *S. canadensis* among different N level environment, which may play an important role in responding to changes in N addition environment and promote to spread in new area.

Nitrogen is often the most limiting nutrient for plant growth in most ecosystems, which is very important for fast-growing plants, especially invasive plants (Uddin and Robinson, 2018; Zhang et al., 2022). Invasive plants have more advantages in N allocation than native plants, which will promote the response of invasive plants to the N environment (Hu et al., 2022; Oduor, 2022). To explore the response of *S. canadensis* under a N environment, transcriptome analysis was performed among different N deposition level environments. Previous studies suggested that N levels can significantly affect the growth of *S. canadensis* (Wan et al., 2018).

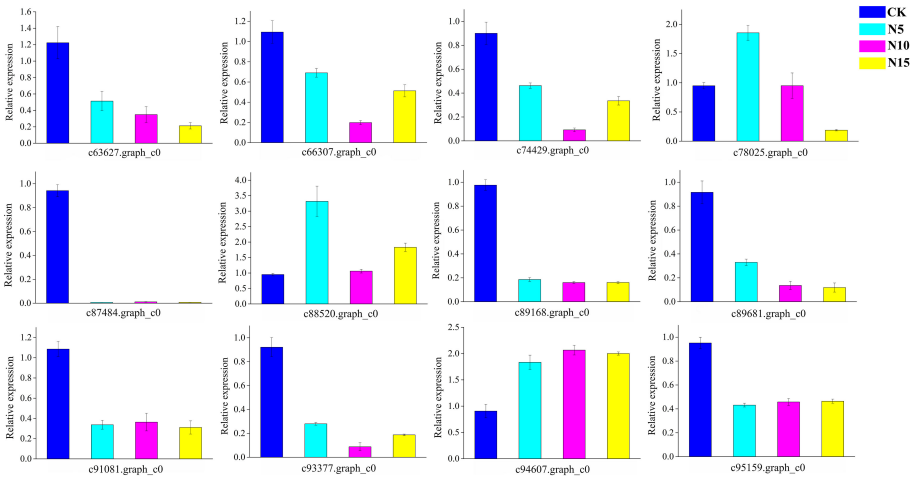

FIGURE 9
The qRT-PCR analyses of randomly selected genes in CK, N5, N10, and N15 group respectively.

The successful invasion of the exotic plant *S. canadensis* may be significantly affected by the N addition environment (Liu X. S. et al., 2022). In this study, most plant growth- and development-related genes were differentially expressed in the N environment comparison groups. Based on the essential functional GO terms related to the N metabolism process, plant growth and photosystem, such as 'nitrate assimilation', 'reactive nitrogen species metabolic process', 'nitrogen cycle metabolic process', 'nitrogen utilization', 'photosystem I reaction center', and 'growth factor activity'. KEGG enrichment analysis showed that many DEGs with the function of plant development-related pathways were significantly enriched, such as plant hormone, sugar metabolism and circadian rhythm-related pathways. As a result of response of other invasive plants under N deposition environment (Huang et al., 2022), N supplement conditions may change the growth, energy metabolism rate and availability of N resources of *S. canadensis*.

Furthermore, according to the gene expression network analysis, in addition to the plant growth- and development-related DEGs, many regulator genes were collected in the different modules, such as histone genes, zinc finger protein genes, E3 ubiquitin-protein ligase genes and transcription factor genes. These DEGs may play regulatory roles in plant growth and development in an N-addition environment.

Conclusion

In this study, we explored the effect of the N environment response of *S. canadensis* in physiology and transcriptome analysis. The physiological data showed that the photosynthetic pigment and soluble sugar contents were elevated by N addition. The antioxidant enzyme activities were altered in different N level environments. Transcriptome analysis showed that photosynthesis- and sugar metabolism process-related genes were also upregulated under N addition. In addition, secondary metabolism-related genes were affected in the N environment, and most of the phenol, flavonoid and sesquiterpenoid and triterpenoid metabolism-related DEGs were downregulated in the N environment. Most monoterpenoid- and diterpenoid-related DEGs were upregulated. As a result, many regulated genes were collected and may play vital roles in *S. canadensis* under N addition. Taken together, our work provides valuable information for the responses of *S. canadensis* to the N deposition environment, and the elevated N level environment may facilitate the fast growth and spread of invasive plant species.

Data availability statement

The datasets presented in this study can be found in online repositories. The names of the repository/repositories and accession number(s) can be found in the article/Supplementary Material.

Author contributions

MW designed the research, analyzed the data and wrote the manuscript. HL provided the methodology and revised the manuscript. YZ and MS performed the experiments. Investigation. BL and TZ participated in the design of the study. All authors contributed to the article and approved the submitted version.

Funding

This research was supported by the science and technology research project of Henan Province (agricultural field): Research on preparation, function and health food of bioactive peptide from Dioscorea opposita Thunb(182102110093).

Conflict of interest

The authors declare that the research was conducted in the absence of any commercial or financial relationships that could be construed as a potential conflict of interest.

Publisher's note

All claims expressed in this article are solely those of the authors and do not necessarily represent those of their affiliated organizations, or those of the publisher, the editors and the reviewers. Any product that may be evaluated in this article, or claim that may be made by its manufacturer, is not guaranteed or endorsed by the publisher.

Supplementary material

The Supplementary Material for this article can be found online at: https://www.frontiersin.org/articles/10.3389/fpls.2023.1005023/full#supplementary-material

References

Asim, A., Gokce, Z. N. O., Bakhsh, A., Cayli, I. T., Aksoy, E., Caliskan, S., et al. (2021). Individual and combined effect of drought and heat stresses in contrasting potato cultivars overexpressing miR172b-3p. *Turkish J. Agric. Forestry* 45, 651–668. doi: 10.3906/tar-2103-60

Bradley, B. A., Blumenthal, D. M., Wilcove, D. S., and Ziska, L. H. (2010). Predicting plant invasions in an era of global change. *Trends In Ecol. Evol.* 25, 310–318. doi: 10.1016/j.tree.2009.12.003

Cao, Y., Luo, Q., Tian, Y., and Meng, F. (2017). Physiological and proteomic analyses of the drought stress response in *Amygdalus mira* (Koehne) yü et Lu roots. *BMC Plant Biol.* 17, 53. doi: 10.1186/s12870-017-1000-z

Carboni, M., Gueguen, M., Barros, C., Georges, D., Boulangeat, I., Douzet, R., et al. (2018). Simulating plant invasion dynamics in mountain ecosystems under global change scenarios. *Global Change Biol.* 24, E289–E302. doi: 10.1111/gcb.13879

Chu, F. F., Cheng, J., Zhang, X. D., Ye, Q., Chen, S. T., Zhou, J. H., et al. (2019). Transcriptome and key gene expression related to carbon metabolism and fatty acid synthesis of *Chlorella vulgaris* under a nitrogen starvation and phosphorus repletion regime. *J. Appl. Phycol.* 31, 2881–2893. doi: 10.1007/s10811-019-01811-y

Chuang, L., Liu, S. Y., Biedermann, D., and Franke, J. (2022). Identification of early quassinoid biosynthesis in the invasive tree of heaven (*Ailanthus altissima*) confirms evolutionary origin from protolimonoids. *Front. Plant Sci.* 13. doi: 10.3389/fpls.2022.958138

Ciereszko, I. (2018). Regulatory roles of sugars in plant growth and development. *Acta Societatis Botanicorum Poloniae* 87, 3583. doi: 10.5586/asbp.3583

Cocozza, C., Bartolini, P., Brunetti, C., Miozzi, L., Pignattelli, S., Podda, A., et al. (2022). Modulation of class III peroxidase pathways and phenylpropanoids in arundo donax under salt and phosphorus stress. *Plant Physiol. Biochem.* 183, 151–159. doi: 10.1016/j.plaphy.2022.05.002

Deng, B., Li, Y. Y., Lei, G., and Liu, G. H. (2019). Effects of nitrogen availability on mineral nutrient balance and flavonoid accumulation in *Cyclocarya paliurus*. *Plant Physiol. Biochem.* 135, 111–118. doi: 10.1016/j.plaphy.2018.12.001

Dentener, F., Drevet, J., Lamarque, J. F., Bey, I., Eickhout, B., Fiore, A. M., et al. (2006). Nitrogen and sulfur deposition on regional and global scales: A multimodel evaluation. *Global Biogeochem. Cycles* 20, 1–21. doi: 10.1029/2005GB002672

Diagne, C., Leroy, B., Vaissiere, A. C., Gozlan, R. E., Roiz, D., Jaric, I., et al. (2021). High and rising economic costs of biological invasions worldwide. *Nature* 592, 571–576. doi: 10.1038/s41586-021-03405-6

Dong, M., Lu, J., Zhang, W., Chen, J., and Li, B. (2006). Canada Goldenrod (*Solidago canadensis*): An invasive alien weed rapidly spreading in China. *Acta Phytotaxon. Sin.* 44, 72–85. doi: 10.1360/aps050068

Dong, L. J., Yang, J. X., Yu, H. W., and He, W. M. (2017). Dissecting *Solidago canadensis*-soil feedback in its real invasion. *Ecol. Evol.* 7, 2307–2315. doi: 10.1002/ece3.2743

Dusenge, M. E., Duarte, A. G., and Way, D. A. (2019). Plant carbon metabolism and climate change: elevated CO_2 and temperature impacts on photosynthesis, photorespiration and respiration. *New Phytol.* 221, 32–49. doi: 10.1111/nph.15283

Fernie, A. R., Bachem, C. W. B., Helariutta, Y., Neuhaus, H. E., Prat, S., Ruan, Y. L., et al. (2020). Synchronization of developmental, molecular and metabolic aspects of source-sink interactions. *Nat. Plants* 6, 55–66. doi: 10.1038/s41477-020-0590-x

Gao, M., Zhang, S., Luo, C., He, X., Wei, S., Jiang, W., et al. (2018). Transcriptome analysis of starch and sucrose metabolism across bulb development in *Sagittaria sagittifolia*. *Gene* 649, 99–112. doi: 10.1016/j.gene.2018.01.075

Grabherr, M. G., Haas, B. J., Yassour, M., Levin, J. Z., Thompson, D. A., Amit, I., et al. (2011). Full-length transcriptome assembly from RNA-seq data without a reference genome. *Nat. Biotechnol.* 29, 644–652. doi: 10.1038/nbt.1883

Gusev, A. P. (2015). The impact of invasive Canadian goldenrod (*Solidago canadensis* l.) on regenerative succession in old fields (the southeast of Belarus). *Russian J. Biol. Invasions* 6, 74–77. doi: 10.1134/S2075111715020034

Heshmati, I., Khorasani, N., Shams-Esfandabad, B., and Riazi, B. (2019). Forthcoming risk of *Prosopis juliflora* global invasion triggered by climate change: Implications for environmental monitoring and risk assessment. *Environ. Monit. Assess.* 191, 72. doi: 10.1007/s10661-018-7154-9

Hu, C. C., Liu, X. Y., Yan, Y. X., Lei, Y. B., Tan, Y. H., and Liu, C. Q. (2022). A new isotope framework to decipher leaf-root nitrogen allocation and assimilation among plants in a tropical invaded ecosystem. *Sci. Total Environ.* 806, 151203. doi: 10.1016/j.scitotenv.2021.151203

Hu, Y. B., Peuke, A. D., Zhao, X. Y., Yan, J. X., and Li, C. M. (2019). Effects of simulated atmospheric nitrogen deposition on foliar chemistry and physiology of hybrid poplar seedlings. *Plant Physiol. Biochem.* 143, 94–108. doi: 10.1016/j.plaphy.2019.08.023

Huang, F. F., Zhou, G. H., Liao, H. X., Fan, Z. X., and Chen, B. M. (2022). Simulated nitrogen deposition induces shifts in growth and resource-use strategies during range expansion of an invasive plant. *Biol. Invasions* 24, 621–633. doi: 10.1007/s10530-021-02668-4

Hui, C., Richardson, D. M., Landi, P., Minoarivelo, H. O., Roy, H. E., Latombe, G., et al. (2021). Trait positions for elevated invasiveness in adaptive ecological networks. *Biol. Invasions* 23, 1965–1985. doi: 10.1007/s10530-021-02484-w

Hura, T., Hura, K., Ostrowska, A., Gadzinowska, J., Urban, K., and Pawłowska, B. (2022). The role of invasive plant species in drought resilience in agriculture: the case of sweet briar (*Rosa rubiginosa* l.). *J. Exp. Bot.*, erac377. doi: 10.1093/jxb/erac377

Jin, H., Yuan, Y., Gao, F., Oduor, A. M. O., and Li, J. (2020). The invasive plant *Solidago canadensis* exhibits partial local adaptation to low salinity at germination but not at later life-history stages. *Am. J. Bot.* 107, 599–606. doi: 10.1002/ajb2.1456

Kayihan, D. S., Aksoy, E., and Kayihan, C. (2021). Identification and expression profiling of toxic boron-responsive microRNAs and their targets in sensitive and tolerant wheat cultivars. *Turkish J. Agric. And Forestry* 45, 411–433. doi: 10.3906/tar-2102-5

Khan, F. S., Gan, Z. M., Li, E. Q., Ren, M. K., Hu, C. G., and Zhang, J. Z. (2022). Transcriptomic and physiological analysis reveals interplay between salicylic acid and drought stress in citrus tree floral initiation. *Planta* 255, 24. doi: 10.1007/s00425-021-03801-2

Lastdrager, J., Hanson, J., and Smeekens, S. (2014). Sugar signals and the control of plant growth and development. *J. Exp. Bot.* 65, 799–807. doi: 10.1093/jxb/ert474

Li, B., and Dewey, C. N. (2011). RSEM: accurate transcript quantification from RNA-seq data with or without a reference genome. *BMC Bioinf.* 12, 323. doi: 10.1186/1471-2105-12-323

Li, J. M., Du, L. S., Guan, W. B., Yu, F. H., and Van Kleunen, M. (2016). Latitudinal and longitudinal clines of phenotypic plasticity in the invasive herb *Solidago canadensis* in China. *Oecologia* 182, 755–764. doi: 10.1007/s00442-016-3699-x

Li, Y. R. Z., Wang, M. D., Teng, K., Dong, D., Liu, Z. C., Zhang, T. J., et al. (2022). Transcriptome profiling revealed candidate genes, pathways and transcription factors related to nitrogen utilization and excessive nitrogen stress in perennial ryegrass. *Sci. Rep.* 12, 3353. doi: 10.1038/s41598-022-07329-7

Liao, L., Dong, T. T., Qiu, X., Rong, Y., Sun, G. C., Wang, Z. H., et al. (2019). Antioxidant enzyme activity and growth responses of *Huangguogan citrus* cultivar to nitrogen supplementation. *Biosci. Biotechnol. Biochem.* 83, 1924–1936. doi: 10.1080/09168451.2019.1634513

Liu, X. S., Cai, J. F., Liu, L., Sun, K., Jiang, F., Shen, Y. L., et al. (2022). Nitrogen addition frequency and propagule pressure influence *Solidago canadensis* invasion into native plant community. *Ecosyst. Health Sustainability*, 8:1, 2052763. doi: 10.1080/20964129.2022.2052763

Liu, Y. J., Liu, M., Xu, X. L., Tian, Y. Q., Zhang, Z., and Van Kleunen, M. (2018b). The effects of changes in water and nitrogen availability on alien plant invasion into a stand of a native grassland species. *Oecologia* 188, 441–450. doi: 10.1007/s00442-018-4216-1

Liu, Y. J., Oduor, A. M. O., Zhang, Z., Manea, A., Tooth, I. M., Leishman, M. R., et al. (2017). Do invasive alien plants benefit more from global environmental change than native plants? *Global Change Biol.* 23, 3363–3370. doi: 10.1111/gcb.13579

Liu, Y. Y., Sun, Y., Muller-Scharer, H., Yan, R., Zhou, Z. X., Wang, Y. J., et al. (2019). Do invasive alien plants differ from non-invasives in dominance and nitrogen uptake in response to variation of abiotic and biotic environments under global anthropogenic change? *Sci. Total Environ.* 672, 634–642. doi: 10.1016/j.scitotenv.2019.04.024

Liu, G., Yang, Y. B., and Zhu, Z. H. (2018a). Elevated nitrogen allows the weak invasive plant *Galinsoga quadriradiata* to become more vigorous with respect to inter-specific competition. *Sci. Rep.* 8, 3136. doi: 10.1038/s41598-018-21546-z

Liu, Z., Yu, H. W., Sun, X., and Ding, J. Q. (2022). Effects of elevated temperature on chemistry of an invasive plant, its native congener and their herbivores. *J. Plant Ecol.* 15, 450–460. doi: 10.1093/jpe/rtab013

Liu, X. J., Zhang, Y., Han, W. X., Tang, A. H., Shen, J. L., Cui, Z. L., et al. (2013). Enhanced nitrogen deposition over China. *Nature* 494, 459–462. doi: 10.1038/nature11917

Luo, X., Xu, X. Y., Zheng, Y., Guo, H., and Hu, S. J. (2019). The role of phenotypic plasticity and rapid adaptation in determining invasion success of *Plantago virginica*. *Biol. Invasions* 21, 2679–2692. doi: 10.1007/s10530-019-02004-x

Luo, X., Zheng, Y., Xu, X. H., Xiao, R., and Guo, H. (2020). The impacts of warming and nitrogen addition on competitive ability of native and invasive populations of *Plantago virginica*. *J. Plant Ecol.* 13, 676–682. doi: 10.1093/jpe/rtaa055

Mao, Q. G., Lu, X. K., Wang, C., Zhou, K. J., and Mo, J. M. (2017). Responses of understory plant physiological traits to a decade of nitrogen addition in a tropical reforested ecosystem. *For. Ecol. Manage.* 401, 65–74. doi: 10.1016/j.foreco.2017.06.047

Mattingly, W. B., and Reynolds, H. L. (2014). Soil fertility alters the nature of plant-resource interactions in invaded grassland communities. *Biol. Invasions* 16, 2465–2478. doi: 10.1007/s10530-014-0678-1

Merow, C., Bois, S. T., Allen, J. M., Xie, Y., and Silander, J. A. (2017). Climate change both facilitates and inhibits invasive plant ranges in new England. *Proc. Natl. Acad. Sci.* 114, E3276–E3284. doi: 10.1073/pnas.1609633114

Midolo, G., Alkemade, R., Schipper, A. M., Benitez-Lopez, A., Perring, M. P., and De Vries, W. (2019). Impacts of nitrogen addition on plant species richness and abundance: A global meta-analysis. *Global Ecol. Biogeogr.* 28, 398–413. doi: 10.1111/geb.12856

Nguyen, M. A., Ortega, A. E., Nguyen, K. Q., Kimball, S., Goulden, M. L., and Funk, J. L. (2016). Evolutionary responses of invasive grass species to variation in precipitation and soil nitrogen. *J. Ecol.* 104, 979–986. doi: 10.1111/1365-2745.12582

Nolf, M., Pagitz, K., and Mayr, S. (2014). Physiological acclimation to drought stress in *Solidago canadensis*. *Physiol. Plantarum* 150, 529–539. doi: 10.1111/ppl.12100

Oduor, A. M. O. (2022). Native plant species show evolutionary responses to invasion by *Parthenium hysterophorus* in an *African savanna*. *New Phytol.* 233, 983–994. doi: 10.1111/nph.17574

Oduor, A. M. O., Adomako, M. O., Yuan, Y., and Li, J.-M. (2022). Older populations of the invader *Solidago canadensis* exhibit stronger positive plant-soil feedbacks and competitive ability in China. *Am. J. Bot.* 109, 1230–1241. doi: 10.1002/ajb2.16034

Panda, S., Kazachkova, Y., and Aharoni, A. (2021). Catch-22 in specialized metabolism: balancing defense and growth. *J. Exp. Bot.* 72, 6027–6041. doi: 10.1093/jxb/erab348

Parepa, M., Fischer, M., and Bossdorf, O. (2013). Environmental variability promotes plant invasion. *Nat. Commun.* 4, 1604. doi: 10.1038/ncomms2632

Payne, R. J., Dise, N. B., Field, C. D., Dore, A. J., Caporn, S. J. M., and Stevens, C. J. (2017). Nitrogen deposition and plant biodiversity: past, present, and future. *Front. Ecol. Environ.* 15, 431–436. doi: 10.1002/fee.1528

Peng, Y., Yang, J. X., Zhou, X. H., Peng, P. H., Li, J. J., Zhang, S. M., et al. (2019). An invasive population of *Solidago canadensis* is less sensitive to warming and nitrogen-addition than its native population in an invaded range. *Biol. Invasions* 21, 151–162. doi: 10.1007/s10530-018-1812-2

Pysek, P., Jarosik, V., Hulme, P. E., Pergl, J., Hejda, M., Schaffner, U., et al. (2012). A global assessment of invasive plant impacts on resident species, communities and ecosystems: the interaction of impact measures, invading species' traits and environment. *Global Change Biol.* 18, 1725–1737. doi: 10.1111/j.1365-2486.2011.02636.x

Qu, R. J., Cao, Y. W., Zhang, H. B., Miao, Y. J., Wei, L., Tang, X. Q., et al. (2021). Transcriptome analysis of nitrogen metabolism, transcription factors, and indigoid biosynthesis in *Isatis indigotica* fort. response to nitrogen availability. *J. Plant Growth Regul.* 40, 1181–1197. doi: 10.1007/s00344-020-10178-1

Questad, E. J., Fitch, R. L., Paolini, J., Hernandez, E., and Suding, K. N. (2021). Nitrogen addition, not heterogeneity, alters the relationship between invasion and native decline in *California grasslands*. *Oecologia* 197, 651–660. doi: 10.1007/s00442-021-05049-9

Quinet, M., Vromman, D., Clippe, A., Bertin, P., Lequeux, H., Dufey, I., et al. (2012). Combined transcriptomic and physiological approaches reveal strong differences between short- and long-term response of rice (*Oryza sativa*) to iron toxicity. *Plant Cell Environ.* 35, 1837–1859. doi: 10.1111/j.1365-3040.2012.02521.x

Ren, G. Q., Yang, H. Y., Li, J., Prabakaran, K., Dai, Z. C., Wang, X. P., et al. (2020). The effect of nitrogen and temperature changes on *Solidago canadensis* phenotypic plasticity and fitness. *Plant Species Biol.* 35, 283–299. doi: 10.1111/1442-1984.12280

Ribeiro, P. C. D., Menendez, E., Da Silva, D. L., Bonieck, D., Ramirez-Bahena, M. H., Resende-Stoianoff, M. A., et al. (2017). Invasion of the Brazilian campo rupestre by the exotic grass *Melinis minutiflora* is driven by the high soil n availability and changes in the n cycle. *Sci. Total Environ.* 577, 202–211. doi: 10.1016/j.scitotenv.2016.10.162

Sandel, B., and Dangremond, E. M. (2012). Climate change and the invasion of California by grasses. *Global Change Biol.* 18, 277–289. doi: 10.1111/j.1365-2486.2011.02480.x

Seabloom, E. W., Borer, E. T., Buckley, Y. M., Cleland, E. E., Davies, K. F., Firn, J., et al. (2015). Plant species' origin predicts dominance and response to nutrient enrichment and herbivores in global grasslands. *Nat. Commun.* 6, 7710. doi: 10.1038/ncomms8710

Shao, K., Bai, Z. Q., Li, M. H., Yu, C., Shao, J. W., Sun, Y. Q., et al. (2020). Sucrose metabolism enzymes affect sucrose content rather than root weight in sugar beet (*Beta vulgaris*) at different growth stages. *Sugar Tech* 22, 504–517. doi: 10.1007/s12355-019-00781-2

Simberloff, D., Martin, J. L., Genovesi, P., Maris, V., Wardle, D. A., Aronson, J., et al. (2013). Impacts of biological invasions: what's what and the way forward. *Trends Ecol. Evol.* 28, 58–66. doi: 10.1016/j.tree.2012.07.013

Sun, K., Cai, J. F., Zhang, Y., Mu, Y. N., Si-Ha, A., Shen, Y. L., et al. (2022). Heterogeneous nitrogen supply with high frequency and ramet damage increases the benefits of clonal integration in invasive *Hydrocotyle vulgaris*. *Front. Plant Sci.* 13, 825492. doi: 10.3389/fpls.2022.825492

Sun, Y. M., Guo, J. J., Li, Y. R., Luo, G. W., Li, L., Yuan, H. Y., et al. (2020). Negative effects of the simulated nitrogen deposition on plant phenolic metabolism: A meta-analysis. *Sci. Total Environ.* 719, 137442. doi: 10.1016/j.scitotenv.2020.137442

Sun, Y. M., Hou, M. L., Mur, L., Yang, Y. H., Zhang, T., Xu, X. Y., et al. (2019). Nitrogen drives plant growth to the detriment of leaf sugar and steviol glycosides metabolisms in stevia (*Stevia rebaudiana* bertoni). *Plant Physiol. Biochem.* 141, 240–249. doi: 10.1016/j.plaphy.2019.06.008

Szymura, M., and Szymura, T. H. (2013). Soil preferences and morphological diversity of goldenrods (*Solidago* l.) from south-western Poland. *Acta Societatis Botanicorum Poloniae* 82, 107–115. doi: 10.5586/asbp.2013.005

Uddin, M. N., and Robinson, R. W. (2018). Can nutrient enrichment influence the invasion of *Phragmites australis*? *Sci. Total Environ.* 613, 1449–1459. doi: 10.1016/j.scitotenv.2017.06.131

Vallano, D. M., Selmants, P. C., and Zavaleta, E. S. (2012). Simulated nitrogen deposition enhances the performance of an exotic grass relative to native serpentine grassland competitors. *Plant Ecol.* 213, 1015–1026. doi: 10.1007/s11258-012-0061-1

Wan, L. Y., Qi, S. S., Dai, Z. C., Zou, C. B., Song, Y. G., Hu, Z. Y., et al. (2018). Growth responses of Canada goldenrod (*Solidago canadensis* l.) to increased nitrogen supply correlate with bioavailability of insoluble phosphorus source. *Ecol. Res.* 33, 261–269. doi: 10.1007/s11284-017-1552-2

Wan, L. Y., Qi, S. S., Zou, C. B., Dai, Z. C., Ren, G. Q., Chen, Q., et al. (2019). Elevated nitrogen deposition may advance invasive weed, *Solidago canadensis*, in calcareous soils. *J. Plant Ecol.* 12, 846–856. doi: 10.1093/jpe/rtz019

Wang, W. X., Shen, C. C., Xu, Q., Zafar, S., Du, B., and Xing, D. Y. (2022). Grain yield, nitrogen use efficiency and antioxidant enzymes of rice under different fertilizer n inputs and planting density. *Agronomy-Basel* 12, 430. doi: 10.3390/agronomy12020430

Wang, C. Y., Zhou, J. W., Liu, J., and Jiang, K. (2017). Differences in functional traits between invasive and native *Amaranthus* species under different forms of n deposition. *Sci. Nat.* 104, 59. doi: 10.1007/s00114-017-1482-4

Wu, M., Ge, Y. M., Xu, C. C., and Wang, J. B. (2020a). Metabolome and transcriptome analysis of hexaploid *Solidago canadensis* roots reveals its invasive capacity related to polyploidy. *Genes* 11, 187. doi: 10.3390/genes11020187

Wu, M., Li, Z., and Wang, J. (2020b). Transcriptional analyses reveal the molecular mechanism governing shade tolerance in the invasive plant *Solidago canadensis*. *Ecol. Evol.* 10, 4397–4406. doi: 10.1002/ece3.6206

Wu, M., Liu, H. Y., Li, B. B., and Zhu, T. (2021). Integrated analysis of mRNA-seq and miRNA-seq reveals the advantage of polyploid *Solidago canadensis* in sexual reproduction. *BMC Plant Biol.* 21, 462. doi: 10.1186/s12870-021-03240-x

Ye, X. Q., Yan, Y. N., Wu, M. , and Yu, F. H. (2019). High capacity of nutrient accumulation by invasive *Solidago canadensis* in a coastal grassland. *Front. Plant Sci.* 10, 575. doi: 10.3389/fpls.2019.00575

Yu, G. R., Jia, Y. L., He, N. P., Zhu, J. X., Chen, Z., Wang, Q. F., et al. (2019). Stabilization of atmospheric nitrogen deposition in China over the past decade. *Nat. Geosci.* 12, 424–429. doi: 10.1038/s41561-019-0352-4

Zandalinas, S. I., Balfagon, D., Gomez-Cadenas, A., and Mittler, R. (2022). Plant responses to climate change: metabolic changes under combined abiotic stresses. *J. Exp. Bot.* 73, 3339–3354. doi: 10.1093/jxb/erac073

Zhang, Y. L., Leng, Z. R., Wu, Y. M., Jia, H., Yan, C. L., Wang, X. H., et al. (2022). Interaction between nitrogen, phosphorus, and invasive alien plants. *Sustainability* 14, 746. doi: 10.3390/su14020746

Zhang, L. H., Sun, S. M., Liang, Y. H., Li, B. Y., Ma, S. Y. , Wang, Z. Y., et al. (2021). Nitrogen levels regulate sugar metabolism and transport in the shoot tips of crabapple plants. *Front. Plant Sci.* 12, 626149. doi: 10.3389/fpls.2021.626149

Zhong, G., Wu, Z., Yin, J., and Chai, L. (2017). Responses of *Hydrilla verticillata* (L.f.) royle and *Vallisneria natans* (Lour.) hara to glyphosate exposure. *Chemosphere* 193, 385–393. doi: 10.1016/j.chemosphere.2017.10.173

Zhu, J. H., Qi, J. Y., Fang, Y. J., Xiao, X. H., Li, J. H. , Lan, J. X., et al. (2018). Characterization of sugar contents and sucrose metabolizing enzymes in developing leaves of *Hevea brasiliensis*. *Front. Plant Sci.* 9, 58. doi: 10.3389/fpls.2018.00058

frontiers | Frontiers in Plant Science

TYPE Original Research
PUBLISHED 23 March 2023
DOI 10.3389/fpls.2023.1125245

Check for updates

OPEN ACCESS

EDITED BY
Girdhar Kumar Pandey,
University of Delhi, India

REVIEWED BY
Haihui Fu,
Jiangxi Agricultural University, China
Yuhua Wang,
Nanjing Agricultural University, China

*CORRESPONDENCE
Qibin Ma
maqibin@scau.edu.cn
Aixia Zhang
907265887@qq.com

†These authors have contributed equally to this work

SPECIALTY SECTION
This article was submitted to Plant Physiology, a section of the journal Frontiers in Plant Science

RECEIVED 16 December 2022
ACCEPTED 28 February 2023
PUBLISHED 23 March 2023

CITATION
Wang H, Li C, Wang L, Zhong H, Xu X, Cheng Y, Nian H, Liu W, Chen P, Zhang A and Ma Q (2023) *GmABR1* encoding an ERF transcription factor enhances the tolerance to aluminum stress in *Arabidopsis thaliana*. *Front. Plant Sci.* 14:1125245. doi: 10.3389/fpls.2023.1125245

COPYRIGHT
© 2023 Wang, Li, Wang, Zhong, Xu, Cheng, Nian, Liu, Chen, Zhang and Ma. This is an open-access article distributed under the terms of the Creative Commons Attribution License (CC BY). The use, distribution or reproduction in other forums is permitted, provided the original author(s) and the copyright owner(s) are credited and that the original publication in this journal is cited, in accordance with accepted academic practice. No use, distribution or reproduction is permitted which does not comply with these terms.

GmABR1 encoding an ERF transcription factor enhances the tolerance to aluminum stress in *Arabidopsis thaliana*

Hongjie Wang[1,2,3,4,5†], Cheng Li[1,2,3,4,5†], Lidan Wang[1,2,3,4,5], Hongying Zhong[1,2,3,4,5], Xin Xu[1,2,3,4,5], Yanbo Cheng[1,2,3,4,5], Hai Nian[1,2,3,4,5], Wenhua Liu[6], Pei Chen[6], Aixia Zhang[6*] and Qibin Ma[1,2,3,4,5*]

[1]The State Key Laboratory for Conservation and Utilization of Subtropical Agro-bioresources, South China Agricultural University, Guangzhou, China, [2]The Guangdong Province Key Laboratory of Plant Molecular Breeding, College of Agriculture, South China Agricultural University, Guangzhou, China, [3]The Guangdong Subcenter of the National Center for Soybean Improvement, College of Agriculture, South China Agricultural University, Guangzhou, China, [4]The Guangdong Provincial Laboratory of Lingnan Modern Agricultural Science and Technology, South China Agricultural University, Guangzhou, China, [5]Zengcheng Teaching and Research Bases, South China Agricultural University, Guangzhou, Guangdong, China, [6]Agro-biological Gene Research Center, Guangdong Academy of Agricultural Sciences, Guangzhou, Guangdong, China

The ethylene response factor (ERF) transcription factors, which is one of the largest transcription factor families in plants, are involved in biological and abiotic stress response and play an important role in plant growth and development. In this study, the *GmABR1* gene from the soybean inbred line Zhonghuang24 (ZH24)×Huaxia 3 (HX3) was investigated its aluminum (Al) tolerance. GmABR1 protein has a conserved domain AP2, which is located in the nucleus and has transcriptional activation ability. The results of real-time quantitative PCR (qRT-PCR) showed that the *GmABR1* gene presented a constitutive expression pattern rich in the root tip, stem and leaf tissues of HX3. After Al stress, the *GmABR1* transcript was significantly increased in the roots. The transcripts of *GmABR1* in the roots of HX3 treated with 50 μM $AlCl_3$ was 51 times than that of the control. The *GmABR1* was spatiotemporally specific with the highest expression levels when Al concentration was 50 μM, which was about 36 times than that of the control. The results of hematoxylin staining showed that the root tips of *GmABR1*-overexpression lines were stained the lightest, followed by the control, and the root tips of *GmABR1* RNAi lines were stained the darkest. The concentrations of Al^{3+} in root tips were 207.40 μg/g, 147.74 μg/g and 330.65 μg/g in wild type (WT), overexpressed lines and RNAi lines, respectively. When $AlCl_3$ (pH4.5) concentration was 100 μM, all the roots of Arabidopsis were significantly inhibited. The taproot elongation of WT, *GmABR1* transgenic lines was 69.6%, 85.6%, respectively. When treated with Al, the content of malondialdehyde (MDA) in leaves of WT increased to 3.03 μg/g, while that of transgenic Arabidopsis increased from 1.66-2.21 μg/g, which was lower than that of WT. Under the Al stress, the Al stress responsive genes such as *AtALMT1* and *AtMATE*, and the

genes related to ABA pathway such as *AtABI1*, *AtRD22* and *AtRD29A* were up-regulated. The results indicated that *GmABR1* may jointly regulate plant resistance to Al stress through genes related to Al stress response and ABA response pathways.

KEYWORDS

***GmABR1*, soybean, Al stress, transgenic *Arabidopsis thaliana*, transcription factor**

1 Introduction

Aluminum (Al) third only to oxygen and silicon is one of the most abundant metallic elements in the earth's crust. When the soil pH is below 5.5, Al is mainly present in the form of Al^{3+} which is highly toxic to plants (Ranjan et al., 2021). Approximately 50% of the world's arable soils are acidic, and Al toxicity is a major factor limiting crop yields under abiotic stress in acidic soils (Kochian et al., 2015). The Al absorbed by plants is first concentrated in the root tips. Previous studies have found that the Al^{3+} content of root tip meristem in Al-tolerant plants is generally lower than that of Al-sensitive plants (Rangel et al., 2009). After some heavy metal ions enter root cells of plants, enzyme activity is inhibited and plant metabolism is blocked (Chen, 2006). The elongation and division of root tip cells were severely inhibited under the action of Al^{3+}. The root tip enlargement, main root coarsening and shortening, lateral root number decreased correspondingly. The photosynthesis of leaves was inhibited with yellowing and curling shape, and smaller leaf area (Chauhan et al., 2021). The root changes of plants may be due to the inhibition of cellulose synthesis in root tip cell wall by Al^{3+} (Matsumoto and Motoda, 2012). Plants exposed to Al for a long time will be inhibited the absorption of water and other nutrients in their roots resulting in plant production and even death (Zhang et al., 2019a).

AP2/ERF transcription factors play an important role in plant abiotic stress. They can specifically bind *cis*-elements in the promoter region of downstream defense genes including activating or inhibiting the expression of downstream stress-responsive genes through positive and negative regulation, and thus participate in the response to plant stress (Kumar and Sharma, 2021). The AP2/ERF transcription factor contains one or two conserved AP2/ERF domains consisting of approximately 58-70 amino acids which are involved in DNA binding (Li et al., 2022). The AP2/ERF domain consists of three β folds and one amphiphilic α helix. There are differences between the two amino acid residues at position 14 and 19 in the second β fold, which makes the AP2/ERF transcription factor specific to bind different *cis*-acting elements (Feng et al., 2020).

The AP2/EREBP transcription factor OPBP1 can regulate the expression of stress-related genes. The overexpression of *OPBP1* in tobacco plants showed strong resistance to *Pseudomonas syringae*pv *tabaci* and *Phytophthora parasiticavar nicotianae* pathogens, and improved the resistance to salt stress (Guo et al., 2004). Soybean gene *GmERF5* was involved in the response to *Phytophthora sojae* infection. The tolerance of transgenic lines to *Phytophthora sojae* infection was significantly improved compared with the control. *GmERF5* was significantly induced. While its promoter activity was activated under the treatments of ethylene (ET), abscisic acid (ABA), *Phytophthora sojae*, salt and drought. The results suggested that *GmERF5* was not only involved in the induced defense response but also involved in ABA-mediated pathways of salt and drought tolerance (Dong et al., 2015). In rice, *OsERF922* was rapidly and strongly up-regulated by ABA, salt and blast fungus. *OsERF922* knockout by RNAi enhanced rice resistance to *magnaporthe oryzae* and increased the expression of several genes regulating plant stress resistance synthase. In contrast, plants that overexpressed *OsERF922* reduced the expression of these defense-related genes and increased susceptibility to *magnaporthe oryzae*. The ABA content of *OsERF922* overexpressed rice was significantly higher than that of control and RNAi lines. *NCED3* and *NCED4* were up-regulated in *OsERF922* overexpressed plants, while *NCED4* was down-regulated in RNAi lines. *OsERF922* may enhance plant resistance to abiotic stress by participating in the ABA pathway (Liu et al., 2012). Abscisic acid repressor ABR1, a member of ethylene responsive element binding factor superfamily of AP2/ERF transcription factors, significantly improves drought resistance of rice, crop quality and yield (Pandey et al., 2005). *Fagopyrum esculentum* can cope with aluminum toxicity by increasing ABA level and antioxidant system in early growth and development. The levels of reactive oxygen species (ROS), endogenous ABA and antioxidant enzyme activity in root of buckwheat seedlings increased after aluminum treatment, which may be mediated by increased ABA levels. After ABA treatment, ROS levels increased, catalase (CAT) and ascorbate peroxidase (APX) activities increased (Salazar-Chavarria et al., 2020). *OsERF71* plays a positive role in drought tolerance of rice by increasing the expression of genes related to ABA signaling pathway and proline synthesis. Overexpression of *OsERF71* decreased the water loss rate of rice, while the RNAi lines of *OsERF71* were sensitive to drought stress and increased the water loss rate. Under drought stress, *OsERF71* regulated the expression of several ABA responsive genes and proline synthesis genes, enhanced the sensitivity and proline accumulation of ABA treatment. *GsERF71* overexpressing Arabidopsis has significantly higher tolerance to carbonate stress induced by $NaHCO_3$ or $KHCO_3$ than that of wild-type plants with greener leaves, longer roots, higher chlorophyll content and lower

MDA content. *GsERF71* increased the tolerance to alkaline stress by up-regulating H^+, ATPase expression and regulating auxin accumulation in transgenic plants (Yu et al., 2017). SHINE (SHN) transcription factor is a branch of AP2/ERF and one of the first reported transcription factors to regulate plant cuticle formation. Cuticle plays an important role in improving plant abiotic stress, such as drought resistance, high temperature resistance, salt resistance, disease resistance (Khoudi, 2023). Recent study showed that the *GsERF1* gene from BW69 wild soybean was induced by aluminum stress and ethylene (Li et al., 2022).

The quality and yield of soybean are greatly affected and limited by acidic soil in a large area of the world. In the past, there were a few reports on the involvement of ERF family genes in Al tolerance in plants. In this study, the ethylene reactive transcription factor *GmABR1* of AP2/ERF family gene was identified using the population of recombinant inbred line derived from Zhonghuang 24 (ZH24) × Huaxia 3 (HX3), and its function tolerant to Al stress was investigated by heterotransformation of Arabidopsis.

2 Materials and methods

2.1 Plant materials and growth conditions

In this experiment, the HX3 soybean cultivar was bred and provided by the Guangdong Subcenter of National Soybean Improvement Center. The tissue expression pattern of *GmABR1* and its response to Al stress were studied using qRT-PCR. The seeds of HX3 were germinated on vermiculite after high temperature sterilization. The culture temperature was 26 °C and the light/darkness was 16 h/8 h (Wang et al., 2019a). The cultures were incubated in 0.5 mM $CaCl_2$ solution (containing 50 μM $AlCl_3$) for 0, 3, 6, 9, 12, 24, 36, 48, 60 and 72 h. With the incubation in 0.5 mM $CaCl_2$ with 0, 25, 50, 75, or 100 μM $AlCl_3$ (pH4.5) for 24 h, all the roots of soybean are taken as samples in Al dose-effect experiments (Han et al., 2022). For tissue expression pattern, the samples of roots, stems, and leaves of soybean seedlings incubated in 0.5 mM $CaCl_2$ (50 μM $AlCl_3$ (pH4.5) for the experimental group, without $AlCl_3$ for the control group) for 60 h were taken and rapidly frozen in liquid nitrogen, and stored at -80°C (Wang et al., 2022).

2.2 Bioinformatics analysis and cloning of the *GmABR1* gene

The *GmABR1* gene in soybean cultivar HX3 was up-regulated in the expression profile of acid-resistant aluminum genes, and the login number on the website of the National Center for Biotechnology Information (NCBI) was XP_003523249.1 by using the NCBI database for searching for the sequence information of the candidate gene. The software DNAMAN 9.0 was used for sequence alignment, phylogenetic tree was constructed by proximity method (NJ) using MAGE 7.0 software (Shu et al., 2022). The total RNA of soybean cultivar HX3 extracted by *Trizol* solution (Vazyme Biotech Co., Ltd., Nanjing, China) was reverse-transcribed into cDNA (HiScript® III RT SuperMix for qPCR, Vazyme Biotech Co., Ltd.; Nanjing, China) (Wang et al., 2022). The full-length of *GmABR1* gene was cloned by using specific primers and high-fidelity DNA polymerase (Phanta Max, Vazyme Biotech Co., Ltd.; Nanjing, China) (Table S2). PCR products were detected by 1% agarose gel electrophoresis (GenStar Kit, GenStar Development Company, Calgary, AB, Canada), and the purified PCR products were inserted into the polyclonal site of the zero-background clone pLB vector (Tiangen Lethal Based Fast Cloning Kit, Beijing, China). The fusion vector GmABR1-pLB was transformed into *Escherichia coli* DH5α (Li et al., 2022). The positive clones of *GmABR1* gene were identified by PCR and enzyme digestion, and the CDS sequence of *GmABR1* gene was obtained by sequencing [Sangon Biotech (Shanghai) Co., Ltd., China] (Wen et al., 2021).

2.3 Construction of *GmABR1* overexpression vector and genetic transformation of Arabidopsis

Using the constructed pLB plasmid as DNA template, the CDS sequence of *GmABR1* amplified by PCR was inserted between the restriction sites of *Xba*I and *Sac*I from the vector pTF101 by using the ClonExpressR II One Step Cloning Kit (C112, Vazyme, Nanjing, China) to construct the vector pTF101-GmABR1. The positive clones of pTF101-GmABR1 were identified by PCR using specific primers. The pTF101-GmABR1 plasmid was transformed into *agrobacterium tumefaciens* GV3101 cells by heat shock method (Li et al., 2022). Genetic transformation of Arabidopsis was subsequently performed using agrobacterium-mediated flower impregnation (Han et al., 2022). After the obtained transgenic plants were identified, the T_3 transgenic positive lines with high expression of *GmABR1* in root tip were selected for subsequent experiments including the analysis of its expression patterns response to Al stress and the phenotypes resistant to Al stress (Liu et al., 2020). The primer information used in this experiment was shown in Table S2.

2.4 Subcellular localization of GmABR1 protein

The subcellular localization of GmABR1 protein was analyzed using the method described by Collings et al. and Dong et al. (Collings, 2013; Dong et al., 2015). The subcellular localization of GmABR1 protein was predicted using a web server Cell-PLoc 2.0 (http://www.csbio.sjtu.edu.cn/bioinf/Cell-PLoc-2/). The specific operation is to cut the *Nco*I and *Spe*I sites on the expression vector pCAMBIA1302-eGFP with restriction endonuclease, and to link the recombinant amplified fragments of CDS sequences containing corresponding restriction sites with T4 ligase. After the construction of the fusion expression vector, the plasmid pCAMBIA1302-eGFP-GmABR1 and the empty plasmid pCAMBIA1302-eGFP were transformed into the cells of *Agrobacterium tumefaciens* GV3101 (contain the virus protein P19) and then injected into the lower epidermal cells of 4-week-

old leaf in *Nicotiana tabacum*. The transformed leaves for 48 hours were observed with a laser confocal microscope (Carl Zeiss, Jena, Germany).

2.5 Transactivation assay of GmABR1 protein

The activation activity of GmABR1 protein was verified by using the method described by Han et al. (Han et al., 2022). The full-length sequence of *GmABR1* was first cloned and inserted it into the *Bam*HI and *Eco*RI restriction endonuclease sites of pGBKT7 vector to form the fusion expression vector pGBKT7-GmABR1. The vectors of pGBKT7 and pGBKT7-GmABR1 were then transformed into yeast Y_2H strain, respectively. The transformed yeast cells were cultured on SD medium which was lacking Trp (SD/-Trp) at 30 °C for 3 days. Then the positive colonies were transferred from SD/-Trp medium to SD/-Trp medium containing 125 μg/L X-α-gal. After cultured for 3 days, whether the colonies appear blue or not can be observed on the selected medium.

2.6 Gene expression analysis by qRT-PCR

Total RNA of samples was extracted from soybean or Arabidopsis tissues using the *Trizol* solution (Vazyme Biotech Co., Ltd., Nanjing, China). qRT-PCR and first strand cDNA synthesis templates were performed with 1 μg of RNA using the HiScriptII first strand cDNA synthesis kit (Vazyme Biotech Co., Ltd., Nanjing, China) (Cai et al., 2018). qRT-PCR was performed using SYBR PremixEx-Taq^{TM} II (Takara Bio Inc., Kusatsu, Japan) and real-time CFX96TM systems (Bio-Rad, Hercules, CA, USA) to detect RNA transcripts of related genes (Wang et al., 2022). The inner reference gene *Actin3* in soybean was used to normalize the data. The expression data were calculated using the comparative cycle threshold method $2^{-\triangle\triangle ct}$. The experiments were repeated at three independent organisms (Xian et al., 2020). The primers used in this assay were listed in Table S2.

2.7 Phenotypic analysis of root growth in Arabidopsis treated with Al

Three homozygous lines from T_3 generation of *GmABR1* transgenic plants were used to measure taproot length as described previously (Yokosho et al., 2016; Li et al., 2022). The seeds of *GmABR1* transgenic Arabidopsis and WT were disinfected with 10% sodium hypochlorite for 10 min respectively, during which they were vortically oscillated, and then cleaned with sterilized water for 5 times. The sterilized seeds were sown on a square plate of 1/2 MS solid medium (pH5.8), placed in a refrigerator at 4°C and vernalized at low temperature for 3-4 d. Then the seeds were germinated and grown in the growth chamber with following conditions: 23°C, 60% relative humidity, 100 mol photons $m^{-2}{\cdot}s^{-1}$, 16 h light and 8 h dark cycles. When root lengths of the seedlings grew to 1-2 cm, the seedlings were selected and transferred to the medium containing different concentrations of $AlCl_3$ (0, 25, 50 and 100 μM; pH 4.5). Phenotypic differences were observed and photographed after 3 days of Al treatment. The data were analyzed by using the software Image J (Zhou et al., 2008).

2.8 Soybean hairy root transformation and hematoxylin staining

The construction of pMU103-GmABR1 interference vector (RNAi vector) is similar to the previous construction method (Kereszt et al., 2007; Ren et al., 2019). The 159 bp coding region sequence of *GmABR1* gene was selected to construct the interference vector. The vector plasmids of pTF101, pTF101-GmABR1, pMU103-GmABR1 were transformed into *Agrobacterium rhizogenes* K599 competent cells by heat shock, respectively. Soybean hair roots from the 5-day's seedlings were used as experimental materials, and then transformed by the method of hypocotyl injection.

In order to analyze the expression of *GmABR1* gene in soybean hairy roots, the hairy root lines were treated with 50 μM $AlCl_3$ solution ($CaCl_2$, pH 4.5) for 6 h, then the roots were cut and dipped into hematoxylin solution for 30 min. The stained roots were taken out and rinsed for 30 min before being observed under stereomicroscope (Li et al., 2022).

2.9 Physiological indices assay

Transgenic *GmABR1* Arabidopsis and WT were treated with 0.5 mM $CaCl_2$ solution containing 50 μM $AlCl_3$ and 0.5 mM $CaCl_2$ solution without $AlCl_3$ (pH 4.5), respectively. After 10 days, the whole plant samples were taken to determine the content of MDA (Choudhury and Sharma, 2014).

The hairy root lines transferred into pTF101 plasmid were used as control. The roots of WT, *GmABR1*-overexpressed soybean and *GmABR1*-RNAi soybean were transferred to 0.5 mM $CaCl_2$ solution (pH 4.5) containing 50 μM $AlCl_3$. After 1 day of treatment, the root tips of 2 cm washed with ddH_2O were taken as samples, weighed and recorded. Put 2 M hydrochloric acid (HCl) into a 2 ml EP tube and soak it in a shaking table for 3-4 days. After extraction and filtration, the content of Al^{3+} in soybean hairy roots was determined by plasma inductances coupled (Umemura et al., 2003).

2.10 Statistical analyses

Each experiment was designed at least three biological replicates. The SPSS Statistics (v.22) and GraphPad Prism 8 softwares were used to analyze and process the data. The statistical significance of the difference for the data was indicated by an asterisk ($^*P < 0.05$; $^{**}P < 0.01$) (Ma et al., 2018; Wang et al., 2022).

10.3389/fpls.2023.1125245

3 Results

3.1 Isolation and bioinformatics analysis of *GmABR1*

The *GmABR1* gene was cloned from soybean cultivar HX3 using specific primers (Table S1). The *GmABR1* gene sequence was obtained from the National Center for Biotechnology Information (NCBI) database with the accession number LOC_100793215. The length of *GmABR1* gene was 1135 bp, and the length of open reading frame was 846 bp. It contains two exons encoding a 282 amino acid protein with an estimated molecular weight of 30.8504 KDa and isoelectric point of 10.0135. Sequence alignment revealed that GmABR1 protein had a conserved DNA-binding domain (AP2 domain) consisting of 60 amino acids between 135-194 amino acid residues, which was inferred to be a typical structure of ERF transcription factors. In plants, many ERF family genes have been reported to be closely associated with biotic and abiotic stresses. Amino acid sequence alignment and phylogenetic tree analysis showed that GmABR1 protein had the highest homology up to 93% with AtERF111 (*At5g64750*) protein in Arabidopsis (Figure 1).

3.2 Subcellular localization and transcriptional activation ability of GmABR1 protein

We detected the localization of GmABR1 protein in tobacco leaf cells. The results of confocal laser microscopy showed that GFP protein stimulated green fluorescence in the whole cell, while

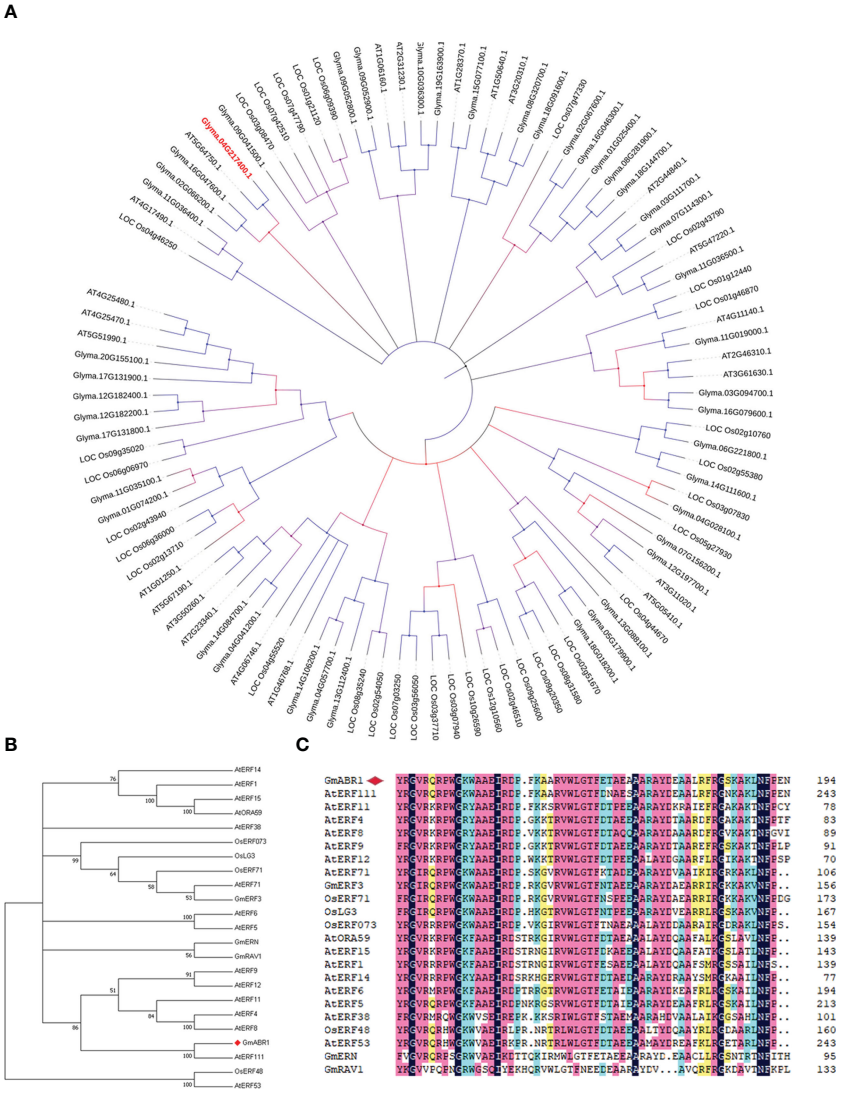

FIGURE 1
Amino acid sequence and phylogenetic analysis of ERF transcription factors. **(A)** Phylogenetic tree analysis of GmABR1 and ERF proteins in representative species of major lineage of plants. **(B)** Phylogenetic analysis of ERF proteins in higher plants. **(C)** Sequence alignment of the AP2 domain in ERF proteins of higher plants. The comparison of amino acid sequences was conducted by the software of DNAMAN9.0. The phylogenetic tree was constructed by the neighbor-joining method using the software of MEGA 7.0. The above involves the amino acid sequences of ERF family from the NCBI database (https://www.ncbi.nlm.nih.gov/). The detailed information of ERF proteins was available from the Table S3.

GmABR1-GFP fusion protein only stimulated green fluorescence in the nucleus, which overlapped with the chromophore of nuclear dye DAPI (Figure 2B). The results showed that the GmABR1 protein is localized in the nucleus.

To determine the transcriptional activity of GmABR1 protein, we combined the ORF of GmABR1 with the pGBKT7 plasmid, and simultaneously transferred the constructed fusion plasmid pGBKT7-GmABR1 and pGBKT7 vector into the receptive cells of yeast strain Y_2H. The results showed that the transformed yeast positive clones of pGBKT7-GmABR1 and pGBKT7 plasmids could grow on SD/-Trp medium. In addition, the yeast monoclonal transformed with pGBKT7-GmABR1 plasmid was blue on SD/-Trp-X-α-Gal solid medium, while the yeast monoclonal transformed with pGBKT7 vector showed no color change (Figure 2A). The results showed that GmABR1 protein had characteristic transcriptional activation.

3.3 Expression patterns of *GmABR1*

The expression pattern of *GmABR1* was studied by using the samples of roots, stems and leaves of soybean HX3. The qRT-PCR results showed that *GmABR1* was mainly expressed in stems, followed by roots and leaves without Al stress. After Al stress, the transcripts of *GmABR1* gene was significantly increased in roots, but no significant change in stems and leaves (Figure 3A). In

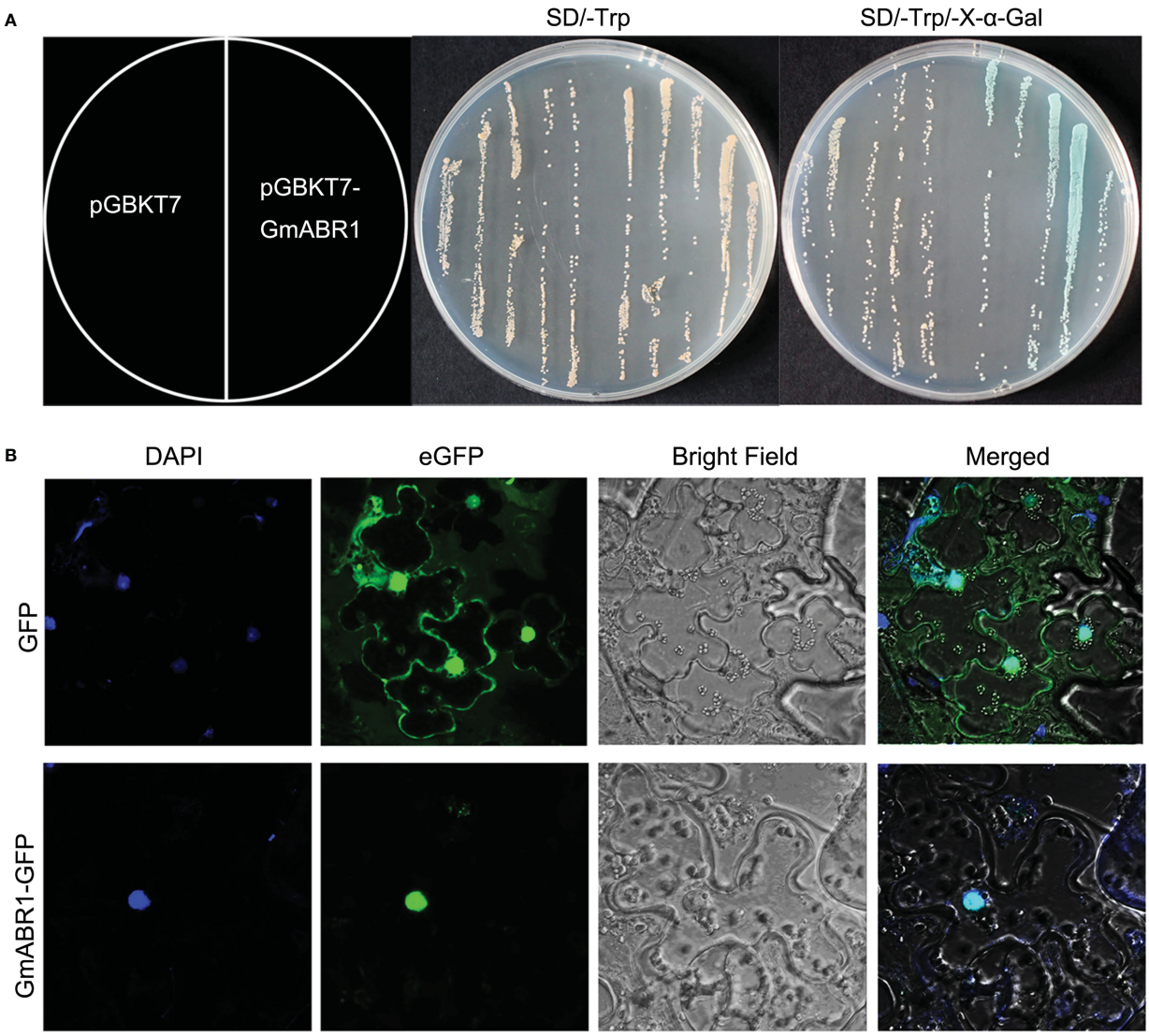

FIGURE 2
Transcriptional activity detection and subcellular localization of GmABR1 protein. **(A)** Transcriptional activation of GmABR1 protein. **(B)** Subcellular localization of GmABR1 protein. The CDS of *GmABR1* sequence was fused with the GAL4 DNA binding region of pGBKT7 vector and expressed in yeast strain Y_2H Gold. After the transformation, the two positive clones were transferred to SD/-TRP solid medium, and the other group was added with substrate X-a-Gal. The pCAMBIA1302-GFP-GmABR1 and pCAMBIA1302-GFP vectors were transformed into *Agrobacterium tumefaciens* GV3101 (contain the virus protein P19) respectively, and then injected into 4-week old *Nicotiana tabacum* L epidermal cells. After cultured for 2 days later, the leaves were observed by laser confocal microscopy (Carl Zeiss, Jena, Germany).

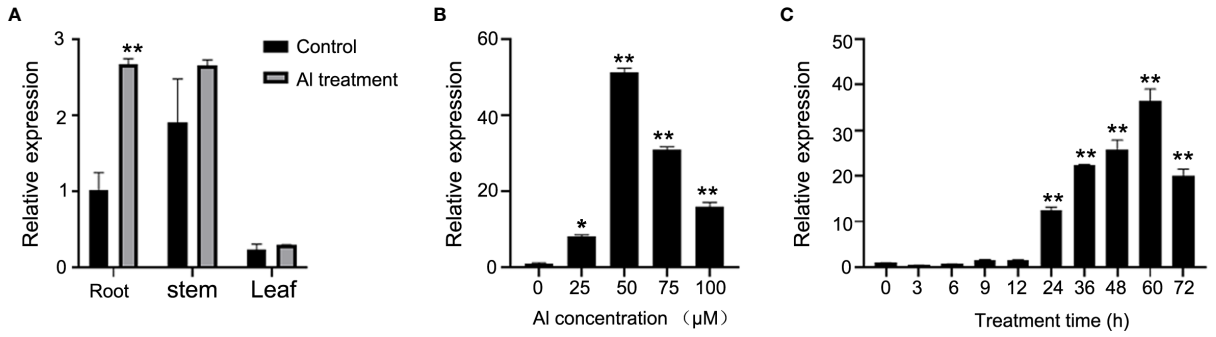

FIGURE 3
Expression pattern analysis of *GmABR1*. **(A)** Tissue expression pattern of *GmABR1*. Samples were obtained from root, stem, and leaf tissues of HX3 seedlings grown in the nutrient solutions containing 0 μM $AlCl_3$ and 50 μM $AlCl_3$, respectively. **(B)** Gene expression of *GmABR1* in the root of soybean cultivar HX3. The soybean cultivar HX3 was cultured for 24 h in the nutrient solutions containing 0, 25, 50, 75 and 100 μM $AlCl_3$, respectively. **(C)** Time course expression pattern of *GmABR1* in the root of soybean cultivar HX3. Using soybean *Actin3* as internal reference gene, three independent replicates were detected by $2^{-\triangle\triangle CT}$ method. The asterisks in figure **A** indicate significant differences between roots and other soybean tissues (*$P < 0.05$; **$P < 0.01$). The asterisk in figure B indicates that there is a significant difference between 0 μM $AlCl_3$ and other Al concentration (25, 50, 75 and 100 μM $AlCl_3$) treatment (*$P < 0.05$; **$P < 0.01$). The asterisk in figure C indicates that there is a significant difference between the Al treatment time of 0 h and the other Al treatments of 3, 6, 9, 12, 24, 36, 48, 60, 72 h (*$P < 0.05$; **$P < 0.01$).

addition, the transcripts of *GmABR1* increased first, then decreased and finally increased with the increase of Al^{3+} concentration. When treated with 50 μM $AlCl_3$, the transcripts of *GmABR1* were 51 times that of the control, while high concentration of $AlCl_3$ inhibited the expression of *GmABR1* (Figure 3B). When treated with 50 μM $AlCl_3$, the *GmABR1* transcripts increased gradually and then decreased along with time, and reached the highest level at 60 h after Al treatment, which was 36 times that of the control (Figure 3C).

3.4 Overexpression of *GmABR1* enhances Al resistance in transgenic Arabidopsis

To investigate the effect of *GmABR1* response to Al stress, *GmABR1* was overexpressed in Arabidopsis and more than 10 homozygous lines were obtained. Three lines with high *GmABR1* transcripts (L1, L4 and L9) were selected for subsequent phenotypic identification (Table S5). The results showed that there was no significant difference in taproot elongation between WT and transgenic lines without Al treatments. After $AlCl_3$ treatments, all lines were significantly inhibited. When $AlCl_3$ concentration was 100 μM, the taproot elongation of WT was 69.6%, while that of transgenic lines was 85.6%. The taproot elongation of *GmABR1* transgenic lines was significantly higher than that of WT (Figures 4A, B). With the increase of $AlCl_3$ concentration, the effect of inhibiting taproot elongation increased. Under the treatment of $AlCl_3$, the concentration of MDA in WT was 1.41 μg/g, and that in *GmABR1* transgenic Arabidopsis was 1.32 μg/g. After 50 μM $AlCl_3$ (pH 4.5) treatment, the MDA content in WT increased to 3.03 μg/g, and the MDA content in transgenic Arabidopsis leaves increased slightly up to 1.66-2.21 μg/g, which was still significantly lower than that in WT (Figure 4C).

3.5 Soybean hairy roots experiment and hematoxylin staining

The effect of *GmABR1* gene on Al stress was studied by soybean hairy roots experiment. Soybean gene *Actin3* was used as internal reference gene, and the hair root lines transformed by pTF101 vector were used as control. The transcription level of *GmABR1* in overexpressed root lines was 6.35 times that of the control, while the transcription level of *GmABR1* in RNAi lines was only 0.60 time that of the control (Figure 5A). After 50 μM $AlCl_3$ treatment, the results of hematoxylin staining showed that the overexpressed lines of *GmABR1* had the lightest root tip coloring, while the RNAi lines of *GmABR1* had the deepest root tip coloring (Figure 5B). The concentration of Al^{3+} in root tips of control, RNAi lines and overexpressed lines was 207.40 μg/g, 147.74 μg/g and 330.65 μg/g, respectively (Figure 5C). The accumulation of Al^{3+} in root tip of RNAi lines was significantly higher than that of *GmABR1*-overexpressed lines.

3.6 *GmABR1* improved the transcription level of Al stress responsive genes in Arabidopsis

To further study the response mechanism of *GmABR1* to Al stress, the relative genes including *AtALMT1*, *AtMATE*, *AtALS3*, *AtSTOP1*, *AtPGIP1* and *AtPGIP2* in Arabidopsis were identified based on previous studies. The qRT-PCR analysis showed that the expression levels of some Al stress-related genes such as *AtALMT1*, *AtMATE*, *AtALS3*, *AtSTOP1*, *AtPGIP1* and *AtPGIP2* in WT and transgenic Arabidopsis were up-regulated after 100 μM $AlCl_3$ (pH4.5) treatment. In particular, the expression levels of *AtALMT1* and *AtMATE* genes were significantly higher than

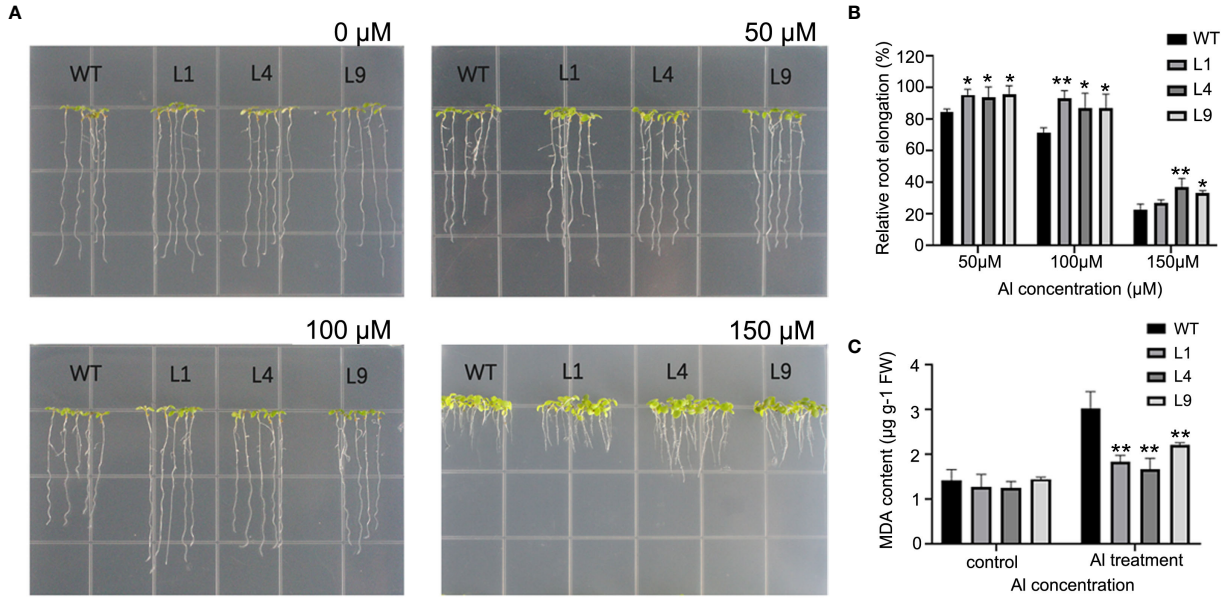

FIGURE 4
Overexpression of *GmABR1* enhances Al resistance in transgenic Arabidopsis. **(A)** Root growth of WT and *GmABR1* transgenic Arabidopsis under 0 μM, 50 μM, 100 μM, 150 μM $AlCl_3$ (pH4.5). **(B)** Relative root elongation of WT and *GmABR1* transgenic Arabidopsis. **(C)** MDA content in leaves of WT and *GmABR1* transgenic Arabidopsis. The asterisk indicated that there was significant difference between WT and *GmABR1* transgenic lines (*$P < 0.05$; **$P < 0.01$). WT: Columbia-0; L1, L4, L9: *GmABR1* transgenic lines of T_3 generation.

those before aluminum treatment, which were 2.9 times and 3.0 times of those before aluminum treatment, respectively (Figure 6).

3.7 Expression changes of ABA responsive genes in Arabidopsis

To further investigate the mechanism of *GmABR1* response to Al stress, the internal reference gene *Tubulin* in Arabidopsis was used as a control. The qRT-PCR analysis showed that after 100 μM $AlCl_3$ (pH 4.5) treatment, the expression levels of *AtABI1*, *AtABI2*, *AtABI4*, *AtABI5*, *AtRD22* and *AtRD29A* were all up-regulated in WT. The up-regulations of *AtABI4*, *AtABI5* and *AtRD22* were 2.9, 3.0 and 2.1 times higher than those before Al stress, respectively. *AtABI1*, *AtABI2* and *AtRD29A* were down-regulated to 0.7, 0.7 and 0.4 times of the pre-treatment levels, respectively (Figure 7).

4 Discussion

Previous studies have shown that AP2/ERF family genes play important biological functions in plants including regulating plant growth and development, and coping with various abiotic stresses. Transcription factor ERF96 is a transcriptional activator that binds GCC and positively regulates Arabidopsis resistance to necrotize pathogens by responding to jasmonic acid and ethylene (Wang et al., 2015). *WRI4* which is mainly expressed in Arabidopsis stem epidermis and encodes an AP2/ERF transcription factor is up-regulated under salt stress and involved in activating epidermal wax biosynthesis to protect plants from environmental stress (Park et al., 2016). *PpeERF2* regulates peach fruit ripening by inhibiting the expression of two ABA biosynthesis genes (*PpeNCED2*, *PpeNCED3*) and cell wall degradation gene (*PpePG1*) (Wang et al., 2019b). The expression of *SlERF5* in tomato is induced not only by low temperature, injury, high salt and drought, but also by plant hormones ethylene and ABA. Transgenic plants overexpressing *SlERF5* showed increased tolerance to drought and high salinity (Wang et al., 2019b).

GmABR1 protein with a highly conserved AP2 domain had the highest homology with ERF111 (*AT5g64750*) protein in Arabidopsis. Previous studies indicated that the *AtERF111* gene was specifically induced by flooding and hypoxia. The root hair length and number of overexpressed *AtERF111* plants increased, which strengthened the hypothesis that *AtERF111* was involved in injury response (Baumler et al., 2019). *AtERF6* plays an active role in antioxidant regulation of Arabidopsis in response to biotic and abiotic stresses (Sewelam et al., 2013). In addition, GmABR1 protein is localized in the nucleus and is self-activating like other ERF transcription factors. We speculate that *GmABR1* has potential functions as a member of the ERF family as a transcription factor (Baumler et al., 2019).

In this study, Al stress can induce high expression of *GmABR1* in cultivated soybean HX3, and it is expressed in soybean roots, stems and leaves (Figure 3). Previous studies have shown that Fe^{3+} and Al^{3+} can form stable complexes or chelates with the components in the dye solution of hematoxylin (Hajiboland et al., 2013). In the dyeing process, oxidation film will form on the surface of the dye solution, and blue precipitation will appear in the dye solution to color the plant nucleus. The content of Al^{3+} in plant can be determined by observing the color depth. Rincon et al. exposed

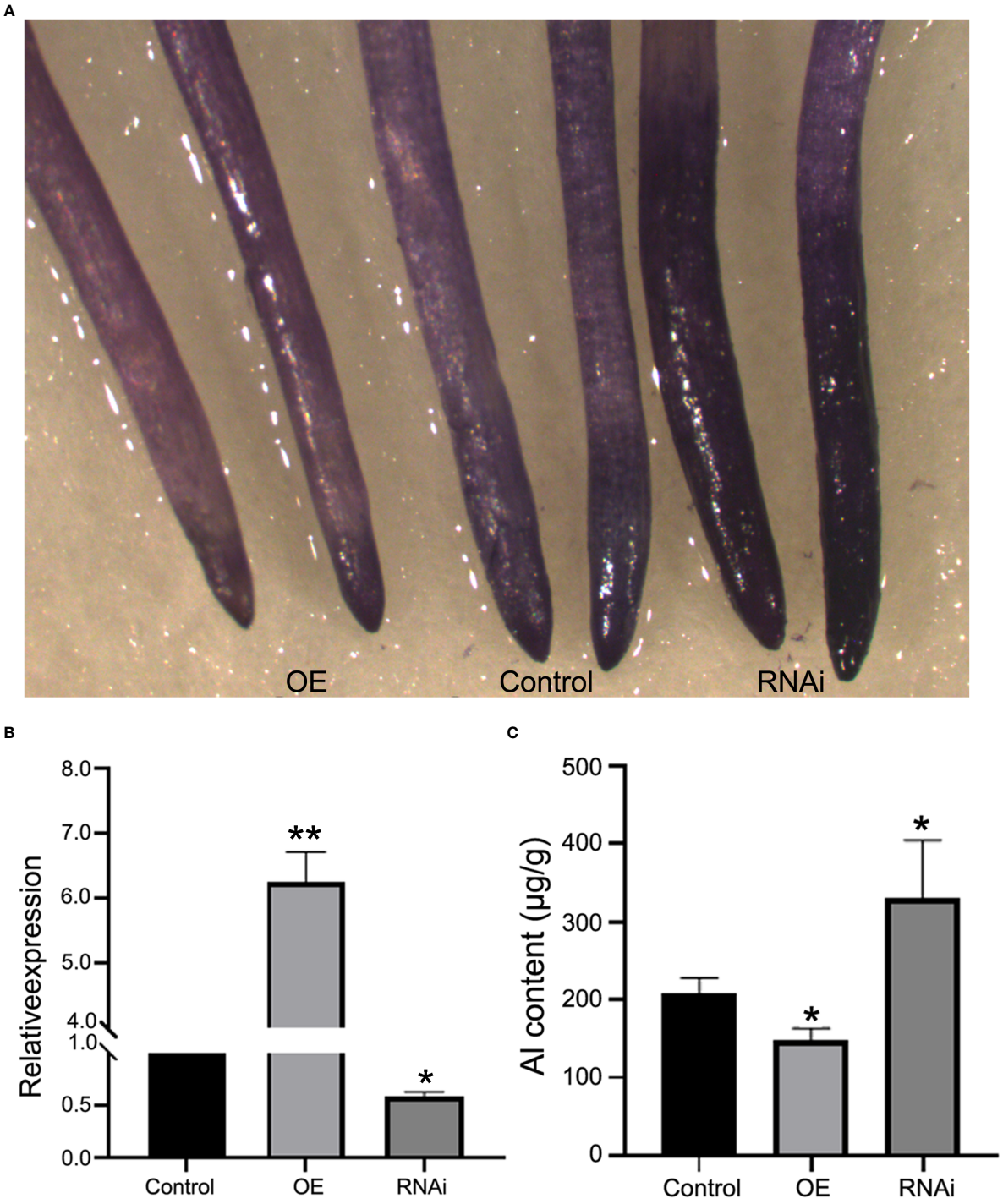

FIGURE 5
Soybean hairy roots experiment and hematoxylin staining. **(A)** Hematoxylin staining of soybean hairy roots. **(B)** Identification of RNA levels in hairy roots of soybean. **(C)** Determination of Al^{3+} content in root tips of soybean hairy root lines. The asterisks in figure B and C indicate significant differences between WT and OE or RNAi lines (*$P < 0.05$; **$P < 0.01$). Control: the lines of transformed pTF101 vector; OE: the lines of transformed pTF101-GmABR1 vector; RNAi: the lines of transformed pMU103-GmABR1 vector.

the roots of whole wheat seedlings to Al for 24 hours with the method of hemoxylin staining, and found that the main difference of Al accumulation between the Al tolerant (Atlas 66) and sensitive (Tam 105) varieties appeared in the growth area 0~2 and 2~5 mm from the root tip (Rincon and Gonzales, 1992). Our study showed that after hemoxylin staining of Al treated hairy roots of soybean, the root tip color of RNAi lines had the deepest color, followed by control lines, and the root tip color of overexpressed lines was stained the lightest (Figure 5A). Furthermore, plasma inductively coupled technique (ICP-AES) was used to determine the root tip

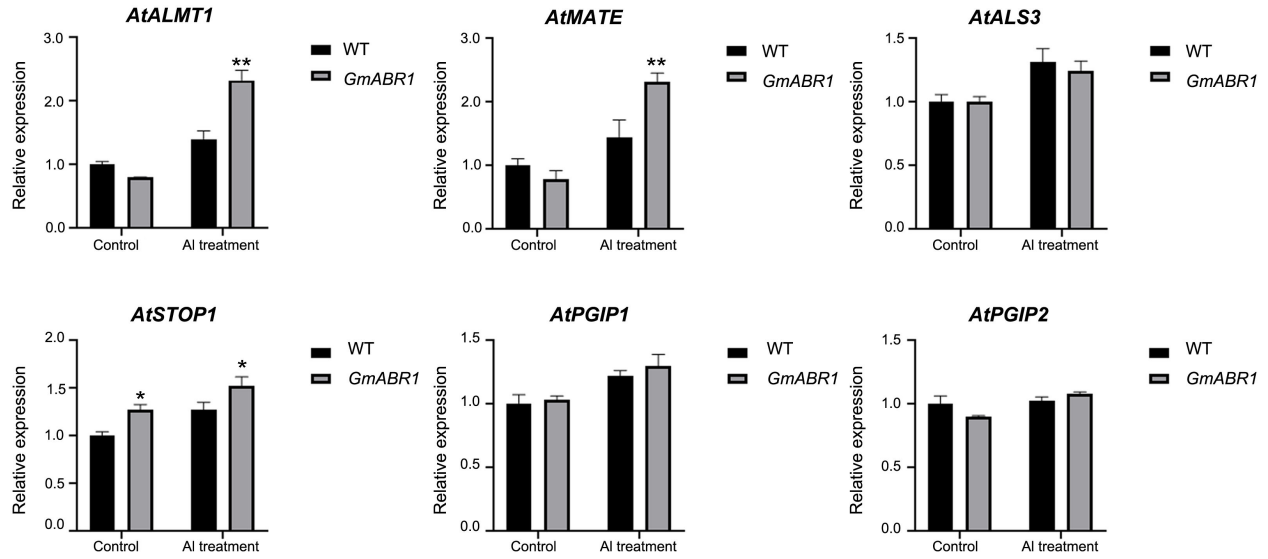

FIGURE 6
Expression patterns of Al stress responsive genes regulated by *GmABR1* in Arabidopsis. Arabidopsis were cultured in solid medium supplemented with 0 and 100 μM $AlCl_3$ (pH4.5) for 7 days, respectively. The expression patterns of Al stress responsive genes by *GmABR1* were detected. Using Arabidopsis *Tubulin* as the internal reference gene, qRT-PCR was used to detect the gene expression level before and after Al treatment. The asterisks indicated that the transcripts of investigated genes in *GmABR1* transgenic lines were significantly different from those of WT treated with and without $AlCl_3$ (*$P < 0.05$; **$P < 0.01$). The information of gene sequences was from the NCBI database (https://www.ncbi.nlm.nih.gov/). qRT-PCR primer information used in this experiment was shown in Table S2.

Al^{3+} data, and the root tip Al^{3+} content of overexpressed lines was the lowest, while the root tip Al^{3+} content of RNAi lines was the highest. The results indicated that *GmABR1* can improve the ability of soybean Al detoxification (Figure 5C). *GmABR1* was heterologous transformed into Arabidopsis, and the relative root elongation of transgenic lines after Al treatment was significantly higher than that of WT (Figure 4). MDA is one of the important products of membrane lipid oxidation, and its content reflects the degree of stress damage to plant cell membrane (Luan et al., 2018). Under Al stress, MDA concentration increased significantly in WT

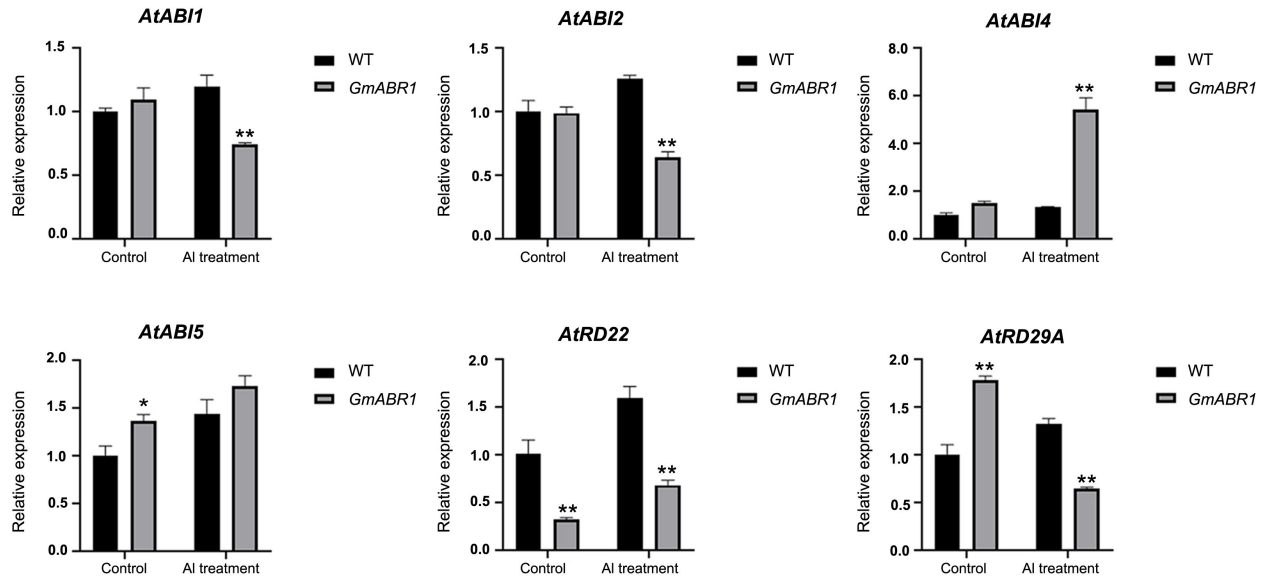

FIGURE 7
Expression patterns of ABA-responsive genes regulated by *GmABR1* in Arabidopsis. Arabidopsis were cultured in solid medium supplemented with 0 and 100 μM $AlCl_3$ (pH4.5) for 7 days, respectively. The expression patterns of Al stress responsive genes by *GmABR1* were detected. Using Arabidopsis *Tubulin* as the internal reference gene, qRT-PCR was used to detect the gene expression level before and after Al treatment. The asterisks indicated that the transcripts of investigated genes in *GmABR1* transgenic lines were significantly different from those of WT treated with and without $AlCl_3$ (*$P < 0.05$; **$P < 0.01$). The information of gene sequences was from the NCBI database (https://www.ncbi.nlm.nih.gov/). qRT-PCR primer information used in this experiment was shown in Table S2.

leaves compared with transgenic plants (Figure 4C). These results suggest that *GmABR1* enhances the tolerance of plants to Al stress.

Previous studies have found that Al-activated secretion of malate and citric acid has important effects on plant Al tolerance. After *MATE* knockdown in Arabidopsis, the transcript level of *MATE* was reduced, and Al-activated root citrate secretion was eliminated. Moreover, *ALMT1* and *MATE* double mutants lacked Al-activated root malate and citrate. Malate secretion mediated by *ALMT1* and citrate secretion mediated by *MATE* evolved independently in Arabidopsis and together contribute to Al tolerance in Arabidopsis (Liu et al., 2009). *STOP1* encodes a zinc finger protein, which is essential for Arabidopsis to resist low pH conditions, and the involvement of *STOP1* is also required for *ALMT1* expression (Iuchi et al., 2007). Liu et al. further demonstrated that the Al tolerance function of *STOP1* also requires *MATE* expression and root citric acid secretion, Arabidopsis *STOP1* gene plays a crucial role in the Al induced expression of *MATE* and *ALMT1* (Liu et al., 2009). Recent studies have reported that *STOP1* transcription is not affected by Al stress, but the expression of Al resistance genes *ALMT1*, *MATE* and *ALS3* downstream of *STOP1* is induced by Al stress. These results suggest that *STOP1* may be regulated by Al at the post-transcriptional or post-translational level (Zhang et al., 2019b). *ALS3* is predicted to encode a factor required for root growth in an Al-toxic environment, and mutational loss of this factor leads to severe Al-dependent consequences. This factor is specific for Al tolerance, as *ALS3* loss-of-function mutants do not show increased sensitivity to other metals, including La and Cu, nor do they exhibit any abnormal growth phenotype in the absence of Al (Larsen et al., 1997). Yuriko et al. found that *PGIP1* and *PGIP2* were strongly inhibited in *STOP1* mutants under Al stress, *PGIP1* and *PGIP2* may play a regulatory role in Al tolerance (Kobayashi et al., 2014). The Al-sensitive gene *ALS3* encodes an ABC transporter-like protein that is required for resistance tolerance to Al to redistribute accumulated Al from sensitive tissues, thereby protecting growing roots from Al toxicity (Larsen et al., 2005).

In present study, the expression levels of *AtALMT1*, *AtMATE*, *AtALS3*, *AtSTOP1*, *AtPGIP1* and *AtPGIP2* genes were up-regulated in WT and transgenic Arabidopsis. The transcription levels of *AtALMT1* and *AtMATE* in transgenic Arabidopsis were significantly increased compared with those before $AlCl_3$ treatment (Figure 6). Therefore, the results indicated that *GmABR1* may increase the secretion of malate and citrate in root tips of transgenic Arabidopsis by inducing the expression of Al stress response genes *AtALMT1* and *AtMATE*, and then increase the resistance of transgenic Arabidopsis to Al stress through external Al exclusion mechanism.

ABA is an important endogenous messenger for plants to cope with stress. Yang et al. found that *AtERF4* is a negative regulator of ethylene and abscisic acid response (Yang et al., 2005). Zhu et al. found that overexpression of *RAP2.6*, a member of the AP2/ERF family, could induce hypersensitivity responses to exogenous ABA and abiotic stress during seed germination and early seedling growth of Arabidopsis. ABA content in *RAP2.6* overexpressing lines decreased after salt treatment (Zhu et al., 2010). The *AtRAP2.6L* homologous apple gene *MdERF113* positively regulates abiotic stress and ABA stress (Rui et al., 2023). In recent years, Arabidopsis TCTP transcription factors have been gradually proved to be relative to abiotic stress signals. Overexpression of *AtTCTP* can enhance drought tolerance of plants by inducing ABA-mediated stomatal closure through interaction with microtubules (Kim et al., 2012). Merlot et al. found that double mutant plants of *ABI1* and *ABI2* loss function alleles were more responsive to ABA than their parental single mutants, while *ABI1* and *ABI2* were jointly involved in the negative feedback regulation of ABA signaling pathway (Merlot et al., 2001). ABI4 is also an important transcription factor in ABA signaling pathway, which can positively regulate *NCED6*, a key gene in ABA biosynthesis (Shu et al., 2016). Some studies have shown that Arabidopsis *ABI5* mutants have enhanced sensitivity to Al, however, it is not related to the regulation of *ALMT1* and *MATE* expression, indicating that ABA signal transduction pathway provides an additional regulatory mechanism for plant Al tolerance. The positive feedback regulatory transcription factor ABI5 can mediate cell wall modification and osmoregulation to enhance plant Al tolerance (Fan et al., 2019). The *RD29A* and *RD22* genes are very sensitive to various abiotic stressors, and their expression is induced by endogenous ABA, which can enhance the ability of plants to resist abiotic stress by participating in ABA pathway (Yamaguchi-Shinozaki and Shinozaki, 1993; Lee et al., 2016). *AtALMT12* is involved in ABA-induced stomatal closure and is a hypothesized target of this pathway with high nitrate and chloride transport capacity, stomatal closure may confer resistance to aluminum (Sasaki et al., 2010). Regulation of stomatal conductance by ABA signals may be an effective strategy to enhance abiotic stress in plants (Hsu et al., 2021).

In this study, the expression levels of *AtABI1*, *AtABI2*, *AtABI4*, *AtABI5*, *AtRD22* and *AtRD29A* genes in WT were all up-regulated after Al treatment. Among them, the transcripts of *AtABI4*, *AtABI5* and *AtRD22* in transgenic lines were significantly up-regulated under Al stress. While the expressions of *AtABI1*, *AtABI2* and *AtRD29A* were down-regulated with lower transcripts of the control treatment (Figure 7). The *RD29A* gene was up-regulated by Al stress in WT plants, but decreased in the transgenic lines. We hypothesized that this pathway has a compensating effect for the acid-resistant Al phenotype of the transgenic lines. Msanne et al. also found contrary to expectations that *RD29A* knockout mutant lines maintained greater root growth, photosynthesis and water use efficiency under salt stress than those of the controls. All transgenes effectively complemented resistance to salt stress-induced root growth inhibition (Msanne et al., 2011). Therefore, the results indicated that *GmABR1* maybe also enhance plant resistance to abiotic stress by participating in the ABA pathway (Xu et al., 2017; Huang et al., 2022).

In summary, the *GmABR1* gene encoding a AP2/ERF transcription factor in soybean was identified in present study, which was induced by Al stress and enriched in the roots, leaves, stems of soybean seedlings. *GmABR1* overexpression increased the tolerance of *GmABR1* transgenic plants to Al stress. The analysis of molecular mechanism showed that the enhanced tolerance to Al stress might due to the comprehensive roles in upregulating and/or downregulating transcripts of the Al stress- and/or ABA-responsive

genes with MDA decrease. Therefore, these results suggested that *GmABR1* may jointly regulate plant resistance to Al stress through the genes related to Al response and/or ABA response pathways.

Data availability statement

The data presented in the study are deposited in the NCBI database (https://www.ncbi.nlm.nih.gov/). The entry numbers of all genes involved in this paper (including the genetic information for making evolutionary trees) can be found in Supplementary Material Table S6. The original contributions presented in the study are included in the article/Supplementary Material, further inquiries can be directed to the corresponding author/s.

Author contributions

QM, AZ and HW conceived of and designed the study. HW, CL, LW, HZ, XX, YC, WL and HN conducted the experiments. HW, CL, LW, PC and QM performed data as well as statistical analysis. HW prepared the manuscript which was edited by QM and AZ. All authors contributed to the article and approved the submitted version.

Funding

This work was supported by the grants from the Project of China-Uruguay Joint Laboratory Cooperation (SQ2018YFE010044), the Guangdong Provincial Science and Technology Innovation Strategy Project (2020B1212060062), the Projects of the National Natural Science Foundation of China (31771816, 31971965 and 31371642), the New Varieties Cultivation of Genetically Modified Organisms (2016ZX08004002-007), the China Agricultural Research System (CARS-04-PS11), the Project of Agricultural Science and Technology Development and Resource and Environmental Protection Management from the Special Rural Revitalization Funds of Guangdong Province (2022KJ153-03), Ministry of Agriculture and Rural Affairs agricultural products quality and safety supervision special (4100-C17106, 21301091702101), the Projects of Key Area Research and Development Program of Guangdong Province (2020B020220008), the project of the Guangdong Provincial Laboratory of Lingnan Modern Agricultural Science and Technology (NZ2021012).

Conflict of interest

The authors declare that the research was conducted in the absence of any commercial or financial relationships that could be construed as a potential conflict of interest.

Publisher's note

All claims expressed in this article are solely those of the authors and do not necessarily represent those of their affiliated organizations, or those of the publisher, the editors and the reviewers. Any product that may be evaluated in this article, or claim that may be made by its manufacturer, is not guaranteed or endorsed by the publisher.

Supplementary material

The Supplementary Material for this article can be found online at: https://www.frontiersin.org/articles/10.3389/fpls.2023.1125245/full#supplementary-material

References

Baumler, J., Riber, W., Klecker, M., Muller, L., Dissmeyer, N., Weig, A., et al. (2019). AtERF#111/ABR1 is a transcriptional activator involved in the wounding response. *Plant J.* 100, 969–990. doi: 10.1111/tpj.14490

Cai, Z., Cheng, Y., Xian, P., Ma, Q., Wen, K., Xia, Q, et al. (2018). Acid phosphatase gene *GmHAD1* linked to low phosphorus tolerance in soybean, through fine mapping. *Theor. Appl. Genet.* 131, 1715–1728. doi: 10.1007/s00122-018-3109-3

Chauhan, D. K., Yadav, V., Vaculik, M., Gassmann, W., Pike, S., Arif, N., et al. (2021). Aluminum toxicity and aluminum stress-induced physiological tolerance responses in higher plants. *Crit. Rev. Biotechnol.* 41, 715–730. doi: 10.1080/07388551.2021.1874282

Chen, L. S. (2006). Physiological responses and tolerance of plant shoot to aluminum toxicity. *Zhi. Wu. Sheng. Li. Yu. Fen. Zi. Sheng. Wu. Xue. Xue. Bao.* 32, 143–155.

Choudhury, S., and Sharma, P. (2014). Aluminum stress inhibits root growth and alters physiological and metabolic responses in chickpea (*Cicer arietinum* l.). *Plant Physiol. Biochem.* 85, 63–70. doi: 10.1016/j.plaphy.2014.10.012

Collings, D. A. (2013). Subcellular localization of transiently expressed fluorescent fusion proteins. *Methods Mol. Biol.* 1069, 227–258. doi: 10.1007/978-1-62703-613-9_16

Dong, L., Cheng, Y., Wu, J., Cheng, Q., Li, W., Fan, S., et al. (2015). Overexpression of *GmERF5*, a new member of the soybean EAR motif-containing ERFtranscription factor, enhances resistance to *Phytophthora sojae* in soybean. *J. Exp. Bot.* 66, 2635–2647. doi: 10.1093/jxb/erv078

Fan, W., Xu, J., Wu, P., Yang, Z., Lou, H., Chen, W., et al. (2019). Alleviation by abscisic acid of Al toxicity in rice bean is not associated with citrate efflux but depends on *ABI5*-mediated signal transduction pathways. *J. Integr. Plant Biol.* 61, 140–154. doi: 10.1111/jipb.12695

Feng, K., Hou, X., Xing, G., Liu, J., Duan, A., Xu, Z. S., et al. (2020). Advances in AP2/ERF super-family transcription factors in plant. *Crit. Rev. Biotechnol.* 40, 750–776. doi: 10.1080/07388551.2020.1768509

Guo, Z. J., Chen, X. J., Wu, X. L., Ling, J. Q., and Xu, P. (2004). Overexpression of the AP2/EREBP transcription factor OPBP1 enhances disease resistance and salt tolerance in tobacco. *Plant Mol. Biol.* 55, 607–618. doi: 10.1007/s11103-004-1521-3

Hajiboland, R., Barcelo, J., Poschenrieder, C., and Tolra, R. (2013). Amelioration of iron toxicity: A mechanism for aluminum-induced growth stimulation in tea plants. *J. Inorg. Biochem.* 128, 183–187. doi: 10.1016/j.jinorgbio.2013.07.007

Han, Z., Wang, J., Wang, X., Zhang, X., Cheng, Y., Cai, Z., et al. (2022). *GmWRKY21*, a soybean WRKY transcription factor gene, enhances the tolerance to aluminum stress in *arabidopsis thaliana*. *Front. Plant Sci.* 13. doi: 10.3389/fpls.2022.833326

Hsu, P. K., Dubeaux, G., Takahashi, Y., and Schroeder, J. I. (2021). Signaling mechanisms in abscisic acid-mediated stomatal closure. *Plant J.* 105, 307–321. doi: 10.1111/tpj.15067

Huang, J., Han, R., Ji, F., Yu, Y., Wang, R., Hai, Z., et al. (2022). Glucose-6-phosphate dehydrogenase and abscisic acid mediate programmed cell death induced by aluminum toxicity in soybean root tips. *J. Hazard. Mater.* 425, 127964. doi: 10.1016/j.jhazmat.2021.127964

Iuchi, S., Koyama, H., Iuchi, A., Kobayashi, Y., Kitabayashi, S., Kobayashi, Y., et al. (2007). Zinc finger protein STOP1 is critical for proton tolerance in arabidopsis and coregulates a key gene in aluminum tolerance. *Proc. Natl. Acad. Sci. U. S.* 104, 9900–9905. doi: 10.1073/pnas.0700117104

Kereszt, A., Li, D., Indrasumunar, A., Nguyen, C., Nontachaiyapoom, S., Gresshoff, P., et al. (2007). *Agrobacterium rhizogenes*-mediated transformation of soybean to study root biology. *Nat. Protoc.* 2, 948–952. doi: 10.1038/nprot.2007.141

Khoudi, H. (2023). SHINE clade of ERF transcription factors: A significant player in abiotic and biotic stress tolerance in plants. *Plant Physiol. Biochem.* 195, 77–88. doi: 10.1016/j.plaphy.2022.12.030

Kim, Y., Han, Y., Hwang, O., Lee, S., Shin, A., Kim, S., et al. (2012). Overexpression of arabidopsis translationally controlled tumor protein gene *AtTCTP* enhances drought tolerance with rapid ABA-induced stomatal closure. *Mol. Cells* 33, 617–626. doi: 10.1007/s10059-012-0080-8

Kobayashi, Y., Ohyama, Y., Kobayashi, Y., Ito, H., Iuchi, S., Fujita, M., et al. (2014). STOP2 activates transcription of several genes for Al- and low pH-tolerance that are regulated by STOP1 in arabidopsis. *Mol. Plant* 7, 311–322. doi: 10.1093/mp/sst116

Kochian, L. V., Pineros, M. A., Liu, J., and Magalhaes, J. V. (2015). Plant adaptation to acid soils: The molecular basis for crop aluminum resistance. *Annu. Rev. Plant Biol.* 66, 571–598. doi: 10.1146/annurev-arplant-043014-114822

Kumar, R., and Sharma, A. K. (2021). Transcription factor stoichiometry in cell fate determination. *J. Genet.* 100, 27. doi: 10.1007/s12041-021-01278-2

Larsen, P. B., Geisler, M. J., Jones, C. A., Williams, K. M., and Cancel, J. D. (2005). *ALS3* encodes a phloem-localized ABC transporter-like protein that is required for aluminum tolerance in arabidopsis. *Plant J.* 41, 353–363. doi: 10.1111/j.1365-313X.2004.02306.x

Larsen, P. B., Kochian, L. V., and Howell, S. H. (1997). Al Inhibits both shoot development and root growth in *als3*, an Al-sensitive arabidopsis mutant. *Plant Physiol.* 114, 1207–1214. doi: 10.1104/pp.114.4.1207

Lee, S. Y., Boon, N. J., Webb, A. A., and Tanaka, R. J. (2016). Synergistic activation of *RD29A via* integration of salinity stress and abscisic acid in *Arabidopsis thaliana*. *Plant Cell Physiol.* 57, 2147–2160. doi: 10.1093/pcp/pcw132

Li, L., Li, X., Yang, C., Cheng, Y., Cai, Z., Nian, H., et al. (2022). *GsERF1* enhances *Arabidopsis thaliana* aluminum tolerance through an ethylene-mediated pathway. *BMC Plant Biol.* 22, 258. doi: 10.1186/s12870-022-03625-6

Liu, D., Chen, X., Liu, J., Ye, J., and Guo, Z. (2012). The rice ERF transcription factor OsERF922 negatively regulates resistance to *Magnaporthe oryzae* and salt tolerance. *J. Exp. Bot.* 63, 3899–3911. doi: 10.1093/jxb/ers079

Liu, J., Magalhaes, J. V., Shaff, J., and Kochian, L. V. (2009). Aluminum-activated citrate and malate transporters from the MATE and ALMT families function independently to confer arabidopsis aluminum tolerance. *Plant J.* 57, 389–399. doi: 10.1111/j.1365-313X.2008.03696.x

Liu, Y. T., Shi, Q. H., Cao, H. J., Ma, Q. B., Nian, H., Zhang, X., et al. (2020). Heterologous expression of a *Glycine soja* C_2H_2 zinc finger gene improves aluminum tolerance in arabidopsis. *Int. J. Mol. Sci.* 21, 2754. doi: 10.3390/ijms21082754

Luan, Y., Cui, J., Li, J., Jiang, N., Liu, P., Meng, J., et al. (2018). Effective enhancement of resistance to *Phytophthora infestans* by overexpression of miR172a and b in *Solanum lycopersicum*. *Planta* 247, 127–138. doi: 10.1007/s00425-017-2773-x

Ma, Q., Xia, Z., Cai, Z., Li, L., Cheng, Y., Liu, J., et al. (2018). *GmWRKY16* enhances drought and salt tolerance through an ABA-mediated pathway in *Arabidopsis thaliana*. *Front. Plant Sci.* 9. doi: 10.3389/fpls.2018.01979

Matsumoto, H., and Motoda, H. (2012). Aluminum toxicity recovery processes in root apices. possible association with oxidative stress. *Plant Sci.* 185-186, 1–8. doi: 10.1016/j.plantsci.2011.07.019

Merlot, S., Gosti, F., Guerrier, D., Vavasseur, A., and Giraudat, J. (2001). The ABI1 and ABI2 protein phosphatases 2C act in a negative feedback regulatory loop of the abscisic acid signalling pathway. *Plant J.* 25, 295–303. doi: 10.1046/j.1365-313x.2001.00965.x

Msanne, J., Lin, J., Stone, J. M., and Awada, T. (2011). Characterization of abiotic stress-responsive *Arabidopsis thaliana RD29A* and *RD29B* genes and evaluation of transgenes. *Planta* 234, 97–107. doi: 10.1007/s00425-011-1387-y

Pandey, G. K., Grant, J. J., Cheong, Y. H., Kim, B. G., Li, L., Luan, S., et al. (2005). ABR1, an APETALA2-domain transcription factor that functions as a repressor of ABA response in arabidopsis. *Plant Physiol.* 139, 1185–1193. doi: 10.1104/pp.105.066324

Park, C. S., Go, Y. S., and Suh, M. C. (2016). Cuticular wax biosynthesis is positively regulated by WRINKLED4, an AP2/ERF-type transcription factor, in arabidopsis stems. *Plant J.* 88, 257–270. doi: 10.1111/tpj.13248

Rangel, A. F., Rao, I. M., and Horst, W. J. (2009). Intracellular distribution and binding state of aluminum in root apices of two common bean (*Phaseolus vulgaris*) genotypes in relation to Al toxicity. *Physiol. Plant* 135, 162–173. doi: 10.1111/j.1399-3054.2008.01183.x

Ranjan, A., Sinha, R., Sharma, T. R., Pattanayak, A., and Singh, A. K. (2021). Alleviating aluminum toxicity in plants: Implications of reactive oxygen species signaling and crosstalk with other signaling pathways. *Physiol. Plant* 173, 1765–1784. doi: 10.1111/ppl.13382

Ren, B., Wang, X., Duan, J., and Ma, J. (2019). Rhizobial tRNA-derived small RNAs are signal molecules regulating plant nodulation. *Science* 365, 919–922. doi: 10.1126/science.aav8907

Rincon, M., and Gonzales, R. A. (1992). Aluminum partitioning in intact roots of aluminum-tolerant and aluminum-sensitive wheat (Triticum aestivum l.) cultivars. *Plant Physiol.* 99, 1021–1028. doi: 10.1104/pp.99.3.1021

Rui, L., Zhu, Z., Yang, Y., Wang, D., Liu, H., Zheng, P., et al. (2023). Functional characterization of *MdERF113* in apple. *Physiol. Plant*, 175, e13853. doi: 10.1111/ppl.13853

Salazar-Chavarria, V., Sanchez-Nieto, S., and Cruz-Ortega, R. (2020). *Fagopyrum esculentum* at early stages copes with aluminum toxicity by increasing ABA levels and antioxidant system. *Plant Physiol. Biochem.* 152, 170–176. doi: 10.1016/j.plaphy.2020.04.024

Sasaki, T., Mori, I. C., Furuichi, T., Munemasa, S., Toyooka, K., Matsuoka, K., et al. (2010). Closing plant stomata requires a homolog of an aluminum-activated malate transporter. *Plant Cell Physiol.* 51, 354–365. doi: 10.1093/pcp/pcq016

Sewelam, N., Kazan, K., Thomas-Hall, S., Kidd, B., Manners, J., Schenk, P., et al. (2013). Ethylene response factor 6 is a regulator of reactive oxygen species signaling in arabidopsis. *PloS One* 8, e70289. doi: 10.1371/journal.pone.0070289

Shu, K., Chen, Q., Wu, Y., Liu, R., Zhang, H., Wang, P., et al. (2016). ABI4 mediates antagonistic effects of abscisic acid and gibberellins at transcript and protein levels. *Plant J.* 85, 348–361. doi: 10.1111/tpj.13109

Shu, W., Zhou, Q., Xian, P., Cheng, Y., Lian, T., Ma, Q, et al. (2022). *GmWRKY81* encoding a WRKY transcription factor enhances aluminum tolerance in soybean. *Int. J. Mol. Sci.* 23, 6518. doi: 10.3390/ijms23126518

Umemura, T., Usami, Y., Aizawa, S., Tsunoda, K., and Satake, K. (2003). Seasonal change in the level and the chemical forms of aluminum in soil solution under a Japanese cedar forest. *Sci. Total. Environ.* 317, 149–157. doi: 10.1016/S0048-9697(03)00364-4

Wang, X., Cheng, Y., Yang, C., Yang, C., Mu, Y., Xia, Q., et al. (2019a). QTL mapping for aluminum tolerance in RIL population of soybean (*Glycine max* l.) by RAD sequencing. *PloS One* 14, e223674. doi: 10.1371/journal.pone.0223674

Wang, X., Liu, S., Tian, H., Wang, S., and Chen, J. G. (2015). The small ethylene response factor ERF96 is involved in the regulation of the abscisic acid response in arabidopsis. *Front. Plant Sci.* 6. doi: 10.3389/fpls.2015.01064

Wang, H., Yin, X., Du, D., Liang, Z., Han, Z., Nian, H., et al. (2022). *GsMYB7* encoding a R2R3-type MYB transcription factor enhances the tolerance to aluminum stress in soybean (*Glycine max* l.). *BMC Genomics* 23, 529. doi: 10.1186/s12864-022-08744-w

Wang, X., Zeng, W., Ding, Y., Wang, Y., Niu, L., Yao, J., et al. (2019b). Peach ethylene response factor PpeERF2 represses the expression of ABA biosynthesis and cell wall degradation genes during fruit ripening. *Plant Sci.* 283, 116–126. doi: 10.1016/j.plantsci.2019.02.009

Wen, K., Pan, H., Li, X., Huang, R., Ma, Q., Nian, H., et al. (2021). Identification of an ATP-binding cassette transporter implicated in aluminum tolerance in wild soybean (*Glycine soja*). *Int. J. Mol. Sci.* 22, 13264. doi: 10.3390/ijms222413264

Xian, P., Cai, Z., Cheng, Y., Lin, R., Lian, T., Ma, Q., et al. (2020). Wild soybean oxalyl-CoA synthetase degrades oxalate and affects the tolerance to cadmium and aluminum stresses. *Int. J. Mol. Sci.* 21, 8869. doi: 10.3390/ijms21228869

Xu, D., Cao, H., Fang, W., Pan, J., Chen, J., Zhang, J., et al. (2017). Linking hydrogen-enhanced rice aluminum tolerance with the reestablishment of GA/ABA balance and miRNA-modulated gene expression: A case study on germination. *Ecotoxicol. Environ. Saf.* 145, 303–312. doi: 10.1016/j.ecoenv.2017.07.055

Yamaguchi-Shinozaki, K., and Shinozaki, K. (1993). The plant hormone abscisic acid mediates the drought-induced expression but not the seed-specific expression of *rd22*, a gene responsive to dehydration stress in *Arabidopsis thaliana*. *Mol. Gen. Genet.* 238, 17–25. doi: 10.1007/BF00279525

Yang, Z., Tian, L., Latoszek-Green, M., Brown, D., and Wu, K. (2005). Arabidopsis ERF4 is a transcriptional repressor capable of modulating ethylene and abscisic acid responses. *Plant Mol. Biol.* 58, 585–596. doi: 10.1007/s11103-005-7294-5

Yokosho, K., Yamaji, N., Mitani-Ueno, N., Shen, R. F., and Ma, J. F. (2016). An aluminum-inducible *IREG* gene is required for internal detoxification of aluminum in buckwheat. *Plant Cell Physiol.* 57, 1169–1178. doi: 10.1093/pcp/pcw065

Yu, Y., Duan, X., Ding, X., Chen, C., Zhu, D., Yin, K., et al. (2017). A novel AP2/ERF family transcription factor from *Glycine soja*, GsERF71, is a DNA binding protein that positively regulates alkaline stress tolerance in arabidopsis. *Plant Mol. Biol.* 94, 509–530. doi: 10.1007/s11103-017-0623-7

Zhang, X., Long, Y., Huang, J., and Xia, J. (2019a). Molecular mechanisms for coping with al toxicity in plants. *Int. J. Mol. Sci.* 20, 1551. doi: 10.3390/ijms20071551

Zhang, Y., Zhang, J., Guo, J., Zhou, F., Singh, S., Xu, X., et al. (2019b). F-box protein RAE1 regulates the stability of the aluminum-resistance transcription factor STOP1 in arabidopsis. *Proc. Natl. Acad. Sci. U. S.* 116, 319–327. doi: 10.1073/pnas.1814426116

Zhou, Q., Tian, A., Zou, H., Xie, Z., Lei, G., Huang, J., et al. (2008). Soybean WRKY-type transcription factor genes, *GmWRKY13*, *GmWRKY21*, and *GmWRKY54*, confer differential tolerance to abiotic stresses in transgenic arabidopsis plants. *Plant Biotechnol. J.* 6, 486–503. doi: 10.1111/j.1467-7652.2008.00336.x

Zhu, Q., Zhang, J., Gao, X., Tong, J., Xiao, L., Li, W., et al. (2010). The arabidopsis AP2/ERF transcription factor RAP2.6 participates in ABA, salt and osmotic stress responses. *Gene* 457, 1–12. doi: 10.1016/j.gene.2010.02.011

Frontiers in
Plant Science

Cultivates the science of plant biology and its applications

The most cited plant science journal, which advances our understanding of plant biology for sustainable food security, functional ecosystems and human health.

Discover the latest Research Topics

See more →

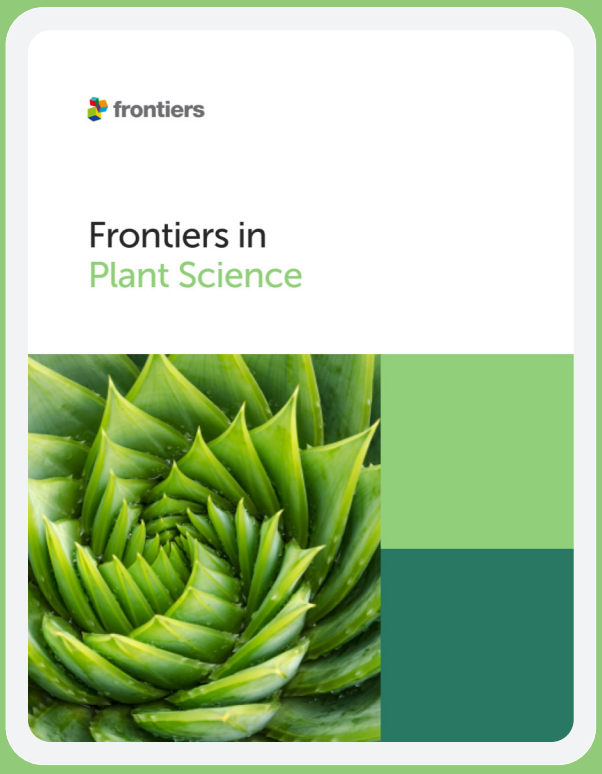

Frontiers

Avenue du Tribunal-Fédéral 34
1005 Lausanne, Switzerland
frontiersin.org

Contact us

+41 (0)21 510 17 00
frontiersin.org/about/contact